FOOD PRESERVATION TECHNOLOGY SERIES

Unit Operations in Food Engineering

Albert Ibarz
Gustavo V. Barbosa-Cánovas

Unit Operations in Food Engineering

FOOD PRESERVATION TECHNOLOGY SERIES

Series Editor
Gustavo V. Barbosa-Cánovas

Innovations in Food Processing
Editors: Gustavo V. Barbosa-Cánovas and Grahame W. Gould

Trends in Food Engineering
Editors: Jorge E. Lozano, Cristina Añón, Efrén Parada-Arias, and Gustavo V. Barbosa-Cánovas

Pulsed Electric Fields in Food Processing: Fundamental Aspects and Applications
Editors: Gustavo V. Barbosa-Cánovas and Q. Howard Zhang

Osmotic Dehydration and Vacuum Impregnation: Applications in Food Industries
Editors: Pedro Fito, Amparo Chiralt, Jose M. Barat, Walter E. L. Spiess, and Diana Behsnilian

Engineering and Food for the 21st Century
Editors: Jorge Welti-Chanes, Gustavo V. Barbosa-Cánovas, and José Miguel Aguilera

Unit Operations in Food Engineering
Albert Ibarz and Gustavo V. Barbosa-Cánovas

Unit Operations in Food Engineering

Albert Ibarz, Ph.D.
University of Lleida
Lleida, Spain

Gustavo V. Barbosa-Cánovas, Ph.D.
Washington State University
Pullman, Washington

CRC PRESS

Boca Raton London New York Washington, D.C.

Library of Congress Cataloging-in-Publication Data

Ibarz, Albert.
[Operaciones unitarias en la engenierâia de alimentos. English]
Unit operations in food engineering / by Albert Ibarz, Gustavo V. Barbosa-Cánovas.
p. cm. -- (Food preservation technology series)
Includes bibliographical references and index.
ISBN 1-56676-929-9
1. Food industry and trade. I. Barbosa-Cánovas, Gustavo V. II. Title. III. Series.
TP370 .I2313 2002
664—dc21 2002017480
CIP

International Standard Book Number 1-56676-929-9
Library of Congress Card Number 2002017480
Printed in the United States of America 1 2 3 4 5 6 7 8 9 0
Printed on acid-free paper

To our families

Preface

One of the primary objectives of the food industry is to transform, by a series of operations, raw agricultural materials into foods suitable for consumption. Many different types of equipment and several stages are used to perform these transformations. The efficient calculation and design of each stage — called unit or basic operation — is one of the main purposes of food engineering.

The systematic study of unit operations began in the chemical engineering field, where calculation tools were developed to describe, based on engineering principles, the changes taking place in each processing step. This knowledge has been applied to food engineering and, at the same time, has been adapted to the particular and distinctive nature of the raw materials used. The goal of any series of operations is not just to obtain optimum production, but also a food product suitable for consumption and of the highest quality. Thus, in the application of unit operations to a food process, exhaustive and careful calculation is essential to obtaining process stages that cause minimum damage to the food that is being processed.

The main objective of this book is to present, in progressive and systematic form, the basic information required to design food processes, including the necessary equipment. The number of food engineering unit operations is quite extensive, but some are rarely applied because they are quite specific to a given commodity or process. This book covers those unit operations that, in the opinion of the authors, are most relevant to the food industry in general. The first chapters contain basic information on transport phenomena governing key unit operations, followed by chapters offering a detailed description of those selected unit operations. To facilitate the understanding of all the studied unit operations, each chapter concludes with a set of solved problems.

We hope this book will be useful as a reference for food engineers and as a text for advanced undergraduate and graduate students in food engineering. We also hope this book will be a meaningful addition to the literature dealing with food processing operations.

Albert Ibarz
Gustavo V. Barbosa-Cánovas

Acknowledgments

The authors wish to express their gratitude to the following institutions and individuals who contributed to making this book possible:

Interministerial Commission of Science and Technology (CICYT) of Spain for supporting the preparation of this book through project TXT96-2223.

The University of Lleida and the Washington State University (WSU) for supplying the facilities and conducive framework for the preparation of this book.

Dr. Jorge Vélez-Ruiz, Universidad de las Américas-Puebla, México for his very important contributions in the preparation of Chapter 7.

María Luisa Calderón (WSU) for her professionalism and dedication in revising the Spanish version of the book from beginning to end. Her commentaries and suggestions were very valuable.

José Juan Rodríguez and Federico Harte (WSU) for their decisive participation in the final review of the Spanish version. Both worked with great care, dedication, enthusiasm, and professionalism.

The "translation team:" Lucy López (Universidad de las Américas-Puebla, México), Jeannie Anderson (WSU), Fernanda San Martín (WSU), and Gipsy Tabilo (WSU) for their incredible dedication to transforming this book into the English version.

All the students who attended our unit operations in food engineering courses; they provided a constant stimulus for conceiving and developing the finished work.

Albert Ibarz, Jr. for his careful collaboration in preparing many of the figures in the book and Raquel Ibarz for her invaluable help and encouragement for making this book a pleasant reality.

Authors

Albert Ibarz earned his B.S. and Ph.D. in chemical engineering from the University of Barcelona, Spain. He is a Professor of Food Engineering at the University of Lleida, Spain and the Vice-Chancellor for Faculty Affairs. His current research areas are: transport phenomena in food processing, reaction kinetics in food systems, physical properties of foods, and ultra high pressure for food processing.

Gustavo V. Barbosa-Cánovas earned his B.S. in mechanical engineering from the University of Uruguay and his M.S. and Ph.D. in food engineering from the University of Massachusetts at Amherst. He is a Professor of Food Engineering at Washington State University and Director of the Center for Nonthermal Processing of Food. His current research areas are: nonthermal processing of foods, physical properties of foods, edible films, food powder technology, and food dehydration.

CONTENTS

1

Introduction to Unit Operations: Fundamental Concepts

1.1 Process

Process is the set of activities or industrial operations that modify the properties of raw materials with the purpose of obtaining products to satisfy the needs of a society. Such modifications of natural raw materials are directed to obtain products with greater acceptance in the market, or with better possibilities of storage and transport.

The primary needs of every human being, individually or as a society, have not varied excessively throughout history; food, clothing, and housing were needed for survival by prehistoric man as well as by modern man. The satisfaction of these necessities is carried out by employing, transforming, and consuming resources available in natural surroundings.

In the early stages of mankind's social development, natural products were used directly or with only small physical modifications. This simple productive scheme changed as society developed, so that, at the present time, raw materials are not used directly to satisfy necessities, but rather are subjected to physical and chemical transformations that convert them into products with different properties.

This way, not only do raw materials satisfy the necessities of consumers, but also those products derived from the manipulation of such raw materials.

1.2 Food Process Engineering

By analogy with other engineering branches, different definitions of food process engineering can be given. Thus, according to one definition, "food process engineering includes the part of human activity in which the knowledge of physical, natural, and economic sciences is applied to agricultural products as related to their composition, energetic content, or physical state."

Food process engineering can also be defined as "the science of conceiving, calculating, designing, building, and running the facilities where the transformation processes of agricultural products, at the industrial level and as economically as possible, are carried out."

Thus, an engineer in the food industry should know the basic principles of process engineering and be able to develop new production techniques for agricultural products. He should also be capable of designing the equipment to be used in a given process. The main objective of food process engineering is to study the principles and laws governing the physical, chemical, or biochemical stages of different processes, and the apparatus or equipment by which such stages are industrially carried out. The studies should be focused on the transformation processes of agricultural raw materials into final products, or on conservation of materials and products.

1.3 Transformation and Commercialization of Agricultural Products

For efficient commercialization, agricultural products should be easy to handle and to place in the market. As a general rule, products obtained directly from the harvest cannot be commercialized as they are, but must undergo certain transformations. Products that can be directly used should be adequately packaged according to requirements of the market. These products are generally used as food and should be conveniently prepared for use.

One problem during handling of agricultural products is their transport from the fields to the consumer. Since many agricultural products have a short shelf life, treatment and preservation methods that allow their later use should be developed. As mentioned earlier, many of these products cannot be directly used as food but can serve as raw material to obtain other products. Developed countries tend to elaborate such products in the harvest zone, avoiding perishable products that deteriorate during transport from the production zone to the processing plant.

1.4 Flow Charts and Description of Some Food Processes

Food processes are usually schematized by means of flow charts. These are diagrams of all processes that indicate different manufacturing steps, as well as the flow of materials and energy in the process.

There are different types of flow charts; the most common use "blocks" or "rectangles." In these charts each stage of the process is represented by a block or rectangle connected by arrows to indicate the way in which the materials flow. The stage represented is written within the rectangle.

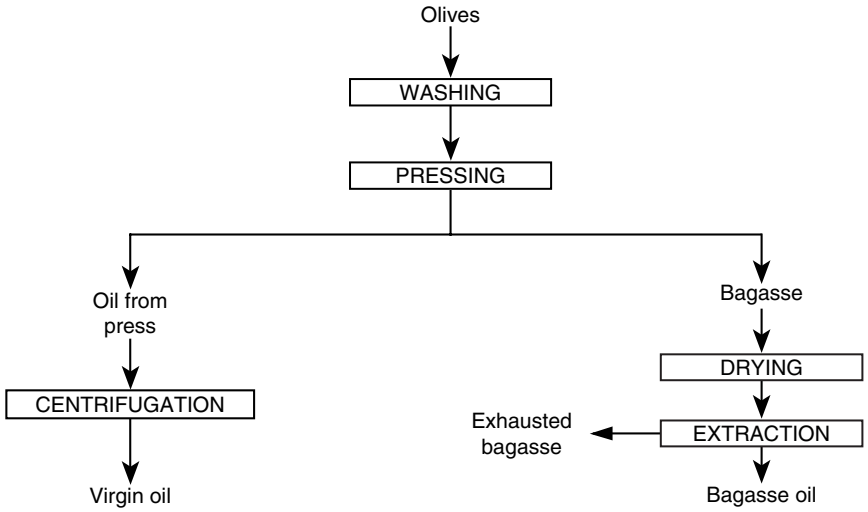

FIGURE 1.1
Extraction of olive oil.

Other types of flow charts are "equipment" and "instrumentation." Figures 1.1, 1.2, and 1.3 show some flow charts of food processes.

1.5 Steady and Unsteady States

A system is said to be under steady state when all the physical variables remain constant and invariable along time, at any point of the system; however, they may be different from one point to another. On the other hand, when the characteristic intensive variables of the operation vary through the system at a given moment and the variables corresponding to each system's point vary along time, the state is called unsteady. The physical variables to consider may be mechanical or thermodynamic. Among the former are volume, velocity, etc., while the thermodynamic variables are viscosity, concentration, temperature, pressure, etc.

1.6 Discontinuous, Continuous, and Semicontinuous Operations

The operations carried out in the industrial processes may be performed in three different ways. In a discontinuous operation the raw material is loaded

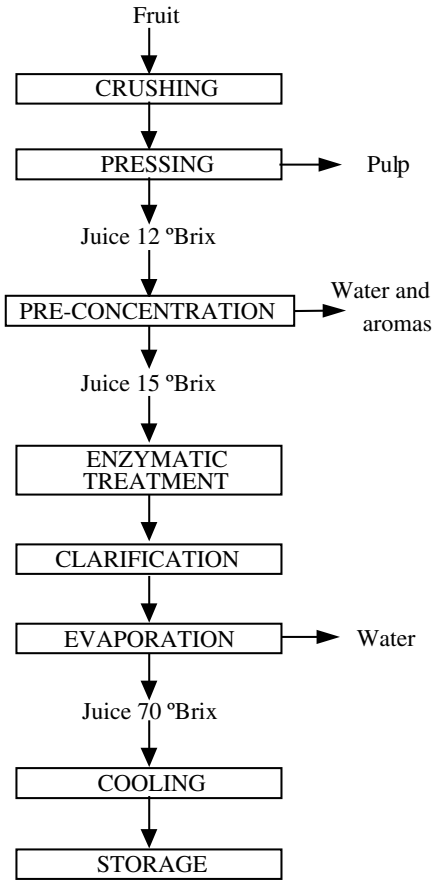

FIGURE 1.2
Production of fruit concentrated juices.

in the equipment; after performing the required transformation, the obtained products are unloaded. These operations, also called "batch" or "intermittent," are carried out in steps:

1. Loading of equipment with raw materials
2. Preparation of conditions for transformation
3. Required transformation
4. Unloading products
5. Cleaning equipment

The batch operation takes place under an unsteady state, since its intensive properties vary along time. An example of this batch process is the crushing of oily seeds to obtain oil.

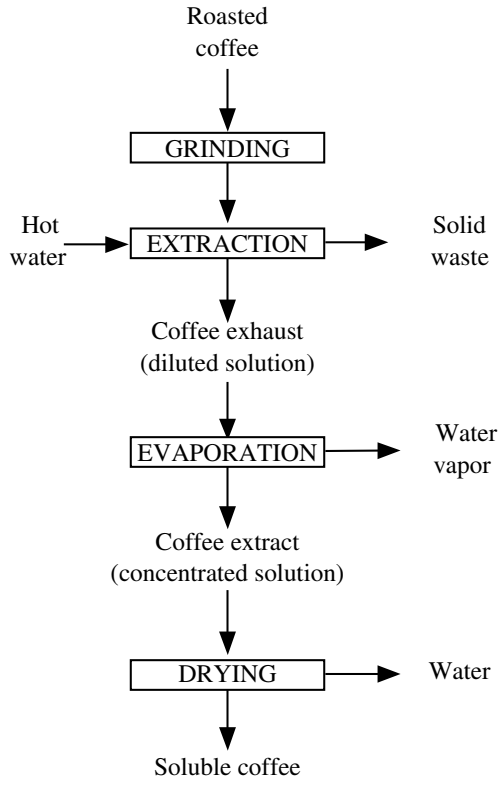

FIGURE 1.3
Elaboration of soluble coffee.

In continuous operations the loading, transformation, and unloading stages are performed simultaneously. Equipment cleaning is carried out every given time, depending on the nature of the process and the materials used. To carry out the cleaning, production must be stopped. Continuous operations take place under steady state, in such a way that the characteristic intensive variables of the operation may vary at each point of the system but do not vary along time. It is difficult to reach an absolute steady state, since there may be some unavoidable fluctuations. An example of a continuous operation is the rectification of an alcohol–water mixture.

In some cases it is difficult to have a continuous operation; this type of operation is called semicontinuous. A semicontinuous operation may occur by loading some materials in the equipment that will remain there for a given time in a discontinuous way, while other materials enter or exit continuously. Sometimes it is necessary to unload those accumulated materials. For example, in the extraction of oil by solvents, flour is loaded and the solvent is fed in a continuous way; after some time, the flour runs out of oil and must be replaced.

These different ways of operation present advantages and disadvantages. Advantages of continuous operation include:

1. Loading and unloading stages are eliminated.
2. It allows automation of the operation, thus reducing the work force.
3. Composition of products is more uniform.
4. There is better use of thermal energy.

Disadvantages of continuous operation are:

1. Raw materials should have a uniform composition to avoid operation fluctuations.
2. Is usually expensive to start the operation, so stops should be avoided.
3. Fluctuations in product demand require availability of considerable quantities of raw materials and products in stock.
4. Due to automation of operation, equipment is more expensive and delicate.

Continuous operation is performed under an unsteady state during starts and stops but, once adequately running, may be considered to be working under steady state. This is not completely true, however, since there could be fluctuations due to variations in the composition of the raw materials and due to modifications of external agents.

When selecting a form of operation, the advantages and disadvantages of each type should be considered. However, when low productions are required, it is recommended to work under discontinuous conditions. When high productions are required, it is more profitable to operate in a continuous way.

1.7 Unit Operations: Classification

When analyzing the flow charts of different processes described in other sections, it can be observed that some of the stages are found in all of them. Each of these stages is called basic or unit operation, in common with many industrial processes. The individual operations have common techniques and are based on the same scientific principles, simplifying the study of these operations and the treatment of these processes.

There are different types of unit operations depending on the nature of the transformation performed; thus, physical, chemical, and biochemical stages can be distinguished:

- Physical stages: grinding, sieving, mixture, fluidization, sedimentation, flotation, filtration, rectification, absorption, extraction, adsorption, heat exchange, evaporation, drying, etc.
- Chemical stages: refining, chemical peeling
- Biochemical stages: fermentation, sterilization, pasteurization, enzymatic peeling

Hence, the group of physical, chemical, and biochemical stages that take place in the transformation processes of agricultural products constitute the so-called unit operations of the food industry, the purpose of which is the separation of two or more substances present in a mixture, or the exchange of a property due to a gradient. Separation is achieved by means of a separating agent that is different, depending on the transferred property.

Unit operations can be classified into different groups depending on the transferred property, since the possible changes that a body may undergo are defined by variations in either its mass, energy, or velocity. Thus, unit operations are classified under mass transfer, heat transfer, or momentum transfer.

Besides the unit operations considered in each mentioned group, there exist those of simultaneous heat and mass transfer, as well as other operations that cannot be classified in any of these groups and are called complementary unit operations.

All the unit operations grouped in these sections are found in physical processes; however, certain operations that include chemical reactions can be included.

1.7.1 Momentum Transfer Unit Operations

These operations study the processes in which two phases at different velocities are in contact. The operations included in this section are generally divided into three groups:

Internal circulation of fluids: study of the movement of fluids through the interior of the tubing; also includes the study of equipment used to impel the fluids (pumps, compressors, blowers, and fans) and the mechanisms used to measure the properties of fluids (diaphragms, venturi meters, rotameters, etc.).

External circulation of fluids: the fluid circulates through the external part of a solid. This circulation includes the flow of fluids through porous fixed beds, fluidized beds (fluidization), and pneumatic transport.

Solids movement within fluids: the base for separation of solids within a fluid. This type of separation includes: sedimentation, filtration, and ultrafiltration, among others.

1.7.2 Mass Transfer Unit Operations

These operations are controlled by the diffusion of a component within a mixture. Some of the operations included in this group are:

Distillation: separation of one or more components by taking advantage of vapor pressure differences.

Absorption: a component of a gas mixture is absorbed by a liquid according to the solubility of the gas in the liquid. Absorption may occur with or without chemical reaction. The opposite process is called desorption.

Extraction: based on the dissolution of a mixture (liquid or solid) in a selective solvent, which can be liquid–liquid or solid–liquid. The latter is also called washing, lixiviation, etc.

Adsorption: also called sorption, adsorption involves the elimination of one or more components of a fluid (liquid or gas) by retention on the surface of a solid.

Ionic exchange: substitution of one or more ions of a solution with another exchange agent.

1.7.3 Heat Transfer Unit Operations

These operations are controlled by temperature gradients. They depend on the mechanism by which heat is transferred:

Conduction: in continuous material media, heat flows in the direction of temperature decrease and there is no macroscopic movement of mass.

Convection: the enthalpy flow associated with a moving fluid is called convective flow of heat. Convection can be natural or forced.

Radiation: energy transmission by electromagnetic waves. No material media are needed for its transmission.

Thermal treatments (sterilization and pasteurization), evaporation, heat exchangers, ovens, solar plates, etc. are studied based on these heat transfer mechanisms.

1.7.4 Simultaneous Mass–Heat Transfer Unit Operations

In these operations a concentration and a temperature gradient exist at the same time:

Humidification and dehumidification: include the objectives of humidification and dehumidification of a gas and cooling of a liquid.

Crystallization: formation of solid glassy particles within a homogeneous liquid phase.

Dehydration: elimination of a liquid contained within a solid. The application of heat changes the liquid, contained in a solid, into a vapor phase. In freeze-drying, the liquid in solid phase is removed by sublimation, i.e., by changing it into a vapor phase.

1.7.5 Complementary Unit Operations

One series of operations is not included in this classification because these are not based on any of the transport phenomena cited previously. These operations include grinding, milling, sieving, mixing of solids and pastes, etc.

1.8 Mathematical Setup of the Problems

The problems set up in the study of unit operations are very diverse, although in all of them the conservation laws (mass, energy, momentum, and stochiometric) of chemical reactions apply. Applying these laws to a given problem is done to perform a balance of the "property" studied in such a problem. In a general way, the expression of the mass, energy, and momentum balances related to the unit time can be expressed as:

$$\left(\text{Property entering the system}\right) = \left(\text{Property exiting the system}\right) + \left(\text{Property that accumulates}\right)$$

This is, that which enters into the system of the considered property is equal to that which leaves what is accumulated. In a schematic way:

$$\mathbf{E} = \mathbf{S} + \mathbf{A}$$

In cases where a chemical reaction exists, when carrying out a balance for a component, an additional generation term may appear. In these cases the balance expression will be:

$$\mathbf{E} + \mathbf{G} = \mathbf{S} + \mathbf{A}$$

When solving a given problem, a certain number of unknown quantities or variables (**V**) are present, and a set of relationships or equations (**R**) is obtained from the balances. According to values of **V** and **R**, the following cases can arise:

- If $\mathbf{V} < \mathbf{R}$, the problem is established incorrectly, or one equation is repeated.
- If $\mathbf{V} = \mathbf{R}$, the problem has only one solution.
- If $\mathbf{V} > \mathbf{R}$, different solutions can be obtained; the best solution is found by optimizing the process.

There are

$$\mathbf{F = V - R}$$

design variables. The different types of problems presented depend on the type of equation obtained when performing the corresponding balances. Thus,

- Algebraic equations have an easy mathematical solution obtained by analytical methods.
- Differential equations are usually obtained for unsteady continuous processes. The solution of the mathematical model established with the balances can be carried out through analytical or approximate methods. In some cases, differential equations may have an analytical solution; however, when it is not possible to analytically solve the mathematical model, it is necessary to appeal to approximate methods of numerical integration (digital calculus) or graphic (analogic calculus).
- Equations in finite differences are solved by means of analogic computers which give the result in a graphic form. In some cases the exact solution can be obtained by numerical methods.

2

Unit Systems: Dimensional Analysis and Similarity

2.1 Magnitude and Unit Systems

The value of any physical magnitude is expressed as the product of two factors: the value of the unit and the number of units. The physical properties of a system are related by a series of physical and mechanical laws. Some magnitudes may be considered fundamental and others derived. Fundamental magnitudes vary from one system to another.

Generally, time and length are taken as fundamental. The unit systems need a third fundamental magnitude, which may be mass or force. Those unit systems that have mass as the third fundamental magnitude are known as absolute unit systems, while those that have force as a fundamental unit are called technical unit systems. There are also engineering unit systems that consider length, time, mass, and force as fundamental magnitudes.

2.1.1 Absolute Unit Systems

There are three absolute unit systems: the c.g.s. (CGS), the Giorgi (MKS), and the English (FPS). In all of these, the fundamental magnitudes are length, mass, and time. The different units for these three systems are shown in Table 2.1. In these systems, force is a derived unit defined beginning with the three fundamental units. The force and energy units are detailed in Table 2.2.

When heat magnitudes are used, it is convenient to define the temperature unit. For the CGS and MKS systems, the unit of temperature is degrees Centigrade (°C), while for the English system it is degrees Fahrenheit (°F). Heat units are defined independently of work units. Later, it will be shown that relating work and heat requires a factor called the mechanical equivalent of heat.

TABLE 2.1

Absolute Unit Systems

Magnitude	System		
	c.g.s. (CGS)	**Giorgi (MKS)**	**English (FPS)**
Length (L)	1 centimeter (cm)	1 meter (m)	1 foot (ft)
Mass (M)	1 gram (g)	1 kilogram (kg)	1 pound-mass (lb)
Time (T)	1 second (s)	1 second (s)	1 second(s)

TABLE 2.2

Units Derived from Absolute Systems

Magnitude	System		
	c.g.s. (CGS)	**Giorgi (MKS)**	**English (FPS)**
Force	1 dyne	1 Newton (N)	1 poundal
Energy	1 erg	1 Joule (J)	1 (pound)(foot)

TABLE 2.3

Technical Unit Systems

Magnitude	System	
	Metric	**English**
Length (L)	1 meter (m)	1 foot (ft)
Force (F)	1 kilogram force (kp or kgf)	1 pound force (lbf)
Time (T)	1 second (s)	1 second (s)
Temperature (θ)	1 degree Centigrade (°C)	1 degree Fahrenheit (°F)

2.1.2 Technical Unit Systems

Among the most used technical systems are the metric and the English systems. In both, the fundamental magnitudes are length, force, and time. In regard to temperature, the unit of the metric system is the Centigrade degree, and that of the English system is the Fahrenheit. Table 2.3 shows the fundamental units of the metric and English systems.

In engineering systems, mass is a derived magnitude, which in the metric system is 1 TMU (technical mass unit) and in the English system is 1 slug.

2.1.3 Engineering Unit Systems

Until now, only unit systems that consider three magnitudes as fundamental have been described. However, in engineering systems, four magnitudes are considered basic: length, time, mass, and force. Table 2.4 presents the different units for the metric and English engineering systems.

TABLE 2.4

Engineering Unit Systems

	System	
Magnitude	**Metric**	**English**
Length (L)	1 meter (m)	1 foot (ft)
Mass (M)	1 kilogram (kg)	1 pound-mass (lb)
Force (F)	1 kilogram force (kp or kgf)	1 pound force (lbf)
Time (T)	1 second (s)	1 second (s)
Temperature (θ)	1 degree Centigrade (°C)	1 degree Fahrenheit (°F)

When defining mass and force as fundamental, an incongruity may arise, since these magnitudes are related by the dynamics basic principle. To avoid this incompatibility, a correction or proportionality factor (g_c) should be inserted. The equation of this principle would be:

$$g_c \times \text{Force} = \text{Mass} \times \text{Acceleration}$$

Observe that g_c has mass units (acceleration/force). The value of this correction factor in the engineering systems is:

$$\text{Metric system: } g_C = 9.81 \frac{(\text{kgmass})(\text{meter})}{(\text{kgforce})(\text{second})^2} = 9.81 \frac{\text{kg} \cdot \text{m}}{\text{kg} \cdot \text{s}^2}$$

$$\text{English system: } g_C = 32.17 \frac{(\text{lbmass})(\text{foot})}{(\text{lbforce})(\text{second})^2} = 32.17 \frac{\text{lb} \cdot \text{ft}}{\text{lbf} \cdot \text{s}^2}$$

2.1.4 International Unit System (IS)

It was convenient to unify the use of the unit systems when the Anglo–Saxon countries incorporated the metric decimal system. With that purpose, the MKS was adopted as the international system and denoted as IS. Although the obligatory nature of the system is recognized, other systems are still used; however, at present many engineering journals and books are edited only in IS, making it more and more acceptable than other unit systems. Table 2.5 presents the fundamental units of this system along with some supplementary and derived units.

Sometimes the magnitude of a selected unit is too big or too small, making it necessary to adopt prefixes to indicate multiples and submultiples of the fundamental units. Generally, it is advisable to use these multiples and

TABLE 2.5

International Unit System

Magnitude	Unit	Abbreviation	Dimension
Length	meter	m	L
Mass	kilogram	kg	M
Time	second	s	T
Force	Newton	N	MLT^2
Energy	Joule	J	ML^2T^{-2}
Power	Watt	W	ML^2T^{-3}
Pressure	Pascal	Pa	$ML^{-1}T^{-2}$
Frequency	Hertz	Hz	T^{-1}

submultiples as powers of 10^3. Following is a list of the multiples and submultiples most often used, as well as the name and symbol of each.

Prefix	Multiplication Factor	IS Symbol
tera	10^{12}	T
giga	10^9	G
mega	10^6	M
kilo	10^3	k
hecto	10^2	h
deca	10^1	da
deci	10^{-1}	d
centi	10^{-2}	c
mili	10^{-3}	m
micro	10^{-6}	μ
nano	10^{-9}	n
pico	10^{-12}	p
femto	10^{-15}	f
atto	10^{-18}	a

It is interesting that, in many problems, concentration is expressed by using molar units. The molar unit most frequently used is the mole, defined as the quantity of substance whose mass in grams is numerically equal to its molecular weight.

2.1.5 Thermal Units

Heat is a form of energy; in this way, the dimension of both is ML^2T^{-2}. However, in some systems temperature is taken as dimension. In such cases, heat energy can be expressed as proportional to the product mass times temperature. The proportionality constant is the specific heat, which depends on the material and varies from one to another. The amount of heat is defined as a function of the material, with water taken as a reference and the specific heat being the unit, so:

$$\text{Heat} = \text{Mass} \times \text{Specific heat} \times \text{Temperature}$$

The heat unit depends on the unit system adopted. Thus:

- Metric system:
  - Calorie: heat needed to raise the temperature of a gram of water from 14.5 to 15.5°C
- English systems:
  - Btu (British thermal unit): quantity of heat needed to raise the temperature of a pound of water one Fahrenheit degree (from 60 to 61°F)
  - Chu (Centigrade heat unit or pound calorie): quantity of heat needed to raise the temperature of one pound of water one degree Centigrade
- International system:
  - Calorie: since heat is a form of energy, its unit is the Joule. The calorie can be defined as a function of the Joule: 1 calorie = 4.185 Joules

Since heat and work are two forms of energy, it is necessary to define a factor that relates them. For this reason, the denominated mechanical equivalent of heat (Q) is defined so that:

$$Q \times \text{Heat energy} = \text{Mechanical energy}$$

so:

$$Q = \frac{\text{Mechanical energy}}{\text{Heat energy}} = \frac{\mathrm{MLT^{-2}L}}{\mathrm{M\theta}} = \mathrm{L^2T^{-2}\theta^{-1}}$$

2.1.6 Unit Conversion

The conversion of units from one system to another is easily carried out if the quantities are expressed as a function of the fundamental units mass, length, time, and temperature. The so-called conversion factors are used to convert the different units. The conversion factor is the number of units of a certain system contained in one unit of the corresponding magnitude of another system. The most common conversion factors for the different magnitudes are given in Table 2.6.

When converting units, it is necessary to distinguish the cases in which only numerical values are converted from those in which a formula should be converted. When it is necessary to convert numerical values from one unit to another, the equivalencies between them, given by the conversion factors, are used directly.

Table 2.6

Conversion Factors

Mass	
1 lb	0.4536 kg
	(1/32.2) slug
Length	
1 inch	2.54 cm
1 foot	0.3048 m
1 mile	1609 m
Surface	
1 square inch	645.2 mm^2
1 square foot	0.09290 m^2
Volume and Capacity	
1 cubic foot	0.02832 m^3
1 gallon (imperial)	4.546 l
1 gallon (USA)	3.786 l
1 barrel	159.241 l
Time	
1 min	60 s
1 h	3600 s
1 day	86,400 s
Temperature difference	
1°C = 1 K	1.8°F
Force	
1 poundal (pdl)	0.138 N
1 lb_f	4.44 N
	4.44×10^5 dina
	32.2 pdl
1 dyne	10^{-5} N
Pressure	
1 technical atmosphere (at)	1 kgf/cm^2
	14.22 psi
1 bar	100 kPa
1 mm Hg (tor)	133 Pa
	13.59 kgf/cm^2
1 psi (lb/in^2)	703 kgf/m^2
Energy, Heat, and Power	
1 kilocalorie (kcal)	4185 J
	426.7 kgfm

Table 2.6 (continued)

Conversion Factors	
1 erg	10^{-7} J
1 Btu	1055 J
1 Chu	0.454 kcal
	1.8 Btu
1 horse vapor (CV)	0.736 kW
	75 kgm/s
1 horse power (HP)	0.746 kW
	33,000 ft lb/min
	76.04 kgm/s
1 kilowatt (kW)	1000 J/s
	1.359 CV
1 kilowatt hour (kW.h)	3.6×10^6 J
	860 kcal
1 atm.liter	0.0242 kcal
	10.333 kgm
Viscosity	
1 poise (P)	0.1 Pa·s
1 pound/(ft.h)	0.414 mPa·s
1 stoke (St)	10^{-4} m^2/s
Mass flow	
1 lb/h	0.126 g/s
1 ton/h	0.282 kg/s
1 lb/(ft^2.h)	1.356 g/s.m^2
Thermal Magnitudes	
1 Btu/(h.ft^2)	3.155 W/m^2
1 Btu/(h.ft^2 °F)	5.678 W/(m^2 K)
1 Btu/lb	2.326 kJ/kg
1 Btu/(lb.°F)	4.187 kJ/(kg.K)
1 Btu/(h.ft. °F)	1.731 W/(m.K)

In cases of conversion of units of a formula, the constants that appear in the formula usually have dimensions. To apply the formula in units different from those given, only the constant of the formula should be converted. In cases in which the constant is dimensionless, the formula can be directly applied using any unit system.

2.2 Dimensional Analysis

The application of equations deducted from physical laws is one method of solving a determined problem. However, it may be difficult to obtain equations

of that type; therefore, in some cases it will be necessary to use equations derived in an empirical form.

In the first case, the equations are homogeneous from a dimensional point of view. That is, their terms have the same dimensions and the possible constants that may appear will be dimensionless. This type of equation can be applied in any unit system when using coherent units for the same magnitudes. On the other hand, equations experimentally obtained may not be homogeneous regarding the dimensions, since it is normal to employ different units for the same magnitude.

The objective of dimensional analysis is to relate the different variables involved in the physical processes. For this reason, the variables are grouped in dimensionless groups or rates, allowing discovery of a relationship among the different variables. Table 2.7 presents the dimensionless modules usually found in engineering problems. Dimensional analysis is an analytical method in which, once the variables that intervene in a physical phenomenon are known, an equation to bind them can be established. That is, dimensional analysis provides a general relationship among the variables that should be completed with the assistance of experimentation to obtain the final equation binding all the variables.

2.2.1 Buckingham's π Theorem

Every term that has no dimensions is defined as **factor π**. According to Bridgman, there are three fundamental principles of the dimensional analysis:

1. All the physical magnitudes may be expressed as power functions of a reduced number of fundamental magnitudes.
2. The equations that relate physical magnitudes are dimensionally homogeneous; this means that the dimensions of all their terms must be equal.
3. If an equation is dimensionally homogeneous, it may be reduced to a relation among a complete series of dimensionless rates or groups. These induce all the physical variables that influence the phenomenon, the dimensional constants that may correspond to the selected unit system, and the universal constants related to the phenomenon treated.

This principle is denoted as Buckingham's π theorem. A series of dimensionless groups is complete if all the groups among them are independent; any other dimensionless group that can be formed will be a combination of two or more groups from the complete series.

Because of Buckingham's π theorem, if the series q_1, q_2, …, q_n is the set of n independent variables that define a problem or a physical phenomenon, then there will always exist an explicit function of the type:

TABLE 2.7

Dimensionless Modules

Modules	Expression	Equivalence
Biot (Bi)	$\frac{hd}{k}$	
Bodenstein (Bo)	$\frac{vd}{D}$	(Re)(Sc)
Euler (Eu)	$\frac{\Delta P}{\rho v^2}$	
Froude (Fr)	$\frac{d_p N}{g}$	
Graetz (Gz)	$\frac{\rho v d^2 \hat{C}_P}{kL}$	(Re)(Pr)(d/L)
Grashof (Gr)	$\frac{g \beta d^3 \Delta T \rho^2}{\eta^2}$	
Hedstrom (He)	$\frac{d\sigma_0 \rho}{\eta'}$	
Nusselt (Nu)	$\frac{h d}{k}$	
Peclet (Pe)	$\frac{\rho v d \hat{C}_P}{k}$	(Re)(Pr)
Power (Po)	$\frac{P}{d_p N^5 \rho}$	
Prandtl (Pr)	$\frac{\hat{C}_P \eta}{k}$	
Reynolds (Re)	$\frac{\rho v d}{\eta}$	
Schmidt (Sc)	$\frac{\eta}{\rho D}$	
Sherwood (Sh)	$\frac{k_g d}{D}$	
Stanton (St)	$\frac{h}{\hat{C}_P \rho v}$	$(Nu)[(Re)(Pr)]^{-1}$
Weber (We)	$\frac{\rho l v^2}{\sigma}$	

$$f(q_1, q_2, \ldots, q_n) = 0 \tag{2.1}$$

This way, a number of dimensionless factors p can be defined with all the variables; hence:

$$\pi_1 = q_1^{a1}, q_2^{a2}, \ldots, q_n^{an}$$

$$\pi_2 = q_1^{b1}, q_2^{b2}, \ldots, q_n^{bn}$$

.....

.....

$$\pi_i = q_1^{p1}, q_2^{p2}, \ldots, q_n^{pn}$$

In this way, i factors π are obtained, each one a function of the variables raised to a power that may be positive, negative, or null. The number of dimensionless factors π will be i, where: $i = n - k$, with n representing the number of independent variables and k denoting the characteristic of the matrix formed by the exponents of the dimensional equations of the different variables and constants in relation to a defined unit system.

These i dimensionless factors $\pi_1, \pi_2, \ldots, \pi_i$ will be related by means of a function:

$$f(\pi_1, \pi_2, \ldots, \pi_i) = 0 \tag{2.2}$$

that can be applied in any unit system. Sometimes it is difficult to find this type of relationship, so a graphical representation that relates the different parameters is used as an alternative.

2.2.2 Dimensional Analysis Methods

The three main methods for dimensional analysis are Buckingham's method, Rayleigh's method, and the method of differential equations. The first two methods will be studied in detail, and the third will be briefly described.

2.2.2.1 Buckingham's Method

The variables that may influence the phenomenon studied are listed first. Dimensional equations of the different variables are established, as are the dimensional constants. When variables have the same dimensions, only one is chosen. The rest of the variables are divided by the chosen variable, obtaining dimensionless groups that will be added to the total obtained. These dimensionless rates are the so-called form factors.

The next step is to build the matrix with the exponents of the magnitudes corresponding to the different variables and dimensionless constants. Thus, for the case of n variables $q_1, q_2, \ldots, q_n$ and the constant g_c:

$$q_1\ q_2\ \cdots\cdots\cdots\cdots q_n\ g_c$$

$$\begin{matrix}\mathrm{L}\\ \mathrm{M}\\ \mathrm{F}\\ \mathrm{T}\\ \theta\end{matrix}\quad\left(\begin{matrix}\text{Matrix of the exponents}\\ \text{of the magnitudes for the}\\ \text{dimensional variables}\\ \text{and constants}\end{matrix}\right)$$

The determinant k is obtained from this matrix. This value represents the minimum number of variables and constants that do not form a dimensionless group.

Next, the i dimensionless groups or factors (π) are formed. Each group is formed by the product of $k + 1$ factors q, with each factor a dimensionless variable or constant, raised to powers that should be determined. k dimensionless factors will be the variables that make the matrix to be of determinant k, in addition to each of the $n - k$ remaining variables with a unit exponent. In this way, the factors π will be:

$$\pi_1 = q_1^{a1} \cdot q_2^{a2} \ldots q_k^{ak} \cdot q_{k+1}$$

$$\pi_2 = q_1^{b1} \cdot q_2^{b2} \ldots q_n^{bn} \cdot q_{k+2}$$

$$\ldots\ldots\ldots\ldots\ldots\ldots$$

$$\ldots\ldots\ldots\ldots\ldots\ldots$$

$$\pi_i = q_1^{p1} \cdot q_2^{p2} - q_n^{pn} \cdot q_{k+i-n}$$

In this set of equations, the magnitudes (q_1, q_2, …, q_k), variables, and constants contain as a whole the total of fundamental magnitudes of the unit system selected. The set of exponents a_1, b_1, …, p_1; a_2, b_2, … p_2, etc., should be such that the groups lack dimensions.

Since the factors π lack dimensions, the magnitudes of each variable are set up in the different dimensionless collections, grouping each magnitude in such a way that it is raised to a power that is a combination of the exponents of the variables in which this magnitude appears. This combination of exponents should be equal to zero, obtaining for each factor π a system of k equations and k unknowns. The systems are solved to determine the exponents of the variables in each dimensionless group.

With these i factors and possible form factors, the following function may be obtained:

$$f\left(\pi_1, \pi_2, \ldots, \pi_i, \ldots\right) = 0 \tag{2.3}$$

In some cases there is no need to form the matrix of exponents or determine its determinant, since by simple observation the minimum number of variables and constants that do not form a dimensionless group can be found.

2.2.2.2 Rayleigh's Method

As in the previous method, the physical variables that participate in the process should initially be identified. Next, one of the variables, generally the variable of greatest interest, is expressed in an analytical way as an exponent function of the remaining variables:

$$q_1 = K\, q_2^{a2}\, q_3^{a3} \ldots q_n^{an} \tag{2.4}$$

where K is a dimensionless constant.

The variables and possible dimensionless constants are substituted by the magnitudes of a unit system, applying the homogeneity conditions for each magnitude. In this way, as many equations as there are fundamental magnitudes in the selected unit system are obtained. If p is the number of such magnitudes, the number of unknowns in this equation system will be $n - 1$:

Equations	p
Unknowns	$n - 1$ exponents

Since the number of unknowns is greater than the number of equations, $(n - 1) - p$ exponents are chosen, while the rest are set up as a function of the exponents. In this way, all the exponents may be established as a function of those $(n - 1 - p)$ selected and are substituted in the last equation. The variables and dimensional constants are grouped in such a way that groups are raised to the same power. Thus, $(n - 1 - p)$ groups that have risen to the selected power are obtained, in addition to one group whose power is the unit. The relationship among dimensionless groups is thus obtained:

$$\pi_1 = f\left(\pi_2, \pi_3, \ldots, \pi_i\right) \tag{2.5}$$

2.2.2.3 Method of Differential Equations

This method is based on the differential equations of momentum, mass, and energy conservation which can be applied to a given problem, as well as those that can be obtained from the boundary conditions. Since this case begins with dimensionally homogeneous equations, if all the terms in each equation are divided by any of them, as many dimensionless groups as terms that had the equation minus one can be obtained.

The advantage of this method is that it is less probable that variables that may have influence on a determined problem will be omitted. This can only occur when an incorrect equation is employed. Also, this method supplies

a more intuitive approach to the physical meaning of the resultant dimensionless groups (Dickey and Fenic, 1976).

2.3 Similarity Theory

For design and building of industrial equipment, two methods are based on the construction of models, which may be mathematical or empirical. The industrial equipment is called prototype.

- Mathematical models: beginning with theoretical aspects, it is possible, sometimes, to design and build a prototype applicable to industrial scale. In practice, this rarely happens.
- Empirical models: in this case experimentation in reduced models is necessary, following directions given by the dimensional analysis.

The values of the prototype are calculated from the values found in the model. A series of similarity criteria must be met in order to pass from the model to the prototype.

The main difference between the two models relies on the fact that the mathematical model is applicable at any scale, while, for the application of the empirical model, a series of similarity criteria between the model and the prototype should be in agreement.

In a general way, the similarity criteria can be expressed according to the following linear equation:

$$m' = km \tag{2.6}$$

where m and m' are measures of the same magnitude in the model and the prototype, respectively. The proportionality constant k receives the name of scale factor.

This type of similarity is applicable to the different magnitudes that encircle the system, such as geometry, force profile, velocity, temperature, and concentration. Therefore, the different similarity criteria will be as follows:

- Geometric similarity refers to the proportionality between the dimensions of the model and the prototype.
- Mechanical similarity, whether static, kinematic, or dynamic, refers to the proportionality among deformations, velocities, and forces, respectively.
- Thermal similarity is relevant if there is proportionality between the temperatures.
- Concentration similarity refers to chemical processes, which require proportionality between concentrations and compositions.

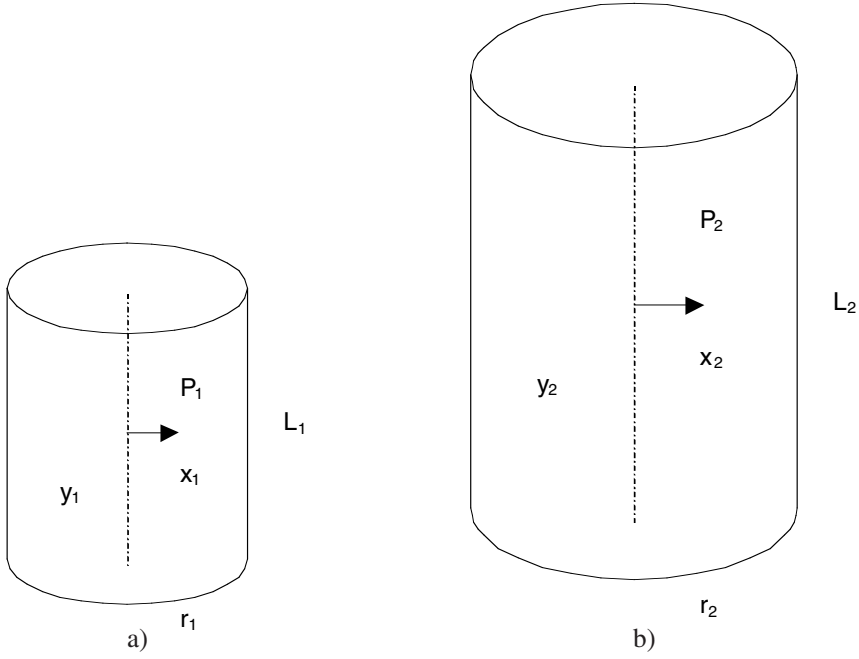

FIGURE 2.1
Geometric similarity (a) and similar figures (b).

The geometric similarity is a previous requisite for the other criteria. In general, each results in a requisite for the following similarities.

Geometric and mechanical similarities will be studied next; thermal and concentration similarities will be briefly discussed. The thermal, concentration, and chemical similarities may be met working at equal temperature and concentration.

2.3.1 Geometric Similarity

Geometric similarity between two systems exists when each point of one of them has a correspondent point in the other. Correspondent points of two systems are those points for which there is a constant ratio for correspondent coordinates.

Figure 2.1 presents two pieces of cylindrical tubing, with radius r_1 and r_2 and lengths L_1 and L_2; the points P_1 and P_2 will correspond if their radial and axial coordinates have a constant ratio:

$$\frac{x_1}{x_2} = \frac{y_1}{y_2} = \frac{r_1}{r_2} = \frac{L_1}{L_2} = k \tag{2.7}$$

Another form used to define geometric similarity is to employ ratios between dimensions that belong to the same system and receive the name of shape factors. Thus:

$$\frac{r_1}{L_1} = \frac{r_2}{L_2} = \omega \tag{2.8}$$

2.3.2 Mechanical Similarity

2.3.2.1 Static Similarity

Static similarity links the proportionality of the deformations. However, this type of similarity can be neglected if materials with enough resistance are employed. When constant tension is applied to solid bodies and geometric similarity is maintained, static similarity exists.

2.3.2.2 Kinematic Similarity

Once the model and the prototype are similar, the proportionality ratios between velocities and times should be sought. In this way, kinematic similarity complies when:

$$\frac{v_1}{v_2} = C \tag{2.9}$$

where v_1 and v_2 are the velocities for correspondent points of the model and the prototype.

2.3.2.3 Dynamic Similarity

Dynamic similarity implies equality of all rates and dimensionless numbers among the significant forces that intervene in analyzed systems. Different equalities that depend on the forces acting on the systems should be complied with in order to have dynamic similarity. Thus, if inertia and friction forces act, then the equality of the Reynolds number should conform. If, in addition, the gravity forces act, then the equality of Froude's module should be complied with. It will be necessary to obey the equality of Weber's module when free liquid–gas surfaces are present, since superficial tensions appear. When pressure forces exist, the equality of Euler's number should be complied with.

A practical study of dynamic similarity is presented next. Consider a mass differential in each of the systems (model and prototype) with different density and viscosity. Inertia forces that move the mass act in both systems and, additionally, are subjected to friction forces. As shown in Figure 2.2, the considered mass is enclosed in a cubic volume that moves within a fluid describing a path L.

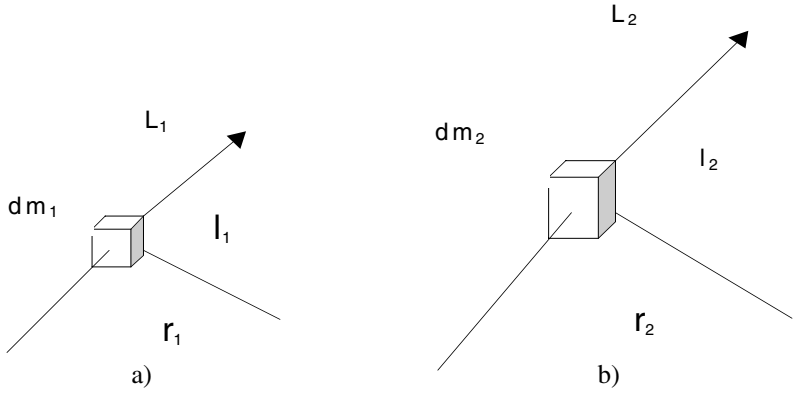

FIGURE 2.2
Movement of a mass within a fluid (a) and dynamic similarity (b).

Inertia forces are normal forces (F_n), hence:

$$F_n = \frac{v^2\,dm}{r} = \frac{v^2\,\rho\,dV}{r} = \frac{v^2\,\rho(dl)^3}{r} \tag{2.10}$$

The friction forces will be tangential and, according to Newton's law:

$$F_t = \eta\,dA\,\frac{dv}{dr} = \eta\left(dl\right)^2\frac{dv}{dr} \tag{2.11}$$

where l is the length, A the area, and η the viscosity. For dynamic similarity to exist, then

$$\frac{F_{n1}}{F_{t1}} = \frac{F_{n2}}{F_{t2}}$$

or

$$\left(\frac{F_n}{F_t}\right)_1 = \left(\frac{F_n}{F_t}\right)_2 \tag{2.12}$$

since

$$\frac{F_n}{F_t} = \frac{v^2\,\rho\left(dl\right)^3}{r}\,\frac{1}{\eta\left(dl\right)^2\frac{dv}{dr}} = \frac{v^2\,\rho\,dl}{r}\,\frac{1}{\eta\,\frac{dv}{dr}} \tag{2.13}$$

Then:

$$\frac{v_1^2 \rho_1 dl_1}{r_1} \frac{1}{\eta_1 \dfrac{dv_1}{dr_1}} = \frac{v_2^2 \rho_2 dl_2}{r_2} \frac{1}{\eta_2 \dfrac{dv_2}{dr_2}}$$

Taking geometric and kinematic similarity ratios into account:

$$r_i = \omega l_i$$

$$l_i = k l_j \qquad dl_i = k\, dl_j$$

$$r_i = k r_j \qquad dr_i = k\, dr_j$$

$$v_i = C v_j \qquad dv_i = C\, dv_j \qquad v_i^2 = C v_j^2$$

When substituting these relationships into the left-hand side of the last equality, one can obtain:

$$\frac{\rho_1 v_1 k}{\eta_1} = \frac{\rho_2 v_2}{\eta_2}$$

but $k = l_1/l_2$, hence:

$$\frac{\rho_1 v_1 l_1}{\eta_1} = \frac{\rho_2 v_2 l_2}{\eta_2} \tag{2.14}$$

That is

$$\left(\mathrm{Re}\right)_1 = \left(\mathrm{Re}\right)_2$$

which points out that the equality of Reynolds module conforms to the model and prototype only when inertia and friction forces exist.

If, in addition, gravity forces act on the systems, then the obtained relations are taken ($(\mathrm{Re})_1 = (\mathrm{Re})_2$), and the following equality is conformed:

$$\left(F_n / F_G\right)_1 = \left(F_n / F_G\right)_2 \tag{2.15}$$

Gravity force is defined as:

$$F_G = g\, dm = g \rho \left(dl\right)^3 \tag{2.16}$$

Considering Equations 2.10 and 2.16, the relationship between the inertia and gravity forces will be defined by:

$$\frac{F_n}{F_G} = \frac{v^2}{r\,g} \tag{2.17}$$

and since $r_i = \omega l_i$, the following relationship applies:

$$\frac{v_1^2}{l_1\,g} = \frac{v_2^2}{l_2\,g} \tag{2.18}$$

which indicates equality in the Froude's module. It must be noted that g cannot be simplified, since a dimensional expression would be obtained. When there are gravity forces, the Froude's modules of the model and the prototype are equal.

When surface tension forces (F_s) intervene, the new relationship to comply with is:

$$\left(F_n/F_s\right)_1 = \left(F_n/F_s\right)_2 \tag{2.19}$$

The surface tension forces are given by:

$$F_s = \sigma l \tag{2.20}$$

where σ is the surface tension. In this way:

$$\frac{F_n}{F_s} = \frac{\rho\, v^2 \left(dl\right)^3}{r}\frac{1}{\sigma\, l} \tag{2.21}$$

from which the following equation is obtained:

$$\frac{\rho_1\, v_1^2 \left(dl_1\right)^3}{r_1}\frac{1}{\sigma_1\, l_1} = \frac{\rho_2\, v_2^2 \left(dl_2\right)^3}{r_2}\frac{1}{\sigma_2 l_2} \tag{2.22}$$

Taking into account the geometric similarity relationships:

$$r_i = \omega\; l_i$$

$$l_i = k\; l_2 \qquad dl_1 = k\; dl_2$$

and substituting them into the last equality and simplifying it, the following can be obtained:

$$\frac{\rho_1 \; v_1^2 \; l_1}{\sigma_1} = \frac{\rho_2 \; v_2^2 \; l_2}{\sigma_2} \tag{2.23}$$

which indicates that the Weber's modules are equal. That is, to have dynamic similarity when surface forces act, the Weber's modules must coincide in the model and prototype.

Finally, the case in which there are pressure forces due to pressure differences is examined below. The new relation to be conformed with is:

$$\left(F_P / F_N\right)_1 = \left(F_P / F_N\right)_2 \tag{2.24}$$

The pressure forces are defined by:

$$F_P = \Delta p \; l^2 \tag{2.25}$$

Consequently:

$$\frac{F_P}{F_N} = \Delta p \; l^2 \frac{r}{\rho \; v^2 \left(dl\right)^3} \tag{2.26}$$

The combination of Equations 2.24 and 2.26 gives:

$$\Delta p_1 l_1^2 \frac{r_1}{\rho_1 \; v_1^2 \left(dl_1\right)^3} = \Delta p_2 l_2^2 \frac{r_2}{\rho_2 \; v_2^2 \left(dl_2\right)^3} \tag{2.27}$$

and according to geometric similarity,

$$r_i = w \; l_i$$

$$l_1 = k \; l_2 \qquad dl_1 = k \; dl_2$$

When substituting these in the last equality and then simplifying it, the following can be obtained:

$$\frac{\Delta p_1}{\rho_1 \; v_1^2} = \frac{\Delta p_2}{\rho_2 \; v_2^2} \tag{2.28}$$

which indicates that there is equality in the Euler's module. That is, when there is dynamic similarity, the Euler's modules of the model and prototype coincide.

Not all the forces described here are always present, so there will only be dynamic similarity in those equalities between the dimensionless modules of the model and prototype referring to the force or forces acting on the system.

Problems

2.1

A fluid food has a viscosity of 6 poises. Obtain the value for viscosity in the international system and in the absolute English system.

By definition, 1 poise is 1 g per cm and s: 1 poise = g/(cm·s)

Conversion to the international system:

$$6\frac{\text{g}}{\text{cm.s}}\frac{1\text{ kg}}{10^3\text{ g}}\frac{100\text{ cm}}{1\text{ m}} = 0.6\frac{\text{kg}}{\text{m.s}} = 0.6\text{ Pa.s}$$

In the international system the viscosity unit is Pa·s, that is equivalent to kg/(m·s).

Conversion to the absolute English system:

$$6\frac{\text{g}}{\text{cm.s}}\frac{1\text{lb}}{453.5\text{g}}\frac{30.48\text{ cm}}{1\text{ft}} = 0.403\frac{\text{lb}}{\text{ft.s}}$$

2.2

Empirical equations are used, in many cases, to calculate individual heat transfer coefficients. Thus, the following expression may be used for the circulation of water in a cylindrical pipe:

$$h = 160\left(1 + 0.01t\right)\frac{\left(\text{v}_m\right)^{0.8}}{\left(d_i\right)^{0.2}}$$

where:

h = film coefficient in Btu/(h·ft²·°F)
v_m = mean velocity of water in ft/s
d_i = interior diameter of the pipe in inches (in)
t = water temperature in (°F)

Perform the adequate unit conversion so this equation can be used in the international system.

When the temperature does not appear as an increment but as temperature in absolute terms, it is recommended to convert it as follows:

$$t\ °\mathrm{F} = 1.8\,t\,°\mathrm{C} + 32°\mathrm{C}$$

hence:

$$h = 160\left(1.32 + 0.018\,t\right)\frac{\left(v_m\right)^{0.8}}{\left(d_i\right)^{0.2}}$$

Simplifying:

$$h = 211.2\,\frac{\left(v_m\right)^{0.8}}{\left(d_i\right)^{0.2}} + 2.88\,\frac{t\left(v_m\right)^{0.8}}{\left(d_i\right)^{0.2}}$$

in which the temperature t is expressed in °C.

The units of the two coefficients that appear in this new equation are:

$$211.2\,\frac{\mathrm{Btu}}{\mathrm{h.ft^2.^oF}}\,\frac{\left(\mathrm{in}\right)^{0.2}}{\left(\mathrm{ft/s}\right)^{0.8}}$$

$$2.88\,\frac{\mathrm{Btu}}{\mathrm{h.ft^2.^oF}}\,\frac{\left(\mathrm{in}\right)^{0.2}}{{}^{\mathrm{o}}\mathrm{C.}\left(\mathrm{ft/s}\right)^{0.8}}$$

The next step is the conversion of these coefficients to the international system:

$$211.2\,\frac{\mathrm{Btu}}{\mathrm{h.ft^2.^oF}}\,\frac{\left(\mathrm{in}\right)^{0.2}}{\left(\mathrm{ft/s}\right)^{0.8}}\,\frac{5.678\ \mathrm{W/\left(m^2.^oC\right)}}{1\ \mathrm{Btu/\left(h.ft^2.^oF\right)}}\left(\frac{0.0254\ \mathrm{m}}{1\ \mathrm{in}}\right)^{0.2}\left(\frac{1\ \mathrm{ft}}{0.3048\ \mathrm{m}}\right)^{0.8} =$$

$$1488\,\frac{\mathrm{W}}{\mathrm{m^2.^oC}}\,\frac{\mathrm{m}^{0.2}}{\left(\mathrm{m/s}\right)^{0.8}}$$

$$2.88\,\frac{\mathrm{Btu}}{\mathrm{h.ft^2.^oF}}\,\frac{\left(\mathrm{in}\right)^{0.2}}{{}^{\mathrm{o}}\mathrm{C.}\left(\mathrm{ft/s}\right)^{0.8}}\,\frac{5.678\ \mathrm{W/\left(m^2.^oC\right)}}{1\ \mathrm{Btu/\left(h.ft^2.^oF\right)}}\left(\frac{0.0254\ \mathrm{m}}{1\ \mathrm{in}}\right)^{0.2}\left(\frac{1\ \mathrm{ft}}{0.3048\ \mathrm{m}}\right)^{0..8} =$$

$$20.3\,\frac{\mathrm{W}}{\mathrm{m^2.^oC}}\,\frac{\mathrm{m}^{0.2}}{{}^{\mathrm{o}}\mathrm{C}\left(\mathrm{m/s}\right)^{0.8}}$$

So the resulting equation is:

$$h = 1488\frac{\left(v_m\right)^{0.8}}{\left(d_i\right)^{0.2}} + 20.3\frac{t\left(v_m\right)^{0.8}}{\left(d_i\right)^{0.2}}$$

which, rearranged, gives:

$$h = 1488\left(1 + 0.01364\,t\right)\frac{\left(v_m\right)^{.0.8}}{\left(d_i\right)^{0.2}}$$

with units: h in W/(m²·°C); v_m in m/s; d_i in m; and t in °C.

2.3

Use a dimensional analysis to obtain an expression that allows the calculation of the power of a stirrer as a function of the variables that could affect it. It is known, from experimental studies, that the stirring power depends on the diameter of the stirrer (D), its rotation velocity (N), the viscosity (η) and density (ρ) of the fluid being stirred, and the gravity acceleration (g).

The power of the stirrer, called P, can be expressed as a function of the other variables: $P = f(D, \eta, g, \rho, N)$

Applying Rayleigh's method:

$$P = K D^a \eta^b g^c \rho^d N^e$$

The number of fundamental magnitudes is three: length (L), mass (M), and time (T). The number of variables is six. Three equations with five unknowns can be obtained. The number of factors π will be: 6 – 3 = 3.

	P	D	η	g	ρ	N
M	1	0	1	0	1	0
L	2	1	–1	1	–3	0
T	–3	0	–1	–2	0	–1
	1	a	b	c	d	e

$$\frac{\mathrm{ML}^2}{\mathrm{T}^3} = K^0\mathrm{L}^a\left(\mathrm{M/LT}\right)^b\left(\mathrm{L/T}^2\right)^c\left(\mathrm{M/L}^3\right)^d\left(\mathrm{L/T}\right)^e$$

Mass (M): $1 = b + d$

Length (L): $2 = a - b + c - 3d$

Time (T): $-3 = -b - 2c - e$

Since there are three equations with five unknowns, two of them can be fixed. If b and c are fixed, the other unknowns can be set up as a function of b and c:

$$d = 1 - b$$
$$e = 3 - b - 2c$$
$$a = 2 + b - c + 3 - 3b = 5 - 2b - c$$

If a, d, and e are substituted in the equation in which power is a function of the different variables, one obtains:

$$P = K D^{5-2b-c}\ \eta^b\ g^c\ \rho^{1-b}\ N^{3-b-2c}$$

The variables are grouped in such a way that they have the same exponent:

$$P = K\ D^5\ \rho N^3\ \left(\rho N D^2/\eta\right)^{-b}\left(DN^2/g\right)^{-c}$$

$$\frac{P}{\rho\, N^3 D^5} = K\left(\frac{\rho\, N\, D^2}{\eta}\right)^{-b}\left(\frac{D\, N^2}{g}\right)^{-c}$$

It can be observed that three dimensionless constants were obtained:

Power's number:

$$\left(Po\right) = \frac{P}{\rho\, N^3 D^5}$$

Reynolds' number:

$$\left(\mathrm{Re}\right) = \frac{\rho\ N D^2}{\eta}$$

Froude's number:

$$\left(Fr\right) = \frac{D\, N^2}{g}$$

The last number expresses the ratio of dynamic action to gravity action.

In general, the power module can be expressed as a function of Reynolds and Froude's numbers, according to an expression of the type:

$$Po = K\left(\mathrm{Re}\right)^m \left(Fr\right)^n$$

2.4

When a fluid circulates through a pipe, mechanical energy losses occur due to friction with the pipe walls' mechanical energy losses by mass unit of the fluid ($\hat{E}_v$), depending on the characteristics of the pipe (internal diameter, roughness, and length) and on the properties of the circulation fluid (density and viscosity), as well as on the circulation velocity (v). Use Buckingham's method to deduce an expression that allows calculation of $\hat{E}_v$ as a function of the mentioned variables.

The number of variables is seven, and the number of fundamental magnitudes is three. Therefore, the number of dimensionless factors π is $\pi = 7 - 3 = 4$.

Energy losses due to friction can be expressed as a function of the remaining variables:

$$\hat{E}_v = K \rho^a \left(d_i\right)^b v^c l^d \varepsilon^e \eta^f$$

Writing all this information in matrix form gives:

	ρ	d_i	v	l	ε	η	$\hat{E}_v$
M	1	0	0	0	0	1	1
L	–3	1	1	1	1	–1	2
T	0	0	–1	0	0	–1	–2
	a	b	c	1	1	1	1

Working with three variables that are fundamental, one establishes them in a way so as to obtain a matrix determinant different from zero. It is determined that the rank of the matrix is equal to three.

Factors π:

1. $\pi_1 = \rho^a (d_i)^b v^c \hat{E}_v$

   The fundamental magnitudes are mass, length, and time:

   Mass (M): $0 = a$

   Length (L): $0 = -3a + b + c + 2$

   Time (T): $0 = -c - 2$

   When solving the system, the values obtained for a, b, and c are $a = 0$; $b = 0$; $c = -2$. Hence, the factor π_1 is $\pi_1 = \hat{E}_v / v^2$.

2. $\pi_2 = \rho^a (d_i)^b v^c$ l

   Mass (M): $0 = a$

   Length (L): $0 = -3a + b + c + 1$

   Time (T): $0 = -c$

   When solving the system, the values obtained for a, b, and c are $a = 0$; $b = -1$; $c = 0$. Hence, the factor π_2 is $\pi_2 = l / d_i$.

3. $\pi_3 = \rho^a (d_i)^b v^c \varepsilon$

   Mass (M): $0 = a$

   Length (L): $0 = -3a + b + c + 1$

   Time (T): $0 = -c$

   When solving the system, the values obtained for a, b, and c are $a = 0$; $b = -1$; $c = 0$. Hence, the factor π_3 is $\pi_3 = \varepsilon/d_i$.

4. $\pi_4 = \rho^a (d_i)^b v^c \eta$

   Mass (M): $0 = a + 1$

   Length (L): $0 = -3a + b + c - 1$

   Time (T): $0 = -c - 1$

   When solving the system, the values obtained for a, b, and c are: $a = -1$; $b = -1$; $c = -1$. Hence, the factor π_4 is $\pi_4 = \eta/(\rho v d_i) = (\mathrm{Re})^{-1}$. Since it is a dimensionless factor, its value is the Reynolds number: $\pi_4 = \mathrm{Re}$.

According to Buckingham's π theorem, one of these dimensionless factors can be expressed as a function of the other three factors. Therefore, it can be written that:

$$\pi_1 = f(\pi_2, \pi_3, \pi_4)$$

that is:

$$\frac{\hat{E}_V}{v^2} = \phi\left(\frac{l}{d_i}, \frac{\varepsilon}{d_i}, \mathrm{Re}\right)$$

Rearranging:

$$\hat{E}_V = v^2 \phi\left(\frac{l}{d_i}, \frac{\varepsilon}{d_i}, \mathrm{Re}\right)$$

It is known that mechanical energy losses per mass unit are proportional to the length, so:

$$\hat{E}_V = v^2 \frac{l}{d_i} \phi\left(\frac{\varepsilon}{d_i}, \mathrm{Re}\right)$$

It is obtained that $\hat{E}_v$ is directly proportional to the squared velocity and to the length, and inversely proportional to the pipe diameter. Likewise, it depends on a function ϕ' that depends on the Reynolds number and the so-called relative roughness, ε/d_i.

Experimentation should be performed to complete this expression. However, the function ϕ' can be substituted by a factor f, called friction factor, in such a way that the energy losses by friction could be obtained from:

$$\hat{E}_V = f \; v^2 \frac{l}{d_i}$$

where the factor f is a function of the Reynolds number and the relative roughness.

2.5

One of the most frequently used devices for batch fermentations is the stirred tank. The power that should be applied to the stirrer (P) is a function of its rotation velocity (N) and diameter (D), density (ρ) and viscosity of the substrate, gravity acceleration (g), and time (t) since the beginning of operation. Demonstrate, using Rayleigh's and Buckingham's methods, that the power module (Po) is a function of the Reynolds (Re) number, Froude's (Fr) number, and time module (Nt), that is:

$$\left(Po\right) = \Phi\left[\left(\mathrm{Re}\right), \left(Fr\right), \left(Nt\right)\right]$$

The modules (Po), (Re), and (Fr) are defined by the expressions:

$$\left(Po\right) = \frac{P}{\rho \, N^3 \, D^5} \qquad \left(\mathrm{Re}\right) = \frac{D^2 \, N \, \rho}{\eta} \qquad \left(Fr\right) = \frac{D \, N^2}{g}$$

The number of variables is seven, while the number of fundamental magnitudes is three; therefore, the number of dimensionless factors π is four.

Rayleigh's Method

The power of the stirrer can be expressed in relation to function of the other variables:

$$P = K \; N^a \rho^b \eta^c D^d \, g^e \, t^f \tag{2.6.1}$$

	P	N	ρ	η	D	g	t
M	1	0	1	1	0	0	0
L	2	0	–3	–1	1	1	0
T	–3	–1	0	–1	0	–2	1
	1	a	b	c	d	e	f

$$\frac{ML^2}{T^3} = K^0 \left(1/T\right)^a \left(M/L^3\right)^b \left(M/LT\right)^c \left(L\right)^d \left(L/T^2\right)^e \left(T\right)^f$$

Mass (M): $1 = b + c$
Length (L): $2 = -3b - c + d + e$
Time (T): $-3 = -a - c - 2e + f$

Since three equations in six unknowns resulted, three of them should be fixed. If c, e, and f are fixed, the other variables are set up as a function of c, e, and f:

$b = 1 - c$
$d = 5 - e - 2c$
$a = 3 - c - 2e + f$

Substituting a, b, and d in Equation 2.6.1 leads to:

$$P = K N^{3-c-2e+f} \rho^{1-c} \eta^c D^{5-2c-3} g^e t^f$$

The variables are grouped in such a way that they have the same exponent:

$$P = K D^5 \rho N^3 \left(\eta/\rho N D^2\right)^c \left(g/DN^2\right)^e \left(Nt\right)^f$$

therefore:

$$\frac{P}{\rho N^3 D^5} = K\left(\rho N D^2/\eta\right)^{-c} \left(DN^2/g\right)^{-e} \left(Nt\right)^f$$

Taking into account the definitions of the power, Reynolds, and Froude's modules, this expression is converted into $(Po) = K\,(Re)^{-c}\,(Fr)^{-e}\,(Nt)^f$ or $(Po) = \Phi[(Re), (Fr), (Nt)]$, which is the focus of this research.

Buckingham's Method

The matrix of the exponents is formed:

	P	N	D	g	ρ	η	t
M	1	0	0	0	1	1	0
L	2	0	1	1	3	–1	0
T	–3	–1	0	–2	0	–1	1

One looks for the rank of the matrix, which can be a maximum of three. There is a determinant different from zero, formed by the columns N, D, and ρ:

$$\text{Det}\begin{vmatrix} N & D & \rho \\ 0 & 0 & 1 \\ 0 & 1 & -3 \\ -1 & 0 & 0 \end{vmatrix} = 1$$

Therefore, the rank of the matrix is three. N, D, and ρ are chosen as fundamental variables.

	N	D	ρ	P	η	g	t
M	0	0	1	1	1	0	0
L	0	1	–3	2	–1	1	0
T	–1	0	0	–3	–1	–2	1
	a	d	b	1	1	1	1

The dimensionless factors π are determined one by one: $\pi_1 = N^a\ \rho^b\ D^d\ P$

Mass (M): $0 = b + 1$
Length (L): $0 = d - 3b + 2$
Time (T): $0 = -a - 3$

When solving this system, one obtains $b = -1$; $d = -5$; $a = -3$, so the dimensionless factor π_1 is:

$$\pi_1 = \frac{P}{N^3\ D^5\ \rho}$$

$\pi_2 = N^a\ \rho^b\ D^d\ \eta$

Mass (M): $0 = b + 1$
Length (L): $0 = d - 3b - 1$
Time (T): $0 = -a - 1$

When solving this system, one obtains $b = -1$; $d = -2$; $a = -1$, so the dimensionless factor π_2 is:

$$\pi_2 = \frac{\eta}{N^2\ D^2\ \rho}$$

$\pi_3 = N^a\ \rho^b\ D^d\ g$

Mass (M): $0 = b$
Length (L): $0 = d - 3b + 1$
Time (T): $0 = -a - 2$

When solving this system, one obtains $b = 0$; $d = -1$; $a = -2$, so the dimensionless factor π_3 is:

$$\pi_3 = \frac{g}{N^2 D}$$

$\pi_4 = N^a \rho^b D^d t$

Mass (M): $0 = b$
Length (L): $0 = d - 3b$
Time (T): $0 = -a + 1$

When solving this system, one obtains $b = 0$; $d = 0$; $a = 1$, so the dimensionless factor π_4 is:

$$\pi_4 = Nt$$

Applying Buckingham's theorem, $\pi_1 = F(\pi_2, \pi_3, \pi_4)$; hence, $(Po) = \Phi[(\mathrm{Re}), (Fr), (Nt)]$, which is the focus of this research.

2.6

A cylindrical 5-m diameter tank that stores concentrated juice (54°Brix) has a 20-cm diameter drainage, placed 50 cm away from the lateral wall of the deposit, and a nozzle 10 cm above the bottom of the tank. When draining the tank, a vortex is formed in such a way that when the liquid level is not high enough, the vortex can reach the outlet pipe, and air can be drawn off together with the juice. The tank should operate at a draining flow of 20 m^3/s. With the purpose of predicting what should be the minimum level of juice in the tank to avoid the vortex reaching the drainage, a study is to be performed with a reduced scale model that will operate with water. Determine the dimensions the model should have, as well as the operation conditions.

Data: It may be supposed that the shape of the vortex depends only on the draining rate and the quantity of liquid in the tank.

Properties of the juice: density 1250 kg/m^3, viscosity 50 mPa·s

H_2 is the level of the juice in the tank required for the vortex not to reach the drainage. Subscript 1 indicates model and subscript 2 indicates the prototype.

Geometric similarity:

$$\frac{d_1}{d_2} = \frac{D_1}{D_2} = \frac{l_1}{l_2} = \frac{h_1}{h_2} = \frac{H_1}{H_2} = k$$

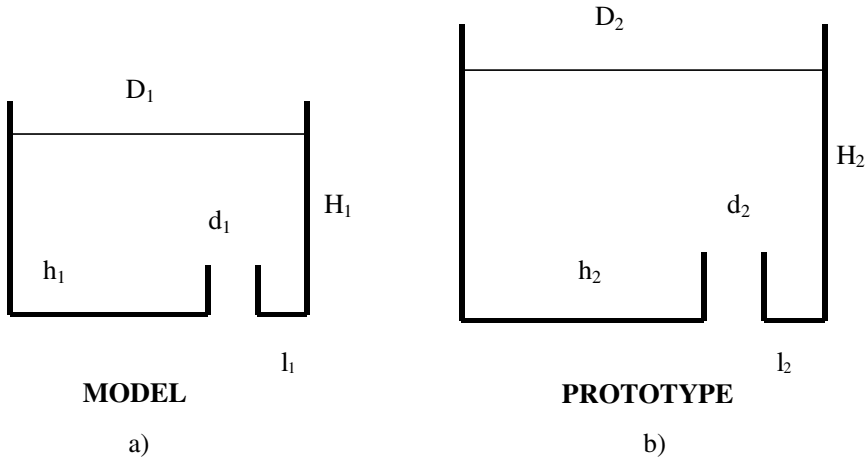

PROBLEM 2.6.

Dynamic similarity:

Since there are inertia, friction, and gravity forces, it should be understood that Reynolds and Froude's numbers for the model and for the prototype are equal:

$$(\mathrm{Re})_1 = (\mathrm{Re})_2 \qquad (Fr)_1 = (Fr)_2$$

From the equality of the Reynolds numbers:

$$\frac{\rho_1 v_1 d_1}{\eta_1} = \frac{\rho_2 v_2 d_2}{\eta_2}$$

hence:

$$\frac{d_1 v_1}{d_2 v_2} = \frac{\eta_1 \rho_2}{\eta_2 \rho_1}$$

From the equality of Froude's numbers:

$$\frac{(v_1)^2}{g d_1} = \frac{(v_2)^2}{g d_2}$$

Therefore:

$$\frac{v_1}{v_2} = \left(d_1/d_2\right)^{1/2}$$

When combining the obtained expressions:

$$\frac{d_1 \left(d_1\right)^{1/2}}{d_2 \left(d_2\right)^{1/2}} = \frac{\eta_1 \rho_2}{\eta_2 \rho_1}$$

Rearranging:

$$\frac{d_1}{d_2} = \frac{\left(\eta_1 \rho_2\right)^{2/3}}{\left(\eta_2 \rho_1\right)^{2/3}}$$

From the data given in the problem and from the properties of water:

$$\eta_1 = 1 \text{ mPa} \cdot \text{s} \qquad \rho_1 = 1000 \text{ kg}/\text{m}^3$$

$$\eta_2 = 50 \text{ mPa} \cdot \text{s} \qquad \rho_2 = 1250 \text{ kg}/\text{m}^3$$

it is obtained that the geometric similarity ratio is $k = d_1/d_2 = 0.0855$.

This factor allows us to obtain the dimensions of the model:

$d_1 = k \cdot d_2 = 0.0855 \cdot 0.2 \text{ m} = 0.017 \text{ m}$
$h_1 = k \cdot h_2 = 0.0855 \cdot 0.1 \text{ m} = 0.0085 \text{ m}$
$D_1 = k \cdot d_2 = 0.085 \cdot 5 \text{ m} = 0.428 \text{ m}$
$l_1 = k \cdot l_2 = 0.0855 \cdot 0.5 \text{ m} = 0.0428 \text{ m}$

Volumetric flow (q) is the product of the linear velocity (v) times the cross-sectional area (S). Since it is expressed as a function of the diameter of the pipe:

$$q = v\,S = v\,\frac{\pi}{4}\,d^2$$

so the flow rate between the model and the prototype will be:

$$\frac{q_1}{q_2} = \frac{v_1 \left(d_1\right)^2}{v_2 \left(d_2\right)^2} = \left(d_1/d_2\right)^{5/2} = k^{5/2}$$

Therefore, the volumetric flow to drain the model is:

$$q_1 = k^{5/2} q_2 = (0.0855)^{5/2} (20\ \mathrm{m^3/s}) = 0.0428\ \mathrm{m^3/s}$$

The minimum level of the liquid in the tank can be expressed as a function of the level in the model, from the value of geometric similarity rate:

$$H_2 = H_1/k = H_1/0.0855 = 11.7\ H_1$$

The value of H_1 can be experimentally obtained in the laboratory, working with the model. Then, with H_1 value, it is possible to obtain the value of H_2, which is the minimum height the juice should reach in the prototype so that the vortex does not reach the drainage pipe.

3

Introduction to Transport Phenomena

3.1 Historic Introduction

Unit operations of the agricultural and food industries constitute the physical, chemical, or biochemical stages that integrate industrial processes by means of which agricultural products are handled or transformed. That these stages are the same as those found in the processes of chemical industries makes the knowledge and advances of unit operations of chemical engineering applicable to the agricultural and food industries when they are adapted to characteristics of the raw material (particularly natural products, which are generally perishable) and particular conditions (hygiene, cleanliness, etc.) normally required by agricultural–industrial processes. The importance of the concepts of process engineering is that they unify the techniques of industries normally considered separate. Thus, the basic principles common to all food industries are unified in a logical way despite their apparent diversity.

Food engineering is a relatively new branch of engineering based on the chemical industry, where process engineering was developed. Chemical engineers have built process technology with dimensions not frequently found, which has been very advantageous. Most of this technology can be applied to the food industry.

The processes can be divided into so-called unit or basic operations common to many processes; thus, the individual study of each unit operation is more efficient than the study of each process. The knowledge of unit operations is vast; the food engineer should take this knowledge and apply it to the development of the food industries.

It should be recalled that the term "unit operation" was established in 1915 by Professor Little of the Massachusetts Institute of Technology (MIT). Because of its historic and conceptual value, it is interesting to recall its definition:

> … every chemical process conducted at any scale can be decomposed in an ordered series of what can be called unit operations, as pulverization, drying, crystallization, filtration, evaporation, distillation, etc. The amount of these unit operations is not very large and, generally, only few of them take place in a determined process.

This simplification reduced the complexity of the study of processes from the almost infinite set of processes that could be imagined to the set of existing unit operations. A given process would be formed by a combination of unit operations.

A new development and growth stage began with the systematic study of these unit operations, adding new operations and generalizing, for many of them, their didactic presentation through dimensional analysis and experimental study. This was a phase of reasoned empiricism in which theory and practice were skillfully combined, and during which the theoretical fundamentals of the different operations were gradually established. This traditional concept of unit operations has been one of the main factors of the extraordinary success of this branch of engineering in the past.

Continuing with the systematization effort, a new generalization period began, grouping unit operations according to the general principles on which they were based. In this way, they were classified within the following sections: fluid treatment, mass transfer by multiple contact, and energy and mass transfer by continuous contact.

Later, because of better knowledge of the fundamentals of unit operations, it was noticed that all of them were based on three phenomena: momentum transport, energy transfer, and mass transfer.

In all three cases, the flow of the transferred property is directly proportional to an impelling force (velocity, temperature, or concentration gradient) and inversely proportional to a resistance that depends on the properties of the system and on operation conditions. Therefore, it is possible to develop an abstract doctrine body from which these three transport phenomena can be taken as particular cases.

3.2 Transport Phenomena: Definition

It can be deduced that all the physical stages constituting the different industrial processes of industrial elaboration are based on momentum transport, energy transfer, and mass transfer. In all processes in which a system is not in equilibrium, the system evolves in such a way that it tends to equilibrium by transferring one or more of the cited properties.

Transport phenomena can be defined as physical phenomena revealed when a system evolves towards an equilibrium state. Some examples to explain this definition may be:

- When, in a fluid stream, there are two points whose velocities, taken normal to its movement, are different, the system will evolve to counteract this velocity difference by means of a momentum transport.

- If, in a solid, there are zones of different temperature, there will be a heat transport from the hottest zone to the coldest one, so the system tends to thermal equilibrium.
- When, within the same phase, there is a concentration difference between two points, a mass transfer will tend to equilibrate this concentration difference.

Actually, in all operations, at least two out of the three phenomena are simultaneously present, but there are some in which one phenomenon normally predominates. Thus, momentum transport predominates in operations of fluid transport, sedimentation, filtration, etc., heat transfer dominates in the design of heat exchangers, condensers, etc., and mass transfer dominates in operations such as absorption, solvent extraction, distillation, etc. In operations such as air–water interaction, drying, crystallization, etc., mass and heat transfer phenomena are equally important.

3.3 Circulation Regimes: Reynolds' Experiment

Before studying the mechanisms of transport phenomena, it is interesting to prove experimentally the existence of such mechanisms. When studying circulation regimes, the experiment carried out by Reynolds in 1833 is extremely important. This experiment consisted of circulating water through transparent tubing with constant cross section, varying the circulation velocity of the liquid by means of a valve placed at the entrance of the pipes. In the middle of the pipes, and in the entrance section, a colored solution was introduced. The variation of the colored vein was observed along the pipes at different circulation velocities of the liquid.

In this type of experiment, the velocity of the liquid is low, the colored vein does not lose its identity while circulating through the center of the pipes, and, although a low and progressive increase of the vein's width can be observed, mixture in a transversal sense is not seen, indicating that the flow takes place as parallel streams with no interference between them. Mass exchange occurs only at the molecular level. As the velocity of the liquid increases, oscillations in the colored filament appear until, at a certain velocity, it breaks into whirlpools and transversally inundates the conduction. Different images of Reynolds' experiment can be observed in Figure 3.1.

Based on these observations, it can be stated that there are two types of well-differentiated circulation regimes in which mass transfer mechanisms are different. For low velocities, liquid moves in a horizontal way with concentric parallel layers and without transversal movement. This regime is called laminar and is characterized by the absence of a global movement perpendicular to the main direction of the stream.

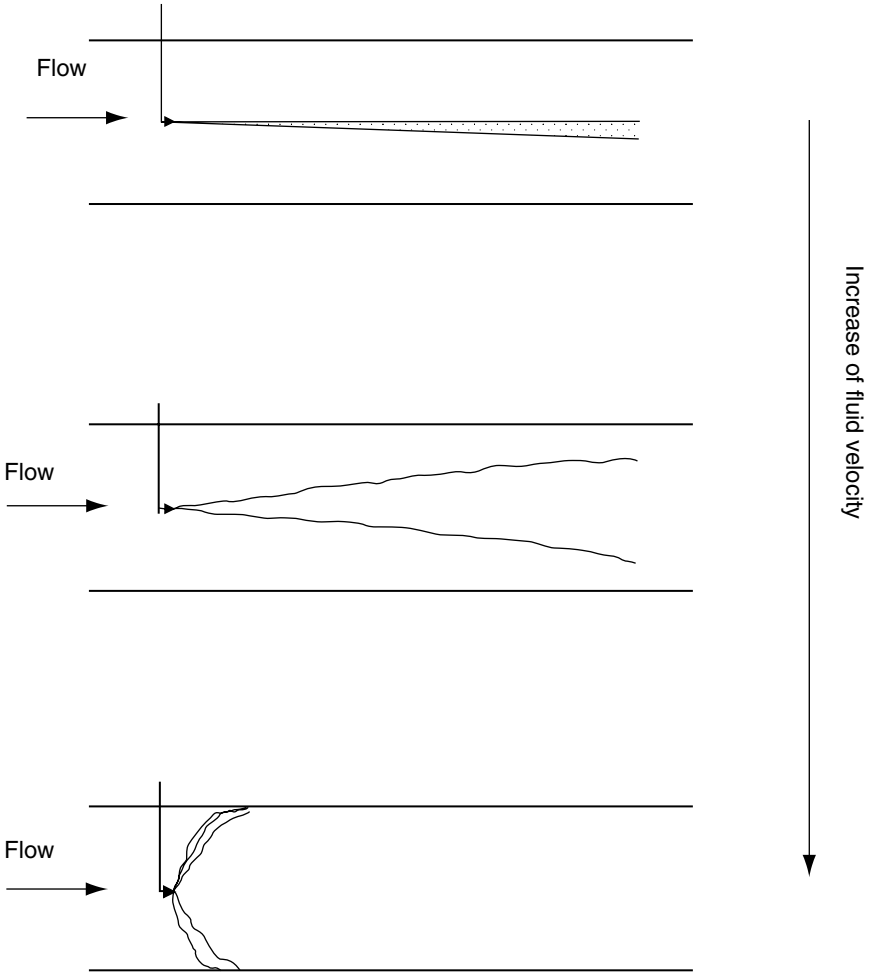

FIGURE 3.1
Reynolds' experiment.

For high velocities, there is movement of the liquid in a transversal way of macroscopic proportions. This type of circulation regime is called turbulent, and is characterized by rapid movement of the liquid in the form of whirlpools with no pre-established direction in the transversal section of the pipe.

The only variable modified in these experiments was velocity, but there may be other variables that could alter the regime, such as diameter of the pipe and the nature of the liquid. Hence, for a better study of circulation regimes, a dimensionless module that relates the magnitudes that characterize the circulation phenomenon is defined, setting up the boundaries of the different regimes. Such a module is called the Reynolds number, which represents the quotient between the inertia and viscosity forces of the moving fluid. In the case of a cylindrical conduit and a Newtonian fluid, it is:

$$\mathrm{Re} = \frac{\rho v d}{\eta} \tag{3.1}$$

where:

Re = Reynolds number (dimensionless)
ρ = density of the fluid (kg/m^3)
v = mean velocity of the fluid (m/s)
d = diameter of the conduit (m)
η = viscosity of the fluid (Pa·s)

The numerical value of the Reynolds number (Re) is used to define the type of circulation regime of a fluid stream. It has been observed that, for values lower than a given Re, called critical, the oscillations of the fluid are unstable and any perturbation disappears quickly. For values higher than this critical Re, the oscillations become stable and of greater amplitude, giving place to a high radial mixture. For Newtonian fluids, the critical Re value is 2100. Values lower than 2100 indicate a laminar regime, while, for greater values, there is a range of Re number values called transition, in which metastable phenomena could appear. The regime is completely turbulent for values higher than 10,000. This study can also be applied to momentum transport and heat transfer.

If the pressure drop (ΔP) in a fluid between the inlet and outlet sections of a conduit is measured in the Reynolds experiment, an increase in the volumetric flow of the fluid will be observed. Figure 3.2 shows the variation of the pressure drop as a function of the Reynolds number. The loss of charge of the

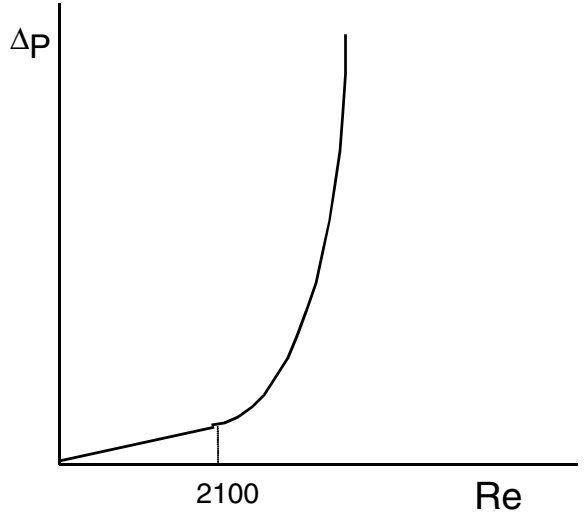

FIGURE 3.2
Variation of the pressure drop in relation to the Reynolds number.

fluid is a result of the energy consumed by the fluid because a momentum transport took place. It can be seen in this figure that, starting from Re = 2100, the loss of charge increases rapidly, which favors the momentum transport process since radial components appear in the velocity of the fluid particles.

In order to study heat transfer, one can consider a tubing in which water with mass flow rate (w) at a temperature t_1 enters, and the same volume of water at temperature t_2, due to the heat gained by the fluid through the tubing wall, exits. The total heat gained will be:

$$q = w\,Cp\left(t_1 - t_2\right) \tag{3.2}$$

When the mass flow rate (w) varies, the exit temperature (t_2) will also vary. A graphical representation of the variation of gained heat as a function of the Reynolds number will yield a graphic similar to that in Figure 3.2. It can be observed that, for a laminar fluid, the exchanged heat increases in direct proportion to the volume of the fluid; however, starting at the critical value of the Reynolds number, a sharp increase is observed. In a laminar regime, heat transfer occurs in radial form, molecule by molecule, but, in a turbulent regime, there are streams or whirlpools that favor radial heat transport.

3.4 Mechanisms of Transport Phenomena

The mechanism of energy transfer by means of electromagnetic waves is called radiation and it can be performed through vacuum, not needing a material media for transmission. However, other forms of energy transfer and of momentum transport are associated with material movement, although there is not a net transfer. Thus, in heat transfer by conduction in a continuous material media, there is no material movement at the macroscopic level, although there is movement at the molecular level due to the motion of free electrons (in metals) or to the vibration of molecules or ions in solids.

Because these different transport phenomena are associated, it is interesting to study them as a whole. Transport of the three previously mentioned properties may take place by means of two well-differentiated mechanisms: molecular transport and turbulent transport.

In molecular transport the transfer of the property is carried out, molecule by molecule, by movement of the individual molecules or by interactions among them. Turbulent transport is produced when large groups of molecules move as aggregates or whirlpools, transporting with them momentum, mass, or energy. These aggregates serve as transportation media and they transfer the property to other groups of molecules that interact with them. Molecular transport can happen alone; turbulent transport never occurs in isolation but is always accompanied by molecular transport.

3.4.1 Mass Transfer

To study the mechanism of mass transfer, suppose a given component of the considered material is transferred from one point to another of the studied system. This mass transfer may take place according to two mechanisms: molecular flow or forced convective flow. When there is a concentration gradient of the considered component between two points of the system, mass transfer is produced by molecular flow. However, when the entire mass moves from one point to another, the transfer is produced by forced convective flow.

According to the physical nature of the media, different situations can occur and the mass transfer is carried out by one or by both of the transport mechanisms considered:

- When there is no concentration gradient of the considered component and if the media is a fluid, there can only be convective transport. Usually, this type of problem is studied as momentum and not as mass transport.
- When there is a concentration gradient of the component and the media is a fluid in repose, the mass transfer is carried out by molecular flow, due only to molecular diffusion. Thus, if one considers a beaker filled with water with a crystal of colorant placed on the bottom, the crystal dissolves, gradually diffusing throughout all the beaker, since the concentration around the crystal is greater than in other zones. This diffusion will take place until equilibrium is reached.
- When there is a concentration gradient and the media is a fluid moving in a laminar regime, mass transfer is carried out by the two mechanisms. Recalling the Reynolds experiment, the colorant is injected into an entrance point P of the tubing (Figure 3.3). At the exit at point Q, the colorant is transferred from the entrance to the exit by forced convection flow, and from the center of the pipe to point Q by molecular flow.

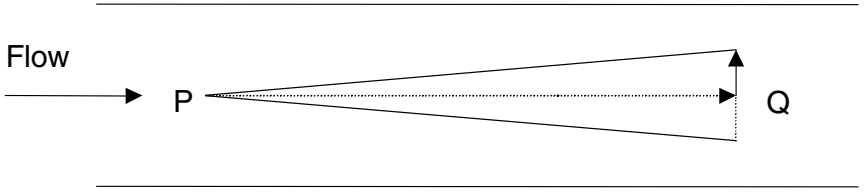

FIGURE 3.3
Simultaneous molecular and forced convective flows.

- When the media is a fluid in which there are turbulence and concentration gradients, the mechanisms of molecular and forced convection mass transport occur simultaneously. Although the phenomenon is complex, it is similar to the previous case, using an analogous model. In this case, consider an effective diffusion that brings together the molecular diffusion due to the gradient and the denominated turbulent diffusion, passing from P to Q by means of turbulent transport by whirlpools.

3.4.2 Energy Transfer

As mentioned at the beginning of this section, energy transfer by radiation occurs by a different mechanism than do those of conduction and convection. It is interesting to mention some aspects of energy transfer by these two mechanisms.

Conduction supposes a molecule-to-molecule flow of energy, due to temperature gradients, by mechanisms that depend on the physical nature of the medium. By analogy with mass diffusion, the principle of these mechanisms can be explained at an atomic-molecular level; however, these mechanisms differ because, in conduction, there is no net mass flux.

If the considered medium is a fluid and there is a temperature gradient, in many cases a density difference will be noticeable. Therefore, there will be a mass flow due to flotation forces associated with an energy flow of the natural convection type. Forced convection exists as well and, as in natural convection, is due to the associated energy of moving fluids; however, in this case the energy applied to move the fluid comes from mechanical devices. Besides convection, energy transfer by conduction will also occur but is less important. In a general way, energy transfer is studied as a convection phenomenon in fluid media, bringing together convection and conduction.

3.4.3 Momentum Transport

To study the mechanisms of momentum transport, an analogous study to the mass transfer study can be carried out. Molecular and forced convection momentum flows can also be considered.

3.4.4 Velocity Laws

In the mechanisms of molecular transport, property transfer occurs due to a potential gradient, which can be a concentration, temperature, or velocity gradient, depending on whether the transferred property is mass, energy, or momentum, respectively.

In molecular transport, the flux density of the property is proportional to the potential gradient. The proportionality constant is an intensive property of the media. Depending on the nature of the property, the proportionality

constant receives different names, as well as the laws of each of the transport phenomena.

Conductivity:

Fick's Law: (flux density of mass) = (diffusivity) (concentration gradient)

Fourier's Law: (flux density of thermal energy) = (thermal conductivity) (temperature gradient)

Newton's Law: (flux density of momentum) = (viscosity) (velocity gradient)

When the transport regime is turbulent, a laminar regime subsists in the inner part of the whirlpools involving molecular transport in this region; normally, the parameters include both phenomena.

3.4.5 Coupled Phenomena

The velocity laws for mass, thermal energy, and momentum transfer are expressed in a similar manner, in which the flux density of the considered property is proportional to the gradient of the impelling force:

$$\vec{J} = k\,\vec{X} \tag{3.3}$$

where

$\vec{J}$ = flux density (quantity of property/$m^2 \cdot s$)
k = proportionality constant
$\vec{X}$ = potential gradient

This equation is applicable to all systems not in equilibrium. The flow of an equal property may be caused by various simultaneous potential gradients, or a given gradient can generate diverse flows. Coupled phenomena or processes are those that occur in systems in which different flows and gradients take place simultaneously. Thus, for example, a temperature gradient, in addition to causing an energy flow, can cause a mass flow (Soret effect of thermodiffusion).

Onsegar generalized the latter expression to a system with R flows and S gradients as:

$$\vec{J}_i = \sum_{j=1}^{S} k_{ij}\,\vec{X}_j \tag{3.4}$$

$$\text{For } i = 1,2,\ldots,R$$

This equation indicates that each flow J_j depends not only on its combined gradient, but also on other gradients acting on the system ($X_{j\neq i}$).

TABLE 3.1

Coupled Phenomena

	Flow Density		
Potential	**Mass**	**Energy**	**Momentum**
Concentration gradient	Diffusion (Fick's law)	Thermodiffusion (Dufour's effect)	
Temperature gradient	Thermodiffusion (Soret's effect)	Thermal conductivity (Fourier's law)	
Velocity gradient			Molecular transport of momentum (Newton's law)

4

Molecular Transport of Momentum, Energy, and Mass

4.1 Introduction

In many cases, it is difficult to describe in a complete and quantitative way the problems set up in engineering. The velocity laws that govern the processes studied may not be exactly known when the behavior of static fluids is studied. However, the behavior of moving fluids sets up complicated problems to be quantified. The work required to pump a fluid through a conduit depends on the momentum losses experienced by the fluid rubbing along the walls, on the circulation regime, and on the type and nature of the fluid.

For transport in one direction under steady state and laminar flow, i.e., molecular transport, the last chapter showed that the velocity expressions or laws may be expressed as: (flux density) = (transport property) (potential gradient).

4.2 Momentum Transport: Newton's Law of Viscosity

Consider a static fluid, between two parallel slabs, of area A separated by a distance y. If, at a given time (t = 0), the lower slab begins to move at a velocity v, a time will come when the velocity profile is stable, as shown in Figure 4.1. Once the steady state is reached, a force F must continue to be applied to maintain the motion of the lower slab. Assuming that the circulation regime is laminar, the force per unit area that should be applied is proportional to the velocity and distance ratio, according to the following equation:

$$\frac{F}{A} = \eta \frac{v}{y} \tag{4.1}$$

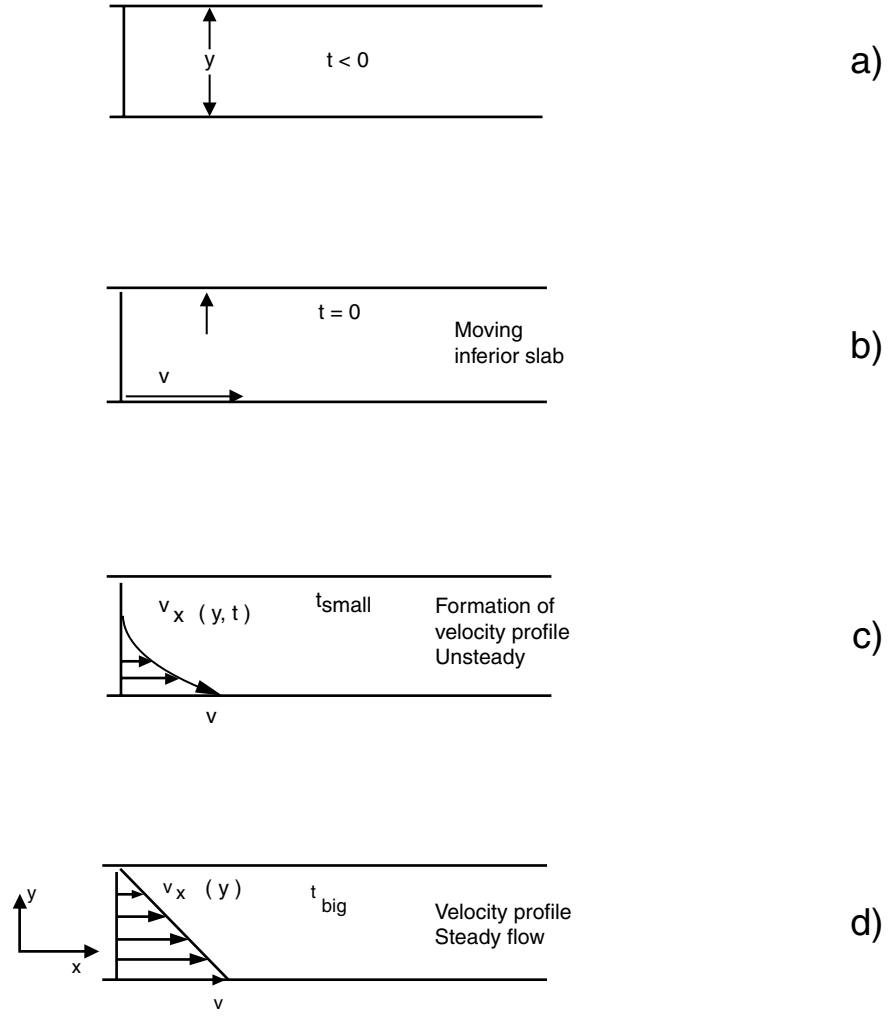

FIGURE 4.1
Velocity profile.

The proportionality constant η is called the viscosity of the fluid.

For certain applications it is convenient to express the latter equation in a more explicit way. The shearing stress exerted in the direction x on the fluid's surface, located at a distance y, by the fluid in the region where y is smaller is designated by τ_{YX}. If the velocity component in the direction x has a value v_x, the last equation may be expressed as:

$$\tau_{YX} = -\eta \frac{d v_X}{d y} \tag{4.2}$$

That is, the shear stress or force per unit area is proportional to the local velocity gradient. This equation is the expression of Newton's law of viscosity. All those fluids that follow this law are termed Newtonian fluids.

The shearing stress shear stress τ_{YX} in a Newtonian fluid, for a distance y from the limit surface, is a measure of the velocity of momentum transport per unit area in a direction perpendicular to the surface. The momentum flux is the amount of momentum per unit area and unit time, which corresponds to a force per unit area. For this reason, τ_{YX} can be interpreted as flux density of momentum x in the direction y.

According to Equation 4.2, the momentum flux goes in the direction of the negative velocity gradient. That is, the momentum is transferred from the fastest moving fluid to the slowest one. Also, shear stress acts in such a direction that it opposes the motion of the fluid.

Another way to express Newton's law of viscosity is:

$$\tau_{YX} = -\nu \frac{d\left(\rho\, v_X\right)}{d\, y} \tag{4.3}$$

where v is the kinematic viscosity, which is the viscosity divided by the density:

$$v = \eta/\rho \tag{4.4}$$

4.3 Energy Transmission: Fourier's Law of Heat Conduction

To study heat transfer, a solid material with the form of a parallele piped with surface A and thickness y is considered. Initially, the temperature of the slab is T_o. At a given time (t = 0), the lower part of the slab suddenly reaches a temperature T_1, higher than T_o, and remains constant over time. The temperature will vary along the slab until reaching the steady state, in which a temperature profile such as that shown in Figure 4.2 is reached. To maintain this profile, a heat flow Q should be sent through the slab.

Values of the temperature difference ($\Delta T = T_1 - T_o$) small enough comply with the following relation:

$$\frac{\dot{Q}}{A} = k \frac{\Delta T}{y} \tag{4.5}$$

This equation indicates that the heat flow per unit area is proportional to the increase of temperature with distance y. This proportionality constant k is called thermal conductivity of the solid slab. This equation also applies

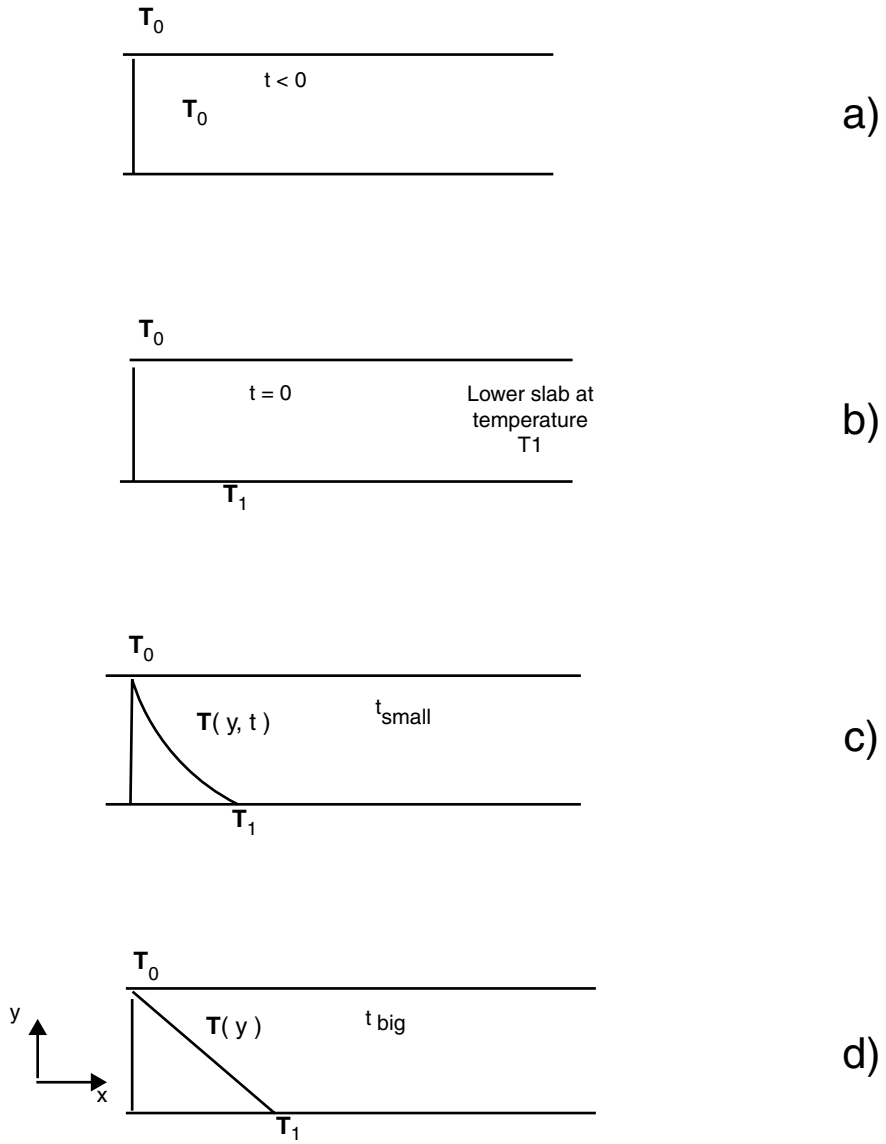

FIGURE 4.2
Development of the temperature profile.

for liquids and gases placed between slabs, provided that there are no convection or radiation processes. Therefore, this equation is applicable to all heat conduction processes in solids, liquids, and gases.

For certain applications it is convenient to express this equation in a differential form. That is, if the thickness y of the solid tends to zero, the limit form of Equation 4.5 will be:

$$q_Y = -k\frac{dT}{dy} \tag{4.6}$$

where q_Y represents the heat flux in the direction y. This equation expresses that heat flow density is proportional to the negative gradient of temperature and is the unidimensional form of Fourier's law of heat conduction.

For other directions, the equations are analogous to that described for direction y. Therefore, Fourier's law is expressed as:

$$\vec{q} = -k\vec{\nabla}T \tag{4.7}$$

that is, the heat flux vector is proportional to the temperature gradient, with opposite direction. It is assumed that the medium is isotropic; i.e., the thermal conductivity has the same value in all the directions of the material.

The units in which heat conductivity is normally expressed are W/(m·K) or kcal/(h·m·°C), and the dimensions are: $[k] = MLT^{-3}\theta^{-1}$.

Besides the thermal conductivity, in the latter equations thermal diffusivity can be used, defined according to the equation:

$$\alpha = \frac{k}{\rho\ \hat{C}_P} \tag{4.8}$$

where $\hat{C}_P$ is the specific heat of the material.

Taking into account the definition of thermal diffusivity, the expression of Fourier's law for one direction is:

$$q_Y = -\alpha\ \frac{d\left(\rho\ \hat{C}_P T\right)}{dy} \tag{4.9}$$

for an isotropic material in which ρ and $\hat{C}_P$ are constants.

4.4 Mass Transfer: Fick's Law of Diffusion

Fick's law of diffusion refers to the movement of a substance through a binary mixture due to the existence of a concentration gradient. The movement of a substance within a binary mixture from high concentration points to points with lower concentrations may be easily deduced by recalling the dissolution of a color crystal in water, as described in Chapter 3. The diffusion of a component due to the existence of a concentration gradient receives the name of ordinary diffusion. There are also other types of diffusion,

according to the property that confers the movement to the component of the mixture; thus, if movement is due to a pressure gradient, it is called pressure diffusion; if it is due to a thermal gradient, the diffusion is thermal. When there is an inequality in the external forces that cause such movement, it is called forced diffusion.

The study of diffusion is more complicated than the cases of momentum and energy transport because diffusion involves the movement of a species within a mixture. In a diffusive mixture, the velocities of the individual components are different and should be averaged to obtain the local velocity of the mixture that is required to define diffusion velocities. To get the expression of Fick's law, it is convenient to define the different forms for expressing concentrations, velocities, and fluxes:

- Mass concentration ρ_i: the mass of species i per unit of mixture volume.
- Molar concentration C_i: the number of moles of the species i per unit of mixture volume. $C_i = \rho_i / M_i$ in which M_i is the molecular weight of species i.
- Mass fraction w_i: the mass concentration of the species i divided by the total molar density of the mixture; $w_i = \rho_i / \rho$.
- Molar fraction X_i: the molar concentration of the species i divided by the total molar density (global concentration) of the mixture: $X_i = C_i / C$.

In the considered mixture, each component moves at a different velocity. If a component i has a velocity v_i with respect to steady coordinate axes, the different types of velocity are defined as follows:

- Mean mass velocity v:

$$\vec{v} = \frac{\sum_{i=1}^{n} \rho_i \vec{v}_i}{\sum_{i=1}^{n} \rho_i} = \frac{\sum_{i=1}^{n} \rho_i \vec{v}_i}{\rho} = \sum_{i=1}^{n} w_i \vec{v}_i \tag{4.10}$$

- Mean molar velocity v^*:

$$\vec{v}^* = \frac{\sum_{i=1}^{n} C_i \vec{v}_i}{\sum_{i=1}^{n} C_i} = \frac{\sum_{i=1}^{n} C_i \vec{v}_i}{C} = \sum_{i=1}^{n} X_i \vec{v}_i \tag{4.11}$$

When considering flow systems, it is convenient to refer to the velocity of the component i with respect to v or v^*, rather than referring to steady coordinate axes. In this way, one obtains the so-called diffusion velocities that represent the movement of the species i with respect to the movement of the fluid stream:

- Diffusion velocity of component i with respect to $\vec{v}$: the velocity of component i with respect to an axis system that moves at velocity v; it is given by the difference $(v_i - v)$.
- Diffusion velocity of the component i with respect to $\vec{v}^*$: the velocity of component i with respect to an axis system that moves at velocity v^*; it is given by the difference $(v_i - v^*)$.

The flux density can be of mass or molar and is a vectorial magnitude defined by the mass or moles that cross through a unit area per unit time. The motion can be referred to as steady axis or as axis moving at velocity v or v^*. In this way, the different forms for expressing the flux density of a component i in a mixture made of n components will be:

- With respect to steady axes:
  Mass flux:

$$\vec{m}_i = \rho_i \vec{v}_i \tag{4.12}$$

  Molar flux:

$$\vec{N}_i = \vec{C}_i \vec{v}_i \tag{4.13}$$

- For moving axes:
  Diffusion mass flux in relation to velocity $\vec{v}$:

$$\vec{j}_i = \rho_i \left(\vec{v}_i - \vec{v}\right) \tag{4.14}$$

  Diffusion mass flux in relation to velocity $\vec{v}^*$:

$$\vec{j}_i^* = \rho_i \left(\vec{v}_i - \vec{v}^*\right) \tag{4.15}$$

  Diffusion molar flux in relation to velocity $\vec{v}$:

$$\vec{J}_i = C_i \left(\vec{v}_i - \vec{v}\right) \tag{4.16}$$

  Diffusion molar flux in relation to velocity $\vec{v}^*$:

$$\vec{J}_i^* = C_i \left(\vec{v}_i - \vec{v}^*\right) \tag{4.17}$$

Some of these forms are rarely applied, such as J_i and j_i*. Most often used in engineering is the molar flux, referred to as steady axis N_i.

Once the different forms in which concentrations, velocities, and flux can be expressed have been reviewed, mass transfer is studied. Consider a binary mixture with components *A* and *B* in which the diffusion of one of the components occurs due to a concentration gradient of the considered component. As for momentum and energy transfer, viscosity and thermal conductivities are defined as proportionality factors between momentum flux and the velocity gradient for viscosity (Newton's law of viscosity), and between heat flux and temperature gradient for thermal conductivity (Fourier's law of heat conduction). In an analogous way the diffusivity $D_{AB} = D_{BA}$ in a binary mixture is defined as the proportionality factor between the mass flux and the concentration gradient, according to the equation:

$$\vec{J}_A^* = -C\, D_{AB}\, \vec{\nabla} X_A \tag{4.18}$$

that is, Fick's first law of diffusion for molar flux. In addition to the concentration gradient, the temperature, pressure, and external forces contribute to the diffusion flux, although their effect is small compared to that of the concentration gradient. This indicates that the diffusion molar flux related to the velocity v* is proportional to the gradient of the molar fraction. The negative sign expresses that this diffusion takes place from higher to lower concentration zones.

It is easy to deduce that the diffusion sum of a binary mixture is zero, i.e.:

$$\vec{J}_A^* + \vec{J}_B^* = 0$$

since, if a component diffuses to one side, the other component diffuses in the opposite way.

When the global concentration is constant, a chemical reaction does not exist, or there is a chemical reaction, but the number of moles does not vary, Equation 4.18 can be transformed into:

$$\vec{J}_A^* = -D_{AB}\, \vec{\nabla} C_A \tag{4.19}$$

There are other ways to express Fick's first law according to the flux and the correspondent concentration gradient considered. Thus, for the mass flux in reference to the steady axes, the gradient considered is that of the mass fraction, so this law is expressed by the equation:

$$\vec{m}_A = w_A \left(\vec{m}_A + \vec{m}_B\right) - \rho D_{AB} \vec{\nabla} w_A \tag{4.20}$$

Of all possible expressions for Fick's first law of diffusion, the one with the greatest importance is that related to the molar flux in steady or fixed axis:

$$\vec{N}_a = X_A\left(\vec{N}_A + \vec{N}_B\right) - CD_{AB}\nabla X_A \tag{4.21}$$

It can be observed that N_A is the result of two vectorial magnitudes, $X_A(\vec{N}A + \vec{N}B)$: the molar flux by convective transport, resulting in the global motion of the fluid, and $(-CD_{AB}\,\vec{\nabla}X_A)$, due to the molecular transport, according to the definition of J_A*.

The units of diffusivity can be expressed, for example, in cm^2/s or m^2/h.

There is a lack of diffusivity data for most mixtures, so it is necessary to use estimated values in many calculations in which diffusivities are required. When possible, experimental data should employed since, generally, they are safer. The order of magnitude for diffusivities is given next for various cases found in practice:

Gas–gas diffusion:	0.776 to 0.096 cm^2/s
Liquid–liquid diffusion:	2×10^{-5} to 0.2×10^{-5} cm^2/s
Diffusion of a gas in a solid:	0.6×10^{-8} to 8.5×10^{-11} cm^2/s
Diffusion of a solid in another solid:	2.5×10^{-15} to 1.3×10^{-30} cm^2/s

Viscosity and thermal conductivity of a pure fluid are only a function of the temperature and pressure, the diffusivity D_{AB} for a binary mixture is a function of temperature, pressure, and composition.

4.5 General Equation of Velocity

The dimensions of the diffusivity D_{AB} are surface per unit time: $D_{AB} = L^2T^{-1}$. If Newton's law of viscosity is considered, the dimensions do not correspond to those of diffusivity: $[\eta] = ML^{-1}T^{-1}$. However, if the kinematic viscosity v is taken, i.e., the relationship between dynamic viscosity and density, it turns out that its dimensions are surface per time unit: $[\nu] = L^2T^{-1}$, that is, the dimensions coincide with those of diffusivity. So ν also receives the name of momentum diffusivity.

In an analogous way, in Fourier's law of heat conduction, the dimensions of thermal conductivity are: $[k] = MLT^{-3}T^{-1}$. However, if the relation $\alpha = k/(\rho\,\hat{C}_p)$ is considered, its dimensions coincide with those of diffusivity: $[\alpha] = L^2T^{-1}$, where α is known as thermal diffusivity.

The analogy of these three magnitudes, D_{AB}, v, and α, is could be observed from the velocity equations for the three transport phenomena in unidirectional systems:

Fick's law:

$$j_{AB} = -D_{AB} \frac{d}{dy}(\rho_A)$$

Newton's law:

$$\tau_{YX} = -\nu \frac{d}{dy}(\rho . v_X)$$

Fourier's law:

$$q_Y = -\alpha \frac{d}{dy}(\rho \hat{C}_P \theta)$$

where ρ and $\hat{C}_P$ remain constant.

In these equations the media is assumed to be isotropic, i.e., the material's viscosity, thermal conductivity, and diffusivity have the same value in any direction. This is acceptable for fluids and most homogeneous solids.

Considering only one direction, the above equations can be grouped into one expression:

$$\Phi_Y = -\delta \frac{d\xi}{dy} \tag{4.22}$$

where Φ_γ is the flux of any of the three properties in the direction y, ξ is the concentration per unit volume of the considered property, and δ is the proportionality factor, called diffusivity. Similar equations will result for the other directions in such a way that the experimental equations of Fick, Newton, and Fourier can be grouped into three general equations, one for each direction. These equations constitute the expressions of molecular transport of the three studied properties.

The analogies expressed by the last equations among momentum, energy, and mass cannot be applied to bi- and tridimensional problems, since shear stresses τ are grouped in a tensorial magnitude, while j_A and q are vectorial magnitudes of three components.

If vectorial notation is used to generalize these equations, for direction x one obtains:

$$\tau_X = -\eta \nabla(v_X) \tag{4.23a}$$

$$q = -k \nabla T_X \tag{4.24}$$

$$j_{AB} = -D_{AB} \frac{d}{dy}(\rho_A) \tag{4.25}$$

For the y and z directions, the only equation that changes is that related to Newton's law; thus, the equations used for direction y and z will be:

$$\tau_Y = -\eta \nabla\left(v_Y\right) \tag{4.23b}$$

$$\tau_Z = -\eta \nabla\left(v_Z\right) \tag{4.23c}$$

Therefore, generalizing, it is obtained:

$$\vec{\Phi} = -\delta \vec{\nabla}\xi \tag{4.26}$$

which expresses that the flux vector is proportional to the gradient of the driving force or potential (for the experimental laws) and concentration of the properties (in the case of more strict laws), and of opposite direction.

5

Air–Water Mixtures

5.1 Introduction

Operations involving air–water mixtures are based on the mass transfer between two phases when two components are present. It is assumed that the liquid phase is constituted of pure water, while the gas phase will be formed by an inert gas that contains water vapor.

The mass transfer takes place exclusively in a gas phase, so the water vapor migrates from the interface to the gas or from the interface to the liquid, occurring, in any case, in the normal way to the surface. The transfer mechanisms involved in these processes are a combination of turbulent transport and diffusion. When there is a phase change, the mass transfer is accompanied by a heat transfer.

The air–water interaction is applied in different processes, the most important of which is air conditioning and water cooling by evaporation. Air humidification and dehumidification operations are based on the air conditioning used in food preservation processes. Also, food drying operations are based on the interaction between air and water, in which the water contained in the food is transferred to the air in vapor form.

5.2 Properties of Humid Air

This section describes the different properties of air–water vapor mixtures useful in calculations of unit operations that involve water transfer between liquid and gas phases. To facilitate the calculations, all properties are usually referred to as the mass or molar unit of dry air.

Molar humidity X_m: the moisture content of air expressed as moles of water per mole of dry air, according to the definition:

$$X_m = \frac{P_V}{P - P_V} \text{ kmoles water vapor/kmoles dry air} \tag{5.1}$$

where:
P_v = partial pressure of water vapor
P = total pressure

Absolute humidity *X*: the moisture content of air expressed in kg of water per kg of dry air. Absolute moisture can be expressed as a function of the partial pressure of the water vapor in the air according to the equation:

$$X = \frac{P_V M_{WATER}}{\left(P - P_V\right) M_{AIR}} \text{ kg water vapor/kg dry air} \tag{5.2}$$

where:
M_{WATER} = 18 kg/kmol
M_{AIR} = 28.9 kg/kmol

Thus, a direct relation between absolute and molar moisture can be found:

$$X = 0.622 \frac{P_V}{P - P_V} = 0.622\ X_m \tag{5.3}$$

When the water vapor partial pressure in the air coincides with the water vapor tension at the temperature of air, it is said that the air is saturated. If P_s is the tension of pure water vapor, then the following is compiled:

$$X_{SATURATION} = 0.622 \frac{P_S}{P - P_S} \tag{5.4}$$

Relative humidity ϕ: the relation between the amount of water vapor contained in a determined air volume and the amount of water vapor that this air volume could contain if it were saturated. From this definition it is easy to see that:

$$\phi = P_V / P_s \tag{5.5}$$

Since for saturated air the water vapor pressure in the air is equal to saturation pressure, the relative humidity is one $\phi = 1$.

The relation between absolute and relative humidities is obtained when combining Equations 5.3 and 5.5:

$$X = 0.622 \frac{P_S \phi}{P - P_S \phi} \tag{5.6}$$

Percentage humidity Y: the relationship between the absolute and saturation humidity:

$$Y = \frac{X}{X_{SAT}} = \frac{P_V\left(P - P_S\right)}{P_S\left(P - P_V\right)} = \phi\frac{\left(P - P_S\right)}{\left(P - P_V\right)} \tag{5.7}$$

Humid volume $\hat{\mathbf{V}}$: the volume occupied by 1 kg of dry air plus the water vapor that it contains:

$$\hat{\mathbf{V}} = \hat{\mathbf{V}}_{\text{DRY AIR}} + \hat{\mathbf{V}}_{\text{WATER VAPOR}}$$

Since all the variables are referred to 1 kg of dry air, the humid volume will contain 1 kg of dry air plus X kg of water vapor. The equation of the ideal gas yields:

$$\hat{V} = \frac{1}{M_{AIR}}\frac{RT}{P} + \frac{X}{M_{WATER}}\frac{RT}{P} = \left(\frac{1}{28.9} + \frac{X}{18}\right)\frac{RT}{P} \tag{5.8}$$

If the air is saturated with humidity, the volume is saturated and is obtained by replacing the absolute humidity with the humidity of saturation.

Density of humid air ρ: the relationship between the mass of humid air and the volume that it occupies:

$$\rho = \frac{m}{V} = \frac{P M_m}{RT} \tag{5.9}$$

where M_m is the mean molecular weight of the dry air and water vapor mixture:

$$M_m = X_{WATER} \cdot M_{WATER} + \left(1 - X_{WATER}\right) \cdot M_{AIR}$$

X_{WATER} is the molar fraction of the water vapor contained in the air, that is, $X_{WATER} = P_V/P$. So:

$$M_m = \frac{P_V}{P}\left(M_{WATER} - M_{AIR}\right) + M_{AIR}$$

If this expression is substituted in Equation 5.9, and considering that $P_V = \phi P_S$, the following expression is obtained:

$$\rho = \frac{P}{RT} M_{AIR} - \frac{\phi P_S}{RT}\left(M_{AIR} - M_{WATER}\right) \tag{5.10}$$

Since the molecular weight of air and of water are 28.9 and 18 kg/kmol, respectively, and the gas constant has a value of 0.082 atm·m³/(kmol·K) or 8.314 Pa·m³/(mol·K), Equation 5.10 is transformed into:

$$\rho = 352.44\frac{P}{T} - 132.93\frac{\phi P_S}{T} \tag{5.11a}$$

in which the pressures should be expressed in atmospheres, although the following equation can be used:

$$\rho = 0.0035\frac{P}{T} - 0.0013\frac{\phi P_S}{T} \tag{5.11b}$$

if the pressure is expressed in Pa. In both expressions, the density is obtained in kg/m³.

Humid specific heat $\hat{S}$: the amount of heat needed to increase by 1°C the temperature of 1 kg of dry air plus the quantity of water it contains:

$$\hat{s} = \hat{C}_{AIR} + X\hat{C}_V \tag{5.12}$$

where:

$\hat{C}_{AIR}$ = specific heat of dry air
$\hat{C}_V$ = specific heat of water vapor

In the most common processes in which air–water interactions are involved, the values of the specific heats vary a little, and mean values are taken:

$$\hat{C}_{AIR} = 1 \text{ kJ/kg} \quad \text{and} \quad \hat{C}_V = 1.92 \text{ kJ/kg °C}$$

This allows one to obtain the humid specific heat by:

$$\hat{s} = 1 + 1.92 \left(\text{kJ/kg dry air °C}\right) \tag{5.13}$$

Humid enthalpy $\hat{\imath}_G$: the enthalpy of dry air plus the enthalpy of the water vapor it contains:

$$\hat{\imath}_G = \hat{\imath}_{AIR} + X\hat{\imath}_V \tag{5.14}$$

where:

$\hat{\imath}_{AIR}$ = enthalpy of 1 kg of dry air
$\hat{\imath}_V$ = enthalpy of 1 kg of water vapor

Enthalpies are state functions; therefore it is necessary to define some reference states. Generally, the enthalpy of liquid water at 0°C and 1 atm is taken as the reference value for water, while for air the reference value corresponds to the enthalpy of dry air at 0°C and 1 atm. For water, a more adequate reference state would be the correspondence to the triple point. However, with this reference state, the water at 0°C and 1 atm has an enthalpy of 0.22 kcal/kg, and since this is a low value, in practice it is usually considered that both reference states coincide.

The enthalpy of 1 kg of dry air with an absolute humidity X and at a temperature T will be calculated by the equation:

$$\hat{i}_G = \hat{C}_{AIR}\left(T - T^*\right) + \hat{C}_V\, X\left(T - T^*\right) + \lambda_0 X$$

where:

T^* = 0°C (reference temperature)

λ_0 = 2490 kJ/kg (latent heat of vaporization for water at 0°C)

When replacing these data, an equation that allows the calculation of the humid enthalpy as a function of temperature and moisture content is obtained:

$$\hat{i}_G = \left(\hat{C}_{AIR} + \hat{C}_V X\right) T + \lambda_0 X \tag{5.15}$$

$$\hat{i}_G = \hat{s}\, T + \lambda_0 X \tag{5.16}$$

Dew temperature T_R: the temperature at which the saturation of air takes place, given the water content. That is, it is the temperature at which condensation of water vapor begins when humid air undergoes a cooling process.

Adiabatic saturation temperature T_S: the temperature at which air is saturated when it is adiabatically cooled. In this adiabatic process, the air undergoes a continuous variation of temperature and moisture content.

Humid temperature T_H: also called wet bulb temperature, the temperature reached by a small water mass under adiabatic and steady conditions, exposed to an air stream of constant temperature, moisture, and velocity (Figure 5.1).

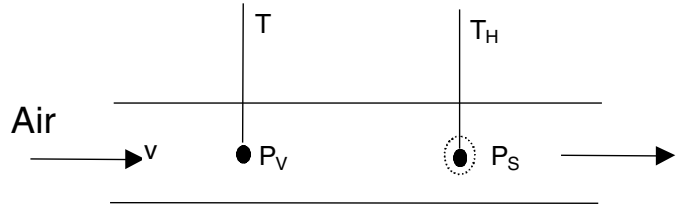

FIGURE 5.1
Humid temperature.

Humid temperature is a function of the temperature T of the air and of the humidity X. Also, from this humid temperature it is possible to determine the absolute humidity of air. In the air–water system, for air velocities between 4 and 10 m/s, the humid temperature coincides with the saturation temperature.

5.3 Mollier's Psychrometric Diagram for Humid Air

The so-called Mollier diagram for humid air is usually employed for the graphic solution of problems in which air–water interaction processes take place, such as air drying and humidification and dehumidification processes, among others. There are different types of psychrometric diagrams depending on which variables are correlated. One of the most used is the $X - T$ chart, in which the absolute humidity against temperature is represented, although the diagram showing the product of the humid specific heat times temperature against the absolute humidity ($\hat{s}T - X$ chart) is used sometimes.

5.3.1 Psychrometric Chart $\hat{s}T - X$

In this chart (see Appendix), the values of the product $\hat{s}T$ are represented in the ordinates, while the values of the absolute humidity X are represented in the abcissas (Figure 5.2). Below, the different straight lines and curves that appear in this chart will be discussed.

Isothermic straight lines: Equation 5.13 was obtained from the definition of humid specific heat. If this equation is multiplied by the temperature, the following is obtained:

$$\hat{s}T = T + 1.92\,TX \tag{5.17}$$

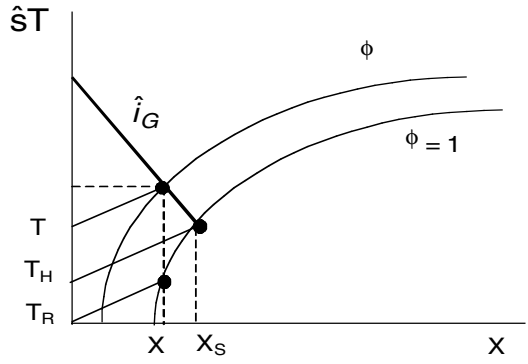

FIGURE 5.2
Psychrometric chart $\hat{s}T$ vs. X.

It can be observed that for each temperature, a straight line with slope 1.92 T and intercept to the origin T can be obtained. It is important to note that, for each temperature value, a different straight line is obtained.

Isoenthalpic straight lines: Equation 5.16 is the expression of the humid enthalpy, which, when rearranged, can be expressed as:

$$\hat{s}T = \hat{\imath}_G - \lambda_0 X \tag{5.18}$$

In the $\hat{s}T - X$ chart, this equation corresponds to the equation of a straight line with slope λ_0 and intercept to the origin $\hat{\imath}_G$. It is evident that the isoenthalpic lines are parallel straight lines, since their slope is $\lambda_0 = 2490$, but they differ in their humid enthalpy value.

Constant relative humidity curves: To obtain this set of curves it is necessary to combine Equations 5.6 and 5.17:

$$X = 0.622 \frac{P_S \phi}{P - P_S \phi} \tag{5.6}$$

$$\hat{s}T = T + 1.92\, TX \tag{5.17}$$

The procedure to follow is:

1. Fix the total pressure for which the chart is built.
2. Fix the relative humidity value.
3. Give values to the temperatures and, by means of the water vapor tables, look for the corresponding values of the vapor pressures.
4. The values of the absolute humidities are obtained, using Equation 5.6, from the different vapor pressure values and the value of the relative humidity fixed in step 2.
5. The values of the product $\hat{s}T$ are calculated, using Equation 5.17, from the temperature values and their corresponding absolute humidities.
6. When plotting the values $\hat{s}T$ against their corresponding absolute humidities X, a curve in which the relative humidity value is constant is obtained.
7. Go back to step 2, changing the relative humidity value and the process with the new value of ϕ. A new curve is obtained from the new value of relative humidity, and so on.

Out of the set of curves obtained, the lower curve corresponds to a value $\phi = 1$, i.e., the saturation curve. It is important to highlight that this curve does not cross the ordinates' origin, since for a total pressure of 1 atm and a temperature of 0°C, the vapor pressure of pure water is 610 Pa, corresponding to an absolute humidity of X = 0.00377 kg water/kg dry air.

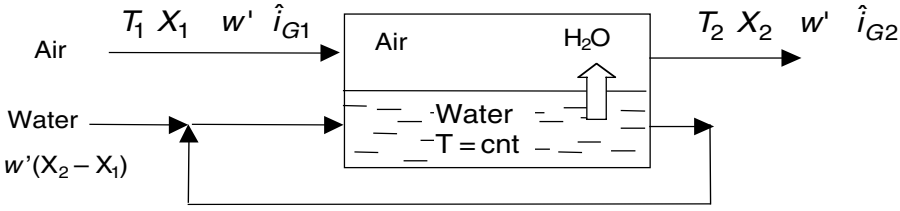

FIGURE 5.3
Adiabatic humidification of air.

Adiabatic humidification straight lines: Assume a process like the one shown in Figure 5.3, in which there is a chamber with water at a constant temperature T, with water recirculation entering the system along with the water added, reaching a temperature almost equal to the temperature of the air leaving the chamber. An air flow w' kg dry air/h with a humidity X_1, temperature T_1, and enthalpy $\hat{i}_{G1}$ is introduced into the chamber. Likewise, an air stream with humidity X_2, temperature T_2, and an enthalpy $\hat{i}_{G2}$ exists in the chamber. To compensate for the evaporated water, a water stream at temperature T and a flow $w'(X_2 - X_1)$ kg water/h is introduced into the system. Since it is an adiabatic process, there will not be heat exchange with the surroundings.

When carrying out a global energy balance of the system, one obtains:

$$w'\hat{i}_{G1} + w'\hat{C}_L\left(X_2 - X_1\right)\left(T - T^*\right) = w'\hat{i}_{G2} \tag{5.19}$$

in which $\hat{C}_L$ is the specific heat of water. If T = 0°C is taken as reference temperature and taking into account that the enthalpy is expressed according to Equation 5.16:

$$\hat{i}_G = \hat{s}\,T + \lambda_0 X \tag{5.16}$$

When substituting in Equation 5.19, one obtains:

$$\hat{s}_1 T_1 + \lambda_0 X_1 + \hat{C}_L T\left(X_2 - X_1\right) = \hat{s}_2 T_2 + \lambda_0 X_2$$

which can be rearranged as:

$$\hat{s}_2 T_2 - \hat{s}_1 T_1 = \left(\hat{C}_L T - \lambda_0\right)\left(X_2 - X_1\right) \tag{5.20}$$

In the $\hat{s}T - X$ chart, this is the equation of a straight line with a slope of $(\hat{C}_L\,T - \lambda_o)$. Generally, the value of the product $\hat{C}_L\,T$ is much smaller than

the latent heat of vaporization, so it can be neglected, and the following is obtained: $\hat{s}_2\ T_2 - \hat{s}_1\ T_1 = -\lambda_0\ (X_2 - X_1)$. If Equation 5.18 is observed, it can be seen that it corresponds to an isoenthalpic line. This indicates that adiabatic humidification straight lines coincide with isoenthalpic lines.

Nonadiabatic humidification straight lines: A process similar to the previous one is considered, but there is no water recirculation, so to maintain a constant temperature T in this water a $\dot{Q}_E$ heat flow is provided; this should compensate for heat losses by evaporation and for losses from the chamber towards the surroundings $\dot{Q}_S$.

When carrying out a global energy balance one obtains:

$$w'\hat{\imath}_{G1} + \hat{C}_L\ w'\left(X_2 - X_1\right)\left(T - T^*\right) + \dot{Q}_E = w'\hat{\imath}_{G2} + \dot{Q}_S \tag{5.21}$$

If the reference temperature is T* = 0°C, and taking into account that:

$$\hat{Q}_E = \frac{\dot{Q}_E}{w'\left(X_2 - X_1\right)} \quad \text{and} \quad \hat{Q}_S = \frac{\dot{Q}_S}{w'\left(X_2 - X_1\right)}$$

are, respectively, supplied and lost heat by the system per unit mass, then Equation 5.21 can be rearranged as:

$$\hat{Q}_E + \left(\hat{C}_L\ T - \hat{Q}_S\right) = \frac{\left(\hat{\imath}_{G2} - \hat{\imath}_{G1}\right)}{\left(X_2 - X_1\right)}$$

Defining $\hat{Q}_0 = \hat{C}_L\ T - \hat{Q}_S$ and taking into account Equation 5.16:

$$\hat{Q}_E + \hat{Q}_0 = \lambda_0 + \frac{\hat{s}_2\ T_2 - \hat{s}_1\ T_1}{X_2 - X_1}$$

or

$$\hat{s}_2 T_2 - \hat{s}_1 T_1 = \left(\hat{Q}_E + \hat{Q}_0 - \lambda_0\right)\left(X_2 - X_1\right) \tag{5.22}$$

which, in the $\hat{s}T - X$ chart, corresponds to the equation of a straight line with slope $(\hat{Q}_E + \hat{Q}_0 - \lambda_0)$ that passes through points with coordinates $(\hat{s}_1 T_1,\ X_1)$ and $(\hat{s}_2 T_2,\ X_2)$.

The quantity $(\hat{Q}_E + \hat{Q}_0)$ represents the amount of heat that should be supplied per kg of evaporated water. This is the heat required to carry out the described process; it is obtained from the slope of the straight line that connects the points representing the states of the air at the entrance and exit of the system.

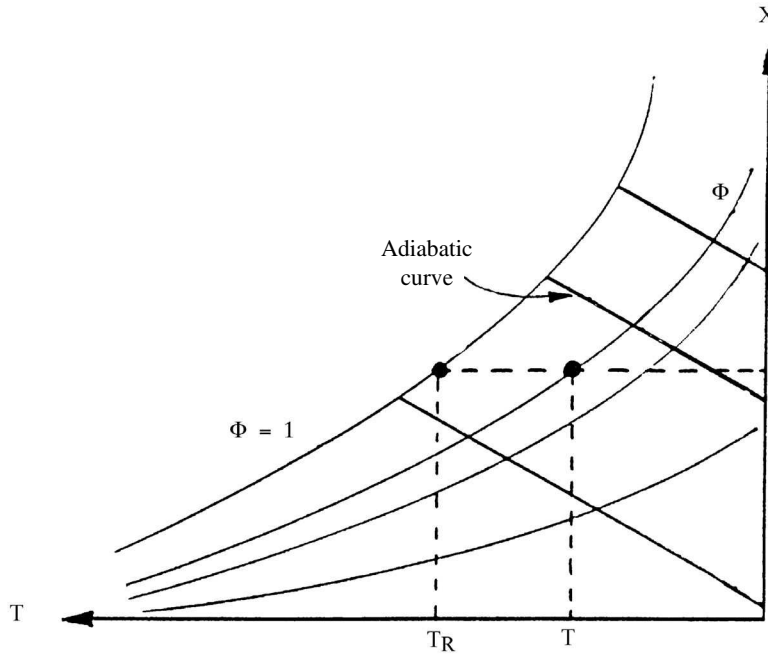

FIGURE 5.4
Psychrometric chart X vs. *T*.

5.3.2 Psychrometric Chart *X – T*

This diagram is the representation of the equations obtained in Section 5.2. In this chart the absolute humidity is represented in the ordinates vs. the temperature in the abscissas (Figure 5.4).

The curves of constant relative humidity are plotted in analog form as the $\hat{s}T - X$ chart. For a total pressure *P*, a relative humidity value is fixed. The values of the water vapor pressures at different temperatures are determined and, by means of Equation 5.6, the corresponding absolute humidities are calculated at these temperatures. Different curves are obtained with different relative humidity values. The upper curve corresponds to the saturation curve ($\phi = 1$). This curve divides the diagram into two zones; the points placed to the left of the curve represent mixtures of air and liquid water and are unstable fogs of air and water vapor. The points placed to the right of the saturation curve are air–water vapor reheated mixtures.

In the $X - T$ chart, the isoenthalpic lines and, consequently, the adiabatic cooling ones as observed in Equation 5.16 are straight lines of negative slope $-\hat{s}/\lambda_0$.

5.4 Wet Bulb Temperature

When a nonsaturated air stream circulates by a water surface, there is a heat transfer from air to water, which causes water evaporation. The water vapor is incorporated into the air. Evaporation causes a decreasing water temperature, whereas air gets closer to saturation conditions. At the end, a steady state is reached in which the heat transfer from the air to water equilibrates with the heat required to evaporate the water. Under these steady conditions, the water is at the wet bulb temperature.

This process is similar to the one described next. Consider a nonsaturated air stream humidity such that its vapor pressure (P_V) is smaller than its saturation pressure. A thermometer measures the temperature T_1 of this air, and another thermometer's bulb is surrounded by a water droplet, as shown in Figure 5.5. The air around the second thermometer is considered to be saturated, i.e., the vapor pressure is that of saturation (P_S). Since the vapor pressure of the air is smaller than the saturation pressure ($P_V < P_S$), water evaporates to the surroundings of the water droplet, causing a decrease in temperature. Therefore, the second thermometer will show a reading T_H lower than T_1 ($T_H < T_1$). T_H is called the wet bulb temperature, while T_1 is called dry bulb temperature.

The flux of evaporated water is:

$$w_{water} = K_G A_G \left(P_S - P_V\right) \tag{5.23}$$

where:

K_G = mass transfer coefficient kg/(m²·s·Pa)
A_G = area of the water droplet

The heat needed to evaporate the water is the latent heat:

$$\dot{Q}_L = \lambda_S w_{WATER} = \lambda_S K_G A_G \left(P_S - P_V\right) \tag{5.24}$$

in which λ_S is the latent heat of vaporization at the temperature of water.

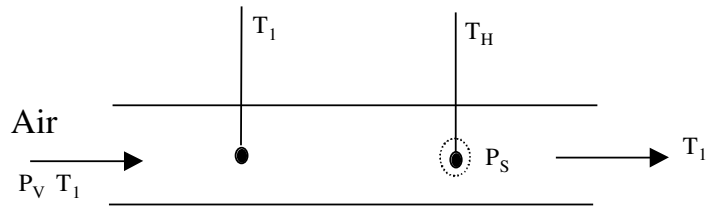

FIGURE 5.5
Welt bulb temperature.

Heat is transferred from the air to the water droplet by radiation and convection mechanisms in such a way that they can be calculated according to the expression:

$$\dot{Q}_S = \left(h_C + h_R\right) A_G \left(T_1 - T_H\right) \tag{5.25}$$

in which h_C and h_R are the heat transfer coefficients by convection and radiation, respectively.

When steady conditions are reached, an equilibrium exists in which the heat transferred from the air to the droplet is equal to the heat required for evaporation:

$$\left(\dot{Q}_L = \dot{Q}_S\right): \quad \lambda_S K_G A_G \left(P_S - P_V\right) = \left(h_C + h_R\right) A_G \left(T_1 - T_H\right)$$

from which the following is deduced:

$$P_S - P_V = -\frac{\left(h_C + h_R\right)}{\lambda_S K_G} \left(T_H - T_1\right) \tag{5.26}$$

This equation is called the psychrometric equation.

In this equation, the heat transfer coefficient by convection h_C, as well as the mass transfer coefficient K_G, depends on the thickness of the gas film. Therefore, an increase in the air velocity causes a decrease of this film and an increase in the values of h_C and K_G. For air velocity values from 5 to 8 m/s, and usual work temperatures, the heat transmitted by convection is much higher than by radiation, so it can be considered that the relation $(h_C + h_R)/K_G$ is practically constant. Under these conditions it is considered that

$$\frac{h_C + h_R}{\lambda_S K_G} = 66\, Pa/°C$$

The wet bulb temperature T_H depends only on the temperature and humidity of the air.

If, in Equation 5.6, which gives the absolute humidity as a function of the vapor pressure, one considers that this pressure P_V is very small in comparison to the total pressure and that it is worked at P = 1 atm, the following can be obtained:

$$X = 0.622\, P_V, \text{ giving } P_V \text{ in atm,}$$

or

$$X = 0.00614\, P_V, \text{ if pressure is given in kPa}$$

When substituting this equation in the psychrometric equation, the following is obtained:

$$\frac{X_S - X_1}{T_H - T_1} = -\frac{0.00614(h_C + h_R)}{\lambda_S K_G} \tag{5.27}$$

This equation relates dry and wet bulb temperatures to air humidity.

5.5 Adiabatic Saturation of Air

In air–water interaction adiabatic processes it is important to determine the conditions of air after its contact with water. Consider a process like the one shown in Figure 5.6, in which an air stream of w' kg of dry air and with temperature, humidity, and enthalpy T_1, X_1, and $\hat{\imath}_{G1}$, respectively, is introduced into a chamber with water at a saturation temperature T_s. If the contact time is sufficiently long, and if the air is sprinkled with water, then the air stream leaving the chamber exits at saturation conditions T_S, X_S, $\hat{\imath}_{GS}$. To compensate for water losses incorporated into the air by evaporation, a water flow equal to $w_L = w'(X_S - X_1)$ at temperature T_S is added continuously.

An energy balance of the system yields the equation:

$$w_L \hat{C}_L \left(T_S - T^*\right) + w' \hat{\imath}_{G1} = w' \hat{\imath}_{GS}$$

in which the reference temperature is $T^* = 0°C$.

The enthalpy is a function of temperature and moisture content, according to Equation 5.16, so:

$$w' \hat{C}_L T_S \left(X_S - X_1\right) + w' \left(\hat{s}_1 T_1 + \lambda_0 X_1\right) = w' \left(\hat{s}_S T_S + \lambda_0 X_S\right)$$

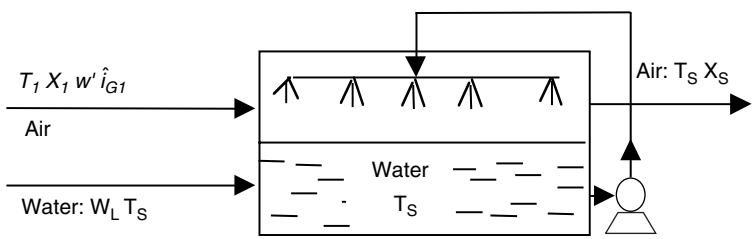

FIGURE 5.6
Adiabatic saturation of air.

The liquid water that evaporates and is incorporated into the air does so at saturation temperature T_S. The humid specific heat at temperature T_S is given by:

$$\hat{s}_S = \hat{s}_1 + \hat{C}_L\left(X_S - X_1\right) \tag{5.28}$$

hence:

$$\hat{C}_L T_S\left(X_S - X_1\right) + \hat{s}_1 T_1 + \lambda_0 X_1 = \hat{s}_1 T_S + \hat{C}_V\left(X_S - X_1\right) T_S + \lambda_0 X_S$$

which, rearranged, is:

$$\left(X_S - X_1\right)\left[\hat{C}_L T_S - \hat{C}_V T_S - \lambda_0\right] = \hat{s}_1\left(T_S - T_1\right)$$

Since the latent heat of evaporation at the saturation temperature T_S is given by:

$$\lambda_S = \lambda_0 + \hat{C}_V T_S - \hat{C}_L T_S \tag{5.29}$$

it is obtained that:

$$X_S - X_1 = -\frac{s_1}{\lambda_S}\left(T_S - T_1\right) \tag{5.30}$$

which is an equation that allows the calculations in adiabatic saturation processes as in functions of the absolute humidity and temperature.

If Equations 5.30 and 5.27 are compared, it can be observed that the adiabatic saturation temperature coincides with that of the wet bulb temperature ($T_S = T_H$) for a total pressure of 101.3 kPa (1 atm) and specific heat given by:

$$\hat{s}_1 = 0.00614\frac{\left(h_C + h_R\right)}{K_G} \tag{5.31}$$

an expression known as the Lewis relation.

From the last comparison, the following psychrometric relation is obtained:

$$b = 0.00614\,\frac{\left(h_C + h_R\right)}{K_G s_1} \tag{5.32}$$

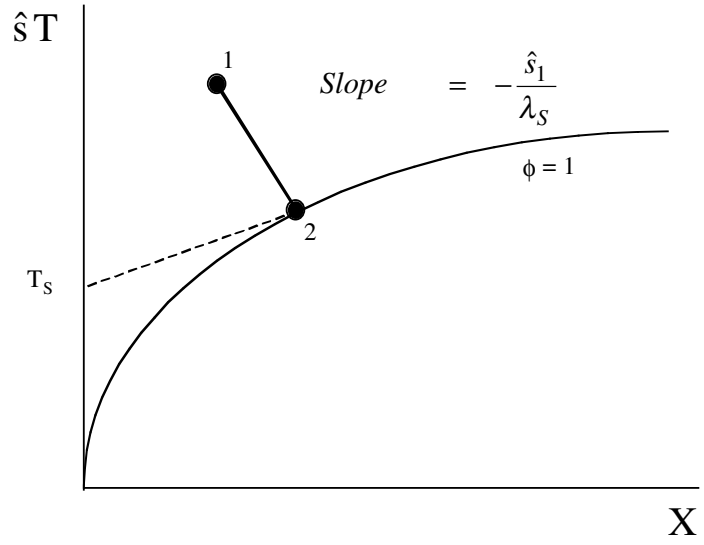

FIGURE 5.7
Adiabatic saturation process for air.

which for the air–water system has a value of 1 kJ/(kg·°C). For other gas–liquid systems this psychrometric relation is greater than one ($b > 1$); also, the wet bulb temperature is higher than the saturation temperature.

In the $\hat{s}T - X$ chart, the conditions of air at the entrance of the chamber are given by point 1 (Figure 5.7). The conditions at the exit point are obtained when drawing a straight line with slope $-\hat{s}/\lambda_S$, whose intersection with the saturation curve (point 2) gives precisely the conditions of the air that leaves the chamber.

Without a psychrometric chart, the adiabatic saturation temperature can be obtained by means of an iterative process, consisting of the following steps:

1. A saturation temperature T_S is supposed.
2. The latent heat λ_S and saturation vapor pressure P_S are calculated according to the above temperature.
3. The corresponding saturation humidity X_S is calculated using Equation 5.30.
4. The saturation humidity X'_S is calculated with Equation 5.4.
5. The saturation humidities X_S and X'_S calculated in steps 3 and 4 are compared. If the values coincide, the calculation is assumed to be complete. On the other hand, if the values do not coincide, a new value of the saturation temperature is taken, beginning again with step 1.

Problems

5.1

Humid air has a dry bulb temperature of 75ºC and a wet bulb temperature of 45ºC. Calculate its absolute and relative humidity, as well as its density.

Solutions

From the psychrometric Equation 5.26, as indicated before, under usual work conditions it is considered that this equation can be expressed as:

$$P_S - P_V = -66\left(T_H - T_1\right)$$

if pressure is given in Pa and temperature in ºC.

For the dry bulb temperature of 75ºC, the saturation pressure is obtained from the saturated water vapor tables (P_V = 38.5 kPa), from which the absolute humidity can be obtained using Equation 5.3:

$$X = 0.622\ \frac{P_V}{P - P_V} = 0.622\ \frac{38.5}{101.23 - 38.5} = 0.382 \frac{\text{kg water}}{\text{kg dry air}}$$

A saturation pressure of 9.8 kPa corresponds to the temperature of 45ºC, from which a saturation humidity X_S = 0.067 kg water/kg dry air is obtained.

Applying the psychrometric equation, $P_V - 9800 = 66\,(75 - 45)$, so P_V = 7820 Pa. The absolute humidity can be determined from this pressure and Equation 5.3:

$$X = 0.622\ \frac{P_V}{P - P_V} = 0.622\ \frac{7.82}{101.23 - 7.82} = 0.052\ \frac{\text{kg water}}{\text{kg dry air}}$$

The relative humidity is obtained from Equation 5.5:

$$\phi = \frac{P_V}{P_S} = \frac{7820\ \text{Pa}}{38500\ \text{Pa}} = 0.20\ (20\%)$$

The humid specific volume is calculated by Equation 5.8, in which the absolute humidity is 0.052 kg water/kg dry air, the temperature is 348 K, and the total pressure is 101.23 kPa, while the constant R is 8.314 × 10^3 Pa·m^3/(kmol·K). With these values a humid volume value of dry air/kg is obtained. Hence, the density will be the inverse of this value:

$$\frac{1}{1.072} = 0.933\ \frac{\text{kg}}{\text{m}^3}$$

The density can be calculated from Equation 5.11b:

$$\rho = 0.0035\,\frac{101230}{348} - 0.0013\,\frac{(0.2)(38500)}{348} = 0.989\ \text{kg/m}^3$$

5.2

A room is kept at a temperature of 21°C by means of a radiator, while the outside temperature is 15°C, with a corresponding wet bulb temperature at 10°C. Calculate the absolute humidity, water vapor pressure, relative humidity, dew temperature, and adiabatic saturation temperature of the air contained in the room.

With the temperatures T_1 = 15°C and T_H = 10°C, it is possible to locate point 1 in the psychrometric chart (Figure 5.P2). When the room is warmed to 21°C, new air conditions are obtained, represented by point 2 in the same chart.

Point 2 is obtained from point 1, by moving up at constant absolute humidity until reaching the 21°C isotherm. The absolute humidity will not vary, since the kg water/kg dry air is constant.

The values asked for in the problem can be obtained from the psychrometric chart:

Absolute humidity:	X = 0.0056 kg water/kg dry air
Relative humidity:	ϕ = 0.37 (37%)
Dew temperature:	T_R = 5.2°C
Adiabatic saturation temperature:	T_S = 12.8°C

The vapor pressure is calculated from Equation 5.3, in which the values of the different variables (X = 0.0056 kg water/kg dry air, P = 101.23 kPa) are substituted to obtain the vapor pressure P_V = 903 Pa.

5.3

The temperature in a warehouse is 30°C and the dew point temperature is 12°C of the air contained in that warehouse. Calculate: (a) the relative humidity that the air will have if it is cooled to 16°C, and (b) the amount of water that will be eliminated from 570 m^3 of air under the indicated conditions if it is cooled to 2°C.

In the psychrometric chart, point 1 (Figure 5.P3) represents the conditions of the air in the warehouse, with T_1 = 30°C and T_R = 12°C and an absolute humidity content of X_1 = 0.0087 kg water/kg dry air. When cooling this air to 16°C, the absolute humidity will not vary ($X_2 = X_1$). Therefore, point 2 is obtained when the vertical straight line of constant absolute humidity X_2 intersects the 16°C isotherm.

This intersection for point 2 corresponds to a relative humidity curve ϕ_2 = 0.77 (77%).

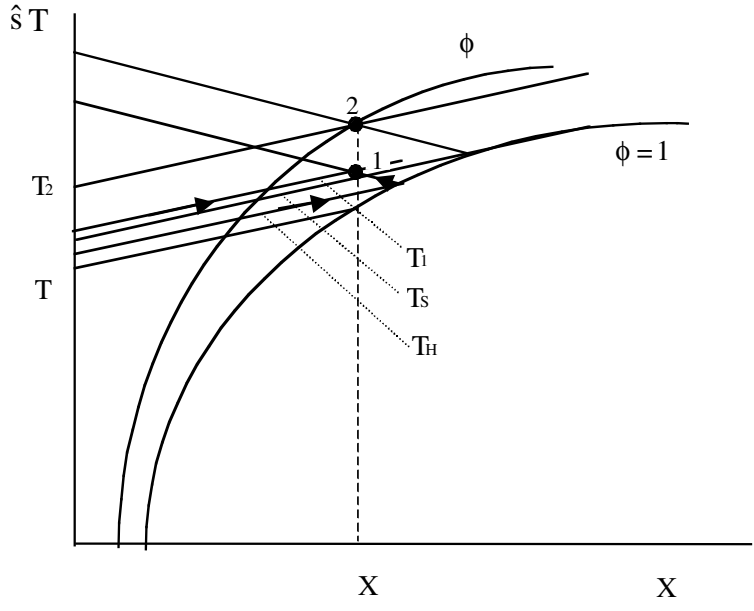

FIGURE 5.P2
Problem 5.2.

The value of this relative humidity could be analytically obtained. Initially, the absolute humidity is calculated from Equation 5.3, using the vapor pressure obtained from water vapor tables for T_R = 12ºC, being P_V = 1390 Pa. These values are substituted in Equation 5.3:

$$X_1 = 0.622 \frac{1.39 \times 10^3}{\left(101.23 - 1.39\right) \times 10^3} = 0.00866 \ \frac{\text{kg water}}{\text{kg dry air}}$$

From water vapor tables, the saturation pressure for 16ºC is P_S = 1832 Pa. Since absolute humidity X_2 is the same as X_1, it is possible to determine the relative humidity from Equation 5.6.

$$0.0087 = 0.622 \frac{1.83 \times 10^3 \, \phi}{\left(101.23 - 1.83 \, \phi\right) \times 10^3}$$

Hence, the relative humidity for the conditions of point 2 is ϕ_2 = 0.76 (76%).

To calculate the kg of water condensed when the temperature decreases to 2ºC, absolute humidities at 16ºC (X_3) and at 2ºC (X_4) are previously determined. The difference (X_3 – X_4) gives the amount of water eliminated per each kg of dry air. Therefore, the kg of dry air contained in the 570 m^3 of humid air is calculated first.

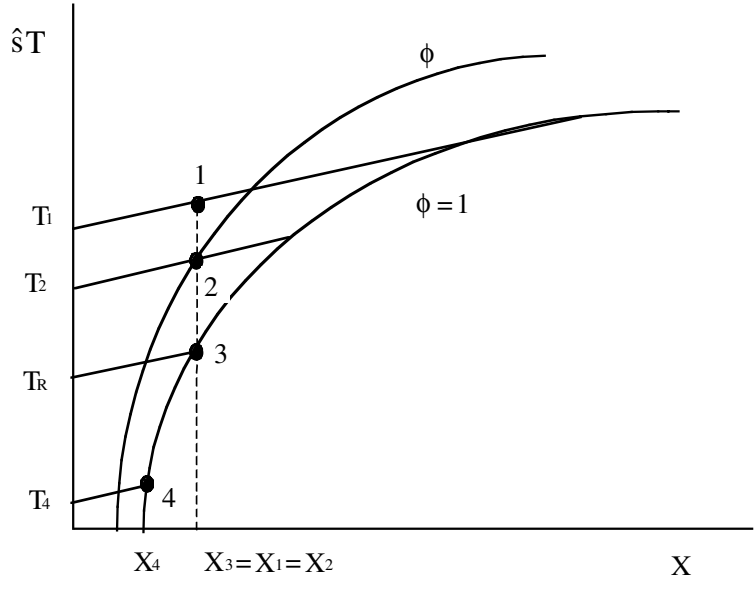

FIGURE 5.P3
Problem 5.3.

The humid volume occupied by 1 kg of dry air at 30ºC is calculated from Equation 5.8:

$$\hat{V} = \left(\frac{1}{28.9} + \frac{0.0087}{18} \right) \frac{\left(8.314 \times 10^3\right)\left(303\right)}{101.23 \times 10^3} = 0.873 \frac{\text{m}^3 \text{ humid air}}{\text{kg dry air}}$$

So, the kg of dry air contained in the 570 m^3 of air will be:

$$570 \text{ m}^3 \text{ humid air} \frac{1 \text{ kg dry air}}{0.873 \text{ m}^3 \text{ humid air}} = 653 \text{ kg dry air}$$

The absolute humidity of point 3 coincides with that of points 1 and 2, while the absolute humidity of point 4 is obtained from the psychrometric chart:

$$X_3 = X_1 = X_2 = 0.0087 \text{ kg water/kg dry air}$$

$$X_4 = 0.0042 \text{ kg water/kg dry air}$$

This allows one to calculate the water eliminated when the air is cooled to 2ºC as:

$$653 \text{ kg dry air } (0.0087 - 0.0042) \frac{\text{kg water}}{\text{kg dry air}} = 2.94 \text{ kg water}$$

5.4

The atmospheric pressure of a July day was 1 atm, the temperature of the air was 32ºC, and its relative humidity was 30%. Determine: (a) the amount of water contained in the air in a 162 m^3 room; (b) the weight of the air–water vapor mixture found in the room; explain (c) why the eggs "sweat" when taken out of the refrigerator (the temperature inside the refrigerator was 8ºC); and (d) calculate the absolute humidity of the air in the room, once saturated, if it was isothermally humidified.

(a) For the temperature T_1 = 32ºC and a relative humidity ϕ = 0.3, point 1 can be fixed in the psychrometric chart corresponding to an absolute humidity of X_1 = 0.0088 kg water/kg dry air. The wet volume can be calculated from Equation 5.8.

$$\hat{V} = \left(\frac{1}{28.9} + \frac{0.0088}{18} \right) \frac{\left(8.314 \times 10^3\right)\left(305\right)}{101.23 \times 10^3} = 0.879 \ \frac{\text{m}^3 \text{ humid air}}{\text{kg dry air}}$$

Since the volume of the room is 162 m^3, and it is humid air, the amount of dry air in the room will be:

$$162 \text{ m}^3 \text{ humid air} \ \frac{1 \text{ kg dry air}}{0.879 \text{ m}^3 \text{ humid air}} = 184.3 \text{ kg dry air}$$

The amount of water in the room can be calculated multiplying this value by the absolute humidity of the air:

$$\left(184.3 \text{ kg dry air}\right) 0.0088 \ \frac{\text{kg water}}{\text{kg dry air}} = 1.622 \text{ kg water}$$

(b) The weight of the air–water mixture is the sum of the values obtained in the last section:

184.3 kg dry air + 1.62 kg water = 185.92 kg humid air

(c) From the psychrometric chart, for T_1 = 32ºC and ϕ = 0.3, the absolute humidity is X_1 = 0.0088 kg water/kg dry air. For this absolute humidity (X_1) and for a relative humidity ϕ = 1, point 3 can be obtained where the 12.3ºC isotherm crosses; that is, the corresponding dew point temperature is T_R = 12.3ºC. Therefore, when cooling the egg to 8ºC, $T_{EGG} < T_R$, water will condense on the surface of the egg.

(d) When air is isothermally humidified until saturation, in the psychometric chart the 32ºC isotherm is followed to go from point 1 to point 2. Hence, the conditions of point 2 are T_2 = 32ºC and ϕ_2 = 1. The correspondent

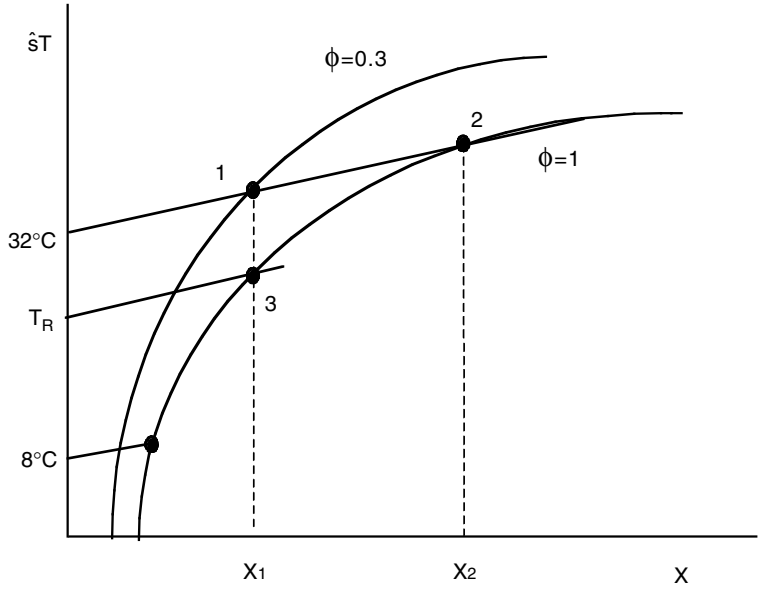

FIGURE 5.P4
Problem 5.4.

abscissa to point 2 is the value of the absolute humidity of the air under these new conditions: X_2 = 0.030 kg water/kg dry air.

5.5

In a dryer, 100 kg/h of water are eliminated from a wet material, using an air stream at 24ºC with an absolute humidity of 0.01 kg water/kg dry air. This air is heated to 69ºC before entering the dryer. At the exit of the dryer there is a thermometer indicating a dry bulb temperature of 54ºC and a wet bulb temperature of 38ºC. a) Determine the consumption of air. b) At the entrance of the dryer the water in the material is at 24ºC, while the vapor that leaves the dryer is at 54ºC. Calculate the heat flow rate that should be supplied to the dryer. Determine, as well, the heat that should be supplied to the preheater.

All the transformations undergone by the air through all the process can be represented in the psychrometric chart (Figure 5.P5). Initially the air has a temperature T_1 = 24ºC, and absolute humidity X_1 = 0.01 kg water/kg dry air, which allows one to determine point 1. In the heater, the air increases its temperature to T_2 = 69ºC, although its absolute humidity remains the same ($X_2 = X_1$), determining in this way point 2. The conditions of the air that leaves the dryer are T_H = 38ºC and T_3 = 54ºC, so point 3 is obtained by drawing the isotherm that passes at 38ºC, when this isotherm intersects the curve ϕ = 1. Then the isoenthalpic is plotted, and the intersection of the

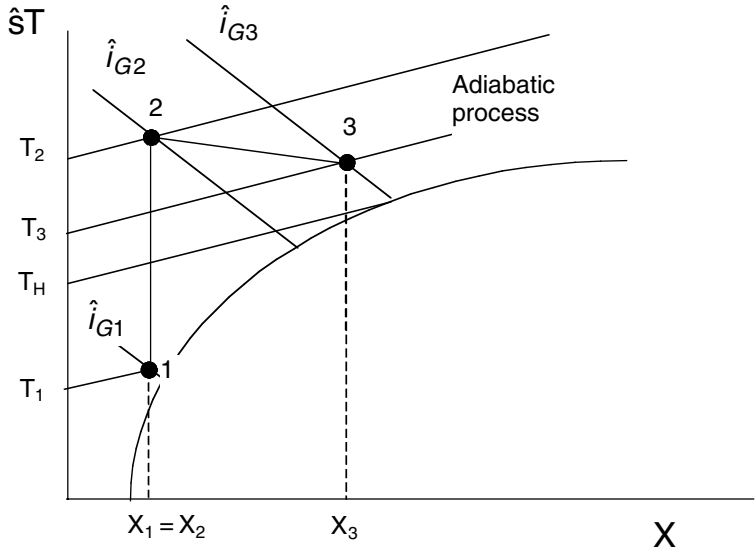

FIGURE 5.P5
Problem 5.5.

isoenthalpic line with the 54ºC isotherm allows one to determine point 3, with a corresponding absolute humidity of X_3 = 0.0375 kg water/kg dry air.

(a) If the flow of dry air that circulates throughout the process is w', from a water balance in the dryer the following is obtained:

$$w'\left(X_3 - X_2\right) = 100 \text{ kg evaporated water/h}$$

$$w' = \frac{100 \text{ kg evaporated water/h}}{\left(0.0375 - 0.01\right) \text{ kg water/kg dry air}} = 3636.36 \text{ kg dry air/h}$$

The humid air flow rate entering the heater is the same that leaves it, that is:

$$w_1 = w_2 = w'\left(1 + X_2\right) = \left(3636.36 + 0.01\right) = 3672.73 \text{ kg humid air/h}$$

(b) It is assumed that the dry material leaves the dryer at a temperature of 24ºC, so the enthalpy associated with this material coincides at the entrance and exit of the dryer. The reference temperature in this case is T^* = 0ºC. If $\dot{Q}_S$ is the heat flow to the dryer, the following is obtained when an energy balance is performed:

$$\dot{Q}_S + w'\hat{i}_{G2} + w_{WATER}\hat{C}_P T_{WATER} = w'\hat{i}_{G3}$$

The enthalpies $\hat{i}_{G2}$ and $\hat{i}_{G3}$ are obtained from the psychrometric chart, and their values are:

$$\hat{i}_{G2} = 95.42 \text{ kJ/kg}$$
$$\hat{i}_{G3} = 151.5 \text{ kJ/kg}$$

When substituting the data in the last equation, the following is obtained:

$$\dot{Q}_S + (3636.36)(95.42) + (100)(4.18)(21) = (3636.36)(151.5)$$
$$\dot{Q}_S = 1.95 \times 10^5 \text{ kJ/h} = 54.2 \text{ kW}$$

If $\dot{Q}_C$ is the heat flow supplied to the heater, from an energy balance one obtains:

$$Q_C = w(i_{G2} - i_{G1})$$

The value of $\hat{i}_{G1}$ is obtained from the psychrometric chart: $\hat{i}_{G1}$ = 49.38 kJ/kg. This value could also be obtained from Equations 5.13 and 5.16:

$$\hat{s} = 1 + 1.92\, X_1 = 1 + 1.92(0.01) = 1.0192 \text{ kJ/(kg} \cdot \text{°C)}$$
$$\hat{i}_G = \hat{s}T + \lambda_0 X_1 = (1.0192)(24) + (2490)(0.01) = 49.36 \text{ kJ/kg}$$

Hence, the heat supplied to the air in the heater will be:

$$\dot{Q}_C = (3636.36)(95.42 - 49.36) = 167490 \text{ kJ/h}$$
$$\dot{Q}_C = 167490 \text{ kJ/h} = 46.5 \text{ kW}$$

6

Rheology of Food Products

6.1 Introduction

Rheology is the science that studies the flow and deformations of solids and fluids under the influence of mechanical forces. To study the rheological behavior of different products, it is necessary to resort to rheometry, which permits knowledge of such behavior and its use in different industry fields. Thus, the rheological measures of a product in the manufacture stage can be useful in quality control. The microstructure of a product can also be correlated with its rheological behavior, allowing development of new materials. Rheometry permits attainment of rheological equations applied in process engineering, particularly unit operations that involve heat and momentum transfer. Finally, knowing the demands of consumers, it is possible to obtain a product that complies with these requirements.

Food industries frequently work with products in a liquid phase in all or some of the industrial operations performed on them (e.g., concentration, evaporation, pasteurization, pumping). Good design of each type of equipment is essential for optimum processing. In the design of every process it is necessary to know the physical characteristics of the streams that form it. One of those characteristics is the rheological behavior of the fluid to be processed, which must be known in order to avoid oversized pumps, pipes, evaporators, etc. that can have negative repercussions on the economy of the process.

Viscosity is used in the calculation of parameters of momentum and energy transport phenomena, as well as in the quality control of some products. For this reason, the rheological constants of processed fluids intervene in the equations of the mathematical model set up for the diverse operations that form a determined process. Such rheological constants should be determined, generally, by means of experimentation in each particular case. Thus, the rheological characterization of the different fluid streams is very important, as is the deduction of the equations that allow direct calculation of the rheological constants as a function of the food considered and the operation variables.

Foods in the liquid phase used in the industrial process or by the consumer include pastes, purées, soft drinks, egg products, milk products, natural fruit juices, and vegetable concentrates and sauces, among others.

6.2 Stress and Deformation

When a force is applied to a body, the observed response is different depending on the material. Thus, when the force is applied to an elastic solid, it deforms, but, when the force stops acting, the solid recovers its initial shape. However, if the product is a Newtonian fluid, when the force stops acting, the fluid continues flowing.

The stress (σ) applied to a material is defined as the force (F) acting per unit area (A). The stress can be normal and tangential. Included in the normal stresses are those of tension and compression. Consider a body, as shown in Figure 6.1. It can be observed that three stresses can be applied on each side of the body, one for each direction. Therefore, there will be nine components of stress, and each one will be named with two subindexes. The first subindex

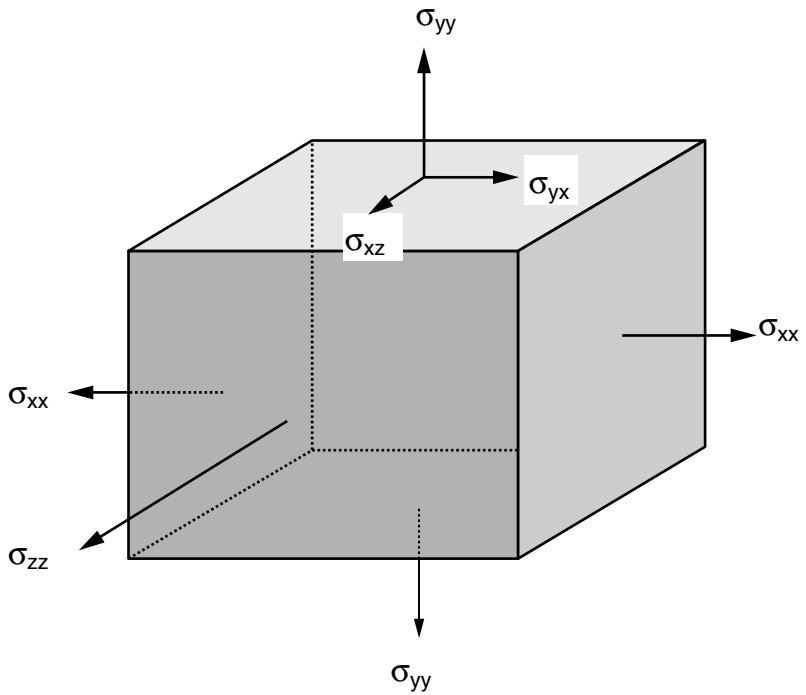

FIGURE 6.1
Stresses on a material.

refers to the section on which it is applied, and the second refers to the direction. Thus, σ_{ij} is a stress applied on section i in the j direction. The nine components of the stress define the stress tensor:

$$\sigma_{ij} = \begin{pmatrix} \sigma_{11} & \sigma_{12} & \sigma_{13} \\ \sigma_{21} & \sigma_{22} & \sigma_{22} \\ \sigma_{31} & \sigma_{32} & \sigma_{33} \end{pmatrix} \tag{6.1}$$

The stress tensor is symmetric, which implies that $\sigma_{ij} = \sigma_{ji}$. Therefore, of the nine components of the stress vector, only six are independent.

The tangential stresses are those in which $i \neq j$, while in the normal stresses $i = j$. The normal tension stresses are positive ($\sigma_{ii} > 0$), while those of compression are negative ($\sigma_{ii} < 0$).

All stresses applied to a material produce a deformation. Deformations can be angular or longitudinal depending on the type of stress applied. Normal stresses cause longitudinal deformations that may be lengthening or shortening depending on whether a tension or compression stress is applied. Tangential stresses produce angular deformations.

If normal tension stress is applied to a bar with initial length L_0, it produces a lengthening of the bar in such a way that the final length is $L = L_0 + \Delta L$ (Figure 6.2). The deformation produced on this bar can be expressed as Cauchy's deformation:

$$\varepsilon_c = \frac{\Delta L}{L_0} = \frac{L}{L_0} - 1 \tag{6.2}$$

Another way to express deformation would be to use Hencky's deformation:

$$\varepsilon_H = \ln\left(L/L_o\right) \tag{6.3}$$

For large deformations, Hencky's deformation definition is preferred over Cauchy's deformation.

Another type of deformation is the simple shear. If a tangential stress is applied to the upper side of a rectangular material, a deformation will occur, as shown in Figure 6.3, where the bottom side remains still. The angle of shear γ is calculated according to the equation:

$$\tan\gamma = \frac{\Delta L}{L} \tag{6.4}$$

In the case of small deformations, the angle of shear in radians coincides with its tangent: $\tan\gamma = \gamma$, called shear strain.

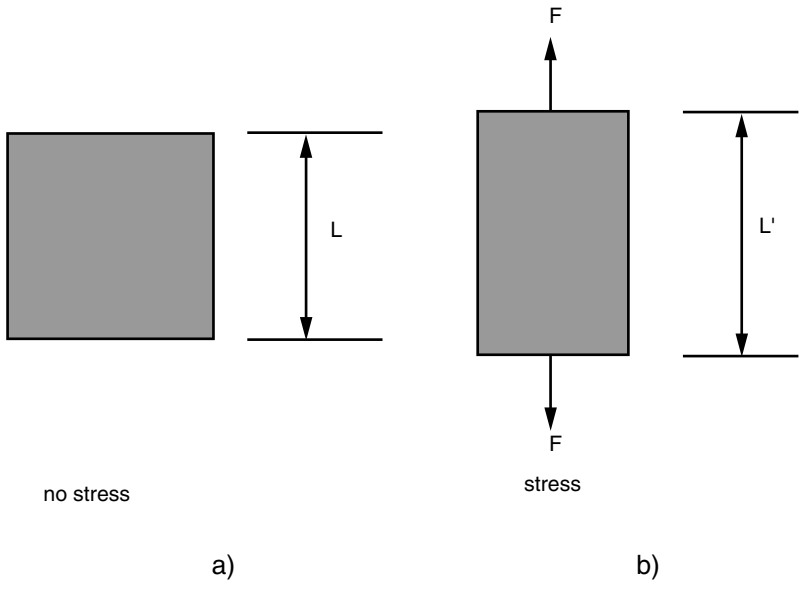

FIGURE 6.2
Deformation due to normal stress.

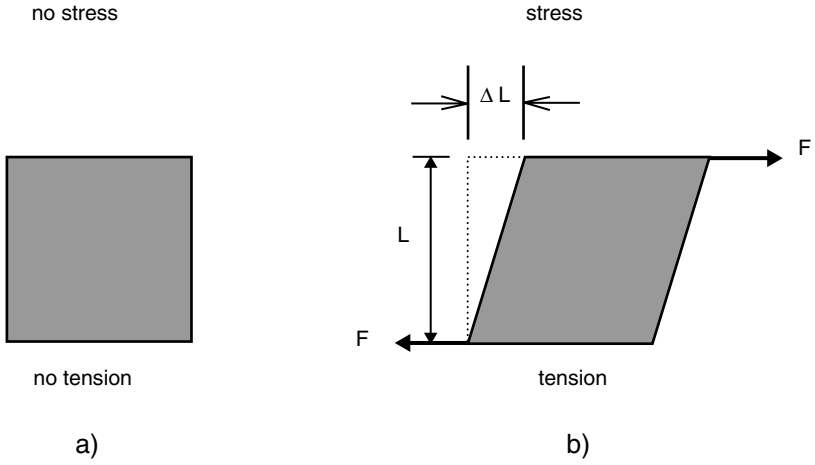

FIGURE 6.3
Shear deformation.

6.3 Elastic Solids and Newtonian Fluids

If tangential stress (σ_{ij}) is applied to a solid material, and if the relationship between the applied stress and the shear deformation or shear (γ) obtained is proportional:

$$\sigma_{ij} = G\gamma \tag{6.5}$$

then the proportionality constant G is called shear or rigidity module. This type of material is called Hooke's solid, which is linearly elastic and does not flow. The stress remains constant until the deformation is eliminated; then, the material returns to its initial form.

The behavior of Hooke's solid can also be studied by applying a normal stress (σ_{ii}) that produces a length change. The normal stress applied is directly proportional to the Cauchy's deformation:

$$\sigma_{ii} = E\varepsilon_C \tag{6.6}$$

where the proportionality constant E is denominated Young's or the elasticity module.

The elastic solids are those that deform when subjected to tensional forces but that they recover their initial shape as such forces dissappear. Solids that do not recover their original shape when the forces stop acting are known as plastic solids. Elastoplastic solids are those in between these two types; i.e., if the applied stresses are lower than a certain value, they behave as elastic solids, but once over this stress value, they can no longer recover their initial shape, behaving then as plastic solids (Figure 6.4).

To study the ideal behavior of fluids, assume a sample contained between two parallel slabs separated by a distance h, as shown in Figure 6.5, in which the lower plate remains fixed, while the upper one moves at a constant velocity v_P. At a given time, this velocity is defined as:

$$v_P = \frac{\delta x}{\delta t}$$

It is necessary to exert a force per unit area (σ_{12}) on the upper plate to keep this velocity. A velocity profile then develops along the height of the fluid, as shown in Figure 6.5. This type of flow is called simple shear. Shear rate ($\dot{\gamma}$) is defined as:

$$\dot{\gamma} = \frac{dv_P}{dy} = \frac{d}{dy}\left(\frac{\delta x}{\delta t}\right) = \frac{d}{dt}\left(\frac{\delta x}{\delta y}\right) = \frac{d\gamma}{dt} \tag{6.7}$$

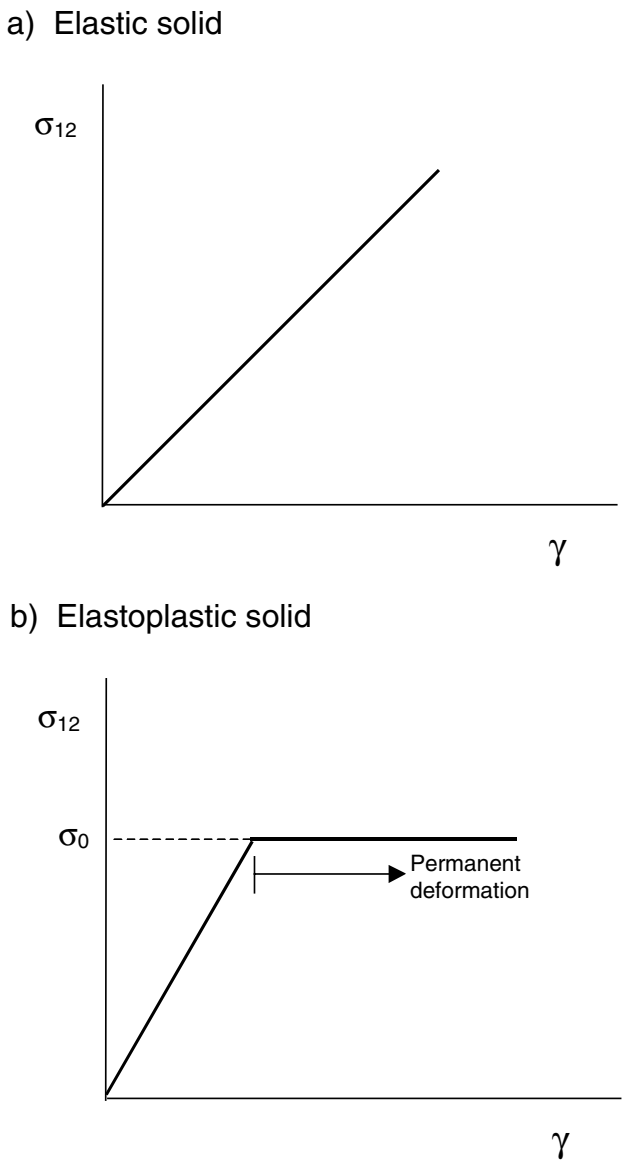

FIGURE 6.4
Deformation curves of solids.

The tangential stress applied σ_{12} and the shear rate $\dot{\gamma}$ are directly proportional, and the proportionality constant is the viscosity (η):

$$\sigma_{12} = \eta \dot{\gamma} \tag{6.8}$$

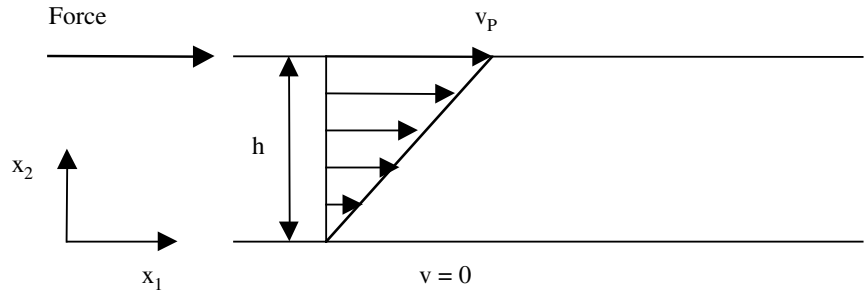

FIGURE 6.5
Velocity profile between parallel slabs.

This expression is known as Newton's law of viscosity.

In the same way that solids that obey Hooke's law of deformation are considered ideal elastic solids, fluids that follow Newton's law of viscosity are considered ideal viscous fluids.

6.4 Viscometric Functions

In order to study the flow of fluids completely, it is necessary to correlate the shear stresses and the shear rates in three dimensions. The shear stress and shear rate must be considered tensors, each of which has nine components. However, for steady state and flow in simple shear, the stress tensor is reduced to:

$$\sigma_{ij} = \begin{pmatrix} \sigma_{11} & \sigma_{12} & 0 \\ \sigma_{21} & \sigma_{22} & 0 \\ 0 & 0 & \sigma_{33} \end{pmatrix} \tag{6.9}$$

Simple shear flow is also called viscometric flow and is the type of flow that occurs in the rotational flow between concentric cylinders, axial flow in a pipe, and rotational flow between parallel plates and between plate and cone.

Only three functions are required to describe the behavior of a fluid's simple shear flow. These are the so-called viscometric functions, including the viscosity function $\eta(\dot{\gamma})$ and the first and second functions of normal stress $\psi_1(\dot{\gamma})$ and $\psi_2(\dot{\gamma})$. These functions are defined as:

$$\eta(\dot{\gamma}) = \phi_1(\dot{\gamma}) = \frac{\sigma_{12}}{\dot{\gamma}} \tag{6.10}$$

$$\psi_1(\dot{\gamma}) = \phi_2(\dot{\gamma}) = \frac{\sigma_{11} - \sigma_{22}}{(\dot{\gamma})^2} \tag{6.11}$$

$$\psi_2(\dot{\gamma}) = \phi_3(\dot{\gamma}) = \frac{\sigma_{22} - \sigma_{33}}{(\dot{\gamma})^2} \tag{6.12}$$

In some cases, the first and second differences of normal stresses are defined as:

$$N_1 = \sigma_{11} - \sigma_{22} \tag{6.13}$$

$$N_2 = \sigma_{22} - \sigma_{33} \tag{6.14}$$

Generally, N_1 is much larger than N_2, and, since the measurement of this last function is difficult, it can be assumed that its value is null.

6.5 Rheological Classification of Fluid Foods

The distinction between liquids and solids was very clear in classical mechanics and separate physical laws were promulgated to describe their behavior; the solids were represented by Hooke's law and the liquids by Newton's law. However, a variety of products exists whose behavior under flow lies between these two extremes. Such is the case for a great quantity of foods. To optimize the use of these foods in the industry, rheological characterization is required.

In a general way, a primary distinction can be made between foods with Newtonian and non-Newtonian behavior, depending on whether their rheological behavior can or cannot be described by Newton's law of viscosity. Also, the behavior of some foods depends on the time that the shear stress acted on them. Fluids for which behavior is a function only of shear stress are called time independent, and their viscosity, at a given temperature, depends on the shear rate. Time dependent fluids are those in which viscosity depends not only on the velocity gradient, but also on the time in which such gradients act. Finally, there are foods that exhibit behaviors of both viscous fluids and elastic solids, i.e., viscoelastic fluids.

The classification of fluid foods can be performed using the viscometric functions defined in the previous section. Thus, for Newtonian fluids, the viscosity function is constant, and its value is the Newtonian viscosity ($\eta(\dot{\gamma}) = \eta$ = constant). In non-Newtonian fluids, this function is not a constant and

may be time independent or dependent, which allows distinguishing between the time independent and dependent non-Newtonian fluids.

In non-Newtonian fluids, one cannot talk about viscosity, since the relationship between the applied shear stress and the shear rate is not constant. The viscosity function is called apparent viscosity, and is a function of the shear rate:

$$\eta_a = \frac{\sigma_{12}}{\dot{\gamma}} = \eta(\dot{\gamma}) \neq \text{constant} \tag{6.15}$$

The first normal stress difference (N_1) can be applied in the study of the viscoelastic behavior of the fluids that present it. In this way, a classification of fluid foods can be made according to the scheme:

- Newtonian flow
- Non-Newtonian flow
  1. Time independent behavior
     - Plastic fluids
     - Pseudoplastic fluids (shear thinning)
     - Dilatant fluids (shear thickening)
  2. Time dependent behavior
     - Thixotopic fluids
     - Antithixotopic or rheopectic fluids
- Viscoelastic behavior

6.6 Newtonian Flow

The viscous flow of a Newtonian fluid implies a nonrecoverable deformation. This behavior is illustrated in Figure 6.5, in which a fluid is contained between two parallel plates. The upper plate moves at a velocity v in relation to the bottom plate. The velocity results from the application of a stress force F per unit area. (It is assumed that the plates have an infinite extension or that the edge effects are negligible.) The layers of fluid in contact with the plates are considered to move at the same velocity as the surface with which they are in contact, assuming that no sliding of the walls takes place. The fluid behaves as a series of parallel layers, or slabs, whose velocities are proportional to the distance from the lower plate. Thus, for a Newtonian fluid, the shear stress is directly proportional to the rate at which velocity changes over distance:

$$\sigma = \frac{F}{A} = \eta \frac{dv}{dy} \tag{6.8}$$

where η is the viscosity coefficient, although generally it is simply called viscosity. It can be said that, for such fluids, the velocity gradient is equal to the shear rate, resulting in a viscosity equation more frequently used as:

$$\sigma = \eta \dot{\gamma} \tag{6.8a}$$

in which $\dot{\gamma}$ is the shear rate.

Simple liquids, true solutions, solvents of low molecular weight, diluted macromolecular dispersions, polymer solutions that do not interact, and pastes with low solids content exhibit ideal Newtonian behavior.

These flow characteristics are exhibited by most beverages, including tea, coffee, beer, wines, and soft drinks. Sugar solutions are also included. Many researchers have studied the viscosity of sucrose solutions since they are often used to calibrate viscometers (Muller, 1973) (see Table 6.1). The viscosity of solutions of sugar mixtures can be easily estimated because it can be approximated by addition.

Milk, which is an aqueous emulsion of 0.0015- to 0.001-mm diameter fat globules of butter and contains around 87% water, 4% fat, 5% sugar (mainly lactose), and 3% protein (mainly casein), is a Newtonian liquid. Fernández-Martín (1972) pointed out that the viscosity of milk depends on temperature, concentration, and physical state of fat and proteins, which in turn are affected by thermal and mechanical treatments. He also found that concentrated milks are non-Newtonian liquids, and concentrated milk presents a slight dependence on shear. Skim milk is less viscous than whole milk,

TABLE 6.1

Viscosity Coefficients of Sucrose Solutions at 20°C

Sucrose %	g/100 g water	Viscosity (mPa·s)
20	25.0	2.0
25	33.2	2.5
30	42.9	3.2
35	53.8	4.4
40	66.7	6.2
45	81.8	9.5
50	100.0	15.5
55	122.2	28.3
60	150.0	58.9
65	185.7	148.2
70	233.3	485.0
75	300.0	2344.0

Source: Muller, H.G., *An Introduction to Food Rheology,* Crane, Riesak & Co., New York, 1973.

since viscosity increases with fat content. The viscosity also increases as nonfat solids increase, but neither relation is simple. The viscosity of milk decreases as temperature increases, as with most liquids.

Oils are normally Newtonian, but at very high values of shear rate they show a different behavior (referred to as pseudoplasticity). This may be due to the alignment of unit cells at high shear stresses, which can cause a decrease in internal friction (Muller, 1973). All oils have a high viscosity due to their molecular structure of long chains. The greater the length of the carbon chain of fatty acids, the greater the viscosity. Polymerized oils have a greater viscosity than nonpolymerized oils. The viscosity of oil also increases with the saturation of the double bonds of carbon atoms.

Generally, it seems that greater molecular interaction results in greater viscosity. The main constituent of castor oil is ricinoleic acid, which contains 18 carbon atoms with a hydroxyl group position 12. The hydroxyl groups form hydrogen bonds, and for this reason the viscosity of castor oil is higher than the viscosity of other similar oils.

Some fruit juices also exhibit a Newtonian flow, such as apple juice with pectin and solids up to 30°Brix and up to 50°Brix, and filtered orange juice of 10 and 18°Brix (Saravacos, 1970). This behavior was identified in the 20 to 70°C temperature range. Juices of different clarified fruits, from which pectinases were removed, such as apple, pear, and peach, presented Newtonian behavior as well (Rao et al., 1984; Ibarz et al., 1987; Ibarz et al., 1989; Ibarz et al., 1992a). A list of products that present this behavior can be found in the review paper by Barbosa–Cánovas et al. (1993).

Another important type of food that presents this behavior are syrups like honey, cereal syrups, and mixtures of sucrose and molasses.

Pryce–Jones (1953) showed that, with the exception of products based on heather (*Calluna vulgaris*) from England, "manuka" (*Leptospermum scoparium*) from New Zealand, and *Eucalyotus ficifolia* from South Africa, most syrups are Newtonian liquids (Rao, 1977).

Munro (1943) showed that the effect of temperature on the viscosity of honey presents three different states. The greatest decrease in viscosity occurs with cold honey heated to room temperature; additional heating reduces the viscosity, and heating above 30°C has practically no effect.

6.7 Non-Newtonian Flow

6.7.1 Time Independent Flow

Although most of the simple gases and liquids experimentally behave as Newtonian fluids in the laminar flow region, various systems, including emulsions, suspensions, solutions of long molecules, and fluids of macromolecular mass, approximate Newtonian behavior only at very low shear

stresses and shear rates. At higher shear levels, such systems may deviate from ideal Newtonian behavior in one or several ways, as illustrated in Figure 6.6. Here, shear stress is schematically shown as a function of the shear rate. The straight line *a* that passes through the origin and has a constant slope represents an ideal Newtonian fluid. Curve *c*, which also passes through the origin, represents a pseudoplastic fluid, or shear thinning fluid. For such materials, the viscosity coefficient is not constant, as in Equation 6.8, but is a function of the shear rate. The viscosity coefficient takes a value at each time; this quantity is known as apparent viscosity.

In a similar way, curve *b* passes through the origin and tends to a straight line near it, but, in contrast to pseudoplastic fluids, the curve is concave towards the axis of shear stress as the shear rate increases. Such materials are called dilatant fluids, or shear thickening, and generally are limited to concentrated suspensions or aqueous pastes.

Another important phenomenon linked to flow is the existence of a threshold value. Certain materials can flow under enough shearing, but do not flow if the shear stress is smaller than a particular value. This is called threshold value, or yield stress (van Wazer et al., 1963). This type of behavior is shown by different materials such as frozen tart and whipped egg yolk, among others. Once the yield stress is exceeded, the shear rate is proportional to the shear stress, as in the case of Newtonian fluids. A fluid that exhibits this behavior is denominated plastic substance or Bingham's body (see curve *d*, Figure 6.6). Materials that exhibit yield stress can also present nonlinearity in the ratio obtained when dividing the shear stress by the shear rate.

The equation for this ratio is called apparent plastic viscosity, η_{pl}, and is given by:

$$\eta_{Pl} = \frac{\sigma - \sigma_0}{\dot{\gamma}} \tag{6.16}$$

where σ_0 is the yield stress. Fluids that exhibit nonlinear flow once the yield stress is exceeded are called pseudoplastic fluids with yield stress (curve *e*, Figure 6.6).

All of these types of flow behavior are referred to as "steady state," or independent time flow (such that equilibrium is reached in a relatively short time during the experiment). The Newtonian, pseudoplastic, and dilatant fluids do not have a yield stress; therefore, they can be called liquids. However, plastic substances exhibit the properties of liquids at shear stress values higher than yield stress, so they can be classified either as liquids or solids.

To express the flow in a quantitative way and adjust the experimental data, in general, the more applied model is a power equation, or the Herschel–Bulkley model:

$$\sigma = k\,\dot{\gamma}^n + c \tag{6.17}$$

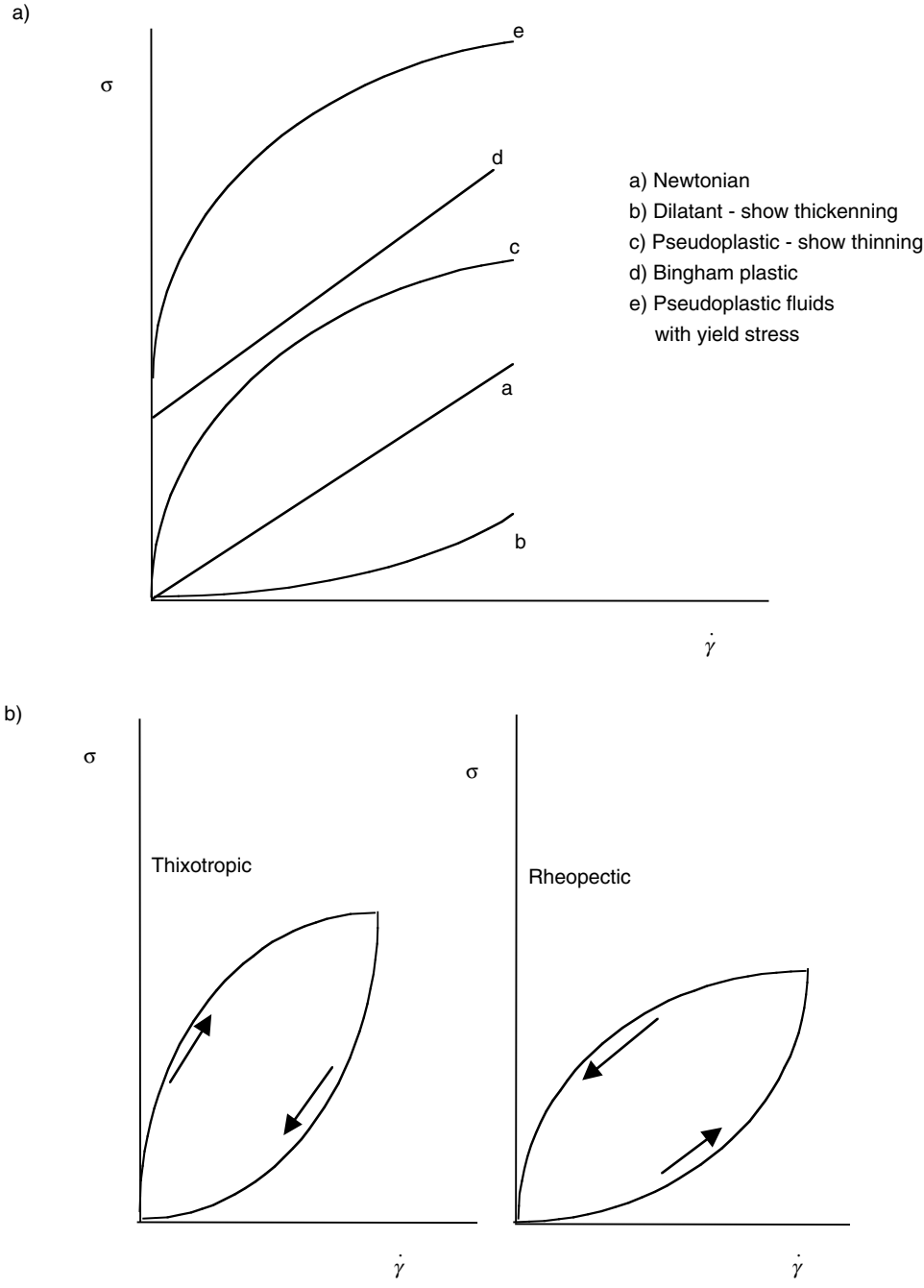

FIGURE 6.6
Rheograms of fluids: (a) time independent Newtonian and non-Newtonian; (b) time dependent non-Newtonian.

This equation includes shear stress (σ), yield stress (c), consistency index (k), shear rate ($\dot{\gamma}$) and index of flow behavior (n) and can represent Newtonian properties of Bingham's body, pseudoplastic or dilatant, depending on the value of the constants.

The dependence with respect to the shear rate points out the existence of a structure within the system. The pseudoplastic behavior indicates the continuous breakage or reorganization of structures, resulting in an increase of resistance when applying a force (Rha, 1978). The pseudoplastic behavior is due to the presence of:

1. Compounds with high molecular weight or long particles at low concentrations
2. High interaction among particles, causing their aggregation or association by secondary bonds
3. Large axial relation and asymmetry of the particles, requiring their orientation along the stream lines
4. Variation of shape and size of the particles, allowing them to pile up
5. Nonrigid or flexible particles that can suffer a change in their geometry or shape

The shear thickening behavior can be explained by the presence of tightly packed particles of different shapes and sizes making the flow more difficult as pressure increases. With an increase of the shear rate, the long and flexible particles can stretch, contributing to dilation (Rha, 1978).

A number of liquid foods exhibit a pseudoplastic behavior to flow. Scientists who have conducted investigations on this topic include Saravacos (1970), who worked with apple, grape, and commercial orange juice, Prentice (1968) with cream, Cornford et al. (1969) with melted samples of frozen whole eggs, and Tung et al. (1970) with unmixed egg white.

In general, fruit and vegetable purées are pseudoplastic fluids. The consistency of these products is an important quality parameter and is usually measured at only one point, using instruments such as the Adams and Bostwick consistometers, the Stormer viscometer, and the flow pipette (Rao, 1977). The consistency of tomato purées depends on the preparation method and the mechanical method to which samples have been subjected, as well as the variety and maturity of the tomatoes.

Harper and El Sarhigi (1965) studied the rheological behavior of tomato concentrates within total solids ranging from 5.8 to 30.0% in weight. The power model adequately describes the flow behavior of these concentrates. Watson (1968) used the power model to characterize the rheological behavior of purées and concentrates of green and ripe apricots.

The rheological properties of other fruit purées have been determined and, in each case, the power model has been used to describe the flow behavior. The products studied are apple sauce (Charm, 1960; Saravacos, 1968), banana purée (Charm, 1960), peach purée (Saravacos and Moyer, 1967; Saravacos,

1968), pear purée (Harper and Leberman, 1962; Saravacos, 1968), and sweet potato (Rao et al., 1975).

It has been found that ketchup and French mustard obey the power law of a yield stress (Higgs and Norrington, 1971). Few products exhibit a dilatant behavior such as that presented by the *Eucalyptus ficifolia*, *Eucalyptus eugenioides*, *Eucalyptus orymbosa*, and *Opuntia eugelmanni* syrups.

6.7.2 Time Dependent Flow

Some materials exhibit time dependent flow characteristics. Thus, as flow time under constant condition increases, such fluids may develop an increase or decrease in viscosity. Increase in viscosity is called rheopecticity, whereas decrease in viscosity is known as thixotropy. Both are attributed to the continuous change of the structure of the material, which may be reversible or irreversible.

The factors that contribute to thixotropy also contribute to the pseudoplasticity, and the factors that cause rheopecticity also cause shear thickening. Thixotropy is due to dependence on time, similar to dependence on shear, and it results from the structural reorganization in a decrease of the resistance to flow. Rheopectic behavior implies the formation or reorganization of the structure that brings with it increasing resistance to flow.

In other words, the phenomenological description of flow characteristics cannot be complete unless time is included, so, in the general case, an axis for time should be added to the flow curves.

Many researchers (Moore, 1959; Ree and Eyring, 1959; Peter, 1964; Cheng and Evans, 1965; Harris, 1967; Frederickson, 1970; Ritter and Govier, 1970; Joye and Poehlein, 1971; Lee and Brodkey, 1971; Mylins and Reher, 1972; Petrellis and Flumerfelt, 1973; Carleton et al., 1974; Lin, 1975; Zitny et al., 1978; Kemblowski and Petera, 1979; Barbosa–Cánovas and Peleg, 1983) have attempted the difficult task of formulating quantitative relationships among shear stress, shear rate, and time.

Cheng and Evans (1965) and Petrellis and Flumerfelt (1973) modified the equation of Herschel–Bulkley with the objective of including a structural parameter that takes into account the effects of time dependence as:

$$\sigma = \lambda\left[c + k\dot{\gamma}^{n}\right] \tag{6.18}$$

where λ is a structural parameter of time, whose value oscillates between one for time zero up to an equilibrium limit value, λ_e that is smaller than one.

According to Petrellis and Flumerfelt (1973), the decrease in the value of the structural parameter λ with time is supposed to obey a kinetics equation of second order:

$$\frac{d\lambda}{dt} = -k_1\left(\lambda - \lambda_e\right)^2 \quad \text{for } \lambda > \lambda_e \tag{6.19}$$

in which the velocity constant, k_1, is a function of the shear rate, which should be determined in an experimental way.

The determination of the kinetic constant k_1 of Equation 6.19 as a function of the shear rate is difficult because the structural parameter λ cannot be obtained in an explicit form from experimental measurements. To overcome this difficulty, the instant and equilibrium structural parameters, λ and λ_e, respectively, are expressed in terms of the apparent viscosity:

$$\frac{d\eta}{dt} = -a_1\left(\eta - \eta_e\right)^2 \tag{6.20}$$

where

$$a_1\dot{\gamma} = \frac{k_1}{c} + k_1\dot{\gamma}^n \tag{6.21}$$

Integrating Equation 6.20 at a constant shear rate, with limit conditions:

For $t = 0$ $\quad \eta = \eta_0$
For $t = t$ $\quad \eta = \eta$

obtains:

$$\frac{1}{\eta - \eta_e} = \frac{1}{\eta_0 - \eta_e} + a_1 \cdot t \tag{6.22}$$

For a given shear rate, when plotting $1/(\eta - \eta_e)$ against time, a straight line with slope a_1 is obtained. If the same procedure is repeated using different shear rates, a relation between a_1 and $\dot{\gamma}$ can be established, and k_1 is obtained from Equation 6.21. Tiu and Boger (1974) employed the kinetic–rheologic model to characterize the thixotropic behavior of a mayonnaise sample.

Another kinetics model is the one given by Figoni and Shoemaker (1983), where it is assumed that the decrease in shear stress is an addition of kinetic functions of first order:

$$\sigma - \sigma_e = \sum\left(\sigma_{0,i} - \sigma_{e,i}\right)\exp\left(-k_i t\right) \tag{6.23}$$

in which σ_e is the equilibrium shear stress, σ_0 the initial time shear stress, and k_i the kinetics constants of structural degradation.

Tung et al. (1970) used the mathematical model of Weltmann (1943):

$$\sigma = A_1 - B_1 \log t \tag{6.24}$$

Another model is that of Hahn et al. (1959):

$$\log(\sigma - \sigma_e) = A_2 - B_2 t \tag{6.25}$$

that describes the thixotropic behavior of egg white, fresh, old, and irradiated with gamma rays. In these equations, σ is the shear stress, σ_e is the equilibrium shear stress, and the coefficients B_1, B_2, A_1, and A_2 denote the initial shear stress. Longree et al. (1966) discussed the rheological properties of a set of milk cream systems based on milk–egg–starch mixtures. The products exhibited a thixotropic behavior and were highly non-Newtonian. Neither the power equation nor that of Casson (1959) yielded adequate results, so other equations were tested. It was found that some data fitted to the equation:

$$\log(\eta - \eta_e) = -c t \tag{6.26}$$

in which η is the viscosity for a time t, η_e is the viscosity at equilibrium, and c is an empirical constant.

Higgs and Norrington (1971) studied the thixotropic behavior of sugared condensed milk. This product behaves as a Newtonian fluid at temperatures between 40 and 55°C, and slightly non-Newtonian behavior is observed at lower temperatures; however, it presented a thixotropic behavior at all temperatures studied. The time coefficient for the thixotropic break B is given by:

$$B = \frac{m_1 - m_2}{\ln(t_2/t_1)} \tag{6.27}$$

where m_1 and m_2 are the slopes of the return curves measured at the end of times t_1 and t_2, respectively, and the thixotropic break coefficient due to the increase of the shear rate M is given by:

$$M = \frac{m_1 - m_2}{\ln(N_2/N_1)} \tag{6.28}$$

where N_1 and N_2 are the angular velocities. The parameters of the power law and the thixotropic coefficients for sugared condensed milk are presented in Table 6.2.

In relaxation studies at a fixed shear rate, many foods initially show a growing shear stress. This phenomenon is known as shear stress overshoot. Dickie and Kokini (1981) have studied the shear stress overshoot in typical food products using the model of Bird–Leider:

$$\sigma_{rz} = m(\dot{\gamma})^n \left[1 + (b\,\dot{\gamma}\,t - 1)\exp\left(-t/a\,n\,\lambda\right)\right] \tag{6.29}$$

TABLE 6.2

Parameters of the Power Law and Thixotropic Coefficients for Sugared Condensed Milk

Temperature (°C)	k (Pa·s^n)	n	B (Pa·s)	M (Pa·s)
25	3.6	0.834	4.08	18.2
40	0.818	1.0	1.20	8.65
55	0.479	1.0	0.529	1.88

where m and n are the parameters of the power law, $\dot{\gamma}$ the sudden imposed shear rate, t the time, a and b the fitting parameters, and λ a constant of time. The time constant in this equation is calculated as a function of the viscosity and the primary coefficient of normal stresses (ψ_1') defined according to:

$$\eta = m\left(\dot{\gamma}\right)^{n-1} \tag{6.30}$$

$$\psi_1' = \tau_{11} - \tau_{12} = m'\left(\dot{\gamma}\right)^{n'-2} \tag{6.31}$$

$$\lambda = \left(\frac{m'}{2m}\right)^{\frac{1}{m'-n}} \tag{6.32}$$

The foods used to study this model were ketchup, mustard, mayonnaise, apple marmalade, unsalted butter, margarine, and ice creams, among others. Kokini (1992) gave the parameters m, n, m', and n' for 15 typical food products (Table 6.3).

A great advantage of this equation is that, for long times, it converges to the power law. Also, it perfectly describes the shear stress overshoot peaks. However, it does not adequately describe the decreasing part of the relaxation curve. For this reason, Mason et al. (1982) modified the model of Bird-Leider model by adding several relaxation terms, obtaining the equation:

$$\sigma_{yx} = m\left(\dot{\gamma}\right)^n \left[1 + \left(b_0\,\dot{\gamma}\,t - 1\right)\frac{\sum b_i \exp\left(-t/\lambda_i\right)}{\sum b_i}\right] \tag{6.33}$$

in which m and n are the parameters of the power law, $\dot{\gamma}$ is the shear rate, t is the time, λ_i is the constants of time, and b_0 and b_i are constants.

TABLE 6.3

Rheological Parameters of Foods

Food	m (Pa·s^n)	n	m' (Pa·s$^{n'}$)	n'	λ (s)
Apple marmalade	222.90	0.145	156.03	0.566	8.21×10^{-2}
Canned candied products	355.84	0.117	816.11	0.244	2.90×10^{0}
Honey	15.39	0.989			
Ketchup	29.10	0.136	39.47	0.258	4.70×10^{-2}
"Acalia" cream	563.10	0.379	185.45	0.127	1.27×10^{3}
Mayonnaise	100.13	0.131	256.40	0.048	2.51×10^{-1}
Mustard	35.05	0.196	65.69	0.136	2.90×10^{0}
Peanut butter	501.13	0.065	3785.00	0.175	1.86×10^{5}
Butter bar	199.28	0.085	3403.00	0.398	1.06×10^{3}
Margarine bar	297.58	0.074	3010.13	0.299	1.34×10^{3}
Pressed margarine	8.68	0.124	15.70	0.168	9.93×10^{-2}
Margarine in tube	106.68	0.077	177.20	0.353	5.16×10^{-1}
Whipped butter	312.30	0.057	110.76	0.476	1.61×10^{-2}
Whipped cheese cream	422.30	0.058	363.70	0.418	8.60×10^{-2}
Whipped dessert garnish	35.98	0.120	138.00	0.309	3.09×10^{1}

Source: Kokini, J.L., Rheological properties of foods, in *Handbook of Food Engineering,* D.R. Heldman and D.B. Lund, Eds., Marcel Dekker, Inc., New York, 1992.

6.8 Viscoelasticity

Some semiliquid products that present, in a joint form, properties of viscous flow and elastic solid are called viscoelastic. Knowing viscoelastic properties is very useful in the design and prediction of the stability of stored samples.

Viscoelastic materials present a characteristic behavior that makes them sharply different from other fluids. Thus, if a Newtonian fluid is allowed to squirt through a pipe, the diameter of the squirt contracts as it exits the pipe, while if it is a viscoelastic fluid, a marked widening of the squirt occurs (Figure 6.7a). This phenomenon is known as the Barus effect.

Another characteristic of these fluids is the Weissenberg effect, which is observed when a fluid in a container is agitated with a small rod. If the fluid is Newtonian or pseudoplastic, a free vortex with a surface profile, as shown in Figure 6.7b, is formed. In the case of viscoelastic fluids, the fluid tends to climb up the small rod.

To describe the viscoelastic behavior, some equations are given, in which the shear stress is a function of the viscous flow and of the elastic deformation. Among these equations, those of Voigt and Maxwell are the most used, depending on whether the behavior is similar to an elastic solid or a viscous fluid.

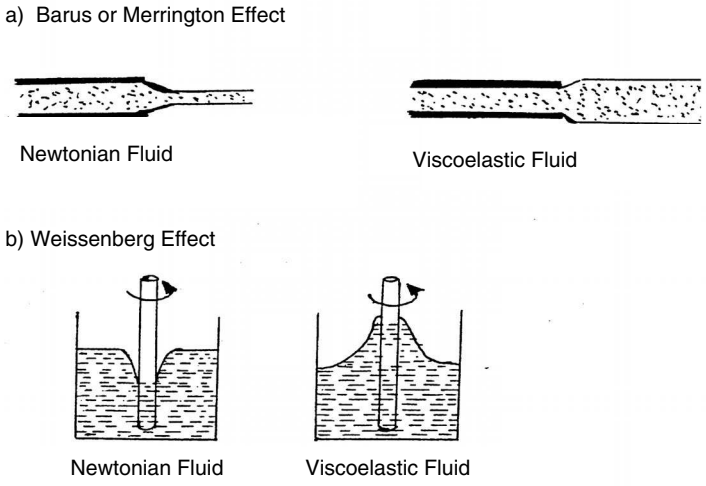

Figure 6.7
Nonlinear viscoelasticity.

The mathematical expression of Voigt's model is:

$$\sigma = G\gamma + \eta\dot{\gamma} \tag{6.34}$$

When the velocity gradient tends to zero, the body behaves as an elastic solid. The quotient between the viscosity and the module G is called the retardation time of the solid:

$$t_E = \eta/G \tag{6.35}$$

and represents the time needed by the shear rate to drop to half of its initial value, when performing at constant stress.

Maxwell's equation is given by:

$$\sigma = \frac{\eta}{G}\frac{d\sigma}{dt} + \eta\dot{\gamma} \tag{6.36}$$

The relation between the viscosity and the module G is called the relaxation time of the fluid:

$$t_R = \eta/G \tag{6.37}$$

and represents the time needed by the stress that results from constant deformation to drop to half of its value.

Generally, the viscoelasticity exhibited by foods is nonlinear and difficult to characterize; therefore, experimental conditions under which the relationship among the variables of deformation, tension, and time can be obtained should be defined.

The viscoelastic behavior of a sample can be studied and characterized in different ways. One way is to study the evolution of the shear stress with time, at a fixed shear rate; it is possible to perform a comparative analysis of different samples from the obtained curves (Elliot and Green, 1972; Elliot and Ganz, 1977; Fiszman et al., 1986).

Viscoelastic materials also present normal stresses being the difference between the first normal stresses used in the characterization of viscoelasticity. Contrary to what occurred with shear stresses, the primary normal stresses do not present overshoot in most semisolid foods.

As indicated by Kokini and Plutchok (1987), the coefficients of the primary normal stresses can be defined under steady state according to the expression:

$$\Psi_1 = \frac{\sigma_{11} - \sigma_{22}}{\dot{\gamma}^2} \tag{6.38}$$

When plotting the coefficient of primary normal stresses under steady state against the shear rate for different semisolid foods using a logarithmic double scale, straight lines are obtained, indicating a behavior in accordance with the power law.

Oscillating tests are also used, in which a shear rate is applied to the sample in an oscillating continuous form, which generates a sinusoidal wave of stresses. For elastic solids, this wave is in phase with the wave of the applied deformation, while for a perfect viscous fluid, there is a 90° out of phase. For viscoelastic materials, the value of the phase-out angle is between 0 and 90°.

Two rheological properties have been defined, the rigidity or storage modulus (G'), which represents the elastic part of the material, and the loss modulus (G''), which represents the viscous character. If γ° and τ° are, respectively, the amplitudes of the deformation and stress waves, and ε the phase-out angle, the G' and G'' moduli are defined by:

$$G' = \left(\tau^\circ/\gamma^\circ\right)\cos\varepsilon \tag{6.39}$$

$$G'' = \left(\tau^\circ/\gamma^\circ\right)\text{sine} \tag{6.40}$$

The complex viscosity for fluid systems is defined as:

$$\eta^* = \left[\left(\eta'\right)^2 + \left(\eta''\right)^2\right]^{1/2} \tag{6.41}$$

in which η' is the viscous component in phase between the stress and the rate of shear, while η'' is the elastic or phase-out component. These viscosity functions are defined by:

$$\eta' = G''/\omega \tag{6.42}$$

$$\eta'' = G'/\omega \tag{6.43}$$

This type of correlation has been used to characterize hydrocolloid solutions (Morris and Ross–Murphy, 1981). Also, in some cases, there are expressions that correlate the different shear properties and viscous functions under steady state with those of the oscillating states (Kokini and Plutchok, 1987).

It is interesting to have a constitutive equation adequately describing the real behavior of samples. One such model is Maxwell's, which combines the viscosity equation of Newton and the elasticity equation of Hooke:

$$\sigma + \lambda\sigma = \eta\dot{\gamma} \tag{6.44}$$

where λ is the relaxation time defined as the quotient between the Newtonian viscosity (η) and the elasticity modulus (G).

In stress relaxation experiments, the sample is subjected to a fix deformation for a period of time and the variation of stress with time is measured. The relaxation measurement is a simple method to obtain a qualitative description of the elastic behavior of a sample. The relaxation time is calculated from the relaxation experienced by the sample after a shear stress has been applied. In some cases, one relaxation time is not enough to describe the rheological behavior of the sample, and it is necessary to use the generalized Maxwell's model, which includes several elements of such a model.

In general, the viscoelasticity presented by foods is nonlinear, so Maxwell's model cannot be applied. For this reason, other constitutive models have been sought, such as the model of Bird–Carreau. This is an integral constitutive model based on Carreau's constitutive theory of molecular networks, in which the whole deformation history of the material is incorporated. In order to apply the Bird–Carreau's model, it is necessary to know the values of the limit viscosity η_0 at shear rate equal to zero, as well as the time constants γ_1 and γ_2 and the constants α_1 and α_2. It is necessary to perform shear tests under steady state and oscillating tests to calculate them. Figure 6.8 shows the graphs obtained in this type of experiment that allow determination of the Bird–Carreau constants (Bird et al., 1977).

From the shear experiment under steady state (Figure 6.8a) η_0 is obtained by extrapolation to $\dot{\gamma} = 0$; the time constant λ_1 is the value of the inverse of the shear rate at the intersection point of the straight line with value η_0 and the tangent to the curve in the non-Newtonian zone, while α_1 is obtained from the slope of the curve $\log \eta - \log \gamma$ in the non-Newtonian zone (Kokini, 1992).

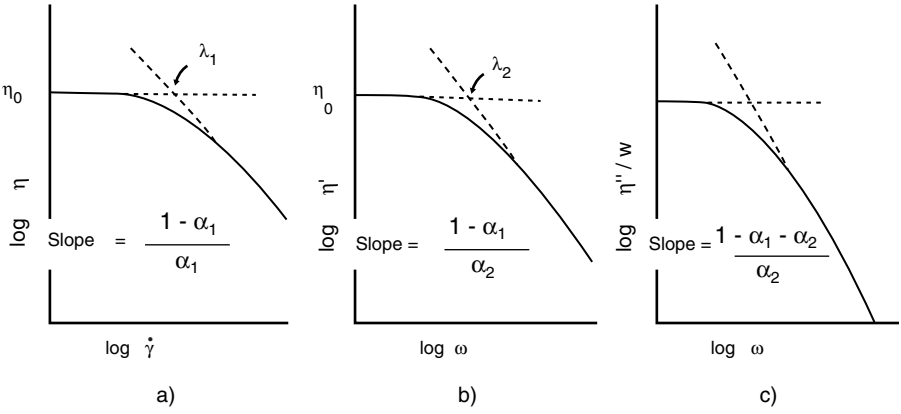

FIGURE 6.8
Determination of the Bird–Carreau constants λ_1, λ_2, x_1, and x_2.

From the oscillating experiments it is possible to obtain graphs of η' and η''/ω against the angular velocity ω in double logarithmic coordinates (Figures 6.8b and 6.8c). The time constant λ_2 is obtained as the inverse of the value of the angular velocity ω at the intersection point of the straight line η_0 and the tangent to the curve of the non-Newtonian zone, while α_2 is obtained from the slope of this curve.

Once these constants are known, it is possible to predict the values of η, η', and η'' (Bird et al., 1977). Thus, the Bird–Carreau model that allows obtaining of the viscosity value η is:

$$\eta = \sum_{p=1}^{\infty} \frac{\eta_P}{1+\left(\lambda_{1P}\,\dot{\gamma}\right)^2} \tag{6.45}$$

where

$$\lambda_{1P} = \lambda_1 \left(\frac{2}{p+1}\right)^{\alpha_1} \tag{6.46}$$

$$\eta_P = \eta_0 \frac{\lambda_{1P}}{\sum \lambda_{1P}} \tag{6.47}$$

For high shear rates, Equation 6.45 becomes:

$$\eta = \frac{\pi\,\eta_0}{Z(\alpha_1)-1}\left[\frac{\left(2\alpha_1\,\lambda_1\,\dot{\gamma}\right)^{\frac{1-\alpha_1}{\alpha_1}}}{2\alpha_1\,\mathrm{sen}\left(\frac{1+\alpha_1}{2\alpha_1}\pi\right)}\right] \tag{6.48}$$

in which $Z(\alpha_1)$ is the function Zeta–Riemann:

$$Z(\alpha_1) = \sum_{k=1}^{\infty} k^{-\alpha_1} \tag{6.49}$$

Expressions that allow calculation of η′ and η″, according to the constitutive model of Bird–Carreau, can be found in the literature (Bird et al., 1977; Kokini, 1992).

Creep and recovery tests have been applied to cream and ice creams (Sherman, 1970). In this case, a constant shear stress is applied for a given time and the variation of the deformation with time is studied (Figure 6.9). The results are expressed in terms of $J(t)$ against time. The function $J(t)$ is the compliance, which is a relation between the deformation generated and the shear stress applied.

$$J(t) = \dot{\gamma}/\tau \tag{6.50}$$

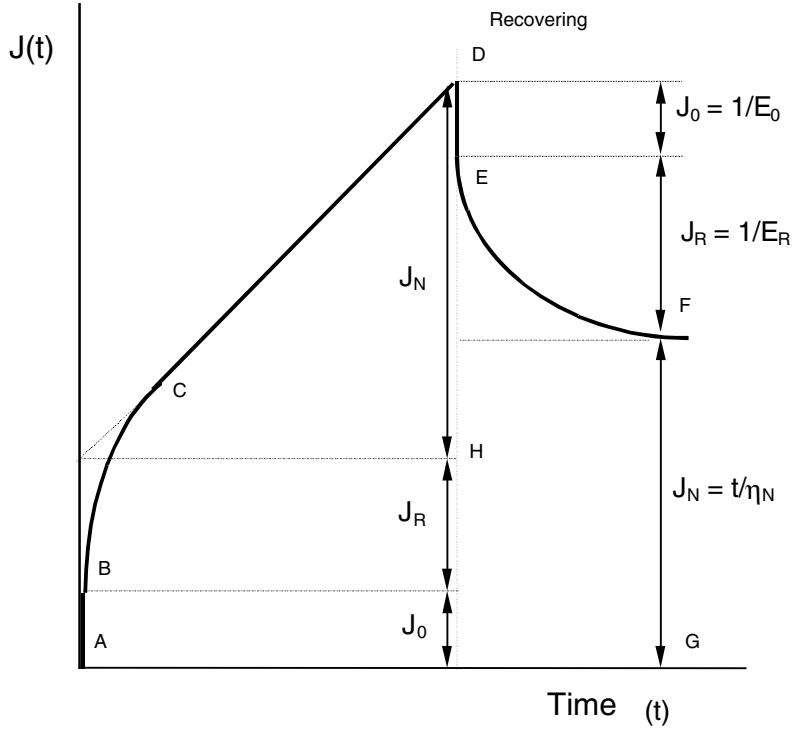

FIGURE 6.9
Curve of a "creep" model. Creep zone: A–B: instantaneous elastic creep; B–C: retarded elastic creep; C–D: Newtonian fluid, recovering zone: D–E: instantaneous elastic recovering; E–F: retarded elastic recovering; F–G: nonrecoverable deformation.

For ice cream and frozen products, the creep compliance against time can be described according to the equation:

$$J(t) = J_0 + J_1\left[1 - \exp\left(-\frac{t}{\theta_1}\right)\right] + J_2\left[1 - \exp\left(-\frac{t}{\theta_2}\right)\right] + \frac{1}{\eta_N} \qquad (6.51)$$

where $J_0 = 1/E_0$ is the instant elastic compliance, E_0 is the instant elastic module, $J_1 = 1/E_1$ and $J_2 = 1/E_2$ are the compliance associated to the retarded elastic behavior, $\theta_1 = \eta_1/E_1$ and $\theta_2 = \eta_2/E_2$ are the retarded times associated to the retarded elasticity, E_1 and E_2 are the retarded elastic modules associated to the retarded elasticity, η_1 and η_2 are the viscosity components associated to retarded elasticity, and η_N is the viscosity associated to the Newtonian flow.

Likewise, it is possible to characterize the viscoelasticity of the samples by studying the development of the shear stress under unsteady state (shear stress overshoot), applying the model of Bird–Leider or the modified model, as stated in the last section.

Another method widely used in the viscoelastic characterization of foods is the use of mechanical models. Thus, for example, mixed and frozen products behave as two bodies of Kelvin–Voight connected in series, while the behavior of melted ice cream can be represented as a unique body of Kelvin–Voigt.

6.9 Effect of Temperature

During manufacture, storage, transport, sale, and consumption, fluid foods are subjected to continuous variations of temperature. For this reason, it is important to know the rheological properties of the products as a function of temperature.

In the case of Newtonian fluids, the expression that correlates viscosity and temperature is an Arrhenius type equation. However, for non-Newtonian fluids, the apparent viscosity is usually related to a fixed shear rate, instead of viscosity (Rao et al., 1984; Vitali et al., 1974; Moresi and Spinosi, 1984):

$$\eta_A = \eta_\infty \exp\left(\frac{E_a}{RT}\right) \qquad (6.52)$$

in which E_a is the flow activation energy, η_∞ is a constant called viscosity of infinite deformation, R is the gas constant, and T is temperature in degrees Kelvin. For non-Newtonian fluids, a consistency index is usually used too,

instead of the apparent viscosity (Harper and El Sarhigi, 1965; Vitali and Rao, 1984a).

Equation 6.52 is the most used for all types of food fluids, although there are others such as the one used by Sáenz and Costell (1986):

$$Y = Y_0 \exp(-BT) \tag{6.53}$$

in which Y is the viscosity or the yield stress, T is the temperature expressed in degrees Celsius, and B is a constant.

In the case of kiwi juice (Ibarz et el., 1991), a linear equation has been applied to describe the variation of the yield stress with temperature.

Temperature can affect different rheological parameters such as viscosity, consistency index, flow behavior index, and yield stress. Generally, the observed effect is the following:

- Viscosity and consistency indexes decrease as temperature increases.
- Flow behavior index is not usually affected by the temperature variation (Sáenz and Costell, 1986; Mizrahi and Berk, 1972; Crandall et al., 1982). However, in some cases a temperature increase could produce an increase in the flow behavior index (Ibarz and Pagán, 1987), changing from pseudoplastic to Newtonian behavior.
- The yield stress can also vary with temperature, so that when temperature increases, yield stress value decreases. Thus, for lemon juices (Sáenz and Costell, 1986) this variation in the yield stress can cause a change in the behavior of juices from pseudoplastic to Newtonian.

6.10 Effect of Concentration on Viscosity

6.10.1 Structural Theories of Viscosity

Bondi (1956) revised the theories of viscosity of liquids. According to the kinetics theory, the viscosity of Newtonian liquids can be obtained by the following equation (after numerous approximations):

$$\eta = \left[0.48(r_1/v)m\Phi_a(r_1)\right]^{1/2} \exp\left[\frac{\Phi_a(r_1)}{kT}\right] \tag{6.54}$$

where r_1 is the interatomic distance characteristic of the liquid density, Φ_a is the attraction component of the interaction energy between a pair of isolated

molecules, m is the molecular weight, v is the molar volume, k is the Boltzman's constant, and T is the temperature.

The advantage of Equation 6.54, as well as similar expressions, is that it relates the viscosity with molecular parameters, especially with the interaction energy between two isolated molecules. However, the mathematical problems when applying basic molecular theory to the liquid viscosity are so difficult that the final equations derived at the present time do not have a practical value for rheologists (van Wazer et al., 1963).

Another approach to the theoretical comprehension of the viscosity of liquids has been developed by Eyring and coworkers (1936) based on the "absolute" theory of velocity processes, which describes the elementary processes that govern the kinetics of chemical reactions. This approach supposes that the liquid is an imperfect molecular reticule, with a number of vacant spaces of the reticule called "holes." According to Eyring, the equation for viscosity can be expressed as:

$$\eta = \frac{hN}{v}\exp\left(\frac{\Delta F}{RT}\right) \tag{6.55}$$

in which ΔF is the free activation energy, h is Planck's constant, N is Avogadro's number, and v is the molar volume.

Brunner (1949) modified this equation to obtain:

$$\eta = \left(\frac{\delta}{v_L}\right)\left(2\pi m kT\right)^{1/2}\exp\left(\frac{\Delta F}{RT}\right) \tag{6.56}$$

where δ is the width of the potential barrier, m is the reduced mass of the activated complex, and v_L is the molecular volume of the liquid.

6.10.2 Viscosity of Solutions

The viscosity of diluted solutions has received considerable theoretical treatment. When talking about viscosity data at high dilution, different functions have been used:

The viscosity rate (also known as relative viscosity):

$$\eta_r = \eta/\eta_0 \tag{6.57}$$

Specific viscosity:

$$\eta_{sp} = \eta_r - 1 = \left(\eta - \eta_0\right)/\eta_0 \tag{6.58}$$

Viscosity number (reduced viscosity):

$$\eta_{red} = \eta_{sp}/C \tag{6.59}$$

Inherent viscosity (logarithm of the viscosity number):

$$\eta_{inh} = \ln\left(\eta_r/C\right) \tag{6.60}$$

Intrinsic viscosity (limit viscosity number):

$$[\eta] = \left[\frac{\eta_{sp}}{C}\right]_{C\to 0} = \left[\left(\ln \eta_r/C\right)\right]_{C\to\infty} \tag{6.61}$$

where η is the viscosity of the solution of concentration C and η_0 is the viscosity of the pure solvent.

According to Einstein, the limit viscosity number, in the case of suspensions of rigid spheres, is 2.5 per volumetric concentration (C_v) measured in cm^3 of spheres per cm^3 of total volume.

For low concentration, the viscosity number is given by the expression:

$$\eta_{red} = 2.5 + 14.1C_v \tag{6.62}$$

Einstein's viscosity relationship has been applied to different solutions and suspensions. For sugar solutions, the first type for which this relationship was tested, the viscosity number experimentally determined was from one to one and a half times greater than the value of 2.5 obtained when assuming that the dissolved sugar was in the form of unsolvated spherical molecules (van Wazer et al., 1963).

The viscosity data as a function of concentration are extrapolated up to infinite dilution by means of Huggins' equation (1942):

$$\eta_{sp}/C = [\eta] + k'[\eta]^2 C \tag{6.63}$$

where k' is a constant for a series of polymers of different molecular weight in a given solvent. The alternative definition of the intrinsic viscosity leads to the equation (Kraemer, 1938):

$$\frac{\ln \eta_r}{C} = [\eta] + k''[\eta]^2\ C \tag{6.64}$$

where $k' - k'' = 1/2$.

At intrinsic viscosity higher than approximately 2, and even lower in some cases, there can be a noticeable dependence of viscosity on the shear velocity in the viscometer. This dependence is not eliminated by extrapolation to infinite dilution, since the measure as a function of the shear velocity and extrapolation at zero rate of shear are also necessary (Zimm and Grothers, 1962).

The theories of the friction properties of polymer molecules in solution show that the intrinsic viscosity is proportional to the effective hydrodynamic volume of the molecule in solution divided by its molecular weight (M). The effective volume is proportional to the cube of a linear dimension of the random coiling of the chain. If $(r)^{1/2}$ is the chosen dimension:

$$[\eta] = \frac{\delta\left(r^2\right)^{3/2}}{M} \tag{6.65}$$

where δ is a universal constant (Billmeyer, 1971).

The effect exerted by concentration on a homogeneous system is to increase the viscosity or consistency index. Two types of correlation can be found in the literature (Harper and El Sahrigi, 1965; Rao et al., 1984), according to a power model and an exponential model, in agreement with the following equations:

$$Y = K_1\left(C\right)^{A_1} \tag{6.66}$$

$$Y = K_2 \exp\left(A_2 C\right) \tag{6.67}$$

in which Y can be the viscosity or the consistency index and C is the concentration of some component of the sample.

Most of the existing information refers to fruit-derived products, in which the effect of the soluble solids, pectin content, total solids, etc. is studied. From the two last equations, the former usually yields good results in purée type foods, while the latter is successfully applied to concentrated fruit juices and pastes (Rao and Rizvi, 1986).

Besides the viscosity and the consistency index, concentration can also affect other parameters. Thus, the yield stress increases as concentration increases. For kiwi juices (Ibarz et al., 1991), as concentration decreases, the yield stress disappears, changing from a plastic to a pseudoplastic behavior.

There are studies showing that concentration does not affect the flow behavior index (Sáenz and Costell, 1986), while in other studies, an increase in concentration decreased its value (Mizrahi and Berk, 1972).

6.10.3 Combined Effect: Temperature–Concentration

From an engineering point of view, it is interesting to find a unique expression that correlates the effect of temperature and concentration on viscosity. The equations generally used are:

$$\eta_a = \alpha_1 (C)^{\beta_1} \exp(Ea/RT) \tag{6.68}$$

$$\eta_a = \alpha_2 \exp(\beta_2 C + Ea/RT) \tag{6.69}$$

in which η_a is the viscosity for Newtonian fluids, or either the apparent viscosity or consistency index for non-Newtonian fluids. The parameters α_i and β_i are constants, C is the concentration, and T the absolute temperature.

Generally, this type of equation is valid in the variables' range for which they have been determined (Rao, 1986; Vitali and Rao, 1984a). These equations have been applied to describe the combined effect of concentration and temperature on different food products (Rao et al., 1984; Vitali and Rao, 1984a; Ibarz and Sintes, 1989; Ibarz et al., 1989; Castaldo et al., 1990; Ibarz et al., 1992a, b).

6.11 Mechanical Models

The rheological behavior of different substances can be described by means of mechanical models. The results obtained with these models can be expressed by means of stress–strain and time diagrams that allow obtaining equations of rheological application. The models used are those of spring and dashpot, as well as combinations of both.

6.11.1 Hooke's Model

Hooke's mechanical model (spring) serves to describe the behavior of ideal elastic solids. This type of model is represented in Figure 6.10, as well as the stress vs. strain curve occurring in the spring.

6.11.2 Newton's Model

The mechanical model of Newtonian fluids is represented by a dashpot, as shown in Figure 6.11. A dashpot is a container filled with fluid in which a piston can freely move up and down. In this model the only resistance that impedes the movement of the piston is the viscosity of the liquid.

6.11.3 Kelvin's Model

Kelvin's mechanical model describes the rheological behavior of ideal viscoelastic materials and corresponds to the Voigt equation (Equation 6.34).

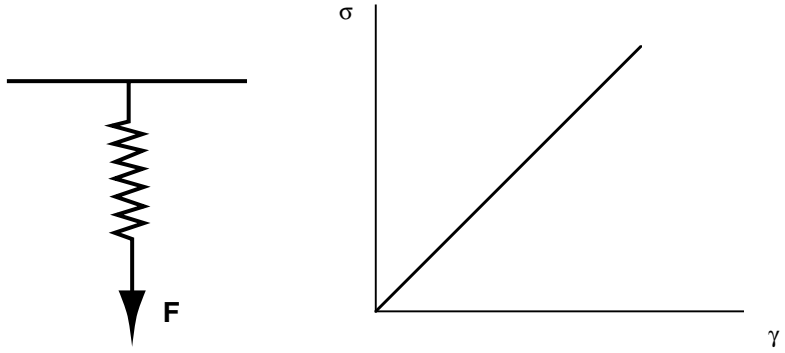

FIGURE 6.10
Hooke's mechanical model.

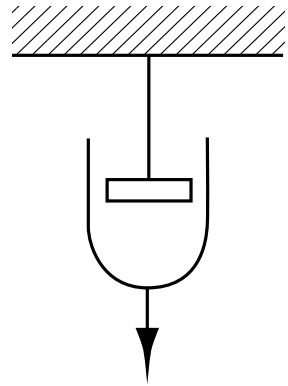

FIGURE 6.11
Mechanical model of a Newtonian fluid.

This model considers a spring and a dashpot together, in parallel; that is, their movement occurs at the same time and at the same velocity. The two elements, spring and dashpot, undergo the same deformation, but not the same stress. This model is represented in Figure 6.12.

In the Kelvin's bodies, when the stress stops acting, the strain will stop, but in a retarded form, according to the expression:

$$\varepsilon = \varepsilon_{max} \exp\left(-t/t_E\right) \tag{6.70}$$

where ε is the relative strain, t is the time, and t_E is the retardation time of the body. The delay to return to the initial state is due to the viscosity of the dashpot.

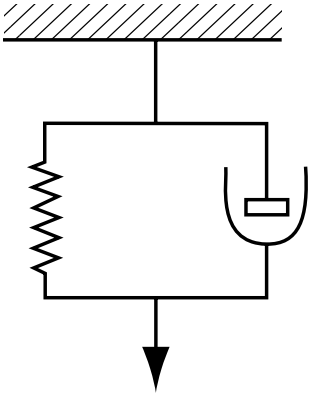

FIGURE 6.12
Mechanical model of the Kelvin's body.

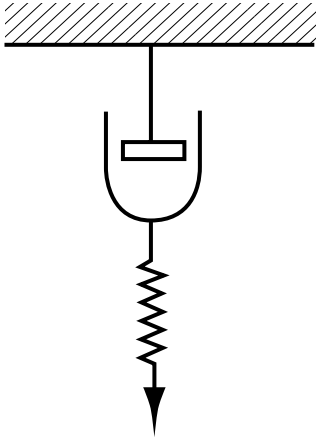

FIGURE 6.13
Maxwell's mechanical model.

6.11.4 Maxwell's Model

This model considers a spring and a dashpot in series, corresponding to the behavior of ideal viscoelastic fluids. Both elements undergo the same stress, but not the same deformation (see Figure 6.13). The change of deformation with time is linear at first because, initially, only the spring is deformed. Then the deformation of the dashpot begins, and once the spring is no longer able to deform, only the dashpot controls the deformation.

If, in a Maxwell's body on which a shear stress σ_M has been applied at a given instant, t_i, the achieved deformation is kept constant, the shear stress slowly ceases because of the viscosity of the dashpot, and it can be expressed according to the equation:

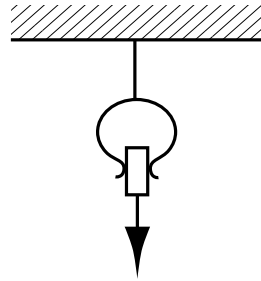

FIGURE 6.14
Saint–Venant's mechanical model.

$$\sigma = \sigma_M \exp\left(-t/t_R\right) \tag{6.71}$$

in which σ_M is the shear stress applied and t_R is the relaxation time of the fluid.

This relaxation phenomenon occurs whenever a material has plastic properties. An ideal solid body does not present relaxation, whereas a perfect viscous fluid presents an instantaneous relaxation. Every solid body that presents this relaxation phenomenon proves that it has a viscous component.

6.11.5 Saint–Venant's Model

This model is based on a slider, which is a type of tweezer holding a piece of material (Figure 6.14). If the applied shear stress is greater than the friction between the slider and the material, it will slide; otherwise, it will stay fixed.

6.11.6 Mechanical Model for the Bingham's Body

The mechanical model that describes the rheological behavior of Bingham's plastics is a combination of a spring and a slider in series and a dashpot in parallel (Figure 6.15).

In addition to these mechanical models, there are more complicated combinations of the three basic models, spring, dashpot, and slider. Thus, Figure 6.16 presents the mechanical model of Burgers that describes the viscoelastic behavior of certain products.

6.12 Rheological Measures in Semiliquid Foods

Scott–Blair (1958) classified the instruments for studying texture, and Rao (1980) classified the instruments for measuring flow properties of fluid foods in three categories: (1) fundamental, (2) empirical, and (3) imitative. The

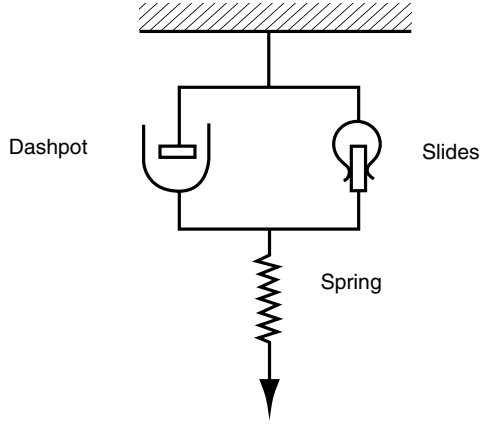

FIGURE 6.15
Mechanical model of the Bingham's body.

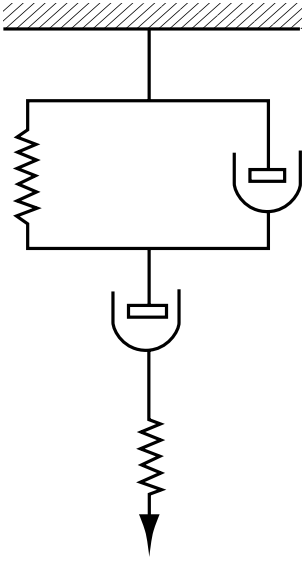

FIGURE 6.16
Mechanical model of Burgers.

fundamental experiments measure defined physical properties and are independent of the instruments. The empirical experiments measure parameters not clearly defined but that have proven useful from past experience. The imitative experiments measure properties under similar conditions to those found in practice (White, 1970).

6.12.1 Fundamental Methods

Different instruments have been used to measure flow properties using fundamental methods. Oka (1960), van Wazer et al. (1963), Sherman (1970), Rao (1977), and Shoemaker et al. (1987) have described several of the commercial instruments and their fundamental equations. The fundamental methods can be classified according to the geometry used: capillary, Couette (concentric cylinder), plate and cone, parallel plates, back extrusion, or squeezing flow. Three requirements are common to the cited geometries: (1) laminar flow of the liquid, (2) isothermal operation, and (3) no slippage in the solid–fluid interphase (van Wazer et al., 1963).

6.12.1.1 Rotational Viscometers

A rotating body immersed in a liquid experiences a viscous drag or retarded force. The quantity of viscous drag is a function of the velocity of the rotation of the body. Using the velocity equations, no difference is obtained whether the body or the container rotates.

Rotational viscometers allow for continuous measurements at a given shear rate or shear stress for long periods of time, allowing determination of whether or not there is time dependence. These attributes are not typical of most capillary viscometers or of other types of viscometers. For these reasons, rotational viscometers are the most used type of instrument for rheological determinations.

6.12.1.2 Concentric Cylinders Viscometers

Although rotational viscometers use a vessel and rotors in the form of spheres, discs, cones, and other particular forms, the most common type is that of concentric coaxial cylinders, schematically shown in Figure 6.17. One cylinder of radius R_b is suspended in a fluid sample in a container of radius R_c. The liquid covers the internal cylinder up to height h. The bottom part of the internal cylinder, or rotor, is separated from the bottom of the vessel by a distance l. Complete descriptions of this type of flow have been given by Oka (1960), van Wazer (1963), Reiner (1971), and Walters (1975), among others.

This is a rheological flow that has been used to characterize the shear behavior of non-Newtonian fluids. Recently, this configuration has also been used to characterize differences of normal stresses (Schowalter, 1978). According to van Wazer et al. (1963), to obtain the fundamental equations, the following assumptions should be made:

1. The liquid is incompressible.
2. The movement of the liquid is under laminar regime.
3. There is steady velocity that is only a function of the radius; it is supposed that the radial and axial flows are equal to zero (neglecting the centrifuge forces).

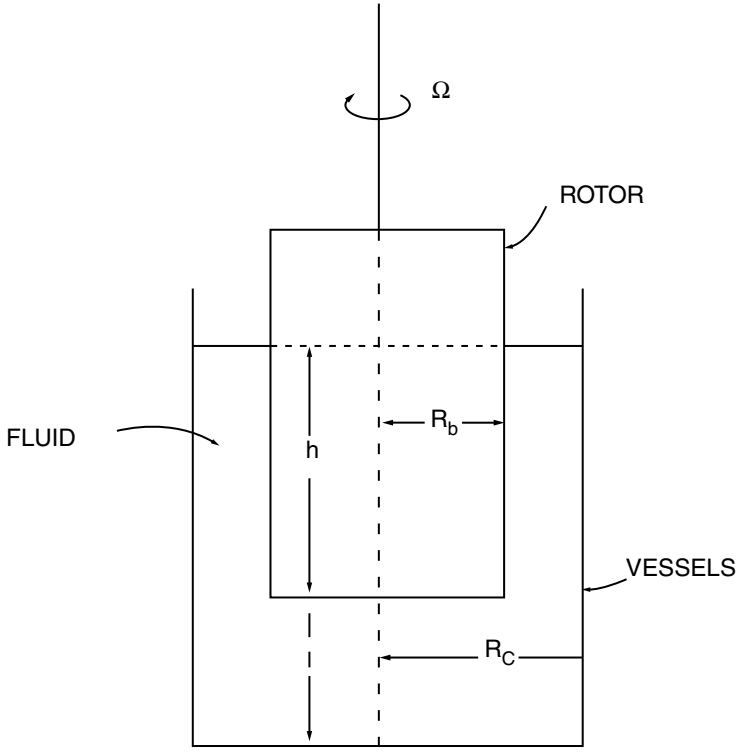

FIGURE 6.17
Concentric cylinders viscometer.

4. There is steady movement; all the derivatives with respect to time of the continuity and movement equations are zero.
5. There is no relative movement between the surface of the cylinders and the fluid in contact with the cylinders, i.e., there is no slippage.
6. The movement is bidimensional (neglecting the final and edge effects).
7. The system is isothermal.

Couette's flow is an example of simple shear flow with a velocity field in which components as cylindrical coordinates are:

$$v(r) = 0 \tag{6.72.a}$$

$$v(\theta) = r\,\omega(r) \tag{6.72.b}$$

$$v(z) = 0 \tag{6.72.c}$$

The only non-null velocity component is the one in the direction θ, $r\omega(r)$ in which $\omega(r)$ is the angular velocity.

According to the velocity field, the stress components are given by:

$$\sigma_{rz} = \sigma_{\theta z} = 0 \tag{6.73}$$

$$\sigma_{r\theta} = \sigma(\dot{\gamma}) \tag{6.74}$$

$$\sigma_{rr} - \sigma_{zz} = \psi_1(\dot{\gamma}) \tag{6.75}$$

$$\sigma_{\theta\theta} - \sigma_{zz} = \psi_2(\dot{\gamma}) \tag{6.76}$$

where σ_{rr}, $\sigma_{\theta\theta}$, σ_{zz}, $\sigma_{r\theta}$, σ_{rz}, and $\sigma_{\theta z}$ are the components of the stress tensor, and $\psi_1(\dot{\gamma})$ and $\psi_2(\dot{\gamma})$ are the components of the function of normal stresses.

It is assumed that the flow occurs between two infinite coaxial cylinders with radii R_i and R_0 ($R_i < R_0$). The internal cylinder rotates with certain angular velocity while the external remains fixed. If the torque per height unit (T') exerted on the fluid in the interior of the cylindrical surface with constant r is calculated, the following relation is obtained:

$$T' = \sigma_{r\theta}(2\pi r)r = 2\pi r^2 \sigma_{r\theta} \tag{6.77}$$

According to Cauchy's first law of movement, the following is obtained:

$$\sigma_{r\theta} = \mu / r^2 \tag{6.78}$$

where μ is a constant. Equalizing Equations 6.74 and 6.77:

$$\sigma_{r\theta} = \frac{T'}{2\pi r^2} = \sigma(\dot{\gamma}) \tag{6.79}$$

If one assumes that the fluid obeys the power law:

$$\sigma = m\dot{\gamma}^n = m\left[\frac{dv}{dr} - \frac{v}{r}\right]^n \tag{6.80}$$

integrating between the ratio of the internal and external cylinders, the following expression is obtained:

$$\int_0^{\omega_i} d\omega = \left[\frac{T'}{2\pi m}\right]^{1/n} \int_{R_0}^{R_i} \frac{dr}{\left(r^{\frac{n+2}{n}}\right)} \tag{6.81}$$

where w_i is the angular velocity at which the internal cylinders spins. Equation 6.81 can be integrated as follows:

$$\omega_i = 2\pi N' = \frac{n}{2}\left[\frac{T'}{2\pi m}\right]^{1/n}\left[\frac{1}{R_i^{2/n}} - \frac{1}{R_0^{2/n}}\right] \tag{6.82}$$

where N' is the number of revolutions per unit time at which the internal cylinder spins. The expression for Newtonian fluids is directly obtained for $n = 1$, from which the Margules' equation for Newtonian viscosity is obtained:

$$\eta = \frac{T'}{4\pi\omega_i}\left[\frac{1}{R_i^2} - \frac{1}{R_0^2}\right] \tag{6.83}$$

When the measured fluid shows a Bingham's plastic behavior, the following expression is obtained:

$$\omega_i = 2\pi N' = \frac{1}{m}\frac{T'}{4\pi}\left[\frac{1}{R_i^2} - \frac{1}{R_0^2}\right] - \frac{\tau_0}{m}\ln\left(R_0 \big/ R_i\right) \tag{6.84}$$

6.12.1.3 Plate–Plate and Cone–Plate Viscometers

Other types of rotational viscometers are of plate and plate and of cone and plate. As indicated, the plate and cone viscometer consists of a flat plate and a cone (Figure 6.18). The angle of the cone, θ_0, is about 3° or less. According to Walters (1975), it is assumed that:

1. Inertia effects are insignificant.
2. The angle of the cone is very small.
3. The cone and the plate have the same radius a.
4. The free surface of the liquid is part of a sphere of radius a and is centered in the cone's vortex.
5. The simple shear flow under steady state is continuous up to the free surface.
6. Surface tension forces are insignificant, and the torque measurement (T) in the fixed plate, as a function of the angular velocity (Ω_1) of the cone, can be used to determine the shear rate which depends on the apparent viscosity, according to the following equations:

$$\dot{\gamma} = \Omega_i\, a/h \tag{6.85}$$

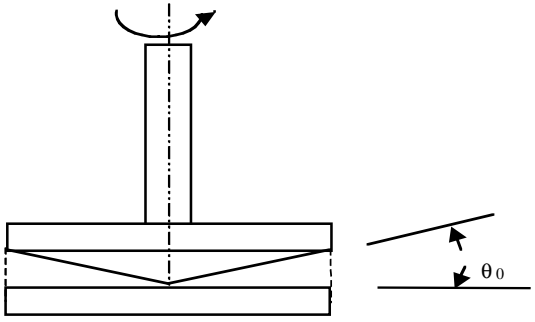

(a)

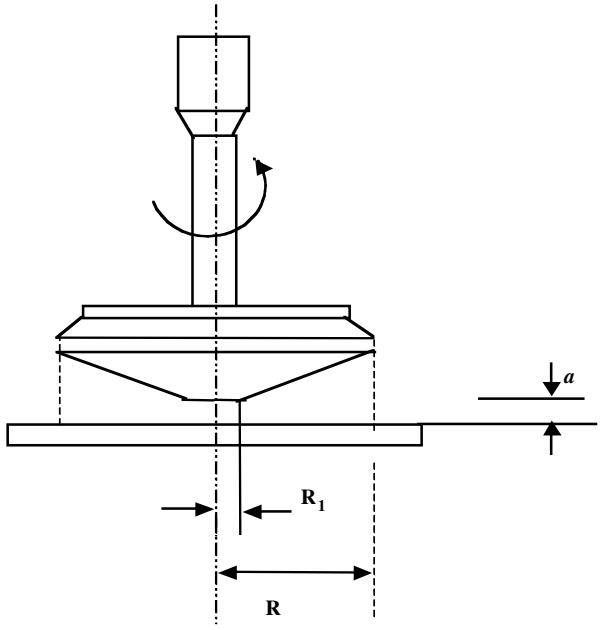

(b)

FIGURE 6.18
Scheme of cone–plate geometry.

$$\sigma = \frac{3T}{2\pi a^3}\left[1+\frac{1}{3}\frac{d\ln T}{3d\dot{\gamma}\,a}\right] \tag{6.86}$$

where a is the radius and h is the distance between the plate and the cone.

For a parallel plates system, the same equations are used to calculate the shear rate and the shear stress. The velocity field is independent of the material's properties for the flow as well as for the flow's torsion of the plate and cone.

Since the mid-1960s, considerable attention has been paid to the situation of combined steady and oscillating flow. Such a situation is interesting in itself, since a rheometric flow can be interpreted relatively simply in terms of certain well-defined functions of the material. It also supplies a much more critical experiment than any rheological equation proposed separately in shear under steady or oscillating state (Walters, 1975; Kokini and Plutchok, 1987).

6.12.1.4 Error Sources

The basic equations obtained in the last section for determination of the relation between σ and γ are based on the existence of a simple flow through the liquid, so numerous assumptions should be complied with to obtain the desired type of flow. An important consideration, therefore, is that these assumptions are valid in practical situations with the limitations that they impose to the operation conditions. The possible error sources affecting the interpretation of the experimental results in the Couette flow are reviewed in this section.

Viscous Heating

When a liquid is sheared, part of the work applied is dissipated as heat. The heating induced by the shearing causes an unavoidable increase of the liquid's temperature, which constitutes a source of error that could be particularly important in the case of highly viscous liquids or at high shear value (Walters, 1975). The symbol β will be used to describe the dependence on temperature of the material's properties ($\beta = 0$ represents materials whose properties are not affected by temperature, and high values of β represent materials whose properties are sensitive to temperature).

It is possible to identify β as the viscosity–temperature relation parameter. The parameter that defines whether the heating induced by the shearing is important in a practical situation is the product $\beta \cdot B(r)$, where $B(r)$ is Brinkman's number. For a Couette's flat flow with a separation between cylinders (gap) of width h, $B(r)$ is given by:

$$B(r) = \frac{\sigma^2 h^2}{\eta K_T T_0} r^2 \tag{6.87}$$

where K_T is the thermal conductivity and T_0 is a reference temperature (K). It can be inferred from this equation that the heating effects should be significant in the higher viscosity and shear rate ranges. A way to minimize such effects is to work with a narrow gap between cylinders.

Imperfections of the Instrument

Reliable viscometric measurements require excellent quality geometry and they should be properly aligned (Walters, 1975).

Perfect alignment in narrow gap rheometry is a difficult task and, for highly viscous liquids, a slight deviation can cause great positive pressure on the region of convergent flow and great negative pressure on the region of divergent flow overimposed to the pressure resulting from normal stresses (Greensmith and Rivlin, 1953). This effect can be eliminated by changing the direction of movement and considering the average pressure during movement in both directions (McKennell, 1960).

Another source of error is the small axial movement of the rotating device during the experiment caused by imperfections of the connection (Adams and Lodge, 1964).

End and Edge Effects

Different authors, such as Oka (1960), van Wazer (1963), and Walters (1975), have highlighted this type of error, which is due to the devices of the instrument having finite dimensions. Consequently, in general, a viscous drag always exists due to the stress at the bottom of the surface of the internal cylinder. Also, the distribution of stresses on the cylindrical surface differs from the distribution on cylinders of infinite length, since the flow is affected by the end of the surface.

The end effect can be considered equivalent to an increase in the effective immersion length from h to $(h + \Delta h)$ (Oka, 1960). Margules' equation for a Newtonian flow becomes:

$$\Omega = \left[\frac{T' h}{4\pi\eta\left(h+\Delta h\right)}\right]\left(\frac{1}{R_i^2} - \frac{1}{R_0^2}\right) \tag{6.88}$$

where Δh, the end correction, is in general a function of R_i, R_0, h, and the ending hollow l. The end correction (Δh) is normally obtained by experimentation when plotting T'/Ω vs. h.

Oka (1960) found a relationship for the end effect that satisfies the Navier–Stokes' equation. The final expression is:

$$\frac{\Delta h}{R_i} = \frac{1}{8}\frac{Ri}{1}\left[1-\left(\frac{R_i}{R_0}\right)^2\right]\left[1+4\frac{1}{R_i}\sum_1^{\infty} A_n \mathrm{I}_2\left(\frac{n\,\pi\,a}{1}\right)+\frac{8}{\pi}\frac{1}{R_i}\sum_1^{\infty} B_n \frac{\operatorname{sen} h\left(K_n h\right)}{K_n R_i}\right] \tag{6.89}$$

where I_2 is the second order modified Bessel's function, K is the nth positive root of the equation $r = (KR_0) = 0$, and A_n and B_n are functions of the dimensionless parameters R_i/R_0, h/R_0 , and $1/R_0$. In this equation the first

term of the second brackets is only due to the end effect of the internal cylinder, the second form is due to the edge effect at the bottom, and the third term is due to the end effect and to the free surface of the fluid in the gap. It is evident that when l is very big compared to R_i and when R_i/R_0 is close to the unit, the term $(\Delta h/R_i)$ is very small. Based on these results, the influence of sphere and end effects may be and probably should be reduced if the gap between the cylinders is as narrow as possible.

Taylor's Vortex

The presence of Taylor's vortexes is a problem that occurs when a sample is analyzed with a coaxial viscometer in which the internal cylinder rotates. The condition for this instability is given by Taylor's number (Schlichting, 1955):

$$T_a = \frac{v_i}{v}\left(\frac{d}{R_i}\right)^{1/2} \geq 41.3 \tag{6.90}$$

in which R_i is the radio of the internal cylinder, d is the gap between cylinders, v_i is the periferic velocity of the internal cylinder, and v is the kinematic viscosity. Three Taylor's numbers can be differentiated for three flow regimes:

$T_a < 41.3$ = Couette laminar
$41.3 < T_a < 400$ = laminar, with Taylor's vortexes
$T_a > 400$ = turbulent

Miscellaneous Sources of Error

Other sources of error are:

1. Inertia effects (This correction depends on $w(r)$, which in turn depends on the apparent viscosity function.)
2. Inherent errors to the interpretation of the experimental results
3. Unstabilities due to the turbulent flow
4. Homogeneity of the tested sample
5. Stability of the tested sample
6. Slippage

6.12.1.5 Oscillating Flow

Oscillating experiments can be carried out using the following geometries: parallel plates, plate and cone, and Couette's system of concentric cylinders. This type of experiment is used to study the viscoelasticity of foods. To do that, a simple harmonic movement of small amplitude is applied to the fixed

parts of the previous measurement systems, which induces an oscillation in the rotor affected by the viscous resistance and the elastic force of the sample contained in the viscometer. The oscillating phase of the rotor is negatively phased out, and the induced amplitude also differs from the applied one.

It is possible to calculate η' and G' (Rao, 1986) from the expressions:

$$\eta' = \frac{-s\left(\theta_1/\theta_2\right)\text{sine}}{\left[\left(\theta_1/\theta_2\right)^2 - 2\left(\theta_1/\theta_2\right)\cos c + 1\right]} \tag{6.91}$$

$$G' = \frac{\omega s\left(\theta_1/\theta_2\right)\left[\cos c - \left(\theta_1/\theta_2\right)\right]}{\left[\left(\theta_1/\theta_2\right)^2 - 2\left(\theta_1/\theta_2\right)\cos c + 1\right]} \tag{6.92}$$

The variables of these expressions are defined in different ways according to the measurement system used. For the Couette system concentric cylinders, the variable is defined as:

$$s = \frac{\left(R_0^2 - R_i^2\right)\left(K - I\omega^2\right)}{4\pi L\, R_i^2\, R_0^2\, \omega} \tag{6.93}$$

In the previous expressions, θ_1 is the angular amplitude of the internal cylinder and θ_2 of the external cylinder, L is the height of the sample contained between the cylinders, I is the inertia moment of the internal cylinder with respect to its axis, ω is the frequency, c is the angle out of phase, and K is the restoration torque constant.

For parallel plates systems, in which the lower plate is subjected to oscillation, the variable s is calculated by the equation:

$$s = \frac{2h\left(K - I\omega^2\right)}{\pi a^2\, \omega} \tag{6.94}$$

h being the distance between plates to their radii, I the moment of inertia of the upper plate with respect to its axis, θ_1 the angular amplitude of the upper plate, θ_2 of the lower plate, and c the upper plate's angle out of phase.

In cone and plate systems in which the plate rotates, s is calculated using the following equation:

$$s = \frac{3\theta_0\left(K - I\omega^2\right)}{2a^2\, \omega} \tag{6.95}$$

where θ_0 is the cone's angle, θ_1 is the angular amplitude of the cone, and θ_2 of the plate, a is the radius of the plate, and c is the cone's angle out of phase.

6.12.1.3 Capillary Flow

When a liquid flows through a pipe it forms a velocity gradient, and a shearing effect occurs. Some methods have been developed to measure the flow properties of fluids by using capillary tubes through which a fluid is forced to flow due to an applied pressure or to hydrostatic pressure. If the volumetric flow, tube dimensions, and applied pressure are known, curves of flow can be plotted and the apparent values of the viscosity can be calculated. Certain assumptions should be made to develop general equations that allow calculating the shear rates and shear stresses for a specific point in the tube.

Rabinowitsch (van Wazer et al., 1963) developed a general equation to calculate the shear rates. This equation, valid for non-Newtonian as well as for Newtonian fluids, is:

$$\dot{\gamma} = \frac{3+b}{4\left(4q/\pi R^3\right)} \tag{6.96}$$

in which

$$b = \frac{d\log\left(4q/\pi R^3\right)}{d\log\left(\Delta PR/21\right)} \tag{6.97}$$

q is the volumetric flow through the capillary of length l and radius R, and P is the applied pressure. The value of the term b can be calculated when plotting $(4q/R^3)$ vs. $(\Delta PR/2\,\mathrm{l})$ in double logarithmic coordinates, b being the slope of the straight line built in such a way. For Newtonian liquids, the slope of the straight line is 1 and the equation reduces to:

$$\dot{\gamma} = 4q/R^3 \tag{6.98}$$

When the slope of the straight line deviates from 1, the fluid does not exhibit a Newtonian character, so the global equation should be used. The flow behavior of a variety of food suspensions has been studied using the capillary tube, e.g., applesauce, baby foods, and tomato purée (Charm, 1960; Saravacos, 1968; Rao et al., 1974).

6.12.1.7 Back Extrusion Viscometry

A way to characterize the rheological behavior of non-Newtonian fluids independent of time is by means of back extrusion tests. Back extrusion is produced when a small rod is submerged in a cylindrical vessel containing the sample to be tested (Figure 6.19). As the small rod penetrates, a sample movement is produced, but in an opposite direction to the rod penetration, hence the name "back extrusion."

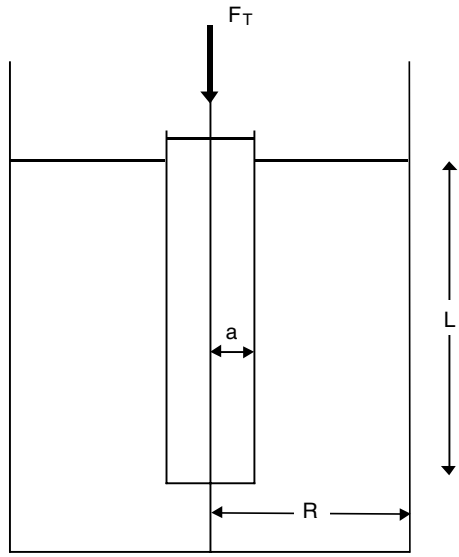

FIGURE 6.19
Position of a small rod and cylindrical vessel in a back extrusion test.

Osorio and Steffe (1987) have applied this type of experiment for the determination of the rheological parameters of fluids that obey the power law. Figure 6.20 shows the graphic obtained in a typical back extrusion experiment, in which the force applied to the small rod is greater each time, so that the length of the small rod that penetrates in the sample increases. The penetration stops at a force F_T, appearing at an equilibrium force F_{Te}.

When calculating the flow behavior index (n), it is necessary to perform two experiments, obtaining its value from the expression:

$$n = \frac{\ln\left[\left(\frac{F_{b_2}}{F_{b_1}}\right)\left(\frac{L_1}{L_2}\right)\right]}{\ln\left(v_1/v_2\right)} \tag{6.99}$$

where the subindexes 1 and 2 refer to the two experiments, v is the velocity of the small rod, L is the length of the small rod submerged in the sample, and F_b is the force corrected with the buoyancy force, defined by:

$$F_b = F_T - \rho g L \pi a^2 \tag{6.100}$$

where a is the radius of the small rod, ρ is the density of the sample, g is the gravitational acceleration, and F_T is the force just before the small rod stops.

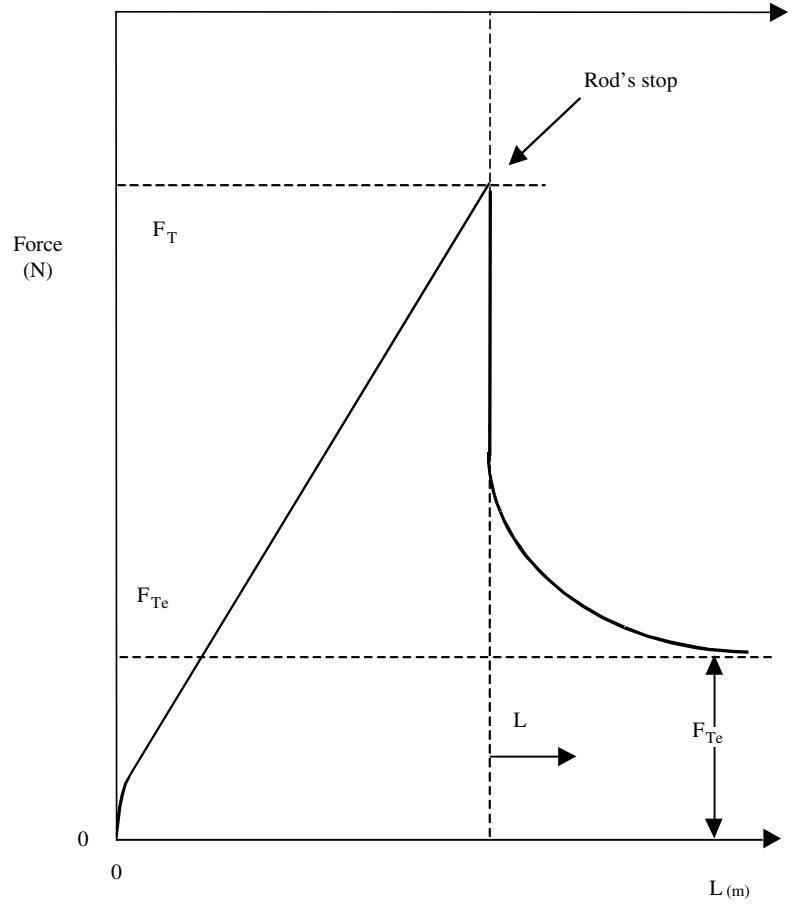

FIGURE 6.20
Typical data of back extrusion for a fluid of the power law.

To calculate the consistency index, the following equation is used:

$$k = \frac{R F_b K}{2\Gamma^2 \pi L R a}\left(\frac{\Phi R}{vK^2}\right) \tag{6.101}$$

where R is the radius of the external vessel, K is the relation between the radii of the small rod and the vessel ($K = a/R$), Φ is the dimensionless flow velocity, and Γ is the dimensionless radius when the stress is null. Φ as well as Γ are functions of K and of the flow behavior index, whose values are given in graphic form or tabulated (Osorio and Steffe, 1987; Steffe and Osorio, 1987).

This type of characterization can also be applied to fluids with Newtonian behavior, assuming that $n = 1$. In the same way, Herschel–Bulkley's and

Bingham's fluids corresponding rheological parameters can be obtained (Osorio, 1985; Osorio and Steffe, 1985). These fluids present a yield stress that is possible to determine using this type of experiment.

It is also possible to apply this technique to the rheological characterization of fluids that present dependence on time; thus, it has been applied to the rheological study of baby food made of macaroni and cheese (Steffe and Osorio, 1987).

6.12.1.8 Squeezing Flow Viscometry

When a fluid material is compressed between two parallel plates, the compressed material flows in a perpendicular direction to the compression force exerted. This is the base of the squeezing flow viscometry and can be used in the rheological characterization of fluids that present slippage problems (Campanella and Peleg, 1987a, b).

Four types of tests, which are at constant volume or constant area of the sample, allow an adequate rheological characterization, combined with the application of constant force or shear rate. Figure 6.21 presents the schemes of these four types of tests. To obtain the parameters of the power law for a determined sample by means of this technique, it is necessary to be sure that the sample does not present viscoelasticity. Next, calculate the consistency index (k) and the flow behavior index (n) for squeezing flow tests of a sample of constant area placed between two circular plates of radius R.

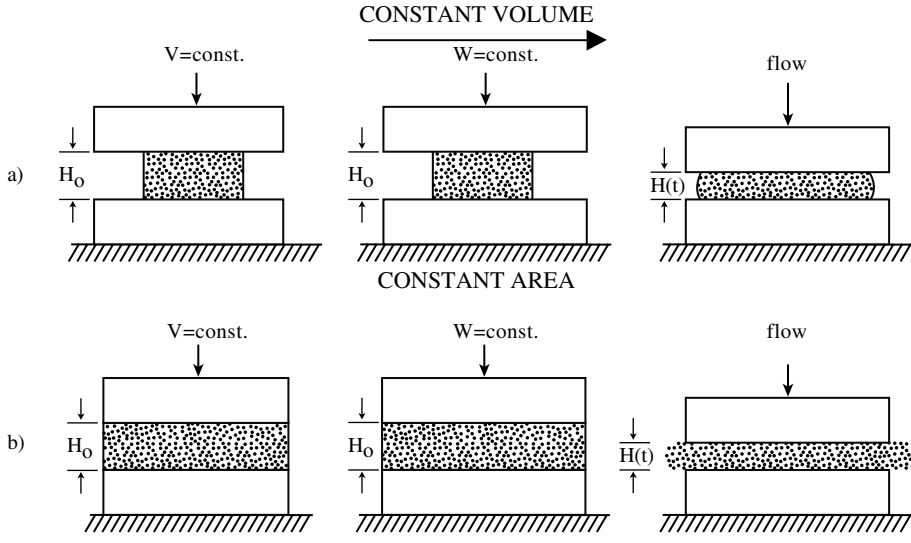

FIGURE 6.21
Types of squeezing flow viscometry tests.

For a constant shear rate (V_d), there is a variation of the sample height $H(t)$ and of the force $F(t)$ with time that can be related according to the expression (Campanella and Peleg, 1987a):

$$F(t) = \frac{3^{\frac{n+1}{2}} \pi R^2 k \left(V_d\right)^n}{\left[H(t)\right]^2} \tag{6.102}$$

from which it is possible to obtain the values of k and n through a nonlinear regression, fitting the experimental data of the variation of $F(t)$ with $H(t)$. These parameters can also be determined by an experiment at constant force. If W is the applied force and H_0 is the initial height of the sample, the variation of $H(t)$ with time is given by the expression (Campanella and Peleg, 1987a):

$$\ln\left[H(t)/H_0\right] = -St \tag{6.103}$$

in which:

$$S = \left[\frac{W}{3^{(n+1)/2} \pi R^2 k}\right]^{1/n} \tag{6.104}$$

To determine the consistency index k and the flow behavior index n, it is necessary to perform at least two experiments, since the slope S of Equation 6.103 contains the two parameters to be determined. Squeezing flow viscometry can also be used to determine the yield stress in products that exhibit it (Campanella and Peleg, 1987).

6.12.2 Empirical Methods

Many instruments have been developed to characterize the consistency of pureés (Rao, 1980). Rotational viscometers with spindles for which mathematical analysis is difficult have been used in empirical tests; the spindles can be needles with protuberances and fins. Kramer and Twigg (1962), Aronson and Nelson (1964), and Rao (1980) describe some of these methods used in the food industry.

6.12.2.1 Adams Consistometer

These instruments measure the consistency of foods based on the degree of extension or flow of the product in all directions in a given time. This type

of instrument has been used in tomato and pumpkin products, cereal cream, and bean pastes (Davis et al., 1954; Lana and Tscher, 1951; Mason and Wiley, 1958).

6.12.2.2 Bostwick Consistometer

This instrument measures the consistency of viscous materials by measuring the distance that a material flows in all directions in a given time. It has been used on ketchup (U.S.D.A., 1953), preserves and canned foods (Davis et al., 1954), and milk pudding (Rutgus, 1958).

6.12.2.3 Tube Flow Viscometer

This viscometer is used to measure the time needed by a determined quantity of fluid to cross a tube or capillary. This type of instrument is especially good for highly mobile materials, as is the Ostwald viscometer. Davis et al. (1954) used this type of viscometer to measure the consistency of tomato paste. They showed that the data obtained with the Adams and the Bostwick consistometers were linearly related and that, with use of the Efflux viscometers, different parameters to those from the consistometer are obtained.

6.12.3 Imitative Methods

In special cases, these methods measure rheological properties under symmetry conditions similar to those presented in practice. This group includes the Brabender Visco Amylograph used in the evaluation of the consistency of flours, starches, and gums (Bhattacharya and Sowbhagya, 1978). The sample is placed in a container and the torque exerted on a rotational spade is measured. The temperature of the sample is raised or lowered at constant velocity and the results are recorded on a mobile registration paper. Also in this group is the Messtometer, which consists of a flow bridge in which the conduits are arranged in a way such that a differential pressure between two reference points is produced. The differential pressure in the flow bridge is given as a function of consistency (Eolkin, 1957).

TABLE 6.4

Rheological Models for Time Independent Viscous Foods

Denomination	Equation	Notes
Newton's Law	$\sigma = \eta\dot{\gamma}$	1 Parameter
Bingham's Model	$\sigma = \eta_{pl}\dot{\gamma} + c$	2 Parameters
Ostwald-de-Waele Nutting's Model or Power Law	$\sigma = \eta(\dot{\gamma})^n$	2 Parameters
Herschel–Bulkley Modified Power Law	$\sigma = \eta(\dot{\gamma})^n + c$	3 Parameters
Casson's Model	$\sigma^{0.5} = k_1 + k_2(\dot{\gamma})^{0.5}$	3 Parameters
Modified Casson's Equation	$\sigma^{0.5} = k_1' + k_2'(\dot{\gamma})^m$	3 Parameters
Elson's Equation	$\sigma = \mu\dot{\gamma} + B\text{sen}h^{-1} + \sigma_0$	3 Parameters
Vocadlo's Model	$\tau = (\tau_0^{1/n} + k\dot{\gamma})^n$	3 Parameters
Shangraw's Model	$\sigma = a\dot{\gamma} + b(1 - \exp(-c\dot{\gamma}))$	2 Parameters
Generalized Model	$\dot{\gamma} = \frac{1}{\eta_0}\left[\frac{1 + \left(\tau_{rz}/\tau_m\right)^{\alpha-1}}{1 + \left(\tau_{rz}/\tau_m\right)^{\alpha-1}\frac{\eta_\infty}{\eta_0}}\right]$	4 Parameters
Sutterby's Model	$\tau_{rz} = -\mu_0\left[\frac{\text{arcsen}\beta\dot{\gamma}}{\beta\dot{\gamma}}\right]^\alpha\dot{\gamma}$	3 Parameters
Springs Truncated Power Law	$\tau_{rz} = -\mu_0\left[\frac{\dot{\gamma}}{\dot{\gamma}_0}\right]^{n-1}\dot{\gamma}$	3 Parameters
Williamson's Model	$\tau = A\frac{\dot{\gamma}}{B + \dot{\gamma}} + \mu_\infty\dot{\gamma}$	3 Parameters
Sisko's Model	$\tau = A\dot{\gamma} + B\dot{\gamma}^n$	3 Parameters

Problems

6.1

The flow behavior of a 47.3°Brix clarified kiwi juice with a certain pectin content was determined, obtaining that the best model to describe such behavior is the power law equation. The rheological constants obtained, at different temperatures, are indicated in the following table:

T (°C)	*K* (mPa·s^n)	*n*
4	2780	0.68
10	2287	0.68
15	1740	0.68
20	1247	0.71
25	1146	0.68
30	859	0.71
35	678	0.73
40	654	0.71
45	557	0.73
50	515	0.73
55	467	0.74
60	404	0.75
65	402	0.74

(a) Calculate the flow activation energy in kJ/mol and)b) calculate the apparent viscosity of the kiwi juice with 47.3°Brix at 37°C, for a velocity gradient of 100 s^{-1}.

(a) The variation of viscosity with temperature can be correlated by an Arrhenius type equation, and in the case of non-Newtonian fluids, the consistency index is used instead of the viscosity:

$$K = K_0 \exp\left(\frac{E_a}{RT}\right)$$

When representing ln*K* against 1/*T*, a straight line is obtained with an intercept origin ordinate of ln(K_0) and a slope of E_a/R. Carrying out this fitting with the data in the table obtains: $K_0 = 3.5 \times 10^{-2}$ mPa·s^a, $E_a/R = 3097$ *K*, so the flow activation energy has a value of 25.75 kJ/mol.

(b) For a pseudoplastic fluid, the apparent viscosity is given by:

$$\eta_a = K\left(\dot{\gamma}\right)^{n-1}$$

For 37°C, it can be taken that the flow behavior index is n = 0.72. The consistency index can be obtained from the Arrhenius equation, with the K_0 and E_a values obtained in the last section, for $T = 310$ *K*. With these data it is obtained that $K = 763.5$ mPa·s^a. The apparent viscosity for a shear rate of 100 s^{-1} is $\eta_a = 210$ mPa·s.

6.2

The industries that process clarified juices without pectin usually concentrate them up to soluble solids content close to 70°Brix, in a multiple evaporation

system. The juice leaves the evaporation stage at 60°C and it should be cooled down to a storage temperature of 5°C by means of a plate heat exchanger followed by one in a spiral shape. The plate heat exchanger only allows fluids with viscosity lower than 1500 mPa·s. to pass through.

The variation of the viscosity with temperature for a clarified peach juice without pectin of 69°Brix can be expressed by means of the equation:

$$\eta = 7.76 \times 10^{-11} \exp\left(6690/T\right)$$

where η is the viscosity in Pa·s and T the absolute temperature. (a) Calculate the flow activation energy. (b) What is the minimum temperature to which a 69°Brix concentrate could be cooled using the plate heat exchanger?

(a) The variation of the viscosity with temperature can be correlated according to an Arrhenius type equation. When comparing the Arrhenius equation with that in the problem's statement, it is possible to obtain:

$$\eta = 7.76 \times 10^{-11} \exp\left(\frac{6690}{T}\right)$$

So E_a/R = 6690 *K*, an equation that allows a flow activation energy of E_a = 55.62 kJ/mol to be obtained.

(b) Since the maximum viscosity allowed by the plate heat exchanger is 1500 mPa·s, the exit temperature of the fluid, once cooled, should be such as to have a fluid viscosity of precisely 1.5 Pa·s at this temperature. The minimum exit temperature is attained when substituting the viscosity value (1.5 Pa·s) in the Arrhenius equation:

$$1.5 = 7.76 \times 10^{-11} \exp\left(\frac{6690}{T}\right)$$

and rearranging it yields T = 282.5 *K* = 9.5°C.

6.3

The influence of the soluble solids content on the rheological behavior of a clarified pear juice without pectin was studied. A 70°Brix concentrated industrial juice was taken and, by means of dilution using distilled water, juices with concentrations within the 30 to 70°Brix range were obtained. It was found that at 25°C all of the juices exhibit a Newtonian behavior, obtaining the following viscosity each sample:

C(°Brix)	30	40	45	50	55	60	65	70
η (mPa·s)	3	5	8	13	19	41	74	233

Obtain an expression that describes the influence of the soluble solids content on viscosity. In one of the stages of the industrial process, the pear juice should circulate through a pipe, having available a centrifuge pump that can propel fluids that have a maximum viscosity of 100 mPa·s. Would this pump be useful to propel a 68°Brix juice at 25°C? What is the maximum concentration that this pump can propel?

The variation of the viscosity with the soluble solids content can be correlated by either of the following expressions:

$$\eta = K_1 \exp(a_1 C) \quad \text{or} \quad \eta = K_2 (C)^{a_2}$$

These equations can be linearized if they are taken in a logarithmic form, and, with the data in the table, it is possible to find the different constants. From the fitting, the folllowing is obtained:

$$\eta = 7.9 \times 10^{-5} \exp(0.106C) \qquad r = 0.975$$

$$\eta = 9.3 \times 10^{-11} (C)^{4.89} \qquad r = 0.940$$

in which the viscosity is given in Pa·s if the soluble solids content is expressed in °Brix. It seems that the exponential model fits better, since its regression coefficient is higher.

If the exponential equation is taken, for a 68°Brix concentration it is obtained that the viscosity of such juice is 106.7 mPa·s. Since this viscosity is higher than 100 mPa·s, the pump could not propel the 68°Brix juice.

The 100 mPa·s viscosity corresponds to a 67.4°Brix juice, according to the exponential equation. For this reason, the available pump could only propel juices with soluble solids contents lower than 67.4°Brix.

6.4

The rheological behavior of a clarified raspberry juice was studied. From a 41°Brix concentrated juice with a pectin content of 0.5 g galacturonic acid/kg juice, different samples up to 15°Brix have been prepared by dilution with distilled water. The rheological behavior of these samples has been studied within the 5 to 60°C temperature range. It was determined that the power law is the model that best describes such behavior, obtaining that the consistency index and the flow behavior index vary with temperature and soluble solids content according to the expressions:

$$K = 1.198 \times 10^{-10} \exp\left(\frac{4560}{T} + 0.196C\right)$$

$$n = 1.123 - 8.52 \times 10^{-3} C$$

where K is in Pa·s^n, T is in Kelvin, and C is in °Brix.

What is the value of the flow activation energy, expressed in kcal/mol and kJ/mol?

An industry that concentrates clarified raspberry juices needs to know the viscosity of a 27°Brix juice that should circulate at 50°C through a stainless steel pipe. If the velocity gradient exerted on such juice along the pipe is 100 s^{-1}, what is the viscosity in mPa·s?

According to the expressions that describe the temperature–concentration combined effect:

$$K = K_1 \exp\left(\frac{E_a}{RT} + K_2 C\right)$$

indicating that

$E_a = 4560\ R$

$E_a = 4560\ K\ 1.987 \times 10^{-3}$ kcal/(mol.K) = 9.06 kcal/mol

$E_a = 4560\ K\ 8.314 \times 10^{-3}$ kJ/(mol.K) = 37.91 kJ/mol

For 27°Brix raspberry juices, the flow behavior index at 50°C (323 K) is n = 0.893, while the consistency index will be K = 32.2 mPa·s^n.

The apparent viscosity of a fluid that obeys the power law is: $\eta_a = K(\dot{\gamma})^{n-1}$. When substituting the obtained data for the consistency and flow behavior indexes in the exponential equation and for a shear rate of 100 s^{-1}, an apparent viscosity of 19.7 mPa·s is obtained.

7

Transport of Fluids through Pipes

7.1 Introduction

The transport of fluids through pipes is very important in many industrial processes and is considered as a unit operation within engineering. In the study of transport, the type of fluid should be known and should be classified:

- According to the behavior presented under the action of external pressures. The fluids may be compressible or incompressible. If the volume of the fluid is independent of its pressure and temperature, then the fluid is incompressible; on the other hand, if the volume varies, the fluid is compressible. Actually, no fluid is incompressible, although liquids may be considered as such. However, gases present a large variation of compressibility with pressure and temperature.
- According to the effects produced by the shear stresses on a fluid. These can be classified as Newtonian and non-Newtonian; whether or not they follow Newton's viscosity law will determine the type of velocities profile of the fluid inside pipes.

Depending on the relation existing between the shear stress (σ) applied to a fluid and its shear rate ($\dot{\gamma}$), the main equations that describe the rheological behavior of a fluid food, as seen in Chapter 6, are:

Newton's equation: $$\sigma = \eta\dot{\gamma} \tag{7.1}$$

Power law: $$\sigma = K\dot{\gamma}^{n} \tag{7.2}$$

Bingham's equation: $$\sigma = \sigma_0 + \eta'\dot{\gamma} \tag{7.3}$$

Herschel–Bulkley's model: $$\sigma = \sigma_0 + K_H\dot{\gamma}^{n} \tag{7.4}$$

where:
- η = viscosity
- K = consistency index
- n = flow behavior index
- σ_o = yield stress
- η' = plastic viscosity

It can be observed that the first three models are variants of the Herschel–Bulkley model if σ_o is zero and n is the unit for the first, if σ_o is zero for the second, and if η' is equivalent to K_H and n is equal to one in the third model.

The fundamental problem presented when studying the flow of fluids inside piping is to know and find equations that relate the pressure loss of the fluid inside the pipe, depending on the flow and on the different properties of the fluid, as well as on the characteristics and dimensions of the pipe. Once these relationships are known by mass and energy balances, it is possible to calculate the power needed to transport the food fluid through the piping.

7.2 Circulation of Incompressible Fluids

As mentioned before, incompressible fluids are those that, when circulating isothermally through a pipe, have the same density at any point, that is, the density remains constant. Although under nonisothermal conditions the density depends on temperature, all the equations for isothermal circulation of incompressible fluids can be applied to isothermal circulation, making a very small error.

7.2.1 Criteria for Laminar Flow

In the circulation of incompressible fluids through pipes, one should have in mind the type of fluid. Fluids can circulate in laminar or turbulent regime, depending on the value of the Reynolds number or module (Re) (Coulson and Richardson, 1979; McCabe et al., 1985), which is dimensionless and defined as:

$$\mathrm{Re} = \frac{v\, d\, \rho}{\eta} \tag{7.5}$$

where:
- v = mean velocity of the fluid in the pipe
- d = internal diameter of the pipe
- ρ = density of the fluid
- η = viscosity of the fluid

This number is a measure of the ratio between the inertia forces and the viscosity or friction forces at each point of a moving fluid. The types of circulation regimes according to the value of the Reynolds number are:

Re < 2100	Laminar regime
2100 < Re < 4000	Transition regime
4000 < Re < 10,000	Practically turbulent regime
10,000 < Re	Turbulent regime

The Reynolds number has been defined in Equation 7.5 for Newtonian fluids; however, for non-Newtonian fluids, this number is defined differently (Charm, 1971; Rao, 1992; Levenspiel, 1993; Singh and Heldman, 1993). Thus, for Bingham plastics, power law fluids, or fluids of the Herschel–Bulkley type, there exist the following equations:

- Bingham plastics

$$\mathrm{Re}_B = \frac{v\, d\, \rho}{\eta'} \tag{7.6}$$

- Power law and Herschel–Bulkley fluids: a generalized Reynolds number Re_G for these fluids is defined as:

$$\mathrm{Re}_G = \frac{d^n\, v^{2-n}\, \rho}{8^{n-1}\, K}\left(\frac{4n}{1+3n}\right)^n \tag{7.7}$$

Newtonian fluids are said to circulate under laminar regime if the Reynolds number is lower than 2100. However, if the fluids are non-Newtonian, a different criterion applies. The critical value of the Reynolds number is defined as the number from which the fluid stops circulating under laminar regime.

For power law fluids, the critical value of the Reynolds number (Steffe and Morgan, 1986) is given by:

$$\left(\mathrm{Re}_G\right)_{Critical} = \frac{6464\, n}{\left(1+3n\right)^2\left(\frac{1}{2+n}\right)^{(2+n)/(1+n)}} \tag{7.8}$$

A plot of this equation is shown in Figure 7.1. The critical value of the Reynolds number shows a maximum of 2400 for a flow index of 0.4. From here, the value decreases to 2100, the correspondent value to a Newtonian fluid (n = 1).

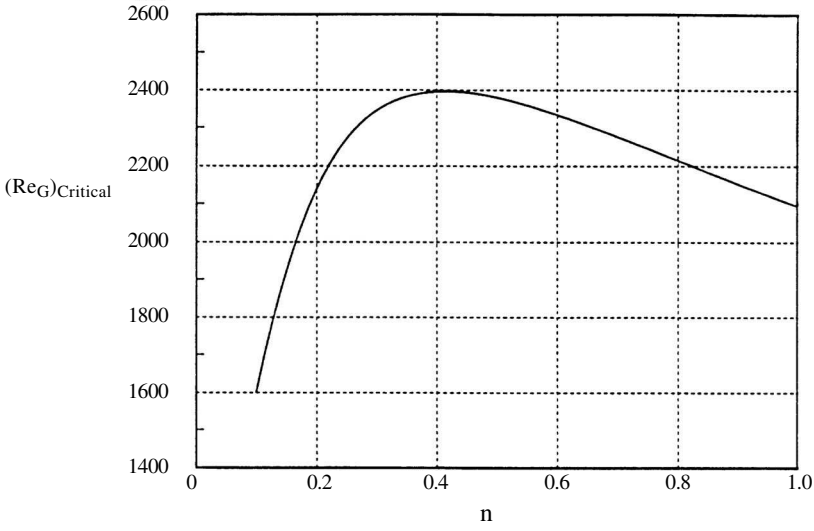

FIGURE 7.1
Variation of the critical Reynolds number with the flow index for power law fluids. (Adapted from Steffe, 1992a).

For Bingham plastics it is necessary to define a parameter m, which is the relation between the yield stress and the shear stress that the fluid exerts on the wall (σ_W) of the pipe through which it flows:

$$m = \sigma_0 / \sigma_w \tag{7.9}$$

The value of the critical Reynolds number for a Bingham plastic can be calculated from the following expression:

$$\left(\mathrm{Re}_B\right)_{Critical} = \frac{He}{8\, m_c}\left(1 - \frac{4m_c}{3} + \frac{m_c^4}{r}\right) \tag{7.10}$$

in which m_c is a critical value of m, obtained from the following relation:

$$\frac{m_c}{\left(1 - m_c\right)^3} = \frac{He}{16,800} \tag{7.11}$$

where He is the Hedstrom number, defined by:

$$He = \frac{\sigma_0\, d^2 \rho}{\left(\eta'\right)^2} \tag{7.12a}$$

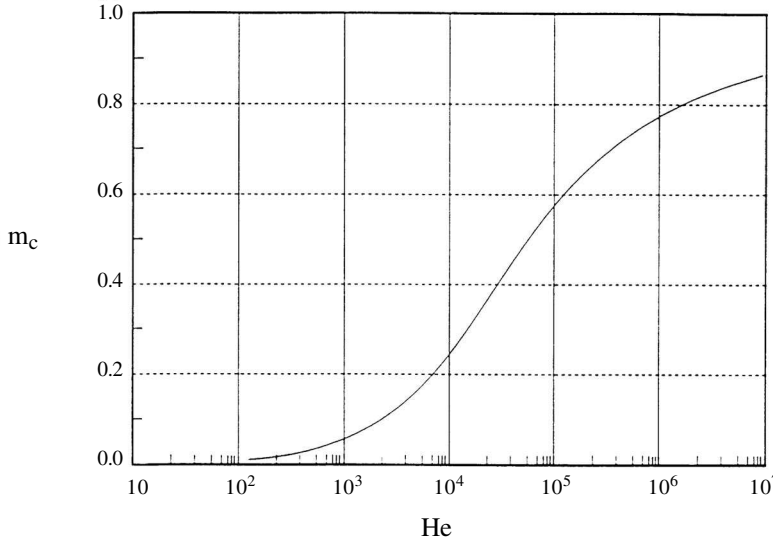

FIGURE 7.2
Variation of m_C with the Hedstrom number for Bingham plastics. (Adapted from Steffe, 1992a).

The variation of the critical value (m_c) with the Hedstrom number correspondent to Equation 7.11 is shown graphically in Figure 7.2. Also, the variation of the critical Reynolds number as a function of the Hedstrom number is shown in Figure 7.3. For high-yield stress values, the correspondent value of the Hedstrom value is high (Figure 7.2), implying that the Reynolds number is high as well (Equation 7.10). Therefore, in these cases it is very difficult for the fluid to circulate under turbulent regime.

For fluids of the Herschel–Bulkley type, the critical value of the generalized Reynolds number can be obtained as a function of the Hedstrom number and the flow index, as can be seen in Figure 7.4 (Hanks and Ricks, 1974; Steffe and Morgan, 1986). When using this graph, the generalized Hedstrom number, defined by the following expression, must be calculated:

$$He_G = \frac{d^2\rho}{K}\left(\sigma_0 / K\right)^{\left(2/n\right)-1} \tag{7.12b}$$

7.2.2 Velocity Profiles

The graph obtained from plotting the variation of the point velocity of the fluid with respect to the radius of the pipe is known as the velocity profile for circular pipes. The velocity profile varies with the value of the Reynolds number.

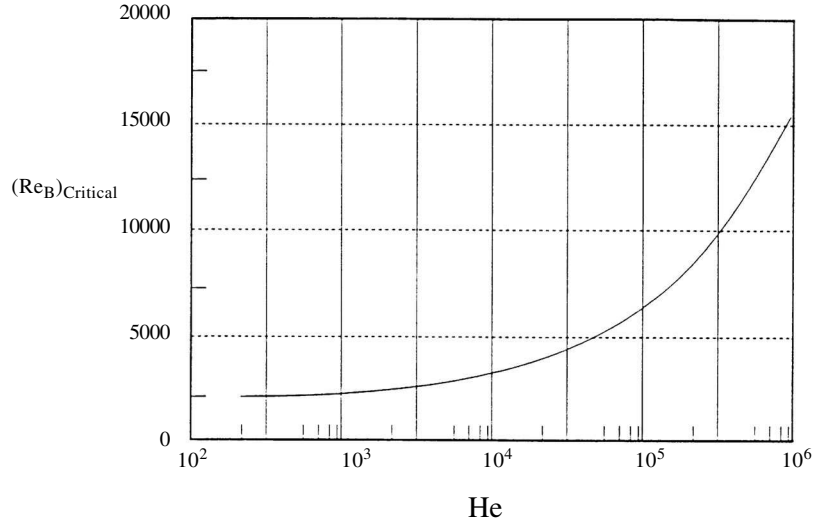

FIGURE 7.3
Variation of the critical Reynolds number with the Hedstrom number for Bingham's plastics. (Adapted from Steffe, 1992a).

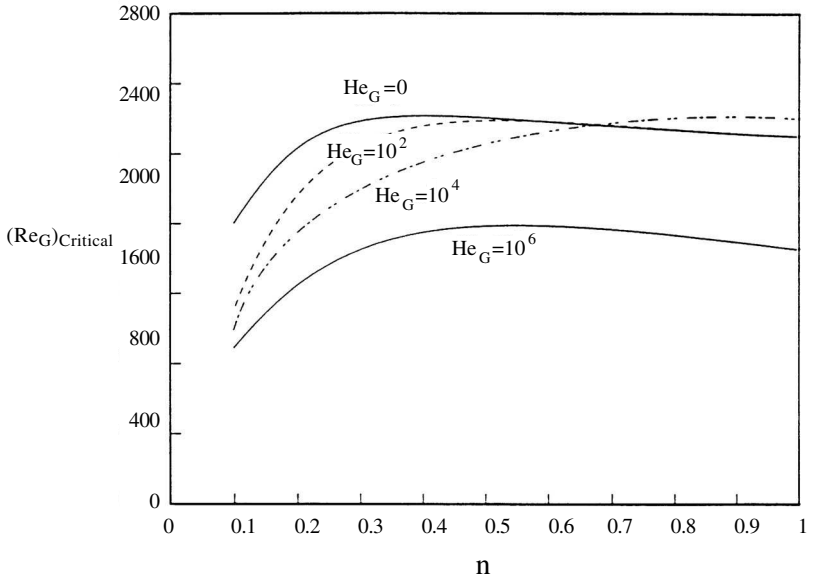

FIGURE 7.4
Critical Reynolds number as a function of the Hedstrom number and the flow index for Herschel–Bulkley fluids.

The velocity profile of a moving fluid depends on the type of flow regime, so different velocity profiles will be obtained depending on whether the flow is laminar or turbulent. Knowledge of this profile is very valuable, since velocity is one of the variables in the kinetic energy term of Bernoulli's equation. Likewise, it is used to calculate the volumetric flow rate.

7.2.2.1 Laminar Regime

The velocity profile in the direction of the stream on the cross section of a fluid circulating through a pipe is not uniform. If the fluid circulates under laminar regime, this profile can be calculated (Coulson and Richardson, 1979; McCabe et al., 1985; Singh and Heldman, 1993) depending on the geometrical characteristics of the pipe through which it flows.

7.2.2.1.1 Newtonian Fluids

The velocity profile presented by a Newtonian fluid circulating under laminar regime by a pipe of a circular cross section is given by the expression:

$$\mathrm{v} = \frac{\left(P_1 - P_2\right)R^2}{4\eta L}\left[1 - \left(\frac{r}{R}\right)\right]^2 \tag{7.13}$$

where:

P_1 = the pressure of the fluid at the entrance of the pipe
P_2 = pressure of the fluid at the outlet of the pipe
R = internal radius of the pipe
r = radius of the pipe at any position
L = length of the pipe

Equation 7.13 indicates that the velocity profile is parabolic. The maximum velocity occurs at the center of the pipe (for $r = 0$), where the effect of the shear stress is minimum:

$$v_{\max} = \frac{\left(P_1 - P_2\right)R^2}{4\,L\,\eta} \tag{7.14}$$

So, when substituting Equation 7.14 in Equation 7.13, a different expression for the point velocity is obtained:

$$v = v_{\max}\left[1 - \left(\frac{r}{R}\right)^2\right] \tag{7.15}$$

The volumetric flow rate for the fluid circulating through the pipe is obtained from the following substitution:

$$q = \int_S v dS = \frac{\left(P_1 - P_2\right) R^4 \pi}{8 L \eta} \tag{7.16}$$

in which S is the flow area or cross-sectional area. This expression is known as the Hagen–Poiseuille equation (Charm, 1971; McCabe et al., 1985; Singh and Heldman, 1993).

The mean circulation velocity is obtained by integrating the volumetric flow and the flow area of all the stream points and filaments (McCabe, 1985):

$$v_m = \frac{\int v dS}{\int dS} = \frac{q}{\Pi R^2} = \frac{\left(P_1 - P_2\right) R^2}{8 L} = \frac{v_{\max}}{2} \tag{7.17}$$

It is also interesting to know the value of the shear stress at each point of a pipe section:

$$\sigma = -\eta \frac{dv}{dr} = \frac{\left(P_1 - P_2\right)\eta}{2L} = \frac{4 v_m \eta}{R^2} r \tag{7.18}$$

indicating that the shear stress profile varies linearly with the radius of the pipe, being maximum at the wall and null at the center of the pipe:

For $r = 0$ $\sigma = 0$

For $r = R$ $\sigma_w = \dfrac{4 v_m \eta}{R}$

7.2.2.1.2 Non-Newtonian Fluids

In an analogous way to the analysis of Newtonian fluids, it is possible to determine the volumetric flow rate and mean velocity for power law fluids, Bingham plastics, and Herschel–Bulkley fluids (Dodge and Metzner, 1959; Skelland, 1967; Heldman, 1975; Toledo, 1993). The equations used to evaluate such parameters are given below.

Velocity profile:

- Power law fluid:

$$v = \frac{n}{n+1}\left(\frac{\Delta P}{2KL}\right)^{1/n}\left[R^{n+1/n} - r^{n+1/n}\right] \tag{7.19}$$

in which ΔP is the difference of pressures between the entrance and exit of the pipe.

- Bingham plastic:

  In this type of fluid, a central vein of maximum velocity is produced, which has a straight profile. The value of the radius r_0 for this central vein is:

$$r_0 = \frac{2\sigma_0 L}{\Delta P} \tag{7.20a}$$

  For $r_0 \le r \le R$, the velocity profile is given by:

$$v = \frac{1}{\eta'}\left[\frac{\Delta P}{4L}\left(R^2 - r^2\right) - \sigma_0\left(R - r\right)\right] \tag{7.20b}$$

- Fluid of the Herschel–Bulkley type:

  As in the case of Bingham plastics, a central vein of flat profile appears, having a maximum velocity. The radius corresponding to this vein, r_0, is obtained from Equation 7.20a, described earlier for Bingham plastics.

- For $r_0 \le r \le R$, the velocity profile will be:

$$\mathrm{v} = \frac{2L}{\Delta P\left(b+1\right)K^b}\left(\left(\sigma_w - \sigma_0\right)^{b+1} - \left(\frac{r\Delta P}{2L} - \sigma_0\right)^{b+1}\right) \tag{7.21}$$

  in which $b = 1/n$.

Volumetric flow rate:

- Power law fluid:

$$q = \pi R^3\left(\frac{n}{3n+1}\right)\left(\frac{\sigma_w}{K}\right)^{1/n} \tag{7.22}$$

- Bingham plastic

$$q = \frac{\pi R^3}{4}\frac{\sigma_w}{\eta'}\left[1 - \frac{4}{3}\left(\frac{\sigma_0}{\sigma_w}\right) + \frac{1}{3}\left(\frac{\sigma_0}{\sigma_w}\right)^4\right] \tag{7.23}$$

  This is called Buckingham's equation.

- Herschel–Bulkley fluid:

$$q = \pi R^3 \frac{\left(\sigma_w - \sigma_0\right)^{m+1}}{\sigma_w^3 K^m}\left[\frac{\left(\sigma_w - \sigma_0\right)^2}{m+3} + \frac{2\sigma_0\left(\sigma_w - \sigma_0\right)}{m+2} + \frac{\sigma_0^2}{m+1}\right] \tag{7.24}$$

in which $m = 1/n$, and n = the flow behavior index.

Mean velocity:
The mean velocity is calculated from the volumetric flow rate, dividing the corresponding equation by the flow area:

$$v_m = \frac{q}{\pi R^2}$$

For the power law fluids, the relation between the point and the mean velocities is given by:

$$\frac{v}{v_m} = \frac{3n+1}{n+1}\left[1 - \left(\frac{r}{R}\right)^{(n+1/n)}\right] \tag{7.25}$$

The variation of the dimensionless velocity profile (v/v_m) as a function of the dimensionless radius (r/R) for this type of fluid can be observed in Figure 7.5. The profile depends on the value of the flow behavior index. For $n = 1$, in which the fluid is Newtonian, the resulting profile is parabolic, as mentioned before. The value of the maximum velocity occurs at the center of the pipe and can be calculated by:

$$\frac{v_{\max}}{v_m} = \frac{3n+1}{n+1} \tag{7.26}$$

For Bingham plastics, the value of the dimensionless velocity is a function of the parameter that relates the shear stresses (Equation 7.9), so there are two expressions. For $1 \geq r/R \geq m$:

$$\frac{v}{v_m} = \frac{2\left[1 - 2m + \frac{2mr}{R} - \left(\frac{r}{R}\right)^2\right]}{1 - \frac{4m}{3} + \frac{m^4}{3}} \tag{7.27a}$$

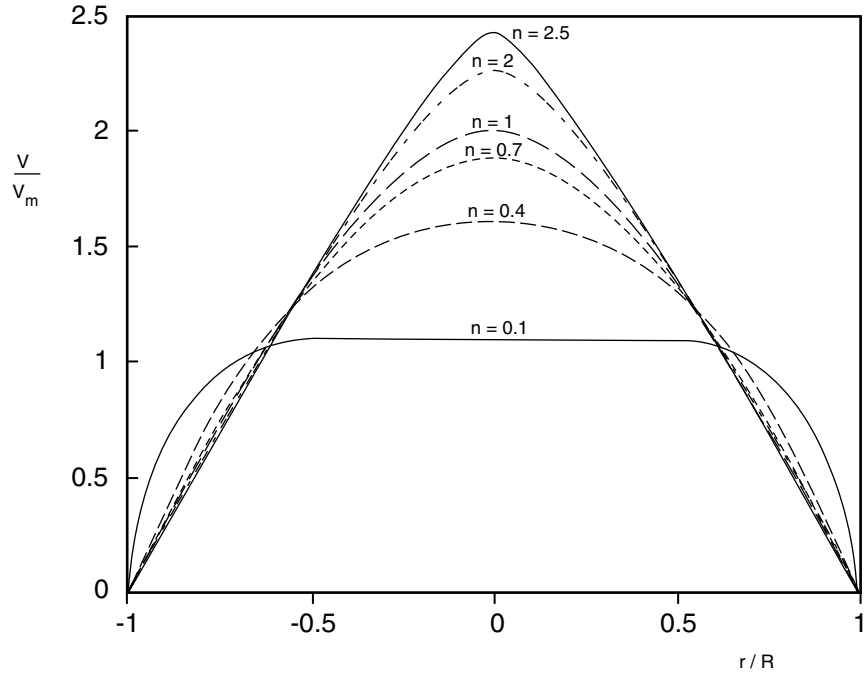

FIGURE 7.5
Velocity profile for power law fluids as a function of the flow behavior index. (Adapted from Steffe, 1992a).

For $r/R \leq m$:

$$\frac{v}{v_m} = \frac{2(1-2m)^2}{1-4m/3+m^4/3} \tag{7.27b}$$

The dimensionless velocity profile for Bingham plastics is graphically represented in Figure 7.6. It can be observed that such a profile depends on the value of m.

7.2.2.2 Turbulent Regime

When a fluid circulates through a pipe under turbulent regime, three zones can be distinguished in the liquid vein. It is assumed that a laminar layer of fluid in contact with the pipe wall develops due to the shear stresses, and this layer is supposed to be in laminar regime. On the contrary, turbulence predominates at the center of the pipe, forming a completely flat front. Between these two zones is one of transition, as shown in Figure 7.7.

As the value of the Reynolds number increases, the thickness of the laminar and transition zones becomes thinner. The laminar sublayer is extremely

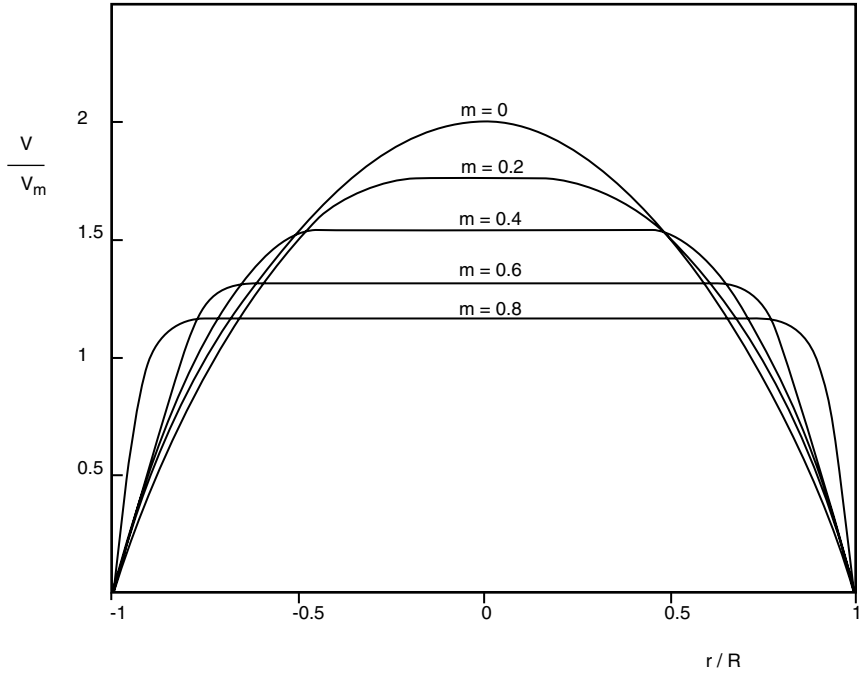

FIGURE 7.6
Velocity profile for Bingham plastics as a function of the parameter *m*. (Adapted from Steffe, 1992a).

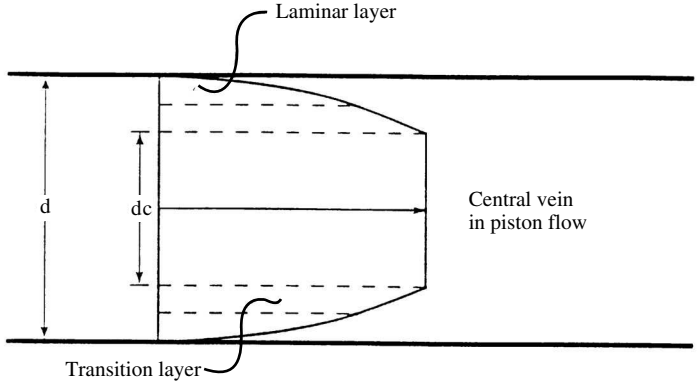

FIGURE 7.7
Velocity profile under turbulent regime.

important, since transport in this layer is performed by molecular mechanisms. Although no theoretical equation has been deduced to obtain the velocity profile for a turbulent regime, an equation that adequately describes such a profile can be obtained experimentally. Thus, the equation that can be used is:

$$v_m = v_{\max}\left(1 - r/R\right)^{1/c} \tag{7.28}$$

in which c is a constant that depends on the value of the Reynolds number and has the following values (Steffe, 1992a):

$c = 6$ for $\mathrm{Re} = 4 \times 10^3$
$c = 7$ for $\mathrm{Re} = 1 \times 10^5$
$c = 10$ for $\mathrm{Re} = 3 \times 10^6$

Equation 7.28 can be applied to many industrial pipes for values of $c = 7$ (Coulson and Richardson, 1979).

The mean velocity can be calculated in an analogous way as for laminar regime, resulting in the following expression:

$$v_m = v_{\max}\frac{2c^2}{(1+c)(1+2c)} \tag{7.29}$$

This equation approximates well to the experimental results, since when plotting $v_m/v_{\max}$ vs. the Reynolds number, a curve that fits to this equation is obtained (Figure 7.8).

For $\mathrm{Re} \geq 10^4$, the relation $v_m/v_{\max}$ can approximate to 0.82, which coincides with the result obtained from Equation 7.29 for a value of $c = 7$.

For power law fluids transported through smooth pipes, the relation $v_m/v_{\max}$ is a function of the generalized Reynolds number and the flow behavior index, as indicated in Figure 7.9 (Dodge and Metzner, 1959).

7.2.2.3 Flow in Noncylindrical Piping

If the transport pipe has a shape other than cylindrical, the equations previously mentioned can be used, with the exception that the diameter of the pipe is substituted by the equivalent diameter. The equivalent diameter (D_e) is defined as four times the hydraulic radius (R_H) that corresponds to the relation between the flow area and the wet perimeter (Charm, 1971; Perry and Chilton, 1973):

$$D_e = 4R_H = 4\frac{\text{Flow area}}{\text{Wet perimeter}} \tag{7.30}$$

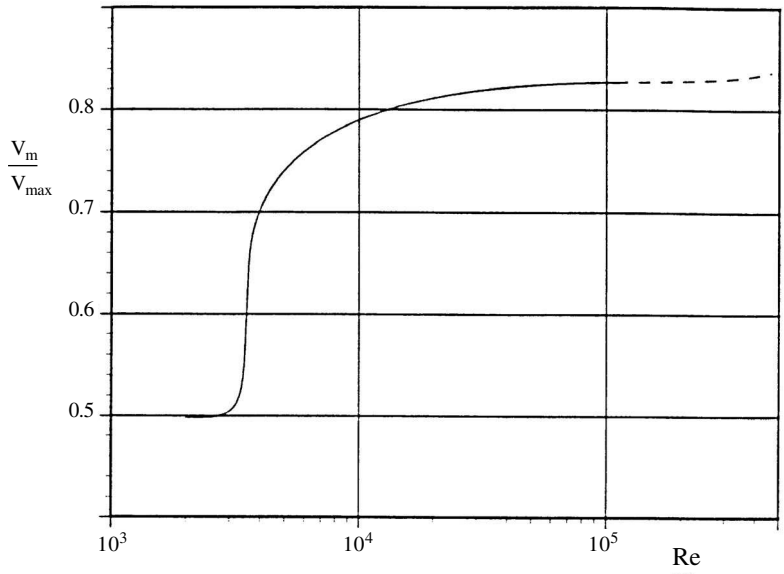

FIGURE 7.8
Variation of (v_m/v_{max}) with the Reynolds number for a turbulent regime

The expressions that allow the calculation of equivalent diameter for piping with cross sections different than circular are given next.

Annular section piping:

$$De = d_0 - de$$

where d_0 corresponds to the internal diameter of the external pipe and de is the external diameter of the internal pipe.

Rectangular section piping:

$$De = 2ab/(a+b)$$

In this case a and b are the width and length, respectively, of the cross section.

Equilateral triangle piping:

$$De = 2h/3$$

where h is the height of the triangle.

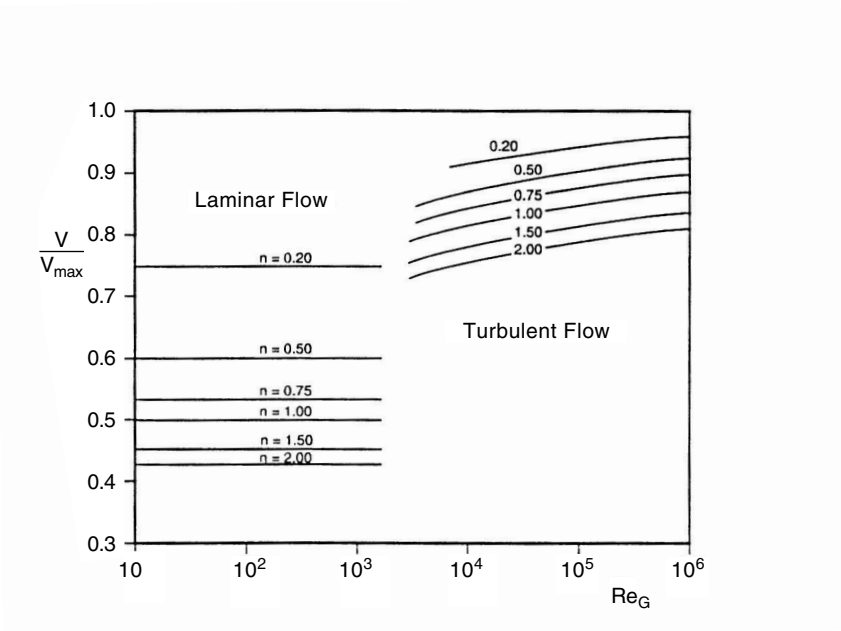

FIGURE 7.9
Variation (v/v_{max}) as a function of the generalized Reynolds number for power law fluids.

7.2.3 Universal Velocity Profiles

Using Prandtl's theory based on the length of the mixture, an equation for the distribution of velocities under turbulent regime can be deduced (Bird et al., 1960; Skelland, 1967; Welty et al., 1976; Coulson and Richardson, 1979).

Three zones are considered in the liquid stream for Newtonian fluids. In the laminar sublayer, the velocity on the wall of the piping is zero. Also, due to the laminar layer's small thickness, it can be assumed that the shear stress is constant and equal to the shear stress on the wall ($\sigma = \sigma_w$):

$$\sigma = \sigma_w = \eta \frac{dv}{dy} \tag{7.31}$$

complying that $v = 0$ for $y = 0$.

Therefore, the velocity profile is linear:

$$v = \frac{\sigma_w}{\eta} y$$

The velocity distribution under turbulent flow can be expressed as a function of the parameters, as defined by the following expressions:

$$v^* = \left(\frac{\sigma_w}{\rho} \right)^{1/2} \tag{7.32}$$

$$v^+ = \frac{v}{v^*} \tag{7.33}$$

$$y^+ = \frac{y\, v^*}{\eta/\rho} \tag{7.34}$$

where:

v^* = friction or shear velocity
v^+, y^+ = the dimensionless velocity and coordinate, respectively

These relations are valid when the velocity (v) varies linearly with y.

For the laminar sublayer, the radius is, practically, the pipe radius and it can be assumed that $r = R$. When substituting the dimensionless equations, as defined in Equation 7.31, it is obtained that:

$$\frac{d\, v^+}{d\, y^+} = 1$$

Integrating with boundary condition $v^+ = 0$ for $y^+ = 0$, it is deduced that, in the laminar sublayer, the velocity distribution will be:

$$v^+ = y^+ \tag{7.35}$$

According to experimental data, this equation is valid for y^+ values between 0 and 5 ($0 < y^+ < 5$).

For the transition zone, the equation that gives the variation of velocity with distance is:

$$v^+ = 5 \ln y^+ - 3.05 \tag{7.36}$$

for $5 < y^+ < 30$ values.

In the turbulent zone the equation to use is:

$$v^+ = 2.5 \ln y^+ + 5.5 \tag{7.37}$$

for $y^+ > 30$.

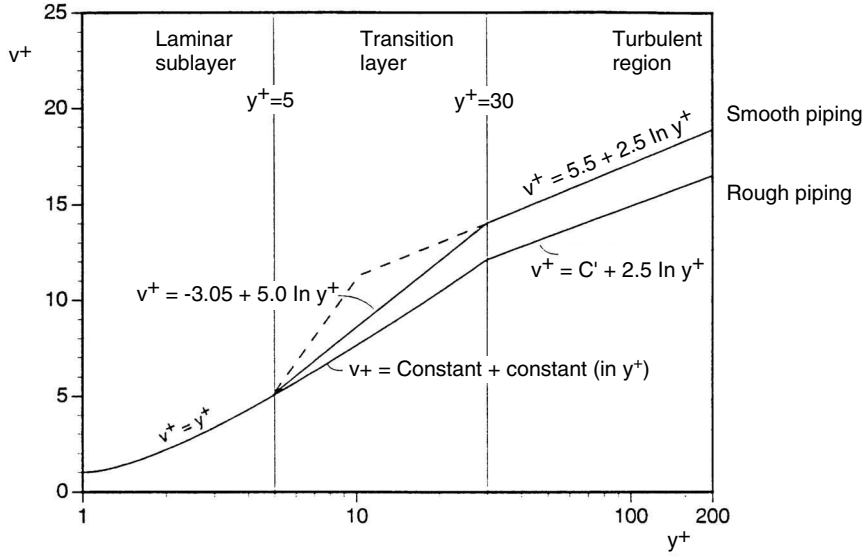

FIGURE 7.10
Universal profile of velocities.

Figure 7.10 presents a graphical representation of the equations of the universal profile of velocities, where the values of v^+ are represented on the ordinates using a decimal scale, and the y^+ values on the abscissas using a logarithmic scale.

The equations of the universal profile of velocities show some inconsistencies, due to their empirical nature. Thus, the turbulent zone (Equation 7.37) foresees a finite gradient of velocity in the center, where it should be zero. These equations are valid for smooth pipes and do not comply well with the transition zone for values of the Reynolds number between 2100 and 10^4. In spite of all the limits, these equations can be used to design dependable equipment.

In the case of pipes that are not smooth, the roughness (ε) should be taken into account. There may be cases of completely rough pipes whose roughness reaches the turbulent zone. In this case, Equation 7.37 is modified to:

$$v^+ = 2.5\ln\left(y^+/\varepsilon\right) - 8.5 \tag{7.38}$$

The universal profile of velocities for non-Newtonian fluids was developed for power law fluids by Dodge and Meztner (1959) and Skelland (1967). In this case the position variable, y^+, is defined by:

$$y^+ = y^n\left(v^*\right)^{2-n}\rho/K \tag{7.39}$$

The velocity profiles are obtained from the following equations. For the laminar sublayer:

$$v^+ = \left(y^+\right)^{1/n} \tag{7.40}$$

For the turbulent sublayer:

$$v^+ = \frac{5.66}{n^{0.75}}\log\left(y^+\right) - \frac{5.66}{n^{1.2}} + \frac{3.475}{n^{0.75}}\left[1.96 + 0.815n - 1.628n\log\left(3 + \frac{1}{n}\right)\right] \tag{7.41}$$

7.3 Macroscopic Balances in Fluid Circulation

Consider that fluid circulates under a steady state. The balances performed are of mass, momentum, energy, and mechanical energy that allow one to obtain the continuity and Bernoulli equations (Foust et al., 1980; McCabe et al., 1985; Steffe and Morgan, 1986; Rao, 1992; Levenspiel, 1993; Singh and Heldman, 1993).

7.3.1 Mass Balance

The mass balance applied to a pipe between two points in sections S_1 and S_2 (Figure 7.11) under steady state can be expressed by:

$$w_1 = w_2 \tag{7.42a}$$

Since this is a process in which there is no accumulation, the mass flow rate (w) in the entrance and exit sections is the same.

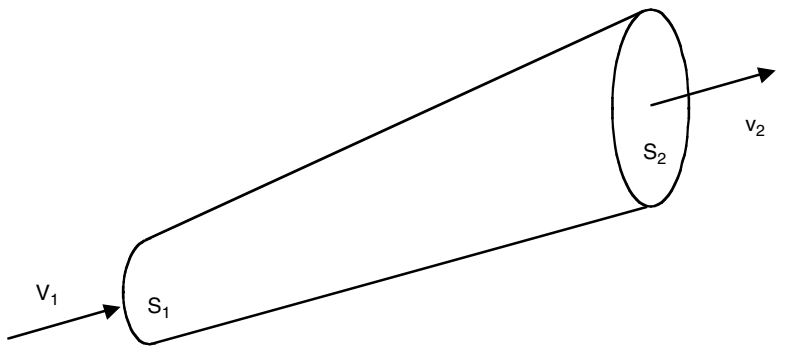

FIGURE 7.11
Pipe section.

Taking into account that the flow or mass flow rate can be expressed as

$$w = \rho S v_m \tag{7.42b}$$

in which S is the cross section of the pipe and v_m is the mean velocity of the fluid, for any section of the pipe:

$$\rho S v_m = C \tag{7.43}$$

in which C is a constant. This expression is known as the continuity equation.

In such an equation a mean velocity should be used, since all the points of the same section do not have the same velocity. For this reason the mean velocity is defined according to the following expression:

$$v_m = \frac{\int_S v\, dS}{S} \tag{7.44}$$

The product of the mean velocity times the density is denominated mass flux:

$$G = v_m \rho \tag{7.45}$$

It is deduced from the continuity equation that, in pipes of constant section, the mass flux is constant too, since $S_1 = S_2$; and if it is an incompressible fluid, or its density remains constant, the mean velocity through a uniform section of piping will be constant.

7.3.2 Momentum Balance

The momentum balance under steady state is based on Newton's second law of movement (Welty et al., 1976; Geankoplis, 1978; Costa et al., 1984; McCabe et al., 1985), which, applied to a pipe section (Figure 7.11), leads to the following expression:

$$w_1 (v_1)_m \beta_1 - w_2 (v_2)_m \beta_2 - P_1 \vec{S}_1 + P_2 \vec{S}_2 + m\vec{g} - \vec{F}_{\text{int}} + \vec{F}_{ext} = 0 \tag{7.46}$$

in which β is the velocity relation:

$$\beta = \frac{1}{S} \int \frac{(v^2)_m\, dS}{(v_m)^2} = \frac{(v^2)_m}{(v_m)^2} \tag{7.47}$$

This coefficient β serves to correct the velocity terms, due to the distribution of velocities in the different sections of the pipe (Harper, 1976; McCabe et al., 1985). For laminar regime, it can be demonstrated that:

$$\left(v^2\right)_m = \frac{\left(v_{\max}\right)^2}{3} \quad \text{and} \quad \left(v_m\right)^2 = \frac{\left(v_{\max}\right)^2}{4}$$

Therefore, β = 4/3.

Also, in such equations, m represents the mass of the fluid and F_{ext} are the external forces that can act on the fluid, causing changes in its momentum. F_{int} are the forces exerted by the fluid on the pipe walls, such as friction and stress forces, among others.

From Equation 7.46, the forces that act on each point of the pipe can be calculated, allowing the design of a fastening system for such pipes.

7.3.3 Total Energy Balance

The energy balance under steady state (Smith and Van Ness, 1975; Foust et al., 1980; Costa et al., 1984) applied to a pipe section is expressed as follows:

$$w_1\left(\hat{H}_1 + \hat{K}_1 + \hat{\phi}_1\right) - w_2\left(\hat{H}_2 + \hat{K}_2 + \hat{\phi}_2\right) + \dot{Q} + \dot{W} = 0 \tag{7.48}$$

where:

$\hat{H}$, $\hat{K}$, $\hat{\phi}$ = enthalpy, kinetic, and potential energies per kg of fluid, respectively
$\dot{Q}$ = quantity of heat flow rate entering the system
$\dot{W}$ = work entering the system

Since, in Equation 7.48 the first three terms are functions of state, reference levels must be defined.

Enthalpy ($\hat{H}$)

The enthalpy per mass unit is a function of pressure and temperature, and its expression is different depending on whether it is a compressible or incompressible fluid. For incompressible fluids:

$$d\hat{H} = \hat{C}_p \, dT \tag{7.49}$$

in which $\hat{C}_p$ is the heat capacity per mass unit at constant pressure, or just specific heat. For compressible fluids, the enthalpy depends also on pressure as well as on temperature, according to the expression:

$$d\hat{H} = \hat{C}p\ dT\ + \hat{V}\ dP \tag{7.50}$$

in which $\hat{V}$ is the volume per mass unit, or specific volume.

Kinetic Energy ($\hat{K}$)

The kinetic energy per mass unit is given by:

$$\hat{K} = \frac{1}{2}\frac{\left(v^3\right)_m}{v_m} \tag{7.51}$$

When it is necessary to express this term as a function of a mean velocity for all the points of the same section, the expression becomes:

$$\hat{K} = \frac{1}{2}\frac{\left(v_m\right)^2}{\alpha} \tag{7.52}$$

in which α is a dimensionless correction factor that depends on the flow regime and on the type of fluid transported.

Under turbulent regime this correction factor can be calculated from the expression:

$$\alpha = \frac{4c^4\left(3+c\right)\left(3+2c\right)}{\left(1+c\right)^3\left(1+2c\right)^3} \tag{7.53}$$

where c is an integer value that is part of the exponent of Equation 7.28. For a turbulent regime with Re = 10^4 and $c = 7$, the value of α is 0.945. Therefore, for the turbulent regime, the value of this parameter is always approximated to one, regardless of the type of fluid.

Under laminar regime, the value of α depends on the type of fluid (Charm, 1971; Osorio and Steffe, 1984; Rao, 1992):

Newtonian fluids: $\alpha = 0.5$

Power law fluids: $$\alpha = \frac{\left(2n+1\right)\left(5n+3\right)}{3\left(3n+1\right)^2} \tag{7.54}$$

Bingham plastics: $$\alpha = \frac{1}{2-m} \tag{7.55}$$

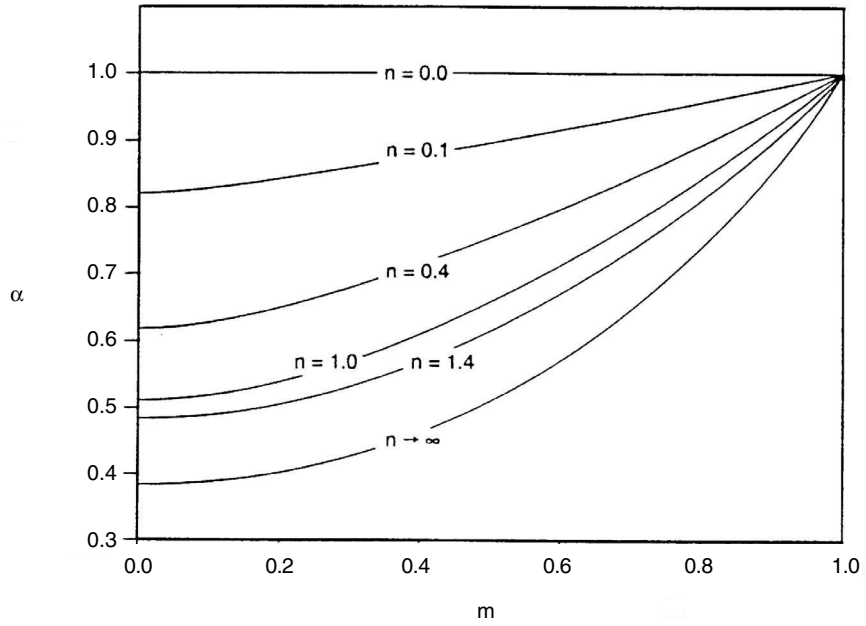

FIGURE 7.12
Kinetic correction factor for Herschel–Bulkley fluids.

Herschel–Bulkley fluids:
$$\alpha = \frac{A}{B} \tag{7.56}$$

where:

$A = [(1 + 3n + 2n^2 + 2n^2m + 2nm + 2n^2m^2)^3][(2 + 3n)(3 + 5n)(3 + 4n)]$

$B = [(2n + 1)^2(3n + 1)^2][18 + n(105 + 66m) + n^2(243 + 306m + 85\,m^2) + n^3(279 + 522m + 350m^2) + n^4(159 + 390m + 477m^2) + n^5(36 + 108m + 216m^2)]$

Figure 7.12 presents the variation of the correction factor α with respect to the value of m for different values of the flow behavior index n, where $m = J_o/J_w$.

Potential Energy ($\hat{\phi}$)

The only potential field considered is the gravitational field, so the potential energy per unit mass is given by:

$$\hat{\phi} = g\,z \tag{7.57}$$

considering $z = 0$ as reference level, giving a $\phi = 0$ magnitude.

When performing an energy balance in a pipe using the continuity equation, the mass flow rate remains constant ($w_1 = w_2 = w$). Hence, if Equation 7.48 is divided by the mass flow rate, it is obtained that:

$$\Delta\left(\hat{H} + \hat{K} + \hat{\phi}\right) - \hat{Q} - \hat{W} = 0 \tag{7.58}$$

in which Δ is the difference operator or increment (exit minus entrance) and all the variables are expressed per unit mass of fluid.

7.3.4 Mechanical Energy Balance

Since real processes are irreversible, the energy balance performed in the last sections is not useful to evaluate mechanical energy losses produced in the pipe. Therefore, an entropy balance is carried out to evaluate these losses. For a steady state regime, this leads to the expression:

$$\Delta\left(\hat{K} + \hat{\phi}\right) + \int_{P_1}^{P_2} \hat{V} dP - \hat{W} + \hat{E}_f = 0 \tag{7.59}$$

in which the term $\hat{E}_f$ represents the mechanical energy losses per mass unit.

This is the so-called Bernoulli equation, and it is very important to calculating the power that needs to be supplied to transport a fluid through a piping system (Coulson and Richardson, 1979; McCabe et al., 1985; Toledo, 1993; Singh and Heldman, 1993). Mechanical energy losses can be evaluated in some cases for which methods or procedures have been developed for their calculation.

In the Bernoulli equation, the value of the term in the integral depends on the type of fluid transported and the type of process performed during the transport. It is necessary to know the relationship between the specific volume and the pressure to evaluate this term.

For incompressible fluids, the specific volume remains constant, hence the term in the integral is:

$$\int_{P_1}^{P_2} \hat{V}\, d\, P = \frac{\Delta P}{\rho} \tag{7.60}$$

In the case of gases, the mean value of the specific volume can be used whenever there are no large temperature or pressure variations. For an adequate calculation of this term, it is necessary to know what type of process is being carried out, whether it is isothermal, adiabatic, polytropic, or some other kind (Smith and Van Ness, 1975).

For incompressible fluids, the more useful form of the Bernoulli equation for calculations related to the transport of fluids can be expressed as:

$$g\Delta z + \frac{\Delta P}{\rho} + \frac{\Delta v^2}{2\alpha} + \hat{E}_f = \hat{W} \tag{7.61}$$

where v is the mean velocity, which will be used hereafter instead of v_m. The parameter α of the kinetic term depends on the circulation regime and on the type of fluid, as indicated previously.

The values that correspond to those unknowns stated in a transport system, such as the power required to move a fluid from one point to another, the height needed to discharge a fluid at point of interest when no pump is available, the discharge volumetric flow rate, the pressure needed at the system entrance, the discharge pressure of the system, the mechanical energy losses due to friction through the different fittings, and the piping (which will be analyzed in the following sections) can be obtained from Equation 7.61.

7.4 Mechanical Energy Losses

7.4.1 Friction Factors

The mechanical energy losses ($\hat{E}_f$) produced during the transport of fluids through a pipe due to the friction between the fluid and the pipe wall can be evaluated by the Bernoulli equation once the other terms are known according to Equation 7.61:

$$\hat{E}_f = \hat{W} - g\Delta z - \frac{\Delta P}{\rho} - \frac{v^2}{2\alpha}$$

Another way to evaluate such mechanical energy losses is from the fluid's properties and the particular characteristics of the pipe involving the so-called friction factor. The friction factor (f) is defined as the relation between the stress exerted by the fluid on the pipe wall (σ_w) and the kinetic energy per volume unit:

$$f = \frac{\sigma_w}{(1/2)\,\rho\, v^2} \tag{7.62}$$

It is important to note that this friction factor, defined according to Equation 7.62, is denominated the Fanning friction factor (f_F). However, some authors, such as Foust et al. (1980), use the Darcy friction factor (f_D). The relation between both is a factor of 4 (Perry and Chilton, 1973; Welty et al., 1976; Harper, 1976; Singh and Heldman, 1993): $f_D = 4\, f_F$. Most commonly used is the Fanning factor, which will be used hereafter. For simpler nomenclature, f will be used instead of f_F.

The load losses per mass unit of fluid are evaluated by the following expression:

$$\hat{E}_f = \frac{F v}{w} = \frac{F v}{v S \rho} \tag{7.63}$$

where F is the force exerted on the wall of the pipe, v is the mean circulation velocity of the fluid, w is the mass flow rate of the fluid, ρ is the density of the fluid, and S is the cross-sectional area of the pipe.

Force can be expressed as a function of the shear stress at the wall (σ_w):

$$F = \sigma_w A = \sigma_w \pi d L \tag{7.64}$$

Since the cross-sectional area of a cylindrical pipe is $S = (\pi/4)d^2$, combining Equations 7.62, 7.63, and 7.64 obtains:

$$\hat{E}_f = 4f \frac{L}{d} \frac{v^2}{2} \tag{7.65}$$

which is called the Fanning equation.

In the same way, the shear stress at the wall can be expressed as a function of mechanical energy losses as follows:

$$\sigma_w = \frac{\hat{E}_f d \rho}{4L} \tag{7.66}$$

7.4.2 Calculation of Friction Factors

The friction factor is a function of the magnitude of the Reynolds number and the absolute rugosity (ε) of the piping. The effect of the rugosity on mechanical energy losses is important, since it greatly affects the friction factor. Rugosity is a parameter that depends on the type and characteristics of the material with which the piping is manufactured. It is linked to the height and shape of the internal protuberances of the pipe; the units of rugosity are given in length (Charm, 1971; Foust et al., 1980; McCabe et al., 1985; Toledo, 1993).

For smooth pipes such as glass and plastics, the rugosity value is zero. Table 7.1 presents some values of the absolute rugosity for clean pipes made of different materials.

Relative rugosity can also be used (Foust et al., 1980) and is defined as the quotient between the absolute rugosity and the internal diameter of the pipe, i.e., (ε/d). Rugosity values, absolute as well as relative, can be obtained from the graph presented in Figure 7.13, in which ε/d is a function of the pipe diameter and the type of material.

TABLE 7.1

Rugosity of Pipes

Material	ε (mm)
Concrete	0.3–3
Cast iron	0.26
Asphalted cast iron	0.12
Galvanized iron	0.15
Wrought iron	0.046
Commercial steel	0.046
Riveted steel	1–10
Drain piping	0.0015

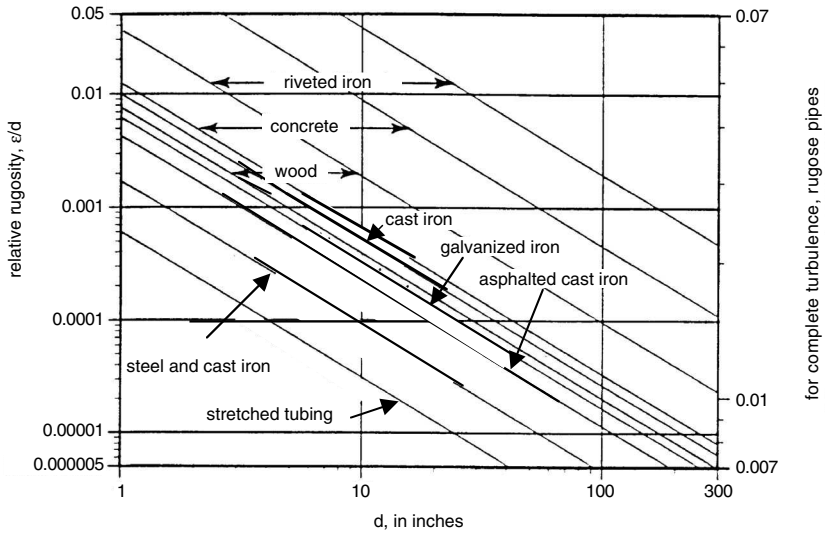

FIGURE 7.13
Values of the relative rugosity coefficient as a function of the diameter and material of the pipe.

Depending on the type of fluid food and the flow regime, there are different types of equations and diagrams that allow calculation of the value of the friction factor.

7.4.2.1 Flow under Laminar Regime

Depending on the type of fluid, different models are used. Therefore, the corresponding equations for Newtonian and non-Newtonian fluids are given next (Skelland, 1967; Foust et al., 1980; Coulson and Richardson, 1979; Steffe et al., 1984; García and Steffe, 1987; Rao, 1992; Steffe, 1992a).

- Newtonian fluids:

$$f = \frac{16}{\mathrm{Re}} \tag{7.67}$$

- Power law fluids:

$$f = \frac{16}{\mathrm{Re}_G} \tag{7.68}$$

in which Re_G is the generalized Reynolds number, defined according to Equation 7.7.

- Bingham plastics: the friction factor is an implicit factor of the Reynolds and Hedstrom numbers and can be calculated from Equation 7.69:

$$\frac{1}{\mathrm{Re}_B} = \frac{f}{16} - \frac{He}{6\left(\mathrm{Re}_B\right)^2} + \frac{\left(He\right)^4}{3f^3\left(\mathrm{Re}_B\right)^8} \tag{7.69}$$

in which Re_B is the Reynolds number for Bingham plastics, while He is the Hedstrom number, as previously defined (Equations 7.6 and 7.12a, respectively).

- Herschel–Bulkley fluids:

$$f = \frac{16}{\Psi \mathrm{Re}_G} \tag{7.70}$$

in which ψ is given by the expression (Steffe et al., 1984; Osorio and Steffe, 1984):

$$\Psi = \left(3n+1\right)^n \left(1-m\right)^{1+n} \left[\frac{\left(1-m\right)^2}{3n+1} + \frac{2m\left(1-m\right)}{2n+1} + \frac{m^2}{n+1}\right]^n \tag{7.71}$$

Since the m factor, or relation between shear stresses, is an implicit function of the generalized Reynolds and Hedstrom numbers (Equations 7.7 and 7.12b, respectively), it can be calculated using the following equation:

$$\mathrm{Re}_G = 2\mathrm{He}_G \left(\frac{n}{3n+1}\right)^2 \left(\frac{\Psi}{m}\right)^{(2/n)-1} \tag{7.72}$$

For Newtonian and power law fluids $m = 0$ and $\psi = 1$, it is possible to calculate the friction factor directly from Equation 7.67 or 7.68. For Bingham and Herschel–Bulkley fluids, if the value of m is not known, it is necessary to solve Equation 7.72 by iteration or by trial and error, using Equations 7.70, 7.71, and the generalized Reynolds number (Equation 7.7) to obtain the value of ψ and, finally, the value of f.

7.4.2.2 Flow under Turbulent Regime

Other equations are used under turbulent regime, theoretically obtained from the denominated universal profile of velocities. However, in the calculation of the friction factor, empirical or semiempirical equations are usually used. As occurs in laminar regime, the equations are dependent on the type of fluid transported.

- Newtonian fluids: one equation often used for rough pipes is the Colebook equation (Welty et al., 1976; Levenspiel, 1993):

$$\frac{1}{(4f)^{1/2}} = -2\log\left[\frac{2.51}{\mathrm{Re}(4f)^{1/2}} + \frac{1}{3.5}\frac{\varepsilon}{d}\right] \tag{7.73}$$

  For a completely developed turbulent regime, the first term within the logarithm is negligible with respect to the second, obtaining a new equation, that of Nikuradse (Skelland, 1967; Welty et al., 1976; Levenspiel, 1993):

$$\frac{1}{(4f)^{1/2}} = 2\log\left(3.7\frac{d}{\varepsilon}\right) \tag{7.74}$$

  Another useful equation for evaluating the friction factor is the following (Levenspiel, 1993):

$$\frac{1}{(4f)^{1/2}} = -2\log\left[\frac{5.62}{\mathrm{Re}^{0.9}} + 0.27\frac{\varepsilon}{d}\right] \tag{7.75}$$

For values of Reynolds numbers between 2.5×10^3 and 10^5 and smooth pipes, Blasius (Levenspiel, 1993) obtained the following correlation:

$$4f = \frac{0.316}{(\mathrm{Re})^{1/4}} \tag{7.76}$$

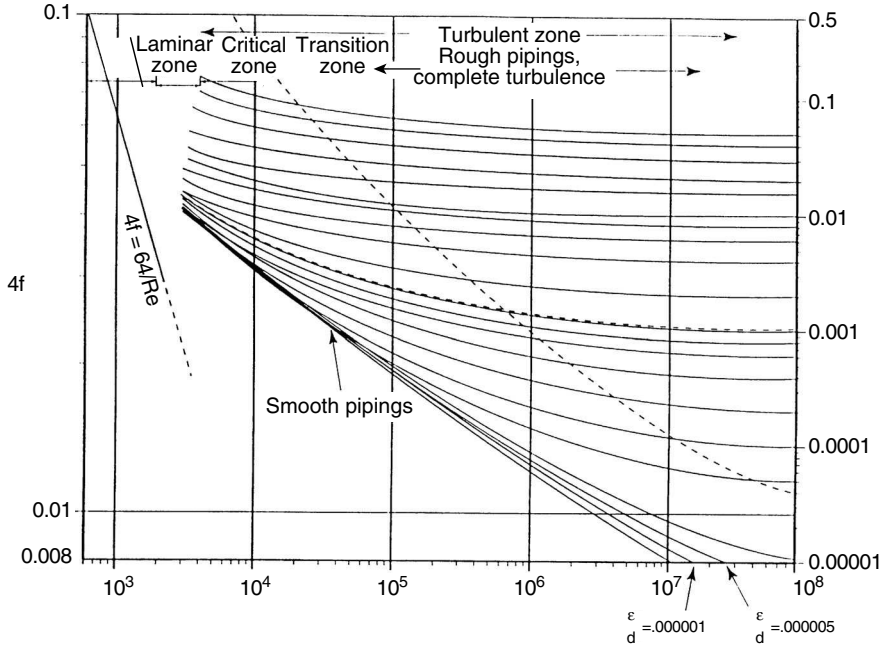

FIGURE 7.14
Moody's diagram for Newtonian fluids.

Another correlation frequently used for smooth pipes (Coulson and Richardson, 1979) is:

$$\frac{1}{(4f)^{1/2}} = 1.80 \log\left(\frac{\mathrm{Re}}{6.81}\right) \tag{7.77}$$

Besides these equations, various researchers have proposed other correlations that can be more or less applied, depending on the particular characteristics of the transport system.

A practical way of calculating the friction factor is from the Moody diagram (Figure 7.14), in which the friction factor ($4f$ or f_D) is a function of the Reynolds number (Re) and the relative rugosity (ε/d). This diagram allows the calculation of the friction factor under laminar or turbulent regime, as well as in the transition zone. It can be observed that, for values of Reynolds numbers smaller than 2100, the variation of $4f$ with Re is linear, which agrees with Equation 7.65. In the turbulent zone, the curves fit with a small error to the equation of Colebrook (Welty et al., 1976; Levenspiel, 1993). In the transition zone, for values of the Reynolds number between 2100 and 4000, a relation that gives good results is:

$$f = 0.71 \times 10^{-9}\left(\mathrm{Re}\right)^2 \tag{7.78}$$

- Power law fluids: the calculation of the friction factor can be performed by the following implicit equation (Skelland, 1967):

$$\frac{1}{(4f)^{1/2}} = \frac{2}{n^{0.75}} \log\left[\mathrm{Re}_G f^{(1-n/2)}\right] - \frac{0.4}{n^{1.2}} \tag{7.79}$$

  In the same way as for Newtonian fluids, the friction factor for power law fluids can be graphically determined by the diagram developed by Dodge and Meztner (1959) (Figure 7.15).

- Bingham plastics: the implicit equation allowing the calculation of the friction factor in this case is:

$$\frac{1}{(4f)^{1/2}} = 2.27 \log(1-m) + 2.27 \log\left[\mathrm{Re}_B f^{1/2}\right] - 1.15 \tag{7.80}$$

  The friction factor can also be obtained from the graph given by Hedstrom (Figure 7.16), in which the friction factor is plotted against the Reynolds number (Re_B), besides being a function of the Hedstrom number. There is an additional parameter that appears in this figure, which is the plasticity number or module (PI), defined by

$$PI = \frac{\sigma_0 \, d}{v \, \eta'} \tag{7.81}$$

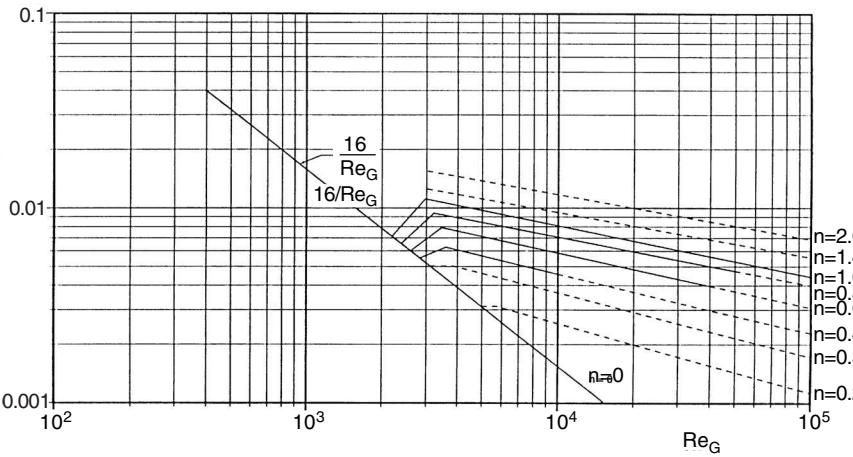

FIGURE 7.15
Diagram of power law fluids. (Adapted from Dodge, D.W. and Metzner, A.B., *AIChET*, 5, 189–197, 1959.)

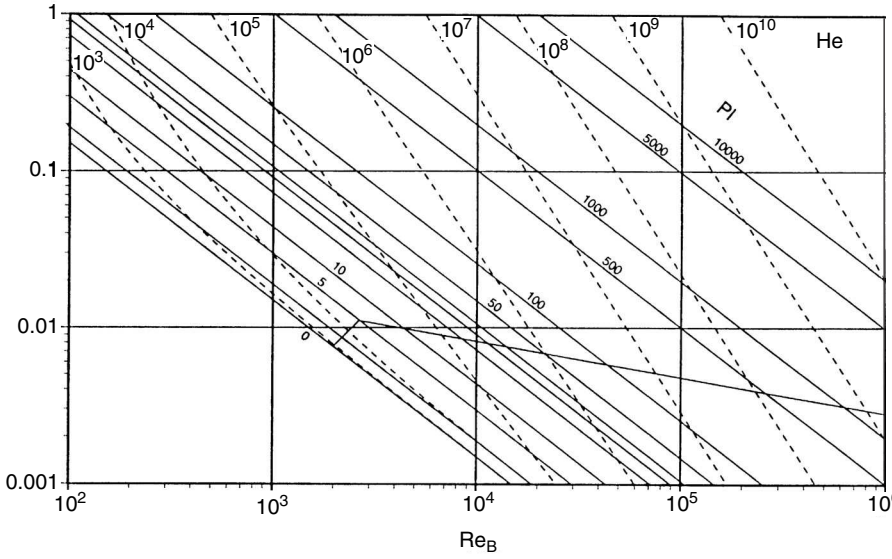

FIGURE 7.16
Hedstrom's diagram for Bingham's plastics. (Adapted from García, E.J. and Steffe, J.F., *J. Food Process. Eng.*, 9, 93–120, 1987.)

- Herschel–Bulkley fluids: it is difficult to find an equation that can be directly applied to this type of fluid in order to calculate the friction factor. However, for values of the flow behavior index of 0.2 and 0.5, the friction factor can be determined using Figures 7.17 and 7.18 (García and Steffe, 1986; Rao, 1992) for a wide range of values of the generalized Reynolds and Hedstrom numbers.

7.4.3 Minor Mechanical Energy Losses

Up to this point, only the way to calculate the mechanical energy losses for straight piping sections has been analyzed. However, all piping sections have a series of elements, known as fittings, that cause additional mechanical energy losses known as minor losses. These losses are due to widening and narrowing of the piping, the presence of valves, and measuring instruments, as well as changes in the flow's direction or diversification of the fluid, generally due to elbows, tees, ys, and crossings (Charm, 1971; Headman, 1975; Geankoplis, 1978; Foust et al., 1980; McCabe et al., 1985; Toledo, 1993).

In general, losses due to each of these elements are small and could be neglected, but, in piping systems containing a considerable number of these fittings, such losses can be very important. There are two ways to calculate these minor losses; one of them is based on the equivalent length of the fitting, while the other uses dimensionless resistance factors.

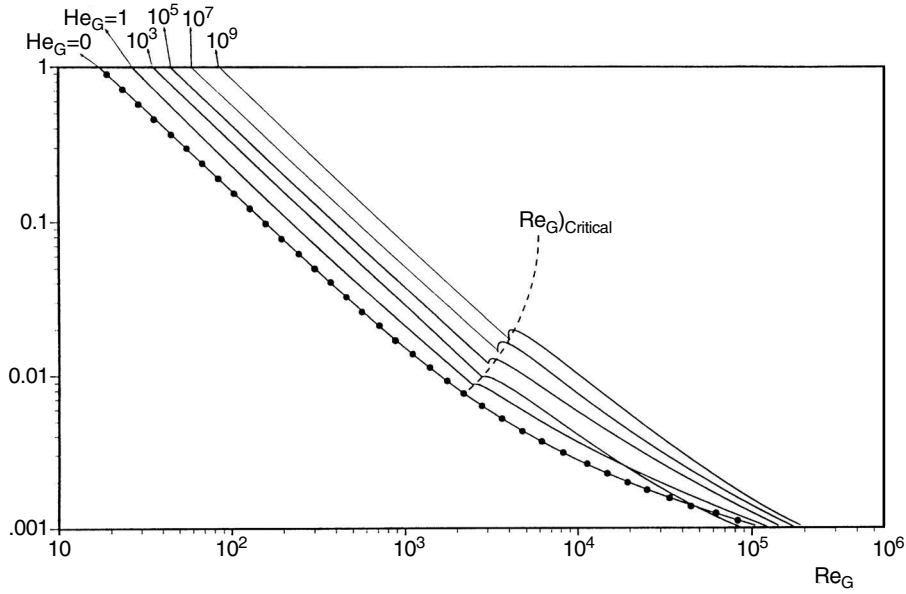

FIGURE 7.17
Friction factors for Herschel–Bulkley fluids (n = 0.2). (Adapted from García, E.J. and Steffe, J.F., *J. Food Process. Eng.*, 9, 93–120, 1987.)

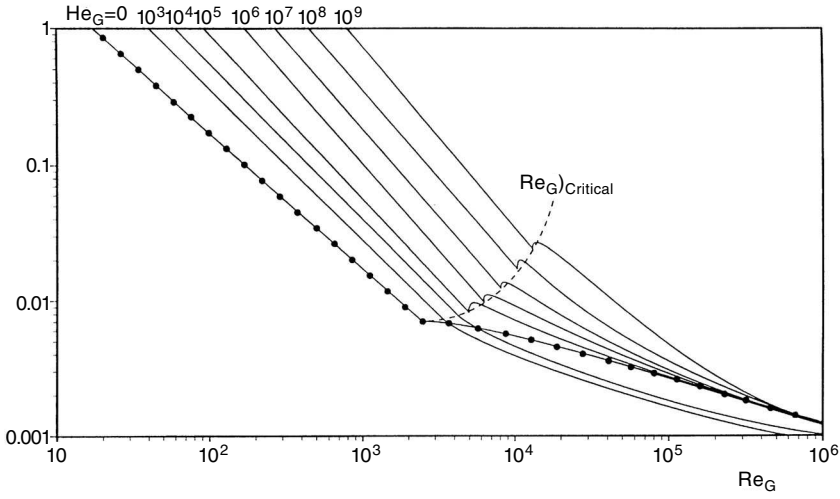

FIGURE 7.18
Friction factor for Herschel–Bulkley fluids (n = 0.5) (Adapted from García, E.J. and Steffe, J.F., *J. Food Process. Eng.*, 9, 93–120, 1987.)

7.4.3.1 Equivalent Length

Equivalent length (L_e) of a fitting is defined as the length of a straight pipe section that will produce the same mechanical energy losses as the fitting placed as part of the piping. In this way, the Fanning equation (Equation 7.65) can be used for calculation of the mechanical loss, substituting the length with the equivalent length:

$$\hat{E}_f = 4f\frac{L_e}{d}\frac{v^2}{2} \tag{7.82}$$

The value of the equivalent length of a fitting can be obtained from tables or nomograms, such as Table 7.2 or Figure 7.19.

Depending on the fitting of interest, the dimensionless value L_e/d is obtained from Table 7.2 and can be directly substituted in Equation 7.82, or from nomograms or a double entrance abacus (Figure 7.19), in which the type of fitting is specified on one axis and the internal pipe diameter on the other axis. When connecting the respective points of these axes, the equivalent length is obtained, corresponding to the intersection point of the connection line and a third axis placed between the two axes mentioned first.

7.4.3.2 Friction Losses Factors

When using the dimensionless friction losses factors k (Foust et al., 1980; Singh and Heldman, 1993), the mechanical energy losses due to each fitting are calculated by means of the following expression:

$$\hat{E}_f = k\frac{v^2}{2} \tag{7.83}$$

The value of the resistance factor depends on the type of fitting present in the pipe. Thus, for a sudden widening in which the fluid circulates through a pipe with a cross section S_1 and a widening of the pipe with cross section S_2 ($S_1 < S_2$), the resistance factor is calculated by the following relation (Geankoplis, 1978; Foust et al., 1980):

$$k = \left(1 - \frac{S_1}{S_2}\right)^2 \tag{7.84}$$

the average velocity that should be used in Equation 7.83 is the one of largest magnitude, which corresponds to section S_1.

For a sudden contraction of the piping in which the fluid goes from a section S_1 to a smaller section S_2, the value of k is obtained from the expression:

$$k = 0.4\left(1 - \frac{S_2}{S_1}\right) \tag{7.85}$$

TABLE 7.2

Equivalent Length of Different Fittings
(for Turbulent Flow Only)

Fittings	L_e/d
45° elbow standard	15
90° elbow standard	30
90° elbow long radius	20
180° return elbow	75
Tee standard:	
Used as elbow, central entrance	90
Used as elbow, entrance by lateral branch	60
Straight passing	20
Check valve, fully open	300
Angle valve, fully open	170
Gate valve:	
Fully open	7
1/4 open	900
1/2 open	200
3/4 open	40
Ordinary entrance	16
Borda entrance	30
Rounded entrance, joints, couplings	Negligible
Sudden widening from d_1 to d_2 ($d_1 < d_2$)	
$\frac{\mathrm{Re}}{32}\left[1-\left(\frac{d_1}{d_2}\right)^2\right]^2$	Laminar flow in d_1
$\frac{f}{4}\left[1-\left(\frac{d_1}{d_2}\right)^2\right]^2$	Turbulent flow in d_1 (f evaluated in d_1)
Sudden reduction from d_2 to d_1 ($d_2 > d_1$)	
$\frac{\mathrm{Re}}{160}\left[1.25-\left(\frac{d_1}{d_2}\right)^2\right]^2$	Laminar flow in d_1
$\frac{f}{10}\left[1.25-\left(\frac{d_1}{d_2}\right)^2\right]^2$	Turbulent flow in d_1 (f evaluated in d_1)

Source: Levenspiel, O., *Flujo de Fluidos. Intercambio de Calor,* Reverté, Barcelona, 1993.

The average velocity used in Equation 7.83, again, is the one of largest magnitude and, in this case, is that corresponding to section S_2. In both cases, the fact of taking the velocity of greater magnitude is because the momentum balances for widening and contractions (Geankoplis, 1978) have been set in such a way that k remains in the terms expressed by Equations 7.84 and 7.85.

In practice, there are tables that allow calculation of the mechanical energy losses of the different fittings. Table 7.3 presents the values of k for some of these.

The calculation of the friction losses factors stated here is valid only for fluids that present a Newtonian behavior. For non-Newtonian fluids, the available information is limited. Steffe et al. (1984) have reported some values

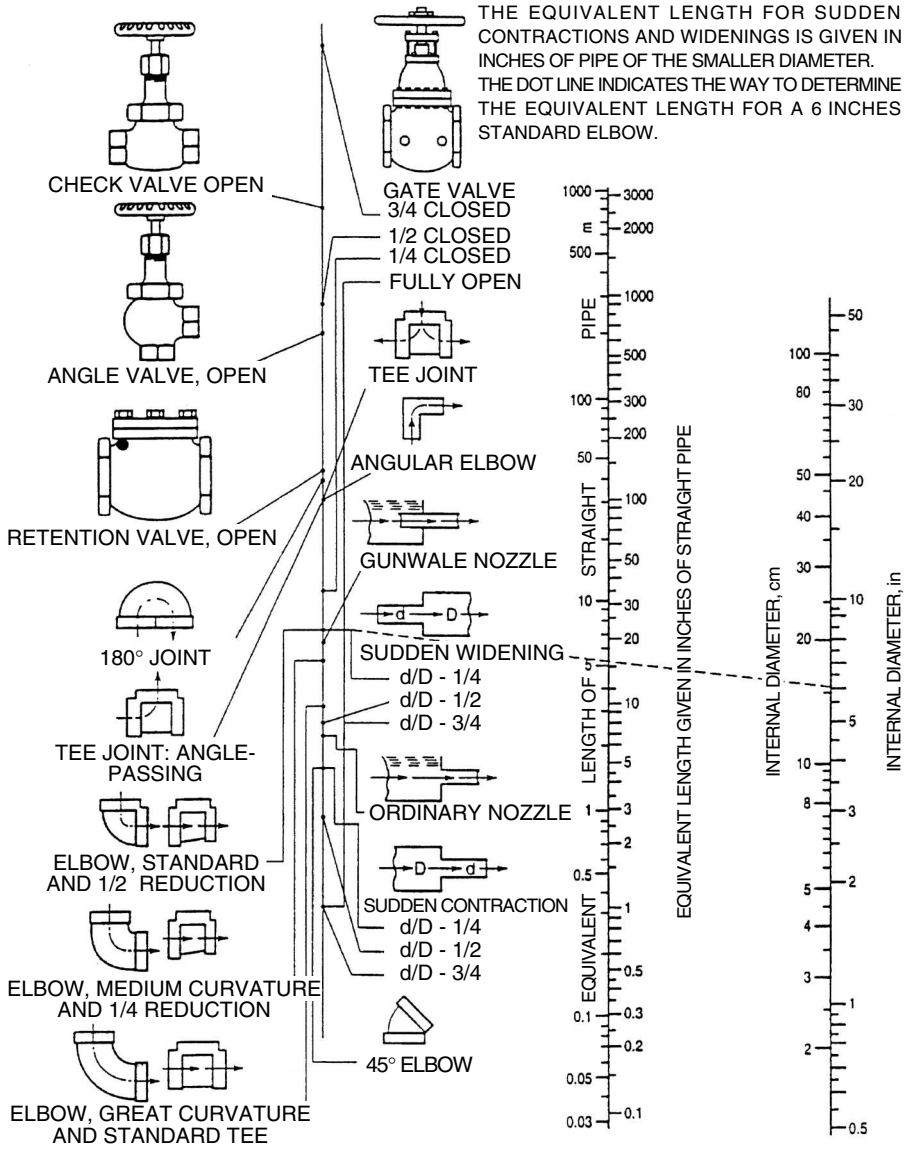

FIGURE 7.19
Abacus for the calculation of the equivalent length of fittings.

of k that show dependence on the circulation regime. Thus, for non-Newtonian fluids that circulate with Reynolds numbers lower than 500, the factors k are calculated by the expression:

$$k_{NN} = \frac{500\,k_N}{\mathrm{Re}} \tag{7.86}$$

TABLE 7.3

Resistance Factors k

Fitting	k	Fitting	k
45° elbow standard	0.35	Ball valve:	
45° elbow great curvature	0.20	5° closed	0.05
90° elbow standard	0.75	10° closed	0.29
90° elbow great curvature	0.45	20° closed	1.56
90° elbow small curvature	1.30	40° closed	17.30
180° curve	1.50	60° closed	206.00
Tee standard:		Butterfly valve:	
With closed fork	0.40	5° closed	0.24
Used as elbow	1.00	10° closed	0.52
With flow division	1.00	20° closed	1.54
Threaded joints	0.04	40° closed	10.80
Handle joint	0.04	60° closed	118.00
Gate valve:		Bottom valve	15.0
Fully open	0.17	Mechanical flowmeters	
3/4 open	0.90	Disk	7.00
1/2 open	4.50	Piston	15.00
1/4 open	24.00	Revolving	10.00
Check valve:		Turbine	6.0
Fully open	9.00	Entrances:	
3/4 open	13.0	Trumpet shaped	0.78
1/2 open	36.0	Sharp edges	0.50
1/4 open	112.0	Slightly rounded	0.23
Diaphragm valve:		Fully rounded	0.04
Fully open	2.30	Exits:	
3/4 open	2.60	Trumpet shaped	1.00
1/2 open	4.30	Sharp edges	1.00
1/4 open	21.00	Rounded	1.00
Angle valve, fully open	2.00		
Retention valve (open):			
Single	2.00		
Ball	70.00		
Disk	10.00		

in which k_N corresponds to the resistance factor of a Newtonian fluid.

Steffe et al. (1984) observed that these factors increase as the generalized Reynolds number decreases, obtaining the following expressions for three types of specific fittings:

Three-way valves: $$k = 30.3\left(\mathrm{Re}_G\right)^{-0.492} \tag{7.87a}$$

Tee fittings: $$k = 29.4\left(\mathrm{Re}_G\right)^{-0.504} \tag{7.87b}$$

Elbows (90°) $$k = 191\left(\mathrm{Re}_G\right)^{-0.896} \tag{7.87c}$$

7.5 Design of Piping Systems

When studying the circulation of fluids through pipes, different problems may appear. Among these, the most frequent are the calculation of mechanical energy losses or pressure drop in the pipe, the calculation of mass flow rate of circulation velocity, and the calculation of the pipe diameter and piping systems.

7.5.1 Calculation of Velocity and Circulation Flow Rate

A typical problem that appears during piping system design is the calculation of the circulation velocity of the fluid, or flow rate, once the characteristics of the fluid and the piping are known, as well as the pressure drop experienced by the fluid. When applying the Bernoulli equation to a piping portion with constant cross section ($\Delta v = 0$) in which there is no work developed by a pump, it is obtained that:

$$g\,\Delta z + \frac{\Delta P}{\rho} + \hat{E}_f = 0$$

This simplification allows the calculation of mechanical energy losses in the piping portion considered.

Once the losses are known, applying the equation of Fanning makes it possible to find the average circulation velocity of the fluid by:

$$v_m = \left(\frac{2d\,\hat{E}_f}{4f\,L} \right)^{1/2} \tag{7.88}$$

This equation allows calculation of the average circulation velocity, as long as the value of the friction factor is known; however, since the friction factor depends on the velocity, the solution of Equation 7.88 can be made by an iterative process, or by using the Kármán graph.

- Iterative process: An average circulation velocity is supposed and the Reynolds module is calculated; with this value and by means of the appropriate equations or adequate graphs (Moody, Dodge–Metzner, etc.), the value of the friction factor is calculated, which, in turn, when substituted in Equation 7.88, allows evaluation of the value of the average velocity. If the calculated velocity coincides with the supposed velocity, then the circulation velocity is obtained. On the other hand, the calculation process is repeated

using the obtained velocity as a departure point, until the values coincide.

The advantage of this procedure is that there are circulation velocities for different situations in a transport system (Geankoplis, 1978) allowing acceleration of the convergence process.

- Kármán's graphic method: In Kármán's graphic method (Foust et al., 1980), $1/(4f)^{1/2}$ is plotted against the value of $\mathrm{Re}(4f)^{1/2}$ (Figure 7.20), in which ε/d appears as a parameter of the curves. It is possible to obtain the circulation velocity of the fluid from this graph without the iterative process.

The following expression is obtained from the Fanning equation:

$$v = \frac{1}{(4f)^{1/2}}\left(\frac{2d\hat{E}_f}{L}\right)^{1/2} \tag{7.89}$$

Also, when combining the Fanning equation with the Reynolds number, it is possible to find the relation:

$$\mathrm{Re}(4f)^{1/2} = \frac{d\rho}{\eta}\left(\frac{2d\hat{E}_f}{L}\right)^{1/2} \tag{7.90}$$

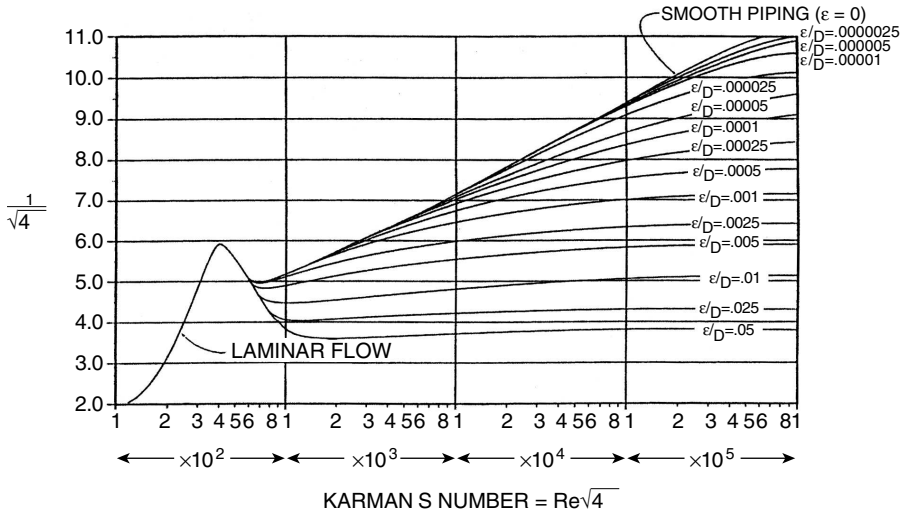

FIGURE 7.20
Kármán's graphic.

The right-handed side of Equation 7.90 can be easily calculated from the problem's data, so the value of $\mathrm{Re}(4f)^{1/2}$ is obtained. This value is looked for in the abscissas of Kármán's graph, and, employing the value of the relative rugosity (ε/d), the correspondent curve allowing calculation of the value of $1/(4f)^{1/2}$ is chosen. The circulation velocity can be calculated from this value and Equation 7.89.

Once the velocity is known, the volumetric flow rate of the fluid is obtained by multiplying the value of the average velocity times the cross sections of pipe. Mass flow rate is obtained by applying Equation 7.42.

7.5.2 Calculation of Minimum Diameter of Piping

When determining the neccesary minimum diameter of a piping of length L, through which a fluid of known characteristics circulates with a volumetric flow rate q and in which a pressure drop ΔP is produced, an iterative process should be performed. The variables to be used, which are unknowns, should be stated as a function of the known data:

$$v = \frac{q}{S} = \frac{4q}{\pi d^2} \tag{7.91}$$

Substituted in the Fanning equation, this gives:

$$d^5 = 4f\frac{8q^2L}{\pi^2\hat{E}_f} \tag{7.92}$$

If Equation 7.91 is substituted in the expression of the generalized Reynolds number, it is obtained that:

$$\mathrm{Re}_G = \left(\frac{4q}{\pi}\right)^{2-n}\frac{\rho}{8^{n-1}K}\left(\frac{4n}{1+3n}\right)^n d^{3n-4} \tag{7.93a}$$

which, for Newtonian fluids (n = 1 and K = η), becomes:

$$\mathrm{Re} = \frac{4}{\pi}\frac{q\rho}{\eta}\frac{1}{d} \tag{7.93b}$$

The iterative process is as follows: a value for $4f$ (around 0.025) is supposed. With this value and Equation 7.92, the diameter is calculated, from which the Reynolds number is calculated using Equation 7.93a. Since the characteristics of the piping are known, then the value of the absolute rugosity ε is known and, with the calculated diameter, the quotient ε/d can be found.

The value of f is calculated using the values of the Reynolds number and the relative rugosity, using the different equations or graphs that exist. If the value obtained coincides with the supposed value, the value of the friction factor is used in Equation 7.92 to calculate the diameter of the piping. On the other hand, the calculation process is repeated using the new $4f$ value found. The iterative process can be accelerated using some numerical method, such as bisection or Newton–Raphson.

7.5.3 Piping Systems

In many transport systems on an industrial scale, situations can exist in which the fluid circulates not only through pipes, but also by several sections. There can be three types of variants in such systems: circulation in parallel, series, or ramified piping. Next, each of these cases is analyzed in detail.

7.5.3.1 Parallel Piping Systems

A set of pipes, as shown in Figure 7.21, is supposed, in which the fluid is distributed through three pipes at a point A, and they converge again at a point B, next to the unloading point. When applying the Bernoulli equation between points A and B, for any section of the system, it is found that:

$$g\left(z_B - z_A\right) + \frac{P_B - P_A}{\rho} + \hat{E}_{fi} = 0$$

from which the following generalization can be made:

$$g\left(z_A - z_B\right) + \frac{P_A - P_B}{\rho} = \hat{E}_{f1} = \hat{E}_{f2} = \hat{E}_{f3} \tag{7.94}$$

That is:

$$\hat{E}_{f1} = \hat{E}_{f2} = \hat{E}_{f3}$$

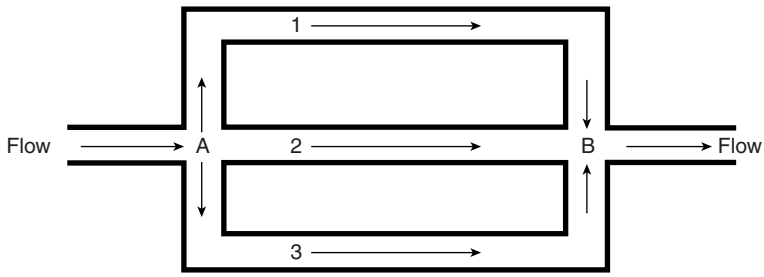

FIGURE 7.21
Parallel piping.

Also, from the continuity equation for a fluid of constant density, it is obtained that:

$$q_A = q_B = q_1 + q_2 + q_3 \tag{7.95}$$

Two types of problems are usually present in this type of parallel piping system. One is the calculation of pressure at point *B* when the characteristics of the fluid and the piping, the pressure at point *A*, and the global circulation flow rates are known. Another problem is the calculation of the volumetric flow rates at each branch and the global one, when the characteristics of the fluid and of the piping and the pressure drop experienced by the fluid between points *A* and *B* are known.

In the first case, an iterative process should be applied, as follows:

1. The flow rate at one branch is supposed, calculating the mechanical energy losses in such a branch using the Fanning equation.
2. The pressure at point *B* (P_B) can be calculated by applying Equation 7.94.
3. The mechanical energy losses are equal for each branch, so those calculated for the first branch will be equal for the other two branches. This allows calculation of the flow rate of each branch, as indicated in Section 7.5.1.
4. The total sum is obtained with the three flow rates of the correspondent branches ($q_1 + q_2 + q_3$) and, if the total coincides with the total flow, which is a known value, the iterative process is finished.

7.5.3.2 Piping in Series

In the global set of piping if sections with different diameters exist, when applying the Bernoulli equation between the extreme points *A* and *B* of all the set of piping, it is obtained that:

$$g\,\Delta z + \frac{\Delta P}{\rho} + \frac{1}{2}\left(\frac{v_n^2}{\alpha_n} - \frac{v_1^2}{\alpha_1}\right) - \hat{W} + \sum_{i=1}^{n} \hat{E}_{fi} = 0 \tag{7.96}$$

in which the subindex *i* represents the portion *i* of the piping, while 1 and *n* refer to the first and last portions, respectively.

The most usual problem in this type of system is the calculation of the global pressure drop by the fluid from its entrance at the first portion until its exit from the last section. In this type of problem it is not necessary to apply any iterative calculation process, since the velocity in each section is evaluated from the continuity equation:

$$v_1 S_1 = v_2 S_2 = v_3 S_3 = \cdots\cdots\cdots = v_n S_n$$

The mechanical energy losses of each section can be calculated with the velocity of each section using the Fanning equation:

$$\hat{E}_{fi} = 4f_i \frac{L_i}{d_i} \frac{v_i^2}{2}$$

where the friction factor is calculated using the appropiate equations or diagrams.

The global pressure drop is determined from the calculated values of $\hat{E}_{Vi}$ using Equation 7.96.

7.5.3.3 Branched Piping

Problems that can appear in this case are varied. In general, the branched pipings are like those presented in Figure 7.22, in which it can be observed that point *A* is where the different branches or pipes of different diameter converge.

For any branch *i* of the system, it is considered that the circulation velocity of the fluid is positive if the direction of the flow is from *A* towards *i*; in the opposite direction it is negative. Usually, point *A* is taken as a reference, so when applying the Bernoulli equation to any of the pipes, it is obtained that:

$$g\left(z_i - z_A\right) + \frac{P_i - P_A}{\rho} + \hat{E}_{fi} = 0$$

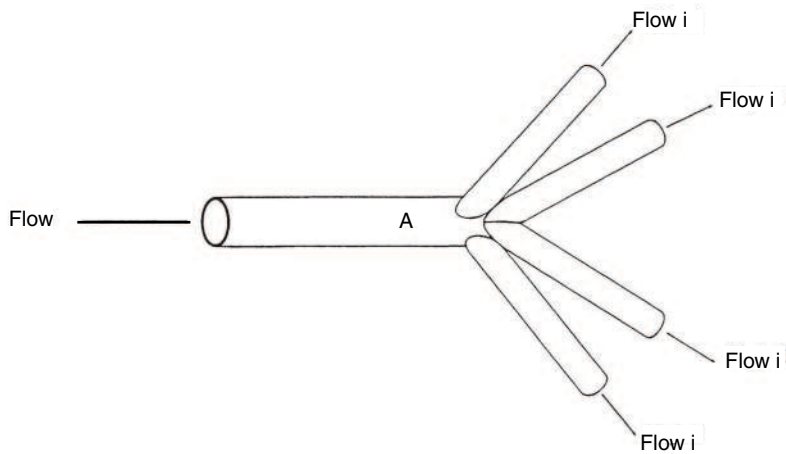

FIGURE 7.22
Branched piping.

That is:

$$\hat{E}_{fi} = \frac{P_A}{\rho} + g z_A - \left(\frac{P_i}{\rho} + g z_i \right) \tag{7.97}$$

Since mechanical energy losses are always positive, then:

$$\left(\frac{P_i}{\rho} + g z_i \right) < \left(\frac{P_A}{\rho} + g z_A \right)$$

The fluid flows from point A to point i, indicating that the circulation velocity v_i is positive. On the other hand, if

$$\left(\frac{P_i}{\rho} + g z_i \right) > \left(\frac{P_A}{\rho} + g z_A \right)$$

the fluid flows in the opposite direction, from point i to point A, indicating that the circulation velocity v_i is negative.

Generally, problems that usually appear are those in which calculation of the pressure at confluence point A and the circulation velocity of the fluid at each of the branches is desired, whenever the characteristics of the fluid and the piping system are known.

To solve this type of problem, the following algorithm can be used:

1. Initially, the velocity in one of the piping branches (v_i) is supposed, so it is possible to calculate the friction factor using the corresponding equations and diagrams.
2. The mechanical energy losses are calculated from the value of the friction factor by means of the Bernoulli equation applied to this ramification.
3. The term of potential and pressure energy can be calculated by Equation 7.97 ($P_A/\rho + gz_A$), and hence the mechanical energy losses in the remaining piping branches can be calculated by applying Equation 7.97 for each section.
4. Once the mechanical energy losses are known, the velocities and circulation flow rates of each portion are calculated as explained in Section 7.5.1.
5. A mass balance is performed by means of the continuity equation at the confluence point A, considering the sign of velocity at each section:

$$\sum v_i S_i = 0$$

If the mass balance is complied with, the supposed velocity is the one looked for, and the problem is completed. On the other hand, if the result of this last equation is positive, then the value of the supposed velocity v_i is decreased and the calculation process is repeated. If such result is negative, the iteration is repeated, but the value of v_i is increased.

7.6 Pumps

In most systems, in order to make liquids circulate through pipes, it is necessary to supply mechanical energy by means of mechanical devices known as pumps. It is necessary to supply energy to the transported fluid because, when liquid circulates through a pipe, there are mechanical energy losses due to the friction force on the pipe wall, and it is also necessary to transform the work supplied by the pump into kinetic energy, either potential or into pressure. The energy required by the system is the term $\hat{W}$ that appears in the mechanical energy balance or Bernoulli equation:

$$g\Delta z + \frac{\Delta P}{\rho} + \frac{\Delta v^2}{2\alpha} + \hat{E}_f = \hat{W}$$

In problems related to pumping fluids, the terms of this equation are generally used in the form of the so-called "loads" (Perry and Chilton, 1973; Coulson and Richardson, 1979; Foust et al., 1980; McCabe et al., 1985; Singh and Heldman, 1993), which are the different energy terms divided by the value of g. It can be observed that the dimensional analysis of these load terms results only in length, whose units are meters in the international system. It can be interpreted, from this observation, that the energy of each term of the equation represents the height to which the mass of 1 kg of fluid can be elevated.

In this way, the Bernoulli equation applied between points 1 and 2 of the system shown in Figure 7.23 leads to the following explicit form:

$$\frac{\hat{W}}{g} = (z_2 - z_1) + \left(\frac{v_2^2}{2\alpha_2 g} - \frac{v_1^2}{2\alpha_1 g}\right) + \frac{P_2 - P_1}{\rho g} + \frac{\hat{E}_f}{g} \tag{7.98}$$

In this expression, $\hat{W}/g$ is usually represented by H, which is the load exerted by the pump on the fluid. Other terms are static load, kinetic or velocity load, pressure load, and loss of load by friction.

7.6.1 Characteristics of a Pump

Explained next are certain characteristic variables that appear on pumps. All of the following definitions will be referred to in Figure 7.23.

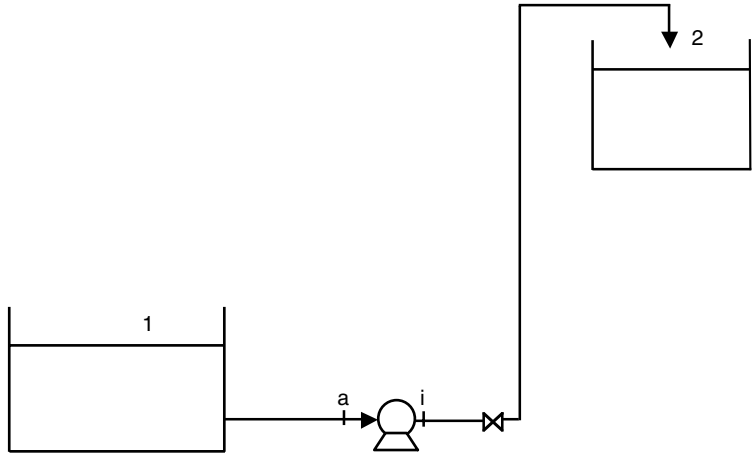

FIGURE 7.23
Fluid transport system.

7.6.1.1 Suction Head

The suction head is identified as the sum of the static, kinetic, and pressure heads at the suction point of the pump (i.e., the value of the energy that the fluid has at the suction point), and is expressed in meters of liquid. Hence:

$$H_a = z_a + \frac{1}{g}\left(\frac{P_a}{\rho} + \frac{v_a^2}{2\alpha}\right) \tag{7.99}$$

Since in real systems it is difficult to know the conditions at the entrance of the pump, a mechanical energy balance can be carried out between points 1 and *a* to evaluate H_a, which generates the following equality:

$$\left(z_a - z_1\right) + \left(\frac{v_a^2}{2\alpha g} - \frac{v_1^2}{2\alpha g}\right) + \frac{\left(P_a - P_1\right)}{\rho g} + \frac{\hat{E}_{f1}}{g} = 0$$

The suction head is expressed as follows:

$$H_a = z_a + \left(\frac{P_a}{\rho g} + \frac{v_a^2}{2\alpha g}\right) = z_1 + \left(\frac{P_1}{\rho g} + \frac{v_1^2}{2\alpha g}\right) - \frac{\hat{E}_{f1}}{g} \tag{7.100}$$

The suction head can be determined if the conditions at point 1 and the friction head losses in the section 1 – *a* are known. It must be noted that the value of the suction head decreases as the circulation flow rate of the liquid increases, since friction losses increase.

7.6.1.2 Impelling Head

Analogous to the suction head, the impelling head is the sum of static, kinetic, and pressure loads at the discharge point of the pump. The impelling head represents the available energy, expressed in meters of liquid, that the fluid has at the exit of the pump to circulate until reaching the final point of the system.

$$H_i = z_i + \frac{1}{g}\left(\frac{P_i}{\rho} + \frac{v_i^2}{2\alpha}\right) \tag{7.101a}$$

When performing a mechanical energy balance between the impelling and final points (point *i* and 2 in Figure 7.23), the following equality is obtained:

$$\left(z_2 - z_i\right) + \left(\frac{v_2^2}{2\alpha g} - \frac{v_i^2}{2\alpha g}\right) + \frac{\left(P_2 - P_i\right)}{\rho g} + \frac{\hat{E}_{f2}}{g} = 0 \tag{7.101b}$$

allowing evaluation of the impelling head from known terms of the transport system; this includes the conditions at the final point and the friction head losses between the impelling and final points:

$$H_i = z_i + \left(\frac{P_i}{\rho g} + \frac{v_i^2}{2\alpha g}\right) = z_2 + \left(\frac{P_2}{\rho g} + \frac{v_2^2}{2\alpha g}\right) + \frac{\hat{E}_{f2}}{g} \tag{7.102}$$

The impelling head increases as the liquid flow rate increases, since it implies an increase of friction losses.

7.6.1.3 Total Head of a Pump

The total head that can be developed by a pump is defined as the difference between the impelling and suction heads:

$$H = H_i - H_a \tag{7.103}$$

So, taking into account the equations obtained before, the total head is expressed according to the equation:

$$H = \left(z_i - z_a\right) + \left(\frac{v_i^2}{2\alpha g} - \frac{v_a^2}{2\alpha g}\right) + \frac{P_i - P_a}{\rho g}$$

which, expressed as a function of points 1 and 2, according to Equations 7.100 and 7.102, leads to:

$$H = (z_2 - z_1) + \left(\frac{v_2^2}{2\alpha_2 g} - \frac{v_1^2}{2\alpha_1 g} \right) + \frac{P_2 - P_1}{\rho\, g} + \frac{\hat{E}_{f2} + \hat{E}_{f1}}{g} \tag{7.103}$$

in which $\hat{E}_{f1} + \hat{E}_{f2} = \hat{E}_f$ are the total losses of mechanical energy. It is obvious that this equation corresponds to the total balance of mechanical energy through the entire transport system, between points 1 and 2 of Figure 7.23. The total head needed to impel the liquid is greater as the flow rate that should circulate through the pipe increases, since load losses increase in proportion to the volume moved.

7.6.1.4 Net Positive Suction Head: Cavitation

Cavitation is a phenomenon produced when the pressure at some point of the liquid stream becomes lower than the vapor pressure of the liquid at the working temperature. This pressure drop causes the liquid to vaporize, and bubbles ("cavities") appear within the liquid stream. This stream carries the bubbles away to zones with greater pressure, where they disappear, causing an increase of the local pressure that can affect and deteriorate the transport system. This cavitation phenomenon causes a decrease of the suction and discharge pressures of the pump, which can empty it.

To avoid cavitation, the pump should work under certain conditions. To know these working conditions, the net positive suction head (NPSH) is defined as the difference between the suction head and the vapor pressure of the liquid (Coulson and Richardson, 1979; McCabe et al., 1985):

$$\text{NPSH} = H_a - h_v \tag{7.104}$$

In this equation the vapor pressure of the liquid, h_v, is expressed in meters. Since food fluids have a high water percentage, the vapor pressure of pure water is usually taken as the value for h_v, which also ensures the most unfavorable situation of this physical phenomenon.

Once NPSH is defined, it is important to distinguish between the two types of NPSH value used in the design and practical application of fluid transport systems:

1. The absolute net positive suction head $(\text{NPSH})_A$ is characteristic of each specific system and depends on the height of each system, the placement of the pump, and the particular characteristics of the piping system. It can be calculated according to the equation:

$$(\text{NPSH})_A = H_a - h_v = z_a + \frac{v_a^2}{2\alpha\, g} + \frac{P_a - P_v}{\rho\ g} \tag{7.105a}$$

$$(\text{NPSH})_A = z_1 + \frac{v_1^2}{2a\, g} + \frac{P_1 - P_v}{\rho g} + \hat{E}_{f1} \tag{7.105b}$$

2. The required net positive suction head $(NPSH)_R$ is characteristic of each pump; the data are specified by the manufacturer, being a function of the pump design and its rotation velocity, in the case of centrifugal pumps. The $(NPSH)_R$ represents the minimal suction head necessary to prevent cavitation for a determined circulation flow rate of the liquid.

To have a good design, $(NPSH)_A$ should be longer than $(NPSH)_R$ to avoid cavitation at any point of the pipe. It is important that the value of the pressure head of the fluid at the suction point exceed the vapor pressure of the liquid, expressed in meters, by at least 1 m.

If cavitation occurs, the circulation flow rate of the liquid is decreased to eliminate this phenomenon by means of a valve placed at the impelling point, or by decreasing the temperature of the liquid, thus decreasing its vapor pressure.

7.6.2 Installation Point of a Pump

One of the more troubling aspects in the design of piping systems is to know where the pump should be placed so the fluid can circulate without presenting cavitation. The installation point should be such that the absolute net positive suction head is at least equal to the required NPSH. It can happen that the $(NPSH)_R$ of a pump is not known. In this case, the pump should be placed at a point where the static pressure of the suction point, P_a, is larger than the vapor pressure of the liquid in circulation.

When applying the mechanical energy equation between points 1 and *a* in Figure 7.23, the total length of the piping system (straight sections plus fittings), which should exist before the suction point of the pump, can be calculated, obtaining in this way the installation point:

$$g(z_a - z_1) + \left(\frac{v_a^2}{2\alpha} - \frac{v_1^2}{2\alpha}\right) + \frac{P_a - P_1}{\rho} + 4f\frac{v^2}{2}\frac{L_T}{d} = 0$$

If the suction pressure is substituted in this equation by the value of the vapor pressure of the liquid ($P_a = P_v$), the maximum total length of the piping between point 1 and that of suction can be calculated.

There can be a case where wrongly calculated fittings are already installed, where cavitation appears: this is $P_a < P_v$. There are different solutions to avoid this cavitation. One is to increase the value of pressure at the suction point by decreasing the height at which the pump is placed, or changing its installation point by decreasing the distance from point 1 to the suction point. Also, decreasing the circulation flow rate, which decreases the mechanical energy losses, can increase the pressure at the suction point. Another way to avoid cavitation is to decrease the vapor pressure of the liquid by decreasing its circulation temperature.

7.6.3 Pump Power

Once the point at which the pump will be placed is calculated, the power needed to make the fluid circulate between the charge and discharge points (1 and 2 in Figure 7.23) should be determined. Hence, the mechanical energy balance is applied again between such points:

$$g\left(z_2 - z_1\right) + \left(\frac{v_2^2}{2\alpha} - \frac{v_1^2}{2\alpha}\right) + \frac{P_2 - P_1}{\rho} + \hat{E}_f = \hat{W}$$

$\hat{W}$ is obtained from this equation, which is the energy or work per mass unit that should be supplied to the fluid to make it circulate from point 1 to point 2.

The pump power is calculated from the following equation:

$$Pot = P_w = \hat{W}\, w \tag{7.106}$$

in which w is the circulation flow rate or mass flow rate of the fluid. In this way, if $\hat{W}$ is expressed in J/kg and w in kg/s, the units of the pump power will be watts (J/s).

7.6.4 Pump Efficiency

The pump's power expressed in the last section corresponds to the theoretical or useful power that the fluid should receive to circulate through the system. However, in real systems it is necessary to apply a higher power than in theoretical systems. This is due to the existence of mechanical energy losses in the mobile parts of the pump (Coulson and Richardson, 1979), because of friction with surfaces, and because of the form of the impellers, leakage, and friction with bearings, among other factors.

The real or propelling power of the pump can be calculated from the theoretical power if the work efficiency of the pump and the engine that moves it are known. If the performance or efficiency of a pump (Φ) is defined as the relation between the energy captured by the fluid and the energy by the engine, then the real power of the pump can be expressed by the following relation:

$$\left[Pow\right]_{Real} \frac{\left[Pow\right]_{Theoretical}}{\Phi} = \frac{\hat{W}w}{\Phi} \tag{7.107}$$

7.6.5 Types of Pumps

The different types of pumps that exist to impel liquids through pipes can be divided into three main groups: positive-displacement, rotary, and centrifugal

pumps (Badger and Banchero, 1970; Perry and Chilton, 1973; Coulson and Richardson, 1979; Foust et al., 1980; McCabe et al., 1985; Singh and Heldman, 1993).

Piston or plunger pumps are the most representative of the positive-displacement pumps, also called alternative pumps. In these pumps, a piston draws the liquid through an inlet check valve and then forces it out through a discharge check valve. Because the discharge flow rate is not continuous with time, double action pumps are used in many cases. The volumetric efficiency concept, defined as the quotient between the volume of the discharged fluid and the volume swiped by the piston, is usually employed in these pumps.

Rotary pumps do not need retention valves to intake and discharge liquids; the spinning parts confined within a shell accomplish this, creating an empty volume space that causes the liquid to penetrate. This volume is then reduced and the liquid expelled. Gear, screw, and vane pumps can be cited among the different types of rotary pumps. Rotary pumps are frequently used to transport food powders such as dehydrated milk and soluble coffee.

Centrifugal pumps, which are most widely used to transport food fluids, are constituted by a series of vanes that spin around an axis inside a shell. The liquid enters through the center and, due to the spin of the vanes, a centrifugal force is conferred, thus achieving the movement of the fluid. The total head developed by a centrifugal pump for a determined flow rate is independent of the fluid density, so the pressure increase (ΔP) developed by the pump will be greater as the fluid density increases. Since the static pressure depends on the liquid's height, according to the expression $\Delta P = g\rho z$, then, in the case in which the pump is filled with air, ΔP will be small, so the fluid cannot be pumped. Thus, to use the pump, it should be previously primed or purged.

Each pump presents certain defined characteristics in which the power, head, and efficiency are a function of the volumetric circulation flow rate. Generally, the manufacturer provides such pump-specific characteristics; hence, the point of service can be determined by calculating the total head of the system. Most of the data provided by pump manufacturers refer to Newtonian fluids.

It is interesting to note that most food fluids exhibit non-Newtonian behavior. Also, almost all of them circulate under laminar regime conditions.

An adequate form to calculate and select pumps is that presented by Steffe and Morgan (1986). The data provided by manufacturers (using Newtonian fluids such as water and oil) can be applied to non-Newtonian fluids if the so-called effective viscosity (η_e) is employed. For a non-Newtonian fluid that circulates under laminar flow, Skelland (1967) defined the effective viscosity from the Hagen–Poiseuille equation, according to the following:

$$\eta_e = \frac{\Delta P}{L}\frac{\pi d^4}{128\, q} \tag{7.108}$$

considering that the relation between the mass (w) and volumetric (q) flow rate is:

$$w = qr$$

and that the pressure drop is related to the mechanical energy losses according to the expression:

$$\Delta P = \hat{E}_f \rho$$

in which $\hat{E}_f$ is given by the Fanning equation.

When combining these equations, the effective viscosity can be expressed as:

$$\eta_e = \frac{4 f w}{16 \pi d} = \frac{f w}{4 \pi d} \tag{7.109}$$

The expressions for the effective viscosity (Equations 7.108 and 7.109) can be employed in the procedure developed by Steffe and Morgan (1986).

The characteristic pump curves provided by the manufacturers are usually given as a function of the kinematic viscosity. The last is defined as the relation between the dynamic viscosity and the density:

$$\nu = \eta / \rho \tag{7.110}$$

One of the units used most often to express the kinematic viscosity is the Stoke (St), defined as:

$$St = \frac{\text{Poise}}{\text{g/cm}^3} = \frac{\text{cm}^2}{\text{s}}$$

Kinematic viscosity can also be expressed in other units as universal saybolt seconds (USS), standard redwood seconds (SRS) and Engler degrees. Table 7.4 presents the equivalencies among different kinematic viscosity units.

Problems

7.1

In pasteurization treatments of fluid foods, devices in which the fluid circulates within a tube at the treatment temperature are usually employed. To ensure a satisfactory pasteurization, it is necessary that the microorganisms that circulate at the maximum velocity remain long enough in order to receive an adequate thermal treatment. A fluid food that has a density of 1250 kg/m^3 circulates through a 26.7 mm internal diameter pipe (3/4 in

TABLE 7.4

Equivalencies between Kinematic Viscosity Units

cSt	USS	SRS	°Engler
7.4	5	44.3	1.58
20.6	100	85.6	3.02
43.2	200	170.0	5.92
87.6	400	338.0	11.70
110.0	500	423.0	14.60
132.0	600	508.0	17.50
176.0	800	677.0	23.35
220.0	1000	896.0	29.20
330.0	2000	1690.0	58.40
550.0	2500	2120.0	73.00
660.0	3000	2540.0	87.60
880.0	4000	3380.0	117.00
1100.0	5000	4230.0	146.00
2200.0	10,000	8460.0	292.00
4400.0	20,000	18,400.0	584.00

Note: For values higher than 300 USS, the following conversion can be used: USS = 4.62 cSt.

Source: Baquero, J. and Llorente, V., *Introducción a la Ingeniería Quírnica*, McGraw-Hill, Mexico, 1985.

nominal diameter) with a 10,000 kg/h mass flow rate. Calculate the value of maximum circulation velocity for the two following cases: (a) clarified juice or 45°Brix peach juice with a viscosity of 9 mPa·s; (b) egg yolk that presents a power law fluid behavior, with K = 880 mPa·s^n and n = 0.20.

The mean velocity is obtained from Equation 7.42:

$$v_m = \frac{w}{S\,\rho} = \frac{4w}{\rho\,\pi\,d^2}$$

When the data are substituted, the velocity obtained is: v_m = 3.97m/s.

(a) For peach juice that behaves as a Newtonian fluid, the magnitude of the Reynolds number is obtained when substituting the data in Equation 7.5:

$$(\mathrm{Re}) = \frac{\left(1250\,\frac{\mathrm{kg}}{\mathrm{m}^3}\right)\left(3.97\,\frac{\mathrm{m}}{\mathrm{s}}\right)(0.0267\mathrm{m})}{9\times10^{-3}\,\frac{\mathrm{kg}}{\mathrm{m}\cdot\mathrm{s}}} = 14{,}718$$

From Figure 7.18, for (Re) = 14,718, the value $v_m/v_{\max}$ = 0.78, so the maximum velocity will be $v_{\max}$ = 5.09 m/s.

(b) In the case of egg yolk that presents a non-Newtonian behavior, the generalized Reynolds number is obtained from Equation 7.7:

$$\mathrm{Re}_G = \frac{(0.0267\mathrm{m})^{0.2}\left(3.97\frac{\mathrm{m}}{\mathrm{s}}\right)^{2-0.2}\left(1250\frac{\mathrm{kg}}{\mathrm{m}^3}\right)}{8^{(0.2-1)}\left(0.88\frac{\mathrm{kg}}{\mathrm{m}\cdot\mathrm{s}}\right)}\frac{\left(4(0.2)\right)^{0.2}}{\left(1+3(0.2)\right)^{0.2}} = 37,828$$

From Figure 7.9, for Re_G = 37,828 and n = 0.2, the value v_m/v_{max} = 0.92; therefore, the maximum velocity is v_{max} = 4.31 m/s.

7.2

A fluid food whose density is 1200 kg/m^3 circulates at 25°C by a 5-cm diameter pipe with a mass flow rate of 5000 kg/h. Determine the kinetic energy flow that the fluid transports if the following fluids circulate: (a) concentrated peach juice (69°Brix) with a viscosity of 324 mPa·s; (b) nonclarified raspberry juice (without pectin elimination) of 41°Brix that has a pseudoplastic behavior, with n = 0.73 and K = 1.6 Pa·s^n; (c) apple purée that presents a Herschel–Bulkley behavior (σ_0 = 58.6 Pa, K = 5.63 Pa·s^n, and n = 0.47). In regard to transport conditions, a relationship between the yield stress and the shear stress on the wall of 0.2 can be supposed; and (d) mayonnaise that behaves as a Bingham's plastic with σ_0 = 85 Pa, η' = 0.63 Pa·s^n. In this case, c = 0.219.

The mean circulation velocity, according to Equation 7.42, is v_m = 0.59 m/s. The kinetic energy flow rate can be obtained by multiplying Equation 7.52 times the mass flux:

$$K = w\frac{1}{2}\frac{(v_m)^2}{\alpha}$$

In this expression, the value of α is unknown.

(a) For the peach concentrate that behaves as a Newtonian fluid, α depends on the Reynolds number; therefore, when substituting data in Equation 7.5 it is obtained that:

$$(\mathrm{Re}) = \frac{(1200)(0.59)(0.05)}{(0.324)} = 109$$

which indicates a laminar flow that corresponds to a value of α = 0.5, so the kinetic energy corresponding to this fluid is:

$$K = 5000\frac{\text{kg}}{\text{h}}\left(\frac{1}{2}\right)\frac{\left(0.59\frac{\text{m}}{\text{s}}\right)^2}{0.5} = 1740.5\frac{\text{kg}\cdot\text{m}^2}{\text{s}^2\cdot\text{h}}$$

or K = 1740.5 J/h.

(b) For the raspberry juice that behaves as a pseudoplastic fluid, α depends on the generalized Reynolds number; therefore, when substituting data in Equation 7.7, it is obtained that:

$$\text{Re}_G = \frac{(0.05)^{0.73}(0.59)^{2-0.73}(1200)}{8^{0.73-1}(1.60)}\frac{\left(4(0.73)\right)^{0.73}}{\left(1+3(0.73)\right)^{0.73}} = 70.8$$

On the other hand, the value of the critical Reynolds number is calculated from Equation 7.8:

$$\text{Re}_G)_{critical} = \frac{6464\,(0.73)}{\left(1+3(0.73)\right)^2\left(\frac{1}{2+(0.73)}\right)^{(2+0.73)/(1+0.73)}} = 2262$$

which indicates a laminar flow for which the value of α is given by Equation 7.54:

$$\alpha = \frac{\left(2(0.73)+1\right)\left(5(0.73)+3\right)}{3\left(3(0.73)+1\right)^2} = 0.536$$

Therefore,

$$K = 5000\left(\frac{1}{2}\right)\left(\frac{0.59^2}{0.536}\right) = 1623.6$$

That is,

$$K = 1623.6\ \text{J/h}$$

(c) For apple purée that behaves as a non-Newtonian fluid with a yield stress, α depends on the generalized Reynolds number, so when substituting in Equation 7.7 it is obtained that Re_G = 62.3, while the critical value of the Reynolds number (Figure 7.4) depends on the Hedstrom number. Therefore, substituting in Equation 7.12b:

$$He_G = \frac{(0.05\text{m})^2\left(1200\frac{\text{kg}}{\text{m}^3}\right)}{5.63\frac{\text{kg}}{\text{m}\cdot\text{s}^{1.53}}}\left(\frac{58.6\text{Pa}}{5.63\text{Pa}\cdot\text{s}^{0.47}}\right)^{\left(\frac{2}{0.47}\right)-1} = 1093.6$$

which corresponds to an $Re_G)_{\text{critical}}$ around 2200, pointing out that the fluid circulates under a laminar regime. To evaluate the correction factor α, two alternatives can be followed. The first one is by means of Equation 7.56, from which it is obtained that α = 0.644; or, Figure 7.12, which is less exact, can be used yielding α ≈ 0.62 to 0.64.

Therefore,

$$K = 5000\left(\frac{1}{2}\right)\left(\frac{0.59^2}{0.644}\right) = 1351.3$$

So for this case,

$$K = 1351.3\ \text{J/h}$$

(d) Finally, for the mayonnaise that presents a Bingham's plastic behavior, the value of the Reynolds number is calculated from Equation 7.6, while α is evaluated by Equation 7.55:

$$\text{Re}_B = \frac{\left(1200\frac{\text{kg}}{\text{m}^3}\right)\left(0.59\frac{\text{m}}{\text{s}}\right)(0.05\text{m})}{0.63\frac{\text{kg}}{\text{m}\cdot\text{s}}} = 56.2$$

$$\alpha = \frac{1}{2 - 0.219} = 0.561$$

obtaining that:

$$K = 5000\left(\frac{1}{2}\right)\left(\frac{0.59^2}{0.561}\right) = 1549.4$$

thus, the mayonnaise flow has an associated kinetic energy: K = 1549.4 J/h.

7.3

Calculate the velocity and the mass flow rate with which an apple purée transported through a 15-cm internal diameter pipe at a temperature of 25°C circulates. The total distance that the purée should travel is 300 m. Between the departure and arriving points, a pressure drop of 250 kPa occurs, and

the arriving point is 5 m higher than the departure point. The purée follows the power law at the work temperature, with a consistency index of 2.4 $Pa \cdot s^n$ and a flow behavior index of 0.44, corresponding to a density of 1200 kg/m^3.

An iterative process, according to the description given in Section 7.5.1, calculates the velocity. The critical Reynolds number corresponding to this flow is obtained from Equation 7.8, yielding $Re_G)_{Critical} = 2396$.

The mechanical energy losses are obtained by applying the Bernoulli equation between the entrance and exit points:

$$\hat{E}_f = \frac{\Delta P}{\rho} - g\Delta z = \frac{250 \times 10^3 \dfrac{kg}{m \cdot s^2}}{1200 \dfrac{kg}{m^3}} - \left(9.8 \frac{m}{s^2}\right)(5m) = 159.3 \frac{J}{kg}$$

The iterative process is as follows:

1. A velocity is supposed from which the value of the generalized Reynolds number is evaluated (Equation 7.7).
2. The value of the friction factor is calculated from the Dodge and Metzner diagram (Figure 7.15) or by Equation 7.67 or 7.68.
3. The velocity is determined from f and Equation 7.88, $v_m = (2d\ \hat{E}_f/4fL)^{1/2}$.
4. If the calculated value does not coincide with that supposed, then the process is repeated.

The equations previously mentioned take the following form:

$$Re_G = 615.73(v)^{1.56} \qquad v_m = \frac{0.19955}{f^{1/2}}$$

The values obtained in each iteration are presented in the table below:

Iteration	$v_{supposed}$ (m/s)	Re_G	$4f$	$v_{calculated}$ (m/s)
1	2.20	2107	0.03038	2.29
2	2.29	2243	0.02854	2.36
3	2.36	2350	0.02723	2.42
4	2.42	2444	0.02619	2.47
5	2.47	2524	0.02536	2.51
6	2.51	2588	0.02473	2.54
7	2.54	2636	0.02428	2.56
8	2.56	2668	0.02400	2.58
9	2.58	2700	0.02370	2.59
10	2.59	2717	0.02356	2.60
11	2.60	2734	0.02341	2.60

The mean circulation velocity is v_m = 2.60 m/s. The mass flow rate is obtained using Equation 6.41:

$$w = \left(1200\frac{\text{kg}}{\text{m}^3}\right)\left(2.6\frac{\text{m}}{\text{s}}\right)\left(\frac{\left(3.1416\times(0.15\text{m})^2\right)}{4}\right) = 55.14\frac{\text{kg}}{\text{s}}$$

thus, w = 198,504 kg/h.

7.4

The rheological behavior of apricot marmalade can be described by the Herschel–Bulkley equation, with a yield stress of 19 Pa, a consistence index of 4.43 Pa·s^n, and a flow behavior index of 0.65. Determine the smaller diameter of a steel pipe that should be employed to transport such marmalade with a mass flow rate of 8000 kg/h. The total length of the pipe is 200 m and mechanical energy losses are 75 J/kg. The density of the marmalade is 1165 kg/m^3.

The volumetric flow rate with which the fluid circulates is:

$$q = \frac{\left(8000\frac{\text{kg}}{\text{h}}\right)\left(\frac{\text{h}}{3600\text{s}}\right)}{1165\frac{\text{kg}}{\text{m}^3}} = 1.907\times10^{-3}\frac{\text{m}^3}{\text{s}}$$

Substitution of volumetric flow rate in Equation 7.92 yields:

$$d^5 = 4f\frac{8\left(1.907\times10^{-3}\frac{\text{m}^3}{\text{s}}\right)^2(200\text{m})}{\pi^2\left(75\frac{\text{m}^2}{\text{s}^2}\right)} = \left(7.86\times10^{-6}\right)(4f)\text{m}^5$$

Re_G and He_G are obtained, as a function of the internal diameter, using Equations 7.93a and 7.12b:

$$\text{Re}_G = 390\ d^{-2.05} \quad \text{and} \quad He_G = 5410.8\ d^2$$

Then, Figure 7.18 is used, since there are no other graphics available, and the iterative process described in Section 7.5.2 is as follows:

1. A value of f is supposed, from which the diameter is evaluated.
2. Re_G and He_G can be calculated using this diameter.
3. f is obtained from Figure 7.18. If the calculated and supposed values coincide, the process ends; otherwise, the iterative process is repeated.

The following table summarizes the results obtained in this problem:

Iteration	$4f$	d (m)	Re_G	He_G	$4f$
1	0.025	0.0455	2.20×10^5	11.2	0.00735
2	0.00735	0.0356	3.64×10^5	6.9	0.00618
3	0.00618	0.0344	3.90×10^5	6.4	0.00610
4	0.00610	0.0343	3.92×10^5	6.4	0.00610

Commercially manufactured pipes (see Appendix, Table A4), which approximate to previously calculated values, are: 1 in diameter and catalogue number 40 corresponds to an internal diameter of 0.02665 m. An internal diameter of 0,03505 m corresponds to a diameter of 1¼ in. and catalogue number 40. Finally, if a diameter is 1¼ in and the catalogue number is 80, the corresponding diameter is 0.03246 m.

Therefore, the stainless steel piping that should be employed in this transport system is 1¼ in, catalog number 40.

7.5

A tomato sauce circulates at 30°C, with a mass flow of 7200 kg/h by an 8-cm internal diameter pipe, from a deposit to a storage tank where it is discharged at a pressure of 150 kPa. The tomato sauce behaves as a Bingham plastic with a yield stress of 14 Pa and a plastic viscosity of 80 mPa·s. Determine what the impelling pressure of the pump placed at the exit of the first deposit should be, if from this point and to the storage tank the sauce should be at a 3 m height and a total length of 20 m. The density of the sauce is 1275 kg/m^3.

The installation scheme is similar to that shown in Figure 7.23.

The circulation velocity calculated from Equation 7.42 is v_m = 0.312 m/s, while the corresponding Reynolds and Hedstrom numbers (Equations 7.6 and 7.12a) are 398 and 17,850, respectively.

Applying the Bernoulli equation (Equation 7.61 or 7.101b) between the impelling point of the pump and the end of the piping, it is obtained that:

1. Since there is not a pump between these two points, then $\hat{W} = 0$.
2. Since the velocity between the impelling and discharge points is the same, then $v_i = v_2$.
3. The simplified expression for Bernouill Equations is:

$$g\left(z_2 - z_i\right) + \frac{P_2 - P_i}{\rho} + \hat{E}_f = 0$$

In this equation, the potential and pressure energies are known and it is only necessary to evaluate the energy losses due to friction from the Fanning equation (Equation 7.65) previously obtaining the value of f (Figure 7.16): Re = 400 and He = 1.78.104, $f \cong 0.33$. A more precise result is obtained by using Equation 7.69: $f = 0.313$.

Therefore, mechanical energy losses are:

$$\hat{E}_f = 4\left(0.313\right)\left(\frac{20\ \text{m}}{0.08\ \text{m}}\right)\left(\frac{\left(0.312\frac{\text{m}}{\text{s}}\right)^2}{2}\right) = 15.23\ \text{J/kg}$$

Substituting in number 3, above. obtains:

$$\left(9.8\frac{\text{m}}{\text{s}^2}\right)\left(3\text{m}\right) + \frac{150\ \text{kPa} - P_i}{1275\frac{\text{kg}}{\text{m}^3}} + 15.23\frac{\text{J}}{\text{kg}} = 0$$

from which P_i is obtained, so the impelling pressure is:

$$P_i = 206.9\ \text{kPa}$$

Since the sauce behaves as a Bingham plastic, the shear stress on the wall should be greater than the yield stress, so the parameter m should be smaller than the unit. If Equation 7.66a is used to calculate the value of σ_w:

$$\sigma_w = \frac{\left(15.23\frac{\text{J}}{\text{kg}}\right)\left(1275\frac{\text{kg}}{\text{m}^3}\right)\left(0.08\text{m}\right)}{4\left(20\text{m}\right)} = 19.42\ \text{Pa}$$

and

$$m = \frac{\sigma_0}{\sigma_w} = \frac{14\ \text{Pa}}{19.42\ \text{Pa}} = 0.721$$

so there will be no problems with the flow of this material.

7.6

Ketchup is transported between two deposits open to atmosphere with a mass flow rate of 10,000 kg/h through a stainless steel pipe of 1½ in catalogue 40. The length of the straight pipe from the impelling point to the second deposit is 12 m, with a check valve and three angular elbows. The final point where the sauce is discharged is 8 m above the level of the pump. Also, the distance between the first deposit and the suction point of the pump is 0.5 m of straight piping, maintaining the level of the deposit at 2 m above it. Under the transport conditions, the ketchup has a density of 1250 kg/m^3 and its rheological behavior can be described by means of the Herschel–Bulkley equation with a yield stress of 32 Pa, a consistency coefficient of 18.7 Pa·s^n and a flow behavior index of 0.28. Determine the power of the pump.

Pipe with a nominal diameter 1½ in type 40 has an internal diameter d = 0.04089 m (see Appendix, Table A4). The equivalent lengths of the fittings can be determined from the abacus of Figure 7.19. Thus, the values obtained are: angular elbow: L_e = 6.5 m; check valve: L_e = 30.7 m. The mass and volumetric flow rates are w = 10,000 kg/h = 2.78 kg/s; q = 133.33 l/min = 35.23 gal USA/min. The mean circulation velocity is v = 1.69 m/s.

The generalized Reynolds number is obtained from Equation 7.7, Re_G = 262. This value points out that the sauce circulates under laminar regime. The generalized Hedstrom number is obtained from Equation 7.12.b, He_G = 3.03.

In order to calculate the friction factor and the parameter m, it is necessary to use Equations 7.70, 7.71, and 7.72. The solution of these equations requires carrying out an iterative calculation, obtaining the following values:

$$m = 0.219; \quad \psi = 0.745; \quad 4f = 0.3279$$

The kinetic parameter α is a function of m = 0.219 and n = 0.28, calculated from Figure 7.12. Its value is 0.79.

The pressure at the pump's suction point is obtained when applying Bernoulli's equation (Equation 7.61) between points 1 and a:

$$\hat{E}_{V1} = 0.3279 \frac{0.5}{0.04089} \frac{(1.69)^2}{2} = 5.73 \text{ J/kg}$$

$$(9.8)(-2) + \frac{P_a - 101.33}{1250} + \frac{(1.69)^2}{2(0.79)} = 0$$

Hence, the suction pressure is P_s = 116.41 kPa.

However, if the more unfavorable case in which the initial deposit is almost empty is considered (Δz = 0), the pressure at the pump's suction point will be P_s = 91.91 kPa. The vapor pressure of water at 25°C is P_v = 3.165 kPa.

The absolute net positive suction head is calculated for the most unfavorable case (when the deposit is almost empty): $(\mathrm{NPSH})_A = P_s - P_v$ = 88.75 kPa.

The pressure at the pump's impelling point is obtained by applying Bernoulli's equation between this point and the ending point (points *i* and 2):

$$\hat{E}_{V2} = 0.3279\,\frac{\left(12+30.7+3\times 6.5\right)}{0.04089}\,\frac{\left(1.69\right)^2}{2} = 712.29\ \text{J/kg}$$

$$\left(9.8\right)\left(8-0\right)+\frac{101.33-P_i}{1250}+\frac{\left(1.69\right)^2}{2\left(0.79\right)}+712.29=0$$

from which the impelling pressure is obtained:

$$P_i = 1089.7\ \text{kPa} = 10.9\ \text{bar} = 158\ \text{psi}$$

The pump's work is obtained applying Bernoulli's equation between the impelling and suction points:

$$\hat{W} = \frac{\left(1089.7-91.91\right)\ \text{kPa}}{1250\ \text{kg/m}^3} = 0.798\ \text{kJ/kg}$$

Hence, the theoretical power of the pump will be:

$$Pot = \hat{W}w = 0.798\ \text{kJ/kg}\times 2.78\ \text{kg/s} = 2.22\ \text{kW}$$

The velocity gradient in the pipe varies from zero in the center up to the maximum value on the wall, which can be calculated from the following expression:

$$\dot{\gamma}_w = \left(\frac{\sigma_W-\sigma_0}{K}\right)^{1/n} = 639\ \text{s}^{-1}$$

The discharge pressure of the pump, at the impelling point, should be at the yield stress and elevate the fluid 8 m between the impelling and the final discharge points (point *i* and 2). Thus,

$$\Delta P > \frac{\sigma_0\,4L}{d}+\rho\,g\left(z_2-z_1\right)$$

$$\Delta P > \frac{\left(32\right)\left(4\right)\left(12+30.7+19.5\right)}{0.04089}+\left(1250\right)\left(9.8\right)\left(8-0\right)$$

$$\Delta P > 2.93\times 10^5\ \text{Pa}$$

Then, the pump's discharge pressure to initiate the flow should be greater than 293 kPa (2.93 bar).

8

Circulation of Fluid through Porous Beds: Fluidization

8.1 Introduction

The flow of fluids through beds of solid particles appears in numerous technical processes. Filtration and flow operations through packed columns, used in distillation, absorption, adsorption, and ionic exchange processes, are examples of this type of circulation. In the case of filtration, the solid particles are deposited in a filter medium, and the fluid passes through the filtrating mass. In other processes, such as adsorption and ionic exchange, the fluid moves through a bed of solid particles that usually does not change its characteristics. The study of the flow of only one fluid phase through a column packed with stationary solid particles is presented in this chapter. A particle bed is considered stationary when none of its characteristics vary.

8.2 Darcy's Law: Permeability

After a series of experiments, Darcy demonstrated that the average velocity in a section of the bed is directly proportional to the pressure drop of the fluid when passing through the bed and inversely proportional to its thickness:

$$v = K \frac{\left(-\Delta P\right)}{L} \tag{8.1}$$

where:

$(-\Delta P)$ = pressure drop through the bed
L = thickness or height of the bed
K = proportionality constant

The constant K depends on the physical properties of the bed and of the fluid that circulates through the bed.

This equation indicates that the relation between the fluid's circulation velocity and the pressure drop it experiences is linear, supposing that the flow is laminar. This is correct, since the velocity through the interstices of the granular is low, and the section of each granule is also small; therefore, the value of the Reynolds number is not high.

All this supposes that the resistance offered by the bed to the fluid flow is mainly due to viscous friction. For this reason, the last equation is usually expressed as:

$$v = \frac{1}{\alpha} \frac{(\Delta P)}{\eta L} \tag{8.2}$$

where η is the fluid viscosity, while the constant $1/\alpha$ is called the permeability coefficient.

The permeability unit is the "Darcy," defined as the permeability of a porous media to a viscous flow to allow crossing of 1 ml/(s.cm^2) of a liquid with a viscosity of 1 cP under a pressure drop of 1 atm/cm.

8.3 Previous Definitions

The porous beds are constituted by a set of solid particles, generally placed randomly. To characterize the structure of such beds, a series of variables should be defined in order to study the circulation of fluids through these beds.

8.3.1 Specific Surface

Also called specific surface area (a_s), it can refer to the entire bed or to the particle. For the bed, it is defined as the area of bed surface exposed to the fluid by unit of bed volume.

$$a_S = \frac{\text{area exposed to the fluid}}{\text{bed volume}} \qquad \text{expressed in } \text{m}^{-1}$$

In an analogous way, the specific surface area of the particles (a_{so}) can be defined as the relation between the area of its surface and its volume:

$$a_{S0} = \frac{\text{particle area}}{\text{particle volume}} \qquad \text{expressed in } \text{m}^{-1}$$

TABLE 8.1

Sphericity of Particles

Form of the Particle	Sphericity
Sphere	1
Cube	0.81
Cylinders	
h = d	0.87
h = 5d	0.70
h = 10d	0.58
Discs	
h = d/3	0.76
h = d/6	0.60
h = d/10	0.47
Beach sand	As high as 0.86
River sand	As low as 0.53
Other types of sand	0.75
Triturated solids	0.5–0.7
Granulated particles	0.7–0.8
Wheat	0.85
Raschig rings	0.26–0.53
Berl chairs	0.30–0.37

Source: Levenspiel, O., *Flujo de Fluidos. Intercambio de Calor,* Revertí, Barcelona, 1993.

In the case of a spherical particle with diameter d_r, the particle's specific surface is $a_{so} = 6/d_r$.

When the particles are not spherical, an equivalent diameter of the particle (d_p) is defined as the diameter of a sphere that would have the same surface area to volume ratio as the particle. This equivalent diameter is related to d_r by the factor Γ in such a way that:

$$d_p = \Gamma d_r$$

In this equation, Γ is the so-called factor of shape or sphericity, whose value depends on the shape of the particle. In the case of spherical particles, this form factor is equal to one. However, for different particles, its value is lower than one. Table 8.1 presents sphericity values for different types of particles.

Also, the equivalent diameter of the particles is related to their specific surface according to the expression:

$$d_p = \frac{6\,\Gamma}{a_{S0}}$$

8.3.2 Porosity

The particle bed is not compact, but rather there are zones free of particles, defining the bed porosity or void fraction (ε) as the volume of the bed not

occupied by the solid material. Due to the bed's porosity, the specific surface of the bed and the particle do not coincide, but they are related according to the equation:

$$a_S = a_{S0}\left(1-\varepsilon\right) \tag{8.3}$$

Values for a_{S0} and ε for different types of particle beds can be found in the literature. It is easy to observe that, as porosity increases, fluid flows more easily through the bed, so permeability increases.

In order to continue studying the characteristics of the bed, it will be assumed that it is composed of particles randomly placed in such ways that channels through which the fluid will circulate are formed. It is also supposed that the length of these channels (L') is the same and that they have the same equivalent diameter (D_e). All the particles are contained in a cylindrical column of diameter D and the height of the bed is L.

A series of variables is presented next and will be used to relate the different characteristics of the bed.

Number of channels per m² of transversal section of bed: n'

Total number of channels in bed: $n = n' \cdot (\pi/4) \cdot D^2$

Interface area of one channel: $\pi \cdot D_e \cdot L'$

Interface area of bed: $\left(n' \dfrac{\pi}{4} D^2\right)\left(\pi D_e L'\right)$

Bed volume: $V_L = \dfrac{\pi}{4} D^2 L$

Bed volume occupied by the particles: $V_L(1 - \varepsilon)$

From these definitions it is possible to find the values of the specific surfaces:

$$a_{S0} = \frac{\left(n' \dfrac{\pi}{4} D^2\right)\left(\pi D_e L'\right)}{\dfrac{\pi}{4} D^2 L \left(1-\varepsilon\right)} = \frac{n' L' \pi D_e}{L\left(1-\varepsilon\right)} \tag{8.4}$$

$$a_S = \frac{\left(n' \dfrac{\pi}{4} D^2\right)\left(\pi D_e L'\right)}{\dfrac{\pi}{4} D^2 L} = \frac{n' L' \pi D_e}{L} \tag{8.5}$$

So, it is easy to correlate specific surfaces of the bed and of the particles by:

$$a_S = a_{S0} \cdot \left(1-\varepsilon\right)$$

It is possible to define the equivalent diameter of a channel as four times the hydraulic radius, that is, the relationship between the area of the cross-sectional area of the channel and the wet perimeter:

$$D_e = 4R_H = 4\,\frac{\text{cross-sectional area}}{\text{wet perimeter}}$$

$$D_e = 4\frac{\left(\text{cross-sectional area}\right)L'\,n}{\left(\text{wet perimeter}\right)L'\,n} = \frac{4\left(\text{volume of one channel}\right)n}{\left(\text{interface area of one channel}\right)n}$$

$$D_e = 4\,\frac{\text{volume of voids}}{\text{total interface area}} = \frac{4\,\dfrac{\pi}{4}D^2\,L\,\varepsilon}{\dfrac{\pi}{4}D^2\,L\,a_S}$$

In this way, the equivalent diameter of a channel will be a function of the fraction of void fraction and of the specific surfaces, which can be expressed as:

$$D_e = \frac{4\,\varepsilon}{a_S} = \frac{4\,\varepsilon}{a_{S0}\left(1-\varepsilon\right)} \tag{8.6}$$

For future applications, it is essential to correlate the fluid's circulation velocity through the channel (v_C) with that corresponding to the flow through the column free of particles (v). To do this, the continuity equation will be applied:

$$\rho S v = \rho S_C v_C$$

where ρ is the density of the fluid, and S and S_C are the cross-sectional areas of the column free of particles and of the whole set of channels, respectively.

Column cross-sectional area: $S = \dfrac{\pi}{4}D^2$

Channel cross-sectional area: the sum of the cross-sectional areas of all the channels; since they are supposed to be equal, this variable will be obtained by multiplying the number of channels by the cross-sectional area of one channel.

$$S_C = n\,\frac{\pi}{4}D_e^2 = n'\,\frac{\pi}{4}D^2\,\frac{\pi}{4}D_e^2$$

When substituting these last expressions in the continuity equation, it is possible to obtain the circulation velocity through one channel as a function of the global velocity as:

$$v_C = \frac{4\ \mathrm{v}}{n\ \pi\ D_e}$$

With Equations 8.4 and 8.6 in mind, it is possible to obtain the number of channels from Equation 8.4 and the equivalent diameter of the channel from Equation 8.6; hence, substituting them in the last expression obtains:

$$v_C = v\ \frac{L'}{L\ \varepsilon} \tag{8.7}$$

In this expression, the velocity of one channel is a function of the global velocity and of the lengths of the bed and the channel, as well as of the porosity.

8.4 Equations for Flow through Porous Beds

When studying the circulation of fluids through porous beds, calculating the pressure drop experienced by the fluid when passing through such a particle bed is very important. This pressure drop will depend on the type of flow with which the fluid circulates, obtaining different equations for laminar or turbulent flows.

8.4.1 Laminar Flow: Equation of Kozeny–Carman

If the flow of fluid through the channels is laminar, then the equation of Fanning could be applied to each channel:

$$\frac{\left(-\Delta P\right)}{\rho} = \frac{64}{\mathrm{Re}}\ \frac{L'\ v_C^2}{2\ D_e}$$

If the Reynolds number is:

$$\left(\mathrm{Re}\right) = \frac{\rho v_C D_e}{\eta}$$

and the circulation velocity of the fluid through the channel v_C is given by Equation 8.7, it is obtained that:

$$\left(-\Delta P\right) = 2v\eta \frac{\left(a_{S0}\right)^2 \left(1-\varepsilon\right)^2}{\varepsilon^3} \frac{\left(L'\right)^2}{L}$$

It can be observed that the pressure drop depends, among other things, on the length of each channel and of the bed. The length of each channel L' is larger than the bed length. If it is supposed that such lengths are proportional $L' = K'L$, and defining a constant $K'' = 2(K')^2$, it results that:

$$\left(-\Delta P\right) = 2v\eta \frac{\left(a_{S0}\right)^2 \left(1-\varepsilon\right)^2}{\varepsilon^3} \frac{\left(K'L\right)^2}{L}$$

and solving for v:

$$v = \frac{\left(-\Delta P\right)}{\eta L} \frac{\varepsilon^3}{K'' \left(1-\varepsilon\right)^2 \left(a_{S0}\right)^2} \tag{8.8}$$

(called the equation of Kozeny–Carman).

When comparing this equation with Darcy's Equation (8.2), permeability is given by:

$$\frac{1}{\alpha} = \frac{1}{K''} \frac{\varepsilon^3}{\left(1-\varepsilon\right)^2 \left(a_{S0}\right)^2}$$

The constant K'' is denominated Kozeny's constant. In beds where the porosity and the specific surface do not vary with the thickness of the bed, it has been found experimentally that this constant has a value of 5 ± 0.5. In fact, its value depends on the type of filling and the porosity, taking different values according to the shape of the particles and the porosity of the bed. In the case in which the particles are spherical, the value of this constant is 4.8 ± 0.3. Values for this constant for different types of filling can be found in the literature.

The value of Kozeny's constant is not the same for all types of filling but depends on the L'/L relationship. Carman has demonstrated that:

$$K'' = K_0\left(L'/L\right)$$

The L'/L relationship is called tortuousness, while K_0 is a factor that depends on the transversal section of the channel. In spite of the fact that the tortuousness and factor K_0 can vary, this variation is such that when one increases, the other decreases, and vice versa, and their product has values close to 5.

In practice, in packed beds, those particles in contact with the wall are less compacted, implying that the resistance offered by the bed to flow is lower than that given by the equation of Kozeny–Carman. Coulson obtained a correction factor K_P in an experimental way, so this effect can be taken into account. Such value is given by the equation:

$$K_P = \left(1 + 0.5\frac{A_P}{a_{S0}}\right)^2 \tag{8.9}$$

in which A_P is the surface of the column wall that contains the bed per unit volume of the bed.

To calculate the real pressure drop, the pressure drop calculated by the equation of Kozeny–Carman should be multiplied by the value of this correction factor K_P:

$$\left(-\Delta P\right)_{REAL} = K_P\left(-\Delta P\right)$$

8.4.2 Turbulent Flow: Equation of Burke–Plummer

It was supposed in the last section that fluid circulates through channels in a laminar way, but the equation obtained is not valid in many cases. For this reason, if the circulation flow is turbulent, Fanning's equation can be applied to the circulation of a fluid by a channel, thus:

$$\frac{\left(-\Delta P\right)}{\rho} = 4f\ \frac{L'(v_C)^2}{2D_e}$$

Taking into account the expressions of the equivalent diameter and the velocity through a channel (Equations 8.6 and 8.7):

$$\frac{\left(-\Delta P\right)}{\rho} = 4f\ \frac{1}{2}\frac{\left(v\,L'\right)^2}{\left(\varepsilon\,L\right)^2}\ \frac{L'\,a_{S0}\left(1-\varepsilon\right)}{4\,\varepsilon}$$

In the same way, if it is supposed that $L' = K'L$, and that the specific surface is related to its diameter by the expression $a_{so} = 6/\mathrm{dP}$, it is obtained that:

$$\frac{\left(-\Delta P\right)}{\rho} = 3\left(K'\right)^3 f\ \frac{\rho\,v^2\left(1-\varepsilon\right)}{d_p\,\varepsilon^3}$$

If a modified friction factor is defined as $f' = f(K')^3$, the following equation is obtained:

$$\frac{\left(-\Delta P\right)}{\rho} = 3f' \frac{\rho v^2 \left(1-\varepsilon\right)}{d_p\, \varepsilon^3} \tag{8.10}$$

This equation is called the Burke–Plummer equation, and the value of f' is obtained experimentally, depending on the Reynolds number. The following section shows how to obtain the value of the modified friction factor.

8.4.3 Laminar-Turbulent Global Flow: Equations of Ergun and Chilton–Colburn

Up to this point, the equations for circulation of laminar and turbulent flows have been obtained separately. Therefore, it will be convenient to obtain only one equation that can be used for both types of circulation regimes at the same time.

When observing the equations of Kozeny–Carman and of Burke–Plummer, it can be seen that the pressure loss per bed unit length will be an expression of the type:

$$\frac{\left(-\Delta P\right)}{L} = a v + b v^2$$

or a linear combination of such equations:

$$\frac{\left(-\Delta P\right)}{L} = \alpha' \frac{36K''\left(1-\varepsilon\right)^3}{\varepsilon^3 {d_p}^2} v + \beta' \frac{3f'\left(1-\varepsilon\right)\rho}{\varepsilon^3 d_p} v^2 \tag{8.11}$$

The constants α' and β' that appear in these equations are obtained by fitting experimental data to the equation. In some cases, the Reynolds number is not only used, but also modified, or the particle Reynolds number is used. The expressions for each are given next:

Reynolds number for one channel:

$$\mathrm{Re} = \frac{\rho\, v_C\, D_e}{\eta} = \frac{4\rho\, v L'}{a_{S0}\left(1-\varepsilon\right)\eta\, L}$$

Modified Reynolds number:

$$\mathrm{Re}' = \frac{\rho\, v}{a_{S0}\left(1-\varepsilon\right)\eta}$$

Reynolds number for a particle:

$$\mathrm{Re}_p = \frac{\rho v d_p}{\eta}$$

When the value of the Reynolds number for a particle is lower than 40 ($\mathrm{Re}_p < 40$), the circulation flow is considered to be laminar, while for higher values ($\mathrm{Re}_p > 40$), the flow is considered to be turbulent.

It is easy to obtain the expression for the modified friction factor as:

$$3f' = \frac{\left(-\Delta P\right) d_p \varepsilon^3}{L\left(1-\varepsilon\right)\rho\, v^2} \tag{8.12}$$

This friction factor is usually obtained from graphics, in which $3f'$ is plotted against $\mathrm{Re}_p/(1-\varepsilon)$ on logarithmic coordinates (Figure 8.1).

It can also be obtained from another type of graphic, in which $f'/2$ is plotted against the modified Reynolds number (Re′) on logarithmic coordinates (Figure 8.2).

From a series of experimental data of modified friction factor ($3f'$) values calculated from Equation 8.10, their correspondent values of Reynolds number for a particle are obtained. A function that correlates $3f'$ with Re_p is:

$$3f' = \phi\left(\mathrm{Re}_p\right)$$

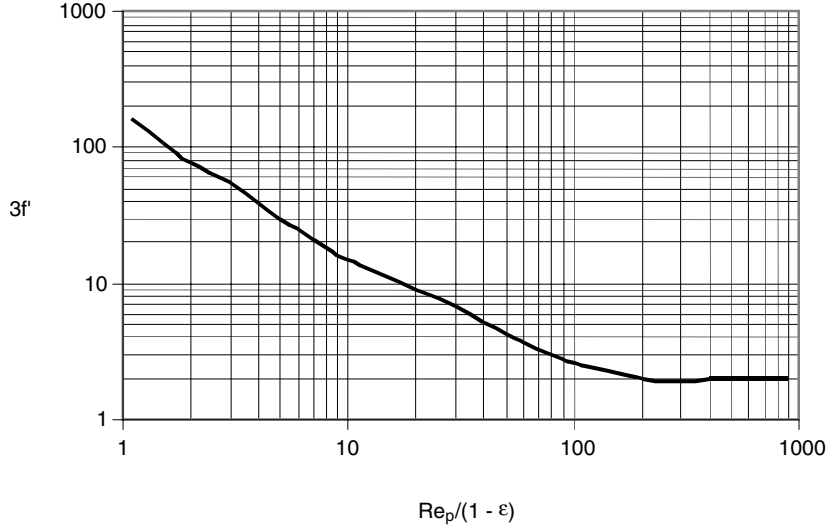

FIGURE 8.1
Modified friction factor ($3f'$) as a function of the particle Reynolds number (Re_p). (Adapted from Foust et al., *Principles of Unit Operations,* John Wiley & Sons, New York, 1980.)

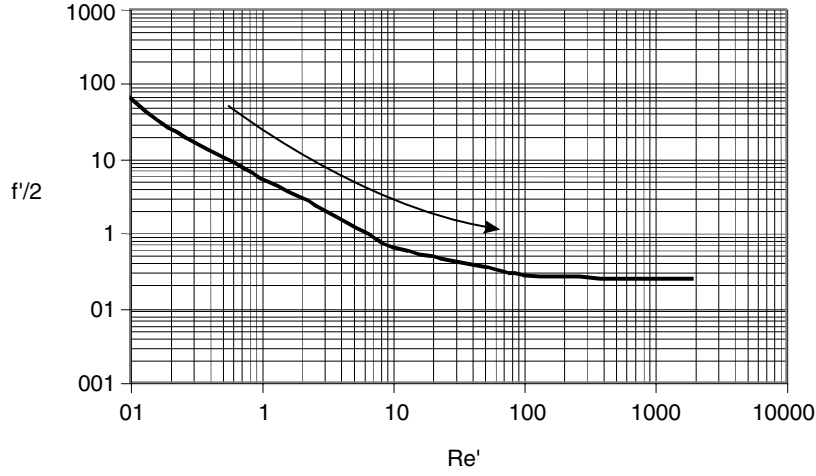

FIGURE 8.2
Modified friction factor (*f'*) as a function of the modified Reynolds number (Re'). (Adapted from Coulson, J.M. and Richardson, J.F., *Ingenicía Quínica,* Tomo Ia Vi, Reverté, 1981.)

The following equation is obtained when fitting experimental data:

$$3f' = \frac{150(1-\varepsilon)}{\mathrm{Re}_p} + 1.75$$

If the values of $3f'$, given by Equation 8.12, and the correspondent particle Reynolds number are substituted in the last equation, the following expression is obtained:

$$\frac{(-\Delta P)}{L} = 150\,\frac{(1-\varepsilon)^2\,\eta}{\varepsilon^3 {d_p}^2}\,v + 1.75\,\frac{(1-\varepsilon)\rho}{\varepsilon^3 d_p}\,v^2 \qquad (8.13)$$

This last expression is called the equation of Ergun, and can be used to calculate the pressure drop experienced by fluid when flowing through a packed bed, independently of the type of circulation flow.

When comparing Equations 8.11 and 8.13, it is easily observed that:

$$36K''\alpha' = 150$$

$$3f'\beta' = 1.75$$

When a gas and a liquid circulate in countercurrent through a column packed with particles, it is convenient to use the so-called equation of Chilton–Colburn, an empiric equation based on the Fanning equation:

$$\frac{(-\Delta P)}{L} = 2f' \frac{\rho v^2}{d_p} \tag{8.14}$$

The modified friction factor f' can be calculated from Figures 8.1 and 8.2, or the following expressions can be used:

For a laminar flow ($Re_p < 40$): $f' = 850/Re_p$

For a turbulent flow ($Re_p > 40$): $f' = \frac{38}{(Re_p)^{0.15}}$

The equation of Chilton–Colburn can be used when a bed is formed by solid particles, but when the particles are hollow, the second term of the equation should be multiplied by a factor K_r, which is given by the equation:

$$K_r = \frac{0.24}{(d_p)^{1/2}}$$

In this equation, d_p is the nominal diameter of the particles in inches.

The voids created in the surrounding area of the wall can also affect the calculation of the pressure drop; therefore, it is necessary to introduce a new correction factor of the wall, K_p, depending on the circulation flow and on the particle diameter to bed diameter ratio (d_p/D). If this ratio is smaller than 1/6, then the wall effect is not considered. Figure 8.3 is used to calculate this new factor K_p, which is plotted against the ratio d_p/D, and there are two curves, one for laminar flow and another for turbulent flow.

Therefore, in general, the real pressure drop the fluid will experience can be obtained by multiplying the pressure drop calculated from the equation of Chilton–Colburn by these two factors, as:

$$(-\Delta P)_{real} = K_r\, K_P (-\Delta P)_{theoretical}$$

8.5 Fluidization

When a fluid circulates through a bed of particles, if the circulation velocity is low, the bed remains static. But if the velocity increases, the bed may expand, causing a rearrangement of the particles with a consequent increase in the porosity of the bed.

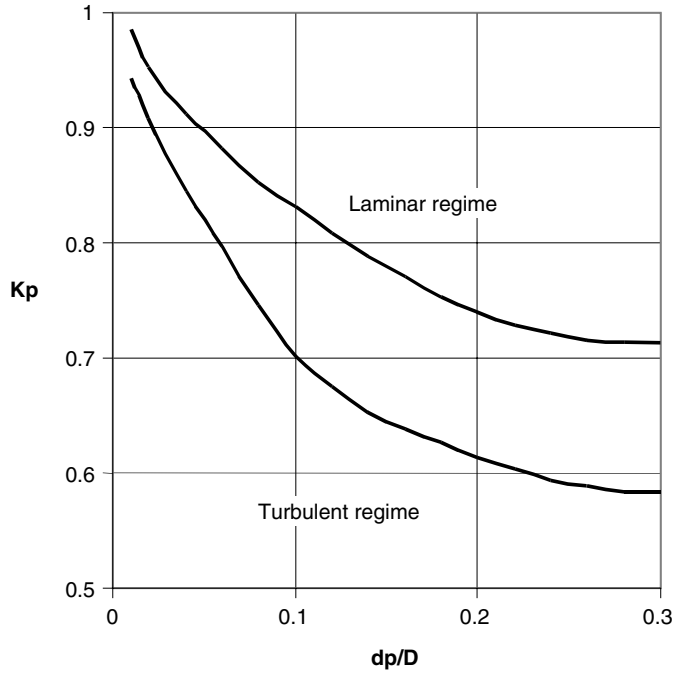

FIGURE 8.3
Correction factor of the wall effect (K_p) as a function of the particle diameter/column diameter (d_p/D). (Adapted from Sawistowski, H. and Smith, W., *Metodos de Calculo en los Procesos de Transferencia de Materia,* Alhambra, Madrid, 1967.)

Imagine a bed of particles through which a fluid circulates, with the circulation velocity of the fluid gradually increased. At low velocities the bed remains static, without height increase, so when the pressure drop is plotted against the circulation velocity on logarithmic coordinates, a straight line is obtained, as represented by the segment *OA* in Figure 8.4.

If the velocity is further increased, the particles begin to separate, but they are still in contact; although the relationship between the pressure drop and the velocity continues to be linear, the slope is smaller (segment *AB*). At point *B*, at which the particles are not in contact, it is said that the bed is fluidized. From this point, if the velocity is increased, there can be a small pressure drop (segment *BC*). If the velocity continues to be increased, the pressure drop will increase linearly with the velocity, but with a smaller slope, until the velocity is high enough to drag the particles, as occurs from point *D* on. The velocity from which fluidization occurs is called minimal velocity of fluidization, whereas velocity corresponding to the drag point is known as drag velocity.

Within the range of velocities where the bed is fluidized, from V_{mf} to exactly before V_D, once the particles have been fluidized, the velocity of the fluid in contact with the particles is higher than the velocity of the fluid that has

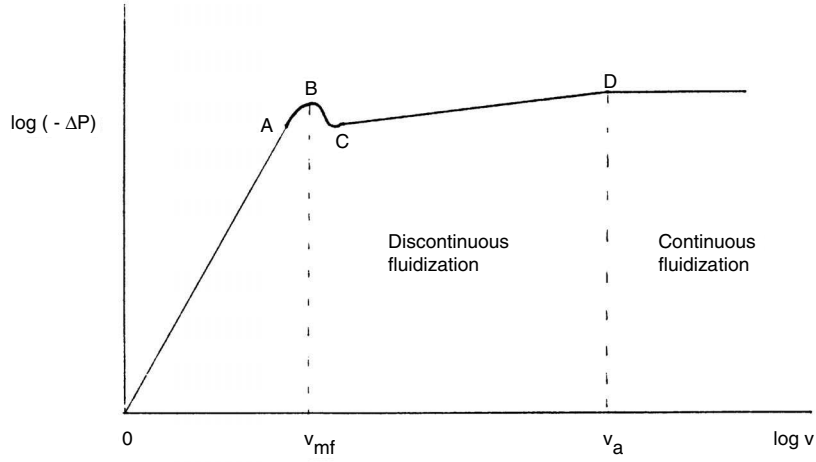

FIGURE 8.4
Pressure drop in fluidized beds.

already passed through the bed. This phenomenon causes the particles to go up and back to the bed instead of being dragged by the fluid. The particles move in a disorderly fashion and it seems as if the bed is boiling. This type of fluidization is known as boiling beds or discontinuous fluidization. On the other hand, when particles are actually dragged, a two-phase circulation occurs. This is called continuous fluidization and is the basis for pneumatic transport.

8.5.1 Minimal Velocity of Fluidization

The point at which the fluidization of the bed occurs is known as minimal velocity of fluidization. At this point there is a dynamic equilibrium between the forces that the gravity field and the fluid exert on the particles. The gravity force exerted on the particles is given by the expression:

$$F_G = (\rho_P - \rho) S\, L\, (1 - \varepsilon)\, g \tag{8.15}$$

where ρ_P and ρ are the densities of the particles and the fluid, respectively; S is the cross-sectional area of the column that contains the particles, L is the height of the bed, ε is the porosity, and g is the gravity constant.

The force exerted by the fluid on the bed of particles is that of pressure, times the cross-sectional area of the bed, and is calculated by the expression:

$$F_P = (-\Delta P) S \tag{8.16}$$

in which (–Δ*P*) is the pressure drop experienced by the fluid when passing through the bed. This expression depends on the circulation flow of the fluid. Therefore, to calculate the minimal velocity of fluidization, the two forces, gravity and pressure, should be equalized, i.e., $F_G = F_P$ or:

$$\left(\rho_P - \rho\right) S\, L \left(1-\varepsilon\right) g = \left(-\Delta P\right) S \tag{8.17}$$

The pressure drop is given by the equation of Ergun as:

$$\frac{\left(-\Delta P\right)}{L} = 150\ \frac{\left(1-\varepsilon\right)^2\ \eta}{\varepsilon^3\, d_p^2}\, v + 1.75\ \frac{\left(1-\varepsilon\right)\rho}{\varepsilon^3\, d_P}\, v^2$$

In spite of the fact that this is the general equation to calculate the pressure drop, it can be simplified, depending on the circulation flow. The different equations that will allow the minimal velocity of fluidization to be calculated, depending on the type of circulation flow of the fluid, are presented next.

8.5.1.1 Laminar Flow

When the circulation flow is laminar, the second term of the right-hand side of the equation of Ergun is negligible compared to the first, so the expression becomes simpler:

$$\frac{\left(-\Delta P\right)}{L} = 150 \frac{\left(1-\varepsilon\right)^2\ \eta}{\varepsilon^3\ d_P^2}\, v$$

When this expression is substituted in Equation 8.17, it is possible to determine the minimal velocity of fluidization under laminar flow as:

$$v_{mf} = \frac{1}{150}\ \frac{\left(\varepsilon_{mf}\right)^3}{\left(1-\varepsilon_{mf}\right)}\ \frac{\rho_P - \rho}{\eta}\, g\, d_p^2 \tag{8.18}$$

8.5.1.2 Turbulent Flow

When the circulation flow is turbulent, the velocity term in the equation of Ergun is negligible compared to the square of the velocity. Therefore, the pressure drop experienced by the fluid can be expressed as:

$$\frac{\left(-\Delta P\right)}{L} = 1.75\ \frac{\left(1-\varepsilon\right)\rho}{\varepsilon^3\, d_P}\, v^2$$

When substituting this expression in Equation 8.17, it is possible to determine the minimal velocity of fluidization under turbulent flow as:

$$\left(v_{mf}\right)^2 = 0.756\left[\frac{\rho_P - \rho}{\rho} g\left(\varepsilon_{mf}\right)^3 d_P\right]^{1/2} \tag{8.19}$$

8.5.1.3 Transition Flow

It can happen that the fluid circulates under a flow higher than the laminar flow, but at which the turbulent flow is not completely developed. In these cases it is necessary to apply the equation of Ergun to calculate the pressure drop regardless of the circulation flow. When substituting the expression of Ergun in Equation 8.17, a second-order equation is obtained, which is necessary to solve in order to find the minimal fluidization velocity:

$$\left(1-\varepsilon\right)\left(\rho_P - \rho\right) g = 150 \frac{\left(1-\varepsilon_{mf}\right)^2 \eta}{\left(\varepsilon_{mf}\right)^3 d_P^2} v_{mf} + 1.75 \frac{\left(1-\varepsilon_{mf}\right)\rho}{\left(\varepsilon_{mf}\right)^3 d_P} \left(v_{mf}\right)^2 \tag{8.20}$$

8.5.2 Minimal Porosity of Fluizidation

In the same way as fluid pressure drop varies with the circulation velocity, the porosity of the bed varies as well. At low velocities, the pressure force is not enough to produce a variation in the structure of the bed, nor in its porosity; but at higher velocities, the bed expands, increasing the void volume.

If the variation of the porosity is plotted against the linear circulation velocity on logarithmic coordinates, a graphic such as that presented in Figure 8.5 is obtained. At low velocities, the porosity does not vary, but a moment comes at which it increases with velocity, presenting a linear variation. The moment at which fluidization begins does not correspond to the point at which the porosity begins to increase, but it occurs at a higher velocity than the minimal fluidization velocity.

The minimal porosity of fluidization can be calculated using graphics that exist for a number of materials (McCabe and Smith, 1968). However, when no data are available, it is possible to use the following expression:

$$\varepsilon_{mf} = 1 - 0.356\left(\log\ d_P - 1\right) \tag{8.21}$$

In this equation the diameter of the particle should be expressed in microns (10^{-6} m), and is valid for d_P values between 50 and 500 μm.

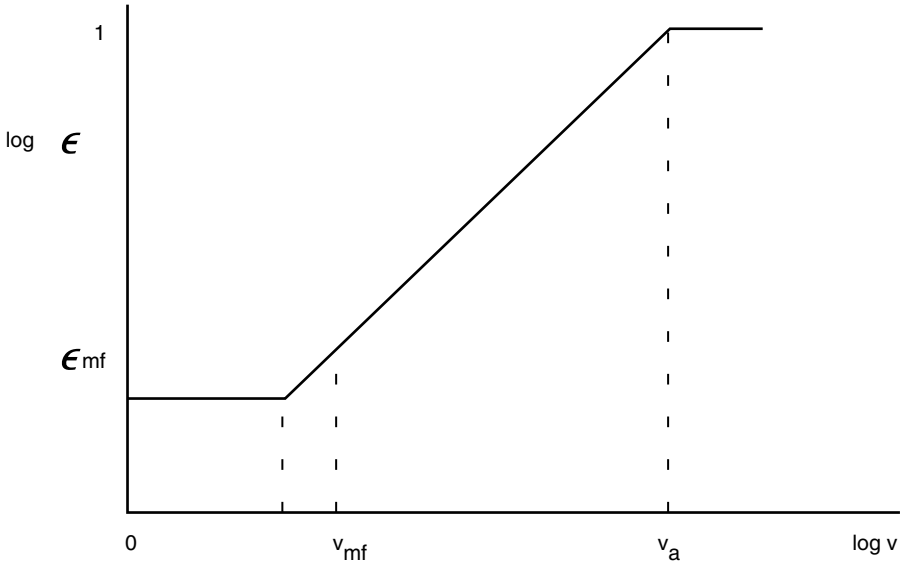

FIGURE 8.5
Porosity of fluidized beds.

8.5.3 Bed Height

When the circulation velocity of the fluid through the porous bed increases, not only does the pressure drop increase, but the porosity increases because the bed height also increases. This bed height increase is tightly bound to the porosity increase, so that the porosity that corresponds to any two heights is related by the expression:

$$L_1\left(1-\varepsilon_1\right)=L_2\left(1-\varepsilon_2\right) \tag{8.22}$$

In a particular case, if a bed porosity ε_0 and height L_0 correspond to a fixed bed, the height and porosity at another given instant are related to the former by the equation:

$$L\left(1-\varepsilon\right)=L_0\left(1-\varepsilon_0\right)$$

If the bed were compact, the particles would occupy the entire bed and there would be no voids, so the expression that correlates the heights becomes simpler:

$$L\left(1-\varepsilon\right)=L_C$$

where L_C is the height of the compact bed.

Problems

8.1

A gas circulates through a bed of cubic particles (5 mm side) at a velocity of 1.2 m/s. The density of the particles is 2050 m kg/m^3 and the apparent density of the bed is 1000 kg/m^3. Calculate: (a) the equivalent diameter of the particle; (b) the void fraction; and (c) the pressure loss experienced by the fluid when passing through one meter of packed bed if the gas density is 0.750 kg/m^3 and its viscosity is 0.018 mPa·s.

(a) The equivalent diameter of the particle is calculated from the expression:

$$d_P = \frac{6\Gamma}{a_{S0}}$$

Since the particles are cubic, the shape factor is $\Gamma = 0.81$, while the specific surface will be:

$$a_{S0} = \frac{6}{l} = \frac{6 \times 25\ \text{mm}^2}{125\ \text{mm}^2} = 1.2\ \text{mm}^{-1}$$

Therefore,

$$d_P = \left(6 \times 0.81/1.2\right)\ \text{mm} = 4.05\ \text{mm}$$

(b) The porosity or void fraction:

$$\varepsilon = \frac{\text{void volume}}{\text{bed volume}} = \frac{\text{bed volume} - \text{volume of particles}}{\text{bed volume}}$$

$$= 1 - \frac{\text{volume of particles}}{\text{bed volume}}$$

If m_P is the total mass of particles and ρ_P its density, then the volume occupied by the particles would be = m_P/ρ_P. In the same way, if m_L is the mass of the bed and ρ_L its density: bed volume = m_L/ρ_L.

The mass of the bed corresponds to the mass of the particles it contains ($m_L = m_P$), while the density of the bed is the so-called apparent density ($\rho_L = \rho_a$).

Therefore:

$$\varepsilon = 1 - \frac{\rho_a}{\rho_p} = 1 - \frac{1000\ \text{kg/m}^3}{2050\ \text{kg/m}^3} = 0.512$$

(c) The pressure drop experienced by the gas when passing through the bed of particles is calculated from the equation of Ergun:

$$\frac{(-\Delta P)}{L} = 150\frac{(1-\varepsilon)^2\,\eta}{\varepsilon^3 d_p^2}\,v + 1.75\,\frac{(1-\varepsilon)\rho}{\varepsilon^3 d_p}\,v^2$$

The following data are substituted in the last equation:

$\varepsilon = 0.512$
$\eta = 1.8 \times 10^{-5}$ Pa·s
$d_p = 4.05 \times 10^{-3}$ m
$\rho = 0.750$ kg/m^3
$v = 1.2$ m/s

hence,

$$(-\Delta P/L) = (350 + 1697)\ \text{Pa/m} = 2047\ \text{Pa/m}$$

To know the type of flow under which the gas circulates, the particle Reynolds number is calculated:

$$\text{Re}_p = \frac{\rho v d_p}{\eta} = \frac{(0.75\ \text{kg/m}^3)(1.2\ \text{m/s})(4.05 \times 10^{-3}\ \text{m})}{1.8 \times 10^{-5}\ \text{Pa s}} = 203$$

so, the gas circulates under turbulent flow.

8.2

A gas that has a viscosity of 0.020 mPa·s circulates through a packed bed with a volumetric flow flux of 4000 m^3/(h.m^2). The bed is packed with cubic particles that have 4 mm per side, with a density of 1300 kg/m^3. A gas cylinder of 5-cm diameter and 50-cm height is used to calculate the apparent density, determining that the particles that occupies the gas cylinder weighs 835 grams. Calculate: (a) the porosity of the system; and (b) if the average density of the gas is 0.85 kg/m^3, the pressure drop it experiences when passing through a 3-m bed of particles.

(a) Calculation of bed porosity:

$$\varepsilon = 1 - \frac{\rho_a}{\rho_p}$$

Apparent density:

$$\rho_a = \frac{m_p}{(\pi/4)DL} = \frac{835\ \text{g}}{(\pi/4)(5^2)(50)\ \text{cm}^3} = 0.8505\ \text{g/cm}^3 = 850.5\ \text{kg/m}^3$$

$$\varepsilon = 1 - \frac{850.5\ \text{kg/m}^3}{1300\ \text{kg/m}^3} = 0.3458$$

Calculation of particle equivalent diameter: since the particles are cubic, the shape factor can be considered as 0.81, also $a_{S0} = \Gamma(6/l)$, therefore:

$$d_p = \Gamma \cdot l = 3.24 \times 10^{-3}\ \text{m}$$

b) The equation of Ergun will be applied to calculate the pressure drop experienced by the gas when passing through 3 m of packed bed. Gas circulation velocity should be calculated first. Since the density of the volumetric flow is the relationship between the volumetric flow rate and the cross-sectional area, it coincides with the velocity:

$$v = \frac{q}{S} = 4000 \frac{\text{m}^3}{\text{h m}^2} \frac{1\ \text{h}}{3600\ \text{s}} = 1.111\ \text{m/s}$$

The following data are substituted in the equation of Ergun:

$\varepsilon = 0.3458$
$\eta = 2 \times 10^{-5}\ \text{Pa}\cdot\text{s}$
$d_p = 3.24 \times 10^{-3}\ \text{m}$
$\rho = 0.850\ \text{kg/m}^3$
$v = 1.11\ \text{m/s}$
$L = 3\ \text{m}$

then:

$$(-\Delta P) = 3(3287 + 8967) = 36{,}762\ \text{Pa}\ (\text{N/m}^2)$$

The particle Reynolds number would be:

$$\text{Re}_p = \frac{\rho v d_p}{\eta} = \frac{(0.85\ \text{kg/m}^3)(1.11\ \text{m/s})(3.24 \times 10^{-3}\ \text{m})}{2 \times 10^{-5}\ \text{Pa s}} = 153$$

So, the gas circulates under turbulent flow.

8.3

In a drying process, air is circulated through a bed of peas contained in a cylindrical column of 85-cm diameter. The bed has a void fraction equal to 0.40. Air circulates with a flow of 5000 m^3/h measured at the entrance to the column (1.5 atm, 90°C) and a viscosity of 0.015 mPa·s. Calculate the pressure drop per unit of bed length experienced by air when passing through the bed of peas.

To calculate the pressure drop experienced by the gas when passing through the packed bed, the equation of Ergun (Equation 8.13) will be applied.

Calculation of air density:

$$\rho = \frac{PW_{AIR}}{RT} = \frac{(1.5\ \text{atm})(29\ \text{kg/mol})}{\left(0.082\ \frac{\text{atm m}^3}{\text{kmol K}}\right)(363\ \text{K})} = 1.461\ \text{kg/m}^3$$

Calculation of velocity:

$$v = \frac{w}{\rho S} = \frac{q}{S} = \frac{5000\ \text{m}^3/\text{h}}{(\pi/4)(0.85\ \text{m})^2}\ \frac{1\ \text{h}}{3600\ \text{s}} = 2.448\ \text{m/s}$$

Calculation of pressure drop; the following data are substituted in the equation of Ergun:

$\varepsilon = 0.40$
$\eta = 1.35 \times 10^{-5}$ Pa·s
$d_P = 0.003$ m
$\rho = 1.461$ kg/m^3
$v = 2.448$ m/s

hence:

$$(-\Delta P)/L = (3098 + 47{,}881)\ \text{Pa/m} = 50{,}979\ \text{Pa/m} = (0.52\ \text{atm})$$

The particle Reynolds number will be:

$$\text{Re}_p = \frac{\rho v d_P}{\eta} = \frac{(1.461\ \text{kg/m}^3)(2.448\ \text{m/s})(0.003\ \text{m})}{1.35 \times 10^{-5}\ \text{Pa s}} = 795$$

So, the gas circulates under turbulent flow.

8.4

Air at 50°C is circulated through a glass column of 10-cm diameter and 1-m height, which is filled with cylindrical hollow glass rings (1 cm × 1 cm) with a wall thickness of 1.5 mm. If the air pressure at the entrance of the column is 730 mm Hg and the pressure drop experienced by the fluid when passing through the bed of solids is 100 cm water (column), calculate the air flow that circulates through the bed of solids. Which is the circulation regime of air?

Data and notes: To determine the porosity of the bed, the column is filled with water reaching a height of 40 cm. Then, rings are added until the height of the water and rings is the same (1 m). The viscosity of air at 50°C can be considered to be 0.20 mPa·s.

To calculate the pressure drop experienced by the gas when passing through the packed bed, the equation of Ergun (Equation 8.13) will be applied. This equation can be expressed as a function of the mass flow density, which is $G = \rho v$

$$\frac{(-\Delta P)}{L} = 150\ \frac{(1-\varepsilon)^2 \eta}{\varepsilon^3 d_p^2}\ \frac{G}{\rho} + 1.75\ \frac{(1-\varepsilon)}{\varepsilon^3 d_p \rho}\ G^2$$

Unknown variables will be calculated first.

Porosity calculation:

$$\varepsilon = \frac{\text{Void volume}}{\text{Bed volume}} = \frac{S(40\ \text{cm}^3)}{S(100\ \text{cm}^3)} = 0.4$$

Cross-sectional area of the column:

$$S = (\pi/4) D^2 = (\pi/4) 0.1^2\ \text{m}^2 = 7.854 \times 10^{-3}\ \text{m}^2$$

Pressure drop:

$$(-\Delta P) = 100\ \text{cm w.c.}\ \frac{9.8 \times 10^4\ N/m^2}{1000\ \text{cm w.c.}} = 9800\ \text{Pa} = 0.0967\ \text{atm}$$

Pressure at the entrance of the column:

$$P_e = (730/760)\ \text{atm} = 0.9650\ \text{atm} \times (1.013 \times 10^5\ \text{Pa/atm}) = 97{,}301\ \text{Pa}$$

Pressure at the exit of the column:

$$P_S = P_e - (-\Delta P) = 0.8639\ \text{atm}$$

Calculation of air density:

$$\rho = \frac{PW_{AIR}}{RT}$$

Density at the entrance:

$$\rho = \frac{(0.9605\ \text{atm})(29\ \text{kg/mol})}{\left(0.082\ \frac{\text{atm m}^3}{\text{kmol K}}\right)(323\ \text{K})} = 1.052\ \text{kg/m}^3$$

Density at the exit:

$$\rho = \frac{(0.8638\ \text{atm})(29\ \text{kg/mol})}{\left(0.082\ \frac{\text{atm m}^3}{\text{kmol K}}\right)(323\ \text{K})} = 0.946\ \text{kg/m}^3$$

Apparent density:

$$\rho_a = 0.999\ \text{kg/m}^3$$

Calculation of particle specific surface:

Since the particles are hollow, the surface of the particle will be formed by the internal and external side areas of the cylinder, to which the areas of the circular crowns of the bases should be added.

Thickness of the particle's wall:	$e = 0.0015$ m
External particle diameter:	$de = 0.01$ m
Internal particle diameter:	$di = de - 2e$
Particle height:	$H = 0.01$ m
Particle surface:	$\pi(de + di)H + 2(\pi/4)(de^2 - di^2)$
Particle volume:	$(\pi/4)\ de^2$
Obtaining:	$a_{S0} = 782\ \text{m}^{-1}$
Particle equivalent diameter:	$d_P = 6\ \Gamma/a_{S0} = 7.673 \times 10^{-3}$ m

It was supposed that the shape factor was equal to one.
Calculation of the mass flux:
The following data are substituted in the equation of Ergun:

$\varepsilon = 0.40$

$\eta = 2 \times 10^{-5}\ \text{Pa}\cdot\text{s}$

$\rho = 0.999\ \text{kg/m}^3$
$L = 1\ \text{m}$
$(-\Delta P) = 9800\ \text{Pa}$
$d_p = 7.673 \times 10^{-3}\ \text{m}$

therefore:

$$9800 = 286.9\ G + 2140.3\ G^2$$

$$G^2 + 0.134\ G - 4.58 = 0$$

This is a second-order equation in which the negative root has no physical meaning. The positive root yields the value of the mass flow rate: G = 2.074 kg/(m²s).

The mass flow rate would be:

$$w = G\ S = 2.074\ \text{kg}/\left(\text{m}^2\text{s}\right)7.854 \times 10^{-3}\ \text{m}^2 = 1.629 \times 10^{-2}\ \text{kg/s}$$

The volumetric flow rate would be:

$$q = \frac{w}{\rho} = \frac{1.629 \times 10^{-2}\ \text{kg/s}}{0.999\ \text{kg/m}^3} = 0.0163\ \text{m}^3/\text{s} = 16.3\ \text{l/s}$$

The particle Reynolds number would be:

$$\text{Re}_p = \frac{G d_p}{\eta} = \frac{\left(2.074\ \text{kg/m}^2\ \text{s}\right)\left(1.673 \times 10^{-3}\ \text{m}\right)}{2 \times 10^{-5}\ \text{Pa s}} = 988$$

Hence, the gas circulates under turbulent flow.

8.5

An air stream is isothermally circulated at 45°C through a particle bed contained in a cylindrical tube of 15-cm diameter. The bed is constituted by cylindrical particles of 3-mm diameter and 4.5-mm height, with a density of 1.4 g/cm³. The air pressure at the entrance of the bed is 1.3 atm and experiences a pressure drop of 75 cm w.c. (cm water column) when passing through 1 m of bed. If the viscosity of the air at 45°C is 0.0195 mPa·s, and the particles contained in 250 cm³ weigh 140 g, calculate: (a) specific surface of the bed and of the particle; (b) air density after passing through 1 m bed; and (c) mass flow rate at which air circulates.

Data: The molecular weight can be considered as 29 kg/kmol.

(a) Calculation of the specific surface of the particle:

$$a_{S0} = \frac{\text{Particle surface}}{\text{Particle volume}}$$

Dimensions of the cylindrical particle:

Diameter: $d_P = 0.003$ m
Height: $H = 0.0045$ m

Particle surface:

$$2(\pi/4)dp^2 + \pi\, d_p\, H = 5.655 \times 10^{-5}\ \text{m}^2$$

Particle volume:

$$(\pi/4)dp^2\, H = 3.181 \times 10^{-8}\ \text{m}^3$$

Therefore:

$$a_{S0} = 1777.74\ \text{m}^{-1}$$

It is possible to calculate the equivalent diameter of the particle from a_{S0} as $d_P = 6\Gamma/a_{s0}$.

If it is supposed that the shape factor is one ($\Gamma = 1$), then the particle's equivalent diameter is $d_P = 3.375 \times 10^{-3}$ m.

Calculation of the void fraction:

Apparent density: $\rho_a = 140\ \text{g}/250\ \text{cm}^3 = 0.56\ \text{g}/\text{cm}^3$

Porosity: $\varepsilon = 1 - (\rho_a/\rho_P) = 1 - (0.56/1.4) = 0.6$

Specific surface of the bed:

$$a_S = a_{S0}(1-\varepsilon) = 1777.74\ \text{m}^{-1}(1-0.6) = 711.1\ \text{m}^{-1}$$

(b) Calculation of air density after passing through 1 m of bed:
The pressure drop experienced by the fluid is 75 cm w.c.:

$$(-\Delta P) = 75\ \text{cm w.c.}\frac{1\ \text{atm}}{1000\ \text{cm c.a.}}\frac{9.8\times10^4\ \text{Pa}}{1\ \text{atm}}\frac{1\ \text{atm}}{101.2\cdot10^3\ \text{Pa}} = 0.0726\ \text{atm}$$

Pressure at the entrance:

$$P_e = 1.3 \text{ atm } \frac{1 \text{ atm}}{1.033 \text{ atm}} = 1.258 \text{ atm}$$

Pressure at the exit:

$$P_s = P_e - \left(-\Delta P\right) = 1.1855 \text{ atm}$$

Density of air after passing through 1 m of packed bed:

$$\rho = \frac{\left(1.1855 \text{ atm}\right)\left(29 \text{ kg/mol}\right)}{\left(0.082 \frac{\text{atm m}^3}{\text{kmol K}}\right)\left(318 \text{ K}\right)} = 1.319 \text{ kg/m}^3$$

Air density at the entrance:

$$\rho = \frac{\left(1.258 \text{ atm}\right)\left(29 \text{ kg/mol}\right)}{\left(0.082 \frac{\text{atm m}^3}{\text{kmol K}}\right)\left(318 \text{ K}\right)} = 1.399 \text{ kg/m}^3$$

Apparent density: $\rho_a = 1.359 \text{ kg/m}^3$

(c) To calculate the mass flow, the circulation velocity should be calculated first using the equation of Ergun. The following data are substituted in the equation of Ergun:

$\varepsilon = 0.60$
$\eta = 1.95 \times 10^{-5} \text{ Pa·s}$
$dp = 3.375 \times 10^{-3} \text{ m}$
$\rho = 1.359 \text{ kg/m}^3$
$(-\Delta P) = 7350 \text{ Pa}$
$L = 1 \text{ m}$

so:

$7350 = 190.2\, v + 1304.94\, v^2$
$v^2 + 0.1458\, v - 5.633 = 0$

This is a second-order equation in which the negative root has no physical meaning. The air linear circulation velocity is obtained from the value of the positive root: $v = 2.30$ m/s.

The mass flow is obtained from the expression: $w = \rho_m\, v\, S = \rho_m\, v\, (p/4)\, D^2$.

$$w = \left(1.359\ \text{kg/m}^3\right)\left(2.30\ \text{m/s}\right)\left(\pi/4\right)\left(0.15\ \text{m}\right)^2\left(3600\ \text{s/h}\right) = 190\ \text{kg/h}$$

8.6

The technique of fluidized bed was applied to sorghum seeds drying in an experimental work. To do this, 95.8 kg of seeds/m^2 of bed cross section were loaded into a column of 0.2 m diameter, through which air was circulated. The air conditions at the entrance of the column were 40°C and 1 atm. It was found that the height of the bed varied with the air circulation flow according to the data in the table:

q (m^3/h)	60	71	79	107	131	149	182	212
h (mm)	135	135	138	152	175	187	215	240

Calculate the minimal fluidization velocity, as well as the height of the bed at that instant.

Data and notes: The sorghum bed has a porosity of 0.38 when no air circulates through the system, and the seeds have a sphericity of 0.98 (shape factor). Also, it was found in a previous experiment that 500 grains of this seed displaced 12 cm^3 of water contained in a glass cylinder.

Bed cross-sectional area: $S = (\pi/4)\, D^2 = (\pi/4)\ (0.2\ \text{m})^2 = 0.03142\ \text{m}^2$

The particle diameter can be calculated, supposing that they are spheres with diameter d_r. The 500 grains have a volume of 12 cm^3.

$$500\left(\pi/6\right)\left(d_r\right)^3 = 12\ \text{cm}^3; \quad \text{then: } d_r = 0.358\ \text{cm}$$

The equivalent diameter of the particle is obtained by multiplying this value by the shape factor: $d_P = d_r\, \Gamma = 0.358\ \text{cm} \cdot 0.98 = 0.351\ \text{cm}$. The pressure drop experienced by the air when passing through the bed will be calculated from the equation of Ergun. The porosity of the bed depends on the height, and is calculated from the expression:

$$\varepsilon = 1 - \frac{L_0\left(1 - \varepsilon_0\right)}{L}$$

where ε_0 and L_0 are the porosity and the height of the bed at initial conditions.

The air density is calculated by the equation:

$$\rho = \frac{\left(1\ \text{atm}\right)\left(29\ \text{kg/mol}\right)}{\left(0.082\ \dfrac{\text{atm m}^3}{\text{kmol K}}\right)\left(313\ \text{K}\right)} = 1.3\ \text{kg/m}^3$$

The volumetric flow is used to calculate the linear velocity: $v = q/S$.

TABLE P8.6

Fluidization Data of Sorghum Seeds

q (m^3/h)	L (m)	ε	v (m/s)	(–ΔP) (N/m^2)
60	0.135	0.38	0.531	395.9
71	0.135	0.38	0.628	447.4
79	0.138	0.393	0.700	488.1
107	0.152	0.449	0.946	554.6
131	0.175	0.522	1.158	503.8
149	0.187	0.552	1.318	541.2
182	0.215	0.611	1.609	576.7
212	0.240	0.651	1.875	637.6

From the data in the table of the problem, it is possible to calculate the linear circulation velocity, the bed porosity, and the pressure drop for each volumetric flow of air (Table P8.6).

The data in the table are plotted in logarithmic coordinates (–Δ*P*) and the porosity against velocity (Figure P8.6). The minimal fluidization velocity can be observed in the plot and it corresponds approximately to 0.90 m/s. For minimal porosity, a value of 0.442 can be obtained.

The height reached by the bed for this porosity would be:

$$L = L_0 \frac{1-\varepsilon_0}{1-\varepsilon} = 135 \frac{1-0.380}{1-0.442} = 150 \text{ mm}$$

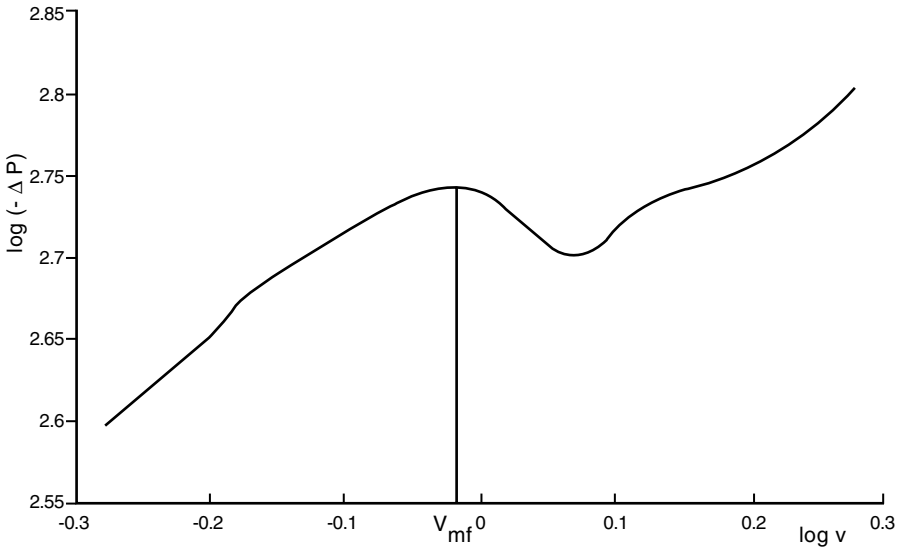

FIGURE P8.6
Pressure drop in a fluidized bed of peas.

8.7

20,000 kg of sand with a mesh size of 0.175 mm (Tyler's series no. 80) are fluidized using an air stream at 350°C and 20 atm pressure in a cylindrical column of 2 m diameter. The density of the particles is 2700 kg/m^3. Under the operation conditions, the viscosity of the air can be taken as 0.021 mPa·s. Calculate: (a) minimal porosity for fluidization; (b) minimal height of fluidized bed; (c) pressure drop experienced by air when passing through the sand bed; and (d) minimal fluidization velocity.

(a) Equation 8.21 is used to calculate the minimal fluidization velocity:

$$\varepsilon_{mf} = 1 - 0.356\left(\log d_P - 1\right) = 0.557$$

(b) The minimal height of the fluidized bed is obtained from the expression:

$$L = L_0 \frac{1-\varepsilon_0}{1-\varepsilon_{mf}}$$

in which L_0 is the height correspondent to a porosity ε_0. If the bed is compact, $\varepsilon_0 = 0$.

Volume of the compact bed: $V_C = (\pi/4)\, D^2\, L_C$

Mass of the compact bed: $m_C = 20{,}000$ kg

Since the density of the particles of the bed is:

$$\rho_P = \frac{m_C}{V_C} = \frac{m_C}{(\pi/4) D^2 L_C}$$

it is possible to calculate the height correspondent to the compact bed:

$$L_C = \frac{m_C}{\rho_C (\pi/4) D^2} = \frac{20{,}000 \text{ kg}}{\left(2700 \text{ kg/m}^3\right)(\pi/4)\left(2^2 \text{ m}^2\right)} = 2.36 \text{ m}$$

Therefore, the bed height at the fluidization point would be:

$$L = 2.36 \frac{1-0}{1-0.557} = 5.33 \text{ m}$$

(c) The gravity and flotation forces due to the displaced fluid equilibrate at the fluidization moment.

$F_G = (\rho_P - \rho)\ S\ L_{mf}(1 - \varepsilon_{mf})\ g$
$F_P = (-\Delta P)\ S$

This is:

$$(-\Delta P) = L_{mf}(\rho_P - \rho)(1 - \varepsilon_{mf})\, g$$

Air density:

$$\rho = \frac{(20\ \text{atm})(29\ \text{kg/mol})}{\left(0.082\ \frac{\text{atm m}^3}{\text{kmol K}}\right)(623\ \text{K})} = 11.35\ \text{kg/m}^3$$

Hence, the pressure drop experienced by the air would be:

$$(-\Delta P) = 5.13\ \text{m}\ (2700 - 11.35)\ \text{kg/m}^3 (1 - 0.54)\ 9.8\ \text{m/s}^2 = 62{,}178\ \text{Pa}$$

(d) The minimal fluidization velocity is calculated from the equation:

$$(\rho_P - \rho)\, g = 150 \frac{(1 - \varepsilon_{mf})\ \eta}{(\varepsilon_{mf})^3 d_P^2} v_{mf} + 1.75\ \frac{\rho}{(\varepsilon_{mf})^3 d_P} (v_{mf})^2$$

When substituting the variables by their values:

$\rho_P = 2700\ \text{kg/m}^3$
$d_P = 1.75 \times 10^{-4}\ \text{m}$
$\rho = 11.35\ \text{kg/m}^3$
$\eta = 2.1 \times 10^{-5}\ \text{Pa·s}$
$\varepsilon_{mf} = 0.557$

a second-order equation is obtained:

$26{,}348.7 = 300{,}476.8\ v_{mf} + 720{,}990.2\ (v_{mf})^2$
$(v_{mf})^2 + 0.417\ v_{mf} - 0.0365 = 0$

The negative root of this equation does not have a physical meaning, so the minimal fluidization velocity would be the positive solution: $v_{mf} = 0.074$ m/s. The particle Reynolds number correspondent to this velocity is:

$$R_{ep} = \frac{\rho v d_P}{\eta} = \frac{(11.53\ \text{kg/m}^3)\ (0.0744\ \text{m/s})(1.75 \times 10^{-4}\ \text{m})}{2.1 \times 10^{-5}\ \text{Pa s}} = 7$$

So, the circulation flow is laminar.

9

Filtration

9.1 Introduction

Filtration is a unit operation whose purpose is the separation of an insoluble solid present in solid–liquid suspension by passing the suspension through a porous membrane that retains the solid particles. The porous membrane is called the filtering medium, while the retained particles in the membrane form a layer known as cake and the liquid that passes through the porous membrane and does not contain solids is called a filtrate.

The desired phase in filtration can occur in the filtrate, cake, or both. When the desired solid part is obtained, the cake should be washed to eliminate the impurities it may contain. Filtration can operate under simple gravity to obtain the flow of filtrate that crosses the filtrating medium, or by applying a pressure higher than the atmospheric pressure to the front part of the filtering medium or vacuum to the back side. These processes are known as pressure filtration and vacuum filtration, respectively.

Filtration is an operation widely used in the industry in general; in the particular case of the food industry, three characteristic types of filtration can be distinguished. The first includes suspensions containing significant amounts of insoluble solids that, when filtered, form a cake on the filtrating medium; thus, obtaining the solid, filtrate, or both could be interesting. Another type of filtration includes suspensions with few insoluble solids that usually are undesired, in which case the filtration is called clarification. Finally, microfiltration should be mentioned. Microfiltration occurs when the size of the solid particles to be separated is around 0.1 mm.

9.2 Fundamentals of Filtration

The study performed next applies to filters in which cakes are formed on the filtering medium. Among these types of filters, the most used are the plate-and-frame press filters.

Initially, the feed or slurry passes through the filtering medium, but, as it filtrates, a cake is formed that increases its thickness, so the feed should pass through not only the filtering medium but also the cake. Hence, the pressure drop along the filter is supposed to be greater with time, resulting in the filtrate flow being smaller with time. This indicates that filtration can be done at constant pressure drop or at constant filtrate flow. In the first case, when maintaining a constant pressure drop, the filtrate flow will decrease along the filtration time. On the other hand, when a constant filtrate flow is desired, the pressure drop will be greater over time. As filtration proceeds, the thickness of the deposited solids increases, becoming a non-stationary circulation of fluids through variable filling height case.

Two zones can be distinguished in the filter: the filtering cake and the filtering medium. The former constitutes a filling that can change its characteristics (specific surface, porosity, etc.), while the filtering medium has fixed characteristics.

In general, for a filter in which a cake is formed, the total pressure drop experienced by the fluid ($-\Delta P$) is the summation of the pressure drop experienced through the filtering medium ($-\Delta P_m$) plus the pressure drop experienced through the cake ($-\Delta P_c$):

$$\left(-\Delta P\right) = -\left(\Delta P_c + \Delta P_m\right) = \left(-\Delta P_c\right) + \left(-\Delta P_m\right) \tag{9.1}$$

9.2.1 Resistance of the Filtering Cake

If a plate-and-frame press filter is considered, the filtering surface is flat and vertical, as shown in Figure 9.1.a. The fluid crosses through a cake of thickness z, in which the pressure drop is ΔP_c. Applying the Bernoulli equation to the cake section obtains:

$$\frac{\Delta P}{\rho} + \frac{\Delta v^2}{2\alpha} + g\,\Delta z + \hat{E}_V = 0 \tag{9.2}$$

According to the conditions of the filter:

$$\frac{\Delta P}{\rho} + \hat{E}_V = 0$$

The circulation of the fluid is laminar, so $\hat{E}_V$ can be obtained from Kozeny's equation as:

$$\hat{E}_V = \frac{\Delta P}{\rho} = \frac{\eta v K'' \left(1-\varepsilon\right)^2 \left(a_{S0}\right)^2}{\rho\, \varepsilon^3} z \tag{9.3}$$

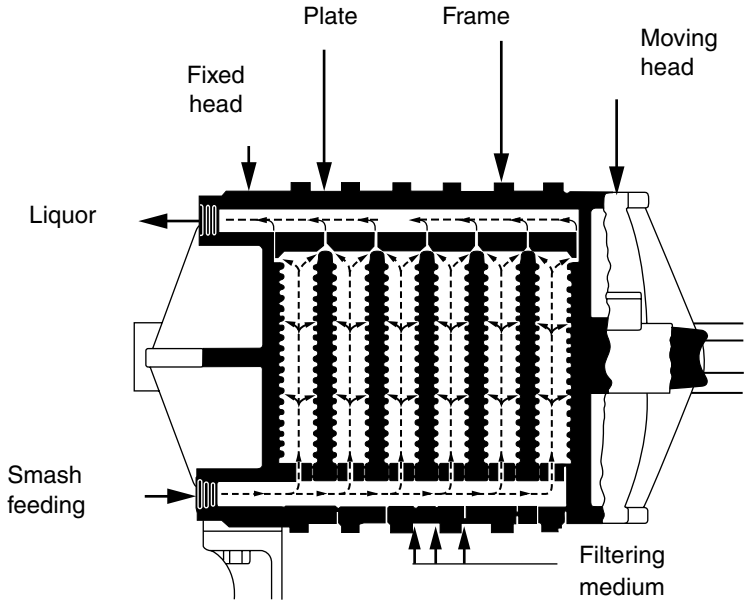

FIGURE 9.1.A
Press-and-frame filter. (Adapted from Ocón, J. and Tojo, G., *Problemas de Ingenieria Quimica*, Aguilar, Madrid, 1968.)

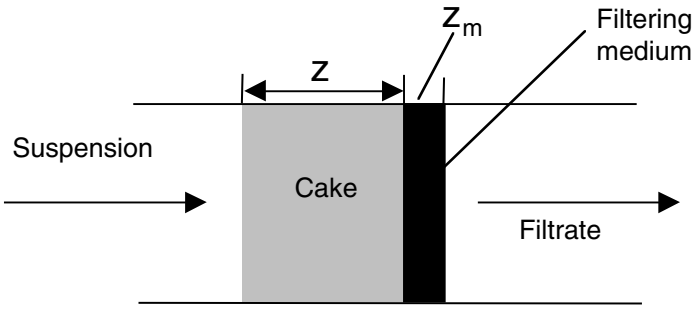

FIGURE 9.1.B
Cake formation scheme.

in which v is the velocity in the free zone given by:

$$v = \frac{1}{A}\frac{dV}{dt} \tag{9.4}$$

where V is the filtrate's volume and A is the cross-sectional area.

Combining the equations mentioned before results in:

$$\frac{1}{A}\frac{dV}{dt} = \frac{\varepsilon^3}{\eta K'' (1-\varepsilon)^2 (a_{S0})^2 z}\left(-\Delta P_{tc}\right) \tag{9.5}$$

The specific resistance of the cake is defined as:

$$\alpha = \frac{K''(1-\varepsilon)(a_{S0})^2}{\varepsilon^3 \rho_S} \tag{9.6}$$

where the units of α are m/kg. α physically represents the pressure drop needed to obtain a unit superficial velocity times volume of filtrate per unit viscosity through the cake containing a unit mass of solid per unit area of filter.

Substituting the expression of the cake's specific resistance in Equation 9.5 obtains:

$$\frac{1}{A}\frac{dV}{dc} = \frac{\left(-\Delta Pc\right)}{\eta \rho_S (1-\varepsilon)\alpha z} \tag{9.7}$$

In order to integrate this equation, the cake's thickness should be a function of the filtrate volume. Hence, some variables will be defined that will allow thickness to be a function of the volume of filtrate.

The cake thickness z is a function of the weight of the deposited dry cake (m_{DC}):

$$m_{DC} = A\, z\, \rho_S (1-\varepsilon) \tag{9.8}$$

To obtain the relationship between the deposited dry cake (m_{DC}) and the volume of filtrate (V), M is defined as the relation between the wet cake and dry cake weight:

$$M = \frac{m_{WC}}{m_{DC}} = \frac{m_{DC} + m_{RL}}{m_{DC}} = 1 + \frac{A\, z\, \varepsilon\, \rho}{A z (1-\varepsilon)\rho_S} \tag{9.9}$$

where the subindexes *WC* and *DC* indicate wet cake and dry cake, respectively, while m_{RL} is the mass of liquid retained by the cake, whose value is:

$$m_{RL} = m_{DC}(M-1) \tag{9.10}$$

If S is the mass fraction of solid in the filtered suspension:

$$S = \frac{\text{solid mass}}{\text{total mass}} = \frac{m_{DC}}{m_{DC}\,M + \rho V} \tag{9.11}$$

Hence:

$$m_{DC} = \frac{\rho V S}{1 - M S} \tag{9.12}$$

This last equation and Equation 9.8 allow one to obtain the relation between thickness of the cake and volume of filtrate:

$$z = \frac{\rho V S}{1 - M S} \frac{1}{\rho_S (1 - \varepsilon) A} \tag{9.13}$$

Substituting and rearranging this expression in Equation 9.7 obtains:

$$\frac{dV}{dt} = \frac{A^2 (-\Delta P c)}{\eta \alpha \dfrac{\rho V S}{1 - M S}} \tag{9.14}$$

In this equation it can be observed that the flow of filtrate is directly proportional to the pressure drop experienced by the fluid when crossing through the cake and inversely proportional to the volume of filtrate. If the pressure drop is kept constant, the filtrate flow decreases with filtration time, since the volume of filtrate increases with time.

9.2.2 Filtering Medium Resistance

The filtrate flow that crosses the filtering medium is the same flow that crosses the cake. The equation of Kozeny can be applied to this zone to calculate the pressure drop $-\Delta P_m$, but actually a resistance of the filtering medium R_f is used, so the filtrate's flow would be:

$$\frac{dV}{dt} = \frac{A (-\Delta P_m)}{\eta R_f} \tag{9.15}$$

The units of R_f are m^{-1}, a resistance that includes various constants of the filter. When compared with Kozeny's equation, this constant is:

$$R_f = \frac{\left(\varepsilon_m\right)^3}{K''_m \left(1-\varepsilon_m\right)^2 \left(a_{S0}\right)^2 z_m} \tag{9.16}$$

in which z_m is the thickness of the filtering medium and all the others are its characteristic variables. The subindex m indicates that these are characteristics of the filtering medium.

It is convenient to consider the resistance offered by the filtering medium as equivalent to the resistance offered by a certain cake thickness z_f that has been deposited due to crossing a volume of filtrate V_f. It is obvious that V_f is a constant fictitious value. Similar to Equation 9.14 obtained for the cake, the filtrate flow can be expressed as a function of this fictitious volume of filtrate according to the expression:

$$\frac{dV}{dt} = \frac{A^2\left(-\Delta P_m\right)}{\eta\alpha \dfrac{\rho V_f S}{1-MS}} \tag{9.17}$$

Comparing this last equation with Equation 9.15, it is observed that:

$$R_f = V_f \frac{\rho S\alpha}{A\left(1-MS\right)} \tag{9.18}$$

in which the resistance of the filtering medium is a function of the fictitious volume of filtrate.

9.2.3 Total Filtration Resistance

As seen before, the total pressure drop experienced by the fluid is the summation of the losses caused when crossing through the cake and the filtering medium.Therefore, the filtrate can be expressed according to the equations:

$$\frac{dV}{dt} = \frac{A^2\left(-\Delta P\right)}{\eta \dfrac{\alpha\rho S}{1-MS}\left(V+V_f\right)} \tag{9.19a}$$

$$\frac{dV}{dt} = \frac{A^2\left(-\Delta P\right)}{\eta\left(\dfrac{\alpha\rho S}{1-MS}V + A R_f\right)} \tag{9.19b}$$

Once these equations are obtained, they should be integrated. Two cases can occur: one when the pressure drop experienced by the fluid is constant and another when operating at a constant volumetric flow.

9.2.4 Compressible Cakes

When the specific resistance of the cake does not change with the cake thickness and is independent of the pressure $-\Delta Pc$, the cake is called incompressible. This happens when the cake is formed by rigid solid particles that keep their shape, in which the values of cake porosity and specific surface of the particles are not affected by the compression applied on the bed.

In general, particles that form the cake are flexible and deformable. In these types of cakes (called compressible), the resistance to flow depends on the pressure drop, which varies along the thickness of the cake. In this case the specific resistance of the cake, α, varies along the cake thickness, and an average value should be used if one wants to integrate Equations 9.19a and b.

Empirical formulas exist that allow one to calculate the specific resistance of the cake α. One of the most used of these equations is given by Almy and Lewis:

$$\alpha = \alpha_0 \left(-\Delta P_c\right)^n \tag{9.20}$$

where α_0 is the specific resistance of the cake when there is no pressure drop, and n is the compressibility factor, whose value varies between 0.1 and 1, with higher values corresponding to the more compressible cakes. Although it has been proved that certain dependence exists, n is supposed to be independent of pressure.

The values of α_0 and n should be obtained experimentally from measurements of α of a known pressure drop in the cake and by plotting into double logarithmic paper the corresponding pairs of values α and ΔP_c. The slope of the fitted straight line will be the value of the compressibility factor n, while the ordinate to the origin allows one to obtain the value of α_0. Another expression that gives the variation of the cake's specific resistance as a function of the pressure drop is Ruth's equation:

$$\alpha = \alpha_0' \left[1 + \beta \left(-\Delta P_c\right)^{n'}\right] \tag{9.21}$$

in which α_0', β, and n' are parameters that should be obtained in an empirical form.

9.3 Filtration at Constant Pressure Drop

When the filtration operation is carried out at a constant pressure drop, it is interesting to know the variation of the volume of filtrate with time. This can be done by integrating Equation 9.19b. This equation can be expressed as separated variables:

$$\left(\frac{\alpha \rho S}{1 - M S} V + A R_f\right) dV = \frac{A^2 \left(-\Delta P\right)}{\eta} dt \tag{9.22}$$

If a new constant C is defined:

$$C = \frac{1 - MS}{\alpha \rho S} \tag{9.23}$$

then Equation 9.22 can be expressed as:

$$\left(\frac{V}{C} + A R_f\right) dV = \frac{A^2 \left(-\Delta P\right)}{\eta} dt$$

If this equation is integrated on the limit condition ($t = 0$, $V = 0$), then:

$$\frac{V^2}{2C} + A R_f V = \frac{A^2 \left(-\Delta P\right)}{\eta} t \tag{9.24}$$

Rearranging:

$$\frac{t}{V} = \frac{\eta}{2 A^2 \left(-\Delta P\right) C} V + \frac{R_f \eta}{A \left(-\Delta P\right)}$$

where, if the new constants K_1 and K_2 are defined as:

$$K_1 = \frac{\eta}{2 A^2 \left(-\Delta P\right) C} \tag{9.25}$$

$$K_2 = \frac{R_f \eta}{A \left(-\Delta P\right)} \tag{9.26}$$

it is obtained that:

$$\frac{t}{V} = K_1 V + K_2 \tag{9.27}$$

corresponding to the equation of a straight line when plotting t/V vs. the volume of filtrate. The slope of this straight line is the constant K_1, while the value of the constant K_2 is the ordinate to the origin.

Obtaining the constants K_1 and K_2 should be performed in experimental form. If a filtration at constant pressure is carried out and the values of the volume of filtrate obtained for different filtration times are recorded, a t/V against V graphic can be built. When adjusting these values by the method of least squares to the straight line given in Equation 9.27, the values of the constants K_1 and K_2 can be obtained from the values of the slope and the ordinate to the origin, respectively.

It is possible to obtain the value of the constant C from K_1 and from C, to obtain the value of the specific resistance α. The value of filtering medium resistance R_f can be obtained from the ordinate to the origin.

Once α and R_f are known, from Equation 9.27, it is possible to determine the filtration time needed to obtain a given volume of filtrate. Similarly, the volume of filtrate can be calculated for a determined time. This can be done from Equation 9.24, which is a second-order equation with respect to the volume of filtrate. When solving this equation, two roots are obtained, one of which has no physical meaning since it is a negative volume. Choosing the adequate root, the volume of filtrate is obtained from the equation:

$$V = A\left[\left(C^2 R_f^2 + \frac{2C\left(-\Delta P\right)}{\eta}\, t\right)^{1/2} - C R_f\right] \tag{9.28}$$

This equation allows calculation of the volume of filtrate as a function of time.

Equation 9.28 can be expressed as a function of the fictitious volume V_f given in Equation 9.18; hence, the following expression is obtained:

$$V = \left(V_f^{\,2} + \frac{2C A^2\left(-\Delta P\right)}{\eta}\, t\right)^{1/2} - V_f \tag{9.29}$$

The flow rate that crosses the cake and the filtering medium is obtained from the derivative of the last equation with respect to time:

$$q = \frac{dV}{dt} = \frac{A C\left(-\Delta P\right)}{\eta\left[C^2 R_f^2 + \dfrac{2C\left(-\Delta P\right)}{\eta}\, t\right]^{1/2}} \tag{9.30}$$

The flow rate is maximum when the filtration time is null, thus:

$$q_{\max} = \frac{A\left(-\Delta P\right)}{\eta R_f} \tag{9.31}$$

9.4 Filtration at Constant Volumetric Flow

Instant volumetric flow can be expressed as the variation of the filtered volume with the filtration time:

$$q = dV/dt$$

If the volumetric flow remains constant, this will be equal to the filtered volume collected during a determined time:

$$q = V/t = \text{constant}$$

Substituting this expression in Equation 9.19b obtains:

$$q = \frac{d\,V}{d\,t} = \frac{A^2\left(-\Delta P\right)}{\eta\left(\frac{\alpha\rho\,S}{1-MS}V + AR_f\right)} = \frac{A^2\left(-\Delta P\right)}{\eta\left(\frac{V}{C} + AR_f\right)} \tag{9.32}$$

This equation allows one to obtain the variation of the pressure drop in order to keep a constant volumetric flow:

$$\left(-\Delta P\right) = \frac{\eta}{CA^2}qV + \frac{\eta R_f}{A}q$$

or:

$$\left(-\Delta P\right) = \frac{\eta}{CA^2}q^2t + \frac{\eta R_f}{A}q \tag{9.33}$$

If new constants K_3 and K_4 are defined as:

$$K_3 = \frac{\eta q^2}{C\,A^2} \tag{9.34}$$

$$K_4 = \frac{\eta R_f\,q}{A} \tag{9.35}$$

it is obtained that:

$$\left(-\Delta P\right) = K_3\,t + K_4 \tag{9.36}$$

Analogous to the last section, using experimental results, if the pressure drop is plotted against filtration time, a series of points is obtained that, when adjusted to a straight line (Equation 9.36), allows one to find the constants K_3 and K_4 from the slope, and the ordinate to the origin, respectively. The values of α and R_f can then be obtained from the values of the constants K_3 and K_4.

The expression that relates the volume of filtrate collected with filtration time and pressure drop can be obtained from Equation 9.32 and written as:

$$\frac{V^2}{C} + A R_f V - A^2 \left(-\Delta P\right) \frac{t}{\eta} = 0$$

When solving this second-order equation, taking the adequate root, the filtered volume as a function of time can be obtained:

$$V = A\left[\left(\frac{C^2 R_f^2}{4} + \frac{C\left(-\Delta P\right)}{\eta} t\right)^{1/2} - \frac{C R_f}{2}\right] \tag{9.37}$$

It can be observed that this expression is similar to the equation obtained for filtration at constant pressure (Equation 9.28).

9.5 Cake Washing

Once the filtration cake is formed, it is usually washed to eliminate the undesirable solids that it may contain. This washing step is carried out on the filter by passing a washing liquid through the cake. This operation is performed at constant pressure drop and volumetric flow, and the washing liquid can follow the same path as the filtrate or a different one. Either way, the washing liquid will contain soluble solids once it has crossed the cake in such way that their concentration will decrease along time.

When the washing liquid follows the same path as the filtrate, the concentration of the washing solids eliminated is up to 90% at an initial period and then abruptly decreases (Figure 9.2). When the washing liquid does not follow the same path as the filtrate, the elimination of the soluble solids is gradual.

In most of the filters, the washing water follows the same path as the filtrate. However, in press-and-frame press filters, the path is different. Figures 9.3 and 9.4 show the filtration and washing operations, respectively, in a press-and-frame filter. It can be observed that the washing area is half of the filtration area, while the resistance of the filtering medium is double for the washing area.

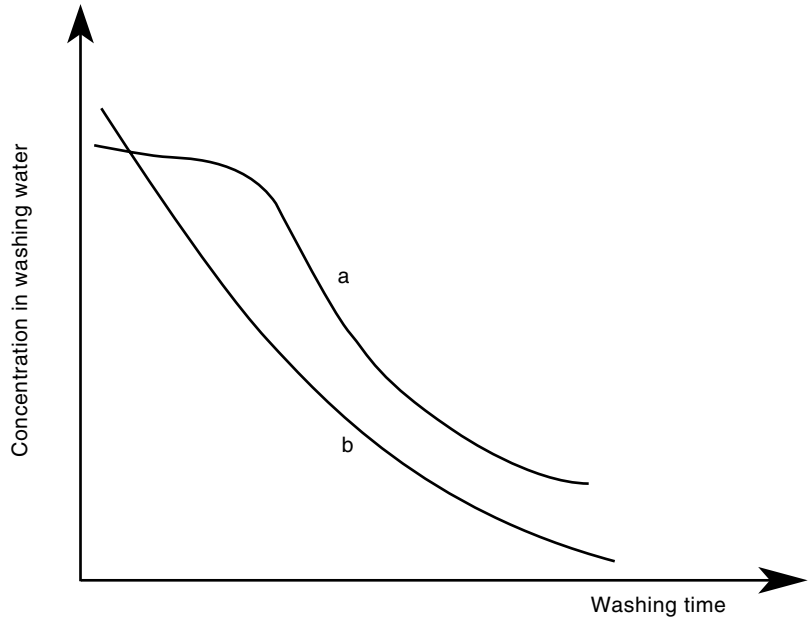

FIGURE 9.2
Concentration of soluble solids in washing water: (a) same path; (b) different path.

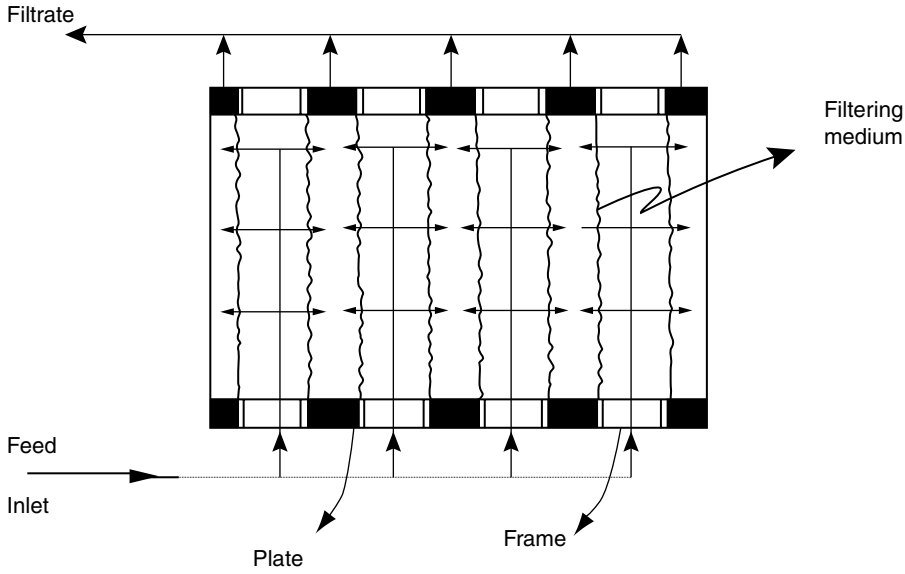

FIGURE 9.3
Filtration operation in a plate-and-frame press filter.

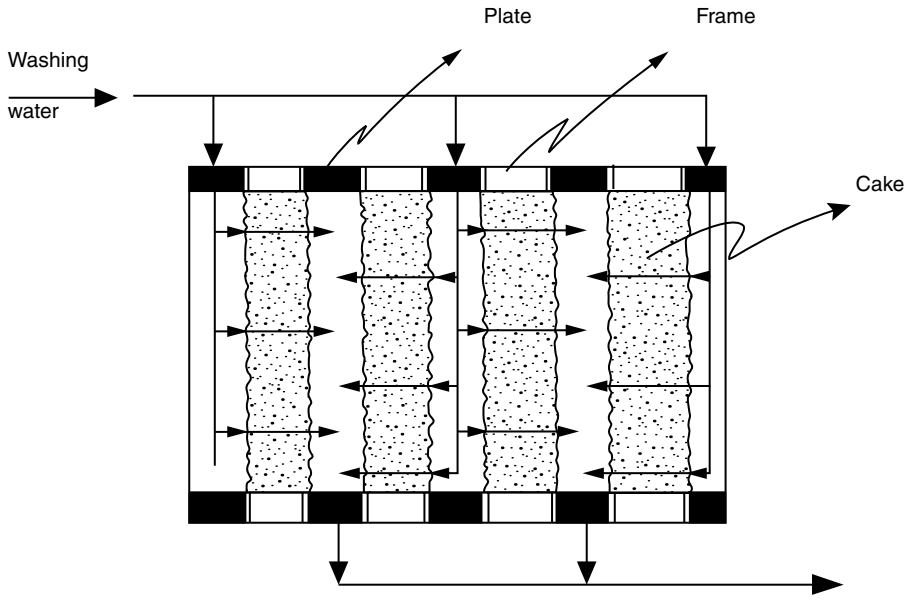

FIGURE 9.4
Washing operation of the cake.

It is important to highlight that the flow of washing liquid coincides with the final flow of filtrate. Thus, if Equation 9.19.b is taken, then:

$$q_L = q_{FINAL} = \frac{\left(Aw\right)^2\left(-\Delta P\right)}{\eta\left(\frac{\alpha\,\rho\,S}{1-MS}V + \mathrm{A}w R_f\right)} \tag{9.38}$$

where Aw is the washing area.

Where the washing area coincides with that of filtration (Aw = A), the expression to calculate the washing flow in which V is the volume of filtered liquid at the end of the filtration operation will be used.

For plate-and-frame press filters, the washing area is half of the filtration area. However, the washing liquid should cross the filtering medium two times. Hence, in Equation 9.38, $2R_f$ should be used instead of R_f, and Aw = A/2. Taking all these remarks into account, the following expression is obtained:

$$q_L = \frac{1}{4}\,\frac{A^2\left(-\Delta P\right)}{\eta\left(\frac{\alpha\,\rho\,S}{1-M\,S} + A R_f\right)} \tag{9.39a}$$

This equation, expressed as a function of K_1 and K_2, defined in Equations 9.25 and 9.26, allows one to express the washing flow as:

$$q_L = \frac{1}{8K_1V + 4K_2} \tag{9.39b}$$

The washing time (t_L) is obtained by dividing the volume of liquid needed for the washing operation by the flow:

$$t_L = V_L / q_L \tag{9.40}$$

where V_L is the volume of liquid that will be used to wash the cake.

9.6 Filtration Capacity

The filtration capacity is defined as the quotient between the volume of filtrate and the time of one filtration cycle:

$$F(c) = \frac{V}{t_{CYCLE}} \tag{9.41}$$

The time of one cycle is the sum of filtration time (t) plus nonoperative time (t'), which includes the washing time (t_L) and a complementary time (t^*) needed for discharge, cleaning, and assembly and adjustment of the filter to begin a new filtration stage.

$$t_C = t + t' = t + t_L + t^* \tag{9.42}$$

9.7 Optimal Filtration Conditions at Constant Pressure

It is evident that during the filtration processes at constant pressure, the filtrate flow decreases as filtration time goes on. For this reason, there will be a time at which continuing the filtration process would not be feasible, so the optimum will be looked for. This optimum occurs at the time at which the filtration capacity is maximum.

Maximum filtration conditions will be obtained by maximizing the filtration capacity function. Hence:

$$\frac{dF(c)}{dV} = 0$$

which is the maximum condition. When the derivative of the filtration capacity with respect to the volume of filtrate is equal to zero, it is possible to obtain the optimum volume. In the same way, the optimum filtration time can be obtained if the function is derived with respect to time. The difference is based on the fact that, for the first case, the time should be expressed as a function of the volume of filtrate, while in the second case, the volume should be expressed as a function of filtration time.

For the particular case in which the nonoperative time, t', is a determined value, the way to obtain the optimum is described next. The filtration time is a function of the volume of filtrate and can be obtained from Equation 9.27:

$$t = K_1 V^2 + K_2 V \tag{9.43}$$

In this way, the filtration capacity can be expressed as:

$$F(c) = \frac{V}{\left(K_1 V^2 + K_2 V\right) + t'}$$

The optimum can be found from the derivative of this expression and equaling it to zero:

$$\frac{dF(c)}{dV} = \frac{d}{dt}\left[\frac{V}{\left(K_1 V^2 + K_2 V\right) + t'}\right] = 0$$

Thus, the following expression is obtained:

$$t' = K_1 V^2 \tag{9.44}$$

This equation indicates the nonoperative time required to obtain an optimum volume of filtrate. If a nonoperative time is given, the volume of filtrate to have an optimum filtration capacity will be:

$$V_{OPTIMUM} = \sqrt{\frac{t'}{K_1}} \tag{9.45}$$

The optimum time will be obtained by substituting this value of volume in Equation 9.42:

$$t_{OPTIMUM} = t' + K_2 \sqrt{\frac{t'}{K_1}} \tag{9.46}$$

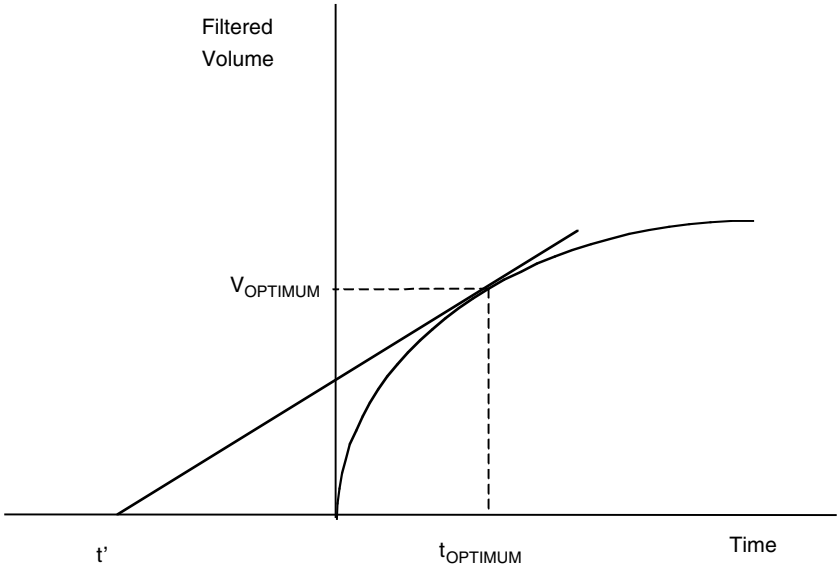

FIGURE 9.5
Graphical method to determine optimum conditions of filtration.

The graphical method of Sbarbaugh allows one to obtain the values of V_{opt} and t_{opt} from the curve in which the filtrate's volume is a function of time (Figure 9.5). To obtain V_{opt} and t_{opt}, the tangent line to the filtration curve from the point (t', 0) is plotted. The tangent point has as coordinates the values of the optimum time and volume of filtrate.

9.8 Rotary Vacuum Disk Filter

Another type of filter widely used in the industry is the rotary filter that operates under vacuum. These filters consist of a cylindrical drum with different sections, which rotates on its axis and in which vacuum is applied to facilitate the crossing of the fluid. The solids are retained in the lateral cylindrical surface (Figure 9.6). As can be observed in this figure, part of the cylinder is submerged in the suspension to be filtered. The cake deposited on the surface is washed by showers of washing liquid. Vacuum is applied to the interior of the drum at the filtration zone as well as in the washing zone, but once out of these zones, vacuum is eliminated to easily separate the cake with a scraper. In this way, the filter can begin the filtration cycle again. This kind of operation is carried out at constant pressure drop and volumetric flow.

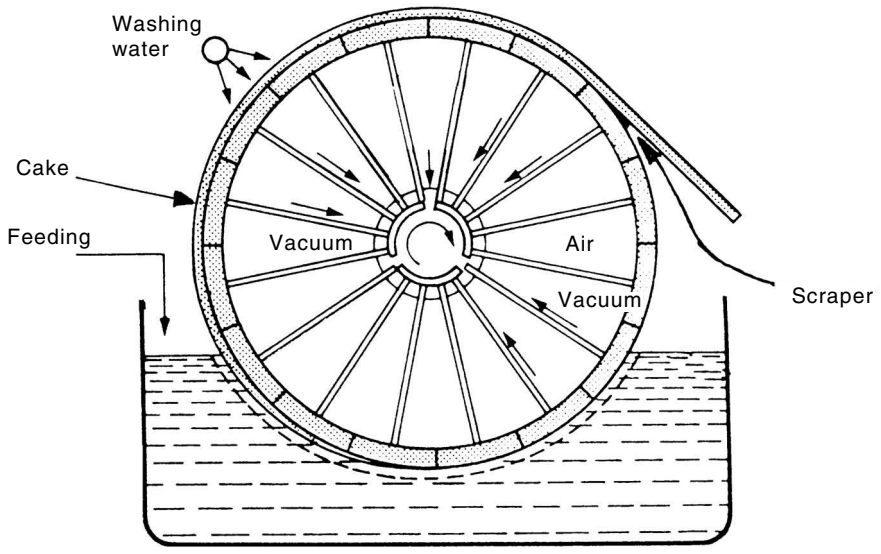

FIGURE 9.6
Rotary vacuum filter.

Mathematical treatment and calculations are performed assuming that the total filtering area (A) is formed by n surfaces A_i, small enough to assume that they behave as a flat filter: $A = n\ A_i$.

The volume filtered (V_i) by one of the sections A_i, since it is a flat filter, can be obtained from Equation 9.28:

$$V_i = A_i\left[\left(C^2R_f^2 + \frac{2C\left(-\Delta P\right)}{\eta}t_S\right)^{1/2} - CR_f\right]$$

where t_s is the time during which the section A_i is submerged, corresponding to the filtration time.

If the filtration drum rotates at a rotation velocity N, and its immersion angle is ϕ, then the time it will be submerged is:

$$t_S = \frac{\phi}{2\pi N} \tag{9.47}$$

in which the angle is given in radians.

The total volume of filtrate is obtained by adding together the volumes of each filtration section considered:

$$V = nV_i = A\left[\left(C^2R_f^2 + \frac{2C\left(-\Delta P\right)}{\eta}\frac{\phi}{2\pi N}\right)^{1/2} - CR_f\right] \tag{9.48}$$

The filtrate flow is a function of the volume of filtrate and is obtained by multiplying the volume of filtrate times the spin velocity of the drum:

$$q = NV = NA\left[\left(C^2R_f^2 + \frac{2C\left(-\Delta P\right)}{\eta}\frac{\phi}{2\pi N}\right)^{1/2} - CR_f\right] \tag{9.49}$$

Sometimes it is interesting to calculate the thickness of the cake deposited on the filter's surface. During one filtration cycle, when a point of the filter surface penetrates into the suspension to be filtered, the insoluble solids begin to deposit. As time goes on, more solids are deposited on this point and, as a consequence, the thickness of the deposited cake increases, depending on the amount of time that this point has been submerged. As was seen in Equation 9.47, such time depends on the immersion angle.

The mass of solids deposited on one of the areas A_i is obtained from Equation 9.13:

$$z = \frac{\rho V_i S}{1 - MS}\frac{1}{\rho_S\left(1-\varepsilon\right)A_i}$$

in which the thickness of the deposited cake is a function of the filtered volume V_i. Such volume is given by Equation 9.48, with A_i representing the filtration area; if the definition of the constant C as a function of the resistance of the cake α is taken into account, then thickness can be obtained by means of the following equation:

$$z = \frac{1}{\rho_S\left(1-\varepsilon\right)\alpha}\left[\left(R_f^2 + \frac{2C\left(-\Delta P\right)}{\eta C}\frac{\phi}{2\pi N}\right)^{1/2} - R_f\right] \tag{9.50}$$

This equation allows one to obtain the cake thickness for an angle of submerged filter of ϕ radians.

Problems

9.1

A plate-and-frame filter that operates under constant pressure requires 1 h to separate 600 l of filtrate of an aqueous suspension. Calculate the filtration capacity if the initial filtration velocity is 60 l/min, 8 l of water are needed to wash the deposited cake, and 35 min are needed to discharge, clean, and assemble the filter.

The filtrate flow is given by Equation 9.19b, which, with the definition of constant C (Equation 9.23), is transformed into:

$$\frac{dV}{dt} = \frac{A^2\left(-\Delta P\right)}{\eta\left(\frac{V}{C} + A R_f\right)}$$

For a filtration at constant pressure drop, $(-\Delta P)$ = constant, the integration of this equation yields:

$$K_1 V^2 + K_2 V - t = 0$$

K_1 and K_2 are defined by Equations 9.25 and 9.26.

For $t = 0$: $(dV/dt) = 0$

$$\left(\frac{dV}{dt}\right)_{t=0} = 60\frac{1}{\text{min}} = \frac{A\left(-\Delta P\right)}{\eta R_f} = \frac{1}{K_2}$$

from which it is obtained that $K_2 = 1000\ \text{s/m}^3$

For $t = 60$ min: $V = 600$ l $= 0.6\ \text{m}^3$, so:

$$K_1\left(0.6\right)^2 + K_2\left(0.6\right) - 3600 = 0$$

obtaining:

$$K_1 = 8333.33\ \text{s/m}^6$$

It is important to point out that the washing flow coincides with the final volume of filtrate; for plate-and-frame filters, Equation 9.39b allows one to calculate the filtrate flow:

$$q_L = \frac{1}{8K_1V + 4K_2}$$

Since, at the end of filtration, 0.6 m^3 was obtained and the constants K_1 and K_2 were previously obtained, then the washing volumetric flow rate will be:

$$q_L = 2.273 \times 10^{-5}\ \text{m}^3/\text{s}$$

The washing time is obtained by dividing the washing volume by the volumetric flow rate:

$$t_L = \frac{80 \times 10^{-3}\ \text{m}^3}{2.273 \times 10^{-5}\ \text{m}^3/\text{s}} = 3520\ \text{s}$$

The filtration capacity is obtained from Equation 9.41, in which the time of one cycle is given by Equation 9.42. Therefore:

$$F(c) = \frac{V}{t + t_L + t^*}$$

in which

$V = 0.6\ \text{m}^3$
$t = 3600\ \text{s}$
$t_L = 3520\ \text{s}$
$t^* = 35 \times 60\ \text{s} = 2100\ \text{s}$

So the filtration capacity is:

$$F(c) = 6.51 \times 10^{-5}\ \text{m}^3/\text{s} = 3.91\ \text{l}/\text{min}$$

9.2

A plate-and-frame press filter is used to filtrate an aqueous suspension. Working under constant filtration velocity, 250 l of filtrate are obtained after 45 min. During this period, the pressure drop increases from 0.40 kg/cm^2 to 3.5 kg/cm^2. If it were desired to work at a constant pressure of 3.5 kg/cm^2, what amount of filtrate would be obtained after 45 min?

The expression that relates the variation of the volume of filtrate to time is given by Equation 9.32:

$$q = \frac{dV}{dt} = \frac{A^2(-\Delta P)}{\eta\left(\frac{V}{C} + AR_f\right)}$$

Since the filtration is at constant volumetric flow, then $q = (dV/dt) =$ constant:

$$q = \frac{250\ \text{l}}{45\ \text{min}} = 5.556\ \text{l/min} = 9.26 \times 10^{-5}\ \text{m}^3/\text{s}$$

It is not necessary to integrate the last equation because it is operated under a constant volumetric flow, but the pressure drop ($-\Delta P$) can be directly obtained as a function of filtration time (Equation 9.36):

$$\left(-\Delta P\right) = K_3\, t + K_4$$

where the constants K_3 and K_4 are given by Equations 9.34 and 9.35:

$$K_3 = \frac{\eta q^2}{C A^2} \qquad K_4 = \frac{\eta R_f\, q}{A}$$

For $t = 0$:

$$\left(-\Delta P\right) = 0.4\ \text{kg/cm}^2 = 39{,}200\ \text{Pa}$$

$$K_4 = \left(-\Delta P\right) = 39{,}200\ \text{Pa}$$

For $t = 45$ min $= 2700$ s:

$$\left(-\Delta P\right) = 3.5\ \text{kg/cm}^2 = 343{,}000\ \text{Pa}$$

$$K_3 = \frac{\left(-\Delta P\right) - K_4}{t} = \frac{\left(343{,}000 - 39{,}200\right)\ \text{Pa}}{2700\ s} = 112.52\ \text{Pa/s}$$

Filtration at constant pressure drop ($-\Delta P$) = 3.5 kg/cm²

When integrating the differential equation, under the limit condition $t = 0$, $V = 0$, a second-order equation is obtained with respect to the volume of filtrate (Equation 9.27):

$$V^2 + 2C\,A\,R_f\,V - \frac{2CA^2\left(-\Delta P\right)t}{\eta} = 0$$

The following is obtained from the expression of K_3:

$$\frac{CA^2}{\eta} = \frac{q^2}{K^3} = \frac{\left(9.26 \times 10^{-5}\ \text{m}^3/\text{s}\right)^2}{112.52\ \text{Pa/s}} = 7.62 \times 10^{-11}\ \frac{\text{m}^6}{\text{Pa}\cdot\text{s}}$$

From the relation:

$$\frac{K_4}{K_3} = \frac{\eta R_f q}{A} = \frac{CA^2}{\eta q^2} = \frac{CA^2 R_f}{q}$$

it is obtained that:

$$C A R_f = q \frac{K_4}{K_3} = \left(9.26 \times 10^{-5}\ \text{m}^3/\text{s}\right) \frac{\left(39{,}200\ \text{Pa}\right)}{\left(112.52\ \text{Pa/s}\right)} = 32.26 \times 10^{-3}\ \text{m}^3$$

The different values obtained are substituted in the second-order equation:

$$V^2 + 2\left(32.26 \times 10^{-3}\right) V - 2\left(7.62 \times 10^{-11}\right)\left(3.5 \times 9.8 \times 10^4\right) 2700 = 0$$

$$V^2 + 0.0645\, V - 0.1411 = 0$$

When solving this equation, the negative root does not have a physical meaning, so only the positive root is taken: $V = 0.345\ \text{m}^3$.

Therefore, after 45 min of filtration at a constant pressure drop of 3.5 kg/cm^2, 345 l of filtrate are obtained.

9.3

An aqueous suspension that contains 7% of insoluble solids is filtered at a rate of 10 ton/h, using a plate-and-frame press filter that works under constant pressure of 3 atm. It was found, experimentally, that the deposited cake contains 50% moisture, the density of the dry solids is 3.5 g/cm^3, and the equivalent diameter of the deposited particles is 0.002 mm. The washing of the cake begins after 10,000 kg/h of feeding have been filtered using 150 l of water, while 30 min are used for the discharge, cleaning, and assembly operations. If the resistance of the filtering medium to filtration is considered negligible, calculate: (a) the specific resistance of the cake; (b) volume of water filtered after one hour; (c) time needed to carry out washing; and (d) filtration capacity.

Data: K″ = 5 can be taken for Kozeny's constant.
Properties of water: Density = 1000 kg/m^3; Viscosity = 1 mPa·s

10,000 kg of the suspension are filtered in 1 h.

Dry solids deposited: W = (10,000) (0.07) = 700 kg

$$M = \frac{\text{weight of wet cake}}{\text{weight of dry cake}} = \frac{100\ \text{kg wet cake}}{50\ \text{kg dry cake}} = 2$$

$$M = \frac{\text{mass of dry solid} + \text{mass of retained liquid}}{\text{mass of dry solid}}$$

If V_T = volume of deposited cake:

$$M = 1 + \frac{V_T \varepsilon \rho}{V_T (1-\varepsilon)\rho_P} = 1 + \frac{\varepsilon \rho}{(1-\varepsilon)\rho_P}$$

Substituting the variables with their values obtains that porosity is ε = 0.778.

Particle's specific surface:

$$a_{S0} = 6/dp = 6/\left(0.002 \times 10^{-3}\ \text{m}\right) = 3 \times 10^{6}\ \text{m}^{-1}$$

The cake-specific resistance is obtained from Equation 9.6:

$$\alpha = \frac{K''(1-\varepsilon)\left(a_{S0}\right)^2}{\varepsilon^3 \rho_S} = \frac{5(1-0.778)\left(3 \times 10^6\ \text{m}^{-1}\right)^2}{(0.778)^3\left(3500\ \text{kg/m}^3\right)} = 6.07 \times 10^9\ \frac{\text{m}}{\text{kg}}$$

For a filtration under constant pressure drop, the volume of filtrate is given by Equation 9.28. Since the resistance of the medium is negligible, $R_f = 0$, the equation can be rearranged as:

$$V = A\left[\left(\frac{2C(-\Delta P)}{\eta} t\right)^{1/2}\right]$$

in which:

$$(-\Delta P) = 3\ \text{atm}\ \frac{9.8 \times 10^4\ \text{Pa}}{1\ \text{atm}} = 2.94 \times 10^5\ \text{Pa}$$

Also, from the definition of the constant C (Equation 9.23):

$$C = \frac{1 - MS}{\alpha \rho S} = \frac{1 - 2 \times 0.07}{(6.07 \times 10^9\ \text{m/kg})(10^3\ \text{kg/m}^3)(0.07)} = 2.024 \times 10^{-12}\ \text{m}^2$$

Volume of filtrate collected in 1 h:

$$V = \frac{W(1 - MS)}{\rho S} = \frac{(700\ \text{kg d.s.})(1 - 2 \times 0.07)}{(1000\ \text{kg/m}^3)(0.07)} = 8.6\ \text{m}^3$$

Thus, the filtration area is obtained from Equation 9.28, with $R_f = 0$

$$8.6\ \text{m}^3 = A\left[\frac{2(2.024 \times 10^{-12}\ \text{m}^2)(2.94 \times 10^5\ \text{Pa})}{(10^{-3}\ \text{Pa s})}(3600\ s)\right]^{1/2}$$

Hence, one filtration area: $A = 4.155\ \text{m}^2$

The washing flow coincides with that of the final filtrate, and since $R_f = 0$, Equation 9.39 becomes simpler:

$$q_L = \frac{1}{4}\frac{C A^2 (-\Delta P)}{\eta V}$$

since:

A $= 4.155\ \text{m}^2$
C $= 2.024 \times 10^{-12}\ \text{m}^2$
V $= 8.6\ \text{m}^3$
η $= 10^{-3}\ \text{Pa} \cdot \text{s}$
$(-\Delta P)$ $= 2.94 \times 10^5\ \text{Pa}$

then:

$$q_L = 2.99 \times 10^{-4}\ \text{m}^3/\text{s}$$

The washing time will be:

$$t_L = \frac{V_L}{q_L} = \frac{(0.15\ \text{m}^3)}{(2.99 \times 10^{-4}\ \text{m}^3/\text{s})} = 502\ \text{s}$$

Calculation of the filtration capacity:

$$F(c) = \frac{V}{t + t_L + t^*} = \frac{8.6\ \text{m}^3}{(3600 + 502 + 1800)\ \text{s}} = 1.457 \times 10^{-3}\ \text{m}^3/\text{s}$$

$$F_C = 1.457 \times 10^{-3}\ \text{m}^3/\text{s} = 87.42\ \text{l/min}$$

9.4

An aqueous solution that contains 10% suspended solids is filtered in a plate-and-frame press filter. In a previous experiment it was determined that the wet cake to dry cake ratio is 2.2, using an incompressible cake with a specific resistance of 2.5×10^{10} m/kg. During filtration at constant pressure of 3 atm, the variation on the amount of filtrate with time is recorded in the following table:

Time (minutes)	8	18	31	49	70	95
Filtrates mass (kg)	1600	2700	3720	4900	6000	7125

From these data, calculate: (a) total area of the filter and resistance of the filtering medium; (b) if the nonoperative time of each filtrating cycle is 26 min, calculate the volume of filtrate recovered at the end of 10 h if the operation is carried out at the optimum filtration cycle; and (c) it is desired to filtrate the same solution but working at constant volumetric flow. If, at the end of 142 min, the pressure drop experienced by the fluid when crossing the cake and the filtering medium is 4.5 atm, calculate the volume of filtrate obtained and the volumetric flow rate at which it circulates.

Data: Water properties: Density = 1000 kg/m^3; Viscosity = 1.2 mPa·s

Filtration at constant pressure drop:

In this type of operation, the variation on the volume of filtrate and time are correlated by a second-order equation (Equation 9.27):

$$K_1 V^2 + K_2 V - t = 0$$

in which the constants K_1 and K_2 are given by Equations 9.25 and 9.26. Equation 9.27 is a straight line if t/V is plotted against V, with a slope K_1 and intercept K_2.

(a) The following table can be constructed with the data stated in the problem:

t (s)	480	1080	1860	2940	4200	5700
V (m^3)	1.6	2.7	3.72	4.9	6.0	7.125
t/V(s/m^3)	300	400	500	600	700	800

The constants K_1 and K_2 can be obtained from the fitting of these data using the method of least squares.

$$K_1 = 90.40 \text{ s/m}^6 \qquad K_2 = 157.58 \text{ s/m}^3$$

The value of constant C is obtained from Equation 9.23:

$$C = \frac{1 - MS}{\alpha \rho S} = \frac{1 - (2.2)(0.1)}{(2.5 \times 10^{10}\ \text{m/kg})(1000\ \text{kg/m}^3)(0.1)} = 3.12 \times 10^{-13}\ \text{m}^2$$

Calculation of the filtration area:

It is possible to obtain such area from the expression of constant K_1 (Equation 9.25)

$$A^2 = \frac{\eta}{2K_1 C(-\Delta P)} = \frac{1.2 \times 10^{-3}\ \text{Pa s}}{2(90.4\ \text{s/m}^6)(3.12 \times 10^{-13}\ \text{m}^2)(3 \times 9.8 \times 10^4\ \text{Pa})}$$

$$= 72.357\ \text{m}^2$$

Then A = 8.506 m².

Calculation of the resistance of the filtration medium:

It is possible to obtain the value from the expression of the constant K_2 (Equation 9.26):

$$R_f = \frac{K_2 A(-\Delta P)}{\eta} = \frac{(157.58\ \text{s/m}^3)(8.506\,\text{m}^2)(3 \times 9.8 \times 10^4\,\text{Pa})}{(1.2 \times 10^{-3}\,\text{Pa s})}$$

$$= 3.284 \times 10^{11}\ \text{m}^{-1}$$

(b) Filtration capacity: it is given by Equation 9.41 that, in this case:

$$F(c) = \frac{V}{t + t'}$$

in which $t' = 26 \times 60\ \text{s} = 1560\ \text{s}$.

Hence, from Equation 9.27:

$$t = K_1 V^2 + K_2 V$$

So the filtration capacity will be:

$$F(c) = \frac{V}{K_1 V^2 + K_2 V + t'}$$

The optimum cycle is obtained from the derivation of this function with respect to the volume of filtrate and equaling it to zero:

$$\frac{d}{dt}\left(F(c)\right) = \frac{K_1 V^2 + K_2 V + t' - V\left(2 K_1 V + K_2\right)}{\left(K_1 V^2 + K_2 V + t'\right)^2} = 0$$

Since the numerator of this expression is equal to zero, then:

$$K_1 V^2 = t'$$

Thus, $V_{opt} = (t'/K_1)^{1/2}$.

Since t' = 1560 s and K_1 = 90.40 s/m^6, the optimum volume of filtrate is V_{opt} = 4.154 m^3.

Filtration time obtained from the expression:

$t = K_1 V^2 + K_2 V$

t = 90.4 s/m^6 (4.154 m^3)^2 + 157.58 s/m^3 · (4.154 m^3)

t = 2215 s = 36 min 55 s

One cycle's time:

$$t_{cycle} = t + t' = 2215 \text{ s} + 1560 \text{ s} = 3775 \text{ s}$$

Number of cycles:

$$\text{n° of cycles} = \frac{(10 \text{ h})(3600 \text{ s/h})}{3775 \text{ s}} = 9.536 \text{ cycles}$$

Nine complete cycles have been completed with +0.536 cycles that correspond to 0.536 cycles × 3775 s/cycle = 2025 s. The volume of filtrate for this time can be obtained by means of a second-order equation: $t = K_1 V^2 + K_2 V_o$

$$2025 = 90.4 V^2 + 157.58 V$$

The negative root of this equation has no physical meaning, so the positive root yields the filtrate's volume obtained during the 2025 s: V = 3.941 m^3.

The volume of filtrate recovered at the end of 10 h of operation will be:

$$V = 9 \text{ cycles} \times 4.154 \text{ m}^3/\text{cycle} + 3.941 \text{ m}^3 = 41.327 \text{ m}^3$$

(c) Filtration under a constant volumetric flow: The volume of filtrate is obtained from Equation 9.37:

$$V = A\left[\left(\frac{C^2 R_f^{\,2}}{4} + \frac{C\left(-\Delta P\right)}{\eta}\, t\right)^{1/2} - \frac{C R_f}{2}\right]$$

The values of the different variables of this equation are:

$A = 8.506\ \text{m}^2$
$C = 3.12 \times 10^{-13}\ \text{m}^2$
$t = 8520\ \text{s}$
$R_f = 3.284 \times 10^{11}\ \text{m}^{-1}$
$(-\Delta P) = (4.5)\ (9.8 \times 10^4)\ \text{Pa}$

Hence, the volume of filtrate is $V = 7.983\ \text{m}^3$.

Filtrate volumetric flow rate:

$$q = \frac{V}{t} = \frac{7.983\ \text{m}^3}{142\ \text{min}} = 0.0562 \frac{\text{m}^3}{\text{min}}$$

$$q = 0.0562\ \text{m}^3/\text{min} = 56.2\ l/\text{min} = 3.373\ \text{m}^3/\text{h}$$

9.5

It is desired to obtain 60 l/min of filtrate from an aqueous suspension that contains 0.25 kg of insoluble solids per each kg of water, using a rotary drum filter. The pressure drop suffered by the fluid is 300 mm of Hg, obtaining a cake that has a 50% moisture content and a filtrate that has a viscosity of 1.2 mPa·s and a density of 1000 kg/m^3. The filter's cycle time is 5 min, with 30% of the total surface submerged. The particles that form the suspension can be considered as spheres with a 6×10^{-3} mm diameter and a 900 kg/m^3 density. If it is supposed that the resistance offered by the filtering medium to filtration is negligible and that a value of 5 can be taken for the Kozeny constant, calculate (a) the specific resistance of the cake; (b) the filter's area; and (c) thickness of the deposited cake.

Suspended solids:

$$S = \frac{0.25\ \text{kg solids}}{\left(1 + 0.25\right)\text{total kg}} = 0.2\ \left(20\%\ \text{solids}\right)$$

$$M = \frac{\text{mass of wet cake}}{\text{mass of dry cake}} = \frac{1 \text{ kg wet cake}}{0.5 \text{ kg dry cake}} = 2$$

Since:

$$M = 1 + \frac{V_C \varepsilon \rho}{V_C (1-\varepsilon) \rho_P}$$

it is possible to obtain the value of porosity using the values of $\rho = 1000$ kg/m^3, $\rho_P = 900$ kg/m^3, and $\varepsilon = 0.4737$.

Particle's specific surface:

$$a_{S0} = \frac{6}{d_P} = \frac{6}{6 \times 10^{-6} \text{ m}} = 10^6 \text{ m}^{-1}$$

The cake specific resistance is obtained from Equation 9.6:

$$\alpha = \frac{K'' (1-\varepsilon)(a_{S0})^2}{\varepsilon^3 \rho_S} = \frac{5(1-0.4737)(10^6 \text{ m}^{-1})^2}{(900 \text{ kg/m}^3)(0.4737)^3} = 2.75 \times 10^{10} \text{ m/kg}$$

Constant C is obtained from Equation 9.23:

$$C = \frac{1 - MS}{\alpha \rho S} = \frac{1 - 2(0.2)}{(2.75 \times 10^{10} \text{ m/kg})(1000 \text{ kg/m}^3)(0.2)} = 1.09 \times 10^{-13} \text{ m}^2$$

Number of rps: $N = 1/(5 \text{ min}) = 0.2 \text{ rpm} = 3.33 \times 10^{-3}$ rps

Drop pressure:

$$(-\Delta P) = \left(\frac{300}{760} \text{ atm}\right)\left(\frac{1.0333 \text{ atm}}{1 \text{ atm}}\right)\left(\frac{9.8 \times 10^4 \text{ Pa}}{1 \text{ atm}}\right) = 39973 \text{ Pa}$$

For a rotary filter, the filtrate volumetric flow rate is obtained from Equation 9.49, which, for the present case, becomes simpler since the resistance of the filtering medium can be neglected ($R_f = 0$):

$$q = NV = NA\left[\left(\frac{2C(-\Delta P)}{\eta}\frac{\phi}{2\pi N}\right)^{1/2}\right]$$

The available data are

$\phi = 0.3 \times 2\pi$ radians;
$\eta = 1.2 \times 10^{-3}$ Pa·s
$q = 60$ l/min $= 10^{-3}$ m^3/s;
$(-\Delta P) = 39{,}972.4$ Pa
$C = 1.09 \times 10^{-13}$ m^2;
$N = 3.33 \times 10^{-3}$ s^{-1}

It is possible to calculate the area of the filter by substituting these data in the equation stated before, thus obtaining $A = 11.73$ m^2.

The cake thickness is obtained from Equation 9.50, but since $R_f = 0$, the equation can be rearranged as:

$$z = \frac{1}{\rho_S (1-\varepsilon)\alpha} \left(\frac{2C(-\Delta P)}{\eta C} \frac{\phi}{2\pi N} \right)^{1/2}$$

in which $(-\Delta P)$, η, ϕ, C, and N have the values indicated above, and also: $\rho_P = 900$ kg/m^3; $\varepsilon = 0.4737$; and $\alpha = 2.75 \times 10^{10}$ m/kg. These data allow one to obtain the cake thickness: $z = 0.018$ m $= 18$ mm.

10

Separation Processes by Membranes

10.1 Introduction

In general, to carry out a separation process or concentration, it is necessary to supply high quantities of energy. However, in the so-called separation processes by membranes, the energy required to perform a separation is small; therefore, these processes have become important in recent years. Certain components of a mixture can be separated in these processes by using a porous membrane selective to the crossing of some of the components of the mixture. Among these processes, inverse osmosis and ultrafiltration, which achieve separation by a semipermeable membrane, must be pointed out. The difference between these processes is difficult to discern, although the membrane in inverse osmosis usually retains molecules of low molecular weight, while in ultrafiltration, molecules with high molecular weights are usually retained. Figure 10.1 shows a classification of the separation processes according to the size of the particle retained.

In general, a stage based on the separation by membranes can be represented according to the scheme in Figure 10.2. Feed (F) with a concentration C_0 of certain components is introduced into the system in which a portion permeates through the membrane, yielding a stream called permeate (P) with a concentration C_P of the component of interest. Certain parts of the feed stream do not cross through the membrane, yielding a reject stream (S) with a concentration C_S.

It is convenient to first define some terms used in the membrane processes.

Retention or Rejection:

$$R = \frac{C_C - C_P}{C_C} = 1 - \frac{C_P}{C_C} \tag{10.1}$$

The retention point of a membrane corresponds to the molecular weight over which all molecules are retained. This concept in ultrafiltration is called molecular weight cut-off. The fact that a value is given to this parameter does not mean that all the molecules of smaller size should cross the membrane;

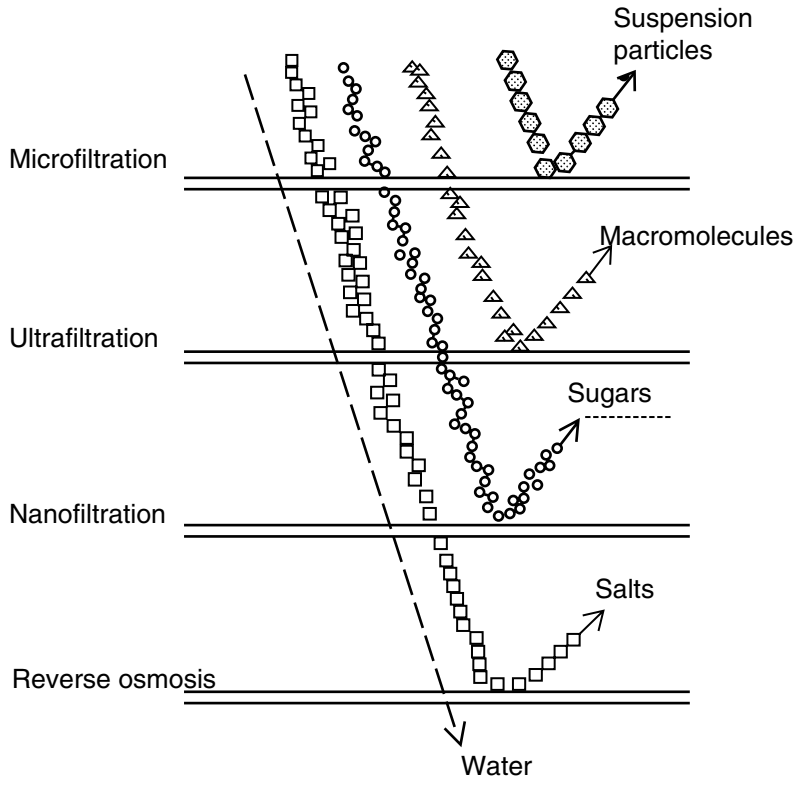

FIGURE 10.1
Classification of the membrane processes. (Adapted from Cheryan, 1986.)

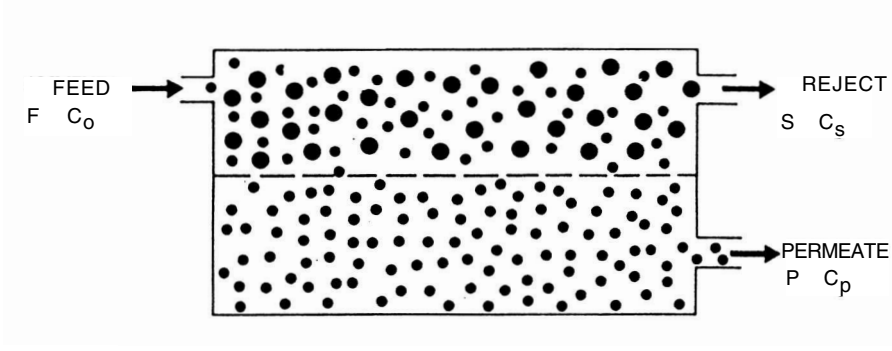

FIGURE 10.2
Basic unit of separation by membrane.

a certain amount of them will be retained. For this reason, when the cut-off value is given, the percentage of rejected molecules of lower molecular weight than this value should also be specified.

Concentration factor (F_c): the quotient between the concentrations of the retained stream and the feed:

$$F_C = \frac{C_S}{C_F} \tag{10.2}$$

Recovery factor (Q): the relation between the permeate obtained and the feed:

$$Q = \frac{P}{F} \tag{10.3}$$

Mass transfer phenomenon through the membrane was observed by the abbot Nollet in 1748, in an experiment in which he kept wine in containers made of animals' stomachs and then submerged them in water. After a certain time, the wine was diluted due to water crossing to the inner part of the container.

This phenomenon is known as osmosis and is based on the fact that, when a semipermeable membrane separates two solutions of different concentration, there is a transfer of solvent from the diluted to the concentrated solution. This produces an increase in the hydrostatic pressure known as osmotic pressure. This process is illustrated in Figure 10.3a. If enough pressure is exerted on the concentrated solution zone to overcome the osmotic pressure, the solute flow is inverted and solvent flows from the concentrated to the diluted solution. This process is known as reverse osmosis (Figure 10.3b).

The equation of van't Hoff, known since 1860, is used to calculate the osmotic pressure and is given by:

$$\pi = iCRT \tag{10.4}$$

in which π is the osmotic pressure, C is the solute molar concentration in the solvent, i is the number of ions for ionic solutes, R is the gases constant, and T is the absolute temperature.

For food fluids containing low molecular weight compounds, the osmotic pressure is high. Table 10.1 shows the osmotic pressures of some of these fluids.

10.1.1 Stages of Mass Transfer

The components transferred through the semipermeable membrane in the ultrafiltration and reverse osmosis processes should overcome a series of resistance from the concentrated solution to the diluted one. Therefore, a series of successive stages occurs during the global mass transfer that can be summarized as follows:

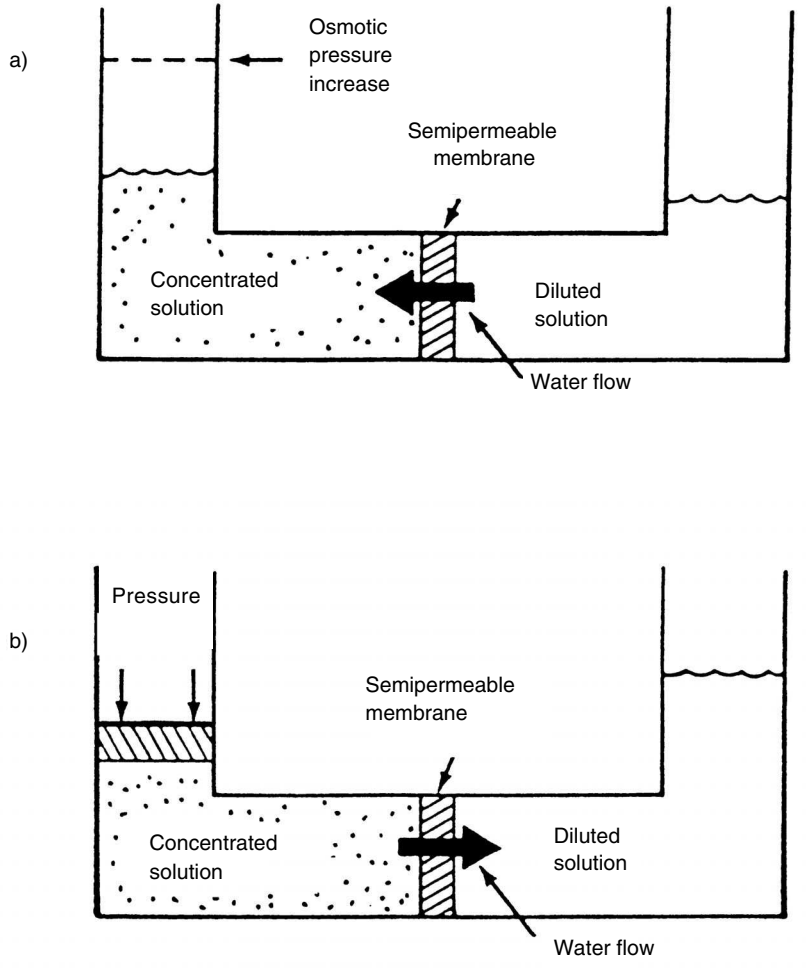

FIGURE 10.3
Scheme of osmosis (a) and reverse osmosis (b) phenomena.

1. Transfer from the concentrated solution to the membrane wall
2. Passage of the component from the solution to the membrane
3. Transfer through the different layers of the membrane, from the wall in contact with the concentrated solution to the wall in contact with the diluted solution
4. Transfer from the membrane wall to the less concentrated liquid

It will be seen later that it is necessary to add one more stage because a polarization layer can be formed.

TABLE 10.1

Osmotic Pressure of Certain Food Fluids at Room Temperature

Food	Concentration	Osmotic Pressure (kPa)
Lactic acid	1% (w/v)	552
Coffee (extract)	28% total solids	3450
Sodium chloride	1% (w/v)	862
Lactose	5% (w/v)	380
Milk	9% nonfat solids	690
Whey	6% total solids	690
Juices		
Apple	15% total solids	2070
Orange	11% total solids	1587
Grape	16% total solids	2070

Source: Cheryan, M. *Ultrafiltration Handbook,* Technomic Publishing Co., Lancaster, PA, 1986.

10.1.2 Polarization by Concentration

In separation processes by membranes, the mass transfer is selective for the solvent that transfers through the membrane. In the first mass transfer stage, solute is transferred from the concentrated solution to the membrane wall and does not cross the membrane, but the solvent does, so the final effect produced is the increase of the solute concentration in the surrounding area of the membrane wall. This layer of higher concentration is called the polarization layer.

If C_m is the solute concentration in the membrane surroundings and C_c is the concentration in the solution, then the polarization factor is defined as the quotient between both concentrations:

$$F_P = \frac{C_m}{C_C} \tag{10.5}$$

The effect of this layer is unfavorable in the global mass transfer process, since the concentration increase in this layer ($C_m > C_c$) causes diffusive streams from this layer into the solution. At the same time, it produces an increase of the osmotic pressure, so the transfer stream will decrease, as will be seen later. Another negative factor is that, due to the increase in concentration, precipitation of the solute occurs on the membrane wall and will interfere in the global mass transfer process.

To avoid these harmful effects, agitation is incorporated into the design of separation processes by membranes, or the fluid is forced to circulate under turbulent regime. In spite of all this, the polarization layer is not completely eliminated.

10.2 Mass Transfer in Membranes

Different models have been developed to explain mass transfer through the membrane. A brief explanation of some models is given next.

10.2.1 Solution Diffusion Model

This model assumes that the different components of the solution (solvent and solute) are dissolved in the membrane when in contact with the wall and then diffuse through the membrane in an independent form. The dissolving stage occurs according to an equilibrium distribution law, so it can be referred to as a partition coefficient analogous to the partition coefficient of other classic operations (for example, liquid–liquid extraction). According to this distribution law, the membrane is selective to solubilization of certain components. The diffusion through the membrane is driven by pressure and concentration gradients between both sides of the membrane wall.

The flow of each component of the solution through the membrane is given by an expression of the type:

$$J_i = -\frac{D_i C_i}{RT}\,\text{grad}\left(\mu_i\right) = -\frac{D_i C_i}{R\,T}\left(\frac{\partial \mu_i}{\partial C_i}\,\text{grad}\,C_i + \overline{V}_i\,\text{grad}\,P_i\right) \qquad (10.6)$$

where:

J_i = flux of the component i
D_i = diffusion coefficient of the component i in the membrane
C_i = concentration of the component i in the membrane
μ_i = chemical potential
$\overline{V}_i$ = partial molar volume
P_i = applied pressure

10.2.2 Simultaneous Diffusion and Capillary Flow Model

This model assumes that the two mechanisms involved in the transfer through the membrane are diffusion and capillary flow and that they occur simultaneously. The diffusion of the components is carried out in an analogous way to that described in the previous model, in that the diffusion through the membrane is due to a chemical potential gradient. The effect of the solution passage from the wall in contact with the concentrated solution to the other side through channels that exist within the membrane should be added to this transfer mechanism. This additional flow is proportional to the pressure gradient existing between both sides of the membrane and occurs in such a way that the concentration does not vary.

The solvent flow is greater than the solute's flow because the diffusion coefficient of the former is much greater than the solute's:

$$D_{solvent} \gg D_{solute}$$

In this model, the flows for the solvent and solute are given by the expression:

$$J_i = J_{Diffusion} + J_{Capillary}$$

in which $J_{Diffusion}$ can be obtained according to the expression given by the solution diffusion model, while $J_{Capillary}$ is the capillary component that can be calculated using the expression:

$$J_{Capillary} = K C_I \text{ grad } P$$

In this expression:

K = constant
C_i = concentration of the component i
P = applied pressure

10.2.3 Simultaneous Viscous and Friction Flow Model

This model assumes that the whole transfer is performed through small channels in the membrane. It can be assumed that these channels are not straight and are equal. It is assumed that the fluid circulates through the membrane channels under laminar regime, so it is possible to apply Fanning's equation to calculate the circulation velocity as a function of the pressure drop experienced by the fluid when crossing the membrane. Hence, the following equation is employed:

$$\frac{(-\Delta P)}{\rho} = \frac{64}{\text{Re}} \frac{(v_c)^2}{2} \frac{\delta}{D_e} \tag{10.7}$$

where δ is the channel length, D_e is the equivalent diameter of each channel, v_c is the velocity at which the fluid circulates through the channel, and Re is the Reynolds number. The Reynolds number may be substituted in Equation 10.7 by its value:

$$\text{Re} = \frac{\rho\, v_c D_e}{\eta}$$

The value of the global velocity can be expressed as a function of the linear velocity of the fluid in each channel if the continuity equation is applied, obtaining:

$$v = v_c \frac{\delta_m \varepsilon}{\delta} \tag{10.8}$$

where:

v = global velocity
δ_m = membrane thickness
δ = channel length
ε = membrane porosity

If, in addition, the tortuousness (τ^o) is defined as the relation between one channel length and the thickness of the membrane ($\tau^o = \delta/\delta_m$), and the equations stated before are combined, then the following equation is obtained:

$$v = \frac{\varepsilon (D_e)^2}{32 \eta \delta_m (\tau^o)^2} \left(-\Delta P\right)$$

Hence, the flux is:

$$J = \rho v = \frac{\rho \varepsilon (D_e)^2}{32 \eta \delta_m (\tau^o)^2} \left(-\Delta P\right) \tag{10.9}$$

10.2.4 Preferential Adsorption and Capillary Flow Model

This model assumes that the membrane presents a preferential adsorption behavior towards some components of the solution, so a layer of these components will form at the interface membrane–solution. Figure 10.4 presents this model in a schematic way for the case of a sodium chloride aqueous solution. It is also assumed that there is a critical pore size that can allow the adsorbed component at the interface to cross and circulate through the membrane channels under capillary flow.

The adsorbed quantity at the interface (Γ) can be calculated as a function of the interface tension (τ) by means of the Gibbs equation:

$$\Gamma = \frac{1}{RT} \frac{d\tau}{d \ln a} \tag{10.10}$$

where a is the activity of the solute.

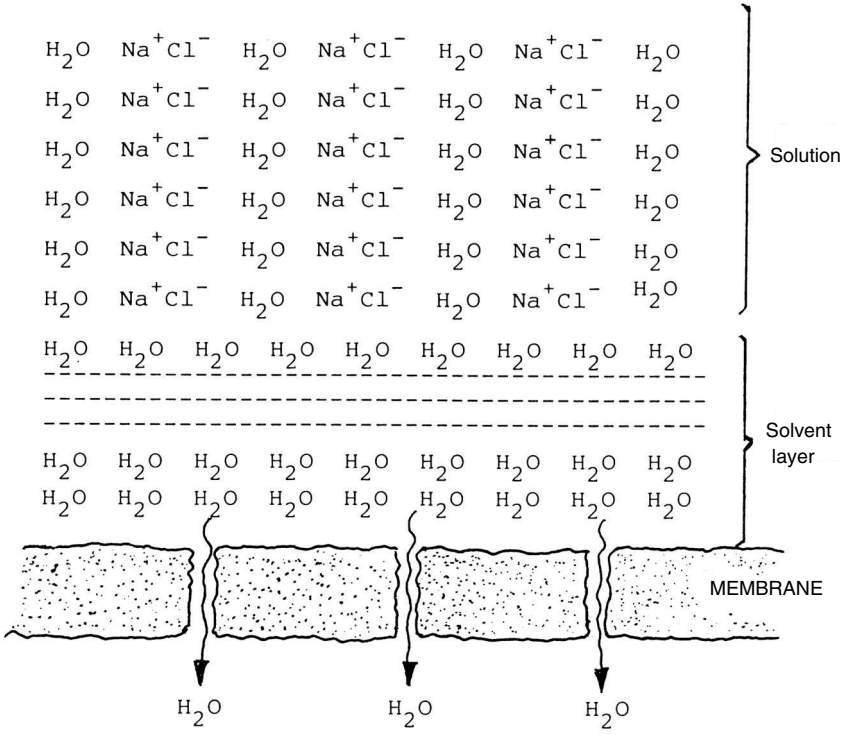

FIGURE 10.4
Preferential adsorption capillary flow model.

10.2.5 Model Based on the Thermodynamics of Irreversible Processes

The general process to describe mass transfer through membranes is obtained by applying the thermodynamics of irreversible processes to the membrane, considering it as a black box, and analyzing the entropy variation that takes place. The increase in entropy is the driving force that produces the transfer through the membrane. In this model, during the transfer of each component, besides the primary driving force that causes it, the flow due to coupled phenomena is also taken into account. In this way, the general expression for the transfer of one of the components is given by the equation:

$$J_i = L_{ii}\,\phi\left(\Delta G_i\right) + \sum_j L_{ij}\,\phi\left(\Delta G_j\right) \tag{10.11}$$

The first addend of the right-hand side expression represents the mass flow of component *i* per unit area due to the difference of free energy between

the two faces of the membrane, where $\phi(\Delta G_i)$ is the driving force, which is a function of the free energy through the membrane for such component i. The proportionality coefficient L_{ii} is a function of the diffusion coefficient of component i. The second addend represents the additional contribution to the transfer of the component i due to the free energy differences of the other components that the flow of component i carries coupled.

According to Onsegar, the values of the coefficients L have restrictions in such a way that they should comply with:

$$L_{ij} = L_{ji}$$
$$L_{ii} - (L_{ij})^2 \geq 0$$

In general, the coupled flows are small compared to the primary flow. Thus, the flow of one component is usually given as a function of only one driving force, the primary.

10.3 Models for Transfer through the Polarization Layer

As indicated in a previous section, the semipermeable membrane hinders the crossing of certain components, so in the interface membrane–solution, an accumulation of these components is produced, building up the so-called polarization layer.

When the solution is made up of macromolecules and presents a high concentration, it can occur that the polarization layer acquires gel properties starting from a given value of the concentration of the rejected compound in this layer (C_g). When such a value is reached, a gelatinous layer begins to form, becoming a new resistance to the flow of the permeate.

This process can be observed in schematic form in Figure 10.5. A solution with a solute concentration C_c permeates through the membrane to the permeate stream, presenting a concentration C_p smaller than C_c. However, the polarization layer produces a concentration increase up to a value C_m right on the membrane wall. If $C_m < C_g$, the gel layer will not be formed, while if $C_m = C_g$, the gel layer will be formed and its thickness will increase as operation time goes on. There are different models to explain transfer through the polarization layer. Two of these models will be explained next.

10.3.1 Hydraulic Model

This model is based on the film theory. It is supposed that, in the surrounding area of the membrane, a layer is formed in which there is a concentration gradient in which the concentration increases from C_c to C_m. This concentration gradient produces a transfer of mass from the polarization layer to the solution. For this reason, when making a balance of the component in the

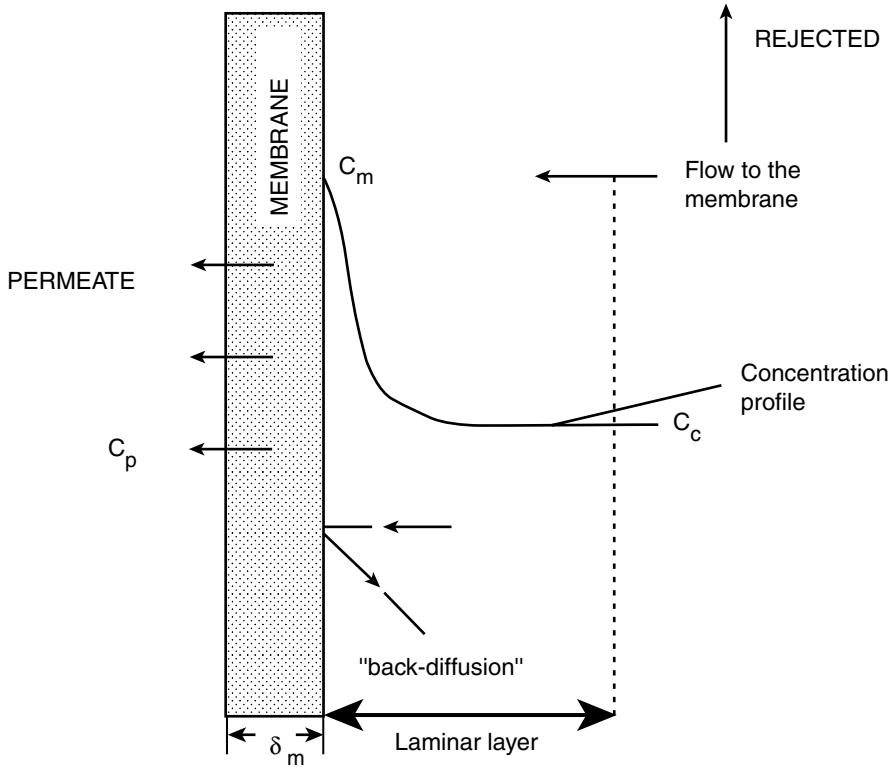

FIGURE 10.5
Polarization layer by concentration.

polarization layer, it is obtained that the amount of the component that crosses the membrane is equal to the amount that arrives at the membrane from the solution, times the global flow, and minus the amount of component transferred by diffusion from the layer to the solution. This balance yields the following expression:

$$C_P J = C J - D_S \frac{dC}{dx} \tag{10.12}$$

in which J is the global flux and D_S is the diffusivity of the solute.

This equation is valid if the following requisites are complied with:

- The diffusion coefficient is independent of the concentration.
- There is a concentration gradient only in the polarization layer, assuming that the transfer from the solution to the layer is carried out by convective mechanisms.
- There are no convection streams due to density differences.

The last equation is a first order nonhomogeneous differential equation that can be integrated on the boundary conditions: for $x = 0$, $C = C_c$ and for $x = \delta_p$, $C = C_m$, where δ_p is the thickness of the polarization layer.

The integration of the differential equation allows calculation of the concentration of the solute in the interface membrane-concentrated solution:

$$C_m = C_P + \left(C_C - C_P\right) \exp\left(\frac{J\delta_P}{D_S}\right)$$

If a transfer coefficient of the solute (k_s) is defined as the relationship between diffusivity and thickness of the polarization layer ($k_s = D_s/\delta_p$), the following is obtained:

$$C_m = C_p + \left(C_c - C_p\right)\exp\left(J/k_S\right) \tag{10.13}$$

The flux of the solvent is obtained by multiplying the global flux by the solvent's concentration:

$$J_{\mathrm{D}} = J C_{\mathrm{D}}$$

which, substituted in Equation 10.13, yields the expression of the concentration on the membrane's side as a function of the flow density of the solvent:

$$C_m = C_P + \left(C_C - C_P\right)\exp\left(\frac{J_D}{C_D k_S}\right) \tag{10.14}$$

The calculation of the solute transfer coefficient k_s can be carried out starting from the Colburn's analogy:

$$j_{\mathrm{D}} = j_{\mathrm{H}}$$

Taking into account the definition of the Colburn's factor for diffusivity:

$$\left(Sh\right) = j_H\left(\mathrm{Re}\right)\left(Sc\right)^{1/3} \tag{10.15}$$

where:

Sh = Sherwood number ($k_S\, d_e/D_S$)
Re = Reynolds number ($\rho\, v\, d_e/\eta$)
Sc = Schmidt number ($\eta/(\rho\, D_S)$)
j_{H} = Colburn factor for heat transfer
d_e = equivalent diameter

TABLE 10.2

Characteristic Geometric Parameters of Reverse Osmosis Modules for Flat, Spiral, and Tubular Configurations

Configuration	a	A_m	d_e	l_c	l_{pd}	l_{pc}
Flat						
Annular	$\frac{\pi}{2}(R_e - R_i)$	$\pi(R_e^2 - R_i^2)$	$2h$	$(R_e - R_i)$	$(R_e - R_i)$	$70\,d_e$
Rectangular	$H\,h$	$H\,L$	$2h$	L	L	$70\,d_e$
Spiral	$H\,h$	$\frac{HL}{N}$	$2h$	L	$\frac{L}{N}$	0
Tubular	$\frac{\pi}{4}D_i^2$	$\frac{\pi D_i L}{N}$	D_i	L	$\frac{L}{N}$	0

Source: Lombardi and Moresi (1987).

The Colburn factor depends on the circulation regime of the fluid in such a way that it can be calculated from the following equations:

Laminar flow (Re < 2100) $$j_H = 0.023(\mathrm{Re})^{-0.2} \tag{10.16}$$

Turbulent flow (Re > 10^4) $$j_H = 1.86(\mathrm{Re})^{-2/3}(d_e/l_c)^{1/3} \tag{10.17}$$

where l_c is a characteristic length that, similar to the equivalent diameter, depends on the type of configuration used. Table 10.2 presents the characteristic geometric parameters of the more common configurations, which are shown in Figure 10.6.

It is difficult to calculate the solute diffusivity in the solution; however, it can be evaluated by means of the correlation of Wilke and Chang:

$$D_S = 7.4 \times 10^{-8} \frac{T(\psi M)^{1/2}}{\eta(\overline{V}_m)^{0.6}} \tag{10.18}$$

where:

$\overline{V}_m$ = molar volume of the solute at boiling temperature (cm^3/mol)
η = solution viscosity (cP)
ψ = association parameter of the solvent (2.6 for pure water)
T = absolute temperature
M = solvent molecular weight

Another way to evaluate solute diffusivity can be by starting from the equation:

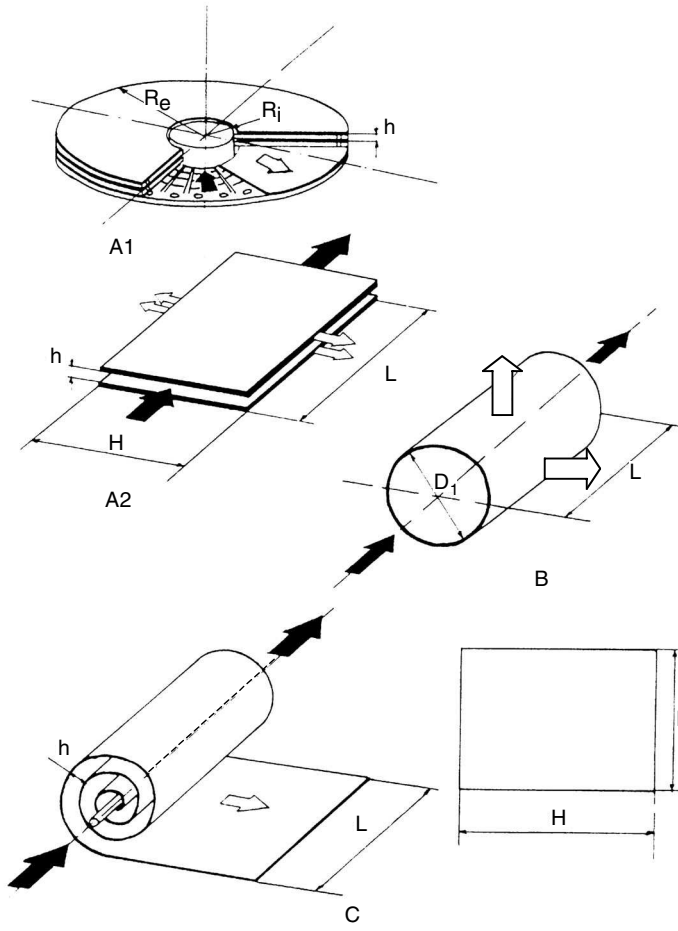

FIGURE 10.6
Geometric configuration of separation modules for membranes: (A1) annular flat; (A2) rectangular flat; (B) tubular; (C) spiral. (Adapted from Lombardi and Moresi, 1987.)

$$D_S = 7.7 \times 10^{-16} \frac{T}{\eta \left(\overline{V}^{1/3} - \overline{V}_0^{1/3} \right)} \tag{10.19}$$

in which diffusivity D_S is expressed in m^2/s, viscosity η in Pa·s, and the temperature T in Kelvin. The value of $\overline{V}_0$ for diffusion of solutes in water is 0.008. The variable $\overline{V}$ is the molecular volume, which is defined as the volume in m^3 of one kmol of substance in liquid form at its boiling temperature. Table 10.3 shows values of the molecular volume for different substances.

TABLE 10.3

Values of Molecular Volume

Substance	$\bar{V}$ (m³/kmol)
Carbon	0.0148
Hydrogen	0.0037
Oxygen	
Double bond	0.0074
In aldehydes and cetones	0.0074
In methyl esters	0.0091
In ethyl esters	0.0099
In ether and other esters	0.0110
In acids	0.0120
Bonded to S, P, N	0.0083

Source: Perry, R.H. and Chilton, C.H., *Chemical Engineer's Handbook*, McGraw–Hill, New York, 1982.

10.3.2 Osmotic Model

This model considers that, for the specific case of ultrafiltration, reverse osmosis and mechanical filtration characteristics are present, so the osmotic factors as well as the variation of the diffusion coefficient and viscosity with concentration should be taken into account. This process is considered a filtration through the polarization layer.

The solvent flow that crosses the membrane is obtained by performing a mass balance in the polarization layer, so such flow will be equal to the amount of solvent arriving at the membrane with the global flow, minus the amount of solvent returning from the polarization layer to the solution, due to back-diffusion by chemical potential difference. Also, the quantity due to the hydraulic contribution caused by the pressure drop through the polarization layer should be added.

In the case that the solution is made of the solvent and one solute, the density of the diffusion molar flow for the solvent can be expressed according to Fick's first law for binary mixtures:

$$N_D = X_D\left(N_D + N_S\right) - C_T D_D \frac{\partial X_D}{\partial x} \tag{10.20}$$

where:

N_D = molar flux of solvent
N_S = molar flux of solute
X_D = molar fraction of solvent
C_T = global molar concentration
D_D = solvent diffusivity
x = distance

The first term of the right-hand side expression in Equation 10.20 is the molar flux of the solvent resulting from the global movement of the solvent, while the second addend is the solvent's flux due to the diffusion superimposed to the global flow. In this equation, the terms for the solvent global flow and diffusion go the same way, since the solvent diffuses in the same direction as the stream. However, for the solute, global flow and diffusion go in opposite ways, since the solute diffuses against the stream.

The osmotic model takes into account the new hydraulic contribution term, so the flux for the solvent would be:

$$N_D = X_D\left(N_D + N_S\right) - C_T D_D\left[\frac{\partial X_D}{\partial x} + X_D \frac{\overline{V}_D}{RT}\frac{\partial P}{\partial x}\right] \tag{10.21}$$

in which $\overline{V}_D$ is the partial molar volume of the solvent and P is the pressure.

10.4 Reverse Osmosis

Reverse osmosis can be defined as a membrane separation process in which the selective retention or rejection of ionic solutes takes place. Retention is due to electrostatic rejection and effects of the dielectric tension in the interface, which causes particles of smaller size than the pore size of the membrane to be retained. In general, it is said that molecules with molecular weights smaller than 300 Da can be rejected, the size of the retained particles being around 1 to 10 Å.

10.4.1 Mathematical Model

Any of the models explained before can be used to describe the transfer phenomenon through the membrane. However, the solution diffusion model is one of the most used, as is the model based on the thermodynamics of irreversible processes.

Regardless of which model is adopted, it is assumed that some requirements should be complied with when the model is applied. Such requirements are:

- Each component crosses the membrane due to the effect of its chemical potential.
- There are no coupled flows phenomena, that is, $L_{ij} = 0$.
- The diffusion coefficient is considered to be independent of concentration, supposing that Fick's Law is complied with.

- It is considered that the total molar concentration is constant in the entire work zone.
- The velocity at which each component is transferred is determined by its diffusion coefficient and by the solution capacity in the membrane.

With these hypotheses, the transfer equation through the membrane is simplified to an expression in which the driving force is due to the chemical potential gradient of the components. Such potential can be expressed in terms of pressure and concentration.

When applying the equation of the solution diffusion model (Equation 10.6) in the case of a solution consisting of the solvent and one solute, it should be taken into account that the chemical potential of the solution is influenced more by the concentration gradient than by the pressure gradient.

For the calculation of the solvent flow through the membrane, it is considered that its concentration gradient is negligible, so the following equation should be integrated:

$$J_D = \frac{D_D C_D}{RT} \overline{V}_D \frac{dP}{dx} \tag{10.22}$$

on the boundary conditions: for $x = 0$, $P = P_c + \pi_c$ and for $x = \delta_m$, $P = P_m + \pi_m$, yielding the following expression:

$$J_D = \frac{D_D C_D \overline{V}_D}{RT} \left(\Delta P - \Delta \pi \right) \tag{10.23}$$

For the calculation of the solute flow through the membrane, it is supposed that the pressure gradient does not affect the transfer of solute, but that it depends exclusively on the concentration gradient of the solute between both faces of the membrane. Hence:

$$J_S = -\frac{D_S C_{Sm}}{RT} \frac{\partial \mu_{Sm}}{\partial C_{Sm}} \frac{dC_{Sm}}{dx} \tag{10.24}$$

in which the subindex *Sm* indicates solute in the membrane. The solute's chemical potential in the membrane is expressed according to the equation:

$$\mu_{Sm} = \mu^{\circ}_{Sm} + RT \ln \left(\gamma_S C_{sm} \right) \tag{10.25}$$

where γ_S is the activity coefficient of the solute.

Therefore, the following equation is obtained for the global flux:

$$J_S = -D_S \frac{dC_{Sm}}{dx} \tag{10.26}$$

that can be integrated on the boundary conditions:

for $x = 0$, $C_{Sm} = C_{Sm}^C$ and for $x = \delta_m$, $C_{Sm} = C_{Sm}^P$, in which C_{Sm}^C is the concentration of the solute within the membrane on the wall on the high-pressure side, while C_{Sm}^P is the low-pressure face. The integration yields to the expression:

$$J_S = \frac{D_S}{\delta_m}\left(C_{Sm}^C - C_{Sm}^P\right)$$

Taking into account a solute partition or distribution coefficient between the membrane and the solution defined by:

$$K_P = \frac{C_{Sm}}{C_S} = \frac{\text{solute concentration in the membrane}}{\text{solute concentration in the solution}}$$

the amount of solute transferred is obtained by the expression:

$$J_S = \frac{K_P D_S}{\delta_m}\left(C_C - C_P\right) \tag{10.27}$$

If one of the membrane properties depends on the pressure or concentration, the following permeability coefficients of the membrane to the solvent and the solute can be defined:

Permeability of the membrane to the solvent:

$$A = \frac{D_D C_D \overline{V}_D}{RT\delta_m} \tag{10.28}$$

Permeability of the membrane to the solute:

$$B = \frac{D_S K_P}{\delta_m} \tag{10.29}$$

Thus, the expressions of the flux of the solvent and solute would be:

$$J_D = A\left(\Delta P - \Delta\pi\right) \tag{10.30}$$

$$J_S = B\left(C_c - C_p\right) \tag{10.31}$$

The solute rejection is given by Equation 10.1:

$$R = \frac{C_C - C_P}{C_C} = 1 - \frac{C_P}{C_C}$$

But the flux of the solvent and the solute are related by the expressions: $J_D = J\ C_D$ and $J_S = J\ C_p$; then:

$$J_S = \frac{J_D}{C_D} C_P$$

Hence, the solute concentration in the transfer stream is expressed by:

$$C_P = \frac{J_S}{J} = \frac{BC_D}{A\left(\Delta P - \Delta\pi\right) + BC_D}\ C_C \tag{10.32}$$

so the solute rejection would be:

$$R = \frac{A\left(\Delta P - \Delta\pi\right)}{A\left(\Delta P - \Delta\pi\right) + BC_D} \tag{10.33}$$

10.4.2 Polarization Layer by Concentration

In previous sections, it was assumed that only the semipermeable membrane puts up resistance to mass transfer. However, a layer is formed in the surrounding area of the membrane due to the accumulation of solute. This layer offers a new resistance to mass transfer, and various harmful effects to such transfer are observed, notably:

- The osmotic pressure increases as the solute concentration increases, so the amount of transferred solvent decreases, since the driving force is smaller. The term $\Delta\pi$ increases in Equation 10.30; therefore, J_D decreases.
- The pumping power should increase to compensate for this drop.

- The amount of solute increases in the transfer stream since the concentration difference that impels such transfer increases. If C_c increases in Equation 10.31, so does J_S.
- Deposits are produced on the membrane's wall, so some pores can be blocked. This fact gives the inconveniences of all processes where dirt is deposited.
- Deposited substances can cause deterioration of the membrane.

Some authors indicate that the polarization by concentration can be measured by the quotient between solute concentration on the membrane surface and in the solution. If the hydraulic model is applied to describe the mass transfer through the polarization layer, Equation 10.14 is obtained:

$$C_m = C_P + \left(C_C = C_P\right) \exp\left(\frac{J}{K_S}\right)$$

In the case that the solute is totally rejected, that is, the solute concentration in the transfer stream is zero, then this equation can be simplified to:

$$C_m = C_C \exp\left(\frac{J}{K_S}\right) \tag{10.34}$$

For some cases with defined geometry, such as parallel or tubular layers under laminar flow, solutions can be found in the literature.

10.4.3 Influence of Different Factors

It is interesting to study the effect that operative effects such as pressure, temperature, and type of solute exert on the global process.

10.4.3.1 Influence of Pressure

Pressure is one of the factors that can greatly affect the transfer of components. Thus, if Equation 10.33, which gives the retained fraction, is observed, it can be deduced that, for high values of the applied pressure, the second addend of the denominator (BC_D) is negligible in comparison to the first addend, so the value of R tends to one. That is, if the term of the applied pressure tends to infinite, then R acquires a value equal to one. However, this is not exact since the value to which R tends is close to one but not exactly one. This is because when the effective pressure increases, the solute flux increases too. This can be graphically observed in Figure 10.7.

Pressure will also affect the solvent flow, since if ΔP in Equation 10.30 increases, the variation of the solvent flow will be linear to the increase of

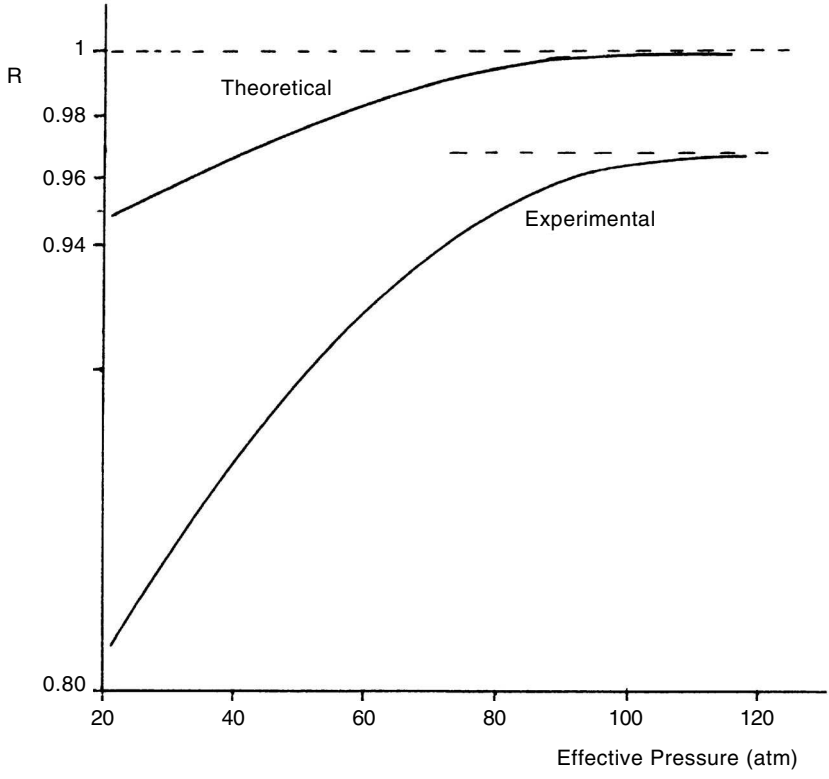

FIGURE 10.7
Influence of pressure on the permeate flow.

the applied pressure. However, in reality, this does not happen exactly, since when the pressure increases, certain compression of the membrane occurs, causing a decrease of its permeability. Also, the polarization by concentration phenomenon increases as the pressure increases, hindering the transfer of solvent.

10.4.3.2 Effect of Temperature

The effect of a temperature increase on the solvent flow is to increase the flow due to an increase of the membrane permeability to the solvent and to a decrease of the solvent viscosity. The variation of permeability A with temperature can be correlated by an Arrhenius-type equation as:

$$A = A_0 \exp\left(-E_o / RT\right) \tag{10.35}$$

where:

A_0 = permeability at 0 °C
A = permeability at t °C
E_o = activation energy of the water impregnated in the membrane (16 to 25 kJ/mol)
R = gas constant
T = absolute temperature

Permeability values are usually given at 20°C, so at any other temperature they should be correlated to those corresponding to this temperature. In this way:

$$A = A_{20} \exp\left[\frac{E_0}{R}\left(\frac{1}{293} - \frac{1}{T}\right)\right] \tag{10.36}$$

A value of 23 kJ/mol is usually taken for E_0 and, since the gas constant is $R = 8.314 \times 10^3$ kJ/(mol K), it is obtained that:

$$A = A_{20} \exp\left[9.45 - \frac{2768}{T}\right] \tag{10.37}$$

Temperature also affects the viscosity of the solvent; thus, when temperature increases, viscosity decreases. The variation of viscosity with temperature can also be correlated by an Arrhenius-type equation:

$$\eta = \eta_o \exp\left(E/RT\right) \tag{10.38}$$

in which

η = solvent viscosity
η_0 = frequency factor
E = flow activation energy

In the case of aqueous solutions, the solvent is water, whose flow activation energy is 16.7 KJ/mol.

In the case of permeability A, as well as in the case of viscosity η, when plotting their logarithms against the inverse of absolute temperature, straight lines whose slopes correspond to the activation energy are obtained (Figure 10.8).

For a given operation in which the effective and osmotic pressures are kept constant, starting from Equation 10.30 and taking into account Equations 10.35 and 10.38, it can be written that:

$$J_D\eta = A\left(\Delta P - \Delta\pi\right)\eta = KA_0 \exp\left(-\frac{E_0}{RT}\right)\eta_0 \exp\left(\frac{E}{RT}\right)$$

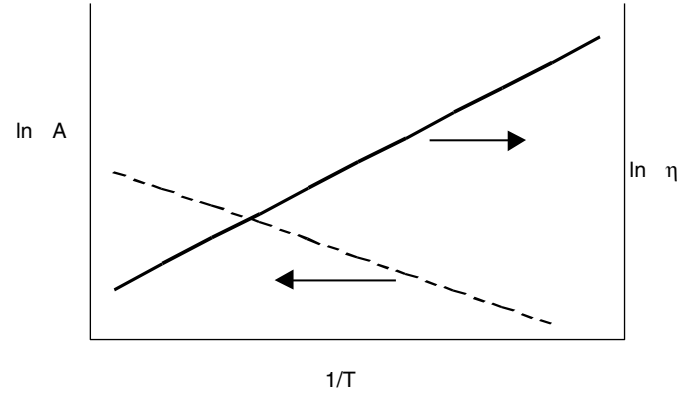

FIGURE 10.8
Influence of temperature on fluid viscosity and membrane permeability.

$$J_D \eta = K A_0 \eta_0 \exp\left(\frac{E - E_0}{RT}\right) \tag{10.39}$$

In this equation, K is a constant. In the case that the activation energy values coincide ($E = E_0$), the product of the flux times the viscosity is constant.

10.4.3.3 Effect of Type of Solute

The type of solute influences the mass transfer in such a way that the retention will be greater as the molecular size is greater. Also, the retention increases as the charge valence of the ion increases. It can also be observed that the flow through the membrane increases when there are molecules that form hydrogen bonds with the membrane, and that the flow is greater as the strength of such hydrogen bonds increases.

It is known that membranes show some selectivity to diverse components, so that the salts from divalent ions are retained better than those with monovalent ions. With regard to the cations, it is known that sodium is better retained than ammonium while, for the anions, chloride is better retained than other ions such as nitrate, perchlorate, and cyanide. All observations stated with respect to selectivity of the solutes have been determined experimentally.

10.5 Ultrafiltration

Similar to reverse osmosis, ultrafiltration is a separation process by membrane capable of selectively retaining solutes that cannot be ionized. This separation is based on the molecular size of the solutes being retained, in

general, for molecules with a molecular weight between 300 and 500,000 Da, which corresponds to molecular sizes between 10 and 200 Å. Unlike reverse osmosis, ultrafiltration is not controlled by osmotic pressure, so separation at low work pressures (from 34 to 690 kPa) can be carried out.

10.5.1 Mathematical Model

In ultrafiltration, the prevailing transfer mechanism through the membrane is selective filtration through the pores. For this reason, rejection presented by the membrane for a given compound is dependent on the molecular weight of the compound, its shape, size, and flexibility, as well as the working conditions.

The permeate flow can be obtained assuming that the membrane works as a molecular sieve, formed by a set of channels of equal size, form, and length, through which solvent and molecules of smaller size than the channels flow. Since the diameter of the channels is small, it is supposed that the permeate that flows circulates under laminar regime, so the Fanning equation can be applied to calculate the flow through the membrane. In this way, the model that best describes the transfer phenomenon through the membrane is the simultaneous viscous flow and friction model.

When applying this model, the calculation of the solvent flux yields to the expression:

$$J_D = \frac{\varepsilon D_e^2 \rho}{32 \eta \delta_m (\tau^o)^2} \left(-\Delta P\right)$$

in which ε is porosity of the membrane, D_e is the equivalent diameter of the channels, δ_m is the membrane thickness, τ° is the tortuousness factor of the channels, ρ and η are the density and viscosity of the fluid, respectively, while $(-\Delta P)$ is the pressure drop experienced by the fluid when crossing the membrane.

If the hydraulic permeability of the membrane is defined as:

$$K_m = \frac{\varepsilon D_e^2 \rho}{32 \delta_m (\tau^o)^2} \tag{10.40}$$

then it is obtained that:

$$J_D = \frac{K_m}{\eta} \left(-\Delta P\right) \tag{10.41}$$

which is an equation that can be expressed as a function of the hydraulic resistance of the membrane R_m, in such a way that:

$$J_D = \frac{(-\Delta P)}{\eta R_m} \tag{10.42}$$

indicating that the solvent's flow is directly proportional to the pressure difference between both sides of the membrane, and inversely proportional to the hydraulic resistance that the membrane puts up to the solvent transfer through itself.

While the last equation is usually used to calculate solvent transfer, factors that account for the probability that a molecule will penetrate a channel can be introduced, in addition to the distribution of the channel's size. It is evident that this complicates the calculation of solvent transfer through the membrane.

The equation of Ferry–Faxen is used to calculate the solute flow, in which the interaction of the molecules with the walls of the membrane's channels is taken into account, as well as the esteric effects, size and shape of the molecules, and cross section of the channels. In this way, the solute flux is expressed according to the equation:

$$J_S = J_D C_c \sigma \tag{10.43}$$

in which σ is a dimensionless constant with a value between 0 and 1. Physically, this constant represents the fraction of solute that passes through the channels whose cross section is such that they could not retain smaller molecules. This factor can be expressed as a function of the probability of a solute molecule to penetrate a channel and of the friction force with the channel walls. Thus, the equation allowing calculation of this constant is given by the expression:

$$\sigma = \left[2(1-\chi)^2 - (1-\chi)^4\right]\left[1 - 2.104\chi + 2.09\chi^3 - 0.95\chi^5\right] \tag{10.44}$$

in which χ is the relationship between the molecular diameter (D_m) and the diameter of the cross section of the membrane channels (D_e), that is, $\chi = D_m/D_e$.

10.5.2 Concentration Polarization Layer

As occurs in reverse osmosis processes, in ultrafiltration, a layer with solute concentration higher than the concentration in the fluid appears next to the membrane in the high-pressure zone. In this case, the problem is bigger, since from a certain concentration it begins to turn into a gel, so that, if the transfer continues, the gel layer increases its thickness as the operation time continues.

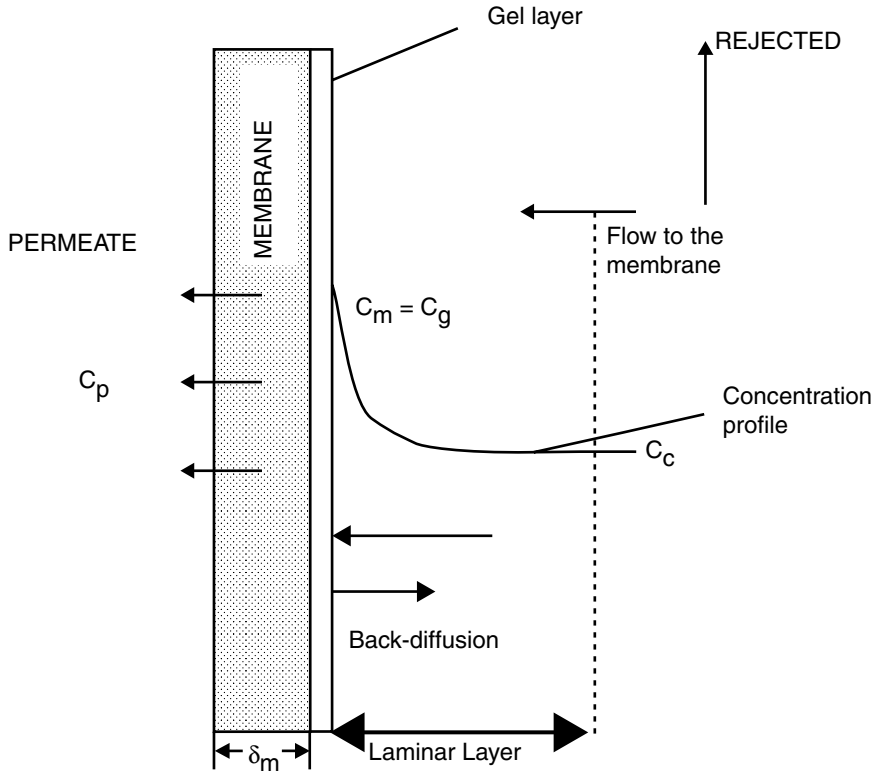

FIGURE 10.9
Concentration polarization layer and gel layer.

The gelled polarized layer offers a new resistance to mass transfer (Figure 10.9), so, if the gel's hydraulic permeability (K_g) is defined, then the solvent flux would be expressed according to the equation:

$$J_D = \frac{\left(-\Delta P\right)}{\eta\left(\frac{1}{K_m} + \frac{1}{K_g}\right)} \tag{10.45}$$

where ($-\Delta P$) is the global pressure difference from the concentrated solution to the permeate stream. For this reason, the solvent flux would be directly proportional to the pressure increase and inversely proportional to the resistance offered by the membrane (R_m) and the gel layer (R_g):

$$J_D = \frac{\left(-\Delta P\right)}{\eta\left(R_m + R_g\right)} \tag{10.46}$$

When it is considered that the solute concentration in the permeate stream is much greater than in the concentrated solution ($C_p \ll C_c$), or when the solution is totally rejected, under steady state, the solute transport stream from the concentrated solution to the polarization layer is equal to the diffusional transport from such layer to the solution:

$$JC = D_S \frac{dC}{dx} \tag{10.47}$$

The integration of this equation yields the following expression:

$$J = k_S \ln\left(\frac{C_g}{C_C}\right) \tag{10.48}$$

where k_S is a global transfer coefficient with a value equal to $k_S = \frac{D_S}{\rho_S}$, in which δ_p is the thickness of the polarization layer. This coefficient is determined as explained in Section 10.3, using Equation 10.15.

In this case, the solute transfer from the gel layer to the solution (back-diffusion) can be expressed as a function of the mass transfer global coefficient, so that:

$$D_S \frac{dC}{dx} = K\left(C_g - C_C\right) \tag{10.49}$$

Where the transfer phenomenon through the gel layer controls the global process, the flux of the solvent will be expressed as:

$$J_D = k_S \ln\left(\frac{C_g}{C_C}\right) \tag{10.50}$$

This equation is similar to the equation obtained for reverse osmosis.

In order to avoid the build-up of concentration polarization layers, the operation should be done at high feeding velocities.

10.5.3 Influence of Different Factors

10.5.3.1 Influence of Pressure

If there were no gel layer, the flow would vary in a linear fashion with pressure. However, this fact is not completely true; therefore, the influence of such a layer should always be taken into account. The influence of pressure in different cases can be seen in Figure 10.10. Thus, when the resistance of

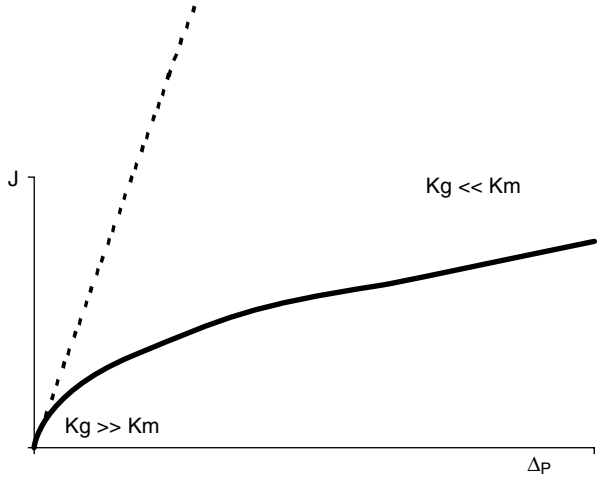

FIGURE 10.10
Influence of pressure on the permeate stream during ultrafiltration.

the gel layer is negligible ($K_g \to \infty$ or $R_g \to 0$), the variation is linear, while if this layer controls the transfer phenomenon ($K_g \ll K_m$ or $R_g \gg R_m$), the amount of transferred mass is independent of pressure.

At first, rejection or retention is independent of the applied pressure, since the parameter σ is only determined by the dimensions of the molecules and the cross section of the membrane pores. However, it has been experimentally observed that rejection decreases when the pressure increases. The explanation for this phenomenon could be that, due to the high pressures applied, the membrane can be elastically deformed, thus increasing the cross-section of the channels and facilitating the passage of the solute through those channels. However, the molecules can also be deformed, yielding the same result.

10.5.3.2 Effect of Temperature

A temperature increase produces a decrease of the solvent viscosity, causing an increase of the solvent flow. If Equation 10.41 is observed for the calculation of solvent flow, when the viscosity η that is in the denominator of the equation decreases, then the flux of the solvent (J_D) will increase. It is accepted that, for each degree Centigrade that temperature increases, the solvent flow increases between 1.1 and 1.7%.

The back-diffusion of the gel layer increases as temperature increases; hence, the critical concentration at which the gel is formed increases too. Thus, the formation of this layer is delayed.

All these reasons indicate that it is convenient to work at high temperatures. However, the resistance of the membranes to temperature determines the limit of the working temperature.

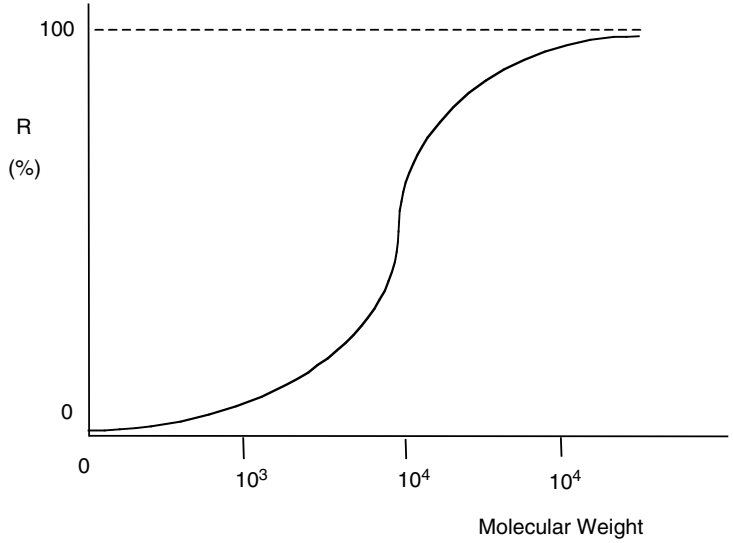

FIGURE 10.11
Influence of the solute's molecular weight on the percentage rejected.

10.5.3.3 Effect of Type of Solute

The retention that the membranes carry out on the molecules of solute is a function of their size and molecular weight. When plotting the variation of the rejected solute percentage against its molecular weight, a sigmoid curve, as shown in Figure 10.11, is obtained. Membranes do not present rejection to solutes with low molecular weight. Rejection increases when the molecular weight is greater than 1000 Da. For values larger than 10^5 Da, the rejection is total.

10.6 Design of Reverse Osmosis and Ultrafiltration Systems

Some difficulties appear in the design of reverse osmosis units that should be taken into account so the resulting unit can be successfully applied to the separation problem stated. Among these difficulties are the following:

- Membranes are usually fragile and cannot stand high working pressures.
- The concentration polarization layer, intended to eliminate, hinders mass transfer and also dirties the membranes.

- Membranes are usually bulky, so designs with a high packing density are usually desirable, their purpose being to reduce the dimensions of the container since it should operate under pressure.
- The high costs implied by membrane replacement should be avoided.

The designs performed to solve these difficulties have yielded different types of modules. Most used are plate-and-frame, tubular, spiral-wound, and thin hollow-fiber.

A certain number of variables, related among them by transfer kinetics equations and equations from balances, are managed in all design process. This allows that, once solved, the best design is obtained. Usually, the design variables are the desired recovery factor, the concentration of the permeate stream, working temperature and pressure, pretreatment operations that should be performed, the methods used to maintain the flow through the membrane, the retained flux, and the final treatments to be applied to obtain the desired concentration degree.

The posed problems can be different, although, in general, the available data are the feed flow and its concentration, the working temperature, the recovery factor or permeate flow, and the type of membrane to use. If the type of membrane is fixed, then it is possible to know the solute rejection as well as the working pressure it can stand. These data should be correlated by adequate equations in order to obtain the concentrations of the permeate and retained streams, as well as the membrane area needed and the pumping power to carry out the desired separation.

Next, two calculation methods that allow solution of design problems of reverse osmosis and ultrafiltration units will be explained. The first method does not take into account the possible effects of the polarization layer, assuming that it does not exist. In the second method, the calculations are performed considering the polarization layer, which means that it is supposed that the permeate stream does not contain solute.

10.6.1 First Design Method

This method is based on the assumption that there is no polarization layer; the basic fundamentals have been applied in some calculations described in the literature (Weber, 1979). It is considered a separation stage such as that shown in Figure 10.2, in which F, P, and S are the flows of the feed, permeate, and retained streams, respectively, with their respective concentrations C_0, C_p, and C_S. Initially, the global and component mass balances should be posed:

$$F = P + S \tag{10.51}$$

$$FC_0 = PC_p + SC_S \tag{10.52}$$

A mean concentration of the concentrated solution is defined as a weighed mean between concentrations corresponding to the feed and retained streams, in such a way that:

$$C_C = \frac{F C_0 + S C_S}{F + S} \tag{10.53}$$

Hence, the mean rejection will be:

$$R = \frac{C_C - C_P}{C_C} \tag{10.54}$$

This equation allows one to obtain the permeate stream concentration as a function of the mean concentration (C_C) and of the rejection as:

$$C_p = C_C \left(1 - R\right) \tag{10.55}$$

However, to calculate C_C, it is necessary to previously know the concentration of the retained stream (C_S), which should be obtained from the solute component balance. To do this, the concentration of the permeate should be known; this is one of the variables that should be determined. Therefore, it is necessary to use an iterative calculation process that begins by assuming that the rejection is total, or that the solute concentration in the permeate is null (C_p).

Therefore, $F\ C_0 = S\ C_S$, obtaining that the mean weighted concentration would be:

$$C_C = \frac{2 F C_0}{2F - P} = \frac{2 C_0}{2 - Q} \tag{10.56}$$

where $Q = P/F$, that is, the so-called recovery factor.

When substituting this value of C_C in Equation 10.55, it is obtained that the concentration of the permeate stream could be expressed as:

$$C_P = \frac{2 C_0}{2 - Q} \left(1 - R\right) \tag{10.57}$$

The calculation stages to be followed to solve a typical problem of separation by membrane will be stated next. The following variables are known as data: feed flow and its composition, permeate flow or recovery factor, rejection factor, pressure drop between the membrane faces, working temperature, and permeability to solvent.

Stages of the calculation procedure:

1. Calculation of the concentration of the permeate stream from Equation 10.57
2. Calculation of the flow of the retained stream from the global balance (Equation 10.51)
3. Calculation of the concentration of the retained stream, from Equation 10.52, of component global balance
4. Calculation of the weighed mean concentration of the concentrated solution, using Equation 10.53
5. Determination of the concentration of the permeate stream, using Equation 10.55
6. Stages 3, 4, and 5 are repeated using this value of the concentration of the permeate stream to obtain a new value of such concentration. If this final value coincides with the latest, then the process is finished; otherwise, steps 3, 4, and 5 are repeated in an iterative way until the values coincide.
7. Calculation of the osmotic pressure of the concentrated solution using as concentration value that of the weighed mean: $\pi = i\, C_c R\, T$
8. Determination of the solvent flux from Equation 10.30: $J_D = A\,(\Delta P - \Delta\pi)$
9. Calculation of the membrane area needed to carry out the separation. To do this, the permeate flow is divided by its flux:

$$A_m = \frac{P}{J_D} \tag{10.58}$$

10. Calculation of the power needed to overcome the pressure drop experienced by the fluid when crossing the membrane by taking the product of the volumetric flow rate of the permeate stream times the value of such pressure drop

The effects of the concentration polarization have not been taken into account in the calculation procedure. However, the polarization layer can produce negative effects, although they can be reduced to a minimum with an adequate regulation of the circulation flows within the operative units. Another factor that should be taken into account is the compressing of the membranes and their footing, which causes the networking pressure to be lower as time goes on, so the stream that crosses the membrane will decrease. All this produces an oversized plant, so at the beginning it will not be necessary to operate at the defined pressures when the membrane is compressed or soiled.

10.6.2 Second Design Method

This method has been described by Lombardi and Moresi (1987) and is based on the assumption that the solute retention by the membrane is total (B = 0). Thus, the concentration of the solution at the membrane wall is obtained from Equation 10.13, in which the solute concentration in the permeate stream is null ($C_p = 0$):

$$C_m = C_C \exp\left(\frac{J}{K_S}\right) \tag{10.34}$$

It is assumed that the known data are the operation conditions, transmembrane pressure and working temperature, feed flow and concentration, and the physical and rheological properties of the solution.

Calculation procedure stages:

1. The osmotic pressure of the solute π_c for the solute concentration on the membrane wall (C_m) is calculated. For the first iteration it will be supposed that this concentration is the concentration of the food ($C_m = C_0$).
2. The physical properties of the solution, density, and viscosity are estimated. It is convenient to point out that, for non-Newtonian fluids, the viscosity that should be used is the effective viscosity for power fluids, which is defined according to the equation:

$$\eta_e = K\left(\frac{8\,\mathrm{v}}{\mathrm{d_e}}\right)^{n-1}\left(\frac{3n+1}{4\,n}\right)$$

   In this equation, K is the consistency index and n is the flow behavior to index.
3. The diffusion coefficient is calculated (D_s).
4. The solvent flux is determined with Equation 10.30.

$$J_D = A\left(\Delta P - \Delta\pi\right)$$

5. The linear velocity of the food is calculated:

$$\mathrm{v} = \frac{F}{\rho a}$$

   in which a is the cross section and depends on the type of device. Table 10.2 shows the expressions that allow calculation of the cross section, according to the type of configuration used.

6. The flow conditions are evaluated depending on the value of the Reynolds number:

$$\mathrm{Re} = \frac{\rho v d_e}{\eta}$$

   The characteristic diameter d_e depends on the configuration used and can be calculated as indicated in Table 10.2.
7. The transfer coefficient k_s is calculated by Equation 10.15, 10.16, or 10.17, depending on the circulation regime.
8. The concentration on the membrane wall is determined using Equation 10.34: $C_m = C_c \exp(J/k_s)$.
9. The osmotic pressure of the solution is calculated with this new value of C_m.
10. The solvent flux is recalculated using Equation 10.30.
11. The obtained value is compared to the value obtained in the previous calculation stage. If the difference between these values is greater than a tolerance previously defined, a new iteration is made starting at step 8. If the difference is lower, the calculation is finished. Usually, the value of the tolerance not to be exceeded by the difference between the flux in two successive stages of the iterative process is taken as 0.05 kg/(m^2 h).
12. The global and component mass balances are carried out (Equations 10.51 and 10.52) to determine the unknown variables.
13. The membrane area needed is calculated by Equation 10.58: $A_m = P/J_D$.

10.7 Operative Layout of the Modules

The global concentrations of the permeate and retained streams can be calculated by the procedure explained in the previous section, as can the membrane area needed. However, the layout of the osmotic unit or module is not indicated, so the configuration of such units can vary. Generally, there are three arrangements for these units: single stage, simple cascades in series, and two stages with recirculation of concentrate. There can also be other types of arrangements, alternating the units in series and in parallel.

10.7.1 Single Stage

The unique stage layout is shown in Figure 10.12. The global and component balances are obtained by Equations 10.51 and 10.52: $F = P + S$ and $F\,C_0 = P\,C_p + S\,C_S$.

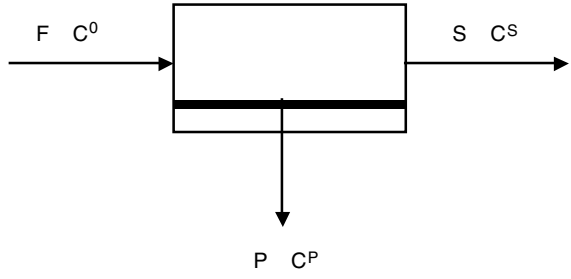

FIGURE 10.12
Single stage of membrane separation.

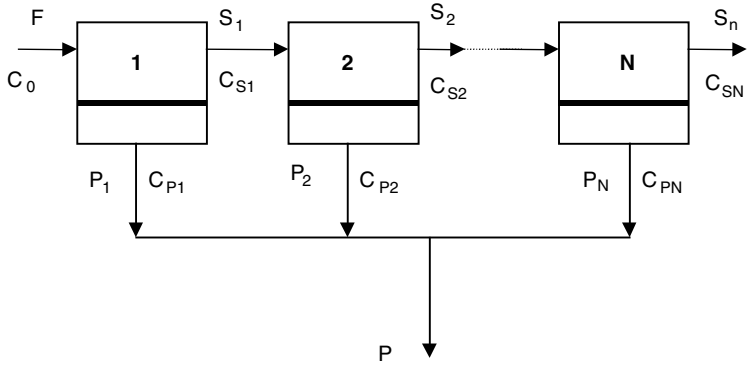

FIGURE 10.13
Single cascade layout.

10.7.2 Simple Stages in Series

In this layout, the units are placed in such a way that the retained stream of one stage is used as feed for the next stage, obtaining a permeate stream in each section that merges later into only one stream. Figure 10.13 shows a scheme of this type of layout.

The global and solute balances should be carried out in each stage according to the mathematical model. For nomenclature, the variables should have a subindex that corresponds to the stage that they leave.

Global balances:

$$F = P + S_N \tag{10.59}$$

$$FC_0 = PC_p + S_N C_{SN} \tag{10.60}$$

Balance at stage *i*:

$$S_{i-1} = P_i + S_i \tag{10.61}$$

$$S_{i-1} C_{Si-1} = P_i C_{Pi} + S_1 C_{si} \tag{10.62}$$

10.7.3 Two Stages with Recirculation

This type of layout is shown in Figure 10.14. It can be observed that, in the first stage, the retained stream is obtained as one of the products, while the permeate stream of this stage feeds the second stage. The permeate stream of the second stage is the final permeate stream, while the retained stream is recirculated and mixed with the fresh feed at the first stage. A maximum yield is achieved in this type of layout if the units work in such a way that the concentration of the retained stream of the second stage coincides with the concentration of the fresh feed ($C_{S2} = C_0$).

The mathematical model for this type of operation is obtained when performing the global and the component balances in each of the two stages.

Balance of the first stage:

$$F + S_2 = P_1 + S_1 \tag{10.63}$$

$$\left(F + S_2\right) C_0 = P_1 C_{p1} + S_1 C_{S1} \tag{10.64}$$

$$C_0 = \left(1 - Q_1\right) C_{S1} + Q_1 C_{P1} \tag{10.65}$$

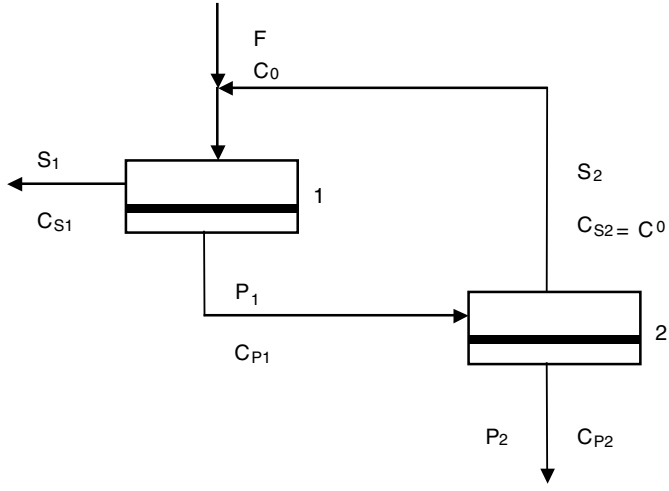

FIGURE 10.14
Two stage system with recirculation of the retained stream.

Balance of the second stage:

$$P_1 = P_2 + S_2 \tag{10.66}$$

$$P_1 C_{P1} = P_2 C_{P2} + S_2 C_0 \tag{10.67}$$

$$C_{P1} = (1 - Q_2) C_0 + Q_2 C_{P2} \tag{10.68}$$

Global recovery:

$$Q = \frac{Q_1 Q_2}{\left[1 - Q_1 (1 - Q_2)\right]} \tag{10.69}$$

Problems

10.1

A salt water stream at 20°C, containing 2.1 g/l of sodium chloride in solution, is desalted by passing it through a reverse osmosis system at a volumetric flow rate of 20,000 l/h. The recovery factor of water is 89% and the osmotic membrane has a rejection of 95% for the sodium chloride at a differential pressure of 4.13 MPa with permeability coefficient to water 2×10^{-4} kg/m^2 s atm^{-1}. Calculate: (a) permeate and retained stream flows; (b) flux and concentration of the water that leaves the osmotic installation; (c) area of the osmotic membrane; and (d) pumping power required to make the osmotic unit work.

$$\Delta P = 4.13 \times 10^6 \text{ Pa} = 40.79 \text{ atm}$$

The device used is a single stage like the one shown in Figure 10.12.

(a) The recovery factor is $Q = 0.89$ and since $Q = P/F$, it is obtained that the permeate stream is P = 17,800 l/h. Also, from the global balance (Equation 10.51) it is possible to obtain the flow of the retained stream S = 2200 l/h.

(b) By following the iterative process described in Section 10.6, iteration begins assuming that the concentration of the permeate stream is null, allowing one to obtain Equation 10.57. C_p is recalculated from this equation. C_S is calculated using the value of C_p and the problem data. The mean concentration of the retained stream C_c is calculated using Equation 10.53. Finally, the value of C_p is obtained by Equation 10.55.

Starting from Equation 10.57:

$$C_P = \frac{(2)(2100)}{2 - 0.89}(1 - 0.95) = 189.2 \text{ mg/l}$$

Iteration	C_p (mg/l)	C_S (mg/l)	C_c (mg/l)	C_p (mg/l)
1	189.2	17,560.2	3632.1	181.6
2	181.6	17,621.6	3638.2	181.9
3	181.9	17,619.2	3637.9	181.9

Hence, the concentration of the transfer stream is C_p = 181.9 mg/l.

Calculation of osmotic pressure:

$$C_c = 3637.9 \text{ mg NaCl/l} = 0.06225 \text{ moles NaCl/l}$$

$$\Delta\pi = (2)(0.06225)(0.082)(293) = 2.99 \text{ atm}$$

The solvent flux (water) is obtained from Equation 10.30:

$$J_D = 2 \times 10^{-4} \frac{\text{kg}}{\text{m}^2 \text{ s atm}} (40.79 - 2.99) \text{ atm} = 7.56 \times 10^{-3} \frac{\text{kg}}{\text{m}^2 \text{ s}}$$

$$J_D = 7.56 \times 10^{-3} \ l \text{ water}/(\text{m}^2 \cdot \text{s})$$

(c) The membrane area is obtained from Equation 10.58:

$$A_m = \frac{P}{J_D} = \frac{17{,}800 \text{ l water/h}}{7.56 \times 10^{-3} \text{ l water}(\text{m}^2 \text{ s})} \frac{1 \text{h}}{3600 \text{s}} = 654 \text{ m}^2$$

(d) Calculation of the pumping power:

$$Pot = (F)(\Delta P)$$

$$Pot = (20 \text{ m}^3/\text{h})(4.13 \times 10^6 \text{ N/m}^2)(1 \text{ h}/3600 \text{ s})(1 \text{ kW}/10^3 \text{ W}) = 23 \text{ kW}$$

10.2

A steam boiler, fed with 8000 l/h of water, is used to cover the energy needs of a food industry. The available water comes from a water stream that has a hardness of $CaCO_3$ of 8 g/l, and to avoid deposits in the boiler, its content should be lowered to 250 ppm. The depuration treatment is carried out in a reverse osmosis system, consisting of a two-stage simple cascade layout and working at a temperature of 25°C and a pressure of 204 atm. The membranes of each unit have a permeability to water of 1.29 × 10^{-6} mol

$H_2O/(cm^2\ s\ atm)$ and permeability to $CaCO_3$ of 9.8×10^{-6} cm/s. If the recovery factors of the first and second stage are 80 and 90%, respectively, calculate: (a) the water flow that should be taken from the water stream to satisfy the needs of the steam device; (b) the flow and concentration of the permeate streams obtained in each stage; and (c) the membrane area required at each stage.

The layout of both stages is as shown in Figure 10.2.

(a) The total recovery factor can be obtained from those corresponding to each stage. Thus:

$$Q_1 = P_1/F_1 = 0.80$$

$$Q_2 = P_2/S_1 = 0.90$$

$$Q = P/F = Q_1 + (1 - Q_1)Q_2 = 0.98$$

The water flow to be treated is $F = P/Q = 8163.3$ l/h.

(b) The molar concentration of the feed and final permeate streams is:

$$C_0 = 8.5\ \text{g/l} = 0.085\ \text{mol}\ CaCO_3/\text{l}$$

$$C_p = 0.25\ \text{g/l} = 2.5 \times 10^{-3}\ \text{mol}\ CaCO_3/\text{l}$$

Global and component balances for the entire system:

$$F = P + S_2$$

$$FC_0 = PC_p + S_2 C_{S2}$$

The following is obtained when substituting the data:

$$S_2 = 163.3\ \text{l/h}$$

$$C_{S2} = 4.127\ \text{mol}\ CaCO_3/\text{l}$$

Balances at the first stage: $F = P_1 + S_1$; $Q_1 = P_1/F$. Hence, when substituting the data: $P_1 = 6530.6$ l/h; $S_1 = 1632.7$ l/h.

Balances at the second stage: $S_1 = P_2 + S_2$; $Q_2 = P_2/S_1$. Thus, when substituting the data: $P_2 = 1469.4$ l/h; $S_2 = 163.3$ l/h.

The flux that crosses the membrane is the sum of the solvent flux plus the solute flux as: $J = J_D + J_S$ and also $J_S = J\ C_P$.

When combining these equations with Equations 10.30 and 10.31, it is obtained that

$$A'\left(\Delta P - iC_S RT\right) = B\left(C_S - C_P\right)\left(\frac{1-C_P}{C_P}\right) \tag{10.70}$$

When applying this equation to the second stage, and substituting all known data, a second-order equation is obtained whose unknown is C_{P2}:

$$\left(C_{P2}\right)^2 - 306\, C_{P2} + 4.127 = 0$$

One of the two roots does not have a physical meaning, while the other root allows one to know the value of the transfer stream concentration in the second stage: C_{p2} = 0.0135 mol $CaCO_3$/l.

Component balance at the second stage: $S_1\ C_{S1} = S_2\ C_{S2} + P_2\ C_{p2}$. When substituting data, the concentration of the permeate stream of the first stage is obtained: C_{S1} = 0.425 mol $CaCO_3$/l.

The following is obtained by applying Equation 10.70 to the first stage: $(C_{p1})^2 - 24{,}121\ C_{p1} + 0.425 = 0$.

One of the roots has no physical meaning, while the other root allows one to obtain the value of the permeate stream concentration of the second stage: $C_{p1} = 2 \times 10^{-5}$ mol $CaCO_3$/l.

(c) In order to calculate the membrane area of each stage, it is necessary to previously calculate the flux. If Equation 10.30 is applied to each stage, it is obtained that:

$$J_{D1} = 1.29 \times 10^{-6}\,\frac{\text{mol water}}{\text{cm}^2\,\text{s atm}}\left(204 - 2 \times 0.425 \times 0.082 \times 298\right)\text{atm}$$

$$= 2.364 \times 10^{-4}\,\frac{\text{mol water}}{\text{cm}^2\,\text{s}}$$

$$J_{D2} = 1.29 \times 10^{-6}\,\frac{\text{mol water}}{\text{cm}^2\,\text{s atm}}\left(204 - 2 \times 4.127 \times 0.082 \times 298\right)\text{atm}$$

$$= 2.95 \times 10^{-6}\,\frac{\text{mol water}}{\text{cm}^2\,\text{s}}$$

The permeate streams contain water and salts. However, since the concentration is very low, it can be considered that these streams contain only water.

Also, when calculating the area, if this consideration is taken, then slightly greater surfaces are obtained. This is positive from the design point of view.

$$P_1 = 6530.6\ l\ \text{water/h} = 100.78\ \text{mol water/s}$$

$$P_2 = 1469.4\ l\ \text{water/h} = 22.68\ \text{mol water/s}$$

Finally, the area is obtained from Equation 10.58: $A_m = P/J_D$; $A_1 = 43\ m^2$; $A_2 = 769\ m^2$.

10.3

The possibility of setting up a plant to concentrate fruit juices is being studied. To do this, it is intended to combine a first reverse osmosis stage that will concentrate juice to an intermediate content of soluble solids, and a second conventional evaporation stage that will concentrate the juice up to 70°Brix. The reverse osmosis system will consist of two stages with recirculation of concentrate. It is known that, when 18,000 kg/h of clarified peach juice of 11.5°Brix are processed, 8950 kg/h of juice whose soluble solids content is 23°Brix are obtained. The permeability of the osmotic membrane to water is 0.0117 mol/(s m^2 atm). The osmotic unit operates at 50°C, under 30 atm of pressure. The effects of the concentration polarization can be considered negligible at these working conditions. Calculate: (a) mass flow rate and concentration of the final permeate stream; (b) the value of the membrane permeability to the soluble solids transport; (c) the concentration of the recirculation stream and the permeate stream that leaves the first stage; and (d) the surface of osmotic membrane needed in each step.

Data and Notes: The calculation of the osmotic pressure assumes that the equation of van't Hoff can be applied and that the soluble solids of the juice are mainly sucrose ($C_{12}H_{22}O_{11}$).

At 50°C, the density of the clarified peach juice varies with the soluble solids content according to the expression:

$$\rho = 0.991 + 3.5 \times 10^{-3}\ C + 2.23 \times 10^{-5}\ C^2\ \text{g/cm}^3$$

for $C > 10$, where C is given in °Brix. For $C < 10$°Brix it can be considered equal to the density of water at 50°C (0.988 g/cm^3).

In the design of a two-stage system with recirculation of the retained stream, its function is optimum when the concentration of the recirculated stream coincides with the concentration of food ($C_{S2} = C_0$).

(a) From the global and component balances applied to the entire system: $F = P_2 + S_1$ and $F\ C_0 = P_2\ C_{p2} + S_1\ C_{S1}$. When substituting the data in the problem, it is obtained that $P_2 = 9050$ kg/h and $C_{p2} = 0.127$°Brix.

(b) The densities of the food streams, final permeate stream, and concentrated juice can be obtained from the expression given in the statement:

$$\rho_{0.127°\text{Brix}} = 0.988 \text{ g/cm}^3$$

$$\rho_{11.5°\text{Brix}} = 1.034 \text{ g/cm}^3$$

$$\rho_{23°\text{Brix}} = 1.084 \text{ g/cm}^3$$

The molar concentrations of the correspondent streams will be $C_0 = C_{S2}$ = 11.5°Brix = 0.3477 mol sucrose/l, C_{S1} = 23°Brix = 0.729 mol sucrose/l, and C_{p2} = 0.127°Brix = 3.7×10^{-3} mol sucrose/l.

As was seen in the previous problem, there is a relationship between the concentration of the retained and permeate streams (Equation 10.70). The following expression is obtained when it is applied to the second stage:

$$A'\left(\Delta P - iC_{S2}RT\right) = B\left(C_{S2} - C_{P2}\right)\left(\frac{1 - C_{P2}}{C_{P2}}\right)$$

The value of the permeability to solute (sucrose) can be obtained using the known values: $B = 2.6 \times 10^{-3}\ l/(s\ m^2) = 2.6 \times 10^{-6}\ m/s$.

(c) Equation 10.70 is used to calculate the concentration of the permeate stream of the first stage, allowing one to obtain a second-order equation: $(C_{p1})^2 - 49.84\ C_{p1} + 0.729 = 0$. One of the roots has no physical meaning, while the other allows one to know the value of the concentration of the transfer stream in the second stage: C_{p1} = 0.0146 mol sucrose/l = 0.506°Brix.

(d) The areas of the osmotic membranes are calculated from the quotient between the flow of the solvent permeate stream and the flux. For this reason, such values should be calculated first:

$$J_{D1} = 1.17 \times 10^{-2} \frac{\text{mol water}}{\text{cm}^2 \text{ s atm}} \left(30 - 0.729 \times 0.082 \times 323\right) \text{ atm}$$

$$= 0.125 \frac{\text{mol water}}{\text{m}^2 \text{ s}}$$

$$J_{D2} = 1.17 \times 10^{-2} \frac{\text{mol water}}{\text{cm}^2 \text{ s atm}} \left(30 - 0.3477 \times 0.082 \times 323\right) \text{ atm}$$

$$= 0.243 \frac{\text{mol water}}{\text{m}^2 \text{ s}}$$

$$J_{D1} = 0.125 \text{ mol water}/\left(\text{s.m}^2\right) = 2.252 \text{ kg}/\left(\text{s m}^2\right)$$

$$J_{D2} = 0.243 \text{ mol water}/\left(\text{s.m}^2\right) = 4.38 \times 10^{-3} \text{ kg}/\left(\text{s m}^2\right)$$

The calculation of P_1 is obtained from the mass global and component balances, applied to the second stage: $P_1 = P_2 + S_2$ and $P_1\ C_{p1} = P_2\ C_{p2} + S_2\ C_{S2}$. When substituting the problem data, it is obtained that $S_2 = 312$ kg/h and $P_2 = 9362$ kg/h.

It can be assumed that the permeate streams are constituted only by solvent (water), since their soluble solids content is very low. Also, if this assumption is considered for the area calculation, slightly higher surfaces are obtained than is positive from a design point of view. Area is obtained from Equation 10.58: $A_m = P/J_D$, $A_1 = 1149$ m^2, and $A_2 = 574$ m^2.

10.4

In a clarification process, apple juice (12°Brix) is fed into an ultrafiltration tubular module. Due to the presence of pectin in the surroundings of the tubular membrane wall, a gelled layer is formed when the concentration of the pectin reaches a value of 4.5% (w/V). Juice circulates inside the tubular membrane at a velocity of 1 m/s. The ultrafiltration tubes have a diameter of 1 cm and a length of 2 m. If the pectin content in the juice fed to the ultrafiltration module is 0.5% (w/V), calculate: (a) the flux of the clarified juice; and (b) the number of tubes needed if it is desired to obtain 100 l/h of such juice.

Data: Juice properties: density 1020 kg/m^3; viscosity 1.2 mPa·s; solute diffusivity 8×10^{-11} m^2/s.

(a) When the gel layer is formed it is assumed that there is a total rejection to pectin, so it does not appear in the permeate stream. For this reason, the calculation of the flux of the clarified juice (permeate stream) will be made using Equation 10.48. It is required in this equation to determine the value of the mass transfer constant by Equation 10.15: $(Sh) = j_H\ (\text{Re})(Sc)^{1/3}$.

Since Colburn's factor j_H depends on the Reynolds number, its value should be calculated first:

$$\text{Re} = \frac{\rho v d_e}{\eta} = \frac{\left(1020 \dfrac{\text{kg}}{\text{m}^3}\right)\left(1 \dfrac{\text{m}}{\text{s}}\right)\left(0.01 \text{ m}\right)}{\left(1.2 \times 10^{-3} \text{ Pa} \cdot \text{s}\right)} = 8500$$

For this value of the Reynolds number (Re = 8500), Colburn's factor can be taken as: $j_H = 0.023(\text{Re})^{-0.2}$. In this way, the Sherwood number will be a function of the Reynolds and Schmidt numbers according to the expression: $(Sh) = 0.023\ (\text{Re})^{0.8}(Sc)^{1/3}$.

Schmidt number:

$$(Sc) = \frac{\eta}{\rho D_S} = \frac{\left(1.2 \times 10^{-3}\ \text{Pa s}\right)}{\left(1020\ \frac{\text{kg}}{\text{m}^3}\right)\left(8 \times 10^{-11}\ \frac{\text{m}^2}{\text{s}}\right)} = 1.47 \times 10^4$$

Hence:

$$(Sh) = 0.023(8500)^{0.8}\left(1.47 \times 10^4\right)^{1/3} = 784$$

It is possible to calculate the mass transfer coefficient from the Sherwood number:

$$k_S = 784\frac{\left(8 \times 10^{-11}\ \text{m}^2/\text{s}\right)}{(0.01\ \text{m})} = 6.27 \times 10^{-6}\frac{\text{m}}{\text{s}} = 6.27 \times 10^{-6}\frac{\text{m}^3}{\text{m}^2\ \text{s}}$$

The flux of the juice will be:

$$J_D = \left(6.27 \times 10^{-6}\frac{\text{m}^3}{\text{m}^2\ \text{s}}\right)\ln\left(\frac{4.5}{0.5}\right) = 1.38 \times 10^{-5}\frac{\text{m}^3}{\text{m}^2\ \text{s}}$$

$$J_D = 1.38 \times 10^{-5}\ \text{m}^3/\left(\text{m}^2\ \text{s}\right) = 49.62\ \text{l}/\left(\text{m}^2\ \text{h}\right)$$

(b) The total area of the ultrafiltration module is obtained using Equation 10.58: $A_m = P/J_D$; $A_m = 2.015\ \text{m}^2$. This is the lateral area of the tubes of the ultrafiltration module, i.e., $A_m = n\pi d_e L$, in which n is the number of tubes. Therefore:

$$n = \frac{\left(2.015\ \text{m}^2\right)}{(0.01\ \text{m})(2\ \text{m})} = 32\ \text{ tubes}$$

It is concluded, from this result, that 32 tubes are needed.

11

Thermal Properties of Food

11.1 Thermal Conductivity

In the heat transfer by conduction processes under steady state, the flow of heat transmitted (Q) through a solid is directly proportional to the transmission area (A) and to the increase of temperature (ΔT), and is inversely proportional to the thickness of the solid (e). The proportionality constant is called thermal conductivity:

$$Q = k\frac{A\,\Delta T}{e}$$

Heat conduction under steady state has been used in different experiments to calculate the thermal conductivity of food, although experiments under unsteady state can also be used. Either way, mathematical relationships are sought that allow calculation of the thermal conductivity of a given food as a function of temperature and composition.

An equation that allows calculation of the thermal conductivity of sugar solutions, fruit juices, and milk is (Riedel, 1949):

$$k = \left(326.8 + 1.0412T - 0.00337\ T^2\right)\left(0.44 + 0.54\ X^m_{WATER}\right) 1.73\ \times 10^{-3} \quad (11.1)$$

in which k is expressed in J/(s·m·°C); T in °C, and X^m_{WATER} is the mass fraction of water. This equation is valid for a temperature range between 0 and 180°C.

Sweat (1974) gives the following equation for different fruits and vegetables:

$$k = 0.148 + 0.493\ X^m_{WATER} \quad (11.2)$$

valid for water contents higher than 60%, although it cannot be used with low-density foods or with foods that have pores (e.g., apples).

In the case of milk, Fernández–Martín (1982) gives a second order polynomial expression with respect to temperature.

$$k = A + BT + CT^2 \tag{11.3}$$

in which the parameters A, B, and C are a function of the fat and nonfat content of milk.

An equation that allows one to obtain the thermal conductivity of cream (Gromov, 1974) is:

$$k = \frac{\left[411.6 - 4.26\ (f - 10)\right] \times 10^{-6}}{1 - 0.0041\ (T - 30)} \rho \tag{11.4}$$

in which thermal conductivity is expressed in kcal/(h·m·°C), and f is the fat content between 10 and 60%; ρ is the density of the sample at the corresponding temperature and composition expressed in kg/m^3; while T is the temperature in °C in the 30 to 70°C range.

Also, Fernández–Martín and Montes (1977) gave an expression for cream:

$$k = \left[12.63 + 0.051\ T - 0.000175\ T^2\right]\left[1 - \left(0.843 + 0.0019\ T\right) X_G^V\right] \cdot 10^{-4} \tag{11.5}$$

where the thermal conductivity is expressed in cal/(s·cm·°C) and temperature in °C in the 0 to 80°C range. Also, f is the fat percentage between 0.1 and 40%, while X_G^V is the volumetric fraction of the fat phase for values lower than 0.52.

If the food composition is known, it is possible to find its thermal conductivity from the equation:

$$k = \sum_i \left(k_i X_i^V\right) \tag{11.6}$$

in which k_i is the thermal conductivity of the component i, and X_i^V is the volumetric fraction of this component.

The volumetric fraction of the component i is given by the expression:

$$X_i^V = \frac{X_i^m / \rho_i}{\sum_i \left(X_i^m / \rho_i\right)} \tag{11.7}$$

in which X_i^m is the mass fraction of the component i and ρ_i is its density.

Table 11.1 presents the thermal conductivity values of some foods. Table 11.2 shows the thermal conductivity of the main pure components of foods, while the conductivity of water and ice as a function of temperature is given in Table 11.3.

TABLE 11.1

Thermal Conductivity of Some Foods

Product	Water Content (%)	Temperature (°C)	Thermal Conductivity (J/s·m·°C)
Oil			
Olive		15	0.189
	—	100	0.163
Soybean	13.2	7–10	0.069
Vegetable and animal	—	4–187	0.169
Sugars	—	29–62	0.087–0.22
Cod	83	2.8	0.544
Meats			
Pork			
Perpendicular to the fibers	75.1	6	0.488
		60	0.54
Parallel to the fibers	75.9	4	0.443
		61	0.489
Fatty meat	—	25	0.152
Lamb			
Perpendicular to the fibers	71.8	5	0.45
		61	0.478
Parallel to the fibers	71.0	5	0.415
		61	0.422
Veal			
Perpendicular to the fibers	75	6	0.476
		62	0.489
Parallel to the fibers	75	5	0.441
		60	0.452
Beef			
Freeze-dried			
1000 mm Hg	—	0	0.065
0.001 mm Hg	—	0	0.035
Lean			
Perpendicular to the fibers	78.9	7	0.476
	78.9	62	0.485
Parallel to the fibers	78.7	8	0.431
	78.7	61	0.447
Fatty	—	24–38	0.19
Strawberries	—	–14–25	0.675
Peas	—	3–17	0.312

11.2 Specific Heat

The specific heat is defined as the energy needed to increase by 1°C the temperature of one unit mass. For foods with a high water content above the freezing point, the following equation can be used (Siebel, 1982):

$$\hat{C}_P = 0.837 + 3.349\ X^m_{WATER} \tag{11.8}$$

TABLE 11.2

Equations for Calculating Thermal Properties

Thermal Property	Component	Equation as a Function of Temperature
k (W/m·°C)	Carbohydrate	$k = 0.20141 + 1.3874 \times 10^{-3}\ T - 4.3312 \times 10^{-6}\ T^2$
	Ash	$k = 0.32962 + 1.4011 \times 10^{-3}\ T - 2.9069 \times 10^{-6}\ T^2$
	Fiber	$k = 0.18331 + 1.2497 \times 10^{-3}\ T - 3.1683 \times 10^{-6}\ T^2$
	Fat	$k = 0.18071 + 2.7604 \times 10^{-3}\ T - 1.7749 \times 10^{-7}\ T^2$
	Protein	$k = 0.17881 + 1.1958 \times 10^{-3}\ T - 2.7178 \times 10^{-6}\ T^2$
$\alpha \cdot 10^6$ (m²/s)	Carbohydrate	$\alpha = 8.0842 \times 10^{-2} + 5.3052 \times 10^{-4}\ T - 2.3218 \times 10^{-6}\ T^2$
	Ash	$\alpha = 1.2461 \times 10^{-1} + 3.7321 \times 10^{-4}\ T - 1.2244 \times 10^{-6}\ T^2$
	Fiber	$\alpha = 7.3976 \times 10^{-2} + 5.1902 \times 10^{-4}\ T - 2.2202 \times 10^{-6}\ T^2$
	Fat	$\alpha = 9.8777 \times 10^{-2} + 1.2569 \times 10^{-4}\ T - 3.8286 \times 10^{-8}\ T^2$
	Protein	$\alpha = 6.8714 \times 10^{-2} + 4.7578 \times 10^{-4}\ T - 1.4646 \times 10^{-6}\ T^2$
ρ (kg/m³)	Carbohydrate	$\rho = 1.5991 \times 10^{3} - 0.31046\ T$
	Ash	$\rho = 2.4238 \times 10^{3} - 0.28063\ T$
	Fiber	$\rho = 1.3115 \times 10^{3} - 0.36589\ T$
	Fat	$\rho = 9.2559 \times 10^{2} - 0.41757\ T$
	Protein	$\rho = 1.3299 \times 10^{3} - 0.51840\ T$
$\hat{C}_P$ (kJ/kg·°C)	Carbohydrate	$\hat{C}_P = 1.5488 + 1.9625 \times 10^{-3}\ T - 5.9399 \times 10^{-6}\ T^2$
	Ash	$\hat{C}_P = 1.0926 + 1.8896 \times 10^{-3}\ T - 3.6817 \times 10^{-6}\ T^2$
	Fiber	$\hat{C}_P = 1.8459 + 1.8306 \times 10^{-3}\ T - 4.6509 \times 10^{-6}\ T^2$
	Fat	$\hat{C}_P = 1.9842 + 1.4733 \times 10^{-3}\ T - 4.8008 \times 10^{-6}\ T^2$
	Protein	$\hat{C}_P = 2.0082 + 1.2089 \times 10^{-3}\ T - 1.3129 \times 10^{-6}\ T^2$

Source: Choi and Okos (1986b).

TABLE 11.3

Equations to Calculate Thermal Properties of Water and Ice

	Temperature Functions[a]	
Water	$k_A = 0.57109 + 1.7625 \times 10^{-3}\ T - 6.7036 \times 10^{-6}\ T^2$	(W/m·°C)
	$\alpha_A = [0.13168 + 6.2477 \times 10^{-4}\ T - 2.4022 \times 10^{-6}\ T^2].10^{-6}$	(m²/s)
	$\rho_A = 997.18 + 3.1439 \times 10^{-3}\ T - 3.7574 \times 10^{-3}\ T^2$	(kg/m³)
	$\hat{C}_{PA1} = 4.0817 - 5.3062 \times 10^{-3}\ T + 9.9516 \times 10^{-4}\ T^2$	(kJ/kg·°C)
	$\hat{C}_{PA2} = 4.1762 - 9.0864 \times 10^{-5}\ T + 5.4731 \times 10^{-6}\ T^2$	(kJ/kg·°C)
Ice	$k_H = 2.2196 - 6.2489 \times 10^{-3}\ T + 1.0154 \times 10^{-4}\ T^2$	(W/m·°C)
	$\alpha_H = [1.1756 - 6.0833 \times 10^{-3}\ T + 9.5037 \times 10^{-5}\ T^2] \times 10^{-6}$	(m²/s)
	$\rho_H = 916.89 - 0.13071\ T$	(kg/m³)
	$\hat{C}_{PH} = 2.0623 + 6.0769 \times 10^{-3}\ T$	(kJ/kg·°C)

[a] $\hat{C}_{PA1}$ = For a temperature range between −40 and 0°C.
$\hat{C}_{PA2}$ = For a temperature range between 0 and 150°C.

Source: Choi and Okos (1986b).

in which $\hat{C}_P$ is expressed in kJ/(kg·°C) and X^m_{WATER} is the mass fraction of the water in food.

An equation given by Charm (1971) is:

$$\hat{C}_P = 2.309\ X^m_{GF} + 1.256\ X^m_s + 4.187\ X^m_{WATER} \tag{11.9}$$

in which X^m_{GF} and X^m_s are the mass fractions of fat and solids, respectively.

For milk at temperatures higher than the final point of fusion of milk fat, the following expression can be used (Fernández–Martín, 1972a):

$$\hat{C}_P = X^m_{WATER} + \left(0.238 + 0.0027\ T\right) X^m_{TS} \tag{11.10}$$

in which the specific heat is expressed in kcal/(kg·°C), temperature T in °C in a range from 40 to 80°C, and X^m_{WATER} and X^m_{TS} are the mass fractions of water and total solids, respectively.

Gromov (1979) gives the next equation for cream:

$$\hat{C}_P = 4.187\, X^m_{WATER} + \left(16.8\ T - 3.242\right)\left(1 - X^m_{WATER}\right) \tag{11.11}$$

expressing the specific heat in J/(kg.K), temperature T in Kelvin, for the 272 to 353 K range, and the fat content between 9 and 40%.

Manohar et al. (1991) gave the following equation for tamarind juices:

$$\hat{C}_p = 4.18 + \left(6.839 \times 10^{-5}\, T - 0.0503\right) C \tag{11.12}$$

in which the specific heat is expressed in kJ/(kg K) if the temperature is given in Kelvin, and C is the soluble solids content expressed in °Brix.

Choi and Okos (1986b) proposed an equation for the case in which the composition of the product is known:

$$\hat{C}_P = \sum_i \left(\hat{C}_{Pi}\, X^m_i\right) \tag{11.13}$$

where $\hat{C}_{Pi}$ is the specific heat of the component i, while X^m_i is the mass fraction of the component i.

The specific heat values of different foods are listed in Table 11.4. Table 11.2 also presents expressions for the calculation of the specific heat of pure components as a function of temperature, while in Table 11.3, equations that allow calculation of the specific heat of water and ice as a function of temperature are given.

11.3 Density

Density is defined as the relation between the mass of a given sample and its volume. Different expressions for the calculation of food density can be found in the literature. Thus, for fruit juices, density can be expressed as a function of the refraction index according to the expression (Riedel, 1949):

TABLE 11.4

Specific Heat for Some Foods

Product	Water (%)	Specific heat (kJ/kg.K)
Meats		
Bacon	49.9	2.01
Beef		
Lean beef	71.7	3.433
Roast beef	60.0	3.056
Hamburger	68.3	3.520
Veal	68.0	3.223
Prawns	66.2	3.014
Eggs		
Yolk	49.0	2.810
Milk		
Pasteurized, whole	87.0	3.852
Skim	90.5	3.977–4.019
Butter	15.5	2.051–2.135
Apples (raw)	84.4	3.726–4.019
Cucumbers	96.1	4.103
Potatoes	79.8	3.517
	75.0	3.517
Fish	80.0	3.600
Fresh	76.0	3.600
Cheese (fresh)	65.0	3.265
Sardines	57.4	3.014
Carrots (fresh)	88.2	3.810–3.935

Source: Reidy, G.A., M.S. thesis, Michigan State University, 1968.

$$\rho = \frac{s^2 - 1}{s + 2} \frac{64.2}{0.206} 16.0185 \tag{11.14}$$

where ρ is the density expressed in kg/m^3 and s is the refraction index.

Some equations express density as a function of temperature and soluble solids content. For clarified apple juices, Constenla et al. (1989) presented the following:

$$\rho = 0.82780 + 0.34708 \exp\left(0.01\ X\right) - 5.479 \times 10^{-4}\ T \tag{11.15}$$

in which density is expressed in g/cm^3, X is the concentration in °Brix, and T is the absolute temperature. This expression can be applied in the 20 to 80°C temperature range and in the 12 to 68.5°Brix range. These same authors expresed the density of these juices as a function of °Brix and density of water:

$$\rho = \frac{\rho_{WATER}}{0.992417 - 3.7391 \times 10^{-3}\ X} \tag{11.16}$$

However, Aguado and Ibarz (1988) gave different expressions for clarified apple juices in the 5 to 70°C temperature range and in the 10 to 71°Brix concentration range. One of these expressions is:

$$\rho = 0.98998 - 5.050 \times 10^{-4}\, T + 5.1709 \times 10^{-3}\, C + 0.0308 \times 10^{-5}\, C^2 \qquad (11.17)$$

where density is expressed in g/cm^3, C in °Brix, and T in °C.

Ibarz and Miguelsanz (1989) reported a similar equation for clarified pear juice in the 5 to 70°C temperature range and in the 10 to 71°Brix concentration range:

$$\rho = 1.0113 - 5.4764 \times 10^{-4}\, T + 3.713 \times 10^{-3}\, C + 1.744 \times 10^{-5}\, C^2 \qquad (11.18)$$

Alvarado and Romero (1989) presented the following expression for different juices, for temperatures from 20 to 40°C and for concentrations from 5 to 30°Brix:

$$\rho = 1002 + 4.61\, C - 0.460\, T + 7.001 \times 10^{-3}\, T^2 + 9.175 \times 10^{-5}\, T^3 \qquad (11.19)$$

in which density is expressed in kg/m^3, C in °Brix, and T in °C.

For sucrose solutions with concentrations between 6 and 65°Brix and a temperature of 20°C, Kimball (1986) reported the equation:

$$\rho = 0.524484 \exp\left[\frac{\left(C + 330.872\right)^2}{170,435}\right] \qquad (11.20)$$

in which density is expressed in g/cm^3 and C in °Brix.

Manohar et al. (1991) presented a second order polynomial equation as a function of the total soluble solids content for tamarind juices:

$$\rho = 1000 + 4.092\, C + 0.03136\, C^2 \qquad (11.21)$$

in which density is obtained in kg/m^3 and the concentration C is expressed in °Brix.

Rambke and Konrad (1970) reported a second order polynomial equation for milk as a function of the dry mass percentage:

$$\rho = a + b\, X_o + c\, X_o^2 \qquad (11.22)$$

where ρ is expressed in g/cm^3 and X_o is the dry mass percentage. The coefficients of this equation for different temperatures are given in Table 11.6.

For temperatures higher than the boiling point, the equation of Berstsch et al. (1982) can be used:

$$\rho = 1040.51 - 0.2655\,T - 0.01\,T^2 - \left(0.967 + 0.969 \times 10^{-2}\,T - 0.478 \times 10^{-4}\,T^2\right) f \tag{11.23}$$

where ρ is expressed in kg/m^3; T is temperature in °C for the range from 65 to 140°C; and f is the fat content for values between 0.02 and 15.5%.

Andrianov et al. (1968) reported the following equation for cream in the 40 to 80°C range and fat content between 30 and 83%:

$$\rho = 1.0435 - 1.17 \times 10^{-5}\,X_G - \left(0.52 \times 10^{-3} + 1.6 \times 10^{-8}\,X_G\right) T \tag{11.24}$$

in which density is expressed in g/cm^3, temperature is in °C, and the fat content X_G is the mass fraction.

Choi and Okos (1986b) suggested an expression as a function of the density of the components of the product:

$$\rho = \frac{1}{\sum_i \left(X_i^m / \rho_i \right)} \tag{11.25}$$

in which X_i^m is the mass fraction of the component i and ρ_i its density.

Tables 11.2 and 11.3 show the expressions that allow calculation of the densities of the pure components as a function of temperature.

11.4 Thermal Diffusivity

A widely used property in calculations of heat transfer by conduction is the thermal diffusivity, defined according to the expression:

$$\alpha = \frac{k}{\rho\,\hat{C}_p} \tag{11.26}$$

The value of the thermal diffusivity of a given food can be calculated if the thermal conductivity, density, and specific heat are known. However, some mathematical expressions allow calculation of the thermal diffusivity according to water content. Thus, Martens (1980) reported the following equation:

$$\alpha = 5.7363 \times 10^{-8}\, X^{m}_{WATER} + 2.8 \times 10^{-10}\, T \tag{11.27}$$

where α is the thermal diffusivity in m^2/s, X^{m}_{WATER} is the water mass fraction, and T is the temperature in Kelvin.

On the other hand, Dickerson (1969) presented an expression in which the food's thermal diffusivity is a function only of the water content and its thermal diffusivity:

$$\alpha = 8.8 \times 10^{-8} \left(1 - X^{m}_{WATER}\right) + \alpha_{WATER}\, X^{m}_{WATER} \tag{11.28}$$

Choi and Okos (1986b) expressed thermal diffusivity as a function of the components, similar to other thermal properties:

$$\alpha = \sum_i \left(\alpha_i\, X^{V}_i\right) \tag{11.29}$$

where α_i is the thermal diffusivity of the component i and X^{V}_i is the volumetric fraction of such component.

Table 11.5 presents thermal diffusivity values for some foods. Tables 11.2 and 11.3 show the expressions that allow calculation of the thermal diffusivities of pure components:

TABLE 11.5

Thermal Diffusivity for Some Foods

Product	Water (%)	Temperature[a] (°C)	Thermal Diffusivity $\times 10^5$ (m^2/s)
Fruits, Vegetables			
Avocado (pulp)	—	24 (0)	1.24
Seed	—	24 (0)	1.29
Whole	—	41 (0)	1.54
Sweet potato	—	35	1.06
	—	55	1.39
	—	70	1.91
Cherries (pulp)	—	30 (0)	1.32
Squash	—	47 (0)	1.71
Strawberries (pulp)	92	5	1.27
Beans (purée)	—	26–122	1.80
Peas (purée)	—	26–128	1.82
String beans (cooked)	—	4–122	1.68
Limes	—	40 (0)	1.07
Apples	85	0–30	1.37
Applesauce	37	5	1.05
	37	65	1.12
	80	5	1.22
	80	65	1.40
	—	26–129	1.67

TABLE 11.5 (continued)

Thermal Diffusivity for Some Foods

Product	Water (%)	Temperature[a] (°C)	Thermal Diffusivity $\times 10^5$ (m^2/s)
Peach	—	27 (4)	1.39
Turnip	—	48 (0)	1.34
Potato			
Pulp	—	25	1.70
Mashed (cooked)	78	5	1.23
Banana (pulp)	76	5	1.18
	76	65	1.42
Grapefruit			
(pulp)	88.8	—	1.27
(albedo)	72.2	—	1.09
Beet	—	14 (60)	1.26
Tomato (pulp)	—	4.26	1.48
Fishes and Meats			
Cod	81	5	1.22
	81	65	1.42
Hipogloso	76	40–65	1.47
Salted meat	65	5	1.32
	65	65	1.18
Ham (smoked)	64	5	1.18
	64	40–65	1.38
Beef			
Loin[b]	66	40–65	1.23
Round	71	40–65	1.33
Tongue	68	40–65	1.32
Water	—	30	1.48
	—	65	1.60
Ice	—	0	11.82

[a] The first temperature is the initial one, and that in parentheses is the one of the surroundings.

[b] Data are applicable if the juices exuded during storage remain in foods.

Source: Singh, R.P., *Food Technol.*, 36(2): 87–91.

TABLE 11.6

Values of the Parameters of Equation 11.22

T	Skim Milk			Whole Milk ($c = 0$)	
(°C)	a	$b \times 10^3$	$c \times 10^5$	a	$b \times 10^3$
5	1.0000	3.616	1.827	1.0010	2.55
20	0.9982	3.519	1.782	1.0080	2.09
35	0.9941	3.504	1.664	1.0137	1.66
50	0.9881	3.568	1.366	0.9953	2.11
60	0.9806	3.601	1.308		

Problems

11.1

Determine the density, thermal conductivity, specific heat, and thermal diffusivity, at 25°C, of a food product that has been chemically analyzed, and whose weight composition is: 77% water, 19% carbohydrate, 3% protein, 0.2% fat, and 0.8% ash.

The method of Choi and Okos is used; therefore, the thermal properties of each component at 25°C are previously calculated. The following table contains the results obtained.

Component	ρ_i (kg/m³)	k_i (W/m·°C)	$\hat{C}_{Pi}$ (kJ/kg·°C)	$\alpha_i \times 10^7$ (m²/s)
Water	994.91	0.6110	4.1773	1.458
Carbohydrate	1591.34	0.2334	1.5942	0.927
Protein	1316.94	0.2070	2.0376	0.797
Fat	915.15	0.2496	2.0180	1.019
Ash	2416.78	0.3628	1.1375	1.332

The volumetric fraction of each component is calculated by means of Equation 11.7. The mass and volumetric fractions of each component are presented next.

Component	X_i^m	X_i^v
Water	0.77	0.8398
Carbohydrate	0.19	0.1296
Protein	0.03	0.0247
Fat	0.002	0.0024
Ash	0.008	0.0036

Thermal conductivity: obtained from Equation 11.6:

$$\mathbf{k} = \sum \left(k_i X_i^v\right) = 0.55 \ \mathrm{W/(m \cdot °C)} = 5.5 \times 10^{-4} \ \mathrm{kJ/(s.m.°C)}$$

Density: obtained from Equation 11.25:

$$\rho = \frac{1}{\sum_i \left(X_i^m / \rho_i \right)} = 1085 \ \mathrm{kg/m^3}$$

Specific heat: obtained from Equation 11.13:

$$\hat{C}_P = \sum_i \left(\hat{C}_{Pi} X_i^m\right) = 3.594 \ \mathrm{kJ/(kg \cdot °C)}$$

Thermal diffusivity: obtained from Equation 11.29:

$$\alpha = \sum_i \left(\alpha_i \; X_i^V\right) = 1.37 \times 10^{-7} \; \mathrm{m^2/s}$$

It can also be calculated by Equation 11.26:

$$\alpha = \frac{k}{\rho \; \hat{C}_P} = 1.41 \times 10^{-7} \; \mathrm{m^2/s}$$

Result:

ρ = 1085 kg/m^3
k = 0.50 W/(m·°C)
$\hat{C}_P$ = 3.94 kJ/(kg·°C)
α = 1.7×10^{-7} m^2/s

12

Heat Transfer by Conduction

12.1 Fundamental Equations in Heat Conduction

In order to study heat conduction in a solid, an energy balance in a volume of the material, assuming that the convection and radiation mechanisms are negligible, is carried out. This balance gives rise to an equation used to calculate temperature profiles in the solid, as well as to obtain the heat flux that crosses it. The transfer of heat per unit time due to conduction is related to the distribution of temperatures by Fourier's law.

The fundamental equation is obtained by carrying out an energy balance in a reference volume of the solid, according to the expression:

$$\begin{pmatrix}\text{Thermal energy}\\ \text{by conduction}\\ \text{input flow rate}\end{pmatrix} + \begin{pmatrix}\text{Thermal energy}\\ \text{generation}\\ \text{flow rate}\end{pmatrix} =$$

$$\begin{pmatrix}\text{Thermal energy}\\ \text{by conduction}\\ \text{output flow rate}\end{pmatrix} + \begin{pmatrix}\text{Thermal energy}\\ \text{accumulation}\\ \text{flow rate}\end{pmatrix} =$$

The resulting expression of the equation depends on the geometry considered, and it is advantageous to derive different expressions according to the type of coordinates with which one is working.

12.1.1 Rectangular Coordinates

A volume of the solid is taken to perform the energy balance, as shown in Figure 12.1. It is supposed that temperature variation is only along the x

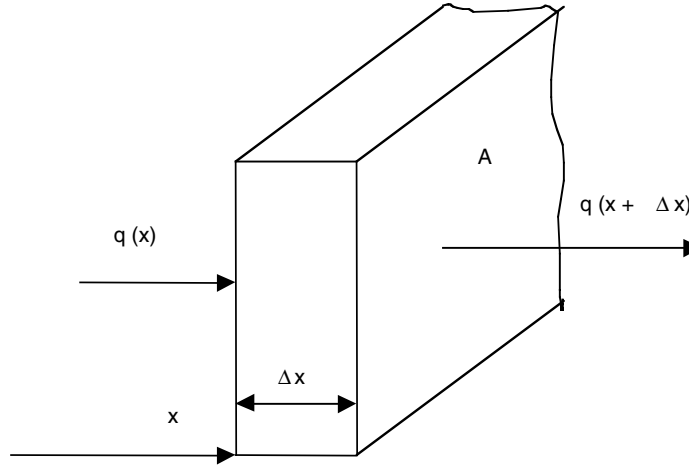

FIGURE 12.1
Volume of a solid in rectangular coordinates.

direction; this means that the solid's temperature is only a function of coordinate x and of time. Also, it is considered that the characteristics of the material are constant in such a way that the thermal conductivity, k, the density, ρ, and the specific heat, $\hat{C}_P$, of the solid are constant.

With these assumptions, the energy balance applied to the volume of material in Figure 12.1 yields the following equation:

$$\rho \hat{C}_P \frac{\partial T}{\partial t} = k \frac{\partial^2 T}{\partial^2 x} + \tilde{q}_G$$

in which:

t = time
T = temperature
$\tilde{q}_G$ = energy generation flow rate per unit volume

There are various terms in this general equation of heat transfer by conduction: the input and output of heat in volume of solid considered, generation, and accumulation.

The input and output terms are governed by Fourier's equation. The generation term does not appear in all cases, but does appear in cases in which chemical or nuclear reactions that generate heat occur in the considered volume, or when there are electric currents applied to such volume that, when passing through resistances, generate heat. When there is a variation in the temperature of the system, a variation in the internal energy will occur, so accumulation terms will appear in the fundamental equation of heat transfer by conduction. In the case where the temperature of the solid remains constant, there will not be an accumulation of energy, yielding to steady state conditions.

The heat balance is applied to a volume of solid like the one presented in Figure 12.1. The different terms of the energy balance are developed next.

- Input term: The heat flow that enters in the solid volume considered, according to the Fourier's equation, is:

$$\dot{Q}_e = q(x)A = -k\,A\frac{\partial\,T(x)}{\partial\,x}$$

  in which A is the cross-sectional area through which the heat flows, $q(x)$ is the heat flow density, and $\dot{Q}_e$ is the heat flow that penetrates the solid through the area A in coordinate position x.
- Output term: Similar to the input term, the output term is:

$$\dot{Q}_S = q(x+\Delta x)A = -k\,A\frac{\partial T(x+\Delta x)}{\partial x}$$

  where $\dot{Q}_S$ is the heat flow that exits off the solid through the A in position $(x + \Delta x)$.
- Generation term: If the energy flow generated per unit of volume of solid is defined, $\tilde{q}_G$, the generation flow would be:

$$\dot{Q}_G = \tilde{q}_G A\Delta x$$

- Accumulation term: The volume of solid at the temperature T has an energy content given by:

$$E = \rho\,A\,\Delta x\,\hat{C}_P\,T$$

  If the solid is considered isotropic, then ρ and $\hat{C}_P$ are constant, so the accumulation flow in direction x is:

$$\dot{Q}_A = \frac{\partial E}{\partial t} = \rho A\,\Delta x\,\hat{C}_P\frac{\partial T}{\partial t}$$

  Therefore, the energy balance applied to the considered volume yields to the expression:

$$-k\,A\frac{\partial T(x)}{\partial x} + \tilde{q}_G\,A\,\Delta x = -k\,A\frac{\partial T(x+\Delta x)}{\partial x} + \rho\,A\,\Delta x\,\hat{C}_P\frac{\partial T}{\partial t}$$

If all the terms of this expression are divided by the volume on which the balance (A, Δx) is applied, then rearranging this equation obtains that:

$$\rho \hat{C}_P \frac{\partial T}{\partial t} = k \frac{\dfrac{\partial T(x+\Delta x)}{\partial t} - \dfrac{\partial T(x)}{\partial t}}{\Delta x} + \tilde{q}_G$$

If the limit $\Delta x \to 0$ is taken, the following equation is obtained:

$$\rho \hat{C}_P \frac{\partial T}{\partial t} = k \frac{\partial^2 T}{\partial x^2} + \tilde{q}_G$$

This is the fundamental equation of heat transfer by conduction following direction x.

This equation can be generalized to include the three directions x, y, and z; thus, the general equation of heat conduction is obtained:

$$\rho \hat{C}_P \frac{\partial T}{\partial t} = k \frac{\partial^2 T}{\partial^2 x} + \frac{\partial^2 T}{\partial^2 y} + \frac{\partial^2 T}{\partial^2 z} + \tilde{q}_G$$

If it is taken into account that the Laplacian operator ∇^2 is defined by:

$$\nabla^2 = \frac{\partial^2}{\partial^2 x} + \frac{\partial^2}{\partial^2 y} + \frac{\partial^2}{\partial^2 z}$$

then the last equation can be expressed as:

$$\rho \hat{C}_P \frac{\partial T}{\partial t} = k \nabla^2 T + \tilde{q}_G \tag{12.1}$$

12.1.2 Cylindrical Coordinates

The general equation of heat conduction for cylindrical coordinates is analogous to the one obtained for rectangular coordinates, with the exception that the Laplacian operator is expressed in a different way. The general equation of heat conduction for cylindrical coordinates would be:

$$\rho \hat{C}_P \frac{\partial T}{\partial t} = k \left[\frac{1}{r} \frac{\partial}{\partial r} \left(r \frac{\partial T}{\partial r} \right) + \frac{1}{r^2} \frac{\partial^2 T}{\partial \phi^2} \right] + \frac{\partial^2 T}{\partial z^2} + \tilde{q}_G \tag{12.2}$$

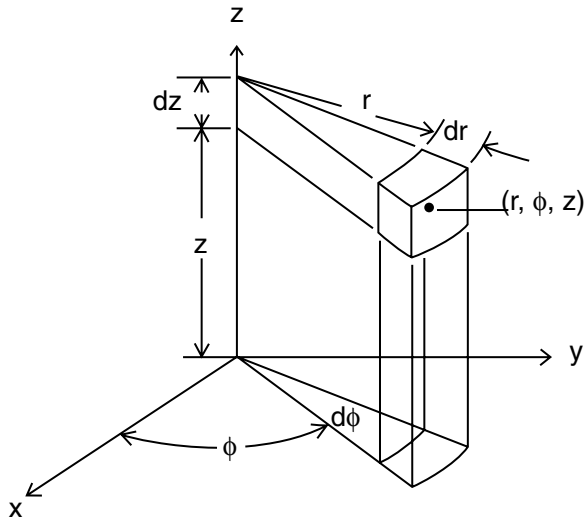

FIGURE 12.2
Cylindrical coordinates system.

in which r, ϕ, and z are the radial, angular, and axial coordinates, respectively, as can be seen in Figure 12.2.

12.1.3 Spherical Coordinates

Similar to the case of cylindrical coordinates, the general expression for heat conduction is obtained by expressing the Laplacian operator in spherical coordinates. If temperature is a function of the three coordinates and of time, the resulting expression is:

$$\rho\hat{C}_P \frac{\partial T}{\partial t} = \tag{12.3}$$

$$= k\left[\frac{1}{r^2}\frac{\partial}{\partial r}\left(r^2\frac{\partial T}{\partial r}\right) + \frac{1}{r^2\,\text{sen}\,\theta}\frac{\partial}{\partial\theta}\left(\text{sen}\,\theta\frac{\partial T}{\partial\theta}\right) + \frac{1}{r^2\,\text{sen}^2\,\theta}\frac{\partial^2 T}{\partial\phi^2}\right] + \tilde{q}_G$$

The meaning of each of the spherical coordinates can be seen in Figure 12.3.

12.2 Heat Conduction under Steady Regime

In a case where no generation of energy in the system is considered, the term $\tilde{q}_G$ of the heat transfer equations disappears. Additionally, if heat conduction

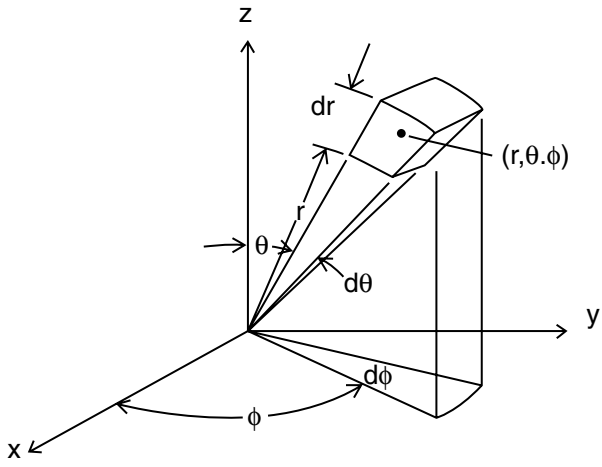

FIGURE 12.3
Spherical coordinates system.

occurs under steady state, the accumulation term, which depends on time, is null, so the general heat conduction equation is transformed into:

$$\nabla^2 T = 0 \tag{12.4}$$

where ∇^2 is the Laplacian operator that, as seen before, has different expressions according to the types of coordinates used.

This equation is called the Laplace equation and is widely used in different engineering areas since it appears in many problems related to the solution of mathematical models set up for different processes.

12.2.1 Monodimensional Heat Conduction

Heat conduction in only one direction will be studied in this section. This means it will be considered that temperature is a function of only one direction or coordinate. In the case of rectangular coordinates, it is considered that the temperature varies along coordinate x, while for spherical and cylindrical coordinates, this temperature variation is assumed along the radial coordinate.

The temperature profile will be obtained along the desired direction in each case by integration of the Laplace equation, obtaining the integration constants by applying boundary conditions to the integrated equation. Once the temperature profile is obtained, the Fourier equation is applied to determine the heat transfer flow.

Among the different cases that can occur, those of heat transmission through flat, cylindrical, and spherical layers will be studied since these are the geometric shapes that appear most frequently.

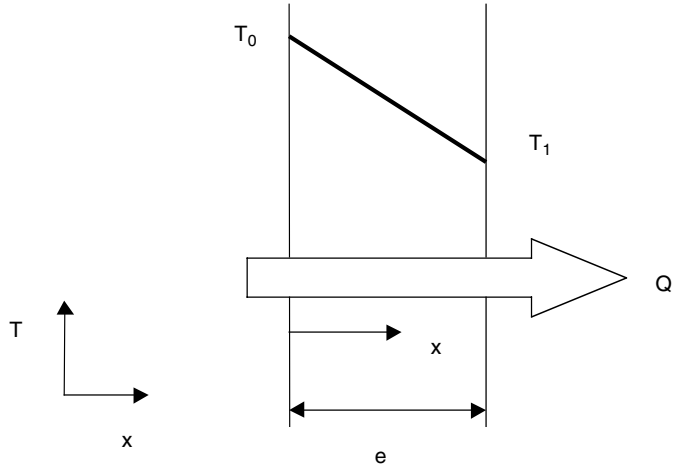

FIGURE 12.4
Temperature profile in a flat wall.

12.2.1.1 Flat Wall

The most common way to decrease heat losses through a wall is to place an insulation layer; therefore, it is important to know the width such a layer should have. In this case, an infinite slab will be assumed, thus avoiding consideration of the end effects. Although this assumption is made, the results obtained can be applied to the case of finite slabs in a reliable way.

If a slab with infinite surface is assumed, with one face at temperature T_0 and the other at T_1, with $T_0 > T_1$, the heat flow goes from T_0 to T_1 (Figure 12.4).

The equation of Laplace for rectangular coordinates in one direction would be:

$$\frac{\partial^2 T}{\partial x^2} = 0$$

Temperature is only a function of position x, so the partial derivatives can be substituted by total derivatives. The following is obtained when integrating this equation:

$$T = C_1 x + C_2$$

where C_1 and C_2 are integration constants whose values are obtained when applying the following boundary conditions:

$$\text{For } x = 0 \qquad T = T_0$$
$$\text{For } x = e \qquad T = T_1$$

so:

$$T = T_0 + \frac{T_1 - T_0}{e} x \tag{12.5}$$

Thus, temperature varies linearly with position. The temperature profile becomes flatter as the thermal conductivity of the solid becomes greater.

To calculate the heat flow that crosses such a slab, the heat flux is multiplied by the area of the slab:

$$\dot{Q} = q A = -k A \frac{dT}{dx}$$

The temperature profile dT/dx can be known, so:

$$\dot{Q} = k A \frac{T_0 - T_1}{e} \tag{12.6}$$

In many cases it is better to express it as:

$$\dot{Q} = \frac{T_0 - T_1}{\left(\frac{e}{k A}\right)} \tag{12.7}$$

This equation is analogous to Ohm's Law, in which $(T_0 - T_1)$ represents the difference of the thermal potential and (e/kA) is the resistance to heat flow.

It is assumed that the medium is isotropic, so the thermal conductivity remains constant. When the thermal conductivity varies linearly with temperature, the same type of equation can be used, but a value of conductivity that is the arithmetical mean between the values corresponding to the temperatures T_0 and T_1 must be used.

Usually, coatings are placed on walls to avoid heat losses through them. Generally, such coatings do not consist of only one material but, rather, several coatings can be used, as shown in Figure 12.5.

For the ith resistance, the temperature between layer i and $i - 1$ will be T_{i-1}, and between layer i and $i + 1$ it will be T_i.

In the same way as for one layer, it can be demonstrated that for the ith layer, the temperature profile is defined by the equation:

$$T\left(x_i\right) = T_{i-1} + \frac{T_i - T_{i-1}}{e_i} x_i \tag{12.8}$$

in which e_i is the thickness of layer i and x_i is the positional coordinate of layer i.

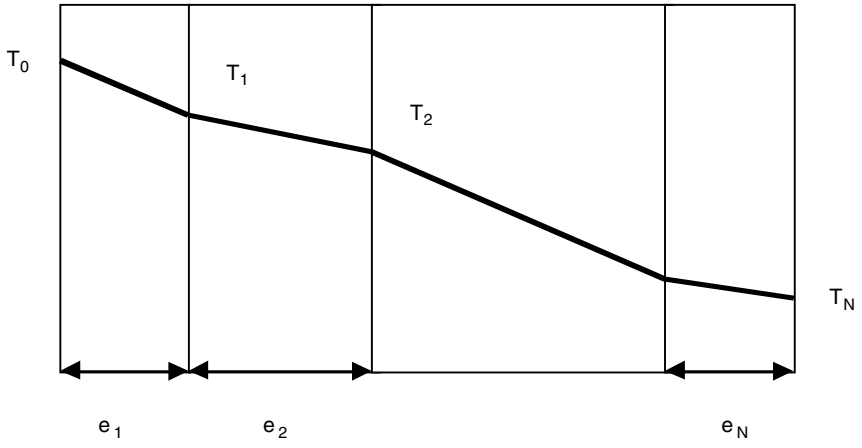

FIGURE 12.5
Set of flat layers in series.

Since there is no energy accumulation, the heat flow that crosses each layer is the same, hence:

$$\dot{Q} = q_i A = \frac{T_0 - T_1}{\left(e_1 / k_1 A\right)} = \frac{T_1 - T_2}{\left(e_2 / k_2 A\right)} = \cdots\cdots = \frac{T_{N-1} - T_N}{\left(e_N / k_N A\right)}$$

Rearranging this equation according to the properties of the ratios:

$$\dot{Q} = \frac{T_0 - T_N}{\sum_{i=1}^{N} \left(e_i / k_i A\right)} \tag{12.9}$$

12.2.1.2 Cylindrical Layer

The most common problem in which a cylindrical body intervenes is in pipes that transport fluids at temperatures higher or lower than room temperature, so they are coated with insulators to avoid heat transfer to the outside. A hollow cylinder of radius r_0 covered with an insulator of thickness e is proposed to study this problem, as shown in Figure 12.6. The temperature of the fluid that circulates inside is T_0, while the temperature of the external medium is T_1.

The fundamental equation of heat conduction (Equation 12.2), if there is no energy generation and under a steady state for the case of heat transmission along the radial coordinate r, becomes:

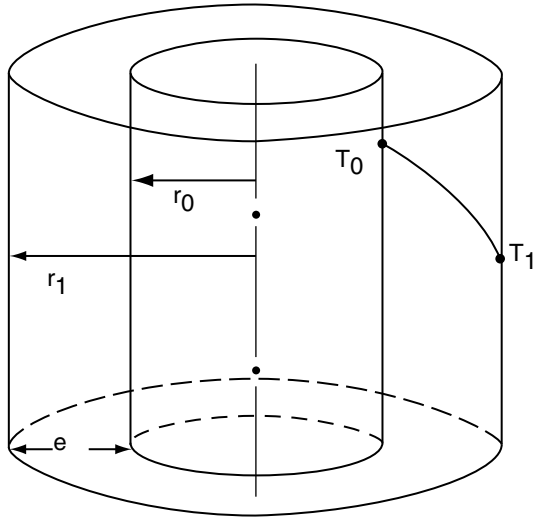

FIGURE 12.6
Temperature profile in a cylindrical layer.

$$\frac{1}{r}\frac{\partial}{\partial r}\left(r\frac{T}{\partial r}\right)=0$$

or:

$$r\frac{T}{\partial r}=C_1$$

where C_1 is a constant.

This equation can be expressed in total derivatives if temperature is a function only of the radial coordinate. The following equation is obtained after integration:

$$T=C_1\ln r+C_2$$

where C_1 and C_2 are integration constants whose values are obtained by applying the following boundary conditions:

$$\text{For } r=r_0 \quad T=T_0$$
$$\text{For } r=r_1 \quad T=T_1$$

Hence:

$$T(r) = T_0 - \left(T_0 - T_1\right)\frac{\ln\left(\dfrac{r}{r_0}\right)}{\ln\left(\dfrac{r_1}{r_0}\right)} \tag{12.10}$$

Heat flux is obtained from Fourier's equation. If the cylinder has a length L, the cross-sectional area of the heat flow will be $A = 2\pi rL$, so such flux would be:

$$\dot{Q} = q\,A = -k\,A\frac{dT}{dr} = -k\,2\,\pi\,r\,L\frac{dT}{dr}$$

In this equation, dT/dr is obtained by differentiating Equation 12.10, yielding:

$$\dot{Q} = k\,2\,\pi\,r\,L\frac{T_0 - T_1}{\ln\left(r_1 \big/ r_0\right)} \tag{12.11}$$

If the numerator and the denominator of the second member are multiplied by the thickness $e = r_1 - r_0$, this equation becomes:

$$\dot{Q} = \frac{T_0 - T_1}{\left(e \big/ k\,A_{ml}\right)} \tag{12.12}$$

in which A_{ml} is the mean logarithmic area between the external and internal cylindrical surfaces:

$$A_{ml} = \frac{A_1 - A_0}{\ln\left(A_1 \big/ A_0\right)}$$

being: $A_0 = 2\pi r_0 L$ and $A_1 = 2\pi r_1 L$.

If instead of only one coating there were N layers, the temperature profile of each layer i would be:

$$T\left(r_i\right) = T_{i-1} - \left(T_{i-1} - T_i\right)\frac{\ln\left(r \big/ r_{i-1}\right)}{\ln\left(r_i \big/ r_{i-1}\right)} \tag{12.13}$$

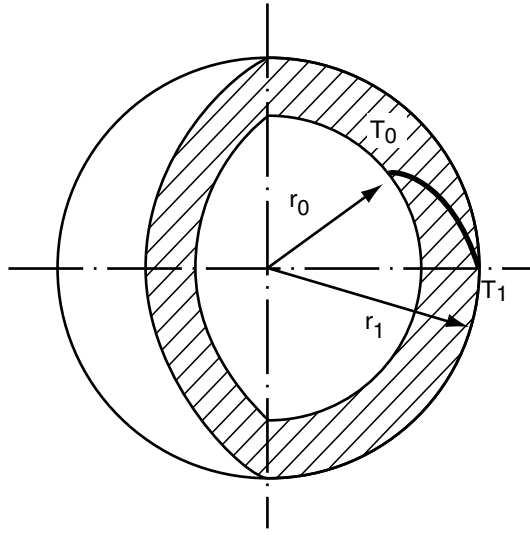

FIGURE 12.7
Thermal profile in a spherical layer.

The heat flow that crosses these layers is expressed as:

$$\dot{Q} = \frac{T_0 - T_N}{\sum_{i=1}^{N} \left(e_i \Big/ k_i \left(A_{ml} \right)_i \right)} \tag{12.14}$$

It can be observed that the equations obtained for heat flux are analogous to those obtained for the case of flat layers, with the difference that, for cylindrical geometry, the area is the logarithmic average instead of the arithmetic one.

12.2.1.3 Spherical Layer

Consider a hollow sphere covered with one layer of a certain material with thickness $e = r_1 - r_0$, as the one shown in Figure 12.7. If temperature is a function only of the radial coordinate and if, also, there is no heat generation and the work is done under steady state, the heat conduction fundamental equation for spherical coordinates (Equation 12.3) becomes:

$$\frac{1}{r^2} \frac{\partial}{\partial r} \left(r^2 \frac{\partial T}{\partial r} \right) = 0$$

The following equation is obtained from the former:

$$r^2 \frac{\partial T}{\partial r} = C_1$$

where C_1 is the integration constant.

Since temperature depends only on the radial coordinate, this equation can be expressed as a total derivative that, integrated, becomes:

$$T = C_2 - \frac{C_1}{r}$$

The integration constants of this equation are obtained by applying the following boundary conditions:

$$\text{For } r = r_0 \quad T = T_0$$
$$\text{For } r = r_1 \quad T = T_1$$

Yielding a temperature profile according to the expression:

$$T(r) = T_0 + (T_1 - T_0)\frac{r_1}{r_1 - r_0}\left(1 - \frac{r_0}{r}\right) \tag{12.15}$$

the heat flow will be:

$$\dot{Q} = \frac{T_0 - T_1}{\left(e/k\, A_{mg}\right)} \tag{12.16}$$

in which e is the layer's thickness and A_{mg} is the mean geometric area of the internal and external spherical areas. This equation was obtained similarly to the previous cases, substituting the expression of the temperature profile in Fourier's equation.

If, instead of considering one layer surrounding the sphere, N layers are considered, the temperature profile in one of the intermediate layers i, will be:

$$T(r_i) = T_{i-1} + (T_i - T_{i-1})\frac{r_i}{r_i - r_{i-1}}\left(1 - \frac{r_{i-1}}{r}\right) \tag{12.17}$$

The expression that allows calculation of the heat flux is:

$$\dot{Q} = \frac{T_0 - T_N}{\sum_{i=1}^{N} \left(e_i/k_i\, A_{mgi}\right)} \tag{12.18}$$

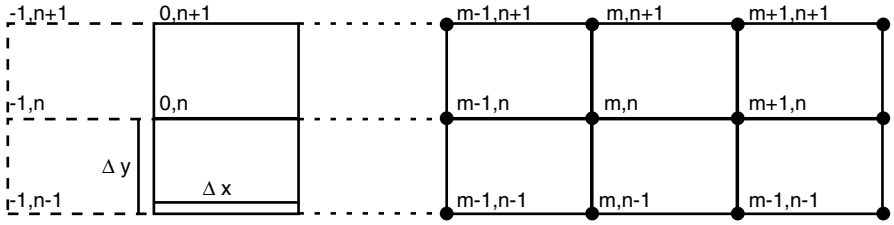

FIGURE 12.8
Division into plots and notation for the numerical solution of bidimensional heat conduction.

This equation is analogous to those obtained for other types of geometry studied, except that the area in the spherical geometry is the mean geometric area of the external and internal surfaces of the spherical layers.

12.2.2 Bidimensional Heat Conduction

Heat conduction in only one direction was studied in previous sections. However, there are cases in which the problem cannot be reduced to monodimensional conduction. If heat conduction occurs in two directions and there is neither heat accumulation nor generation, the following equation is obtained for rectangular coordinates:

$$\frac{\partial^2 T}{\partial x^2} + \frac{\partial^2 T}{\partial y^2} = 0 \tag{12.19}$$

It can be observed that temperature depends on coordinates x and y.

This equation can be solved in different ways, although it is convenient to express it as finite differentials. Once expressed this way, analytical and numerical methods are applied to solve the equation. In addition to these methods, there are graphical and analogic methods that allow solution of Laplace's equation (Equation 12.4) in two directions.

In order to express Equation 12.19 in finite differentials, the solid in which an energy balance will be carried out is divided according to an increment of x and another of y (Figure 12.8), the two directions in which temperature varies.

The nodes resulting from the division are indicated according to direction x by subindex m and in direction y by subindex n.

The temperature around any node can be expressed as a function of the node. Taylor series expansion up to the third term including it yields:

$$T_{m+1,n} = T_{m,n} + \left(\frac{\partial T}{\partial x}\right)_{m,n} \Delta x + \frac{1}{2}\left(\frac{\partial^2 T}{\partial x^2}\right)_{m,n} (\Delta x)^2$$

$$T_{m-1,n} = T_{m,n} - \left(\frac{\partial T}{\partial x}\right)_{m,n} \Delta x + \frac{1}{2}\left(\frac{\partial^2 T}{\partial x^2}\right)_{m,n} (\Delta x)^2$$

$$T_{m,n+1} = T_{m,n} + \left(\frac{\partial T}{\partial y}\right)_{m,n} \Delta y + \frac{1}{2}\left(\frac{\partial^2 T}{\partial y^2}\right)_{m,n} (\Delta y)^2$$

$$T_{m,n-1} = T_{m,n} - \left(\frac{\partial T}{\partial y}\right)_{m,n} \Delta y + \frac{1}{2}\left(\frac{\partial^2 T}{\partial y^2}\right)_{m,n} (\Delta y)^2$$

The first and second derivatives of temperature at point (m, n) according to directions x and y can be obtained from this set of equations:

$$\left(\frac{\partial T}{\partial x}\right)_{m,n} = \frac{T_{m+1,n} - T_{m-1,n}}{2\,\Delta x}$$

$$\left(\frac{\partial T}{\partial y}\right)_{m,n} = \frac{T_{m,n+1} - T_{m,n-1}}{2\,\Delta y}$$

$$\left(\frac{\partial^2 T}{\partial x^2}\right)_{m,n} = \frac{T_{m+1,n} - 2\,T_{m,n} + T_{m-1,n}}{(\Delta x)^2}$$

$$\left(\frac{\partial^2 T}{\partial y^2}\right)_{m,n} = \frac{T_{m,n+1} - 2\,T_{m,n} + T_{m,n-1}}{(\Delta y)^2}$$

If these expressions are substituted in Equation 12.19 it is obtained that:

$$\frac{T_{m+1,n} - 2\,T_{m,n} + T_{m-1,n}}{(\Delta x)^2} + \frac{T_{m,n+1} - 2\,T_{m,n} + T_{m,n-1}}{(\Delta y)^2} = 0$$

In the case that the division is carried out in such a way that the increments in the directions x and y are equal, $\Delta x = \Delta y$, this equation can be expressed as:

$$T_{m,n} = \frac{1}{4}\left(T_{m+1,n} + T_{m-1,n} + T_{m,n+1} + T_{m,n-1}\right) \tag{12.20}$$

This equation indicates that temperature in one node is the arithmetic mean of the nodes around it.

The surrounding conditions can be expressed as an algebraic equation; thus, if temperature at the wall of the solid is T_0, it can be expressed as:

$$T_{0,n} = T_0 \quad \text{for } n = 0, 1, 2, \ldots, N$$

Also, since a maximum or minimum condition exists on the wall:

$$\left(\frac{\partial T}{\partial x}\right)_{0,n} = 0 \qquad n = 0, 1, 2, \ldots, N$$

which, expressed as finite differences, becomes:

$$T_{-1,n} = T_{1,n} \qquad n = 0, 1, 2, \ldots, N$$

This equation indicates that there are points outside the system that have the same temperature as those symmetric with respect to the wall belonging to the system.

Once this series of equations is stated, the problem should be solved; different methods can be used to do that. Next, two numerical methods to solve the equations are explained: Liebman's method and the relaxation method.

12.2.2.1 Liebman's method

As obtained previously (Equation 12.20), the temperature at one node is the arithmetic mean of the temperatures around it. Liebman's method distinguishes two types of alternating points (Figure 12.9), those marked with a circle and those marked with a cross. In order to find the temperature of the

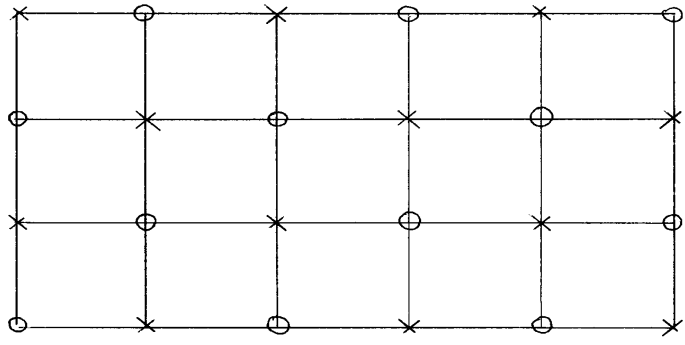

FIGURE 12.9
Division of solids by Liebman's method.

points, first the temperatures of alternated points are given a value, for example, those marked with a circle. The temperatures corresponding to the points marked with a cross can be calculated from the assumed temperatures using Equation 12.20. This process is repeated until the temperatures of two consecutive calculations coincide. At this point, the temperatures of each node are the temperatures sought and the temperature profile is obtained.

12.2.2.2 Relaxation method

In this method, the temperatures of all the nodes in the mesh are assumed. It is very difficult to guess correctly and comply with Equation 12.20 on the first attempt; however, it is possible to obtain a residual such as the following:

$$R = T_{m+1,n} + T_{m-1,n} + T_{m,n+1} + T_{m,n-1} - 4T_{m,n}$$

Once the values of the temperatures are supposed, the value of the residual of each node will be obtained and should tend to be zero, indicating that the supposed temperatures are the desired ones. Since this is difficult to do, temperatures should be successively corrected, according to the expression:

$$\left(T_{m,n}\right)^{*} = T_{m,n} + \frac{R_{m,n}}{4}$$

The residuals of each point are calculated again using the corrected temperatures and the process is repeated until the residuals are negligible. In this case, the temperatures at each point are the temperatures sought.

Once the temperatures of all the points are calculated using one of these methods, the temperature profile is known. It is possible to calculate the heat flux that crosses a given area from such a profile using the following expression:

$$\dot{Q} = \int_{S} k \nabla T \, dS \tag{12.21}$$

in which dS is the cross-sectional area. Calculation of heat flux can be difficult, so graphical methods are used.

In short, the general problem in bidimensional heat conduction is the calculation of the distribution of temperatures and, once they are known, the calculation of the heat flux. Two numerical methods have been shown to calculate the heat distribution or temperature profile, but other methods, such as graphical, analog, and matrix, are explained elsewhere.

12.2.3 Tridimensional Heat Conduction

When heat conduction in a solid is such that three directions should be considered, the same techniques developed for bidimensional conduction

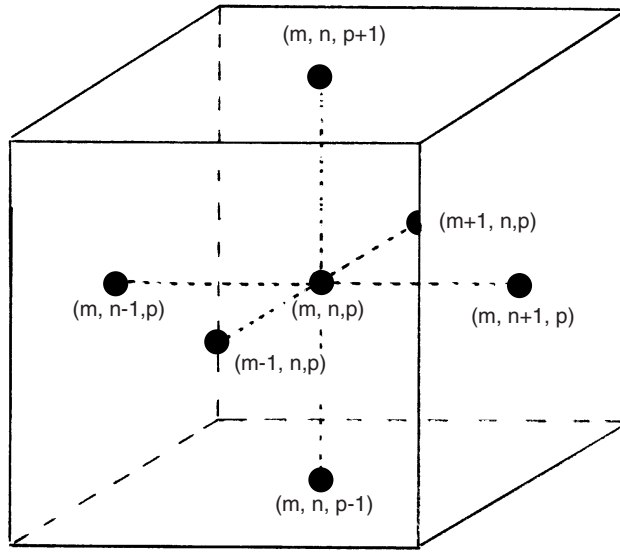

FIGURE 12.10
Division into plots for tridimensional heat conduction.

can be applied. Consider a parallelepiped (Figure 12.10) through which heat is transmitted under steady state, with all the conditions surrounding it known. When a heat balance expressed as finite differences is applied, the temperature of the point with coordinates (m, n, p) when the increments of the three space coordinates are equal ($\Delta x = \Delta y = \Delta z$) is:

$$T_{m,n,p} = \\ = \frac{1}{6}\left(T_{m+1,n,p} + T_{m-1,n,p} + T_{m,n+1,p} + T_{m,n-1,p} + T_{m,n,p+1} + T_{m,n,p-1}\right) \tag{12.22}$$

This equation indicates that the temperature of a node for tridimensional problems without heat generation and under steady state is the arithmetic mean of the temperature of the surrounding nodes. The procedure is analogous to the case of bidimensional heat conduction.

12.3 Heat Conduction under Unsteady State

In all the cases studied in Section 12.2, it was assumed that the temperature of any point of the solid remains constant with time. However, there are cases in which temperature inside the solid, besides changing with position, also changes with time. Such is the case of freezing and thawing, in which it is desirable to know the time needed to reach a certain temperature at a determined point of the solid, or to know the temperature of such a point after some time. It should be taken into account that the process is developed under unsteady state regime.

The following is obtained from the heat conduction fundamental equation in the case of rectangular coordinates (Equation 12.1):

$$\rho \hat{C}_P \frac{\partial T}{\partial t} = k \nabla^2 T + \tilde{q}_G$$

Taking into account that thermal diffusivity α is defined by:

$$\alpha = \frac{k}{\rho \hat{C}_P}$$

Equation 12.1 is transformed into:

$$\frac{\partial T}{\partial t} = \alpha \nabla^2 T + \tilde{q}_G \tag{12.23}$$

This equation is valid for any type of coordinates, but the Laplacian ∇^2 operator should be expressed in the adequate form in each case.

The mathematical treatments in the following sections will be done in rectangular coordinates, but it should be noted that, for other types of coordinates, the mathematical treatment is similar. In all cases presented next, it will be assumed that there is no heat generation.

12.3.1 Monodimensional Heat Conduction

If a semi-infinite solid, as shown in Figure 12.11, in which the thickness in direction x is infinite, is considered, it can be supposed that the heat flow crossing such a solid does so exclusively in the x direction. If there is no heat generation inside the solid, Equation 12.23 can be expressed as:

$$\frac{\partial T}{\partial t} = \alpha \frac{\partial^2 T}{\partial x^2} \tag{12.24}$$

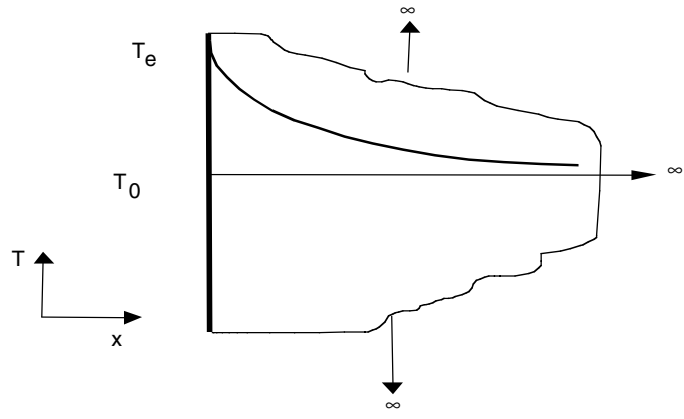

FIGURE 12.11
Semi-infinite solid.

This equation is difficult to solve, but different methods such as analytical, numerical, or graphical can be applied. Some of these methods will be explained next.

12.3.1.1 Analytical Methods

The analytical solution of Equation 12.24 is obtained when the boundary conditions that allow integration of such an equation are specified. This integration is possible only in some cases, such as semi-infinite solids. If, at the beginning, the solid has a temperature T_0 and at a given time the wall reaches a temperature T_e, it is considered that the temperature of a point far away from the wall continues to be T_0 at any instant. Therefore, the conditions to integrate Equation 12.24 are:

Initial condition:	For $\forall\ x$	$t = 0$	$T = T_0$
Boundary condition:	For $\forall\ t$	$x \to \infty$	$T = T_0$
	For $\forall\ t$	$x = 0$	$T = T_e$

The boundary conditions assume that the wall is always at a constant temperature T_e, thus it is an isothermal condition.

The solution of Equation 12.24 is obtained under these boundary conditions, and it can be demonstrated that the equation describing the temperature distribution in the slab is:

$$\frac{T_e - T}{T_e - T_0} = erf\left(\frac{x}{2\sqrt{\alpha t}}\right) \tag{12.25}$$

In this equation, *erf* is the error function of Gauss, defined by:

$$erf(\eta) = \frac{2}{\sqrt{\pi}} \int_0^{\eta} \exp\left(-\eta^2\right) d\eta \tag{12.26}$$

where:

$$\eta = \frac{x}{2\sqrt{\alpha t}}$$

Gauss's error function can be tabulated for the different values of position x. Such values are presented in Table 12.1.

TABLE 12.1

Gauss's Error Function

$$erf(\eta) = \frac{2}{\sqrt{\pi}} \int_0^{\eta} \exp\left(-\eta^2\right) d\eta$$

$$\eta = \frac{x}{2\sqrt{\alpha t}}$$

η	erf (η)	η	erf (η)
0.00	0.00000	1.00	0.84270
0.04	0.45110	1.10	0.88020
0.08	0.09008	1.20	0.91031
0.12	0.13476	1.30	0.93401
0.16	0.17901	1.40	0.95228
0.20	0.22270	1.50	0.96610
0.24	0.25670	1.60	0.97635
0.28	0.30788	1.70	0.98379
0.32	0.34913	1.80	0.98909
0.36	0.38933	1.90	0.99279
0.40	0.42839	2.00	0.99532
0.44	0.46622	2.10	0.99702
0.48	0.50275	2.20	0.99814
0.52	0.53790	2.30	0.99886
0.56	0.57162	2.40	0.99931
0.60	0.60386	2.50	0.99959
0.64	0.63459	2.60	0.99976
0.68	0.66278	2.70	0.99987
0.72	0.69143	2.80	0.99993
0.76	0.71754	2.90	0.99996
0.80	0.74210	3.00	0.99998
0.84	0.76514	3.20	0.999994
0.88	0.78669	3.40	0.999998
0.92	0.80677	3.60	1.00000
0.96	0.82542		

Another case in which it is possible to find an analytical solution to Equation 12.24 is when the semi-infinite solid has a simple geometry, for example, for infinite slabs with finite thickness or for cylinders with infinite height. It is also possible to find analytical solutions for spherical solids.

The case of heat transmission through an infinite slab with thickness $2X_o$ will be studied next. Initially, the slab is at a temperature T_0 and immersed in a fluid at a temperature T_e. In this case, the surrounding condition is convection, since there is heat transfer from the fluid to the solid's wall by a convection mechanism, while within the solid the heat is transferred by conduction. In this way, it can be written that:

$$h\left(T_e - T_w\right) = -k\left(\frac{\partial T}{\partial x}\right)_w \tag{12.27}$$

in which T_w is the temperature of the slab wall in contact with the fluid at a given time and h is the individual convective heat transfer coefficient between the fluid and the solid.

The boundary conditions to obtain an analytical solution are:

Initial condition:	For $\forall\ x$	$t = 0$	$T = T_0$
Boundary condition:	For $t \to \infty$	$x = x_0$	$T = T_e$
	For $\forall\ t$	$x = 0$	$\frac{\partial T}{\partial x} = 0$

This last boundary condition is because an optimum, maximum, or minimum condition should exist in the center of the slab ($x = 0$), depending on whether the solid becomes cooler or hotter.

The analytical solution of the problem becomes easier if the variables are expressed in a dimensionless way. Hence, the following adimensional temperature, time, and position variables are defined:

$$Y = \frac{T_e - T}{T_e - T_0} \tag{12.28a}$$

$$\tau = \left(Fo\right) = \frac{\alpha t}{\left(x_0\right)^2} \tag{12.28b}$$

$$n = \frac{x}{x_0} \tag{12.28c}$$

It should be noted that the adimensional time variable is an expression of the Fourier number.

The substitution of the adimensional variables in Equation 12.24 yields:

$$\frac{\partial T}{\partial t} = \frac{\partial^2 Y}{\partial n^2} \tag{12.29}$$

on the boundary conditions:

$$\begin{array}{llll} \text{For} & \forall\, n & t = 0 & Y = 1 \\ \text{For} & n = 1 & t \to \infty & Y = 0 \\ \text{For} & n = 0 & \forall \tau & \dfrac{\partial Y}{\partial n} = 0 \end{array}$$

Equation 12.29 can be solved by separation of variables, obtaining the solution:

$$Y = 4\sum_{i=1}^{\infty} \frac{\text{sen}\, A_i}{2\, A_i + \text{sen}\left(2\, A_i\right)} \cos\left(A_i\, n\right) \exp\left(-\, A_i\, \tau\right) \tag{12.30}$$

In this expression, A_i are the infinite solutions of the equation:

$$A_i\, \text{tg}\left(A_i\right) = \frac{1}{m} \tag{12.31}$$

where $\frac{1}{m}$ is Biot's number, defined according to:

$$\left(Bi\right) = \frac{1}{m} = \frac{h x_0}{k} \tag{12.32}$$

These solutions are valid for values of Biot's number between 0.1 and 40, where there is a combined conduction–convection mechanism for heat transmission.

This analytical solution was obtained for an infinite slab with thickness $2x_0$. Analogous solutions can be obtained for a cylinder of radius x_0 and infinite height, as well as for a sphere of radius x_0, although the solution of Equation 12.29 is more complex.

Analytical solutions are usually represented as graphs (Figures 12.12, 12.13 and 12.14), making the solution to different problems easier to calculate. It should be noted that these figures are the graphical solution of a dimensionless equation expressed as partial derivatives (Equation 12.29) under specific boundary conditions. For this reason, these graphs can be used for all problems expressed in these types of differential equations and boundary conditions.

Besides these solutions, a numerical method allows one to evaluate the temperature in the center of the solid. As noted previously, it is difficult to

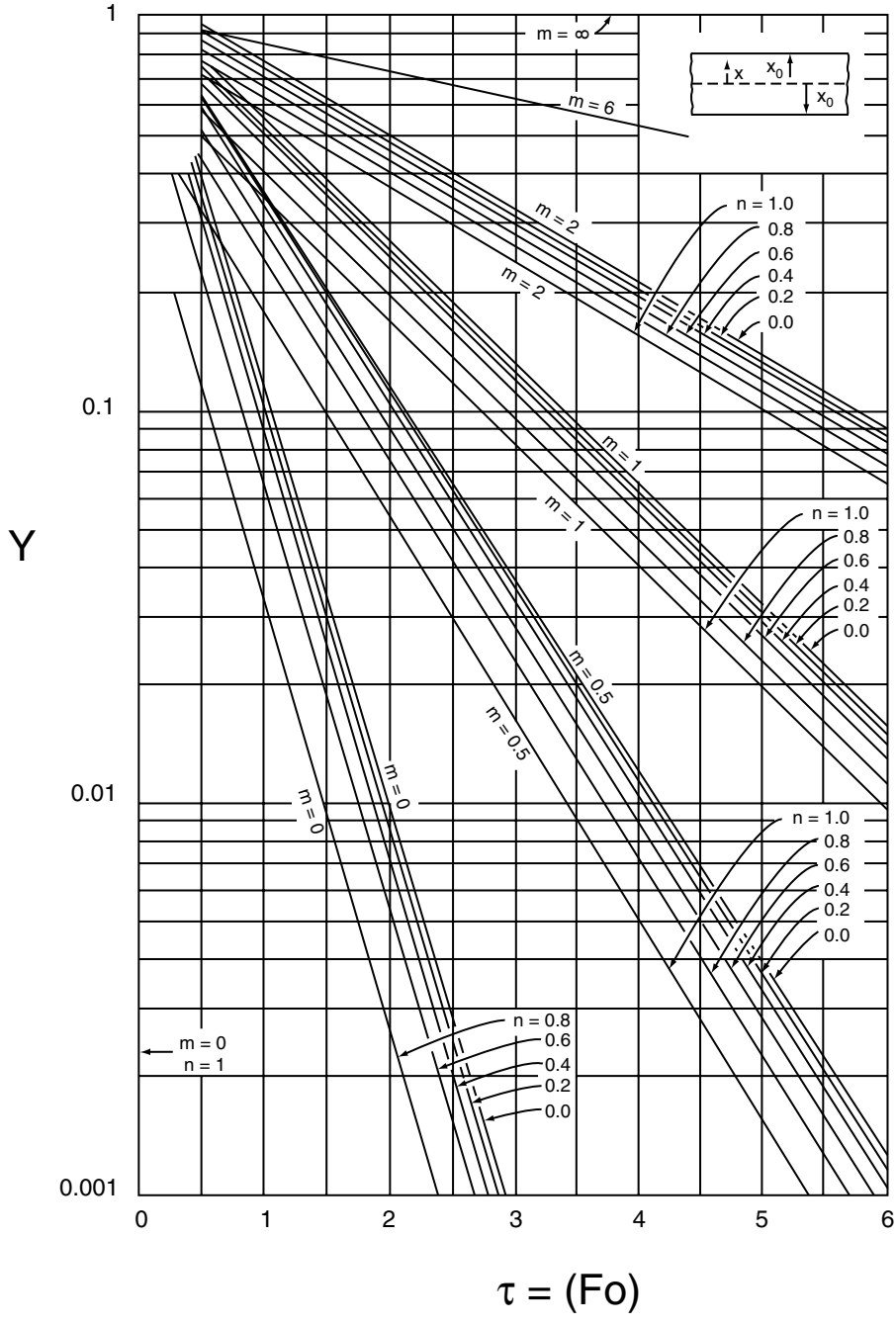

FIGURE 12.12
Dimensionless temperature as a function of time and position for an infinite slab.

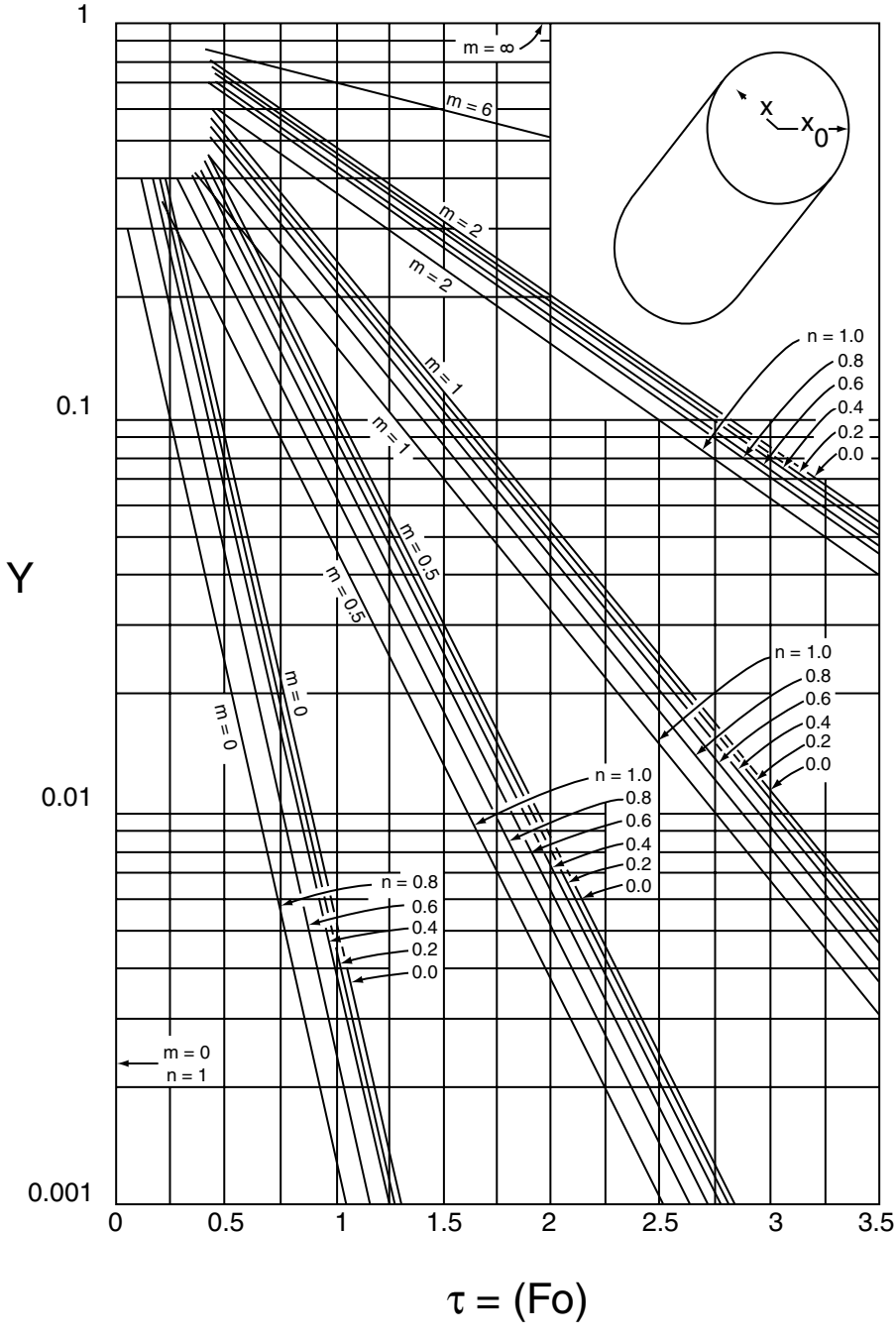

FIGURE 12.13
Dimensionless temperature as a function of time and position for a cylinder with infinite height.

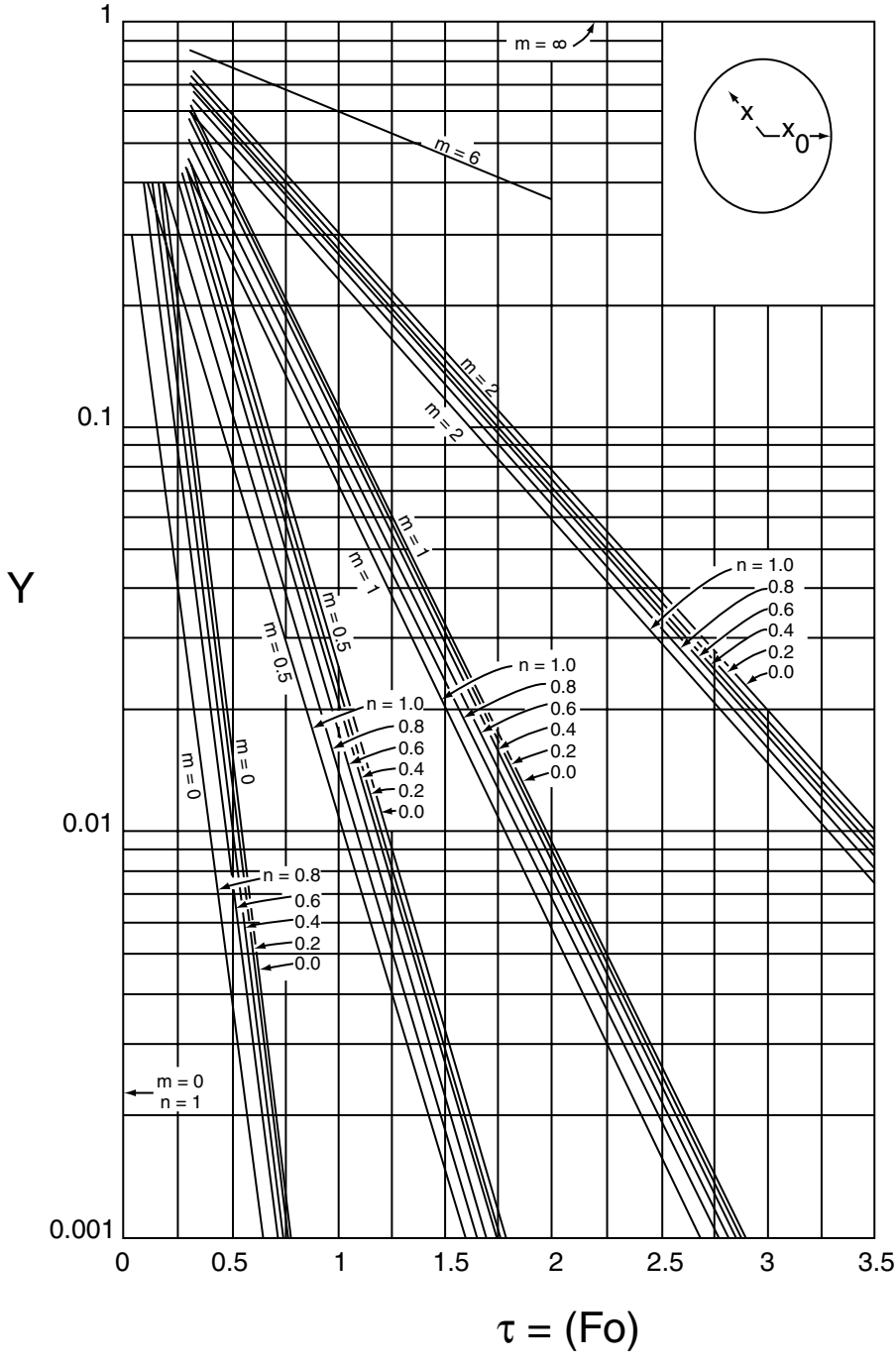

FIGURE 12.14
Dimensionless temperature as a function of time and position for a sphere.

obtain an exact solution to this type of problem. However, for simple geometries, a series is obtained as a solution to the problem. For the specific case where the value of the Fourier number (F_o) is larger than 0.2, only the first term of the series is important. In this way, the solution to Equation 12.24 is a function of the Fourier number, according to the expression:

$$Y = \frac{T_e - T_f}{T_e - T_0} = C_1 \exp\left(-\xi^2 Fo\right) \tag{12.33}$$

where T_f is the temperature at the center of the solid at time t, while T_e and T_0 are the temperatures of the external fluid and initial of the solid, respectively. The parameters C_1 and ξ of this equation can be found in Table 12.2 and are a function of the value of Biot's number and the type of solid considered. It should be taken into account that the Fourier number is defined according to the expression:

$$(Fo) = \frac{\alpha t}{L^2} \tag{12.34}$$

where α is the thermal diffusivity, L is the characteristic length of the solid, and t is the time.

In those cases in which the value of Biot's number is lower than 0.1, convection controls the heat transfer process. Since convection is the controlling mechanism, the temperature of the solid will be uniform. It is possible to obtain the following solution to the problem from an energy balance:

$$Y = \frac{T_e - T_f}{T_e - T_0} = \exp\left(-\frac{h\,A\,t}{m\,\hat{C}_P}\right) \tag{12.35a}$$

where A is the surface area of the solid, $\hat{C}_P$ is its specific heat, and m is the mass of the solid, while T_e and T_0 are the temperatures of the external fluid and initial of the solid, and T_f is the temperature of the solid at time t. If the expressions of Biot's and Fourier's numbers are taken into account (Equations 12.32 and 12.34), the last equation can be expressed in a dimensionless form as:

$$Y = \frac{T_e - T_f}{T_e - T_0} = \exp\left[-(Bi)(Fo)\right] \tag{12.35b}$$

12.3.1.2 Numerical and Graphical Methods

Besides the analytical method obtained in the previous section for solution of problems under unsteady state, numerical or graphical methods can be

TABLE 12.2

Coefficients for the First Term of the Solutions for Monodimensional Heat Conduction under Unsteady State

	Infinite Slab		Infinite Cylinder		Sphere	
Bi	**ξ**	C_1	**ξ**	C_1	**ξ**	C_1
0.01	0.0998	1.0017	0.1412	1.0025	0.1730	1.0030
0.02	0.1410	1.0033	0.1995	1.0050	0.2445	1.0060
0.03	0.1732	1.0049	0.2439	1.0075	0.2989	1.0090
0.04	0.1987	1.0066	0.2814	1.0099	0.3450	1.0120
0.05	0.2217	1.0082	0.3142	1.0124	0.3852	1.0149
0.06	0.2425	1.0098	0.3438	1.0148	0.4217	1.0179
0.07	0.2615	1.0114	0.3708	1.0173	0.4550	1.0209
0.08	0.2791	1.0130	0.3960	1.0197	0.4860	1.0239
0.09	0.2956	1.0145	0.4195	1.0222	0.5150	1.0268
0.10	0.3111	1.0160	0.4417	1.0246	0.5423	1.0298
0.15	0.3779	1.0237	0.5376	1.0365	0.6608	1.0445
0.20	0.4328	1.0311	0.6170	1.0483	0.7593	1.0592
0.25	0.4801	1.0382	0.6856	1.0598	0.8448	1.0737
0.30	0.5218	1.0450	0.7465	1.0712	0.9208	1.0880
0.40	0.5932	1.0580	0.8516	1.0932	1.0528	1.1164
0.50	0.6533	1.0701	0.9408	1.1143	1.1656	1.1441
0.60	0.7051	1.0814	1.0185	1.1346	1.2644	1.1713
0.70	0.7506	1.0919	1.0873	1.1539	1.3525	1.1978
0.80	0.7910	1.1016	1.1490	1.1725	1.4320	1.2236
0.90	0.8274	1.1107	1.2048	1.1902	1.5044	1.2488
1.0	0.8603	1.1191	1.2558	1.2071	1.5708	1.2732
2.0	1.0769	1.1795	1.5995	1.3384	2.0288	1.4793
3.0	1.1925	1.2102	1.7887	1.4191	2.2889	1.6227
4.0	1.2646	1.2287	1.9081	1.4698	2.4556	1.7201
5.0	1.3138	1.2402	1.9898	1.5029	2.5704	1.7870
6.0	1.3496	1.2479	2.0490	1.5253	2.6537	1.8338
7.0	1.3766	1.2532	2.0937	1.5411	2.7165	1.8674
8.0	1.3978	1.2570	2.1286	1.5526	2.7654	1.8921
9.0	1.4149	1.2598	2.1566	1.5611	2.8044	1.9106
10.0	1.4289	1.2620	2.1795	1.5677	2.8363	1.9249
20.0	1.4961	1.2699	2.2881	1.5919	2.9857	1.9781
30.0	1.5202	1.2717	2.3261	1.5973	3.0372	1.9898
40.0	1.5325	1.2723	2.3455	1.5993	3.0632	1.9942
50.0	1.5400	1.2727	2.3572	1.6002	3.0788	1.9962
100.0	1.5552	1.2731	2.3809	1.6015	3.1102	1.9990

applied. The numerical solution would be applied to simple cases such as slabs. To do this, the solid is divided into cells and temperature variation in each cell with time is observed. The equation for the heat balance under unsteady state, without heat generation, for rectangular coordinates in one direction only is:

$$\frac{\partial T}{\partial t} = \alpha \frac{\partial^2 T}{\partial x^2} \tag{12.24}$$

This equation can be expressed as finite differences, so its partial derivatives are expressed as:

$$\frac{\partial T}{\partial t} = \frac{T(x, t+\Delta t) - T(x, t)}{\Delta t} \tag{12.36}$$

$$\frac{\partial^2 T}{\partial x^2} = \frac{T(x+\Delta x, t) - 2\,T(x, t) + T(x-\Delta x, t)}{(\Delta x)^2} \tag{12.37}$$

Substitution of these derivatives in the last equation yields:

$$T(x, t+\Delta t) - T(x,t) = \frac{\Delta t}{(\Delta x)^2}\ \alpha \left[T(x+\Delta x, t) - 2\,T(x, t) + T(x-\Delta x, t)\right]$$

If Fourier's number, which is defined by Equation 12.34,

$$(Fo) = \frac{\alpha\,\Delta t}{(\Delta x)^2}$$

is substituted in the last equation, an expression that gives the temperature of one cell in the solid for a given time ($t + \Delta t$) later than time t is obtained:

$$T(x, t+\Delta t) = Fo\left[T(x+\Delta x, t) + T(x-\Delta x, t) + \left(\frac{1}{Fo} - 2\right) T(x, t)\right] \tag{12.38}$$

The selection of the value of Fourier's number is limited, since for values of F_0 greater than ½, errors accumulate as the calculation process advances. The selection of the value of F_0 fixes the time increase Δt since:

$$\Delta t = Fo\frac{(\Delta x)^2}{\alpha} \tag{12.39}$$

In the case where a value of F_0 = ½ is selected, the following is obtained:

$$T(x, t+\Delta t) = \frac{1}{2}\left[T(x+\Delta x, t) + T(x-\Delta x, t)\right] \tag{12.40}$$

which points out that the temperature of a cell is the arithmetic mean of the temperatures of the adjacent cells in the last time period.

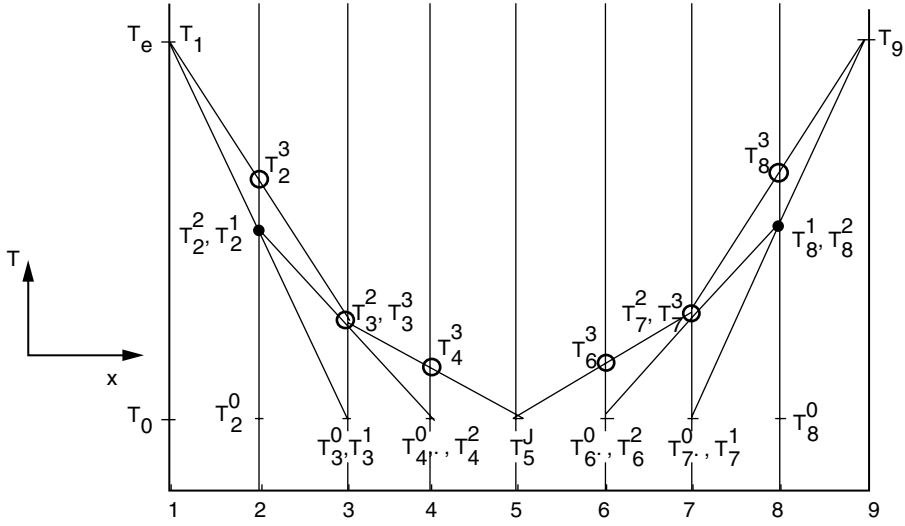

FIGURE 12.15
Division of a solid and evolution of the temperature profile.

If, at the beginning, the solid of Figure 12.15 was at temperature T_0 and the external faces were exposed to a temperature T_e, the way to operate would be explained next. The solid is divided into an odd number of cells (in this case, nine); the temperature profiles for the different time periods are the following:

For	t = 0	$T_1 = T_9 = T_e$
		$T_2 = T_3 = \ldots = T_8 = T_0$
For	$t = 0 + \Delta t$	$T_1 = T_9 = T_e$
		$T_2 = T_8 = (T_0 + T_e)/2$
		$T_3 = T_4 = \ldots = T_7 = T_0$
For	$t = 0 + 2\Delta t$	$T_1 = T_9 = T_e$
		$T_2 = T_8$ do not change
		$T_3 = T_7 = (T_2 + T_8)/2$
		$T_4 = T_5 = T_6 = T_0$

and so on, until reaching the fixed Δt.

When Fourier's number is selected as $F_o = ½$, a simple graphical solution for the heat conduction problems under unsteady state is obtained. The graphical method based on this procedure is called Binder–Schmidt's method.

According to Equation 12.40, the temperature of a cell is the arithmetic mean between the temperatures of the adjacent cells at a previous time

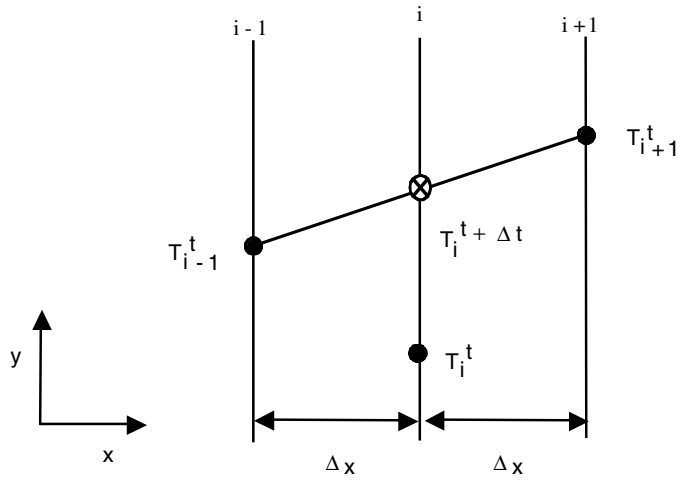

FIGURE 12.16
Graphic method of Binder–Schmidt.

period, so the temperature of the intermediate cell can be obtained graphically by connecting the temperatures on their sides (Figure 12.16).

The Binder–Schmidt method assumes that the solid is divided into equal x increments (Δx), but can only be applied to monodimensional heat conduction problems. Figure 12.15 shows this graphical method developed for a slab divided into cells in such a way that there are only nine sections. The solid is initially at a temperature T_0 and both external faces are exposed to a temperature T_e. The variation of the temperature profile for the first four time increments can be observed in Figure 12.15. The temperature of each cell is indicated by T_i^j, in which the subindex i indicates the position of the plot and the subindex j indicates the time period.

12.3.2 Bi- and Tridimensinal Heat Conduction: Newman's Rule

Heat transfer by conduction under unsteady state has been studied in previous sections for infinite solids. However, in practice, the slabs and cylinders do not have a length–thickness ratio large enough to be considered as solids of infinite dimensions. The way in which this problem can be solved is simple. The method is called Newman's rule since he demonstrated that, for a heating or cooling solid parallelepiped, the solution that describes the temperature variation as a function of time and position can be expressed as:

$$Y = Y_X\, Y_Y\, Y_Z \tag{12.41}$$

where Y is the adimensional temperature defined in Equation 12.28a, and the variables Y_X, Y_Y, and Y_Z are the dimensionless values of temperatures

according to directions x, y, and z, respectively, considering the other two directions as infinite. The assumption is that the parallelepiped is made of three semi-infinite slabs of finite thickness that correspond to each of the three dimensions of the parallelepiped.

A finite cylinder can be considered the intersection of an infinite length cylinder and a semi-infinite slab. In this way, the solution is given by:

$$Y = Y_C\, Y_L \tag{12.42}$$

in which Y_C is the adimensional value of temperature for a cylinder of infinite length, while Y_L corresponds to a semi-infinite slab.

Problems

12.1

The heating fluid in a pasteurization process is heated to the processing temperature in an oven with a three-layer wall. The first wall is made of refractory bricks, the second of insulating bricks, and the third is a 6.3-mm steel veneer for mechanical protection. The temperature of a refractory brick in contact with the oven is 1371°C, while the external temperature of the steel veneer is 38°C. Calculate the thickness of the brick layers if the total heat loss through the oven wall is 1570kJ/(h.m^2).

Data: Properties of the materials:

Material	Maximum Temperature of Use (°C)	Thermal Conductivity (W·m^{-1}°C^{-1})	
		38°C	1100°C
Refractory brick	1425	3.03	6.23
Insulating brick	1093	1.56	3.03
Steel	—	45.00	—

Since the maximum temperature the insulating brick can stand is 1093°C, this will be the temperature that one of the layers should have to minimize the total thickness. Therefore, T_1 = 1093°C.

The temperature profile in a layer is given by Equation 12.8:

$$T\left(x_i\right) = T_{i-1} + \frac{T_i - T_{i-1}}{e_i} x_i$$

The heat flux is expressed according to Equation 12.6:

$$\frac{\dot{Q}}{A} = q = -k\frac{dT}{dx} = k\frac{T_{i-1} - T_i}{e_i}$$

Refractory brick:

$$T = T_0 + \frac{T_1 - T_0}{e_1} x$$

$$q = -k_1 \frac{T_1 - T_0}{e_1} \Rightarrow \frac{T_1 - T_0}{e_1} = \frac{-q}{k_1} = \frac{-15750\,\mathrm{W/(m^2)}}{6.23\,\mathrm{W/(m\cdot{}^oC)}} = -2528\,\frac{^o\mathrm{C}}{\mathrm{m}}$$

If:

$$\left.\begin{array}{l} T = T_1 = 1093^o\mathrm{C} \\ x = e_1 \end{array}\right\} \Rightarrow 1093 = 1371 - 2528\, e_1 \Rightarrow e_1 \approx 0.11\,\mathrm{m}$$

The thickness of the refractory brick layer is 0.11 m.
Insulating brick:

$$T = T_1 + \frac{T_2 - T_1}{e_2} x$$

If the thermal conductivity k of a material varies linearly with temperature, $k = a + bT$, it can be demonstrated that for any intermediate temperature:

$$k_m = \frac{1}{2}\left(k_{T1} + k_{T2}\right)$$

$$k_2 = \frac{1}{2}\left[\left(k_{insul}\right)_{1093^oC} + \left(k_{insul}\right)_{38^oC}\right] = 2.30\,\mathrm{W/(m\cdot{}^oC)}$$

so:

$$q = -k_2 \frac{T_2 - T_1}{e_2} \Rightarrow \frac{T_2 - T_1}{e_2} = \frac{-q}{k_2} = \frac{-15750\,\mathrm{W/(m^2)}}{2.3\,\mathrm{W/(m\cdot{}^oC)}} = -6847.8\,\frac{^o\mathrm{C}}{\mathrm{m}}$$

Applying the limit condition:

$$T = T_2 \quad x = e_2$$

$$T_2 = 1093 - 6874.3\, e_2$$

Temperature T_2 should be known to calculate the thickness e_2.

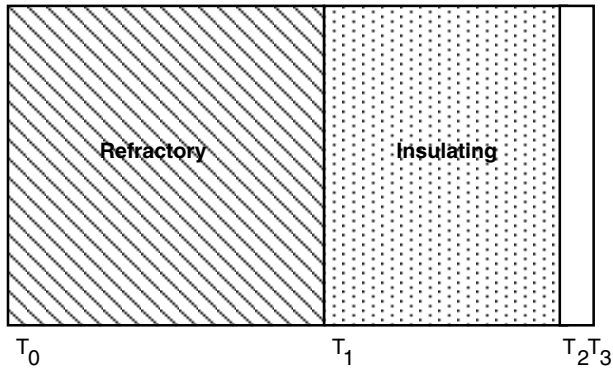

FIGURE P12.1
Problem 12.1.

Steel veneer:

$$T = T_2 + \frac{T_3 - T_2}{e_3}\, x$$

$$q = -k_3 \frac{T_3 - T_2}{e_3} \Rightarrow \frac{T_3 - T_2}{e_3} = \frac{-q}{k_3}$$

$$T_2 = T_3 + q\frac{e_3}{k_3}$$

$$T_2 = 38^{\circ}\mathrm{C} + 15750 \frac{\mathrm{W}}{\mathrm{m}^2}\ \frac{0.0063\mathrm{m}}{45\,\mathrm{W}/\left(\mathrm{m}\cdot{}^{\circ}\mathrm{C}\right)} = 40.2^{\circ}\mathrm{C}$$

Hence:

$$40.2 = 1093 - \left(6847.8\right) e_2 \Rightarrow e_2 = 0.154\ \mathrm{m}$$

The thickness of the insulating layer is 0.154 m.

12.2

A new material is being tested to insulate a refrigerating chamber; its thermal conductivity should be determined, so a hollow sphere of the material is built. An electrical resistance of 15 W is placed in the center of the sphere, and the temperatures of the surfaces are measured with thermocouple once the steady conditions are reached. Calculate: (a) the thermal conductivity of the material; and (b) the temperature in an intermediate point of the sphere wall.

Data: Internal radius of the sphere: 3 cm; external radius: 8 cm. Temperatures: internal wall: 98°C; external wall: 85°C.

Under steady state, the temperature profile is given by Equation 12.15:

$$T = T_0 + \left(T_1 - T_0\right) \frac{r_1}{r_1 - r_0}\left(1 - \frac{r_0}{r}\right)$$

The heat flow per time unit will be constant and equal to:

$$\dot{Q} = q\,A = -k\,A\frac{dT}{dr} = -k\,4\;\; r^2\frac{dT}{dr} = 4\;\; k\left(T_0 - T_1\right)\frac{r_1 r_0}{r_1 - r_0}$$

(a) Thermal conductivity of material:

$$k = \frac{\dot{Q}\left(r_1 - r_0\right)}{4\left(T_0 - T_1\right) r_1\, r_0}$$

$$\dot{Q} = 15\ W = 15\ \mathrm{J/s}$$

$$r_1 = 0.08\ \mathrm{m};\quad r_0 = 0.03\ \mathrm{m}$$

$$T_0 = 98^{\circ}\mathrm{C};\quad T_1 = 85^{\circ}\mathrm{C}$$

$$k = \frac{\left(15\ \mathrm{W}\right)\left(0.08 - 0.03\right)\mathrm{m}}{4\pi\left(98 - 85\right)^{\circ}\mathrm{C}\,\left(0.08\ \mathrm{m}\right)\left(0.03\ \mathrm{m}\right)} \approx 1.91\frac{\mathrm{W}}{\mathrm{m}\cdot{}^{\circ}\mathrm{C}}$$

(b) Temperature in an intermediate point:
If it is assumed that:

$$r_m = \frac{r_0 + r_1}{2} \qquad r_m = 0.055\ \mathrm{m}$$

$$T_m = T_0 + \left(T_1 - T_0\right)\frac{r_1}{r_1 - r_0}\left(1 - \frac{r_0}{r_m}\right)$$

Substituting the data in the corresponding units:

$$r_0 = 0.03\ \mathrm{m} \qquad T_0 = 98^{\circ}\mathrm{C}$$

$$r_1 = 0.08\ \mathrm{m} \qquad T_1 = 85^{\circ}\mathrm{C}$$

$$r_m = 0.055\ \mathrm{m}$$

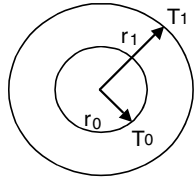

FIGURE P12.2
Problem 12.2.

$$T_m = 98 + (85 - 98)\frac{0.08}{0.08 - 0.03}\left(1 - \frac{0.03}{0.055}\right)$$

$$T_m = 98 - 9.5 = 88.5^{\circ}\text{C}$$

12.3

Combustion smoke circulates through a square chimney 45 m high, so the internal wall is at 300°C, while the external wall is at 30°C. If the dimensions of the chimney are those indicated in the attached figure, calculate the temperature at the center of the chimney wall.

Due to the symmetry of the cross section of the chimney, the calculation of the temperature at the points of the center of the wall thickness is equal to calculating the corresponding temperature of the points indicated as *a*, *b*, *c*, and *d* in the fourth side of the chimney. It can be observed that the grid defined is such that $\Delta x = \Delta y = 0.25$ m.

In this problem, since the points where temperature should be calculated are few, the general equation can be applied to obtain such temperatures (Equation 12.20):

$$T_{m,n} = \frac{1}{4}\left(T_{m+1,n} + T_{m-1,n} + T_{m,n+1} + T_{m,n-1}\right)$$

For the four points considered:

$$\left.\begin{aligned} 4T_a &= 30 + T_b + 30 + T_b \\ 4T_b &= 300 + 30 + T_a + T_c \\ 4T_c &= 300 + 30 + T_b + T_d \\ 4T_d &= 300 + 30 + T_c + T_c \end{aligned}\right\} \qquad \left.\begin{aligned} 4T_a &= 60 + 2T_b \\ 4T_b &= 330 + T_a + T_c \\ 4T_c &= 330 + T_b + T_d \\ 4T_d &= 330 + 2T_c \end{aligned}\right\}$$

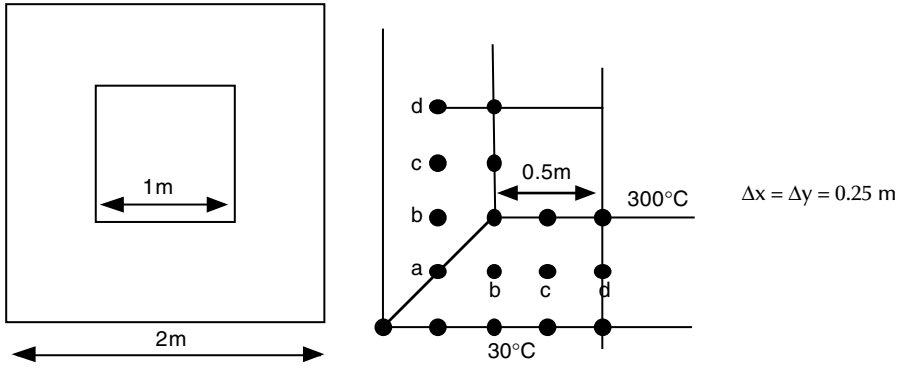

FIGURE P12.3
Problem 12.3.

Therefore, a system of four equations with four unknowns is obtained that, when solved, allows one to know the temperatures of the intermediate points of the wall:

$$T_a = 87^\circ\text{C} \qquad T_b = 144^\circ\text{C} \qquad T_c = 159^\circ\text{C} \qquad T_d = 162^\circ\text{C}$$

Liebman's Method:

Initially, the temperature of two points T_a and T_c is assumed, and the temperature of the other two points (T_b and T_d) is calculated from the general equation. The temperature of the two first points is recalculated using the new temperatures, repeating the iterative process until the temperatures of two consecutive iterations coincide.

It is supposed that $T_a = T_c = 180^\circ\text{C}$. The following table shows the results of different iterations.

Iteration	T_a (°C)	T_b (°C)	T_c (°C)	T_d (°C)
0	180		180	
1		172.5		172.5
2	101.25		168.75	
3		150		166.88
4	90		161.72	
5		145.43		163.36
6	87.72		159.70	
7		144.35		162.35
8	87.18		159.18	
9		144.09		162.09
10	87.05		159.05	
11		144.02		162.02
12	87.01		159.01	

Relaxation Method:

Initially, the temperatures of all the points are assumed, and the value of the residual is calculated as:

$$R_{m,n} = T_{m+1,n} + T_{m-1,n} + T_{m,n+1} + T_{m,n-1} - 4T_{m,n}$$

The value of these residuals should be zero. If not, the temperature is corrected at each point using the expression:

$$T^{*}_{m,n}(i+1) = T_{m,n}(i) + \frac{1}{4}R_{m,n}(1) \qquad i = n^{\circ} \text{ iteration}$$

The following table presents the results of the iterative process of this method:

Iteration		***a***	***b***	***c***	***d***
1	T	180	180	180	180
	R	–300	–30	–30	–30
2	T	105	172.5	172.5	172.5
	R	–15	–82.5	–15	–15
3	T	101.25	151.88	168.75	168.75
	R	–41.25	–7.5	–24.38	–7.5
4	T	90.94	150	162.66	166.88
	R	–3.76	–16.4	–3.77	–12.18
5	T	90	145.9	161.72	163.83
	R	–8.2	–1.88	–7.15	–1.88
6	T	87.95	145.43	159.93	163.36
	R	–0.94	–3.84	–0.93	–3.58
7	T	87.72	144.47	159.7	162.47
	R	–1.94	–0.46	–1.86	–0.48
8	T	87.24	144.36	159.24	162.35
	R	–0.24	–0.96	–0.25	–0.92
9	T	87.18	144.12	159.18	162.12
	R	–0.48	–0.12	–0.48	–0.24
10	T	87.05	144.09	159.06	162.06
	R	–0.02	–0.25	–0.09	–0.12
11	T	87.05	144.03	159.04	162.03
	R	–0.12	–0.035	–0.1	–0.04
12	T	87.02	144.02	159.02	162.02
	R	–0.04	–0.04	–0.04	–0.04

T = Temperature

R = Residual

12.4

A solid vegetable body of great dimensions is at 22°C. One of the stages of a vegetable preservation process consists of cooking the vegetable in a tank with boiling water at 100°C. Calculate the temperature of a point placed at 15 mm under the surface after 10 min.

Data: Properties of the vegetable: density: 700 kg/m^3; specific heat: 3.89 kJ/(kg·°C); thermal conductivity: 0.40 W/(m·°C).

This stage consists of a large solid heating under steady state. Since it is a solid of large dimensions, the problem is considered as heat conduction in semi-infinite solids.

$$\frac{\partial T}{\partial t} = \frac{\partial^2 T}{\partial x^2}$$

$$\alpha = \frac{k}{\rho \hat{C}p} = \frac{0.40 \text{ J}/(\text{s}\cdot\text{m}\cdot^{\circ}\text{C})}{\left(700\frac{\text{kg}}{\text{m}^3}\right)\left(3890\frac{\text{J}}{\text{kg}\cdot^{\circ}\text{C}}\right)} = 1.46\times10^{-7}\frac{\text{m}^2}{\text{s}}$$

Since it is a cooking stage in a boiling water tank, the convection coefficient can be considered high enough ($h \to \infty$) to suppose that the temperature at the surface of the solid is equal to the temperature of the water at the time when the vegetable is first immersed.

Since the tank contains boiling water ($h \to \infty$), it is assumed that $T_w \approx T_e$. The last differential equation can be integrated on the boundary conditions that allow obtaining Equation 12.25:

$$\frac{T_e - T}{T_e - T_0} = erf\left(\frac{x}{2\sqrt{\alpha t}}\right)$$

where *erf* is the Gauss error function:

$$\frac{x}{2\sqrt{\alpha t}} = \frac{15\times10^{-3}\text{ m}}{2\sqrt{\left(1.46\times10^{-7}\frac{\text{m}^2}{\text{s}}\right)(10\text{min})\left(\frac{60\text{ s}}{1\text{ min}}\right)}} = 0.8013$$

The Gauss error function is interpolated between the values of the correspondent table (Table 12.1), obtaining:

$$erf\left(0.8013\right) = 0.74286$$

$$\frac{T_e - T}{T_e - T_0} = 0.74286$$

Since T_0 = 22°C and T_e = 100°C, it is obtained that $T \approx$ 42.1°C.

12.5

An industry that processes potatoes acquires them in a region where the climate is variable. The commercial agent in charge of buying the potatoes found out that some days before harvesting, a strong cool wind came from the north and was blowing for 10 h with a temperature of –10°C. Potatoes deteriorate if their surface reaches 0°C. If the average soil depth of the potatoes is 10 cm and, at the beginning of the frost, the soil was at a temperature of 5°C, what will the commercial agent advise regarding the potato purchase?

Data: physical properties of soil: density: 1600 kg/m^3; specific heat: 3.976 kJ/(kg °C); thermal conductivity: 1 W/(m °C).

Thermal diffusivity:

$$\alpha = \frac{k}{\rho \hat{C}p} = \frac{1\ \mathrm{J/(s \cdot m \cdot ^oC)}}{(1600\ \mathrm{kg/m^3})(3976\ \mathrm{J/kg \cdot ^oC})} = 1.57 \times 10^{-7}\ \frac{\mathrm{m^2}}{\mathrm{s}}$$

The heat transfer is carried out in a semi-infinite solid, yielding:

$$\frac{T_e - T}{T_e - T_0} = erf\left(\frac{x}{2\sqrt{\alpha t}}\right)$$

If

$$\eta = \frac{x}{2\sqrt{\alpha t}} = \frac{10 \times 10^{-2}\ \mathrm{m}}{2\sqrt{\left(1.57 \times 10^{-7}\ \frac{\mathrm{m^2}}{\mathrm{s}}\right)\left(10\ \mathrm{h}\ \frac{3600\ \mathrm{s}}{1\mathrm{h}}\right)}} = 0.6651$$

the Gauss' error function takes a value of *erf*(0.6651) = 0.65534; hence:

$$\frac{T_e - T}{T_e - T_0} = 0.65534$$

Since T_e = –10°C and T_0 = 5°C, it is obtained that T = –0.2°C, indicating that the potatoes will be affected and, therefore, it is advisable not to acquire them.

12.6

It is intended to process sausages in an autoclave. The sausage can be considered equivalent to a cylinder 30 cm in length and 10 cm in diameter. If

the sausages are initially at 21°C and the temperature of the autoclave is kept at 116°C, calculate the temperature in the center of a sausage 2 h after its introduction into the autoclave.

Data: Surface heat transfer coefficient in the autoclave to the surface of the sausage is 1220 W/(m² °C). Sausage properties: density: 1070 kg/m³; specific heat: 3.35 kJ/(kg °C); thermal conductivity: 0.50 W/(m-°C).

Since the sausage has a cylindrical shape, it is considered formed from the intersection of a cylinder of infinite height of radius r_0 and an infinite slab of thickness $2x_0$

$$\left.\begin{array}{l} r_0 = 5 \text{ cm} \\ 2x_0 = \text{h} = 30 \text{ cm} \end{array}\right\} \quad \begin{array}{l} r_0 = 5 \text{ cm} \\ x_0 = 15 \text{ cm} \end{array}$$

According to Newman's rule, $Y = Y_c\, Y_L$, in which:

$$Y = \frac{T_e - T_A}{T_e - T_0} = \frac{116 - T_A}{116 - 21}$$

T_A is the temperature in the geometric center of the sausage, whose coordinates are $(r, x) = (0, 0)$.

Calculation of Y_C:

$$n_c = \frac{r}{r_0} = \frac{0}{5} = 0$$

$$m_c = \frac{k}{h\, r_0} = \frac{0.50 \ \dfrac{\text{W}}{\text{m}\cdot{}^{\circ}\text{C}}}{\left(1220 \dfrac{\text{W}}{\text{m}^2\,{}^{\circ}\text{C}}\right)\left(5\times10^{-2}\text{m}\right)} = 0.00082 \approx 0$$

$$\tau_c = \frac{k\,t}{\rho\, \hat{C}p\, r_0^2} = \frac{\left(0.50 \dfrac{\text{W}}{\text{m}\cdot{}^{\circ}\text{C}}\right)\left(7200 \text{ s}\right)}{\left(1070 \dfrac{\text{kg}}{\text{m}^3}\right)\left(3350 \dfrac{\text{J}}{\text{kg}\cdot{}^{\circ}\text{C}}\right)\left(5\times10^{-2}\right)^2 \text{ m}^2} = 0.4$$

From Figure 12.13, $Y_c = 0.17$.

Calculation of Y_L:

$$n_L = \frac{x}{x_0} = \frac{0}{15} = 0$$

$$m_L = \frac{k}{h x_0} = \frac{0.50 \dfrac{\text{W}}{\text{m}\cdot{}^\circ\text{C}}}{\left(1220 \dfrac{\text{W}}{\text{m}^2\,{}^\circ\text{C}}\right)\left(15\times10^{-2}\ \text{m}\right)} = 0.0027 \approx 0$$

$$\tau_L = \frac{k\ t}{\rho\ \hat{C}_p x_0^2} = \frac{\left(0.50 \dfrac{\text{W}}{\text{m}\cdot{}^\circ\text{C}}\right)(7200\ \text{s})}{\left(1070 \dfrac{\text{kg}}{\text{m}^3}\right)\left(3350 \dfrac{\text{J}}{\text{kg}\cdot{}^\circ\text{C}}\right)\left(15\times10^{-2}\ \text{m}\right)^2} = 0.0446$$

$Y_L \approx 0.98$ (from Figure 12.12); therefore:

$$Y = Y_c\, Y_L = (0.17)(0.98) = 0.1666$$

$$Y = \frac{T_e - T_A}{T_e - T_0}$$

$$0.1666 = \frac{116 - T_A}{116 - 21}$$

Hence:

$$T_A = 100.2^\circ\text{C}$$

12.7

A boiling water bath is used during the manufacture of sausages at the cooking stage. It can be considered that the sausages have a cylindrical shape of 5-cm diameter and 50-cm length. Initially, the sausage is at 22°C and, when it is immersed in the boiling water bath, its surface instantaneously reaches the temperature of the bath. Estimate the time that should elapse from when the sausage is introduced in the bath until the geometric center reaches 85°C.

Data: Thermal properties of the sausage: thermal conductivity: 0.44W/(m°C); density: 1260 kg/m^3; specific heat: 2.80 kJ/(kg·°C).

Thermal diffusivity:

$$\alpha = \frac{k}{\rho \hat{C}_P} = \frac{0.44\ \text{J}/\left(\text{s}\cdot\text{m}\cdot{}^\circ\text{C}\right)}{\left(1260 \dfrac{\text{kg}}{\text{m}^3}\right)\left(2.80\times10^3 \dfrac{\text{J}}{\text{kg}\cdot{}^\circ\text{C}}\right)} = 1.247\times10^{-7}\ \frac{\text{m}^2}{\text{s}}$$

The sausage can be considered an object formed from the intersection of an infinite slab of 50 cm of thickness and a cylinder of 5 cm of diameter and infinite length. Newman's rule can be applied as:

$$Y = Y_c\, Y_L = \frac{T_e - T}{T_e - T_0} = \frac{100 - 85}{100 - 22} = 0.1923$$

A time that makes the product $Y_c \cdot Y_L$ to be exactly 0.1923 has to be determined.

Slab: $x_0 = 25$ cm

$$\tau_L = \frac{\alpha t}{(x_0)^2} = \frac{\left(1.247 \times 10^{-7}\ \mathrm{m^2/s}\right)}{\left(0.25\ \mathrm{m}\right)^2}\left(\frac{60\ \mathrm{s}}{1\ \mathrm{min}}\ t_L\ \mathrm{min}\right) \approx 1.2 \times 10^{-4}\ t_L$$

$$n_L = \frac{x}{x_0} = 0$$

$$m_L = \frac{k}{h\, x_0} = 0 \quad \left(\text{since } h \to \infty\right)$$

Cylinder: $r_0 = 2.5$ cm

$$\tau_c = \frac{\alpha \cdot t}{\left(r_0\right)^2} = \frac{1.247 \times 10^{-7}\ \mathrm{m^2/s}}{\left(0.025\ \mathrm{m}\right)^2}\left(\frac{60\,\mathrm{s}}{1\,\mathrm{min}}\ t_c\ \mathrm{min}\right) \approx 0.012\ t_c$$

$$n_c = \frac{r}{r_0} = 0$$

$$m_L = \frac{k}{h r_0} = 0$$

τ_L and τ_C should be given in minutes.

The problem is solved by iteration, assuming a time and determining with graphs Y_C and Y_L, whose product yields 0.1923. The following table shows the values of the iterative process.

t (min)	τ_L	τ_C	Y_L	Y_C	Y
60	7.18×10^{-3}	0.718	≈1	0.0273	0.0273
30	3.59×10^{-3}	0.359	≈1	0.20	0.20
35	4.19×10^{-3}	0.419	≈1	0.152	0.152
32	3.84×10^{-3}	0.384	≈1	0.19	0.19

obtaining $t \approx 32$ min.

Since the height of the sausage is much greater than its diameter, it could be assumed to be a cylinder of infinite height, so $Y \approx Y_C = 0.1923$. It is graphically obtained that, for this Y, the value of the dimensionless time is $\tau_C = 0.012$.

From this value, the following time is obtained: t = 0.4/0.012 ≈ 33 min.

12.8

A piece of meat with the shape of a parallelepiped of dimensions 1 m × 1 m × 6 cm is submerged in a tank containing water at 3°C. The initial distribution of temperatures along the width of the meat piece is:

Distance from the surface (cm):	0	1	2	3
Temperature °C:	27	24	23	22

Determine the distribution of temperatures after ½ h.

Data and notes: The convective heat transfer coefficient from the piece of meat to water is high enough to assume that the temperature on the wall of the meat at the initial time is the arithmetic mean of the temperatures of the bath and the meat's wall. After the first time period, assume that the wall reaches the temperature of the bath.

Thermal conductivity of the meat:	0.56 W/(m·°C)
Specific heat of the meat:	3.35 kJ/(kg·°C)
Density of the meat:	1200 kg/m^3

The piece of meat will be considered an infinite slab with a 6-cm thickness, so heat transfer is carried out through this thickness. The monodimensional heat balance is:

$$\frac{\partial T}{\partial t} = \alpha \frac{\partial^2 T}{\partial x^2}$$

This equation is solved by finite differences, obtaining that the temperature at a point for a given time is a function of the temperature of the adjacent points during the last period, according to the expression:

$$T(x,t+\Delta t) = (Fo)\left[T(x+\Delta x,t) + T(x-\Delta x,t) + \left(\frac{1}{Fo} - 2\right)T(x,t)\right]$$

where:

$$\frac{1}{Fo} = \frac{(\Delta x)^2}{\alpha\, \Delta t}$$

The Binder–Schmidt method assumes (F_o) = ½ and Δx = 0.01 m; therefore, the time period Δ*t* will be:

$$\Delta t = \frac{(\Delta x)^2 \rho \hat{C}_p (Fo)}{k} = \frac{(0.01\ \text{m})^2 \left(1200 \frac{\text{kg}}{\text{m}^3}\right)\left(3350 \frac{\text{J}}{\text{kg}^\circ\text{C}}\right)}{2\left(0.56 \frac{\text{J}}{\text{s m}^\circ\text{C}}\right)} = 359\ \text{s}$$

that is, $\Delta t = 359\ \text{s} \approx 0.1\ \text{h}$.

Since it is desired to determine the temperature distribution at the end of ½ h, the number of time periods will be:

$$n^\circ \Delta t = \frac{0.5\ \text{hours}}{\Delta t} = \frac{0.5}{0.1} = 5\ \text{periods}$$

Since $1/(F_o) = ½$,

$$T(x, t + \Delta t) = \frac{1}{2}\left[T(x + \Delta x, t) + T(x - \Delta x, t)\right]$$

The following table presents the values of the temperatures of the different layers as a function of time:

Time (hours)	T_1(°C)	T_2(°C)	T_3(°C)	T_4(°C)	T_5(°C)	T_6(°C)	T_7(°C)
Before cooling	27	24	23	22	23	24	27
0	15	24	23	22	23	24	15
0.1	3	19	23	23	23	19	3
0.2	3	13	21	23	21	13	3
0.3	3	12	18	21	18	12	3
0.4	3	10.5	16.5	18	16.5	10.5	3
0.5	3	9.75	14.25	16.5	14.25	9.75	3

Figure P12.8 shows the plotting of the solid in different layers.

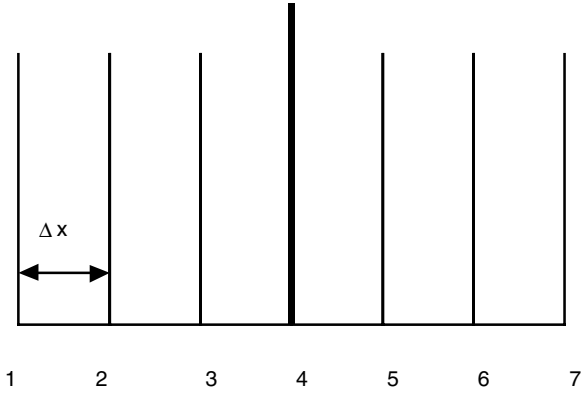

FIGURE P12.8
Problem 12.8.

13

Heat Transfer by Convection

13.1 Introduction

Every moving fluid carries an associated energy that causes heat to be transferred from one point to another; these points are at different temperatures due to such movement. This type of heat transmission is called convection.

If a fluid is in contact with a solid that is at a greater temperature, the fluid receives heat that is transferred within it by movement of the particles of the fluid. This movement causes heat transport by convection to happen, and it can occur in natural or forced form. The first case occurs when there is no mechanical agitation and is attributed to density differences at different points of the fluid caused by the effect of temperature. On the other hand, forced convection occurs when the movement of the fluid is produced mechanically using devices such as agitators and pumps, among others.

Heat transfer by convection is very important when studying the heat exchange between two fluids separated by a wall in such a way that one of them gives up heat to the other, so that the first fluid cools while the second heats up. The devices in which this heat transmission is performed are called heat exchangers.

13.2 Heat Transfer Coefficients

13.2.1 Individual Coefficients

If one considers a fluid that circulates through a solid pipe or around a solid surface, the heat transfer from the solid to the fluid (or vice versa) depends on the fluid–solid contact area and on the temperature difference. Thus, for a system like that shown in Figure 13.1, in which a solid of differential area dA at a temperature T_S is in contact with a fluid at temperature T_f, then $T_S > T_f$. There is heat transmission from the solid to the fluid in a way such that the heat flow will be proportional to dA and $(T_S - T_f)$. This is:

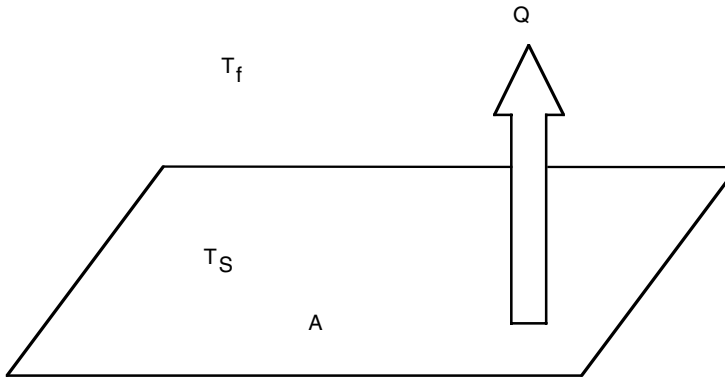

FIGURE 13.1
Heat transfer by convection.

$$dQ \propto dA\left(T_S - T_f\right)$$

A proportionality coefficient h is defined in such a way as:

$$dQ = h\,dA\left(T_S - T_f\right) \tag{13.1}$$

This proportionality constant is called the individual convective heat-transfer coefficient, or film coefficient, and depends on the physical and dynamical properties of the fluid. Some relations between these properties can be found by means of dimensional analysis that, complemented with later experimentation, allows one to obtain equations to calculate such coefficients.

The individual convective heat-transfer coefficient h depends on the physical properties that affect flow (density, ρ, and viscosity, η), its thermal properties (specific heat, $\hat{C}_P$, and thermal conductivity, k), the characteristic length L of the transmission area (in the case of cylindrical pipe, its diameter d), gravity acceleration g, the velocity v at which the fluid circulates, the temperature difference between the solid and the fluid ($T_S - T_f$), and the cubic or volumetric expansion coefficient β (that, in the case of an ideal gas, coincides with the inverse of the absolute temperature).

A relation among the different dimensionless groups is obtained by applying a dimensional analysis:

$$Nu = \phi\left[\left(\mathrm{Re}\right)\left(Pr\right)\left(Gr\right)\right] \tag{13.2}$$

in which the dimensionless groups are defined as follows:

Nusselt number: $$(Nu) = \frac{h\,d}{k} \tag{13.3}$$

Reynolds number: $$(\mathrm{Re}) = \frac{\rho\, v\, d}{\eta} \tag{13.4}$$

Prandtl number: $$(\mathrm{Pr}) = \frac{\hat{C}_P\,\eta}{k} \tag{13.5}$$

Grashof number: $$(Gr) = \frac{\beta\, g\, \Delta T\, d^3\, \rho^2}{\eta^2} \tag{13.6}$$

Sometimes it is possible to express the relationship among dimensionless groups as a function of the Peclet and Graetz numbers that are combinations of Reynolds and Prandtl numbers and that are used in forced convection problems.

Peclet number: $$(Pe) = (\mathrm{Re})(Pr) = \frac{\rho\, v\, d\, \hat{C}_P}{k} \tag{13.7}$$

Graetz number: $$(Gz) = (\mathrm{Re})(Pr)(d/L) = \frac{\rho\, v\, d^2\, \hat{C}_P}{k\, L} \tag{13.8}$$

In natural convection, velocity depends on the flotation effects, so the Reynolds number can be omitted in Equation 13.2, whereas in forced convection, the Grashof number is the one that can be omitted. Thus:

Natural convection: $Nu = \phi\,[(Pr)(Gr)]$
Forced convection: $Nu = \phi\,[(\mathrm{Re})(Pr)] = \phi\,(Gz)$

It is interesting that, within a wide temperature and pressure range, for most of the gases the Prandtl number is practically constant; thus it can be omitted, yielding to simpler equations for the calculation of the individual heat transfer coefficients.

Once the relationships among the different dimensionless groups are found, final equations that allow calculation of the film coefficients can be obtained by experimentation. In spite of the fact that, in the literature there are numerous expressions to calculate such individual coefficients, a series of expressions commonly used in practice will be given below.

13.2.1.1 Natural Convection

As stated before, the Nusselt number is only a function of the Grashof and Prandtl numbers for free or natural convection. The equation that relates these three numbers is:

$$Nu = a\left(Gr\,Pr\right)^{b} \tag{13.9}$$

in which the values of the parameters a and b depend on the system and working conditions.

Configuration	*Gr.Pr*	a	b
Vertical plates and cylinders			
Length > 1 m			
Laminar	$< 10^4$	1.36	1/5
Laminar	$10^4 < Gr\,Pr < 10^9$	0.55	1/4
Turbulent	$> 10^9$	0.13	1/3
Spheres and horizontal cylinders			
Diameter < 0.2 m			
Laminar	$10^3 < Gr\,Pr < 10^9$	0.53	1/4
Turbulent	$> 10^9$	0.13	1/3
Horizontal plates (heated upwards cooled downwards)			
Laminar	$10^5 < Gr\,Pr < 2 \times 10^7$	0.54	1/4
Turbulent	$2 \times 10^7 < Gr\,Pr < 3 \times 10^9$	0.55	1/3
(heated upwards cooled downwards)			
Laminar	$3 \times 10^5 < Gr\,Pr < 3 \times 10^{10}$	0.27	1/4

When the fluid is air in laminar flow, the equations to be used are:

Horizontal walls:

$$h = C\left(\Delta t\right)^{1/4} \tag{13.10}$$

Upwards: $C = 2.4$

Downwards: $C = 1.3$

Vertical walls: $\left(L > 0.4\,\mathrm{m}\right)$: $h = 1.8\left(\Delta T\right)^{1/4}$ (13.11)

Vertical walls: $\left(L > 0.4\,\mathrm{m}\right)$: $h = 1.4\left(\Delta T/L\right)^{1/4}$ (13.12)

Horizontal and vertical pipes: $h = 1.3\left(\Delta T/d\right)^{1/4}$ (13.13)

In all these expressions, d and L should be given in meters to obtain the value of the film coefficient in J/(s m^2 °C).

13.2.1.2 Forced Convection

The properties of the fluid should be calculated at a mean global temperature in all the expressions stated next.

13.2.1.2.1 Fluids inside Pipes

Flow in turbulent regime:

One of the more used equations is the Dittus–Boelter equation:

$$Nu = 0.023(\mathrm{Re})^{0.8}(Pr)^{n} \tag{13.14}$$

n = 0.4 for fluids that heat up

n = 0.3 for fluids that cool down

This equation is valid for Re > 10^4 and 0.7 < Pr < 160.

In some cases it is convenient to use an expression that includes the number of Stanton (St):

$$(St) = \frac{h}{\hat{C}_p\, \rho v} \tag{13.15}$$

in such a way that the equation to use is:

$$(St)(Pr)^{2/3} = 0.023(\mathrm{Re})^{-0.2} \tag{13.16}$$

The second member of this equation is denominated factor j_H of Colburn.

For viscous fluids that move at Re < 8000 and Pr < 10^4, the equation of Sieder–Tate is usually used:

$$Nu = 0.027(\mathrm{Re})^{0.8}(Pr)^{1/3}(\eta/\eta_w)^{0.14} \tag{13.17}$$

All the properties of the fluid are calculated at a mean temperature, except η_w, which is calculated at the mean temperature of the wall.

Another equation that includes the viscosity term at the temperature of the wall is:

$$(Nu) = 0.023(\mathrm{Re})^{0.8}(Pr)^{2/3}(\eta/\eta_w)^{0.14} \tag{13.18}$$

As indicated before, the value of the Prandtl number is practically constant in the case of gases circulating inside the pipes, so the equation that can be used is simpler:

$$(Nu) = 0.021(\mathrm{Re})^{0.8} \tag{13.19}$$

Flow in transition regime:

For $2100 < \mathrm{Re} < 10^4$, the following expression is used:

$$(Nu) = 0.116\left[(\mathrm{Re})^{2/3} - 125\right]\left[1 + (d/L)^{2/3}\right](\eta/\eta_W)^{0.14} \tag{13.20}$$

Flow in laminar regime:

Heat transfer to a fluid, in a laminar regime ($\mathrm{Re} < 2100$), takes place almost exclusively by conduction. Also, the distribution of velocity is parabolic, so the equations to be used are different from those stated before. However, it is convenient to obtain a similar expression to those used for a turbulent regime, one of the most common being:

$$(Nu) = 1.86\left[(\mathrm{Re})(Pr)(d/L)\right]^{1/3}(\eta/\eta_W)^{0.14} \tag{13.21}$$

or:

$$(Nu) = 1.86\,(Gz)^{1/3}\,(\eta/\eta_W)^{0.14} \tag{13.22}$$

13.2.1.2.2 Fluids Flowing on the Exterior of Solids

Some of the most common expressions will be presented below.

Flow in turbulent regime:

For gases: $$(Nu) = 0.26\,(\mathrm{Re})^{0.6}(Pr)^{0.3} \tag{13.23}$$

For liquids: $$(Nu) = \left[0.35 + 0.47\,(\mathrm{Re})^{0.52}\right](Pr)^{0.3} \tag{13.24}$$

In the case of liquids that move by the annular space of concentric tubes, the equation of Davis can be used:

$$(St) = 0.029\,(\mathrm{Re})^{-0.2}\,(Pr)^{-2/3}(\eta/\eta_W)^{0.14}(d_0/d_i)^{0.15} \tag{13.25}$$

where d_0 and d_i are the external and internal diameters of the circular ring, respectively. Sometimes, equations for flow inside tubes are used instead of Equation 13.25, changing the diameter of the pipe for the equivalent diameter.

Flow in laminar regime:

The following equation can be used for liquids in which 0.2 < Re < 200:

$$\left(Nu\right) = 0.86\left(\mathrm{Re}\right)^{0.43}\left(Pr\right)^{0.3} \tag{13.26}$$

For liquids that circulate at Re > 200 and gases at 0.1 < Re < 10^3, the next expression is used:

$$\left(Nu\right) = \left[0.35 + 0.56\left(\mathrm{Re}\right)^{0.52}\right]\left(Pr\right)^{0.3} \tag{13.27}$$

In case the Prandtl number is 0.74, the equation that can be used is:

$$\left(Nu\right) = 0.24\left(\mathrm{Re}\right)^{0.6} \tag{13.28}$$

13.2.1.2.3 Heating or Cooling of Flat Surfaces

For Re > 20,000, taking as characteristic length the length of the flat surface in the same direction as the flow, the following expression is used:

$$\left(Nu\right) = 0.036\left(\mathrm{Re}\right)^{0.8}\left(Pr\right)^{1/3} \tag{13.29}$$

For air over smooth slabs:

$$h = 5.7 + 3.9\,v \qquad \left(v > 5\ \mathrm{m/s}\right) \tag{13.30a}$$

$$h = 7.4\left(v\right)^{0.8} \qquad \left(5 < v < 30\ \mathrm{m/s}\right) \tag{13.30b}$$

in which v is the velocity of the fluid in m/s and h is obtained in J/(m^2 s °C).

13.2.1.3 Convection in Non-Newtonian Fluids

Many food fluids do not present Newtonian behavior, so the equations given previously to calculate film coefficients cannot be used. Few data can be found in the literature to calculate such coefficients for non-Newtonian fluids. Some equations that can be used are presented next.

13.2.1.3.1 Circulation in Plug Flow

When a fluid circulates in plug flow by a pipe, and for values of the Graetz number higher than 500, the following expression is useful:

$$(Nu) = \frac{8}{\pi} + \frac{4}{\pi}(Gz)^{1/2} \tag{13.31}$$

13.2.1.3.2 Circulation in Turbulent Regime

When the flow behavior of the fluid can be described by the power law, the following equation can be used:

$$(Nu) = 1.75\left(\frac{3n+1}{4n}\right)^{1/3}(Gz)^{1/3} \tag{13.32}$$

Also, besides all the expressions given here, more can be found in the literature; some of them will be seen in detail in the section that corresponds to film coefficients of shell and tube heat exchangers.

It is important to point out, too, that in all those expressions in which the viscosity of the fluid at the temperature of the wall (η_w) appears, it is necessary to perform an iterative process to calculate the film coefficient. This is because, in order to obtain the value of η_w, it is necessary to know previously the value of the temperature on the exchanger wall; for that, the value of the film coefficient is needed.

13.2.2 Global Coefficients

The last section presented methods to calculate the heat-transfer coefficients from a solid surface to a fluid or vice versa. However, there are cases in practice in which a fluid is cooled or heated by means of another fluid that cools down or heats up, and both fluids are separated by a solid surface. In this case, it is necessary to find a heat-transfer coefficient that allows calculation of the heat transferred from one fluid to another through a solid wall.

Suppose a system (Figure 13.2) in which a hot fluid at temperature T transfers heat to another cool fluid at temperature t through a solid surface. Heat transfer is carried out from the hot to the cold fluid. Initially, heat is transferred by convection from the fluid at temperature T to the surface at temperature T_w. Heat is transferred by conduction through the solid, so there is a temperature drop from T_w to t_w. Then heat is transferred by convection from the wall to the cold fluid at temperature t. The area of the solid surface in contact with the hot fluid is called A_h, while that in contact with the cold fluid will be A_F. In case the surface is flat, these areas coincide and $A_h = A_C$. However, in general, these areas do not coincide. Next, the heat transfer process described is studied.

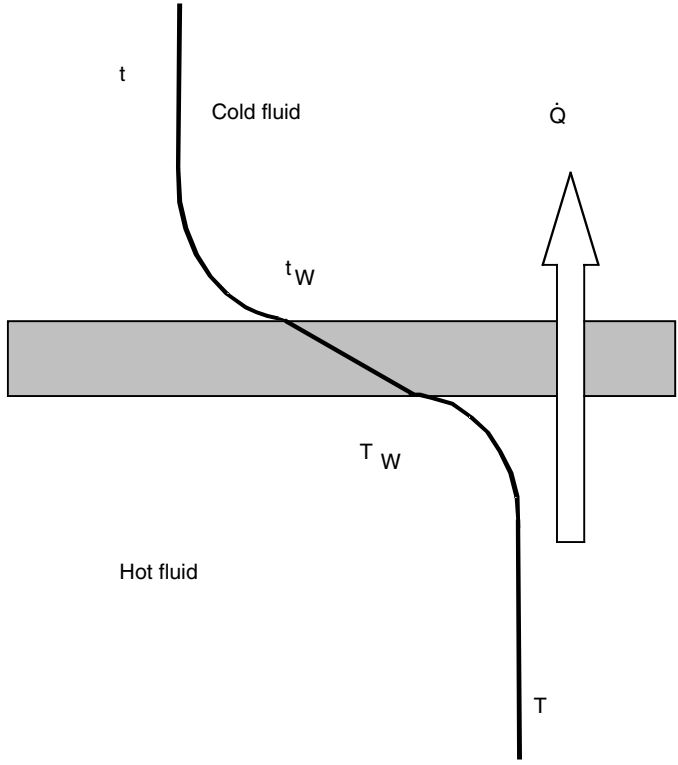

FIGURE 13.2
Heat exchange between fluids separated by a solid.

Heat convection on the side of the hot fluid:

$$\dot{Q} = h_h \left(T - T_W\right) A_h = \frac{T - T_W}{\dfrac{1}{h_h A_h}} \tag{13.33}$$

in which h_h is the individual heat-transfer coefficient in the hot fluid.

Heat conduction through the solid surface:

$$\dot{Q} = \frac{k}{e}\left(T_W - t_W\right) = \frac{T_W - t_W}{\dfrac{e}{k A_{ml}}} \tag{13.34}$$

in which k is the thermal conductivity of the solid, e is the thickness of the solid, and A_{ml} is the logarithmic mean area, defined by:

$$A_{ml} = \frac{A_c - A_h}{\ln\left(A_c / A_h\right)} \tag{13.35}$$

Heat convection on the side of the cold fluid:

$$\dot{Q} = h_h \left(t_W - t\right) A_c = \frac{t_W - t}{\dfrac{1}{h_c\, A_c}} \tag{13.36}$$

in which h_c is the individual convective heat-transfer coefficient in the cold fluid.

The heat flow transferred is the same in each case, so:

$$\dot{Q} = \frac{T - T_W}{\dfrac{1}{h_h\, A_h}} = \frac{T_W - t_W}{\dfrac{e}{k\, A_{m\,l}}} = \frac{t_W - t}{\dfrac{1}{h_c\, A_c}} \tag{13.37}$$

Due to the properties of the ratios, the last equation can be expressed as the quotient between the sum of the numerators and of the denominators, in such a way that:

$$\dot{Q} = \frac{T - t}{\dfrac{1}{U_h\, A_h}} = \frac{T - t}{\dfrac{1}{U_c\, A_c}} \tag{13.38}$$

where U_h and U_c are the heat-transfer global coefficients referring to the areas in contact with the hot and cold fluid, respectively. These global coefficients are defined by the expressions:

$$\frac{1}{U_h} = \frac{1}{h_h} + \frac{e}{k\dfrac{A_{m\,l}}{A_h}} + \frac{1}{h_c \dfrac{A_c}{A_h}} \tag{13.39a}$$

$$\frac{1}{U_c} = \frac{1}{h_n \dfrac{A_h}{A_c}} + \frac{e}{k\dfrac{A_{m\,l}}{A_c}} + \frac{1}{h_c} \tag{13.39b}$$

It can be observed that the expression $1/(U.A)$ represents the global resistance to heat transfer from the hot to the cold fluid. This resistance is the sum of three resistances in series: those due to the hot fluid, to the solid wall, and to the cold fluid.

TABLE 13.1

Dirt Factors

Product	*R* (m² °C/kW)	Product	*R* (m² °C/kW)
Water		Liquids	
Distilled	0.09	Brine	0.264
Sea	0.09	Organic	0.176
River	0.21	Fuel oil	1.056
Boiler	0.26	Tars	1.76
Very hard	0.58		
Gases			
Steam		Air	0.26–0.53
Good quality	0.052	Solvents' vapor	0.14
Bad quality	0.09		

In fact, the calculation of this coefficient is more complicated, since the fluids can leave sediments on the solid surface. For this reason, two new resistances appear in the last equations: R_h and R_c, which are the resistance due to the deposits or sediments of the hot and cold fluids, respectively. So the heat-transfer global coefficient, if the deposits or sediments are taken into account, can be expressed as:

$$\frac{1}{U_F} = \frac{1}{U} + R_h + R_c \tag{13.40}$$

In this equation, U is the global coefficient calculated by either Equation 13.39a or b, and U_F is the heat-transfer global coefficient that includes the resistance due to deposits. Table 13.1 shows the typical values of soiling factors for water and other types of fluids.

The calculation of the heat-transfer global coefficients is performed as indicated, although approximated values of this coefficient can be found in the literature for different types of devices and operations (Kreith and Black, 1983).

The value of the coefficient on the internal side of the tubes is obtained in reference to the internal area, although sometimes it can be interesting to know the value of the heat-transfer coefficient in reference to the external area. If h_i and h_{ie} are the film coefficients of the fluid that circulates inside the pipe, referring to the internal and external area respectively, then the following is complied with:

$$h_{ie} = h_i \frac{d_e}{d_i} \frac{\phi_{te}}{\phi_{ti}}$$

where d_e and d_i are the external and internal diameters of the tubes, respectively.

The relation of viscosities defines the coefficient ϕ_t:

$$\phi_t = \frac{\eta}{\eta_W} \tag{13.41}$$

therefore:

$$\frac{\phi_{ti}}{\phi_{te}} = \frac{\eta_{We}}{\eta_{Wi}}$$

where η_{We} is the viscosity of the fluid at the external temperature of the wall of the tubes and η_{Wi} corresponds to the internal temperature.

13.3 Concentric Tube Heat Exchangers

This is the simplest type of heat exchanger, consisting of two tubes of different diameter arranged one inside the other. A fluid circulates inside the internal tube, while another fluid circulates through the circular ring. The hot or cold fluid can circulate indiscriminately by the interior tube or by the circular ring, although if the hot fluid circulates by the internal tube, the heat transfer is better.

These exchangers can operate in two ways: in parallel and in countercurrent (Figure 13.3). In the first case, the cold fluid and the hot fluid circulate in the same direction, while in countercurrent the fluids circulate in opposite ways.

13.3.1 Design Characteristics

The setup of the mathematical model will be performed from the energy balances for the hot and cold fluid and through the exchange surface. This study will be made for the two operation methods mentioned before.

13.3.1.1 Operation in Parallel

Suppose a system like that shown in Figure 13.4, in which the fluid enters by section 1 and exits by section 2. The circulation flows are w_h and w_c, and the specific heats are $\hat{C}_P)_h$ and $\hat{C}_P)_c$ for the hot and cold fluids, respectively. The heat flow transferred by the hot fluid is captured by the cold fluid, and in the case that there are no heat losses outside, the following is complied with:

$$\dot{Q} = w_h \left(\hat{C}_P\right)_h \left(T_{\text{in}} - T_{\text{out}}\right) = w_c \left(\hat{C}_P\right)_c \left(t_{\text{in}} - t_{\text{out}}\right) \tag{13.42}$$

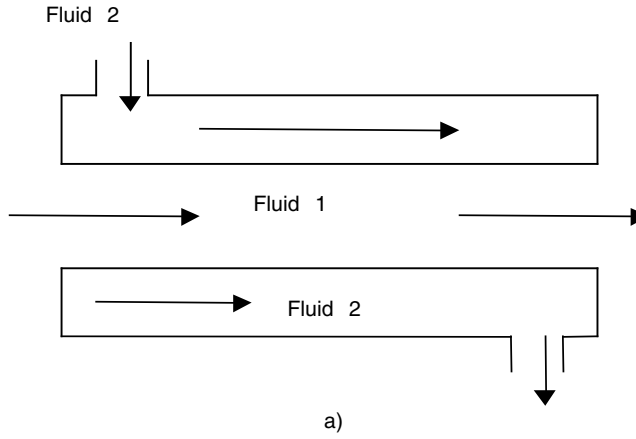

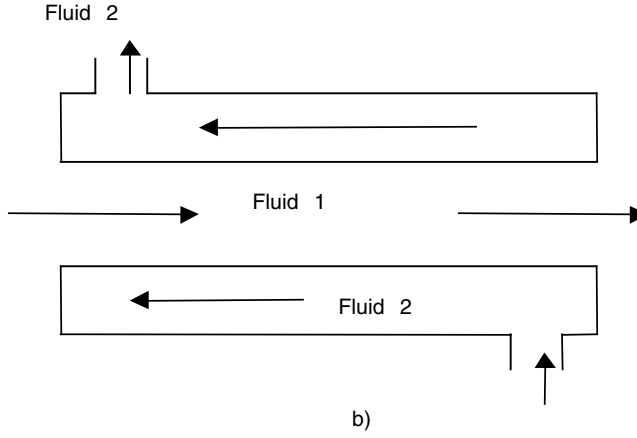

FIGURE 13.3
Concentric tube heat exchanger: a) parallel flow; b) countercurrent flow.

w being the mass flow of each stream, T the temperature of the hot fluid, t the temperature of the cold fluid, and $\hat{C}_P$ the specific heat of the hot (h) and cold (c) fluid, respectively.

Consider a surface differential (dA) of the heat exchanger (Figure 13.4). The temperatures of the fluids are T and t at the inlet of this element of the exchanger, with ($T + dT$) and ($t + dt$) being those at the outlet.

When an energy balance is performed on this part of the exchanger, the following is obtained for the hot fluid:

$$w_h\left(\hat{C}_P\right)_h T = d\,\dot{Q} + w_h\left(\hat{C}_P\right)_h \left(T - dT\right)$$

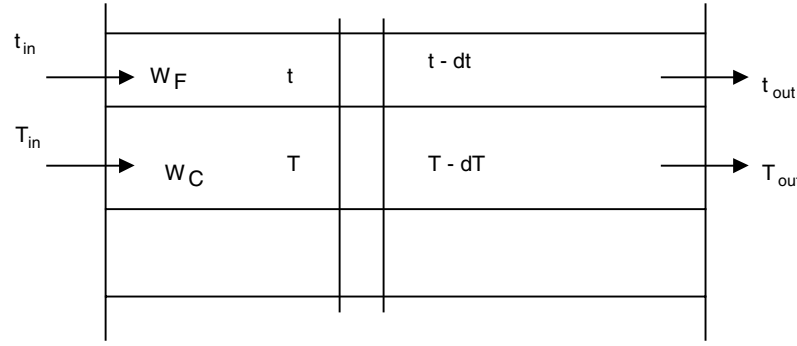

FIGURE 13.4
Concentric tube heat exchanger; fluids flow.

$$d\dot{Q} = U(T - t)dA$$

hence:

$$d\dot{Q} = U(T - t)dA = -w_h\left(\hat{C}_P\right)_h dT \tag{13.43}$$

In an analogous way, for the cold fluid:

$$d\dot{Q} = U(T - t)dA = w_c\left(\hat{C}_P\right)_c dt \tag{13.44}$$

To calculate the exchange area, the last equations should be integrated and arranged as separated variables:

$$\frac{U}{w_h\left(\hat{C}_P\right)_h}dA = \frac{-dT}{T - t} \tag{13.45}$$

$$\frac{U}{w_c\left(\hat{C}_P\right)_c}dA = \frac{dt}{T - t} \tag{13.46}$$

The integration of these equations allows calculation of the area of the exchanger:

$$A = \int dA = \int \frac{w_h\left(\hat{C}_P\right)_h}{U}\frac{-dT}{T - t} \tag{13.47a}$$

$$A = \int dA = \int \frac{w_c\left(\hat{C}_P\right)_c}{U}\frac{dt}{T - t} \tag{13.47b}$$

Integration is not as simple as it seems, since the heat-transfer global coefficient U, in general, is not constant because its value depends on the fluid and flow properties, which vary along the heat exchanger as the temperature changes.

The following expression can be obtained from the differential equations on separated variables previously obtained:

$$\frac{-d(T-t)}{T-t} = -d\ln(T-t) = U\left(\frac{1}{w_h\,\hat{C}_P)_h} + \frac{1}{w_c\,\hat{C}_P)_c}\right)dA$$

If it is supposed that the heat-transfer global coefficient is constant (U = constant) and the difference between both fluids is defined as $\Delta T = T - t$, when integrating the whole area it is obtained that:

$$\ln\left(\frac{\Delta T_1}{\Delta T_2}\right) = U\,A\left(\frac{1}{w_h\,\hat{C}_P)_h} + \frac{1}{w_c\,\hat{C}_P)_c}\right)$$

The following expression is obtained from the global balance (Equation 13.42):

$$\left(\frac{1}{w_h\,\hat{C}_P)_h} + \frac{1}{w_c\,\hat{C}_P)_c}\right) = \frac{\Delta T_1 - \Delta T_2}{\dot{Q}}$$

so the heat flow transferred through the area of the exchanger is:

$$\dot{Q} = U\,A(\Delta T)_{m\,l} \tag{13.48}$$

$(\Delta T)_{ml}$ being the logarithmic mean temperature difference:

$$(\Delta T)_{ml} = \frac{\Delta T_1 - \Delta T_2}{\ln\left(\frac{\Delta T_1}{\Delta T_2}\right)} \tag{13.49}$$

If the heat-transfer global coefficient is not constant, the transmission area should be calculated by graphical or numerical integration of:

$$A = -\int \frac{w_h\,\hat{C}_P)_h\,d\,T}{U(T-t)} = \int \frac{w_c\,\hat{C}_P)_c\,d\,t}{U(T-t)} \tag{13.50}$$

It should be taken into account that the relationship between the temperature of the fluids, t and T, is given by the heat balance between the inlet and outlet section and any section in the exchanger:

$$w_h \left(\hat{C}_P\right)_h \left(T_{\text{in}} - T\right) = w_c \left(\hat{C}_P\right)_c \left(t - t_{\text{in}}\right)$$

However, it can be mathematically demonstrated that, if the heat-transfer global coefficient, U, varies linearly with ΔT or with one of the temperatures T or t, the value of the heat flow transferred through the exchange area is:

$$\dot{Q} = A \left(U\ \Delta T\right)_{m\,lc} \tag{13.51}$$

where $(U\ \Delta T)_{mlc}$ is the crossed logarithmic mean, defined by the expression:

$$\left(U\,\Delta T\right)_{m\,lc} = \frac{U_2\,\Delta\,T_1 - U_1\,\Delta\,T_2}{\ln\left(\dfrac{U_2\,\Delta\,T_1}{U_1\,\Delta\,T_2}\right)} \tag{13.52}$$

The calculation of the crossed logarithmic mean implies previous knowledge of the value of the heat-transfer global coefficient at the ends of the exchanger.

13.3.1.2 Countercurrent Operation

In this case, as indicated by its name, the fluids circulate in countercurrent (Figure 13.3). It can be demonstrated, in an analogous way to the parallel operation, that the equations obtained from the heat balance are:

For a constant U: $\dot{Q} = U\,A\left(\Delta\,T\right)_{m\,l}$

If U varies linearly with temperature: $\dot{Q} = A\left(U\ \Delta T\right)_{m\,lc}$

For the same heat requirement, that is, the same values of inlet and outlet temperatures, the logarithmic mean of the temperatures is higher for countercurrent operations than for parallel operations. For this reason, the surface required to perform the desired heat transfer will be smaller in countercurrent operation. It is important to point out that, in the calculation of the logarithmic mean temperature, the temperature increments in each section vary with respect to the operation in parallel, since in this case $\Delta T_1 = T_{\text{in}} - t_{\text{out}}$ and $\Delta T_2 = T_{\text{out}} - t_{\text{in}}$.

13.3.2 Calculation of Individual Coefficients

The different expressions presented in Section 13.2.1 are used to calculate individual or film coefficients, although one of the most used is the Dittus–Boelter equation (Equation 13.14). In these equations, the diameter used to calculate the Reynolds and Nusselt numbers is the inside diameter of the interior tube. The equivalent diameter is used for the fluid that circulates by the annular space.

The equivalent diameter for a pipe of section other than circular is defined as four times the hydraulic radius, which is the quotient between the cross-sectional area and the wet perimeter:

$$D_e = 4r_H = 4\frac{\text{cross-sectional area}}{\text{wet perimeter}} \tag{13.53}$$

In the case of a circular ring (Figure 13.5), the wet perimeter is considered only that part corresponding to the heat exchange area, that is, the perimeter "wet" by the heat transfer:

$$D_e = 4\, r_H = 4\frac{(\pi/4)\left(d_0^2 - d_e^2\right)}{\pi\, d_e}$$

Hence:

$$D_e = \frac{\left(d_0^2 - d_e^2\right)}{d_e} \tag{13.54}$$

where d_0 is the internal diameter of the external tube and d_e is the external diameter of the internal tube.

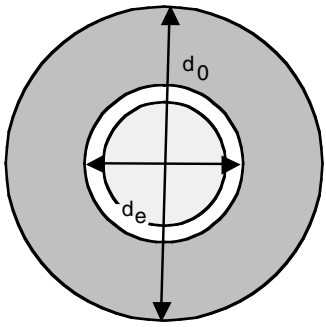

FIGURE 13.5
Cross section of a concentric tube heat exchanger.

13.3.3 Calculation of Head Losses

Regarding the circulation of fluids inside pipes, head losses can be calculated from Fanning's equation (Equation 7.65). Diameter appears in this last expression, that, in the case of the internal pipe, coincides with its internal diameter. However, the equivalent diameter should be used in the case of the circular ring and varies from that obtained in the last section, since the wet perimeter is different:

$$D_e = 4\, r_H = 4\frac{(\pi/4)\left(d_0^2 - d_e^2\right)}{\pi\left(d_0 - de\right)} = d_0 - d_e \tag{13.55}$$

The friction factor can be calculated from the different equations found in Section 7.4.2 of Chapter 7. These equations vary depending on the circulation regime and are different according to the value of the Reynolds number.

13.4 Shell and Tube Heat Exchangers

In cases in which it is necessary to have a big transfer surface to perform the heat transfer from one fluid to another, use of a set of tubes contained in a shell is recommended (Figure 13.6). The set of tubes is called a bundle; a supporting plate fastens them. In this type of heat exchanger, one fluid circulates inside the tubes and the other one outside the tubes and inside the shell. Usually, this last fluid is forced to change direction due to the presence of supporting plates. Such plates or baffles can be perpendicular or horizontal to the tube bundle. In the first case they are called deflectors; different types of deflectors are shown in Figure 13.7 (orifice, disk and doughnut, and segmental baffles). The distance between baffles determines the velocity of the fluid, generally 0.2 times the value of the diameter of the shell. Also, the percent of the diameter of the shell not occupied by the deflector is called bypassing.

When the supporting plates placed inside the shell are slabs parallel to the tubes, they divide the shell into a set of passes in such a way that the fluid circulating outside the tubes changes direction in two consecutive passes. In the same way, the direction change of the fluid that circulates inside the tube bundle is called a pass. Different types of shell and tube heat exchangers with different fluid passes are represented in Figure 13.6.

On the other hand, the tubes can be arranged as triangles, squares, or rotated squares (Figure 13.8). The square arrangement allows an easier cleaning of the external parts of the tubes. The triangular arrangement makes the turbulence of the fluid easy, so the heat transfer coefficient increases, although the head losses increase too.

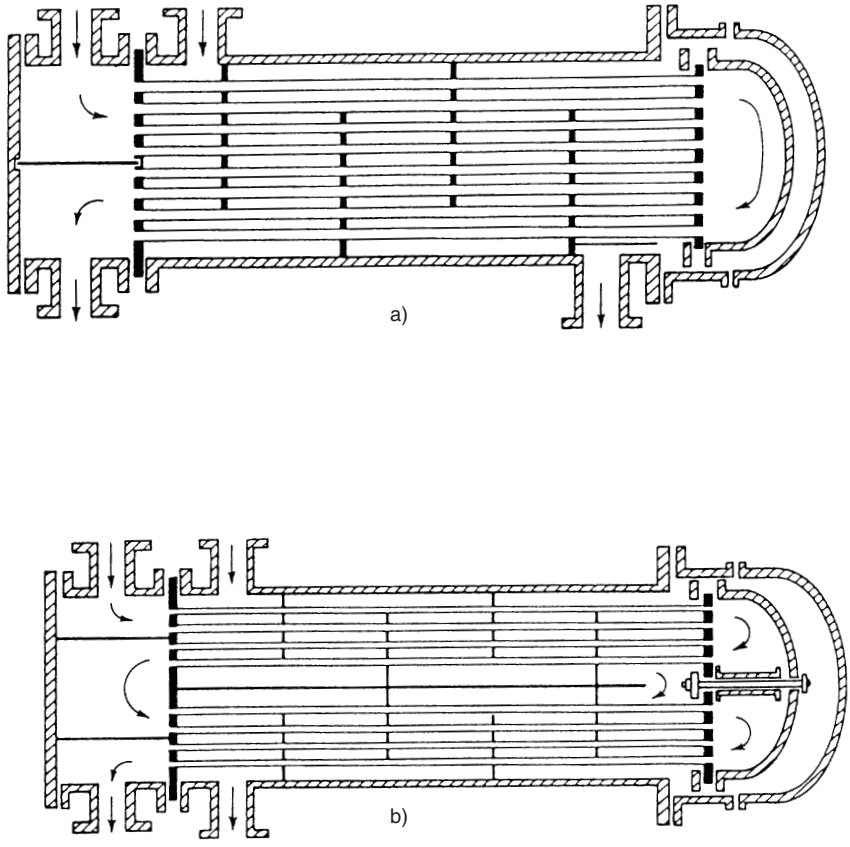

FIGURE 13.6
Shell and tube heat exchanger: (a) ½ configuration heat exchanger; (b) ¾ configuration heat exchanger.

13.4.1 Design Characteristics

Certain considerations regarding which fluid is advisable to circulate inside and which outside the tubes should be taken into account for the design of shell and tube heat exchangers.

In general, to reduce heat losses to the exterior, the hot fluid should circulate inside the tube bundle. However, since it is easier to clean the inside of the tubes, it is preferable to circulate the dirtiest fluid or the one that leaves more deposits or sediments inside the tube bundle. In case both fluids produce similar dirtiness, it is preferable to circulate the one with greater pressure inside the tubes, since the cost of a pressured shell is high. For viscous fluids, it is preferable to make them circulate inside the tubes, since, in general, this type of fluid deposits dirt. When they circulate in laminar regime, it is preferable to make them circulate through the outside, since the

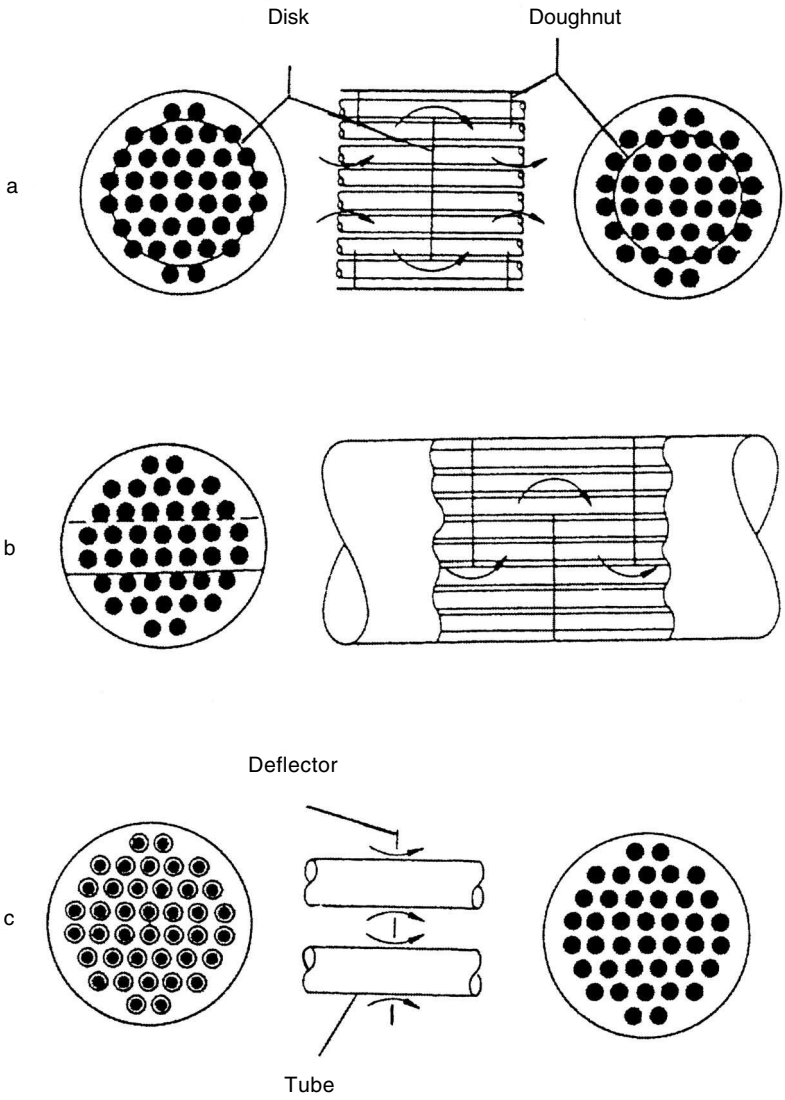

FIGURE 13.7
Types of baffles and shell and tube heat exchangers: (a) with disk and doughnut baffles; (b) segmental baffles; (c) orifice baffles. (Adapted from Kreith, F. and Black, W.Z., *La Transmisión del Calor Principios Fundamentales*, Alhambra, Madrid, 1983.)

baffles will help to increase the turbulence and, therefore, will increase the heat transfer. If the fluids are corrosive, they will be circulated inside the tubes, since if they circulate outside, the use of an anticorrosive will be needed to avoid the deterioration of the outside part of the tubes and the shell.

With these considerations in mind, the setup of the mathematical model needed to design these type of heat exchangers will be presented below. The

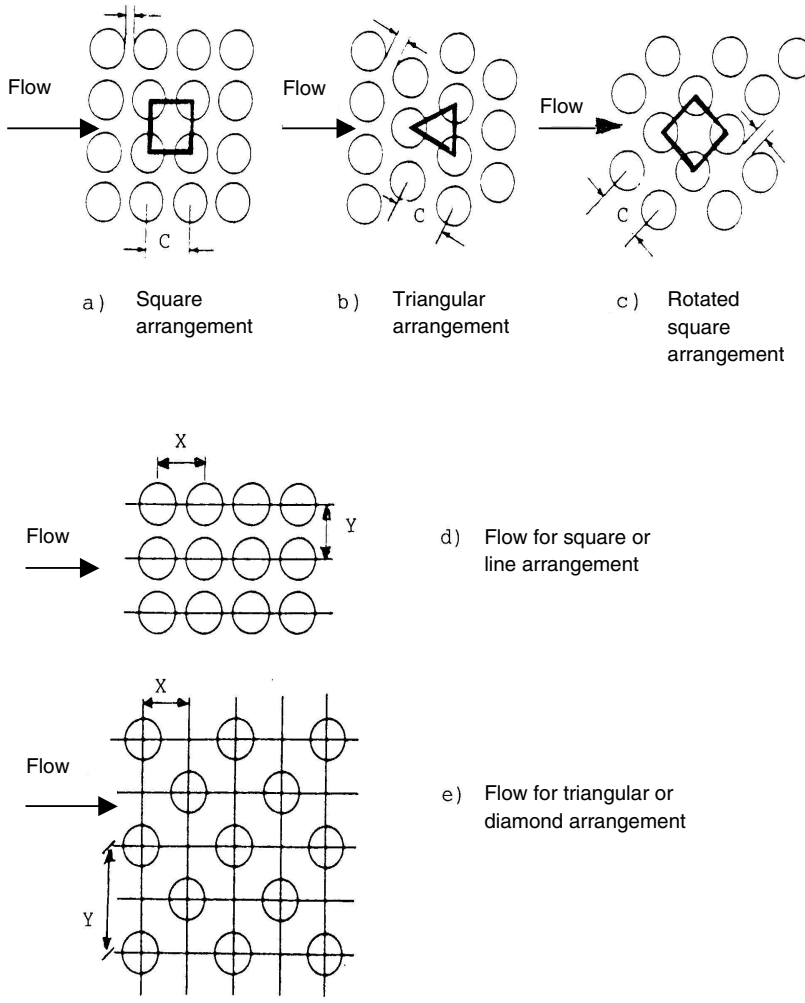

FIGURE 13.8
Tube bundle arrangement.

global heat transfer balances for these heat exchangers are equal to those for the double tube heat exchanger:

$$\dot{Q} = w_h \left(\hat{C}_P\right)_h \left(T_{\text{in}} - T_{\text{out}}\right) = w_c \left(\hat{C}_P\right)_c \left(t_{\text{in}} - t_{\text{out}}\right) \tag{13.42}$$

Regarding the equation of heat transfer velocity through the exchange area, it is difficult to apply an expression like that used for concentric tube heat exchangers, since in this case the fluid that circulates by the shell experiences continuous direction changes; parallel or countercurrent operations

do not pertain. However, it is considered that the velocity equation is similar to the equation for double tube heat exchangers, although the logarithmic mean temperature difference will be affected by a correction factor. Hence:

$$\dot{Q} = U A \left(\Delta T\right)_{ml} F \tag{13.56}$$

The logarithmic mean temperature difference is calculated as if the operation is performed in countercurrent:

$$\left(\Delta T\right)_{m\,l} = \frac{\left(T_{\text{in}} - t_{\text{out}}\right) - \left(T_{\text{out}} - t_{\text{in}}\right)}{\ln\left(\dfrac{T_{\text{in}} - t_{\text{out}}}{T_{\text{out}} - t_{\text{in}}}\right)} \tag{13.57}$$

The factor F that corrects such logarithmic mean temperature difference is dimensionless and depends on the inlet and outlet temperature of the fluids and the type of heat exchanger.

13.4.2 Calculation of the True Logarithmic Mean Temperature Difference

As mentioned before, the heat transfer velocity equation is affected by a factor *F*, due to the geometry of the system. This factor corrects the logarithmic mean temperature increase $(\Delta T)_{ml}$, obtaining at the end the true value of this expression. A series of considerations related to the functioning of this type of heat exchanger should be made for the calculation of this factor. The following assumptions are made:

- The temperature of the fluid in any cross section is considered to be the same.
- The heat transfer coefficient is constant.
- The heat transfer is equal at each pass.
- The specific heat of each fluid is constant.
- The mass flow of each fluid is constant.
- There are no phase changes due to condensation or evaporation.
- Heat losses to the exterior are negligible.

The following dimensionless factor can be defined if the heat exchanger of Figure 13.9 is considered:

$$Z = \frac{T_{\text{in}} - T_{\text{out}}}{t_{\text{out}} - t_{\text{in}}} = \frac{w_c \left(\hat{C}_P\right)_c}{w_h \left(\hat{C}_P\right)_h} \tag{13.58}$$

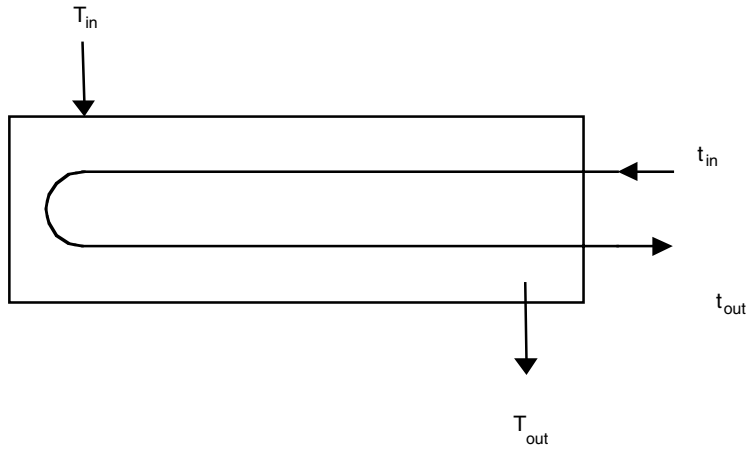

FIGURE 13.9
Shell and tube heat exchanger ½ configuration.

It can be observed that this is a relationship between the heat capacities by hour, that is, the heat required to increase the flow per hour in 1°C for each fluid.

Also, a new dimensionless temperature factor can be defined according to the expression:

$$\varepsilon = \frac{t_{out} - t_{in}}{T_{in} - t_{in}} \tag{13.59}$$

This temperature relationship indicates the heating or cooling efficiency and can vary from zero, for the case of constant temperature of one of the fluids, to the unit, when the inlet temperature of the hot fluid (T_{in}) coincides with the temperature of the cold fluid at the outlet (t_{out}).

The correction factor F is a function of these dimensionless parameters and of the type of heat exchanger: $F = F(Z, \varepsilon, \text{type})$. Figures 13.10 and 13.11 show the graphic correlation for the different types of shell and tube heat exchangers.

When applying the correction factors, whether the hot fluid circulates by the shell and the cold one by the tube bundle or vice versa is not important. If the temperature of one of the fluids remains constant, the flow direction is not important, since in this case $F = 1$.

13.4.3 Calculation of Individual Coefficients

In order to calculate the heat transfer global coefficient, the film coefficients inside and outside the tubes should be previously known. The way to calculate individual coefficients will be explained below.

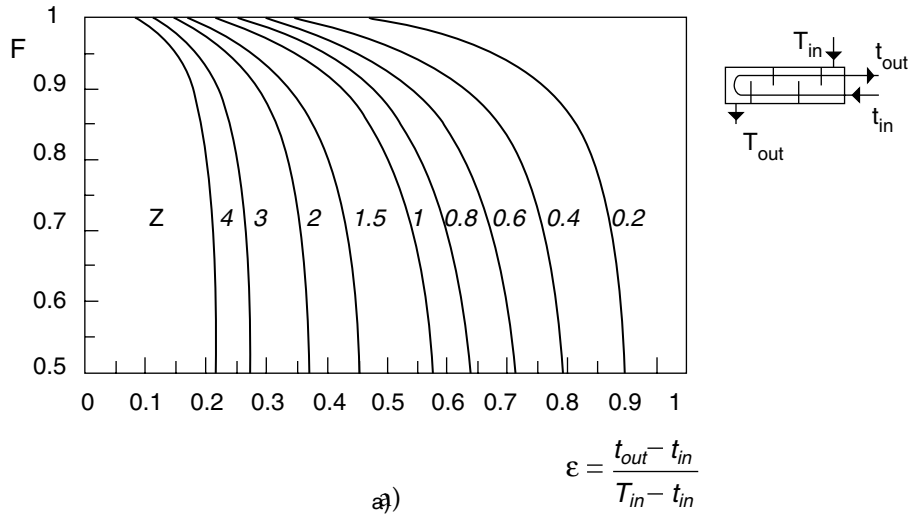

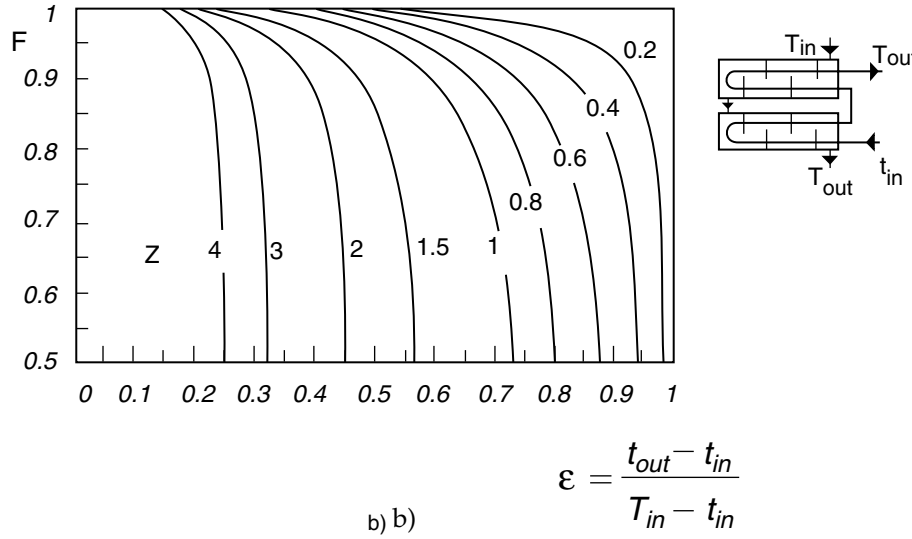

FIGURE 13.10
F factor for shell and tube exchangers: (a) one shell crossing, two or more tubes; (b) two shell crossings, four or more tubes. (Adapted from Coulson, J.M. and Richardson, J.F., *Ingeniería Química,* Vols. I and VI, Reverté, Barcelona, 1979.)

13.4.3.1 Coefficients for the Inside of the Tubes

The way to calculate the coefficient of the inside of the tubes was indicated in Section 13.2.1, and any of the expressions presented there can be used. One of the most used is that of Sieder–Tate (Equation 13.17), as is the factor j_H of Colburn (Equation 13.16):

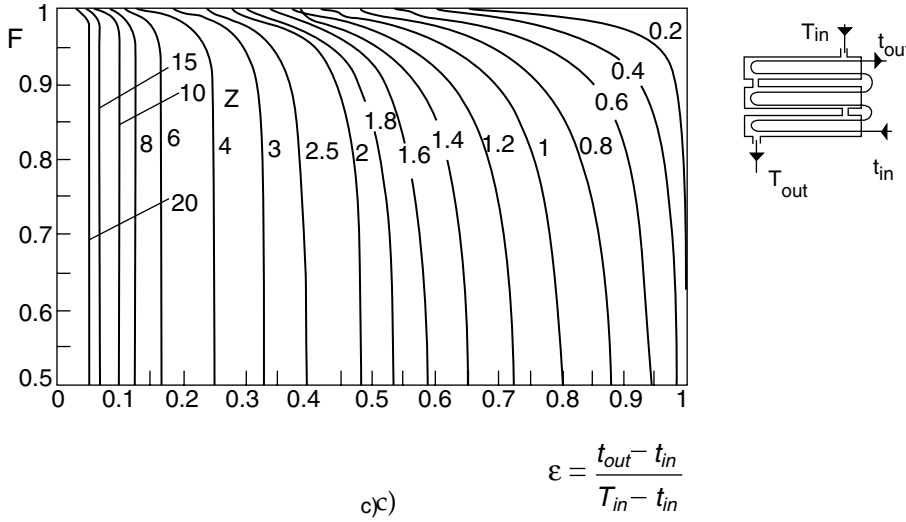

c)

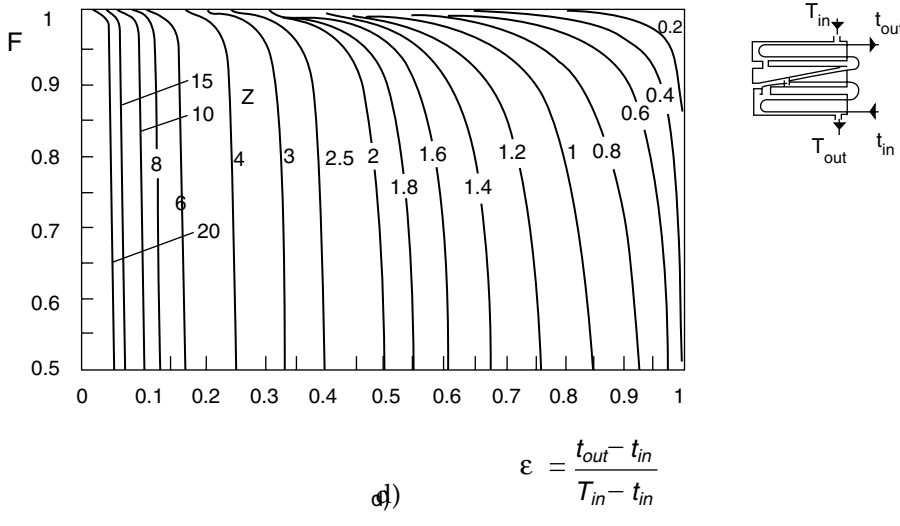

d)

FIGURE 13.11
F factor for shell and tube heat exchangers: (c) three shell crossings; (d) four shell crossings. (Adapted from Coulson, J.M. and Richardson, J.F., *Ingeniería Química*, Vols. I and VI, Reverté, Barcelona, 1979.)

$$j_H = (Nu)(Pr)^{-1/3}(\eta/\eta_w)^{-0.14} = 0.027(\mathrm{Re})^{0.8} \tag{13.17}$$

The Reynolds number appears in all these expressions, which is defined by:

$$(\mathrm{Re}) = \frac{\rho v d_i}{\eta} = \frac{G_t d_i}{\eta} \tag{13.60}$$

where v is the linear circulation velocity of the fluid inside a tube, and G_t is the mass flow density of the fluid that circulates inside a tube.

The value of G_t is calculated from the global mass flow of the fluid (w), the cross section of a tube (a_t), the total number of tubes in the bundle (N_t), and their number of passes (n). Hence:

$$G_t = \frac{w}{N_t a_t / n} \tag{13.61}$$

13.4.3.2 Coefficients on the Side of the Shell

The calculation of the coefficient for the side of the shell is more complicated than in the last case, since it cannot be calculated using the expressions set up in other sections. This is due to different causes, one of which is that the fluid in the shell continuously changes direction. Also, turbulence that depends on the type of distribution of the tubes is created. Thus, in the case of a flow perpendicular to the tubes, the resistance of the square arrangement is lower than the resistance of the diamond arrangement (Figure 13.8). For this reason, it can be said that the value of the heat transfer coefficient for the shell side depends on the Reynolds number, the type of deflectors, and the tube arrangement used.

Different methods to calculate the coefficient on the side of the shell can be found in the literature. One of these methods, suggested by Kern, uses the concept of the equivalent diameter for the shell, in the case of flow parallel to the tubes. The expression that allows calculation of the equivalent diameter is different according to the arrangement of the tube bundle.

For a square arrangement:

$$D_e = \frac{4\left[Y^2 (\pi/4) d_e^2\right]}{\pi d_e} \tag{13.62a}$$

For a triangle arrangement:

$$D_e = \frac{4\left[X Y (\pi/4) d_e^2\right]}{\pi d_e} \tag{13.62b}$$

in which d_e is the external diameter of the tubes, and X and Y are defined by Figure 13.8.

The equation that allows calculation of the film coefficient is:

$$(Nu) = 0.36(\mathrm{Re})^{0.55} (Pr)^{1/3} (\eta/\eta_w)^{0.14} \tag{13.63}$$

in which the equivalent diameter defined by any of Equations 13.62a and b should be used in the Nusselt number. The Reynolds number is calculated according to the expression:

$$\left(\mathrm{Re}\right) = \frac{G_c D_e}{\eta} \tag{13.64}$$

with G_c denoting the mass flux referred to the maximum area (A_c) for the transversal flow. The expression that allows calculation of this area is:

$$A_c = \frac{D_c B C'}{n Y} \tag{13.65}$$

where n is the number of passes that the fluid experiences in the shell, B is the separation between the deflector plates, D_c is the internal diameter of the shell, Y is the distance between the centers of the tubes, and C' is the distance between two consecutive tubes ($C' = Y - d_e$).

The value of G_c is obtained from the mass flow w and the area A_c:

$$G_c = \frac{w}{A_c} \tag{13.66}$$

In the case of flow of gases through tube bundles, one of the most used equations is:

$$\left(Nu\right) = 0.33 C_h \left(\mathrm{Re}_{\max}\right)^{0.5} \left(Pr\right)^{0.3} \tag{13.67}$$

in which C_h is a constant that depends on the tube arrangement and whose values for different arrangements are given in Table 13.2. In this equation, the maximum flux value should be used to calculate the Reynolds number in such a way that its value is obtained from Equation 13.66.

Different correlations that allow calculation of heat transfer coefficients for fluids that flow perpendicularly to the tube bundle can be found in literature for different types of heat exchangers (Foust et al., 1968).

There are other expressions that allow calculation of the coefficients for the fluid that circulates on the shell side, using the heat transfer factor j_H, in such a way that:

$$j_H = \left(Nu\right)\left(Pr\right)^{-1/3} \left(\eta/\eta_w\right)^{-0.14} \tag{13.68}$$

in which j_H is obtained from the empirical equations that take into account the type of circulation regime, influence of bypassing the deflectors, and arrangement of the tube bundle.

TABLE 13.2

C_h and C_f Factors for Shell and Tube Heat Exchangers

	$X = 1.25d_0$				$X = 1.5d_0$			
	Linear		Diamond		Linear		Diamond	
RE_{MAX}	C_h	C_f	C_h	C_f	C_h	C_f	C_h	C_f
$Y = 1.25\ d_0$								
2000	1.06	1.68	1.21	2.52	1.06	1.74	1.16	2.58
20,000	1.00	1.44	1.06	1.56	1.00	1.56	1.05	1.74
40,000	1.00	1.20	1.03	1.26	1.00	1.32	1.02	1.50
$Y = 1.5\ d_0$								
2000	0.95	0.79	1.17	1.80	0.95	0.97	1.15	1.80
20,000	0.96	0.84	1.04	1.10	0.96	0.96	1.02	1.16
40,000	0.96	0.74	0.99	0.88	0.96	0.85	0.98	0.96

Source: Coulson, J.M. and Richardson, J.F., *Ingeniería Química,* Vols. I and VI, Reverté, Barcelona, 1999.

The most used expressions to calculate the factor j_H are explained below.

For turbulent regime ($2100 < Re < 10^6$):

$$j_H = a\left(\mathrm{Re}\right)^b \tag{13.69}$$

in which a and b are parameters that depend on the deflector and type of arrangement, respectively. The values of a for different values of deflector bypassing are:

Deflector bypassing	5	25	35	45
a	0.31	0.35	0.30	0.27

The value of b will be:

$b = 0.55$ for triangular and normal square arrangements
$b = 0.56$ for rotated square arrangement

For laminar regime ($Re < 2100$):

$$j_H = a\left(\mathrm{Re}\right)^{0.43} \tag{13.70}$$

where the parameter a is a function of the deflector bypassing:

Deflector bypassing	15	25	35	45
a	0.84	0.69	0.64	0.59

13.4.4 Calculation of Head Losses

Head losses of the fluid that circulates inside the tubes should be differentiated from those of that circulating outside.

13.4.4.1 Head Losses inside Tubes

When calculating the pressure drop inside the tubes, the pressure drop due to friction (ΔP_t) should be distinguished from the pressure drop due to changing from one pass to the next (ΔP_r). The pressure drop due to the tubes can be calculated from the equation of Fanning:

$$\Delta P_t = (4f)\frac{L}{d_i} n \frac{G_t^2}{2\rho} \tag{13.71}$$

in which L is the length of the tubes, d_i is their internal diameter, G_t is the mass flux with which the fluid circulates through each tube, and f is the friction factor depending on the Reynolds number and the relative roughness, as well as on the circulation regime.

The pressure drop for the direction change (180°C) is calculated by the equation:

$$\Delta P_r = 4\frac{\rho v^2}{2} = 4\frac{G_t^2}{2\rho} \tag{13.72}$$

If there are n passes, the total head loss is:

$$\Delta P = \Delta P_t + n\,\Delta P_r \tag{13.73}$$

13.4.4.2 Head Losses on the Shell Side

The equation used to calculate head losses on the shell side is:

$$\Delta P_c = \frac{f' G_c^2 D_c \left(N_c + 1\right)}{2\rho D_e} \tag{13.74}$$

where D_c is the internal diameter of the shell, D_e is the equivalent diameter of the shell (Equations 13.62a and b), and N_c is the number of baffles, so $(N_c + 1)$ is the number of times the fluid crosses the shell.

If L is the length of the shell and B is the distance between baffles, then it is complied that: $N_c + 1 = l/B$.

The parameter f' is the friction coefficient and depends on the Reynolds number, the type of tube arrangement, and the baffle bypassing. This friction factor can be calculated from graphs (Figure 13.12).

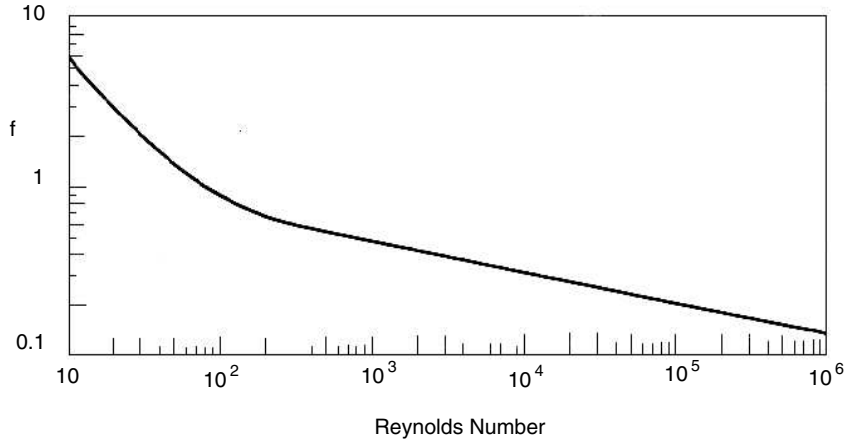

FIGURE 13.12
Friction factor for the shell fluid. (Adapted from Coulson, J.M. and Richardson, J.F., *Ingeniería Química*, Vols. I and VI, Reverté, Barcelona, 1979.)

TABLE 13.3

Plate-type Heat Exchanger Arrangements

- Flow in parallel, in which the stream is divided into various substreams and, once passed through the plates, converges again
- *Z* arrangement, in which both streams flow in parallel, but the outlet is at the opposite side to the inlet
- *U* arrangement, in which both streams flow in parallel, but the outlet and inlet points are on the same side of the heat exchanger

Head losses can also be calculated from the following equation:

$$\Delta P_c = C_f \, m \frac{\rho \, v_c^2}{6} \tag{13.75}$$

In this equation, v is the circulation velocity of the fluid through the shell, m is the number of rows of tubes, and C_f is a factor that depends on the type of tube arrangement, whose value can be obtained from data in Table 13.3.

13.5 Plate-Type Heat Exchangers

The plate-type heat exchangers are constituted by a series of corrugated plates made by simple stamp and drilled on the ends to allow or direct the

flow of liquid to be heated or cooled. These plates are placed one in front of the other in such a way that the fluids can circulate between them. Also, they are compressed by screws so that they can support the internal pressure. Some rubber gaskets should be placed between the plates and in their edges, to avoid fluid leakage or mixings. These gaskets limit the area in which these heat exchangers can be used. Once the set of plates is ready, the arrangement of the drilled holes on each plate directs the pass of the fluids, as can be observed in Figure 13.13.

According to how the plates are arranged, different forms for the pass of fluid can be obtained. Thus, plates can be combined in such a way that distributions like those shown in Figure 13.14 can be formed; these are discussed briefly below:
There are other types of arrangements which are more complex. Some examples are shown in Figure 13.14.

The applications of these types of heat exchangers are very flexible, since when the arrangement of the plates or drilled holes is changed, the flow characteristics in such heat exchangers change too. Also, it is possible to perform operations with various fluids in the same heat exchanger by inserting a connecting grid that allows the inlet or outlet of selected fluids, as can be observed in Figure 13.13. One example of this case is milk pasteurizers, in which milk can be gradually heated or cooled in one heat exchanger using hot or cold water streams and taking advantage of the heat carried by milk that should be cooled after heating. Other processes in which plate-type heat exchangers are used in a similar way as that described here can be found in the industry.

One of the problems of any heat exchanger is soiling: deposits formed on the walls decrease the transfer of heat, which can prevent the heat exchanger from meeting the specifications for which it was designed, if it is not adequately scaled. This can be a serious problem in a tubular heat exchanger, since it needs to be cleaned to function adequately again. However, plate-type heat exchangers have the advantage of easily expanding by adding new plates, which allows a longer time between cleanings. Also, the soiling process in these heat exchangers is slower, since fluids circulate with high turbulence and the surfaces of plates are smoother, avoiding low velocity zones.

In plate-type heat exchangers, turbulence is reached for values of the Reynolds number from 10 to 500, since folds on plates break the film stagnated on the heat transfer surface. Corrugation of plates, besides holding each other and keeping a constant separation between them, produces a high turbulence in the fluid that circulates between the plates. On the other hand, corrugation allows a considerable increase in the transfer surface per plate. All these factors contribute to high heat transfer coefficients; under similar conditions, this coefficient is ten times higher in a plate-type heat exchanger than the heat transfer coefficient for a fluid circulation inside a tube of a conventional tube heat exchanger. Thus, for the same exchange capacity, the transfer area is much lower in plate-type heat exchangers.

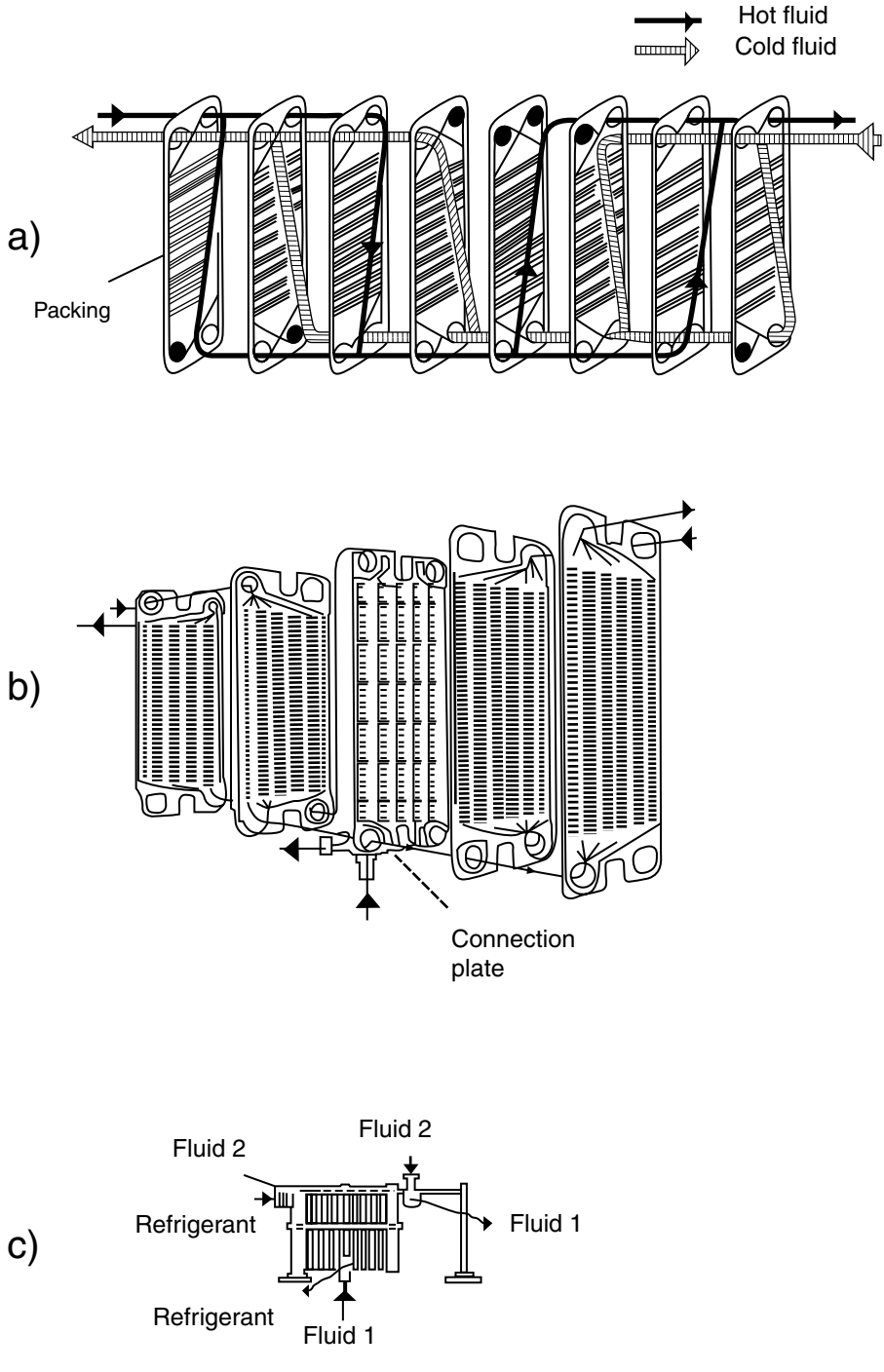

FIGURE 13.13
Plate-type heat exchanger.

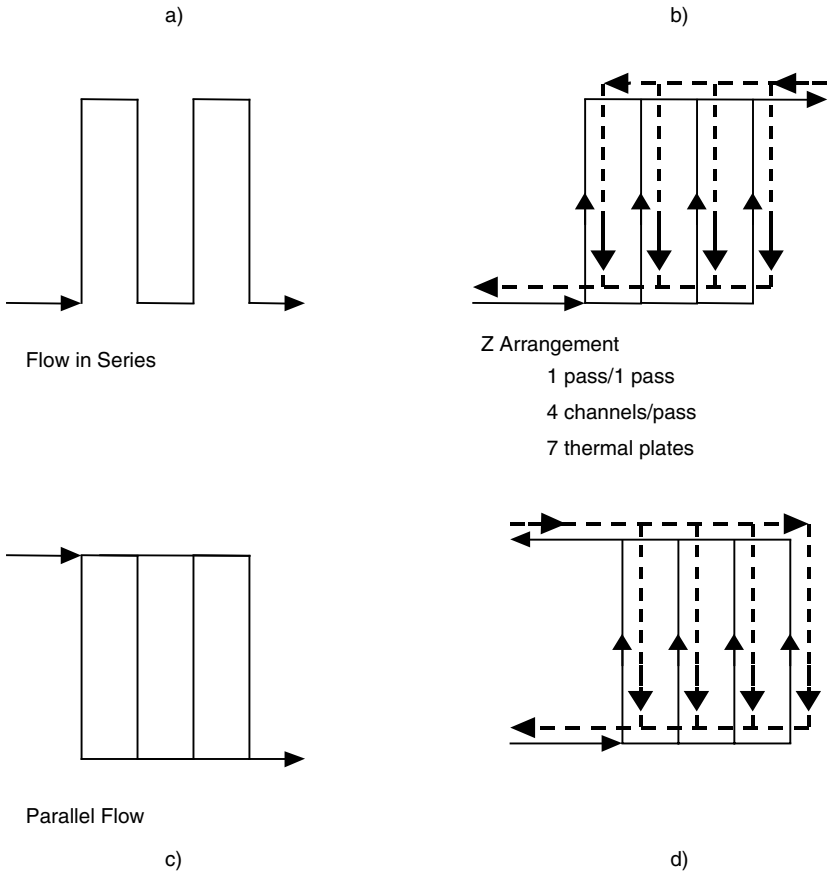

FIGURE 13.14
Fluid circulation for different arrangements.

In spite of these advantages, plate-type heat exchangers have some limitations with respect to tube-heat exchangers. Thus, it is possible to build plate-type heat exchangers that can withstand 20 atm as maximum pressure; in extreme cases the gaskets can withstand 260°C as maximum. In addition, the pressure drop in this type of heat exchanger is greater than in tube exchangers. These limitations define the application of plate-type heat exchangers.

13.5.1 Design Characteristics

Consider a heat exchanger formed by four plates like the one shown in Figure 13.15. It can be observed that one of the fluids circulates through a channel receiving heat from the other fluid through the plates. This is one of the simpler cases involving plate-type heat exchangers. However, in general they are constituted by a greater number of plates placed one next to

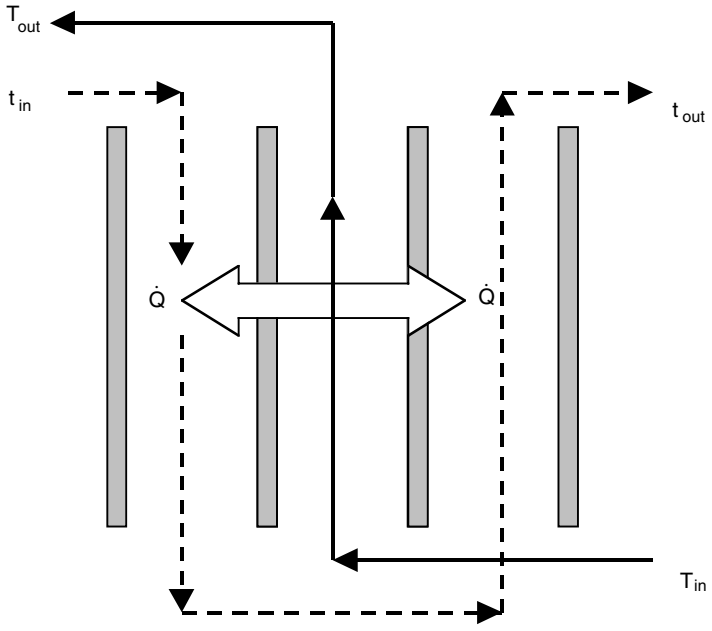

FIGURE 13.15
Basic unit of a plate-type heat exchanger.

the other, and fluids flow according to the arrangements shown in Figure 13.14 or with more complicated arrangements.

In any case, the basic equations used to set up the mathematical model are similar to those of other types of heat exchangers. Thus, the fundamental equations are:

Global energy balance: The cold fluid increases its temperature and absorbs the heat flow given up by the hot fluid:

$$\dot{Q} = w_h \left(\hat{C}_P\right)_h \left(T_{\text{in}} - T_{\text{out}}\right) = w_c \left(\hat{C}_P\right)_c \left(t_{\text{out}} - t_{\text{in}}\right) \tag{13.76}$$

Heat transfer equation: The following equation can be applied to a system like the one shown in Figure 13.15:

$$\dot{Q} = U\left(2A_p\right)\left(\Delta T\right)_{ml} \tag{13.77}$$

in which U is the global heat-transfer coefficient, A_P is the area of one plate, and $(\Delta T)_{ml}$ is the logarithmic mean temperature difference, taken as if the fluids circulate in countercurrent. For more complex systems, the velocity equation is similar to the last one but includes a correction factor F for the

logarithmic mean temperature difference, and its value depends on the passing system of the fluids and the number of transfer units. Therefore:

$$\dot{Q} = U A_t \left(\Delta T\right)_{ml} F \tag{13.78}$$

In this equation, A_t is the total heat transfer area of the exchanger.

The total area is the product of the area of one plate times the number of plates in which there is heat transfer:

$$A_t = N \cdot A_p \tag{13.79}$$

The plates through which heat is transferred are called **thermal plates**. It should be indicated that the plates at the end of the heat exchanger and the intermediate ones that distribute the fluids are not thermal, since in these plates there is no heat exchange between the fluids. Therefore, if there are N thermal plates, the number of channels by which fluids circulate is $N + 1$.

13.5.2 Number of Transfer Units

The *number of transfer units* (*NTU*) is defined as the relationship between the temperature increase experienced by the fluid being processed and the logarithmic mean temperature increase:

$$NTU = \frac{T_{\text{in}} - T_{\text{out}}}{\left(\Delta T\right)_{ml}} \tag{13.80}$$

From the velocity equation and from the total heat flow transferred (Equations 13.76 and 13.77) it is obtained that:

$$\dot{Q} = U\left(2A_p\right)\left(\Delta T\right)_{ml} = w_h \left(\hat{C}_P\right)_h \left(T_{\text{in}} - T_{\text{out}}\right) \tag{13.81}$$

Hence, the number of transfer units can be expressed as:

$$NTU = \frac{2A_p U}{w_h \left(\hat{C}_P\right)_h} \tag{13.82}$$

Considering a global mean heat-transfer coefficient and the total area:

$$NTU = \frac{A_t U_m}{w_h \left(\hat{C}_P\right)_h} \tag{13.83}$$

The number of transfer units is also called execution factor, thermal length, or temperature ratio. This factor is needed to evaluate the correction factor *F* of the logarithmic mean temperature difference, as will be seen later. Also, depending on the value of this factor, the type of plates that should be used in the heat exchanger for a given process can be chosen. Thus, for low values of *NTU*, short and wide plates should be used, which are characterized by low heat transfer coefficients and small pressure drops in each pass. On the other hand, for high *NTU* values, long and narrow plates with deep folds on their surfaces are used, and small hollows between plates are left in order to have narrow channels.

Likewise, the plates in which folds are formed by channels that have obtuse angles yield high *NTU* values for each plate while, if the angle formed by the folds is acute, the value of *NTU* of the plate is low, offering smaller resistance to the flow of the fluid that passes between plates.

13.5.3 Calculation of the True Logarithmic Mean Temperature Difference

In this type of heat exchanger, the true increment or logarithmic mean temperature difference is determined in a similar way to the case of shell and tube heat exchangers. The logarithmic mean temperature increase is defined as if the operation were carried out in countercurrent (Equation 13.57).

The temperature increase should be corrected with a factor *F*, whose value can be graphically obtained once the number of transfer units (*NTU*) and the passes system of the hot and cold fluids through the channels of the heat exchangers are known. *F* can be calculated from Figure 13.16, from the *NTU* and the type of passes of the fluids (Marriott, 1971; Raju and Chand, 1980).

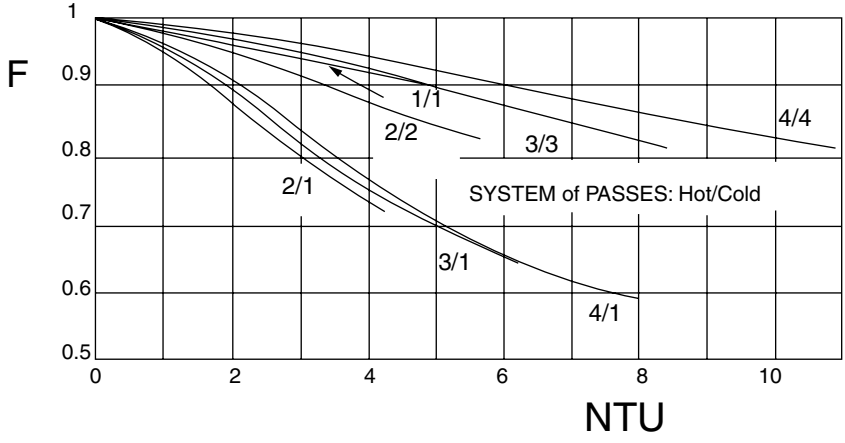

FIGURE 13.16
Correction factors *F* for different systems of passes. (Adapted from Marriott, J. *Chem. Eng.*, 5, 127–134, 1971.)

In these heat exchangers the correction factor can have high values, close to one, and in addition to high heat transfer coefficients, very high performances can be obtained. In plate-type heat exchangers, the temperature difference between the hot stream at the inlet point (T_{in}) and the cold fluid at the outlet point (t_{out}) can be as small as 1°C, whereas for a shell and tube heat exchanger this difference is close to 5°C.

13.5.4 Calculation of the Heat Transfer Coefficients

There is an expression for plate-type heat exchangers that relates Nusselt, Reynolds, and Prandtl numbers according to the equation:

$$(Nu) = C(\mathrm{Re})^x (Pr)^y (\eta/\eta_w)^z$$

where C is a constant.

The values of the constant and exponents of this equation are experimentally determined and are only valid for each type of plate for which they were obtained. Also, they depend on the circulation regime. In these heat exchangers, it is considered that the fluid circulates in laminar regime when the value of the Reynolds number is lower than 400, while for values higher than 400, the fluid circulates in turbulent regime.

In turbulent regime (Re > 400), these variables range between the following values (Marriott, 1971):

C = 0.15 to 0.40
x = 0.65 to 0.85
y = 0.30 to 0.45 (generally 0.333)
z = 0.05 to 0.20

The Reynolds number depends on the system of passes by which different fluids flow. Thus, for flow-in series, in which each fluid passes through each channel as one stream, the Reynolds number is defined according to the equation:

$$(\mathrm{Re}) = \frac{\rho v D_e}{\eta} = \frac{G D_e}{\eta} \tag{13.84a}$$

where v is the linear circulation velocity of the fluid and G its correspondent global mass flux, while D_e is the equivalent diameter.

When the system of passes is in parallel flow, the streams of each fluid are subdivided into substreams (Figure 13.14) that cross the channels between plates. The Reynolds number is given by:

$$(\mathrm{Re}) = \frac{(G/n)De}{\eta} \tag{13.84b}$$

In this equation, n is the number of channels of each type of fluid. If n_c is the number of channels for the hot fluid, the Reynolds number for this fluid is calculated applying the last equation for $n = n_h$. For the cold fluid, the same equation is applied using $n = n_c$, where n_c is the number of channels in which the stream of this fluid is divided.

One of the most used equations for the calculation of the individual heat transfer coefficients in turbulent regime is:

$$(Nu) = 0.374(\mathrm{Re})^{2/3}(Pr)^{1/3}(\eta/\eta_w)^{0.15} \tag{13.85}$$

An equation easy to apply in turbulent regime and that uses the mean values of Reynolds and Prandtl numbers is (Bunopane et al., 1963; Usher, 1970):

$$(Nu) = 0.2536(\mathrm{Re})^{0.65}(Pr)^{0.4} \tag{13.86}$$

The geometry of plates is not taken into account in all these equations. However, some equations include geometric factors, such as pass length (L) and the spacing between plates (b). One of these is that of Troupe et al. (1960):

$$(Nu) = (0.383 - 0.0505^{L/b})(\mathrm{Re})^{0.65}(Pr)^{0.4} \tag{13.87}$$

Other equations have been proposed for the calculation of film coefficients when working in laminar regime (Re < 400), one of them being a variation of the Sieder–Tate equation (Marriott, 1971):

$$(Nu) = C\left(\mathrm{Re}\, Pr\, \frac{D_e}{L}\right)^{1/3}(\eta/\eta_w)^{0.14} \tag{13.88}$$

where the value of the constant C ranges between 1.86 and 4.5, depending on the geometry of the system.

Another equation used in laminar regime is (Jackson and Troupe, 1964; Raju and Chand, 1980):

$$h = 0.742\hat{C}_p G(\mathrm{Re})^{-0.62}(Pr)^{-2/3}(\eta/\eta_w)^{0.14} \tag{13.89}$$

The equivalent diameter D_e that appears in the Reynolds and Nusselt numbers is defined as four times the hydraulic radius, which in turn is the ratio between the area through which the fluid flows between the plates and the wet perimeter:

$$D_e = 4r_H = 4\frac{ab}{2a} = 2b \tag{13.90}$$

In this equation, a is the width of the plates and b is the distance between them.

It is interesting to point out that, for a tube heat exchanger, the equivalent diameter coincides with the pipe diameter. Therefore, from the heat exchange standpoint, the plate-type heat exchanger will be equal to a tube heat exchanger whose diameter is equal to double the thickness of the packings. If one takes into account that the thickness is usually 2 to 5 mm, it turns out that the plate-type heat exchanger behaves like one with tubes of 4 to 10 mm of diameter. In spite of the fact that a tube heat exchanger with these characteristics would be ideal for the desired heat exchange, it is very difficult to achieve, since mechanical difficulties arise during the building process.

For the calculation of individual coefficients, graphs exist in which the values of such coefficients correlate with the so-called specific pressure drop (Figure 13.17).

The specific pressure drop (J) is defined as the ratio between the pressure drop and the number of transfer units:

$$J = \frac{\Delta P}{NTU} \tag{13.91}$$

As Figure 13.17 shows, in most of the plate-type heat exchangers the variation of the film coefficients due to the specific pressure drop is similar. Curve A refers to special plates that have a spacing greater than usual, designed for operations in which the value of NTU is very low, or for

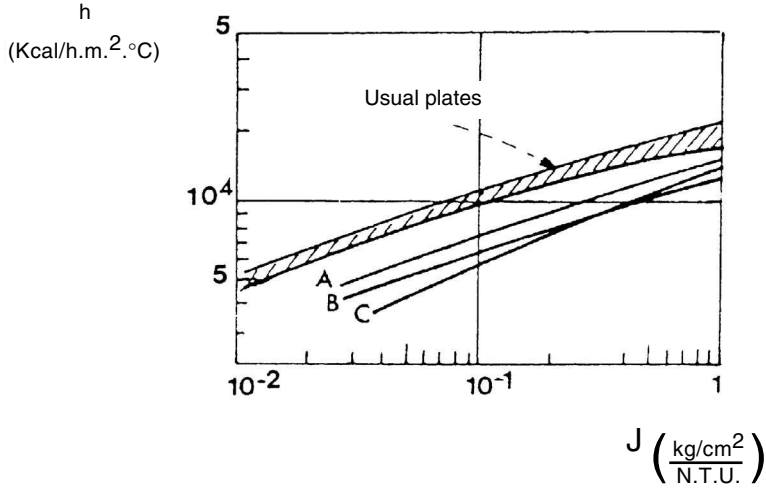

FIGURE 13.17
Variation of individual heat transfer coefficients with the specific pressure drop. (Adapted from Marriott, J. *Chem. Eng.*, 5, 127–134, 1971.)

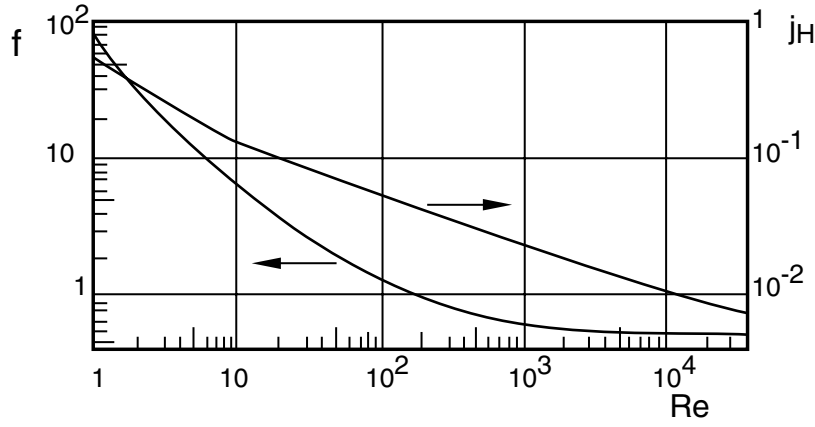

FIGURE 13.18
Variation of the friction factor f and j_H with the Reynolds number.

processes in which fluids with high solids content should be treated. Curve *B* is used for similar cases, in which plates have fewer foldings per unit area and, therefore, fewer contact points. Finally, Curve *C* is used for smooth plates with stamped waves that have a small effect on the fluid flow.

The film coefficients can also be obtained from the Colburn coefficient j_H for heat transfer. Figure 13.18 shows graphically the value of j_H as a function of Reynolds number for one type of plate.

Once the individual coefficients are obtained, the global heat transfer coefficient must be calculated according to the global equation:

$$\frac{1}{U} = \frac{1}{h_C} + \frac{e}{k_p} + \frac{1}{h_F} + R_h + R_c \tag{13.92}$$

In this equation, e is the thickness of the plate wall, k_p is the thermal conductivity of the material of which the plate is made, and R_h and R_c are the soiling factors of the hot and cold fluids, respectively.

13.5.5 Calculation of Head Losses

It is extremely important to know the head or pressure losses experienced by the fluids when flowing through plate-type heat exchangers, since when such drop is known, the type of plates for the heat exchanger can be chosen. Variations of the Fanning equation can be used to calculate the pressure drop. One of these equations is:

$$\Delta P = 2 f \frac{G^2 L}{g D_e \rho} \tag{13.93}$$

In this equation, G is the mass flux of the fluid, L is the length of the plate or the distance that each fluid should cross when passing through the channel between two plates, g is the gravitational constant, and f is the friction factor.

The friction factors calculated from the flowing linear velocity of the fluids, in turbulent regime, are 10 to 60 times higher in the flow through channels in a plate-type heat exchanger than in the flow through a tube for similar Reynolds numbers.

For the turbulent circulation regime, the friction factor can be calculated from the following equation (Cooper, 1974; Raju and Chand, 1980):

$$f = \frac{2.5}{(\mathrm{Re})^{0.3}} \tag{13.94}$$

The friction factor depends on the type of plate. Figure 13.18 shows graphically the variation of the friction factor with Reynolds number.

13.5.6 Design Procedure

In the design of heat exchangers, it is generally desirable to calculate the area of heat exchange or the number of thermal plates required to perform an operation in which the inlet and outlet temperatures of one of the fluids, the inlet temperature of the other fluid, the mass flow of both streams, the physical properties of both fluids, and the characteristics of the plates to use are known.

The design of a plate-type heat exchanger is complex, so in order to find a solution for the mathematical model, it is necessary to use computer programs. However, there are simpler methods that allow one to obtain a good approximation for the design of these heat exchangers, even in such cases in which the circulating fluids behave as non-Newtonian fluids.

A design method based on the use of correction factors F of the logarithmic mean temperature difference is explained next. A series of hypotheses should be made to solve the mathematical model stated. It will be assumed that the following conditions are complied with:

- Heat losses to the surroundings are negligible.
- No air bags are formed inside the heat exchanger.
- The overall heat transfer coefficient is constant along the heat exchanger.
- The temperature inside each channel only varies along the direction of flow.
- In parallel flow, the global stream is equally divided among all the channels.

These assumptions allow one to solve the problem set up at the beginning of the section for fluids flowing in series or in parallel.

Next, the steps to calculate the number of plates in the design of a desired heat exchanger will be explained:

Data:

T_e, T_s, t_e, w_h, w_c

Physical properties of the fluids: k, ρ, η, $\hat{C}_P$ (obtained from tables, graphs, or equations)

Characteristics of the plates: k_p, L, a, b, e (given by the manufacturer)

Calculation steps:

1. Calculation of the total heat flow transferred by the hot fluid and gained by the cold one, using Equation 13.76:

$$\dot{Q} = w_h \left(\hat{C}_P\right)_h \left(T_e - T_s\right)$$

2. Calculation of the outlet temperature of the cold fluid, from Equation 13.76:

$$t_{\text{out}} = t_{\text{in}} + \frac{\dot{Q}}{w_c \left(\hat{C}_P\right)_c}$$

3. Calculation of the physical properties of the fluids at the mean temperatures, using tables, graphs, or the adequate equations.
4. Calculation of the logarithmic mean temperature difference $(\Delta T)_{ml}$.
5. Determination of the *number of transfer units* (*NTU*) with Equation 13.80
6. Calculation of the correction factor F of the logarithmic mean temperature using Figure 13.16
7. Determination of the Reynolds number of each stream, using Equations 13.84a and b, depending on the arrangement of the flow (series or parallel)
8. Calculation of the individual heat transfer coefficients h by Equations 13.85 to 13.89, depending on the circulation regime. They can also be determined from Figure 13.17 or 13.18
9. Calculation of the overall heat transfer coefficients U using Equation 13.92, once the film coefficients are known and the soiling factors have been estimated.

10. Calculation of the total heat transfer area from Equation 13.78:

$$A_t = \frac{\dot{Q}}{U\left(\Delta T\right)_{ml} F}$$

11. Determination of the number of thermal plates from the total area and the area of each plate: $N = A_t/A_p$

These steps are common for the calculation of heat exchangers that work either in series or parallel. However, in the case of an operation in parallel, an iterative process for the calculation of the number of thermal plates should be carried out. This is because in step 7, the number of channels of the hot (n_h) and cold (n_c) streams should be assumed in order to calculate the corresponding Reynolds number, which allows continuation of following calculation steps until the number of thermal plates is obtained. Once this number N is known, the number of total channels will be known: $n = N + 1$. In the case that N is odd, the number of channels is even, so the values of n_c and n_f are equal ($n_h = n_c = (N + 1)/2$). On the other hand, if N is even, the number of channels is odd, so the number of channels of a type is higher than the other type in one unit. Once the values of n_h and n_c are obtained from N, they are compared with those assumed in step 7. If the assumed and calculated values coincide, then the process is finished; otherwise, the process is repeated from steps 7 to 11. The iterative process is repeated until such values coincide.

13.6 Extended Surface Heat Exchangers

In many cases, heat exchangers whose surface has been extended by means of *fins* are used to improve the heat transfer. Fins can have different shapes (Figure 13.19), such as longitudinal, circular, spiral, or tang, among others, and can be made of material the same as or different from that of the tubes. In any case, a good contact between the tube and the fin should be ensured. Fins are widely used in cooling processes, especially when it is desirable to eliminate heat by using fluids that are bad conductors, such as gases.

A fin will not always noticeably improve heat transfer, since the transfer depends on the resistance that more greatly affects this transfer. Thus, the general expression that relates the global heat transfer coefficient in reference to the internal area with the different resistance, neglecting the possible soiling effects, is obtained.

$$\frac{1}{U_i A_i} = \frac{1}{h_e A_e} + \frac{e}{k A_{ml}} + \frac{1}{h_i A_i} \tag{13.95}$$

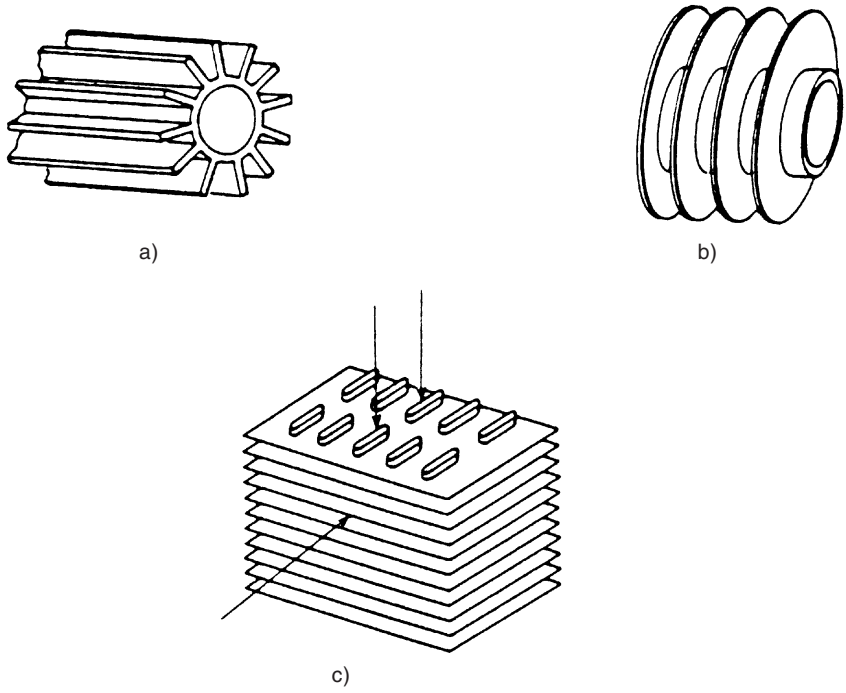

FIGURE 13.19
Different types of fins: (a) longitudinal; (b) transversal; (c) tubes with continuous fins.

The left-hand side of this equation represents global resistance to the heat transfer and is the summation of three resistances: those due to two fluids, plus the resistance offered by the metallic wall. Generally, the resistance exerted by the metal is not high if compared to the other two resistances, so it can be considered negligible.

If Equation 13.95 is observed, it can be seen that A_e is the external area. Therefore, if fins extend, then the value of $1/(h_e A_e)$ is decreased, so the global resistance decreases in such a way that heat transfer is favored. This heat removal will be more or less important depending on the values acquired by the individual heat transfer coefficients of the fluids. If the external coefficient h_e is very small compared to h_i, the external resistance will be much greater than the internal resistance; therefore, if the external area A_e is increased, the global resistance decreases almost proportionally with the increase of the external area. On the other hand, if h_i is much smaller than h_e, the resistance of the internal fluid will be much greater than that of the external; therefore, the increase in the external area will slightly influence the global resistance, and then fins do not always noticeably increase heat transfer.

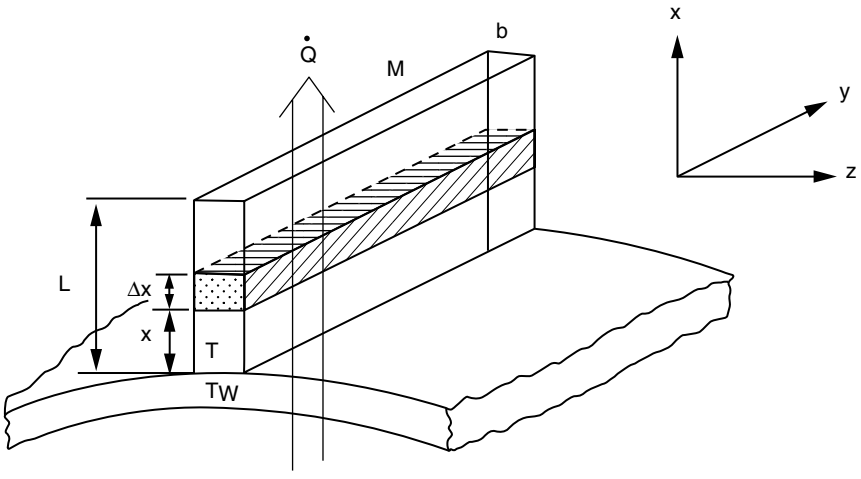

FIGURE 13.20
Longitudinal fin; geometric characteristics and direction of the heat flow.

13.6.1 Mathematical Model

Among the different types of fins, only the problem of the longitudinal fins will be set up. This model is similar for the other types of fins, although the mathematical solution has not been performed in all cases because it is difficult to obtain.

Consider the fin shown in Figure 13.20. Its dimensions are those indicated; T_w is the temperature at the base of the fin and is constant. An energy balance can be accomplished by assuming the following:

- Heat transfer by conduction along the fins occurs only in the radial direction, so temperature is a function only of this coordinate.
- A fin dissipates heat by convection to the outside only along its lateral area and not by its edges. That is, it dissipates heat through the lateral area to the sides.
- The heat flux driven to the outside at any point of the fin, with a temperature T, is expressed as $q = h_e\ (T - T_e)$, where T_e is the temperature of the external fluid and h_e is the individual convective heat transfer coefficient within the external fluid.

The following equation is obtained when carrying out an energy balance in a differential element of the fin with a height Δx:

$$M b q(x) - M b q(x + \Delta x) - 2 M \Delta x h_e (t - T_e) = 0 \tag{13.96}$$

If the last expression is divided by the differential of the fin's volume (*M.b*. Δx) and is taken as the limit for $\Delta x \to 0$, the following equation results:

$$\frac{dq}{dx} = -\frac{2}{b} h_e \left(t - T_e\right) \tag{13.97}$$

Taking into account that the heat flux, according to Fourier's law, is:

$$q = -k\frac{dT}{dx}$$

then the following is obtained from Equation 13.97:

$$k\frac{d^2T}{dx^2} = \frac{2h_e}{b}\left(T - T_e\right) \tag{13.98}$$

This equation can be integrated on the boundary conditions:

For $x = 0$, $T = T_w$.
For $x = L$, $dT/dx = 0$.

This last condition is a maximum or minimum since at the end of the fin the temperature will be maximum or minimum depending on whether it heats or cools.

The integration of the differential equation on the boundary conditions stated before yields the following expression:

$$\frac{T - T_e}{T_W - T_e} = \frac{\cosh\left[\left(L - x\right)\left(\frac{2\,h_e}{k\,b}\right)^{1/2}\right]}{\cosh\left[L\left(\frac{2\,h_e}{k\,b}\right)^{1/2}\right]} \tag{13.99}$$

13.6.2 Efficiency of a Fin

The efficiency of a fin is defined as the ratio between the heat dissipated by the surface of the fin and the heat that would be dissipated if the entire surface were at the temperature of the base (T_w):

$$\eta = \frac{\text{heat dissipated by the fin's surface}}{\text{heat that would be dissipated if the surface were at } T_w}$$

In the case presented in the last section for longitudinal fins, the expression that can be used to obtain the efficiency of a fin is:

$$\eta = \frac{\int_0^L \int_0^M h_e \left(T - T_e\right) dy\, dx}{\int_0^L \int_0^M h_e \left(T_W - T_e\right) dy\, dx} \tag{13.100}$$

The integration of this expression yields the equation:

$$\eta = \frac{\tan h \left[L \sqrt{\frac{2\, h_e}{k\, b}} \right]}{L \sqrt{\frac{2\, h_e}{k\, b}}} \tag{13.101}$$

This last equation can be expressed in graphical form (Figure 13.21) representing the efficiency against the adimensional product $L(2h_e/k\,b)^{1/2}$. It can be observed that the value of this product depends on the ratio h_e/k in such a way that when it is small, the efficiency of the fin tends to be one. On the other hand, when the values of h_e are high, the efficiency decreases to very low values, so the use of fins is neither needed nor efficient, as indicated before.

The increase of temperatures between a given section and the external fluid appears in the expression that defines the efficiency (Equation 13.93)

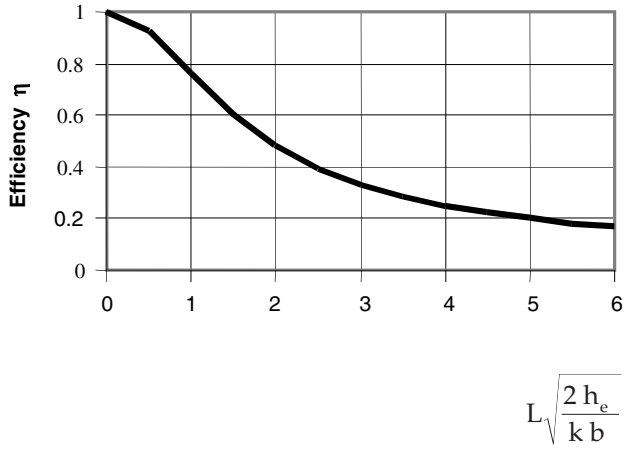

FIGURE 13.21
Efficiency of a longitudinal fin.

so that $\Delta T = T - T_e$. The value of ΔT varies from the base of the fin up to its end, so the solution of the last integral should take into account this variation. This was considered when obtaining the last expression of efficiency. However, if an average of the difference between the temperature of the fin and the fluid is used ($(\Delta T)_m = T - T_e$, where T_m is a mean temperature of the fin), the integration of the expression of the efficiency will be:

$$\eta = \frac{\int_0^L \int_0^M h_e \left(T_m - T_e\right) dy\, dx}{\int_0^L \int_0^M h_e \left(T_W - T_e\right) dy\, dx} = \frac{T_m - T_e}{T_W - T_e} = \frac{\left(\Delta T\right)_m}{\left(\Delta T\right)_W} \tag{13.102}$$

where $(\Delta T)_W = T_W - T_e$.

This last equation points out that the efficiency of this type of fin can be expressed as a relationship between the average temperature increase of the fin and the fluid and the difference between the temperature of the fin's base and the fluid.

The mathematical model and its solution, as well as the expression of the temperature profile along the fins and its efficiency, performed here for longitudinal fins, can be similarly done for other types of fins.

13.6.3 Calculation of Extended Surface Heat Exchangers

The calculation of the global heat transfer coefficient in heat exchangers with fins depends on the presence of fins, since the heat transferred from the metal surface to the fluid will be the addition of two flows, one through the area of the naked tube and the other through the surface of the fin. Therefore, the global coefficient referred to the internal area will be expressed as:

$$U_i = \frac{1}{\dfrac{A_i}{h_e\left(\eta A_a + A_e\right)} + \dfrac{e\, A_i}{k\, A_{m\,l}} + \dfrac{1}{h_i}} \tag{13.103}$$

in which A_i represents the internal surface of the tube, A_a the fin's surface, A_e that of the naked tube, and h the efficiency of the fin.

Obtaining U_i is not so easy, since the calculation of h_e adds more difficulties than in the cases of heat exchangers made of naked tubes. This is due to the fact that the flow outside the fins is modified, so the film coefficient will be different from the coefficient of a smooth tube. The values of h_e for the case of tubes with fins should be experimentally obtained for the different types of fins. Generally, the manufacturers of this type of heat exchangers should provide these data.

13.7 Scraped Surface Heat Exchangers

Scraped surface heat exchangers consist of two concentric tubes in which, generally, a high viscosity fluid circulates inside the internal tube. The internal surface of this tube is scraped by a set of blades inserted in a central axis that spins at a certain number of revolutions. This type of heat exchanger is used in the food industry and is known as the Votator heat exchanger.

The design of this type of heat exchanger assumes that the heat transferred from the surface of the tube to the viscous fluid or vice versa is carried out by conduction under unsteady state. It is considered that such heat transfer by conduction is similar to conduction in a semi-infinite solid. Thus, the equation that relates the temperature T of a point of the fluid at a distance x from the wall with time can be expressed as:

$$\frac{T_w - T}{T_w - T_0} = fer\left(\frac{x}{2\sqrt{\alpha t}}\right) \tag{13.104}$$

In this equation, T_w is the temperature of the wall, T_0 is the initial temperature of the considered point, while *fer* is the so-called Gauss' error function, and α is the thermal diffusivity of the fluid.

If there are P scraping blades inserted in the central axis, which spin at a frequency N, the time that a blade takes to pass at the same point of the fluid is $t_N = 1/(P\,N)$. Heat transfer by conduction within the viscous fluid occurs during this period.

The total heat transferred from the wall to the fluid during this period is:

$$Q_T = h_i\, A\left(T_P - T_0\right) t_N \tag{13.105}$$

where h_i is the individual convective heat transfer coefficient for the viscous fluid and A is the heat transfer area.

On the other hand, if an infinitesimal time is considered, the heat flow can be expressed according to Fourier's equation that, in the tube's wall, for $x = 0$ is:

$$dq = -k\left(\frac{\partial T}{\partial x}\right)_{x=0}$$

If it is known that:

$$\frac{d}{dx}\, fer\left(\frac{x}{2\sqrt{\alpha t}}\right) = \frac{1}{\sqrt{\pi \alpha t}} \exp\left(\frac{-x^2}{4\alpha t}\right)$$

the temperature gradient for $x = 0$ can be obtained from Equation 13.104:

$$\left(\frac{\partial T}{\partial x}\right)_{x=0} = \frac{T_w - T_0}{\sqrt{\pi \alpha t}}$$

Hence:

$$dq = k\frac{T_w - T_0}{\sqrt{\pi \alpha t}}$$

Since:

$$dq = \frac{1}{A}\frac{dQ}{dt}$$

$$\frac{1}{A}\frac{dQ}{dt} = k\frac{T_w - T_0}{\sqrt{\pi \alpha t}}$$

This equation with separable variables can be integrated on the boundary condition:

For $t = t_N$, $Q = Q_T$

obtaining:

$$Q_T = A2k\left(T_w - T_0\right)\sqrt{\frac{t_N}{\pi \alpha}}$$

It is easy to deduce the following when comparing the last expression with Equation 13.105:

$$h_i = 2\sqrt{\frac{k^2}{\pi t_N \alpha}}$$

Since $\alpha = k/(\rho \hat{C}_P)$ and $t_N = 1/(P\ N)$, the individual coefficient for the viscous fluid is:

$$h_i = 2\sqrt{\frac{k\rho \hat{C}_P PN}{\pi}} \tag{13.106}$$

There are other equations for the calculation of the individual coefficient on the internal side besides the last expression. Thus, for heat exchange between hot and cold water, an equation relates the coefficient h_i with the spinning velocity of the rotor:

$$\log N = 8.36 \times 10^{-5} h_i + 0.164 \tag{13.107}$$

for values between 5 and 31.67 rps.

Another equation used to calculate h_i is:

$$(Nu) = 4.9\,(\mathrm{Re})^{0.57}(Pr)^{0.47}\left(\frac{d_i\,N}{v}\right)^{0.17}\left(\frac{d_i}{L}\right)^{0.37} \tag{13.108}$$

for N values between 1.5 and 7.5 rps.

13.8 Agitated Vessels with Jacket and Coils

The calculation of this type of equipment requires previous knowledge of the individual coefficient of the fluid contained inside the vessel and of the fluid that circulates inside the coil or the jacket.

13.8.1 Individual Coefficient inside the Vessel

Helicoidal coils: For the case of baffled agitators and for values of Reynolds number between 300 and 4×10^5, the following expression is used:

$$\frac{h\,D_T}{k} = 0.87\left(\frac{D_P^2\,N\,\rho}{\eta}\right)^{0.62}\left(\frac{\hat{C}_P\,\eta}{k}\right)^{1/3}\left(\frac{\eta}{\eta_w}\right)^{0.14} \tag{13.109}$$

In the case of flat-baffle disk turbine agitators and values of the Reynolds module between 400 and 2×10^5, the following equation is used:

$$\frac{h\,d_0}{k} = 0.17\left(\frac{D_P^2\,N\,\rho}{\eta}\right)^{0.67}\left(\frac{\hat{C}_P\,\eta}{k}\right)^{0.37}\left(\frac{D_P}{D_T}\right)^{0.1}\left(\frac{d_0}{D_T}\right)^{0.5} \tag{13.110}$$

The following variables are defined in these expressions:

D_T = Internal diameter of the vessel
D_p = Diameter of the agitator's baffle
d_o = External diameter of the coil tube
N = Spinning velocity of the agitator

Jackets: The following expression is used to calculate the coefficient of the fluid inside the agitated vessel:

$$\frac{h\,D_T}{k} = a\left(\frac{D_P^2\,N\,\rho}{\eta}\right)^b\left(\frac{\hat{C}_P\,\eta}{k}\right)^{1/3}\left(\frac{\eta}{\eta_w}\right)^m \tag{13.111}$$

in which a, b, and m depend on the type of agitator used. The values of these parameters are given in the next table.

Agitator	a	b	m	Re
Baffles	0.36	2/3	0.21	300 to 3×10^5
Helical	0.54	2/3	0.14	2000
Anchor	1	1/2	0.18	10 to 300
Anchor	0.36	2/3	0.18	300 to 4×10^4
Flat-baffles disk turbine	0.54	2/3	0.14	40 to 3×10^5
Helical coil	0.633	1/2	0.18	8 to 10^5

13.8.2 Individual Coefficient inside the Coil

The calculation of this individual coefficient is performed as in the case of pipes, and the value obtained should be multiplied by the value of the coefficient γ, defined by the equation:

$$\gamma = 1 + 3.5\frac{d_i}{D_S} \tag{13.112}$$

In this equation, d_i is the internal diameter of the coil tube and D_S is the diameter of the coil.

13.8.3 Individual Coefficient in the Jacket

Generally, condensing vapor circulates through the jacket; the individual heat transfer coefficients usually have high values between 8000 and 9000 W/(m²°C). The calculation of this coefficient can also be made, assuming that the jacket is a circular ring and using one of the equations given in Section 13.2.3.

13.9 Heat Exchange Efficiency

Heat exchange efficiency is defined as the relation between the real heat flow and the maximum heat flow possible. This value could be obtained in a heat exchanger working in countercurrent and with an infinite area. Assuming

no heat losses to the outside, two cases can occur for a heat exchanger with infinite area:

- $w_h\ (\hat{C}_P)_h < w_c\ (\hat{C}_P)_c$, where the outlet temperature of the hot fluid is equal to the temperature of the cold fluid at the inlet
- $w_c\ (\hat{C}_P)_c < w_h\ (\hat{C}_P)_h$, in which case the outlet temperature of the cold fluid coincides with the inlet temperature of the hot fluid

According to these statements, it can be said that the efficiency relates the heat flow of the processed fluid with the maximum possible flow, with a limit not to contradict the second law of thermodynamics.

The expression that defines the efficiency is:

$$\varepsilon = \frac{w_h \left(\hat{C}_P\right)_h \left(T_{\text{in}} - T_{\text{out}}\right)}{\left(w_h\ \hat{C}_P\right)_{\text{min}} \left(T_{\text{in}} - t_{\text{in}}\right)} = \frac{w_c\ \hat{C}_P)_c \left(t_{\text{out}} - t_{\text{in}}\right)}{\left(w_h\ \hat{C}_P\right)_{\text{min}} \left(T_{\text{in}} - t_{\text{in}}\right)} \tag{13.113}$$

in which $(w_h\ \hat{C}_P)_{\text{min}}$ is the lower value of $w_h\ (\hat{C}_P)_h$ and $w_c\ (\hat{C}_P)_c$.

If thermal capacity per unit time of any fluid is defined as the product of the mass flow times its specific heat, that is:

$$C = w_h\ \hat{C}_P \tag{13.114}$$

then, Equation 13.113 can be expressed as:

$$\varepsilon = \frac{C_h \left(T_{\text{in}} - T_{\text{out}}\right)}{C_{\text{min}} \left(T_{\text{in}} - t_{\text{in}}\right)} = \frac{C_c \left(t_{\text{out}} - t_{\text{in}}\right)}{C_{\text{min}} \left(T_{\text{in}} - t_{\text{in}}\right)} \tag{13.115}$$

In any case, if the efficiency of a determined heat exchanger is known, it is possible to know the heat flow transferred by knowing only the inlet temperatures of the hot and cold fluids:

$$\dot{Q} = \varepsilon\ C_{\text{min}} \left(T_{\text{in}} - t_{\text{in}}\right) \tag{13.116}$$

since it can be observed from Equation 13.113 that:

$$\dot{Q} = C_h \left(T_{\text{in}} - T_{\text{out}}\right) = C_c \left(t_{\text{out}} - t_{\text{in}}\right) = \varepsilon\ C_{\text{min}} \left(T_{\text{in}} - t_{\text{in}}\right) \tag{13.117}$$

It can be seen that it is possible to calculate the heat flow transferred without knowing the outlet temperatures of the fluids (needed in conventional calculations of heat exchangers) by using Equation 13.117, since for the calculation of the heat flow transferred through the exchange area, the logarithmic mean temperature $(\Delta T)_{ml}$ should be calculated first.

Next, an example of the calculation system using the efficiency for a countercurrent system will be presented. Consider the heat flow transferred in a

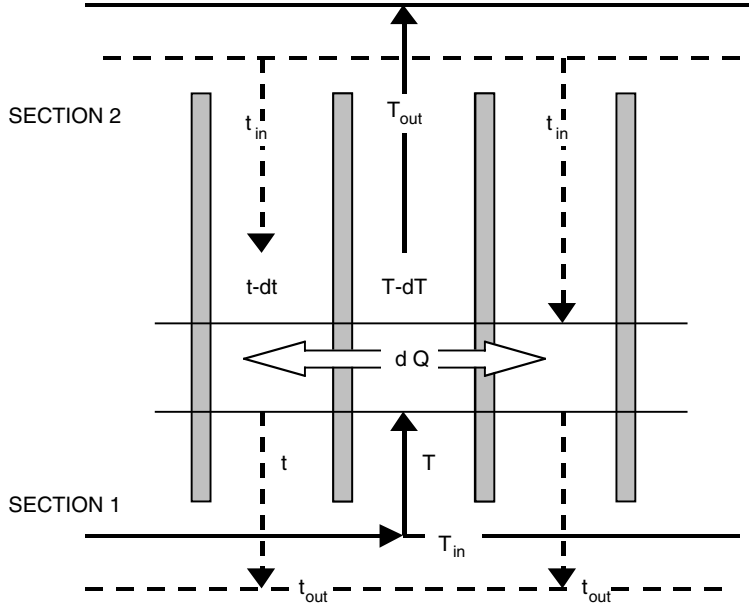

FIGURE 13.22
Heat transfer for circulation of fluids in countercurrent.

differential area *dA* for the system shown in Figure 13.22. An energy balance in this differential area, taking into account the heat transfer velocity is:

$$d\dot{Q} = C_h\, dT = C_c\, dt = U_m\, dA\left(T - t\right) \tag{13.118}$$

If the energy balance is performed between section 1 and any other, it is obtained that:

$$C_h\left(T_{\text{in}} - T\right) = C_c\left(t_{\text{out}} - t_{\text{in}}\right)$$

Hence:

$$T - t = T_{\text{in}} - \frac{C_c}{C_h}\, t_{\text{out}} + \left(\frac{C_c}{C_h} - 1\right) t \tag{13.119}$$

Substituting this expression in Equation 13.118 yields:

$$\frac{U_m\, d\, A}{C_c} = \frac{dt}{T_{\text{in}} - \dfrac{C_c}{C_h}\, t_{\text{out}} + \left(\dfrac{C_c}{C_h} - 1\right) t}$$

This equation can be integrated on the boundary conditions:

$$\text{For } A = 0,\ t = t_{out}$$
$$\text{For } A = A,\ t = t_{in}$$

obtaining:

$$U_m A\left(\frac{C_c - C_h}{C_c C_h}\right) = \ln\left[\frac{T_{in} - t_{out}}{T_{in} - \frac{C_c}{C_h}\ t_{out} + \left(\frac{C_c}{C_h} - 1\right) t_{in}}\right]$$

or:

$$-U_m A\left(\frac{C_c - C_h}{C_c C_h}\right) = \ln\left[\frac{\left(T_{in} - t_{in}\right) - \frac{C_c}{C_h}\left(t_{out} - t_{in}\right)}{\left(T_{in} - t_{in}\right) - \left(t_{out} - t_{in}\right)}\right]$$

Equation 13.115 can be expressed as:

$$\frac{t_{out} - t_{in}}{T_{in} - t_{in}} = \varepsilon\ \frac{C_{min}}{C_c}$$

that, substituted in the last equation, allows one to obtain the efficiency value according to the expression:

$$\varepsilon = \frac{1 - \exp\left(-U_m A \frac{C_c - C_h}{C_c C_h}\right)}{\frac{C_{min}}{C_h} - \frac{C_{min}}{C_c}\exp\left(-U_m A \frac{C_c - C_h}{C_c C_h}\right)} \tag{13.120}$$

Two cases can occur:

1. If $C_h < C_c$, then: $C_{min} = C_h$ and $C_{max} = C_c$.
   So:

$$\varepsilon = \frac{1 - \exp\left(-\frac{U_m A}{C_h}\left(1 - \frac{C_h}{C_c}\right)\right)}{1 - \frac{C_h}{C_c}\exp\left(-\frac{U_m A}{C_h}\left(1 - \frac{C_h}{C_c}\right)\right)} \tag{13.121}$$

2. If $C_c < C_h$, then: $C_{min} = C_c$ and $C_{max} = C_h$.
   Then:

$$\varepsilon = \frac{1-\exp\left(-\frac{U_m A}{C_c}\left(\frac{C_c}{C_h}-1\right)\right)}{\frac{C_c}{C_h}-\exp\left(-\frac{U_m A}{C_c}\left(\frac{C_c}{C_h}-1\right)\right)} = \frac{1-\exp\left(-\frac{U_m A}{C_c}\left(1-\frac{C_c}{C_h}\right)\right)}{1-\frac{C_c}{C_h}\exp\left(-\frac{U_m A}{C_c}\left(1-\frac{C_c}{C_h}\right)\right)} \tag{13.122}$$

Therefore, for both cases, efficiency can be expressed according to the following equation:

$$\varepsilon = \frac{1-\exp\left(-\frac{U_m A}{C_{min}}\left(1-\frac{C_{min}}{C_{max}}\right)\right)}{1-\frac{C_{min}}{C_{max}}\exp\left(-\frac{U_m A}{C_{min}}\left(1-\frac{C_{min}}{C_{max}}\right)\right)} \tag{13.123}$$

This equation takes into account the definition of the number of heat transfer units and defines the parameter β as the relationship between the minimum and maximum thermal capacities per unit time:

$$NTU = \frac{U_m A}{C_{min}} \tag{13.124}$$

$$\beta = \frac{C_{min}}{C_{max}} \tag{13.125}$$

In this way, the heat transfer efficiency can be expressed as a function of these parameters according to the equation:

$$\varepsilon = \frac{1-\exp\left[-NTU\left(1-\beta\right)\right]}{1-\beta\exp\left[-NTU\left(1-\beta\right)\right]} \tag{13.126}$$

For the case of flow in parallel, the treatment would be similar to the countercurrent flow. Therefore, the efficiency is expressed as:

$$\varepsilon = \frac{1 - \exp\left[-NTU\,(1+\beta)\right]}{1+\beta} \tag{13.127}$$

It is observed that, for operations in parallel as well as in countercurrent, the efficiency is a function of two dimensionless parameters, the *number of heat transfer units* (*NUT*), and the ratio between the maximum and minimum thermal capacities per unit time (β).

These efficiency expressions, developed for parallel and countercurrent flow cases, can be obtained for any type of heat exchanger. The final equations are usually given in graphical form, in which efficiency ε is plotted in the ordinates and the number of heat transfer units *NTU* in the abscissas, with β the constant parameter of each curve (Figures 13.23, 13.24, and 13.25). Different efficiency diagrams for different types and arrangements of plate-type heat exchangers can be found in the literature (Raju and Chand, 1980).

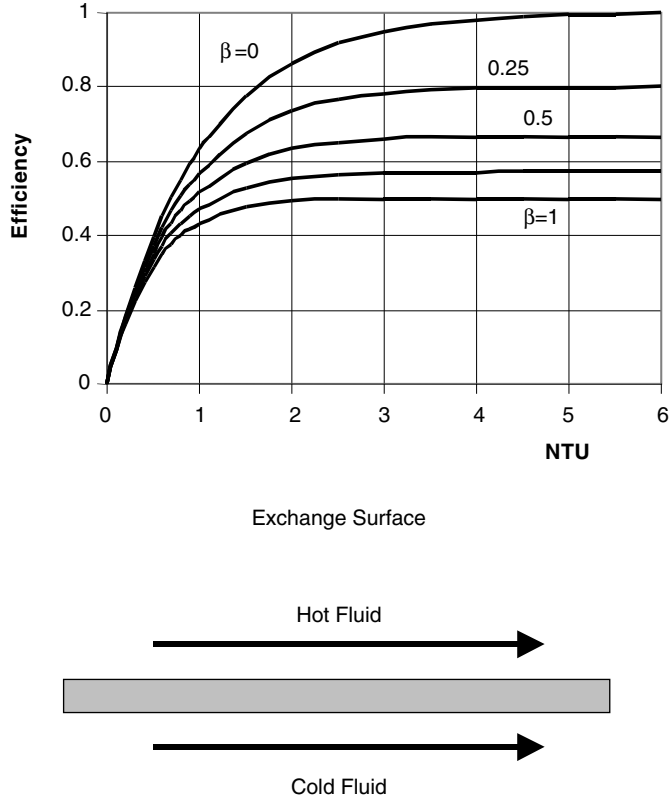

FIGURE 13.23
Efficiency diagram for parallel flow.

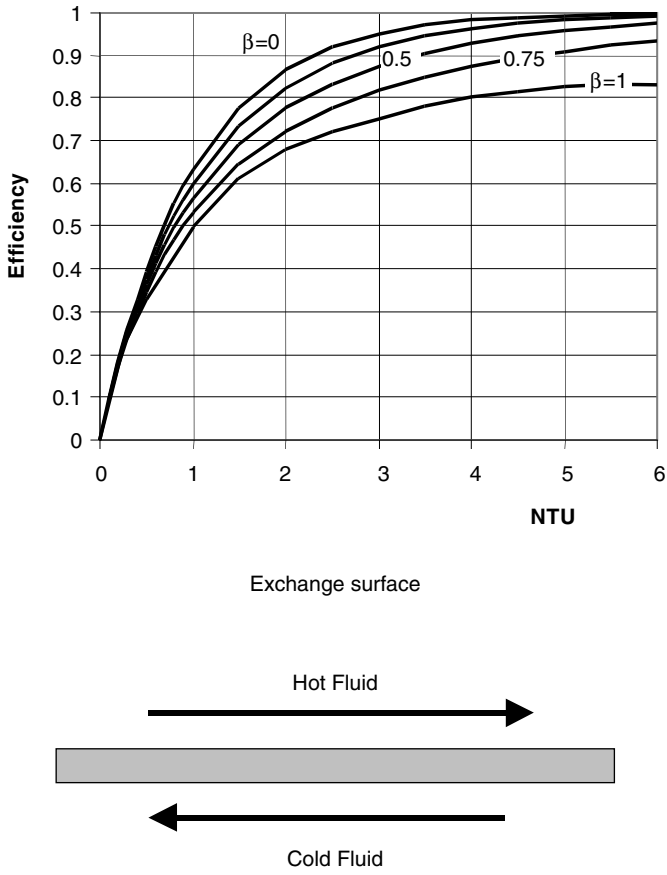

FIGURE 13.24
Efficiency diagram for countercurrent flow.

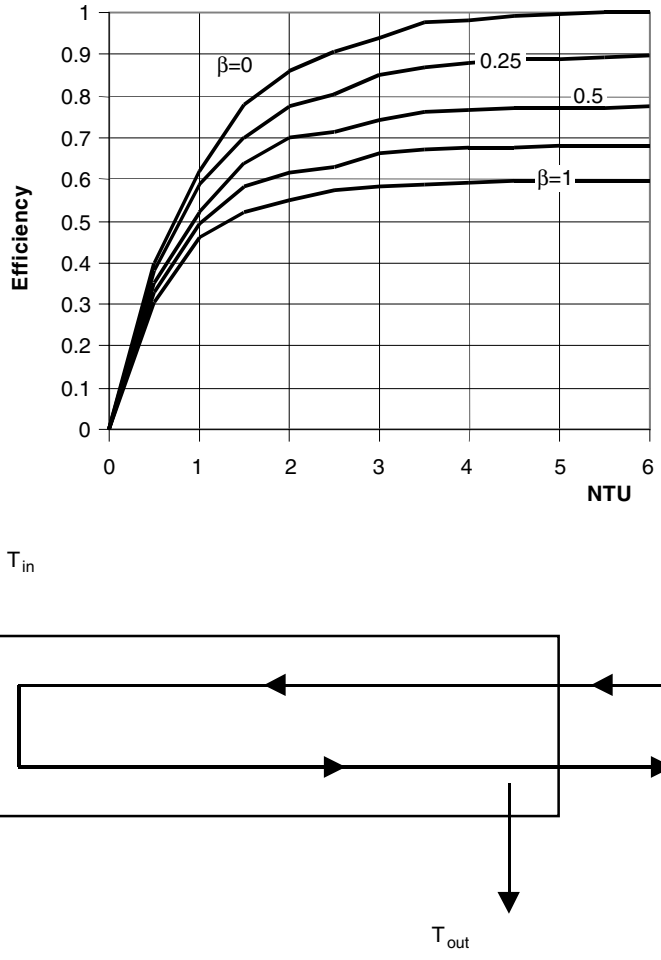

FIGURE 13.25
Efficiency diagram for shell and tube heat exchanger.

Problems

13.1

It is desired to heat 12,000 kg/h of smashed tomatoes from 18°C to 75°C using a concentric tube heat exchanger. Tomato circulates through a stainless steel tube AISI 304 standard of 2 in, while on the outside it condenses saturated steam at 105°C. If the resistance imposed by the film of condensate and the tube wall can be considered negligible, calculate the length that the heat exchanger should have to perform the heating.

Data: Properties of the smashed tomatoes in the operation temperature range: specific heat 3.98 kJ/(kg°C); thermal conductivity 0.5 W/(m°C);

density 1033 kg/m^3. Viscosity varies with temperature according to the expression $\eta = 1.75 \times 10^{-4} \exp(4000/T)$ mPa·s, in which T is the absolute temperature.

Dimensions of the 2 in steel tube: internal diameter 5.25 cm; external diameter 6.03 cm.

Assume that the global heat transfer coefficient varies linearly with temperature.

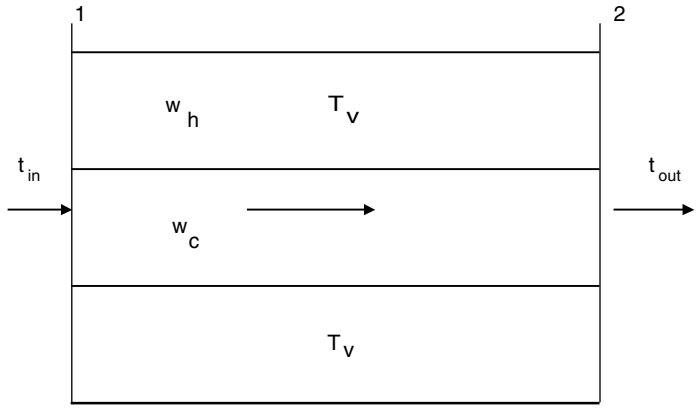

FIGURE P13.1
Problem 13.1.

The condensation latent heat, obtained from saturated steam tables for T_v, is λ_v = 2242 kJ/kg. The condensation heat of steam is given to the tomato to increase its temperature from 18°C to 75°C.

$$w_h \lambda_v = w_c \left(\hat{C}_P\right)_c \left(t_{out} - t_{in}\right)$$

$$w_h \left(2242 \frac{kJ}{kg}\right) = \left(12000 \frac{kg}{h}\right)\left(3.98 \frac{kJ}{kg^\circ C}\right)(75 - 18)^\circ C$$

$$w_h = 1214.2 kg/h$$

According to the problem statement, the resistance offered to heat transfer by the condensed steam and by the wall can be considered as negligible, so $U = h_i$. Since the global heat transfer coefficient varies linearly with temperature, $U = a + bT$, the heat flow that crosses the lateral section of the metal pipe is:

$$\dot{Q} = A\left(U \Delta T\right)_{m l c} = \pi \ d_i L \left(U \Delta T\right)_{m l c}$$

$$\left(U\Delta T\right)_{mlc} = \frac{U_2\Delta T_1 - U_1\Delta T_2}{\ln\left(\dfrac{U_2\Delta T_1}{U_1\Delta T_2}\right)}$$

$$U_1 = h_1;\ \Delta T_1 = T_v - t_{\text{in}} = \left(105-18\right)^{\circ}\text{C} = 87^{\circ}\text{C}$$

$$U_2 = h_2;\ \Delta T_2 = T_v - t_{\text{out}} = \left(105-75\right)^{\circ}\text{C} = 30^{\circ}\text{C}$$

The individual heat transfer coefficients are calculated by using the equation of Sieder–Tate:

$$h = \frac{0.027\ k}{d}\left(\text{Re}\right)^{0.8}\left(Pr\right)^{0.33}\left(\eta/\eta_W\right)^{0.14}$$

Calculation of the maxx flux of the tomato stream:

$$G = \frac{w_t}{\dfrac{\pi}{4}d_i^2} = \frac{4\left(12{,}000\ \text{kg/h}\right)}{\pi\left(5.25\times10^{-2}\right)^2\text{m}^2}\cdot\left(\frac{1\ \text{h}}{3600\ \text{s}}\right) = 1539.8\frac{\text{kg}}{\text{m}^2\cdot\text{s}}$$

The temperature of the metal wall will coincide with the temperature of steam condensation, since there is no resistance due to the metal wall and the condensation layer: $T_w = T_v = 105°\text{C}$.

The calculation of (Re), (Pr), h_1 and h_2 require knowledge of the viscosity values at the corresponding temperatures. For this reason, the following expression is used:

$$\eta = 1.75\times10^{-4}\exp\left(4000/\text{T}\right)$$

The following table presents the values of (Re), (*Pr*), and η calculated using the previous equations:

t (°C)	*T* (K)	*h* (mPa·s)	Re	*Pr*	h_1 W/(m² °C)	h_2 W/(m² °C)
18	291	163.2	496	1298	892 $L^{-1/3}$	
75	348	17.2	4700	136.8		1283
105	378	6.9				

It can be observed that at the inlet, $(\text{Re})_1 = 496$, so the expression for laminar flow should be used to calculate h_1:

$$Nu = 1.86\left[\left(\text{Re}\right)\left(Pr\right)\left(d/L\right)\right]^{1/3}\left(\eta/\eta_w\right)^{0.14}$$

Then:

$$h_1 = \frac{1.86\,k}{d_i}\left[(\mathrm{Re})\,(Pr)\,(d_i)\right]^{1/3}\left(\eta/\eta_w\right)^{0.14}\,L^{-1/3}$$

For calculation of h_2 it is necessary to know the length of the heat exchanger, so the problem should be solved by iteration. The following is obtained when substituting the values of the variables: $h_1 = 892\ L^{-1/3}\ W/(m^2°C)$.

The calculation of h_2 can be performed by the equation of Sieder–Tate (13.1).

The length of the heat exchanger is calculated by the expression:

$$L = \frac{\dot{Q}}{\pi\ d_i\left(U\,\Delta T\right)_{m\,l\,c}}$$

where:

$$\dot{Q} = w_h\,\lambda_v = 756.18\ \mathrm{kW}$$

and

$$d_i = 5.25\times10^{-2}\ \mathrm{m}$$

Substitution of these values in the expression of the heat exchanger length yields:

$$L = \frac{160.62\ \ln\left(3.91\,L^{1/3}\right)}{3.91 - L^{-1/3}}$$

Calculation of L is done by iteration, so an initial length is supposed and substituted in the right-hand term, thus obtaining the length that should coincide with the supposed one. The length of the heat exchanger is $L = 129$ m.

13.2

A water pipe made of 2″ steel tubing crosses a 30 m room that is kept at –18°C. The temperature of the water at the inlet point is 15°C, and the pipe is insulated with a 6-cm thick cover made of fiberglass. Calculate: (a) the minimal water flow to avoid freezing; (b) the time needed by water to freeze inside the pipe in case water circulation stops, assuming that the global heat transfer coefficient remains constant.

Data: tube = air convection coefficient = 12 W/(m²°C); thermal conductivity of fiber glass = 0.07 W/(m·°C); fusion latent heat of ice at 1 atm = 335 kJ/kg; thermal conductivity of water = 0.60 W/(m·°C).

Steel pipe: thermal conductivity = 45 W/(m °C).

Internal diameter is 52.5 mm. External diameter is 60.3 mm

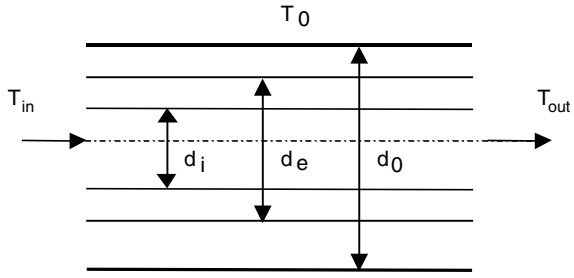

FIGURE P13.2
Problem 13.2.

d_i = 0.0525 m
d_e = 0.0603 m
d_0 = 0.1803 m

Insulation thickness: e_a = 6 cm = 0.06 m
Pipe thickness: $e_p = (d_e - d_i)/2$ = 3.9 mm = 0.0039 m

(a) Water should have a temperature higher than 0°C at the outlet point to prevent freezing. The heat flow rate given by water is:

$$\dot{Q} = w\,\hat{C}p\left(T_{\text{in}} - T_{\text{out}}\right)$$

where w is the maximum flow at which water circulates, T_e = 15°C, and $T_S \geq$ 0°C. Such heat flow rate is lost through the lateral wall according to the expression:

$$\dot{Q} = U_i\,A_i\left(\Delta T\right)_{ml}$$

In this equation, U_i is the global heat transfer coefficient referred to the internal area, A_i is the heat transfer internal area, and $(\Delta T)_{ml}$ is the logarithmic mean temperature difference:

$$\left(\Delta T\right)_{ml} = \frac{\left(T_{\text{in}} - T_0\right) - \left(T_{\text{out}} - T_0\right)}{\ln\left(\dfrac{T_{\text{in}} - T_0}{T_{\text{out}} - T_0}\right)} = \frac{\left(15+18\right) - \left(0+18\right)}{\ln\left(\dfrac{15+18}{0+18}\right)} = 24.8^{\circ}\text{C}$$

$A_i = \pi\, d_i\, L = \pi$ (0.0525 m) (30 m) = 4.948 m^2
$A_e = \pi\, d_e\, L = \pi$ (0.0603 m) (30 m) = 5.683 m^2
$A_0 = \pi\, d_0\, L = \pi$ (0.1803 m) (30 m) = 16.993 m^2

$$A_{ml_1} = \frac{A_e - A_i}{\ln \frac{A_e}{A_i}} = 5.307 \text{ m}^2; \quad A_{ml_2} = \frac{A_0 - A_e}{\ln \frac{A_0}{A_e}} = 10.326 \text{ m}^2$$

Calculation of U_i:

$$\frac{1}{U_i} = \frac{1}{h_i} + \frac{e_p}{k_p \frac{A_{ml_1}}{A_i}} + \frac{e_a}{k_a \frac{A_{ml_2}}{A_i}} + \frac{1}{h_0 \frac{A_0}{A_i}}$$

$$\frac{1}{U_i} = \frac{1}{h_i} + \frac{0.0039 \text{ m}}{\left(45 \frac{\text{W}}{\text{m}^\circ\text{C}}\right)\left(\frac{5.307 \text{ m}^2}{4.948 \text{ m}^2}\right)} + \frac{0.06 \text{ m}}{\left(0.07 \frac{\text{W}}{\text{m}^\circ\text{C}}\right)\left(\frac{10.326 \text{ m}^2}{4.948 \text{ m}^2}\right)}$$

$$+ \frac{1}{\left(12 \frac{\text{W}}{\text{m}^{2\circ}\text{C}}\right)\left(\frac{16.993 \text{ m}^2}{4.948 \text{ m}^2}\right)}$$

$$\frac{1}{U_i} = \frac{1}{h_i} + 0.435 \qquad U_i = \frac{h_i}{1 + 0.43\, h_i} \frac{\text{W}}{\text{m}^{2\circ}\text{C}}$$

It is necessary to calculate the value of the convective coefficient for the inside of the pipe h_i, which can be done by using the equation of Dittus–Boelter for fluids that cool down:

$$h_i = 0.023 \frac{k}{d_i} (\text{Re})^{0.8} (\text{Pr})^{0.3}$$

$$(\text{Re}) = \frac{\rho\, v d_i}{\eta} = \frac{w 4}{\pi d_i \eta} = 4 \frac{\left(w \frac{\text{kg}}{\text{h}}\right)\left(\frac{1 \text{ h}}{3600 \text{ s}}\right)}{\pi (0.0525 \text{ m})(10^{-3} \text{ Pa} \cdot \text{s})} = 6.74\, w$$

$$(Pr) = \frac{\hat{C}p\, \eta}{k} = \frac{\left(4.185 \frac{\text{kJ}}{\text{kg}^\circ\text{C}}\right)\left(10^{-3} \text{ Pa.s}\right)}{\left(0.6 \times 10^{-3} \frac{\text{kJ}}{\text{s} \cdot \text{m} \cdot ^\circ\text{C}}\right)} \approx 7$$

$$h_i = 0.023 \frac{0.6 \text{ W/(m°C)}}{0.0525 \text{ m}} (6.74\, w)^{0.8} (7)^{0.3} = 2.17\, w^{0.8}$$

$$h_i = 2.17\, w^{0.8} \text{ W/(m°C)}$$

From the energy balance: $w\hat{C}_P (T_{in} - T_{out}) = U_i A_i (\Delta T)_{ml}$

$$\left(w \frac{\text{kg}}{\text{h}}\right)\left(\frac{1 \text{ h}}{3600 \text{ s}}\right)\left(4.185 \frac{\text{kJ}}{\text{kg°C}}\right)(15-0)\text{°C} =$$

$$\left(\frac{h_i}{1+0.435\, h_i} \frac{10^{-3} \text{ kJ}}{\text{s·m·°C}}\right)(4.948 \text{m}^2)(24.8\text{°C})$$

Hence:

$$w = \frac{7.04\, h_i}{1+0.435\, h_i} \text{ kg/h}$$

From the substitution of the expression of h_i as a function of the flux w, it is obtained that:

$$w = \frac{15.27\, w^{0.8}}{1+0.94\, w^{0.8}}$$

This equation is solved by iteration, yielding: w = 14.43 kg/h.

For this flow: (Re) = (6.74) (14.43) = 97.

Since the regime is laminar, the equation of Dittus–Boelter cannot be used to calculate h_i. Instead, another expression for laminar regime should be tried:

$$h_i = 1.86 \frac{k}{d_i}\left(\text{Re}\, Pr \frac{d_i}{L}\right)^{1/3}$$

$$h_i = 1.86 \frac{0.6 \text{ W/(m·°C)}}{0.0525 \text{ m}}\left(6.74\, w 7 \frac{0.0525 \text{ m}}{30 \text{ m}}\right)^{1/3}$$

$$h_i \approx 9.26\, w^{1/3} \text{ W/(m}^2 \text{ °C)}$$

The following equation is obtained when substituting the last expression in the energy balance:

$$w = \frac{65.19\ w^{1/3}}{1 + 4.03\ w^{1/3}}$$

After solving by iteration: w = 14.69 kg/h.

This means that if water circulates with a flow lower than 14.69 kg/h, it can freeze inside the pipe.

For w = 14.69 kg/h, it is obtained that:

$$h_i \approx 22.7\ \mathrm{W}/\left(\mathrm{m}^2 \cdot {}^{\circ}\mathrm{C}\right)$$

$$U_i \approx 2.1\ \mathrm{W}/\left(\mathrm{m}^2 \cdot {}^{\circ}\mathrm{C}\right)$$

(b) In case the circulation of water stops, there will be a mass of water inside the pipe:

$$m = \rho\ V = \rho\ \frac{\pi}{4} d_i^2\ L = \frac{\pi}{4}\left(10^3\ \frac{\mathrm{kg}}{\mathrm{m}^3}\right)\left(0.0525\ \mathrm{m}\right)^2\left(30\ \mathrm{m}\right)$$

$$m = 64.94\ \mathrm{kg}$$

The time that this mass of water needs to cool to 0°C can be obtained from the energy balance under unsteady state. The heat output term is equal to the accumulation:

$$U_i\ A_i\left(T_i - T_0\right) = -m\hat{C}p\ \frac{dT_i}{dt}$$

If this equation is integrated on the boundary conditions,

For: t = 0, $T_i = T_{i0}$.

For: t= t, $T_i = T_C$ = 0°C.

The following is obtained:

$$t = \frac{m\hat{C}p}{U_i\ A_i} \ln\left(\frac{T_{i0} - T_0}{T_C - T_0}\right)$$

If it initially is assumed that $T_{i0} = (T_{in} + T_{out})/2 = 7.5°C$, then:

$$t = \frac{(64.94\ \text{kg})(4.185\ \text{kJ}/(\text{kg}\cdot{}^{\circ}\text{C}))}{2.1\times10^{-3}\ \text{kJ}/(\text{s}\cdot\text{m}^2\cdot{}^{\circ}\text{C})(4.948\text{m}^2)}\ \ln\left(\frac{7.5+18}{0+18}\right) = 9110\ \text{s} = 2.53\ \text{h}$$

The heat flow rate that should be eliminated to freeze this water is:

$$\dot{Q}_c = \frac{\lambda\, m}{t_c} = U_i\ A_i\ (T_C - T_0)$$

$$t_C = \frac{\lambda\, m}{U_i A_i (T_c - T_0)}$$

$$= \frac{(335\ \text{kJ}/\text{kg})(64.94\ \text{kg})}{(2.1\times10^{-3}\ \text{kJ}/(\text{s m}^2{}^{\circ}\text{C}))\ (4.948\text{m}^2)(0+18)^{\circ}\text{C}} = 116315\ \text{s}$$

The time that water needs to freeze is $t_C = 32.31$ h.

13.3

A thermally insulated heat exchanger is made of two concentric steel tubes. The external diameter of the inner tube is 6 cm and has a wall thickness of 5 mm, while the internal diameter of the external tube is 10 cm. A fluid circulates through the internal tube with a mass flow of 1000 kg/h and is heated from 22 to 78°C by circulating 100kg/h of steam in countercurrent at 1 atm. Determine:

(a) Temperature of the heating fluid at the outlet point
(b) Individual convective heat transfer coefficient for the fluid being processed
(c) Area of the heat transfer surface
(d) Length of the heat exchanger

Data: The resistance offered by the steel tube to heat transfer can be considered negligible.

Fluid properties: specific heat 4.185 kJ/(kg·°C); viscosity: 1.2 mPa·s; density: 1000 kg/m^3; thermal conductivity: 0.56 W/(m°C); steam's latent heat: 2256 kJ/kg.

For the work conditions of the heat exchanger, it can be considered that, for steam condensation, the individual convective heat transfer coefficient is 870 W/(m^2°C), while for liquid water at temperature higher than 75°C this coefficient can be considered as equal to 580 W/(m^2°C).

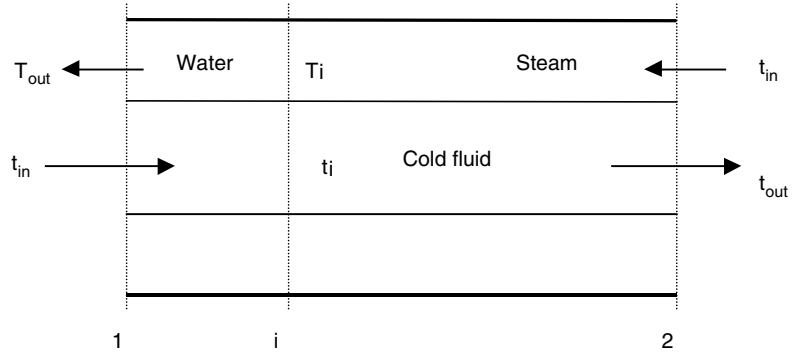

FIGURE P13.3
Problem 13.3.

$t_{in} = 22°C$
$d_e = 6$ cm
$t_{out} = 78°C$
$d_i = d_e - 2_e = 5$ cm
$T_{in} = 100°C$

(a) Steam's heat condensation:

$$\dot{Q}_h = w_h \lambda = \left(100 \frac{\text{kg}}{\text{h}}\right)\left(2256 \frac{\text{kJ}}{\text{kg}}\right)$$

$$\dot{Q}_h = 225{,}600 \text{ kJ/h}$$

Heat gained by the cold fluid:

$$\dot{Q}_c = w_c \hat{C}p_c \left(t_{out} - t_{in}\right) = (1000)(4.185)(78 - 22)$$

$$\dot{Q}_c = 234{,}360 \text{ kJ/h}$$

Since $\dot{Q}_h \leq \dot{Q}_c$, the vapor condenses at an intermediate point and from there lowers its temperature leaving the heat exchanger at a temperature lower than 100°C. The following is complied at the point where the steam begins to condense:

$$w_h \lambda = w_c \hat{C}p_c \left(t_{out} - t_i\right)$$

$$(100)(2256) = (1000)(4.185)\left(78 - t_i\right) \Rightarrow t_i = 24.1°C$$

When the fluid condenses, T_i = 100°C, and water gives heat up to a temperature T_{out}, complying that:

$$w_h\left(\hat{C}_P\right)_h\left(T_i - T_{\text{out}}\right) = w_c\left(\hat{C}_P\right)_c\left(t_i - t_{\text{in}}\right)$$

$$(100)(4.185)\left(100 - T_{\text{out}}\right) = (1000)(4.185)\left(24.1 - 22\right) \Rightarrow T_{\text{out}} = 79^{\circ}\text{C}$$

(b) Calculation of h_i:

$$G = \frac{w}{S} = \frac{1000\ \text{kg/h}}{\frac{\pi}{4}\cdot\left(0.05\right)^2\text{m}^2}\cdot\frac{1\text{h}}{3600\ \text{s}} \approx 141.5\ \text{kg/}\left(\text{m}^2\cdot\text{s}\right)$$

$$(\text{Re}) = \frac{\rho v d}{\eta} = \frac{G d_i}{\eta} = \frac{\left(141.5\ \text{kg/m}^2\cdot\text{s}\right)\left(0.05\ \text{m}\right)}{1.2\times10^{-3}\text{Pa}\cdot\text{s}} \approx 5.9\times10^3$$

$$\left(Pr\right) = \frac{\hat{C}p\,\eta}{k} = \frac{\left(4.185\ \text{kJ/kg}\cdot^{\circ}\text{C}\right)\left(1.2\times10^{-3}\text{Pa}\cdot\text{s}\right)}{\left(0.56\times10^{-3}\ \text{kJ/s}\cdot\text{m}\cdot^{\circ}\text{C}\right)} = 9$$

Applying the equation of Dittus–Boelter:

$$\left(Nu\right) = \frac{h\cdot d}{k} = 0.023\left(\text{Re}\right)^{0.8}\left(Pr\right)^{0.4}$$

$$\frac{h\left(0.05\ \text{m}\right)}{0.56\ \text{W/}\left(\text{m}\cdot^{\circ}\text{C}\right)} = 0.023\left(5.9\times10^3\right)^{0.8}\left(9\right)^{0.4} \Rightarrow h_i \approx 645\ \text{W/}\left(\text{m}^2\cdot^{\circ}\text{C}\right)$$

$$h_{ie} = h_i\cdot\frac{d_i}{d_e} = 645\left(\frac{5}{6}\right) = 537.5\ \text{W/}\left(\text{m}^2\cdot^{\circ}\text{C}\right)$$

(c) The heat exchanger is divided into two zones for the calculation of the area: condensation and cooling.

Steam condensation zone:

$$\frac{1}{U_e} = \frac{1}{h_e} + \frac{e}{k\left(d_{ml}/d_e\right)} + \frac{1}{h_i\left(d_i/d_e\right)} = \frac{1}{h_e} + \frac{1}{h_{ie}} = \frac{h_{ie} + h_e}{h_e\,h_{ie}}$$

$$U_e = \frac{h_{ie} \cdot h_e}{h_{ie} + h_e} \qquad U_e = \frac{(537.5) \cdot (870)}{537.5 + 870} \approx 332 \text{ W}/(\text{m}^2 \cdot ^\circ\text{C})$$

$$\dot{Q}_h = w_h \lambda = (100)(2256) = 225{,}600 \text{ kJ/h}$$

$$\dot{Q}_h = U_e A'_e (\Delta T_{ml}) = 22{,}600 \text{ kJ/h}$$

$$\Delta T_{ml} = \frac{(T_i - t_i) - (T_{in} - t_{out})}{\ln\left(\frac{T_i - t_i}{T_{in} - t_{out}}\right)} = \frac{(100 - 24.1) - (100 - 78)}{\ln\left(\frac{100 - 24.1}{100 - 78}\right)} = 43.5^\circ\text{C}$$

$$A'_e = \frac{(225{,}600 \text{ kJ/h})}{(332 \times 10^{-3} \text{ kJ/sm}^2{}^\circ\text{C})(43.5^\circ\text{C})} \approx 4.34 \text{ m}^2$$

Zone of the condensed water:

$$\dot{Q}_e = w_h \hat{C}_{P_i} (T_i - T_{out}) = (100)(4.185)(100 - 79) = 8789 \text{ kJ/h}$$

$$U_e = \frac{(537.5)(580)}{(537.5) + (580)} = 279 \text{ W}/(\text{m}^2{}^\circ\text{C})$$

$$\Delta T_{ml} = \frac{(T_i - t_i) - (T_{out} - t_{in})}{\ln\left(\frac{T_i - t_i}{T_{out} - t_{in}}\right)} = \frac{(100 - 24.1) - (79 - 22)}{\ln\left(\frac{100 - 24.1}{79 - 22}\right)} \approx 66^\circ\text{C}$$

$$A''_e = \frac{(8789 \text{ kJ/h})}{(279 \times 10^{-3} \text{ kJ/s} \cdot \text{m}^2 \cdot ^\circ\text{C})(66^\circ\text{C})} \approx 0.13 \text{ m}^2$$

Total area: $A_T = A'_e + A''_e = 4.47$ m^2.

(d) The heat exchanger length can also be divided in two parts.

$$A_e = \pi d_e L$$

$$L' = \frac{A'_e}{\pi d_e} = \frac{(4.34)}{\pi (0.06)} = 23.03 \text{ m}$$

$$L'' = \frac{A_e''}{\pi\, d_e} = \frac{(0.13)}{\pi\,(0.06)} = 0.70 \text{ m} = 70 \text{ cm}$$

The total length of the heat exchanger is: $L_T = L' + L'' \approx 23.7$ m.

13.4

It is desired to have a water stream of 4 kg/s at 90°C in an industrial facility where sausages are dried. The stream will be used to condition the drying air. A heat exchanger that has 2 tube passes (50 tubes per pass) per 1 shell is available to heat water up to 90°C. Oil circulating outside the tubes at 3.5 kg/s is used as heating fluid and its temperature at the inlet point is 250°C.

If the inlet temperature of water is 18°C and the tubes by which it circulates are made of steel with an external diameter of 3 cm and an internal diameter of 2.85 cm in a diamond arrangement, determine: (a) the heat transfer coefficient for the inside of the tubes; (b) the area of the heat transfer surface; and (c) length of the tubes.

Data and notes: The resistance to heat flow offered by the surface of the tubes can be considered negligible. The heat transfer coefficient on the oil side is 580 W/(m²·°C).

Properties of water: density = 1000 kg/m³; specific heat: 4.185 kJ/(kg·°C); thermal conductivity = 0.65 W/(m·°C); viscosity = 1 mPa·s.

Properties of oil: density = 850 kg/m³; specific heat = 2.1 kJ/(kg°C); viscosity: 30 mPa·s; thermal conductivity = 0.14 W/(m°C).

$$w_c = 4\frac{\text{kg}}{\text{s}} = 14{,}400 \text{ kg/h}$$

$$w_h = 3.5\frac{\text{kg}}{\text{s}} = 12{,}600 \text{ kg/h}$$

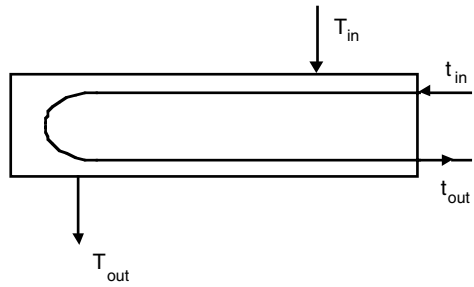

FIGURE P13.4
Problem 13.4.

$$\dot{Q} = w\,\hat{C}_p\,(\Delta t) = U_e\,A_e\,\Delta T_{ml}\,F$$

$$\dot{Q} = \left(14{,}400\,\frac{\text{kg}}{\text{h}}\right)\left(\frac{4{,}185\ \text{kJ}}{\text{kg}\cdot{}^{\circ}\text{C}}\right)(90-18)^{\circ}\text{C} = \left(12{,}600\,\frac{\text{kg}}{\text{h}}\right)\left(\frac{2.1\ \text{kJ}}{\text{kg}\cdot{}^{\circ}\text{C}}\right)(250-T_{\text{out}})$$

from which the following is obtained: T_s = 85.4°C.

$$\left.\begin{aligned} Z &= \frac{T_{\text{in}}-T_{\text{out}}}{t_{\text{out}}-t_{\text{in}}} = \frac{250-85{,}4}{90-18} \approx 2.3 \\ \varepsilon &= \frac{t_{\text{out}}-t_{\text{in}}}{T_{\text{in}}-t_{\text{in}}} = \frac{90-18}{250-18} = 0.31 \end{aligned}\right\} \xrightarrow{\text{Graph}} F \approx 0.83$$

$$d_{\text{internal}} = 2.85\times10^{-2}\ \text{m}$$

Cross-flow section per tube:

$$S = \frac{\pi}{4}d_i^2 = 6.38\times10^{-4}\ \text{m}^2$$

$$G = \frac{w}{S_T} = \frac{4\,\text{kg/s}}{50\left(6.38\times10^{-4}\right)} \approx 125.4\,\frac{\text{kg}}{\text{s}\cdot\text{m}^2}$$

$$(\text{Re}) = \frac{G\,d_i}{\eta} = \frac{(125.4)\left(2.85\times10^{-2}\right)}{10^{-3}} = 3574 \Rightarrow \text{turbulent flow}$$

$$(Nu) = \frac{h\,d_i}{k} = 0.027\,(\text{Re})^{0.8}\,(Pr)^{1/3}\,(\eta/\eta_{\text{w}})^{0.14}$$

It is taken that $(\eta/\eta_w) = 1$;

$$(Pr) = \frac{\hat{C}p\,\eta}{k} = \frac{(4.185\,\text{kJ/kg}\cdot{}^{\circ}\text{C})(10^{-3}\,\text{kg/m}\cdot\text{s})}{(0.65\times10^{-3}\,\text{kJ/s}\cdot\text{m}\cdot{}^{\circ}\text{C})} = 6.44$$

Substitution in the last equation yields:

$$\frac{h\left(2.85\times10^{-2}\ \text{m}\right)}{0.65\,\frac{\text{W}}{\text{m}\cdot{}^{\circ}\text{C}}} = 0.027\left(3.57\times10^{3}\right)^{0.8}(6.44)^{1/3} \Rightarrow h_c = 796.5\,\frac{\text{W}}{\text{m}^2\cdot{}^{\circ}\text{C}}$$

$$h_{t0} = h_t \frac{d_i}{d_e} = 756.7 \frac{\text{W}}{\text{m}^2.^\circ\text{C}} \qquad \frac{1}{U_e} = \frac{1}{h_n} + \frac{1}{h_{t0}}$$

$$\frac{1}{U_e} = \frac{1}{580} + \frac{1}{756.7} \Rightarrow U_e = 328.3 \frac{\text{W}}{\text{m}^{2\circ}\text{C}}$$

The heat flow rate transferred through the exchange area is:

$$\dot{Q} = U_e A_e (\Delta T)_{\text{ml}} F$$

The logarithmic mean temperature is:

$$(\Delta\text{T})_{\text{ml}} = \frac{(T_{\text{in}} - t_{\text{out}}) - (T_{\text{out}} - t_{\text{in}})}{\ln\left(\frac{T_{\text{in}} - t_{\text{out}}}{T_{\text{out}} - t_{\text{in}}}\right)} = \frac{(250 - 90) - (85.4 - 18)}{\ln\left(\frac{250 - 90}{85.4 - 18}\right)} \approx 107^\circ\text{C}$$

The heat flow rate exchanged by one of the fluids is:

$$\dot{Q} = \left(14400 \frac{\text{kg}}{\text{h}}\right)\left(4.185 \frac{\text{kJ}}{\text{kg}.^\circ\text{C}}\right)(90 - 18)^\circ\text{C} = 4,339,008 \text{ kJ/h}$$

Equaling the last result to the heat transferred through the exchange area yields:

$$\left(4,339,008 \frac{\text{kJ}}{\text{h}}\right)\left(\frac{1 \text{ h}}{3600 \text{ s}}\right) = \left(328.3 \frac{\text{W}}{\text{m}^{2\circ}\text{C}}\right) A_e \ (107^\circ\text{C})(0.83)$$

Hence, the following is obtained: $A_e \approx 41.34$ m².
Lateral area of a tube: $\pi\, d_e\, L$

$$A_e = 2 \times 50 \times A_{\text{tube}} = 2 \times 50\, \pi\, d_e L \quad \begin{cases} 2 \text{ passes} \\ 50 \text{ tubes/pass} \end{cases}$$

$$41.34 \text{ m}^2 = 2(50)\pi(0.03 \text{ m})\, L$$

Thus, the tube's length is $L = 4.39$ m.
If the equation of Dittus–Boelter (Eq. 13.14) were applied to the calculation of the individual coefficient h_t, the following would be obtained:

$$h_t = 748.6 \text{ W}/\left(\text{m}^{2\circ}\text{C}\right) \Rightarrow h_{t0} \approx 711.1 \text{ W}/\left(\text{m}^{2\circ}\text{C}\right)$$

in which the global coefficient would be U_e = 319.5 W/(m²°C).

Hence, the following area and length of the tube would be obtained:

$$A_e = 42.48 \text{ m}^2 \Rightarrow L \approx 4.51 \text{ m}$$

13.5

Tartrates present in white wine should be eliminated to avoid later precipitation problems in the bottle. For this reason, previous to bottling, the wine is cooled to 4°C to cause precipitation of tartrates that are then separated from the wine. It is desired to cool 1000 kg/h of white wine from 16 to 4°C in a wine cellar, using a ½ shell and tube heat exchanger, with 18 tubes arranged in squares, and with a distance between the centers equal to 1.5 times the diameter of the tubes. The shell has a diameter of 20 cm and is equipped with baffles that have a baffle cut of 15% and a baffle spacing of 25 cm. A 1200 kg/h stream of water with glycol at –6°C is used as refrigerating fluid, circulating outside the tubes. Due to the possible deposit of tartrates, the soiling factor should be considered as 0.00043 (m²°C)/W. Calculate: (a) global heat transfer coefficient; (b) total heat transfer area; and (c) tube length.

Data: characteristics of the tubes: internal diameter = 10 mm; thickness = 1.5 mm; Thermal conductivity = 40 W/(m°C).

Consider that the properties of both fluids are similar and equal to those of water.

$$d_i = 0.01 \text{ m}$$
$$d_e = 0.013 \text{ m}$$
$$X = Y = 1.5 d_e = 0.0195 \text{ m}$$
$$C' = Y - d_e = 0.0065 \text{ m}$$

Square arrangement:

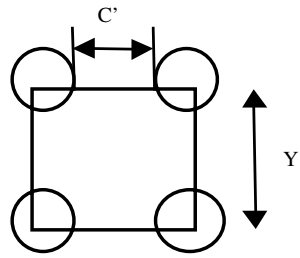

FIGURE P13.5
Arrangements of tubes.

Energy balance:

$$w_h \hat{C}p_h \left(T_{\text{in}} - T_{\text{out}}\right) = w_c \hat{C}p_c \left(t_{\text{out}} - t_{\text{in}}\right)$$

$$\left(1000 \text{ kg/h}\right)\left(4.185 \text{ kJ / kg}^{\circ}\text{C}\right)\left(16-4\right)^{\circ}\text{C} =$$

$$\left(1200 \text{ kg/h}\right)\left(4.185 \text{ kJ / kg}^{\circ}\text{C}\right)\left(t_{\text{out}} - \left(-6\right)\right)^{\circ}\text{C}$$

Hence: $t_{\text{out}} = 4^{\circ}\text{C}$
Coefficient on the tube side:

$$\left(Nu\right) = \frac{h_i d_i}{k} = 0.027 \left(\text{Re}\right)^{0.8} \left(\text{Pr}\right)^{1/3}$$

$$G_t = \frac{4\, w\, n}{N_t \pi\, d_i^2} = \frac{4\left(1000 \text{ kg/h}\right) 2}{18\, \pi \left(0.01\right)^2 \text{m}^2} \frac{1 \text{ h}}{3600\ s} \approx 393 \frac{\text{kg}}{\text{m}^2 \text{ s}}$$

$$\left(\text{Re}\right) = \frac{G_t\, d_i}{\eta} = \frac{\left(393 \frac{\text{kg}}{\text{m}^2 \text{ s}}\right)\left(0.01 \text{ m}\right)}{10^{-3} \text{Pa} \cdot \text{s}} = 3930$$

$$\left(Pr\right) = \frac{\hat{C}p\, \eta}{k} = \frac{\left(4.185 \frac{\text{kJ}}{\text{kg}\,^{\circ}\text{C}}\right)\left(10^{-3} \text{ Pa} \cdot \text{s}\right)}{\left(0.58 \times 10^{-3} \frac{\text{kJ}}{\text{s.m.}^{\circ}\text{C}}\right)} = 7.2$$

Therefore:

$$\frac{h_i \left(0.01 \text{ m}\right)}{0.58 \text{ W/}\left(\text{m}\cdot^{\circ}\text{C}\right)} = 0.027 \left(3930\right)^{0.8} \left(7.2\right)^{1/3}$$

obtaining:

$$h_i = 2270 \frac{\text{W}}{\text{m}^2 \cdot^{\circ}\text{C}}$$

Coefficient of the shell:

$$D_e = \frac{4\left[Y^2 - \frac{\pi}{4} d_e^2\right]}{\pi\, d_e} = \frac{4\left[0.0195^2 - \frac{\pi}{4} 0.013^2\right]}{\pi\ 0.013} = 0.0242 \text{ m}$$

$$G_e = \frac{w n Y}{D_c B C'} = \frac{(1200\ \text{kg/h})(1)(0.0195\ \text{m})}{(0.20\ \text{m})(0.25\ \text{m})(0.0065\ \text{m})} \frac{1\text{h}}{3600\text{s}} = 20 \frac{\text{kg}}{\text{m}^2\,\text{s}}$$

$$(\text{Re}) = \frac{G_c D_e}{\eta} = \frac{(20\ \text{kg/m}^2\text{s})(0.0242\ \text{m})}{10^{-3}\ \text{Pa}\cdot\text{s}} = 484$$

$$(Pr) = 7.2$$

$$\frac{h_e D_e}{k} = 0.36(\text{Re})^{0.55}\ (Pr)^{1/3}$$

$$\frac{h_e(0.0242\ \text{m})}{0.58\ \text{W/(m}\cdot{}^\circ\text{C)}} = 0.36(484)^{0.55}\ (7.2)^{1/3}$$

obtaining:

$$h_e = 499.3 \frac{\text{W}}{\text{m}^2.{}^\circ\text{C}}$$

Overall heat transfer coefficient:

$$\frac{1}{U_e} = \frac{1}{499.3} + \frac{1.5 \times 10^{-3}}{(40)\left(\frac{0.01134}{0.013}\right)} + \frac{1}{(2270)\left(\frac{0.01}{0.013}\right)} + 0.00043$$

$$d_{ml} = \frac{d_e - d_i}{\ln(d_e/d_i)} = \frac{(0.013 - 0.01)\text{m}}{\ln(0.013/0.01)} = 0.01134\ \text{m}$$

Hence:

$$U_e = 328 \frac{\text{W}}{\text{m}^2{}^\circ\text{C}}$$

Heat transfer through the exchange area:

$$\dot{Q} = U_e\, A_e\, \Delta T_{ml}\, F$$

$$\Delta T_{ml} = \frac{(T_e - t_S) - (T_S - t_e)}{\ln\left(\frac{T_e - t_S}{T_S - t_e}\right)} = \frac{(16-4) - (4-(-6))^\circ\text{C}}{\ln\frac{12}{10}} \approx 11^\circ\text{C}$$

Calculation of F:

$$Z = \frac{T_{in} - T_{out}}{t_{out} - t_{in}} = \frac{16 - 4}{4 - (-6)} = \frac{12}{10} = 1.2$$

$$\varepsilon = \frac{t_{out} - t_{in}}{T_{in} - t_{in}} = \frac{4 - (-6)}{16 - (-6)} = \frac{10}{22} \approx 0.455$$

The following is obtained for a ½ shell and tube heat exchanger: $F \approx 0.81$.
Heat transfer area:

$$A_e = \frac{\dot{Q}}{U_e \Delta T_{ml} F} = \frac{w_h \hat{C}p_h (T_{in} - T_{out})}{U_e \Delta T_{ml} F}$$

$$A_e = \frac{(1000 \text{ kg/h})\left(\frac{1 \text{ h}}{3600 \text{ s}}\right)\left(4.185 \frac{\text{kJ}}{\text{kg °C}}\right)(16 - 4)\text{°C}}{(328 \times 10^{-3} \text{ kJ/sm}^2\text{°C})(11\text{°C})(0.81)} = 4.773 \text{ m}^2$$

External heat exchange area: $A_e = 4.773$ m²
Length of tubes:

$$A_e = N_t \pi d_e L$$

$$L = \frac{A_e}{N_t \pi d_e} = \frac{4.773 \text{ m}^2}{18 \pi (0.013 \text{ m})} = 6.49 \text{ m}$$

13.6

A hot air stream at 95°C is required in a drying process. For this reason, 3500 kg/h of air at 15°C is circulated inside a tubular heat exchanger whose shell has a 0.5m diameter, while outside, combustion gases entering the heat exchanger at 400°C and leaving at 100°C circulate. The heat exchanger has 1 shell pass and 2 tube passes, with a total of 400 tubes arranged in squares. The distance between the tubes' centers is two times the diameter of the tubes, and they have baffles with a 25% cut placed every 25 cm. If the heat transferred by radiation is considered negligible, calculate: (a) flow rate of combustion gases; (b) individual heat transfer coefficients for both fluids; (c) total heat transfer area; and (d) length that the tubes should have.

Data: tubes characteristics = thermal conductivity = 44 W/(m·°C); internal diameter = 11 mm; external diameter = 12.5 mm.

Consider that the properties of both fluids are similar and their values are presented in the following table:

T (°C)	k (W/m·°C)	η (mPa·s)	$\hat{C}_P$ (kJ/kg·°C)
0	0.023	0.0180	0.996
250	0.046	0.0265	0.979
500	0.058	0.0350	0.963

Air mean temperature:

$$t_m = \frac{t_{in} + t_{out}}{2} = \frac{15 + 95}{2} = 55^{\circ}\text{C}$$

Combustion gases mean temperature:

$$T_m = \frac{T_{in} + T_{out}}{2} = \frac{400 + 100}{2} = 250^{\circ}\text{C}$$

Properties of the fluids at these mean temperatures:

Fluid	T (°C)	k (W/m·°C)	η (mPa·s)	$\hat{C}_P$ (kJ/kg·°C)
Air	55	0.028	0.0189	0.992
Gases	250	0.046	0.0265	0.979

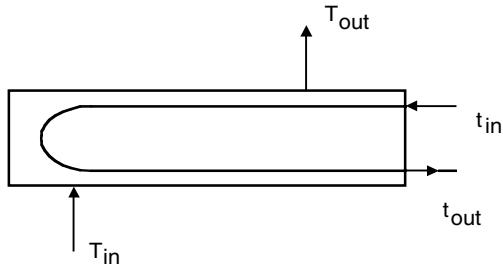

FIGURE P13.6A
Tubes and shell heat exchanger ½.

(a) Energy balance:

$$w_h \left(\hat{C}_P\right)_h \left(T_{in} - T_{out}\right) = w_c \left(\hat{C}_P\right)_c \left(t_{out} - t_{in}\right)$$

$$w_h \left(0.97 \frac{\text{kJ}}{\text{kg}\cdot^{\circ}\text{C}}\right)(400 - 100)^{\circ}\text{C} = \left(3500 \frac{\text{kg}}{\text{h}}\right)\left(0.992 \frac{\text{kJ}}{\text{kg}\,^{\circ}\text{C}}\right)(95 - 15)^{\circ}\text{C}$$

Flow rate of combustion gases: w_h = 945.7 kg/h

(b) The heat transfer individual coefficients would be calculated from the following expression:

$$(Nu) = 0.33\ C_h (\mathrm{Re})^{0.6}\ (Pr)^{0.3}$$

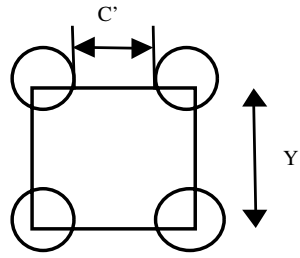

FIGURE P13.6B
Arrangement of tubes.

For the combustion gases that circulate through the shell
Maximum mass flow:

$$G_h = \frac{w_h}{A_C}$$

$$A_C = \frac{D_C\ B\ C'}{nY} = \frac{D_C\ B\ (Y - d_0)}{n\ Y}$$

$$Y = 2d_0 = 2 \times 12.5 \times 10^{-3}\ \mathrm{m} = 0.025\ \mathrm{m}$$

$$B = 25\ \mathrm{cm} = 0.25\ \mathrm{m} \qquad D_c = 0.5\,\mathrm{m} \qquad \mathrm{n} = 1\ \text{shell pass}$$

Hence, $A_C = 0.0625\ \mathrm{m}^2$
The mass flux is, then:

$$G_h = \frac{945.7\ \mathrm{kg/h}}{0.0625\ \mathrm{m}^2} = 15{,}131.2\ \frac{\mathrm{kg}}{\mathrm{m}^2 \cdot \mathrm{h}} = 4.20\ \frac{\mathrm{kg}}{\mathrm{m}^2\ \mathrm{s}}$$

The equivalent diameter for a square arrangement is:

$$D_e = \frac{4\left(Y^2 - \dfrac{\pi}{4} d_0^2\right)}{\pi\pi\ d_0} = 0.051\ \mathrm{m}$$

Calculation of the Reynolds number:

$$(\mathrm{Re})_{\text{máx}} = \frac{G_h D_e}{\eta} = \frac{\left(4.20 \frac{\text{kg}}{\text{m}^2\,\text{s}}\right)(0.051\ \text{m})}{0.0265 \times 10^{-3}\,\text{Pa}\cdot\text{s}} = 8083$$

Prandtl number:

$$(Pr) = \frac{\hat{C}p\,\eta}{k} = \frac{\left(0.979\ \frac{\text{kJ}}{\text{kg}\cdot{}^{\circ}\text{C}}\right)\left(0.0265 \times 10^{-3}\,\text{Pa}\cdot\text{s}\right)}{\left(0.046 \times 10^{-3}\ \frac{\text{kJ}}{\text{s}\cdot\text{m}\cdot{}^{\circ}\text{C}}\right)} = 0.65$$

Calculation of the coefficient C_h:

$$\left.\begin{aligned} Y &= 2d_0 \\ X &= Y = 2d_0 \end{aligned}\right\}$$

The values that correspond to $Y = X = 1.5\ d_0$ are taken from Table 13.2.

For: Re = 2000, $C_h = 0.95$.
For: Re = 20,000, $C_h = 0.96$.

The value $C_h = 0.95$ is taken.
The individual heat transfer coefficient for the combustion gases can be found from the obtained values:

$$h_n = \frac{k}{D_e}\,0.33\,\left(\mathrm{Re}_{\max}\right)^{0.6}(Pr)^{0.3}\,C_h$$

$$h_n = \frac{0.046\ \frac{\text{W}}{\text{m}\cdot{}^{\circ}\text{C}}}{0.051\ \text{m}}\,0.33\,(8083)^{0.6}(0.65)^{0.3}(0.95)$$

yielding:

$$h_c = 54.9\ \frac{\text{W}}{\text{m}^2\,{}^{\circ}\text{C}}$$

The calculation of the individual coefficient for the air that circulates inside the tubes is done using the following expression: $(\mathrm{Nu}) = 0.021(\mathrm{Re})^{0.8}$.
If w_t is the air mass flow, the air flux that circulates inside the tube is:

$$G_t = \frac{w_t}{N_t\, a_t / n} = \frac{w n 4}{N_t\, \pi d_i^2}$$

where:

w_t = 3500 kg/h mass flow
n = 2 tube passes
N_t = 400 total number of tubes
a_t = $\pi/4\, d_i^2$ transversal section of a tube

Substitution of data yields the mass flux:

$$G_t = \frac{(3500\ \text{kg/h})(2)(4)}{(400)\,\pi\,(11\times10^{-3})^2\ \text{m}^2} = 184{,}146.2\ \frac{\text{kg}}{\text{h}\cdot\text{m}^2} = 55.15\ \frac{\text{kg}}{\text{m}^2\,\text{s}}$$

$$(\text{Re}) = \frac{G_t\, d_i}{\eta} = \frac{(51.15\ \text{kg/m}^2\,\text{s})(11\times10^{-3}\ \text{m})}{0.0189\times10^{-3}\ \text{Pa}\cdot\text{s}} = 29{,}971$$

$$(Nu) = \frac{h_t\, d_i}{k} = 0.021\,(29{,}971)^{0.8}$$

Therefore, the individual coefficient on the tube side can be obtained:

$$h_t = \frac{0.028\ \text{W/(m}\cdot{}^{\circ}\text{C)}}{11\times10^{-3}\,\text{m}}\,0.021\,(29{,}971)^{0.8}$$

$$h_t = 204\ \frac{\text{W}}{\text{m}^2\,{}^{\circ}\text{C}}$$

(c) Calculation of the total external area of the tubes:

$$A_e = \frac{\dot{Q}}{U_e\,(\Delta T)_{ml}\,F}$$

$$d_{ml} = \frac{d_0 - d_i}{\ln\left(\frac{d_0}{d_i}\right)} = \frac{(12.5-11)\times10^{-3}}{\ln\left(\frac{12.5}{11}\right)}\ \text{m} = 11.73\times10^{-3}\ \text{m}$$

$$e = \frac{d_0 - d_i}{2} = \frac{(12.5-11)\times10^{-3}}{2}\ \text{m} = 7.5\times10^{-4}\ \text{m}$$

The global coefficient referring to the external area is calculated from the following equation:

$$\frac{1}{U_e} = \frac{1}{549\ \frac{\text{W}}{\text{m}^2\ ^\circ\text{C}}} + \frac{\left(7.5\times10^{-4}\ \text{m}\right)\left(12.5\times10^{-3}\ \text{m}\right)}{\left(44\ \frac{\text{W}}{\text{m}\cdot^\circ\text{C}}\right)\left(11.73\times10^{-3}\text{m}\right)}$$

$$+\frac{12.5\times10^{-3}\ \text{m}}{\left(204\ \frac{\text{W}}{\text{m}^2\ ^\circ\text{C}}\right)\left(11\times10^{-3}\ \text{m}\right)}$$

Obtaining:

$$U_e = 42\ \frac{\text{W}}{\text{m}^2\ ^\circ\text{C}}$$

Calculation of the factor F: $F = F\cdot(Z, E, \text{type})$.

$$\left.\begin{aligned} Z &= \frac{T_{\text{in}} - T_{\text{out}}}{t_{\text{out}} - t_{\text{in}}} = \frac{400-100}{95-15} = 3.75 \\ \varepsilon &= \frac{t_{\text{out}} - t_{\text{in}}}{T_{\text{in}} - t_{\text{in}}} = \frac{95-15}{400-15} = 0.21 \end{aligned}\right\} \xrightarrow{\text{Graph}} \text{F} \approx 0.83$$

Calculation of $(\Delta T)_{ml}$:

$$\left(\Delta\text{T}\right)_{ml} = \frac{\left(400-95\right)-\left(100-95\right)}{\ln\left(\frac{400-95}{100-15}\right)} = 172.2^\circ\text{C}$$

Calculation of the total heat flow rate transferred:

$$\dot{Q} = w_c\hat{C}p\Big)_c\ \left(t_s - t_e\right) = \left(3500\frac{\text{kg}}{\text{h}}\right)\left(0.992\ \frac{\text{kJ}}{\text{kg}\cdot^\circ\text{C}}\right)\left(95-15\right)^\circ\text{C}$$

$$\dot{Q} = 277{,}760\ \text{kJ/h}$$

Total external area:

$$A_e = \frac{\dot{Q}}{U_e\left(\Delta T\right)_{ml} F} = \frac{\left(277{,}760\ \text{kJ/h}\right)\left(\frac{1\ \text{h}}{3600\ \text{s}}\right)}{\left(42\times10^{-3}\ \frac{\text{kJ}}{\text{s m}^2\ ^\circ\text{C}}\right)\left(172.2^\circ\text{C}\right)\left(0.83\right)} = 12.853\ \text{m}^2$$

(d) Calculation of the tube length: $A_e = \pi\, d_0\, L\, N_t$

where:

L = tube length
d_0 = external diameter of the tubes
N_t = 400 tubes

$$L = \frac{A_e}{\pi\, d_0\, N_t} = \frac{12.853\ \text{m}^2}{\pi\left(12.5 \times 10^{-3}\ \text{m}\right)\left(400\right)} = 0.818\ \text{m}$$

L = 81.8 cm.

13.7

It is desired to refrigerate a must that is at 25°C, to send it to a jacketed vessel where its fermentation will be carried out at a controlled temperature of 16°C. In order to perform this refrigeration, 20,000 kg/h of must are fed into a plate-type heat exchanger that operates in parallel, handling a 1/1 hot fluid to cold fluid ratio, using fluid at 3°C as refrigerant fluid. If the temperature at which water leaves the heat exchanger is 14°C, calculate: (a) flow of refrigeration water; (b) heat transfer coefficients; and (c) number of thermal plates.

Data: characteristics of the plates: stainless steel: AISI 316; dimensions = 75 cm × 25 cm × 1.5 mm; surface = 0.165 m²; gasket thickness = 5 mm; thermal conductivity = 16 W/(m°C).

Assume that, in the range of work temperature, the thermal properties of the fluids do not vary:

Water: thermal conductivity = 0.58 W/(m·°C); viscosity = 1 mPa·s; density = 1000kg/m³; specific heats = 4.185 kJ/(kg°C).

Must: thermal conductivity = 0.52 W/(m·°C); viscosity = 1.2 mPa·s; density = 1030 kg/m³; specific heat = 4.06 kJ/(kg°C).

The following figures show a schema of the plate-type heat exchanger and the dimensions of a channel between two plates.

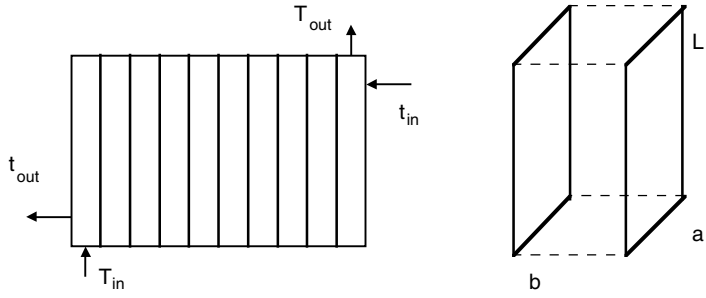

FIGURE P13.7
Problem 13.7.

(a) Energy balance:

$$\dot{Q} = w_h \left(\hat{C}_P\right)_h \left(T_{\text{in}} - T_{\text{out}}\right) = w_c \left(\hat{C}_P\right)_c \left(t_{\text{out}} - t_{\text{in}}\right)$$

$$\left(20{,}000 \frac{\text{kg}}{\text{h}}\right)\left(4.06 \frac{\text{kJ}}{\text{kg}\cdot{}^{\circ}\text{C}}\right)(25-16)^{\circ}\text{C} = w_c \left(4.185 \frac{\text{kJ}}{\text{kg}\cdot{}^{\circ}\text{C}}\right)(14-3)^{\circ}\text{C}$$

$$w_c \approx 15{,}874.9 \text{ kg/h}$$

b) Data managing: $D_e = 4r_H = 2b = 2 \times 5$ mm = 10 mm = 0.01 m

$$S = a.b = (0.25 \text{ m})\left(5 \cdot 10^{-3} \text{ m}\right) = 1.25 \times 10^{-3} \text{ m}^2$$

Flow density of the fluids: $G = w/S$

$$G_h = \frac{20000}{1.25 \cdot 10^{-3}} \cdot \frac{1}{3600} = 4444.44 \ \frac{\text{kg}}{\text{m}^2 \text{ s}}$$

$$G_c = \frac{15873}{1.25 \cdot 10^{-3}} \cdot \frac{1}{3600} = 3527.76 \ \frac{\text{kg}}{\text{m}^2 \text{ s}}$$

Prandtl number:

$$(Pr) = \frac{\hat{C}p\,\eta}{k}$$

Hot fluid:

$$(Pr)_h = 9.4$$

Cold fluid:

$$(PR)_c = 7.2$$

Reynolds number:

$$(\text{Re}) = \frac{(G/n)\,D_e}{\eta}$$

Hot fluid:

$$\left(\mathrm{Re}\right)_h = \frac{37,037}{n_h}$$

Turbulent if $n_c < 93$.
Cold fluid:

$$\left(\mathrm{Re}\right)_c = \frac{35,277.6}{n_c}$$

Turbulent if $n_c < 89$.

Individual coefficients:

$$\left(Nu\right) = \frac{h\,D_e}{k} = 0.374\left(\mathrm{Re}\right)^{0.668}\ \left(Pr\right)^{0.333}$$

Hot fluid:

$$h_h = 51,546.6\left(n_h\right)^{-0.668}\ \mathrm{W}/\left(\mathrm{m}^2.^{\circ}\mathrm{C}\right)$$

Cold fluid:

$$h_c = 40,935.1\left(n_c\right)^{-0.668}\ \mathrm{W}/\left(\mathrm{m}^2\ ^{\circ}\mathrm{C}\right)$$

Global coefficient:

$$\frac{1}{U} = \frac{1}{h_h} + \frac{1}{h_c} + \frac{1.5\cdot 10^{-3}\ \mathrm{m}}{16\ \mathrm{W}/\left(\mathrm{m}^2.^{\circ}\mathrm{C}\right)}$$

$$\Delta T_{ml} = \frac{\left(T_{\mathrm{in}} - t_{\mathrm{out}}\right) - \left(T_{\mathrm{out}} - t_{\mathrm{in}}\right)}{\ln\left(\dfrac{T_{\mathrm{in}} - t_{\mathrm{out}}}{T_{\mathrm{out}} - t_{\mathrm{in}}}\right)} = \frac{\left(25-14\right) - \left(14-3\right)}{\ln\left(11/13\right)} = 12^{\circ}\mathrm{C}$$

$$NTU = \frac{T_{\mathrm{in}} - T_{\mathrm{out}}}{\Delta T_{ml}} = \frac{25-16}{12} = 0.75$$

From the graph (Fig.13.16): $F = F\ (NTU$, type of pass), obtaining $F \approx 0.96$.
From the thermal balance: $\dot{Q} = w_h\ (\hat{C}_P)_h\ (T_{in} - T_{out})$
From the velocity equation: $\dot{Q} = U\ A_T\ \Delta T_{ml} F$
The total area is obtained from the equation:

$$A_T = \frac{w_h \left(\hat{C}_P\right)_h \left(T_{in} - T_{out}\right)}{U\ \Delta T_{ml} F}$$

Substitution of data yields:

$$A_T = \frac{17{,}621.5}{U} \text{m}^2$$

The number of thermal plates is:

$$N = \frac{A_T}{A_P}$$

It is necessary to perform an iterative calculation process:

It is supposed that the number of channels for fluids (n_h, and n_c) and heat transfer coefficients are calculated (h_h, h_c, and U). Next, the total area is calculated and, with it, the number of thermal plates. The total number of channels $n = n_h + n_c = N + 1$. If the number of channels obtained coincides with the number supposed, then the process ends. On the other hand, the process should be performed again. Table P13.7 presents the values of the different variables in each stage of the iterative calculation.

TABLE P13.7

Variables of the Iterative Calculation Process of the Number of Thermal Plates

n_h	n_c	Re_h	Re_c	h_h	h_c (W/m²·°C)	U	A_T (m²)	N	n_h	n_c
30	30	1235	1176	5315	4221	1928	9.140	56	29	28
28	28	1277	1260	5434	4420	1985	8.877	54	28	27
28	27	1323	1307	5566	4529	2024	8.706	53	27	27
27	27	1372	1307	5703	4529	2043	8.630	53	27	27

Heat transfer coefficients:

Must:

$$h_c = 573\ \frac{\text{W}}{\text{m}^2\ ^\circ\text{C}}$$

Water:

$$h_h = 4529 \ \frac{\text{W}}{\text{m}^2\ ^\circ\text{C}}$$

Global:

$$U = 2043 \ \frac{\text{W}}{\text{m}^2\ ^\circ\text{C}}$$

Number of thermal plates: $N = 53$.
Operation in series: $n_h = n_c = 1$.

$(\text{Re})_c = 35{,}278$
$(\text{Re})_h = 37{,}037$
$(Pr)_c = 7.2$
$(Pr)_h = 9.4$
$h_c = 40{,}935\ \text{W/m}^2\ ^\circ\text{C}$
$h_h = 51{,}547\ \text{W/m}^2\ ^\circ\text{C}$
$U = 7269\ \text{W/m}^2\ ^\circ\text{C}$
$A_T = 2.424\ \text{m}^2$

Number of thermal plates: $N = 15$ thermal plates.

13.8

A viscous food fluid is at 15°C, and it is desired to increase its temperature to 40°C to introduce it to a plate-type pasteurizer at a flow rate of 3000 kg/h. To carry out such heating, a scraped surface concentric tube heat exchanger, with four blades inserted in a central axis that rotates at 6 rpm, will be used. 10,000 kg/h of hot water that circulate by the annular section are introduced at 98°C. If the heat exchanger is perfectly insulated to avoid heat losses to the outside, calculate its length.

Data: The thickness of the central axis and of the blades can be considered as negligible.

Properties of the food fluid: specific heat = 3.35 kJ/(kg·°C); thermal conductivity = 0.52 W/(m·°C); density = 1100 kg/m^3; viscosity = 1.6 Pa·s.

Water properties: specific heat = 4.185 kJ/(kg·°C); viscosity = 1 mPa·s; thermal conductivity = 0.58 W/(m·°C); density = 1000 kg/m^3.

The tubes are made of stainless steel and their thermal conductivity is 23 W/(m·°C). The internal tube has an internal diameter of 22 cm and a wall thickness of 8 mm. The external tube has an internal diameter of 30 cm.

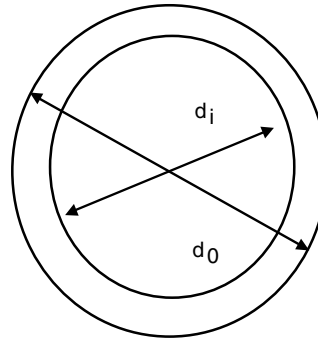

FIGURE P13.8
Problem 13.8. d_i = 22 cm = 0.22 m
$d_e = d_i + 2_e$ = 23.6 cm - 0.236 m
d_0 = 30 cm = 0.3 m

Internal tube section:

$$S_i = \frac{\pi}{4} \cdot d_i^2 = 0.0380 \text{ m}^2$$

Annular section:

$$S_a = \frac{\pi}{4} \left(d_0^2 - d_e^2 \right) = 0.02694 \text{ m}^2$$

Equivalent diameter of the annular section:

$$D_e = 4 r_H = 4 \cdot \frac{\frac{\pi}{4}\left(d_0^2 - d_e^2 \right)}{\pi \, d_e} = \frac{d_0^2 - d_e^2}{d_e} = 0.1454 \text{ m}$$

Mass flux for water:

$$G_h = \frac{w_n}{S_a} = \frac{10{,}000 \text{ kg/h}}{0.02694} \cdot \frac{1 \text{ h}}{3600 \text{ s}} = 103.1 \frac{\text{kg}}{\text{m}^2 \cdot \text{s}}$$

The heat transfer coefficient for water is calculated from the equation of Dittus–Boelter (Eq. 13.14) for fluids that cool down:

$$\left(Nu \right) = \frac{h \, D_e}{k} = 0.023 \left(\text{Re} \right)^{0.8} \left(Pr \right)^{0.3}$$

Prandtl number:

$$(Pr) = \frac{\hat{C}p\,\eta}{k} = \frac{\left(4.185\ \frac{\text{kJ}}{\text{kg}\cdot{}^{\circ}\text{C}}\right)\left(10^{-3}\ \text{Pa}\cdot\text{s}\right)}{\left(0.58\times10^{-3}\ \frac{\text{kJ}}{\text{s m}\ {}^{\circ}\text{C}}\right)} = 7.2$$

Reynolds number:

$$(\text{Re}) = \frac{\rho v D_e}{\eta} = \frac{G_h D_e}{\eta} = \frac{\left(103.1\frac{\text{kg}}{\text{m}^2\ \text{s}}\right)\left(0.1454\ \text{m}\right)}{10^{-3}\ \text{Pa}\cdot\text{s}} \approx 1.5\times10^4$$

Substitution in the equation of Dittus–Boelter:

$$h_e = \frac{\left(0.58\ \frac{\text{W}}{\text{m}\cdot{}^{\circ}\text{C}}\right)}{\left(0.1454\ \text{m}\right)} 0.023\left(1.5\cdot10^4\right)^{0.8}\left(7.2\right)^{0.3} \approx 363\ \frac{\text{W}}{\text{m}^2\cdot{}^{\circ}\text{C}}$$

The individual heat transfer coefficient for the food fluid is calculated from the following equation (Eq. 13.106):

$$h_i = 2\left(\frac{k\rho\hat{C}p\,PN}{\pi}\right)^{1/2}$$

$$h_i = 2\left(\frac{\left(0.52\frac{\text{W}}{\text{m}\cdot{}^{\circ}\text{C}}\right)\left(1100\frac{\text{kg}}{\text{m}^3}\right)\left(3.35\times10^3\ \frac{\text{J}}{\text{kg}\cdot{}^{\circ}\text{C}}\right)(4)\left(6\ \text{min}^{-1}\frac{1\ \text{min}}{60\ \text{s}}\right)}{\pi}\right)^{1/2}$$

obtaining:

$$h_i = 988\ \frac{\text{W}}{\text{m}^2\ {}^{\circ}\text{C}}$$

Global heat transfer coefficient referred to the internal area:

$$\frac{1}{U_i} = \frac{1}{988\ \frac{\text{W}}{\text{m}^2\ {}^{\circ}\text{C}}} + \frac{8\cdot10^{-3}\ \text{m}}{\left(23\ \frac{\text{W}}{\text{m}\cdot{}^{\circ}\text{C}}\right)\left(\frac{0.228\ \text{m}}{0.22\ \text{m}}\right)} + \frac{1}{\left(363\ \frac{\text{Wl}}{\text{m}^2\cdot{}^{\circ}\text{C}}\right)\left(\frac{0.236\ \text{m}}{0.22\ \text{m}}\right)}$$

in which D_{ml} is:

$$D_{ml} = \frac{d_e - d_i}{\ln\left(d_e/d_i\right)} = \frac{0.236 - 0.22}{\ln\left(0.236/0.22\right)} = 0.228 \text{ m}$$

yielding:

$$U_i = 255 \ \frac{\text{W}}{\text{m}^2\ ^\circ\text{C}}$$

From the energy balance:

$$\left(10{,}000\ \frac{\text{kg}}{\text{h}}\right)\left(4.185\ \frac{\text{kJ}}{\text{kg}\cdot^\circ\text{C}}\right)\left(98 - T_{\text{out}}\right)^\circ\text{C} = \left(3000\ \frac{\text{kg}}{\text{h}}\right)\left(3.35\ \frac{\text{kJ}}{\text{kg}\cdot^\circ\text{C}}\right)\left(40 - 15\right)^\circ\text{C}$$

results that the temperature is T_s = 92°C.

From the velocity equation:

$$\dot{Q} = U_i\, A_i\, \Delta T_{ml} = U_i\, \pi\ d_i\, L\, \Delta T_{ml}$$

where:

$$\dot{Q} = w_c\, \hat{C}p_c \left(t_{\text{out}} - t_{\text{in}}\right) = 251{,}250\ \text{kJ/h}$$

if the fluids circulate in countercurrent:

$$\Delta T_m = \frac{\left(T_{\text{in}} - t_{\text{out}}\right) - \left(T_{\text{out}} - t_{\text{in}}\right)}{\ln \dfrac{T_{\text{in}} - t_{\text{out}}}{T_{\text{out}} - t_{\text{in}}}} = \frac{\left(98 - 40\right) - \left(92 - 15\right)}{\ln \dfrac{98 - 40}{92 - 15}} \approx 67^\circ\text{C}$$

$$A_i = \frac{\left(251{,}250\ \text{kJ/h}\right)\left(1\ \text{h}/3600\ \text{s}\right)}{\left(255\times10^{-3}\ \dfrac{\text{kJ}}{\text{s}\ \text{m}^2\ ^\circ\text{C}}\right)\left(67^\circ\text{C}\right)} = 4.085\ \text{m}^2$$

the length of the heat exchanger being:

$$L = \frac{4.085\ \text{m}^2}{\pi\left(0.22\ \text{m}\right)} = 5.91\ \text{m}$$

If the fluids circulate in parallel:

$$\Delta T_{ml} = \frac{\left(T_{\text{in}} - t_{\text{in}}\right) - \left(T_{\text{out}} - t_{\text{out}}\right)}{\ln \dfrac{T_{\text{in}} - t_{\text{in}}}{T_{\text{out}} - t_{\text{in}}}} = \frac{\left(98 - 15\right) - \left(92 - 40\right)}{\ln \dfrac{98 - 15}{92 - 40}} \approx 66.3^{\circ}\text{C}$$

$$A_i = \frac{\left(251250 \text{ kJ/h}\right)\left(1 \text{ h}/3600 \text{ s}\right)}{\left(255 \times 10^{-3} \dfrac{\text{kJ}}{\text{s m}^2\,^{\circ}\text{C}}\right)\left(66.3^{\circ}\text{C}\right)} = 4.128 \text{ m}^2$$

the length of the heat exchanger being:

$$L = \frac{4.128 \text{ m}^2}{\pi\left(0.22 \text{ m}\right)} = 5.97 \text{ m}$$

If the following equation is used to calculate h_i, the length L should be determined by iteration:

$$\left(Nu\right) = \frac{h_i d_i}{k} = 4.9\left(\text{Re}\right)^{0.57} \left(Pr\right)^{0.47} \left(\frac{d_i \cdot N}{v}\right)^{0.17} \left(\frac{d_i}{L}\right)^{0.37}$$

$$\left(\text{Re}\right) = \frac{G_c \cdot d_i}{\eta} = \frac{w_c\, d_i}{S_i\, \eta} = \frac{\left(3000 \dfrac{\text{kg}}{\text{h}}\right)\left(\dfrac{1 \text{ h}}{3600 \text{ s}}\right)\left(0.22 \text{ m}\right)}{\left(0.038 \text{ m}^2\right)\left(1.6 \text{ Pa} \cdot \text{s}\right)} = 3$$

$$\left(Pr\right) = \frac{\hat{C}p\eta}{k} = \frac{\left(3.35 \dfrac{\text{kJ}}{\text{kg}\cdot^{\circ}\text{C}}\right)\left(1.6 \text{ Pa} \cdot \text{s}\right)}{\left(0.52.10^{-3} \dfrac{\text{kJ}}{\text{s m}\,^{\circ}\text{C}}\right)} = 10{,}308$$

$$\left(\frac{d_i N}{v}\right) = \frac{\left(0.22 \text{ m}\right)\left(6 \text{ min}^{-1}\right)}{0.02 \text{ m/s}} \left(\frac{1 \text{ min}}{60 \text{ s}}\right) \approx 1.104$$

The linear velocity of circulation is:

$$v = \frac{w_c}{\rho S} = \frac{3000 \text{ kg/h}}{\left(1100 \dfrac{\text{kg}}{\text{m}^3}\right)\left(0.038 \text{ m}^2\right)} \left(\frac{1 \text{ h}}{3600 \text{ s}}\right) \approx 0.020 \text{ m/s}$$

When substituting these data in the former equation, the coefficient h_i can be obtained:

$$h_i = \frac{0.52\ \text{W/m·°C}}{0.22\ \text{m}}\ 4.9\ (3)^{0.57}\ (10308)^{0.47}\ (1.104)^{0.17}\left(\frac{0.22}{L}\right)^{0.37}$$

Therefore:

$$h_i = 968\ L^{-0.37}\ \text{W/m}^2\text{·°C}$$

The calculation of L should be made by iteration:

$$\frac{1}{U_i} = \frac{1}{h_i} + 2.904 \times 10^{-3}$$

Since:

$$L = \frac{w_c\ (C_P)_c\ (t_s - t_e)}{\pi\ d_i\ \Delta T_{ml}\ U_i}$$

In countercurrent, $L = (1507/U_i)$ m; in parallel, $L = (1523/U_i)$ m.

Table P13.8 presents the values of the variables of the different stages of the iterative process.

Hence, the length of the heat exchanger obtained is:

Operation in parallel: $L = 7.68$ m

Operation in countercurrent: $L = 7.78$ m

TABLE P13.8

Variables of the Iterative Calculation Process of the Length of the Scraped-Surface Heat Exchanger

	L_s (m)	h_i (W/m²°C)	U_i (W/m²°C)	L_c (m)
Countercurrent	6	499	204	7.39
	7.39	462	197	7.64
	7.64	456	196	7.68
	7.68	455	196	7.68
Parallel	7	471	199	7.66
	7.66	456	196	7.77
	7.77	453	196	7.78

13.9

A hot 40°Brix sugar solution is employed in one of the elaboration stages of preserved fruits. Heating is carried out by introducing 1000 kg of this solution in a cylindrical agitated vessel of 1 m of diameter, perfectly insulated. This vessel has a baffle of 30 cm of diameter that rotates at 120 rpm. A helicoidal coil is submerged in the vessel, made of stainless steel tubes of 12 mm of internal diameter, 1 mm of wall thickness, and 15 m of total length. Saturated steam at 3 atm circulates inside the coil and condenses; its convective heat transfer coefficient is 9300 W/(m²°C). If the solution is initially at 16°C, calculate: (a) overall heat transfer coefficient; (b) the time required by the solution to reach 60°C; (c) the flow and quantity of steam required to carry out heating; (d) rate of temperature increase of the solution when it is at 50°C; and (e) if it is supposed that the global heat transfer coefficient is constant, what is the temperature of the solution after 50 min?

Data and notes: The resistance put up by the coil surface to heat transfer can be considered negligible.

Properties of the sugar solution: thermal conductivity = 0.814 W/(m·°C); specific heat = 2.85 kJ/(kg·°C); viscosity = $\eta = 3.7 \times 10^{-7} \exp(2850/T)$ Pa·s; T in Kelvin; density = $\rho = 1.191 - 4.8 \times 10^{-4} \times T$ g/cm³; T in °C.

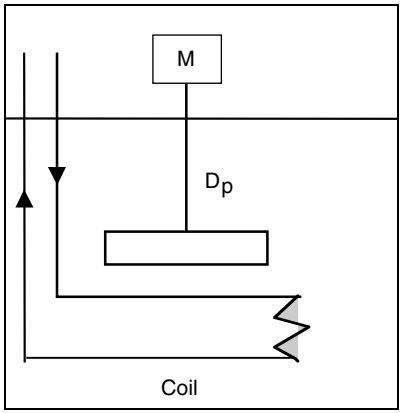

FIGURE P13.9A
Problem 13.9a.

For condensed saturated steam at 3 atm, the following is obtained from tables (see Appendix Table A1): T = 132.9°C.

$$\left.\begin{aligned} \hat{H}_w &= 2721 \text{ kJ/kg} \\ \hat{h}_w &= 558 \text{ kJ/kg} \end{aligned}\right\} \lambda_w = 2163 \frac{\text{kJ}}{\text{kg}}$$

D_T = 1 m

D_P = 0.3 m

$d_i = 12 \times 10^{-3}$ m
$d_e = 14 \times 10^{-3}$ m
$L = 15$ m

Heating is done from 16 to 60ºC; therefore the properties of the solution will be taken at a mean temperature $t_m = 38$°C.

Properties at 38 ºC:

$\eta \approx 3.53 \times 10^{-3}$ Pa·s
$\rho \approx 1.173$ g/cm^3 = 1173 kg/m^3

Calculation of the coefficient h_e:

$$\frac{h_e D_T}{k} = 0.87 \left(\frac{D_P^2 N \rho}{\eta} \right)^{0.62} \left(\frac{\hat{C}p\, \eta}{k} \right)^{1/3} \left(\frac{\eta}{\eta_w} \right)^{0.14}$$

$$(\mathrm{Re}) = \frac{D_P^2 N \rho}{\eta} = \frac{(0.3^2\ \mathrm{m}^2)(2\ \mathrm{s}^{-1})(1173\ \mathrm{kg/m}^3)}{5.53 \times 10^{-3}\ \mathrm{Pa \cdot s}} = 5.98 \times 10^4$$

$$(Pr) = \frac{\hat{C}p\, \eta}{k} = \frac{\left(2.85 \frac{\mathrm{kJ}}{\mathrm{kg\ ^oC}}\right)(3.53 \times 10^{-3}\ \mathrm{Pa \cdot s})}{\left(0.814 \times 10^{-3} \frac{\mathrm{kJ}}{\mathrm{s\ m^2\ ^oC}}\right)} = 12.4$$

Substitution yields:

$$\frac{h_e\,(1\ \mathrm{m})}{0.814\ \mathrm{W/m^2.^oC}} = 0.87 (5.98 \times 10^4)^{0.62} (12.4)^{1/3} (3.53 \times 10^{-3})^{0.14} (\eta_w)^{-0.14}$$

obtaining:

$$h_e = 680.6\, (\eta_w)^{-0.14}\ \mathrm{W/(m^2\ ^oC)} \qquad \text{(P.13.9.1)}$$

To obtain h_e, it is necessary to know T_W, the temperature of the coil surface, to calculate η_W, the viscosity of the solution at the wall temperature.

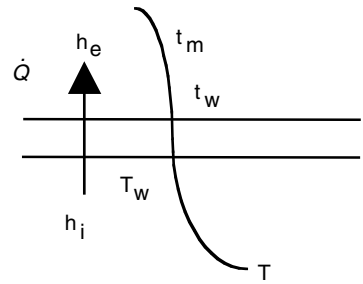

FIGURE P13.9B
Problem 13.9b.

Heat transfer is:

$$\dot{Q} = h_i\, A_i\left(T - T_W\right) = h_e \cdot A_e\left(t_w - t_m\right)$$

Since it is supposed that the surface does not offer resistance to heat transfer: $T_W \approx t_W$

Hence:

$$t_{\mathrm{w}} = \frac{h_i\, A_i\, T + h_e\, A_e\, t_{\mathrm{w}}}{h_i\ A_i + h_e\, A_e} = \frac{h_i\, d_i\, T + h_e\, d_e\, t_{\mathrm{w}}}{h_i\, d_i + h_e\, d_e}$$

$$t_{\mathrm{w}} = \frac{\left(9300\right)\left(12\times10^{-3}\right)\left(132.9\right) + h_e\left(14\times10^{-3}\right)\left(38\right)}{\left(9300\right)\left(12\times10^{-3}\right) + h_e\left(14\times10^{-3}\right)}$$

Obtaining:

$$t_{\mathrm{w}} = \frac{14,832 + 0.532\, h_e}{112 + 14\times10^{-3}\ h_e} \qquad \text{(P13.9.2)}$$

An iteration is needed to calculate h_e. A value is supposed for t_w and the viscosity is calculated at this temperature, which allows one to calculate h_e using Equation (P13.9.1). t_w is calculated by substituting this value in Equation (P13.9.2). If the calculated value coincides with the supposed value, then the problem is solved; if not, the process is repeated until it coincides. The following table presents the results of the iteration:

Iteration	t_W (°C)	$\eta_W \cdot 10^4$ (Pa·s)	h_e (W/(m²°C))	t_W (°C)
1	100	7.70	1857	114.6
2	114.6	5.78	1933	114.1
3	114.1	5.83	1931	114.1

Then,

$$h_e = 1931\ \frac{\mathrm{W}}{\mathrm{m}^2\,{}^{\mathrm{o}}\mathrm{C}}$$

(a) Calculation of the global coefficient U_e:

$$\frac{1}{U_e} = \frac{1}{h_e} + \frac{1}{h_i\left(d_i/d_e\right)}$$

$$\frac{1}{U_e} = \frac{1}{1931} + \frac{1}{\left(9300\right)\left(12/14\right)} \Rightarrow U_e \approx 1554\ \frac{\mathrm{W}}{\mathrm{m}^2\,{}^{\mathrm{o}}\mathrm{C}}$$

(b) Energy balance:

Accumulation term:

$$A = \mathrm{m}\,\hat{C}p\frac{dt}{d\theta}$$

Input term:

$$E = U_e A_e \left(T - t\right)$$

T = temperature of condensing steam
t = temperature of the solution in the vessel
θ = time

Equaling these two terms:

$$m\,\hat{C}p\frac{dt}{d\theta} = U_e\,A_e\left(T - t\right)$$

This is a differential equation in separated variables, which, integrated on the boundary condition ($\theta = 0 \quad t = t_0$), yields the following equation:

$$\ln\left(\frac{T - t_0}{T - t}\right) = \frac{U_e\,A_e}{m\,\hat{C}p}\;\theta$$

This expression allows calculation of the heating time for a determined temperature, or vice versa:

Time:

$$\theta = \frac{m\,\hat{C}p}{U_e\,A_e}\;\ln\left(\frac{T - t_0}{T - t}\right)$$

Temperature:

$$t = T - \left(T - t_0\right)\;\exp\left(-\frac{U_e\,A_e\,\theta}{m\,\hat{C}p}\right)$$

where:
m = 1000 kg
T = 132.9°C $\quad t_0$ = 16°C
$A_e = \pi\,d_e L$ = 0.6527 m²
$\hat{C}_p$ = 2.85 kJ/kg°C

For t = 60°C

$$\theta = \frac{\left(10^3\ \text{kg}\right)\left(2.85\ \frac{\text{kJ}}{\text{kg}\,^\circ\text{C}}\right)}{\left(1554\times10^{-3}\ \frac{\text{kJ}}{\text{s m}^2\,^\circ\text{C}}\right)\left(0.6597\text{m}^2\right)}\ln\left(\frac{132.9-16}{132.9-60}\right)=1313\ \text{s}$$

obtaining a time equal to: θ = 1313 $s \approx 22$ min

(c) Steam flow rate and quantity condensed

$$w_v\,\lambda_w = \frac{m}{\theta}\,\hat{C}p\,\left(t-t_0\right)$$

$$w_v\left(2163\ \text{kJ/kg}\right)=\left(\frac{1000\ \text{kg}}{1313\ \text{s}}\right)\left(\frac{3600\ \text{s}}{1\ \text{h}}\right)\left(2.85\ \frac{\text{kJ}}{\text{kg}\,^\circ\text{C}}\right)\left(60-16\right)^\circ\text{C}$$

Steam flow rate: $w_v \approx 159$ kg/h

Mass of steam: $V = w_v = 58$ kg

(d) Velocity at which temperature increases:

$$\frac{dt}{d\theta}=\frac{U_e\,A_e}{m\,\hat{C}p}\,\left(T-t\right)$$

$$\frac{dt}{d\theta}=\frac{\left(1931\times10^{-3}\ \frac{\text{kJ}}{\text{s m}^2\,^\circ\text{C}}\right)\left(\frac{3600\ \text{s}}{1\ \text{h}}\right)\left(0.6597\ \text{m}^2\right)}{\left(1000\ \text{kg}\right)\left(2.85\ \frac{\text{kJ}}{\text{kg}\,^\circ\text{C}}\right)}\left(132.9-50\right)^\circ\text{C}$$

$$\approx\ 133.4^\circ\text{C/h}$$

(e) Temperature at 50 minutes

$$t=132.9-\left(132.9-16\right)\ \exp\left(-\frac{\left(1931\times10^{-3}\ \frac{\text{kJ}}{\text{s m}^2\,^\circ\text{C}}\right)\left(0.6597\ \text{m}^2\right)\left(3000\ \text{s}\right)}{\left(1000\ \text{kg}\right)\left(2.85\ \frac{\text{kJ}}{\text{kg}\,^\circ\text{C}}\right)}\right)$$

Thus, temperature is t = 102.3°C.

Since it is assumed that the processing is done at atmospheric pressure, water becomes steam and there is no liquid phase. However, since it is a sugar solution, it is possible that it boils at 100ºC, due to the increase of the boiling point produced by the soluble solids.

13.10

12,000 kg/h of a fluid at 15°C, whose specific heat is 3.817 kJ/(kg°C), is being processed in a food industry. In order to improve the energy performance, it is desired to install a heat exchanger to increase the temperature of the fluid to 72°C, using a water stream of 20,000 kg/h that comes from the condensation of steam at 1 atm. Calculate the surface of a heat exchanger for circulation in parallel and in countercurrent, if the overall heat transfer coefficient is 1750 W/(m²°C).

Operation in parallel:

Energy balance:

$$\dot{Q} = w_c \left(\hat{C}_P\right)_c \left(t_{\text{out}} - t_{\text{in}}\right) = w_h \left(\hat{C}_P\right)_h \left(T_{\text{in}} - T_{\text{out}}\right)$$

Since steam condenses at 1 atm $\Rightarrow T_e = 100$°C.

Substitution yields:

$$\left(12{,}000\frac{\text{kg}}{\text{h}}\right)\left(3.817\frac{\text{kJ}}{\text{kg}\cdot{}^{\circ}\text{C}}\right)(72-15)^{\circ}\text{C} = \left(20{,}000\frac{\text{kg}}{\text{h}}\right)\left(4.185\frac{\text{kJ}}{\text{kg}\cdot{}^{\circ}\text{C}}\right)(100-T_{\text{out}})$$

The following is obtained: $T_{\text{out}} = 68.8$°C. This is impossible because $T_s < T_e$, which is contrary to the thermodynamics laws.

Operation in countercurrent:

$$C_h = \left(20{,}000\frac{\text{kg}}{\text{h}}\right)\left(4.185\frac{\text{kJ}}{\text{kg}\,^{\circ}\text{C}}\right) = 83{,}700\ \frac{\text{kJ}}{\text{h}\,^{\circ}\text{C}}$$

$$C_c = \left(12{,}000\frac{\text{kg}}{\text{h}}\right)\left(3.817\frac{\text{kJ}}{\text{kg}\,^{\circ}\text{C}}\right) = 45{,}804\ \frac{\text{kJ}}{\text{h}\,^{\circ}\text{C}}$$

Then $C_{\min} = C_c$; $C_{\max} = C_h$.

Hence:

$$\beta = \frac{C_{\min}}{C_{\max}} = 0.547$$

The performance or efficiency of the heat transfer is:

$$\varepsilon = \frac{C_c\left(t_{\text{in}} - t_{\text{out}}\right)}{C_{\min}\left(t_{\text{in}} - T_{\text{in}}\right)} = \frac{15-72}{15-100} = \frac{57}{85} = 0.671$$

The value of *NTU* can be found from efficiency graphs (Fig. 13.24):

$$\left.\begin{array}{l}\varepsilon = 0.671\\ \beta = 0.547\end{array}\right\} \xrightarrow{\text{Graph}} NTU \approx 1.5$$

since:

$$NTU = \frac{U\,A}{C_{\min}}$$

The heat exchange area is:

$$A = \frac{C_{\min}\,NTU}{U} = \frac{\left(45{,}804\ \frac{\text{kJ}}{\text{h}\,^{\circ}\text{C}}\right)\left(\frac{1\ \text{h}}{3600\ \text{s}}\right)(1.5)}{1.75\ \frac{\text{kJ}}{\text{s}\,\text{m}^2\,^{\circ}\text{C}}} \approx 10.906\ \text{m}^2$$

The area can also be calculated from the heat transfer velocity through the exchange area equation:

$$\dot{Q} = U\,A\,\Delta T_{ml}$$

$$\dot{Q} = \left(12{,}000\frac{\text{kg}}{\text{h}}\right)\left(3.817\frac{\text{kJ}}{\text{kg}\cdot^{\circ}\text{C}}\right)(72-15)^{\circ}\text{C} = 2{,}610{,}828\ \text{kJ/h}$$

$$(\Delta T)_{ml} = \frac{(T_{\text{in}} - t_{\text{out}}) - (T_{\text{out}} - t_{\text{in}})}{\ln\left(\frac{T_{\text{in}} - t_{\text{out}}}{T_{\text{out}} - t_{\text{in}}}\right)} = \frac{(100-72)-(68.8-15)}{\ln\left(\frac{100-72}{68.8-15}\right)}$$

Obtaining: $(\Delta T)_{ml} = 39.5^{\circ}\text{C}$.

Since $U = 1750\ \text{W}/(\text{m}^2{}^{\circ}\text{C})$, then the area is:

$$A = \frac{\left(2{,}619{,}828\ \frac{\text{kJ}}{\text{h}}\right)\left(\frac{1\ \text{h}}{3600\ \text{s}}\right)}{\left(1.75\frac{\text{kJ}}{\text{s}\,\text{m}^2\,^{\circ}\text{C}}\right)(39.5^{\circ}\text{C})} = 10.492\ \text{m}^2$$

The small difference found can be due to the error made during the graphical determination of *NTU*.

14

Heat Transfer by Radiation

14.1 Introduction

Energy transfer by radiation is basically different from other energy transfer phenomena because it is not proportional to a temperature gradient and does not need a natural medium to propagate. Also, its transfer is simultaneous with convection.

Any molecule possesses translation, vibrational, rotational, and electronic energy under quantum states. Passing from one energetic level to another implies an energy absorption or emission. Passing to a higher energy state implies energy absorption by a molecule; on the other hand, a molecule emits energy as radiation when passing to a lower energy level. Since the energy levels as quantums, the absorption or emission of energy is in the form of photons that have a double nature particle-wave.

Any body at a temperature higher than absolute zero can emit radiant energy; the amount emitted depends on the temperature of the body. As the temperature of a body increases, energy levels are excited first, followed by electronic levels. A temperature increase implies that the radiation spectrum moves to shorter wavelengths or is more energetic.

The corpuscle theory states that radiant energy is transported by photons and is a function of its frequency ν, according to the expression:

$$E = h\nu \tag{14.1}$$

in which the proportionality constant h is the so-called Planck's constant, whose value is $h = 6.6262 \times 10^{-34}$ J·s.

The wave theory considers radiation as an electromagnetic wave, relating frequency to wavelength according to the following equation:

$$\nu = c/\lambda \tag{14.2}$$

where λ is the wavelength of the radiation and c is the value of light speed under vacuum conditions (2.9979×10^8 m/s).

So-called thermal radiation, which includes the ultraviolet, visible, and infrared spectrum, corresponds to wavelengths of 10^{-7} to 10^{-4} m.

14.2 Fundamental Laws

Prior to the description of the different laws that rule the radiation phenomenon, it is convenient to define a black body, which is a body that absorbs and emits the maximum quantity of energy at a determined temperature, but reflects none.

14.2.1 Planck's Law

The energy emitted by a black body at a given temperature T is a function of the wavelength. In this way, if q_λ is considered the spectral emissive power expressed in $J/(m^3 \cdot s)$, then:

$$q^e_{b,\lambda} = \frac{C_1}{\lambda^5 \left[\exp\left(\frac{C_2}{\lambda T} \right) - 1 \right]} \tag{14.3}$$

in which $q^e_{n,\lambda}$ is the radiation energy emitted per unit time and volume at a wavelength λ by a black body that is at a temperature T. The superscript e refers to emission, while the subscripts b and λ refer to black body and wavelength, respectively. The constants C_1 and C_2 are defined by:

$$C_1 = 2\pi c^2 h = 3.742 \times 10^{-16}\ J/(m^2 \cdot s)$$
$$C_2 = hc/k = 1.438 \times 10^{-2}\ m \cdot K$$

in which k is the Boltzmann's constant, which has a value of 1.3806×10^{-23} J/K.

14.2.2 Wien's Law

The emissive power of a black body at a determined temperature shows variation with the wavelength in such a way that it passes through a maximum. Also, if the temperature of emission increases, it is observed that the maximum corresponds to a lower wavelength, while the value of the emissive power is higher.

In order to find the wavelength corresponding to the maximum emission, the derivative of Planck's law with respect to the wavelength (Equation 14.3) should be equaled to zero:

$$\frac{d\left(q^e_{b,\lambda}\right)}{d\lambda} = 0$$

Hence:

$$\lambda_{max} \cdot T = 2.987 \times 10^{-3}\ \mathrm{m} \cdot K \tag{14.4}$$

This expression confirms what was indicated before.

14.2.3 Stefan–Boltzmann Law

The flux of the radiation energy, or the total radiation energy per unit area, emitted by a black body is obtained by integrating Planck's equation on all the wavelengths. This integration shows that such energy depends only on temperature and is proportional to its fourth power:

$$q_n^e = \sigma T^4 \tag{14.5}$$

σ being the Stefan–Boltzmann constant with a value of:

$$\sigma = \frac{2\,\pi^5\ k^4}{15\ c^2\ h^3} = 5.67 \times 10^{-8}\ \ \mathrm{J}/\left(\mathrm{s.m}^2 \cdot K^4\right) \tag{14.6}$$

14.3 Properties of Radiation

As can be observed from the discussion in the last section, radiation energy depends on wavelength. This makes the behavior of bodies to emission and absorption of radiating energy dependent on this energy. The properties that show this dependence are called monochromatic properties. These properties can depend on the direction in which radiation is transmitted, called directional properties. However, some mean total properties independent of wavelength and direction can be considered, simplifying the calculations and difficulties of the treatment of problems in which radiation energy intervenes.

14.3.1 Total Properties

It is considered that all properties have an equal mean value for all wavelengths and directions. Radiation received by a body can experience some of the following phenomena: part of it can be absorbed, part of it transmitted, and part of it reflected.

If q is the total flow density of radiation received by a body, it can be written that:

$$q = q^r + q^t + q^a \tag{14.7}$$

in which superscripts *r*, *t*, and *a* stand for reflected, transmitted, and absorbed, respectively.

The fraction of energy reflected, transmitted, or absorbed has different names, thus:

- Reflectivity or reflection factor (*r*): Fraction of radiation received by a body that is reflected:

$$r = \frac{q^r}{q} \tag{14.8}$$

- Transmissivity or transmission factor (*t*): fraction of radiation received by a body that is transmitted:

$$t = \frac{q^t}{q} \tag{14.9}$$

- Absorptivity or absorption factor (*a*): fraction of radiation received by a body that is absorbed:

$$a = \frac{q^a}{q} \tag{14.10}$$

The following expression can be easily obtained from the last equations: $r + t + a = 1$.

The emissivity of a body is defined as the ratio between the quantity of radiation emitted by such a body and a quantity that a black body could emit at the same temperature:

$$e = \frac{q^e}{q_b^e} = \frac{q^e}{\sigma T^4} \tag{14.11}$$

It should be pointed out that all these properties have a mean value that is the same for all directions and wavelengths.

The following is complied with by bodies in which all the energy received is reflected: $r = 1$, $t = 0$, and $a = 0$; hence, they are called perfect mirrors. Those in which all the energy is transmitted ($r = 0$, $t = 1$, and $a = 0$) are known as transparent bodies, while those that absorb all the energy received ($r = 0$, $t = 0$, and $a = 1$) are denominated black bodies.

It is found, in a black body, that $q^e = q_b^e$. So, if this value is substituted in Equation 14.11, it is obtained that emissitivity is equal to one. This means that, in black bodies, emissivity as well as absorptivity is equal to one ($a = e = 1$).

14.3.2 Monochromatic Properties: Kirchhoff's Law

If the properties for each wavelength (λ) are considered instead of the mean value for all wavelengths (and independent of them), then reflectivity, transmissivity, absorptivity, and emissivity are defined according to the following expressions:

$$r_\lambda = \frac{q_\lambda^r}{q_\lambda} \tag{14.12a}$$

$$t_\lambda = \frac{q_\lambda^t}{q_\lambda} \tag{14.12b}$$

$$a_\lambda = \frac{q_\lambda^a}{q_\lambda} \tag{14.12c}$$

The following is also complied with: $r_\lambda + t_\lambda + a_\lambda = 1$.
Monochromatic emissivity can be defined the same as total emissivity:

$$e_\lambda = \frac{q_\lambda^e}{q_{b,\lambda}^e} \tag{14.13}$$

The mean value of each of these properties, as a function of the monochromatic properties, is obtained according to the following equations:

$$r = \frac{\int_0^\infty r_\lambda\, q_\lambda\, d\lambda}{\int_0^\infty q_\lambda\, d\,\lambda} \tag{14.14a}$$

$$t = \frac{\int_0^\infty t_\lambda\, q_\lambda\, d\lambda}{\int_0^\infty q_\lambda\, d\,\lambda} \tag{14.14b}$$

$$a = \frac{\int_0^\infty a_\lambda\, q_\lambda\, d\lambda}{\int_0^\infty q_\lambda\, d\,\lambda} \tag{14.14c}$$

$$e = \frac{\int_0^\infty e_\lambda q^e_{b,\lambda} d\lambda}{\int_0^\infty q^e_{b,\lambda} d\lambda} = \frac{1}{\sigma T^4} \int_0^\infty e_\lambda \, q^e_{b,\lambda} d\lambda \tag{14.14d}$$

Now, suppose a cavity at a temperature T that emits a flux q; inside the cavity is a body with absorptivity a and emissivity e. When thermal equilibrium is reached, it is complied that the energy absorbed and emitted by the body is equal. That is, $a \cdot q = q^e$.

If it is a black body, then $a = 1$, so: $1 \cdot q = q^e_b$. Thus, if these two equations are divided, then:

$$a = \frac{q^e}{q^e_b}$$

When comparing this expression with Equation 14.11, one can see that it is the same, coinciding with the total emissivity ($a = e$). If monochromatic properties are used instead of total properties, then an analogous expression can be obtained ($a_\lambda = e_\lambda$).

It was stated that under thermal equilibrium in a black body the emissivity is equal to the absoptivity, which is known as Kirchhoff's law. It should be pointed out that a body in which the monochromatic properties are constant for the whole wavelength range is called a gray body. Also, in gray bodies, it is always complied that the absorptivity and emissivity are equal, even if they are not under thermal equilibrium.

14.3.3 Directional Properties

It is evident that a body emitting radiation does not necessarily do so in the same way in all directions. For this reason, the radiation properties of a body will be different depending on the direction considered.

If a point on a differential area dA that emits energy in a determined direction (Figure 14.1) is considered, then the solid angle ($d\omega$) displayed at such area is:

$$d\omega = \frac{dA \cos\theta}{r^2} \tag{14.15}$$

in which θ is the angle formed by the director vector of surface dA and the vector of the direction from the emission point in such differential area, while r is the distance that separates a point from the area. If one desires to obtain the solid angle displayed from the point to the whole space, then Equation 14.15 should be integrated for a whole sphere, obtaining that $\omega_{SPHERE} = 4\pi$.

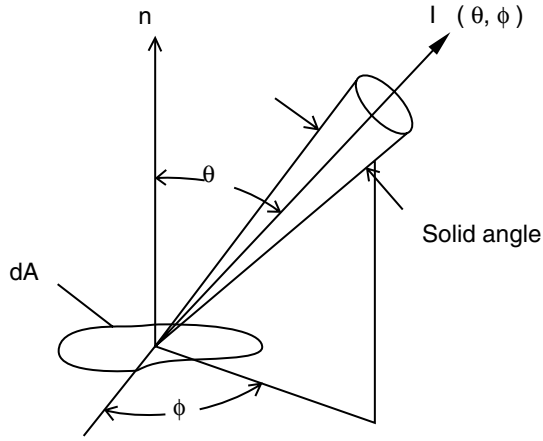

FIGURE 14.1
Solid angle displayed by *dA*.

It is convenient to define the intensity of radiation of an emitter, which depends on the direction considered. In this way, the intensity of radiation emitted by a point is defined as the radiant energy per unit time, unit solid angle, and unit area projected in a direction normal to the surface:

$$I(\theta,\phi) = \frac{dq}{\cos\theta\, d\,\omega} \tag{14.16}$$

where dq is the flux emitted by the emitter, θ and ϕ are the angular coordinates that define the direction of emission, and $d\omega$ is the solid angle.

If it is desired to obtain the total flux emitted in all directions, the following integration should be done:

$$q = \int I(\theta,\phi)\cos\theta\, d\omega \tag{14.17}$$

In order to perform such integration, it is necessary to know the intensity of emission. Thus, if the emitter behaves in such a way that the intensity of emission is the same in all directions, then the emission is diffuse. On the other hand, it is said that the emission is specular if its behavior is similar to a mirror, that is, it emits in specular directions with respect to the radiation received.

In the case of a diffuse emitter, the intensity of radiation is independent of the angular coordinates of emission. If the intensity of radiation is defined as $I = I(\theta,\phi)$, then the total flux emitted in all directions is:

$$q = \int I(\theta,\phi)\cos\theta\, d\omega = \pi\, I \tag{14.18}$$

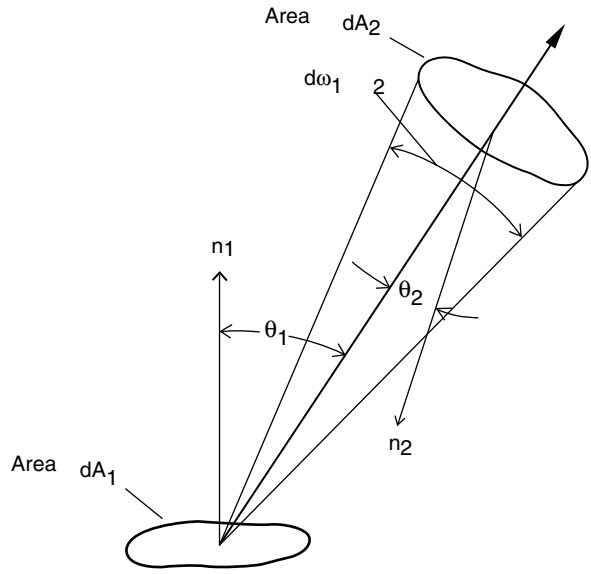

FIGURE 14.2
View factor.

14.4 View Factors

When the energy exchanged by any two bodies is studied, it is evident that the energy emitted by one is not completely absorbed by the other, since it can only absorb the portion that it intercepts. For this reason, view factors, also called direct view factors, shape factors, geometric factors, or angular factors, should be defined.

14.4.1 Definition and Calculation

Consider two bodies of differential areas, dA_1 and dA_2 (Figure 14.2). The view factor of the first body with respect to the second is defined as the fraction of the total energy emitted by dA_1 that is intercepted by dA_2.

The following expression defines the view factor of dA_1 with respect to dA_2:

$$F_{dA_1,\,dA_2} = \frac{q^e_{1,2}}{q^e_1} = \frac{\cos\theta_1 \cos\theta_2 \; dA_2}{\pi r^2} \tag{14.19}$$

where θ_1 and θ_2 are the angles that each of the director vectors (n_1 and n_2) make with r, which is the straight line that connects the centers of the areas (dA_1 and dA_2).

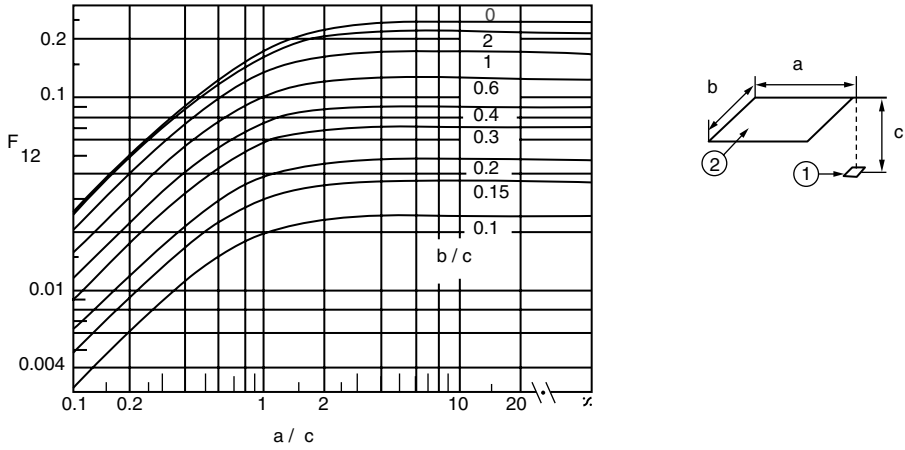

FIGURE 14.3
View factor from a differential area to a parallel rectangle. (Adapted from Costa et al., *Ingeniería Química*, 4. *Transmisión de Calor*, Alhambra, Madrid, 1986.)

If the second body is not a differential but has an area A_2, the view factor between dA_1 and this area is calculated by the expression:

$$F_{dA_1,A_2} = \int_{A_2} \frac{\cos\theta_1 \cos\theta_2 \, dA_2}{\pi r^2} \tag{14.20}$$

The view factor between two surfaces that have infinite areas is obtained from the expression:

$$F_{A_1,A_2} = \frac{1}{A_1} \int_{A_1} \int_{A_2} \frac{\cos\theta_1 \cos\theta_2 \, dA_2 \, dA_1}{\pi r^2} \tag{14.21}$$

The mathematical calculation of view factors is difficult. However, graphs that facilitate this task can be found in the literature for specific cases (Figures 14.3, 14.4, 14.5, 14.6, and 14.7).

14.4.2 Properties of View Factors

View factors comply with different properties that are listed next. They are useful for different applications to solve problems in which exchange of radiant energy takes place.

Reciprocity relationship: For any two areas it is complied that the product of the area of the first body times the factor with which it views the second body is equal to the product of the area of the second body times the factor with which it views the first body.

$$A_i F_{i,j} = A_j F_{j,i} \tag{14.22}$$

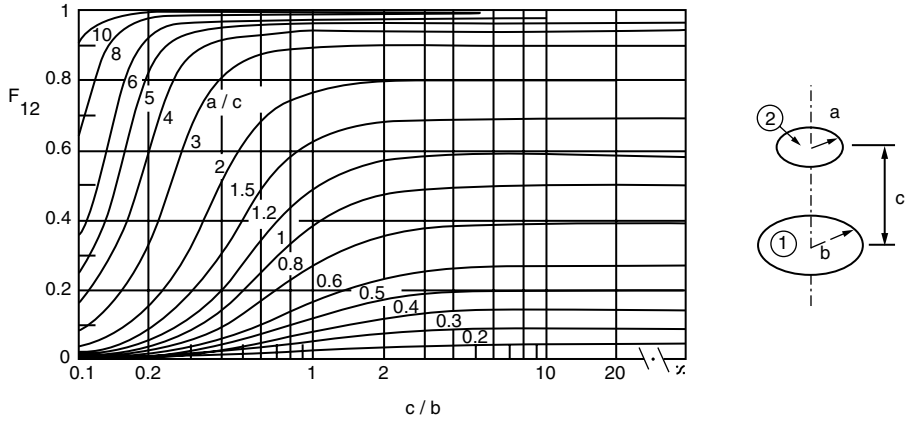

FIGURE 14.4
View factor between parallel circular surfaces. (Adapted from Costa et al., *Ingeniería Química,* 4. *Transmisión de Calor,* Alhambra, Madrid, 1986.)

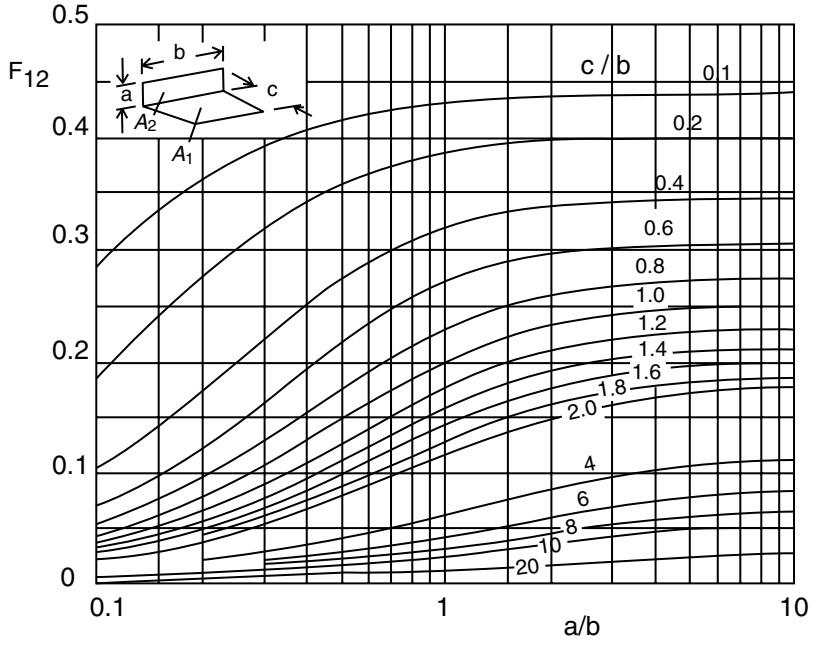

FIGURE 14.5
View factors for perpendicular rectangles with a common edge. (Adapted from Costa et al., *Ingeniería Química,* 4. *Transmisión de Calor,* Alhambra, Madrid, 1986.)

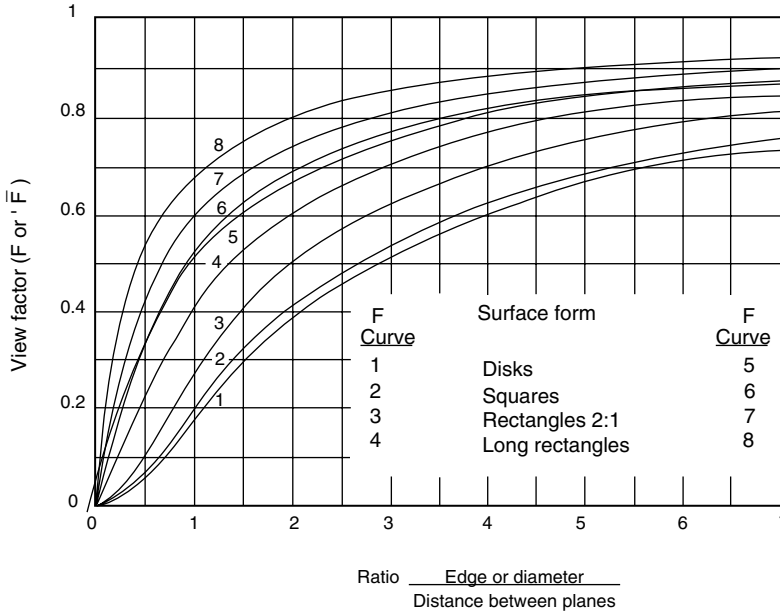

FIGURE 14.6
View and refractory factor between parallel planes. (Adapted from Costa et al., *Ingeniería Química,* 4. *Transmisión de Calor,* Alhambra, Madrid, 1986.)

Conservation principle: For a closed system formed by N surfaces, it is complied that the addition of the geometric factors of a surface, with respect to all the surfaces that surround it, is equal to one, since the addition of all the fractions of energy emitted by such a surface that are intercepted by the other surfaces is equal to one.

$$F_{i,1} + F_{i,2} + F_{i,3} + \cdots + F_{i,N} = 1 \tag{14.23}$$

For those bodies that cannot see themselves (plane or convex surfaces), the view factors with respect to themselves are null, since the radiation emitted cannot be intercepted by the body itself.

$$F_{i,i} = 0$$

The shape factor of a black surface completely surrounded by another black surface is equal to one, since all the energy emitted by the first body is captured by the second.

Additive relationship: The view factor of a single surface A_i with respect to a composite surface $A_{(jkl)}$ complies with:

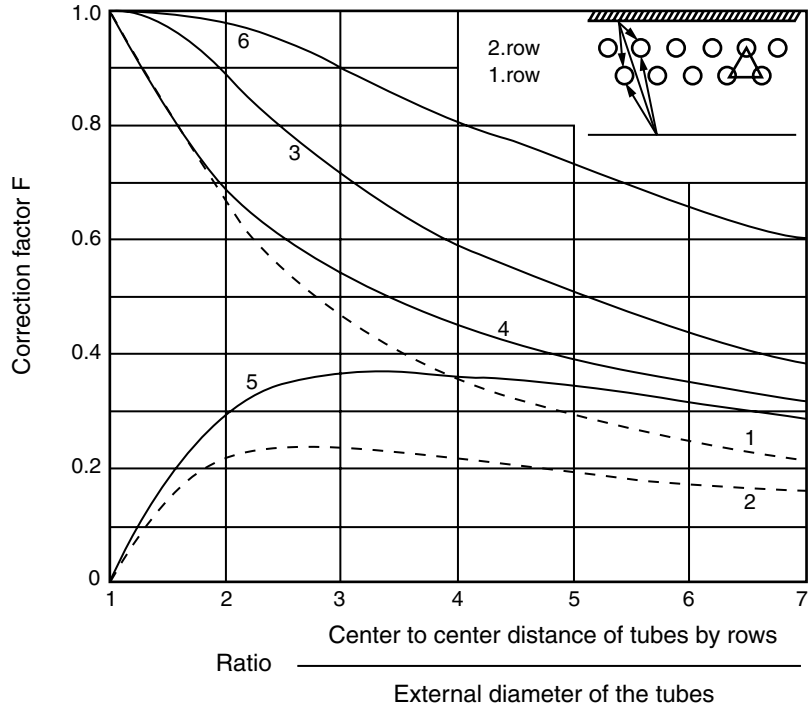

FIGURE 14.7
Correction factor F for radiation to a tube bundle: (1) direct to the first row; (2) direct to the second row; (3) total to one row (one row); (4) total to the first row (two rows); (5) total to the second row (two rows); (6) total to two rows (two rows). (Adapted from Costa et al., *Ingeniería Química*, 4. *Transmisión de Calor*, Alhambra, Madrid, 1986.)

$$A_i F_{i,(jkl)} = A_i F_{i,j} + A_i F_{i,k} + A_i F_{i,l} \tag{14.24}$$

In this case the second surface is composed by three other surfaces:

$$A_{(jkl)} = A_j + A_k + A_l$$

14.5 Exchange of Radiant Energy between Surfaces Separated by Nonabsorbing Media

Some cases of exchange of radiant energy between bodies not separated by a material medium are presented next. That is, there is no possibility for the medium that separates two bodies to intercept the radiation emitted by one of the bodies.

14.5.1 Radiation between Black Surfaces

Suppose two black bodies with surface area A_1 and A_2 and at temperatures T_1 and T_2. The energy flow rate that leaves each of them and that is intercepted by the other one can be obtained from the expressions:

$$\dot{Q}_{1,2} = F_{12} A_1 \sigma T_1^4$$

$$\dot{Q}_{2,1} = F_{21} A_2 \sigma T_2^4$$

The net flow rate received by each body is:

$$\dot{Q}_{net} = F_{12} A_1 \sigma \left(T_1^4 - T_2^4\right) \tag{14.25a}$$

$$\dot{Q}_{net} = F_{21} A_2 \sigma \left(T_2^4 - T_1^4\right) \tag{14.25b}$$

Taking into account the reciprocity property, it can be seen that these expressions coincide, except that one will be positive and the other negative, depending on whether it is receiving or emitting net heat by radiation. Thus, if $T_1 > T_2$, then $\dot{Q}_1$ will be positive, meaning that the surface A_1 emits net radiation, while A_2 will have the same value but with a negative sign.

14.5.2 Radiation between a Surface and a Black Surface Completely Surrounding It

Consider a body whose surface area A_1 is completely surrounded by a black surface A_2, T_1 and T_2 being the temperature of each of these bodies. The radiant energy emitted by each one and intercepted by the other body is:

$$\dot{Q}_{1,2} = F_{12} A_1 e_1 \sigma T_1^4$$

$$\dot{Q}_{2,1} = F_{21} A_2 a_1 \sigma T_2^4$$

The net heat is:

$$\dot{Q}_{net} = F_{12} A_1 e_1 \sigma T_1^4 - F_{21} A_2 a_1 \sigma T_2^4 \tag{14.26}$$

Taking into account the reciprocity property, and if surface area A_1 does not view itself ($F_{12} = 1$), the net heat emitted or captured by A_1 is:

$$\dot{Q}_{net} = A_1 \sigma \left(e_1 T_1^4 - a_1 T_2^4\right) \tag{14.27}$$

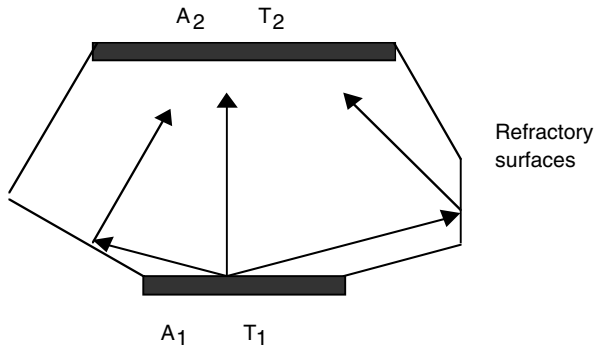

FIGURE 14.8
Radiation between two black surfaces separated by refractory surfaces.

The following is implied as if it were a gray body where $a = e$:

$$\dot{Q}_{net} = A_1 \sigma e_1 \left(T_1^4 - T_2^4\right)$$

In the case of a black body, the expression is simplified, since its emissivity is equal to one.

14.5.3 Radiation between Black Surfaces in the Presence of Refractory Surfaces: Refractory Factor

Generally, in the design of industrial equipment (ovens, heaters, etc.), the radiation emitter and receptor are not alone; rather, there is another type of surface called refractory. Under steady state, refractory surfaces emit all the radiation that they have absorbed, as long as there are no heat losses through the refractory surface. Therefore, no net heat flow is associated to the radiation exchange in refractory surfaces. A surface that emits all the radiation that it receives is called adiabatic. A refractory wall is adiabatic if all the heat absorbed by radiation is emitted.

Consider two surfaces A_1 and A_2 joined by refractory walls to study this case (Figure 14.8). Consider also that all of them maintain the same temperature. The transfer of radiant energy from A_1 to A_2, or vice versa, includes not only the direct transfer, but also heat transfer that comes from the refractory walls.

The heat emitted by A_1 that reaches A_2 is:

$$\dot{Q}_{1,2} = F_{12} A_1 \sigma T_1^4 + F_{1R} A_1 \sigma T_1^4 \frac{F_{R2}}{1 - F_{RR}}$$

where

$$\frac{F_{R2}}{1-F_{RR}}$$

is a factor that represents the fraction of energy emitted by the refractory walls that reaches surface A_2.

A refractory factor ($\bar{F}$) between surfaces A_1 and A_2 is defined according to the expression:

$$\overline{F}_{12} = F_{12} + \frac{F_{R2}}{1-F_{RR}} \tag{14.28}$$

Thus, the heat that comes out of one surface and reaches the other will be expressed according to the equations:

$$\dot{Q}_{1,2} = \overline{F}_{12} A_1 \sigma T_1^4$$

$$\dot{Q}_{2,1} = \overline{F}_{21} A_2 \sigma T_2^4$$

Therefore, the net heat exchanged by both surfaces is:

$$\dot{Q}_{net} = \overline{F}_{12} A_1 \sigma T_1^4 - \overline{F}_{21} A_2 \sigma T_2^4 \tag{14.29}$$

The refractory factors comply with the same properties as normal view factors, so:

$$\dot{Q}_{net} = \overline{F}_{12} A_1 \sigma \left(T_1^4 - T_2^4\right) \tag{14.30}$$

14.5.4 Radiation between Nonblack Surfaces: Gray Factor

In case the radiation energy is exchanged between bodies that are not black, it should be taken into account that the energy emitted by a body is calculated by the Stefan–Boltzmann equation multiplied by the emissivity. Also, the energy received by one of these bodies is affected by the absorption coefficient. All these factors complicate the mathematical treatment, although, in engineering, it is assumed that the bodies are gray to simplify the problem. This is equivalent to considering the absorption coefficient independent of the wavelength of the incident radiation and, therefore, of the temperature and other characteristics of the emitter. The emissivity and absorption coefficients in gray bodies are equal.

For the case of two surfaces A_1 and A_2 joined by any number of refractory zones, the net radiant energy flow exchanged can be expressed according to:

$$\dot{Q}_{net} = \Im_{12} A_1 \sigma \left(T_1^4 - T_2^4\right) \tag{14.31}$$

where $\Im_{12}$ is a shape factor, called gray factor, that depends on the view factors of the surfaces and the refractory factor, as well as on the emissivity and surface area of the bodies considered.

The gray factor is defined as:

$$\Im_{12} = \frac{1}{\frac{1}{F_{12}} + \left(\frac{1}{e_1} - 1\right) + \frac{A_1}{A_2}\left(\frac{1}{e_2} - 1\right)} \tag{14.32}$$

This equation allows one to obtain the value of the gray factor and is a general expression that, in some cases, may be simplified. Thus, for the case of two big parallel planes that exchange radiant energy, the refractory factor is equal to one, and the surface areas are equal, obtaining that:

$$\Im_{12} = \frac{1}{\frac{1}{e_1} + \frac{1}{e_2} - 1}$$

14.6 Coefficient of Heat Transfer by Radiation

In cases of heat transfer by conduction and convection, the heat flow is proportional to the temperature increase and to the transfer area, so the proportionality constant is the thermal conductivity in the case of heat conduction, and the individual film coefficient in the case of heat convection. Thus:

Heat conduction: $\dot{Q} = (k/e)\, A\, (T_0 - T_1)$
Heat convection: $\dot{Q} = h\, A\, (T_w - T_f)$

In the case of radiation, the heat flow is calculated by the Stefan–Boltzmann equation. However, sometimes it is convenient to express it in a similar way to heat conduction and convection. In this way, the heat flow by radiation is:

$$\dot{Q} = h_R A \left(T_1 - T_2\right) \tag{14.33}$$

in which h_R is called the coefficient of heat transfer by radiation and has the same units as film coefficients. This coefficient can be calculated from graphs or tables. Table 14.1 shows the values of the coefficient of heat transfer by

TABLE14.1a

Values for $(h_C + h_R)$ for Steel Pipes towards their Surroundings[a]

d_0	$(T_S - T_G)$ (°C)													
(cm)	10	25	50	75	100	125	150	175	200	225	250	275	300	325
2.5	11.03	11.66	12.68	13.76	14.96	16.29	17.08	19.18	20.92	22.61	24.44	26.34	28.29	30.28
7.5	10.00	10.54	11.01	12.49	13.66	14.87	16.13	17.87	19.93	21.12	22.92	24.77	26.67	28.67
12.5	9.51	10.04	10.93	11.91	13.12	14.44	15.57	17.18	18.79	20.49				
25.5	9.13	9.65	10.58	11.60	12.75	14.04	15.17	16.80	18.50					

[a] Units of $(h_C + h_R)$ kcal/(h m^2 °C)

Source: Costa et al., *Ingeniería Química, 4. Transmisión de Calor,* Alhambra, Madrid, 1986.

TABLE14.1b

Values of $(h_C + h_R)$ for Steel Pipes towards their Surroundings[a]

d_0	$(T_S - T_G)$ (°F)														
(in)	30	50	100	150	200	250	300	350	400	450	500	550	600	650	700
1	2.16	2.26	2.50	2.73	3.00	3.29	3.60	3.95	4.34	4.73	5.16	5.60	6.05	6.51	6.99
3	1.97	2.05	2.25	2.47	2.73	3.00	3.31	3.69	1.03	4.73	4.85	5.26	5.71	6.19	6.08
5	—	1.95	2.15	2.36	2.61	2.90	3.20	3.54	3.90						
10	1.80	1.87	2.07	2.29	2.54	2.80	3.12	3.47	3.84						

[a] Units of $(h_C + h_R)$ Btu/(h ft^2 °F)

Source: Perry, R.H. and Chilton, C.H., *Chemical Engineer's Handbook,* New York, McGraw–Hill, 1973.

radiation, along with convective coefficients, for the case of pipes whose surfaces can lose heat by both mechanisms.

In the specific case of black surfaces with a view factor equal to one, the net heat flow is given by:

$$\dot{Q} = \sigma A\left(T_1^4 - T_2^4\right)$$

When comparing this expression with Equation 14.33, an expression to calculate the transfer coefficient by radiation can be obtained:

$$h_R = \sigma \frac{T_1^4 - T_2^4}{T_1 - T_2} = \sigma\left(T_1^3 + T_1^2\, T_2 + T_1\, T_2^2 + T_2^3\right) \tag{14.34}$$

In the case of radiation between gray surfaces or surfaces whose view factor is different from one, the appropriate equations should be taken into account.

14.7 Simultaneous Heat Transfer by Convection and Radiation

Heat transfer, in practice, occurs by more than one mechanism at the same time. Thus, in the case of heat transfer from a hot surface to the exterior, convection and radiation perform this transmission simultaneously. Consider a hot surface at a temperature T_S, which is surrounded by a fluid at a temperature T_G, with T_w denoting the temperature of the walls. The heat transfer mechanisms are radiation and convection, so the heat flow transferred from the hot surface will be the sum of heat transferred by radiation plus the heat transferred by convection:

$$\dot{Q}_{TOTAL} = Q_R + Q_C$$

$$\dot{Q}_R = h_R\, A\left(T_S - T_w\right)$$

$$\dot{Q}_C = h_C\, A\left(T_S - T_G\right)$$

Hence:

$$\dot{Q}_{TOTAL} = h_R\, A\left(T_S - T_w\right) + h_C\, A\left(T_S - T_G\right)$$

In the case where the temperature of the fluid T_G is the same as the temperature of the wall:

$$\dot{Q}_{TOTAL} = \left(h_R + h_C\right) A \left(T_S - T_w\right) \tag{14.35}$$

The values of the coefficients h_R and h_C should be calculated previously. The individual coefficient of heat transfer by convection h_C is calculated from graphs or equations obtained empirically and based on a dimensional analysis. The coefficient h_R can be obtained from graphs or equations, as indicated in the previous section.

Problems

14.1

The use of solar energy to heat an air stream that will be used to dry barley is studied in a seed experimental center. Hence, a black solar collector (5 m × 10 m) was placed on the roof of the building. The surroundings can be considered a black body that has an effective radiactive temperature of 32°C. Heat losses by conduction to the outside can be neglected, while losses due to convection can be evaluated from the individual coefficient of heat transfer, which in turn is calculated according to the expression: $h = 2.4\ (\Delta T)^{0.25}$ W/(m^2 K). In this equation ΔT is the difference of temperatures between the surface of the collector and its surroundings. If the incident solar energy produces in the collector a radiant flux of 800 W/m^2, calculate the temperature at which the thermal equilibrium in the collector is reached.

The temperature at which thermal equilibrium is reached is obtained when all the heat that reaches the collector is equal to all the heat that leaves the collector. Heat inlet will be by direct radiation of the sun and by the radiant energy coming from the surroundings, whereas heat by radiation and by convection will come out of the collector.

Suppose that the temperature of the collector at which equilibrium is reached is T_1 and the temperature of the surroundings is T_2 = 32 °C, and that the area of the collector is A_1 and A_2 is the area of the surroundings. The energy balance in the collector leads to the expression:

$$q_{sun} A_1 a_1 + a_1 F_{21} A_2 e_2 \sigma T_2^4 = a_2 F_{12} A_1 e_1 \sigma T_1^4 + A_1 h \left(T_1 - T_2\right)$$

The solar collector and the surroundings are black bodies, so their emissivities (e) and the absorption coefficient (a) have a value equal to one. The surroundings completely encircle the collector, so if the reciprocity property

is applied, $F_{12}A_1 = F_{21}A_2$, and if it is supposed that the solar collector has a plane area value, $F_{12} = 1$ is obtained. Substitution in the last equation yields:

$$q_{sun} + \sigma T_2^4 = \sigma T_1^4 + h\left(T_1 - T_2\right)$$

Rearrangement of terms and substitution of data gives.

$$800\frac{\text{W}}{\text{m}^2} = \left(5.67 \times 10^{-8}\frac{\text{W}}{\text{m}^2\,\text{K}^4}\right)\left(T_1^4 - 305^4\right)K^4 + 2.1\,(T_1 - 305)^{1.25}\,\frac{\text{W}}{\text{m}^2}$$

This equation should be solved by iteration, obtaining T_1 = 359 K (= 86ºC).

14.2

It is desired to grill some fillets that have an emissivity of 0.45, using a grill made of a 50 cm × 90 cm metallic base, with a grate placed 25 cm above the base; the opening between the grate and the base is completely closed by refractory sheets. Fillets are placed so that they cover the whole grate, while vegetal charcoal is placed on the base, estimating that their absorptivity and emissivity are 1 and 0.85, respectively.

The temperature of charcoal during the grilling process is 800°C and the temperature of the environment is 25°C. Heat exchanged by convection between charcoal and fillets is 600 W. If heat transfer from the bottom part of the charcoal and the upper side of the fillets towards the surroundings is neglected, determine the temperature acquired by the fillets under thermal equilibrium.

When carrying out a heat balance in the meat, it is obtained that the heat entering by radiation and convection from the charcoal is equal to the heat exiting the meat by radiation:

$$a_2\,\bar{F}_{12}\,A_1\,e_1\,\sigma T_1^4 + \dot{Q}_C = a_1\,\bar{F}_{21}\,A_2\,e_2\,\sigma T_2^4$$

Subscripts 1 and 2 refer to the charcoal and fillets, respectively. Due to the geometry of the system, $A_1 = A_2$ and $\bar{F}_{12} = \bar{F}_{21}$. Also, $a_1 = 1$, since charcoal is considered a black body, and the fillets are considered gray bodies ($a_2 = e_2$). Taking this into account, it is obtained that the temperature of the fillets is expressed according to the equation:

$$T_2 = \sqrt[4]{e_1\,T_1^4 + \frac{\dot{Q}_C}{\bar{F}_{12}\,A_1\,e_2\,\sigma}}$$

The refractory view factor $\bar{F}_{12}$ is calculated from Figure 14.6, where curve 7 is taken for a rectangle 2:1:

$$\text{Ratio} = \frac{\text{edge length}}{\text{distance between planes}} = \frac{90\ \text{cm}}{25\ \text{cm}} = 3.6$$

Hence, $\bar{F}_{12} = 0.82$.
Substitution of data yields:

$$T_2 = \sqrt[4]{(0.85)(1073)^4\,\text{K}^4 + \frac{600\ \text{W}}{(0.82)(0.45\ \text{m}^2)(0.45)\left(5.67 \times 10^{-8}\ \frac{\text{W}}{\text{m}^2\,\text{K}^4}\right)}}$$

$T_2 = 1044.6$ K (= 771.6°C).

14.3

Saturated steam at 2.1 kg/cm² circulates inside a pipe of 3 cm of external diameter and 2.5 mm of wall thickness, so the temperature outside the wall of the tube is 120°C. To avoid heat losses to the exterior that could cause steam to condense, the pipes are insulated with a 4-cm thick insulator, whose thermal conductivity is 0.1 kcal/(hm°C). If the pipe is inside a room at 25°C, calculate: (a) the amount of heat dissipated per m of pipe when it is not insulated; (b) the temperature of the external surface of insulator that covers the pipe; and (c) the percentage of heat loss saved by the insulation.

(a) For the noninsulated pipe, the heat dissipated to the exterior is due to simultaneous convection and radiation, the exchange area being $A_e = \pi\, d_e\, L$. The heat flowrate exchanged per m of pipe is:

$$\frac{\dot{Q}}{L} = \pi d_e \left(h_C - h_R\right)\left(T_w - T_G\right)$$

where:

$$T_w - T_G = 120°\text{C} - 25°\text{C} = 95°\text{C}$$

The calculation of $(h_c - h_R)$ should be interpolated in Table 14.1, obtaining a value of:

$$\left(h_c + h_R\right) = 14.59\,\text{kcal}/\left(\text{h m}^2\,{}^\circ\text{C}\right)$$

Therefore, the heat flow rate per m of pipe exchanged with the surroundings is:

$$\frac{\dot{Q}}{L} = \pi(0.03\ \text{m})\left(14.59\ \frac{\text{kcal}}{\text{h m}^2\,{}^\circ\text{C}}\right)(95^\circ\text{C}) = 130.6\ \frac{\text{kcal}}{\text{h m}}$$

(b) When the pipe has an insulating cover, the heat per m of pipe that flows through the insulation is the same amount dissipated to the outside by radiation and convection:

$$\frac{\dot{Q}}{L} = \frac{\pi\left(d_0 - d_e\right)}{\ln\left(d_0 / d_e\right)} \frac{k}{e_A}\left(T_w - T_0\right)$$

$$= \pi d_0 \left(h_C + h_R\right)\left(T_w - T_G\right)$$

where d_0 and d_e are the external diameters of the pipe and the insulator ($d_0 = d_e + 2e_A$), e_A being the thickness of the insulator. T_w and T_0 are the temperatures of the external wall of the pipe and the insulator, respectively.

Substitution yields:

$$\frac{\pi(11-3)\times 10^{-2}\ \text{m}}{\ln\left(11/3\right)} \frac{0.1 \dfrac{\text{kcal}}{\text{h m °C}}}{0.04\ \text{m}}\left(120 - T_0\right)\text{°C} = \pi(0.11\ \text{m})\left(h_C + h_R\right)\left(T_w - 25\right)\text{°C}$$

Rearranging:

$$T_0 = \frac{168 + 25\left(h_C + h_R\right)}{1.4 + \left(h_C + h_R\right)}$$

This equation is solved by iteration, so T_0 is supposed and $(T_0 - T_G)$ is calculated. This value is used to determine $(h_C - h_R)$ from Table 14.1, which in turn allows one to calculate the temperature T_0 using the last equation. Thus, the following is obtained:

$$T_0 = 37°\text{C}$$

$$\left(h_C - h_R\right) = 9.73\ \text{kcal}/\left(\text{h m}^2\,°\text{C}\right)$$

Using these data, the heat flow lost per m of pipe is:

$$\frac{\dot{Q}}{L} = \pi\ (0.11\ \text{m})\left(9.73 \frac{\text{kcal}}{\text{h m}^2\ °\text{C}}\right)(37 - 25)\text{°C} = 40.4 \frac{\text{kcal}}{\text{h m}}$$

(c) When observing the heat losses per unit time and length of pipe in the last two sections, it is easy to obtain that the percentage of loss saved with insulation is 69%.

14.4

It is desired to heat 10,000 kg of a product in an electric oven shaped with a 3 m × 4 m floor. A row of cylindrical resistances (4 m long and 2 cm of diameter) was placed on its roof in such a way that the distance between their centers is 6 cm. The temperature reached by the resistance is 1500°C, and they are in a plane 2.5 m above the product to be heated. If the oven has refractory walls that are perfectly insulated from the exterior, determine the time needed to heat the product from 20 to 500°C.

Data: emissivity of the resistance = 0.70; emissivity of the load = 0.90; specific heat of the product = 1.046 kJ/(kg°C).

First, the heat flow from the electric resistance to the product is calculated. Since the walls of the oven are refractory, T_1 is the temperature of the resistance and T is the temperature of the product. Then, according to Equation 14.31:

$$\dot{Q}_{1P} = \Im_{1P} A_1 \sigma\left(T_1^4 - T^4\right)$$

in which $\Im_{1P}$ is the gray factor defined by Equation 14.32. The refractory factor in this equation is calculated as if they were two parallel surfaces separated by refractors, although it should be corrected with a factor F, since the emission is actually by the resistance.

It is supposed that there exists an imaginary plane parallel to the product at 2.5 m. This implies calculation of the geometric factor between 3 × 4 m² parallel planes separated by 2.5 m.

Using the ratio: smaller side/distance between planes = 3/2.5 = 1.2 and, using Figure 14.6 curve 7, it is obtained that $\bar{F} \cong 0.64$.

The correction factor F is obtained from Figure 14.7 (radiation to a tube bundle). The radiation plane with respect to the tubes is supposed:

$$\frac{\text{distance between the center of the tubes}}{\text{external diameter of the tubes}} = \frac{6\text{ cm}}{2\text{ cm}} = 3$$

Using this value in the abscissas and the total curve at one row (curve 3), it is obtained that $F = 0.72$.

The value of the refractory factor is $\bar{F}_{1P} = (0.64)(0.72) = 0.46$.

The areas are $A_1 = A_P = 12$ m². The gray factor is obtained by Equation 14.32:

$$\Im_{12} = \frac{1}{\dfrac{1}{0.46} + \left(\dfrac{1}{0.7} - 1\right) + \dfrac{12}{12}\left(\dfrac{1}{0.9} - 1\right)} = 0.369$$

The value of the heat flow rate exchanged by the resistance and the product is calculated using Equation 14.31:

$$\dot{Q}_{1P} = (0.369)(12\,\mathrm{m}^2)\left(5.67 \times 10^{-8}\,\frac{\mathrm{W}}{\mathrm{m}^2\,\mathrm{K}^4}\right)(1773^4 - T^4)\,\mathrm{K}^4$$

$$\dot{Q}_{1P} = 2.51 \times 10^{-7}\,(1773^4 - \mathrm{T}^4)W$$

The heat irradiated by the resistance goes to the product that accumulates this heat by increasing its temperature. When performing an energy balance in the product, it is obtained that:

$$\dot{Q} = m\hat{C}_P\frac{dT}{dt} = 2.51 \times 10^{-7}\,(1773^4 - T^4)W$$

where m is the mass of the product. Substitution of data given in the statement of the problem yields:

$$(10{,}000\ \mathrm{kg})\left(1.046 \times 10^3\,\frac{\mathrm{J}}{\mathrm{kg}\,^\circ\mathrm{C}}\right)\frac{dT}{dt} = 2.51 \times 10^{-7}\,(1773^4 - T^4)W$$

This expression allows one to obtain an equation in separated variables to calculate time:

$$t = 4.17 \times 10^{13}\int_{293}^{773}\frac{dT}{(1773^4 - T^4)}$$

Integration yields:

$$t = \frac{4.17 \times 10^{13}}{2 \times 1773^3}\left[\frac{1}{2}\ \ln\left(\frac{1773+T}{1773-T}\right) + \arctan\left(\frac{T}{1773}\right)\right]_{293}^{773} = 53{,}700\ \mathrm{s}$$

Therefore, 14 h and 55 min are required to carry out the heating process indicated in the problem.

15

Thermal Processing of Foods

15.1 Introduction

One of the main problems in food engineering deals with the inactivation of microorganisms present in foods, not only to prevent their contaminating potential, but also to preserve foods for as long as possible. In order to achieve the inactivation of spore and vegetative forms, foods are thermally treated inside containers or in continuous form and are packed later in aseptic containers. It is important to obtain a high-quality final product by minimizing losses in nutrients or sensorial properties.

The thermal processing of packed products is carried out in equipment that uses steam or hot water as the heating fluid. In aseptic processing, the products are first thermally treated, then carried to a previously sterilized container, and finally sealed under sterile environment conditions. This is a technique used in fluids such as milk and fruit juices, although recently it has also been applied to particulate food products. Aseptic processing presents different advantages with respect to traditional thermal treatment in containers, since the food undergoes less deterioration, processing times are shorter, energy consumption is reduced, and the quality of the treated product is improved and more uniform.

Pasteurization and sterilization can be distinguished within thermal treatments. The former refers to the thermal destruction of specific pathogen microorganisms, although the resulting product is unstable if not stored under refrigeration. Sterilization is a process by which products are made stable without refrigerated storage.

15.2 Thermal Death Rate

The death rate for any microorganism in a determined medium and thermally treated at certain fixed temperature follows a first-order kinetics. Thus, if N is the number of microorganisms, its variation with time is expressed as:

$$\frac{dN}{dt} = -kN \tag{15.1}$$

This equation can be integrated considering the boundary condition that, for the initial time, there are N_o microorganisms, yielding:

$$N = N_0 \exp(-kt) \tag{15.2}$$

in which N is the number of microorganisms present at a time t, and k is the death rate constant.

The value of the rate constant depends on the type of microorganism, the medium, and the temperature. Also, for a specific microorganism, the value depends on the state of the microorganism, vegetative or spores. These constants are much greater for vegetative forms than for spore forms, indicating that spores are much more difficult to destroy. The values of the thermal death constant of vegetative forms are around 10^{10} min^{-1}, while spore form values are approximately 1 min^{-1}.

15.2.1 Decimal Reduction Time *D*

Decimal reduction time is usually employed in calculations of thermal treatment problems and can be defined as the treatment time required to reduce the number of microorganisms to the tenth part, represented as D_T. In thermal treatment calculations it is assumed that this time is independent of the initial concentration of microorganisms, but that it depends on temperature, type of microorganism, and culture or food media in which microorganisms grow.

The following expression is obtained from Equation 15.2:

$$D_T = \frac{2.303}{k} \log_{10}\left(\frac{N}{N_0}\right)$$

and since $N = 0.1\ N_0$, the decimal reduction time is expressed as a function of the rate constant of thermal death as:

$$D_T = \frac{2.303}{k} \tag{15.3}$$

and treatment time is expressed according to Equation 15.4:

$$t = D_T \log_{10}\left(\frac{N_0}{N}\right) \tag{15.4}$$

15.2.2 Thermal Death Curves

Equation 15.2 can become a linear equation if it is expressed in logarithmic form:

$$\ln\left(\frac{N}{N_0}\right) = -k\,t \tag{15.5}$$

If N/N_0 is plotted in semilogarithmic coordinates against time, a straight line with slope $-k$ and ordinate to the origin 1 is obtained. This straight line is called a thermal death curve and, for each microorganism, it is determined by the treatment temperature so that, if the temperature is different, the slope of the straight line will also be different, since the death rate constant varies. Thus, if temperature increases, the slope is greater (Figure 15.1).

This is common for thermal treatment of microorganisms, but it may not be true in the case of spore forms. When N/N_0 is plotted against time in semilogarithmic coordinates, curves and not straight lines are obtained, as can be seen in Figure 15.1.

Some curves show thermal death curves for some microorganisms present in milk, while Figure 15.3 shows curves for thermal inactivation of some enzymes. Some curves show a thermal death curve which represents how to obtain the value of the decimal reduction time for a specific treatment temperature.

15.2.3 Thermal Death Time Constant *z*

Thermal treatments are carried out at different temperatures, depending in each case on the needs or facilities of each industry. For this reason, thermal treatments are not necessarily performed at the temperatures at which thermal death data were obtained. Therefore, a relationship between thermal death time and temperature should be found. This relationship is given as a graph in Figure 15.5, where thermal death time (TDT) or decimal reduction (D_T) are plotted in semilogarithmic coordinates against temperature. It can be observed that a straight line with negative slope ($-m$) is obtained. The value of the slope is:

$$m = \frac{\log D_{T_1} - \log D_{T_2}}{T_1 - T_2} \tag{15.6}$$

in which D_{T1} is the decimal reduction time at temperature T_1, while D_{T2} is the time corresponding to temperature T_2.

The parameter z is defined as the inverse of slope m and measures the variation of the thermal death rate with temperature, representing the temperature increase required to reduce the treatment time to the tenth part or, in turn, D_T.

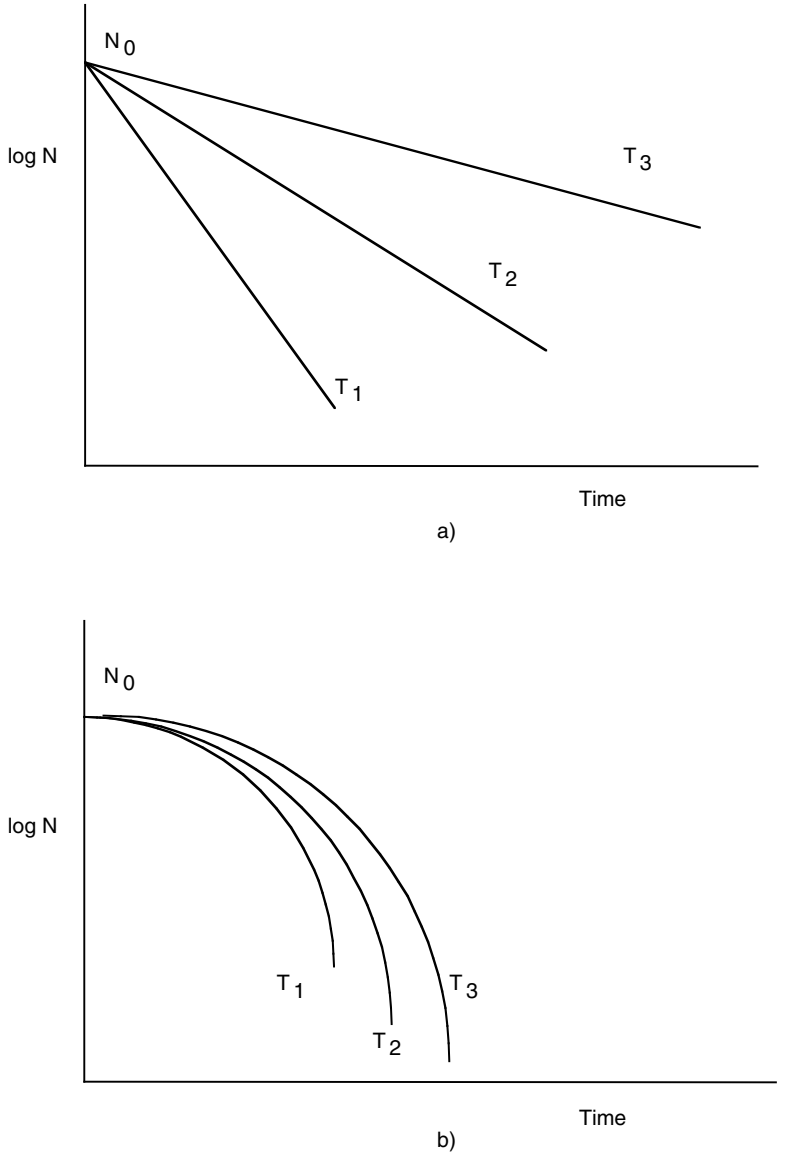

FIGURE 15.1
Thermal death curves for microorganisms: $T_1 > T_2 > T_3$. (a) vegetative form; (b) spore forms.

The relationship between two treatment times and their corresponding temperatures can be easily obtained from the equation:

$$\frac{\log t_1 - \log t_2}{\log 10} = \frac{T_2 - T_1}{z} \tag{15.7a}$$

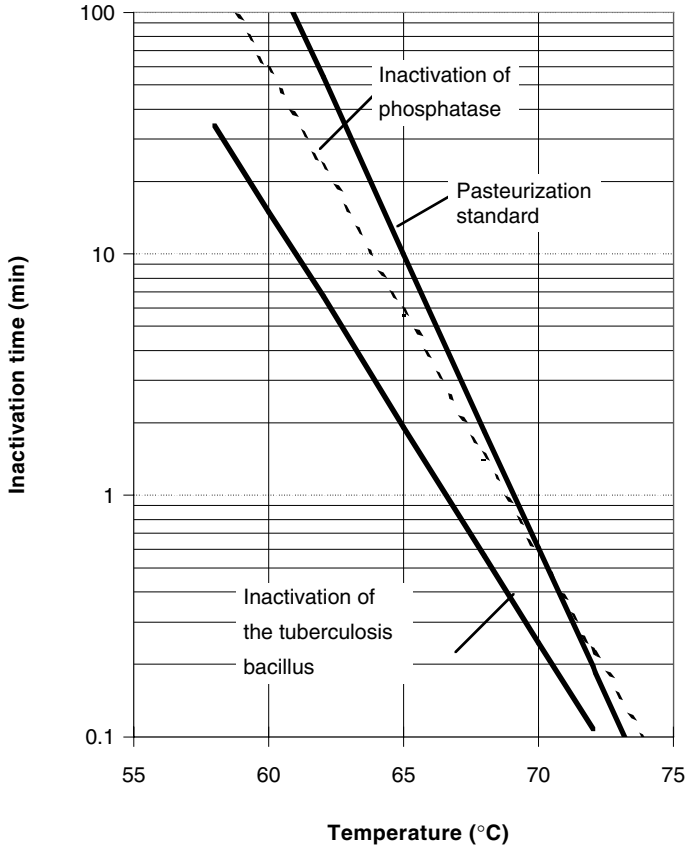

FIGURE 15.2
Thermal death curves for milk microorganisms. (Adapted from Earle, R.L., *Ingenieria de los Alimentos*, 2nd ed., Acribia, Zaragoza, Spain, 1983.)

or as a function of the decimal reduction times:

$$\frac{\log D_{T_1} - \log D_{T_2}}{\log 10} = \frac{T_2 - T_1}{z} \tag{15.7b}$$

If one of these temperatures is the one of reference, then:

$$t_1 = t_R 10^{\frac{T_R - T_1}{z}} \tag{15.8a}$$

$$D_1 = D_R 10^{\frac{T_R - T_1}{z}} \tag{15.8b}$$

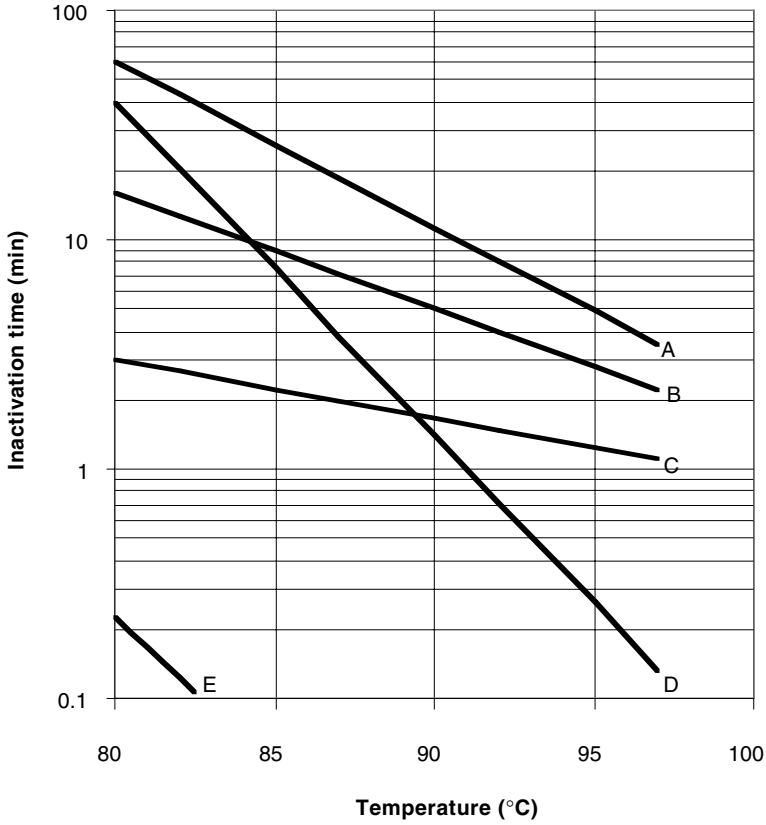

FIGURE 15.3
Thermal inactivation curves for biological factors: (A) pectinesterase (citric products); (B) polygalacturonase (citric products); (C) ascorbic oxidase (peach); (D) *clostridium pasteuranum* (6D); (E) molds and yeast (12D). (Adapted from Toledo, R.T. and Chang, S.-Y., *Food Technol.*, 44(2), 75, 1990.)

The value of z is used to calculate the lethal efficiency rate L that measures lethality at a temperature T with respect to the reference temperature T_R:

$$L = 10^{\frac{T-T_R}{z}} \tag{15.9}$$

Therefore, treatment time t_T, as well as decimal reduction time D_T, at any temperature T, can be expressed as a function of the lethal rate:

$$t_T = \frac{t_R}{L} \tag{15.10a}$$

$$D_T = \frac{D_R}{L} \tag{15.10b}$$

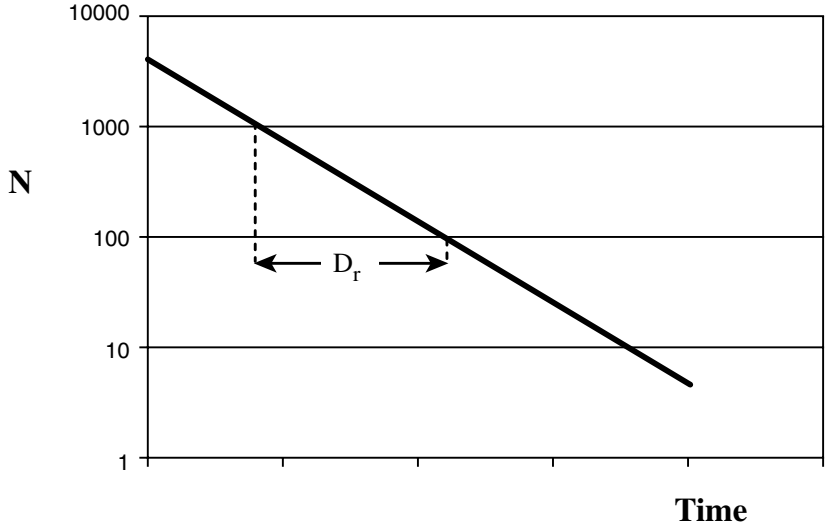

FIGURE 15.4
Thermal death time (TDT) curve; obtaining decimal reduction time.

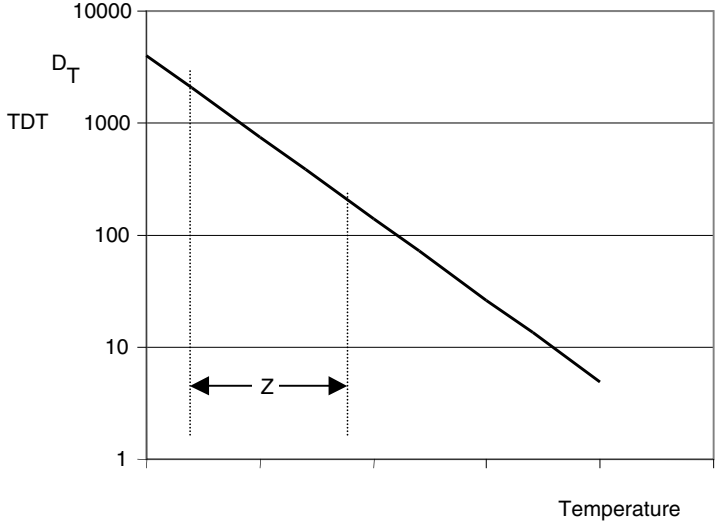

FIGURE 15.5
Thermal death curve TDT or D_T.

15.2.4 Reduction Degree *n*

It can be easily observed in Equation 15.2 that an infinite time of treatment is required in order to obtain a null concentration of microorganisms at the end of a thermal treatment. This points out that it is impossible to achieve

a complete sterilization of the product. For this reason, a final concentration N_F is defined to ensure that the treated product is commercially sterile. Therefore, complete sterilization of a product cannot be discussed; rather, focus will be on commercial sterility.

The decimal logarithm of the ratio between the initial amount of microorganisms N_0 and the amount of microorganisms at a given time, at which N_F is obtained, is called reduction degree.

$$n = \log_{10}\left(\frac{N_0}{N_F}\right) \tag{15.11}$$

This n value is arbitrary and depends on the type of microorganism, although the safety of thermal treatment is greater as the value of the reduction degree is greater. Table 15.1 presents the values of n for different microorganisms that cause deterioration in foods. It can be observed that this value is different depending on the type of microorganism. Those microorganisms with higher values indicate that it is necessary to reduce the microorganisms' content to lower levels than those that present a lower reduction degree to ensure commercial sterility. Values of the rate parameters for degradation of food components can be found in the literature (Lund, 1975).

TABLE 15.1

Destruction or Thermal Degradation Time of Thermo-Sensitive Microorganisms, Enzymes, Vitamin B_1, and Clorophylls

Food	Microorganism or Thermo-sensitive factor	T_R (°C)	D_T (min)	F_R (min)	z (°C)	n
Low acid (pH > 4.6)	*B. stearothermophilis*	121	4–5	15	9.5–10	5
	C. thermosaccharolitico	121	2–5	15	10	5
	C. nigrificans	121	2–5	15	10	5
	C. botulinum	121	0.1–0.3	2.5–3	10	12
	C. sporogenes	121	0.1–1.5	5	10	5
Acid (4 < pH < 4.6)	*B. coagulans*	121	0.01–0.07	—	10	5
	B. polymixa and *macerans*	100	0.1– 0.5	1.3–10 (F_{93})	14–17.5	—
	C. pasteurianum	100	0.1–0.5	1.3–10 (F_{93})	8	5
Very acid (pH < 4)	*Lactobacillus*, *Leuconostoc*	65	0.5–6.0	0.1 (F_{93})	5–11	—
	Yeast and molds	121	5×10^{-8}	10^{-6}	5–8	20
Sweet corn and green beans	Peroxidase	121	1.22	5.1	11–52	4
Spinach	Catalase	121	2.3×10^{-7}	9.3×10^{-7}	8.3	4
Pea	Lipoxigenase	121	1.7×10^{-7}	7×10^{-6}	8.7	4
Pear	Polyphenoloxidase	121	3.2×10^{-8}	1.3×10^{-7}	5.6	4
Papaya	Polygalacturonase	121	4.4×10^{-6}	1.7×10^{-8}	6.1	4
Spinach and green beans	Vitamin B_1	121	140	5.6	25	0.04
	Chlorophyll a	121	12.8	0.50	51–87	0.04
	Chlorophyll b	121	14.3	0.57	98–111	0.04

15.2.5 Thermal Death Time *F*

The treatment time needed to reach a reduction degree n at a given temperature T is called thermal death time, F_T. The value of this treatment time can be obtained from Equation 15.5:

$$F_T = nD_T \tag{15.12}$$

This means that the treatment time is obtained by multiplying the decimal reduction time by the reduction degree. This equation is known as the survival law, or the first law of thermal death of microorganisms, or the first law of degradation of one quality factor of a food that can be thermally destroyed. The value of this parameter F is called thermal death time.

The treatment time to reach a given reduction degree n depends on temperature in such a way that, when temperature increases, the time required to achieve such reduction decreases. If treatment time and temperature are plotted in semilogarithmic coordinates, a straight line is obtained. If the reduction degree is higher, for example $n + 1$, a straight line with the same slope as for the degradation degree n is obtained, although parallel and with a higher ordinate to the origin. On the other hand, if the reduction degree is $n - 1$, the straight line will have the same slope, although its ordinate to the origin will be lower.

Generally, the thermal death time F of a certain microorganism is given as a function of a reference temperature T_R and a reduction degree n.

The reference temperature usually taken is 121.1°C (250°F), labeling F_0 to the value of F corresponding to this temperature. This means that F_0 is the time required to reduce the given population of a microbial spore with a z of 10°C at 121.1°C. F_C is defined as the value of F in the center of the container, and F_S is the integrated lethality of the heat received by all the points of the container:

$$F_S = nD_R \tag{15.13}$$

in which D_R is the decimal reduction time at 121.1°C. In systems where the food to be treated is rapidly heated, the value of F_S can be considered equal to F_0 or F_C. In practice, the value of F_0 is obtained by summing the lethal rates at 1-min intervals from the heating and cooling curves of a product during thermal processing. In cases where the heating process is slow, the time required for the thermal processing is corrected by the following equation:

$$B = f_h \log\left(\frac{j_h I_h}{g}\right) \tag{15.14}$$

where B is the time of thermal processing corrected for the time needed by the treatment device to reach the processing temperature, f_h are the minutes required by a semilogarithmic heating curve to cross one logarithmic cycle,

j_h is the heating lag factor, I_h is the difference in temperature between the treatment device and the food at the beginning of the process, and g is the difference between the temperature of the treatment device and the maximum temperature attained at a given point of the food, which is usually the slowest heating point (Stumbo et al., 1983; Karel et al., 1975a). Each of these parameters is defined next:

$$I_h = T_E - T_i \tag{15.15}$$

$$j_h = \frac{T_E - T_{ip}}{T_E - T_i} \tag{15.16}$$

$$g = T_E - T \tag{15.17}$$

where:

T_E = temperature of treatment or sterilizing device
T = temperature at a given point of the food
T_i = initial temperature of the food
T_{ip} = temperature obtained at the intersection of the prolongation of the straight part of the semilogarithmic heating curve and the vertical line corresponding to the start of the process, called apparent initial temperature

Besides these parameters, analogous functions can be defined for the cooling stage. In this way, I_c is the difference between the temperature at the end of the heating process (T_f) and the temperature of the cooling water (T_w). The cooling lag factor j_c, corresponding to the cooling curve, is similar to the factor j_h and is defined as:

$$j_c = \frac{T_w - T_{ip}}{T_w - T_i} \tag{15.18}$$

where T_i is the initial temperature of the product at the start of the cooling process and T_{ip} is the apparent initial temperature.

15.2.6 Cooking Value *C*

Thermal processing not only affects the microorganisms present in food, but also affects a food's general quality. For this reason, a cooking value *C*, which is a concept similar to that of lethality, is applied to degradation of sensory attributes. The reference temperature for this value is 100ºC, with typical values of z within the range of 20 to 40ºC.

$$C = C_{100}\, 10^{\frac{100 - T}{z}} \tag{15.19}$$

15.2.7 Effect of Temperature on Rate and Thermal Treatment Parameters

The thermal death of microorganisms follows a first-order kinetics in such a way that, when treatment temperature increases, the rate constant increases; consequently, the thermal death rate increases too. The effect of temperature on the rate constant can be described by the Arrhenius equation:

$$k = K_0 \exp\left(\frac{-Ea}{RT}\right) \tag{15.20}$$

in which k is the rate constant, K_0 is the frequency factor, Ea is the activation energy, R is the gas constant, and T is the absolute temperature.

The relationship between two rate constants for two temperatures T_1 and T_2 can be expressed as:

$$\frac{k_2}{k_1} = \exp\left[\frac{Ea}{R}\left(\frac{1}{T_1} - \frac{1}{T_2}\right)\right] \tag{15.21a}$$

or:

$$\log\left(\frac{k_2}{k_1}\right) = \frac{Ea}{2.303R}\left(\frac{1}{T_1} - \frac{1}{T_2}\right) \tag{15.21b}$$

Since $k = 2.303/D$:

$$\log\left(\frac{k_2}{k_1}\right) = \log\left(\frac{D_1}{D_2}\right)$$

From Equation 15.7:

$$\frac{D_1}{D_2} = 10^{\frac{T_2 - T_1}{z}}$$

Hence:

$$\log\left(\frac{k_2}{k_1}\right) = 10^{\frac{T_2 - T_1}{z}}$$

The combination of these equations yields:

$$\frac{T_2 - T_1}{z} = \frac{Ea}{2.303R}\left(\frac{1}{T_1} - \frac{1}{T_2}\right)$$

The value of z can be obtained as a function of the activation energy and the temperatures:

$$z = \frac{2.303\,R}{Ea\,T_1\,T_2} \tag{15.22}$$

15.3 Treatment of Canned Products

The importance of treatment temperature on thermal death time was explained in the previous section. In canning, treatments are performed in devices where the container goes from room temperature to a treatment temperature so that, after a given time, adequate sterilization levels are accomplished. In these devices, the product to be treated increases its temperature until reaching the process or holding temperature, and then goes through a cooling stage.

15.3.1 Heat Penetration Curve

In thermal treatment it is important to know the point within the canned product that has the lowest temperature, i.e., the lowest heating point. This point receives the lower degree of thermal treatment and can not undergo an adequate thermal treatment. For this reason, it is necessary to know the heat penetration curve at this point, which shows its change of temperature with heating time.

The construction of the heat penetration curve for a given product and container is usually obtained experimentally, although in some cases it can be generated by analytical methods. The latter assumes that heat penetrates the food by conduction, which is only true for solid foods, and calculates the temperature of the geometric center as a function of time. However, this is not complied with liquid foods because heat transmission is not carried out only by conduction, and its convective component should be taken into account. Also, the lowest heating point does not coincide with the geometric center.

When a container with food is placed in a thermal treatment device at a temperature T_E, it can be observed that the temperature of the food increases gradually. It is important to know the evolution of the temperature at the lowest heating point (T_C), since this is the point that receives the lowest thermal treatment, and it should be ensured that the microbial load is adequately eliminated. When heat transfer is performed by conduction, the lowest heating point coincides with the geometric center. However, if there are convective streams inside the container during heating, the lowest heating point does not correspond to the geometric center and is located on the vertical axis, but closer to the bottom of the container.

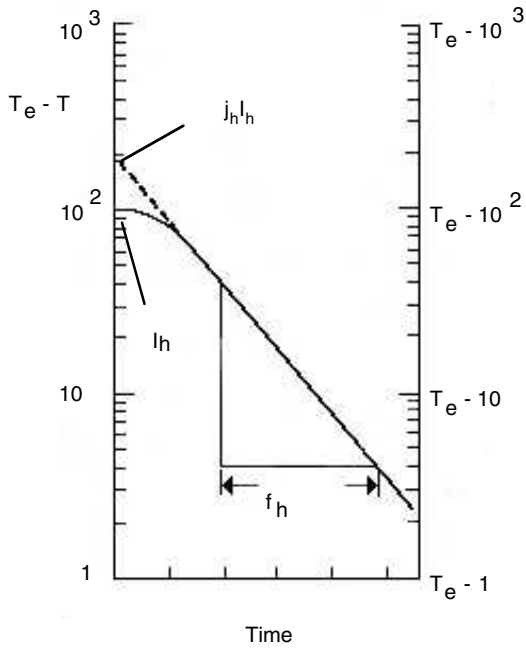

FIGURE 15.6
Heat penetration curve.

The plot of the variation in temperature of a food as a function of heating time is used to characterize heat penetration in foods. The temperature of the geometric center, T_C or T, is taken as the food temperature, and a linear function is obtained when plotting the logarithm of $g = (T_e - T)$ vs. heating time. In a semilogarithmic graph, $(T_e - T)$ is represented on the left ordinates' axis, and the values of $T = T_e - g$ on the right ordinates' axis (Figure 15.6). Log cycles of $T_e - 1$ to $T_e - 10$ and to $T_e - 100$ appear on this last axis.

The temperature of the product against time can be represented in semilogarithmic form based on this graph. This can be done by turning the semilogarithmic paper 180° and labeling the top line with a number equivalent to $T_e - 1$. The next log cycle is labeled with a number equivalent to $T_e - 10$, and the third cycle with a number equivalent to $T_e - 100$. This type of graph is represented in Figure 15.7.

When canned foods are placed inside the thermal treatment equipment, an induction period exists before the temperature of the food begins to rise. This makes the heat penetration curve in Figures 15.6 and 15.7 nonlinear at the beginning of the operation.

It is possible to determine the apparent initial temperature T_{ip} from Figure 15.7 by extending the straight line of the curve until it intersects with the ordinate axis. This temperature, along with the initial temperature T_i and that of the treatment equipment T_E, is used to calculate j_h. The value of f_h is

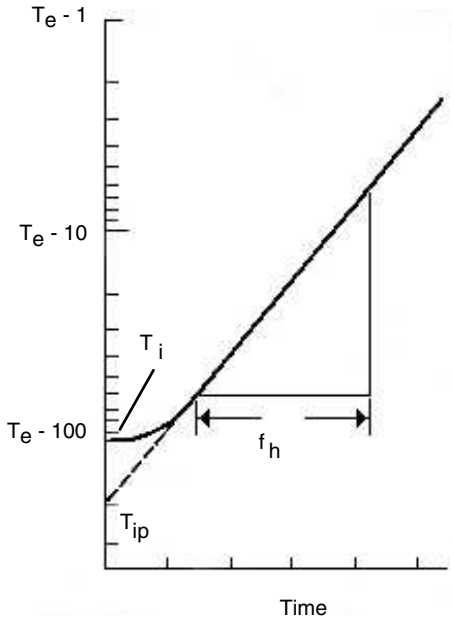

FIGURE 15.7
Graph of the heat penetration curve data.

obtained from the straight part of the heat penetration curve taking the inverse of the slope of this straight line for one log cycle on the heating curve.

15.3.2 Methods to Determine Lethality

15.3.2.1 Graphical Method

The level of sterilization is expressed as a treatment time and temperature for each type of product, shape, and size of container. If the product is treated at a fixed temperature, the treatment time can be directly obtained from Equation 15.10. However, the temperature of the product varies, not only with position, but also with time. For this reason, it is commonly established that time should be measured from the instant when the work temperature is reached until the end of the heating process.

If temperature varies with treatment time, integration is needed to obtain the reduction degree required:

$$\log\left(\frac{C_0}{C}\right) = \int_0^t \frac{dt}{D_T} \tag{15.23}$$

It is necessary to know how the treatment or decimal reduction time varies at each temperature with heating time in order to solve the integral term of Equation 15.23. Thus, it is necessary to previously know the variation of temperature with time (heat penetration curve). Different solving methods exist; however, only the TDT curve method will be used in this book.

In order to ensure an adequate thermal treatment, the integral term of Equation 15.23 should be greater than the reduction degree n previously established for each type of microorganism and product:

$$\int_0^t \frac{dt}{D_T} = \int_0^t \frac{L}{D_R}\, dt \geq n \tag{15.24a}$$

Since the treatment or thermal death time at a determined temperature is a function of the decimal reduction time ($F_T = n\, D_T$), it is obtained that:

$$\int_0^t \frac{dt}{F_T} = \int_0^t \frac{L}{F_R}\, dt \geq 1 \tag{15.24b}$$

The value of the integral term can be graphically solved by plotting $1/t_T$ vs. time and obtaining the area below the curve between two times, in such a way that its value is at least 1. In the case of using the decimal reduction time, $1/D_T$ should be plotted against time, and the value of the area should be greater than the reduction degree n (Figure 15.8).

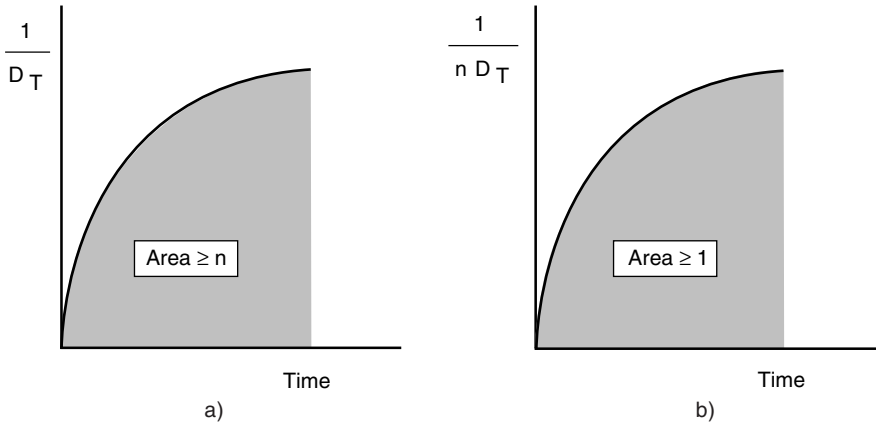

FIGURE 15.8
Graphical method to evaluate lethality.

Equations 15.8a and 15.8b are used to obtain the values of treatment or decimal reduction times for each temperature.

15.3.2.2 Mathematical Method

The mathematical method uses Equation 15.14 to calculate the processing time. This time can be obtained if the values of f_h, the temperature difference $T_e - T_i$, the thermal induction factor j_h, as well as the g value of the temperature difference between the treatment equipment T_e and the slowest heating point at the end of thermal processing are known. The three first parameters can be determined from the heat penetration curve (Figure 15.7), while factor g is not so easily obtained, since the final temperature to ensure an adequate food sterility level cannot be known in advance.

This method was originally developed by Ball and is based on the integration of the lethal effects produced by the time–temperature relationship. The method can be applied when the heat penetration curve, in semilogarithmic coordinates, is a straight line after an initial induction period. The equation developed by Ball (Equation 15.14) takes into account the lethal effects of the cooling stage. A parameter U is defined as the time required to accomplish a certain degree of microbial inactivation at the temperature of the treatment equipment, equivalent to the value F of the process:

$$U = F F_R = F 10^{\frac{T_R - T_e}{z}} \tag{15.25}$$

where F_R is the time at temperature T_R, equivalent to 1 min at 121°C (Stumbo et al., 1983).

Stumbo and Longley (1966) suggested the incorporation of another parameter f_h/U, and tables showing this parameter as a function of g for different values of z have been published (Stumbo et al., 1983). Table 15.2 shows one example for the case of z = 10°C. To obtain these tables, Stumbo used data of different points of the container in order to have different values of j_c. It is assumed in these tables that heat transfer occurs only by conduction, and nonarbitrary assumptions regarding the shape of the temperature profiles at the cooling stage are made. The range of j_c and rounding errors in numeric calculations limits the use of this method. There are graphs in the literature that allow one to obtain the value of g at the end of the treatment. In these graphs, f_h/U is plotted vs. log g in semilogarithmic coordinates for different values of z, and different curves can be obtained depending on the value of j (Toledo, 1980; Teixeira, 1992).

The processing time calculated by this method assumes that, when the containers are placed in the treatment equipment, the temperature of the latter is T_e. This only occurs in equipment that operates in a continuous form. However, in batch processing there is a "come-up" time until the equipment

TABLE 15.2

Relationships f_h/U:g for Values of z = 10 °C

	Values of g (°C) when j is:								
f_h/U	**0.4**	**0.6**	**0.8**	**1.0**	**1.2**	**1.4**	**1.6**	**1.8**	**2.0**
0.2	2.27×10^{-5}	2.46×10^{-5}	2.64×10^{-5}	2.83×10^{-5}	3.02×10^{-5}	3.20×10^{-5}	3.39×10^{-5}	3.58×10^{-5}	3.76×10^{-5}
0.4	7.39×10^{-3}	7.94×10^{-3}	8.44×10^{-3}	9.00×10^{-3}	9.50×10^{-3}	1.00×10^{-2}	1.06×10^{-2}	1.11×10^{-2}	1.16×10^{-2}
0.6	4.83×10^{-2}	5.24×10^{-2}	5.66×10^{-2}	6.06×10^{-2}	6.44×10^{-2}	6.83×10^{-2}	7.28×10^{-2}	7.67×10^{-2}	8.06×10^{-2}
0.8	0.126	0.136	0.148	0.159	0.171	0.182	0.194	0.205	0.217
1	0.227	0.248	0.269	0.291	0.312	0.333	0.354	0.376	0.397
2	0.85	0.92	1.00	1.07	1.15	1.23	1.30	1.38	1.45
3	1.46	1.58	1.69	1.81	1.93	2.04	2.16	2.28	2.39
4	2.01	2.15	2.30	2.45	2.60	2.74	2.89	3.04	3.19
5	2.47	2.64	2.82	3.00	3.17	3.35	2.53	3.71	3.88
6	2.86	3.07	3.27	3.47	3.67	3.88	4.08	4.28	4.48
7	3.21	3.43	3.66	3.89	4.12	4.34	4.57	4.80	5.03
8	3.49	3.75	4.00	4.26	4.51	4.76	5.01	5.26	5.52
9	3.76	4.03	4.31	4.58	4.86	5.13	5.41	5.68	5.96
10	3.98	4.28	4.58	4.88	5.18	5.48	5.77	6.07	6.37
20	5.46	5.94	6.42	6.89	7.37	7.84	8.32	8.79	9.27
30	6.39	6.94	7.56	8.11	8.72	9.33	9.89	10.5	11.1
40	7.11	7.72	8.39	9.06	9.72	10.4	11.1	11.7	12.4
50	7.67	8.39	9.11	9.83	10.6	11.3	12.0	12.7	13.4
60	8.22	8.94	9.72	10.5	11.2	12.0	12.7	13.5	14.3
70	8.67	7.78	10.2	11.1	11.8	12.6	13.4	14.2	15.0
80	9.01	9.89	10.7	11.6	12.3	13.2	14.0	14.8	15.6
90	9.44	10.28	11.2	12.0	12.8	13.7	14.5	15.3	16.2
100	9.78	10.7	11.6	12.4	13.3	14.1	15.0	15.8	16.7

reaches the treatment temperature. In order to take into account the contribution of this come-up time to global lethality, Ball (1923) assumed that 40% of this period contributes to thermal processing. In this way, the real processing time is:

$$t_R = B - 0.4\,t_l \tag{15.26}$$

in which t_l is the come-up time required by the equipment to reach the treatment temperature T_e.

15.4 Thermal Treatment in Aseptic Processing

Different types of treatment equipment are used for the aseptic packaging of food products, where food is thermally treated to reduce its microbial load in an adequate form and then packaged under aseptic conditions. This process consists of three stages. The first is a heating stage, where the food goes from its initial temperature to the treatment temperature. In the second stage, the food receives a thermal treatment at a constant temperature, which is called the holding stage. The third part is a cooling stage. Once the food is treated, it is placed in a sterile container sealed in an aseptic environment. Heat exchangers are used in the heating and cooling stages and can be any one of the different types described in Chapter 13. During the holding stage, food usually circulates through a cylindrical pipe receiving heat from the wall of a tube of a heat exchanger, generally of concentric tubes.

In the treatment equipment, the residence time of a fluid in the treatment equipment should be at least the minimum time required so as to reduce the microbial load in the reduction degree desired.

The residence time, in any treatment equipment, is the relationship between the volume of the device V and the volumetric flow q:

$$t = \frac{V}{q} \tag{15.27}$$

In the case of fluid foods circulating in tubular equipment, the residence time is obtained by the expression:

$$t = \frac{L}{\mathrm{v}} \tag{15.28}$$

in which L is the tube length and v the linear circulation velocity of the fluid through the tube.

Generally, in aseptic processing it is necessary to calculate the length of the holding tube by using Equation 15.28. In this equation, the velocity depends on the circulation regime and type of fluid. For Newtonian fluids that circulate under turbulent regime, a mean velocity (v_m) is used. However, if the fluid circulates under laminar regime (Re < 2100), the maximum velocity, which is a function of the mean velocity, should be used:

$$v_{\max} = 2v_m \tag{15.29}$$

If the fluid shows a rheological behavior according to the power law, Figure 7.9 of Chapter 7 should be used to calculate the maximum velocity as a function of the mean velocity.

Calculation problems can arise in aseptic processing when the product to be treated consists of two phases, with particles suspended within a fluid, as in the case of soups. In these cases, the problem lies with the fact that, when the fluid phase has already reached the processing temperature, the solid particles have a lower temperature. In order to ensure adequate thermal processing, calculations should be made with respect to the slowest heating points, which coincide with the geometric center of the solid particles. This causes the residence times in the holding tube to be greater and particles to need a greater thermal treatment. Also, solid particles can become damaged (Ohlsson, 1994).

It is important to know the heat transfer to the interior of the particles and to obtain the evolution of the temperature at their geometric center with processing time. This is a heating process under unsteady state, and one of the methods described in Section 12.3 of Chapter 12 should be applied. Therefore, the heat transfer coefficient from the fluid to the particles should be previously evaluated. Equations exist in the literature that allow one to calculate heat transfer coefficients of fluids circulating by the exterior of solids. Thus, for fluids that circulate outside spheres, an expression that relates Nusselt, Reynolds, and Prandtl numbers is (Ranz and Marshall, 1952):

$$(Nu) = 2 + 0.6(\mathrm{Re})^{0.5}(Pr)^{1/3} \tag{15.30}$$

If the fluid and the particles circulate at the same velocity, then the Reynolds number is cancelled and (Nu) = 2.

According to Chandarana et al. (1990), if the fluid is water, then the following expression can be employed:

$$(Nu) = 2 + 1.33 \times 10^{-3}(\mathrm{Re})^{1.08} \tag{15.31}$$

This equation is valid for 287 < (Re) < 880.

If the fluid that circulates outside the particles is a starch solution, then Equation 15.32 should be used:

$$\left(Nu\right) = 2 + 2.82 \times 10^{-3} \left(\mathrm{Re}\right)^{1.16} \left(Pr\right)^{0.89} \tag{15.32}$$

This equation is valid for 1.2 < (Re) < 27 and 9.5 < (*Pr*) < 376.

In all these equations, the velocity that should be used in the calculation of the Reynolds number is the relative velocity with which particles circulate inside the tube with respect to the fluid.

In the case of fluids with suspended particles, equations that allow the direct calculation of processing times can also be applied. Hence, the distribution of temperatures in the particles should be obtained first. The *F* value is related to the diffusivity, size of particle (*R*), and position in the tubing (*r*) by means of the equation:

$$F(t) = j \exp\left(-B\,t\right)$$

$$F_0 = \frac{E\left[A \exp\left(-B\,t_p\right)\right]}{B} 10^{\frac{T_A - T_R}{z}}$$

$$A = j\ 2.3^{\frac{T_A - T_R}{z}} \tag{15.33}$$

in which T_A is the external temperature of the particle, T_R is the reference temperature, and t_p is the processing time; $E(x)$ is the exponential integral, while *j* and *B* can be obtained by the relationships given in Table 15.3 for different types of particles, in which α is the thermal diffusivity of the particle and η_l is the viscosity of the carrying fluid.

TABLE 15.3

Parameters for the Calculation of *F* in Equation 15.33

Geometry of the Particle	Position in the Particle	*j*	*B*
Sphere of radius *R*	Center	2	$\frac{\pi^2 \alpha}{R^2}$
	Any	$\frac{2}{\pi}\frac{R}{r}\mathrm{sen}\frac{\pi r}{R}$	
Parallelepiped (2*X*)(2*Y*)(2*Z*)	Center	2.0641	
	Any	$2.0641 \cos\frac{\pi}{2}\frac{x}{X} \cos\frac{\pi}{2}\frac{y}{Y} \cos\frac{\pi}{2}\frac{z}{Z}$	$\frac{\pi^2\alpha}{4}\left(\frac{1}{X^2}+\frac{1}{Y^2}+\frac{1}{Z^2}\right)$
Cylinder (2*R*)(2*L*)	Center	2.0397	$\frac{\alpha}{4}\left(\frac{\pi^2}{L^2}+\frac{\eta_l^2}{R^2}\right)$

15.4.1 Residence Times

In tubular devices in which the fluid circulates under plug flow, the residence time of the microorganisms on the fluid coincides with the mean residence time. For this reason, the calculation of thermal treatments will not present problems. However, it can occur that the fluid does not circulate under plug flow. In this case there will be microorganisms entering the equipment at the same time, but with different residence times.

Thus, for example, if the fluid circulates under laminar regime through a cylindrical pipe, then there exists a parabolic velocity profile in such a way that those microorganisms that enter through the central stream will have a higher velocity than microorganisms traveling close to the walls, and the residence time of the former will be shorter. This can cause the treatment to be inadequate, since the residence time of these microorganisms is shorter than the mean residence time. For this reason, it is essential to know the maximum velocity and to use it for the calculations, since it corresponds to the minimum residence time in the treatment equipment. Figure 15.9 shows different velocity profiles in tubular devices for different circulation regimes in pipes and presents a scheme of an agitated vessel.

15.4.2 Dispersion of Residence Times

In real thermal treatment equipment, the microorganisms that enter at the same instant do not stay in the equipment during the same time. It is convenient to know the dispersion of the residence times to carry out an adequate calculation of treatment time. Some parameters that will be used in other sections are defined next. The residence time of a microorganism in the equipment is the time interval between the inlet and the outlet. Age is the time that passes from the inlet to a given instant. Function of distribution of internal ages (I) is the curve that represents the distribution of ages inside the treatment equipment, while function of distribution of external ages (E) is the curve representing the distribution of ages of microorganisms that leave the treatment equipment, i.e., the residence times. In order to determine these functions, it is necessary to use experimental techniques. One of these techniques, the tracer-response, consists of introducing a tracer into the entering stream and measuring its concentration at the exit.

The more common entrance functions are those of step and impulse (or delta). In the first function, a tracer is introduced at a certain concentration at a given instant and is maintained along all the experiment. On the other hand, in the delta or impulse entrance, a certain level of tracer is introduced at once (Figure 15.10). In this figure, C_t is the concentration of the tracer at a given instant t, while C_0 is the total concentration.

The response functions of each entrance function are represented by F and C, for step and impulse, respectively. It should be pointed out that all the functions defined in this section should be normalized.

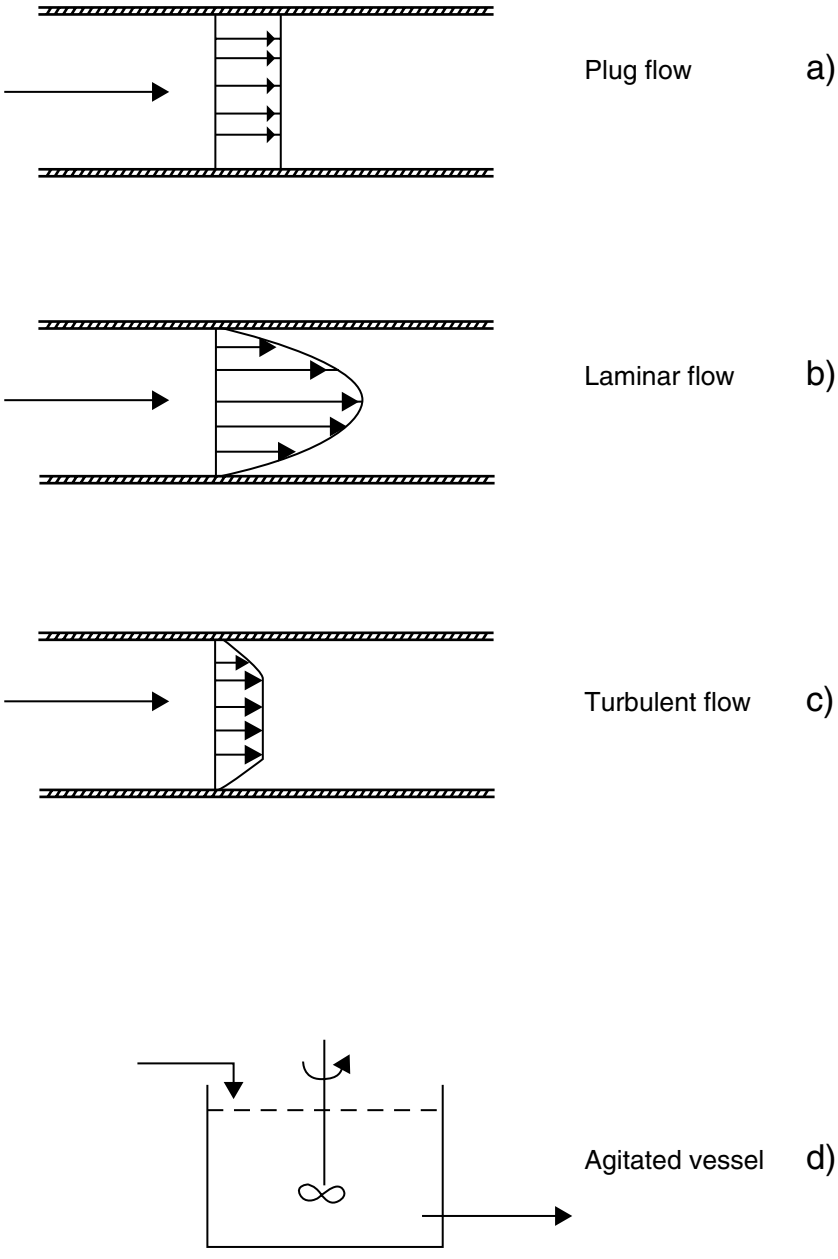

FIGURE 15.9
Flow of fluids in tubing and in an agitated vessel.

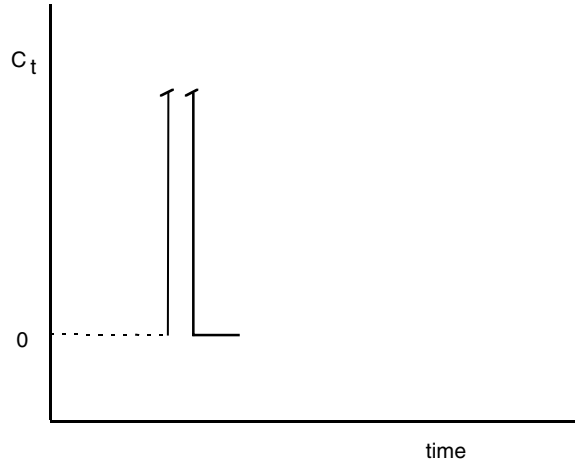

FIGURE 15.10
Entrance of tracer as impulse.

The relationships between the different functions of entrance and response are the following:

$$I = 1 - F \tag{15.34a}$$

$$E = C \tag{15.34b}$$

$$E = \frac{dF}{d\theta} = -\frac{dI}{d\theta} \tag{15.34c}$$

in which θ is a dimensionless time variable defined as the quotient between time t and the mean residence time t_M.

The function that will be used in the following sections for continuous thermal treatment calculations is the function of distribution of external ages E.

15.4.3 Distribution Function *E* under Ideal Behavior

The circulation of a food in thermal treatment equipment is considered ideal when such equipment is a perfect mixing agitated vessel or a tubular equipment with either laminar or plug flow through it. The expressions for the function of distribution of external ages for each of the equipment mentioned is given next as a function of the real and dimensionless time variable:

Perfect mixing agitated vessel:

$$E = \frac{1}{t_M}\exp\left(-\frac{t}{t_M}\right) \tag{15.35a}$$

$$E_\theta = \exp(-\theta) \tag{15.35b}$$

Tubular equipment with plug flow:

$$E = \delta(t - t_M)$$

which is known as delta distribution function or Dirac.

Tubular equipment with laminar flow:

$$E = \frac{t_M^2}{2t^3} \tag{15.36a}$$

$$E = \frac{1}{2\theta^3} \tag{15.36b}$$

Figure 15.11 presents all these functions E as a response of an impulse entrance.

It is possible to obtain distribution functions of external ages for non-Newtonian fluids. Thus, for fluids that follow the power law, the function is expressed as:

$$E = \frac{2n}{3n+1}\frac{t_M^3}{t^3}\left(1 - \frac{n+1}{3n+1}\frac{t_M}{t}\right)^{\frac{n-1}{n+1}} \tag{15.37}$$

in which n is the index of flow behavior.

For Bingham plastics that circulate in pipes, a velocity profile has been created in which the central stream circulates under plug flow. The distribution function of external ages is:

$$E = \frac{(1-m)t_0\, t_M^3}{t^3}\left[1 - m + \frac{m}{\sqrt{1 - \sigma_0 \frac{t_M}{t}}}\right] \tag{15.38}$$

in which:

$$m = \frac{r}{R} = \frac{\sigma_0}{\sigma_{WALL}} \quad \text{and} \quad t_0 = \frac{m^2 + 2m + 3}{6}$$

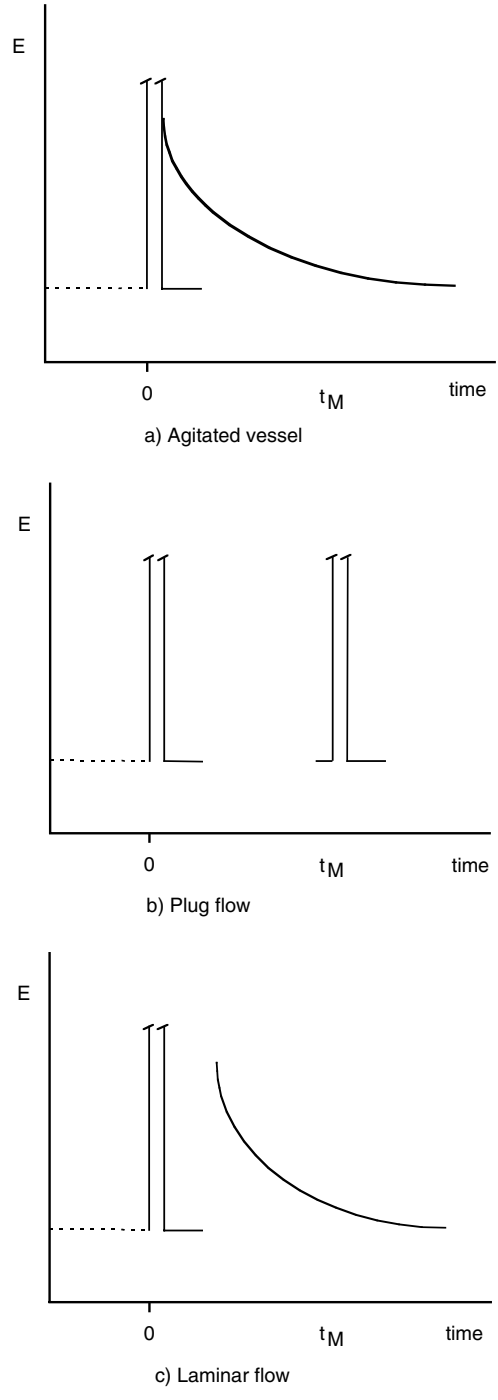

FIGURE 15.11
Distribution function of external ages for different types of flow.

σ_0 being the yield stress, σ_{WALL} the value of the shear stress on the wall, and t_0 a parameter that represents the residence time of the fluid in the central stream under plug flow.

15.4.4 Distribution Function *E* under Nonideal Behavior

The distribution function of external ages is the residence time of each element of the fluid in the treatment equipment. This function depends on the path followed by the fluid inside the container. If it is considered a container for thermal treatment, in which the food enters with a volumetric flow q, the distribution function of external ages can be represented according to what is indicated in Figure 15.12. In order to normalize this function, the area below the curve should have a value equal to one:

$$\int_0^\infty E\,dt = 1 \tag{15.39}$$

The fraction of fluid that leaves the container between any two times t_1 and t_2 will be:

$$E\,\Delta t = a\left(t_2 - t_1\right) \tag{15.40}$$

where a is the mean value of the distribution function of external ages in this time interval.

The fraction of fluid that leaves at a time smaller than t_1 is:

$$\int_0^{t_1} E\,dt$$

while the fraction that exists at times greater than t_1 is:

$$\int_{t_1}^\infty E\,dt = 1 - \int_0^{t_1} E\,dt$$

As indicated before, the function E should be experimentally obtained by injecting a tracer and observing the response. For the specific case in which the tracer is introduced as an impulse function in the food stream, it should be operated as indicated next. If V is the volume of the thermal treatment device through which a stream with volumetric flow q circulates, an amount M of tracer is introduced at a determined time. The amount of tracer is analyzed in the outlet stream. If C_i is this concentration, then it is tabulated

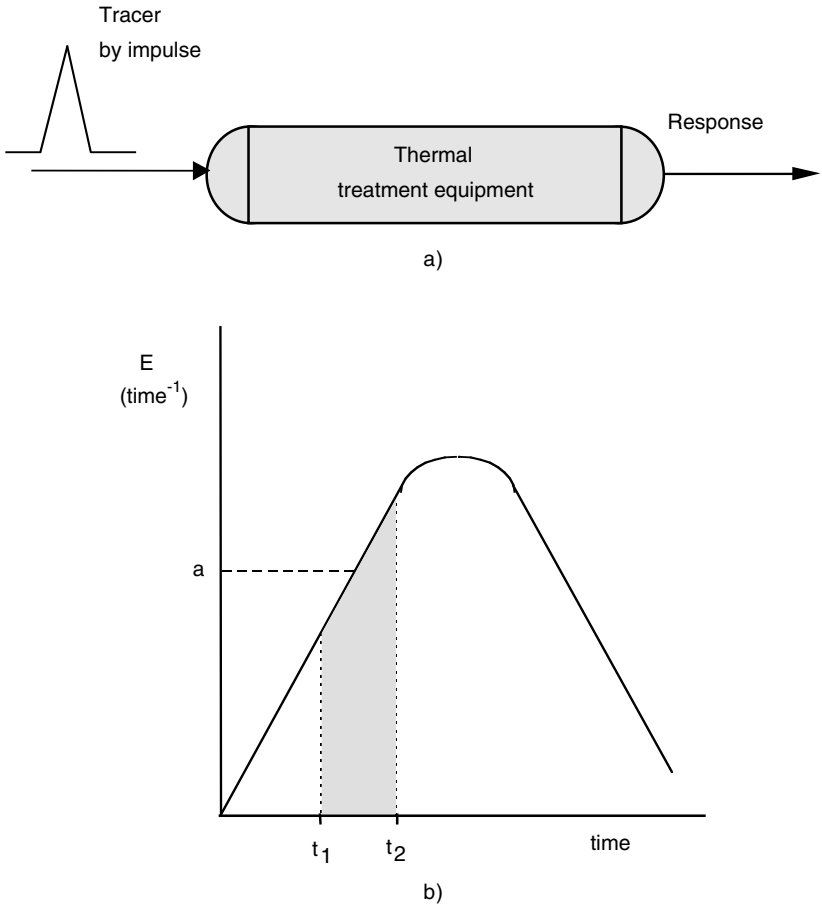

FIGURE 15.12
Obtaining the curve of external ages.

or plotted against time to obtain the distribution function of the tracer's concentration.

The area below this curve will be:

$$\int_0^\infty C_i \, dt = \sum_i C_i \, \Delta t = \frac{M}{q} \tag{15.41}$$

in which M is the total quantity of tracer injected.

The curve E is obtained from this curve, but since it should be normalized, the concentration obtained at each time is divided by the area given by Equation 15.39:

$$E = \frac{C_i}{\int_0^\infty C_i\,dt} = \frac{qC_i}{M} \tag{15.42}$$

It is interesting to point out that many thermally treated food fluids contain suspended solid particles. In these cases, the distribution curves of external ages show a double node, in such a way that the response curve begins to appear at times greater than half of the mean residence time.

Since mean residence times are required in later calculations, they must be determined. Also, the variance gives an idea of the dispersion of the residence times, since such dispersion is greater as the variance is greater. For this reason, equations that allow calculation of the mean and the variance will be stated.

The mean permits one to calculate the mean residence time t_M. In general, this value is calculated from the equation:

$$t_M = \frac{\int_0^\infty t_i C_i\,dt}{\int_0^\infty C_i\,dt} \tag{15.43}$$

In case the number of measurements is discrete, the integrals can be substituted by summations:

$$t_M = \frac{\sum_0^\infty t_i C_i \Delta t}{\sum_0^\infty C_i \Delta t} \tag{15.44}$$

For continuous functions with discrete measurements with equal time intervals, the distribution function of external ages can be used in the calculation of the mean:

$$t_M = \int_0^\infty t_i E\,dt = \sum_0^\infty t_i E_i \Delta t \tag{15.45}$$

The variance can be obtained from the expression:

$$\sigma^2 = \frac{\int_0^\infty t_i^2 C_i \, dt}{\int_0^\infty C_i \, dt} - t_M^2 \tag{15.46}$$

When the number of values is discrete, the integral can be substituted by a summation:

$$\sigma^2 = \frac{\sum_0^\infty t_i^2 C_i \, \Delta t}{\sum_0^\infty C_i \, \Delta t} - t_M^2 \tag{15.47}$$

For continuous curves or discrete measurements at equal time intervals, the variance can be calculated by the following equation:

$$\sigma^2 = \int_0^\infty t_i^2 E \, dt - t_M^2 = \sum_0^\infty t_i^2 E_i \, \Delta t_i - t_M^2 \tag{15.48}$$

15.4.5 Application of the Distribution Models to Continuous Thermal Treatment

The destruction of microorganisms or of some thermosensitive factors of food occurs in the thermal treatment equipment. Such destruction follows a first order kinetics; therefore, the equipment can be considered a reactor in which a first-order reaction is performed.

The following expression can be applied for the calculation of the mean concentration C_M in the stream that leaves the thermal treatment equipment as a function of the inlet concentration C_0:

$$C_M = C_0 \int_0^\infty \left(\frac{C}{C_0} \right)_t E \, dt \tag{15.49}$$

Since the destruction kinetics is of first order:

$$C = C_0 \exp(-k t)$$

then substitution in Equation 15.49 yields:

$$C_M = C_0 \int_0^\infty \exp\left(-k\,t\right)_t E\,dt \tag{15.50}$$

When the number of values is discrete, the latter equation can be expressed using a summation:

$$C_M = C_0 \sum_0^\infty \left[\exp\left(-k\,t\right)\right]_t E\,\Delta t \tag{15.51}$$

Equation 15.50 or 15.51 allows calculation of thermal treatments of products that circulate in a continuous form through the thermal treatment equipment.

For the case of ideal behavior (perfect mixing agitated vessel, plug flow, and laminar flow through pipes), there are analytical solutions to Equation 15.50. These solutions are given next for these three cases.

The distribution function of external ages for a fluid that is treated in a perfect mixing agitated vessel is given by Equation 15.35, which should be substituted in Equation 15.50 and an integration should then be performed:

$$C_M = C_0 \int_0^\infty \exp\left(-k\,t\right)_t \left[\frac{1}{t_M}\exp\left(-\frac{t}{t_M}\right)\right] dt \tag{15.52}$$

Integration yields:

$$C_M = C_0 \frac{1}{1+k\,t} \tag{15.53}$$

For circulation under plug flow, the distribution function of external ages is the delta function of Dirac (Equation 15.36) that, substituted in Equation 15.50, yields:

$$C_M = C_0 \int_0^\infty \exp\left(-k\,t\right)_t \left[\delta\left(t - t_M\right)\right] dt = \exp\left(-k\,t_M\right) \tag{15.54}$$

For circulation under laminar flow, the distribution function of external ages is given by Equation 15.37. The following expression is obtained by substituting it in Equation 15.50:

$$C_M = C_0 \int_0^\infty \exp\left(-k\,t\right)_t \left(\frac{t_M^2}{2t^3}\right) dt \tag{15.55}$$

Problems

15.1

A thermocouple located in the slowest heating point of a crushed tomato can gives the following temperature–time variation:

Time (min):	0	10	20	30	40	50	60
Temperature (°C):	60	71	85	100	107	110	113

The can is placed in the center of a pile subjected to a sterilization process in an autoclave in which the processing temperature is kept at 113°C. Determine the processing time, assuming that the lethal effect of the cooling period is negligible.

Data and notes: the temperature increment needed to decrease the treatment time to the tenth part (Z) for a reduction degree of 12 for *Bacillus coagulans* is 10°C. The time required to obtain this reduction degree at 121°C is 3 min.

The treatment time for a given temperature is calculated from Equation 15.11, in which the following is complied, according to the data given in the statement:

$$T_R = 121°C \qquad F_R = 3 \text{ minutes} \qquad z = 10°C \qquad n = 12$$

In order to solve the problem, the conditions given by Equation 15.24 should be complied with. First, the effect produced during the heating time has to be evaluated by calculating the values of process time required and decimal reduction at each temperature. It is known that, for a given temperature, Equation 15.8 is useful to calculate D_T from F_T.

Beginning with the data in the table of the problem statement and Equations 15.8 and 15.12, it is possible to obtain Table 15.P1:

TABLE 15.P1

Values of Thermal Death Time and Decimal Reduction as a Function of Heating Time

$t_{heating}$ (min)	T (°C)	F_T (min)	D_T (min)	$1/F_T$ (min^{-1})	$1/D_T$ (min^{-1})
0	60	3.8×10^6	3.2×10^5	2.7×10^{-7}	3.2×10^{-6}
10	71	3×10^5	2.5×10^4	3.3×10^{-6}	4×10^{-5}
20	85	1.2×10^4	992	8.4×10^{-5}	10^{-3}
30	100	378	31.5	2.7×10^{-3}	0.032
40	107	75.4	6.3	0.013	0.159
50	110	37.8	3.2	0.027	0.320
60	113	18.9	1.6	0.053	0.635

The lethality for sterilization is obtained by plotting $1/F_T$ against time, or $1/D_T$ (Figure 15.8) against time, and graphically integrating the functions obtained. When performing this integration between the initial and final heating times (60 min) it is obtained that:

$$\int_0^{60} \frac{d\,t}{F_T} = 0.65 < 1$$

$$\int_0^{60} \frac{d\,t}{D_T} = 7.8 < 12$$

This indicates that it is not possible to achieve sterilization of the product with this heating time, so it is required to continue heating at 113°C during a period of time such that the value of the lethality sterilization level complies with the conditions in Equation 15.24.

For F_T, 1 – 0.65 = 0.35 is needed to comply with Equation 15.24b, so the additional time is:

$$t_{113} = (0.35)(18.9 \text{ min}) = 6.62 \text{ min}$$

If the decimal reduction time D_T were used instead, what is needed for sterilization is 12 – 7.8 = 4.2; therefore, the additional time is:

$$t_{113} = (4.2)(1.58 \text{ min}) = 6.64 \text{ min}$$

15.2

A cylindrical can of 6 cm diameter and 15 cm height contains 250 g of pea cream and has a microbial load of 10^5 spores of *Clostridium sporogenes* per each kg of cream. In order to decrease the spore content, the can is subjected to a sterilization process in an autoclave that condenses steam at 121°C. The lowest heating point initially is at 71°C and the temperature along the thermal treatment evolves in the following way:

t (s)	600	800	1000	1400	1600	2000	2200	2400	2600
T (°C)	94	103	109	113.5	116	118	110	82	65

At 121°C, the *Clostridium sporogenes* spores present the following values: z = 10°C and F = 1.67 min. Calculate: (a) the viable spores per kg of cream that exist in the lowest heating point when it reaches the maximum temperature; (b) the microbial load at such point after 45 min of treatment.

The treatment time at different temperatures that is being acquired by the product is calculated from Equation 15.8. According to the data given in the statement of the problem, it is found that:

$$T_R = 121°C \quad F_R = 3 \text{ min} \quad z = 10°C$$

Also, *C. sporogenes*: $n = 5$
Since $D_T = F_T \cdot n$, it is possible to obtain the following table (Table 15.P2):

TABLE 15.P2

Values of Thermal Death Time and Decimal Reduction as a Function of Heating Time

$t_{heating}$ (s)	T (°C)	F_T (min)	D_T (min)	$1/F_T$ (min^{-1})	$1/D_T$ (min^{-1})
600	94	837	167	10^{-3}	5.9×10^{-3}
800	103	105	21	9.5×10^{-3}	0.047
1000	109	26.5	5.3	0.038	0.189
1400	113.5	9.4	1.88	0.107	0.532
1600	116	5.3	1.06	0.189	0.947
2000	118	3.3	0.67	0.300	1.500
2400	82	13,265	2653	7.5×10^{-5}	0.0004
2600	65				

The level of lethality for sterilization is obtained by integration from the beginning of heating up to 2000 s, which corresponds to the time of maximum temperature.

$$\int_0^{2000} \frac{dt}{D_T} = \log\left(\frac{C_0}{C}\right) = 13.29$$

Therefore, the concentration of *C. sporegenes* in the product after 2000 s is:

$$C = C_0 \times 10^{-13.29} = 5.1 \times 10^{-9} \text{ spores/kg}$$

For a time equal to 45 min, integration should be performed between the initial time and 2700 s:

$$\int_0^{2700} \frac{dt}{D_T} = \log\left(\frac{C_0}{C}\right) = 16.34$$

Hence, $C = 4.6 \times 10^{-12}$ spores/kg.

15.3

A packed food is thermally treated in equipment whose processing temperature is 130ºC. It has been obtained that the evolution of temperature at the slowest heating point with processing time is:

t (min)	0	6.5	10	12	16.5	23	28	36	44
T (°C)	30	40	50	60	80	100	110	120	125

If the initial microbial load is 10 CFU/container and it is desired to reduce it to 10^{-5} CFU/container, calculate the processing time. The target microorganism for this thermal process has a decimal reduction time of 2 min for a reference temperature of 121ºC, and to reduce the treatment time to the tenth part it is required to increase the temperature to 10ºC.

This problem will be solved by the method of Ball, using Equation 15.14. The heat penetration curve, similar to that in Figure 15.7, will be plotted in order to calculate the apparent initial temperature. The data of the table included in the statement of the problem are graphically represented in semilogarithmic coordinates, as shown in Figure 15.P3. Hence, T_{ip} = –70ºC. I_h and j_h are calculated from this temperature and Equations 15.15 and 15.16.

$$I_h = T_e - T_i = 130 - 30 = 100^{\circ}\mathrm{C}$$

$$j_h = \frac{T_e - T_{ip}}{T_e - T_i} = \frac{130 - (-70)}{130 - 30} = 2$$

The value of f_h can also be obtained from Figure 15.P3, since it is the inverse of the slope of the straight part of the heat penetration curve. Therefore, it is obtained that f_h = 28 min.

The value of F for this process is then calculated:

$$F = D_T \log\left(\frac{N_0}{N}\right) = (2\,\mathrm{min})\log\left(\frac{10}{10^{-5}}\right) = 12\,\mathrm{min}$$

The value of the parameter U is calculated from Equation 15.25:

$$U = F\,10^{\frac{T_R - T_e}{z}} = (12\ \mathrm{min})10^{\frac{121-130}{10}} = (12\ \mathrm{min})(0.1259) = 1.51\ \mathrm{min}$$

Therefore:

$$\frac{f_h}{U} = 18.53$$

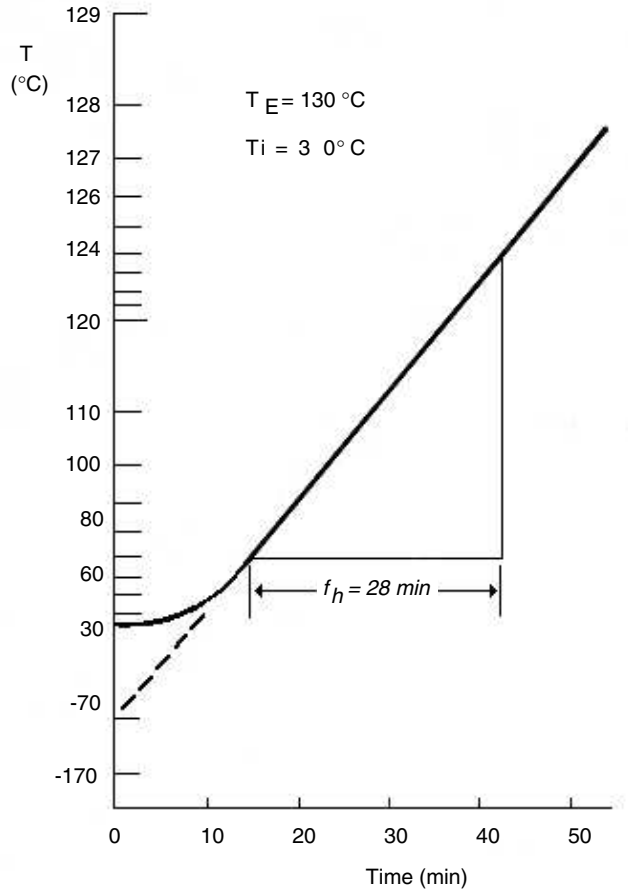

FIGURE 15.P3
Heat penetration curve.

Interpolation in Table 15.2, using the latter quotient (18.53) and $j = 2$, yields a value of $g = 8.84$°C.

Now Equation 15.14 can be applied, since all the variables are known:

$$B = (28\ \text{min})\log\left(\frac{(2)(100)}{8.84}\right) = (28\ \text{min})(1.355) \approx 38\ \text{min}$$

This means that the processing time is 38 min.

15.4

A baby food based on apple purée is thermally treated at a rate of 1500 kg/h employing an aseptic packaging process. The product is heated from 22 to 90°C in a plate heat exchanger. Then it is introduced into a concentric tube

heat exchanger that has an internal diameter of 5 cm. Condensing steam circulates by the annular space that allows maintenance of the product temperature at 90ºC while it remains in the heat exchanger. Commercial sterilization of the product, at 90ºC, is achieved if it remains for 90 s at such temperature. Determine the length that the residence tube should have to ensure that the food receives an adequate thermal treatment.

Data: food properties: density = 1200 kg/m^3; it behaves as a power law fluid with a consistency index of 2.4 Pa·s^n and presents a flow behavior index of 0.5.

The length of the residence tube is obtained from Equation 15.28, where the time is 90 s, which is the time needed to ensure an adequate thermal treatment for the product. The velocity to be used in this equation is the maximum velocity, which in turn is a function of the mean velocity at which the product circulates inside the pipe.

The mean circulation velocity of the product is obtained from the continuity equation:

$$v_m = \frac{4w}{\rho \pi d^2} = \frac{4\left(1500\dfrac{\text{kg}}{\text{h}}\dfrac{1\text{h}}{3600\text{s}}\right)}{\left(1200\dfrac{\text{kg}}{\text{m}^3}\right)\pi\left(0.05\text{m}\right)^2} = 0.556\,\frac{\text{m}}{\text{s}}$$

Since it is a fluid that rheologically behaves according to the power law, the value of the generalized Reynolds number should be previously calculated using Equation 7.7 given in Chapter 7:

$$\text{Re}G = \frac{\left(0.05\text{m}\right)^{0.5}\left(0.556\dfrac{\text{m}}{\text{s}}\right)^{2-0.5}\left(1200\dfrac{\text{kg}}{\text{m}^3}\right)}{8^{0.5-1}\left(2.4\ \text{Pa.s}^{0.5}\right)}\left(\frac{4\cdot(0.5)}{1+3\cdot(0.5)}\right)^{0.5} \approx 117$$

This value means, according to Figure 7.1 (Chapter 7), that the product circulates inside the pipe under laminar regime. Since the product exhibits a power law rheological behavior, it is obtained, from Figure 7.9 (Chapter 7) and a flow behavior index $n = 0.5$, that the mean velocity/maximum velocity relationship is:

$$\frac{v_m}{v_{\max}} = 0.6$$

Hence, the value of the maximum velocity is:

$$v_{\max} = 0.926\,\frac{\text{m}}{\text{s}}$$

Therefore, the length of the residence tube should be:

$$L = \left(0.926\ \frac{\text{m}}{\text{s}}\right)(90\,\text{s}) = 83.34\ \text{m}$$

15.5

An aseptic processing system is used to treat a vegetable soup that contains small pieces of meat in suspension. It can be assumed that the carrier fluid is an aqueous solution and the meat particles are spheres with diameters equal to 12 mm that circulate at a velocity of 0.002 m/s with respect to the carrier fluid. The fluid has a temperature of 150ºC at the entrance of the residence tube, while the meat particles have a uniform temperature of 90ºC. In order to process the soup adequately, a microbial reduction degree of 12 in the center of the particles should be attained. If the volumetric flow with which the soup circulates is 30 l/min, calculate the length that the residence tube should have in order to achieve the desired microbial reduction if the internal diameter of the tube is 4.5 cm.

Data: properties of the aqueous solution: density = 1000 kg/m^3; thermal conductivity = 0.58 W/(m ºC); viscosity = 1.5 mPa·s; specific heat = 4.1 kJ/(kg ºC); thermal diffusivity of meat = 1.3×10^{-7} m^2/s.

The microorganism contained in the soup has a decimal reduction time of 1.5 s at 121ºC, and, in order to reduce the treatment time to the tenth part, it is necessary to increase the temperature to 10ºC.

When the soup enters the holding tube, the carrier fluid has a temperature higher than the temperature of the meat particles, so inside the tube there will be heat transfer from the fluid to the particles. Thus, the temperature of such particles will progressively increase. It is required to calculate the evolution of temperature at the particles' geometric center in order to determine the lethality required for the product to be adequately processed.

The heating process occurs under unsteady state, so the temperature of the particles' center should be calculated according to the description in Section 12.3 (Chapter 12). Initially, the individual heat transfer coefficient will be calculated using Equation 15.31, since the fluid is an aqueous solution. The Reynolds, Prandtl, and Nusselt numbers are:

$$(\text{Re}) = \frac{(1000\,\text{kg/m}^3)(0.002\,\text{m/s})(0.012\,\text{m})}{1.5 \times 10^{-3}\,\text{Pa}\cdot\text{s}} = 16$$

$$(Pr) = \frac{(4100\,\text{J/(kg°C)})(1.5 \times 10^{-3}\,\text{Pa}\cdot\text{s})}{0.58\,\text{J/(s.m.°C)}} = 10.8$$

$$(Nu) = 2 + 2.82 \times 10^{-3}(16)^{1.16}(10.6)^{0.89} = 2.575$$

The individual heat transfer coefficient by convection is

$$h = 249\,\mathrm{W/(m^2\,^oC)}$$

In order to apply the method described in Section 12.3, the following dimensionless numbers should be calculated:

$$m = \frac{k}{h\,r_0} = \frac{\left(0.58\ \mathrm{W/(m^oC)}\right)}{\left(249\,\mathrm{W/(m^2{}^oC)}\right)\left(0.006\ \mathrm{m}\right)} \approx 0.4$$

$$n = \frac{r}{r_0} = 0$$

$$(Fo) = \frac{\alpha\, t}{(r_0)^2} = 3.417 \times 10^{-3}\, t, \text{ expressing the time } t \text{ in seconds}$$

Figure 12.14 is used to calculate the temperature of the slowest heating point. Table 15.P5 shows the different data obtained for the times assumed.

The graphical method described in Section 15.3.3 is used to calculate lethality. In order to calculate the thermal death times, it is supposed that the desired reduction degree is n = 12, hence:

$$F_R = nD_R = (12)(1.5\ \mathrm{s}) = 18\ \mathrm{s}$$

Calculation of lethal velocity is made by Equation 15.9, while the global lethality is calculated using Equation 15.24. The last columns of Table 15.P5 present the values of these parameters for the different processing times. In this table it is observed that a time between 80 and 100 s yields an integral value equal to 1; this time is 85 s.

$$\int_0^{85} \frac{L_{dt}}{F_R} = 1$$

TABLE 15.P5

Calculation of the Global Lethality

Time (s)	(Fo)	T (°C)	$L = 10^{\frac{T-121}{10}}$	$\frac{L}{F_R}$ (s⁻¹)	$\int_0^t \frac{L}{F_R}\cdot dt$
0	0	90			
30	0.103	102	0.0126	0.0007	
60	0.205	114	0.1995	0.0111	0.175
80	0.273	120	0.7943	0.0441	0.743
100	0.342	13.6	1.8197	0.1011	2.118

The linear circulation velocity in the residence tube is calculated from the continuity equation:

$$v = \frac{4q}{\pi d^2} = \frac{4\left(30\dfrac{\text{l}}{\text{min}}\dfrac{1\,\text{m}^3}{10^3\,\text{l}}\dfrac{1\,\text{min}}{60\,\text{s}}\right)}{\pi\left(0.045\,\text{m}\right)^2} \approx 0.314\,\text{m/s}$$

Since it is a laminar regime, the relationship between the maximum and the mean velocities is (Equation 15.29): $v_{max} = 2\ v = 0.628$ m/s. Thus, the length of the residence tube is:

$$L = \left(0.628\frac{\text{m}}{\text{s}}\right)\left(85\,\text{s}\right) = 53.38\,\text{m}$$

15.6

Milk flowing at 1000 kg/h that contains the tuberculosis bacillus with a concentration equal to 10^8 CFU/cm^3, is fed into a tubular thermal treatment equipment with the objective of reducing the microorganism content down to 0.01 CFU/cm^3. The tubular section has an internal diameter of 1 in., and the density of milk is 1030 kg/m^3. The product is held at 71°C during the thermal treatment. Determine the length of the tubular section of treatment if the distribution of external ages follows the δ function of Dirac.

What would be the final microbial load if the treatment equipment were a 500 l perfect mixing agitated vessel?

The treatment time, for a temperature of 71°C = 159.8°F and according to Figure 15.2, should be $F_{71C} = 0.17$ min = 10.2 s.

It is assumed that the reduction degree is $n = 12$, so the decimal reduction time is $D_T = 10.2/12 = 0.85$ s.

The destruction constant of the tuberculosis bacillus is:

$$k = \frac{2.303}{D_T} = 2.71\,\text{s}^{-1}$$

The distribution function of external ages, for the tubular equipment, is the delta of Dirac, $\delta(t - t_M)$, while the mean concentration at the outlet is given by Equation 15.54:

$$10^{-2} = 10^8 \exp(-2.71.t_M)$$

Hence, $t_M = 8.5$ s, which is the mean residence time in the equipment.

The circulation velocity of milk is calculated from the continuity equation:

$$v = \frac{4w}{\rho \pi d^2} = 0.532 \frac{\text{m}}{\text{s}}$$

The length of the tubular equipment is:

$$L = \left(0.532 \text{ m/s}\right)\left(8.5 \text{ s}\right) = 4.52 \text{ m}$$

For the agitated vessel, the distribution function of external ages is given by Equation 15.35, while the mean concentration at the exit of the vessel is calculated by Equation 15.53. In this case, the residence time is obtained by dividing the volume of the vessel by the fluid's circulation volumetric flow:

$$t = \frac{V}{q} = \frac{\rho V}{w} = 1854 \text{s}$$

The concentration of the tuberculosis bacillus in the milk that leaves the agitated vessel is (Equation 15.53):

$$C = \frac{10^8 \text{ CFU/cm}^3}{1 + \left(2.71 \text{s}^{-1}\right)\left(1854 \text{s}\right)} = 2 \times 10^4 \text{ CFU/cm}^3$$

15.7

A *food fluid* that contains 10^8 CFU/cm^3 of a pathogenic microorganism is treated in tubular equipment at 120°C. The fluid circulates under plug flow regime with a mean residence time equal to 15 s, achieving a reduction degree of 12. Determine the microbial load of the fluid that leaves the treatment equipment. Calculate the microbial load of this fluid if it were treated in sterilizing equipment in which the distribution of external ages is given by the following table.

t (s)	0	5	10	15	20	25	30	35
E (s^{-1})	0	0.03	0.05	0.05	0.04	0.02	0.01	0

It can be obtained, from the definition of reduction degree $n = \log (C_0/C)$, for $n = 12$ and $C_0 = 10^8$ CFU/cm^3, that $C = 10^{-4}$ CFU/cm^3.

Initially, the microorganism inactivation kinetics constant should be calculated. Since the equipment is tubular, Equation 15.45 is applied:

$$10^{-4} = 10^8 \exp(-k \cdot 15 \text{ s})$$

Hence, $k = 1.84$ s^{-1}.

The mean residence time for the distribution of external ages given in the statement can be calculated from Equation 15.28:

$$t_M = 5 \times \left(5 \times 0.03 + 10 \times 0.05 + 15 \times 0.05 + 20 \times 0.04 + 25 \times 0.02 + 30 \times 0.01\right)$$
$$= 5 \times 3 = 15 \text{ s}$$

Although a mean time t_M = 15 s is obtained, which is equal to that of the tubular equipment, the mean concentration at the outlet will be different, as can be observed next.

The mean concentration at the outlet is calculated using Equation 15.51. Results are shown in Table 15.P7:

TABLE 15.P7

t (s)	E_t (s^{-1})	exp(–kt)	exp(–kt)$E_t\Delta t$
5	0.03	10^{-4}	1.5×10^{-5}
10	0.05	10^{-8}	2.5×10^{-9}
15	0.05	10^{-12}	2.5×10^{-13}
20	0.04	10^{-16}	2.0×10^{-17}
25	0.02	10^{-20}	1.0×10^{-21}
30	0.01	10^{-24}	5.0×10^{-26}
Total			1.50×10^{-5}

Therefore:

$$C_M = \left(10^8 \text{ CFU}/\text{cm}^3\right)\left(1.5 \times 10^{-5}\right) = 1500 \text{ CFU}/\text{cm}^3$$

This concentration, practically, is due to the contribution of the fraction that leaves at 5 s. Although the mean residence time is 15 s, which is equal to the time of the plug flow, the number of CFU is markedly higher, which demonstrates the great influence of the distribution of the residence times.

15.8

A food fluid that contains 10^7 CFU of a pathogenic microorganism per l is thermally treated in pasteurizing equipment that uses water as heating fluid. The hot water keeps the food's temperature at 75°C. From previous experiments, it is known that, at this temperature, the time needed to reduce the initial microorganism population in the food fluid to the tenth part is 6 s. Calculate the concentration of microorganisms in the fluid that leaves the pasteurizing equipment, if it behaves in such a way that the distribution of external ages (E_t) is:

(a) Exponentially decaying:

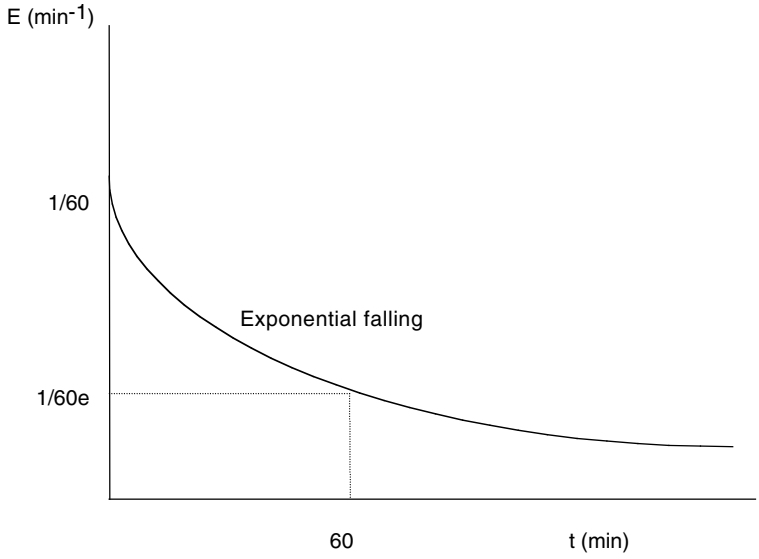

(b) Dirac's function, in which the response time to impulse is 45 s.
(c) Step function:

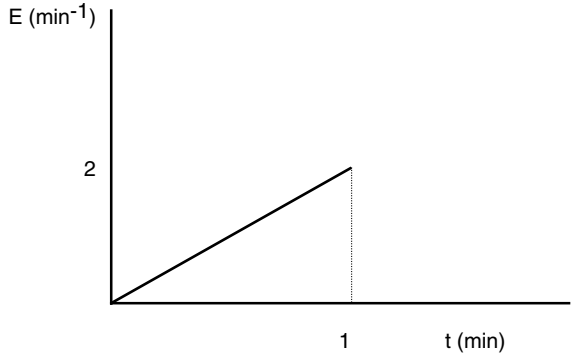

The kinetics of the thermal destruction of microorganisms is of first order, and it is known that the kinetics constant is related to the decimal reduction time by Equation 15.3, obtaining that:

$$k = \frac{2.303}{D_T} = \frac{2.303}{6\,\mathrm{s}} = 0.384\,\mathrm{s}^{-1} \cong 23\,\mathrm{min}^{-1}$$

(a) In this case, the falling of E_t is exponential, so the type of equation is: $E_t = a \exp(-bt)$, in which a and b are constants that must be determined.

For $t = 0$

$$E = a = \left(\frac{1}{60}\right)\text{s}^{-1}$$

For $t = 60$ s

$$\frac{1}{60e} = \left(\frac{1}{60}\right)\exp\left(-b60\right)$$

obtaining that $b = \left(\frac{1}{60}\right)\text{s}^{-1}$.

The equation of distribution of external ages is:

$$E = \left(\frac{1}{60}\right)\exp\left(-\frac{t}{60}\right) \qquad \text{if it is expressed in s}^{-1}$$

$$E = \exp\left(-t\right) \qquad \text{if it is expressed in min}^{-1}$$

When compared to Equation 15.33, it is observed that the residence time is:

$$t_M = 60 \text{ s} = 1 \text{ min},$$

and also that it is a perfect mixing agitated vessel.

The mean concentration of microorganisms at the outlet is obtained from Equation 15.53:

$$C_M = C_0 \frac{1}{k t_M + 1} = 10^7 \frac{1}{\left(23 \text{ min}^{-1}\right)\left(1 \text{ min}\right) + 1} = 4.17 \times 10^5 \text{ CFU/l}$$

(b) For a distribution of external ages following the delta function of Dirac with $t_M = 45$ s, $\delta = t - 45$ if it is expressed in s^{-1}, or $\delta = t - 0.75$ if it is expressed in min^{-1}. The mean concentration of microorganisms at the outlet is obtained by means of Equation 15.54:

$$C_M = \exp\left(-23 \times 0.75\right) = 0.32 \text{ CFU/l}$$

(c) The distribution given in the graph can be expressed according to the equation $E = 2t$ min^{-1}, for times between 0 and 1 min.

In this case, the mean concentration at the outlet is calculated by Equation 15.50:

$$\int_0^{\infty} \exp(-k\,t)\; 2t\; dt$$

Since after 1 min the microorganisms that have entered at the same time have already exited, this integration should be performed between 0 and 1 min. Thus, the following is obtained from this integration:

$$C_M = 2C_0\left[\frac{1}{k^2} - \frac{k+1}{k^2}\exp(-k)\right]_0^{\infty}$$

$$C_M = 2\left(10^7\ \text{CFU/l}\right)\left(1.89 \times 10^{-3}\right) = 3.78 \times 10^4\ \text{CFU/l}$$

16

Food Preservation by Cooling

16.1 Freezing

Freezing is one of the most widely used methods of food preservation because of two main reasons. The first is that many microorganisms cannot grow at the low temperatures used in freezing. Also, when a food is frozen, part of the water is transformed into ice, thus decreasing the food's water activity (a_w). This a_w decrease influences the growth of many microorganisms, since they cannot develop in low water activity conditions.

Food freezing can be carried out in different ways and, depending on the method, the quality of the frozen food may vary. Thus, if freezing is instantaneous, there will be many points in the food where formation of ice begins. This means that there are many nucleation sites and the ice crystals formed are small; therefore, the food tissues are slightly affected. On the other hand, if freezing is slow, there are few nucleation sites and the small number of ice crystals formed will grow with time. This will cause larger crystals to form, which can affect the final quality of the frozen product.

When freezing a food, it is important to know how the temperature of the food varies during the freezing process. It is well known that the temperature of pure water varies with time as it freezes (Figure 16.1). The freezing temperature of pure water is 0°C, so, if beginning with water at a higher temperature, initially a temperature decrease below 0°C exists. This means that there will be a subcooling; later, due to the beginning ice formation, fusion heat will be released and the temperature increases again to 0°C. At this point, temperature remains constant until all of the water becomes ice. Then, the temperature decreases again with a higher slope, since the thermal conductivity of ice is greater than that of liquid water.

In foods, this process is different from the freezing of pure water (Figure 16.2). If T_f is the temperature at which the freezing of the product begins, the temperature initially decreases below that temperature. Once the first ice crystals are formed, the temperature increases to a value equal to T_f. However, the temperature does not remain at that point, but rather continuously decreases slightly due to the transformation of water into ice and the increasing concentration of soluble solids coming from food in the unfrozen

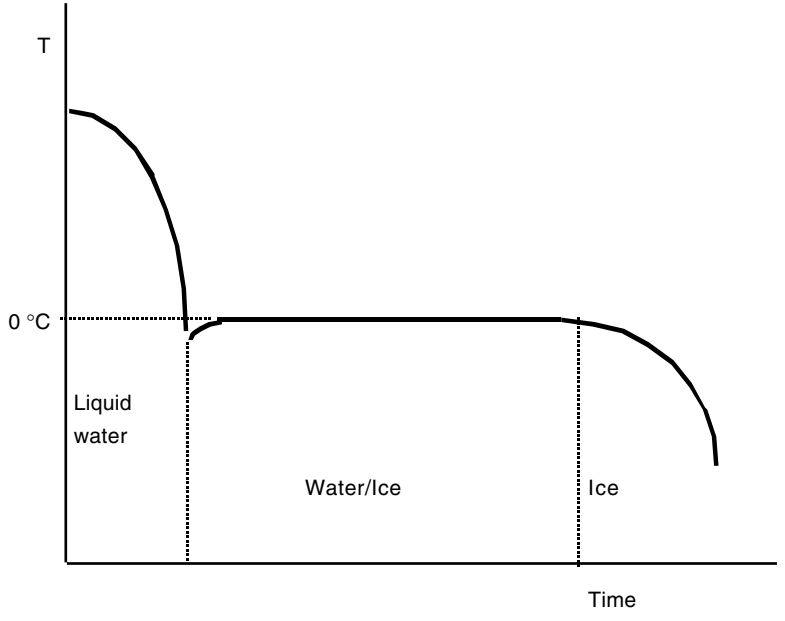

FIGURE 16.1
Pure water freezing.

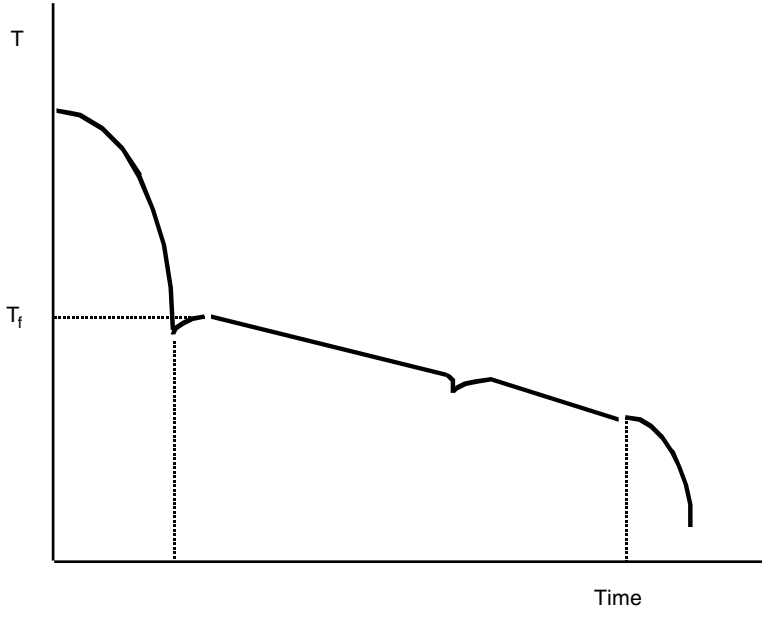

FIGURE 16.2
Freezing of a food product.

water fraction. There is a moment when the crystallization of any of the solids may begin and crystallization heat is released, in this way increasing the temperature. Finally, a temperature at which it is not possible to freeze more water will be reached, since the soluble solids content is such that unattainably low temperatures are required. This is the final freezing point of the product, after which the product decreases in temperature until reaching the temperature of the freezing medium.

It is important to point out that, in frozen products, not all the water can be frozen. A portion of unfrozen water remains, which is known as bound water. Also, the time that passes from when the food reaches the initial freezing temperature T_f until reaching the final freezing point is known as freezing time. This parameter is required for calculation of freezing processes and is needed for the design of freezers.

Different types of freezers in the food industry are used depending on the freezing desired. One type is the plate or contact freezer, in which the product to be frozen is shaped as a parallelepiped and placed between plates that are at lower temperatures than the freezing temperature of the product. Heat transfer from the food to the plates achieves the freezing of the product. In this type of freezer, the process is usually slow, so ice crystal growth will prevail over nucleation.

Other freezers use refrigerant fluids in which the food to be frozen is placed. Freezing can be more or less rapid depending on the type of fluid and its temperature. Thus, if the fluid is liquid nitrogen, there will be a great number of nucleation sites and small ice crystals will be formed; since the temperature is very low, nucleation will prevail over growth and freezing times will be short. On the other hand, if cold air is used as fluid, freezing is slow and crystal growth will prevail over nucleation. Therefore, the type of freezer to be used depends on need and on the desired quality of the product.

16.2 Freezing Temperature

Freezing temperature is the temperature at which the first ice crystals begin to form, i.e., the temperature at which ice crystals and liquid water coexist in equilibrium. For pure water, this temperature corresponds to 0°C (273 K). However, the water in foods contains soluble solids, and it is known that these solids cause a decrease in the freezing point of water. For this reason, the temperature at which the freezing of a food begins is lower than 0°C. It is evident that the concentration of soluble solids in the unfrozen water portion of a food increases as freezing develops, causing the freezing temperature to vary with time. Therefore, for calculation purposes, it is common practice to take the temperature at which the first ice crystals appear as the initial freezing temperature.

At the beginning of freezing, the aqueous solution is diluted, so as a first approximation, the initial freezing temperature can be calculated by applying the Raoult's law:

$$T_f = K_w \frac{m_S}{M_S} \tag{16.1}$$

in which:

m_S = g solute/100 g water
M_S = molecular weight of the solute
K_w = 18.6 (cryogenic constant of water)

It should be pointed out that, for foods, M_S is an equivalent molecular weight of the solutes contained in the food.

Empirical equations exist in the literature that allow one to determine the initial freezing temperature of certain foods only as a function of their moisture content (Levy, 1979). When the moisture content of a food is known, the molar fraction of water can be calculated. An equation that allows calculation of the initial freezing temperature is:

$$T_f = \frac{T_{0w}\,\lambda}{1 - R\,T_{0w} \ln X} \tag{16.2a}$$

where:

T_{0w} = freezing temperature of pure water (273 K)
λ = latent heat of freezing of water (6003 kJ/kmol)
R = gas constant (8.314 kJ/kmol K)
X = molar fraction of unfrozen water

Table 16.1 presents the values of the initial freezing temperature for some foods.

16.2.1 Unfrozen Water

During the freezing process, a fraction of unfrozen water always exists in a food. Also, as previously mentioned, there is bound water not in the form of ice at the final freezing point. It is important to determine the amount of unfrozen water, since this affects not only the properties of the product, but also the enthalpy needed for freezing to occur.

If at a given instant the mass fractions of unfrozen water and solids in a food are x_w and x_S, respectively, then the molar fraction of nonfrozen water can be calculated from the following expression:

TABLE 16.1

Initial Freezing Temperature of Some Foods

Product	Moisture Content (%)	Freezing Temperature (°C)
Meat	55–70	–1.0 to –2.2
Fruits	87–95	–0.9 to –2.7
Cranberry	85.1	–1.11
Plum	80.3	–2.28
Raspberry	82.7	–1.22
Peach	85.1	–1.56
Pear	83.8	–1.61
Strawberry	89.3	–0.89
Egg	74	–0.5
Milk	87	–0.5
Fish	65–81	–0.6 to –2.0
Isotonic		–1.8 to –2.0
Hypotonic		–0.6 to –1.0
Vegetables	78–92	–0.8 to –2.8
Onion	85.5	–1.44
Asparagus	92.6	–0.67
Spinach	90.2	–0.56
Carrot	87.5	–1.11
Juices		
Cranberry	89.5	–1.11
Cherry	86.7	–1.44
Raspberry	88.5	–1.22
Strawberry	91.7	–0.89
Apple	87.2	–1.44
Apple purée	82.8	–1.67
Apple concentrate	49.8	–11.33
Grape must	84.7	–1.78
Orange	89.0	–1.17
Tomato pulp	92.9	–0.72

Sources: Heldman, D.R., *Food Freezing. Handbook of Food Engineering,* Heldman, D.R. and Lund. D.B., Eds., Marcel Dekker, New York, 1992; Mufart, A., *Ingeniería Industrial Alimentaria,* Acribia, Zaragoza, Spain, 1994; Plank, R., *El Empleo del Frío en la Industria de la Alimentación,* Reverté, Barcelona, 1980.

$$X = \frac{\left(x_w/18\right)}{\left(x_w/18\right)+\left(x_S/M_S\right)} \tag{16.3a}$$

In this equation it is necessary to know the equivalent molecular weight of the solids. Therefore, the unfrozen water is:

$$x_w = \frac{18 x_S X}{M_S\left(1-X\right)} \tag{16.3b}$$

Hence, the mass fraction of the ice formed (x_I) is the initial mass fraction of the moisture content of the food (x_{0w}) less the mass fraction of unfrozen water:

$$x_I = x_{0w} - x_w$$

The molar fraction of unfrozen water can be calculated using Equation 16.2a, which, when appropriately expressed, yields the molar fraction of unfrozen water as a function of the freezing temperature:

$$\ln X = \frac{\lambda}{R}\left[\frac{1}{T_{0w}} - \frac{1}{T_F}\right] \tag{16.3c}$$

16.2.2 Equivalent Molecular Weight of Solutes

The so-called equivalent molecular weight of solids appears in different equations presented in the previous section. It is necessary to determine this variable for freezing calculations. Equation 16.1 can be used when considering an ideal diluted solution whenever the initial freezing temperature is known. In the same way, another equation that allows one to determine M_S is Equation 16.3b, if the mass and molar fractions of unfrozen water are known, as well as the mass fraction of solids.

Also, there are empiric equations (Chen, 1985) that allow the calculation of the equivalent molecular weight for specific foods:

Orange and apple juices:

$$M_S = \frac{200}{1 + 0.25 x_S}$$

Meat:

$$M_S = \frac{535.4}{x_{0w}}$$

Cod:

$$M_S = \frac{404.9}{x_{0w}}$$

16.3 Thermal Properties of Frozen Foods

The thermal properties of a food appear as variables in the different equations used to calculate freezing times and to design processing systems. Therefore, it is essential to know the value of these properties in order to solve the different problems that could be set up. In spite of the numerous references on properties of frozen foods reported in the literature, it is necesary to have equations that allow their calculation.

16.3.1 Density

When a food is frozen, its density decreases due to the fraction of ice that it contains. An equation allowing calculation of the density of a frozen product is:

$$\frac{1}{\rho} = \frac{x_w}{\rho_w} + \frac{x_I}{\rho_I} + \frac{x_S}{\rho_S} \tag{16.4}$$

in which x_w, x_I, and x_S are the mass fractions of unfrozen water, ice, and total solids, respectively. The densities of water, ice, and total solids can be calculated from the equations given by Choi and Okos (1986). It should be pointed out that calculating the density of the total solids requires knowing the composition of this fraction.

16.3.2 Specific Heat

The specific heat of the frozen product is a function of its content of unfrozen water, ice, and total solids, according to the following expression:

$$\left(\hat{C}_P\right)_F = \left(\hat{C}_P\right)_w \left(x_w + x_I + x_S\right) \tag{16.5}$$

However, Choi and Okos (1986) presented a general equation in which the specific heat of the product is expressed as the sum of the specific heats of each component times its mass fraction.

These equations should be used for calculation of the enthalpies of frozen foods. However, in freezing, in general, the initial temperature of the food does not correspond to the freezing temperature, but to a higher one. Therefore, it is also important to determine the specific heat of the unfrozen food. An equation to calculate the specific heat of the unfrozen food as a function of its moisture content is:

$$\left(\hat{C}_P\right)_{NF} = \left(\hat{C}_P\right)_w \left(0.3 + 0.7\ x_{0w}\right) \tag{16.6}$$

There are other equations in the literature, some of which are specific for some products (Mafart, 1994; Levy, 1979). However, it is appropriate to apply the equations of Choi and Okos whenever the composition of the food is known.

16.3.3 Thermal Conductivity

Calculation of the thermal conductivity of frozen foods may be more complicated than the calculation of density of specific heat, since thermal conductivity depends not only on the water content and conductivity of the aqueous and solid phases, but also on the structure of the product. Thus, Kopelman (1966) considered that three different structure models could exist in foods. In one model, it is considered that the food is a homogeneous system made of two components in a dispersed form. A second model considers a homogeneous system made of two components, in which the solid fraction is arranged in the form of fibers in two directions. The third model assumes a homogeneous system in which the solid fraction is arranged as parallel slabs in one direction. Thus, Kopelman (1966) presents different equations that allow calculation of the thermal conductivity of the product depending on the type of structure.

The conductivity of the liquid phase is usually higher than the conductivity of the fraction of solids; thus, for a homogeneous system in which both phases are dispersed, the thermal conductivity of a food is calculated by the equation (Heldman, 1992):

$$k = k_L \frac{1 - \left(X_S^V\right)^2}{1 - \left(X_w^V\right)^2 \left(1\ -\ X_S^V\right)} \tag{16.7}$$

In this equation, k_L is the thermal conductivity of the liquid, while X_S^V and X_w^V are the volumetric fractions of solids and water, respectively.

If the conductivity of the liquid and solid phases is similar, the following expression should be used:

$$k = k_L \frac{1 - Q}{1 - Q\left(1\ -\ X_S^V\right)} \tag{16.8}$$

where:

$$Q = \left(X_S^V\right)^2 \left[1 - \frac{k_S}{k_L}\right]$$

k_S being the thermal conductivity of the solid fraction.

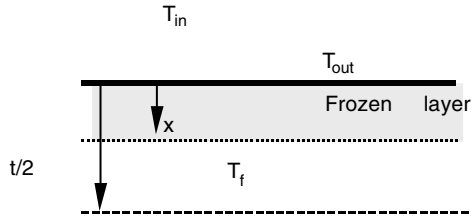

FIGURE 16.3
Freezing front of a slab.

For systems in which the solids are in the form of striated fibers or slabs, conductivity depends on whether it is considered parallel or perpendicular to such fibers or slabs.

16.4 Freezing Time

Calculation of freezing time is one of the most important parameters within the design of freezing stages, since it represents the time that the food will be inside the freezing equipment. In principle, it represents the time needed by the geometric center of the food to change its initial temperature down to a given final temperature, lower than freezing temperature, also called effective freezing time. Sometimes, the so-called nominal freezing time is employed. Nominal freezing time is the time passed between when the surface of the food reaches 0°C until the geometric center reaches a temperature 10°C lower than the initial freezing temperature.

Calculation of freezing time can be complex, since the freezing temperature of the food changes continuously along the process, as mentioned before. However, as a first approximation, the time elapsed from when the food is at its freezing temperature until the whole food is frozen can be calculated.

In order to do this calculation, a slab with infinite dimensions, but of finite thickness, is supposed. This implies that the heat transfer will be only in one direction. This body is initially at a temperature T_f and is introduced into a freezer in which the external temperature is T_e. A freezing front is formed along the freezing process that advances from the surface at a temperature T_s towards the center of the slab (distance x) (Figure 16.3). When performing an energy balance, the outlet-heat term should be equal to energy dissipated because of freezing.

Heat is transmitted through the frozen layer by conduction, and from the surface to the exterior by convection, so the outlet-heat term per unit time can be expressed as:

$$Q_S = A\frac{k}{x}\left(T_F - T_S\right) = A\,h\left(T_F - T_e\right) = A\frac{T_F - T_e}{\frac{x}{k} + \frac{1}{h}}$$

The term of energy dissipated by freezing is expressed as:

$$Q_D = A\rho\lambda_I\frac{dx}{dt}$$

In these equations, A is the area of the slab, k and ρ are the thermal conductivity and density of the frozen layer, while h is the coefficient of heat transfer by convection to the exterior.

When equaling these equations, it is obtained that:

$$\rho\lambda_I\frac{dx}{dt} = \frac{T_f - T_e}{\frac{x}{k} + \frac{1}{h}}$$

This equation, with separable variables, can be integrated on the following boundary conditions:

For $t = 0$ $x = 0$

For $t = t_F$ $x = e/2$

t_C being the freezing time and e the thickness of the slab. The integrated equation allows calculation of the freezing time:

$$t_F = \frac{\rho\lambda_I}{T_F - T_e}\left(\frac{e^2}{8k} + \frac{e}{2h}\right) \tag{16.9}$$

This expression is known as Plank's equation and is valid only for the freezing period. This means that it is assumed that the food was initially at its freezing temperature. Also, λ_I is the latent heat of the frozen fraction and is calculated by multiplying the latent heat of pure water λ times the mass fraction of frozen water: $\lambda_I = x_H\lambda$.

For cylinders of infinite length and spheres, freezing time is obtained in an analogous way, although the resulting expression differs on the values of coefficients 8 and 2 that affect the conductivity and the coefficient of convection. Thus, for cylinders, these values are 16 and 4, while for spheres, such values are 24 and 6. Also, the characteristic dimension will not be the thickness but the radius.

If it is taken into account that the numbers of Fourier, Biot, and Stefan are defined by the equations:

Fourier's number:

$$(Fo) = \frac{k}{\rho \hat{C}_P (e)^2}$$

Biot's number:

$$(Bi) = \frac{he}{k}$$

Stefan's number:

$$(Ste) = \frac{\hat{C}_P (T_f - T_e)}{\lambda}$$

then the equation is transformed into an expression that correlates these three modules:

$$(Fo) = \frac{1}{8}\frac{1}{(Ste)} + \frac{1}{2}\frac{1}{(Bi)(Ste)}$$

This equation is valid for infinite slabs with finite thickness and can be generalized for spheres and cylinders of infinite height:

$$(Fo) = \frac{R}{(Ste)} + \frac{P}{(Bi)(Ste)} \tag{16.10}$$

The values for the parameters P and R for slabs, infinite cylinders, and spheres in this equation are presented in Table 16.2.

The equation of Plank is an approximation for the calculation of freezing processes. Although it cannot be used for the exact calculation of freezing times, it is useful in order to obtain an approximation of these times.

TABLE 16.2

Parameters P and R of Equation 16.10

Geometry	*P*	*R*	Dimension
Infinite slab	1/2	1/8	thickness *e*
Infinite cylinder	1/4	1/16	radius *r*
Sphere	1/6	1/24	radius *r*

In practice, there are cases in which the product to be frozen has a finite geometry. Equation 16.10 can be used in such cases, although the parameters P and R will differ from the values given in Table 16.2. The calculation of these parameters is very complex. Thus, for the case of a parallelepiped of thickness e, width a, and length l, the dimensionless length parameters $\beta_1 = a/e$ and $\beta_2 = l/e$ are defined in such a way that the values of P and R are calculated from the following equations (Plank, 1980):

$$P = \frac{\beta_1 \beta_2}{2\left(\beta_1 \beta_2 + \beta_1 + \beta_2\right)} \tag{16.11a}$$

$$R = \frac{(M-1)(\beta_1 - M)(\beta_2 - M)\ln\left(\frac{M}{M-1}\right) - (N-1)(\beta_1 - N)(\beta_2 - N)\ln\left(\frac{N}{N-1}\right)}{8L} + \frac{2\beta_1 + 2\beta_2 - 1}{72}$$

$$L = \sqrt{(\beta_1 - \beta_2)(\beta_1 - 1) + (\beta_1 - 1)^2} \tag{16.11b}$$

$$M = \frac{\beta_1 + \beta_2 + 1 + L}{3}$$

$$N = \frac{\beta_1 + \beta_2 + 1 - L}{3}$$

Plank's equation is useful to determine the freezing times, but only in an approximate way. This equation was developed assuming that, at the beginning of the freezing process, the food was at the freezing temperature. However, generally, the food is usually at a temperature higher than the freezing temperature. The real time should be the sum of the time calculated by Plank's equation plus the time needed by the surface of the product to decrease from an initial temperature to the freezing temperature. The method described for heat transfer under unsteady state should be used to calculate the additional time, using the properties of the unfrozen food.

Some works for calculating such time can be found in the literature. One of these is presented by Nagaoka et al. (1955), in which the calculation of freezing time is performed using the following expression:

$$t_F = \frac{\rho\, \Delta\hat{H}}{T_F - T_e}\left(\frac{\mathrm{Re}_l^2}{k} + \frac{Pl}{h}\right)\left[1 + 0.008\,(T_i - T_F)\right] \tag{16.12}$$

In this equation, T_i is the food's temperature at the start of freezing, while $\Delta\hat{H}$ is the difference between the food's enthalpy at the initial temperature and at the end of the freezing process.

The enthalpy increase experienced by food during the freezing process can be evaluated by means of the equation:

$$\Delta \hat{H} = \left(\hat{C}_P\right)_{Nf}\left(T_i - T_f\right) + x_I\, \lambda_w + \left(\hat{C}_P\right)_f\left(T_f - T_f\right) \tag{16.13}$$

In this expression, the first addend of the right-hand side of the equation represents the heat that should be eliminated from the product from the initial temperature to the freezing temperature. The second addend represents the heat released during the phase change of the frozen water fraction, while the third is the heat eliminated so the food can pass from the freezing temperature to the final T_f. This temperature must not necessarily coincide with the temperature of the freezing medium, but can be slightly higher, although in case they coincide, it is complied that $T_f = T_e$. Also, λ_w is the latent heat of fusion of pure water, while the specific heat of the food before and after freezing can be calculated from Equations 16.6 and 16.5, respectively.

This is a simple method to calculate the increase of enthalpy. Empirical equations can be found in literature that also allow one to calculate such enthalpy variation (Chen, 1985; Levy, 1979; Succar and Hayakawa, 1983). Also, Riedel (1956, 1957a, b) has developed diagrams that allow one to calculate enthalpies for different products (meat, eggs, fruits, and juices) as a function of the water content and the fraction of frozen water.

Another modification to Plank's equation is that given by Cleland and Earle (1976, 1982), in which they define a new dimensionless number:

Plank's number:

$$\left(Pk\right) = \frac{\left(\hat{C}_P\right)_w \left(T_i - T_f\right)}{\Delta H}$$

in which $(\hat{C}_P)_w$ stands for the specific heat of the unfrozen water.

Plank's equation (Equation 16.10) is used to calculate the freezing time, in which the values of the parameters P and R depend on the type of geometry. The following equations are used for slabs:

$$P = 0.5072 + 0.2018\left(Pk\right) + \left(Ste\right)\left[0.3224\left(Pk\right) + \frac{0.0105}{\left(Bi\right)} + 0.0681\right] \tag{16.14a}$$

$$R = 0.1684 + \left(Ste\right)\left[0.0135 + 0.274\left(Pk\right)\right] \tag{16.14b}$$

The following expressions are used for cylinders:

$$P = 0.3751 + 0.0999(Pk) + (Ste)\left[0.4008(Pk) + \frac{0.071}{(Bi)} - 0.5865\right] \quad (16.15a)$$

$$R = 0.0133 + (Ste)[0.3957 + 0.0415(Pk)] \quad (16.15b)$$

For spherical geometry, the equations to be used are:

$$P = 0.1084 + 0.0924(Pk) + (Ste)\left[0.231(Pk) - \frac{0.3114}{(Bi)} + 0.6739\right] \quad (16.16a)$$

$$R = 0.0784 + (Ste)[0.0386(Pk) - 0.1694] \quad (16.16b)$$

In addition to these modifications, these authors introduced a parameter called equivalent dimension of heat transfer, which takes into account the shape of the product to be frozen. However, the correction due to this factor yields lower freezing times, so it might be better not to make such a correction and to remain in a conservative position.

Freezing time is calculated for regular shaped foods in all of the methods previously described. However, there can be cases of freezing of nonregular shaped products. In order to solve this problem, a dimensionless factor is defined which is a function of Biot's number and form factors β_i. The equations that allow the calculation of this factor can be found in the literature (Cleland et al., 1987a,b; Cleland, 1992). Thus, for example, in the case of an ellipsoid shaped body, in which the axis has the dimensions r, $\beta_1 r$, $\beta_2 r$, the parameter E is calculated according to the expression (Cleland, 1992):

$$E = 1 + \frac{1 + (2/Bi)}{\beta_1^2 + (2\beta_1/Bi)} + \frac{1 + (2/Bi)}{\beta_2^2 + (2\beta_2/Bi)} \quad (16.17)$$

The value of the characteristic dimension r of the irregular object is found by taking the shorter distance from the surface to the lowest cooling point. The parameters β_1 and β_2 are obtained from the following equations:

$$A_x = \pi \beta_1 r^2$$

$$V = \frac{4}{3} \pi \beta_1 \beta_2 r^3$$

In these equations, A_X is the smaller transversal section that contains the thermal center, while V is the volume of the considered body. The calculation of the freezing time of a food, whatever its geometry, is obtained by dividing the calculated freezing time by the value of this factor E.

16.5 Design of Freezing Systems

In the design of freezing systems, it is necessary to know the amount of energy that should be eliminated from the food to change from the initial to the final temperature of the frozen product. To do this, one must know the enthalpy of the food at the beginning and end of the freezing process. Since enthalpy is a function of state, it should be given with respect to a reference temperature that, in the case of freezing processes, is –40°C. This means that, at this temperature, the enthalpy of any product is considered null.

In order to calculate the power needed to carry out the freezing process, it is necessary to determine the variation of enthalpy experienced by the product, since it is introduced in the freezer until the product reaches the final temperature. This can be achieved by using Equation 16.13.

Another factor that should be calculated is the power that the freezing equipment should have to perform a given process. Such power is the total energy to be eliminated from the food per unit time and a measure of the capacity of the freezing system. Freezing power is calculated by the following equation:

$$Pow = \frac{m\Delta\hat{H}}{t} \tag{16.18}$$

Here, m is the total quantity of food to be frozen, $\Delta\hat{H}$ the increase of enthalpy experienced by the food from the initial to the final temperature, and t the time the food stays in the freezing equipment. This time usually coincides with freezing time calculated in the previous section.

If the equation given by Nagaoka et al. (Equation 16.12) is used to calculate the freezing time, power can be calculated by the following expression:

$$Pow = \frac{m\left(T_f - T_e\right)}{\rho\left(\frac{\mathrm{Re}^2}{k} + \frac{Pe}{h}\right)\left[1 + 0.008\left(T_i - T_f\right)\right]} \tag{16.19}$$

It is not necessary to know the enthalpy increase experienced by the food; therefore, neither the values of specific heat nor the unfrozen water fraction are needed.

16.6 Refrigeration

Refrigeration can be defined as the process in which heat is eliminated from a material at a temperature higher than the temperature of its surroundings. In a general way, refrigeration is a term used to denominate food storage at temperatures lower than 15°C and above the freezing point. These processes have been applied to food preservation. So-called natural refrigeration has been used since ancient times, taking advantage of the fact that snow, ice, and brines allow temperatures lower than environmental temperatures. It should be pointed out that some food products have been and are still kept in storages whose temperature is different from the ambient temperature and is constant with time. However, denominated mechanical refrigeration, in which mechanical and electrical devices are used to achieve temperatures lower than the temperature of the surroundings, is discussed in this chapter.

Once foods are obtained from their natural source, they present problems such as perishability and limited commercial life, since these foods can be altered, mainly due to three mechanisms:

- Live organisms that contaminate and deteriorate foods, not only microorganisms (parasites, bacteria, and molds), but also insects in different stages of their vital cycle
- Biochemical activities performed within foods such as respiration, browning, and overripeness, which in most cases are due to the enzymes present in food. These activities can reduce the food's quality and are present in vegetables after harvest and in animal foods after slaughter.
- Physical processes, such as loss of moisture that yields dehydration

A decrease of storage temperature implies a decrease in the rate of deterioration reactions, so the food increases its shelf life. The rate of deterioration will be lower as the temperature is lower, which points out that it is desirable to decrease the temperature to the minimum whenever it is higher than freezing. However, this is not always possible. It has been observed that, at low temperatures, even above freezing temperature, undesirable reactions can take place in some foods. Thus, some fruits can present internal and core browning during storage, e.g., pears. It is recommended to store them at 3 to 4°C, since if they are stored at 0°C, browning can occur. It is not advisable to store potatoes below 3°C because imbalances in the starch–sugar system that produce the accumulation of sugars can occur and, consequently, the potatoes will deteriorate. Table 16.3 presents storage temperatures below which deterioration problems can occur in some types of foods.

Another important parameter to consider during food storage under refrigeration is the relative humidity. If humidity is lower than the so-called relative humidity of equilibrium, there is a water loss from the food to the exterior, leading to dehydration of the product. On the other hand, if the

TABLE 16.3

Deterioration of Fruits and Vegetables under Storage Conditions

Product	Critical Temperature of Storage (°C)	Type of Deterioration between the Critical and Freezing Temperature
Olive	7	Internal browning
Avocado	4–13	Brown discoloration in pulp
Cranberry	2	Rubbery texture, red pulp
Eggplant	7	Scald on surface
		Rotting
Sweet potato	13	Internal discoloration, spot
		Rotting
Squash	10	Rotting
Green beans	7	Spot and redness
Lime	7–9	Spot
Lemon	14	Spot, red mark
		Membranous staining
Mango	10–13	Gray discoloration of peel
		Unequal ripeness
Melon	7–10	Spot, peel putrefaction
		No ripeness
Apple	2–3	Internal and core browning, scald, moist breaking
Orange	3	Spot, brown marks
Papaya	7	Spot, Rotting
		No ripeness
Potato	3	Mahogany browning
		Sweetening
Cucumber	7	Spot, Rotting
Pineapple	7–10	Green color upon ripening
Banana	12–13	Opaque color upon ripening
Grapefruit	10	Scald, spot
"Quingombó"	7	Discoloration, spot, embedded zone, rotting.
Watermelon	4	Spot, unpleasant odor
Tomato		
Ripe	7–10	Rotting, softening, soaked water
Green	13	Light color upon ripening, rotting

Source: Lutz, J.M. and Hardenburg, R.E., *Agricultural Handbook No. 66,* USDA, Washington, D.C., 1968.

relative humidity of the environment is higher, then water condensation on the food surface can occur, in many cases facilitating microbial growth and deterioration of the product. Tables 16.4 and 16.5 show, respectively, temperatures and relative humidities for the optimum storage of different foods.

16.7 Refrigeration Mechanical Systems

The second law of thermodynamics indicates that heat flows only in the decreasing direction of temperature. However, industrial refrigeration

TABLE 16.4

Storage Temperature under Normal Atmosphere

T (°C)	Product
Just above the freezing point	Animal tissues: mammal meat, fish, chicken
	Fruits: apricots, lemons (yellow), pears, nectarines, oranges (Florida), plums, berries, apples (some varieties), peaches
	Vegetables: asparagus, beets, peas, radishes, broccoli, brussels sprouts, carrots, celery, cauliflower, corn, spinach
	Milk
	Egg (with shell)
2–7 °C	Fruits: melons, oranges (except Florida), apples (some varieties), ripe pineapples
	Vegetables: early potatoes
> 7 °C	Fruits: avocados, bananas, grapefruits, mangos, lemons (green), limas, green pineapples, tomatoes
	Vegetables: green beans, cucumbers, sweet potatoes, late potatoes

Source: Karel et al. 1975a.

TABLE 16.5

Recommended Relative Humidity

Relative Humidity	Product
Less than 85%	Butter, cheese, coconut, dried fruits, garlic, nuts, dry onions, egg (shell), dates
85–90%	Animal tissues: mammal meat (except veal), chicken
	Fruits: banana (yellow), citric, pineapples, nectarines, plums, peaches, tomatoes
	Vegetables: sweet potatoes, early potatoes
90–95%	Animal tissues: veal, fish
	Fruits: apples (90%), berries, pears, bananas (green)
	Vegetables: green beans, cucumbers, sweet corn, late potatoes, vegetable leaves, green peas, edible roots

Source: Karel et al. 1975a.

processes have eliminating heat from low temperature points towards points with higher temperature as their objective. In order to achieve this, the denominated refrigeration cycles, in which a fluid circulates in different stages in a closed cycle, are used. The most important refrigeration system is vapor compression. A simple scheme of this cycle is given in Figure 16.4. Vapor compression is a closed cycle in which the fluid that circulates is called refrigerant.

Supposing that the cycle begins at point 1, the compressor suction point, the fluid in a vapor state receives energy from the compressor and goes to point 2 through a polytropic compression at which the fluid increases its pressure and temperature and, at the same time, its enthalpy. This fluid decreases its energy content in a condenser by an isobaric process, passing

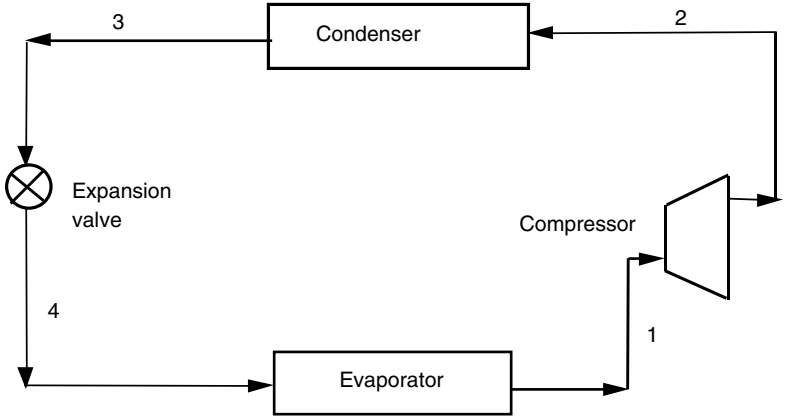

FIGURE 16.4
Refrigeration cycle system. (Adapted from Stoecker, W.F. and Jones, J.W., *Refrigeration and Air Conditioning*, McGraw–Hill, New York, 1982.)

to a liquid state (point 3). Then it flows through an expansion valve in an isoentropic process, with a decrease in pressure (point 4), obtaining a liquid–gas mixture. This mixture changes to a saturated vapor state in an evaporator where the fluid receives heat, changing an isobaric process, then changing to the conditions of point 1, where the cycle begins again. It should be pointed out that the global system takes heat from the environment in the evaporator and releases heat in the condenser.

The global process can be represented in a pressure–enthalpy diagram (Figure 16.5). The fluid receives the compression work during compression stages 1 to 2, and may be the most expensive stage of all the system. This compression work can be evaluated by the enthalpy difference between the discharge and suction points of the compressor. Thus, the compression work per unit mass of fluid is:

$$\hat{W}_C = \hat{H}_2 - \hat{H}_1 \tag{16.20}$$

If it is desired to obtain the theoretical power of the compressor, work should be multiplied by the mass flow rate of the fluid that circulates through the system:

$$Pow = w\hat{W}_C = w\left(\hat{H}_2 - \hat{H}_1\right) \tag{16.21}$$

As can be observed, the circulation flow of the fluid determines to some extent the size of the compressor to be used, since the compression power required will be greater as the flow becomes greater

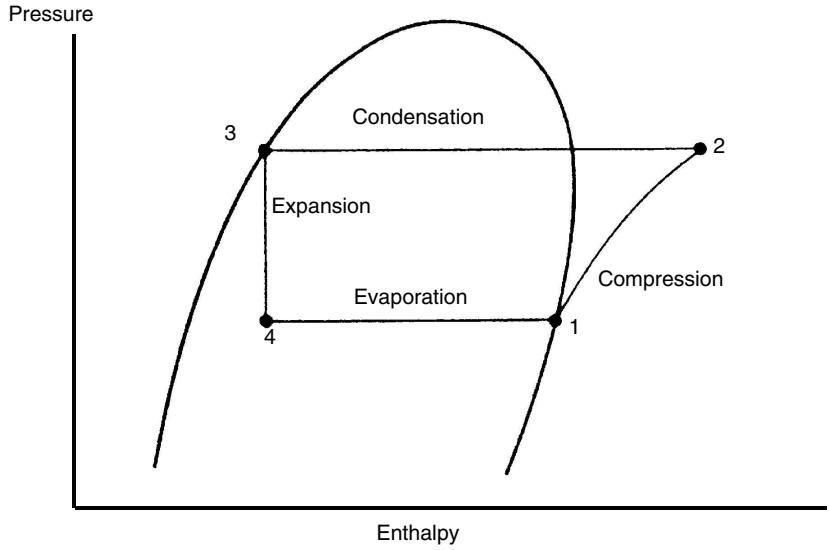

FIGURE 16.5
Vapor compression cycle.

The amount of energy released by the fluid in the condenser is determined from the enthalpies of points 2 and 3. In this way, the heat flow released by the fluid is:

$$\dot{Q}_S = w\left(\hat{H}_3 - \hat{H}_2\right) \tag{16.22}$$

In this equation, w is the mass flow rate of the fluid and $\hat{H}$ is the enthalpy per unit mass of fluid. Since point 2, where the fluid leaves the compressor, has a greater enthalpy than point 3, heat with negative sign is obtained. Hence, it is heat released by the fluid and its value is used for sizing the condenser and calculating the amount of cooling fluid to use.

Evaporation stages 4 to 1 represent the refrigerant effect of the system. At these stages the heat transferred from the environment to the fluid is:

$$\dot{Q}_E = w\left(\hat{H}_1 - \hat{H}_4\right) \tag{16.23}$$

This heat is absorbed by the fluid and represents the refrigerant capacity, which is the essential aim of the process.

There is an important parameter in these processes, the coefficient of performance (ϕ), defined as the refrigerant effect divided by the work externally

provided. Since this work is only that of compression, the performance coefficient of the refrigeration system is:

$$\phi = \frac{\hat{H}_1 - \hat{H}_4}{\hat{H}_2 - \hat{H}_1} \tag{16.24}$$

The power per kilowatt of refrigeration is the inverse of the coefficient of performance; an efficient refrigeration system should have a low power value, but a high performance coefficient value (Stoecker and Jones, 1982).

In some refrigeration systems, the fluid that feeds the compressor is overheated steam, thus ensuring that no refrigerant in a liquid state enters the compressor. In order to achieve this, the saturated vapor that leaves the evaporator passes through a heat exchanger, in which the fluid that gives heat is the flow that leaves the condenser. Besides the cited effect, the liquid of the condenser is subcooled, preventing the formation of bubbles before it passes through the expansion valve.

16.8 Refrigerants

Various fluids are used as refrigerant fluids. The fluids used in vapor compression systems are called primary refrigerants, while secondary refrigerants are those used for transportation at low temperatures from one place to another.

Generally, solutions with freezing temperatures below 0°C are used as secondary refrigerants. Aqueous solutions of ethyleneglycol, propyleneglycol, and calcium chloride are among the most commonly used. The properties of these solutions are similar, although propyleneglycol has the advantage of not being dangerous if it comes into contact with food.

There are many primary refrigerants that have been used and are used in industry. Table 16.6 presents a list of some of those. For the hydrocarbons and halocarbons, the numerical designation is determined as follows: the first digit from right to left is given by the number of fluorine atoms present in the molecule, the second digit (the middle) corresponds to the number of hydrogen atoms in the molecule plus one, and the third digit corresponds to the number of carbon atoms minus one. For inorganic compounds, the last two digits represent their molecular weight.

Selection of the type of refrigerant depends on the process in which the refrigerant will be used. Sometimes leaks can occur in a refrigeration system, and if the refrigerant comes into contact with the food, it can become contaminated. Thus, if a food is allowed to be in contact with ammonia for a long time, its taste and aroma may be affected. Although halocarbons do not

TABLE 16.6

Some Types of Refrigerants

Type	Number	Chemical Name	Formula
Halocarbons	11	Trichlorofluoromethane	CCl_3F
	12	Dichlorodifluoromethane	CCl_2F_2
	13	Chlorotrifluoromethane	$CCLF_3$
	22	Chlorodifluoromethane	$CHClF_2$
	40	Chloromethyl	CH_3Cl
	113	Triclorotrifluoroethane	CCl_2FCClF_2
	114	Dichlorotetrafluoroethane	$CClF_2CClF_2$
Hydrocarbons	50	Methane	CH_4
	170	Ethane	C_2H_6
	290	Propane	C_3H_8
Inorganic	717	Ammonia	NH_3
	718	Water	H_2O
	729	Air	
	744	Carbon dioxide	CO_2
	764	Sulfur dioxide	SO_2

Source: Stoecker, W.F. and Jones, J.W., *Refrigeration and Air Conditioning*, McGraw–Hill, New York, 1982.

cause serious problems when in contact with foods (Stoecker and Jones, 1982), these compounds produce deleterious effects on the atmospheric ozone layer; therefore, their use is limited and some have been banned.

16.9 Multipressure Systems

A multipressure system has two or more low pressure points. A low pressure point is the pressure of the refrigerant between the expansion valve and the inlet to the compressor. Multipressure systems can be found in the dairy industry (Stoecker and Jones, 1982), in which an evaporator operates at –35°C to strengthen or harden ice cream, whereas another evaporator operates at 2°C to cool milk.

In refrigeration systems, a stream that is a mixture of liquid and vapor can be obtained between the condenser and the evaporator due to its passage through an expansion valve. The fraction of gas can be separated from the liquid fraction by separation tank. Thus, in Figure 16.6, point 1 indicates the conditions of a saturated liquid that, when expanded produces a mixture 3, which can be separated into a liquid 4 and a vapor 6. This vapor is fed into the compressor, while the liquid is driven through an expansion valve to the evaporator; the system needs, therefore, two compressors. Systems with only one compressor are not commonly used since they are not efficient (Stockier and Jones, 1982).

To compress a gas, at the outlet of the compressor, besides having a greater pressure, the gas increases its temperature as well. In many cases, with the

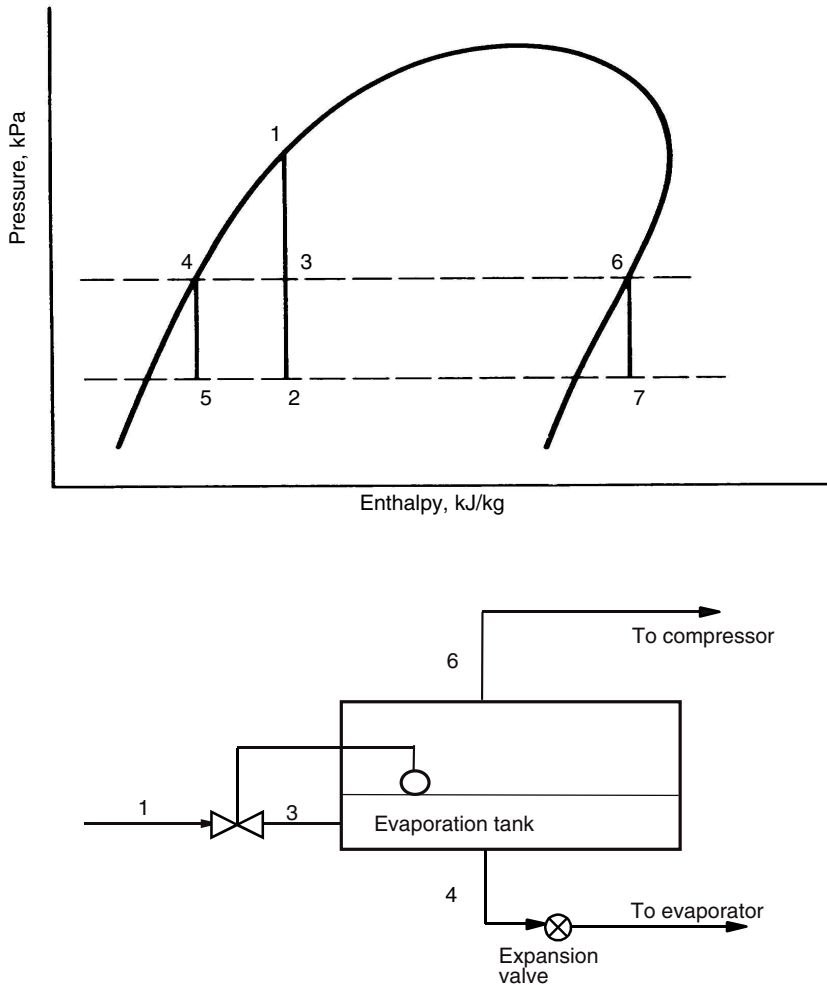

FIGURE 16.6
Expansion process with gas separation. (Adapted from Stoecker, W.F. and Jones, J.W., *Refrigeration and Air Conditioning*, McGraw–Hill, New York, 1982.)

objective of improving the process performance, two compressors with intermediate refrigeration of the vapor are used, thus reducing the overheating produced and obtaining a saturated vapor. This method is usually replaced in refrigeration systems by an alternative, shown in Figure 16.7, in which liquid refrigerant from the condenser is used as refrigeration fluid for the intermediate refrigerator. The compressor of the first stage discharges vapor that bubbles in the liquid of the intermediate refrigerator, leaving a saturated vapor (point 4) that has a lower temperature than the point 2 of discharge. In this type of system, if p_S is the suction pressure of the first compressor

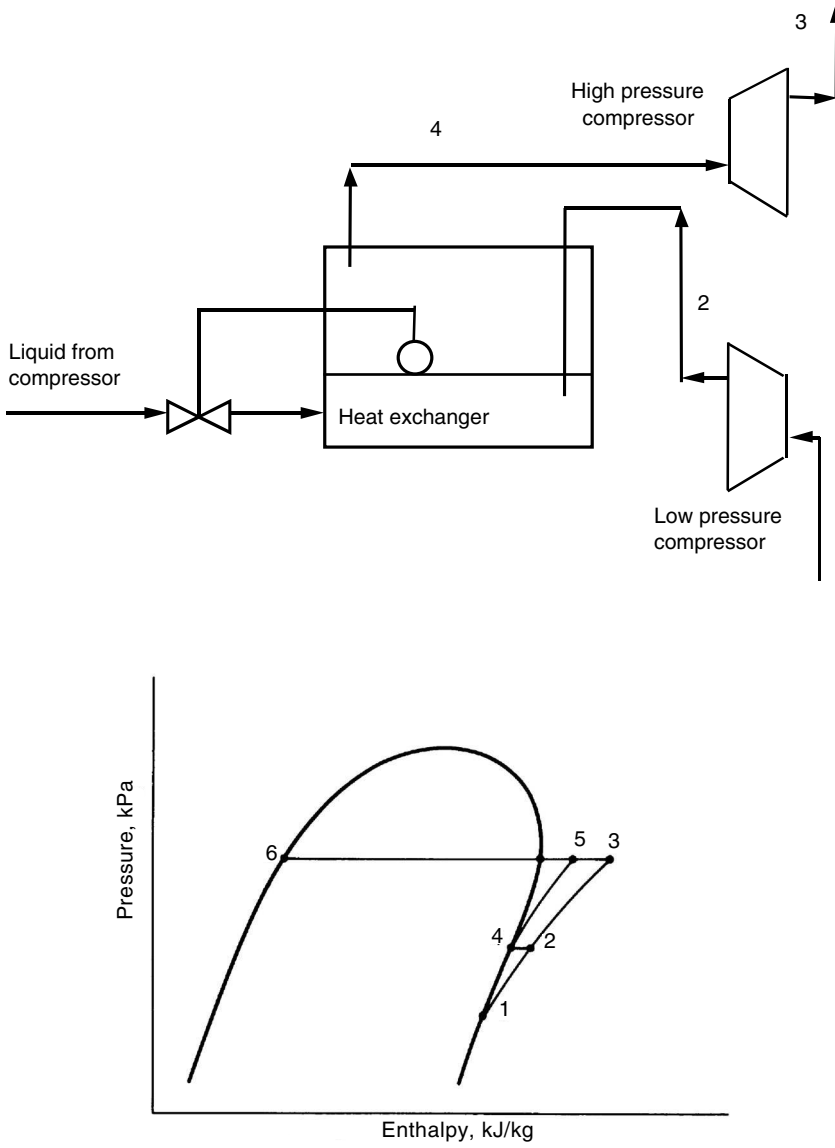

FIGURE 16.7
Intermediate refrigeration with liquid refrigerant. (Adapted from Stoecker, W.F. and Jones, J.W., *Refrigeration and Air Conditioning*, McGraw–Hill, New York, 1982.)

and p_D is the discharge of second compressor, the intermediate pressure (p_i) is calculated as the geometric mean of these two pressures as:

$$p_i = \sqrt{p_S\, p_D} \tag{16.25}$$

This pressure is the discharge pressure of the first compressor and the suction pressure of the second, as well as the pressure at which the intermediate refrigerator should operate in order to maintain the optimum global economy of the system.

16.9.1 Systems with Two Compressors and One Evaporator

One common way to obtain a low temperature evaporator is by using a two-stage compression with an intermediate refrigerator and separation of gas (Figure 16.8). This system requires less power than one with simple compression, and usually the power savings justify the extra cost of the equipment.

It can be observed that the fluid that circulates in different sections of the installation is the same, hence:

$$w_1 = w_2 = w_7 = w_8 \tag{16.26a}$$

$$w_3 = w_6 \tag{16.26b}$$

For the solution of problems with this type of system, different balances should be performed:

Energy balance in the evaporator:

$$\dot{Q}_E = w_1\left(\hat{H}_1 - \hat{H}_8\right) \tag{16.27}$$

Balance in the intermediate refrigerator:

$$w_2\hat{H}_2 + w_6\hat{H}_6 = w_3\hat{H}_3 + w_7\hat{H}_7 \tag{16.28}$$

Taking into account Equation 16.26, it is obtained that:

$$w_3\left(\hat{H}_3 - \hat{H}_6\right) = w_2\left(\hat{H}_2 - \hat{H}_7\right) \tag{16.29}$$

Power of the compressors:

First compressor: $$\left(Pow\right)_1 = w_1\hat{W}_1 = w_1\left(\hat{H}_2 - \hat{H}_1\right) \tag{16.30}$$

Second compressor: $$\left(Pow\right)_2 = w_3\hat{W}_2 = w_3\left(\hat{H}_4 - \hat{H}_3\right) \tag{16.31}$$

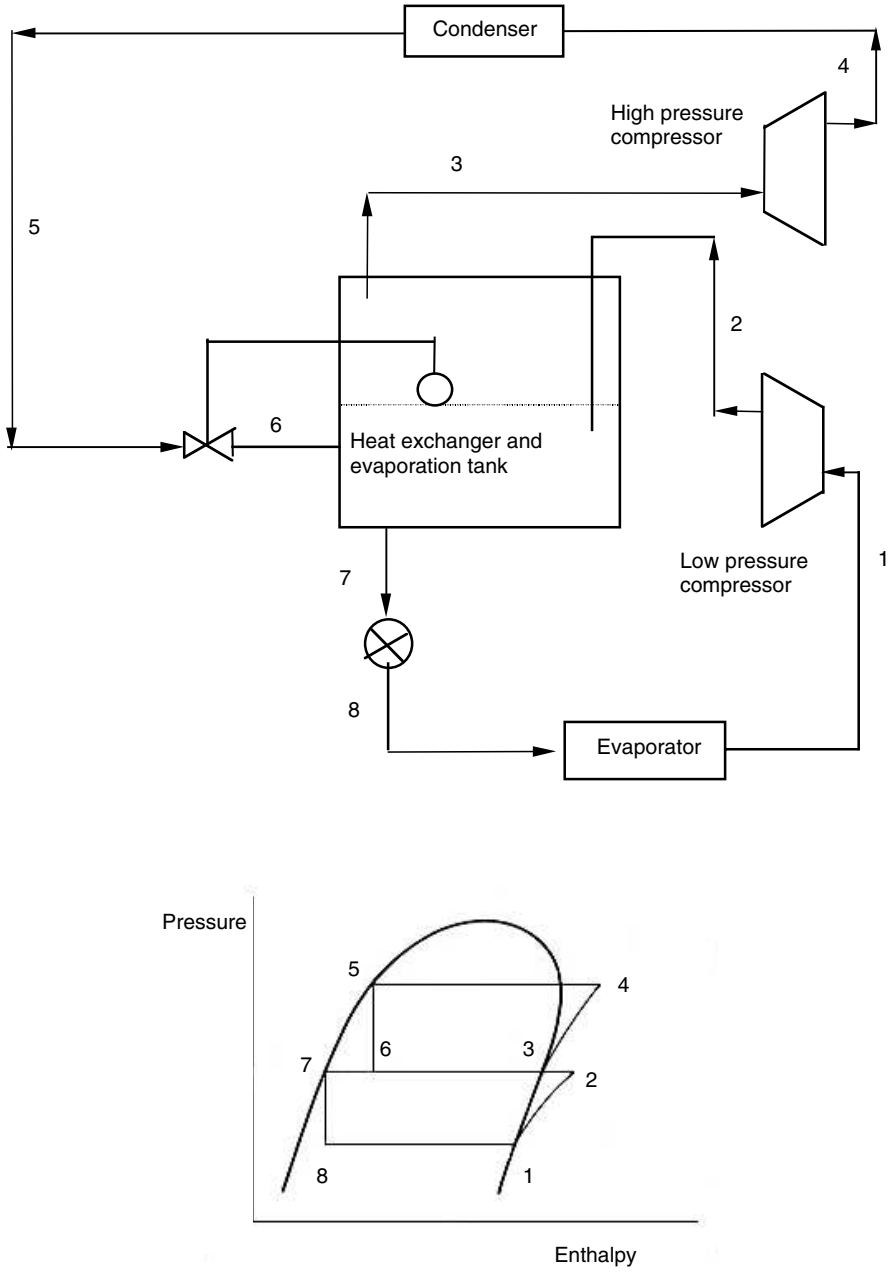

FIGURE 16.8
Operation with two compressors and one evaporator. (Adapted from Stoecker, W.F. and Jones, J.W., *Refrigeration and Air Conditioning*, McGraw–Hill, New York, 1982.)

16.9.2 Systems with Two Compressors and Two Evaporators

Systems that have two compressors and two evaporators operating at different temperature are common in the refrigeration industry. Different refrigeration temperatures are often required in different processes of the same plant. Evaporators at two different temperatures can operate in an efficient way in a two-stage system that uses an intermediate refrigerator and vapor separator (Figure 16.9). It should be pointed out that the intermediate pressure of the system corresponds to the saturation temperature T_3 of the second evaporator and is fixed by this temperature.

The solution of problems should be carried out through mass and energy balances in the different parts of the system.

The following is complied with in this system:

$$w_1 = w_2 = w_7 = w_8 \tag{16.32}$$

Balances in the evaporators:

$$\dot{Q}_{E1} = w_1\left(\hat{H}_1 - \hat{H}_7\right) \tag{16.33}$$

$$\dot{Q}_{E2} = w_6\left(\hat{H}_3 - \hat{H}_6\right) \tag{16.34}$$

Balances in the second evaporator and intermediate refrigerator:

$$w_2\hat{H}_2 + w_5\hat{H}_5 + \dot{Q}_{E2} = w_3\hat{H}_3 + w_7\hat{H}_7 \tag{16.35}$$

$$w_2 + w_5 = w_3 + w_7 \tag{16.36}$$

Since $w_2 = w_7$, it is also true that $w_3 = w_5$; hence:

$$w_3\left(\hat{H}_3 - \hat{H}_5\right) = w_2\left(\hat{H}_2 - \hat{H}_7\right) + \dot{Q}_{E2} \tag{16.37}$$

Power of the compressors:

First compressor: $$\left(Pow\right)_1 = w_1\hat{W}_1 = w_1\left(\hat{H}_2 - \hat{H}_1\right) \tag{16.38}$$

Second compressor: $$\left(Pow\right)_2 = w_3\hat{W}_2 = w_3\left(\hat{H}_4 - \hat{H}_3\right) \tag{16.39}$$

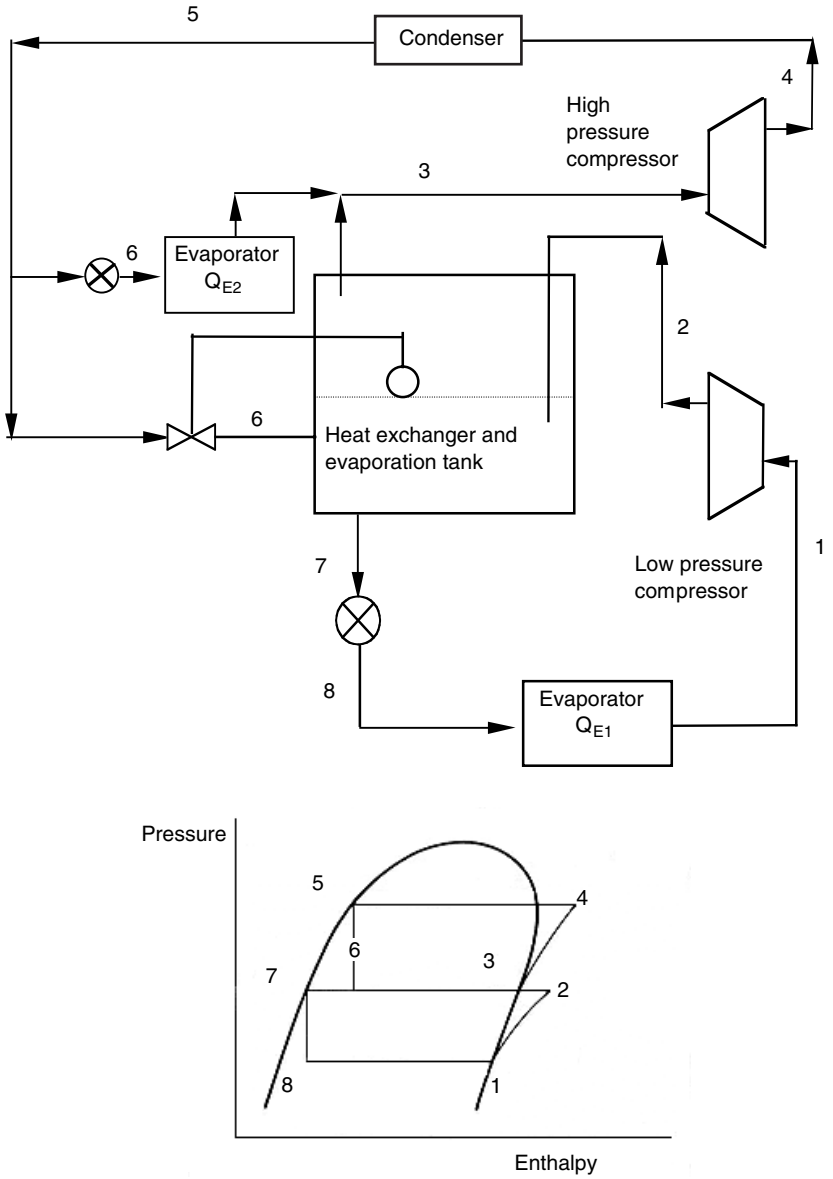

FIGURE 16.9
Operation with two compressors and two evaporators. (Adapted from Stoecker, W.F. and Jones, J.W., *Refrigeration and Air Conditioning*, McGraw–Hill, New York, 1982.)

Problems

16.1

A 3-cm thick slab of lean meat is placed inside a freezer in which the temperature is –25°C. The coefficient of heat transfer by convection from the surface of the meat is 15 J/(s·m²·°C). Determine the time needed to freeze the meat slab if 70% of its weight is water.

Data: properties of lean meat: thermal conductivity = 1.7 J/(s·m·°C); specific heat = 2.1 kJ/(kg·°C); density = 995 kg/m³.

According to Table 16.1, the initial freezing temperature for lean meat is T_f = –2.2°C.

The molar fraction of water at the freezing point is obtained from Equation 16.3c:

$$\ln X_{0w} = \frac{6003}{8.314}\left[\frac{1}{273} - \frac{1}{270.8}\right] \qquad X_{0w} = 0.9787$$

The equivalent molecular weight of the solutes is calculated by Equation 16.3b:

$$M_S = \frac{(18)(0.3)(0.9787)}{(0.7)(1 - 0.9787)} = 355.18 \text{ kg / kmol}$$

The molar fraction of unfrozen water at –25°C is obtained from Equation 16.3c:

$$\ln X_w = \frac{6003}{8.314}\left[\frac{1}{273} - \frac{1}{248}\right] \qquad X_w = 0.7660$$

The mass fraction of unfrozen water is obtained from Equation 16.3b:

$$x_S = \frac{(18)(0.3)(0.766)}{(355.18)(1 - 0.766)} = 0.04976$$

The mass fraction of frozen water is:

$$x_I = x_{wi} - x_w = 0.65024$$

The effective latent heat is calculated from the ice fraction in the meat:

$$\lambda_I = x_I \lambda = (0.65024)(6003) = 3903.4 \text{ kJ / kmol} = 216.86 \text{ kJ / kg}$$

Then, the equation of Plank is applied to determine the freezing time. For this reason, it is necessary to determine previously the numbers of Biot and Stefan:

Biot's number:

$$(Bi) = \frac{he}{k} = \frac{(15)(0.03)}{(1.7)} = 0.2647$$

Stefan's number:

$$(Ste) = \frac{\hat{C}_P\left(T_f - T_e\right)}{\lambda_I} = \frac{(2.1)(-2.2-(-25))}{(216.86)} = 0.2208$$

The Fourier number is obtained from Plank's equation for a slab:

$$(Fo) = \frac{1}{8}\frac{1}{(0.2208)} + \frac{1}{2}\frac{1}{(0.2647)(0.2208)} = 9.120$$

The freezing time is obtained by solving the Fourier number for t:

$$t_f = (Fo)\frac{\rho\hat{C}_P(e)^2}{k} = (9.12)\frac{(995)(2.1)(0.03)^2}{(0.0017)} = 10,089 \text{ s}$$

$$t_f = 2 \text{ h } 48 \text{ min}$$

16.2

4-kg blocks of beaten egg yolk contained in a rectangular geometry of 5 cm thickness, 20 cm width, and 40 cm length are introduced into a continuous belt freezer in which air circulates at –25°C. The yolks are introduced into the freezer at 20°C and leave at –10°C. Determine the time needed to freeze the yolks. If each yolk block moves 1 m each minute inside the freezer, what length should the freezer's band have? Calculate the power that the freezer should have if 100 yolk blocks are treated simultaneously.

Data: Composition in weight of egg yolk: 48.4% water, 16% *F* proteins, 34% lipids, 0.5% hydrocarbons, and 1.1% ash. Individual coefficient of heat transfer by convection: 20 J/(s·m²·°C).

The thermal properties of yolk at 20°C are calculated by the equations of Choi and Okos, so the properties of its components are determined first:

Component	k (J/s·m·°C)	$\hat{C}_P$ (kJ/kg·°C)	ρ (kg/m³)	X_i^m	X_i^V
Water	0.6037	4.177	995.7	0.484	0.4931
Protein	0.2016	2.032	1319.5	0.160	0.1230
Fat	0.1254	2.012	917.2	0.340	0.3761
Carbohydrates	0.2274	1.586	1592.9	0.005	0.0021
Ash	0.3565	1.129	2418.2	0.011	0.0070

$$k = (0.6037)(0.4931) + (0.2016)(0.123) + (0.1254)(0.3761) + (0.2274)(0.0021) + (0.3565)(0.007)$$

$$\hat{C}_P = (4.177)(0.484) + (2.032)(0.16) + (2.012)(0.34) + (1.586)(0.005) + (1.129)(0.011)$$

$$\rho = (1/995.7)(0.484) + (1/1319.5)(0.16) + (1/917.2)(0.34) + (1/1592.9)(0.005) + (1/2418.2)(0.011)$$

where

k = 0.3726 J/(s·m·C)
$\hat{C}_p$ = 3.051 kJ/(kg·°C)
ρ = 1014.5 kg/m³

The properties of frozen yolk will be determined at –10°C. The fraction of unfrozen water should be calculated previously at this temperature. The temperature at which yolk begins to freeze is –0.5°C.

The molar fraction of water in yolk when freezing begins is calculated by Equation 16.3c:

$$\ln X_{0w} = \frac{6003}{8.314}\left[\frac{1}{273} - \frac{1}{272.5}\right]$$

This value allows calculation of the equivalent molecular weight of the solutes by means of Equation 16.3b:

$$M_S = \frac{(18)(0.516)(0.9952)}{(0.484)(1-0.9952)} = 3944.8 \text{ kg/kmol}$$

The molar fraction of unfrozen water at –10°C is obtained from Equation 16.c:

$$\ln X_w = \frac{6003}{8.314}\left[\frac{1}{273} - \frac{1}{263}\right] \qquad X_w = 0.9043$$

The mass fraction of unfrozen water is obtained from Equation 16.3.b:

$$x_S = \frac{(18)(0.516)(0.9043)}{(3944.8)(1-0.9043)} = 0.0223$$

The mass fraction of frozen water is $x_I = x_{wi} - x_w = 0.4617$.

The thermal properties of the components at –10°C are shown in the following table:

Component	k (J/s·m·°C)	$\hat{C}_P$ (kJ/kg·°C)	ρ (kg/m³)	X_i^m	X_i^V
Water	0.5541	4.234	996.8	0.0223	0.0220
Protein	0.1666	1.996	1335.1	0.160	0.1177
Fat	0.2083	1.969	929.8	0.340	0.3591
Carbohydrates	0.1871	1.529	1602.2	0.005	0.0031
Ash	0.3153	1.073	2426.6	0.011	0.0045
Ice	22.922	2.002	918.2	0.4617	0.4938

The properties of yolk at –10°C are obtained by applying the equations of Choi and Okos:

$$k = 1.240 \text{ J/(s.m.°C)}; \quad \hat{C}_p = 2.027 \text{ kJ/(kg.°C)}; \quad \rho = 987 \text{ kg/m}^3$$

The generalized equation of Plank (Equation 16.10) will be used to calculate the freezing time, but the numbers of Biot and Stefan should be determined first using the properties of yolk at –10°C.

Biot's number:

$$(Bi) = \frac{he}{k} = \frac{(20)(0.05)}{(1.240)} = 0.8065$$

Stefan's number: the effective latent heat is calculated from the fraction of ice that the yolk contains:

$$\lambda_I = x_I \lambda_w = (0.4617)(6003)(1/18) = 154 \text{ kJ/kg}$$

so the module of Stefan is:

$$(Ste) = \frac{\hat{C}p\,(T_f - T_e)}{\lambda_I} = \frac{(2.027)(-0.5)-(-25))}{(154)} = 0.3225$$

The parameters P and R are obtained from Equations 16.11a and b, in which $\beta_1 = (20)/(5) = 4$ and $\beta_2 = (40)/(5) = 8$; hence, $P = 0.3636$ and $R = 0.0993$

Fourier's number is obtained from the equation of Plank for a slab:

$$(Fo) = \frac{0.0993}{(0.3225)} + \frac{0.3636}{(0.8065)(0.3225)} = 1.706$$

The freezing time is obtained when solving the equation of Fourier's number for t:

$$t_f = (Fo)\frac{\rho\hat{C}p(e)^2}{k} = (1.706)\frac{(982)(2.027)(0.05)^2}{(0.00117)} = 7256 \text{ s}$$

This time corresponds to the time needed to freeze the product if it is initially at the freezing temperature. For this reason, the time required by the surface of the product to change from 20°C to –0.5°C should be calculated. The rule of Newman should be applied to a parallelepiped geometry; however, the width and length of the yolk blocks are really greater than the thickness. For this reason, it will be supposed that the heat transfer predominates on this direction. Using dimensionless modules:

$$Y = \frac{T_e - T_f}{T_e - T_i} = \frac{-25-(-0.5)}{-25-20} = 0.544$$

$$m = \frac{k}{h(e/2)} = \frac{(0.372)}{(20)(0.025)} = 0.744$$

$$n = 1$$

The dimensionless time module is obtained graphically: $\tau = 0.5$. This module allows the calculation of the time needed to decrease the temperature to the initial point of freezing:

$$t = \frac{\tau(e/2)^2\rho\hat{C}p}{k} = \frac{(0.5)(0.025)^2(1014.5)(3.051\times1000)}{0.372} = 2591 \text{ s}$$

The total time is:

$$t_{TOTAL} = t_f + t = (7256)(2591) = 9840 \text{ s} = 164 \text{ min}$$

The residence time of the food in the freezer should be at least the freezing time (164 min). If v is the velocity with which the yolk blocks move inside the freezer, then the length that the egg yolk should cross in the freezer is:

$$L = t_{TOTAL}\, v = (164)(1) = 164 \text{ m}$$

The total freezing time calculated from Plank's equation is an approximation, so it will be calculated from the equation of Nagaoka et al. (Equation 16.12). For this reason, the enthalpy variation experienced by the product should be previously calculated from Equation 16.13:

$$\Delta\hat{H} = (3.051)(20 - (-0.5)) + (154) + (2.027)(-0.5 - (-10)) = 235.8 \text{ kJ/kg}$$

Substitution of data in Equation 16.12 yields the total freezing time:

$$t_T = \frac{(982)\left(235.8 \times 10^3\right)}{-0.5 - (-25)}\left(\frac{(0.0993)(0.05)^2}{1.240} + \frac{(0.3636)(0.05)}{20}\right)\left[1 + 0.008\,(10 - (-0.5))\right]$$

Hence:

$$t_T = 12202 \text{ s} \equiv 203.4 \text{ min}$$

Therefore, the total length is L = (203.4 min) (1 m/min) = 203.4 m.

It can be observed that the freezer's band length calculated by this method is greater, and the one obtained by the Plank's equation is just estimated.

The total mass to freeze is m = (100)(4) = 400 kg.

The power of the freezer is calculated applying Equation 16.18:

$$Pow = \frac{m\Delta\hat{H}}{t_{TOTAL}} = \frac{(400)(235.8)}{(12,202)} = 7.73 \text{ kW}$$

16.3

An industrial facility requires 100 kW of freezing power. In order to meet such requirements, a standard system of the vapor compression cycle was installed, using ammonia as refrigerant fluid. This cycle operates at a condensation temperature of 30ºC and an evaporation temperature of –10ºC. Calculate: (a) the circulation mass flow rate of refrigerant fluid; (b) the power

needed by the compressor; (c) the coefficient of performance; and (d) the power per kilowatt of refrigeration.

This is a vapor compression cycle, so the global process is like the one shown in the pressure–enthalpy diagram of Figure 16.5.

The enthalpy at point 1 is determined in the diagram or in the ammonia tables (Appendix A3) and corresponds to a saturated vapor at –10ºC:

$$\hat{H}_1 = 1450.2 \text{ kJ/kg}$$

$$p_1 = 291.6 \text{ kPa}$$

The enthalpy of point 2 is determined by the isoentropic line that passes over point 1 and cuts the isobaric line that corresponds to a temperature of 30ºC:

$$\hat{H}_2 = 1650 \text{ kJ/kg}$$

$$p_2 = 1173 \text{ kPa}$$

The enthalpy of point 3 corresponds to saturated liquid at 30ºC, and can be obtained from tables: $\hat{H}_3$ = 341.8 kJ/kg. Also: $\hat{H}_4 = \hat{H}_3$ = 341.8 kJ/kg.

(a) The refrigeration power represents the heat flow absorbed in the evaporator. From Equation 16.23:

$$w = \frac{\dot{Q}_E}{\hat{H}_1 - \hat{H}_4} = \frac{100 \text{ kW}}{(1450.2 - 341.8) \text{ kJ/kg}} = 0.090 \text{ kg/s} \approx 324.8 \text{ kg/h}$$

that is, the refrigerant flow.

(b) The power needed by the compressor is calculated from Equation 16.21:

$$Pow = w\left(\hat{H}_2 - \hat{H}_1\right) = (0.09 \text{ kg/s})((1650 - 1450.2)\text{kJ/kg}) \approx 18 \text{ kW}$$

(c) The coefficient of performance is obtained from Equation 16.24:

$$\phi = \frac{\hat{H}_1 - \hat{H}_4}{\hat{H}_2 - \hat{H}_1} = \frac{w\left(\hat{H}_1 - \hat{H}_4\right)}{w\left(\hat{H}_2 - \hat{H}_1\right)} = \frac{100 \text{ kW}}{18 \text{ kW}} = 5.56$$

(d) The refrigeration power or compressor power per kilowatt of refrigeration is the inverse of the coefficient of performance:

$$\text{Refrigeration power} = \frac{18\ \text{kW}}{100\ \text{kW}} = 0.18$$

16.4

The refrigeration requirements in an industry are for 400 kW, so a system of two compressors with intermediate refrigerator and vapor elimination is installed. The system uses ammonia as refrigerant fluid. If the evaporation temperature is –20ºC and the condensation temperature is 30ºC, calculate the power of the compressors.

The system installed is the one described in Figure 16.8. According to the statement of the problem, the suction pressure of the first compressor p_S and the discharge pressure of the second compressor p_D correspond to the saturation pressure at the temperatures of the evaporator and condenser, respectively. From ammonia tables (Appendix A3): T_S = –20ºC corresponds to p_S = 190.7 kPa and T_D = 30ºC corresponds to p_D = 1168.6 kPa.

The intermediate pressure for an economic optimum is obtained from Equation 16.25:

$$p_i = \sqrt{p_S\, p_D} = \sqrt{(190.7)(1168.6)} = 472.1\ \text{kPa}$$

The enthalpies for the different points representative of the system can be obtained from the tables and graphs for ammonia:

Point 1: saturated vapor at –20ºC has an enthalpy: $\hat{H}_1$ = 1437.2 kJ/kg.

Point 2: placed on the isoentropic line that passes over point 1 and cuts the isobaric line p_i = 472.1 kPa. Hence, $\hat{H}_2$ = 1557.5 kJ/kg.

Point 3: to saturated vapor at the pressure p_i = 472.1 kPa, correspond a temperature $T_3 \approx 2.5$ºC and an enthalpy: $\hat{H}_3$ = 1464.3 kJ/kg.

Point 4: placed on the isoentropic line that passes over point 3 and cuts the isobaric line at the discharge pressure of the second compressor p_D = 472.1 kPa. The conditions of point 4 are obtained from the point where the two lines cross, yielding an enthalpy: $\hat{H}_4$ = 1590 kJ/kg.

Point 5: corresponds to saturated liquid at 30ºC, and from tables it is possible to obtain the value of its enthalpy: $\hat{H}_5$ = 341.8 kJ/kg.

Point 6: a liquid–vapor mixture at a pressure of 472.1 kPa, but with the same enthalpy as point 5: $\hat{H}_6 = \hat{H}_5$ = 341.8 kJ/kg.

Point 7: a saturated liquid at 472.1 kPa. The value of its enthalpy can be obtained by interpolation in tables: $\hat{H}_7$ = 211.6 kJ/kg.

Point 8: a liquid–vapor mixture at –20ºC, but with the same enthalpy as that of point 7: $\hat{H}_8 = \hat{H}_7$ = 211.6 kJ/kg.

Once the values of the different points representative of the system have been obtained, it is possible to determine the different variables that intervene.

The circulation mass flow rate of the refrigerant fluid in the first compressor is obtained from the energy balance in the evaporator (Equation 16.27):

$$w_1 = \frac{\dot{Q}_E}{\hat{H}_1 - \hat{H}_8} = \frac{400 \text{ kW}}{(1437.2 - 211.6) \text{ kJ/kg}} = 0.326 \text{ kg/s} \approx 1175 \text{ kg/h}$$

Also, it is known (Equations 16.26a and b) that different streams in the system have the same circulation mass flow rate. Thus:

$$w_1 = w_2 = w_7 = w_8 \quad \text{and} \quad w_3 = w_6$$

When carrying out the energy balance in the intermediate refrigerator, Equation 16.29 is obtained, which allows calculations of the circulation flow rate of the refrigerant fluid in the second compressor:

$$w_3 = \frac{w_2\left(\hat{H}_2 - \hat{H}_7\right)}{\left(\hat{H}_3 - \hat{H}_6\right)} = \frac{0.326(1557.5 - 211.6)}{(1464.3 - 341.8)} = 0.391 \text{ kg/s} \approx 1409 \text{ kg/h}$$

The power of the compressors is obtained from Equations 16.30 and 16.31:

$$(Pow)_1 = w_1\left(\hat{H}_2 - \hat{H}_1\right) = (0.326)(1557.5 - 1437.2) = 39.2 \text{ kW}$$

$$(Pow)_2 = w_3\left(\hat{H}_4 - \hat{H}_3\right) = (0.391)(1590 - 1464.3) = 49.2 \text{ kW}$$

The total compression power for the system is Pow = 88.4 kW.

17

Dehydration

17.1 Introduction

Dehydration, or drying, is one of the unit operations most commonly used for food preservation. It has been used since prehistoric times because it allows for food products with longer lives. As time went on, the demand for food increased as population increased, which resulted in the increased importance of preservation by drying within the food sector. The development of the drying industry has been linked to the demand for foods to feed soldiers in wars around the world. Dehydration is especially useful for military purposes, since it reduces the weight and size of foods. The advances achieved within the military field have been transferred to the drying industry in general, yielding greater advances of the food drying industry as a whole.

To a greater or lesser extent, water in food is eliminated during dehydration processes, thus achieving better microbiological preservation, as well as retarding many undesirable reactions. Although food preservation has great importance, dehydration also can decrease packaging, handling, storage, and transport costs because it decreases a food's weight and, in some cases, its volume.

Although the terms drying and dehydration may be used as synonyms, they are not. A food is considered to be dehydrated if it does not contain more than 2.5% water, while a dried food may contain more than 2.5% water (Barbosa–Cánovas and Vega–Mercado, 1996).

Except for freeze-drying, osmotic drying, and vacuum drying, the removal of water from a food is achieved in most cases by blowing a dry air flow, which eliminates water from the surface of the product to the air stream. The food drying process not only decreases the water content of the food, but also can affect other physical and chemical characteristics such as destruction of nutrients and enzymatic and nonenzymatic reactions, among others.

In the drying process, it is important to know the mechanisms related to the movement of water inside and outside the food. This movement can be due to capillary forces, water diffusion due to concentration gradients, diffusion

on the surface, diffusion of water vapor in the pores filled with air, or flow due to pressure gradients or to vaporization and condensation of water.

17.2 Mixing of Two Air Streams

In air drying processes, the gaseous stream that leaves the dryer usually has an energy content that makes reuse possible, even when its moisture content is higher than the moisture content of the air entering the dryer. For this reason, the recirculation of air leaving the dryer is common practice and allows the global drying process to be cheaper. In most cases, a hot and wet air stream is partially recirculated and mixed with a fresh air stream. The heat and material balances for this operation can be expressed as:

$$w_C X_C + w_H X_H = (w_C + w_H) X_m \tag{17.1}$$

$$w_C H_C + w_H H_H = (w_C + w_H) H_m \tag{17.2}$$

In these equations, w is the air flow, X is moisture content, and H is enthalpy, with the subscripts C and H representing cold and hot, respectively, while the subscript m refers to the conditions of the mixture. This type of process can be seen in the moisture–enthalpy diagram (Figure 17.1); note

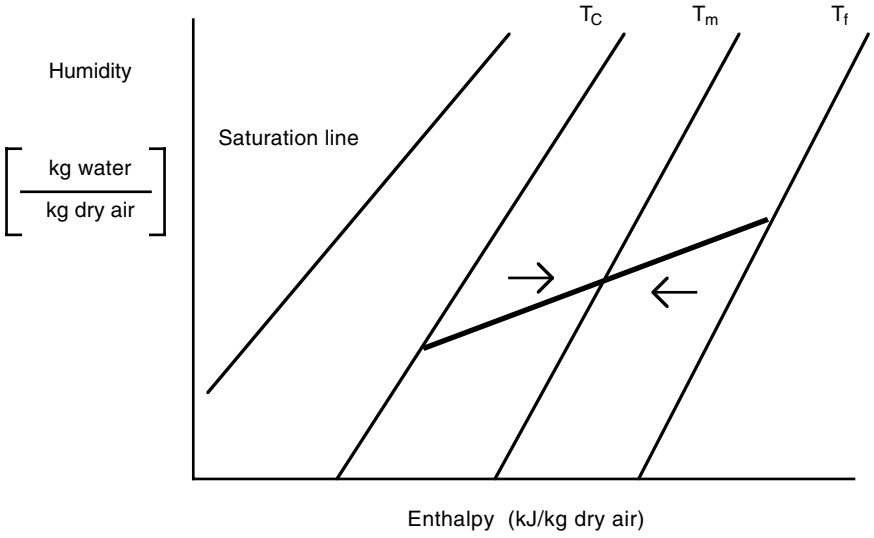

FIGURE 17.1
Representation of the mixing of two air streams.

that the differences in enthalpy between the mixed stream and the initial streams are proportional to the mass flows.

17.3 Mass and Heat Balances in Ideal Dryers

17.3.1 Continuous Dryer without Recirculation

A dryer of this type consists mainly of a chamber in which the air and the solids to be dried flow in countercurrent (Figure 17.2). The solids are introduced at a mass flow rate w_S (kg of dry solids/h), with a moisture content of Y_E at a temperature T_{SE}, leaving the dryer at a temperature T_{SS} with a moisture content Y_S. The air stream enters the dryer with a flow w' (kg of dry air/h), at a temperature T_{AE} with a humidity X_E (kg water/kg dry air), and it leaves the dryer at a temperature T_{AS}, with a humidity X_S.

The following is obtained when performing a mass balance for water:

$$w_S\left(Y_E - Y_S\right) = w'\left(X_S - X_E\right) \tag{17.3}$$

while the energy balance yields the expression:

$$\dot{Q}_E + w'\hat{\imath}_E + w_S\,\hat{h}_E = \dot{Q}_S + w'\hat{\imath}_S + w_S\,\hat{h}_S \tag{17.4}$$

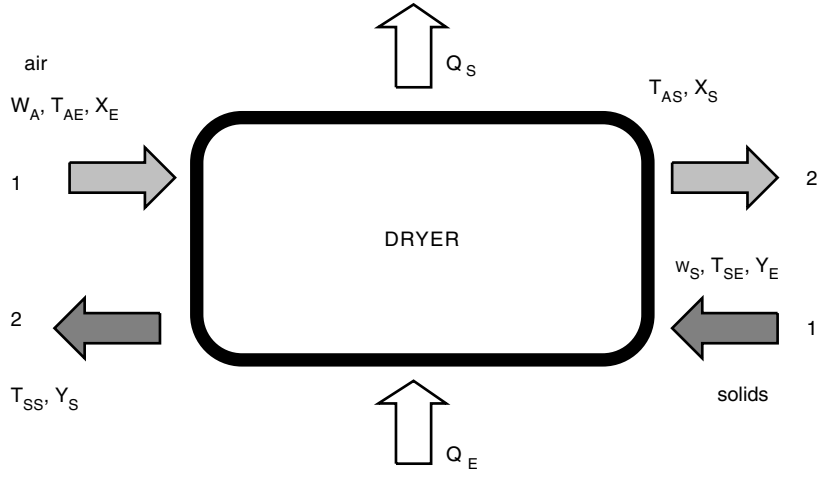

FIGURE 17.2
Continuous ideal dryer without recirculation.

In this equation, $\dot{Q}_E$ and $\dot{Q}_S$ are the heat flows given and lost in the dryer, respectively, $\hat{h}$ is the enthalpy of the solids, and $\hat{\imath}$ is the enthalpy of the air given by Equation 5.16:

$$\hat{\imath} = \hat{s}\left(T - T^*\right) + \lambda_0 \cdot X = \left(1 + 1.92\ X\right)\left(T - T^*\right) + \lambda_0 X \tag{17.5}$$

where $\hat{s}$ is the wet specific heat of air. The enthalpy of the air is:

$$\hat{h} = \left(\hat{C}_P\right)_S \left(T - T^*\right) + Y\ \left(\hat{C}_P\right)_w \left(T - T^*\right) \tag{17.6}$$

Here, $(\hat{C}_P)_S$ is the specific heat of the solids, and $(\hat{C}_P)_w$ is the specific heat of the water in the product. In these last equations, T^* is a reference temperature, usually taken as 0°C.

17.3.2 Continuous Dryer with Recirculation

As described in the last section, the air stream leaving the dryer contains more water than at the inlet, but its temperature is still high. For this reason, the energy contained in this stream is usually used by recirculation. However, since its water content would not permit a good application in the dryer, this stream is mixed with a stream of fresh dry air and, before introducing the mixture in the dryer, it passes through a heater to increase its enthalpy content (Figure 17.3).

A mass balance in the heater yields:

$$w_1' X_1 + w_6' X_2 = \left(w_1' + w_6'\right) X_4 \tag{17.7}$$

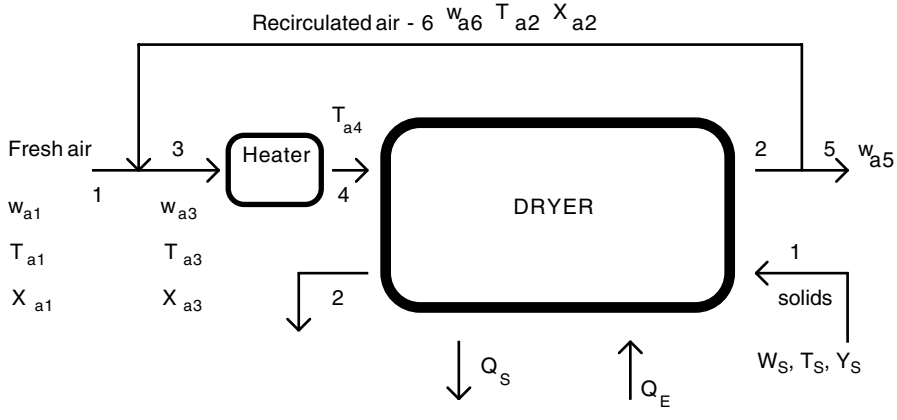

FIGURE 17.3
Ideal continuous dryer with recirculation.

Here, w_1' is the fresh dry air flow, w_6' is the recirculated air, X_1 is the moisture content of fresh air, X_2 is the moisture content of the recirculated air, and X_4 is the moisture content of the mixture leaving the heater.

The mass balance in the dryer leads to the expression:

$$\left(w_1'+w_6'\right)X_4 + w_S' Y_E = \left(w_1 + w_6'\right)X_2 + w_S' Y_S \tag{17.8}$$

The enthalpy balances can be performed in the same way for the heater, dryer, or complete system.

17.4 Dehydration Mechanisms

Drying is defined as the removal of moisture from a product, and in most practical situations the main stage during drying is the internal mass transfer. The mechanisms of water transfer in the product during the drying process can be summarized as follows (Van Arsdel and Copley, 1963): water movement due to capillary forces, diffusion of liquid due to concentration gradients, surface diffusion, water vapor diffusion in pores filled with air, flow due to pressure gradients, and flow due to water vaporization–condensation. In the pores of solids with rigid structure, capillary forces are responsible for the retention of water, whereas in solids formed by aggregates of fine powders, the osmotic pressure is responsible for water retention within the solids as well as in the surface.

The type of material to be dried is an important factor to consider in all drying processes, since its physical and chemical properties play a significant role during drying due to possible changes that may occur and because of the effect that such changes may have in the removal of water from the product.

A hygroscopic material is one that contains bound water that exerts a vapor pressure lower than the vapor pressure of liquid water at the same temperature. It is expected that products made mainly of carbohydrates will behave in a hygroscopic way, since the hydroxyl groups around the sugar molecules allow formation of hydrogen bonds with water molecules. The interaction between the water molecules and the hydroxyl groups causes solvation or solubilization of sugars. In water soluble proteins, as in most of the globular proteins, the polar amino acids are uniformly distributed in the surface, while the hydrophobic groups are located towards the inside of the molecule. This arrangement allows formation of hydrogen bonds with water, which explains the solubility of this type of proteins.

17.4.1 Drying Process

In drying processes, data are usually obtained as the change in the weight of the product over time (Figure 17.4). However, drying data can sometimes be expressed in terms of drying rate.

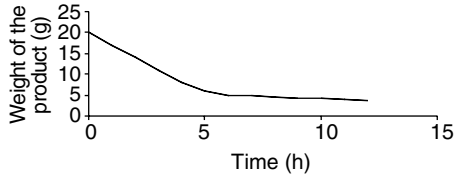

FIGURE 17.4
Variation of the product's weight in a drying process.

The moisture content of the product is defined as the relationship between the amount of water in the food and the amount of dry solids, expressed as:

$$Y_t = \frac{w_T - w_S}{w_S} \tag{17.9}$$

In this equation, w_T is the total weight of the material at a determined given time, w_S is the weight of dry solids, and Y_t is the moisture expressed as water weight/dry solid weight. A very important variable in the drying process is the so-called free moisture content, Y, defined as:

$$Y = Y_t - Y_{eq} \tag{17.10}$$

In this equation, Y_{eq} is the moisture content when equilibrium is reached. A typical drying curve is obtained by plotting the free moisture content against drying time (Figure 17.5).

The drying rate, R, is proportional to the change in moisture content with time:

$$R \propto \frac{dY}{dt} \tag{17.11}$$

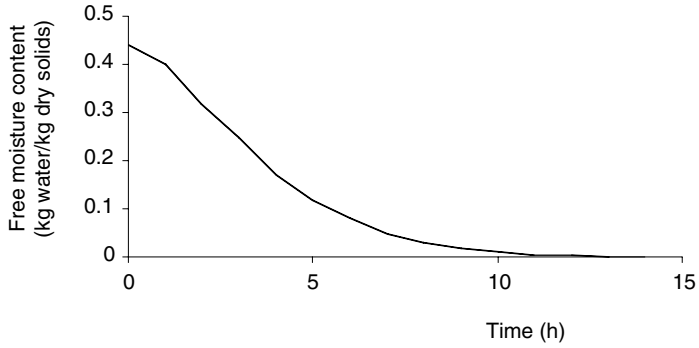

FIGURE 17.5
Free moisture content as a function of drying time.

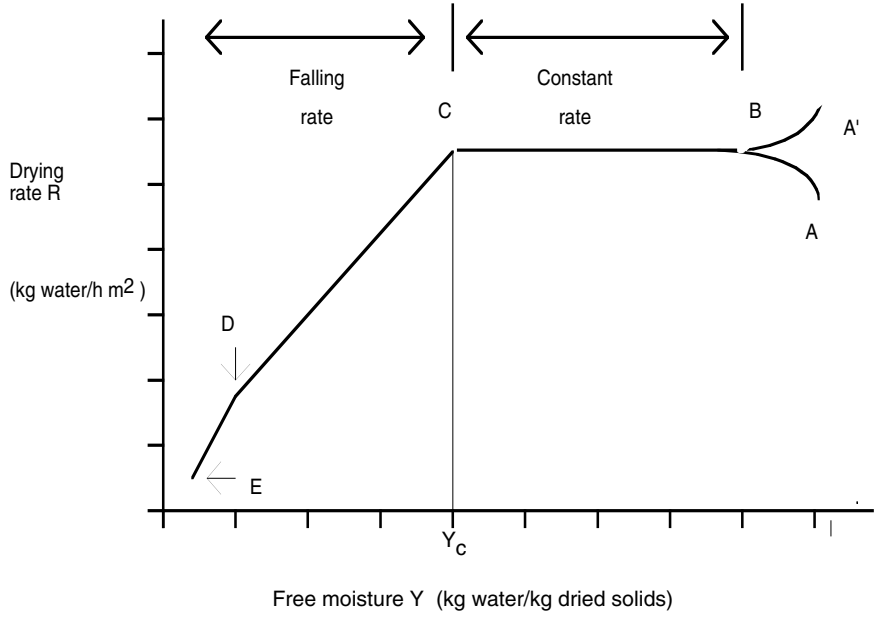

FIGURE 17.6
Drying rate curve. (Adapted from Barbosa–Cánovas, G.V. and Vega–Mercado, H., *Dehydration of Foods*, Chapman and Hall, New York, 1996.)

The value of dY/dt for each point in the curve can be obtained from Figure 17.5 by the value of the tangent to the curve at each of the points.

The drying rate can be expressed as (Geankoplis, 1983):

$$R = -\frac{w_S'}{A}\frac{dY}{dt} \tag{17.12}$$

Here, w_S' is the flow of dry solids and A is the area of the drying surface. When plotting the drying rate vs. time, a curve similar to the curve in Figure 17.4 is obtained.

The drying process of a material can be described by a series of stages in which the drying rate plays a key role. Figure 17.6 shows a typical drying rate curve in which points A and A' represent the initial point for a cold and hot material, respectively. Point B represents the condition of equilibrium temperature of the product surface. The elapsed time from point A or A' to B is usually low and commonly neglected in the calculation of drying time. The section B to C of the curve is known as the constant drying rate period and is associated with the removal of unbound water in the product. In this section, water behaves as if the solid were not present. Initially, the surface of the product is very wet, with a water activity value close to one. In porous solids, the water removed from the surface is compensated by the flow of water from the interior of the solid. The constant rate period continues, while

the evaporated water at the surface can be compensated for by the internal water. The temperature at the surface of the product corresponds approximately to the wet bulb temperature (Geankoplis, 1983).

The falling rate period starts when the drying rate cannot be kept constant any longer and begins to decrease and the water activity on the surface becomes smaller than one. In this case, the drying rate is governed by the internal flow of water and water vapor. Point *C* represents the start of the falling rate period, which can be divided into two stages. The first stage occurs when the wet points on the surface decrease continuously until the surface is completely dry (point *D*), while the second stage of the falling rate period begins at point *D*, where the surface is completely dry and the evaporation plane moves to the interior of the solid. The heat required to remove moisture is transferred through the solid to the evaporation surface, and the water vapor produced moves through the solid in the air stream going towards the surface. Sometimes there are no marked differences between the first and second falling rate periods. The amount of water removed during this period may be small, while the time required may be long since the drying rate is low.

17.4.2 Constant Rate Drying Period

The transport phenomena that take place during the constant drying rate period are mass transfer of steam to the environment (from the surface of the product through an air film that surrounds the material) and heat transfer through the solid. The surface of the material remains saturated with water during the drying process, since the rate at which water moves from the interior of the solid is fast enough to compensate for the water evaporated at the surface. If it is assumed that there is only heat transfer by convection from the hot air to the surface of the solid, and mass transfer from the surface to the hot air (Figure 17.7), it is obtained that:

$$q = h A\left(T - T_W\right) \tag{17.13}$$

$$N_a = k_y\left(X_W - X\right) \tag{17.14}$$

In these equations, h is the heat transfer coefficient, A is the area being dried, T_W is the wet bulb temperature, T is the drying temperature, N_a is the flux of water vapor, X_W is the moisture content of air at the solid surface, X is the moisture content of the dry air stream, and k_y is the mass transfer coefficient.

The heat needed to evaporate water at the surface of the product can be expressed as:

$$q = N_a M_a \lambda_W A \tag{17.15}$$

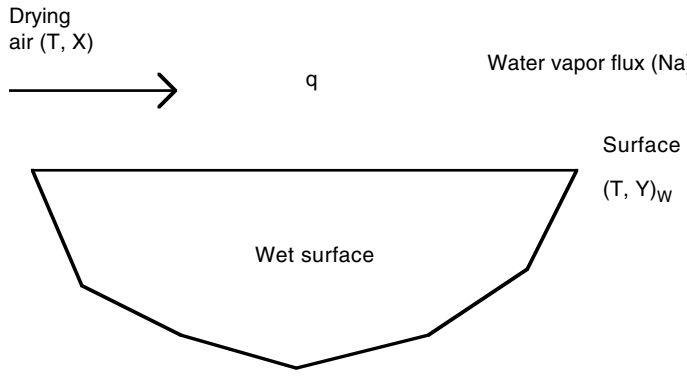

FIGURE 17.7
Heat and mass transfer during drying. (Adapted from Barbosa–Cánovas, G.V. and Vega–Mercado, H., *Dehydration of Foods,* Chapman and Hall, New York, 1996.)

where M_a is the molecular weight of water and λ_W is the latent heat of vaporization at the temperature T_W.

The drying rate during the constant rate period is expressed as (Okos et al., 1992):

$$R_C = k_y M_b \left(X_W - X\right) \tag{17.16}$$

or

$$R_C = \frac{h\left(T - T_W\right)}{\lambda_W} = \frac{q}{\lambda_W A} \tag{17.17}$$

In these equations M_b is the molecular weight of air, X_W is the humidity corresponding to the wet bulb temperature, and X is the humidity of the air within the gaseous stream. If there is no heat transfer by conduction or radiation, the temperature of the solid at the wet bulb temperature is equal to the temperature of the air during the constant rate drying period.

In drying calculations it is essential to know the mass transfer coefficient, which can be evaluated by the following expression (Okos et al., 1992):

$$\frac{k_y l}{D_{AB}} = 0.664\left(\mathrm{Re}\right)^{1/2}\left(Sc\right)^{1/3} \tag{17.18}$$

This equation is valid for laminar flow parallel to a flat plate, with l denoting the length of the plate in the flow direction; the Reynolds and Schmidt numbers are defined by the expressions:

$$\left(\mathrm{Re}\right) = \frac{\rho v d}{\eta} \qquad \left(Sc\right) = \frac{\eta}{\rho D_{AB}} \tag{17.19}$$

where D_{AB} is the molecular diffusivity of the air–water mixture, d the characteristic length or diameter, v the velocity of the fluid, ρ the density, and η the viscosity.

The heat transfer coefficient can be obtained by the equation (Geankoplis, 1983):

$$h = 0.0204\left(G\right)^{0.8} \tag{17.20}$$

In this expression, G is the mass flux of air expressed in kg/(m² h), yielding the heat transfer coefficient in W/(m² °C). The heat transfer coefficient in a slab can be expressed as a function of the Nusselt number, according to an expression of the type (Chirife, 1983):

$$\left(Nu\right) = \frac{hd}{k} = 2 + \alpha\left(\mathrm{Re}\right)^{1/2}\left(Pr\right)^{1/3} \tag{17.21}$$

The Prandtl number is defined as:

$$\left(Pr\right) = \frac{\hat{C}_P\,\eta}{k} \tag{17.22}$$

where k is the thermal conductivity, α is a constant, and $\hat{C}_P$ is the specific heat.

17.4.3 Falling Rate Drying Period

This period occurs after drying at a constant rate; as its names indicates, the drying rate R decreases when the moisture content is lower than the critical moisture content Y_C. Equation 17.12 should be solved by integration in order to solve this type of problem, and this can be calculated by a graphical integration method when plotting $1/R$ vs. Y.

The movement of water in the solid can be explained by different mechanisms (Barbosa–Cánovas and Vega–Mercado, 1996) such as diffusion of liquid due to concentration gradients, diffusion of water vapor due to partial vapor pressure, movement of liquid due to capillary forces, movement of liquid due to gravity forces, or surface diffusion. The movement of water through the food depends on its porous structure as well as on the interactions of water within the food matrix. Only some of the theories listed will be described next. Development of all of these theories can be found in the literature (Barbosa–Cánovas and Vega–Mercado, 1996; Chen and Johnson, 1969; Bruin and Luyben, 1980; Fortes and Okos, 1980; Geankoplis, 1983).

17.4.3.1 Diffusion Theory

The main mechanism in drying solids is water diffusion in solids of fine structure and in capillaries, pores, and small holes filled with water vapor.

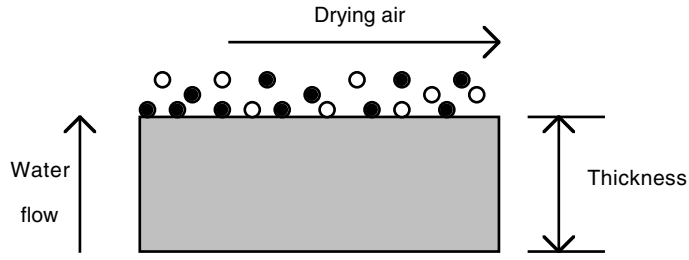

FIGURE 17.8
Surface diffusion and water vapor transport mechanism. (Adapted from Bruin, S. and Luyben, , K.Ch.A.M., in *Advances in Drying*, Vol. 1, Mujumdar, A.S., Ed., Hemisphere Publishing, New York, 1980.)

The water vapor diffuses until it reaches the surface, where it passes to the global air stream. Fick's law applied to a system like the one shown in Figure 17.8 can be expressed as:

$$\frac{\partial Y}{\partial t} = D_{eff}\,\frac{\partial^2 Y}{\partial x^2} \tag{17.23}$$

In this equation, Y is the moisture content of the product, t is the time, x is the dimension in the direction of transfer, and D_{eff} the coefficient of diffusion.

Depending on the type of geometry considered, the solution to Fick's equation takes different forms. The solutions for simple geometry such as slab, cylinder, and sphere are given next.

Slab:

$$\Gamma = \frac{Y - Y_s}{Y_o - Y_s} = \frac{8}{\pi^2}\sum_{n=1}^{\infty}\frac{1}{h_n^2}\,e^{\left(\frac{-h_n^2\,\pi^2 D_{eff}\,t}{4\,L^2}\right)} \tag{17.24a}$$

$$h_n = 2n - 1$$

In this equation, Y is the moisture content at the time t, Y_0 is the initial moisture content, Y_S is the moisture at the surface, and L is the thickness of the slab.

Cylinder:

$$\Gamma = \frac{Y - Y_s}{Y_o - Y_s} = \frac{4}{r_a^2}\sum_{n=1}^{\infty}\frac{1}{\beta_n^2}\,e^{\left(-\beta_n^2\,D_{eff}\,t\right)} \tag{17.24b}$$

Here, r_a is the radius of the cylinder and β_n are the roots of the Bessel function of first type and order zero.

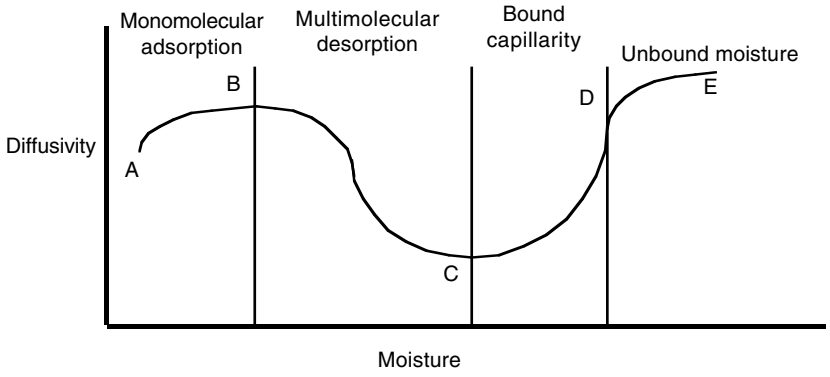

FIGURE 17.9
Relationship between moisture content and diffusivity. (Adapted from Barbosa–Cánovas, G.V. and Vega–Mercado, H., *Dehydration of Foods*, Chapman and Hall, New York, 1996.)

Sphere:

$$\Gamma = \frac{Y - Y_s}{Y_o - Y_s} = \frac{6}{\pi^2} \sum_{n=1}^{\infty} \frac{1}{n^2} e^{\left(\frac{-n^2 D_{eff}^2 t}{r^2} \right)} \tag{17.24c}$$

where r is the radius of the sphere.

The effective diffusion coefficient (D_{eff}) is determined experimentally from drying data; when the term $\ln\Gamma$ is plotted against time, the slope of the linear section gives the value of D_{eff} (Okos et al., 1992).

The relationship between diffusivity and moisture is presented in Figure 17.9. Region *A* to *B* represents the monomolecular adsorption at the surface of the solid and consists of the movement of water by diffusion of the vapor phase. Region *B* to *C* involves the multimolecular desorption, where moisture begins to move in the liquid phase. Microcapillarity plays an important role in region *C* to *D*, where moisture easily emigrates from water-filled pores. In region *D* to *E*, moisture exerts its maximum vapor pressure and the migration of moisture is due essentially to capillarity.

Effective diffusivity values for some food products are given in Table 17.1.

17.5 Chamber and Bed Dryers

The main objective of food dehydration is to lengthen the commercial life of the final product. For this reason, moisture content is reduced to levels so as to limit microbial growth and to retard deteriorating chemical reactions. Hot air is used in most drying processes, a type of operation used since historic times.

TABLE 17. 1

Effective Diffusivity of Some Food Products

Food (m^2/s)	T(°C)	D_{effect}
Whole milk, foam	50	2.0E–9
	40	1.4E–9
	35	8.5E–10
Apples	66	6.40E–9
Freeze-dried apples	25	2.43E–10
Raisins	25	4.17E–11
Potatoes	54	2.58E–11
	60	3.94E–11
	65.5	4.37E–11
	68.8	6.36E–11
Pears (slabs)	66	9.63E–10
Veal, freeze-dried powder	25	3.07E–11
Carrot cubes	40	6.75E–11
	60	12.1E–11
	80	17.9E–11
	100	24.1E–11

Source: Okos et al., in Heldman, D.R. and Lund, D.B., *Handbook of Food Engineering,* Marcel Dekker, New York, 1992.

The basic configuration of an atmospheric dryer is a chamber in which the food is introduced and equipped with a fan and pipes that allow the circulation of hot air through and around the food. Water is eliminated from the surface of the food and driven outside the dryer, with the air stream that leaves it, in a simple operation. Air is heated at the inlet of the dryer by heat exchangers or directly with a mixture of combustion gases. This type of dryer is widely used in the production of cookies, dried fruits, chopped vegetables, and food for domestic animals.

In general, the drying process depends on the heat and mass transfer characteristics of the drying air and food. Two types of phenomena are involved in the drying process in an atmospheric dryer: heating the product and reducing its moisture content, both as a function of time. Figure 17.10 presents moisture and temperature profiles as a function of drying time.

Some types of dryers expose the food to a direct hot air stream that heats the product and eliminates water vapor. However, the nature of some foods does not allow direct exposure to hot air, so heating is carried out by heat exchangers that prevent direct contact between the product and the heating medium. The first type of dryer is called a direct dryer, while the second is called an indirect dryer. In atmospheric drying operations, direct dryers are usually employed.

17.5.1 Components of a Dryer

The basic configuration of a dryer consists of a feeder, heater, and collector. The final arrangement of these components is characteristic of each type of dryer. Figure 17.11 shows a basic scheme of an atmospheric dryer:

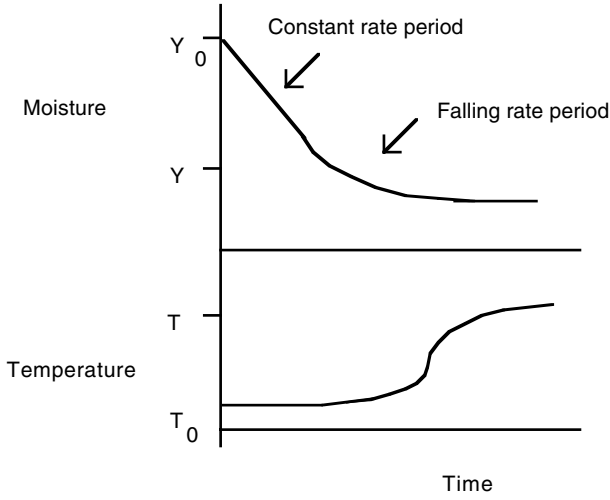

FIGURE 17.10
Moisture and temperature profiles in food dehydration.

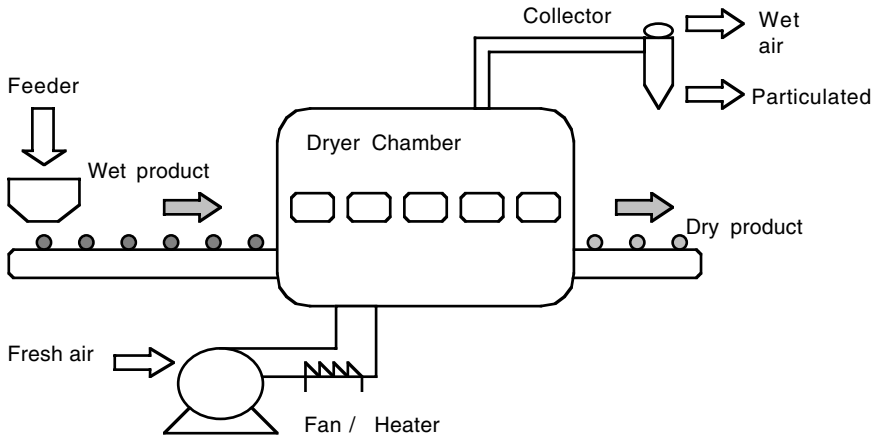

FIGURE 17.11
Basic configuration of an atmospheric dryer. (Adapted from Barbosa–Cánovas, G.V. and Vega–Mercado, H., *Dehydration of Foods,* Chapman and Hall, New York, 1996.)

Feeder: The most common feeders for foods are screw conveyors, rotatory slabs, vibrating trays, and rotatory air chambers. In some cases, special feeders are needed, for example, bed dryers in which it is necessary to ensure a uniform distribution of material.

Heater: In some direct heaters, air is heated by mixing with combustion gases. In indirect heaters, the air and the product are heated in a heat exchanger. The cost of direct heating is lower than that

for indirect heating, but some products can be damaged by gases. The maximum possible temperature of air in a direct heater ranges from 648 to 760°C, while for an indirect heater the maximum temperature is 425°C.

Collector: The separation of products as powder or particulate in the air stream can be achieved by cyclones, bag filters, or wet washers.

17.5.2 Mass and Heat Balances

17.5.2.1 Discontinuous Dryers

The conditions of the air do not remain constant in a drying chamber or tray dryer during a drying process. Heat and mass balances are used to estimate conditions of the air leaving the drier. A heat balance for a tray dryer is like the one shown in Figure 17.12, considering a differential length dL_t and a section of thickness z, which can be expressed as:

$$dq = G\hat{C}_S(z\,b)dT \tag{17.25}$$

In this equation, G is the mass flux of air, b the distance between trays, z the thickness of the trays, q the flux of heat, T the temperature, and $\hat{C}_S$ the specific wet heat of the air–water mixture.

The flux of heat can also be expressed as:

$$dq = h(z\,dL_t)(T - T_W) \tag{17.26}$$

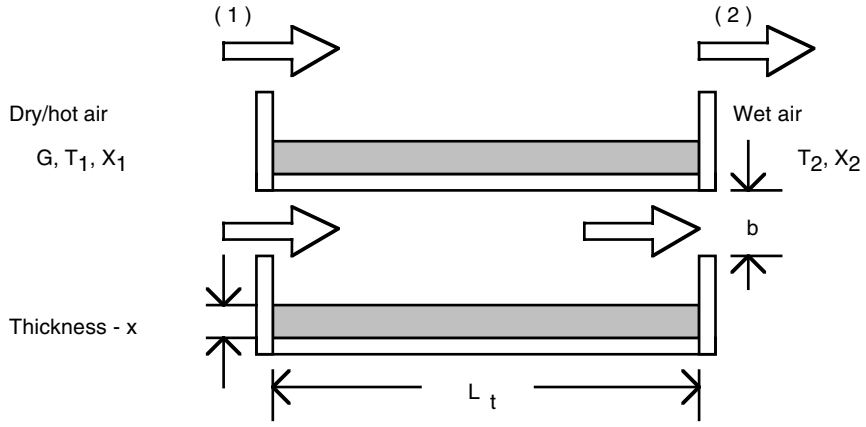

FIGURE 17.12
Tray dryer. (Adapted from Barbosa–Cánovas, G.V. and Vega–Mercado, H., *Dehydration of Foods*, Chapman and Hall, New York, 1996.)

Here, h is the heat transfer coefficient, T_W is the wet bulb temperature, and L_t is the length of the tray. Assuming that h and $\hat{C}_S$ are constants, when combining these two equations, the following can be obtained by integration:

$$\frac{h L_t}{G \hat{C}_s b} = \ln\left(\frac{T_1 - T_W}{T_2 - T_W}\right) \tag{17.27}$$

in which T_1 and T_2 are the temperatures of air at the inlet and outlet of the tray, respectively. The mean logarithmic temperature is defined by:

$$\Delta T_{ml} = \left(T - T_W\right)_{ml} = \frac{\left(T_1 - T_W\right) - \left(T_2 - T_W\right)}{\ln\left(\frac{T_1 - T_W}{T_2 - T_W}\right)} \tag{17.28}$$

Combining Equations 17.27 and 17.28:

$$\left(T - T_W\right)_{ml} = \frac{\left(T_1 - T_W\right)\left(1 - \exp\ \frac{-h L_t}{G \hat{C}_s b}\right)}{\left(\frac{h L_t}{G \hat{C}_s b}\right)} \tag{17.29}$$

The heat flow reaching the product surface from the hot air can be expressed as:

$$\dot{Q} = \frac{Q}{t} = h z L_t \Delta T_{ml} \tag{17.30}$$

This heat is used to evaporate water from the surface of the food. The total heat required to change from an initial moisture content Y_1 to a final moisture corresponding to the critical moisture content Y_C is:

$$Q = \left(z L_t x \rho\right) \lambda_W \left(Y_1 - Y_C\right) \tag{17.31}$$

When equaling the last two equations and taking into account Equation 17.29, it is obtained that the drying time for the constant rate period is given by:

$$t_c = \frac{x \rho_s L_t \lambda_W \left(Y_1 - Y_c\right)}{G \hat{C}_s b \left(T_1 - T_W\right)\left(1 - \exp\left(\frac{-h L_t}{G \hat{C}_s b}\right)\right)} \tag{17.32}$$

In this expression, Y_1 is the initial moisture content of the product, Y_c is the critical moisture content, x is the thickness of the bed, ρ_s is the density of the solid, and λ_W is the latent heat of vaporization at the temperature T_W.

Calculation of the drying time for the falling rate period is determined as explained next. The equation that describes the drying rate in this period is:

$$R = \frac{-w_S}{A}\frac{dY}{dt} \tag{17.33}$$

in which w_S is the amount of solids. This rate can also be expressed according to the equation (Barbosa–Cánovas and Vega–Mercado, 1996):

$$R = \frac{h}{\lambda_W}\left(T - T_W\right)_M \tag{17.34}$$

in which the drying rate is expressed as a function of a mean temperature increment. Combining these equations and assuming that the drying velocity is a linear function of Y, when integrating on the boundary condition $t = 0$, $Y = Y_C$ and $t = t_D$, $Y = Y_F$, the drying time for the falling rate is obtained (Geankoplis, 1983):

$$t_D = \frac{w_S \lambda_W Y_C \ln\left(\dfrac{Y_C}{Y_F}\right)}{Ah\left(T - T_W\right)_M} \tag{17.35}$$

If the mean difference of temperatures is logarithmic, it can be substituted in Equation 17.29 and it is obtained that:

$$t_D = \frac{x\rho_s L_t \lambda_W Y_C \ln\left(\dfrac{Y_C}{Y_F}\right)}{G\hat{C}_s b\left(T_1 - T_W\right)\left(1 - \exp\left(\dfrac{-hL_t}{G\hat{C}_s b}\right)\right)} \tag{17.36}$$

where Y_F represents the final moisture of the product.

The total drying time to change from a moisture content Y_1 to a final moisture content Y_F is obtained by adding the times calculated with Equations 17.32 and 17.36, the total drying time being equal to $t_S = t_C + t_D$.

17.5.2.2 Discontinuous Dryers with Air Circulation through the Bed

Another type of discontinuous dryer is one in which drying air is circulated through a bed of food. Figure 17.13 presents this type of dryer. It is supposed

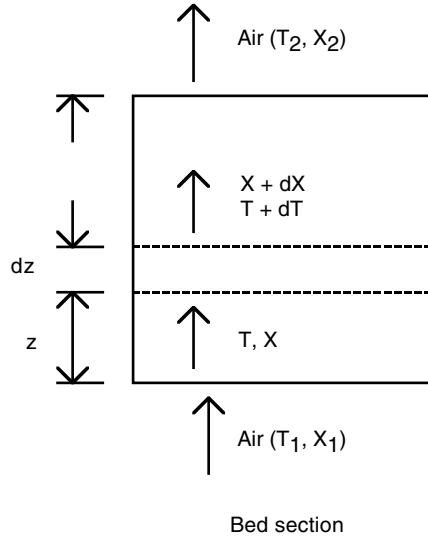

FIGURE 17.13
Drying due to air circulation through the bed. (Adapted from Barbosa–Cánovas, G.V. and Vega–Mercado, H., *Dehydration of Foods,* Chapman and Hall, New York, 1996.)

that the system is adiabatic, that there are no heat losses, and that the air circulates with a mass flux G, entering at a temperature T_1, with a humidity X_1, while at the outlet, air has a temperature T_2 and a humidity X_2.

The global drying velocity can be expressed as:

$$R = G\left(X_2 - X_1\right) \tag{17.37}$$

while, for a bed's height differential dz, the heat flux transmitted by air is:

$$dq = G\hat{C}_S A\,dT \tag{17.38}$$

Here, A is the crossing section. The heat transferred to the solid can be expressed according to the equation:

$$dq = h\,a\,A\left(T - T_W\right)dz \tag{17.39}$$

where a is the specific surface of the bed particles. Such specific surface is determined depending on the type of particle; thus:

Spherical particles:
$$a = \frac{6\left(1-\varepsilon\right)}{D_P} \tag{17.40}$$

Cylindrical particles: $$a = \frac{6(1-\varepsilon)(1+0.5D_C)}{D_C l} \tag{17.41}$$

In these equations, l is the length of the particle, D_c is the diameter of the cylinder, D_p is the diameter of a sphere, and ε is the fraction of holes (porosity) in the solid. Supposing that h and $\hat{C}_S$ are constants, when equaling Equations 17.38 and 17.39 and integrating, it is obtained that:

$$\frac{haz}{G\hat{C}_S b} = \ln\left(\frac{T_2 - T_w}{T_1 - T_w}\right) \tag{17.42}$$

Considering $w_s = A\rho_s/a$, the expressions for drying times are (Geankoplis, 1983; Barbosa–Cánovas and Vega–Mercado, 1996):

Constant rate period:

$$t_C = \frac{\rho_s \lambda_w (Y_1 - Y_c)}{hA(T - T_w)_M} \tag{17.43}$$

or

$$t_C = \frac{\rho_s (Y_1 - Y_c)}{aK_y M_B (X_W - X)} \tag{17.44}$$

in which K_y is the mass transfer coefficient, M_B is the molecular weight, and X_W is the humidity of air at the temperature T_W.

Falling rate period:

$$t_D = \frac{\rho_S \lambda_W Y_C \ln\left(\frac{Y_c}{Y_F}\right)}{ha(T - T_w)_M} \tag{17.45}$$

or

$$t_D = \frac{\rho_S Y_C \ln\left(\frac{Y_c}{Y_F}\right)}{aK_y M_B (X_W - X)} \tag{17.46}$$

The difference of temperatures through the bed can be taken as the logarithmic mean (Equation 17.29) that, when substituted in Equations 17.43 and 17.45, yields:

Constant rate period:

$$t_C = \frac{x\rho_S \lambda_W \left(Y_1 - Y_c\right)}{G\hat{C}_s \left(T_1 - T_W\right)\left(1 - \exp\left(\frac{-hax}{G\hat{C}_S}\right)\right)} \tag{17.47}$$

Falling rate period:

$$t_D = \frac{x\rho_S \lambda_W Y_C \ln\left(\frac{Y_c}{Y_F}\right)}{G\hat{C}_s \left(T_1 - T_W\right)\left(1 - \exp\left(\frac{-hax}{G\hat{C}_S}\right)\right)} \tag{17.48}$$

where x is the thickness of the bed.

The heat transfer coefficient for circulation of drying air can be evaluated by equations (Geankoplis, 1983):

$$h = 0.151\frac{\left(G_t\right)^{0.59}}{\left(D_P\right)^{0.41}} \quad \frac{D_p G_t}{\eta} > 350 \text{ for } IS \tag{17.49}$$

$$h = 0.214\frac{\left(G_t\right)^{0.49}}{\left(D_P\right)^{0.51}} \quad \frac{D_p G_t}{\eta} < 350 \text{ for } IS \tag{17.50}$$

The equivalent diameter (D_P) for a cylindrical particle is:

$$D_P = \left(D_C\, l + 0.5 D_C^2\right)^{1/2} \tag{17.51}$$

17.5.2.3 Continuous Dryers

The equation that allows calculation of drying time for the constant rate period in a dryer in which the solid food and air circulate in countercurrent is (Geankoplis, 1983):

$$t_c = \left(\frac{G}{w_S}\right)\left(\frac{w_S}{A}\right)\frac{1}{K_y M_B}\ln\left(\frac{X_W - X_c}{X_W - X_1}\right) \tag{17.52}$$

in which A/w_S is the surface exposed to drying. This equation can be expressed as:

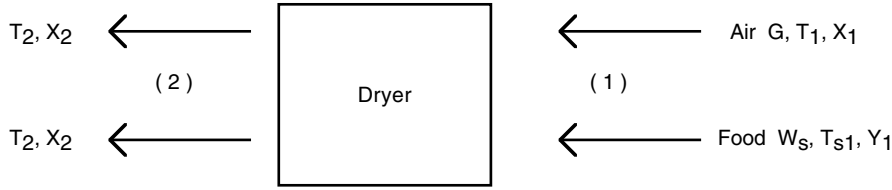

FIGURE 17.14
Drying operation for concurrent flow.

$$t_c = \left(\frac{G}{w_S}\right)\left(\frac{w_S}{A}\right)\frac{1}{K_y M_B}\left(\frac{X_1 - X_C}{\Delta X_{ML}}\right) \tag{17.53}$$

Here, ΔX_{ML} is the logarithmic mean difference of moisture content:

$$\Delta X_{ML} = \frac{(X_1 - X_w) - (X_c - X_w)}{\ln\left(\dfrac{X_w - X_c}{X_w - X_1}\right)} \tag{17.54}$$

in which the critical moisture content is (Geankoplis, 1983):

$$X_C = X_2 + \frac{w_S}{G}\left(Y_c - Y_2\right) \tag{17.55}$$

The drying time for the falling rate period is obtained from the equation:

$$t_D = \left(\frac{G}{w_s}\right)\left(\frac{w_s}{A}\right)\frac{Y_c}{Y_2 + \left(X_w - X_2\right)\left(\dfrac{G}{w_s}\right)K_y M_B}\ \ln\left(\frac{Y_c\left(X_w - X_c\right)}{Y_2\left(X_w - X_1\right)}\right) \tag{17.56}$$

In the case of concurrent flow, as shown in Figure 17.14, hot air comes into contact with the wet food at the inlet, so the mass balance is expressed as:

$$G X_1 + w_S Y_1 = G X_2 + w_S Y_2 \tag{17.57}$$

or

$$G\left(X_2 - X_1\right) = w_S\left(Y_1 - Y_2\right) \tag{17.58}$$

These equations are expressed as follows in terms of critical values:

$$G\left(X_C - X_1\right) = w_S\left(Y_1 - Y_C\right) \tag{17.59}$$

$$X_C = X_1 + \frac{w_s}{G}\left(Y_1 - Y_C\right) \tag{17.60}$$

17.6 Spray Drying

This type of drying is used for foods dissolved in water and includes the formation of droplets that, when later dried, yield dry food particles. Initially, the fluid food is transformed into droplets dried by spraying a mist into a continuous hot air medium. Open cycles are most commonly used in this type of drying, as shown in Figure 17.15. The drying air is heated using a dry medium and, after drying, is cleaned using cyclones before releasing it to the atmosphere. In this type of operation, the air leaving the system can still contain heat.

A second type of arrangement is the use of a closed circuit with a heating medium (air, CO_2, etc.). Air is used in the drying process, then is cleaned,

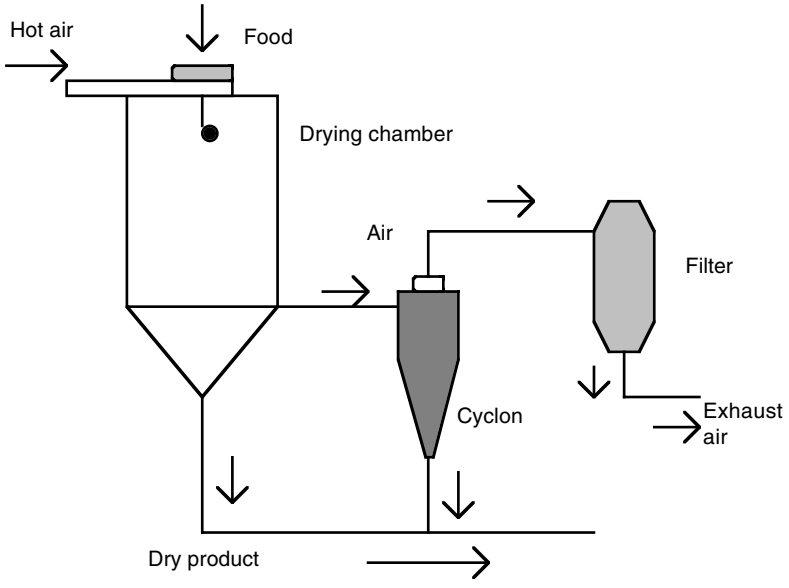

FIGURE 17.15
Open cycle, spray drying under concurrent flow. (Adapted from Barbosa–Cánovas, G.V. and Vega–Mercado, H., *Dehydration of Foods*, Chapman and Hall, New York, 1996.)

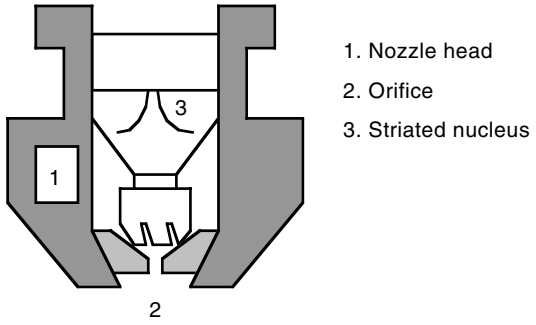

FIGURE 17.16
Striated pressure nozzle. (Adapted from Masters, K., *Spray Drying Handbook,* 5th ed., Longman Group Limited, U.K., 1991.)

dried, and used again in a continuous process. The efficiency of this type of drying is higher than for open systems. In a closed circuit system, the dry product is the only one leaving the system, while in open circuits, hot air is also released to the exterior and may contain microparticles.

This type of drying includes atomization of food into drying media in which moisture is eliminated by evaporation. Drying is performed until the moisture content fixed for the product is reached. This type of drying is controlled by the flow and temperature conditions of the product as well as of the air at the inlet. Spray drying was used for the first time around 1900 for dry milk and was later applied to eggs and coffee.

The most important characteristic of spray drying is the formation of droplets and their contact with air. Breaking the food stream into droplets produces the atomization of food. Different types of atomizers will be explained next. (Barbosa–Cánovas and Vega–Mercado, 1996).

17.6.1 Pressure Nozzles

Pressure nozzles are used to form droplets, since it is possible to control the food flow and the atomization characteristics by varying the pressure. The mean size of the droplets formed is proportional to the food flow and its viscosity. Figure 17.16 shows one type of pressure nozzle.

The fundamental principle of this type of nozzle is the conversion of pressure energy into kinetic energy. The liquid layers are broken under the influence of the physical properties of the liquid and by the friction effects with air. The power required by a pressure nozzle is proportional to the feed rate and pressure of the nozzle (Barbosa–Cánovas and Vega–Mercado, 1996):

$$P_k = 0.27 \frac{\Delta P}{\rho} \tag{17.61}$$

where ΔP is the total pressure drop and ρ is the density of food. The conversion of pressure into kinetic energy in a centrifugal pressure nozzle results in a rotatory movement of the liquid that can be expressed as (Marshall, 1954):

$$E_h = 19.2\ w\ \Delta P \tag{17.62}$$

where w is the mass flow rate and E_h is the energy or power. The flow of liquid in the orifice of a centrifugal pressure nozzle can be expressed as:

$$2\left(\pi\, r_1^2\, V_{inlet}\right) = 2\left(\pi\, b\, r_2\, U_r\right) \tag{17.63}$$

$$V_{inlet} = \frac{w_1}{2\pi r_1^2 \rho} \tag{17.64}$$

or

$$\frac{U_r}{V_{inlet}} = \frac{r_1^2}{r_2\, b} \tag{17.65}$$

In these equations, b is the thickness of the liquid film in the orifice, r_1 is the radius of the inlet channel, r_2 is the radius of the orifice, V_{inlet} is the velocity of the liquid at the inlet, U_r is the vertical component of the atomization velocity, and w_1 is the mass flow rate of the liquid.

The velocity of the liquid leaving the nozzle is expressed as:

$$V_{outlet} = \sqrt{U_h^2 + U_v^2} \tag{17.66}$$

When expressed in terms of pressure drop through the nozzle:

$$V_{outlet} = C_v\left(2\,g\,h\right)^n = C_v\left(2\,g\frac{P}{\rho}\right)^n \tag{17.67}$$

Here, U_h and U_v are the horizontal and vertical components of velocity, $n = 0.5$, for turbulent flow, C_v is a velocity coefficient, g is the gravitational constant, n is a constant, and h is the head pressure. The performance of a pressure nozzle is affected by pressure and the density and viscosity of the liquid. Masters (1991) proposed a correlation between flow changes through the injector and the pressure and density changes according to the expression:

$$\frac{w_2}{w_1} = \left(\frac{P_2}{P_1}\right)^{0.5} = \left(\frac{\rho_1}{\rho_2}\right)^{0.5} \tag{17.68}$$

TABLE 17.2

Effect of Some Process Variables on Droplet Size

Variable	Effect
Nozzle capacity	
Feed rate below the designed rate	Incomplete atomization
Feed rate below minimum	Size of droplets decreases
Specified feed rate	Size of droplets increases
Big spraying angle	Small droplets
Pressure increase	Size of droplets decreases
Viscosity	
Increase	Thick atomization
Very high	Impossible operation
High surface tension	Makes atomization difficult
Orifice size	Droplet size = $k\,D^2$ D = orifice diameter k = constant

Source: Barbosa–Cánovas, G.V. and Vega–Mercado, H., *Dehydration of Foods,* Chapman and Hall, New York, 1996.

The effect of viscosity on the flow is not clearly defined, although it can be determined in an experimental form. The effect of process variables such as capacity of the nozzle, atomization angle, pressure, viscosity, surface tension, and diameter of the orifice on the droplet size are given in Table 17.2.

Industrial dryers containing multinozzles are installed to permit high feeding velocities and to provide equal conditions in each nozzle for a better uniformity of atomization. The configurations of the nozzles should present the following conditions: easy access to remove the nozzles, uniform distribution, possibility of isolation, and visibility of each nozzle. Some of the possible configurations are shown in Figure 17.17.

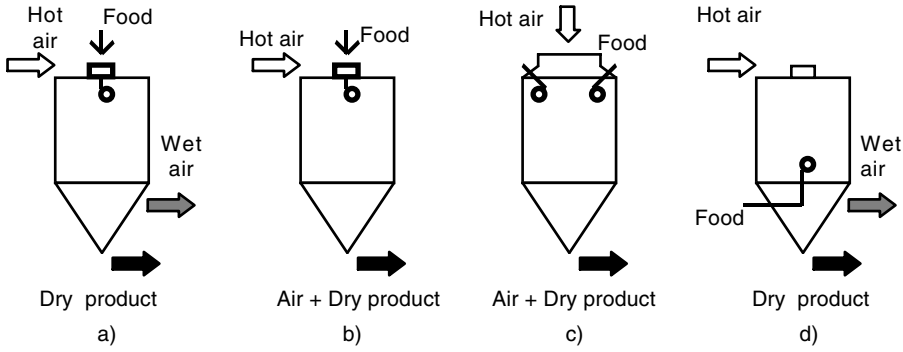

FIGURE 17.17
Configuration of pressure nozzles in industrial dryers. (Adapted from Barbosa–Cánovas, G.V. and Vega–Mercado, H., *Dehydration of Foods,* Chapman and Hall, New York, 1996.)

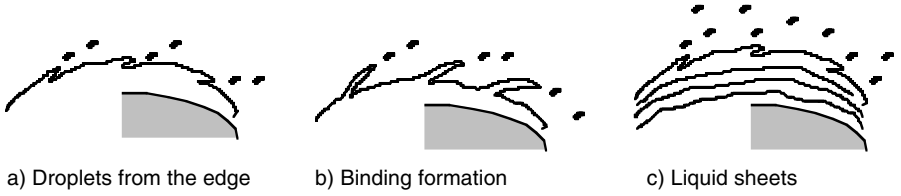

FIGURE 17.18
Atomization with disks without blades. (Adapted from Barbosa–Cánovas, G.F. and Vega–Mercado, H., *Dehydration of Foods,* Chapman and Hall, New York, 1996.)

17.6.2 Rotary Atomizers

Rotary atomizers differ from pressure nozzles because liquid achieves velocity without high pressure. Also, the feed rate can be controlled with disks while, in the case of nozzles, the pressure drop as well as the diameter of the orifice change simultaneously. Figure 17.18 shows the physical behavior of the food for the atomization mechanism in the case of disks. The formation and release of droplets from the edge of the disk, taking into account a low velocity of feed and disk, are shown in Figure 17.18a. Atomization consists of one droplet and two satellites. An increase in the velocity of the disk and the food produces a change in the mechanism of formation of droplets (Figure 17.18b). The arrangement of the liquid in layers (Figure 17.18c) appears when the bindings of the liquid join each other and extend beyond the edge of the disk.

In disks with blades (Figure 17.19a), the disintegration of the liquid takes place on the edge of the disk due to the friction effect between the air and the surface of the liquid. The liquid emerges as a thin film from the blade. The optimum size of a droplet for a given feed depends on rotation without

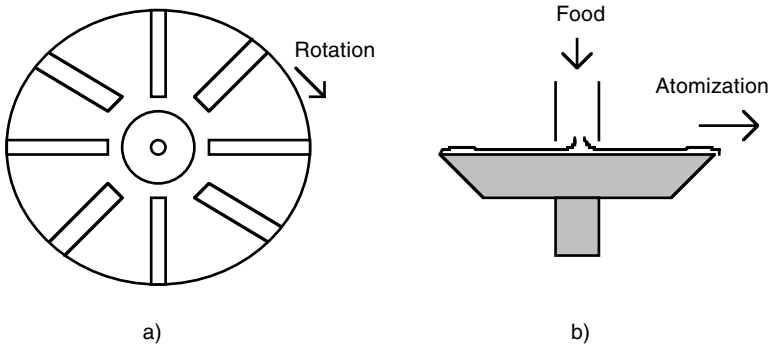

FIGURE 17.19
Rotary atomizers: (a) disk with blades; (b) plane disk with sharp edge. (Adapted from Barbosa–Cánovas, G.V. and Vega–Mercado, H., *Dehydration of Foods,* Chapman and Hall, New York, 1996.)

vibration, centrifugal force, soft and complete wetting of the blade's surface, and a uniform distribution and feed.

The acceleration along the blade stops when the liquid reaches the edge of the disk, so the velocity of the liquid can be expressed as (Barbosa–Cánovas and Vega–Mercado, 1996):

$$U_r = 0.0024\left(\frac{\rho\pi^2 N^2 D w^2}{\eta h^2 n^2}\right)^{0.33} \tag{17.69}$$

$$U_t = \pi D N \tag{17.70}$$

$$U_{res} = \sqrt{U_r^2 + U_t^2} \tag{17.71}$$

$$\alpha = \tan^{-1}\left(\mathrm{Ur}/\mathrm{Ut}\right) \tag{17.72}$$

In these equations, U_r is the radial component of velocity, U_r is the tangential component, U_{res} is the result of stopping velocity, α is the angle of the released liquid, D is the diameter of the disk, N is the rotation velocity of the atomizer, n is the number of blades, h is the height of blades, and η is the viscosity. The effect of process variables such as disk speed, feed rate, liquid viscosity, surface tension, and density of the liquid on the size of the droplet for a rotary atomizer is given in Table 17.3.

The distribution size of atomization in a rotary atomizer can be expressed as:

$$D_{mean} = \frac{K w^a}{N^b d^{0.6}\left(n h\right)^d} \tag{17.73}$$

in which the values of K, a, b, and d are a function of the disk speed and the load rate of the blade. Table 17.4 presents the values of these constants.

Rotary atomizers are generally installed in the center of the roof in spray dryers to let enough contact time between the droplet and the hot air pass and to allow evaporation of the liquid (Shaw, 1994).

The relationship between the size of the wet droplet and the size of the dry particle is expressed according to the equation:

$$D_{WET} = \beta D_{DRY} \tag{17.74}$$

in which D_{WET} is the size of the droplet during atomization, D_{DRY} is the size of the dry particle, and β is the change of shape factor. This last factor is a function of the type of product and temperature and it is useful to change the scale of a dryer (Masters, 1991).

TABLE 17.3

Effect of Process Variables on the Size of Droplets for a Rotary Atomizer

VARIABLE	Effect	
Disk speed Constant feed	$\frac{D_1}{D_2} = \left[\frac{N_2}{N_1}\right]^p$	D = diameter of the disk N = disk speed, rpm p = 0.55–0.80
Feed rate Constant disk speed	$\frac{D_1}{D_2} = \left[\frac{q_1}{q_2}\right]^s$	q = feed rate s = 0.1–0.12
Viscosity of the liquid	$\frac{D_1}{D_2} = \left[\frac{\eta_1}{\eta_2}\right]^r$	η = viscosity r = 0.2
Surface tension	$\frac{D_1^2}{D_2} = \left[\frac{\sigma_1}{\sigma_2}\right]^s$	σ = surface tension s = 0.1–0.5
Density of the liquid	$\frac{D_1}{D_2} = \left[\frac{\rho_2}{\rho_1}\right]^t$	ρ = density t = 0.5

Source: Barbosa–Cánovas, G.V. and Vega–Mercado, H., *Dehydration of Foods,* Chapman and Hall, New York, 1996.

TABLE 17.4

Values of Constants of Equation 17.73

Disk speed (m/s)	Load Rate of the Blade (kg/h m)	*a*	*b*	*d*	$K*10^4$
Normal 85–115	Low 250	0.24	0.82	0.24	1.4
Normal to high 85–180	Normal 250–1500	0.2	0.8	0.2	1.6
Very high 180–300	Normal to high 1000–3000	0.12	0.77	0.12	1.25
Normal to high 85–140	Very high 3000–60,000	0.12	0.8	0.12	1.2

Source: Masters, K., *Spray Drying Handbook,* 5th ed., Longman Group Limited, U.K., 1991.

17.6.3 Two-Fluid Pneumatic Atomizers

The atomization of a liquid using a gas at high velocity is known as pneumatic atomization. The mechanism involves high velocity of a gas that allows creation of high friction forces, causing the liquid to break into droplets. The formation of droplets takes place in two stages: first the liquid is broken into

filaments and long drops, and then the filaments and large drops are broken into droplets. Formation of droplets is affected by the properties of the liquid (surface tension, density, and viscosity), as well as by those of the gas flow (velocity and density).

Air and vapor are the primary gas media used in pneumatic atomization. In the case of closed systems, inert gases are usually employed. In order to achieve optimum friction conditions, high velocities between air and liquid are required. Such conditions are obtained by expansion of the gas phase at sonic and ultrasonic velocities, before contact with the liquid or by direct gas flow on a thin film of liquid in the nozzle. Pneumatic nozzles include an internal mixing and an internal and external combined mixing. The power requirement for an isoentropic expansion is expressed as:

$$P = 0.402\, w_A\, T \left\{ 0.5\, M_a^2 + 2.5 \left[1 - \left(\frac{P_1}{P_2} \right)^{0.286} \right] \right\} \tag{17.75}$$

In this equation, w_A is the mass flow rate of air, T is the absolute temperature, M_a is the module of Mach, and P_1 and P_2 are the initial and final pressures, respectively. The mean atomization size obtained in a pneumatic atomizer can be expressed as:

$$D = \frac{A}{\left(V^2\, \rho_a \right)^{\alpha}} + B \left(\frac{w_{air}}{w_{liq}} \right)^{-\beta} \tag{17.76}$$

where V is the relative velocity between air and liquid, α and β are a function of the nozzle, A and B are constants, w_{air} is the mass flow rate of air, and w_{liq} is the mass flow rate of liquid. Table 17.5 shows the effects of the process variables on droplets for pneumatic atomizers.

TABLE 17.5

Effect of Process Variables on Droplets for Pneumatic Atomizers

Variable	Effect
Mass ratio air/liquid	
Rate increase	Decrease of droplet size
$w_{air}/w_{liq} < 0.1$	Deteriorating atomization
$w_{air}/w_{liq} \geq 10$	Upper limit for effective rate
	Increase to create particles of smaller size
Relative rate	
Increase of air rate	Decrease of droplet size
Viscosity	
Increase of fluid viscosity	Increase of droplet size
Increase of air viscosity	Decrease of droplet size

Source: Masters, K., *Spray Drying Handbook,* 5th ed., Longman Group, U.K., 1991.

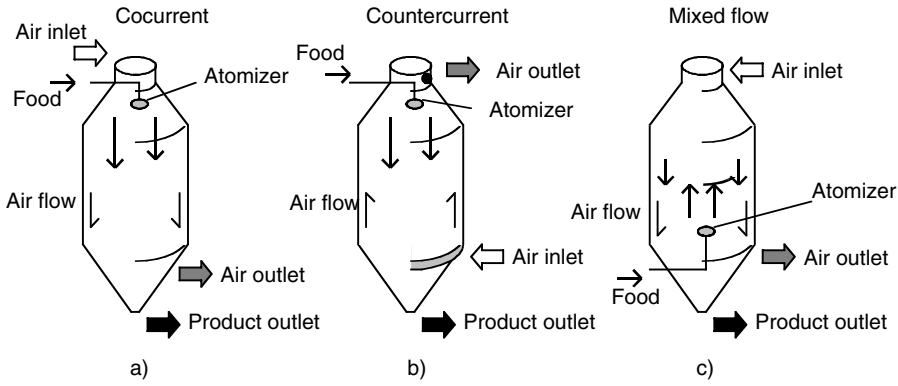

FIGURE 17.20
Classification of dryers according to atomization movement. (Adapted from Barbosa–Cánovas, G.V. and Vega–Mercado, H., *Dehydration of Foods*, Chapman and Hall, New York, 1996.)

17.6.4 Interaction between Droplets and Drying Air

The distance traveled by a drop until it is completely affected by air depends on its size, shape, and density. Since the common atomizers are independent of air flow while in fine atomizers, such flow should be taken into account (Barbosa–Cánovas and Vega–Mercado, 1996). Atomization movement can be classified according to dryer design as cocurrent, countercurrent, or mixed flow (Figure 17.20).

The atomization movement can be explained for a simple droplet. The forces that act on a droplet are:

$$\frac{\pi}{6} D^3 \rho_w \frac{dV}{dt} = \frac{\pi}{6} D^3 \left(\rho_w - \rho_a\right) g - 0.5 C_d \rho_a V_r^2 A \tag{17.77}$$

in which D is the diameter of the droplet, C_d is the dragging coefficient, V_r is the relative velocity of the droplet with respect to the air, A is the area of the droplet, ρ_W is the density of the droplet, and ρ_a is the density of air. Masters (1991) discussed the atomization movement under different flow conditions. The temperature profile inside the dryer is an important aspect and is a function of the type of flow (Masters, 1991; Barbosa–Cánovas and Vega–Mercado, 1996).

17.6.5 Heat and Mass Balances

In food drying by atomization, the liquid that should be removed is, in most cases, water, although the removal of organic solvents in closed cycle operations is also common. If a system like the one shown in Figure 17.21 is considered, the heat and mass balances yield the following equations.

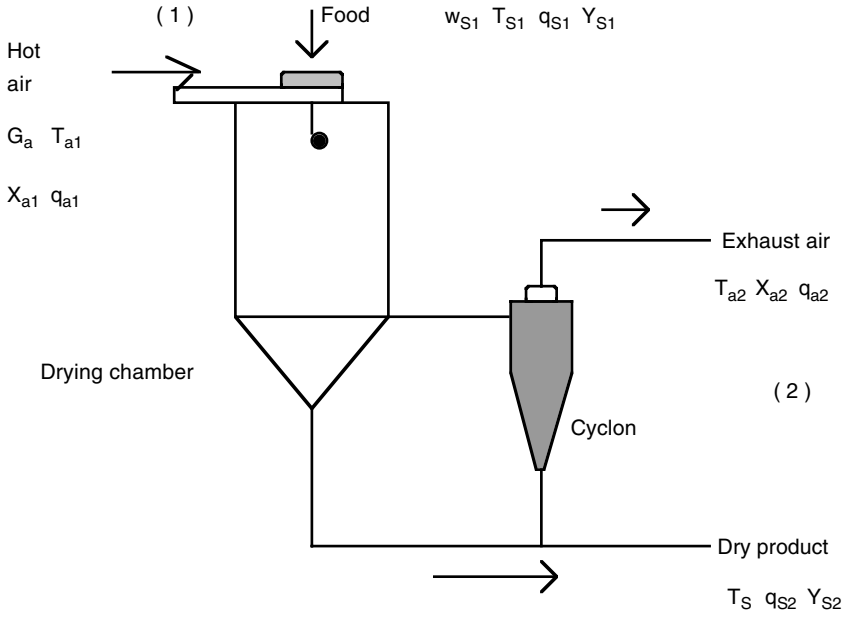

FIGURE 17.21
Data of a dryer for heat and mass balances (w_s, dry solids rate; T_s, solids temperature; q_s, solids enthalpy; Y_s, solids moisture content; G_a, dry air flow rate; T_a, air temperature; X_a, air moisture content; q_a, enthalpy).

A mass balance applied to the whole system yields:

$$w_S\left(Y_{S1} - Y_{S2}\right) = G_a\left(X_{a2} - X_{a1}\right) \tag{17.78}$$

in which w_S is the mass flow rate of dry solids, Y_{S1} is the moisture content of the solid that enter to the dryer, Y_{S2} is the moisture content of the solid leaving the dryer, G_a is the mass flow rate of dry air, X_{a1} is the humidity of the air entering the dryer, and X_{a2} is the humidity of the air leaving the dryer.

A balance of enthalpies yields the equation:

$$w_S\, q_{S1} + G_a\, q_{a1} = w_S\, q_{S2} + G_a\, q_{a2} + q_L \tag{17.79}$$

In this equation, q_{S1} and q_{S2} are enthalpies of the solids at the inlet and outlet, respectively, while q_{a1} and q_{a2} are the enthalpies of air at the inlet and outlet of the dryer, and q_L represents the heat losses.

The performance of a spray dryer is measured in terms of thermal efficiency, which is related to the heat input required to produce a unit weight of dry product with the desired specifications. Global thermal efficiency (ϕ_{global}) is defined as the fraction of total heat supplied to that used in the dryer during the evaporation process:

$$\phi_{\text{global}} = 100\frac{(T_1 - T_2)}{(T_1 - T_0)} \tag{17.80}$$

where T_1 is the temperature of the hot air at the inlet, T_2 is the temperature corresponding to the outlet, and T_0 is the temperature of the atmospheric air. The evaporation efficiency ($\phi_{\text{evaporation}}$) is defined as the rate of actual evaporation capacity to the capacity obtained in an ideal case of air exhausting at the saturation temperature:

$$\phi_{\text{evaporation}} = 100\frac{(T_1 - T_2)}{(T_1 - T_{sat})} \tag{17.81}$$

17.7 Freeze Drying

Freeze drying was developed to overcome the loss in conventional drying operations of compounds responsible for aroma in foods (Barbosa–Cánovas and Vega–Mercado, 1996). The freeze drying process consists mainly of two stages: (1) the product is frozen, and (2) the product is dried by direct sublimation of ice under reduced pressure. This type of drying was initially introduced on a large scale in the 1940s to produce dry plasma and blood products. After that, antibiotics and biological materials were prepared on an industrial scale by freeze drying. Figure 17.22 shows the basic sketch of a freeze drying system.

Freeze drying has been shown to be an effective method for extending the mean life of foods; it consists of two important characteristics:

1. Absence of air during processing, which, together with low temperature, prevents deterioration due to oxidation or modifications of the product
2. Drying at a temperature lower than room temperature, which allows products that decompose or experience changes in their structure, texture, appearance, or aroma as a consequence of high temperatures to be dried under vacuum with minimum damage

Freeze-dried products that have been adequately packaged can be stored for unlimited time, maintaining most of the physical, chemical, biological, and sensorial properties of the fresh product. Quality losses due to enzymatic and nonenzymatic browning reactions are also reduced; however, the oxidation of lipids, caused by low moisture levels achieved during drying, is higher in freeze dried products. Packing the products in packages impermeable to oxygen can control this lipid oxidation. Nonenzymatic browning occurs

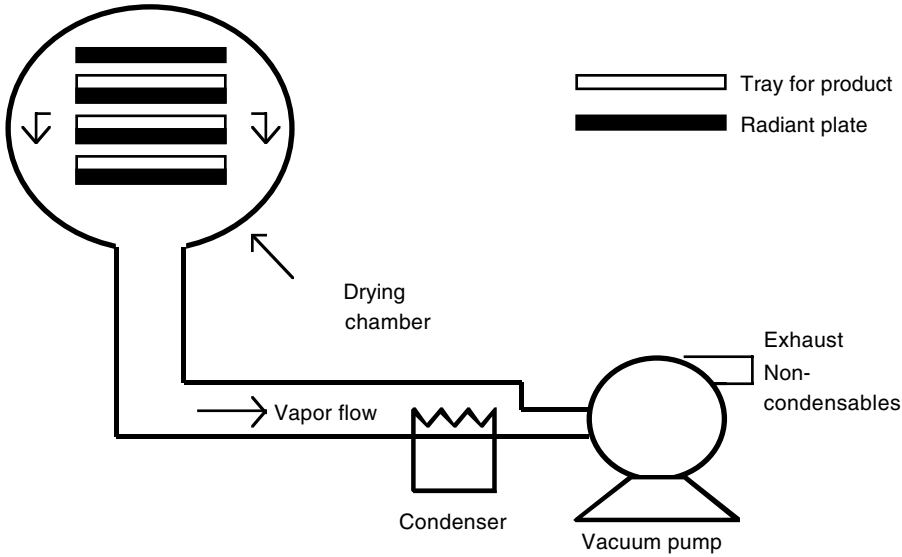

FIGURE 17.22
Freeze drying basic system. (Adapted from Barbosa–Cánovas, G.F. and Vega–Mercado, H., *Dehydration of Foods*, Chapman and Hall, New York, 1996.)

slightly during drying, since the reduction of the moisture content of the product during the process is almost instantaneous. The use of low temperatures also reduces the denaturalization of proteins in this type of drying (Okos et al., 1992).

Freeze-dried products can recover their original shape and structure by adding water because the spongy structure of these products allows their rapid rehydration. The characteristics of the rehydrated product are similar to those of a fresh product. The porosity of freeze-dried products allows a more complete and rapid rehydration than in air-dried foods. However, one of the greatest disadvantages of freeze drying is the energy cost and long drying time period. Coffee and tea extracts, vegetables, fruits, meats, and fish are obtained by freeze drying. These products have 10 to 15% of their original weight and do not require refrigeration. Products with moisture content lower than 2% can also be obtained.

As indicated previously, the freeze drying process consists of two stages: freezing and drying. Freezing must be very quick, with the objective of obtaining a product with small ice crystals and in an amorphous state. The drying stage is performed at low pressures in order to sublime the ice. Figure 17.23 presents a diagram of water phases of freeze drying, while Figure 17.24 presents the drying stages.

Three important design variables should be considered for freeze drying: (1) vacuum inside the drying chamber; (2) radiant energy flow applied to the food; and (3) the temperature of the condenser. The initial drying rate is high, since the resistance to mass and energy flow is low. However, a thin

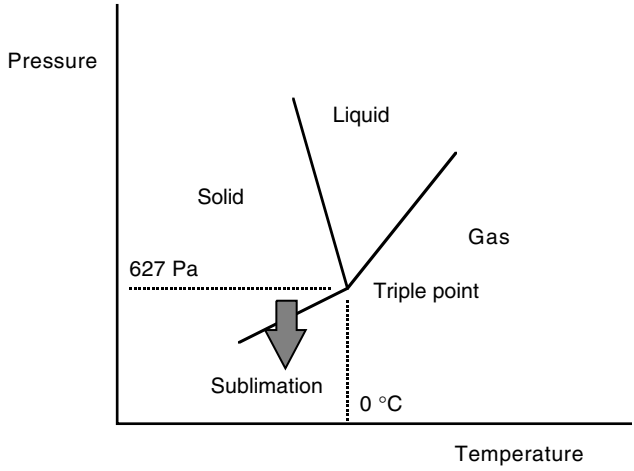

FIGURE 17.23
Diagram of water phases. (Adapted from Barbosa–Cánovas, G.V. and Vega–Mercado, H., *Dehydration of Foods,* Chapman and Hall, New York, 1996.)

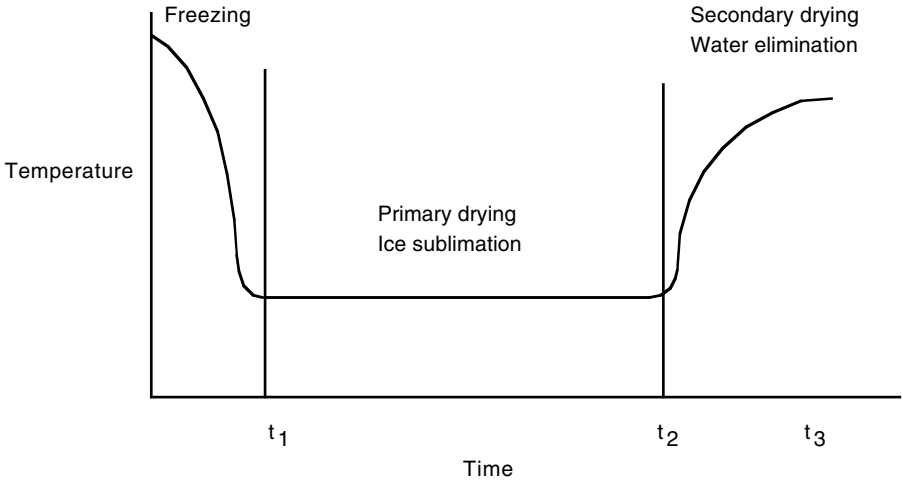

FIGURE 17.24
Freeze drying stages. (Adapted from Barbosa–Cánovas, G.V. and Vega–Mercado, H., *Dehydration of Foods,* Chapman and Hall, New York, 1996.)

layer around the frozen product accumulates and causes the drying rate to decrease as it progresses. This layer acts as an insulator and affects the heat transfer towards the ice front. Also, the mass transfer from the ice front decreases as the thickness of the dry layer increases, due to the reduction of diffusion from the sublimation interface towards the surface of the product.

17.7.1 Freezing Stage

The freezing temperature and time of food products is a function of the solutes in solution that it contains. The freezing temperature for pure water remains constant at the freezing point until water is frozen. The freezing temperature of foods is lower than for pure water, since the solutes concentrate in the nonfrozen water fraction and the freezing temperature continuously decreases until the solution is frozen. The whole mass of the product becomes rigid at the end of the freezing process, forming a eutectic that consists of ice crystals and food components. It is necessary to reach the eutectic state to ensure the removal of water by sublimation only — not because of a combination of sublimation and evaporation.

The permeability of the frozen surface can be affected by the migration of soluble components during the freezing stage. However, removal of the thin layer on the surface of the frozen product, or freezing under conditions that inhibit the separation of the concentrated phase, gives place to better drying rates (Barbosa–Cánovas and Vega–Mercado, 1996).

17.7.2 Primary and Secondary Drying Stages

Two stages can be distinguished during the freeze drying process. The first stage involves ice sublimation under vacuum: ice sublimates when energy corresponding to the latent heat of sublimation is supplied. The vapor generated in the sublimation interface is eliminated through the pores of the product due to low pressure in the drying chamber; the condenser prevents the vapor from returning to the product. The driving force of sublimation is the pressure difference between the water vapor pressure in the ice interface and the partial water vapor pressure in the drying chamber. The energy required to sublimate ice is supplied by radiation or conduction through the frozen product, or by irradiation of water molecules using microwaves.

The second drying stage begins when the ice in the product has been removed and moisture comes from water partially bound to the material being dried. The heating rate should decrease at this moment in order to keep the temperature of the product under 30 to 50°C, which will prevent the material from collapsing. If the solid part of the material is too hot, the structure collapses, resulting in a decrease of the ice sublimation rate in the product (Barbosa–Cánovas and Vega–Mercado, 1996).

17.7.3 Simultaneous Heat and Mass Transfer

The mass and heat transfer phenomena during freeze drying can be summarized in terms of diffusion of vapor from the sublimation front and heat radiation and conduction from the radiation slab. A steady state model will be supposed in the development of this section in order to facilitate calculations.

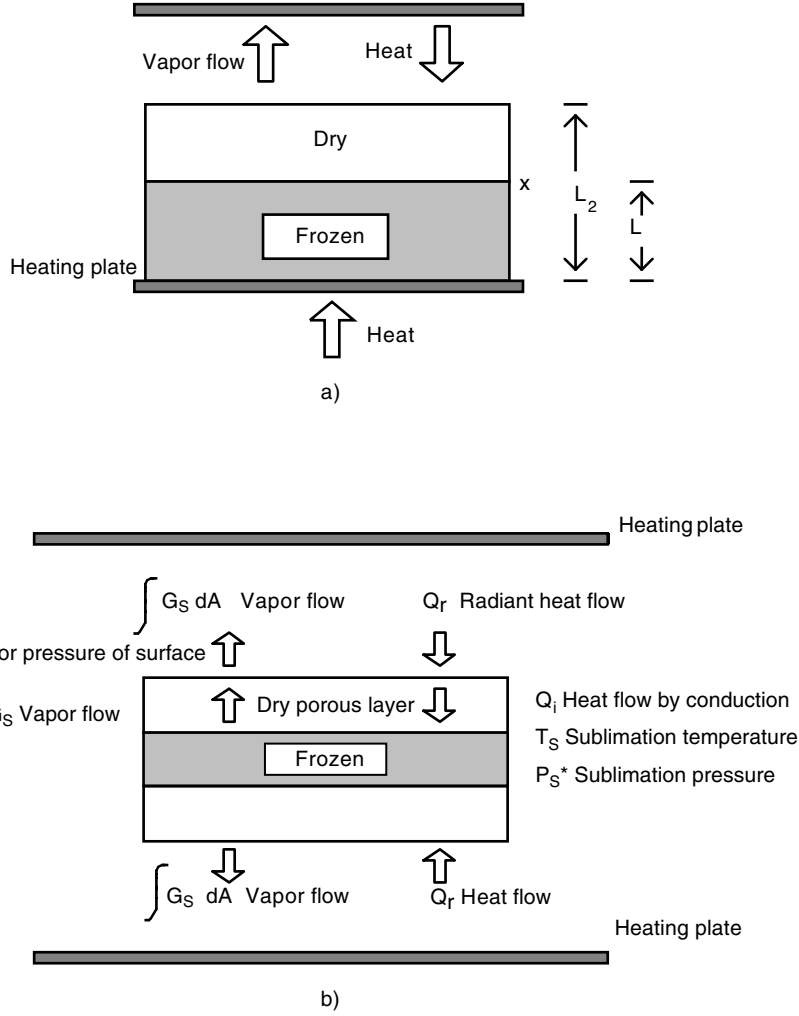

FIGURE 17.25
Heat and mass flows during freeze drying: (a) drying by one side; (b) symmetric arrangement (drying by both sides). (Adapted from Barbosa–Cánovas, G.V. and Vega–Mercado, H., *Dehydration of Foods*, Chapman and Hall, New York, 1996.)

The energy required to maintain sublimation is assumed to be equal to the radiant or conductive flow due to the temperature gradient between the frozen product and the heat source in the drying chamber. Water sublimates below the triple point under pressures of 627 Pa or less. The sublimation interface is located above the ice front, and the elimination of water takes place close to or at the sublimation interface. Figure 17.25 shows the heat and mass flows during drying of frozen slabs.

TABLE 17.6

Thermal Conductivity and Sublimation Temperature of Freeze Dried Products

Product	k (W/m K)	Product	T_{sub} (°C)
Coffee extract (25%)	0.033	Coffee	–23
Gelatin	0.016	Shrimp	–18
Milk	0.022	Whole egg	–17
Apple	0.016–0.035	Apple	–7
Peach	0.016	Chicken	–21
Turkey	0.014	Salmon	–29
Mushrooms	0.010	Veal	–14
Veal	0.035–0.038	Carrot	–25

Source: Schwartzberg, H., Freeze Drying — Lecture Notes, Food Engineering Dept., Univ. of Massachusetts, Amherst, 1982.

The heat flow due to convection or conduction at the sublimation surface, for Figure 17.25a, can be expressed as (Barbosa–Cánovas and Vega–Mercado, 1996):

$$q = h\left(T_e - T_s\right) = k\,\frac{\left(T_s - T_f\right)}{\left(L_2 - L_1\right)} \tag{17.82}$$

In this equation, q is the heat flux, h is the external coefficient of heat transfer by convection, T_e is the external temperature of vaporization of the gas, T_S is the temperature of the surface of the dry solid, T_f is the sublimation temperature of the ice front, k is the thermal conductivity of the dry solid, and $(L_2 - L_1)$ is the thickness of the dry layer. Thermal conductivity and sublimation temperature values for some freeze-dried products are given in Table 17.6.

The flux of vapor from the sublimation front is given by Okos et al. (1992):

$$N_a = \frac{D'\left(P_{fw} - P_{sw}\right)}{RT\left(L_2 - L_1\right)} = K_g\left(P_{sw} - P_{ew}\right) \tag{17.83}$$

in which N_a is the flux of vapor, D' is the mean effective diffusivity of vapor into the dry layer, R is the gas constant, T is the mean temperature of the dry layer, P_{fw} is the partial vapor pressure in equilibrium with the ice sublimation front, P_{SW} is the partial vapor pressure at the surface, P_{ew} is the partial vapor pressure within the external gas phase, and K_g is the external mass transfer coefficient.

Equations 17.82 and 17.83 can be combined, expressing q and N_a in terms of the external operation conditions (Barbosa–Cánovas and Vega–Mercado, 1996):

$$q = \frac{T_e - T_f}{\left(\frac{1}{h} + \frac{\left(L_2 - L_1\right)}{k}\right)} \tag{17.84}$$

and

$$N_a = \frac{\left(P_{fw} - P_{ew}\right)}{\left(\frac{1}{K_g} + \frac{RT\left(L_2 - L_1\right)}{D'}\right)} \tag{17.85}$$

The constants h and K_g depend on the velocity of the gas and the dryer, while k and D' depend on the nature of the dry material. T_e and P_{ew} are given by the operation conditions. These last two equations can be related through the latent heat of sublimation (ΔH_S) as:

$$q = \Delta H_S N_a \tag{17.86}$$

Combination of Equations 17.82, 17.85, and 17.86 yields:

$$\frac{k\left(T_s - T_f\right)}{\left(L_2 - L_1\right)} = \frac{\Delta H_s \left(P_{fw} - P_{ew}\right)}{\left(\frac{1}{K_g} + \frac{RT\left(L_2 - L_1\right)}{D'}\right)} \tag{17.87}$$

or

$$h\left(T_e - T_s\right) = \frac{\Delta H_s \left(P_{fw} - P_{ew}\right)}{\left(\frac{1}{K_g} + \frac{RT\left(L_2 - L_1\right)}{D'}\right)} \tag{17.88}$$

An increase of T_e or T_s causes an increase in the drying rate, as can be observed from Equations 17.87 and 17.88. The temperature T_S is limited by the sensitivity to heat of the material; T_f should be lower than the collapse temperature of the material. Sensibility is defined in terms of the degradation reactions, while the collapse temperature is defined in terms of deformation of the porous structure of the dry layer.

The drying rate can be expressed as:

$$N_a = \left(\frac{L}{2M_a V_s}\right)\frac{-dx}{dt} \tag{17.89}$$

in which L is the total thickness of the product, x is the thickness of the dry layer, t is the time, M_a is the molecular weight of water, and V_S is the volume of occupied solid per unit of water mass (per kg of water), expressed as $V_S = 1/(Y_0\,\rho_S)$, where Y_0 is the initial moisture content and ρ_S is the density of the dry solid. An analogous deduction was considered by Schwartzberg (1982) to describe the freeze drying process, in which he considered the mass and heat transfer through both faces of the product (Figure 17.25b). The vapor flow in the system can be expressed as:

$$G_s = \frac{K_P\left(P_s^* - P_o\right)}{x} \tag{17.90}$$

$$= \frac{K_p\left(P_s^* - P_c^*\right)}{x} \tag{17.91}$$

$$= \rho\frac{\left(Y_o - Y_f\right)}{\left(1+Y_o\right)}\frac{dx}{dt} \tag{17.92}$$

In this equation, P_S^* is the vapor pressure in the sublimation interface, P_0 is the partial water pressure at the surface, P_C^* is the pressure in the condenser that should be equal to P_0, unless the non-condensable are introduced in the dryer, K_P is the permeability of the dry layer, ρ is the density of the frozen layer of the slab, Y_0 is the moisture content of the food (mass of water or mass of dry solid), Y_f is the initial moisture content, x is the thickness of the dry layer, and t is the drying time. The first part of Equation 17.92 represents the change in water content per unit of volume of frozen product. The change of thickness of the dry layer is a function of time, keeping constant the surface area. Table 17.7 presents values of permeability for some freeze-dried foods.

The drying time is obtained by integration of Equation 17.92, yielding:

$$t_S = \rho\frac{\left(Y_o - Y_f\right)}{2K_p\left(1+Y_o\right)}\frac{a^2}{\left(P_s^* - P_o\right)} \tag{17.93}$$

where a is the thickness of half of the slab.

TABLE 17.7

Permeability of Freeze-Dried Foods

Product	Permeability (10^{-9} kg/m s μmHg)
Coffee (20% solids)	4.0–8.6
Coffee (30% solids)	3.0
Whole milk	2.7–5.3
Apple	3.3–6.0
Potato	1.3
Fish	8.7
Banana	1.1
Veal	0.7–4.4
Tomato (22°Brix)	2.1
Carrot	2.0–5.6

Source: Schwartzberg, K., Freeze Drying — Lecture Notes. Food Engineering Dept., Univ. of Massachusetts, Amherst, 1982.

The heat required for sublimation is supposed to be equal to the radiant energy and can be expressed as:

$$Q_r = Q_i = G_s H_s \tag{17.94}$$

in which Q_i is the internal flow inside the slab and H_S is the mean latent heat of vapor (Barbosa–Cánovas and Vega–Mercado, 1996). The internal heat flow can be expressed as:

$$Q_i = \frac{K_t\left(T_o - T_s\right)}{x} \tag{17.95}$$

In this equation, K_t is the thermal conductivity of the dry layer, T_0 is the temperature of the surface of the slab, and T_S is the sublimation temperature. Substitution of Equation 17.92 by G_S in Equation 17.95 yields:

$$\frac{K_t\left(T_o - T_s\right)}{x} = \rho\frac{\left(Y_o - Y_f\right)}{\left(1 + Y_o\right)} H_s \frac{dx}{dt} \tag{17.96}$$

Assuming that T_0, T_s, and K_t remain constant:

$$t_S = \rho\frac{\left(Y_o - Y_f\right)}{\left(1 + Y_o\right)} H_s \frac{a^2}{K_t\left(T_o - T_s\right)} \tag{17.97}$$

The combination of mass and heat transfer relationships for drying time t_S yields a relation that is a function of the properties of the dry layer and the operation conditions during freeze drying:

$$\left(P_s^* - P_o\right) = \left(\frac{-K_t}{K_p H_s}\right)\left(T_s - T_o\right) \tag{17.98}$$

This can be a straight-line equation if P_S^* and T_S are considered as variables, T_o and P_o are fixed, and K_t and K_p are independent of P_s^* and T_s (Schwartzberg, 1982). The values of P^* can be calculated from the sublimation equation as follows:

$$\ln P^* = 30.9526 - \frac{6153.1}{T} \tag{17.99}$$

where T is the absolute temperature. Equations 17.98 and 17.99 can be used together to define the final operation conditions during the freeze drying process.

Another very important variable is the surface temperature, T_0. The value of such a variable is controlled by the heat transfer rate from the heating plate, whose temperature is T_p:

$$Q_r = F_{op}\sigma\left(T_p^4 - T_o^4\right) \tag{17.100}$$

In this equation, σ is the Stefan–Boltzman's constant and F_{op} is the shape or vision factor, defined as:

$$F_{op} = \frac{1}{\left(\frac{1}{\varepsilon_o} + \frac{1}{\varepsilon_p} - 1\right)} \tag{17.101}$$

where ε_0 is the emissivity of the surface of the product and ε_P is the emissivity of the radiant plate. Assuming that $\varepsilon_0 \approx 1$, it is obtained that $F_{op} \approx \varepsilon_0$; the combination of Equations 17.95, 17.97, and 17.100 yields:

$$T_p^4 = T_o^4 + \frac{K_t\left(T_o - T_s\right)}{\left(\frac{2\,K_t\left(T_o - T_s\right)\left(1 + Y_o\right)}{H_s\,\rho\left(Y_o - Y_f\right)}t + x^2\right)^{0.5}} \tag{17.102}$$

17.8 Other Types of Drying

17.8.1 Osmotic Dehydration

The concentration of foods by immersion in a hypertonic solution is known as osmotic dehydration. Osmosis consists of molecular movement of certain components of a solution through a semipermeable membrane towards a less concentrated solution.

Water losses in food during osmotic dehydration can be divided into two periods (Barbosa–Cánovas and Vega–Mercado, 1996): (1) a period lasting about 2 h with a high water removal rate, and (2) a period, from 2 to 6 h, with a falling rate of water removal. The temperature and concentration of the osmotic solution affect the water loss rate of the product. Compared to air drying or freeze drying, osmotic dehydration is quicker since water elimination occurs without phase change.

The difference in chemical potential through the semipermeable membrane between the product and the osmotic solution is the driving force for mass transfer. The chemical potential μ_i is related to water activity according to the expression:

$$\mu_i = \mu_i^o + RT \ln a_w \tag{17.103}$$

in which μ_i^o is the reference chemical potential, R is the gas constant, and T is the absolute temperature. The mass transfer continues until the water activities of the osmotic solution and the food are equal. The main mechanism through which mass transfer takes place is by diffusion due to the concentration gradient existing between the food and the osmotic solution. The diffusion rate of water can be estimated by the modified law of Fick (Barbosa–Cánovas and Vega–Mercado, 1996) and depends on the geometry of the product to be dried.

The temperature variable has a great effect on the osmotic dehydration process, since an increase of temperature intensifies water removal and penetration of the osmotic solution into the tissue. The water and solute content of the food is a function of time; Figure 17.26 shows this variation for fruit dehydration, in which a decrease in water content and an increase in sugar content can be observed over time.

The selection of the solute of the osmotic solution is also very important; three main factors should be taken into account: (1) the sensory characteristics of the product, (2) the cost of the solute, and (3) the molecular weight of the solute. In general, the solutes used most in osmotic dehydration processes are sodium chloride, sucrose, lactose, fructose, and glycerol. Table 17.8 presents the uses and advantages of some osmotic solutes.

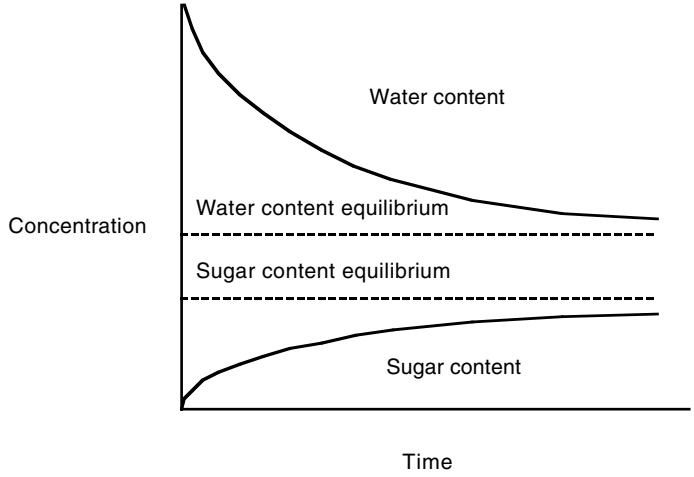

FIGURE 17.26
Water and sugar contents during osmotic dehydration. (Adapted from Barbosa–Cánovas, G.V. and Vega–Mercado, H., *Dehydration of Foods,* Chapman and Hall, New York, 1996.)

TABLE 17.8

Uses and Advantages of Some Osmotic Solutes

Name	Uses	Advantages
Sodium chloride	Meats and vegetables Solutions higher than 10%	High a_W depression capacity
Sucrose	Fruits	Reduces browning and increases retention of volatiles
Lactose	Fruits	Partial substitution of sucrose
Glycerol	Fruits and vegetables	Improves texture
Combination	Fruits, vegetables, and meats	Adjusted sensorial characteristics; combines the high a_W depression capacity of salts with the high capacity of water elimination of the sugar

Source: Barbosa–Cánovas, G.V. and Vega–Mercado, H., *Dehydration of Foods,* Chapman and Hall, New York, 1996.

17.8.2 Solar Drying

The practice of drying harvested foods by scattering them in thin layers exposed to the sun is called open solar drying or natural solar drying. This technique is used to process grapes, figs, plums, coffee beans, cocoa beans, sweet peppers, pepper, and rice, among others. This type of drying has some limitations such as:

- Lack of control of the drying process that can give rise to an excessive drying of the food, loss of grains or beans due to germination, and nutritional changes
- Lack of uniformity in drying
- Contamination due to molds, bacteria, rodents, birds, and insects

For this reason, solar dryers have been developed based on the use of energy from the sun and also of hot air to dry the food. Thus, natural convection solar dryers exist that do not require any type of mechanical or electric energy, as well as forced convection dryers that require the use of fans to blow hot air.

17.8.3 Drum Dryers

These dryers consist of hollow metal cylinders that rotate on their horizontal axis and are internally heated with steam, hot water, or another heating medium. Drum dryers are used to dry pastes and solutions; potato flakes are obtained using these dryers. Figure 17.27 shows different types of drum dryers.

The global drying rate of the food film placed on the drum surface can be expressed as (Heldman and Singh, 1981):

$$\frac{dX}{dt} = \frac{U\,A\,\Delta T_m}{\lambda} \tag{17.104}$$

In this equation, ΔT_m is the mean logarithmic difference between the drum surface and the product, U is the global heat transfer coefficient, A is the area of the drying surface, λ is the latent heat of vaporization at the temperature of the drying surface, and X is the moisture content.

17.8.4 Microwave Drying

Microwaves are high-frequency waves. The advantages of microwave heating over convection or conduction heating are:

- Only the product to be heated absorbs energy.
- There are no losses due to heating of the surrounding media (air and walls).
- Deep penetration of the heating source results in more uniform and effective heating.

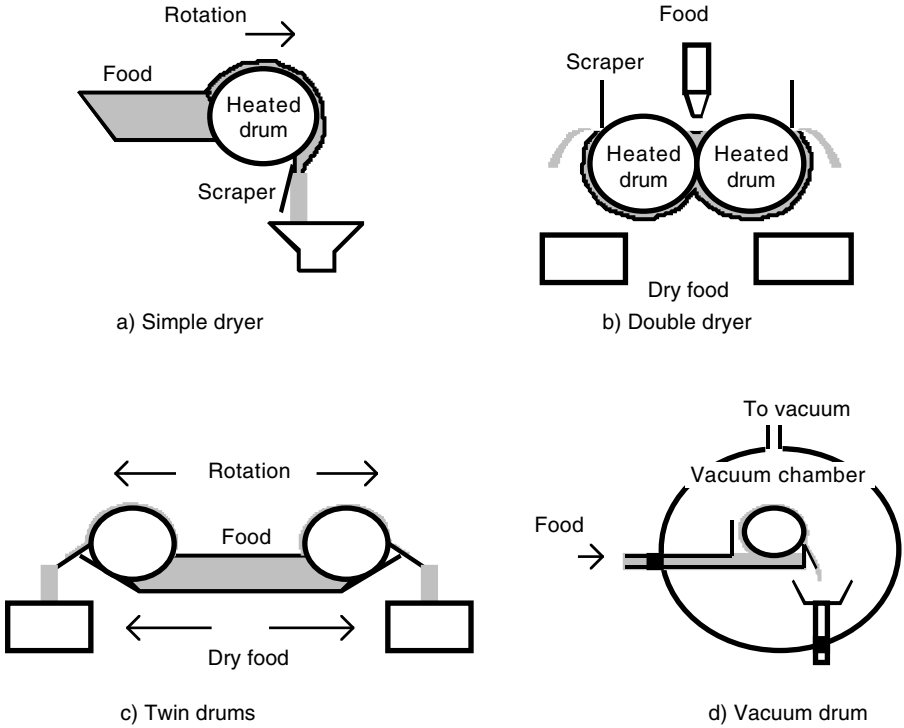

FIGURE 17.27
Drum dryers. (Adapted from Barbosa–Cánovas, G.V. and Vega–Mercado, H., *Dehydration of Foods*, Chapman and Hall, New York, 1996.)

Microwaves are used in the food industry for drying potato chips, blanching vegetables, quick thawing frozen fish, precooking chicken and bacon, and elimination of molds in dry fruits and milk products.

17.8.5 Fluidized Bed Dryers

The particles that form a bed can be fluidized if the pressure drop through the bed is equal to the weight of the bed, reaching the expansion and suspension in air of the particle. The system behaves as a fluid when its Froude number is smaller than one (Karel, 1975b), in which the air velocity is generally within the 0.05 to 0.075 m/s range. In fluidized beds, the particles do not present contact points between them, which facilitates a more uniform drying.

Problems

17.1

It is desired to dry a solid that contains 0.075 kg of water/kg of dry solid to a moisture content of 0.005 kg of water/kg of dry solid. Thus, 645 kg/h of a solid are fed to a dryer that is completely thermally insulated, in which air flows under countercurrent. Air is introduced at 100ºC and humidity of 0.010 kg of water/kg of dry air and leaves the dryer at 45ºC. If the solids are introduced at 25ºC and leave the dryer at 70ºC, calculate the air flow rate needed to carry out this drying operation. The specific heat of the solids is 1.465 kJ/kg K.

The type of dryer used is continuous with recirculation, like the one shown in Figure 17.2. If the dryer is thermally insulated, it can be assumed that there are no heat intakes or losses to the exterior. This means

$$\dot{Q}_E = \dot{Q}_S = 0$$

The dry solid's flow rate entering into the dryer is:

$$W_s = 645/\left(1+0.075\right) = 600 \text{ kg dry solid/h}$$

The enthalpies of the air streams are obtained from Equation 17.5:

$$\hat{i}_E = \left(1+1.92\times 0.010\right)\left(100-0\right)+2490\times 0.01 = 126.82 \text{ kJ/kg dry air}$$

$$i_S = \left(1+1.92\,X_S\right)\left(45-0\right)+2490\,X_S = 4+2576.4\,X_S \text{ kJ/kg dry air}$$

The enthalpies of the solids are obtained from Equation 17.6:

$$\hat{h}_E = 1.465\left(25-0\right)+0.06\times 4.185\left(25-0\right) = 44.47 \text{ kJ/kg dry solid}$$

$$\hat{h}_S = 1.465\left(70-0\right)+0.005\times 4.185\left(70-0\right) = 104.02 \text{ kJ/kg dry solid}$$

Substitution in Equation 17.4 yields:

$$w'126.82+\left(600\right)\left(44.47\right) = w'\left(45+2576.4\,X_S\right)+\left(600\right)\left(104.2\right)$$

It is obtained from the mass balance (Equation 17.3) that:

$$600\left(0.075-0.005\right) = w'\left(X_S-0.01\right)$$

When solving the last two equations, it is obtained that the humidity of the air leaving the dryer is X_S = 0.0264 kg of water/kg dry air, while the

flow of dry air that should be introduced into the dryer is w' = 2567 kg dry air/h.

17.2

A 60 × 60 cm and 3 cm depth tray contains a granular wet product that is desired to be dried with an air stream. The air stream is hot and provides enough heat to dry the product by a convection mechanism. The air at 65ºC flows at a rate of 5 m/s, with a humidity level of 0.02 kg of water/kg of dry air. If it is considered that the sides and bottom of the tray are completely insulated, determine the constant drying rate.

The following properties are obtained for air at 65ºC and absolute humidity of 0.02 kg of water/kg of dry air from the psychrometric diagram:

$$\text{Temperature } T_W = 32.5°\text{C} \qquad X_W = 0.034 \text{ kg of water/kg of dry air}$$

The wet volume is obtained from Equation 5.8:

$$V_H = \left(\frac{1}{28.9} + \frac{0.02}{18} \right) \frac{(0.082)(273+65)}{1} = 0.9898 \text{ m}^3/\text{kg dry air}$$

so the density of humid air is:

$$\rho = \frac{1+0.02}{0.9898} = 1.031 \text{ kg/m}^3$$

The mass flux is:

$$G = \rho v = (1.031)(6)(3600) = 22269.6 \frac{\text{kg}}{\text{m}^2\,\text{h}}$$

The convective heat transfer coefficient can be calculated from Equation 17.20:

$$h = 0.0204 \left(22,269.6\right)^{0.8} = 61.35 \text{ W/(m}^2\,°\text{C)}$$

For T_W = 32.5ºC, the latent heat is λ_W = 2423.4 kJ/kg.

The drying rate can be calculated from Equation 17.17:

$$R = \frac{h(T - T_W)}{\lambda_W} = \frac{(61.35)(3600)(65 - 32.5)}{(2423.4)(1000)} = 2.96 \frac{\text{kg}}{\text{h}\,\text{m}^2}$$

Since the surface being dried has an area of 0.36 m^2, the total evaporation rate is 1.066 kg water/h.

17.3

A porous solid with a critical moisture content of 0.22 kg of water/kg dry solid is subjected to a drying process to reduce its moisture from 0.22 to 0.15 kg of water/kg solid in 4 h. The thickness of the solid is 6 cm and the drying process only takes place on one of the faces of the solid. Calculate the drying time required by a solid with similar characteristics, but with a thickness of 8 cm and with the drying process taking place simultaneously on the two faces exposed to the air stream.

Initially, the value of the effective diffusivity through the solid should be calculated. The solution to Fick's equation given in Equation 17.24a can be used for a solid with such geometry. It is considered that $Y_S = 0$, and that all the water reaching the surface evaporates immediately.

$$\Gamma = \frac{Y}{Y_o} = \frac{8}{\pi^2} e^{\left(\frac{-h_n^2 \pi^2 D_{eff}\, t}{4\, L^2}\right)}$$

where $h_n = 1$, $Y = 0.15$; $Y_0 = Y_C = 0.22$; $L = 0.06$ m, and $t = 14{,}400$ s. The effective diffusivity can be obtained by substituting these data in the last equation:

$$D_{eff} = 1.75 \times 10^{-8} \ \text{m}^2/\text{s}$$

For the second part of the problem, since the type of product is the same, the value obtained for diffusivity can be employed as well as the expression given before. However, it should be taken into account that drying takes place on both faces of the slab; therefore, the thickness should be half of its value, that is, $L = 0.04$ cm. Calculations using the new thickness and the value of the effective diffusivity obtained previously yield a drying time of 6419 s or 1.78 h.

17.4

A food product is obtained in the form of spherical particles of 15 mm diameter and moisture content of 1.5 kg water/kg dry solid. The equilibrium moisture content is 0.01 kg water/kg dry solid. In order to reduce the moisture content of this product to 0.2 kg water/kg dry solid, it is placed in a dryer on a porous mesh forming a bed 5 cm thick. The apparent density of the bed is 560 kg/m^3, while the dry solids have a density of 1400 kg/m^3. Air at a velocity of 0.8 m/s is circulated through the bed. Air at the inlet is 120°C with a moisture content of 0.05 kg water/kg dry air. If the critical moisture content is 0.5 kg water/kg dry solids, calculate the total drying time.

Free moisture content:

Initial: $Y_1 = 1.5 - 0.01 = 1.59$ kg water/kg dry solid

Final: $Y = 0.02 - 0.01 = 0.01$ kg water/kg dry solid

Critical: $Y_C = 0.5 - 0.01 = 0.49$ kg water/kg dry solid

Conditions of air at the inlet (from the psychrometric chart):

$T_1 = 120°C$ $X_1 = 0.05$ kg water/kg dry solid

$T_W = 49°C$ $X_W = 0.083$ kg water/kg dry solid $\lambda_W = 2382$ kJ/kg

Humid air volume (Equation 5.8):

$$V_H = \left(\frac{1}{28.9} + \frac{X}{18}\right)\frac{RT}{P} = \left(\frac{1}{28.9} + \frac{0.05}{18}\right)\frac{(0.082)(273+120)}{1}$$

$$= 1.205 \text{ m}^3/\text{kg dry air}$$

Density of the humid air entering:

$$\rho = \frac{(1+0.05)}{1.205}\frac{\text{kg/kg dry air}}{\text{m}^3/\text{kg dry air}} = 0.872 \left(\text{kg dry air} + \text{water}\right)/\text{m}^3$$

The air flux is:

$$G = v\rho = 0.8\frac{\text{m}}{\text{s}}0.872\frac{\text{kg dry air + water}}{\text{m}^3}\frac{1 \text{ kg dry air}}{1.05 \text{ kg dry air + water}}$$

$$G = 0.6644\frac{\text{kg dry air}}{\text{s.m}^2} = 2392\frac{\text{kg dry air}}{\text{h.m}^2}$$

The air that circulates through the bed gains water, and this content is greater at the outlet than at the inlet. A mean moisture content value is estimated, which can be 0.07 kg water/kg dry air, so the mean mass flux density for air is:

$$G_t = G(1+0.07) = 2559\frac{\text{kg dry air + water}}{\text{h.m}^2}$$

Also, the humid heat is calculated with this assumed mean moisture:

$$\hat{s} = 1 + (1.92)(0.07) = 1.1344 \text{ kJ}/(\text{kg dry air °C})$$

The hollow fraction (porosity) should be calculated from the density of the particles and the apparent density of the bed:

$$\varepsilon = 1 - \frac{\rho_a}{\rho_S} = 1 - \frac{560}{1400} = 1 - 0.4 = 0.6$$

The specific surface of the bed is calculated by Equation 17.40:

$$a = 6\frac{(1-0.6)}{0.015} = 160\ \frac{\text{m}^2}{\text{m}^3}$$

In order to estimate the viscosity of the air, a mean temperature of 93ºC is considered, yielding a value of $\eta = 2.15 \times 10^{-5}$ Pa·s.

The Reynolds number is:

$$(\text{Re}) = \frac{G_t D_p}{\eta} = \frac{\left(\frac{2559}{3600}\frac{\text{kg}}{\text{s.m}^2}\right)(0.015\ \text{m})}{2.15 \times 10^{-5}\ \text{Pa} * \text{s}} = 496$$

The convective heat transfer coefficient is calculated from Equation 17.49:

$$h = 0.151\frac{(2559)^{0.59}}{(0.015)^{0.41}} = 86.6\ \text{W}/(\text{m}^2 \cdot ^\circ\text{C})$$

The drying time is obtained from Equations 17.47 and 17.48:

Constant rate period: $t_C = 1.44$ h

Falling rate period: $t_D = 0.66$ h

So the total drying time is $t = 2.1$ h.

17.5

A 2-cm thick veal slab is dried using a freeze drying process. Initially, the product has a moisture content of 75%, and it is desired to dry it until it reaches 5% moisture content. The initial density of the veal is 1050 kg/m^3. If the sublimation pressure is kept at 260 μmHg, and a pressure of 100 μmHg is maintained in the condenser, calculate the drying time. Suppose that $K_P = 0.75 \times 10^{-9}$ kg/(m·s·μmHg).

According to the problem statement:

$$a = 0.01 \text{ m} \qquad P_0 = P_0^*$$

$$Y_0 = 0.75/0.25 = 3 \qquad Y_f = 0.05/0.95 = 0.0526$$

Using Equation 17.93:

$$t_S = \rho \frac{\left(Y_o - Y_f\right)}{2K_p\left(1 + Y_o\right)} \frac{a^2}{\left(P_s^* - P_o\right)} = 1050 \frac{\left(3 - 0.0526\right)}{2\left(0.75 \times 10^{-9}\right)\left(1 + 4\right)} \frac{\left(100\right)^2}{\left(260 - 100\right)}$$

Hence, the drying time is:

$$t_S = 322,372 \text{ s} = 89.55 \text{ h}.$$

18

Evaporation

18.1 Introduction

Evaporation is a unit operation that consists of the elimination of water of a fluid food by means of vaporization or boiling. Several foods are obtained as aqueous solutions and, in order to facilitate their preservation and transport, they are concentrated during a water elimination stage. This elimination can be performed in different ways, although evaporation is one of the most used methods. The equipment used to remove this water from the food product is called an evaporator.

An evaporator consists mainly of two chambers, one for condensation and another for evaporation. Steam condenses in the condensation chamber, giving off the latent heat of condensation, which is contained in the evaporation chamber. The evaporated water leaves the evaporation chamber at boiling temperature, obtaining at the same time a stream of concentrated solution.

Figure 18.1 shows a scheme of an evaporator. The mass flow of steam is w_V, while that of food is w_A, obtaining a stream of vapor V and another of concentrated solution (or liquid) w_C. The removed vapor V is driven to the condenser where it condenses. It is important to note that many food solutions are heat sensitive and can be adversely affected if exposed to high temperatures. For this reason it is convenient to operate under vacuum conditions in the evaporation chamber, which causes the boiling temperature of the aqueous solution to decrease, and the fluid to be affected by heat to a lesser extent. If it is desired to operate under vacuum, a vacuum pump is needed. Also, a barometric column to compensate for the pressure difference with the exterior is needed in the condenser to condense the vapor released in the evaporation chamber.

The capacity of the evaporator (V) is defined as the amount of water evaporated from the food per unit time. The consumption (w_V) is the amount of heating steam consumed per unit time. The economy (E) is the amount of solvent evaporated per unit of heating steam:

$$E = \frac{\text{capacity}}{\text{consumption}} = \frac{V}{w_V} \tag{18.1}$$

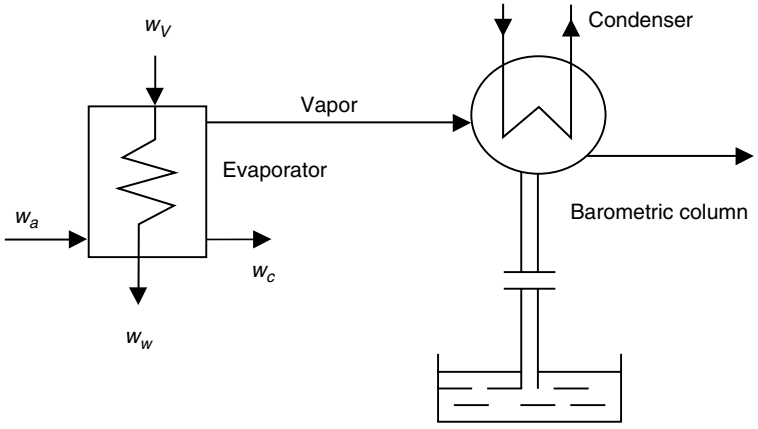

FIGURE 18.1
Scheme of the installation of an evaporator.

18.2 Heat Transfer in Evaporators

Figure 18.2 presents a scheme of a single-effect evaporator including the different variables of each stream. The condensation chamber is fed with a saturated vapor stream w_V that has a temperature T and an enthalpy $\hat{H}_w$. Vapor condenses and the only heat given off is that of condensation, so a stream w_V of liquid water leaves this chamber at the condensation temperature T, and with enthalpy $\hat{h}_w$, which corresponds to the enthalpy of water at the boiling point. The condensation heat flow $\dot{Q}$ is transferred through the exchange area of the evaporator to the food stream in the evaporation chamber.

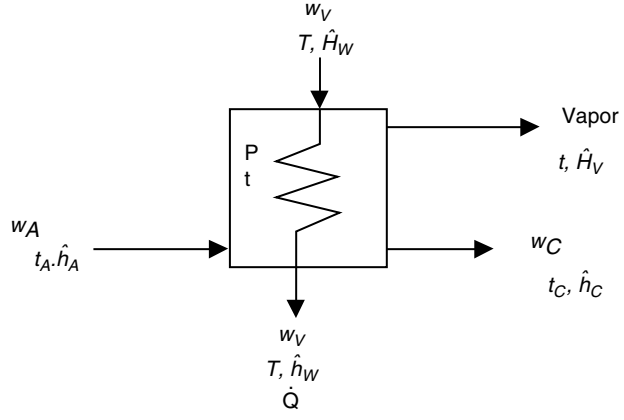

FIGURE 18.2
Simple evaporator.

A stream w_A is fed into the evaporation chamber at a temperature t_A with enthalpy $\hat{h}_A$. Due to the heat released by the condensed vapor ($\dot{Q}$), a concentrated stream w_C is obtained, with temperature t_C and enthalpy $\hat{h}_C$. Also, a vapor stream V is obtained, at a temperature T_V and with enthalpy $\hat{H}_V$. Note that the temperatures of the concentrated and vapor streams are equal and correspond to the boiling temperature of the concentrated solution that leaves this chamber.

The energy balances that should be performed are:

Condensation chamber: $$w_V \hat{H}_w = w_V \hat{h}_w + \dot{Q} \tag{18.2}$$

Evaporation chamber: $$w_A \hat{h}_A + \dot{Q} = w_C \hat{h}_C + V \hat{H}_V \tag{18.3}$$

Exchange area: $$\dot{Q} = U A \Delta T = U A \left(T - t\right) \tag{18.4}$$

where U is the overall heat transfer coefficient and A is the area of the evaporator.

18.2.1 Enthalpies of Vapors and Liquids

In the notation used here, the enthalpies per unit mass of vapor streams will be designated by $\hat{H}$, and those of liquid by $\hat{h}$.

The enthalpy per unit mass of vapor at a temperature T can be expressed as the summation of the enthalpy at saturation ($\hat{H}_{sat}$) plus the integral between the boiling temperature T_b and the enthalpy at T of the specific heat times dT:

$$\hat{H} = \hat{H}_{SAT} + \int_{Te}^{T} \left(\hat{C}_P\right)_V \, dT \tag{18.5}$$

The term $\hat{H}_{SAT}$ is the enthalpy of the vapor at its condensation temperature. The specific heat of the water vapor $(\hat{C}_P)_V$ depends on the pressure, although its value is close to 2.1 kJ/(kg·°C).

Since enthalpy is a function, the state of the enthalpy of a liquid should be expressed as a function of a reference temperature. If this temperature is t^* and the liquid is at a temperature t, it is obtained that:

$$\hat{h} = \int_{t^*}^{t} \hat{C}_P \, dT = \hat{C}_P \left(t - t^*\right) \tag{18.6}$$

Tables used for the calculation of these enthalpies can be found in the literature. Generally, the reference temperature is the freezing temperature of water (0°C).

The enthalpy of the liquid at its boiling temperature is called $\hat{h}_{SAT}$. The latent heat of condensation or evaporation (λ) will be the difference between the saturation enthalpies of the vapor and the liquid, since the evaporation and condensation temperatures are the same.

$$\lambda = \hat{H}_{SAT} - \hat{h}_{SAT} \tag{18.7}$$

The numerical values of the enthalpies of saturated vapor and of the liquid can be obtained from saturated water vapor tables, and the latent heat of condensation can be calculated. However, this value can be obtained in an approximate way from the equation of Regnault as follows:

$$\lambda = 2538 - 2.91\ T \text{ kJ/kg} \tag{18.8}$$

where T is in °C.

The enthalpies of the liquid streams, food ($\hat{h}_A$) and concentrated ($\hat{h}_C$), that appear in Equation 18.3 are expressed as:

$$\hat{h}_A = \int_{t^*}^{t_A} \left(\hat{C}_P\right)_A dT = \left(\hat{C}_P\right)_A \left(t_A - t^*\right) \tag{18.9}$$

$$\hat{h}_C = \int_{t^*}^{t_C} \left(\hat{C}_P\right)_C dT = \left(\hat{C}_P\right)_C \left(t_C - t^*\right) \tag{18.10}$$

The enthalpy of the vapor in Equation 18.3 will be different if the solution being concentrated presents or does not present a boiling point rise. In case of no increase in the boiling point of the concentrated solution, the enthalpy of the vapor will be the sum of the saturated liquid plus the latent heat:

$$\left(\hat{H}_V\right)_{SAT} = \hat{C}_P\left(t_b - t^*\right) + \lambda \tag{18.11}$$

where t_b is the boiling temperature of the solution.

In case of an increase in the boiling point, the boiling temperature of the solution (t_e) will be greater than that of pure water (t), so the vapor enthalpy will be:

$$\hat{H}_V = \hat{C}_P\left(t_b - t^*\right) + \lambda + \left(\hat{C}_P\right)_V \left(t - t_b\right) \tag{18.12}$$

In order to simplify the calculations, the reference temperature usually selected is the boiling point of pure water, $t^* = t_b$, which makes the enthalpy of the vapor leaving the evaporation chamber coincide with the latent heat

of condensation if there is no increase in the boiling point. Also, the enthalpy of the concentrated stream will be annulled, since $t_C = t_b = t$.

18.2.2 Boiling Point Rise

Water boils at a fixed temperature whenever the pressure remains constant. If the pressure varies, the boiling point varies too. For aqueous solutions, the boiling temperature depends not only on pressure, but also on the amount of solute contained, in such a way that the presence of the solute causes the boiling temperature to increase. The determination of the boiling point rise presented by food solutions is very important for the calculation of evaporators. For this reason, expressions and means to calculate the increase in boiling temperature will be given next.

For diluted solutions that comply with the law of Raoult, the boiling point increment can be calculated by the expression:

$$\Delta T_b = \frac{1000\ Kb\ X}{M_S} \tag{18.13}$$

where M_S is the molecular weight of the solute, X is the ratio of kg solute/kg solvent, and Ke is the so-called boiling constant of the solvent.

For aqueous solutions the following equation can be used:

$$\Delta T_b = 0.52C \tag{18.14}$$

where C is the molal concentration of the solute.

A general expression that allows the calculation of the boiling point rise considering an ideal solution is the equation:

$$\Delta T_b = \frac{-t_b}{1 + \dfrac{\lambda}{R\ t_b\ \ln\ X_w}} \tag{18.15}$$

If the solutions are diluted, the following equation can be used:

$$\Delta T_b - \frac{R t_b^2}{\lambda}\left(1 - X_w\right) \tag{18.16}$$

In these two last equations, X_w is the mass fraction of water, λ is the latent heat of evaporation, R is the gas constant, and t_b is the boiling temperature of pure water.

For real solutions, the boiling point rise can be calculated by the empirical rule of Dühring, which states that the boiling point of the solution is a linear

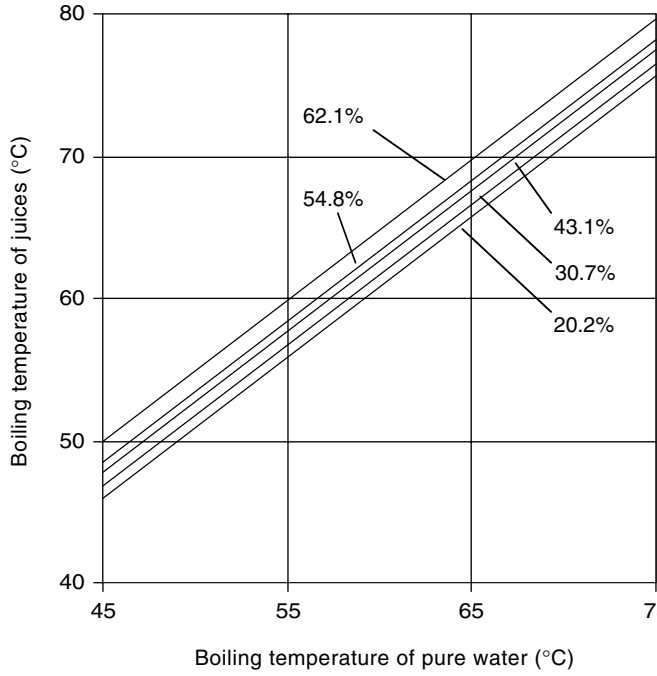

FIGURE 18.3
Diagram of Dühring for tamarind juices. (Adapted from Manohar, B. et al., *J. Food Eng.*, 13, 241–258, 1991.)

function of the boiling point of the pure solvent at the same pressure. For a given concentration of solute, the plots of the boiling temperatures of the solution against those corresponding to the pure solvent yield straight lines. Figures 18.3 and 18.4 present the diagram of Dühring for two aqueous systems.

In the case of sugar solutions, empirical correlations exist that allow the boiling point increase of the solutions to be obtained. One of these expressions is (Crapiste and Lozano, 1988):

$$\Delta T_b = \alpha C^{\beta} P^{\delta} \exp(\gamma C) \tag{18.17}$$

in which C is the concentration of the solution in °Brix, P is the pressure in mbar, and α, β, δ, and γ are empirical constants whose values depend on the solute. Table 18.1 shows the values of these parameters for sucrose, reducing sugars, and fruit juice solutions.

This equation has been modified for juices by adding a new term to the exponential term in such a way that the final expression is (Ilangantileke et al., 1991):

$$\Delta T_b = 0.04904\, C^{0.029} P^{0.113} \exp\left(-0.03889\, C + 6.52 \times 10^{-4} C^2\right) \tag{18.18}$$

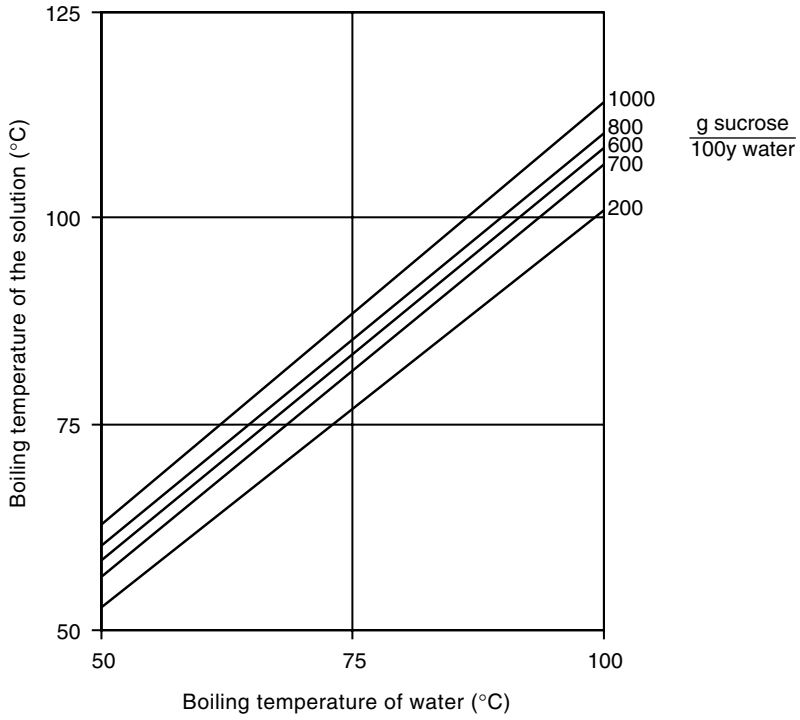

FIGURE 18.4
Diagram of Dühring for aqueous solutions of sucrose.

TABLE 18.1

Parameters α, β, δ, and γ

Sample	$\alpha \times 10^2$	β	δ	$\gamma \times 10^2$
Sucrose	3.061	0.094	0.136	5.328
Reducing sugars	2.227	0.588	0.119	3.593
Juices	1.360	0.749	0.106	3.390

Source: Crapiste, G.H. and Lozano, J.E., *J. Food Sci.*, 53(3), 865–868, 1988.

18.2.3 Heat Transfer Coefficients

The calculation of the overall heat transfer coefficient can be obtained from the expression:

$$\frac{1}{U\,A} = \frac{1}{h_w\,A'} + \frac{e_p}{k_p\,A_m} + \frac{1}{h_c\,A''} \tag{18.19}$$

TABLE 18.2

Global Heat Transfer Coefficients for Different Types of Evaporators

Evaporator	U (W/m²·°C)
Long tube vertical	
Natural circulation	1000–3500
Forced circulation	2300–12000
Short tube	
Horizontal tube	1000–2300
Calandria type (propeller calandria)	800–3000
Coiled tubes	1000–2300
Agitated film (Newtonian liquids)	
Viscosity 1 mPa·s	2300
100 mPa·s	1800
10^4 mPa·s	700

Source: McCabe, W.L. and Smith, J.C., *Operaciones Básicas de Ingeniería Química*, Reverté, Barcelona, Spain, 1968.

in which h_w is the individual convective heat transfer coefficient for the condensing vapor, while h_c is the coefficient corresponding to the boiling solution. The parameters e_P and k_P are the thickness of the solid through which heat transfer occurs and its thermal conductivity, respectively. In this type of operation, it is assumed that the areas are the same, so the expression is simplified to:

$$\frac{1}{U} = \frac{1}{h_w} + \frac{e_P}{k_P} + \frac{1}{h_c} \tag{18.20}$$

In case there is deposition on the heat transfer surface, the resistance offered (R_D) should be taken into account. Hence, the real overall coefficient U_D is:

$$\frac{1}{U_D} = \frac{1}{U} + R_D \tag{18.21}$$

Although the calculation of the theoretical overall coefficient should be made by Equation 18.20, values for this coefficient can be found in the literature, depending on the type of evaporator. Table 18.2 shows the values for this coefficient.

18.3 Single Effect Evaporators

Figure 18.5 shows a single-effect evaporator with all the streams and variables. In order to perform the calculation of this type of evaporator, mass and energy balances should be conducted.

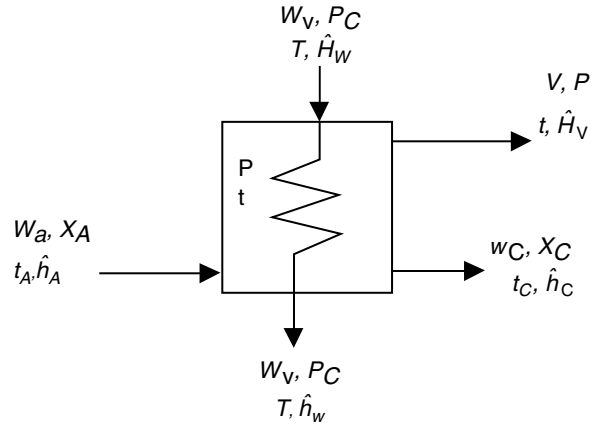

FIGURE 18.5
Single effect evaporator.

Mass balances: A global balance and a component balance are carried out.

$$w_A = w_C + V \tag{18.22}$$

$$w_A X_A = w_C X_C \tag{18.23}$$

where X_A and X_C are the mass fractions of solute in the food and in the concentrated solution streams, respectively.

Energy balances: Balances around the condensation and evaporation chambers are performed, in addition to the equation of heat transfer rate through the exchange area. These balances are similar to those performed previously and are given in Equations 18.2, 18.3, and 18.4. If the expressions for the enthalpies of the liquid and the vapor given in Section 18.2.1 are taken into account, then:

Condensation chamber:

$$w_V\left(\hat{H}_w - \hat{h}_w\right) = w_V \lambda_w = \dot{Q} \tag{18.24}$$

Evaporation chamber:

$$w_A\left(\hat{C}_P\right)_A\left(t_A - t_b\right) + \dot{Q} = w_C\left(\hat{C}_P\right)_C\left(t_C - t_b\right) + V\left[\lambda_V + \left(\hat{C}_P\right)_V\left(t - t_b\right)\right] \tag{18.25}$$

Exchange area:

$$\dot{Q} = U A \Delta T = U A\left(T - t\right) \tag{18.4}$$

Note that $t_C = t$; that is, the temperatures of the streams leaving the evaporation chamber are equal, and the boiling point rise of the solution $\Delta T_b = t - t_b$. When combining Equations 18.24 and 18.25, it is obtained that:

$$w_V \lambda_V = w_C \left(\hat{C}_P\right)_C \Delta T_b + V\left[\lambda_V + \left(\hat{C}_P\right)_V \Delta T_b\right] - w_A \left(\hat{C}_P\right)_A \left(t_A - t_b\right) \quad (18.26)$$

In case there is no boiling point rise ($\Delta T_e = 0$), the previous equation becomes:

$$w_V \lambda_V = V \lambda_V - w_A \left(\hat{C}_P\right)_A \left(t_A - t_b\right) \quad (18.27)$$

18.4 Use of Released Vapor

The vapor released in the evaporation chamber contains energy that may be used for other industrial purposes. Such vapor has a temperature lower than that of steam, so its latent heat of condensation is greater; for this reason, it is very important to take advantage of this latent heat. There are different methods for using this energy, among which are vapor recompression, thermal pump, and multiple effect. The first and second methods mentioned will be briefly studied here, while in the following section the multiple-effect method will be studied in detail.

18.4.1 Recompression of Released Vapor

One way to use the energy contained in released vapor is to compress and use it as heating steam. There are two methods in practice to compress this vapor: mechanical compression and thermocompression.

18.4.1.1 Mechanical Compression

This type of operation consists of compressing the vapor released in the evaporation chamber using a mechanical compressor. The vapor leaving the evaporation chamber at a temperature t_1 and a pressure P_1 is compressed to a pressure P_2, corresponding to the pressure of the steam used in the condensation chamber (Figure 18.6). In the enthalpy–entropy Mollier diagram for steam (Figure 18.7), the condition of the released vapor can be represented by point 1. Mechanical compression, generally, is an isoentropic process, so a perpendicular straight line is followed until reaching the isobar corresponding to pressure P_2. The condition of this steam can be found in Mollier's diagram, where it is obtained that the outlet temperature of the

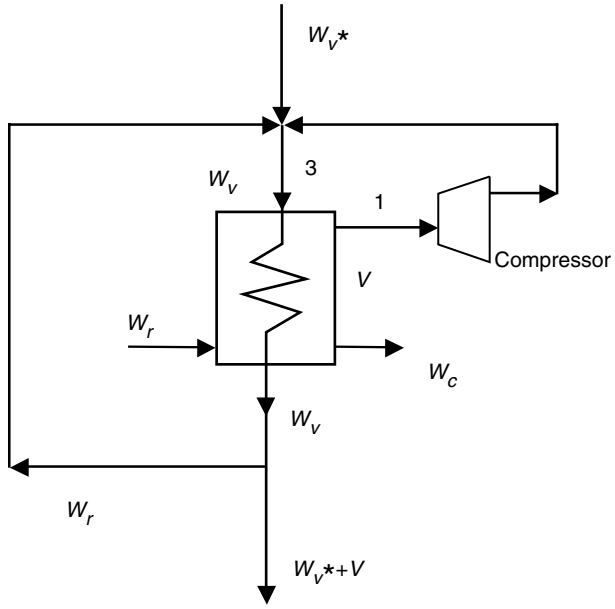

FIGURE 18.6
Simple evaporator with mechanical compression of released vapor.

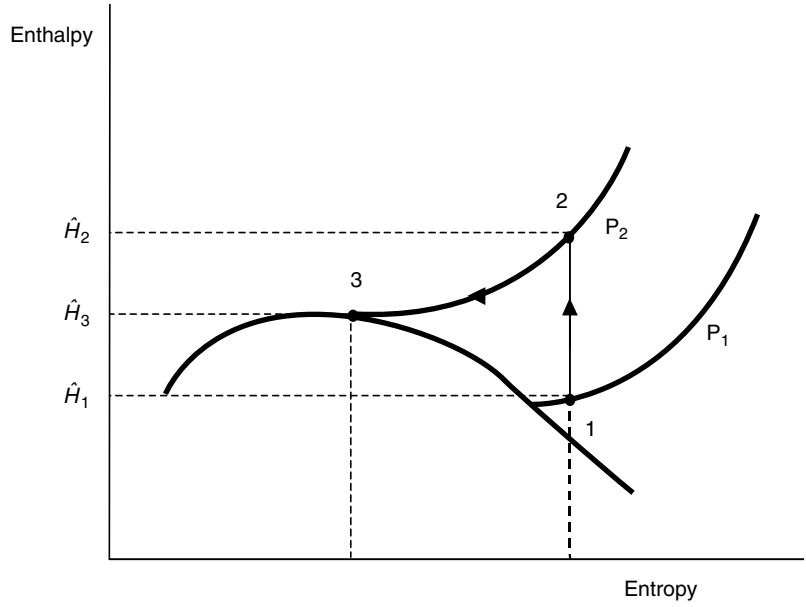

FIGURE 18.7
Evolution of released vapor during mechanical compression.

compressor is t_2, its pressure is P_2, and its enthalpy is $\hat{H}_2$. It can be observed that the vapor obtained after compression is a reheated steam, so before mixing it with the saturated steam coming from the boiler, its temperature is lowered by recirculating a stream w_R. In this way, the condensation chamber can be fed with saturated steam.

As can be observed in Figure 18.6, in this type of operation the balances around the evaporation chamber are not affected. However, additional balances should be performed in the condensation chamber.

Energy and mass balances:

$$w_V = V + w_R + w_V^* \tag{18.28}$$

$$w_V \hat{H}_w = V \hat{H}_1 + w_R \hat{h}_w + w_V^* \hat{H}_w \tag{18.29}$$

$$\dot{Q} = w_V \lambda_W \tag{18.30}$$

The calculation of the evaporator is similar to that described in the single effect, although in this case these additional balances should be taken into account.

18.4.1.2 Thermocompression

Another way to use the energy of the released vapor is to use a jet which carries away part of the vapor and joins the steam coming from the boiler. Figure 18.8 represents a diagram of the evaporator jet system. The jet is a device that functions, due to the effect of Venturi, in such a way that a steam jet carries away part of the vapor released in the evaporation chamber. The vapor entering the condensation chamber is saturated, although its pressure is intermediate between steam and the released vapor. If the jet is fed with a steam flow w_V^* that has a pressure P_W and an enthalpy $\hat{H}^*$, then this steam carries away a fraction of vapor V, which is at pressure P_1, temperature t_1, and has an enthalpy $\hat{H}_1$. The vapor that leaves the jet will have a pressure P_C and an enthalpy $\hat{H}_w$, with a mass flow rate w_V. Similarly to mechanical compression, the balances around the evaporation and condensation chambers are unaltered. However, new balances should be carried out in the jet.

Balances around the jet:

$$w_V^* + aV = w_V \tag{18.31}$$

$$w_V^* \hat{H}^* + aV \hat{H}_1 = w_V \hat{H}_w \tag{18.32}$$

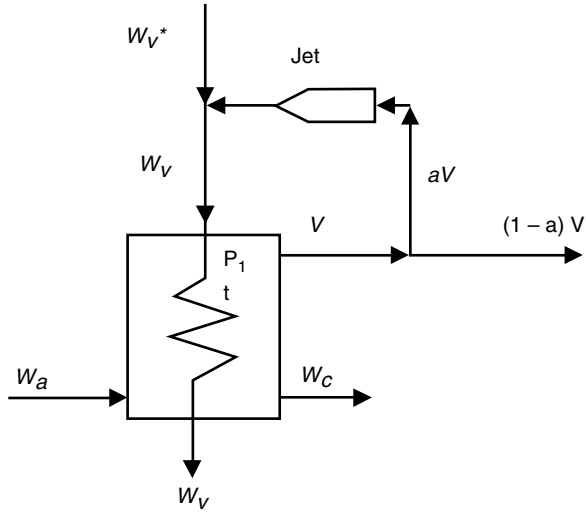

FIGURE 18.8
Simple evaporator with thermocompression of released vapor.

An empirical equation correlates the different variables and allows calculations of this type of compression. Thus, the expression to be used is (Vián and Ocón, 1967):

$$\frac{aV}{w_V^*} + 1 = R\frac{\log\left(P_w / P_1\right)}{\log\left(P_C / P_1\right)} \tag{18.33}$$

in which R is the thermal performance of the jet.

18.4.2 Thermal Pump

The so-called thermal pump is usually employed in heat sensitive products in which high temperature can adversely affect the product. Low boiling temperatures can be achieved with this device. Figure 18.9 presents a scheme of this installation, while Figure 18.10 shows a temperature–entropy diagram for the heating fluid.

This installation has two evaporators. The evaporation chamber of the first is fed with the fluid to be concentrated, obtaining a vapor stream V that is used as heating fluid for the second evaporator. The condensation chamber of the first evaporator is fed with a vapor, which could be NH_3, that condenses. This liquid exits the condensation chamber (point 1), expands in a valve (point 2), and is employed to feed the evaporation chamber of the

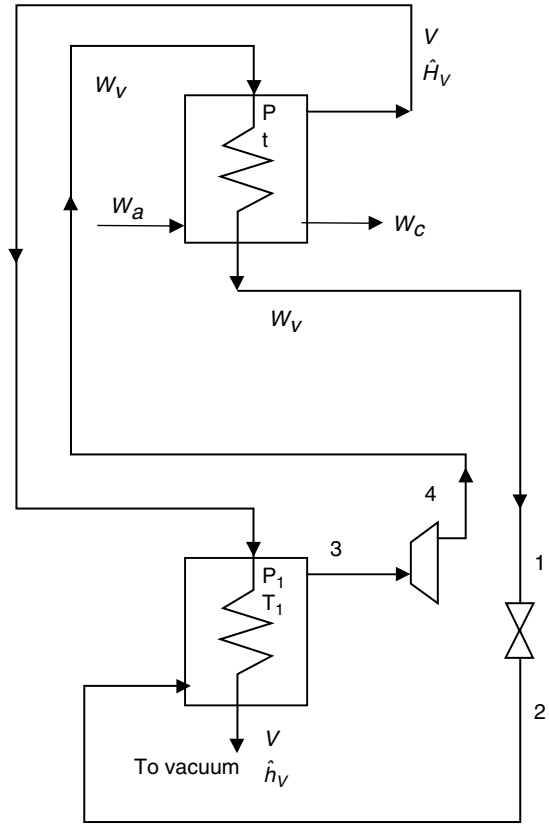

FIGURE 18.9
Installation with thermal pump.

other evaporator, thus yielding a vapor stream (point 3) fed to a mechanical compressor, with the objective of raising its pressure and obtaining a more energetic vapor (point 4). This vapor is used as heating vapor for the first evaporator. It should be pointed out that the circuit followed by the heating vapor is a closed circuit.

This type of installation is usually employed to concentrate juices, for example, orange juice, that are affected by high temperatures.

18.4.3 Multiple Effect

One of the most usual ways of employing the vapor released in the evaporation chamber is by using it as heating fluid in another evaporator. Figure 18.11 shows a diagram of a triple-effect evaporation system. It can be observed that the vapor released in the first evaporator is used as heating fluid in the second one, while the vapor liberated in this effect is used to

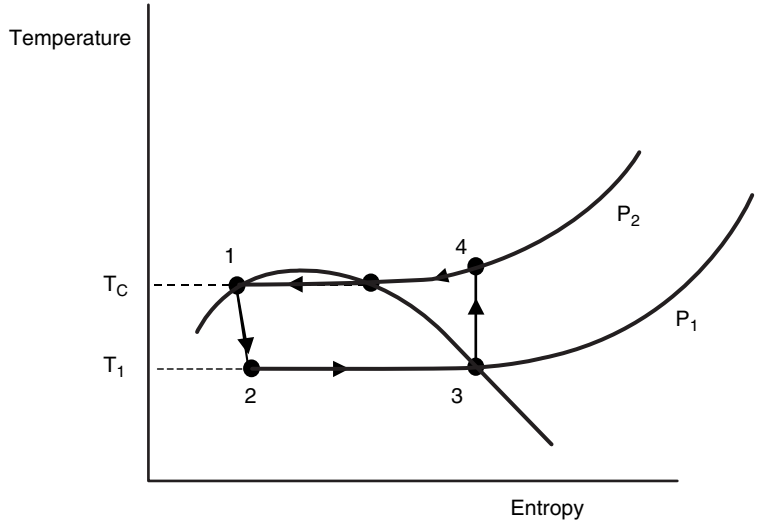

FIGURE 18.10
Evolution of the heating fluid in the temperature–entropy diagram for the thermal pump.

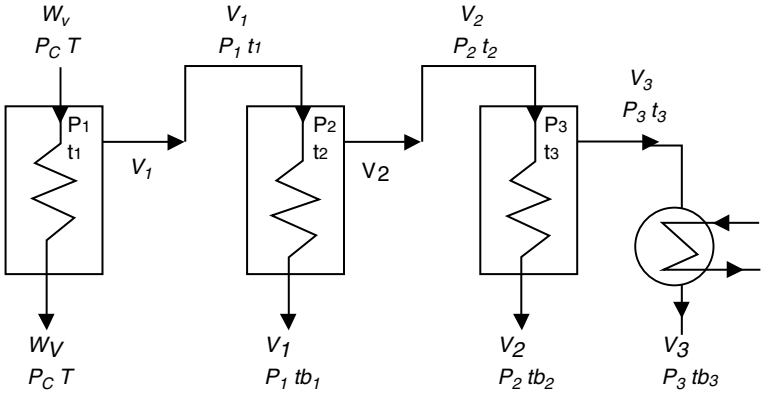

FIGURE 18.11
Scheme of released vapor use in a triple effect evaporator.

heat the third effect. Finally, the vapor released in the last effect is driven to the condenser.

For notation, the different streams have subscripts corresponding to the effect that they are leaving. The vapor released during the different effects is, each time, at a lower temperature and a lower pressure:

$$T > t_1 > t_{b1} > t_2 > t_{b2} > t_3 > t_{b3}$$

$$P_C > P_1 > P_2 > P_3$$

where t_1, t_2, and t_3 are the boiling temperatures of the solutions leaving the evaporation chambers of the first, second, and third effects, respectively. The temperatures t_{b1}, t_{b2}, and t_{b3} are the boiling temperatures of pure water at pressures P_1, P_2, and P_3, respectively.

The evaporation chamber of the first effect is at a pressure P_1 and temperature t_1. The vapor that leaves this effect V_1 does so at these conditions and is used as heating fluid in the second effect, where it is supposed to enter in saturated conditions, i.e., at its boiling temperature t_{b1}. The pressure in the condensation chamber of the second effect is still P_1, while the temperature is t_{b1}. The evaporation chamber of the second effect is at pressure P_2 and temperature t_2, the same as those of the vapor V_2 leaving this chamber. This vapor condenses in the condensation chamber of the second effect at a temperature t_{b2} and a pressure P_2. The evaporation chamber of the third effect is at a pressure P_3 and a temperature t_3; thus, the vapor V_3 leaving this effect has the same characteristics. This vapor is driven to a condenser where it condenses at the temperature t_{b3}, which corresponds to that of pressure P_3.

When there is no boiling point rise of the solutions that pass through the evaporator, the temperatures of the evaporation chamber of one effect and that of condensation of the following effect will be equal ($t_i = t_{bi}$).

Note that, in this type of installation, vacuum pumps are required to reach adequate temperatures in the chambers of each effect. A more detailed study, which allows the calculation of multiple-effect evaporators, is performed in the following section.

18.5 Multiple-Effect Evaporators

Only the case of a triple-effect evaporator will be studied; however, the mathematical treatment in other cases for multiple effects is similar.

18.5.1 Circulation of Streams

As previously mentioned, the vapor released in the evaporation chamber of one effect is employed as heating fluid for the next effect. However, depending on the circulation system of the solutions to be concentrated, different passing systems are obtained.

18.5.1.1 Parallel Feed

The food is distributed in different streams fed into each of the effects (Figure 18.12A), while the concentrated solution stream of each effect is gathered in only one stream, which will be the final concentrate.

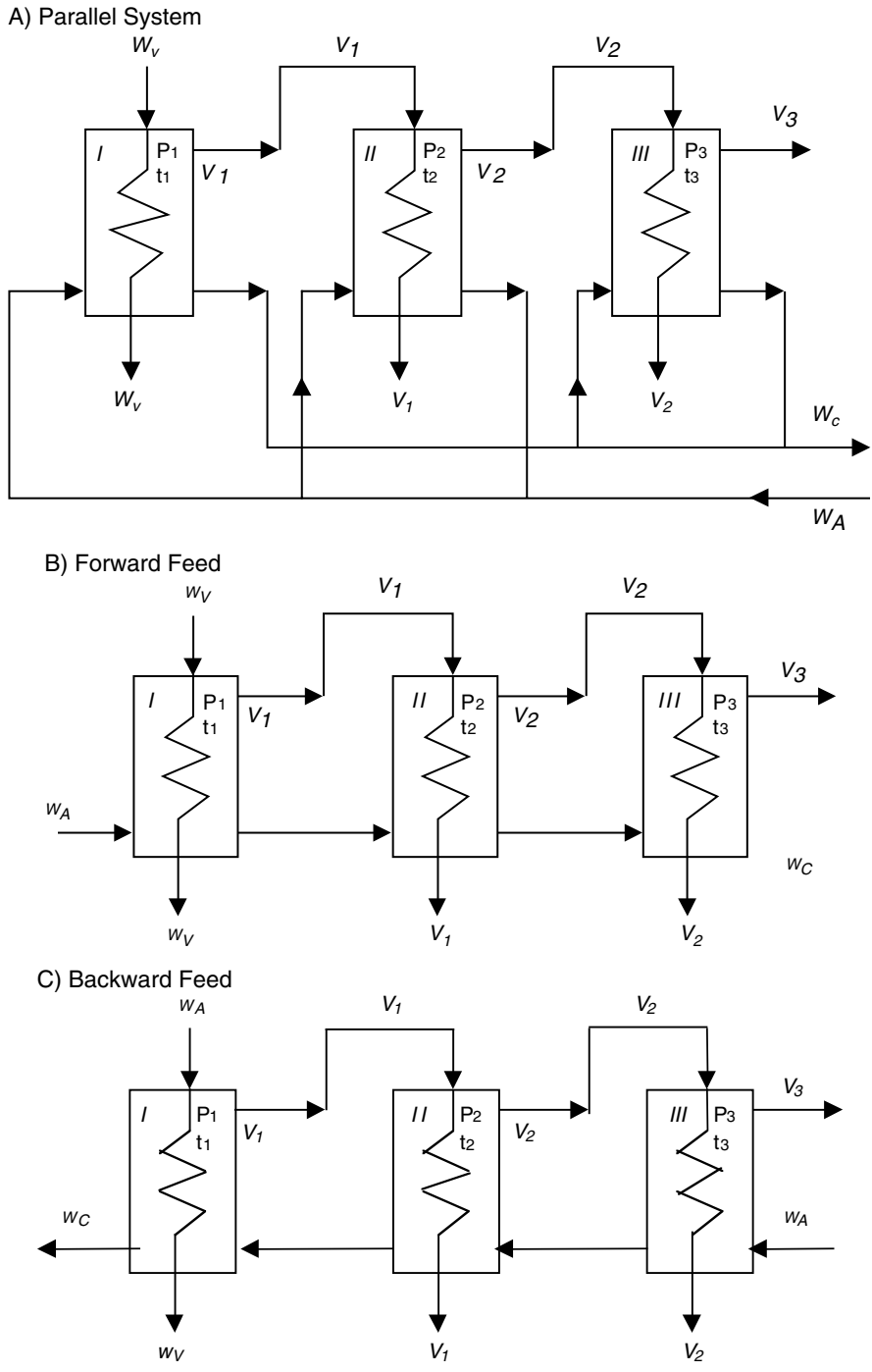

FIGURE 18.12
Circulation systems of fluid streams for triple effect evaporators.

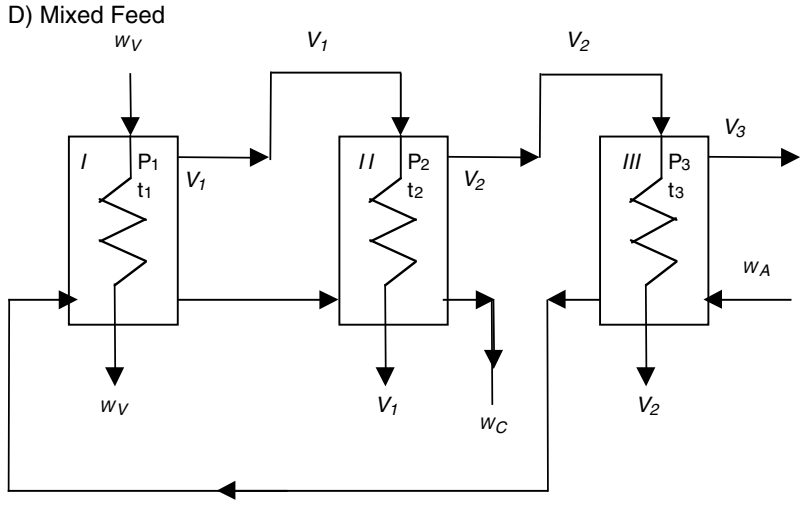

FIGURE 18.12 (continued)

18.5.1.2 Forward Feed

The diluted stream is fed into the first effect, while the concentrate stream leaving each effect is fed into the following effect (Figure 18.12B). It can be observed that the vapor and concentrate streams of each effect are parallel flows. This pass system is frequently used for solutions that can be thermally affected, since the most concentrated solution is in contact with the vapor at the lowest temperature.

18.5.1.3 Backward Feed

The flows of the solutions to concentrate and of vapor are countercurrent (Figure 18.12C). The diluted solution is fed into the last effect, where the vapor has less energy, and the concentrated solution leaving this effect is used to feed the previous effect and so on. This type of arrangement should be carefully used in the case of food solutions, since the solution with the highest concentration gains heat from the vapor at the highest temperature, which may affect the food.

18.5.1.4 Mixed Feed

In this type of arrangement, the diluted solution can be fed into any of the effects, while the concentrated solutions can be used to feed a previous or following effect. Figure 18.2D shows a mixed-feed arrangement in which the diluted solution is fed into the third effect, while the solution leaving this effect is used to feed the first one. The food stream feeding the second effect is the concentrated solution that leaves the first effect, obtaining the final concentrated solution at the second effect.

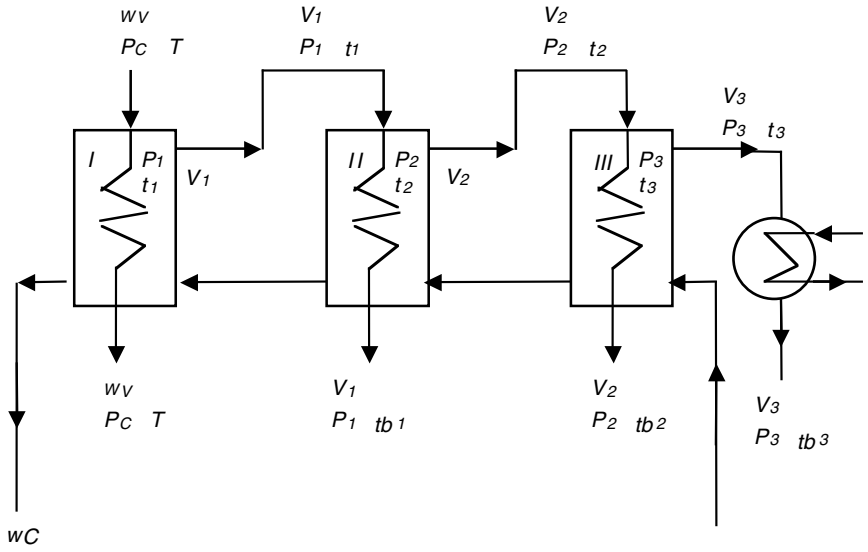

FIGURE18.13
Backward feed triple effect evaporator.

18.5.2 Mathematical Model

Of the different cases that can be studied, this section will examine only the triple-effect evaporator in which the pass system is a backward feed (Figure 18.13). The mathematical model here and its solution are similar for any type of circulation and number of effects.

In order to set up the mathematical model, the global and component mass balances should be performed, as well as the enthalpy balances and equations for rate of heat transfer through the exchange area in each effect.

The reference temperatures for calculating the enthalpies of the different streams are the boiling temperatures of pure water at the pressure in the evaporation chamber of each effect t_{bi}. The boiling point rise of each effect is the difference between the boiling temperature of the solution leaving the chamber of each effect and the boiling temperature of pure water at the pressure in this chamber $\Delta T_{bi} = t_i - t_{bi}$.

The notation used here implies that the streams leaving an effect will have the subscript corresponding to each effect.

Mass balances:

$$w_A = w_C + V_1 + V_2 + V_3 \tag{18.34}$$

$$w_A X_A = w_C X_C \tag{18.35}$$

$$w_2 = w_A - V_2 - V_3 \tag{18.36}$$

$$w_3 = w_A - V_3 \tag{18.37}$$

Enthalpy balances:

The enthalpy balances performed around each effect lead to the following equations:

$$w_V \hat{H}_W + w_2 \hat{h}_2 = w_V \hat{h}_W + w_C \hat{h}_C + V_1 \hat{H}_{V1}$$

$$V_1 \hat{H}_{V1} + w_3 \hat{h}_3 = V_1 \hat{h}_{V1} + w_2 \hat{h}_2 + V_2 \hat{H}_{V2}$$

$$V_2 \hat{H}_{V2} + w_A \hat{h}_A = V_2 \hat{h}_{V2} + w_3 \hat{h}_3 + V_3 \hat{H}_{V3}$$

Substitution of the expressions of the enthalpies of each stream and rearrangement yields:

$$\begin{aligned} w_V\left(\hat{H}_w - \hat{h}_w\right) = w_C\left(\hat{C}_P\right)_C\left(t_C - t_{b1}\right) + V_1\left[\lambda_{V1} + \left(\hat{C}_P\right)_V\left(t_1 - t_{b1}\right)\right] \\ - w_2\left(\hat{C}_P\right)_2\left(t_2 - t_{b1}\right) \end{aligned} \tag{18.38}$$

$$\begin{aligned} V_1\left[\lambda_{V1} + \left(\hat{C}_P\right)_V\left(t_1 - t_{b1}\right)\right] = w_2\left(\hat{C}_P\right)_2\left(t_2 - t_{b2}\right) + V_2\left[\lambda_{V2} + \left(\hat{C}_P\right)_V\left(t_2 - t_{b2}\right)\right] \\ - w_3\left(\hat{C}_P\right)_3\left(t_3 - t_{b2}\right) \end{aligned} \tag{18.39}$$

$$\begin{aligned} V_2\left[\lambda_{V2} + \left(\hat{C}_P\right)_V\left(t_2 - t_{b2}\right)\right] = w_3\left(\hat{C}_P\right)_3\left(t_3 - t_{b3}\right) + V_3\left[\lambda_{V3} + \left(\hat{C}_P\right)_V\left(t_3 - t_{b3}\right)\right] \\ - w_A\left(\hat{C}_P\right)_A\left(t_A - t_{b3}\right) \end{aligned} \tag{18.40}$$

These are general equations, which means that it is assumed that there is a boiling point rise. However, when there is no boiling point rise, the equations are simplified.

Even when the vapor leaving the evaporation chambers is reheated, it is assumed that, when it enters the condensation chamber of the next effect, it enters as saturated vapor. This simplifies the latter equations to:

$$w_V\lambda_w = w_C\left(\hat{C}_P\right)_C\left(t_C - t_{b1}\right) + V_1\left[\lambda_{V1} + \left(\hat{C}_P\right)_V \Delta T_{b1}\right] - w_2\left(\hat{C}_P\right)_2\left(t_2 - t_{b1}\right) \tag{18.41}$$

$$V_1\lambda_{V1} = w_2\left(\hat{C}_P\right)_2 \Delta T_{b2} + V_2\left[\lambda_{V2} + \left(\hat{C}_P\right)_V \Delta T_{b2}\right] - w_3\left(\hat{C}_P\right)_3\left(t_3 - t_{b2}\right) \tag{18.42}$$

$$V_2\lambda_{V2} = w_3\left(\hat{C}_P\right)_3 \Delta T_{b3} + V_3\left[\lambda_{V3} + \left(\hat{C}_P\right)_V \Delta T_{b3}\right] - w_A\left(\hat{C}_P\right)_A \left(t_A - t_{b3}\right) \quad (18.43)$$

Rate of heat transfer equations:

The heat transferred through the exchange area of each effect is obtained from the following equations:

$$\dot{Q}_1 = w_V\lambda_w = U_1 A_1\left(T - t_1\right) \quad (18.44)$$

$$\dot{Q}_2 = V_1\lambda_{V1} = U_2 A_2\left(t_{b1} - t_2\right) \quad (18.45)$$

$$\dot{Q}_3 = V_2\lambda_{V2} = U_3 A_3\left(t_{b2} - t_3\right) \quad (18.46)$$

It is assumed that the vapor entering the condensation chambers is saturated and the only heat that dissipates is the condensation heat.

18.5.3 Resolution of the Mathematical Model

Generally, the data available in evaporator problems are the flow rate of food to concentrate, as well as its composition and temperature. Also, the composition of the final concentrated solution is known. The characteristics of the vapor of the steam boiler are known; generally the pressure and, since it is saturated vapor, its temperature and latent heat can be obtained from thermodynamics tables. The pressure of the evaporation chamber of the third effect is usually known; therefore, its characteristics are also known. It is possible to obtain the boiling point rise by Dühring diagrams or adequate equations once the composition of the streams leaving the evaporation chambers is known.

A ten-equation system is obtained from the mass and enthalpy balances as well as from the rate equations:

$$w_A = w_C + V_1 + V_2 + V_3 \quad (18.34)$$

$$w_A X_A = w_C X_C \quad (18.35)$$

$$w_2 = w_A - V_2 - V_3 \quad (18.36)$$

$$w_3 = w_A - V_3 \quad (18.37)$$

$$w_V\lambda_w = w_C\left(\hat{C}_P\right)_C \left(t_C - t_{b1}\right) + V_1\left[\lambda_{V1} + \left(\hat{C}_P\right)_V \Delta T_{b1}\right] - w_2\left(\hat{C}_P\right)_2 \left(t_2 - t_{b1}\right) \quad (18.41)$$

$$V_1\lambda_{V1} = w_2\left(\hat{C}_P\right)_2 \Delta T_{b2} + V_2\left[\lambda_{V2} + \left(\hat{C}_P\right)_V \Delta T_{b2}\right] - w_3\left(\hat{C}_P\right)_3 \left(t_3 - t_{b2}\right) \quad (18.42)$$

$$V_2\lambda_{V2} = w_3\left(\hat{C}_P\right)_3 \Delta T_{b3} + V_3\left[\lambda_{V3} + \left(\hat{C}_P\right)_V \Delta T_{b3}\right] - w_A\left(\hat{C}_P\right)_A \left(t_A - t_{b3}\right) \quad (18.43)$$

$$\dot{Q}_1 = w_V\lambda_w = U_1 A_1\left(T - t_1\right) \quad (18.44)$$

$$\dot{Q}_2 = V_1\lambda_{V1} = U_2 A_2\left(t_{b1} - t_2\right) \quad (18.45)$$

$$\dot{Q}_3 = V_2\lambda_{V2} = U_3 A_3\left(t_{b2} - t_3\right) \quad (18.46)$$

Since the number of unknowns is larger than the number of equations, there are infinite solutions. It is assumed that the area of each effect is equal in order to solve the problem. Also, the heat flow rate transferred through each effect is similar, and can be assumed to be equal ($\dot{Q}_1 = \dot{Q}_2 = \dot{Q}_3$).

Since it is complied that $\dot{Q}_i/A_i$ = constant, then:

$$\frac{T - t_1}{\frac{1}{U_1}} = \frac{t_{b1} - t_2}{\frac{1}{U_2}} = \frac{t_{b2} - t_3}{\frac{1}{U_3}} \quad (18.47)$$

Due to one property of the ratios, they will be equal to the sum of the numerators divided by the sum of the denominators:

$$\frac{T - t_1}{\frac{1}{U_1}} = \frac{t_{b1} - t_2}{\frac{1}{U_2}} = \frac{t_{b2} - t_3}{\frac{1}{U_3}} = \frac{T - t_{b3} - \sum T_{bi}}{\sum\left(\frac{1}{U_i}\right)} \quad (18.48)$$

where ΔT_{bi} is the boiling point rise experienced by the solution in the *i*th effect.

These assumptions allow solution of a system of ten equations, although an iterative process is needed to solve the mathematical model.

18.5.4 Calculation Procedure

The calculation procedure requires an iterative method, which is simpler when there is no boiling point rise.

18.5.4.1 Iterative Method when there is Boiling Point Rise

The calculation steps are:

1. Assume that the flow of heat transfer at each stage is the same. Also, assume that the exchange areas of the different stages are equal.
2. Determine w_C by Equations 18.34 and 18.35 as the total flow of released vapor ($V_1 + V_2 + V_3$).
3. Assume that the flows of eliminated vapor in each effect are equal: $V_1 = V_2 = V_3$.
4. Calculate the concentrations X_2 and X_3.
5. Use the concentration of each solution to determine their correspondent specific heats: $(\hat{C}_P)_i$.
6. Calculate the boiling point rise in each effect. Such rises are calculated with the concentration of the solution leaving the effect.
7. Calculate the unknown temperatures of the evaporation and condensation chambers using Equation 18.48.
8. Calculate the latent heat of condensation λ_w, λ_{V1}, λ_{V2}, and λ_{V3} of the saturated steams at temperatures T, t_{b1}, t_{b2} and t_{b3}.
9. Solve the equation systems obtained from enthalpy and mass balances, Equations 18.34 through 18.43. This operation allows determination of w_w, w_2, w_3, V_1, V_2, and V_3.
10. Obtain the areas of each effect A_1, A_2, and A_3 from the rate equations (Equations 18.44, 18.45, and 18.46).
11. Check whether the areas obtained are different by less than 2% with respect to the mean value A_m, in which case the iterative process is finished.
12. If the areas are different, recalculate X_2 and X_3 using the values of V_2 and V_3 obtained in step 9.
13. Recalculate the boiling point rise with the new concentrations.
14. Determine the new temperatures of the different evaporation and condensation chambers using the following expressions:

$$\left(T - t_1\right)_j = \left(T - t_1\right)_{j-1}\left(\frac{A_1}{A_m}\right) \tag{18.49}$$

$$\left(t_{b1} - t_2\right)_j = \left(t_{b1} - t_2\right)_{j-1}\left(\frac{A_2}{A_m}\right) \tag{18.50}$$

$$\left(t_{b2} - t_3\right)_j = \left(t_{b2} - t_3\right)_{j-1}\left(\frac{A_3}{A_m}\right) \tag{18.51}$$

These equations point out that the temperature rise between the condensation and evaporation chambers of each effect in an iterative stage j is equal to the rise existing between such chambers in the previous calculation stage $j - 1$, multiplied by the ratio between the area of each effect and the mean area. Two pairs of values are obtained for each unknown temperature, so the value taken is the arithmetic mean.

15. Continue the calculations beginning with step 8 until the values of the areas of each effect coincide.

18.5.4.2 Iterative Method when there is No Boiling Point Rise

The calculation steps are listed below:

1. Assume that the heat flows transferred in each stage are the same. Also, assume that the exchange areas of the different stages are equal.
2. Determine w_C and the total flow of released vapor ($V_1 + V_2 + V_3$) by Equations 18.34 and 18.35.
3. Assume that the flows of vapor eliminated in each effect are equal: $V_1 = V_2 = V_3$.
4. Calculate the concentrations X_2 and X_3.
5. Use the concentration of each solution to determine their correspondent specific heats: $(\hat{C}_P)_i$.
6. Calculate the unknown temperatures of all evaporation and condensation chambers using Equation 18.48.
7. Use temperatures T, t_{b1}, t_{b2}, and t_{b3} to calculate the latent heat of condensation of saturated steams λ_w, λ_{V1}, λ_{V2}, and λ_{V3} at these temperatures.
8. Solve the equation systems obtained from the enthalpy and mass balances, Equations 18.34 through 18.43, which will allow calculation of w_w, w_2, w_3, V_1, V_2, and V_3.
9. Obtain the areas of each effect A_1, A_2, and A_3 from the rate equations (Equations 18.44, 18.45, and 18.46).
10. Check whether the areas obtained are different by less than 2% with respect to the mean value A_m, in which case the iterative process is finished.
11. If the areas are different, recalculate X_2 and X_3 using the values of V_2 and V_3 obtained in step 9.

12. Calculate the new temperatures of the different evaporation and condensation chambers using Equations 18.49, 18.50, and 18.51. Two pairs of values are obtained for each unknown temperature, so the value taken is the arithmetic mean.
13. Continue from step 7 until the values of the areas of each effect coincide.

18.6 Evaporation Equipment

Different types of equipment are used for evaporation processes: those in which the fluid circulates by pumps and those that do not need these devices. The former are called forced circulation evaporators, and the latter are called natural circulation evaporators. Also, there are long tube evaporators of ascending and descending film, as well as plate and expanded flow evaporators. A brief description of each type is given next.

18.6.1 Natural Circulation Evaporators

There are different types of evaporators based on the natural circulation of fluids, with the simplest being the open evaporator. There are also tube evaporators, usually short, based on this principle.

18.6.1.1 Open Evaporator

These evaporators are the simplest, consisting mainly of a container open to the atmosphere in which fluid is heated directly, or by a heating coil or external jacket. Often, evaporators have a low evaporation rate, hence showing a poor thermal economy. Sometimes, to allow operation under vacuum, the container may have a hermetic seal.

The main advantage of these evaporators is that they are useful when low capacity units are required. However, heating is not effective in large capacity units, since the ratio of heat transfer surface to volume of liquid is low. Also, heat transfer is reduced in units that have internal coils, since they make the circulation of liquid difficult.

This type of evaporator is used in the food industry to concentrate tomato pulp, prepare soups and sauces, and boil marmalades and confectionery products.

18.6.1.2 Short Tube Horizontal Evaporator

These evaporators are formed by a chamber, the bottom of which is crossed by a bundle of interior horizontal tubes (Figure 18.14) that circulate steam acting as heating fluid. Above the tubes is a space that allows the separation by gravity of drops carried away by the vapor released in the base.

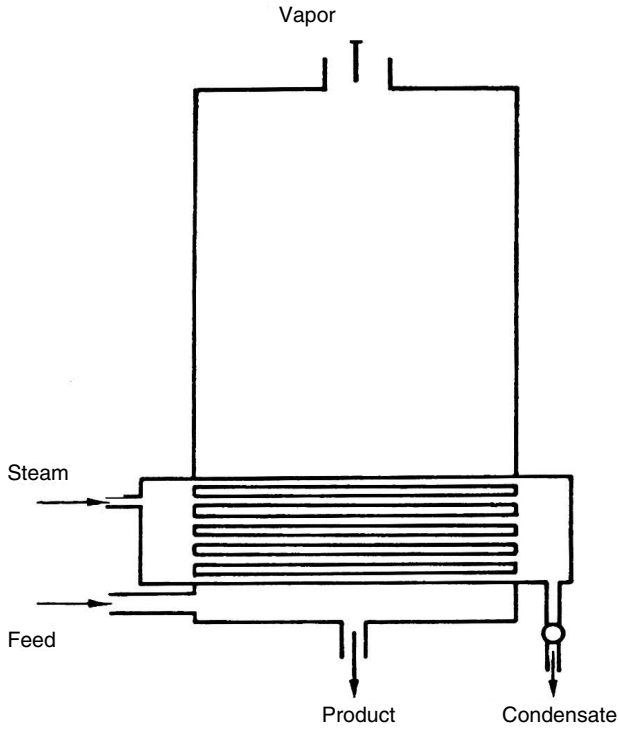

FIGURE 18.14
Short tube horizontal evaporator. (Adapted from Brennan, J.G. et al., *Los Operaciones de la Ingeniería de los Alimentos*, Acribia, Zaragoza, Spain, 1980.)

Impact slabs are arranged in order to facilitate the separation and carrying away of drops. Since the tube bundle makes the circulation of liquid difficult, such evaporators present poor global heat transfer coefficients. They are usually employed for the concentration of low viscosity liquids.

18.6.1.3 Short Tube Vertical Evaporator

Figure 18.15 shows a scheme of this type of evaporator in which the heating steam condenses outside tubes vertically arranged inside the evaporation chamber. The tube sheet, called the calandria, has a large central return tube through which a liquid colder than the liquid that circulates in the heating ascending tubes, thus forming natural circulation streams. The length of the tubes usually ranges between 0.5 and 2 m, with a diameter of 2.5 to 7.5 cm, while the central tube presents a transversal section between 25 and 40% of the total section occupied by the tubes.

These evaporators show adequate evaporation velocities for noncorrosive liquids with moderate viscosity. The units can be equipped with basket calandria that facilitate cleaning, since they can easily be dismounted.

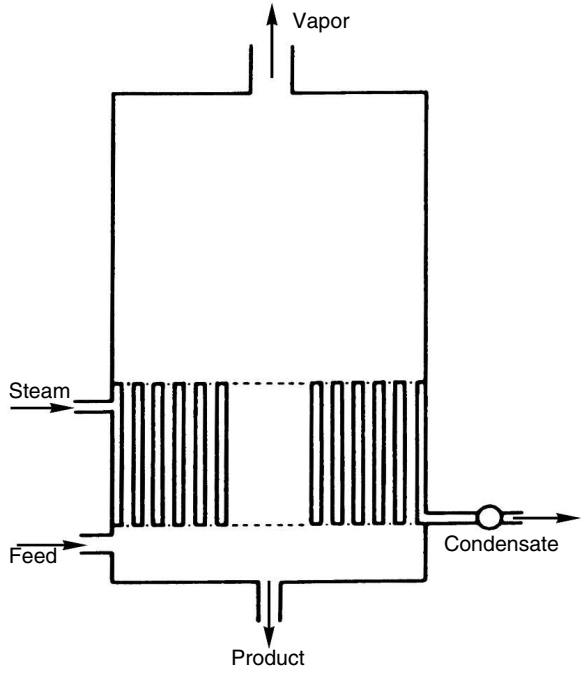

FIGURE 18.15
Short tube vertical evaporator. (Adapted from Brennan, J.G. et al., *Los Operaciones de la Ingeniería de los Alimentos,* Acribia, Zaragoza, Spain, 1980.)

Short tube vertical evaporators are usually employed for the concentration of sugar cane and beet juices, as well as in the concentration of fruit juices, malt extracts, glucose, and salt.

18.6.1.4 Evaporator with External Calandria

In this type of evaporator (Figure 18.16), the tube bundle is located outside the vapor separator. The evaporator usually operates at reduced pressures and has easy access to the tube bundle. Also, a plate heat exchanger can substitute for the calandria, which is useful in case crusts form, since the plates are easy to dismount and clean.

Since these evaporators can operate under vacuum, they are used to concentrate heat sensitive foods such as milk, meat extracts, and fruit juices.

18.6.2 Forced Circulation Evaporators

Circulation in these evaporators is achieved by a pump that impels the food through the calandria into a separation chamber, where vapor and concentrate are separated (Figure 18.17). The pump causes the fluid to circulate at a velocity between 2 and 6 m/s; when it passes through the tube bundle,

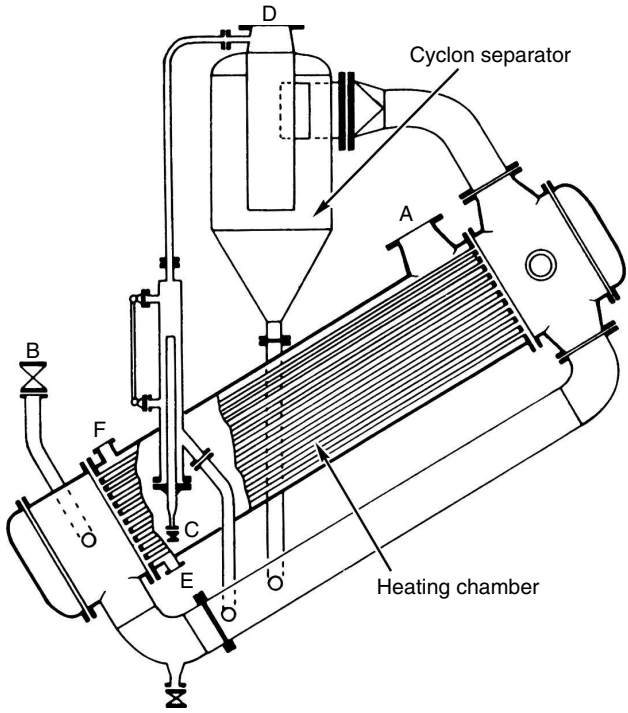

FIGURE 18.16
Evaporator with exterior calandria: A, vapor inlet; B, liquid feed inlet; C, concentrated liquid outlet; D, vapor outlet; E, condensate outlet; F, noncondensable gases outlet. (Adapted from Brennan, J.G. et al., *Los Operaciones de la Ingeniería de los Alimentos,* Acribia, Zaragoza, Spain, 1980.)

the fluid gains enough heat to reheat it, but the liquid is subjected to a static charge that prevents boiling inside the tubes. However, when the fluid reaches the chamber, there is a sudden evaporation, and the impact plate facilitates the separation of the liquid phase from vapor.

These evaporators are capable of concentrating viscous liquids when the pump impels the liquid at an adequate velocity. For this reason, centrifugal pumps are used if the liquids present low viscosity. If the liquids have a higher viscosity, then positive displacement pumps should be used.

18.6.3 Long Tube Evaporators

Some evaporators consist of a vertical chamber made of a tubular exchanger and a separation chamber. The diluted liquid is preheated to almost boiling temperature before entering the tubes. Once inside the tubes, the liquid begins to boil, and the expansion due to vaporization yields the formation of vapor bubbles that circulate at high velocity and carry away the liquid, which continues concentrating as it moves forward. The liquid–vapor mixture

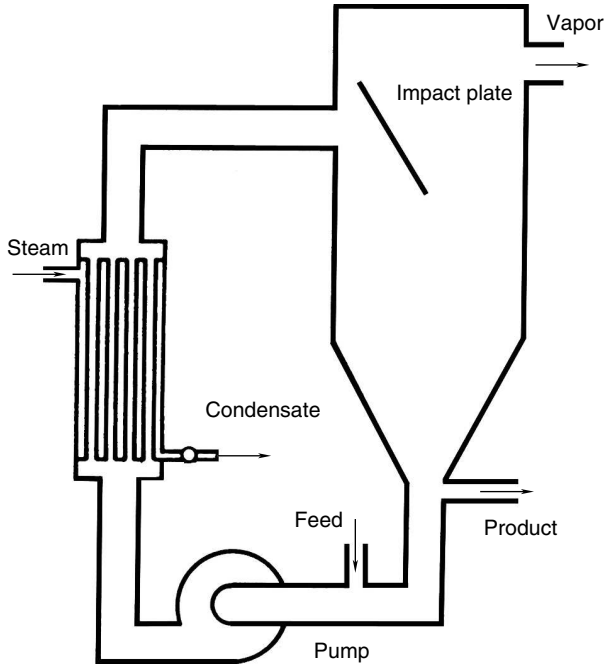

FIGURE 18.17
Forced circulation evaporator. (Adapted from Brennan, J.G. et al., *Los Operaciones de la Ingeniería de los Alimentos,* Acribia, Zaragoza, Spain, 1980.)

then enters the separation chamber, where baffle plates facilitate vapor separation. The concentrated liquid obtained can be directly extracted or mixed with nonconcentrated liquid and recirculated, or it can go into another evaporator where concentration can be increased.

Long tube evaporators can be of ascending film, falling film, or ascending–falling film. In ascending film evaporators, the liquid enters the bottom of the tubes; vapor bubbles that ascend through the center of the tube begin to form, creating a thin film on the tube wall that ascends at great velocity. In falling film evaporators, the feed is performed at the top of the tubes, so the vapor formed descends through the center of the tubes as a jet at great velocity. When high evaporation velocities are desired, ascending–falling film evaporators are used, where ascending film evaporation is used to obtain an intermediate concentration liquid with a high viscosity. This liquid is then further evaporated in tubes, where it circulates as falling film.

Generally, overall heat transfer coefficients are high. In film evaporators, the residence time of the liquid treated in the heating zone is short since it circulates at great velocity. The product is thus not greatly affected by heat; therefore, these evaporators are useful for evaporation of heat-sensitive liquids. Descendent film evaporators are widely used to concentrate milk products.

18.6.4 Plate Evaporators

Plate evaporators consist of a set of plates distributed in units in which vapor condenses in the channels formed between plates. The heated liquid boils on the surface of the plates, ascending and descending as a film. The liquid and vapor mixture formed goes to a centrifugal evaporator.

These evaporators are useful to concentrate heat sensitive products, since high treatment velocities are achieved, allowing good heat transfer and short residence times of the product in the evaporator. Also, plate evaporators occupy little space on the floor and are easily manipulated for cleaning, since setup and dismount are easy and quick. Plate evaporators are usually employed to concentrate coffee, soup broth, light marmalades, and citric juices.

Besides the evaporators described here, there are other types, such as expanded flow, scrape surface and those based on the functioning of the thermal pump used for evaporation of products very sensitive to heat.

Problems

18.1

A salt solution is concentrated from 5 to 40% in weight of salt. For this reason, 15,000 kg/h of the diluted solution are fed to a double-effect evaporator that operates under backward feed. The steam used in the first effect is saturated at 2.5 atm, maintaining the evaporation chamber of the second effect at a pressure of 0.20 atm. If feed is at 22°C, calculate: a) steam flow rate needed and economy of the system; b) heating area of each effect; c) temperatures and pressures of the different evaporation and condensation chambers.

Data: consider that only the 40% salt solution produces a boiling point rise of 7°C. The specific heat of the salt solutions can be calculated by the expression: $\hat{C}_P = 4.18 - 3.34\ X$ kJ/(kg·°C), where X is the mass fraction of salt in the solution. The global heat transfer coefficients of the first and second effect are, respectively, 1860 and 1280 W/(m² °C). Specific heat of water vapor is 2.1 kJ/(kg·°C).

The diagram of the double-effect evaporator is represented in Figure 18.P1.

Properties of the saturated steam:

$$P_w = 2.5 \text{ at} = 2452 \text{ mbar} \qquad T = 126.8°\text{C}$$

$$\hat{h}_w = 533 \text{ kJ/kg}$$

$$\hat{H}_w = 2716 \text{ kJ/kg} \qquad \lambda_w = 2183 \text{ kJ/kg}$$

$$P_2 = 0.2 \text{ atm} = 196 \text{ mbar} \qquad t_{b2} = 59.7°\text{C}$$

$$\hat{h}_{V2} = 250 \text{ kJ/kg}$$

$$\hat{H}_{V2} = 2609 \text{ kJ/kg} \qquad \lambda_{V2} = 2359 \text{ kJ/kg}$$

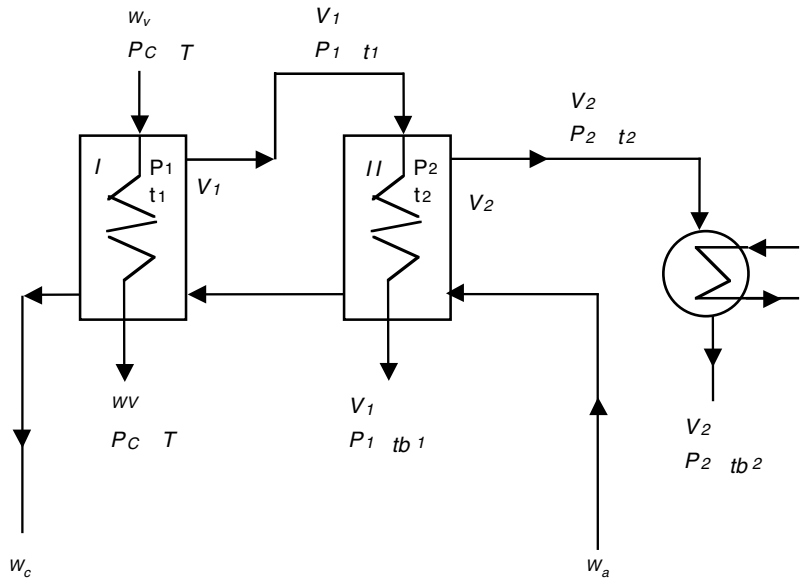

FIGURE 18.P1
Backward feed double effect evaporator.

Global and component mass balances:

$$15{,}000 = w_C + V_1 + V_2$$
$$(15{,}000)(0.05) = w_C(0.40)$$

obtaining:

$$w_C = 1875 \text{ kg/h} \quad \text{and} \quad V_1 + V_2 = 13{,}125 \text{ kg/h}$$

Initially, it is assumed that $V_1 = V_2 = 6562.5$ kg/h, supposing that the composition of the stream w_2 is $X_2 = 0.09$.

The specific heats of each stream are obtained from the equation given in the problem statement:

For $X_A = 0.05$, $\hat{C}_{PA} = 4.01$ kJ/(kg·°C).
For $X_C = 0.40$, $\hat{C}_{PC} = 2.84$ kJ/(kg·°C).
For $X_1 = 0.09$, $\hat{C}_{P1} = 3.88$ kJ/(kg·°C).

According to the statement of the problem, boiling point rise is only in the first effect, while it can be neglected in the second one, yielding that $t_2 = t_{b2} =$ 59.7°C.

In order to perform the calculation process, it is supposed that the areas and the heat flows transferred through these exchange areas are equal for the two effects, complying with (Equation 18.48):

$$\frac{\dot{Q}}{A} = \frac{T - t_{b2} - \Delta T_{b1}}{\frac{1}{U_1} + \frac{1}{U_2}} = \frac{(127.2 - 59.7 - 7)\,^{\circ}\mathrm{C}}{\left[\frac{1}{1860} + \frac{1}{1280}\right]\frac{\mathrm{m}^2\,^{\circ}\mathrm{C}}{\mathrm{W}}}$$

Hence, $\dot{Q}/A = 45{,}569$ W/m^2.

The temperature t_{e1} is obtained from the heat transfer rate equation in the second effect:

$$\dot{Q}/A = U_2\left(t_{b1} - t_2\right) \qquad t_{b1} = 95.3^{\circ}\mathrm{C}$$

The boiling temperature in the first effect is:

$$t_1 = t_{b1} + \Delta T_{b1} = 95.3 + 7 = 102.3\,^{\circ}\mathrm{C}$$

It is possible to find the properties of the saturated steam from the temperature $t_{b1} = 95.3°C$ and the saturated steam tables:

$$t_{b1} = 95.3^{\circ}\mathrm{C} \qquad P_1 = 855 \text{ mbar}$$

$$\hat{h}_{V1} = 399.3 \text{ kJ/kg}$$

$$\hat{H}_{V1} = 2668 \text{ kJ/kg} \qquad \lambda_{V1} = 2268.7 \text{ kJ/kg}$$

Enthalpy balances applied to both effects yield:

1st effect:

$$2183\, w_V = \left(2268.7 + (2.1)\cdot(7)\right)V_1 + (2.84)(1875)(102.3 - 95.3) - 3.88\, w_2(59.7 - 95.3)$$

2nd effect:

$$2268.7\, V_1 = 2359.4\, V_2 - (4.01)(15{,}000)(22 - 59.7)$$

Together with the following balance equations:

$$w_2 = w_A - V_2$$

$$V_1 + V_2 = 13{,}125$$

A four-equation system with four unknowns is obtained, which, when solved, yields:

$$w_V = 8102 \text{ kg/h} \qquad w_2 = 9056.5 \text{ kg/h}$$

$$V_1 = 7181.5 \text{ kg/h} \qquad V_2 = 5943.5 \text{ kg/h}$$

The value of the areas through which heat is transferred can be obtained by means of the equations of heat transfer rate through such areas:

1st effect:

$$8102\left(2183/3600\right) = 1.86\ A_1\left(126.8 - 102.3\right)$$

2nd effect:

$$7181.5\left(2268.7/3600\right) = 1.28\ A_2\left(95.3 - 59.7\right)$$

$$A_1 = 107.81 \text{ m}^2 \qquad A_2 = 99.32 \text{ m}^2$$

The mean area is A_m = 105.56 m^2. Since these areas differ by more than 2%, the calculation procedure should begin again, rectifying the intermediate temperatures t_1 and t_{e1}, since the other temperatures remain the same:

$$t_{b1} - 59.7 = \left(95.3 - 59.7\right)\left(A_2/A_m\right) \qquad t_{b1} = 93.8°\text{C}$$

$$126.8 - t_1 = \left(126.8 - 102.3\right)\left(A_1/A_m\right) \qquad t_1 = 101.3°\text{C}$$

Hence, t_{b1} = 101.3 – 7 = 94.3°C.

Since they are different, the mean value of each temperature is taken: t_{b1} = 94°C and t_1 = 101°C.

The new enthalpies for 94°C can be found in the saturated steam tables:

$$t_{b1} = 94°\text{C} \qquad P_1 = 815 \text{ mbar}$$

$$\hat{h}_{V1} = 393.8 \text{ kJ/kg}$$

$$\hat{H}_{V1} = 2666 \text{ kJ/kg} \qquad \lambda_{V1} = 2272.2 \text{ kJ/kg}$$

The four-equation system stated above is solved again using the new value of λ_{V1}, yielding:

$$w_V = 8090 \text{ kg/h} \qquad w_2 = 9051 \text{ kg/h}$$

$$V_1 = 7176 \text{ kg/h} \qquad V_2 = 5949 \text{ kg/h}$$

The areas are recalculated from the velocity equations:

$$A_1 = 102.22 \text{ m}^2 \qquad A_2 = 103.16 \text{ m}^2$$

(a) Economy of the system:

$$E = \frac{V_1 + V_2}{w_V} = \frac{13{,}125}{8090} = 1.62$$

(b) Area per effect:

$$A_m = 102.7 \text{ m}^2$$

(c) 1st effect:

$$P_C = 2452 \text{ mbar} \qquad T = 126.8°\text{C}$$

$$P_1 = 815 \text{ mbar} \qquad t_1 = 101.0°\text{C}$$

2nd effect:

$$P_1 = 815 \text{ mbar} \qquad t_{b1} = 94.0°\text{C}$$

$$P_2 = 196 \text{ mbar} \qquad t_2 = 59.7°\text{C}$$

18.2

A double-effect evaporator, operating under forward feed, is used to concentrate clarified fruit juice from 15 to 72 °Brix. The steam available from the boiler is saturated at 2.4 atm, and the vacuum pressure in the evaporation chamber of the second effect is 460 mm Hg. The diluted juice is fed into the evaporation chamber at a temperature of 50°C and a mass flow rate of 3480 kg/h. If the overall heat transfer coefficients for the first and second effects are 1625 and 1280 W/(m²·°C), respectively, determine: (a) steam flow rate from the boiler and economy of the system; (b) heating surface for each effect; and (c) temperatures and pressures in the condensation and evaporation chambers for each effect.

Data: properties of the fruit juices: the boiling point rise can be calculated according to the expression $\Delta T_b = 0.014\ C^{0.75}\ P^{0.1}\exp(0.034\ C)°C$, where C is the soluble solids content in °Brix and P is the pressure in mbar. The specific heat is a function of the mass fraction of water according to the equation:

$$\hat{C}_P = 0.84 + 3.34X_{WATER} \text{ kJ}/\left(\text{kg} \cdot °\text{C}\right)$$

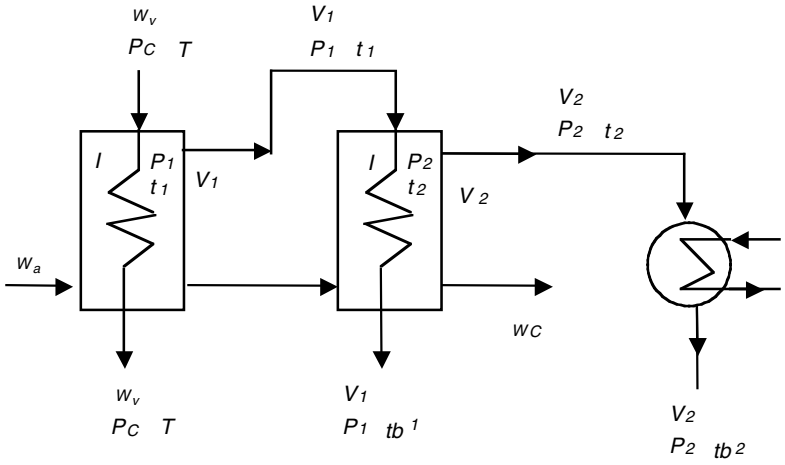

FIGURE 18.P2
Forward feed double-effect evaporator.

There is a vacuum pressure of 460 mm Hg in the evaporation chamber of the second effect, so its pressure is $P_2 = 300$ mm Hg.

Properties of the saturated steam:

$$P_w = 2.4 \text{ atm} = 2353 \text{ mbar} \qquad T = 125.5°\text{C}$$

$$\hat{h}_w = 527 \text{ kJ/kg}$$

$$\hat{H}w = 2713 \text{ kJ/kg} \qquad \lambda_w = 2186 \text{ kJ/kg}$$

$$P_2 = 300 \text{ mmHg} = 400 \text{ mbar} \qquad t_{b2} = 75.8°\text{C}$$

$$\hat{h}_{V2} = 317 \text{ kJ/kg}$$

$$\hat{H}_{V2} = 2637 \text{ kJ/kg} \qquad \lambda_{V2} = 2320 \text{ kJ/kg}$$

Figure 18.P2 shows a diagram of the double-effect evaporator that works under forward feed.

Global and component mass balances:

$$3480 = w_C + V_1 + V_2$$

$$(3480)(0.15) = (0.72)w_C$$

Yielding:

$$w_C = 725 \text{ kg/h} \quad \text{and} \quad V_1 + V_2 = 2755 \text{ kg/h}$$

Initially it is supposed that $V_1 = V_2 = 1377.5$ kg/h, which makes one assume that the composition of the stream w_2 is $X_2 = 0.248$, corresponding to a content of 24.8 °Brix.

The boiling point rises are calculated by the equation given in the data section. The concentration used is that of the stream leaving each effect:

1st effect:

$$C_1 = 24.8°\text{Brix} \qquad P_1 = ?$$

2nd effect:

$$C_2 = 72.0°\text{Brix} \quad P_2 = 400 \text{ mbar}$$

obtaining:

$$\Delta T_{b1} = 0.36\left(P_1\right)^{0.1} \qquad \Delta T_{b2} = 7.3°\text{C}$$

The boiling temperature of the second effect is:

$$t_2 = t_{b2} + \Delta T_{b2} = 75.8 + 7.3 = 83.1°\text{C}$$

P_1 should be known in order to obtain ΔT_{e1}, but it can be estimated. In case P_1 = 1000 mbar, the boiling point rise is ΔT_{e1} = 0.7°C.

The specific heat of each stream is obtained from the equation given in the statement of the problem:

For C_A = 15°Brix:

$$\hat{C}_{PA} = 3.68 \text{ kJ/}\left(\text{kg} \cdot °\text{C}\right)$$

For C_C = 75°Brix:

$$\hat{C}_{PC} = 1.78 \text{ kJ/}\left(\text{kg} \cdot °\text{C}\right)$$

For C_1 = 24.8°Brix:

$$\hat{C}_{P1} = 3.35 \text{ kJ/}\left(\text{kg} \cdot °\text{C}\right)$$

In order to perform the calculation procedure, it is supposed that the areas and the heat flows transferred through these exchange areas are equal for both effects, complying with:

$$\frac{\dot{Q}}{A} = \frac{T - t_{b2} - \Delta T_{b1} - \Delta T_{b2}}{\frac{1}{U_1} + \frac{1}{U_2}} = \frac{(125.5 - 75.8 - 0.7 - 7.3)^{\circ}\text{C}}{\left(\frac{1}{1625} + \frac{1}{1280}\right)\frac{\text{m}^2\,^{\circ}\text{C}}{\text{W}}}$$

Hence, $\dot{Q}/A$ = 29,858 W/m^2.

Temperature t_{e1} is obtained from the heat transfer rate equation for the second effect:

$$\dot{Q}/A = U_2(t_{e1} - t_2)$$

$$t_{b1} = 106.4^{\circ}\text{C}$$

and the boiling point in the first effect is:

$$t_1 = t_{b1} + \Delta T_{b1} = 106.4 + 0.7 = 107.1^{\circ}\text{C}$$

The properties of saturated steam can be found using the temperature t_{b1} = 106.4°C from the saturated steam tables:

$$t_{b1} = 106.4^{\circ}\text{C} \qquad P_1 = 1271 \text{ mbar}$$

$$\hat{h}_{V1} = 447 \text{ kJ/kg}$$

$$\hat{H}_{V1} = 2685 \text{ kJ/kg} \qquad \lambda_{V1} = 2238 \text{ kJ/kg}$$

If the boiling point rise in the first effect is recalculated using pressure P_1 = 1271 mbar, a slightly different value is obtained, so the same boiling point rise obtained before is taken.

Application of enthalpy balances to both effects yields:

1st effect:

$$(2186)w_V = (2238 + (2.1)(0.7)V_1 + w_1(3.35)(107.1 - 106.4) - (3480)(50 - 106.4)$$

2nd effect:

$$(2238)V_1 = V_2(2319 + (2.1)(0.7) + (725)(1.78)(83.1 - 75.8) - w_1(3.35)(107.1 - 75.8)$$

With the equations of the balances:

$$w_1 = w_A - V_1$$

$$V_1 + V_2 = 2755$$

a four-equation system with four unknowns is obtained that, when solved, yields:

$$w_V = 1726 \text{ kg/h} \qquad w_1 = 2120 \text{ kg/h}$$

$$V_1 = 1360 \text{ kg/h} \qquad V_2 = 1395 \text{ kg/h}$$

These new values are used to calculate the soluble solids content in the stream w_1, obtaining 24.6°Brix, which allows calculation of the specific heat and the boiling point rise: $\hat{C}_{P1}$ = 3.36 kJ/(kg·°C) and ΔT_{b1} = 0.7°C.

The value of the areas through which heat is transferred can be obtained by the equations of heat transfer rate through such areas:

1st effect:

$$(1725) \times (2186)/(3600) = (1.625) A_1 (125.5 - 107.1)$$

2nd effect:

$$(1360) \times (2238)/(3600) = (1.28)\ A_2 (106.4 - 83.2)$$

$$A_1 = 35.05 \text{ m}^2 \qquad A_2 = 28.35 \text{ m}^2$$

The mean area is A_m = 31.70 m². Since these areas are different by more than 2%, the calculation procedure should begin again, rectifying the intermediate temperatures t_1 and t_{b1} (Equations 18.49 to 18.51), as the other temperatures do not vary:

$$t_{b1} - 83.1 = (106.4 - 83.1)(A_2/A_m) \qquad t_{b1} = 103.9°\text{C}$$

$$125.5 - t_1 = (125.5 - 107.1)(A_1/A_m) \qquad t_1 = 105.2°\text{C}$$

With this temperature, it is obtained that:

$$t_{b1} = 105.2 - 0.7 = 104.6°\text{C}$$

Since they are different, the mean value of each one is taken, so:

$$t_{b1} = 104.2°\text{C} \quad \text{and} \quad t_1 = 104.9°\text{C}$$

The new enthalpies for 104.2°C can be found in the saturated steam tables:

$$t_{b1} = 104.2°\text{C} \qquad P_1 = 1177 \text{ mbar}$$
$$\hat{h}_{V1} = 437 \text{ kJ/kg}$$
$$\hat{H}_{V1} = 2682 \text{ kJ/kg} \qquad \lambda_{V1} = 2245 \text{ kJ/kg}$$

The four-equation system stated above is solved again, using the new value of λ_{V1}, yielding:

$$w_v = 1720.8 \text{ kg/h} \qquad w_2 = 2118.6 \text{ kg/h}$$
$$V_1 = 1361.4 \text{ kg/h} \qquad V_2 = 1393.6 \text{ kg/h}$$

The areas are recalculated from the rate equations:

$$A_1 = 31.22 \text{ m}^2 \qquad A_2 = 31.43 \text{ m}^2$$

(a) Mass flow rate of steam from the boiler:

$$w_V = 1720.7 \text{ kg/h}$$

Economy of the system:

$$E = \frac{V_1 + V_2}{w_V} = \frac{2755}{1720.8} = 1.6$$

b) Area per effect:

$$A_m = 31.33 \text{ m}^2$$

c) 1st effect:

$$P_C = 2353 \text{ mbar} \qquad T = 125.5°\text{C}$$
$$P_1 = 1177 \text{ mbar} \qquad t_1 = 104.9°\text{C}$$

2nd effect:

$$P_1 = 1177 \text{ mbar} \qquad t_{b1} = 104.2°\text{C}$$
$$P_2 = 400 \text{ mbar} \qquad t_2 = 83.1°\text{C}$$

18.3

Tamarind is an important culinary condiment used as an acidifying ingredient. Due to the cost of transport, it is convenient to obtain tamarind as a concentrated juice through an evaporation stage. An Indian industry desires to obtain 1000 kg/h of a 62°Brix of concentrated juice beginning with 10°Brix. For this reason, the possibility of installing a single effect with mechanical compression of steam or a double effect operating under forward feed is studied. The global heat transfer coefficients of the first and second effect are 2100 and 1750 W/(m² °C), respectively. The food is at 22°C, while the 62°Brix juice cannot withstand temperatures higher than 70°C. The industry has a saturated steam stream at 1.8 kg/cm² used to carry out the juice concentration. Calculate: (a) the 10 °Brix juice flow that can be concentrated and the consumption of steam at 1.8 kg/cm for both options; (b) the compression power, for the first option, if the isentropic performance of the compressor is 88%; (c) the more profitable option, if the cost of each m² of evaporator is $22 U.S., of each kW of compression power is $4 U.S., of each kW.h is $0.08 U.S., and of each kg of steam at 1.8 kg/cm² is 1 cent. Consider that the amortization of the equipment is estimated in 1 year.

Data and notes: juices with soluble solids content lower than 18°Brix do not present an appreciable boiling point rise. The plant functions 300 days a year, 16 hours daily. Specific heat of the tamarind juices:

$$\hat{C}_p = 4.18 + \left(6.84 \times 10^{-5} T - 0.0503\right) X_S \text{ kJ}/\left(\text{kg} \cdot \text{K}\right)$$

where X_S is the percentage of soluble solids and T is the temperature in Kelvin.

Single effect evaporation with mechanical compression:

The diagram of this type of installation corresponds to Figure18.6. The temperature in the evaporation chamber is t_1 = 70°C, while the boiling temperature of pure water is obtained from the graph of Dühring (Figure 18.3): t_{e1} = 66°C (ΔT_{b1} = 4°C).

The following conditions can be obtained from saturated steam tables:

$P_C = 1.8 \text{ atm} = 1765 \text{ mbar}$ $\quad T_C = 116.3°\text{C}$

$\hat{h}_w = 488 \text{ kJ/kg}$

$\hat{H}_w = 2700 \text{ kJ/kg}$ $\quad \lambda_w = 2212 \text{ kJ/kg}$

$t_{b1} = 66°\text{C}$ $\quad P_1 = 262 \text{ mbar} = 0.27 \text{ atm}$

$\hat{h}_{V1} = 276 \text{ kJ/kg}$

$\hat{H}_{V1} = 2619 \text{ kJ/kg}$ $\quad \lambda_{V1} = 2343 \text{ kJ/kg}$

The vapor that leaves the evaporation chamber is reheated to a temperature of t_1 = 70°C, with an enthalpy:

$$\hat{H}_1 = \hat{H}_{V1} + \hat{C}_{PV} \cdot \Delta T_{b1} = 2619 + (2.1)(4) = 2627.4 \text{ kJ/kg}$$

The compression of the vapor that leaves the evaporation chamber is an isentropic process (Figures 18.6 and 18.7) from point 1 at a 262 mbar isobar to point 2 at the 1765 mbar isobar. The conditions of point 2 corresponding to the vapor outlet at the compressor can be obtained by means of the graph:

$$P_2 = P_C = 1765 \text{ mbar} \qquad t_2 = 270°\text{C}$$
$$\hat{H}_2 = 3009 \text{ kJ/kg}$$

Vapor (V) with these conditions is reheated and mixed with the vapor coming out of the boiler (w'_V) that is saturated at the same pressure, yielding a reheated vapor mixture. In order to avoid this, part of the condensate (w_R) is recirculated to obtain a saturated vapor at point 3 (w_V), which is fed to the condensation chamber of the evaporator (Figures 18.6 and 18.7).

The specific heats of the food and concentrate streams are calculated at their respective concentrations:

Food:

$$C_A = 10°\text{Brix} \qquad \hat{C}_{PA} = 3.88 \text{ kJ/(kg} \cdot °\text{C)}$$

Concentrate:

$$C_C = 62°\text{Brix} \qquad \hat{C}_{PC} = 2.52 \text{ kJ/(kg} \cdot °\text{C)}$$

Mass balances:

$$w_A = w_C + V \qquad w_A = 1000 + V$$
$$w_A X_A = w_C X_C \qquad w_A 0.1 = w_C 0.62$$

obtaining:

$$w_A = 6200 \text{ kg/h} \qquad V = 5200 \text{ kg/h}$$

If an enthalpy balance is performed in the evaporator, it is possible to obtain the amount of the vapor w_V that gets into the evaporation chamber:

$$2212\ w_V = (5200)(2343) + (2.1)(4) + (100)(2.52)(4) - (6200)(3.88)(22 - 66)$$

$$w_V = 6010.2\ \text{kg/h}$$

When performing the mass and enthalpy balances around point 3, where the streams of steam from the boiler (w'_V), compressed vapor ($V_2 = V$), and recirculated condensate (w_R) get together, it can be obtained that:

$$6010.2 = w'_V + w_R + 5200$$

$$(6010.2)(2700) = w'_V (2700) + w_R (488) + (5200)(3009)$$

Solution of this system yields:

$$w'_V = 83.8\ \text{kg/h}$$

$$w_R = 726.4\ \text{kg/h}$$

The area of the evaporator is obtained from the heat transfer rate equation:

$$w_V \lambda_w = U_1 A (T_C - t_1)$$

$$(6010.2)(2212)/(3600) = (2.1) A (116.5 - 70)$$

Hence, the area is:

$$A = 37.82\ \text{m}^2$$

The theoretical compression power is obtained from the expression:

$$(Pow)_T = V (\hat{H}_2 - \hat{H}_1)$$

$$(Pow)_T = (5200/3600)(\text{kg/s})(3009 - 2627.4)\text{kJ/kg}$$

$$(Pow)_T = 551.2\ \text{kJ/kg}$$

The real power is obtained by dividing the theoretical power by the isentropic performance:

$$(Pow)_R = (551.2/0.88) = 62.4\ \text{kJ/kg}$$

The annual operation cost is calculated from the expression:

$$C = C_A\, A + C_P \left(Pow\right)_R C_{POWxh}\, h_T + C_V\, w'_V\, h_T$$

where C_A, C_P, C_V, and $C_{POW_{xh}}$ are the cost per m^2 of evaporator area, cost per compression power installed, cost of the waste of steam coming from the boiler, and operation cost of the compressor, respectively, while h_T denotes the annual operation hours.

Operation hours:

$$h_T = \left(16\right)\left(300\right) = 4800 \text{ h}$$

The annual cost is:

$$C = \left(22\right)\left(37.82\right) + \left(4\right)\left(626.4\right) + \left(0.08\right)\left(626.4\right)\left(4800\right) + \left(0.017\right)\left(83.8\right)\left(4800\right)$$

Hence: C = U.S. $250,713.

Forward feed double-effect evaporator:

This type of evaporator is similar to the one presented in Figure 18.P1. A vapor at a pressure P_C = 1.8 atm = 1765 mbar enters the condensation chamber of the first effect, while in the second effect the boiling temperature of the 62°Brix juice is t_2 = 70°C, so the boiling temperature of pure water is t_{b2} = 66°C (ΔT_{b2} = 4°C).

The following is obtained from the saturated steam tables:

$$P_C = 1.8 \text{ atm} = 1765 \text{ mbar} \qquad T_C = 116.3°\text{C}$$

$$\hat{h}_w = 488 \text{ kJ/kg}$$

$$\hat{H}_w = 2700 \text{ kJ/kg} \qquad \lambda_w = 2212 \text{ kJ/kg}$$

$$t_{b2} = 66°\text{C} \qquad P_2 = 262 \text{ mbar} = 0.27 \text{ atm}$$

$$\hat{h}_{V2} = 276 \text{ kJ/kg}$$

$$\hat{H}_{V2} = 2619 \text{ kJ/kg} \qquad \lambda_{V2} = 2343 \text{ kJ/kg}$$

The global and component mass balances yield:

$$w_A = 6200 \text{ kg/h} \qquad V_1 + V_2 = 5200 \text{ kg/h}$$

Initially it is supposed that $V_1 = V_2 = 2600$ kg/h, allowing the concentration of stream w_1 to be obtained, leaving the first effect: $C_1 = 17.2$°Brix, pointing out that there will not be an appreciable boiling point rise ($\Delta T_{b1} = 0$).

The specific heats of the different juice streams are:

Food:

$$C_A = 10°\text{Brix} \qquad \hat{C}_{PA} = 3.88 \text{ kJ}/(\text{kg} \cdot °\text{C})$$

Stream:

$$C_1 = 17.2°\text{Brix} \qquad \hat{C}_{P1} = 3.75 \text{ kJ}/(\text{kg} \cdot °\text{C})$$

Concentrate:

$$C_C = 62°\text{Brix} \qquad \hat{C}_{PC} = 2.52 \text{ kJ}/(\text{kg} \cdot °\text{C})$$

To perform the calculation process, it is supposed that the areas and heat flows transferred through such exchange areas are equal in both effects, complying with:

$$\frac{\dot{Q}}{A} = \frac{T - t_{b2} - \Delta T_{b2}}{\frac{1}{U_1} + \frac{1}{U_2}} = \frac{(116.3 - 66 - 4)°\text{C}}{\left(\frac{1}{2100} + \frac{1}{1750}\right)\frac{\text{m}^2 \, °\text{C}}{\text{W}}}$$

Thus, $\dot{Q}/A = 44{,}196$ W/m^2.

Temperature t_{e1} is obtained from the heat transfer rate equation in the second effect:

$$\dot{Q}/A = U_2(t_{b1} - t_2) \qquad t_{e1} = 95.3°\text{C}$$

and the boiling temperature in the first effect is:

$$t_1 = t_{b1} + \Delta T_{b1} = 95.3 + 0 = 95.3°\text{C}$$

It is possible to find the properties of saturated steam, using the temperature $t_{b1} = 95.3$°C, from saturated steam tables:

$$t_{b1} = 95.3°\text{C} \qquad P_1 = 855 \text{ mbar}$$

$$\hat{h}_{V1} = 399.3 \text{ kJ/kg}$$

$$\hat{H}_{V1} = 2668 \text{ kJ/kg} \qquad \lambda_{V1} = 2268.7 \text{ kJ/kg}$$

Thus, applying enthalpy balances to both effects:

1st effect:

$$(2212)w_V = (2268.7)V_1 + w_1(3.75)(0) - (6200)(3.88)(22 - 95.3)$$

2nd effect:

$$V_1(2268.7) = V_2(2343 + (2.1)(4) + (1000)(2.52)(70 - 66) - w_1(3.75)(95.3 - 66)$$

besides the equations of the balances:

$$w_1 = w_A - V_1 = 6200 - V_1$$
$$V_1 + V_2 = 2600$$

A four-equation system with four unknowns is obtained, which, when solved, yields:

$$w_V = 3425 \text{ kg/h} \qquad w_1 = 3637.8 \text{ kg/h}$$
$$V_1 = 2562.2 \text{ kg/h} \qquad V_2 = 2637.8 \text{ kg/h}$$

The composition of stream w_1 is recalculated, obtaining C_1 = 17°Brix, so there is no boiling point rise in the first effect ($\Delta T_{b1} = 0$), and its specific heat is almost the same as the one calculated before.

The value of the areas through which heat is transferred can be obtained from the heat transfer rate equations through such areas:

1st effect:

$$(3425)(2212)/(3600) = (2.16)A_1(116.3 - 95.3)$$

2nd effect:

$$(2562.2)(2268.7)/(3600) = (1.28)A_2(95.3 - 70)$$

$$A_1 = 47.72 \text{ m}^2 \qquad A_2 = 36.47 \text{ m}^2$$

and a mean area A_m = 42.10 m². Since these areas are different by more than 2%, the calculation procedure should begin again, rectifying the intermediate temperatures t_1 and t_{b1}, since the other temperatures remain the same:

$$t_{b1} - 70 = (95.3 - 70)(A_2/A_m) \qquad t_{b1} = 92.0°C$$

$$116.3 - t_1 = (116.3 - 95.3)(A_1/A_m) \qquad t_1 = 92.5°C$$

Since $\Delta T_{b1} = 0$, it is complied that $t_{e1} = t_1$.

Since they are different, the mean value of both is taken, thus: $t_{e1} = t_1 = 92.3°C$.

The new enthalpies for the temperature 92.3°C can be found in the saturated steam tables:

$$t_{b1} = 92.3°C \qquad P_1 = 770 \text{ mbar}$$

$$\hat{h}_{V1} = 387 \text{ kJ/kg}$$

$$\hat{H}_{V1} = 2662 \text{ kJ/kg} \qquad \lambda_{V1} = 2275 \text{ kJ/kg}$$

The four-equation system stated above is solved using the new value of λ_{V1}, obtaining:

$$w_V = 3405.4 \text{ kg/h} \qquad w_1 = 3632.3 \text{ kg/h}$$

$$V_1 = 2567.7 \text{ kg/h} \qquad V_2 = 2632.3 \text{ kg/h}$$

The areas are recalculated from the rate equations:

$$A_1 = 41.52 \text{ m}^2 \qquad A_2 = 41.58 \text{ m}^2$$

Thus, the mean area by effect is:

$$A_m = 41.55 \text{ m}^2$$

The annual cost is obtained from the expression:

$$C = C_A 2 A_m + w_V C_V h_T$$

Hence:

$$C = (22)2(41.55) + (3405.4)(0.017)(4800)$$

$$C = \text{U.S. } \$279{,}709$$

According to the result obtained, it is better to install one effect with vapor recompression, since the annual cost is lower.

19

Distillation

19.1 Introduction

Distillation is a unit operation with the objective of separation or fractionation, by vaporization, of a mixture of miscible and volatile liquids into its components. Such fractionation is made possible by taking advantage of the different vapor pressures of the components of the mixtures at certain temperatures. The distillation process is one of the more important unit operations in the chemical and petroleum industries, although it is also used in the food industries, for example, the alcohol industry, among others.

When there is interaction between the liquid and vapor phases, distillation is called rectification. When this interaction is not present, the operation is called simple distillation. When phases interact during rectification, the gas phase becomes richer in the more volatile (lighter) component, while the liquid phase becomes richer in the heaviest component. The contact between phases can be performed under equilibrium stages or by means of continuous contact. Other types of distillation are azeotropic and extractive distillation.

19.2 Liquid–Vapor Equilibrium

The transfer of material reaches a limit when equilibrium between phases is achieved; in other words, at that moment, the net transfer of one of the components ceases. Therefore, in order to reach a driving force for mass transfer, equilibrium should be avoided. It is very important to know when equilibrium between two phases occurs in order to evaluate the driving forces. The composition of a vapor in equilibrium with a liquid of a given composition is experimentally determined by an equilibrium distiller, called a boil-meter.

If binary mixtures formed by A and B are considered, with A the most volatile component, the graphic representation of equilibrium requires a

three-dimensional diagram. To make this clearer, a section at constant temperature and pressure are considered, obtaining an isothermal and an isobaric diagram, respectively.

Gibbs' phases rule is applied to a closed binary system in equilibrium: $L = C - F + 2$, where L is the number of degrees of freedom, C is the number of components, and F is the number of phases. In the case of a binary distillation, the number of components and phases is two, so the degrees of freedom will also be two. Thus, if two variables of the system are specified (temperature and composition, temperature and pressure, or pressure and composition), it will be determined by obtaining the values from the corresponding equilibrium diagram.

At constant pressure, two curves can be observed in the isobaric diagram or boiling point diagram. The upper curve reflects the variation of the composition of vapor with the boiling temperature of the liquid and is called the dew or condensation curve. The bottom curve, called the bubble or boiling point curve, shows the relationship between boiling temperature and the composition of the liquid at constant pressure. Both curves define three zones in the diagram (Figure 19.1). The first zone is located under the bubble-point curve; any point in the zone represents a liquid phase system. The second

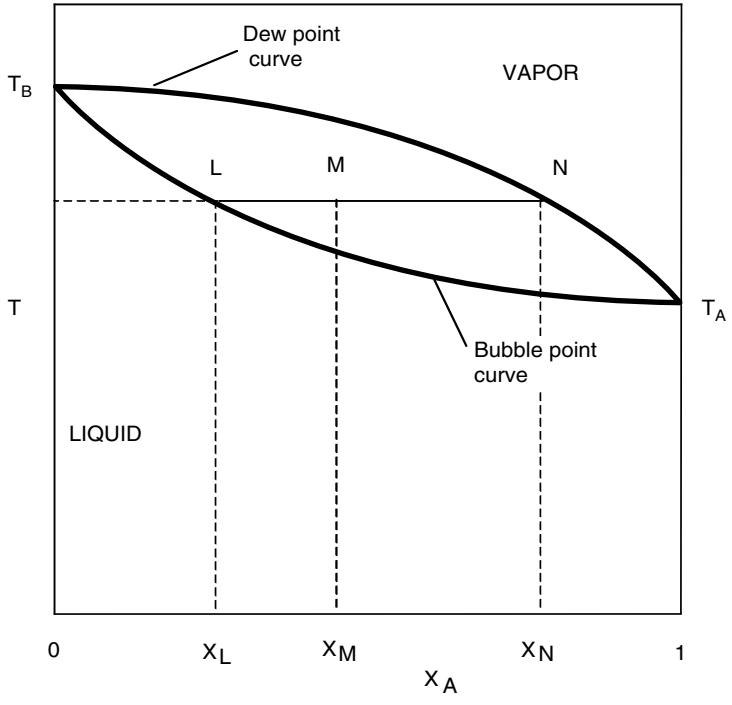

FIGURE 19.1
Temperature–composition diagram.

zone, in which any point indicates that the system represented is under vapor phase, is located over the dew-point curve. The third zone is located between both curves, dew point and bubble point, in which any point represents a system that consists of a mixture of two phases. Thus, point *M* of the diagram in this third zone represents a state in which the system is constituted by a mixture of a liquid of composition x_L and a vapor of composition x_N, with the global composition of the system x_M. The straight line *LN* is called the distribution line. The relative amount of both phases is related by the segments:

$$\frac{\text{moles of liquid}}{\text{moles of vapor}} = \frac{\overline{MN}}{\overline{ML}}$$

Systems exist in which the isobaric diagrams deviate from the ideal behavior in such a way that they show curves such as those in Figure 19.2. It can be observed that a minimum in the evaporation curve corresponding to the boiling point temperature of a mixture of composition x_Z is lower than that of the pure volatile component. The mixture of composition x_Z is known as azeotropic mixture or, simply, azeotrope. It can be seen that, in these types of mixtures, the pure components cannot be obtained in only one distillation stage, since, even when beginning with mixtures with composition higher or lower than x_Z, the azeotrope is always obtained as one of the two final streams. A binary system that behaves as azeotrope is water–ethanol. Besides this type of azeotrope with a minimum, there are azeotropic systems with a maximum.

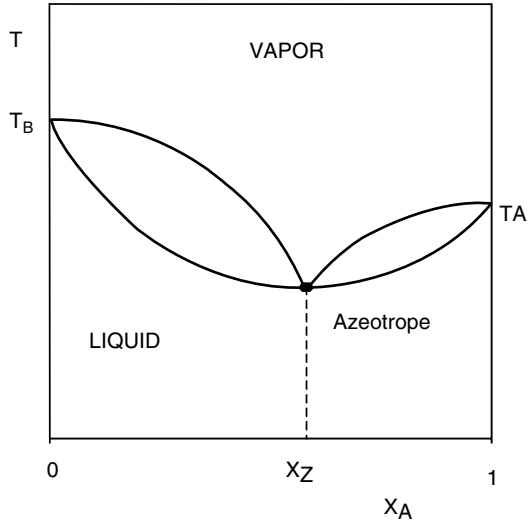

FIGURE 19.2
T–X diagram for an azeotropic binary system.

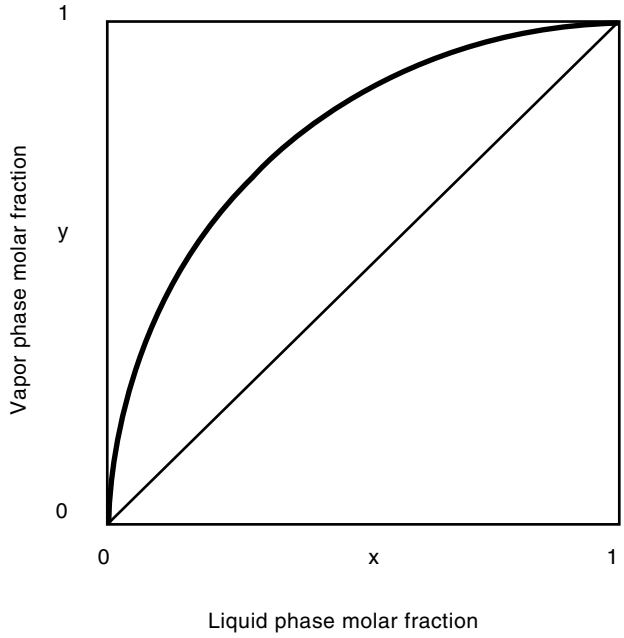

FIGURE 19.3
y–x equilibrium diagram.

Since industrial distillations take place basically at constant pressure, it is more adequate to represent the liquid–vapor compositions with a composition (*x–y*) diagram called an equilibrium diagram (Figure 19.3). Compositions are given in molar fractions representing those corresponding to the liquid phase on the abscissa, while the molar fractions of the gas phase are represented on the ordinate. In this diagram, the temperature of each point varies along the curve, and the union lines are represented by points. Since vapor is richer in the most volatile component, the curve is located over the diagonal. Separation of the components is easier as the distance between the equilibrium curve and the diagonal becomes greater and the difference between the composition of the liquid and the vapor increases.

The variation of pressure with composition at a constant temperature is represented with isothermal diagrams. Three zones are also observed in these diagrams: liquid, vapor, and liquid–vapor mixtures.

19.2.1 Partial Pressures: Laws of Dalton, Raoult, and Henry

Suppose a binary mixture of components *A* and *B*. The partial pressure P_A exerted by component *A* in such a mixture in vapor phase is the pressure that such a component would exert at the same temperature if it were occupying the same volume alone. The total pressure is the sum of the partial pressures of all the components:

$$P = \sum P_i$$

This equation represents the known law of Dalton for ideal mixtures, and it can be deduced that the partial pressure exerted by a component is proportional to the molar fraction of the component in the vapor phase:

$$P_i = y_i P \tag{19.1}$$

The law of Raoult relates the partial pressure of each component in the vapor phase with the molar fraction in the liquid phase in such a way that the proportionality factor is the vapor pressure of the pure component (P^o) at the same temperature:

$$P_i = x_i P^o \tag{19.2}$$

This relationship is normally complied with only at high values of x_i.

Ideal liquid–liquid solutions follow the laws of Raoult and Dalton over all concentration ranges of the components. In an ideal solution, two volatile liquids that dissolve without absorbing or releasing heat are mixed in such a way that their volumes result additive.

Henry's law relates the partial pressure exerted by the components in the vapor phase over the solution with the molar fraction in the liquid phase:

$$P_i = x_i H \tag{19.3}$$

H is the so-called Henry's constant. This law can be stated as follows: at constant temperature, the solubility of a gas in a liquid is directly proportional to the partial pressure of the gas in equilibrium with the solution. Once the constant temperature is assumed, the concentration of a gas dissolved in a liquid is directly proportional to the pressure that the gas exerts on the solution with which it is in equilibrium.

The law of Henry is complied, for a binary mixture in which A is the solute and B is the solvent, when x_A is small, i.e., for diluted solutions in which B is complied for small x_B values. If Henry's law can be applied to one component for a certain concentration range, it can be thermodynamically deduced that the law of Raoult can be applied to the other component in the same range of concentrations. For ideal solutions, both laws are equal and the constant of Henry coincides with the vapor pressure of the component under pure state.

The relationships stated above allow calculation of the equilibrium compositions in ideal liquid–vapor systems where the vapor pressures of the pure substances are known at different temperatures. Thus, for a binary system, given x_A, it is possible to calculate the composition y_A in the vapor

phase which is in equilibrium with x_A. When combining the expressions of the laws of Dalton and Raoult, the following equation is obtained:

$$P_A = x_A \frac{P_A^0}{P} \tag{19.4}$$

The molar fraction x_A can be calculated as:

$$P = P_A + P_B = x_A P_B^0 + x_B P_B^0 = x_A P_A^0 + \left(1 - x_A\right) P_B^0 \tag{19.5}$$

obtaining:

$$x_A = \frac{P - P_B^0}{P_A^0 - P_B^0} \tag{19.6}$$

19.2.2 Relative Volatility

Volatility can also be used to relate the equilibrium compositions between gas and liquid phases. The volatility of a component is defined as the relation between the partial pressure in the gas phase and its molar fraction in the liquid phase:

$$\alpha = \frac{P_i}{x_i} \tag{19.7}$$

For a binary mixture, the relative volatility of one component with respect to the other is defined as the ratio between the volatilities of each one of the components:

$$\alpha = \frac{\alpha_A}{\alpha_B} = \frac{P_A x_B}{P_B x_A} \tag{19.8}$$

and since:

$$P_A = y_A P \qquad P_B = y_B P$$

$$y_B = 1 - y_A \qquad x_B = 1 - x_A$$

the relative volatility is:

$$\alpha_{AB} = \frac{y_A \left(1 - x_A\right)}{x_A \left(1 - y_A\right)} \tag{19.9}$$

This equation permits one to obtain the value of the molar fraction in the liquid phase:

$$y_A = \frac{\alpha_{AB}\, x_A}{1+\left(\alpha_{AB}-1\right) x_A} \tag{19.10}$$

It is possible to build the equilibrium curve from this equation because, when values are given to the composition in the liquid phase, the corresponding value in the gas phase is obtained.

The fractionation of the mixture will be easier as the value of relative volatility becomes greater. When this value is 1, no separation will be achieved. In an ideal system, the absolute volatility of each component is equal in number to the vapor pressure of the pure component. Therefore, the relative volatility is $\alpha_{AB} = P_A^o/P_B^o$.

Relative volatility varies with temperature so that when the latter decreases, the former increases. When calculating the equilibrium curve from the relative volatility, an average value should be taken along the column. This is valid if the volatilities on the upper and lower extremes of the column differ by less than 15%. When this is not true, the equilibrium curve should be built for different sections so that the relative volatility is the same in each section.

In some cases, the equilibrium relationship between both phases is given by an equation of the type $y_i = K\, x_i$, in which K_i is, in many cases, constant for a wide range of temperatures.

19.2.3 Enthalpy Composition Diagram

The mixing, latent, and sensible heats of the components of the mixture should be taken into account in some distillation problems. In the case of binary mixtures, all magnitudes and equilibrium data can be represented in graphic form in the so-called enthalpy–composition diagram.

In this type of diagram, the molar composition (or mass composition) of the more volatile component is represented on the abscissa, and the specific enthalpies (kJ/kg or kJ/kmol) corresponding to each composition are represented on the ordinate. These enthalpies are referred to as the reference state of liquid water at 0°C and 1 atm.

Figure 19.4 presents a typical enthalpy–composition diagram for a binary mixture. The molar or mass fraction of the vapor (y) and of the liquid (x) are represented on the abscissa, while the enthalpies of vapor $\hat{H}$ and of liquid $\hat{h}$ are represented on the ordinate. When representing the enthalpy of the saturated liquid $\hat{h}$ against the composition, the line corresponding to the saturated liquid or bubble-point curve is obtained. If the enthalpy of the vapor $\hat{H}$ is represented, then the saturated vapor line or dew point curve is obtained.

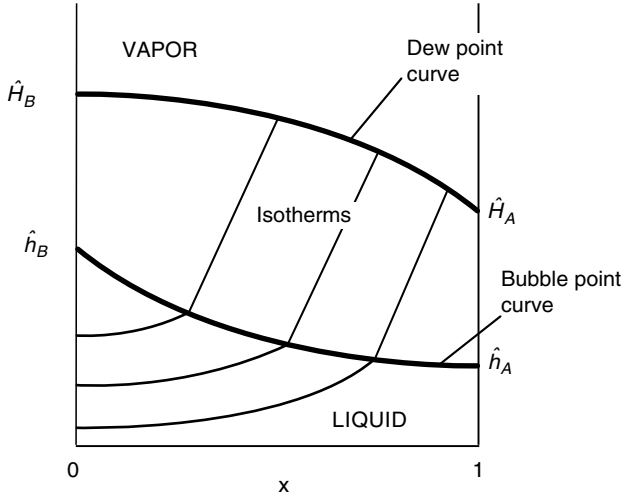

FIGURE 19.4
Enthalpy–composition diagram.

19.3 Distillation of Binary Mixtures

There are different distillation methods for binary mixtures. Simple and flash distillation will be described in this section, while continuous and discontinuous rectification methods are described in detail in later sections.

19.3.1 Simple Distillation

The simple open or differential distillation works in a batch fashion in one stage only (Figure 19.5), as follows: a kettle is loaded with the mixture to be distilled and vapors are formed by supplying heat. Vapors are withdrawn continuously so that condensate does not return to the kettle. Initially, the vapors formed will contain a high percentage of the most volatile component. The composition of the mixture in the kettle varies continuously so that the fraction of the heaviest component increases and there is no steady state. Since heat is supplied to the kettle at a constant rate, the boiling temperature of the load will increase as it becomes poor in the most volatile component. In order to obtain the mathematical model of this operation, the balances detailed next should be performed.

A global molar balance is carried out:

$$\frac{d(L+V)}{dt} = -D \tag{19.11}$$

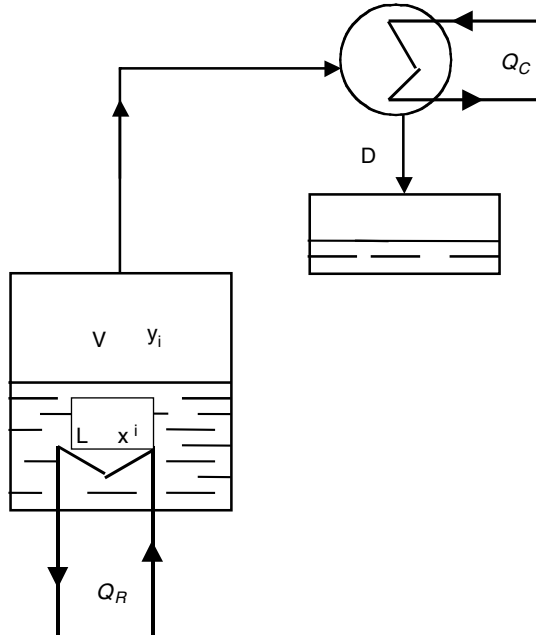

FIGURE 19.5
Simple distillation.

where L and V are the molar quantities of liquid and vapor respectively in the kettle, while D is the amount of distillate obtained. The molar density of vapor is much lower than that of liquid, and where V is not so high, the last equation can be expressed as: $dL/dt = -D$.

Balance of the volatile component:

$$\frac{d\left(Lx + Vy\right)}{dt} = -Dy \tag{19.12}$$

but, since $dL/dt = -D$,

$$\begin{aligned} L\frac{dx}{dt} + x\frac{dL}{dt} &= y\frac{dL}{dt} \\ \left(y-x\right)\frac{dL}{dt} &= L\frac{dx}{dt} \end{aligned} \tag{19.13}$$

A differential time range is complied with:

$$\frac{dL}{L} = \frac{dx}{y-x} \tag{19.14}$$

This is a differential equation with separable variables. If one begins with L_0 moles of composition x_0, the integration of this equation yields the expression:

$$\ln\left(\frac{L}{L_0}\right) = \int_{x_0}^{x} \frac{dx}{y-x} \tag{19.15}$$

This expression is called Rayleigh's equation. The integral term can be calculated graphically or numerically if the equilibrium relationship between the compositions of the vapor and liquid phases is known for the initial and final temperatures. If $1/(y-x)$ is plotted against x, then the value of the integral term between the compositions x_0 and x, initial and final, respectively, is obtained.

When the equilibrium relationship is linear, that is, if $y = mx + c$ is complied with, the integral term has an analytical solution:

$$\frac{L}{L_0} = \left(\frac{y-x}{y_0-x_0}\right)^{1/(m-1)} \tag{19.16}$$

If the equilibrium relationship is $y = Kx$, the following equation is obtained:

$$\frac{L}{L_0} = \left(\frac{x}{x_0}\right)^{1/(K-1)} \tag{19.17}$$

When it can be assumed that the relative volatility is constant, the integral term also has an analytical solution, obtaining the expression:

$$\ln\left(\frac{Lx}{L_0 x_0}\right) = \alpha \ln\left(\frac{L(1-x)}{L_0(1-x_0)}\right) \tag{19.18}$$

19.3.2 Flash Distillation

Flash distillation, also called closed or equilibrium distillation, consists of the evaporation of a certain amount of liquid in such a way that the vapor generated is in equilibrium with the residual liquid. The vapor is withdrawn and condensed separately. Flash distillation is schematized in Figure 19.6. A mixture with L_0 mol and composition x_0 is introduced in a chamber where the pressure is lower than that of the mixture. In this way, V mol of vapor with composition y and L mol of liquid with composition x are separated. The compositions y, x of the separated phases are in equilibrium.

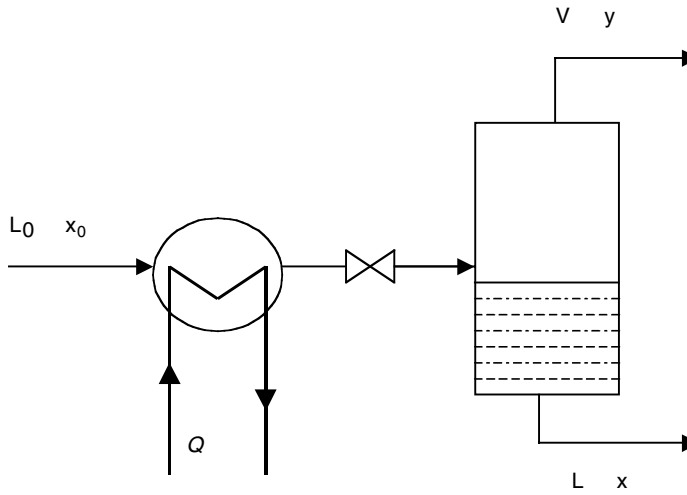

a)

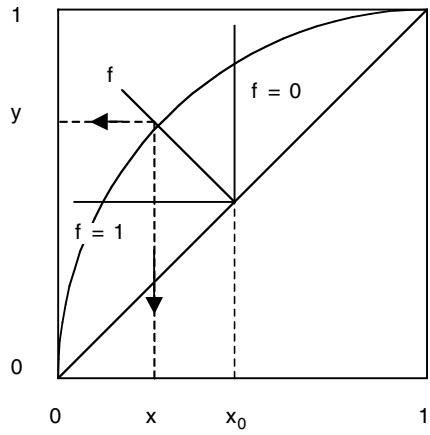

b)

FIGURE 19.6
Flash distillation: (a) installation sketch; (b) operation on the equilibrium diagram.

The following expressions are obtained from the global balance and the volatile component:

$$L_0 = V + L$$

$$L_0 x_0 = V y + L x$$

Hence:

$$y = -\left(\frac{L}{V}\right)x + \left(\frac{L+V}{V}\right)x_0 \tag{19.19}$$

If f is the fraction of mol of feed vaporized, $f = V/L_0$; then:

$$y = -\frac{1-f}{f}x + \frac{x_0}{f} \tag{19.20}$$

The $y - x$ diagram corresponds to the equation of a straight line that connects the composition of the initial mixture with the separated vapor and liquid streams. Therefore, if it is desired to know the compositions of such streams, a straight line with slope $-(1-f)/f$ is plotted from the diagonal of abscissa x_0. The desired compositions are obtained at the point where this straight line cuts across the equilibrium curve (Figure 19.6).

Where $f = 0$, no vapor stream is generated and the mixture is not separated. If $f = 1$, the whole mixture is vaporized, obtaining only a phase change without fractionation of the mixture.

19.4 Continuous Rectification of Binary Mixtures

In every distillation process the vapor formed in the kettle is richer in the more volatile component than in the remaining liquid. However, the vapor contains a certain amount of both components and the distillate is rarely a pure substance. In order to increase the concentration of the more volatile component in the vapor and to separate the less volatile one, the vapor is brought into contact with a stream of boiling liquid that runs down the column. A stream of liquid with a high concentration of the volatile component, called reflux, is introduced at the top of the column. The most volatile components are concentrated in the vapor phase and the least volatile in the liquid phase. This way, the vapor phase becomes richer in the most volatile component as it goes up the column, while the liquid phase becomes richer in the heavier component as it descends the column.

The separation achieved in the mixture between the top and bottom products depends on the relative volatilities of the components, number of contact stages, and reflux ratio. This process is called rectification and is performed in fractionating columns that operate in a continuous mode. Figure 19.7 shows a typical diagram of a rectification column. In these columns, heat $\dot{Q}_R$ is supplied to the kettle, generating a stream of vapor that rises. The vapor withdrawn from the top of column V_D is condensed and driven in a liquid

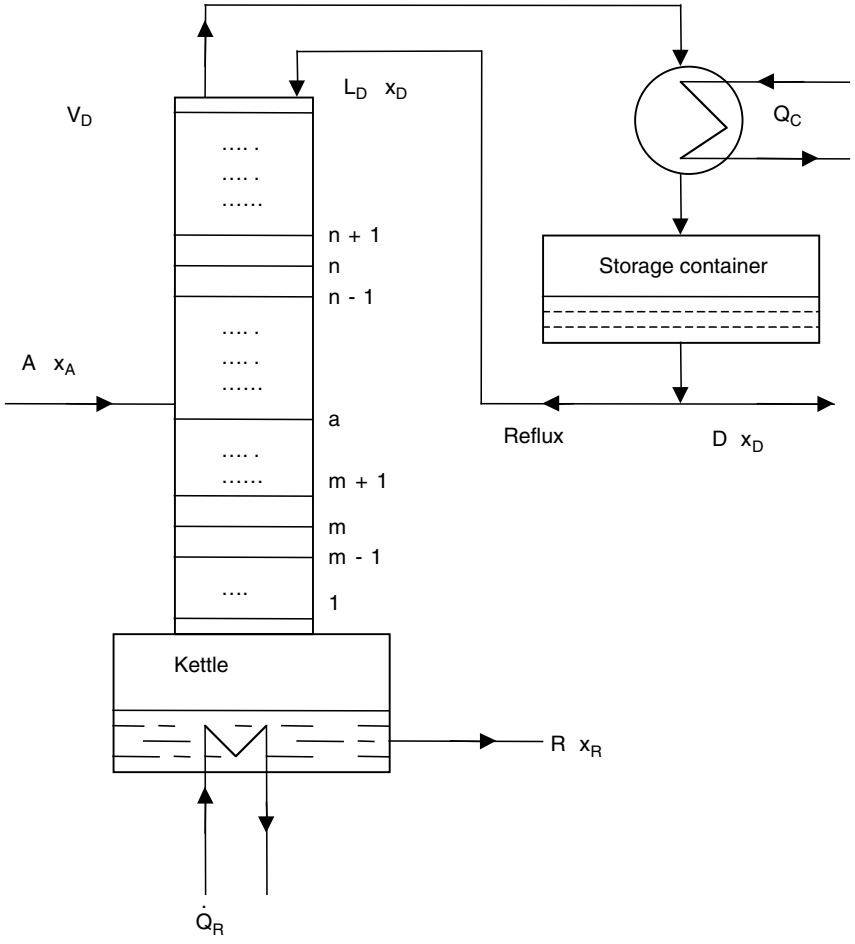

FIGURE 19.7
Rectification column.

state to a storage container. Part of this condensate is obtained as distillate product D, rich in the most volatile component, while part L_D is returned to the column by introducing it at the top in the form of reflux. Liquid coming from the column reaches the kettle, withdrawing the excess as waste stream R, rich in the heaviest component. The column is fed in a continuous form by a stream A, which is the mixture to be distilled. The plate in which feed is introduced divides the column into two parts; the top is the rectification, or enrichment, zone and the bottom is the exhaust zone. In the rectification or enrichment zone, vapor becomes richer in the most volatile component, eliminating part of the heaviest component from the vapor going up the column. In the exhaust zone, the most volatile component is eliminated from the liquid going down the column.

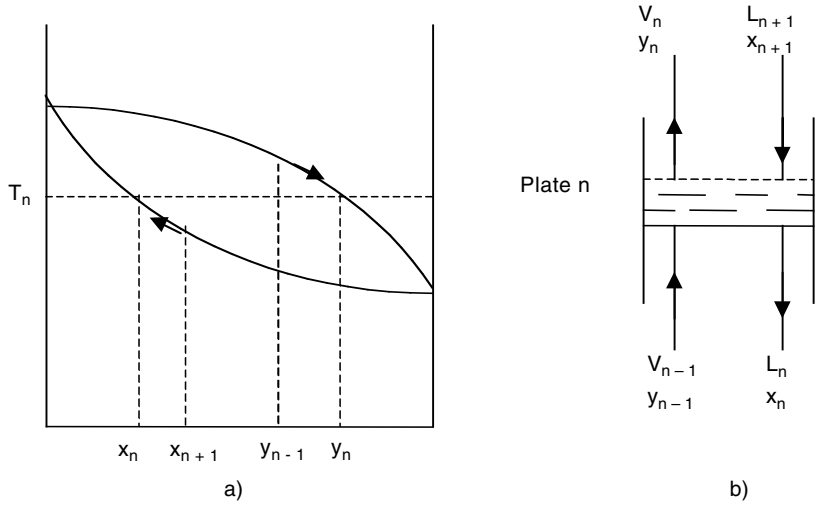

FIGURE 19.8
Evolution of the concentrations of phases in a plate *n*.

The system tends to reach equilibrium in each plate of the column. Vapor going up and liquid going down in each plate are not in equilibrium. The heaviest component condenses from the vapor going up, and its latent heat of condensation is used to vaporize part of the most volatile component from the reflux stream, so the vapor becomes richer in the most volatile component, while the reflux stream becomes poorer in the most volatile component. The result is that the streams leaving each plate tend to the equilibrium. Figure 19.8 shows the process towards equilibrium in a plate at a temperature T_n.

19.4.1 Calculation of the Number of Plates

When designing equipment to yield a given fractionation, a mathematical model to calculate the number of plates is needed. Other basic factors to design a distillation unit are number of plates, diameter of the column, heat to be supplied to the kettle, and heat to be removed from the condenser. Analysis of the functioning of the columns of plates is based on the setup and solution of mass and energy balances.

19.4.1.1 Mathematical Model

In order to set up the mathematical model, it is assumed that the column is perfectly isolated; heat losses to the exterior are considered null. Also, an ideal system is one in which mixing heat is considered zero. The balances will be applied to a rectification column such as that shown in Figure 19.7. The mathematical model will be obtained when carrying out the balances

around the different parts of the column. Also, molar units will be used to make calculations of distillation problems easier. The enthalpies of the vapor streams are represented by $\hat{H}$, while those of liquid are indicated by $\hat{h}$. The different compositions and variables have the subscripts of the corresponding streams.

Global balance around the column:
The global and component molar balances, as well as the energy global balance, allow one to obtain:

Global balance:

$$A = D + R \tag{19.21}$$

Volatile component balance:

$$Ax_A = Dx_D + Rx_R \tag{19.22}$$

Energy balance:

$$A\hat{H}_A + \dot{Q}_R = D\hat{h}_D + R\hat{h}_R + \dot{Q}_D \tag{19.23}$$

where A, D, and R are the molar streams of the feed, distillate, and waste, respectively.

Balances around the condenser:
The balances performed around the condenser are:

$$V_D = L_D + D \tag{19.24}$$

$$V_D y_D = L_D x_D + Dx_D \tag{19.25}$$

If condensation is total, it complies with $y_D = x_D$

$$V_D\hat{H}_D = \left(L_D + D\right)\hat{h}_D + \dot{Q}_D \tag{19.26}$$

The heat removed in the condenser is:

$$\dot{Q}_D = V_D\,\hat{H}_D - \left(L_D + D\right)\hat{h}_D = V_D\left(\hat{H}_D - \hat{h}_D\right) \tag{19.27}$$

When the vapor entering the condenser V_D is at its dew point, the enthalpies of the vapor $\hat{H}_D$ and of the liquid $\hat{h}_D$ are at their saturation point, thus complying with $\hat{H}_D - \hat{h}_D = \lambda_C$, which is the latent heat of condensation of the

vapor mixture that reaches the condenser. Therefore, the amount of heat eliminated in the condenser is:

$$\dot{Q}_D = \lambda_C V_D \tag{19.28}$$

Balances around the kettle:
When performing the balances around the kettle, it is obtained that:

$$L_1 = R + V_R \tag{19.29}$$

$$L_1 x_1 = R x_R + V_R y_R \tag{19.30}$$

$$L_1 \hat{h}_1 + \dot{Q}_R = R \hat{h}_R + V_R \hat{H}_R \tag{19.31}$$

Thus, the heat that should be supplied to the kettle is:

$$\dot{Q}_R = R \hat{h}_R + V_R \hat{H}_R - L_1 \hat{h}_1 \tag{19.32}$$

It is important to point out that the enthalpies of the different streams that appear in the last equation depend not only on temperature, but also on composition. Therefore:

$$\hat{h}_R = \hat{h}_R(x_R, T_R) \qquad \hat{H}_R = \hat{H}_R(y_R, T_R) \qquad \hat{h}_1 = \hat{h}_1(x_1, T_1)$$

It is easy to observe in Equation 19.32 that heat $\dot{Q}_R$ is not obtained directly from the condensation heat of the mixture in the kettle, since it is the difference between the enthalpies of the vapor and the liquid of the waste, but at the same composition y_R and temperature T_R:

$$\lambda_R = \hat{H}_R(y_R, T_R) - \hat{h}_R(y_R, T_R)$$

When the enthalpy of the liquid is only a function of temperature, assuming the sensible heats as negligible, it is complied that:

$$\dot{Q}_R = \lambda_R V_R \tag{19.33}$$

Balances around the enrichment zone:
The balances are applied between a plate n (excluding it) and the upper part of the column.

$$V_n - L_{n+1} = V_D - L_D = D \tag{19.34}$$

$$V_n y_n - L_{n+1} x_{n+1} = V_D y_D - L_D x_D = D x_D \tag{19.35}$$

$$V_n \hat{H}_n - L_{n+1} \hat{h}_{n+1} = V_D \hat{H}_D - L_D \hat{h}_D \tag{19.36}$$

Balances around the exhaust zone:
The balances are carried out between a plate *m* (including it) and the bottom of the column.

$$V_m + R = L_{m+1} \tag{19.37}$$

$$V_m y_m + R x_R = L_{m+1} x_{m+1} \tag{19.38}$$

$$V_m \hat{H}_m + R \hat{h}_R = L_{m+1} \hat{h}_{m+1} - \dot{Q}_R \tag{19.39}$$

Balances around the feed plate:
The balances applied to this plate yield the following equations:

$$A = V_a - L_{a+1} + L_a - V_{a-1} = D - R \tag{19.40}$$

$$A x_A = V_a y_a - L_{a+1} x_{a+1} + L_a x_a - V_{a-1} y_{a-1} \tag{19.41}$$

$$A \hat{H}_A = V_a \hat{H}_a - L_{a+1} \hat{h}_{a+1} + L_a \hat{h}_a - V_{a-1} \hat{H}_{a-1} \tag{19.42}$$

19.4.1.2 Solution of the Mathematical Model: Method of McCabe–Thiele

Once the mathematical model is set up, the next step is to solve it with the corresponding data. Generally, data include feed flow A and the compositions of feed x_A, of the waste x_R, and of the distillated x_D.

There are three solution methods for the mathematical model. One is the Ponchon–Savarit method, in which the enthalpy diagram is employed. The Lewis–Sorel method analytically determines the number of theoretical stages by step-by-step calculation. However, only the McCabe–Thiele method will be described in detail in this section.

In order to apply the method of McCabe–Thiele to calculate the number of theoretical plates of a distillation column, the following hypotheses must be verified:

- The specific heats of all liquids and vapors are constant and equal.
- The latent heats of vaporization are constant and equal.
- The mixing heats are null.
- The column works in an adiabatic form.

If, in the enthalpy–composition diagram, the lines of saturated vapor and liquid are parallel straight lines, then the liquid and vapor flows in each zone are constant. This is complied by binary mixtures of organic substances in which the molar latent heats are similar. If the stated hypotheses are complied, then it will also be complied that, since the molar heat of vaporization is constant, when V_{n-1} mol of vapor condense, they will give off a quantity of heat sufficient to vaporize V_n mol, hence $V_{n-1} = V_n$. This means the molar flow of vapor is constant along all the sections of the zone considered. It can be demonstrated that $L_n = L_{n+1}$ from the enthalpy balance. In general, V_n and L_n are constant in the enrichment zone, and V_m and L_m are constant in the exhaust zone.

Feed condition is an important datum in distillation operations. The fraction of feed in liquid form is defined as q. Therefore, when feed enters into the feed plate, the fraction $q.A$ will join the liquid stream that goes down the column. If the hypotheses stated before are taken into account, then the following is obtained when performing a balance in this plate:

$$L_m = L_n + q\,A \tag{19.43}$$

$$V_m = V_n + (q-1)A \tag{19.44}$$

The enthalpy balance in this plate yields (Equation 19.42):

$$A\hat{H}_A = V_a\hat{H}_a - L_{a+1}\hat{h}_{a+1} + L_a\hat{h}_a - V_{a-1}\hat{H}_{a-1}$$

When it is complied that the liquid and vapor streams are constant in each zone, and from the previous equations, it is obtained that:

$$A\left(\hat{H}_A + (q+1)\hat{H}_a - q\,\hat{h}_a\right) = V_n\left(\hat{H}_a - \hat{H}_a\right) + L_n\left(\hat{h}_a - \hat{h}_a\right) = 0$$

hence:

$$q = \frac{\hat{H}_a - \hat{H}_A}{\hat{H}_a - \hat{h}_a} \tag{19.45}$$

When the temperature of the feed plate T_a is the same as that of feed T_A, it is observed that the condition of feed q is the relationship between the heat needed to evaporate one mol of feed and the molar latent heat of feed:

$$q = \frac{\text{heat to evaporate 1 mol of feed}}{\text{molar latent heat of feed}}$$

The molar balances of the enrichment zone permit one to obtain Equation 19.35, taking into account that the hypotheses stated before are complied with: $V_n = V_D$ and $L_n = L_D$. It is obtained that:

$$y_n = \frac{L_D}{V_D} x_{n+1} + \frac{D x_D}{V_D} \tag{19.46a}$$

This expression is the equation of a straight line in the $y - x$ equilibrium diagram, known as the enrichment line. This straight line relates the composition of the vapor in plate n with that of the liquid of the above plate $n + 1$.

If the reflux relation $r = L_D/D$ is defined as the relationship between the molar streams of the liquid going back to the column as reflux and that of distillate stream (the previous equation), another way to express the enrichment line can be as:

$$y_n = \frac{r}{r+1} x_{n+1} + \frac{x_D}{r+1} \tag{19.46b}$$

In the x–y diagram, this straight line passes through points (x_D, x_D) and (0, $Dx_{D/}V_D$), and has slope L_D/V_D.

Equation 19.38 was obtained from the balance of the most volatile component around the exhaust zone. If the hypotheses of McCabe–Thiele are taken into account, and if Equations 19.43 and 19.44 are substituted in the last equation, it is obtained that:

$$y_m = \frac{L_n + q A}{V_n + (q-1)\ A} x_{m+1} - \frac{R x_R}{V_n + (q-1) A} \tag{19.47}$$

This expression is the equation of a straight line in the x–y equilibrium diagram that passes by the point (x_R, x_R) and has a slope equal to L_m/V_m. Also, it correlates the composition of the vapor leaving plate m with the composition of the liquid coming from the plate $m + 1$ above.

The intersection point of the enrichment and exhausting operating lines is obtained when solving the system formed by Equations 19.46a and 19.47. The following is obtained when solving such a system:

$$y = \frac{q}{q-1} x - \frac{x_A}{q-1} \tag{19.48}$$

where the equation of a straight line represents the geometric place where the operating lines intersect as a function of the condition q of the feed. This

equation is called line q. Line q passes over the point (x_A, x_A) and has a slope $m = q/(q-1)$. Therefore, if the enrichment operating line is known when joining the point of intersection of the enrichment line on line q with the point (x_R, x_R), the exhaust operating line is obtained.

Depending on the condition of the feed, the value of q as well as the slope of line q will be different:

$q > 1$ subcooled liquid	$1 < m < \infty$
$q = 1$ liquid at bubble point	$m = \infty$
$0 < q < 1$ liquid–vapor mixture	$\infty > m > 0$
$q = 0$ vapor at dew point	$m = 0$
$q < 0$ overheated vapor	$1 > m > 0$

The number of plates or theoretical stages can be determined, according to the McCabe–Thiele method, as follows:

The operating lines are plotted in the x–y diagram. Steps are drawn, beginning on the top from point (x_D, x_D) between the operating line of the enrichment zone and the equilibrium curve, to exceeding line q of feed. The steps are drawn from this point, using the operating line of the exhaust zone until the point (x_R, x_R) is exceeded. The fraction of a stage that can appear is taken as a whole (Figure 19.9).

It is convenient to evaluate, out of infinite solutions, the optimum plate at which feed should be introduced, i.e., that which gives rise to the least number of plates. The optimum condition is achieved by introducing feed when the intersection point of the operating lines (x_a^*, y_a^*) is exceeded.

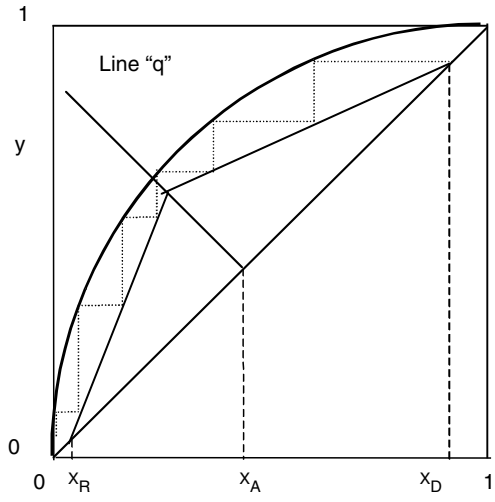

FIGURE 19.9
Calculation of the number of plates by the McCabe–Thiele method.

The McCabe–Thiele method assumes that the molar flow rate in each zone of the column is constant. In most cases, it can be supposed that this is true, since the molar heats of many systems differ by less than 10%. This method cannot be applied in cases in which the operating lines show a marked curvature. It should also not be applied when the relative volatility is lower than 1.3 or higher than 5, or when the reflux ratio is lower than 1.1 (the minimum) or when more than 25 plates are required.

19.4.2 Reflux Ratio

As stated above, the reflux relationship is defined as the quotient between the amount of reflux returned to the column at the top in liquid form and the amount of distillated product obtained: $r = L_D/D$. The enrichment line can be expressed as a function of the reflux relationship (Equation 19.46b) as:

$$y_n = \frac{r}{r+1} x_{n+1} + \frac{x_D}{r+1} \tag{19.46b}$$

Therefore, if the reflux relationship varies, the slope of the operating line will be modified, yielding a variation in the number of plates required for a given fractionation. When the reflux relationship r is known, the enrichment line can be obtained by joining the points with coordinates (x_D, x_D) and $(0, x_D/(r + 1))$.

When all the distillate is returned to the column as reflux, it is said that the column works at total reflux. Since no distillate ($D = 0$) is obtained, the operating line for the enrichment zone has a slope equal to one and ordinate to an origin equal to zero. Thus, this line has an equation $y = x$, coinciding with the diagonal.

If the reflux relationship decreases, it is implied that the number of plates will increase as the slope of the operating line decreases. If r decreases, then, at a given moment, the operating line intersects the equilibrium line on the point at which the value of composition is exactly x_A. If the reflux relationship decreases below this value, it is not possible to reach the feed plate.

When the enrichment operating line intersects the equilibrium line, the number of plates to reach a feed with composition x_A is infinite.

19.4.2.1 Minimum Reflux Relationship

As discussed earlier, there is a value of the reflux relationship below which it is not possible to perform a given separation. This value is called the minimum reflux ratio and it depends on the condition of feed, i.e., on line q. In general, the value of the minimum reflux ratio can be obtained by drawing the operating line from point (x_D, x_D) on the diagonal to the point at which the line q intersects the equilibrium curve. The minimum reflux ratio r_m is obtained from the slope of this line.

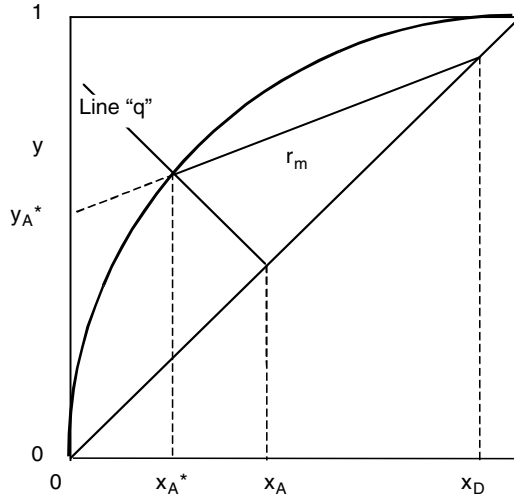

FIGURE 19.10
Minimum reflux relationship.

For a normal binary system, in which the equilibrium curve is like the one shown in Figure 19.10, line q intersects the equilibrium curve at the point (x_A^*, y_A^*). The slope of the straight line that connects the points (x_D, x_D) and (x_A^*, y_A^*) is:

$$\left(\frac{L}{V}\right)_{\min} = \frac{r_m}{r_m - 1} = \frac{x_D - y_A^*}{x_D - x_A^*}$$

Hence, the minimum reflux ratio is:

$$r_m = \frac{x_D - y_A^*}{y_A^* - x_A^*} \tag{19.49}$$

If the feed is a liquid at its bubble point, then $q = 1$, so line q is vertical and intersects the equilibrium curve at $y_A^*, x_A^* = x_A$, so the minimum reflux ratio is:

$$r_m = \frac{x_D - y_A^*}{y_A^* - x_A} \tag{19.50}$$

If the feed is a vapor at its dew point, then $q = 0$, resulting in a horizontal line q and intersecting the equilibrium curve at point: $y_A^* = x_A$, x_A^*; hence:

$$r_m = \frac{x_D - x_A}{x_A - x_A^*} \tag{19.51}$$

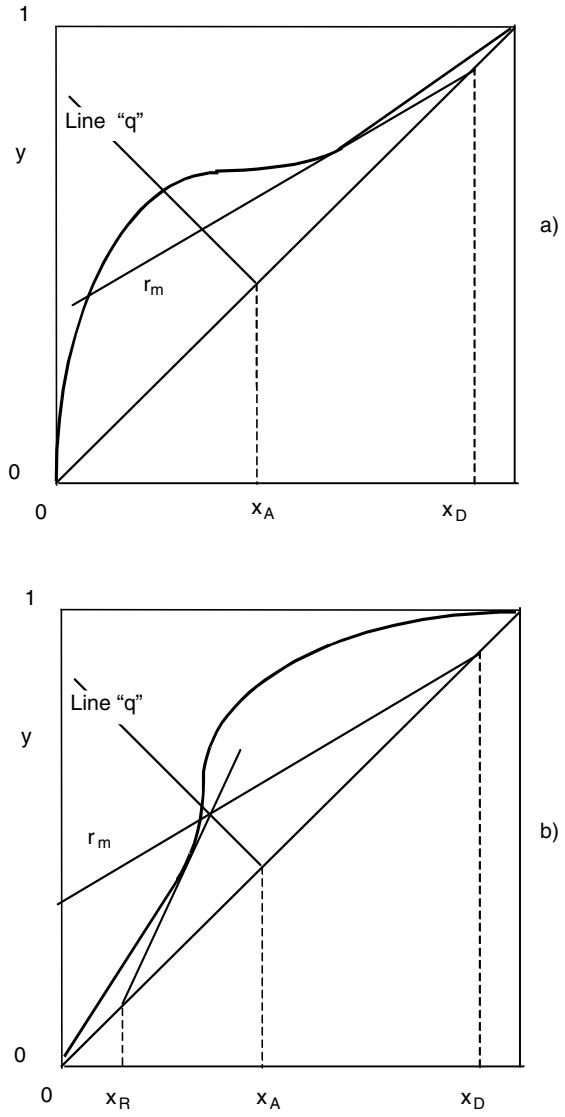

FIGURE 19.11
Obtaining the minimum reflux ratio in special systems.

In cases such as that shown in Figure 19.11, in which, if a line were drawn from point (x_D, x_D) to the point where line q intersects the equilibrium curve, the operating line would be above the equilibrium curve, operation would not be possible. In these cases, the minimum reflux ratio is obtained from the slope of the line tangent to the equilibrium curve, drawn from the point at the diagonal (x_D, x_D).

If the inflection is placed in the lower zone of the curve and the tangent to the equilibrium curve is drawn from (x_R, x_R) and at the point that intersects line q, it is connected to point (x_D, x_D) to obtain the operating line, giving the minimum reflux ratio (Figure 19.11).

If the equilibrium curve is concave upwards, the minimum reflux relationship can be calculated analytically; in the particular case when the relative volatility is constant, the following expression is obtained:

$$r_m = \frac{1}{\alpha - 1}\left(\frac{x_D}{x_A^*} - \alpha \ \frac{1 - x_D}{1 - x_A^*}\right) \tag{19.52}$$

This is the equation of Fenske–Underwood.

19.4.2.2 Number of Plates for Total Reflux

When all of the distillate obtained in the overhead condenser is returned as liquid reflux, the operating line coincides with the diagonal, and the number of plates required to obtain a determined separation is minimal. When the relative volatility is constant, the method of Fenske can be applied to obtain the number of plates needed for a given fractionation working under total reflux.

The number of theoretical plates N for the case of binary mixtures with two components A and B is obtained from the expression:

$$N + 1 = \frac{\log\left(\left(\frac{x_A}{x_B}\right)_D \left(\frac{x_B}{x_A}\right)_R\right)}{\log \alpha_{AB}} \tag{19.53}$$

where α_{AB} is the relative volatility of A with respect to B (Equation 19.8).

19.4.3 Multiple Feed Lines and Lateral Extraction

Sometimes two or more feed mixtures of the same substances of different composition should be distilled to obtain the same products (Figure 19.12). In order to solve this problem by means of the McCabe–Thiele method, the enrichment line above feed A_1 is built as usual. On the other hand, the enrichment line between both feedings is drawn from the intersection of line q_1, representing the feed richer in the most volatile component, with the upper operating line, with slope L_1/V_1. Here, L_1 and V_1 are the streams of liquid and vapor in this zone of the column. These streams are calculated to perform a molar balance around the upper feed plate:

$$L_1 = L + q_1 A_1$$

$$V_1 = V + (q_1 - 1) A_1$$

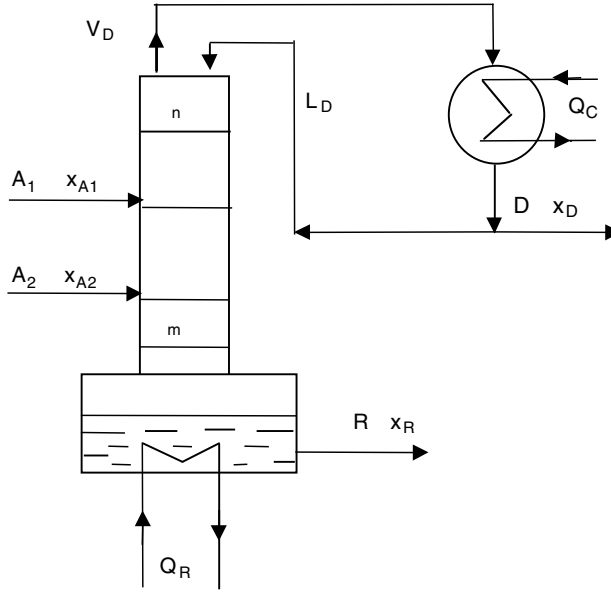

a) Installation scheme

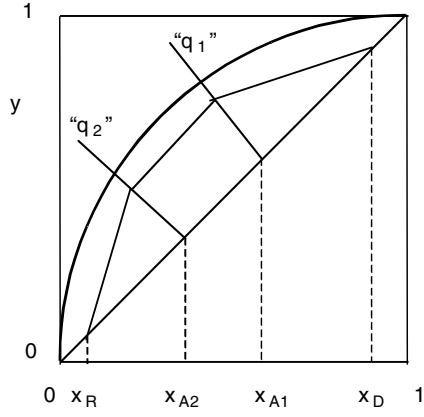

b) Operation on the equilibrium diagram

FIGURE 19.12
Rectification with multiple feeding.

The operating line for the exhaust zone is drawn by connecting point (x_R, x_R), with the point resulting from the intersection between the operating line between both feedings and the line q_2 representing the condition of feed A_2. Once a reflux relationship is fixed, the minimum number of plates is

obtained by the usual method, and feeds are introduced in the stage shown in the *x–y* equilibrium diagram by the respective line *q* (Figure 19.12).

Lateral extraction refers to any stream of product different from the top or waste products. In Figure 19.13, stream *E* represents a lateral extraction.

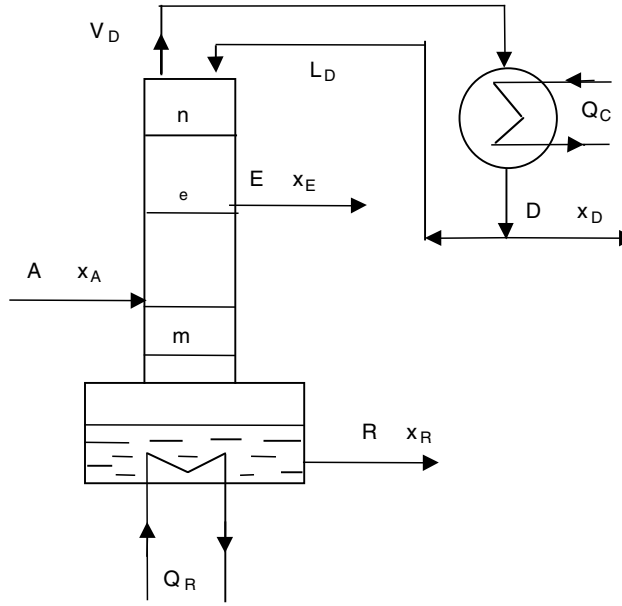

a) Installation sketch.

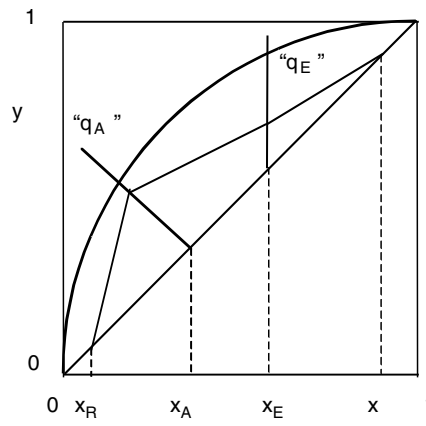

b) Operation on the equilibrium diagram.

FIGURE 19.13
Rectification with lateral extraction.

The number of plates in the column and the extraction plate are obtained by drawing the steps between the operating and equilibrium lines. Similar to the case of multiple feedings, the equations of the operating lines for the different sections of the column should have been previously plotted. For this reason, it is supposed that the lateral extraction is performed in liquid form, in such a way that the stream is at its bubble point. The equations for the operating lines are:

Zone above the lateral extraction:

$$y_n = \frac{L_D}{V_D} x_{n+1} + \frac{D x_D}{V_D} \tag{19.46a}$$

Zone between the lateral extraction and the feeding:

$$y = \frac{L_D - E}{V_D} x + \frac{D x_D + E x_E}{V_D} \tag{19.54}$$

Zone below feeding:

$$y = \frac{\left(L_D - E\right) + q A}{V_D + \left(q - 1\right) A} x - \frac{R x_R}{V_D + \left(q - 1\right) A} \tag{19.55}$$

It is sufficient to calculate the first two straight lines, because if the point where the second operating line (Equation 19.54) intersects the line q is connected to the point (x_R, x_R), then the exhaust line is obtained.

19.4.4 Plate Efficiency

The number of plates needed to perform a given separation can be calculated as described earlier. However, it is assumed that the streams leaving each plate are in equilibrium, which is not true. For this reason, a greater number of plates will be required to carry out the proposed distillation. For calculation of the real number of plates or stages, three types of efficiency can be used: global, Murphree's, and local.

Global efficiency is defined as the quotient between the number of theoretical stages (N_{TS}) and the real number of stages (N_{RS}) needed for a determined rectification:

$$\eta = \frac{N_{TS}}{N_{RS}} 100(\%) \tag{19.56}$$

However, it is usually considered that equilibrium is reached in the kettle and that one stage is discounted, so the global efficiency will be:

$$\eta = \frac{N_{TS} - 1}{N_{RS} - 1} 100(\%) \tag{19.57}$$

The efficiency of Murphree is a function of each plate and can be defined as the ratio between the actual change achieved in composition and the change that would take place if equilibrium were achieved:

$$\eta_{MV} = \frac{y_n - y_{n-1}}{y_n^* - y_{n-1}} 100(\%) \tag{19.58}$$

where y_n is the actual concentration of the vapor phase that leaves the plate, n, y_{n-1} is the actual concentration of the vapor phase that enters the plate, and n, y_n^* is the concentration of the vapor in equilibrium with the liquid that leaves the plate n.

The efficiency of Murphree can also be defined by refering to the liquid phase:

$$\eta_{ML} = \frac{x_{n+1} - x_n}{x_{n+1} - x_n^*} 100(\%) \tag{19.59}$$

The efficiency of Murphree can have values greater than one (higher than 100%), since the vapor produced from the liquid that reaches the plate is richer in the most volatile component than the vapor released from the liquid leaving the plate. A vapor with a mean composition richer than the one corresponding to equilibrium may be produced; this happens frequently in large columns.

Local efficiency is defined similarly to Murphree's efficiency, but considering only one point of the plate. Local efficiency is scarcely used in practice, since the variations of concentration at different points of the plate must be known.

19.4.5 Diameter of the Column

In order to calculate the diameter of the plate column, it is necessary to take into account previous considerations. Since the liquid that runs down and the vapor that goes up circulate inside the column under countercurrent flow, the phenomenon called flooding can occur. In plate columns, flooding occurs because the pressure loss experienced by the vapor stream and the liquid flow is high enough to prevent the liquid stream from running down through the pipes from one plate to the plate below without causing the level of the liquid in the plates to exceed the separating distance between them.

The velocity at which flooding occurs is obtained by the equation of Souders–Brown:

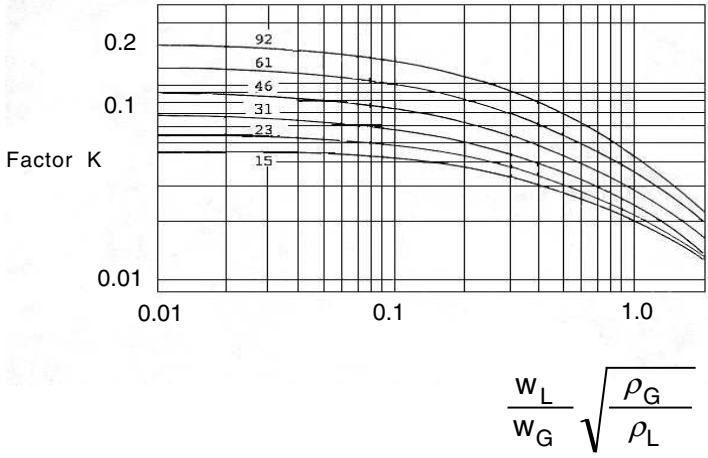

FIGURE 19.14
Factor *K* for plate flooding. (Adapted from King, 1980.)

$$v_{FLO} = K\sqrt{\frac{\rho_L - \rho_G}{\rho_G}} \tag{19.60}$$

where ρ_L and ρ_G are the density of the liquid and vapor, respectively, and *K* is a coefficient that is a function of different variables.

The value of coefficient *K* can be obtained for perforated and bell plates from Figure 19.14, in which the values of *K* are represented on the ordinates vs. $(w_L/w_G)\sqrt{(\rho_G/\rho_L)}$.

The different curves correspond to distances between plates and w_L and w_G, and are the mass flow rates of the liquid and vapor streams, respectively.

In plate columns, the gas stream that usually goes up carries away drops of liquid from one plate to the one above. In the same way, the liquid stream carries away bubbles to the plates below. This causes a decrease in the efficiency of the plates and increases the flow between stages. In order to evaluate this effect, dragging ψ is defined as the ratio between mol of liquid carried away per mol of total liquid that runs down. The value of ψ is correlated with the percentage of flooding and with the relationship $(w_L/w_G)\sqrt{(\rho_G/\rho_L)}$ (Figure 19.15). It is recommended that columns at values of ψ lower than 0.15 be operated in this manner.

Calculation of the diameter of the column begins by obtaining the value of the function:

$$(w_L/w_G)\sqrt{(\rho_G/\rho_L)}$$

From Figure 19.14, the value of the flooding coefficient *K* is obtained for a given distance between plates. The flooding percentage ϕ is obtained for a

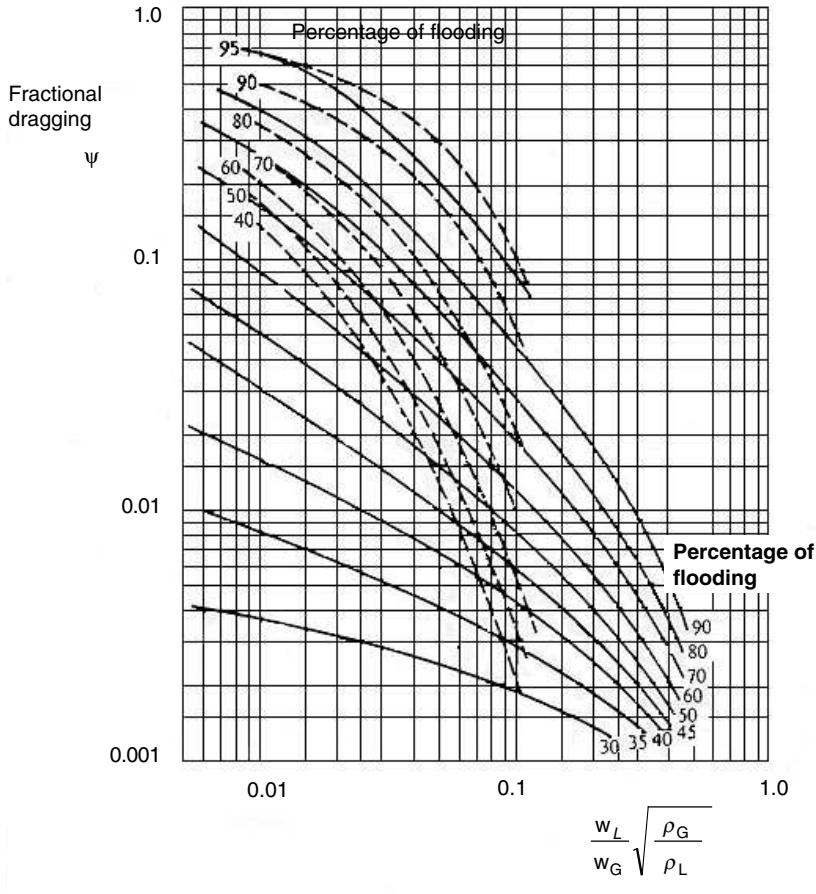

FIGURE 19.15
Dragging correlation: perforated plates, bubbling bell plates. (Adapted from King, 1980.)

dragging ψ value around 0.1 from Figure 19.15. Since not all of the plate section is effective, it can be assumed that only 70% of it is active. For this reason, the real circulation velocity of the gas stream is:

$$v = 0.7\, v_{FLO} = 0.7\, K \sqrt{\frac{\rho_L - \rho_G}{\rho_G}} \tag{19.61}$$

If the vapor flow rate circulating through the column is *V*, then the transversal section of the column is obtained by dividing this value among the flux, which in turn is the product of the circulation velocity times density.

When combined with Equation 19.60, the diameter of the column for cylindrical section columns is obtained from the following equation:

$$D_C = \frac{4V}{\pi \rho_G \, \mathrm{v}} = \frac{4V}{\pi \rho_G \, 0.7 \phi K} \sqrt{\frac{\rho_G}{\rho_L - \rho_G}} \tag{19.62}$$

19.4.6 Exhaust Columns

In cases in which the purpose is to separate a small amount of the most volatile component from the heaviest component, so-called exhaust columns are used. In these columns, the feed stream is introduced in liquid form at the top of the column, so there is no enrichment zone, but only an exhaust zone. The feed stream acts as a reflux ensuring rectification inside the column. In this type of operation, the vapors leaving the column by the top are condensed and obtained as distillate stream.

Assuming that the hypotheses of McCabe–Thiele are complied with, the liquid stream circulates by the column that coincides with the feed stage, while the vapor stream coincides with the distillate stream:

$$L_m = A$$

$$V_m = D = A - R$$

Hence, the operating line is given by the equation:

$$y_{m+1} = \left(\frac{A}{A-R} \right) x_{m-1} - \left(\frac{R}{A-R} \right) x_R \tag{19.63}$$

which is the equation of a straight line crossing the point (x_R, x_R) of a diagonal with a slope equal to $A/(A-R)$.

In order to calculate the number of stages, only one operating line should be drawn — the exhaust line. This line crosses the point with coordinates (x_R, x_R) in the x–y equilibrium diagram. Also, this straight line passes through the point that has an ordinate $y = 1$ and an abscissa corresponding to:

$$x = 1 + \frac{R}{A}\left(x_R - 1\right) \tag{19.64}$$

Once one has obtained this operating line, steps are drawn between the equilibrium curve and the straight line, beginning at point (x_R, x_R), until reaching the composition of feed.

19.5 Discontinuous Rectification

In certain situations, the amount of feed to distillate is not high and continuous operation may be very expensive. In this case, it is preferable to carry out a batch or discontinuous distillation. In a batch operation, the kettle or pot is loaded with the mixture for distillation and heated in such a way that the vapors formed are circulated through the rectification column. The composition of the distillate depends on the composition of the load, the number of plates, and the reflux ratio used.

When the process begins, the distillate is rich in the most volatile component, while the mixture in the kettle becomes poorer in this component. As distillation proceeds, the distillate stream becomes poorer in the most volatile component and the waste or residue becomes richer in the heaviest component.

Batch operation can be performed in such a way that the composition of the distillate is constant, so the reflux rate should be changed continuously. It can also be operated so that the reflux ratio remains constant; thus, the composition of the distillate will decrease. In order to solve the problems set up here, it will be assumed that the hypotheses of McCabe–Thiele are complied with.

The columns used in this type of distillation are the same as for continuous operation, but without feed stream. It should be pointed out that the amount of distillate obtained at a given instant (D) is a function of the flow of the distillate stream $D(t)$ according to the following expression:

$$D = \int_0^t D(t)\, dt \tag{19.65}$$

while the mean composition of the distillate (x_D) is a function of the composition of the distillate stream:

$$x_D = \frac{\int_0^t x_D(t)\, D(t)\, dt}{\int_0^t D(t)\, dt} \tag{19.66}$$

19.5.1 Operation with Constant Distillate Composition

It is assumed that the kettle is initially loaded with R_0 mol of the mixture to be separated; where the content of the most volatile component is x_{0R}, a distillate D of composition x_D will be obtained after a certain time of operation, while R mol of composition x_R will remain in the kettle. When performing a global balance and a balance of the most volatile component around the whole column, it is obtained that:

$$R_0 = R + D$$

$$R_0 x_{0R} = R x_R + D x_D$$

hence,

$$R = R_0 \frac{x_D - x_{R_0}}{x_D - x_R} \tag{19.67}$$

where R_0, x_{0R}, and x_D are constants, while x_R and R vary over time.

When the operation is developed at constant composition of the distillate (x_D = constant), the reflux ratio should be varied. When heating of the loaded mixture begins, a vapor stream (V_D) rising along the column is formed, and a distillate is obtained by using a head condenser, returning part of the distillate as reflux (L_D); the other part accumulates in a distillate receiver. After a certain time of operation t, R mol of mixture remain in the pot, while an amount of distillate D is obtained. The condensing vapor V_D gives rise to streams L_D and $D(t)$:

$$V_D = L_D + D(t)$$

If the amount of heat supplied to the kettle is constant ($\dot{Q}_C$ = constant), then the vapor flow V_D will be constant. However, L_D should vary in order to keep the composition of the distillate constant. Variations of L_D imply variations in the reflux ratio.

The variation of R with time can be obtained by a differential balance along the column:

$$\frac{dR}{dt} = -D(t) = -(V_D - L_D) = -V_D + L_D$$

$$\frac{d(R x_R)}{dt} = -D(t)\, x_D$$

$$R \frac{dx_R}{dt} + x_R \frac{dR}{dt} = (-V_D + L_D) x_D$$

Substitution of the values of R and dR/dt in the last expression yields:

$$dt = \frac{R_0}{V_D} (x_D - x_{R_0}) \frac{dx_R}{\left(\frac{-V_D + L_D}{V_D}\right)(x_D - x_R)^2}$$

This equation can be integrated on the boundary condition: for the initial time $t = 0$, the composition of the mixture in the pot is x_{R0}:

$$t = \frac{R_0}{V_D}\left(x_D - x_{R_0}\right)\int_{x_R}^{x_{R_0}} \frac{dx_R}{\left(\frac{-V_D + L_D}{V_D}\right)\left(x_D - x_R\right)^2} \tag{19.68}$$

This equation allows calculation of the operation time for a column in which the number of plates is known and where it is desired to obtain a waste or residue of composition x_R. To calculate the value of the integral term, different operating lines with slope $(L_D/V_D)_i$ should be drawn from the point of the diagonal (x_D, x_D). Using the equilibrium diagram, the number of stages is traced to obtain in each case a residue value equal to x_{iR}. The intersection of each operating line with the ordinate's axis yields the value of $x_D/(r_i + 1)$, allowing determination of the value of the reflux ratio r_i. The integral term can be evaluated from the data obtained in a graphical or numerical form, thus solving the problem.

If the heat flow supplied to the kettle is constant, then the vapor flow rate created will also be constant, so:

$$\dot{Q}_C = V_{D.}\,\lambda \tag{19.69}$$

where λ is the molar latent heat.

If the reflux is continuously adjusted along the operation in such a way that the composition of the distillate stream does not vary, the following is complied with at any instant:

$$r = \frac{dL_D}{dD(t)}$$

and the total amount of reflux that flows down the column can be obtained from the integration of the expression:

$$dL_D = r\,dD(t) \tag{19.70}$$

Also, the heat supplied to the condenser in order to produce reflux during the whole distillation process is:

$$\dot{Q}_C = \lambda\int_0^{L_D} dL_D = \lambda\int_{r_1}^{r_2} r\,dD(t) \tag{19.71}$$

This equation can be integrated if the relationship that exists between the reflux ratio and the distillate stream is known.

19.5.2 Operation under Constant Reflux Ratio

If the column works at constant reflux, then the composition of the distillate stream varies along the distillation time. If the heat supplied to the kettle or pot is constant, then the vapor flow V_D will be constant. Hence, since the reflux ratio is constant, the flow L_D that circulates through the column will be constant as well.

The global and component balances yield the expression:

$$R\frac{dx_R}{dt}+x_R\frac{dR}{dt}=\left(-V_D+L_D\right)x_D$$

Thus:

$$R\frac{dx_R}{dt}+x_R\frac{dR}{dt}=x_D\frac{dR}{dt}$$

At a given instant it is complied that:

$$\frac{dR}{R}=\frac{dx_R}{x_D-x_R}$$

This equation can be integrated on the boundary condition: for the initial time $t = 0$, the composition of the residue is x_{0R}, allowing one to obtain the equation of Rayleigh:

$$\ln\left(\frac{R}{R_0}\right)=\int_{x_R}^{x_{R_0}}\frac{dx_R}{x_D-x_R}$$

The integral term can be solved by a graphical or numerical integration. The way to solve the integral for the case when the number of plates or theoretical stages and the reflux ratio are known, or when the relationship (L_D/V_D) is known, is described next. The value of the composition of the distillate x_{iD} is fixed, and a straight line with a slope L_D/V_D is drawn from the point of the diagonal that corresponds to such value of the distillate. A number of steps equal to the number of plates in the column are drawn between this line and the equilibrium line, thus obtaining the value that corresponds to the composition of the residue x_{iR}.

The operation is repeated for different values of composition of the distillate, using lines that have the same slope as the first, obtaining in each case the value that corresponds to the composition of the residue. For each value of composition of the residue, a value of $1/(x_D - x_R)$ is obtained and these values are plotted against those of residue. The value of the integral term of

the equation of Rayleigh can be evaluated by a graphical or numerical integration. This integration between the values of residue of composition x_{0R} and x_R allows one to calculate the amount of mixture that remains in the kettle.

Determination of the operation time required to perform a global balance obtains:

$$\frac{dR}{dt} = -D(t) = -V_D + L_D = \text{constant}$$

The operation time is obtained from the integration of the previous differential equation:

$$t = \frac{R_0 - R}{V_D\left(1 - \frac{L_D}{V_D}\right)} \tag{19.72}$$

But, taking into account that the heat supplied to the kettle is $\dot{Q}_C = V_D\lambda$, then:

$$t = \frac{R_0 - R}{\frac{\dot{Q}_C}{\lambda}\left(1 - \frac{L_D}{V_D}\right)} \tag{19.73}$$

19.6 Steam Distillation

In general, heat is supplied to a distillation column in an indirect way by a heat exchanger. However, there are cases in which steam distillation is used, for example, when one of the components of the mixture is water and is taken away as residue, or when water forms a second unmixable phase. This type of distillation is also used when the mixture to be separated has a high boiling point and can give place to thermal decomposition of the components. Steam is passed directly through the liquid mixture contained in the distiller, but the solubility of steam in the liquid should be very low. This way, distillation can be done without a kettle, although the column requires more plates (Figure 19.16). The enrichment section of the column is not affected; however, the global heat and mass balances around the exhaust zone are affected.

If C is the steam flow fed to the column, then the global, most volatile component and energy balances around the exhaust zone are expressed as:

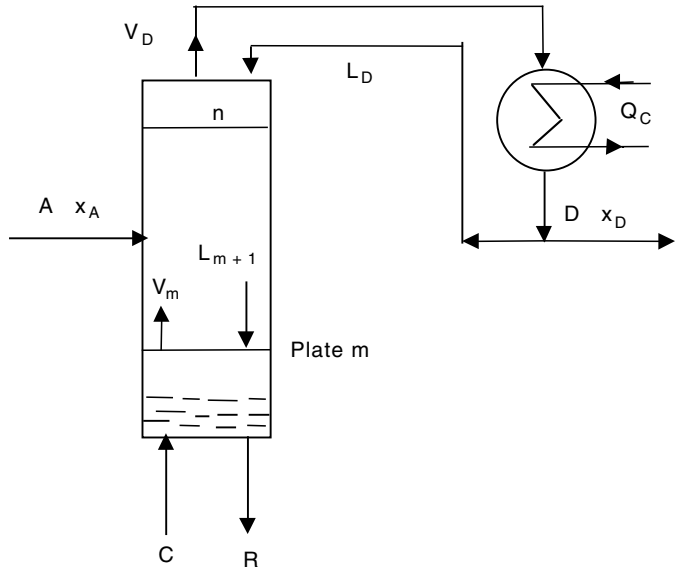

FIGURE 19.16
Steam distillation.

$$L_{m+1} + C = V_m + R$$

$$L_{m+1} x_{m+1} = V_m y_m + R x_R$$

$$L_{m+1} \hat{h}_{m+1} + C \hat{H}_C = V_m \hat{H}_m + R \hat{h}_R$$

Taking into account the hypotheses complied with when the McCabe–Thiele method is applied: $L_{m+1} = R$ and $V_m = C$. Hence, the exhaust line is expressed as:

$$y_m = \frac{R}{C}\left(x_{m+1} - x_R\right) \tag{19.74}$$

It can be observed that, for $x_{m+1} = x_R$, the value of the ordinate to the origin is null ($y_m = 0$), implying that, in the equilibrium diagram, the exhaust line passes through point (x_R, 0) instead of point (x_R, x_R).

According to the hypotheses of McCabe–Thiele, it can be supposed that the latent heats of the mixtures are equal. However, in general, if λ_m is the latent heat of the mixture and λ_C is the latent heat of the steam, and if the sensible heats are neglected, then it is complied that:

$$\lambda_m V_m = C \lambda_C$$

Therefore:

$$L_{m+1} + C = V_m + R$$

$$L_{m+1} = C\frac{\lambda_C}{\lambda_m} + R - C$$

Thus, the exhaust line will be expressed according to the equation:

$$y_m = \frac{R + C\left(\frac{\lambda_C}{\lambda_m} - 1\right)}{C\left(\lambda_C \diagup \lambda_m\right)} x_{m+1} - \frac{R x_R}{C\left(\lambda_C \diagup \lambda_m\right)} \tag{19.75}$$

Problems

19.1

An aqueous solution contains 30% in weight of ethanol. A simple distillation is used to recover 80% of the alcohol contained in such a solution. Determine the composition of the waste solution.

The molecular weight of water and ethanol are 18 and 46 kg/kmol, respectively, so a molar fraction $x_0 = 0.144$ corresponds to an initial mass fraction of 0.3.

The alcohol that remains in the kettle at a given time is equal to the initial quantity minus the distillated quantity:

$$L x - L_0 x_0 - D x_D = L_0 x_0 - 0.8 L_0 x_0 = 0.2 L_0 x_0$$

Substitution in the equation of Rayleigh (Equation 19.15) yields:

$$\ln\left(\frac{x}{0.2 x_0}\right) = \int_x^{x_0} \frac{dx}{y - x}$$

This equation allows calculation of the composition in the kettle. A value of x is supposed, the logarithmic term is calculated, and the right-hand term of the equality is obtained by graphical or numerical integration. When the values of these two terms coincide, the value of x that complies with it is the composition of the residual liquid.

Table 19.P1 can be constructed from the equilibrium data for the ethanol–water system:

TABLE 19.P1

Data for the Solution of the Equation of Rayleigh

x	y	$\ln(x/0.2x_0)$	Integral
0.01	0.103		
0.03	0.235	0.408	0.366
0.04	0.270	0.328	0.322
0.05	0.325	0.552	0.285
0.10	0.444	1.245	0.126

19.2

A rectification column is available to recover 90% of the ethanol contained in an aqueous mixture, with a composition in weight for which the volatile component is 50%. Feed is introduced as a liquid–vapor mixture containing 50% liquid. When the column operates with a reflux ratio 50% higher than the minimum, a waste stream containing 90% water weight is obtained. Determine: (a) molar composition of the distillate; (b) feed plate;. and (c) number of plates required if the global efficiency of the column is 80%.

The equilibrium diagram is obtained from the equilibrium data of the ethanol–water system (Table 19.P2):

TABLE 19.P2

Equilibrium Data of the Ethanol–Water System

x	y	x	y
0.01	0.103	0.50	0.652
0.03	0.235	0.60	0.697
0.05	0.325	0.70	0.753
0.10	0.444	0.80	0.818
0.20	0.529	0.85	0.856
0.30	0.573	0.87	0.873
0.40	0.613	0.894	0.894

where x and y are the molar fractions of ethanol in the liquid and vapor phases, respectively.

The molar fractions of feed and residue can be obtained from the compositions in weight and molecular weights of water and ethanol:

$$x_A = 0.281 \qquad x_R = 0.042$$

A = 100 kmol/h is taken as the calculation basis for the feed stream.

The quantity of alcohol in the distillate stream is $D\,x_D = 0.9\,A\,x_A$.

The global and component balances around the column (Equations 19.21 and 19.22) give:

$$100 = D + R$$

$$(110)(0.281) = D x_D + R(0.042)$$

$$D x_D = 0.9(110)(0.281)$$

Solution yields:

$$R = 66.9 \text{ kmol/h} \qquad D = 33.1 \text{ kmol/h} \qquad x_D = 0.764$$

Since feed contains 50% liquid, then $q = 0.5$. For this reason, the equation of line q of feed condition (Equation 19.48) is:

$$y = -x + 0.562$$

A straight line is drawn to join the point of the diagonal x_D with the point where line q intersects the equilibrium curve, obtaining the straight line that gives the minimum reflux ratio. This line has an ordinate to the origin:

$$\frac{x_D}{r_m + 1} = 0.4$$

from which the minimum reflux ratio, $r_m = 0.91$, is obtained. Since the operating reflux ratio is 50% higher than the minimum, then $r = 1.365$.

Operating line for the enrichment zone (Equation 19.46):

$$y = 0.577\,x + 0.323$$

The exhaust line is obtained by connecting the diagonal (x_R, x_R) with the intersection point of line q and the enrichment line.

The number of theoretical stages is obtained by drawing steps between the equilibrium and the operating lines. The number of theoretical stages is obtained graphically (Fig. 19.P2): $N_{TS} = 10$ (9 plates + kettle), with the eighth plate, counting from the top, the one in which the feed stream should be introduced.

If it is supposed that equilibrium is reached in the kettle, the number of real stages is obtained from Equation 19.57:

$$N_{RS} = 1 + \frac{10 - 1}{0.8} = 13 \text{ theoretical plates } (12 \text{ plates} + \text{kettle})$$

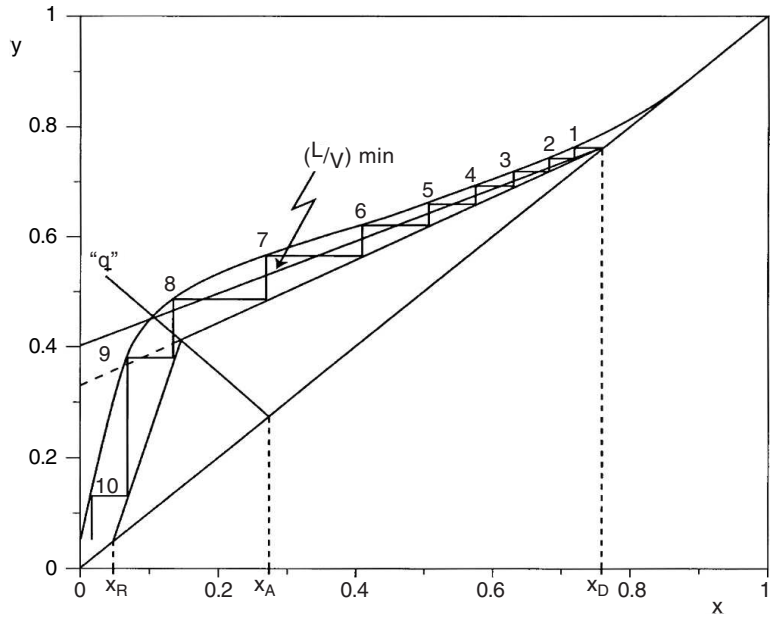

FIGURE 19.P2
Problem 19.2

19.3

A binary mixture containing 40% of the volatile component is subjected to a continuous fractionated distillation. It is desired to obtain a distillate of which the molar fraction of the volatile component is 0.90, and a base product with a molar fraction of the heaviest component is equal to 0.93. The relative volatility of the volatile component with respect to the heaviest one can be considered constant and equal to 2.85. The column works with a reflux relationship 75% higher than the minimum. Calculate: (a) equilibrium data; (b) number of theoretical stages if the feed is saturated vapor: in which plate should the feed stream be introduced?; and 9c) if the feed is a liquid at 20°C, find the equation of line q of the feed condition.

Data:

Component	Molecular Weight (kg/kmol)	Boiling Temperature (°C)	Specific Heat (kJ/kg·°C)	Latent Heat (MJ/kmol)
Volatile	40	75	1.85	30
Heavy	18	100	4.185	40

(a) Equilibrium data obtained from relative volatility:

$$y = \frac{\alpha x}{1 + (\alpha - 1)x}$$

Equilibrium data in Table 19.P2 are obtained by giving values to x.

TABLE 19.P2

Equilibrium Data of the Binary Mixture

x	y	x	y
0.000	0.000	0.600	0.810
0.050	0.130	0.700	0.869
0.100	0.241	0.800	0.919
0.200	0.416	0.900	0.963
0.300	0.550	0.950	0.982
0.400	0.655	1.000	1.000
0.500	0.740		

(b) Since the feed is a saturated vapor, $q = 0$, so line q passes through point (x_A, x_A) and is parallel to the abscissa axis.

The points that represent the feed, distillate and residue are plotted in the equilibrium diagram:

$$x_A = 0.4 \qquad x_D = 0.90 \qquad x_R = 0.07$$

The straight line that gives the minimum reflux ratio is obtained by joining the point (x_D, x_D) with the intersection of line q and the equilibrium curve. The slope of this straight line allows obtaining the minimum reflux ratio:

$$\left(\frac{L}{V}\right)_{\min} = \frac{r_m}{1 + r_m} = 0.704 \qquad r_m = 2.38$$

The operating reflux ratio is obtained from:

$$r = 1.75\, r_m = 4.17$$

Hence, with this value, it is obtained that the enrichment line is given by:

$$y = 0.807\, x + 0.174$$

The exhaust line is obtained by joining the intersection point of line q and the enrichment line with point (x_R, x_R).

Steps are drawn between the equilibrium curve and the operating lines (Fig. 19.P3), yielding $N_{TS} = 7$. The feed is introduced in the fifth plate starting from the top of the column.

(c) The value of q is obtained from Equation 19.45, but it is necessary to obtain the values of the enthalpies of the vapor and liquid at the feed plate.

Temperature of feed plate:

$$T_A = (0.4)(75) + (0.6)(100) = 90°\text{C}$$

Since the feed is at 20°C, it is a subcooled liquid.

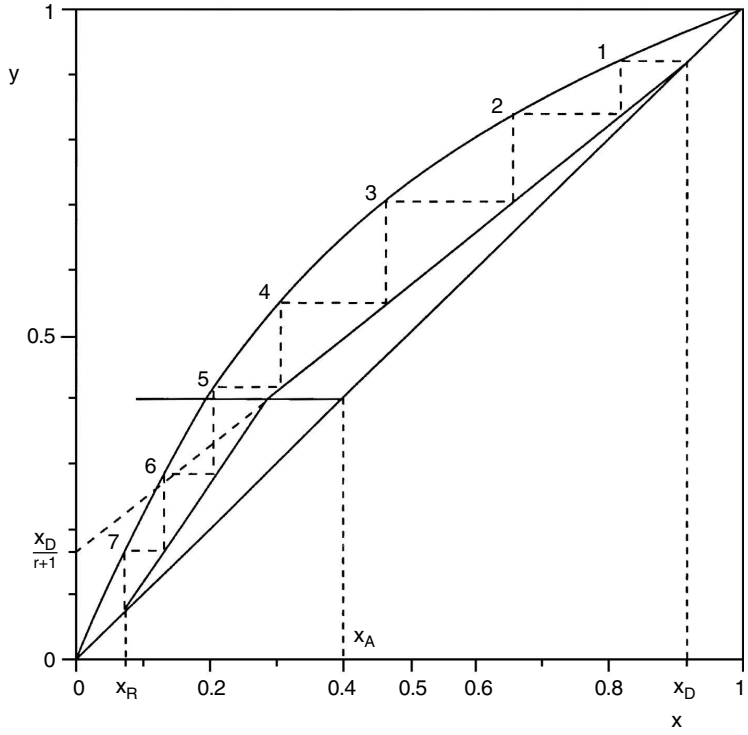

FIGURE 19.P3
Problem 19.3.

The reference temperature for the calculation of enthalpies is $T^* = 0°\text{C}$.

Specific heats:

Volatile:

$$\hat{C}_P = (1.85)(40) = 74 \ \ \text{kJ}/(\text{kmol K})$$

Heavy:

$$\hat{C}_P = (4.185)(18) = 75.33 \ \text{kJ}/(\text{kmol K})$$

Mixture:

$$\hat{C}_P = (0.4)(74) + (0.6)(75.33) = 74.8 \ \text{kJ}/(\text{kmol K})$$

Latent heat:

$$\lambda_A = ((0.4)(30) + (0.6)(40))10^3 = 36,000 \ \text{kJ}/\text{kmol}$$

Liquid's enthalpy:

$$\hat{h}_a = \hat{C}_P \ (T_a - T^*) = (74.8)(90 - 0) = 6732 \ \text{kJ}/\text{kmol}$$

Vapor's enthalpy:

$$\hat{H}_a = \lambda_A + \hat{h}_a = 42,732 \ \text{kJ}/\text{kmol}$$

Food's enthalpy:

$$\hat{H}_A = \hat{C}_P \ (T_A - T^*) = (74.8)(20 - 0) = 1496 \ \text{kJ}/\text{kmol}$$

The value of q is obtained from Equation 19.45:

$$q = \frac{42,732 - 1496}{36,000} = 1.145$$

Since this value is greater than one, it is a subcooled liquid. Line q is obtained from Equation 19.48: $y = 7.88\ x - 2.75$.

19.4

A rectification column is used to separate a mixture made of CS_2 and CCl_4. Two mixtures with different composition are available, so it is desired to feed each one of them into different plates. One of the mixtures is equimolar and is fed at a rate of 100 kmol/h, while the other has an 80% molar content of CS_2 and is fed at a rate of 60 kmol/h. Both streams are introduced as liquids at their boiling point. It is desired to obtain two residue streams, one of 30 mol/h with a 30% molar content of CS_2 and another with only 2% molar content of CS_2. The distillate has a 95% molar content of CS_2. The column operates with a reflux ratio of 2. It can be assumed that the hypotheses of McCabe–Thiele are complied with. Determine: (a) the number of theoretical stages require; (b) in which theoretical plate the 80% CS_2 feed

should be introduced; and (c) the theoretical plate from which the 30% CS_2 residue stream can be extracted.

For the CS_2–CCl_4 system, the volatile component is carbon sulphide. The equilibrium data at 760 mm Hg are shown in Table 19.P4.

Feed is introduced in liquid form, so $q = 1$ in both feeds. Line q will, in both cases, be parallel to the ordinate axis. Also, one of the residues is obtained from the kettle, but the other one is obtained at an intermediate plate, in both cases in liquid form.

TABLE 19.P4

Equilibrium Data for the System CS_2–CCl_4

T (°C)	*x*	*y*	*T* (°C)	*x*	*y*
76.7	0.000	0.000	59.3	0.391	0.634
74.9	0.030	0.082	55.3	0.532	0.747
73.1	0.062	0.156	52.3	0.663	0.829
70.3	0.111	0.266	50.4	0.757	0.878
68.6	0.144	0.333	48.5	0.860	0.932
63.8	0.259	0.495	46.3	1.000	1.000

The global and component molar balances yield:

$$A_1 + A_2 = D + R_1 + R_2$$

$$A_1 x_{A1} + A_2 x_{A2} = D x_D + R_1 x_{R1} + R_2 x_{R2}$$

Substituting data:

$$100 + 60 = D + 30 + R_2$$

$$(100)(0.5) + (60)(0.8) = D\,0.95 + (30)(0.3) + R_2\,0.02$$

Solution of this equation system gives:

$$D = 92.9 \text{ kmol/h} \qquad R_2 = 37.1 \text{ kmol/h}$$

Since the reflux ratio is 2 ($L_D/D = 2$), then:

$$L_D = 2\,D = 185.8 \text{ kmol/h}$$

$$L_1 = L_D + A_1 = 185.5 + 60 = 245.8 \text{ kmol/h}$$

$$L_2 = L_1 + A_2 = 245.8 + 100 = 345.8 \text{ kmol/h}$$

$$L_3 = L_2 - R_1 = 345.8 - 30 = 315.8 \text{ kmol/h}$$

$$V_D = L_D + D = 185.8 + 92.9 = 278.7 \text{ kmol/h}$$

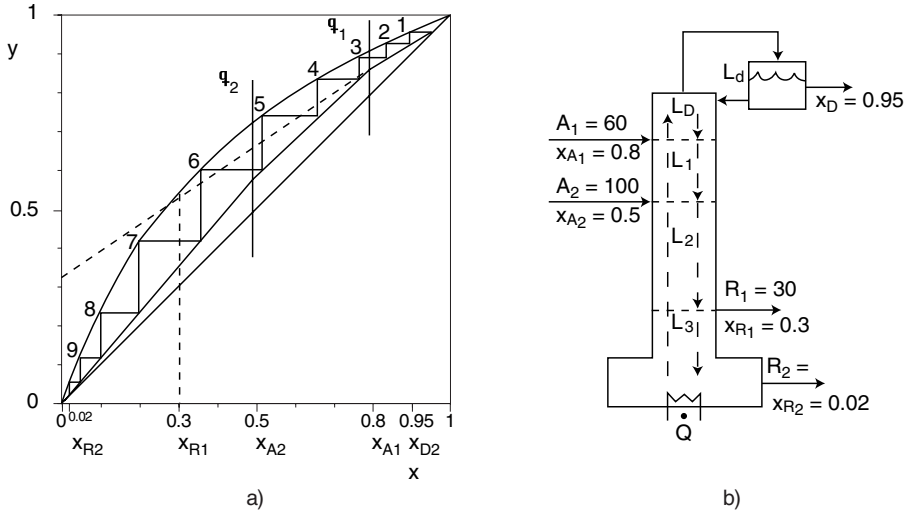

FIGURE 19.P4

Since all of the feed and residue streams are in liquid state, the vapor stream that goes up the column is the same for all zones: $Vi = V_D$.

The slopes of the operating straight lines are:

1st enrichment straight line:	$L_D/V_D = 0.666$
2nd enrichment straight line:	$L_1/V_D = 0.882$
1st exhaust straight line:	$L_2/V_D = 1.24$
2nd exhaust straight line:	$L_3/V_D = 1.132$

The different operating lines are constructed as follows. The first enrichment line (slope 0.666) is drawn from the point of the diagonal (x_D, x_D). The intersection of this line and line q_1 is a point at which the second enrichment line passes, which is drawn with a slope equal to 0.882. This second line intersects q_2 at a certain point from which the first exhaust line is built (slope = 1.24).The intersection of the last line and line q_3 is a point that, when joined with (x_{R2}, x_{R2}), allows one to obtain the second exhaust line.

The number of theoretical stages is obtained by drawing steps between the equilibrium curve and the different operating lines (Fig. 19.P4): $N_{TS} = 10$ (9 stages + kettle).

Figure 19.P4 presents the graphical method to obtain the number of theoretical plates.

Feed with 80% content:	A_1 in the third plate
Feed with 50% content:	A_2 in the sixth plate
Residue with 30% content:	R_1 in the seventh plate

19.5

An aqueous ethanol solution, containing 40% in weight of the volatile component, is continuously fed to a rectification column with an objective to obtain two streams containing 88% and 5% in weight of ethanol. Also, it is desired to obtain a third stream containing 30% of the alcohol that is introduced, with feed its ethanol content 75% in weight. Calculate the number of theoretical plates, as well as the feed and lateral extraction plates, if a reflux ratio of 2 is used and the feed is a liquid at its boiling point.

The percentage in weight composition should be converted to molar fractions. For this reason it is necessary to know the molecular weight of the components, which in this case are 18 and 46 kg/kmol for water and ethanol, respectively:

Feed:	$x_A = 0.207$
Distillate:	$x_D = 0.742$
Residue:	$x_R = 0.020$
Lateral extraction:	$x_E = 0.540$

It is taken as a calculation basis that the column is fed with $A = 100$ kmol/h.

The alcohol leaving the column with the lateral stream is 30% of that introduced with feed:

$$E x_E = 0.3 A x_A$$

$$E(0.54) = (0.3)(100)(0.207) \qquad E = 11.5 \text{ kmol/h}$$

The distillate and residue streams are obtained when performing global and component balances around the column:

$$100 = D + R + 11.5$$

$$(100)(0.207) = D(0.742) + R(0.020) + (11.5)(0.54)$$

Hence:

$$D = 17.62 \text{ kmol/h} \qquad R = 70.88 \text{ kmol/h}$$

The liquid recirculated to the column as reflux and the vapor that leaves the column by the top are:

$$L_D = r D = (2)(17.62) = 35.24 \text{ kmol/h}$$

$$V_D = L_D + D = D\,(r+1) = (17.62)(3) = 52.86 \text{ kmol/h}$$

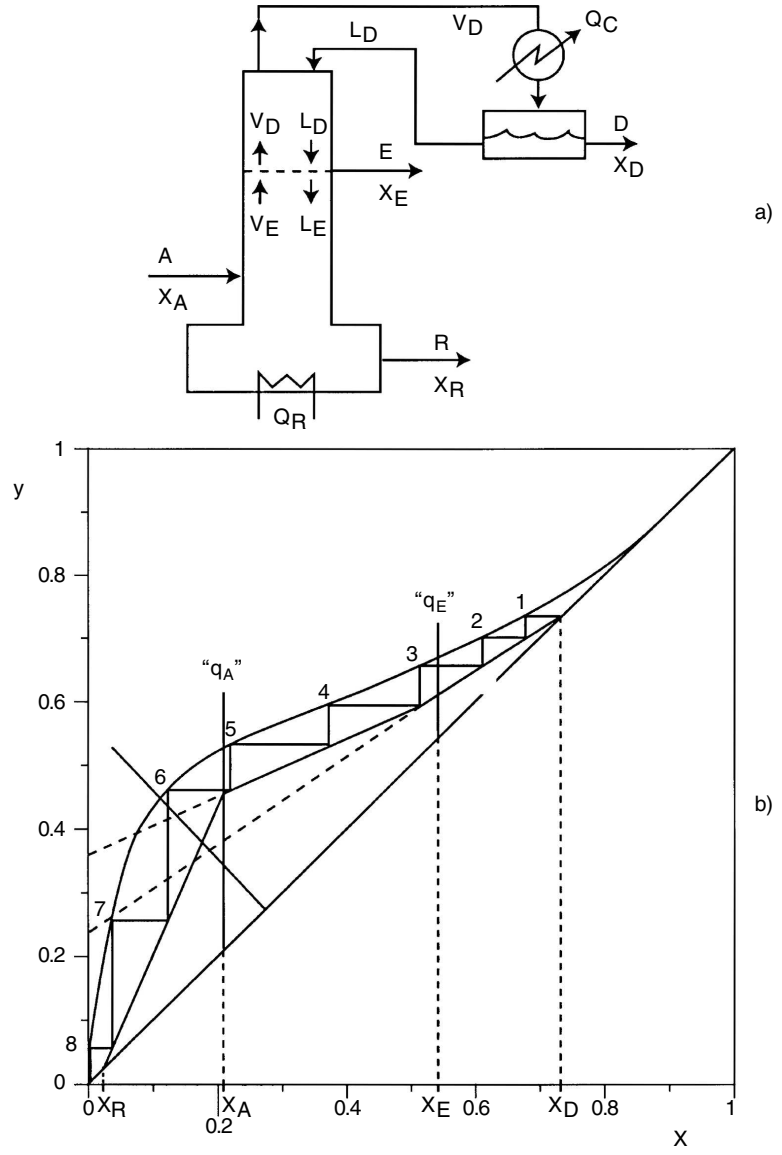

FIGURE 19.P5

Feed as well as lateral extraction are liquids at their boiling point, so their lines q are parallel to the ordinate axis and pass through the points of the diagonal x_A and x_E, respectively. Also, they will not affect the vapor stream that circulates along the column:

$$V_n = V_E = V_D = 52.86 \text{ kmol/h}$$

The liquid stream flow rate that circulates through the column between the lateral extraction and the feed plate is $L_E = L_D - E = 23.74$ kmol/h.

The different operating lines for the different column sections are:

- Between the lateral extraction and the top of the column:

$$y = \frac{r}{r+1}x + \frac{x_D}{r+1} \qquad y = 0.667x + 0.247$$

- Between the feed plate and the lateral extraction:

$$y = \frac{L_E}{V_D}x + \frac{Dx_D + Ex_E}{V_D} \qquad y = 0.449x + 0.365$$

The exhaust line is built by connecting the point of the diagonal x_R with the intersection of the last straight line and the feed line q''_A ($x = 0.207$).

The number of theoretical stages is obtained by drawing steps between the three operating lines and the equilibrium curve. Operating in this way (Figure 19.P5), the number of theoretical stages is $N_{TS} = 8$ (7 plates + kettle). The feed plate is the sixth from the top, while the lateral extraction is made at the third plate from the top.

19.6

A rectification column with a separating power of 6 theoretical stages is used in a discontinuous operation to distill a binary mixture. The initial composition of the mixture is 60% of the most volatile component. The column operates at constant composition of the distillate, which has a molar content equal to 98%. Distillation is interrupted when 83% of the loaded volatile component is obtained as distillate. If the volatility of the most volatile component with respect to the heaviest is 2.46, calculate the reflux ratio required at the beginning and the end of the operation.

Equilibrium data are obtained from the relative volatility:

$$y = \frac{\alpha x}{1 + (\alpha - 1)x}$$

The equilibrium data of the mixture are obtained by giving values to x (Table 19.P6a):

TABLE 19.P6a

Equilibrium Data of the Binary Mixture

x	0.0	0.1	0.2	0.3	0.4	0.5	0.6	0.7	0.8	0.9	1.0
y	0.0	0.215	0.380	0.513	0.621	0.711	0.787	0.852	0.908	0.956	1.0

The equilibrium diagram of this binary system is obtained by plotting y against x. Setup of the global balance and the balance of the most volatile component yields an expression that binds the total amount of distillate obtained as a function of the composition of the residue, and vice versa:

$$D = R_0 \frac{x_{R0} - x_R}{x_0 - x_R} \qquad x_R = \frac{R_0 x_{R0} - D x_D}{R_0 - D}$$

At the beginning of the operation, the composition of the residue is x_{R0} = 0.6. In order to obtain the final composition of the operation, it should be taken into account that 83% of the most volatile component is recovered. If it is supposed that, at the beginning, the column is loaded with R_0 = 100 kmol, the amount of the most volatile component that goes to the distillate is:

$$D x_D = 0.83 R_0 x_{R0}$$

$$D(0.98) = (0.83)(100)(0.6) \qquad D = 49.8 \text{ kmol}$$

Thus, the composition of the residue at this moment is:

$$x_R = \frac{(100)(0.6) - (49.8)(0.98)}{(100) - (49.8)} = 0.207$$

Since the composition of the distillate is fixed, the reflux ratio should vary along the process in order to maintain the distillate with a fixed composition. Different operating lines will be drawn for different reflux ratios, and six steps (six plates) between the operating line and the equilibrium curve should be drawn. This procedure allows one to obtain a residue composition for each case, as well as Table 19.P6b:

TABLE 19.P6b

$x_D/r + 1$	r	x_R
0.45	1.18	0.725
0.40	1.20	0.665
0.30	2.27	0.545
0.20	3.90	0.46
0.10	8.80	0.31
0.05	18.6	0.26

The values of the reflux ratio can be plotted against those of the reflux composition (Figure 19.P6), and the reflux ratios at the beginning and end of the process can be obtained by interpolation and extrapolation:

$$x_{R0} = 0.6 \qquad r_i = 1.7$$

$$x_R = 0.207 \qquad r_i = 32$$

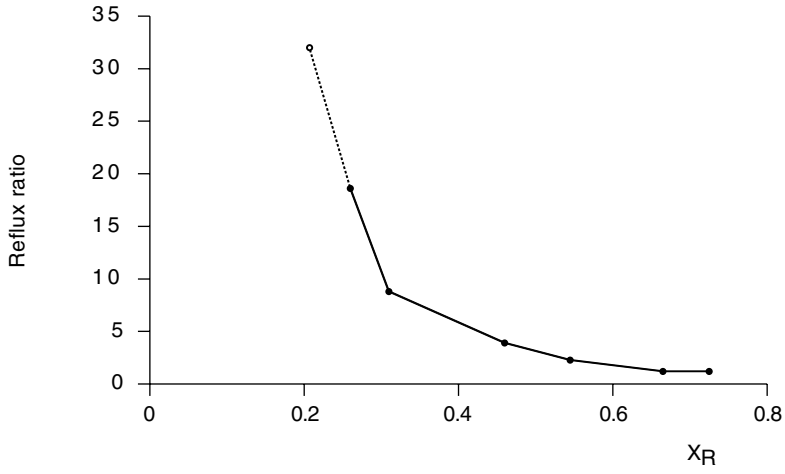

FIGURE 19.P6

20

Absorption

20.1 Introduction

Absorption is a unit operation related to mass transfer between phases; it is used to separate one or more components of a gas mixture by absorption (dissolution) into an adequate liquid. This operation, based on mass transfer in one interface, is controlled to a great extent by the diffusion velocity.

Absorption may be a purely physical phenomenon in which gases dissolve in the liquid solvent. Thus, for example, carbon dioxide can be eliminated from a gas mixture by passing it through water, in which anhydrous carbon dioxide dissolves, yielding carbonic water. However, in other cases, besides the gas dissolution in a solvent, a chemical reaction that influences the absorption velocity takes place, although generally this is not the controlling stage. Examples of absorption with chemical reaction are the elimination of sulfur dioxide by absorption into water or absorption of carbon dioxide in a sodium hydroxyl solution.

The reverse operation, in which the solute passes from the liquid to the gas phase, is called desorption or stripping. Desorption processes are used in the food industry when elimination of the hydrocarbons present in the oils obtained by extraction with solvents is desired.

Absorption is generally carried out in plate or packed columns. In the former case, mass transfer is performed in each plate, reaching equilibrium whenever it is supposed that efficiency is total. For packed columns, mass transfer is performed along the whole column on a continuous basis. The most frequent way of operation consists of circulating the gas and liquid streams under countercurrent flow, since the greater concentration gradient is obtained in this way, accelerating the absorption process.

Sometimes absorption can be carried out in spray, bubble, or wet-wall columns, although stirred tanks and other types of equipment are also used. In spite of the great variety of apparatus used in absorption processes, the calculation of packed columns will be studied in detail in this chapter, with a few considerations of plate columns.

20.2 Liquid–Gas Equilibrium

The principle on which absorption and desorption processes are based is the concentration difference of the component to be transferred, existing between the phases and equilibrium state. The mass transfer will be greater the more distant the system is from the equilibrium conditions.

Suppose a mixture of gases in which one component is soluble in a liquid. When the gas mixture comes into contact with this liquid at a given pressure and temperature, the component dissolves into the liquid until reaching a point where there is no net transfer of the component. This point determines the equilibrium for fixed conditions. Either way, the partial pressure of the component P_i in the gas phase is a function of its concentration in the liquid phase C_i (Figure 20.1). The curve resulting from plotting P_i against C_i is the equilibrium curve at a fixed temperature. Point A represents the conditions of a component i desired to be recovered by absorption. Its partial pressure in the gas phase is higher than that at equilibrium (P_e), so part of the component passes to the solvent phase, that is, it is absorbed. In a closed system, or if working in columns with parallel streams, the partial pressure will decrease, while the concentration of the solute will increase in the solvent until reaching a point in the equilibrium curve where mass transfer from the gas to liquid phase stops.

Any point above the equilibrium curve represents a system in which the solute transfer is carried out from the gas phase to the liquid phase, that is, absorption occurs. On the other hand, when the conditions of a system are

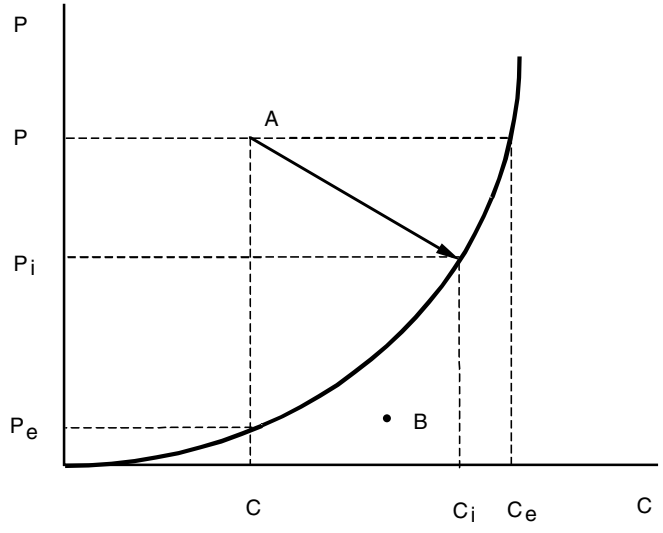

FIGURE 20.1
P–C equilibrium in absorption diagram.

represented by a point below the equilibrium curve (point *B*), the system evolves in such a way that the component is transferred from the liquid to the gas phase and a desorption process takes place.

Equilibrium data required for absorption calculations include the solubility of the gaseous solute in the solvent. Data must also include temperature, concentration of gas in the solvent, pressure of the solute in the gas phase, and total pressure. When the total pressure is low, it does not have much influence on equilibrium data; however, high pressures can have a noticeable effect on gas solubility.

The equilibrium curve of any system depends on pressure and temperature conditions, in addition to the conditions of the system's nature. Of these variables, temperature exerts a greater influence on the solubility of a gas in a liquid. Generally, if the temperature increases, the solubility of the gas in the liquid decreases, according to the law of van't Hoff. Therefore, for a given system, the equilibrium curve will be different, depending on temperature in such a way that a curve obtained at a higher temperature is above a curve at a lower temperature.

If the liquid and gas phases behave ideally, then they comply with the law of Raoult. If the liquid solution does not behave in an ideal way, the law cannot be applied. However, for low solute concentrations in the liquid (diluted solutions), the law of Henry is complied with:

$$P_i = H C_i \tag{20.1}$$

In many cases, Henry's law is valid when the partial pressure is lower than 1 atm. However, for higher pressures, the law of Henry is only applicable for a limited range of concentration.

The constant of Henry varies greatly with temperature and, in general, such variation can approximate a relationship of the type:

$$\log H = A + \frac{B}{T} \tag{20.2}$$

where T is the absolute temperature, while A and B are constants.

As explained above, the law of Henry is applied to diluted solutions, i.e., when molar fraction in the solute is lower than 0.1. This law is usually used for the calculations of equilibrium condition in the design of absorption columns.

It is very useful to represent equilibrium data in molar ratios, defined according to the following equations for calculation of absorption and desorption processes:

Gas phase:
$$Y = \frac{P_i}{P - P_i} \tag{20.3}$$

Liquid phase: $$X = \frac{C_i}{C_T - C_i} \tag{20.4}$$

where P and P_i are the total pressure and the component pressure of i in gas phase, respectively, while C_T is the total concentration in liquid phase, also called molar density, and C_i is the concentration of component i in the liquid phase.

If x and y are the molar fractions of the component in the liquid, then they are bonded to the molar ratios according to the expressions:

$$X = \frac{x}{1-x} \qquad x = \frac{X}{1+X} \tag{20.5}$$

$$Y = \frac{y}{1-y} \qquad y = \frac{Y}{1+Y} \tag{20.6}$$

For those ideal systems in which the law of Raoult is complied with:

$$P_i = x_i P_0 = y_i P$$

the equilibrium curve, expressed in molar ratios, is given by the equation:

$$Y_i = \frac{1}{\frac{P}{P_0}\frac{1+X_i}{X_i} - 1} \tag{20.7}$$

20.3 Absorption Mechanisms

Suppose a gaseous mixture in which one component is absorbed by a liquid, as shown in Figure 20.2. The liquid descends over the surface of a solid, while the gas mixture rises. The partial pressure of the gas is slightly higher than that of the liquid with which it is in equilibrium. If P is the partial pressure of the gas, then the concentration of the liquid in equilibrium is C_e. Gas transfer to the liquid phase takes place at a pressure P with a concentration C. The pressure profile in the gas phase and the concentration profile in the liquid phase are shown in Figure 20.2. As the interface is approached, the partial pressure decreases to P_i, which corresponds to the interface, and C_i is the concentration at the interface for the liquid stream. The concentration in the liquid phase decreases from C_i to C. The concentration C of the liquid is in equilibrium with the pressure P_e of the gas.

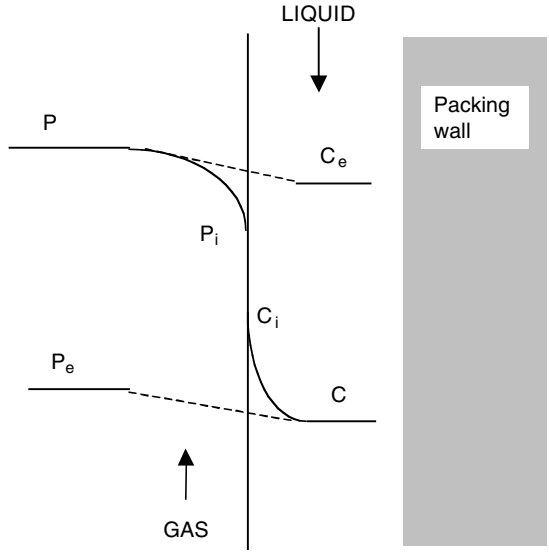

FIGURE 20.2
Mechanism of absorption.

Different models have been proposed to explain mass transfer between phases, although the double film theory, given by Whitman in 1923, is the simplest and postulates the clearest concepts.

20.3.1 Double Film Theory

The double film model assumes that the mass transfer within the global mass in each phase is carried out through convective streams and that no concentration gradients exist within each phase, except in proximity to the interface. It is supposed that, on both sides of interface, there is a static thin film of fluid (laminar sublayers) through which transfer occurs only by molecular diffusion. The direction of mass transfer through the interface does not depend on the difference of concentrations, but on the equilibrium relationship. In the interface, the composition of gas and liquid are in equilibrium. Figure 20.3 shows the concentration profile according to this theory.

In each of these laminar layers, the concentration gradient decreases, being null outside of them. In this model the transfer is considered a stationary process.

20.3.2 Basic Mass Transfer Equations

When, in a homogeneous mixture made of more than one component, a concentration gradient exists from one point to another, there is a tendency to transfer mass in such a way as to have uniform concentrations.

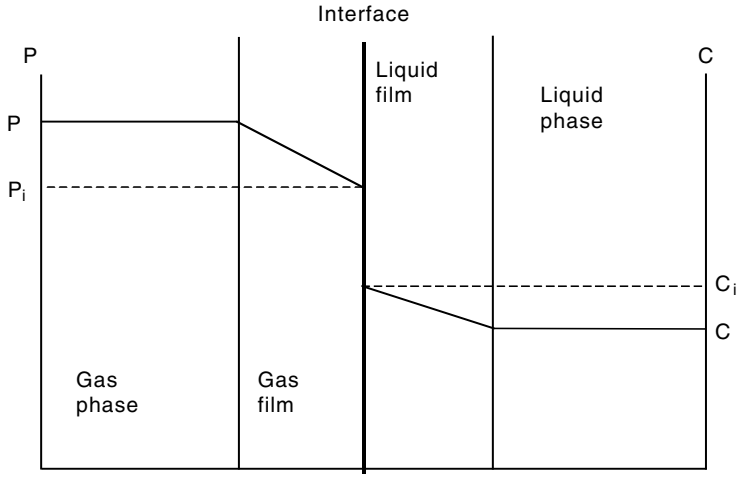

FIGURE 20.3
Concentration profiles in double film.

The net diffusion rate, according to the law of Fick, is proportional to the concentration gradient in the considered point:

$$N_i = -D\frac{\partial C}{\partial z} \tag{20.8}$$

where C is the concentration, z the distance or position, D the diffusivity, and N_i the diffusion flux rate.

The rate of diffusion is high in gases and much slower in liquids. When applying the diffusion theory, it is convenient to use integrated forms of the previous equation, since Equation 20.8 is only applicable to the considered point.

20.3.2.1 Diffusion in the Gas Phase

If a two-component mixture (A and B) is supposed within the gas phase in which A diffuses through B and B is stationary, then when integrating Equation 20.8, if diffusivity is constant, the diffusion flux rate (N_A) is given by:

$$N_A = \left(\frac{D_V}{L}\right)\left(C_G - C_G^i\right) \tag{20.9}$$

where L is the thickness of the layer through which component A diffuses, D_V the diffusivity of A through B, C_G the concentration within the gas (for $L = 0$), and C_G^i the concentration in the interface.

For ideal gases, the concentration in the gas phase is related to the partial pressure according to the equation of the ideal gases, allowing transformation of Equation 20.9 and expressing it as:

$$N_A = \left(\frac{D_V}{RTL}\right)\left(P - P_i\right) \tag{20.10}$$

If an individual mass transfer coefficient in the gas phase is defined:

$$k_g = \frac{D_V}{RTL} \tag{20.11}$$

then the mass transfer diffusion rate (mass flux) through the gas mass is:

$$N_A = k_g\left(P - P_i\right) \tag{20.12}$$

20.3.2.2 Diffusion in the Liquid Phase

The diffusion rate in liquids is much slower than in gases. For diluted solutions, the basic equation giving the mass flux is expressed as:

$$N_A = -\left(\frac{D_L}{L}\right)\left(C - C_i\right) \tag{20.13}$$

where L is the thickness of the liquid film through which diffusion takes place, D_L is the diffusivity in the liquid phase, and C_i and C are the concentrations at the interface and within the liquid, respectively. If a mass transfer individual coefficient for the liquid phase is defined as:

$$k_l = \frac{D_L}{L} \tag{20.14}$$

then the mass flux through the liquid mass is:

$$N_A = k_l\left(C_i - C\right) \tag{20.15}$$

20.3.3 Absorption Velocity

In an absorption process under steady state, the mass flux through the gas film will be the same as the transfer through the liquid film. Therefore, the general equation for the mass transfer is:

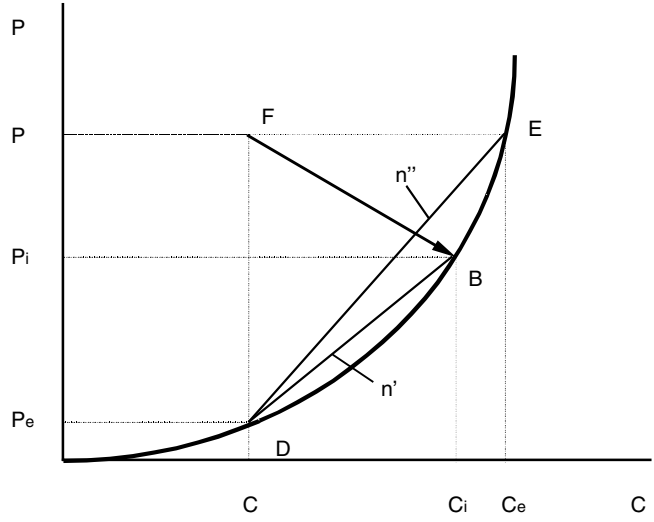

FIGURE 20.4
Relationship of the mass coefficients.

$$N_A = k_g\left(P - P_i\right) = k_l\left(C_i - C\right) \tag{20.16}$$

where P is the partial pressure of the component in the gas phase and P_i is the partial pressure at the interface, while C is the concentration of such component within the liquid and C_i is the concentration at the interface. Figure 20.4 presents these compositions in a pressure–composition diagram.

The slope of the joining line, which allows determination of the concentrations at the interface when the concentrations of the gas and liquid phases are known, is obtained by rearranging Equation 20.16:

$$\frac{P - P_i}{C - C_i} = -\frac{k_l}{k_g} \tag{20.17}$$

Point F represents the conditions in the global mass of the gas and the liquid. Point E represents a concentration C_e in the liquid in equilibrium with the partial pressure P within the gas. Point B represents the concentration C_i in the liquid interface in equilibrium with the partial pressure P_i of the gas interface. Point D represents a pressure P_e in the gas phase that is in equilibrium with a concentration C in liquid phase.

The driving force that causes mass transfer in the gas phase is $(P - P_i)$. The mass transfer driving force in the liquid phase is $(C - C_i)$.

If point F, which gives the concentrations within the gas and liquid phases (C,P), is known, then when drawing a straight line with a slope $-k_l/k_g$, point B

will be obtained where this line crosses the equilibrium curve. Point *B* gives the compositions of the gas and liquid interfaces (C_i,P_i).

In order to determine k_g and k_l, the values of concentration at the interface should be known, which can be difficult to measure. Therefore, it is more adequate to use the mass transfer global coefficients in the gas (K_G) and the liquid (K_L) phases. The mass flux as a function of these global coefficients is expressed as:

$$N_A = K_G\left(P - P_e\right) = K_L\left(C_e - C\right) \tag{20.18}$$

In order to obtain the relationships among the different transfer coefficients, the slopes of the lines that join point $D(C,P_e)$ with points $B(C_i,P_i)$ and $E(C_e,P)$ should be observed in Figure 20.4:

Slope of the straight line DB: $$n' = \frac{P_i - P_e}{C_i - C} \tag{20.19}$$

Slope of the straight line DE: $$n'' = \frac{P - P_e}{C_e - C} \tag{20.20}$$

The mass flux could be expressed as follows from Equations 20.16 and 20.18:

$$N_A = \frac{P - P_i}{\frac{1}{k_g}} = \frac{C_i - C}{\frac{1}{k_l}} = \frac{P - P_e}{\frac{1}{K_G}} = \frac{C_e - C}{\frac{1}{K_L}} \tag{20.21}$$

If the values of the slopes n' and n'' are taken into account, then the combination of Equations 20.9, 20.20, and 20.21 yields:

$$N_A = \frac{P - P_i}{\frac{1}{k_g}} = \frac{P_i - P_e}{\frac{n'}{k_l}} = \frac{P - P_e}{\frac{1}{K_G}} = \frac{P - P_e}{\frac{n''}{K_L}} \tag{20.22}$$

Thus, rearranging according to the properties of the fractions:

$$\frac{1}{k_g} + \frac{n'}{k_l} = \frac{1}{K_G} = \frac{n''}{K_L} \tag{20.23}$$

When the law of Henry is complied with, $n' = n'' = H$, where H is Henry's constant.

The fact that the gas is more or less soluble causes the equilibrium curve to vary and the resistance to mass transfer to be placed in one phase or the

other. Thus, in the case of very soluble gases, the gas phase controls the process and the concentration in the liquid interface is considered to coincide with that of the global liquid ($C_i = C$). Therefore, $P_i = P_e$, which points out that there is no resistance in the liquid phase (k_l is very high) and it is obtained that $k_g = K_G$. When the gas presents a very low solubility in the liquid, pressure P_i coincides with that within the gas ($P_i = P$) and, therefore, $C_i = C_e$, which points out that there is no resistance in the gas phase (k_g is very high). Hence, $k_l = K_L$, so mass transfer is controlled by the liquid phase. If the gas absorbed is a pure gas, the pressure at the gas interface coincides with the partial pressure within the gas ($P_i = P$), so this situation is similar to the latter. Thus, the coefficients k_l and k_g can be determined by using a pure gas.

20.4 Packed Columns

The most common equipment used for gas absorption processes is the packed column. This essentially consists of a tower or cylindrical column with upper and lower outlets for the gas and the liquid and a bed of inert solid particles that fill up the column, called packing. As a general rule, the packed towers operate under countercurrent flow. The liquid or solution is introduced into the column by means of a distributor. The liquid is uniformly spread in such a way as to wet the packing evenly. The gas or gas mixture is introduced at the bottom, ascending through the interstices of the packing, hence circulating under countercurrent with the liquid. Packing proportionates a greater contact surface among both phases, favoring the absorption of the gas by the liquid.

Steps to follow during absorption tower design are:

1. Selection of the solvent
2. Obtainment of equilibrium data
3. Mass balance
4. Enthalpy balance
5. Selection of packing
6. Calculation of the column diameter
7. Calculation of packing height
8. Calculation of pressure drop

20.4.1 Selection of the Solvent

The ideal solvent is one that is neither volatile nor corrosive, in addition to not being viscous or foaming. Also, it should be stable, not flammable, and should not present an infinite solubility for the solute.

Generally, it is difficult to find a solvent that complies with all these requirements, so the solvent will be chosen in each case according to the most convenient alternative. However, liquids that present a greater solubility for the solute will be preferred. In the cases of physical absorption, the cheapest and most noncorrosive solvent is selected. When the absorption is with chemical reaction, the solvent should present a large absorption capacity. Data to select the solvent are available in the literature, generally in specialized encyclopedias.

20.4.2 Equilibrium Data

It is important to know the equilibrium data in an exact and correct form, since they determine the circulation rate of the liquid for a specified recovery of solute.

The best data for a given system are those experimentally obtained, although sometimes it is not possible to obtain these data, so generalized expressions should be used for the system of interest. Such equilibrium data can be found in many cases in the literature, as in technical encyclopedias and handbooks, tables (international critical tables), and, in some cases, scientific journals specializing in the topic.

20.4.3 Mass Balance

When applying the mass balances around the absorption column (Figure 20.5), molar ratios are used, so G' and L' are defined as the inert gas and solvent flow rates in the column:

G' = inert gas molar flow rate (kmol/h)
L' = solvent molar flow rate (kmol/h)

The molar ratios are defined as:

$$\text{molar ratio} = \frac{\text{solute moles}}{\text{inert gas moles}}$$

Y will be used to designate the molar ratio for the gas phase, while X will be used for the liquid phase.

The solute balance along the column demonstrates that the quantity of solute lost by the gas is equal to the quantity gained by the liquid.

Global balance of solute between sections 1 and 2:

$$G'\left(Y_1 - Y_2\right) = L'\left(X_1 - X_2\right) \tag{20.25}$$

from which the following is obtained:

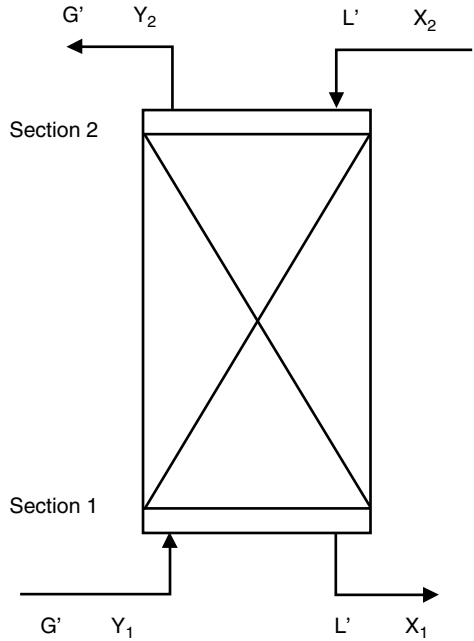

FIGURE 20.5
Absorption column.

$$Y_1 - Y_2 = \frac{L'}{G'}\left(X_1 - X_2\right) \tag{20.26}$$

This equation is a straight line in the equilibrium diagram with molar ratios, which crosses points (X_1,Y_1) and (X_2,Y_2) and has a slope equal to (L'/G'). This straight line that joins points 1 and 2 is called the operating line (Figure 20.6a).

As a general rule, data in absorption processes are G', Y_1, Y_2, and X_2 and unknowns are L' and X_1. For an absorption process, the equilibrium curve is below the operating line; however, in desorption processes, the operating line is placed below the equilibrium curve.

As stated earlier, point 2 is generally a known datum, and point 1 will vary along the horizontal $Y = Y_1$, according to the solvent flow rate L'. When $X_1 = (X_1)_e$, the operating line crosses the equilibrium curve at the point $((X_1)_e, Y_1)$, yielding an operating line in which the ratio (L'/G') is minimum, complying that:

$$\left(\frac{L'}{G'}\right)_{\min} = \frac{Y_1 - Y_2}{\left(X_1\right)_e - X_2} \tag{20.27}$$

Hence, the composition of the outlet liquid $(X_1)_e$ will be in equilibrium with that of the inlet gas (Y_1). In order to reach this point, the height of the tower should be infinite. For equilibrium curves of nonideal cases, as shown

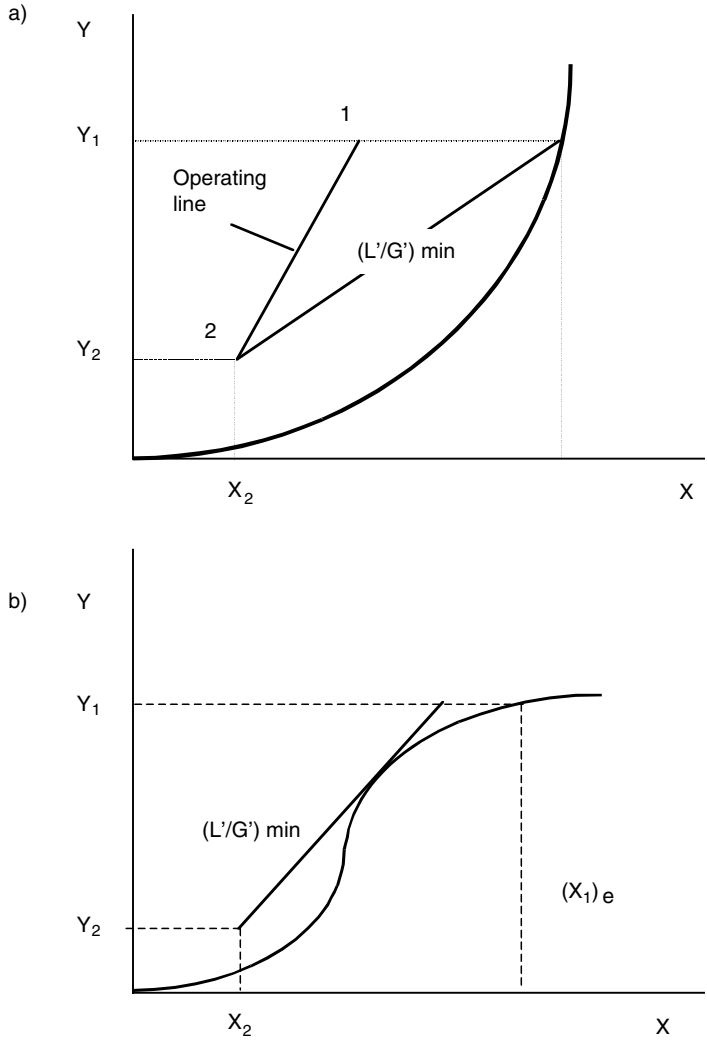

FIGURE 20.6
Operating lines of minimal conditions: (a) ideal system; (b) nonideal system.

in Figure 20.6b, if it is desired to obtain $(L'/G')_{min}$, then, when joining points (X_2, Y_2) and $((X_1)_e, Y_1)$, the straight line will cross the equilibrium curve, so that operation could not be performed. In these cases, the operating line of $(L'/G')_{min}$ is drawn as a tangent to the equilibrium curve.

As a general rule, the absorption processes are carried out empirically, using a ratio 25% higher than the minimum:

$$\frac{L'}{G'} = 1.25\left(\frac{L'}{G'}\right)_{min}$$

20.4.4 Enthalpy Balance

Generally, absorption processes are performed isothermally, and it is not necessary to set up an energy balance. However, in some cases, for example, absorption with chemical reaction, heat release occurs. This leads to a temperature rise of the liquid which will affect the equilibrium curve.

For gas absorption under nonisothermal conditions, sometimes it is assumed that the liquid gains the heat developed and that the temperature of the gas is not affected. This assumption drives the design of a tower with a higher temperature than that required. The enthalpy balance is used to calculate the temperature profile along the column and allows building an equilibrium curve in the *Y*–*X* diagram corresponding to the operation.

If an adiabatic column is assumed: $\dot{Q}_{lost} = 0$.

$$\dot{Q}_{generated} = \dot{Q}_{solution} + \dot{Q}_{reaction} = R\left(\Delta\hat{H}_{sol} + \Delta\hat{H}_{reac}\right)$$

The amount of solute transferred is *R*:

$$R = L'\left(X_1 - X_2\right) = G'\left(Y_1 - Y_2\right) \tag{20.28}$$

When applying an energy balance between sections 1 and 2 of the column, the accumulation term is null and under steady state:

$$\left\{\text{inlet term}\right\} = L_2\,\hat{h}_2 + G_1\,\hat{H}_1$$

$$\left\{\text{outlet term}\right\} = L_1\,\hat{h}_1 + G_2\hat{H}_2$$

$$\left\{\text{generation term}\right\} = R\left(\Delta\hat{H}_{sol} + \Delta\hat{H}_{reac}\right)$$

If $\hat{C}_{P,L}$ and $\hat{C}_{P,G}$ are the heat capacities of the liquid and gas phases respectively, the enthalpies in the liquid phase are:

$$\hat{h}_1 = \left(\hat{C}_{P,L}\right)_1 T_1 \quad \text{and} \quad \hat{h}_2 = \left(\hat{C}_{P,L}\right)_2 T_2$$

Thus, the energy balance is:

$$L_2\left(\hat{C}_{P,L}\right)_2 T_2 + G_1\hat{H}_1 + R\left(\Delta\hat{H}_d + \Delta\hat{H}_r\right) = L_1\left(\hat{C}_{P,L}\right)_1 T_1 + G_2\hat{H}_2 \tag{20.29}$$

therefore:

$$T_1 = \frac{L_2\left(\hat{C}_{P,L}\right)_2 T_2}{L_1\left(\hat{C}_{P,L}\right)_1} + \frac{R\left(\Delta\hat{H}_d + \Delta\hat{H}_r\right)}{L_1\left(\hat{C}_{P,L}\right)_1} + \frac{G_1\hat{H}_1 - G_2\hat{H}_2}{L_1\left(\hat{C}_{P,L}\right)_1} \tag{20.30}$$

Besides considering that the column works adiabatically, assume that the following hypotheses are complied with:

- The heat capacities $(\hat{C}_{P,L})_1$ and $(\hat{C}_{P,L})_2$ are equal and correspond to the solvent:

$$\left(\hat{C}_{P,L}\right)_1 = \left(\hat{C}_{P,L}\right)_2 = \hat{C}_{P,L}$$

- The enthalpies of the gas phase are taken as approximately those of saturated wet air:

$$\hat{H}_1 = \hat{H}_2 \approx \hat{H}_{wet\ air\ (saturated)}$$

- Temperature in sections 1 and 2 is constant along the whole section: $G_1\hat{H}_1 \approx G_2\hat{H}_2$. This term is usually neglected.

Hence:

$$T_1 = T_2 \frac{L_2}{L_1} + \frac{R\left(\Delta\hat{H}_d + \Delta\hat{H}_r\right)}{L_1\hat{C}_{P,L}} \tag{20.31}$$

The values of the liquid stream are approximately equal in both sections: $L_1 \approx L_2 \rightarrow L$.

Thus, for temperature T_1 it is obtained that:

$$T_1 = T_2 + \frac{R\left(\Delta\hat{H}_d + \Delta\hat{H}_r\right)}{L\hat{C}_{P,L}} \tag{20.32}$$

A temperature T_i corresponds to any section of the column i, expressed as:

$$T_i = T_2 + \frac{R_i\left(\Delta\hat{H}_d + \Delta\hat{H}_r\right)}{L\hat{C}_{P,L}} \tag{20.33}$$

where:

$$R_i = L'\left(X_i - X_2\right) \tag{20.34}$$

Therefore, the temperature T_i is a function of the composition of the liquid in section i (X_i) and of section 2 (X_2). Equation 20.33 relates temperature with the composition of the liquid, so the real equilibrium curve should be built from such an expression.

In order to construct the real equilibrium curve, values are given to X_i, and the corresponding temperature T_i is obtained by Equation 20.33. This temperature is used to find the set of isotherms T, the point of such curve that has an abscissa X_i, and its equilibrium Y is obtained.

20.4.5 Selection of Packing Type: Calculation of the Column Diameter

The selection of packing is very important, since its influence is decisive on the height and diameter of the column. The packing of a column will produce an increase of the contact surface between the gas and liquid phases, causing a greater mass transfer between both phases. The characteristics that should be complied with by the packing are:

1. To be chemically inert for the fluids that circulate in the tower
2. To have enough mechanical resistance without excessive weight
3. To allow adequate passing of both streams without originating excessive retention of liquid or pressure drop
4. To proportionate good contact between phases
5. To have relatively low cost

There are different types of packing (Figure 20.7; Table 20.1), which can be classified as:

Rings: Different rings range in size by ½ in increments. Rings are generally made of ceramic or steel, but may also be plastic, glass, and other materials. If rings are smaller than 3 in, they are arranged at random. If they are larger than 3 in, they are placed following an order.

- Raschig: the simplest and most common form, a piece of tubing of small thickness, with height equal to the diameter
- Lessing: similar to Raschig rings, but with a transversal partition wall to increase the contact surface, with a maximum size of 6 in.
- Cross: has two partition walls forming a cross
- Spiral: the partition wall made of a simple, double, or triple spiral
- Pall: similar to Raschig rings, but with side openings

Saddles:

- Berl: resembling an equation saddle, generally made of plastic or ceramic and measuring ½ to 3 in. More Berl saddles can be placed per unit volume than rings. The disadvantage is that Berl saddles can fit within one another, this way reducing the transfer area.
- Intalox: similar in shape to Berl packing saddles, cannot fit within one another

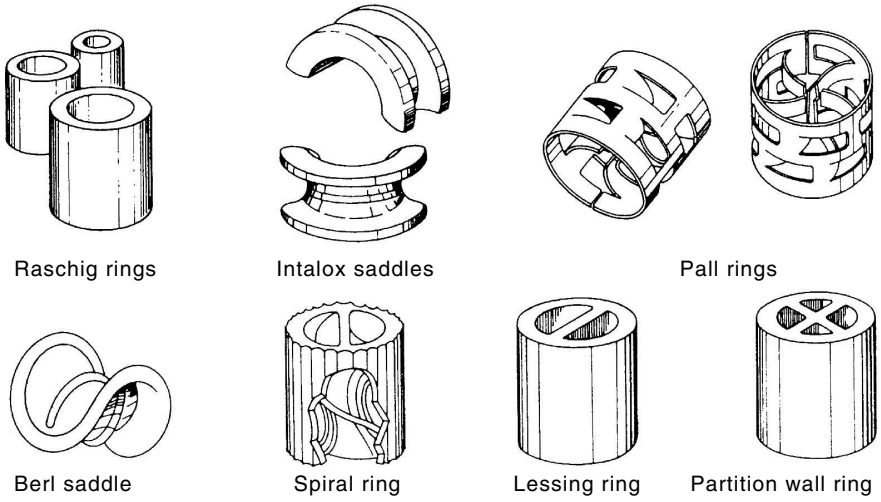

FIGURE 20.7
Different types of packing. (Adapted from Costa, J. et al., *Curso de Quimíca Técnica,* Reverté, Barcelona, 1984.)

TABLE 20.1

Approximate Properties of Different Packings

Packing	Nominal size (in.)	Number per m^2	Specific surface a (m^2/m^3)	Porosity (100 g)	a/ε^3 (m^2/m^3)
Raschig rings	3	1720	72	94	87
(Ceramic I)	2	5420	102	94	123
	1	44,600	206	93	258
	1/2	354,000	416	91	555
Raschig rings	3	1560	62	78	131
(Graphite)	2	5290	95	74	236
	1	42,200	187	74	464
	1/2	338,000	373	74	925
Raschig rings	4	733	52	74	129
(Ceramic II)	2	5420	95	73	245
	1	43,000	190	71	532
	1/2	335,000	368	71	1030
	1/4	2,870,000	795	72	2140
Berl saddles	2	8600	115	77	253
(Ceramic)	1	71,700	243	70	708
	1/2	510,000	465	66	1620
	1/4	4,620,000	1150	65	4200

Other types:

- Other materials used as packing are nickel hanks, wood or metal bars, and pieces of stone, among others. The use of these types of packing is limited to certain processes.

Each packing material has a characteristic dimension, d_P. The channeling of the wall is minimal when $d_p < D/8$, with D the diameter of the column. When d_P is smaller than this value, channeling of liquid on the tower wall is avoided. Redistributors should be placed along the column in order to avoid channels.

20.4.5.1 Packing Static Characteristics

The set of particles that form packing is characterized by the area of the specific surface or unit surface (a) and the void fraction (ε).

Unit surface or specific surface of the bed (a_s): the area exposed to the fluid by the whole packing per unit volume of bed; units are (length)$^{-1}$.

$$a_s = \frac{\text{m}^2 \text{ of surface}}{\text{m}^3 \text{ of packing bed}}$$

Void fraction (ε): the fraction of volume of the bed not occupied by the packing; also called porosity, it is dimensionless. The fraction of volume occupied by the material is $1 - \varepsilon$.

$$\varepsilon = \frac{\text{m}^3 \text{ not occupied by packing}}{\text{m}^3 \text{ of packing}}$$

ε tends to one when packing tends to occupy the whole bed.

Packing factor: defined as the quotient between the specific surface and the fraction of hollows into the cube:

$$\text{packing factor} = \frac{a_s}{\varepsilon^3}$$

Apparent density: the quotient between the total weight of the packing and the volume it occupies:

$$\rho_a = \frac{\text{packing weight}}{\text{occupied volume}}$$

Specific surface of each particle (a_p) $\equiv a_{s_0}$: the area exposed by each particle of packing to the fluid per volume of particle:

$$a_s = a_p(1-\varepsilon) = a_{s_0}(1-\varepsilon)$$

20.4.5.2 Packing Dynamic Characteristics

An important factor for the circulation of both phases through packing is the pressure drop experienced by the gas phase along the column. This pressure drop depends on the liquid phase flow, as well as the gas velocity, since the pressure drop is different depending on whether packing is more or less wet. For this reason, the wet flow or moistening flow (L_m or L_h) is defined as follows:

$$L_m = \frac{\text{volumetric flow rate}}{\text{wet perimeter}} \left(\frac{\text{m}^3/\text{s}}{\text{m}} \right)$$

where the wet perimeter is the relationship between the wet surface and the wet height:

$$\text{wet perimeter} = \frac{\text{wet surface}}{\text{wet height}} = \frac{S z a}{z} = S a$$

where:

S = transversal section of the column (m^2)
z = height of the column (m)
a = specific surface of packing (m^2/m^3)

Therefore, the wet flow is:

$$L_m = \frac{L_V}{S a} = \frac{w_L}{\rho_L S a} \tag{20.35}$$

where L_V is the volumetric flow rate of liquid, w_L is the mass flow rate of fluid, and ρ_L is the density of liquid.

When the gas circulates through the bed, if it is not wet, $L_m = 0$. Then, when plotting the head loss $\Delta P/z$ against the gas flow (velocity of gas V_G) in double logarithmic coordinates, a straight line with slope 1.8 to 2 is obtained (Figure 20.8).

If liquid is introduced countercurrently to the gas flow, then $L_m \neq 0$. As the velocity of the gas increases, the pressure drop (ΔP) per length of packing (z) increases in a power form (from point 1 to point 2). When a certain gas velocity is reached, large load loss increases; this point is called the loading point (point 2). The gas velocity can increase up to a point V_G from which load loss is infinite. This means the pressure drop of the gas is equal to the liquid load and does not flow down. This point is called the flooding point (point 3).

The loading and flooding points will determine the diameter and height of the column. It is desirable to work under conditions where the wet flow is small (a_s = large specific surface) so that the gas velocity is high.

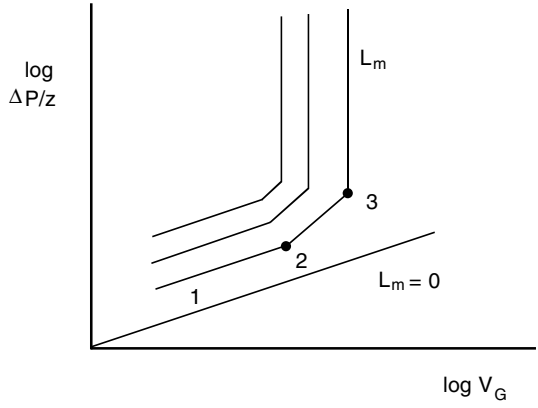

FIGURE 20.8
Pressure drop of the gas as a function of moistening.

20.4.5.3 Determination of Flooding Velocity

It has been proved that good functioning is reached when working at points near load velocity, but not exceeding it. For this reason, it is interesting to calculate the value of the velocity of the load point. Calculation of the loading point is difficult, but not calculation of the flooding point. It has been experimentally observed that the velocity of the loading point is two-thirds that of flooding:

$$G_{LOADING} \approx 0.6 G_{FLOODING} \tag{20.36}$$

where the mass flux is defined as $G = v_G \rho_G$.

There are two methods for calculating the flooding rate: the graphic of Lobo or the equation of Sawistowsky.

Graphic of Lobo

This graph relates the flooding rate with the different physical properties of the phase and packing, as well as the liquid and gas flows for different types of packing (Figure 20.9). Double logarithmic coordinates are used, in which

$$\frac{w_L}{w_G}\sqrt{\frac{\rho_G}{\rho_L}}$$

is represented on the abscissa, while a function of the flooding rate $\psi(V_G)$ is represented on the ordinate and defined according to the expression:

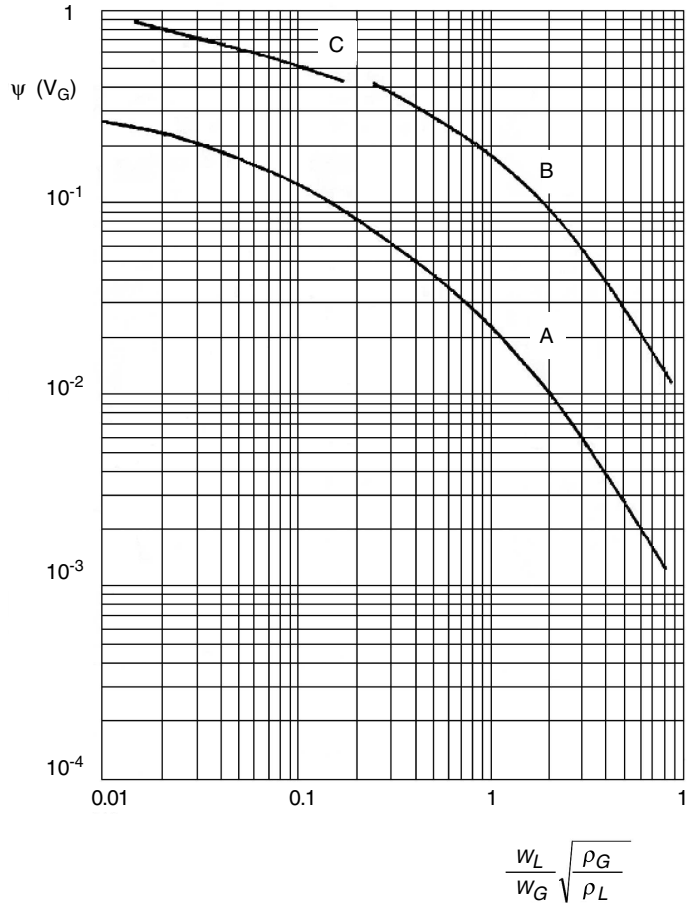

FIGURE 20.9
Flooding graph of Lobo. A) Saddles and rings in random fashion; B) ordered rings; C) screens.

$$\psi\left(V_G\right) = \frac{\left(G_{FLOOD}\right)^2 a}{\rho_L \rho_G \varepsilon^3 g}\left(\frac{\eta_L}{\eta_{WATER}}\right)^{0.2} \tag{20.37}$$

The variables are:

a/ε^3 = packing factor
η_L = viscosity of liquid (Pa·s)
η_{water} = viscosity of water at 20°C (Pa·s)
ρ_G = density of gas (kg/m^3)
ρ_L = density of liquid (kg/m^3)
G = mass flux of gas (kg/s m^2)

Equation of Sawistowsky

The equation of Sawistowsky is an empirical equation used to calculate the flooding rate.

$$\ln\left(\frac{(G_{FLOOD})^2}{g}\frac{a}{\varepsilon^3}\left(\frac{\eta_L}{\eta_{water}}\right)^{0.2}\frac{1}{\rho_G\rho_L}\right) = -4\left(\frac{L}{G}\right)^{1/4}\left(\frac{\rho_G}{\rho_L}\right)^{1/2} \qquad (20.38)$$

where:

G = gas mass flux (kg/s m^3)
G' = molar flow rate of inert (mol/s)
L = mass liquid flux (kg/m^2)

20.4.5.4 Determination of Packing Type

The type of packing that causes optimal wet flow should be selected. Hence, the graph of Morris–Jackson (Figure 20.10) should be used, in which

$$\frac{q_G}{q_L}\sqrt{\frac{\rho_G}{\rho_{air}}}$$

at the loading point is plotted against the wet flow L_m for different packings, q being the volumetric flow rate of the streams. The packing with greater wet flow is chosen for the same value of the ordinate. As a general rule, the velocity of the gas in the column is usually about 1 m/s, varying from 0.3 to 5 m/s.

According to what has been presented in this section, the way to select the packing and to calculate the diameter of the column is as follows:

1. Once w_G, w_L, ρ_G, and ρ_L are determined by the graph of Morris–Jackson, the packing with greater wet flow L_m is chosen.
2. The flooding rate is obtained from the graph of Lobo or the equation of Sawistowsky.
3. The loading rate is calculated from the flooding rate:

$$V_{LOAD} \approx 0.6V_{FLOOD}$$

4. Since G and $V_{G\text{-}LOAD}$ are known, the transversal section of the column is calculated, along with the diameter.

$$S = \frac{1}{\rho_G}\frac{w_G}{V_{G-LOAD}} \qquad S = \frac{\pi}{4}D^2$$

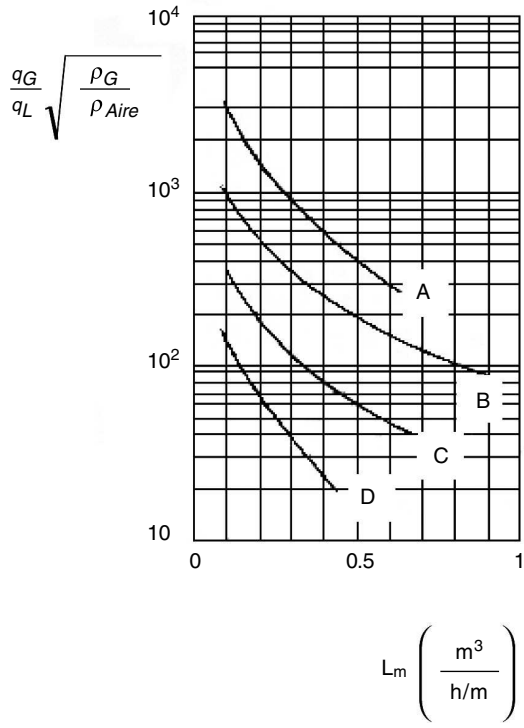

FIGURE 20.10
Loading flows for different types of packing. (Graph of Morris–Jackson.) (A) 2 × 2 × 3/8 in. sawn wood bars; (B) 3 × 3 × 3/8 in. stoneware rings randomly arranged; (C) 2 × 2 × 1/4 in. stoneware rings randomly arranged; 2 × 2 × 3/16 in. stoneware rings randomly arranged; 2 × 2 × 1/16 in. stoneware rings randomly arranged; (D) 1 × 1 × 1/32 in. stoneware rings randomly arranged; 1 × 1 × 1/16 in. metallic rings randomly arranged.

Once the type of packing is selected (stage 1) and the diameter of the column is obtained (stage 4), the following proofs are made:

$D/d_p \geq 8$. In the contrary case, a smaller packing is selected, but with L_m as large as possible.

The last stages are repeated to calculate $V_{G\text{-}LOAD}$; with the same section S, L_m is calculated and compared with the one used, $L_m < L_{m\text{-}graph}$.

The velocity of the gas phase should be between 0.3 and 5 m/s.

20.4.6 Calculation of the Column Height

Once the type of solvent and type of packing have been selected, and the equilibrium data and the diameter of the column are obtained, the next step is to calculate the height of the column.

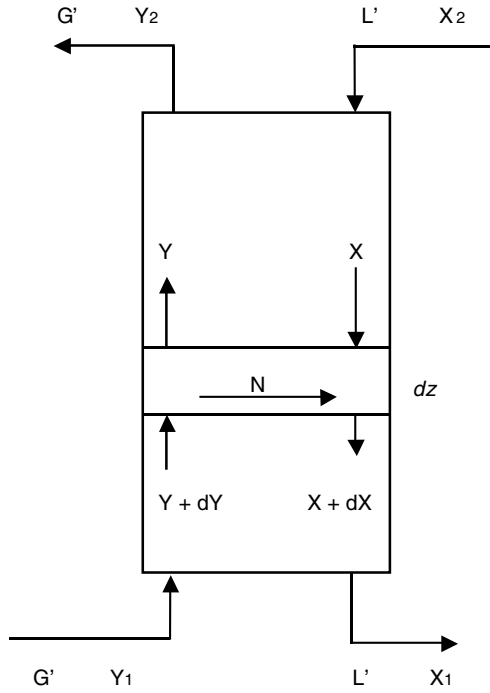

FIGURE 20.11
Absorption packed columns.

20.4.6.1 Concentrated Mixtures

To solve the mathematical model presented, it will be assumed that the following hypotheses are complied with:

- The column works under an adiabatic and isotherm regime.
- Only one solute is transferred.
- It is a concentrated mixture with a concentration higher than 20%.
- The total pressure is constant and pressure drops are negligible.

When performing a mass balance between two transversal sections separated by *dz* (Figure 20.11):

$$G'\left(Y+dY\right)+L'X=G'Y+L'\left(X+dX\right)$$
$$G'\,dY=L'\,dX \tag{20.39}$$

If a balance is made between section 1 and any height, then:

$$G'Y_1 + L'X = G'Y + L'X_1$$
$$Y - Y_1 = \frac{L'}{G'}\left(X - X_1\right) \tag{20.40}$$

The last expression is the equation of the operating line.

If the section of the column is S, then the amount or flux transferred in a height dz is:

$$\text{flow of transferred mass} = N S a dz \tag{20.41}$$

Taking into account Equation 20.39:

$$N\ S\ a\ dz = G'dY = L'dX \tag{20.42}$$

Since the mass flux (N) can be expressed in different ways (Equations 20.16 and 20.18):

$$N = k_g\left(p - p_i\right) = k_l\left(c_i - c\right)$$
$$N = K_G\left(p - p_e\right) = K_L\left(c_e - c\right)$$

Also, as mentioned in Section 20.2:

$$p = \frac{Y}{1+Y}P \rightarrow p_i = \frac{Y_i}{1+Y_i}P \qquad p_e = \frac{Y_e}{1+Y_e}P$$
$$c = \frac{X}{1+X}\rho_m \rightarrow c_i = \frac{X_i}{1+X_i}\rho_m \qquad c_e = \frac{X_e}{1+X_e}\rho_m$$

Hence:

$$G'\,dY = k_g\ a\ S\ dz\left(\frac{Y}{1+Y} - \frac{Y_i}{1+Y_i}\right)P = K_G\ a\ S\ dz\left(\frac{Y}{1+Y} - \frac{Y_e}{1+Y_e}\right)P \tag{20.43}$$

$$L'dX = k_l\ a\ S\ dz\left(\frac{X_i}{1+X_i} - \frac{X}{1+X}\right)\rho_m = K_L\ a\ S\ dz\left(\frac{X_e}{1+X_e} - \frac{X}{1+X}\right)\rho_m \tag{20.44}$$

Four differential equations with separable variables are obtained, and each allows determination of the packing height.

$$z = \frac{G'}{S}\int_{Y_2}^{Y_1} \frac{(1+Y)(1+Y_i)}{k_g\, a\, P(Y-Y_i)}\, dY \tag{20.45}$$

$$z = \frac{G'}{S}\int_{Y_2}^{Y_1} \frac{(1+Y)(1+Y_e)}{K_G\, a\, P(Y-Y_c)}\, dY \tag{20.46}$$

$$z = \frac{L'}{S}\int_{X_2}^{X_1} \frac{(1+X)(1+X_i)}{k_l\, a\, \rho_m(X_i-X)}\, dX \tag{20.47}$$

$$z = \frac{L'}{S}\int_{X_2}^{X_1} \frac{(1+X)(1+X_e)}{K_L\, a\, \rho_m(X_e-X)}\, dX \tag{20.48}$$

Any of these equations allows calculation of the height of packing, but since they do not present an analytical solution, they should be solved in numerical or graphical form. The products ($k_g a$), ($k_l a$), ($K_G a$), and ($K_L a$) are volumetric coefficients of mass transfer.

The operating line in the *Y*–*X* diagram is a straight line and the equilibrium line is a curve. It is easy to determine X_e and Y_e from the diagram, but not the interface X_i and Y_i, since the line between the operating and equilibrium lines is a curve. If this diagram is used, then the packing height can only be calculated from Equations 20.46 and 20.48. The use of Equations 20.45 and 29.47 requires use of the *P*–*C* diagram.

Packing height can be calculated using only the *P*–*C* diagram, from Equations 20.45, 20.46, 20.47, and 20.48, having as variables the pressure and concentration (*p* and *C*). For this reason, a change of variables should be performed: *p* instead of *Y*, and *C* instead of *X:*

$$Y = \frac{p}{P-p} \rightarrow dY = \frac{P}{(P-p)^2}\, dp \tag{20.49}$$

$$X = \frac{c}{\rho_m - c} \rightarrow dX = \frac{\rho_m}{(\rho_m - c)^2}\, dc \tag{20.50}$$

Thus, Equations 20.45 to 20.48 change to:

$$z = \frac{G'}{S}\int_{p_2}^{P_1} \frac{p}{(k_g a)(P-p)^2(p-p_i)}\, dP \tag{20.51}$$

$$z = \frac{G'}{S}\int_{p_2}^{p_1} \frac{P}{\left(K_G a\right)\left(P-p\right)^2\left(p-p_e\right)}\,dP \tag{20.52}$$

$$z = \frac{L'}{S}\int_{C_2}^{C_1} \frac{dC}{\left(k_l a\right)\rho_m\left(1-\frac{c}{\rho_m}\right)^2\left(C_i - C\right)} \tag{20.53}$$

$$z = \frac{L'}{S}\int_{C_2}^{C_1} \frac{dC}{\left(K_L\, a\right)\rho_m\left(1-\frac{c}{\rho_m}\right)^2\left(C_e - C\right)} \tag{20.54}$$

Equations 20.51 and 20.53 are calculated directly from the *P*–*C* diagram, since the relationship $-k_l/k_g$ is easy to determine:

$$-\frac{k_l}{k_g} = \frac{p-p_i}{C-C_i}$$

If Equations 20.52 and 20.54 are used, the calculation is difficult because it requires calculation of K_G and K_L; however, it becomes easier if the law of Henry is complied with. There are some cases in which the calculation of the packing's height is simpler, as when the gas or liquid phases control the process.

20.4.6.2 Diluted Mixtures

Mixtures are considered diluted when the molar ratio in the gas as well as in the liquid phase is lower than 20%, i.e., $Y \le 0.2$ and $X \le 0.2$. The following assumptions can be made in this case:

$$1+Y \approx 1 \qquad y = \frac{Y}{1+Y} \approx Y$$

$$1+X \approx 1 \qquad C = \frac{X}{1+X}\rho_m \approx X\rho_m$$

Supposing that the individual volumetric coefficients ($k_g a$) and ($k_l a$) are practically constant, as well as the total pressure *P* and the molar density ρ_m along the column, then Equations 20.45 and 20.47 become simpler, obtaining:

$$z = \frac{G'/S}{k_g a\, P}\int_{Y_2}^{Y_1} \frac{dY}{Y-Y_i} \tag{20.55}$$

$$z = \frac{L'/S}{k_l a \rho_m} \int_{X_2}^{X_1} \frac{dX}{X_i - X} \tag{20.56}$$

In principle, Equations 20.46 and 20.48 cannot be simplified since ($K_G a$) and ($K_L a$) are not constant. Only when the law of Henry is applied, or when one of the phases controls the process of gas ($k_g = K_G$) or liquid ($k_l = K_L$), such equations can be expressed as:

$$z = \frac{G'/S}{K_G a P} \int_{Y_2}^{Y_1} \frac{dY}{Y - Y_e} \tag{20.57}$$

$$z = \frac{L'/S}{K_L a \rho_m} \int_{X_2}^{X_1} \frac{dX}{X_e - X} \tag{20.58}$$

When observing Equations 20.55 to 20.58, the packing height can be expressed as the product of two groups, one of which is an integral term. The integral term has no units, while the other has length units. In this way, the first term is called the height of the transfer unit, and the second is the number of transfer units.

$$\text{packing height} = (HTU)(NTU) = (H)(N)$$

where:
$N = (NTU)$ = number of transfer units
$H = (HTU)$ = height of transfer units

Thus, the number of gas phase transfer units forming Equation 20.55 is:

$$N_g = \left(NTU\right)_g = \int_{Y_2}^{Y_1} \frac{dY}{\left(Y - Y_i\right)} \tag{20.59}$$

Height of the transfer units in the gas phase:

$$H_g = \left(HTU\right)_g = \frac{G'/S}{k_g a P} \tag{20.60}$$

The number of total transfer units, referred to as the gas phase, taken from Equation 20.56, is:

$$N_G = (NTU)_{G.T} = \int_{Y_2}^{Y_1} \frac{dY}{Y - Y_e} \tag{20.61}$$

Height of total transfer unit referred to the gas phase:

$$H_G = (HTU)_{G.T} = \frac{G'/S}{K_G\, a\, P} \tag{20.62}$$

The number of transfer units in the liquid phase, from Equation 20.57, is:

$$N_l = (NTU)_l = \int_{X_2}^{X_1} \frac{dX}{X_i - X} \tag{20.63}$$

Height of transfer unit in liquid phase:

$$H_l = (HTU)_l = \frac{L'/S}{k_l\, a\, \rho_m} \tag{20.64}$$

The total number of transfer units referred to the liquid phase, from Equation 20.58, is:

$$N_L = (NTU)_{L.T} = \int_{X_2}^{X_1} \frac{dX}{X_e - X} \tag{20.65}$$

Height of one total transfer unit referred to the liquid phase:

$$H_L = (HTU)_{L.T} = \frac{L'/S}{K_L\, a\, \rho_m} \tag{20.66}$$

Then, the total height of packing is the product of the height of one transfer unit times the corresponding number of transfer units:

$$\text{packing height} = H_g N_g = H_l N_l = H_G N_G = H_L N_L \tag{20.67}$$

20.4.6.3 Calculation of the Number of Transfer Units

There are different methods for calculating the number of transfer units. The most used methods are studied next.

Graphical or numerical integration:

The number of transfer units in the gas or liquid phase is given by the following expressions:

$$N_g = \int_{Y_2}^{Y_1} \frac{dY}{Y - Y_i} \qquad N_l = \int_{X_2}^{X_1} \frac{dX}{X_i - X}$$

In order to perform the graphical or numerical integration, X_i or Y_i should be known according to the equation used.

$1/Y - Y_i$ is plotted against Y in the first case and $1/X_i - X$ against X in the second case. N_g or N_l is calculated by a graphical integration.

X_i and Y_i are calculated using the joining straight line (tie line) obtained from:

$$N = k_g\left(p - p_i\right) = k_l\left(C_i - C\right)$$

$$N = k_g P\left(Y - Y_i\right) = k_l \rho_m \left(X_i - X\right)$$

For any point of the operating line $(X,Y)_1$, the corresponding point at the interface $(X_i,Y_i)_1$ is calculated by applying the equation of the joining line (tie line):

$$Y - Y_i = -\frac{k_l \rho_m}{k_g P}\left(X - X_i\right)$$

This line is almost straight in the case of diluted mixtures. The process is repeated successively, allowing one to carry out the graphical or numerical integration mentioned above.

Method of the mean driving force:

This method consists of taking mean values of the driving forces, so the number of transfer units is:

$$N_g = \frac{Y_1 - Y_2}{\left(Y - Y_i\right)_{mean}} \qquad N_l = \frac{X_1 - X_2}{\left(X_i - X\right)_{mean}} \tag{20.68}$$

When the equilibrium line is a straight line, the mean value used in the denominators is equal to the logarithmic mean:

$$N_g = \frac{Y_1 - Y_2}{\left(Y - Y_i\right)_{Lm}} \qquad N_e = \frac{X_1 - X_2}{\left(X_i - X\right)_{Lm}} \tag{20.69}$$

The same occurs in the case of total number of transfer units:

$$N_G = \frac{Y_1 - Y_2}{(Y - Y_e)_{m.l}} \qquad N_L = \frac{X_1 - X_2}{(X_e - X)_{m.l}}$$

When $(Y - Y_i)$ or $(X_i - X)$ does not vary much within the column, the logarithmic mean can be substituted with the arithmetic mean.

There are cases in which the equilibrium line is not a straight line along the whole operating section. However, the equilibrium curve can be divided into different ranges within which the line is straight, so the previous method can be applied to the different sections. The number of transfer units obtained for each section is added to obtain the total number of transfer units.

Analytical method:

When the mixtures are diluted and the law of Henry is complied with, the values of N_G and N_L can be analytically calculated. It is complied that $Y_e = H X$, where H is the constant of Henry, and because they are diluted mixtures:

$$N_G = \int_{Y_2}^{Y_1} \frac{dY}{Y - Y_e}$$

The following is obtained from the mass balance, i.e., from the operating line:

$$X = \frac{G'}{L'}(Y - Y_2) + X_2$$

Hence:

$$Y_e = H\left(\frac{G'}{L'}(Y - Y_2) + X_2\right)$$

If the absorption factor is defined as:

$$A = \frac{L'/G'}{H} \tag{20.70}$$

$$N_G = \int_{Y_2}^{Y_1} \frac{dY}{Y - H\left(\frac{G'}{L'}(Y - Y_2) + X_2\right)} = \frac{\ln\left(\frac{Y_1 - H X_2}{Y_2 - H X_2}\left(1 - \frac{1}{A}\right) + \frac{1}{A}\right)}{1 - \frac{1}{A}} \tag{20.71}$$

then, in order to obtain the total number of transfer units referred to the liquid phase:

$$N_L = \int_{X_2}^{X_1} \frac{dX}{X_e - X} = \frac{\ln\left(\dfrac{X_2 - Y_1/H}{X_1 - Y_1/H}(1-A) + A\right)}{1-A} \tag{20.72}$$

20.4.6.4 Calculation of the Height of the Transfer Unit

As has been explained previously, the groups that multiply the integral term of the equations represent the value of the height transfer unit. Different expressions in literature allow calculation of the values of the height transfer unit in the gas and liquid phases:

$$H_g = \beta\left(\frac{G^{0.41}\,\eta_g^{0.26}.\eta_l^{0.46}\,\sigma^{.0.5}}{L^{0.46}\,\rho_g^{1.33}\,\rho_l^{0.5}\,D_g^{0.67}\,d_P^{\;0.55}}\right) \tag{20.73}$$

$$H_l = \beta\left(\frac{\eta_e^{0.88}\,\sigma^{0.5}}{L^{0.05}\,\rho_L^{1.33}\;D_L^{0.5}\,d_P^{\;0.55}}\right) \tag{20.74}$$

Semmelbauer gave these relationships, where $\beta = 30$ for Raschig rings and $\beta = 21$ for Berl saddles. These equations are valid within ranges that depend on the type of packing (Coulson and Richardson, 1979). Morris and Jakson (1953) reported values for the heights of mass transfer for different types of packing (Table 20.2). On the other hand, there are nomograms that allow calculation of the height of transfer for Pall rings and Intalox saddles (Coulson and Richarson, 1979).

If the individual transfer heights (H_g,H_l) are known, then the global height can be obtained from:

$$H_G = H_g + \frac{n'\rho_m}{L'/G'\,P}\,H_l \tag{20.75}$$

$$H_L = \frac{P}{n''G'/L'\rho_m}H_g + \frac{n'}{n''}H_l \tag{20.76}$$

If the law of Henry is complied with, then $n' = n'' = H$.

TABLE 20.2

Height of Transfer Units for Raschig Rings

Packing	Diameter (mm)	Height (mm)	Thickness (mm)	Height of One Transfer Unit	
				H_g (m)	H_l (m)
Raschig arranged					
Ceramic	100	100	9.5	1.8	0.7
	75	75	9.5	1.1	0.6
	75	75	6.4	1.4	0.6
	50	50	6.4	0.7	0.6
	50	50	4.8	0.8	0.6
Raschig randomly arranged					
Ceramic	50	50	4.8	0.5	0.6
	38	38	4.8	0.3	0.6
	25	25	2.5	0.2	0.5
	19	19	2.5	0.15	0.5
	13	13	1.6	0.1	0.5
Metallic	50	50	1.6	0.5	0.6
	25	25	1.6	0.2	0.5
	13	13	0.8	0.1	0.5
	75	75	9.5	0.8	0.7
	50	50	6.4	0.5	0.6
Carbon	50	50	6.4	0.5	0.6
	25	25	4.8	0.2	0.5
	13	13	3.2	0.1	0.5

20.5 Plate Columns

Besides packed towers, in some cases plate columns are used to conduct certain absorption processes. Thus, in cases in which, due to the loss of charge causes, the use of packed towers with diameters higher than 1 m is needed, plate towers should be used instead. Plate columns are also used when solid deposits that block fluid passing through packing can occur. Another case in which plate columns are used is when the liquid flow is such that flooding of the packed column is likely to occur.

Plate columns employed for gas absorption are similar to those employed for distillation, although efficiency of absorption processes is lower than that of distillation, between 20 and 80%. It is preferable to use packed columns when corrosive fluids are used. Absorption columns function similarly to those of distillation, although in absorption processes there is no reflux. Figure 20.12 shows the sketch of a plate column for absorption.

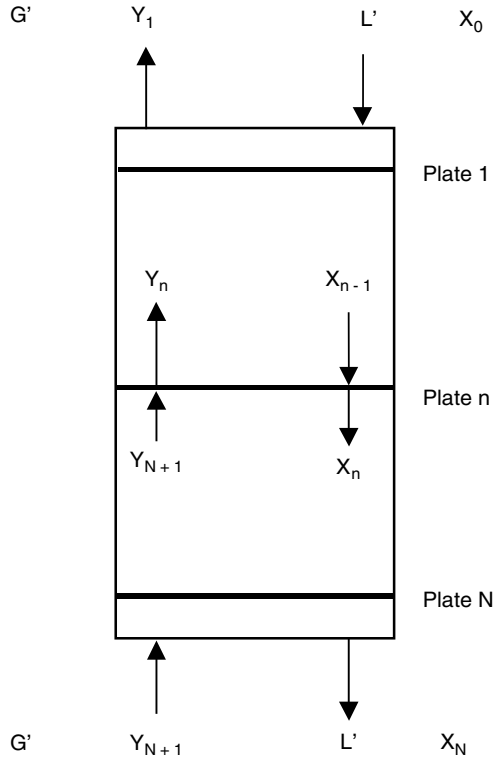

FIGURE 20.12
Absorption plate column: nomenclature.

The total number of plates is N. The following is obtained when performing a solute balance between the excluded plate n and the top of the column:

$$Y_n = \frac{L'}{G'} X_{n-1} + \left(Y_1 - \frac{L'}{G'} X_0 \right) \tag{20.77}$$

This is the equation, with a slope equal to L'/G', which relates the composition of the gas leaving a plate with that of the liquid entering the same plate. The ordinate to the origin is given by the conditions of the top of the column:

$$Y_1 - \frac{L'}{G'} X_0$$

The number of theoretical plates to carry out a determined absorption processes can be obtained by plotting the operating line and equilibrium curve in the Y–X diagram by drawing steps according to the graphical

method of McCabe–Thiele. When the equilibrium line is straight, the number of plates can be calculated in an analytical way, according to the method of Kremser.

A solute balance around plate n yields:

$$G' Y_{n+1} + L' X_{n-1} = G' Y_n + L' X_n$$

If equilibrium is reached in such a plate, and since $Y_e = m X$, then:

$$Y_n = m X_n$$

and in plate $n - 1$:

$$Y_{n-1} = m X_{n-1}$$

Hence:

$$G' Y_{n+1} + L' \frac{Y_{n-1}}{m} = G' Y_n + L' \frac{Y_n}{m}$$

Therefore:

$$Y_n = \frac{Y_{n+1} + A Y_{n-1}}{1 + A}$$

where

$$A = \frac{L' / G'}{m}$$

is called the absorption factor (Equation 20.70).

Since $Y_0 = m X_0$, it can be demonstrated that:

$$\frac{Y_{N+1} - Y_1}{Y_{N+1} - m X_0} = \frac{A^{N+1} - A}{A^{N+1} - 1} \tag{20.78}$$

which is known as the equation of Kremser.

For the case of desorption or stripping processes, it is obtained that:

$$\frac{X_{N+1} - X_1}{X_{N+1} - X_0} = \frac{S^{N+1} - S}{S^{N+1} - 1} \tag{20.79}$$

where $S = 1/A$ is the desorption factor.

In order to obtain a high absorption, either the number of plates in the column or the absorption factor should be large. The optimum value of the

absorption factor is 1.3. The number of theoretical plates to carry out absorption can be calculated from the equation of Kremser. This equation can be found as a graph in the literature (Coulson and Richardson, 1979).

The relationship between the number of theoretical plates and the number of transfer units, when comparing the plate and packed columns, is:

$$N_G\left(1-\frac{1}{A}\right)=N_{TS}\ln A \tag{20.80}$$

in which:

N_G = number of transfer units (packed columns)
N_{TS} = number of theoretical stages (plate columns)

A rapid estimation of the number of theoretical plates is that given by Douglas:

$$N_{TS}+2=6\log\frac{y_{n+1}}{y_1} \tag{20.81}$$

Problems

20.1

An air stream is contaminated with an organic substance that is to be eliminated. For this reason, 800 kg/h of air are introduced through the bottom of a packed tower with Raschig rings randomly arranged, circulating under countercurrent flow with 3000 kg/h of a mineral oil. Calculate: (a) the diameter of the tower that corresponds to the flooding rate; (b) the diameter of the tower when the rate is 0.5 times that of flooding. Data: Properties of the fluids: liquid: density = 900 kg/m^3; viscosity = 40 mPa·s; gas: density = 1.1 kg/m^3. For the packing used: (a/ε^3) = 400 m^2/m^3.

(a) The flooding velocity can be calculated from the equation of Sawistowsky:

$$\ln\left(\frac{V_{FLOOD}^2}{g}\frac{a}{\varepsilon^3}\left(\frac{\eta_L}{\eta_{WATER}}\right)^{0.2}\frac{\rho_G}{\rho_L}\right)=-4\left(\frac{w_L}{w_G}\right)^{1/4}\left(\frac{\rho_G}{\rho_L}\right)^{1/8}$$

where w is the mass flow rate indicated by the subscripts G and L, gas and liquid, respectively.

Substitution yields:

$$\ln\left(\frac{V_{FLOOD}^2}{0.8}400\left(\frac{40}{1}\right)^{0.2}\left(\frac{1.1}{900}\right)\right)=-4\left(\frac{3000}{800}\right)^{1/4}\left(\frac{1.1}{900}\right)^{1/8}$$

Hence, the flooding rate is: V_{FLOOD} = 0.929 m/s.

The tower's diameter can be calculated if the cross section is known, which can be obtained from the continuity equation:

$$S = \frac{w_G}{\rho_G \, v_{FLOOD}} = \frac{(800/3600)}{(1.1)(0.929)} = 0.218 \text{ m}^2$$

The diameter of the column is:

$$D = \sqrt{4 \; S/\pi} = 0.526 \text{ m}$$

(b) Using V_G = 0.5 V_{FLOOD} = 0.465 m/s, and operating similarly to the last section, the column's diameter D = 0.744 m is obtained.

20.2

It is desired to dry an air stream with an absolute humidity of 0.011 kg of water/kg of dry air to a humidity of 0.002 kg of water/kg of dry air for use in a seed drying process. An absorption tower packed with Raschig rings of 2 in and a 50% in weight sodium hydroxide solution are used. If the flow of the absorbent solution is 25% larger than the minimal, calculate the height the tower should have in order to carry out this operation, knowing that the height of one transfer unit is 60 cm.

Equilibrium data for this system are presented in the following table:

X	0	1	2	3	4	5	6	7	8	9	10	12	16
$Y \times 10^4$	0	4	11	28	67	100	126	142	157	170	177	190	202

Units: X in mol H_2O/mol NaOH
Y in mol H_2O/mol dry air

The molecular weight of water, air, and sodium hydroxide are taken as 18, 29, and 40 kg/kmol, respectively.

Calculation of the molar ratios in the gas phase for the inlet and outlet sections:

$$Y_1 = 0.011 \frac{\text{kg } H_2O}{\text{kg dry air}} \frac{1 \text{ kmol } H_2O}{18 \text{ kg } H_2O} \frac{29 \text{ kg dry air}}{1 \text{ kmol dry air}} = 0.0177 \frac{\text{kmol } H_2O}{\text{kmol dry air}}$$

$$Y_2 = 0.002 \frac{\text{kg } H_2O}{\text{kg dry air}} \frac{1 \text{ kmol } H_2O}{18 \text{ kg } H_2O} \frac{29 \text{ kg dry air}}{1 \text{ kmol dry air}} = 0.00322 \frac{\text{kmol } H_2O}{\text{kmol dry air}}$$

The molar ratio for the liquid stream that enters the column is:

$$X_2 = \frac{50\ \text{kg}\ H_2O}{50\ \text{kg NaOH}} \frac{1\ \text{kmol}\ H_2O}{18\ \text{kg}\ H_2O} \frac{40\ \text{kg NaOH}}{1\ \text{kmol NaOH}} = 2.22 \frac{\text{kmol}\ H_2O}{\text{kmol NaOH}}$$

The value of $(L'/G')_{min}$ could be obtained from the slope of the straight line joining the point of the column head (X_2,Y_2) with the point on the equilibrium curve that has as its ordinate $Y_1 = 177 \times 10^{-4}$. However, this line would cut the equilibrium curve, so it will be impossible to carry out the operation. In this case, the tangent to the equilibrium curve is drawn from the column head point (X_2,Y_2), with the slope of the tangent line equaling the value of $(L'/G')_{min}$.

Graphically (Figure 20.P2), it is obtained that

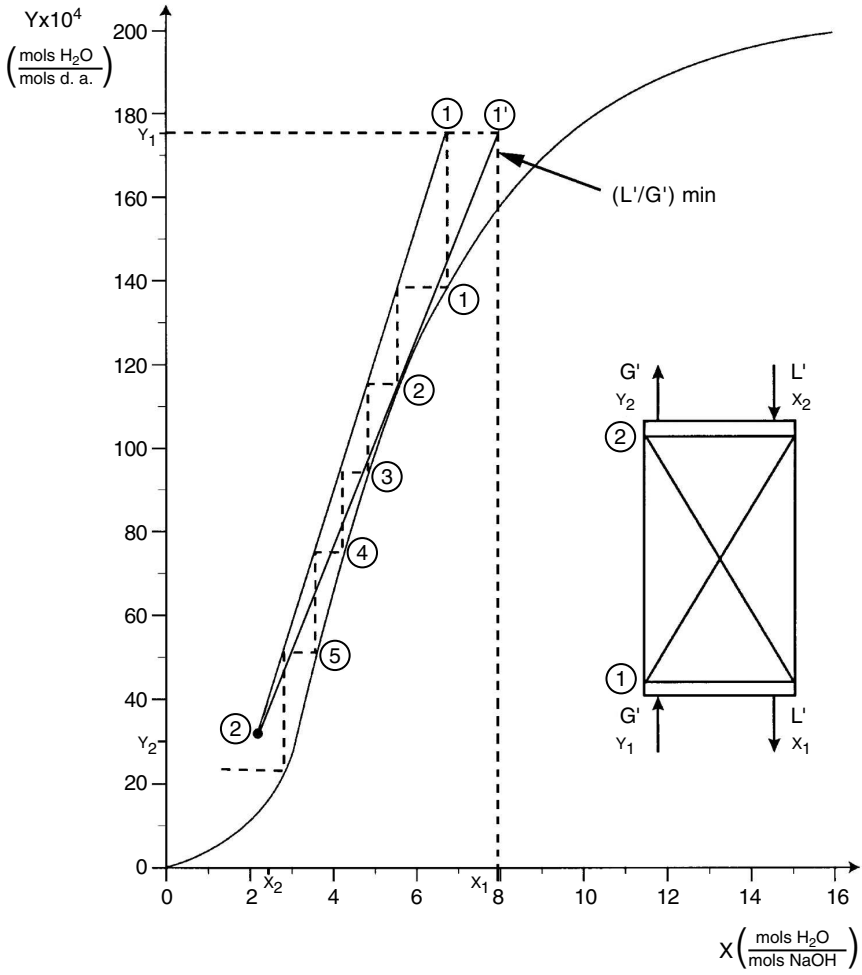

FIGURE 20.P2
Graphic solution of Problem 20.2.

$$\left(L'/G'\right)_{\min} = 2.54 \times 10^{-3} \text{ kmol NaOH/kmol dry air}$$

Since the operation is done at a reflux ratio 25% greater than the minimum, the work relationship is:

$$\frac{L'}{G'} = 1.25\left(\frac{L'}{G'}\right)_{\min} = 0.00318 \frac{\text{kmol NaOH}}{\text{kmol dry air}}$$

The molar ratio for the liquid stream leaving the column is obtained from a global balance: G' ($Y_1 - Y_2$) = L' ($X_1 - X_2$) in a way such that, when substituting the data, it is obtained that X_1 = 6.8 kmol H_2O/kmol NaOH.

The number of transfer units is obtained by drawing steps between the operating line and the equilibrium curve. In this way, it is obtained that *NTU* = 5.7. The column height is calculated by multiplying the value of the height of a transfer unit by the number of transfer units:

$$z = (60 \text{ cm})(5.7) = 342 \text{ cm}.$$

20.3

Oil with a molecular weight of 175 kg/kmol has 5% in weight of a hydrocarbon with a molecular weight of 58 kg/kmol. In order to eliminate 99% of the hydrocarbon, 50 kg/h of the oil–hydrocarbon mixture is fed to a packed column through which steam circulates under countercurrent flow. The column works at 70°C and 5.4 atm with circulation flux for oil and steam of 120 and 18 kg/(h.m^2), respectively. For the type of packing and working conditions used in this process, the height of one transfer unit is 80 cm. If the vapor pressure of the hydrocarbon at 70°C is 6.7 atm and it is supposed that Raoult's law is complied by the mixture, determine: (a) the equilibrium ratio between the two phases, expressed in molar ratios; (b) the diameter of the column; and (c) the height of the column required to perform the operation stated.

(a) When combining the laws of Dalton and Raoult, it is obtained that:

$$y = \frac{P_V^0}{P} x$$

where x and y are the molar fractions of the liquid and gas phases, respectively. If it is desired to obtain the equilibrium data in molar ratios, the last equation should be transformed by expressing the molar fractions as a function of the molar ratios:

$$y = \frac{Y}{1+Y} \qquad x = \frac{X}{1+X}$$

In this way, the equilibrium relationship is:

$$Y = \frac{\left(\frac{P_V^0}{P}\right)X}{1+\left(1-\frac{P_V^0}{P}\right)X} = \frac{\left(\frac{6.7}{5.7}\right)X}{1+\left(1-\frac{6.7}{5.7}\right)X} = \frac{1.241\ X}{1-0.241\ X}$$

The equilibrium curve is obtained and plotted giving values to X and obtaining their corresponding Y values.

(b) It is supposed that the flow density of the liquid stream given in the statement of the problem is of pure oil: L_{OIL} = 120 kg oil/(h.m^2).

Since at the inlet there is 5% hydrocarbon in the oil–hydrocarbon mixture, from each 50 kg/h of mixture introduced, 2.5 kg/h correspond to hydrocarbon and 47.5 kg/h to pure oil. This indicates that the flow rate of pure oil circulating in the column is w_{OIL} = 47.5 kg/h.

The cross section is:

$$S = \frac{w}{L} = \frac{47.5\ \text{kg/h}}{120\frac{\text{kg}}{\text{h.m}^2}} = 0.396\ \text{m}^2$$

which corresponds to a column diameter:

$$D = 0.71\ \text{m} = 71\ \text{cm}\ .$$

(c) At the top of the column, the liquid stream has 5% hydrocarbon, which corresponds to a molar fraction equal to:

$$x_2 = 0.137\,\text{kmol hydrocarbon/kmol total}$$

For this reason, its corresponding molar ratio is:

$$X_2 = 0.159\,\text{kmol hydrocarbon/kmol oil}$$

For the gas phase, the stream that leaves the column has the hydrocarbon eliminated from the liquid phase, which is 99% of that at the inlet:

$$(0.99)(0.25) = 2.475\ \text{kg hydrocarbon/h} = 0.0427\ \text{kmol hydrocarbon/h}$$

Steam is the inert gas of such a gas stream:

$$G' = 18\frac{\text{kg steam}}{\text{h m}^2}0.396\ \text{m}^2\frac{1\ \text{kmol H}_2\text{O}}{18\ \text{kg H}_2\text{O}} = 0.396\ \text{kmol H}_2\text{O/h}$$

The molar ratio of the hydrocarbon in the gas phase at the inlet is:

$$Y_2 = \frac{0.0427\ \text{kmol hydrocarbon/h}}{0.396\ \text{kmol H}_2\text{O/h}} = 0.1078\ \frac{\text{kmol hydrocarbon}}{\text{kmol H}_2\text{O}}$$

At the bottom of the column, the liquid stream that exits contains 1% of the hydrocarbon at the inlet: (0.01)(2.5) = 0.025 kg hydrocarbon/h. In this stream, the amount of oil is still 47.5 kg/h. When calculations are made in a similar way as for the top of the column, it is obtained that:

$$x_1 = 0.00159\ \text{kmol hydrocarbon/kmol total}$$

$$X_1 = 0.0016\ \text{kmol hydrocarbon/kmol oil}$$

It is supposed that steam is pure in this section: $Y_1 = 0$.

The value of Y_2 could have been calculated by a global balance around the whole column:

$$G\left(Y_1 - Y_2\right) = L\left(X_1 - X_2\right)$$

The molar flow rate of oil circulating through the column is:

$$L = 47.5\ \text{kg oil/h} = 0.2714\ \text{kmol/h}$$

Substitution in the mass balance yields:

$$\left(0.396\right)\left(Y_2 - 0\right) = \left(0.2714\right)\left(0.159 - 0.0016\right)$$

$$Y_2 = 0.1079\ \text{kmol hydrocarbon/kmol steam}$$

The number of transfer units is calculated by the equilibrium diagram. The operating line is plotted by joining points (X_1, Y_1) – (X_2, Y_2). Next, the steps between the operating line and the equilibrium curve are drawn (Figure 20.P3), and it is obtained that NTU = 6.25. The column height is calculated by multiplying the value of the transfer unit height times the number of units:

$$z = (0.8\ \text{m})(6.25) = 5\ \text{m}$$

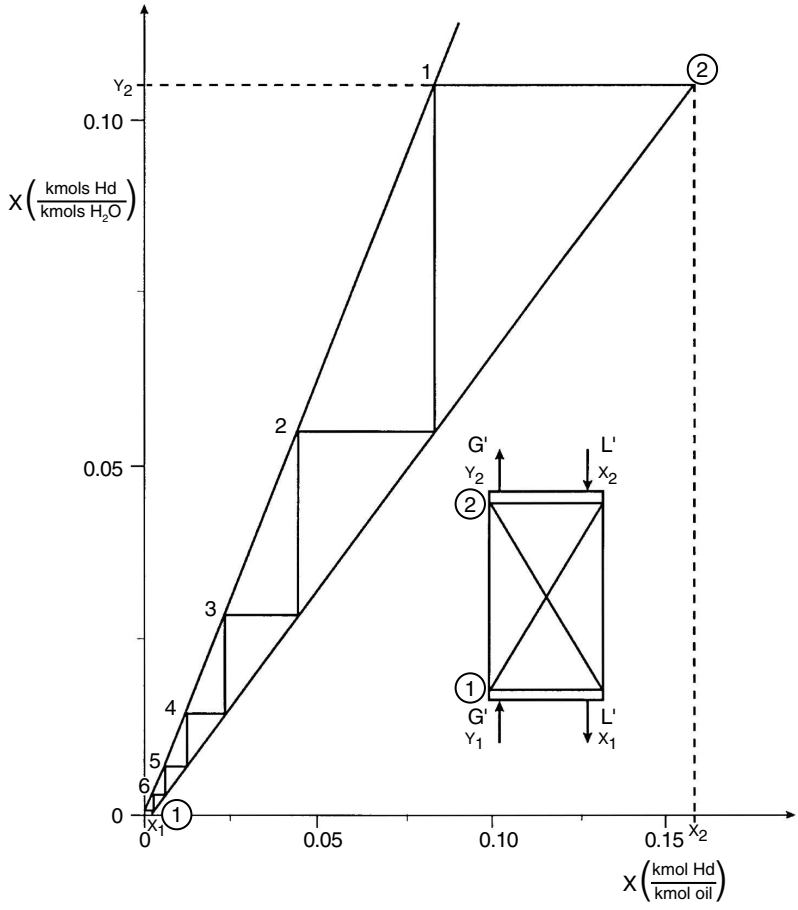

FIGURE 20.P3
Graphical solution for Problem 20.3.

20.4

It is desired to use the combustion gases from an oil fraction in a drying process. It was observed that the mixture of gases, after eliminating steam, contains 6% of SO_2 and 94% of dry air on a molar basis. In order to remove the SO_2, 453.6 kg/h of the gas mixture are fed to a tower packed with Raschig rings of 1 in. The column works at 50% of its flooding rate, using a water flow two times the minimum flow required to carry out the desired operation in an infinite height column. The column works under isothermal conditions at 30°C and 1 atm of pressure. If it is desired that the gas stream leaving the column not exceed 0.1% molar of SO_2, determine the diameter and the height of the column.

Data: equilibrium data at 30°C:

P_{SO_2} (mm Hg)	0.6	1.7	4.7	8.1	11.8	19.7	36.0	52.0	79
$C_{SO_2}\left(\frac{\text{kg So}_2}{100\text{ kg H}_2\text{O}}\right)$	0.02	0.05	0.10	0.15	0.20	0.30	0.50	0.70	1

The individual mass transfer coefficients can be calculated from the equations:

$$\left(k_y a\right) = 0.1\, G^{0.776} L^{0.2} \text{ kmols}/\left(\text{h.m}^3 \cdot \text{molar fraction}\right)$$

$$\left(k_x a\right) = 0.65\, L^{0.82} \text{ kmols}/\left(\text{h.m}^3 \cdot \text{molar fraction}\right)$$

where G and L are the mass flux of the gas and liquid streams, respectively, expressed in kg/(h.m^2). Properties of the liquid stream: density = 944.4 kg/m^3; viscosity = 1 mPa·s.

Equilibrium data in molar fractions or molar ratios can be obtained from data in the table, so the convenient conversions should be performed:

Molar fractions:

$$y = \frac{P_{SO_2}}{760} \qquad x = \frac{C/64}{\frac{100}{18} + \frac{C}{64}}$$

Molar ratios:

$$Y = \frac{P_{SO_2}}{760 - P_{SO_2}} \qquad X = \frac{C/64}{100/18}$$

Equilibrium data are shown in Table 20.P4a.

The molar ratios related to the gas phase, for the inlet and outlet streams, are:

$$Y_1 = 0.0638 \text{ kmol SO}_2/\text{kmol inert gas}$$

$$Y_2 = 0.001 \text{ kmol SO}_2/\text{kmol inert gas}$$

The molar ratio in liquid phase in equilibrium with Y_1 is obtained by interpolation in the following table:

TABLE 20.P4a

Equilibrium Data

Molar Fractions		Molar Ratios	
$y \times 10^2$	$x \times 10^3$	$Y \times 10^2$	$X \times 10^3$
$\left(\frac{\text{kmol } SO_2}{\text{kmol total gas}}\right)$	$\left(\frac{\text{kmol } SO_2}{\text{kmol } SO_2 + H_2O}\right)$	$\left(\frac{\text{kmol } SO_2}{\text{kmol inert gas}}\right)$	$\left(\frac{\text{kmol } SO_2}{\text{kmol } H_2O}\right)$
0.079	0.0565	0.079	0.056
0.224	0.141	0.224	0.141
0.620	0.281	0.622	0.281
1.070	0.422	1.077	0.422
1.566	0.564	1.577	0.563
2.59	0.844	2.661	0.844
4.74	1.41	4.972	1.406
6.84	1.97	7.345	1.969
10.4	2.8	11.601	2.813

$$X_{e1} = 0.00176 \text{ kmol } SO_2/\text{kmol } H_2O$$

The total molar flow rate of gases w_G^M and of inert gas G' are:

$$w_G^M = 453.6 \frac{\text{total kg}}{\text{h}} \frac{\text{total kmol}}{\left((0.06)(64)+(0.94)(29)\right)\text{kg}} = 14.59 \text{ total kmol/h}$$

$$G' = 14.59 \frac{\text{total kmol}}{\text{h}} \frac{94 \text{ kmol air}}{100 \text{ kmol total}} = 13.71 \text{ kmol air/h}$$

A mass balance, in which the composition of the liquid at the outlet must be that of equilibrium with Y_1, should be performed to calculate the minimal flow of inert liquid:

$$G(Y_1 - Y_2) = L_{\min}(X_{e1} - X_2)$$

$$13.71(0.0638 - 0.001) = L_{\min}(0.00176 - 0)$$

Hence: $L_{\min}$ = 489.2 kmol H_2O/h. Since the circulation flow of the liquid should double the minimal, then $L = 2\ L_{\min}$ = 978.4 kmol H_2O/h.

The value of X_1 is obtained from the balance around the whole column:

$$13.71(0.0638 - 0.001) = 978.4(X_1 - 0)$$

$$X_1 = 0.00088 \text{ kmol } SO_2/\text{kmol } H_2O$$

The amount of SO_2 transferred is incorporated into the liquid stream leaving the column; this is the difference between the amount in the gas stream that enters and the amount that exits the column:

SO_2 at inlet:

$$4.59\frac{\text{total kmol}}{\text{h}}\ \frac{6\ \text{kmol SO}_2}{100\ \text{total kmol}}\ \frac{64\ \text{kg SO}_2}{\text{kmol SO}_2}=56.03\ \text{kg SO}_2/\text{h}$$

SO_2 at outlet:

$$3.71\frac{\text{kmol air}}{\text{h}}\ \frac{0.1\ \text{kmol SO}_2}{99.9\ \text{kmol air}}\ \frac{64\ \text{kg SO}_2}{\text{kmol SO}_2}=0.878\ \text{kg SO}_2/\text{h}$$

SO_2 transferred to water:

$$\left(56.03-0.878\right)=55.15\ \text{kg SO}_2/\text{h}$$

It is evident, therefore, that the flow of the liquid at inlet and at outlet will vary:

Inlet: $w_L^2=978.4\ \text{kmol H}_2\text{O/h}=17{,}611.2\ \text{kg H}_2\text{O/h}$

Outlet:
$$w_L^1=\left(17{,}611.2+55.15\right)\ \text{kg aqueous solutions/h}$$
$$=17{,}666.35\ \text{kg aqueous solutions/h}$$

the mean circulation flow rate being w_L = 17,638.8 kg/h.

It is assumed that the gas stream is practically air, so the density of this stream is calculated through the equation of the ideal gases:

$$\rho_G=\frac{(29)(1)}{(0.082)(303)}=1.167\ \text{g/l}$$

The graph of Lobo (Figure 20.9) is used to obtain the flooding flux for the liquid stream:

Abscissa: $$\frac{w_L}{w_G}\sqrt{\frac{\rho_G}{\rho_L}}=\frac{(17{,}666.35)}{(453.6)}\sqrt{\frac{(1.167)}{(1000)}}=1.334$$

the corresponding ordinate for the abscissa in Lobo's graph is:

$$\frac{G_{FLOOD}^2\,a}{g\,\varepsilon^3}\left(\frac{\eta_L}{\eta_{\text{WATER}}}\right)^{0.2}\frac{1}{\rho_G\,\rho_L}=0.015$$

For 1 in Raschig rings: $\varepsilon = 0.73$
$a = 190\ \text{m}^{-1}$

Viscosity: Water 20°C: $\eta_{WATER} = 1\ \text{mPa}\cdot\text{s}$
Liquid at 30°C: $\eta_L = 1.02\ \text{mPa}\cdot\text{s}$

Densities: $\rho_G = 1.167\ \text{kg/m}^3$ $\rho_L = 994.41\ \text{kg/m}^3$
$g = 9.8\ \text{m/s}^2 = 1.27\ \text{m/h}^2$

The value of the gas flow density for flooding conditions can be found using the data above:

$$G_{FLOOD} = 2123.5\ \text{kg}/\left(\text{h m}^2\right)$$

The operating flux is:

$$G = 0.5G_{FLOOD} = 1061.8\ \text{kg}/\left(\text{h m}^2\right)$$

The area of the transversal section of the column is calculated for the least favorable conditions:

$$S = \frac{w_G}{G} = \frac{453.6}{1061.8} = 0.427\ \text{m}^2$$

from which the diameter of the column is:

$$D = 0.737\ \text{m}$$

The following expression is used to calculate the height of the column:

$$z = \frac{G'/S}{\left(k_g a\right)P}\int_{Y_2}^{Y_1}\frac{dY}{Y - Y_i} = H_g N_g$$

In order to determine the height of the transfer unit, H_g, k_g should be expressed as a function of k_y. The mass flux is:

$$N = k_g\left(p - p_i\right) = k_y\left(y - y_i\right)$$

in which p are the partial pressures and y the molar fractions in the gas phase, the subscript i being the interface. When applying the law of Dalton, it is easy to obtain:

$$N = k_g P\left(y - y_i\right) = k_y\left(y - y_i\right)$$

Therefore:

$$k_g\, P = k_y$$

P being the total work pressure.

To calculate ($k_y\, a$), it is necessary to previously determine the mass flux of the liquid and gas streams:

$$L = \frac{w_L}{S} = \frac{17{,}638.8}{0.427} = 41{,}367\,\frac{\text{kg}}{\text{h m}^2}$$

Hence:

$$\left(ky\, a\right) = 0.10\left(1061.8\right)^{0.776}\left(41{,}367\right)^{0.2} = 187.2\ \text{kmol}\Big/\left(\text{h.m}^3 \cdot \Delta\text{y}\right)$$

Therefore, the height of the transfer unit is calculated by the expression:

$$H_g = \frac{G'/S}{\left(k_y\, a\right)} = \frac{\left(13.71\ \text{kmol air/h}\right)\Big/\left(0.427\ \text{m}^2\right)}{187.23\,\dfrac{\text{kmol}}{\text{h.m}^3\ \Delta\text{y}}} = 0.172\ \text{m}$$

To calculate the number of transfer units, the integral term of the equation is expressed as a function of the molar fractions in such a way that:

$$N_g = \int_{Y_2}^{Y_1} \frac{dY}{Y - Y_i} = \int_{y_2}^{y_1} \frac{\left(1 - y_i\right)}{\left(1 - y\right)\left(y - y_i\right)}\, dy = \int_{y_2}^{y_1} \phi\left(y\right) d\text{y}$$

This equation is solved by graphical or numerical integration.

The equilibrium curve is plotted in molar fractions. Also, the operating line is obtained in molar fractions from the mass balance between the top of the column and any section in the column:

$$G'\left(\frac{y}{1-y} - \frac{y_2}{1-y_2}\right) = L'\left(\frac{x}{1-x} - \frac{x_2}{1-x_2}\right)$$

where:

$$y_2 = \frac{Y_2}{1 + Y_2} = \frac{0.001}{1 + 0.001} = 9.99 \times 10^{-4}$$

$$x_2 = 0$$

Hence, the operating line in molar fractions is:

$$3.71\left(\frac{y}{1-y} - 0.000999\right) = 978.4\ \frac{x}{1-x}$$

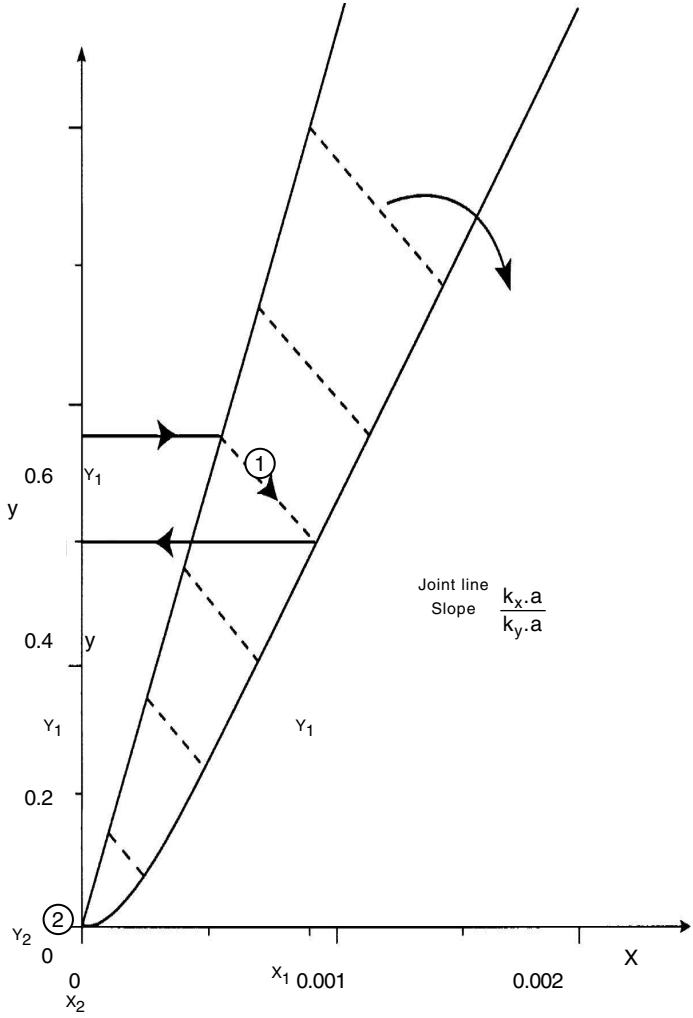

FIGURE 20.P4A
Graphical calculations of y_i.

The procedure to obtain the values of the gas composition at the interface y_i, corresponding to their respective compositions y, using Figure 20.P4a is: for each value of y on the operating line, a straight joining line is drawn to the equilibrium curve, obtaining the value of y_i. The slope of the tie line is $-(k_x/k_y)$.

The value of the slope of the joining straight line is obtained from the statement of the problem using the data obtained for G and L:

$$\left(k_x a\right) = 0.65\left(41{,}367\right)^{0.82} = 3968 \ \text{kmol}/\left(\text{h.m}^3 \cdot \Delta\text{x}\right)$$

$$\left(k_y a\right) = 0.10\left(1061.8\right)^{0.776}\left(41{,}367\right)^{0.2} = 187.2 \ \ \text{kmol}/\left(\text{h.m}^3\Delta\text{y}\right)$$

Thus, the slope is:

$$-\left(k_x/k_y\right) = -\left(k_x\, a/k_y\, a\right) = -21.9$$

Table 20.P4b is generated when operating as indicated before, allowing one to obtain, by numerical or graphical integration, the value of the integral term.

TABLE 20.P4b

y	y_i	ϕ(y)
0.001	0.0005	2001
0.01	0.0067	306
0.02	0.0148	193
0.03	0.0230	144
0.04	0.0315	119
0.05	0.0400	101
0.06	0.0485	88

The number of transfer units is obtained by solving the integral between the values y_1 and y_2, so the function $\phi(y)$ is plotted against y (Figure 20.P4b), graphically or numerically obtaining the value of the area under the curve, between $y_1 = 0.60$ and $y_2 = 0.01$.

From this integration, it is obtained that:

$$N_g = 15$$

Thus, the height of the column is:

$$z = \left(0.172\right)\left(15\right) = 2.57 \text{ m}$$

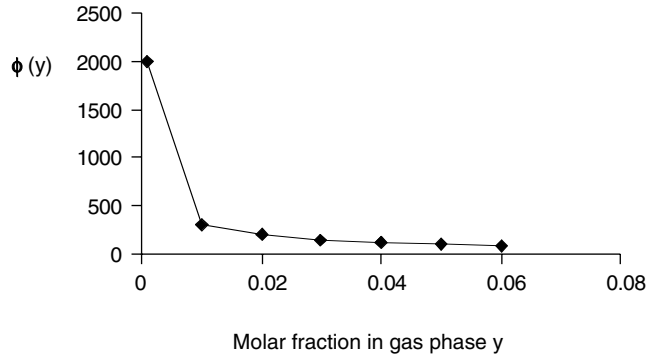

FIGURE 20.P4B
Graphical calculation of N_g.

21

Solid–Liquid Extraction

21.1 Introduction

Solid–liquid extraction is a basic operation to separate one or more components contained in a solid phase by a liquid phase or solvent. The components transferred from the solid to the liquid phase are called solutes, while the insoluble solid is called inert.

Solid–liquid extraction has different names depending on the objective of the process. Thus, it may be known as lixiviation, washing, percolation, etc. It is usually described as "leaching" or "extraction solvent" in English-language literature. The purpose of this operation can be diverse, since in some cases it is necessary to eliminate from a solid an undesirable component by dissolving it into a liquid, which is called washing. However, in other cases, it is desired to obtain a valuable component contained in a solid by dissolving it into a liquid, which is called lixiviation. The term "percolation" refers to the way that the operation is carried out, which is by pouring a liquid onto a solid.

There are different ways in which the solute is contained in the inert solid. Thus, it may be a solid dispersed in insoluble material or it may cover the surface. It may also be a liquid adhered or retained within the solid or contained in its molecular structure.

Important applications of the solid–liquid extraction in the food industry include: extraction of animal and vegetable oils and lipids, washing precipitates, obtaining extracts from animal or vegetable materials, obtaining sugar, and manufacturing tea and instant coffee, among others.

This type of operation may be performed in one or multiple stages. A stage refers to equipment in which the phases are in contact for a determined time, so that the mass transfer among the components of the phases is carried out, tending to equilibrium over time. Once the equilibrium is reached, a mechanical separation of phases is applied. It is difficult to reach equilibrium in one stage, so it is necessary to define the efficiency in order to calculate the real stages. Efficiency of one stage is the quotient between the change in composition actually achieved and the change that should have been achieved for an equilibrium situation under the working conditions.

The ways of operation used in extraction processes can be continuous or batch. One or more stages can be employed for batch operations, with new solvent in each stage, or under countercurrent. A simple stage consists of an agitated mixer, where the solid and the solvent are in contact for a given time. Then the mixture is transferred to a separator, where the phases, called extract and exhausted solids, are obtained after a specified standing time. The extraction and separation stages can be carried out in one piece of equipment instead of two; this type of equipment is called an extractor.

21.2 Solid–Liquid Equilibrium

As in other unit operations, the equilibrium to which a process tends during the operation, as well as the rate needed to reach equilibrium, should be considered by studying the different factors that affect it. It is considered that the extraction mechanism of a solute contained in a solid particle by means of a liquid occurs in three successive stages until equilibrium is reached:

1. Phase change of the solute occurs when the solute changes from solid to liquid phase. The solution of the solute occurs through a solid–liquid interphase. Even when the theory of the limiting layer can be applied to study this stage, this layer has not yet formed. Therefore, this solution phenomenon is considered to be instantaneous and does not affect the global extraction rate.
2. In the next stage, the solute is diffused in the solvent contained in the pores of the solid. In most cases, the solute is within the solid particles, so the solvent should fill the pores of the inert solid to be in contact with the solute. The transfer of the solute from the interior of the solid particles to the surface occurs due to the concentration gradient that exists between the solid–liquid interphase and the external surface of the solid. The solvent inside the pores remains almost stationary; therefore, the transfer of solute from zones with greater concentration to the exterior is performed only by molecular diffusion. Mass transfer rate in this stage is expressed as:

$$N_S = -D_L \frac{dC}{dz}$$

where:

N_S = mass flux in $kg \cdot m^{-2} \cdot s^{-1}$
D_L = diffusivity of the solute through the solvent in $m^2 \cdot s^{-1}$
C = concentration of the solute in $kg \cdot m^{-3}$
z = distance inside the pore in m

Hence, increasing the mass transfer can be achieved by raising the temperature, thus causing a diffusivity increase. Also, if the particles are crushed, the length of pore decreases, thus increasing the mass transfer rate. In some cases, the solvent can break the structure of inert solids, producing fine particles that can block the pores and make the penetration of the solvent difficult. In other cases, for example, in the extraction of sugar from beet, solute dissolution takes place through the cellular walls allowing sugar molecules to pass through the walls while retaining undesirable components. However, if crushing is large enough to break the cellular structure, such components will dissolve and contaminate the sugar solution.

3. Once the solute reaches the particle's surface, it transfers to the solution due to a concentration gradient. Mass transfer is performed simultaneously by molecular and turbulent transport. Mass transfer rate at this stage is expressed as:

$$N_S = \frac{dM}{A\,dt} = K_L\left(C_S - C\right)$$

where:

M = mass of solute transferred (kg)
A = particle-solution contact surface (m^2)
t = time (s)
C_S = solute concentration at the solid's surface ($kg \cdot m^{-3}$)
C = solute concentration in the solution at a determined instant ($kg \cdot m^{-3}$)
K_L = mass transfer coefficient ($m \cdot s^{-1}$)

Increase of the mass transfer rate can be achieved by stirring the solution, since this way the coefficient K_L increases.

Each of the stages described has its own transfer rate, with the slowest the one that controls the extraction process. As stated earlier, the dissolution of the solid during the first stage is considered to be instantaneous, so it will not affect the process. Generally, the second stage controls the transfer rate since it usually develops slowly

In order to increase the global transfer rate, different factors are usually affected, including size of particle, temperature, and stirring of the fluid, influences already described. In addition to the mentioned factors, the type of solvent, which increases the transfer rate, should also be taken into account. A selective solvent with a viscosity low enough to circulate easily within the solid should be used.

It is evident that mass transfer takes place until equilibrium is reached; thus, it is necessary to define the concept of equilibrium. Equilibrium is reached when the solute is totally dissolved, thus obtaining a solution with

uniform concentration. (It should be highlighted that this is not a true equilibrium, since the solvent might contain more solute.) When the solute content in the solid is high enough, it is considered that equilibrium is reached when the solution in contact with the solid is saturated.

If the system has reached equilibrium, two phases will separate when it is left to stand:

1. Extract or overflow, which is the separated solution, solute, and solvent, also called miscella
2. Exhausted solids or underflow, which is the residue formed by the inert solids and the solution retained within them. If equilibrium has been reached, this solution will have the same solute concentration as the extract; if the solution is saturated, the inert solids can also contain undissolved solute.

The different variables used throughout this chapter are defined as:

E = mass flux of overflow (kg/h)
R = mass flux of underflow (kg/h)
Y_i = mass fraction of component i in overflow
X_i = mass fraction of component i in underflow
i = solute (S), solvent (D), or inert component (I)

Since the inert component cannot dissolve in the solvent, there will be no inert component in the overflow, so $Y_I = 0$.

The composition of any stream is expressed as the mass fraction with two subscripts; the first indicates the component, and the second the stream. Thus, for example, X_{SR} is the mass fraction of the solute in the stream R; Y_{DE} is the mass fraction of the solvent in stream E.

21.2.1 Retention of Solution and Solvent

In solid–liquid extraction, the composition of the overflow is the same as that of the liquid retained within the solid. In order to solve the different problems related to this type of operation, it is essential to know the amount of liquid retained within the solid and its variation with the composition of the solution. Hence, experiments should be carried out to obtain these data.

Solution retention is defined as the amount of solution retained per unit mass of inert solid:

$$r = \frac{\text{kg solution}}{\text{kg inert solid}}$$

In the same way, solvent retention can be defined as the amount of solvent retained per unit mass of inert solid. Retention data are usually presented

in graphic form by using triangular diagrams or diagrams in rectangular coordinates free of inert solids.

21.2.2 Triangular and Rectangular Diagrams

The solution of solid–liquid extraction operations can be performed by mass and energy balances, taking into account the concept of ideal stage. However, energy balances are not important in these extraction processes, so mass balances are employed. Calculations can be done by algebraic or graphical methods. The most frequently used diagrams in these types of operations will be described next.

21.2.2.1 Triangular Diagram

This type of diagram is a right triangle (Figure 21.1) in which the vertex of the right angle represents the inert component (*I*), while the other two vertexes represent the solvent (*D*) and the solute (*S*). The mass fraction of the solvent is plotted against the mass fraction of the solute for the underflow phase. The hypotenuse of the triangle represents the overflow or extract since it does not contain inert component. For any point, the mass fraction of the solute is obtained on the horizontal axis, while that corresponding to the solvent is obtained on the vertical axis. The mass fraction of inert component can be obtained from the difference of one minus the sum of the other two fractions.

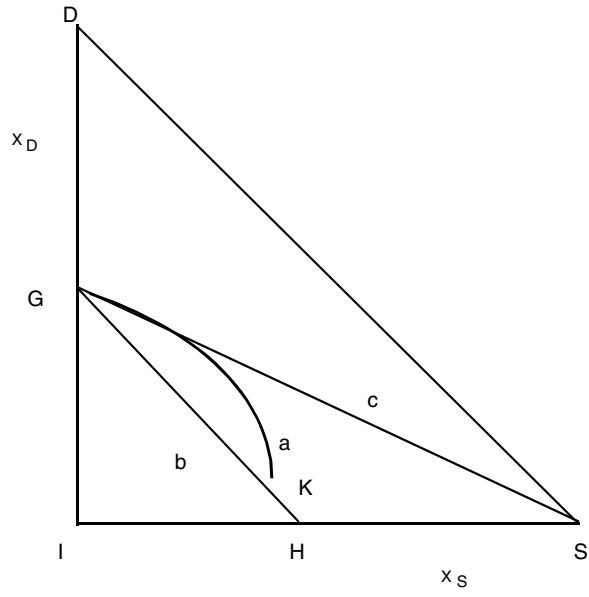

FIGURE 21.1
Triangular diagram: (a) retention curve; (b) constant retention of solution; (c) constant retention of solvent.

The underflow data should be obtained experimentally, which allows representation of the retention curve (*GK*). Generally, the data experimentally obtained are:

y_S = kg solute/kg solution

r = kg solution/kg inert

The mass fractions of solute and solvent are obtained from these data:

$$X_S = \frac{y_S}{1+\frac{1}{r}} \frac{\text{kg solute}}{\text{total kg}} \tag{21.1}$$

$$X_D = \frac{1-y_S}{1+\frac{1}{r}} \frac{\text{kg solvent}}{\text{total kg}} \tag{21.2}$$

The retention curve is obtained by plotting the values of X_S against those of X_D (Figure 21.1). If the amount of retained solution is constant, then the retention line is:

$$X_D = \frac{r}{r+1} - X_S \tag{21.3}$$

which is the equation of a straight line with an ordinate to the origin equal to $r/(r + 1)$ and a slope equal to –1, that is, a straight line parallel to the hypotenuse.

When the amount of solvent retained by the inert solids is constant, the retention curve is:

$$X_D = \frac{r}{r+1}\left(1 - X_S\right) \tag{21.4}$$

which is the equation of a straight line that passes through the point (1,0), the vertex *S*.

When equilibrium is reached during a solid–liquid extraction, the concentration of the overflow phase (Y_S,Y_D) is the same as the concentration of the liquid retained by the solids of the underflow. Thus:

$$Y_S = \frac{X_S}{X_S + X_D}$$

$$Y_D = \frac{X_D}{X_S + X_D}$$

Hence, the following relationship is obtained:

$$X_s/Y_S = X_D/Y_D$$

or:

$$\frac{X_S - 0}{Y_S - 0} = \frac{X_D - 0}{Y_D - 0}$$

This last expression corresponds to a straight line that passes through the points (0,0), (X_S,X_D), and (Y_S,Y_D); since the compositions of the overflow and underflow are those corresponding to equilibrium, such lines are called tie lines or join lines. For any line passing through the vertex *I*, the intersection with the retention curve determines the composition of the underflow, while the intersection with the hypotenuse corresponds to the composition of the overflow.

For a solid–liquid extraction in which the solute is in solid phase, the amount of solute that can be dissolved is limited by the saturation of the solution. For this reason, the diagram can be divided in two zones for a determined temperature: one of saturation and another of nonsaturation (Figure 21.2). If the concentration of the saturated solution (Y_{SAT}) corresponds to point *A* on the hypotenuse, then the line *IA* represents the mixture of inert solid and saturated solution. Solutions on the zone above this line will be nonsaturated lines, while the zone below this line corresponds to saturated solutions. Any point *N* of the nonsaturated zone represents a ternary mixture, so that the separated overflow has a composition Y_1, obtained from the intersection of lines *IN* and the hypotenuse *DS*. Points in the saturated zone (e.g., point *P*) will yield an overflow of saturated solution (Y_{SAT}), while the solute retained by the inert solid has a concentration *X*, obtained from the intersection of the straight lines *AP* and *IS*.

If the solute is initially in liquid phase, it may be miscible in the solvent in any proportion. In this case, all the points on the hypotenuse represent single-phase systems, while the triangle's interior represents nonsaturated solutions. When the solute is not miscible in all proportions in the solvent, three zones (Figure 21.3), defined by the saturation of the solute in the solvent (Y_{2SAT}) and by the solute's saturation (Y_{1SAT}), appear. The zone between the two saturation lines is usually where solid–liquid extraction operations are performed. Zones 1 and 3 are made of a nonsaturated liquid phase and inert solids, while zone 2 is formed by inert solids and two liquid saturated phases with compositions (Y_{1SAT}) and (Y_{2SAT}).

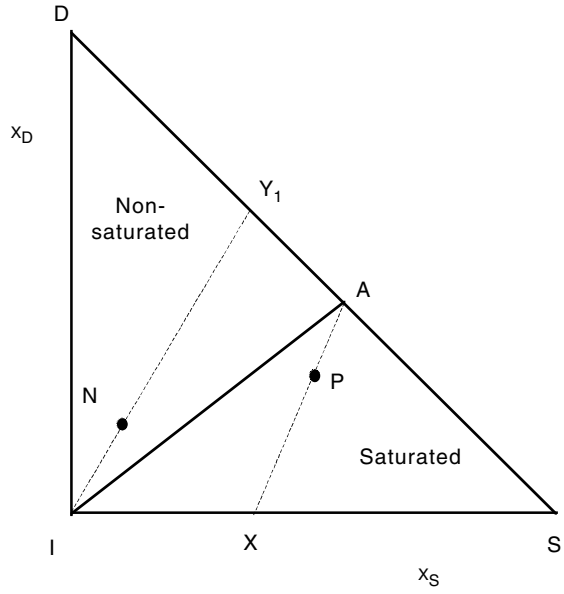

FIGURE 21.2
Triangular diagram: saturation zones for the overflows.

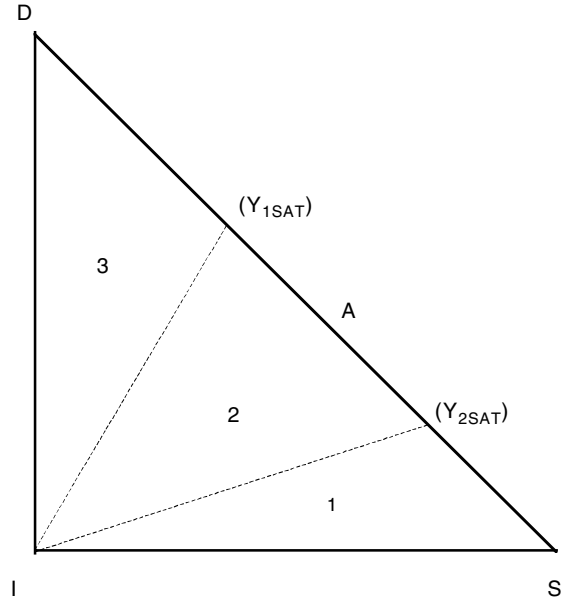

FIGURE 21.3
Triangular diagram: saturation zones for partially miscible solutes.

21.2.2.2 Rectangular Diagram

This diagram is also called a diagram of coordinates free of inert solids, since the variables are referred to on an inert-free basis. The fraction of inert component N is represented on the ordinates:

$$N = \frac{X_I}{X_S + X_D} \tag{21.5}$$

The fractions of underflow (X') and overflow (Y') free of inert solids are represented on the abscissas:

For the underflow:
$$X' = \frac{X_S}{X_S + X_D} \tag{21.6}$$

For the overflow:
$$Y' = \frac{Y_S}{Y_S + Y_D} \tag{21.7}$$

Since the overflow does not contain inert solids, it is complied that $N = 0$, so the overflow line coincides with the abscissa's axis (Figure 21.4).

The composition of the underflow phase is obtained from the retention curve (GK). In the case of constant retention of solution, the underflow line will be parallel to the abscissa axis (straight line GH). In the case of constant solvent retention, the underflow line will be a straight line that passes through the point (1,0) (straight line GS).

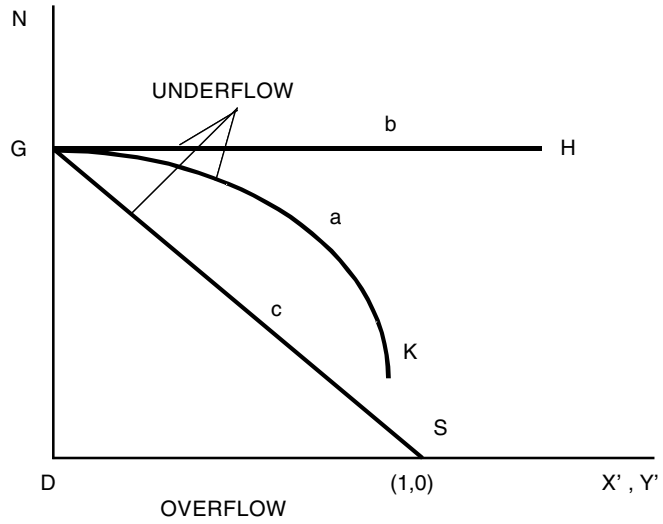

FIGURE 21.4
Rectangular diagram: (a) retention curve; (b) constant retention of solution; (c) constant retention of solvent.

21.3 Extraction Methods

The extraction of solutes contained in a solid phase can be performed in different forms. This section presents three types of operation: single stage, multistage concurrent system, and continuous countercurrent multistage system.

21.3.1 Single Stage

The single-stage method is a batch operation. A food (R_A) is in contact with all the solvent (D) to obtain an underflow R_1, which contains the inert solid and the solution retained in the solids, and the overflow E_1 that contains the formed solution (Figure 21.5a).

This is considered an ideal stage, so the overflow and underflow streams are in equilibrium. In these types of operations, generally, the data available are the feed stream or amount of food R_A and its composition X_{SRA}, and the amount of solvent D and its composition Y_{DD}. On the other hand, the amount of overflow and underflow, as well as their composition, should be determined.

Mass balances should be set up to determine these variables and the mathematical model solved by algebraic or graphical methods.

Global balance: $R_A + D = R_1 + E_1 = M$

Solute balance: $R_A X_{SRA} + D Y_{SD} = R_1 X_{SR1} + E_1 Y S_{E1} = M X_{SM}$

Solvent balance: $R_A X_{DRA} + D Y_{DD} = R_1 X_{DR1} + E_1 Y_{DE1} = M X_{DM}$

The representative point M, called the pole, is fictitious and can be found in the triangular diagram from the intersection of the straight lines $R_A D \cap R_1 E_1$ that join the food with the solvent and the overflow with the underflow, respectively (Figure 21.5b). To solve the stated problem, the M pole should be placed on the straight line $R_A D$, having the following coordinates:

$$X_{SM} = \frac{R_A X_{SRA} + D Y_{SD}}{R_A + D} \tag{21.8}$$

$$X_{DM} = \frac{R_A X_{DRA} + D Y_{DD}}{R_A + D} \tag{21.9}$$

The compositions of the overflow phase E_1 and underflow phase R_1 are obtained by drawing the "tie" that passes through the pole M. That is, point E_1 of composition Y_{SE1} and Y_{DE1} is obtained from the hypotenuse by joining points I and M, while point R_1 with composition X_{SR1} and X_{DR1} is obtained

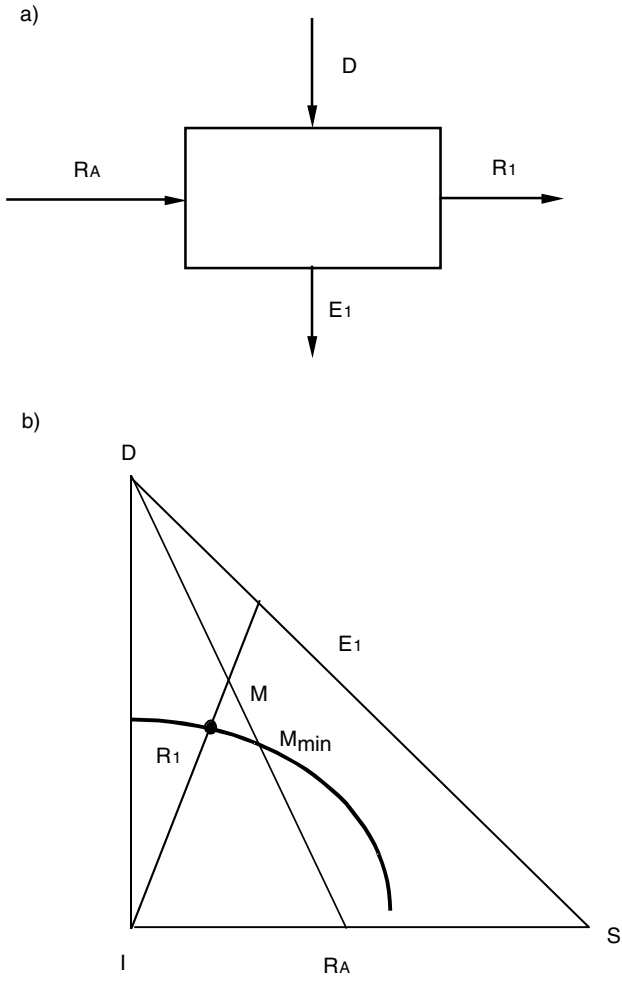

FIGURE 21.5
Single-stage system: (a) scheme of the contact; (b) operation on the triangular diagram.

on the retention curve. The quantities R_1 and E_1 can be obtained from the mass balance stated.

In extraction operations, it is important to know the flow or minimal amount of solvent required to carry out the extraction of solute. This amount (D_{MIN}) is obtained when the pole M is placed exactly on the retention curve. However, in this case, $E_1 \cdot (E_1M) = R_1 \cdot (R_1M)$; if $M = M_{MIN}$, it is complied that R_1 coincides with M; therefore, $(R_1M) = 0$, and since (E_1M) is different from zero, then it should be complied that the amount $E_1 = 0$. This means that no overflow will be obtained; therefore, it is necessary to work with solvent flows greater than the minimum.

The solution of the problem can also be obtained by using the rectangular diagram. The nomenclature used in this diagram, which is free of inert components, will be defined first. Thus:

E' = flow or amount of the overflow phase free of inert solids of stream E
R' = flow or amount of underflow free of inert solids of the stream R
Y'_j = ratio of solute to solute plus solvent of stream j for overflow
X'_j = ratio of solute to solute plus solvent of stream j for underflow
N_j = ratio of inert solid's solute plus solvent for stream j

The mass balances in this case are:

Global balance: $R'_A + D' = R'_1 + E'_1 = M'$
Solute balance: $R'_A X'_{RA} + D' Y'_D = R'_1 X'_{R1} + E'_1 Y'_{E1} = M' X'_M$
Solvent balance: $R'_A N_{RA} + D' N_D = R'_1 N_{R1} + E'_1 N_{E1} = M' N_M$

As in the triangular diagram, in this case M' is a fictitious pole that will be placed on the intersection of R_AD and R_1E_1, its coordinates being:

$$X'_M = \frac{R'_A X'_{RA} + D' Y'_D}{R'_A + D'} \tag{21.10}$$

$$N_M = \frac{R'_A N_{RA} + D' N_D}{R'_A + D'} \tag{21.11}$$

Once the pole M' is located, the compositions of the overflow and underflow are obtained by drawing the tie line (vertical line) that passes through M'. The composition of the overflow is obtained on the abscissas, while that of underflow is obtained on the retention curve. When the overflow solution is in equilibrium with the solution retained by the inert solids, it is complied that $X'_{R1} = Y'_{E1}$.

Once the compositions of the overflow and underflow phases are obtained, amounts corresponding to these phases are obtained from the mass balances.

If the solvent is pure, then $N' = Y'_D = 0$. That is, the point that represents the solvent stream is the origin of the coordinates. When the solvent is not pure, this point will be placed inside the diagram.

These graphical methods allow solution of any type of problem arising from a single-stage system. However, when the retention of solution or solvent is constant, the mathematical model can be solved by analytical methods.

For a constant solution retention, it can be considered that L is the total amount of solution retained. The amount of overflow E_1 is obtained from a

balance of solute plus solvent. Thus, the amount of solute plus solvent that enters the system is:

With the food: $R_A\left(1-X_{IRA}\right)$
With the solvent: $D\left(1-Y_{ID}\right)$

while the amount of solute plus solvent that leaves the system is:

With the upperflow: E_1
With the lowerflow: L

Therefore,

$$R_A\left(1-X_{IRA}\right)+D\left(1-Y_{ID}\right)=E_1+L$$

This expression allows one to obtain the amount of overflow.

Since the composition of the overflow coincides with that of the retained solution, the composition Y_{SE1} can be obtained from a solute balance:

$$R_A X_{SRA}+DY_{SD}=\left(L+E_1\right)Y_{SE1} \tag{21.12}$$

Hence:

$$Y_{SE1}=\frac{R_A X_{SRA}+DY_{SD}}{R_A\left(1-X_{IRA}\right)+D\left(1-Y_{SD}\right)} \tag{21.13}$$

When the solvent is pure, it is complied that $Y_{SD} = Y_{ID} = 0$ and, if, additionally, the food does not contain any solvent $X_{SRA} = 1 - X_{IRA}$, then:

$$Y_{SE1}=\frac{R_A X_{SRA}}{R_A X_{SRA}+D} \tag{21.14}$$

When the solvent retention is constant, L'' is defined as the total amount of the retained solvent, with R_A'', D'', and E_1'' denoting the amount of food, solvent, and overflow, respectively. The following is obtained from the mass balance:

$$R_A''+D''=L''+E_1''$$

If the ratios of solute to solvent in the stream j of underflow and overflow are X_j'' and Y_j'', respectively, when performing a solute balance it is obtained that:

$$R''_A X''_{RA} + D'' Y''_D = \left(L'' + E''_1\right) Y''_{E1}$$

so the ratio of solute in the overflow is:

$$Y''_{E1} = \frac{R''_A X''_{RA} + D'' Y''_D}{R''_A + D''} \tag{21.15}$$

When the solvent is pure ($Y''_D = 0$ and $D'' = D$), and if, additionally, the food does not contain any solvent ($R''_A = 0$), the only solute that enters the system is $R_A.X_{SRA}$. Hence:

$$Y''_{E1} = \frac{R''_A X''_{RA}}{D} \tag{21.16}$$

so the solute fraction in the overflow is:

$$Y_{SE1} = \frac{R_A X_{SRA}}{R_A X_{SRA} + D} \tag{21.17}$$

21.3.2 Multistage Concurrent System

This method of operation consists of repeating the single-stage method in successive stages in such a way that the underflow obtained in each stage is fed to the following stage. The global amount of solvent to use is subdivided into various fractions, using one fraction in each stage (Figure 21.6a). For this type of operation it is complied that:

$$D_T = \sum D_i$$

$$E_T = \sum E_i$$

Therefore, the maximum yield is obtained when the amount of solvent introduced in each stage is equal, that is, $D_i = D_T/n$.

The mass balances for the first stage are:

Global balance: $R_A + D_1 = R_1 + E_1 = M_1$

Solute balance: $R_A X_{SRA} + D_1 Y_{SD} = R_1 X_{SR1} + E_1 Y S_{E1} = M_1 X_{SM}$

Solvent balance: $R_A X_{DRA} + D_1 Y_{DD} = R_1 X_{DR1} + E_1 Y_{DE1} = M_1 X_{DM}$

in which the pole M_1 is placed at the intersection of the straight lines $R_A D_1$ and $R_1 E_1$ (Figure 21.6b), having as coordinates:

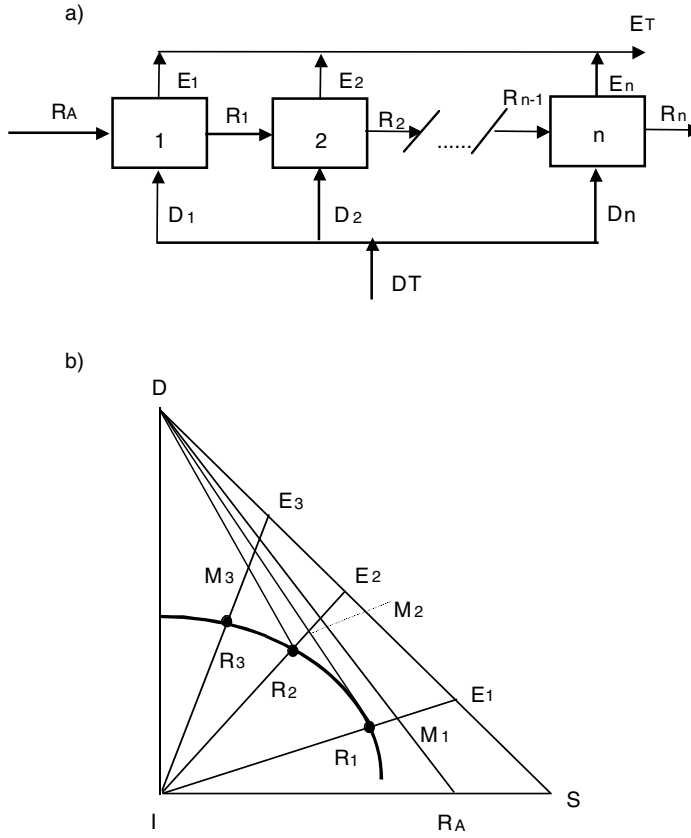

FIGURE 21.6
Multistage concurrent system: (a) scheme of the system; (b) operation on the triangular diagram.

$$X_{SM1} = \frac{R_A X_{SRA} + D_1 Y_{SD}}{R_A + D_1} \tag{21.18}$$

$$X_{DM1} = \frac{R_A X_{DRA} + D_1 Y_{DD}}{R_A + D_1} \tag{21.19}$$

that allow placement of the pole M_1 once the locations of R_A and D_1 are known. The tie line that passes through M_1 will determine the composition of E_1 on the hypotenuse, and of the underflow R_1 on the retention curve.

Operating in an analogous way for a stage *i*, the corresponding mass balances are:

Global balance: $R_{i-1} + D_i = R_i + E_i = M_i$

Solute balance: $R_{i-1}X_{SRi-1} + D_iY_{SDi} = R_iX_{SRi} + E_iY_{SEi} = M_i X_{SMi}$

Solvent balance: $R_{i-1}X_{DRi-1} + D_iY_{DDi} = R_iX_{DRi} + E_iY_{DEi} = M_iX_{DMi}$

in which M_i is the pole of stage i, placed on the intersection of the straight lines ($R_{i-1}D_i$) and ($R_i E_i$), having as coordinates:

$$X_{SMi} = \frac{R_{i-1}X_{SRi-1} + D_i Y_{SDi}}{R_{i-1} + D_i} \tag{21.20}$$

$$X_{DMi} = \frac{R_{i-1}X_{DRi-1} + D_i Y_{DDi}}{R_{i-1} + D_i} \tag{21.21}$$

The tie line that passes through this pole will determine the compositions of overflow E_i and underflow R_i, from which the M_{i+1} can be obtained by repeating the operation successively until the last stage. Figure 21.6b shows the process that should be followed in a triangular diagram, using pure solvent in each stage.

In practice, three types of problems usually occur. The solution method for each case is given next.

First case. It is desired to determine the composition X_{SRn} of the underflow R_n when the amount of feed stream R_A and the total amount of solvent to use D_T are known, as well as their corresponding compositions (X_{SRA} and Y_{SD}) and the number of stages n.

Since D_T is the total amount of solvent, the amount of solvent to use during each stage is $D_i = D_T/n$. The composition of the food X_{SRA} and the solvent Y_{SD} allow placement of the feed R_A and solvent D_i points on the triangular diagram. The pole M_1 will be determined on the straight line R_AD_1, beginning with the coordinates obtained in the balances. When drawing the tie line that passes through M_1, point E_1 is determined on the hypotenuse and R_1 on the retention curve. The latter will feed the second stage. The process is repeated for n stages, in the last stage obtaining points E_n and R_n, which correspond to the compositions of the final streams.

Second case. It is desired to determine the number of stages n required to perform an extraction, from which the amount of feed R_A and its composition X_{SRA} are known. Also, the composition of the final underflow X_{SRn} is known, as is the amount of solvent to use in each stage D_i, as well as its composition Y_{SDi}.

It is possible to place the feed R_A and solvent D_i points based on the compositions X_{SRA} and Y_{SDi}. The pole M_1 is placed on the straight line R_AD_i; E_1 and R_1 will be obtained when tracing the tie line that passes through M_1. The pole M_2 will be placed on the straight line R_1E_1, obtaining R_2 and E_2 when drawing the tie line that passes through M_2. The process is repeated

several times until drawing the tie line that passes through the pole M_n obtaining an underflow with a solute content equal to or lower than that fixed for the final underflow X_{SRn}. The number of stages n is the number of tie lines plotted.

Third case. It is desired to determine the number of stages n when the amount of feed R_A and its composition X_{SRA} are known, as well as the composition X_{SRn} of the final underflow, and the total amount of solvent D_T to use and its composition Y_{SD}.

The way to solve the problem is to assume a number of stages n, which will determine the amount of solvent to use in each stage ($D_i = D_T/n$). Next, the number of equilibrium stages is obtained as in the second case. If this number of stages coincides with the number assumed, then the problem is solved. On the other hand, another value of n should be assumed and the calculation procedure repeated until the number of stages assumed coincides with the calculated number.

Until now, only the calculation method using the triangular diagram has been presented; however, the rectangular diagram with coordinates free of inert solids could also be used. In this diagram, the operation is analogous to that explained for the triangular diagram. The mass balances for a stage i are:

Global balance: $$R'_{i-1} + D'_i = R'_i + E'_i = M'_i$$

Solute balance: $$R'_{i-1}X'_{Ri-1} + D'_i Y'_{Di} = R'_i X'_{Ri} + E'_i Y'_{Ei} = M'_i X'_{Mi}$$

Solvent balance: $$R'_{i-1} N_{Ri-1} + D'_i N_{Di} = R'_i N_{Ri} + E'_i N_{Ei} = M'_i N_{Mi}$$

The pole M'_i is placed on the intersection of $R_{i-1}D_i$ and R_iE_i, its coordinates being:

$$X'_{Mi} = \frac{R'_{Ri-1} X'_{Ri-1} + D'_i Y'_{Di}}{R'_{i-1} + D'_i} \tag{21.22}$$

$$N_{Mi} = \frac{R'_{Ri-1} N_{Ri-1} + D'_i N_{Di}}{R'_{i-1} + D'_i} \tag{21.23}$$

Place the pole M_1 on the straight line R_AD_i, draw the vertical straight line (tie line) that passes through this pole, and determine R_1 and E_1. Place pole M_2 on the straight line R_1D_2, determining R_2 and E_2 by tracing the vertical line that passes through M_2. This process is repeated until the last stage.

The graphical methods to solve problems using triangular as well as rectangular diagrams have been explained here. However, in the two particular cases in which the retention of solute and solvent are constant, the mathematical model set up with mass balances has an analytical solution.

If the retention of solution is constant, it can be considered that L is the flux of solution retained along the different stages. The solute balance for the first stage is:

$$R_A X_{SRA} + D_i Y_{SD} = (E_1 + L) Y_{SE1}$$

As in the case of single-stage contact, the balance of solute plus solvent for the first stage yields the following expression:

$$R_A (1 - X_{IRA}) + D_i (1 - Y_{ID}) = (L + E_1)$$

Thus, the content of solute in the overflow E_1 is:

$$Y_{SE1} = \frac{R_A X_{SRA} + D_i Y_{SD}}{R_A (1 - X_{IRA})) + D_i (1 - Y_{ID})} \tag{21.24}$$

This equation coincides with the one obtained for extraction using single-stage contact.

In general, the balances of solute and solute plus solvent for a stage i of the system are:

Solute: $L Y_{SEi-1} + D_i Y_{SDi} = (L + E_i) Y_{SEi}$

Solute + solvent: $L + D_i (1 - Y_{IDi}) = L + E_i$

The latter balance indicates that the flux of overflow E_i is:

$$E_i = D_i (1 - Y_{ID})$$

Since the flow of solvent D_i that enters in each stage is the same, as is its composition, the flow of overflow E_i that leaves stage i is constant. This means that $E_i = E$ = constant for $i = 2,3,\ldots,n$.

The flow of overflow is constant for all the stages except the first. The flow of overflow for the first stage is obtained from a mass balance for this stage:

$$E_1 = R_A (1 - X_{IR}) + E - L$$

Generally, the solvent does not contain inert solids ($Y_{IDi} = 0$), so $E = D_i$ and the solute balance is:

$$L Y_{SEi-1} + D_i Y_{SDi} = L Y_{SEi} + D_i Y_{SEi}$$

If a constant k is defined as the relationship $k = L/D_i$, the latter equation can be expressed as:

$$(k+1)Y_{SEi} - kY_{SEi-1} = Y_{SD}$$

This is a linear equation in finite differentials of the first order. The solution of this equation is the sum of a particular solution plus a complementary one:

$$Y_{SEi} = (Y_{SEi})_P + (Y_{SEi})_C$$

The particular solution is $(Y_{SEi})_P = Y_{SD}$.

The complementary solution is obtained in a similar manner as for the solution of linear differential equations, assuming that the second member of the initial equation is zero. Thus, it is obtained that:

$$(Y_{SEi})_C = C\left(\frac{k}{k+1}\right)^{i-1} \tag{21.25}$$

where C is a constant. The general solution is:

$$Y_{SEi} = Y_{SD} + C\left(\frac{k}{k+1}\right)^{i-1}$$

where the constant C is obtained by applying the boundary condition:

$$\text{For } i = 1, \qquad Y_{SE1} = \frac{R_A X_{SRA} + D_i Y_{SD}}{R_A(1 - X_{IRA}) + D_i} \tag{21.26}$$

Hence, the final solution is:

$$Y_{SEi} = Y_{SD} + \frac{R_A(X_{SRA} + X_{IRA}Y_{SD} - Y_{SD})}{R_A(1 - X_{IRA}) + D_i}\left(\frac{k}{k+1}\right)^{i-1} \tag{21.27}$$

When the feed does not contain solvent, this equation is reduced to:

$$Y_{SEi} = Y_{SD} + \frac{R_A X_{SRA}(1 - Y_{SD})}{R_A X_{SRA} + D_i}\left(\frac{k}{k+1}\right)^{i-1}$$

When the flow of retained solvent is constant, it is called L''; R''_A, D''_i and E''_i are the amounts of solvent in the feed, solvent, and overflow streams, respectively. Also, X''_j and Y''_j are the ratios of solute to solvent in the overflow and underflow streams, respectively. When performing a balance of solute around the first stage, it is obtained that:

$$Y''_{E1} = \frac{R''_A X''_{RA} + D''_1 Y''_D}{R''_A + D''_1}$$

If this balance is performed for any stage i, the following is obtained:

$$L'' Y''_{Ei-1} + D''_i Y''_D = \left(L'' + E''_i\right) Y''_{Ei}$$

Defining a new parameter $k'' = L''/D''_i$, this equation transforms into:

$$\left(k'' + 1\right) Y''_{Ei} - k'' Y''_{Ei-1} = Y''_D \tag{21.28}$$

This is a linear equation in finite differences of the first order and is solved in a similar way as for constant retention of solution, for the boundary condition:

$$\text{For } i = 1, \qquad Y''_{E1} = \frac{R''_A X''_{RA} + D''_1 Y''_D}{R''_A + D''_1}$$

The final solution is given by the expression:

$$Y''_{Ei} = Y''_D + \frac{R''_A \left(X''_{RA} - Y''_D\right)}{R''_A + D''_i} \left(\frac{k''}{k'' + 1}\right)^{i-1} \tag{21.29}$$

When the feed does not contain solvent, it is complied that $R''_A = 0$ and X''_{RA} tends to zero; the latter equation reduces to the expression:

$$Y''_{Ei} = Y''_D + \frac{R''_A X_{SRA}}{D''_i} \left(\frac{k''}{k'' + 1}\right)^{i-1} \tag{21.30}$$

21.3.3 Continuous Countercurrent Multistage System

In this type of extraction, feed R_A and solvent D enter the multistage system on opposite sides, as indicated in Figure 21.7. The separation efficiency in this type of operation is greater than in other forms of contact. In continuous countercurrent multistage contact, the flow rate of lower flow runs out of

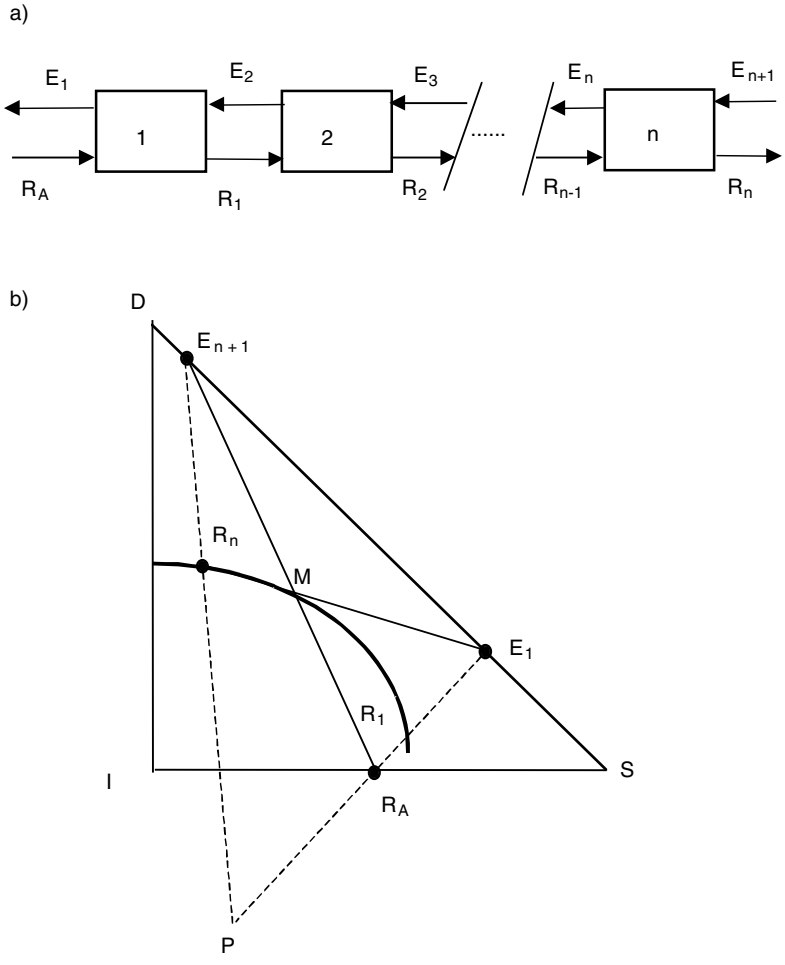

FIGURE 21.7
Continuous countercurrent multistage system: (a) flow of streams; (b) location of point *M* and pole *P*.

solute from the first to the last stage, while the flow rate of upper flow gets richer in solute from the last to the first stage.

The study of this operation using a triangular diagram is performed next. The mass balance applied to the whole system yields the equation:

$$R_A + E_{n+1} = R_n + E_1 = M \tag{21.31}$$

where M is a point in the diagram that represents the flow of a fictitious stream. This point is located on the intersection of the straight lines $R_A E_{n+1}$ and $R_n E_1$, and the value of its coordinates can be obtained from the solute and solvent balances:

$$X_{SM} = \frac{R_A X_{SRA} + E_{n+1} Y_{SEn+1}}{R_A + E_{n+1}} \tag{21.32}$$

$$X_{DM} = \frac{R_A X_{DRA} + E_{n+1} Y_{DEn+1}}{R_A + E_{n+1}} \tag{21.33}$$

The global mass balance can be expressed as:

$$R_A - E_1 = R_n - E_{n+1} = P \tag{21.34}$$

in which P is a pole representing the flow of a fictitious stream that is the difference between the underflow and overflow fluxes on both sides of the system. The pole P is placed on the straight line that joins the points R_A and E_1, besides being located on the line that passes through R_n and E_{n+1}.

The mass balance between the first stage and an intermediate stage i yields:

$$R_A + E_{i+1} = R_i + E_1$$

or:

$$R_A - E_1 = R_i - E_{i+1}$$

Observe that the left-hand side of the equation is the value of the pole P, so this equation can be transformed into a general expression:

$$R_A - E_1 = R_1 - E_2 = \ldots\ldots = R_i - E_{i+1} = \ldots\ldots = R_n - E_{n+1} = P \tag{21.35}$$

This means that the difference between the flows of underflow and overflow remains constant along the system. The position of this pole P can be any position within the plane, but it can also be infinite, as in the case where the straight lines ($R_A E_1$) and ($R_n E_{n+1}$) are parallel.

The solution method for the different types of problems that can occur within the calculation of the number of equilibrium stages is presented next.

First case. It is desired to calculate the number of stages n when the compositions of the streams on both extremes of the system are known. Thus, the known variables are X_{SRA}, Y_{SEn+1}, X_{SRn}, and Y_{SE1}. Knowledge of these compositions allows plotting the points R_A, E_{n+1}, R_n, and E_1 in a triangular diagram. Once these points are located, the straight lines that pass through ($R_A E_1$) and ($R_n E_{n+1}$) are drawn and the intersection of these two straight lines corresponds to the pole P.

Second case. It is desired to determine the number of stages n when the compositions of feed X_{SRA}, solvent Y_{SEn+1}, and underflow X_{SRn} are known, as

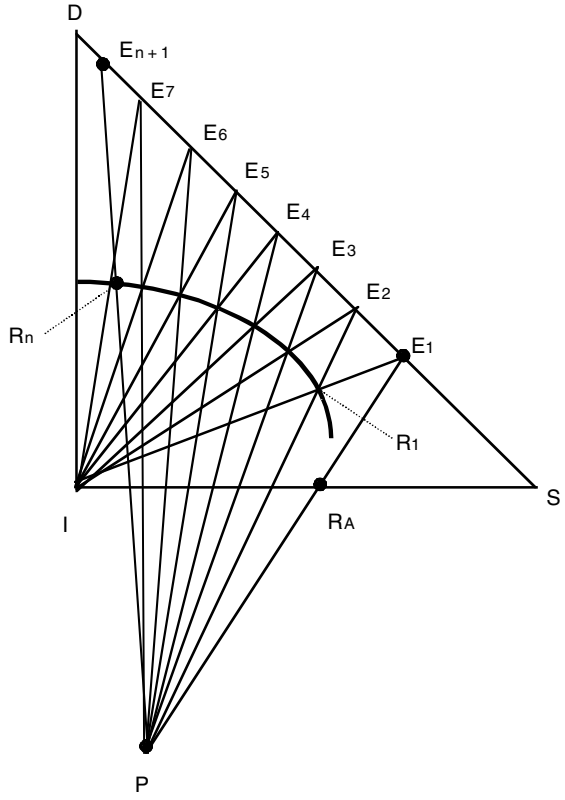

FIGURE 21.8
Continuous countercurrent multistage system: determination of the number of stages.

well as the solvent to feed ratio E_{n+1}/R_A. From these data, it is possible to plot the points that represent the feed R_A and the solvent E_{n+1}. Pole M is placed on the straight line ($R_A E_{n+1}$), taking into account its coordinates. Since the composition of the final underflow X_{SRn} is known, it is possible to plot R_n on the retention curve. The straight line that passes through R_n and point M will determine, on the hypotenuse, the point corresponding to the overflow E_1. Pole P will be placed on the intersection of the straight lines ($R_A E_1$) and ($R_n E_{n+1}$).

Once the pole P is plotted, the number of stages is obtained by drawing the tie line that passes through E_1, which determines R_1 on the retention curve (Figure 21.8). Then, R_1 is joined with pole P and the line extended until it crosses the hypotenuse at point E_2. The tie line that passes through E_2 is drawn, which in turn determines R_2 on the retention curve. The process is repeated successively until a tie line intersects the retention curve on a composition value equal to or lower than X_{SRn}. The number of stages required

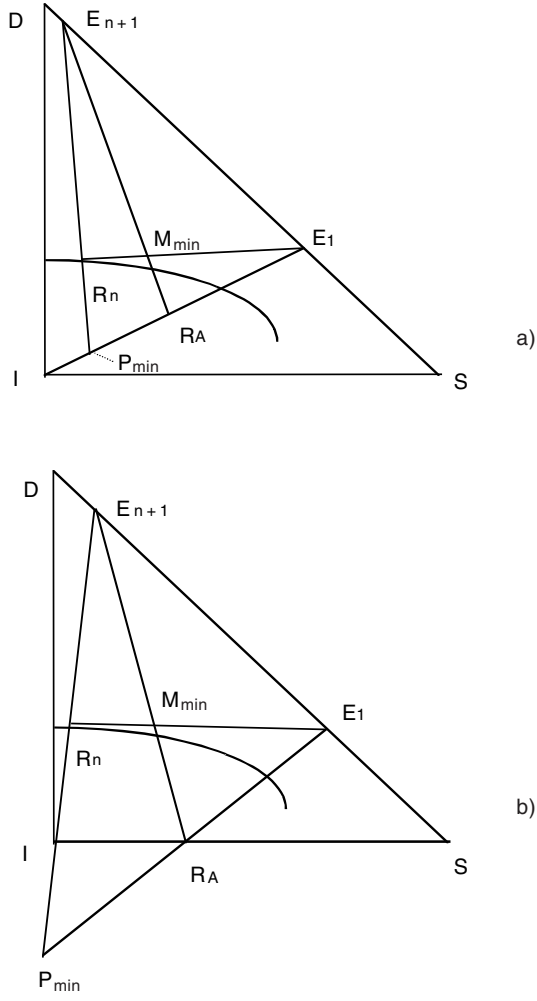

FIGURE 21.9
Minimal flow rate of solvent conditions in continuous countercurrent multistage operation.

to carry out the desired extraction is determined according to the number of tie lines traced.

It is important to know the conditions to perform a given separation with a minimal flow rate of solvent. To calculate this minimal flow rate, the poles M and P should be placed in such a way that the final overflow E_1 is in equilibrium with the feed, or the final underflow R_n is in equilibrium with the solvent E_{n+1} (Figure 21.9).

When using the rectangular diagram, the mass balances are similar, obtaining the expressions:

$$R'_A + E'_{n+1} = R'_n + E'_1 = M'$$

$$R'_A - E'_1 = \ldots\ldots = R'_i - E'_{i+1} = \ldots\ldots = R'_n - E'_{n+1} = P'$$

It can be observed that poles M' and P' also appear in these equations. The former is placed on the intersection of the straight lines $R_A E_{n+1}$ and $R_n E_1$, while pole P' is placed on the intersection of lines $R_A E_1$ and $R_n E_{n+1}$.

The problems are solved in a similar way to that for the triangular diagram. Thus, the points that represent feed, solvent, and final overflow and underflow must be plotted, as well as pole P'. The tie line that crosses E_1 (vertical straight line) determines point R_1 on the retention curve. The straight line that joins P' with R_1 allows one to obtain E_2 on the abscissa axis. The process continues until passing through R_n, so the number of stages is equal to the number of tie lines traced. The minimal solvent flow rate is obtained when any operating line coincides with a tie line.

As in the cases related to single- and multistage contact, when the retention of solution and solvent is constant, the mathematical model set up with the mass balances has an analytical solution.

It is considered, for constant retention of solution, that L is the flow rate of solution retained, which is constant along all stages. The balance of solute plus solvent for the whole system of extractors yields the following expression:

$$E_{n+1} + R_A\left(1 - X_{IRA}\right) = E_1 + L$$

As in the case of a multistage concurrent system, it can be demonstrated that except for the first stage, $E_i = E$ = constant for $i = 2, 3, \ldots, n$. If a solute balance is performed for the whole system, it is obtained that:

$$R_A X_{SRA} + E Y_{SEn+1} = L Y_{SEn} + E_1 Y_{SE1}$$

Hence:

$$Y_{SE1} = \frac{R_A X_{SRA} + E Y_{SEn+1} - L Y_{SEn}}{R_A\left(1 - X_{IRA}\right) + E - L}$$

If the balance is performed for any stage i of the system, then:

$$L Y_{SEi+1} + E Y_{SEi-1} = \left(E + L\right) Y_{SEi}$$

Defining the constant $k = L/E$, the latter equation is expressed as:

$$Y_{SEi+1} - \left(1 + k\right) Y_{SEi} + k Y_{SEi-1} = 0 \tag{21.36}$$

This equation in finite differences can be expressed as:

$$\Big(\big(E-1\big)\big(E-k\big)\Big)Y_{SEi-1}=0 \tag{21.37}$$

where E is the operator (do not confuse with overflow E) that complies:

$$E\,Y_{SEi}=Y_{SEi+1}$$

The solution of the equation in differences presents the solution:

$$Y_{SEi}=C_1+C_2\,k^{(i-1)}$$

In order to obtain the value of the parameters C_1 and C_2, the boundary conditions are applied:

For $i = 1$, $C_1 = Y_{SE1} - C_2$.

For $i = n + 1$, $C_2=\dfrac{Y_{SEn+1}-Y_{SE1}}{k^n-1}$.

Substitution of these values in the latter equation yields:

$$Y_{SEi}=\frac{1}{1-k^n}\Big(Y_{SEn+1}-Y_{SE1}\,k^n+\big(Y_{SE1}-Y_{SEn+1}\big)\,k^{i-1}\Big) \tag{21.38}$$

This equation is valid for $k \neq 1$. For $k = 1$, the equation to use is:

$$Y_{SEi}=Y_{SE1}-\frac{Y_{SE1}-Y_{SEn+1}}{n}\,\big(i-1\big) \tag{21.39}$$

These equations are used for $i = n$ to calculate the number of stages required to carry out the extraction of solute from a food of composition X_{SRA} until obtaining an underflow R_n that retains a solution of composition Y_{SEn}; this solution has the same concentration as the overflow E_n.

When the retention of solvent is constant, L'' is defined as the flow of solvent retained, and R''_A, E''_{n+1}, and E''_1 are the fluxes of solvent in feed, solvent, and overflow, respectively. X''_j and Y''_j are the solute to solvent ratios in stream j of underflow and overflow, respectively.

The global balances of solvent and solute yield the following expressions:

Solvent: $R''_A+E''_{n+1}=L''+E''_1$

Solute: $R''_A\,X''_{RA}+E''_{n+1}\,Y''_{En+1}=L''\,Y''_{En}+E''_1Y''_{E1}$

The solvent streams in the overflows are equal for the different stages, except for the first one:

$$E''_i = E'' = \text{constant} \qquad \text{for} \quad i = 2, 3, \ldots, n$$

Hence:

$$Y''_{Ei} = \frac{R''_A X''_{RA} + E'' Y''_{En+1} - L'' Y''_{En}}{R''_A + E'' - L''}$$

If the solute balance is performed for any stage i:

$$L'' Y''_{Ei-1} + E'' Y''_{Ei+1} = \left(L'' + E''\right) Y''_{Ei}$$

Defining a constant $k'' = L''/E''$:

$$Y''_{Ei+1} - \left(1 - k''\right) Y''_{Ei} + k'' Y''_{Ei-1} = 0 \tag{21.40}$$

which is a linear equation in finite differences, similar to the one obtained for a constant solution retention. It is solved in a similar way, obtaining that:

$$\text{for } k'' \neq 1, \qquad Y''_{Ei} = \frac{1}{1 - \left(k''\right)^n}\left(Y''_{En+1} - Y''_{E1}\,(k'')^n\,\left(Y''_{E1} - Y''_{En+1}\right)\left(k''\right)^{i-1}\right) \tag{21.41}$$

$$\text{for } k'' = 1, \qquad Y''_{Ei} = Y''_{E1} - \frac{Y''_{E1} - Y''_{En+1}}{n}\left(i - 1\right) \tag{21.42}$$

Beginning with a known feed X''_{RA} and using the equations obtained, it is possible to calculate the number of stages with $i = n$ required to obtain an underflow in which the retained liquid has a composition Y''_{En}.

21.4 Solid–Liquid Extraction Equipment

The equipment used to carry out solid–liquid extraction processes varies a great deal, so a clear classification is difficult. Some authors classify equipment according to the size of the particles on which the extraction of the solute will be carried out. Others classify them depending on the volatility of the solvent or whether it is desired to recover the solvent or not. As a

general rule, in the food industry the particles of the material that contain the solute are not very fine, but their size is greater than 200 mesh (0.074 mm of light). Taking into account this fact, extractors are classified according to the contact method in three main groups. It should be noted that this classification does not include all types of extractors.

21.4.1 Batch Percolators

This type of extractor consists mainly of an open deposit or container with a false bottom. The solid particles are placed in the container on the false bottom, which is usually a type of filter or grid. The solvent is distributed on the surface of the solid in such a way that the solvent percolates. The resulting solution crosses the false bottom so that it can be recovered as overflow or extract. In many cases, the solvent is added in such an amount that the solids or load are submerged in the solvent.

Generally, these extractors are used in small industrial plants for extraction of sugar from beets, oil from oleaginous seeds and dry fruits, coffee from roasted and milled grains, tea soluble from dehydrated leaves, etc.

In many cases it is required to use volatile solvents, as in the extraction of oil from seeds, or to work under pressure to achieve a better percolation of solvent through the solid particles. For these reasons, and because of hygienic considerations, these types of extractors are closed.

Figure 21.10 shows a batch percolator, and its functions can be observed as described earlier. When the used solvent is volatile, the incorporation of the solvent recovered should be included, as well as a recycling system with the objective of obtaining a concentrated solution (extract).

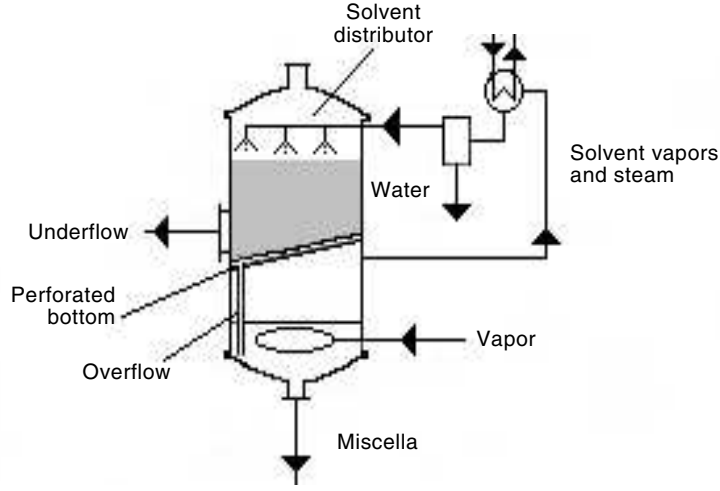

FIGURE 21.10
Batch percolator. (Adapted from Coulson, J.M. and Richardson, J.F., *Ingeniería Quimíca*, Vols. I and VI, Reverté, Barcelona, 1979.)

This figure presents a batch percolator for oil extraction from seeds. It consists of a closed cylindrical container divided into two zones by a slanted division. Seeds are loaded in the top zone and sprayed with solvent using a distributor. The solvent passes through the seed bed and extracts the oil. The extract or overflow passes to the lower section where it is boiled with the water extracted from seeds. The solvent vapors and the steam go to a condenser and then the condensate passes to a separator to eliminate water and return the solvent to the extraction chamber.

21.4.2 Fixed-Bed Multistage Systems

There are cases in which the extraction rate is high and it is possible to perform the desired extraction in one stage. However, this does not happen frequently, so it is required to circulate the solvent under countercurrent through a series of tanks containing the solid. Thus, the fresh solvent is introduced into the tank containing the most nearly exhausted material, flows through the different tanks, and leaves the system through the recently loaded tank. A series of this type of tank is called a diffusion battery.

When the solvent is volatile or the solids bed is not very permeable, it is required to use closed containers that operate under pressure to help the solvent cross the solids bed. In these cases, the series of extraction tanks is called a Robert diffusion battery. The processes in which this type of extractor is used are extraction of coffee, tea, oil, and sugar from beets.

21.4.3 Continuous Percolators

This type of percolator has a moving bed, and most of them operate under countercurrent. Some moving bed extractors or continuous percolators are described next.

Bollmann extractor. This extractor, also called Hansa–Mühle, consists of a bucket elevator unit in a vertical chamber. As shown in Figure 21.11, buckets are loaded with solid at the top right side of the extractor and sprayed with a "half miscella" solution as they descend. In this zone of the extractor, the solid and the solution descend concurrently. The miscella recovered at the right bottom of the extractor is called full miscella. The buckets with partially exhausted solids rise through the left side of the extractor and are sprayed with pure solvent at a determined place in the top zone of the extractor. In this zone, the solid and the solvent circulate under countercurrent in such a way that a half miscella is obtained in the bottom while the bucket with exhausted solids is discharged through the top. This type of extractor is usually employed in processes of extracting oil from seeds.

Hildebrandt extractor. This is an immersion extractor, since the solid is always immersed in the solvent. It consists mainly of three elements placed in such a way that they form a *U*, as shown in Figure 21.12. Solids are fed through one of the vertical branches and conveyed to the bottom by a screw.

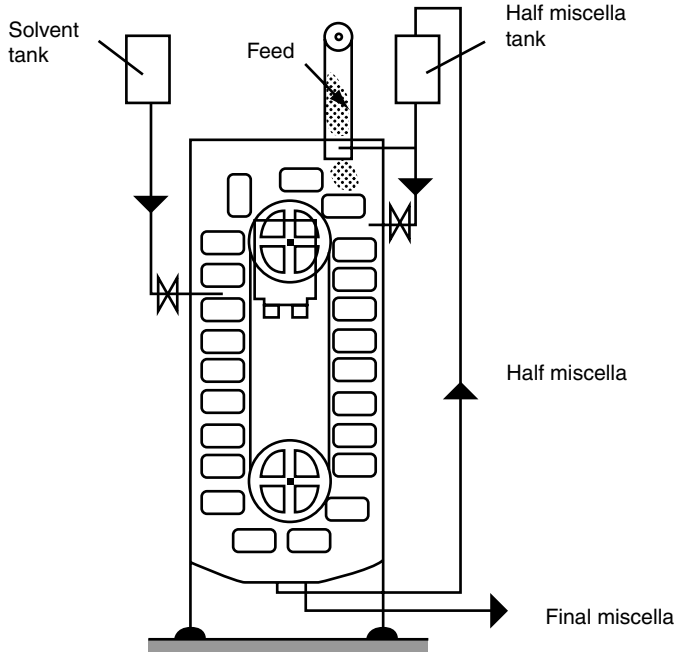

FIGURE 21.11
Bollman extractor. (Adapted from Vian, A. and Ocón, J., *Elementos de Ingeniería Química,* Aguilar, Madrid, 1967.)

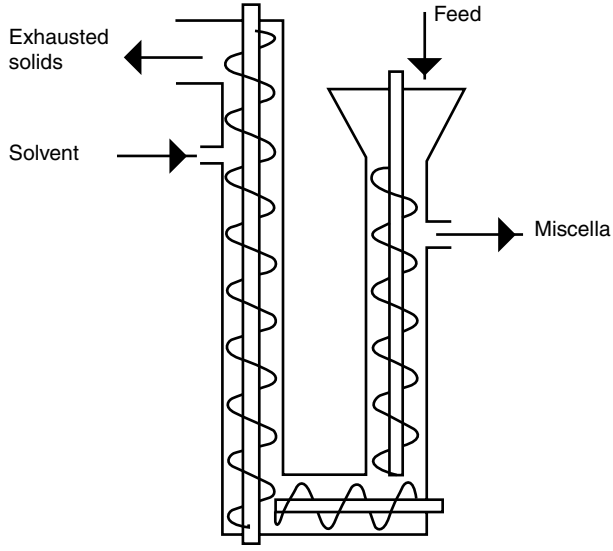

FIGURE 21.12
Hildebrandt extractor. (Adapted from McCabe, W.L., Smith, J.D., and Harriott, P., *Operaciones Unitarias en Ingeniería Quimica,* McGraw–Hill/Interamericana de España, Madrid, 1991.)

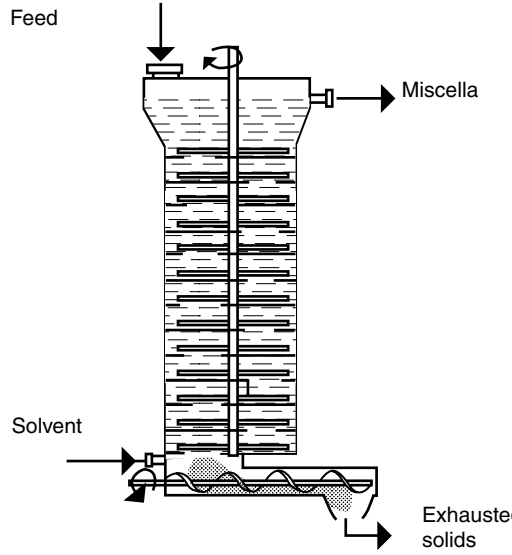

FIGURE 21.13
Bonotto extractor. (Adapted from Brennan, J.G. et al., *Los Operaciones de la Ingeniería de los Alimentos,* Acribia, Zaragoza, Spain, 1980.)

A horizontal branch transports them to the other vertical branch, where they ascend until being discharged at the top. The solids' movement is achieved using screws with a perforated helix surface. The solvent is fed through the branch by which the solids ascend, so the liquid and solid streams circulate countercurrently. A filter at the outlet conduit prevents the solid from coming out with the liquid stream. These extractors are used for sugar extraction from beets and oil from soy flakes, but at the present time construction of this type of extractor is limited.

Bonotto extractor. This extractor consists of a vertical column divided into compartments by horizontal plates (Figure 21.13). Each plate has an opening placed alternately on two consecutive plates. A vertical axle contains rotating blades placed between plates that wipe the solids and cause them fall to the lower plate through the opening. The solids are fed through the top of the column and go downwards, while the solvent enters at the bottom, so the miscella exits through the top of the column. Liquid and solid flows are countercurrent. These extractors are used to extract oil from seeds and dry fruits. Other extractors are based on this extraction principle by immersion in a column, although with some variants, such as Allis Chalmer, Oliver, etc.

Rotocel extractor. This equipment is based on percolation extraction. It consists of a closed cylindrical vertical chamber in which a cylindrical tank divided into compartments rotates. The bottom of the tank is wedge shaped and perforated (Figure 21.14). The solids are charged in these compartments at a determined point and successively sprayed with miscellas that are more diluted each time, until they are sprayed with pure solvent. The liquid

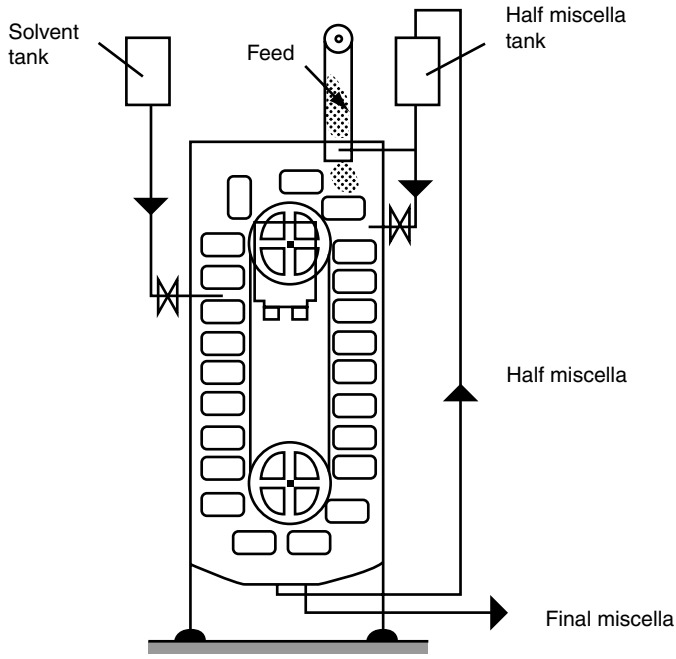

FIGURE 21.14
Rotocel extractor. (Adapted from Vian, A. and Ocón, J., *Elementos de Ingeniería Química*, Aguilar, Madrid, 1967.)

crosses the bed and is collected at the bottom, and the miscella obtained from one compartment is used as solvent for the preceding compartment. There is a drain zone after solids are sprayed with pure solvent, and finally the exhausted solids are discharged. This type of extractor is used for sugar and oil extraction.

21.4.4 Other Types of Extractors

In addition to the extractors described, a series of extractors employed in the oil extraction industry can be partially included in some of the groups stated earlier. Some examples are explained in this section.

Vertical immersion column extractor. This extractor consists of a vertical column, (Figure 21.15) in which the solid is fed into the top, and a conical screw axle that impels the solid material in an ascending and descending movement. The solid that reaches the bottom of the column is driven to a second column by a conveyor screw. In this second column, the solid is extracted by a perforated bucket elevator and then fed into the top of the second column, draining through the buckets and flooding the first column. The highest part of the column has a truncated cone shape and is wider than the rest of the unit, making it easier to clarify and extract the solution. The exhausted solids are eliminated at the top of the second column.

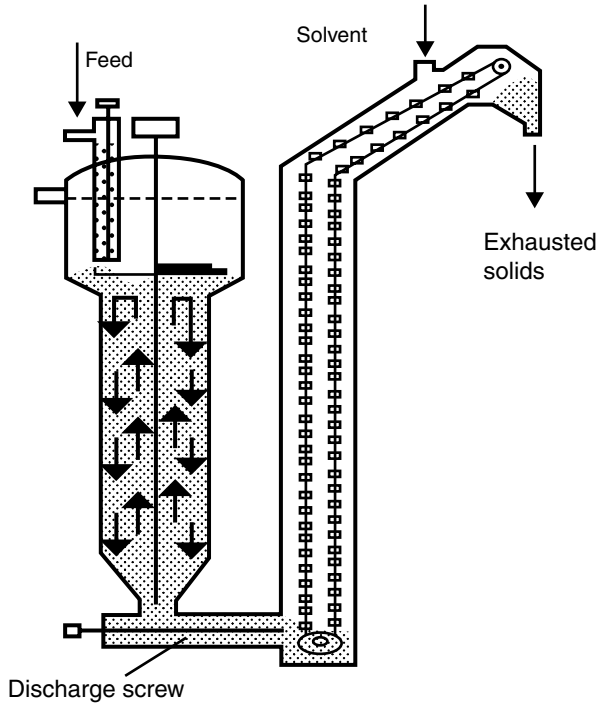

FIGURE 21.15
Vertical immersion column extractor. (Adapted from Bernardini, E., *Technologia de Aceites y Grasas*, Alhambra, Madrid, 1981.)

C.M.B percolation extractor. This is a moving-bed percolation extractor consisting of a metal chamber that contains a perforated-bucket chain (Figure 21.16). The buckets contain the solid, which is sprayed with intermediate solution coming from the bottom from the chamber. The solution drains through the solid while the buckets move. Fresh solvent is sprayed near the end of the chain. Once the solvent is drained through and the solids are exhausted, the bucket is discharged. Then the empty bucket is filled with new solids, and the extraction process begins again. The final miscella is collected at the bottom of the chamber at the section corresponding to the back of the solids feed zone. It can be observed that, in this process, the solvent and solid flow countercurrent due to a series of pumps that take the miscella to the different buckets. This extractor is widely used because it is simple and easy to operate. The De Smet extractor is similar to this one, but there the solid is transported on a conveyor belt.

Soxhlet Extractor. This apparatus is usually employed in laboratory experiments, although it is used in low-capacity facilities; Figure 21.17 shows this type of extractor. It can be observed that the solvent is boiled in a bioiler and the condensed vapors are sent to the container where the solid is placed. The overflow is sent back to the cauldron where solvent vapors are produced and used for new extractions. In this way, the boiler accumulates the solute.

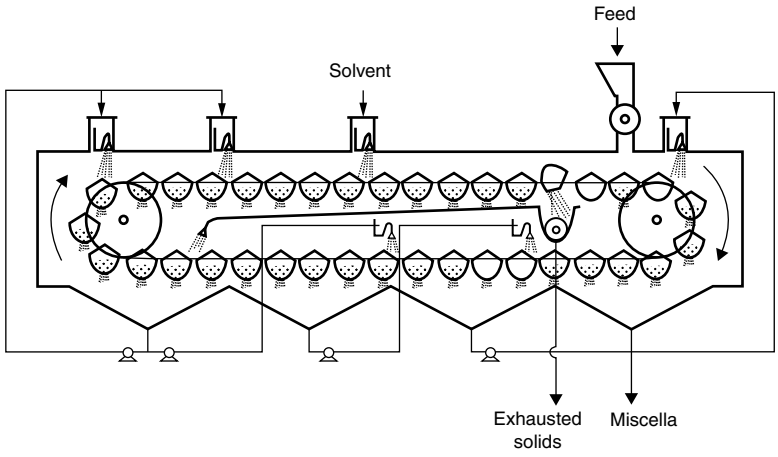

FIGURE 21.16
Percolation extractor. (Adapted from Bernardini, E., *Technología de Aceites y Grasas,* Alhambra, Madrid, 1981.)

Besides these extractors, there are other types that function by immersion or percolation, such as Anderson, Luigi, etc., described elsewhere in the literature. It is important to highlight an extractor that combines two types of extractors in series: the first works by percolation and the second by immersion.

21.5 Applications to the Food Industry

Solid–liquid extraction is a unit operation with diverse applications in the food industry. This section will explain some processes that use extraction with solvent as the main base.

Extraction of sugar from beets. Sugar can be obtained from sugar beet using water as the extraction liquid. The extractors used are generally a diffusion battery or Hildebrandt or Bonotto extractors.

In order to facilitate the extraction operation, beets are cut in long V-shaped slices to form the bed and are then immersed in water. The liquid may have difficulties crossing the bed, so it is convenient to introduce water under pressure. The cellular structure should not be damaged since undesired components, besides sugar, can be extracted. Also, the temperature should be controlled, because if it is too high, undesired nonsugared compounds can be extracted. In general, the final extract obtained contains approximately 15% of dissolved solids. The extract should be purified by a sedimentation and filtration process and then concentrated in evaporators that work under pressure. The crystals are separated by centrifugation, finally obtaining sugar.

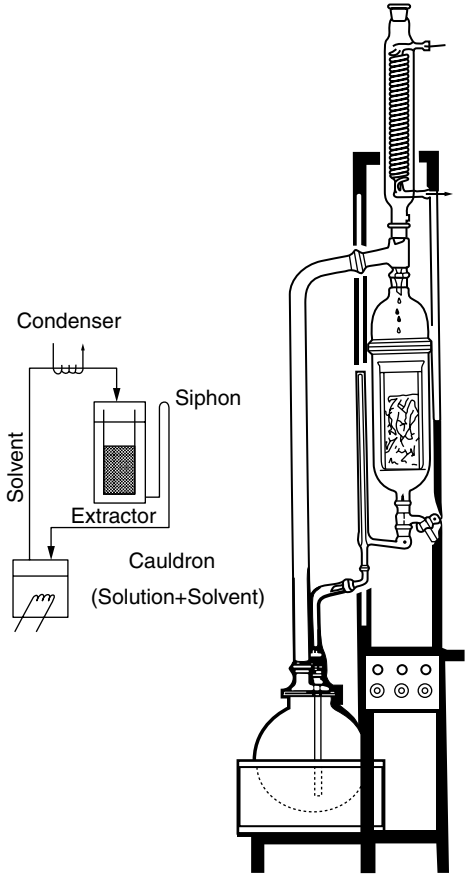

FIGURE 21.17
Soxhlet extractor.

Elaboration of instant coffee. The extraction process is one of the most important stages in the production of instant coffee. The extraction is usually done on roasted and crushed beans, using water as the extractive fluid, obtaining a final solution that contains around 25 to 30% of solids. The solution is then taken to an atomizer, which yields instant coffee grains as a final product. Coffee extraction is carried out in equipment especially designed for this process, consisting of extractors that work under countercurrent, multistage systems, and fixed beds. The solid recently charged is extracted with water at 100°C and, as the process continues, the temperature of the water is increased. High temperatures favor the hydrolysis of insoluble carbohydrates, which in this way become soluble, increasing the soluble solids content in the final solution. However, very high temperatures can hydrolyze substances that may confer undesirable aromas and flavors to the extract.

Elaboration of instant tea. An initial stage to obtain instant tea is extraction with hot water, an operation carried out in fixed-bed extractors, using water at 70°C in the first stages and reaching 90°C during the last. Vacuum is applied to the extractor to facilitate the operation, filling it with dehydrated leaves and re-establishing the pressure with a carbon dioxide stream. The final extract has a solids concentration between 2.5 and 5%, which is too low. For this reason, a distillation that eliminates the volatile products is performed until the final product is obtained. The residual solution, free from aromas, is concentrated by vacuum evaporation, obtaining a solution that contains 25 to 50% of soluble solids. The aromatic fraction obtained during the distillation stage is added to the concentrated solution. Next, instant tea is obtained during a drying stage by freeze drying or atomization. The initial extraction stage can also be performed in moving-bed extractors similar to the Rotocel type under countercurrent and continuously.

Extraction of vegetable oils. The process of extraction with solvent is very important in order to obtain vegetable oils and can be used as an alternative to or in combination with a squeezing operation. After the extraction process, the overflow should be filtered to eliminate suspended solids. The filtrated solution that contains oil, solvent, and water is driven to an evaporation tower to eliminate the solvent, which can be recycled. The oil, water, and residual solvent mixture is conveyed to a steam distillation tower, where oil free from solvent is obtained, while vapors are condensed and taken to a separator where water is eliminated and solvent recovered.

On the other hand, the exhausted solids, called flakes, together with those coming from the filtration stage, contain solvent; since in most cases this will be employed as cattle feed, it is essential to eliminate the solvent retained. The flour is taken to a dryer where the last traces of solvent are removed. The process described or similar processes are used to obtain oil from vegetable products such as oil seeds or dry fruits. Olives, cotton, peanuts, rape, copra, hemp, sunflower, linseed, palm, castor, sesame, soy, and tung seeds, among others, are usually employed. Oil can also be obtained from corn germ, tomato seed, olive bagasse, grape pips, etc.

One factor that influences extraction operations is the type of solvent used. There is a great variety of solvents, but the most used are hexane, heptane, ciclohexane, benzene, trichloroethylene, and carbon sulfur. The last two solvents have a density higher than that of water, so they can stand below a water layer without producing hazardous vapors; however, carbon sulfur is very flammable and the trichloroethylene is toxic. Even though the trichloroethylene has a high extractive power, its use is limited because it cannot remain as residue in the exhausted flour used for cattle fodder due to its high toxicity.

In some countries, tri- and dichloroethylene are not permitted in the food industry because of their carcinogenic properties. The maximum concentration allowed in the environment so as not to have pathologic consequences for people is less than 100 ppm. When trichloroethylene comes into contact with water at high temperature, it decomposes into hydrochloric acid, which

is corrosive for facilities made of ferric materials. Therefore, adequate periodic maintenance and cleaning with alkaline solutions should be carried out to eliminate acid remainders. The vapors of carbon sulfur are also toxic, and it is also corrosive. For these reasons, and despite benzene, heptane, and analogous fractions presenting a lower extractive power, they are preferred. However, it has been proven that benzene causes health problems. Besides these solvents, petroleum ether, acetone, ethylic, and isopropilic alcohols can be used, among others. Thus, ether is used in cocoa butter extraction, while acetone is used to extract gosipol from cottonseeds.

One byproduct of the rice industry is rice bran with a content of lipid material, which can be obtained by an extraction process with solvent. Since this product is made of small particles slightly permeable to solvents, the equipment used to extract oil should be special extractors of the immersion type or those that work under pressure. Also, the installation should have adequate filters to separate the miscella of the small solid particles. The flour of corn germ presents the same problems and should be processed in the same way.

Another useful byproduct is the residue from the production of concentrated tomato. Such residue contains mainly peel and seeds; peel can be used to produce flour to feed animals, while oil and flour can be obtained from tomato seeds by an extraction with solvent procedure. Before the extraction stage, seeds receive a thermal, crushing, and rolling treatment. The products obtained with the extraction are raw oil and exhausted flour. The former is used to elaborate food products, while flour has high protein content and is used to formulate compound fodders.

One type of oil obtained by extraction with solvent is oil from grape pips. A difficulty presented by this type of extraction is that oil is strongly trapped within the cells that contain it, in addition to having a woody composition. For this reason, pips should be treated previously with heating and humidification and, later, with rolling. Once the rolled particles are obtained, they are ready for extraction. A double extraction is performed to obtain a better yield. A percolation extractor is used during the first stage, and an immersion extractor is used in the second stage.

Extraction processes in fishes. Extraction with solvent has other applications besides those already stated, including obtaining oil from whole fish or from specific organs, such as liver.

Not all fish production is suitable for direct human consumption, but great quantities are used to produce preserves and also to obtain oil and flours. Fish receives a series of treatments during the obtaining of oil and flour, among which an extraction with solvent stage is included. Initially, fish is cooked to coagulate proteins and sterilize raw material. Next, there is a pressing stage that yields a cake and a solution that contains water and oil. This solution is centrifuged to separate the water and oil; the cake obtained during the press stage is dried, and flour that still contains oil components is produced. Oil components can be extracted with a solvent; in this way, flour with a high protein content and an oil-solvent stream, from which it is possible to separate the new oil fraction, are obtained.

The equipment used in this extraction is classified as the immersion type, since it is difficult for the solvent to cross through the cake. Appropriate filtration equipment is also required to achieve a good separation of the miscella and solid particles. Many marine species receive treatment of this type, especially sardines, anchovies, herrings, etc. from which oil is extracted, as well as cod liver oil with its high vitamin content.

Other applications. In addition to processes applied to obtain oils, many others have the objective of obtaining specific final products. One of these products is the pectin fraction of fruits, used to elaborate jams and marmalades. A byproduct of the fruit juice industry is the exhausted pulp, which contains pectin that can be extracted with an acid solution and later precipitation with alcohol.

Paprika is a culinary condiment used as colorant in many food products. It is possible to extract paprika pigments with hexane, obtaining a colorant called oleoresin of paprika composed of seed and colorant oil. Such oleoresin presents great advantages over the fresh product, since it has the same colorant power, but with a volume between 5 to 10% of the volume of paprika, allowing a more precise dosage and a clear advantage in transportation. Extraction is usually carried out in continuous De Smet-type extractors; the miscella obtained is concentrated during an evaporation stage and later vapor distillation until a product with an oleoresin content of 99.25% is obtained. This product contains gums that are eliminated by centrifugation. Oleoresin without gum is driven to a dryer to eliminate the solvent, obtaining a final product that contains less than 10 ppm of hexane.

It is possible to obtain different alcohol liquors using solid–liquid extraction processes, if ethanol is used as extractive solvent, for solid substances such as oranges, coffee, and anise, as well as a great quantity of medicinal herbs. These extraction processes are also applied in the manufacture of different colorants and pigments used in the food industry.

Problems

21.1

It is desired to extract oil contained in flour that has 10% oil and the rest inert material. Thus, 500 kg of flour and 3000 kg of an organic solvent are fed into a single-stage system. If the amount of solvent retained by the solids is 0.8 kg/kg of inert solids, calculate: (a) the composition of the overflow and the underflow; (b) the amount of overflow and underflow; and (c) the percentage of oil extracted.

The retention curve is obtained from the equation:

$$X_D = \frac{r}{r+1} - X_S = 0.444 - X_S$$

(a) To solve the problem, it is necessary to determine placement of point *M*, so a solute balance should be carried out:

$$X_{SM} = \frac{R_A X_{SRA} + D Y_{SD}}{R_A + D} = \frac{(500)(0.1) + (3000)(0)}{(500) + (3000)} = 0.014$$

$$X_{DM} = \frac{R_A X_{DRA} + D Y_{DD}}{R_A + D} = \frac{(500)(0) + (3000)(1)}{(500) + (3000)} = 0.857$$

This allows placement of point *M* on the triangular diagram. This point belongs to the straight lines that cross $R_A D$ and $R_1 E_1$. Since the underflow and overflow leaving this stage are in equilibrium, the tie line that crosses the vertex *I* and point *M* is traced. The underflow R_1 is obtained on the retention line, and the overflow E_1 is obtained on the hypotenuse of the triangular diagram (Fig. 21.P1):

Underflow R_1:	$X_S = 0.007$	$X_D = 0.437$
Overflow E_1:	$Y_S = 0.016$	$Y_D = 0.984$

Since retention of solution by the inert solid is constant, the composition of the overflow and retained solution can be calculated from the expression:

$$Y_{SE1} = \frac{R_A X_{SRA}}{R_A X_{SRA} + D} = \frac{(500)(0.1)}{(500)(0.1) + (3000)} = 0.0164$$

(b) The amount of overflow and underflow are obtained from the global and solute balances:

$$(550) + (3000) = R_1 + E_1$$

$$(550)(0.1) + (3000)(0) = R_1(0.007) + E_1(0.016)$$

Hence:

$$R_1 = 813.2 \text{ kg} \qquad E_1 = 2686.8 \text{ kg}$$

(c) The amount of oil extracted is that which passes to the overflow stream:

$$E_1 Y_{SE1} = (2686.8)(0.016) = 44.1 \text{ kg extracted oil}$$

Initially, the food's oil content is $R_A X_{SRA}$ = 50 kg oil.

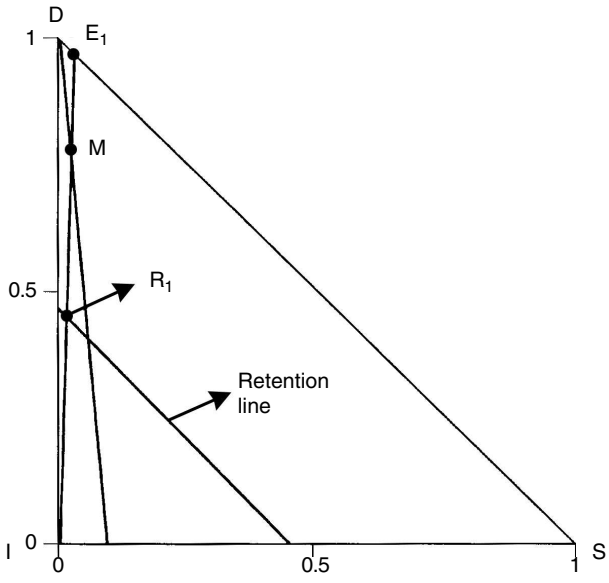

FIGURE 21.P1
Graphical method to obtain underflow and overflow concentrations.

Therefore, the percentage of oil extracted, with respect to the original amount in the food, is:

$$\frac{E_1 Y_{SE1}}{R_A X_{SRA}} 100 = \frac{44.1 \text{ kg oil}}{50 \text{ kg oil}} 100 = 88\%$$

21.2

Fish flour that contains 38% in weight of oil is subjected to an extraction process with ether using a three-stage extractor that operates under concurrent. It has been found that the solution retained by the inert solid is a function of the composition of the solution according to the expression:

$$r = 0.6 + 0.3\ y_S + 7\ y_S^2 \left(\text{kg retained solution/kg inert}\right)$$

where y_s is the weight fraction of solute in the retained solution.

1000 kg/h of fish flour are fed into the extraction system, using 750 kg of ether in each stage. Calculate: (a) the retention curve; (b) the global composition of the extract; (c) the composition of the underflow that leaves the third stage; and (d) the amount of oil recovered.

(a) The retention curve can be determined from the equation given in the statement of the problem (Equations 21.1 and 21.2):

$$X_S = \frac{y_S}{1+1/r} \qquad X_D = \frac{1-y_S}{1+1/r}$$

As values are given to y_S, the respective values of r are obtained, and both are used to determine the retention curve. Data are shown Table 21.P1:

TABLE 21.P1

Retention Data

y_S $\left(\frac{\text{kg solute}}{\text{kg solution}}\right)$	r $\left(\frac{\text{kg retained sol.}}{\text{kg inert}}\right)$	X_S $\left(\frac{\text{kg solute}}{\text{total kg}}\right)$	X_D $\left(\frac{\text{kg solvent}}{\text{total kg}}\right)$
0	0.6	0	0.375
0.1	0.7	0.041	0.371
0.2	0.94	0.097	0.388
0.3	1.32	0.171	0.398
0.4	1.84	0.259	0.389
0.5	2.50	0.357	0.357
0.6	3.30	0.461	0.307
0.7	4.24	0.566	0.243
0.8	5.32	0.673	0.168
0.9	6.54	0.781	0.087
1.0	7.9	0.888	0

$X_S - X_D$ data are plotted in the triangular diagram, obtaining the retention curve.

According to the statement of the problem:

$$D_1 = D_2 = D_3 = 750 \text{ kg} \quad \text{with} \quad Y_{SD} = 0 \quad Y_{DD} = 1$$

$$R_A = 1000 \text{ kg} \quad \text{with} \quad X_{SRA} = 0.38 \quad X_{IRA} = 0.62$$

The problem must be solved stage by stage (Fig. 21.P2). Thus, the steps to follow are: determine the point M_i of each stage on the straight line that joins feed with solvent, draw the tie line that crosses the vertex I and the point M_i, obtain the composition of underflow R_i on the retention curve, and obtain the composition of the overflow E_i on the hypotenuse. Abscissa of points M_i:

$$X_{SMi} = \frac{R_{i-1} X_{SRi-1} + D_i Y_{SDi}}{R_{i-1} + D_i}$$

1st stage:

Point M_1 is located on the abscissa as $X_{SM1} = 0.217$ and is placed on the straight line $R_A D_1$. The compositions of overflow and underflow leaving the first stage can be obtained by tracing the tie line that crosses M_1:

Underflow R_1: $X_{SR1} = 0.21$ $X_{DR1} = 0.39$ $X_{IR1} = 0.40$

Overflow E_1: $Y_{SE1} = 0.34$ $Y_{DE1} = 0.66$

The amount of overflow and underflow are obtained from the global and solute balances in this stage:

$$(1000) + (750) = R_1 + E_1$$
$$(1000)(0.38) + (750)(0) = R_1(0.21) + E_1(0.34)$$

obtaining:

$$E_1 = 96.2 \text{ kg/h} \qquad R_1 = 1653.8 \text{ kg/h}$$

2nd stage:

Point M_2 is located on the abscissa as $X_{SM2} = 0.144$ and is placed on the straight line R_1D_3. The compositions of overflow and underflow leaving the second stage can be obtained from plotting the tie line that crosses M_2:

Underflow R_2: $X_{SR2} = 0.10$ $X_{DR2} = 0.38$ $X_{IR2} = 0.52$

Overflow E_2: $Y_{SE2} = 0.20$ $Y_{DE2} = 0.80$

The amount of overflow and underflow are obtained from the global and solute balances in this stage:

$$(1653.8) + (750) = R_2 + E_2$$
$$(1653.8)(0.21) + (750)(0) = R_2(0.10) + E_2(0.20)$$

obtaining:

$$E_2 = 1069.2 \text{ kg/h} \qquad R_2 = 1334.6 \text{ kg/h}$$

3rd stage:

Point M_3 is located on the abscissa as $X_{SM3} = 0.064$ and is placed on the straight line R_2D_2. The composition of overflow and underflow leaving the third stage can be obtained from plotting the tie line that crosses M_3:

Underflow R_3: $X_{SR3} = 0.04$ $X_{DR3} = 0.37$ $X_{IR3} = 0.59$

Overflow E_3: $Y_{SE3} = 0.10$ $Y_{DE3} = 0.90$

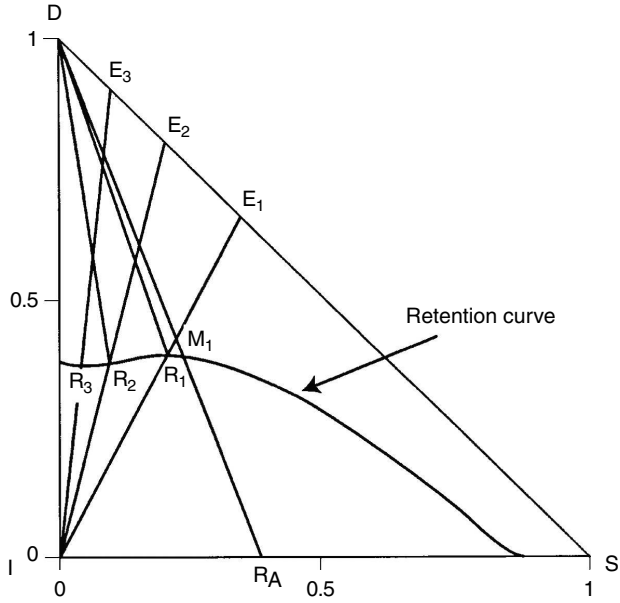

FIGURE 21.P2
Graphical solution of Problem 21.2.

The amount of overflow and underflow are obtained from the global and solute balances in this stage:

$$(1334.6)+(750)=R_3+E_3$$

$$(1334.6)(0.10)+(750)(0)=R_3(0.04)+E_3(0.10)$$

obtaining:

$$E_3=834.6\ \text{kg/h} \qquad R_3=1250\ \text{kg/h}$$

(b) The composition of the final overflow or extract is a weighted average of the extracts of each stage:

$$Y_{SE}=\frac{E_1 Y_{SE1}+E_2 Y_{SE2}+E_2 Y_{SE3}}{E_1+E_2+E_3}=0.165$$

$$Y_{DE}=0.835$$

(c) The composition of the final underflow R_3 is:

$$X_{SR3}=0.04 \qquad X_{DR3}=0.37 \qquad X_{IR3}=0.59$$

(d) The recovered oil is the oil passed to the underflow: $E \cdot Y_{SE}$.

$$E = E_1 + E_2 + E_3 = 2000 \text{ kg/h}$$

Recovered oil: $E Y_{SE} = (2000)(0.165) = 330 \text{ kg oil/h}$

Percentage of recovered oil: $\frac{E Y_{SE}}{R_A X_{SRA}} 100 = \frac{(330)}{(380)} 100 = 86.84\%$

21.3

Cod liver oil is obtained from crushed livers by extraction with an organic solvent. A sample that contains 0.335 kg of oil per each kg of exhausted liver is fed into a multistage extractor that operates under countercurrent, where pure organic solvent is employed. It is desired to recover 90% of the oil in the final overflow, with a composition 60% in weight of oil. If retention of the solution is 2 kg per each 3.2 kg of insoluble solids, calculate the number of ideal stages required to carry out the desired extraction.

Calculations are made assuming that 100 kg of food is introduced into the extractor: R_A = 100 kg.

The food composition is:

$$X_{SRA} = \frac{0.335 \text{ kg solute}}{(1 + 0.335) \text{ total kg}}$$

$$X_{DRA} = 0 \qquad X_{IRA} = 0.749$$

Solute in food: $R_A X_{SRA} = 25.1 \text{ kg oil}$

Inert solids in food: $R_A X_{IRA} = 74.9 \text{ kg inert solids}$

According to the retention data in the statement of the problem:

$$r = \frac{2 \text{ kg solution}}{3.2 \text{ kg inert solids}} = 0.625 \frac{\text{kg solution}}{\text{kg inert solids}}$$

The amount of oil in the final underflow is 10% of the original amount of oil contained in food:

$$R_n X_{SRn} = 0.1 R_A X_{SRA} = 2.51 \text{ kg oil}$$

The kg of solution retained by underflow is calculated from retention:

$$0.625\frac{\text{kg solution}}{\text{kg inert solids}}74.9 \text{ kg inert solids} = 46.81 \text{ kg solution}$$

Thus, the amount of solvent in the final underflow is:

$$\left(46.81 - 2.51\right) \text{kg solvent} = 44.3 \text{ kg solvent}$$

The total amount of final underflow is the sum of that contained in the solute, solvent, and inert solids:

$$R_n = \left(2.51 + 44.3 + 74.9\right) = 121.85 \text{ kg}$$

The composition of the underflow is:

$$X_{SRn} = \frac{2.51 \text{ kg solute}}{121.85 \text{ total kg}} = 0.021$$

$$X_{DRn} = \frac{44.3 \text{ kg solvent}}{121.85 \text{ total kg}} = 0.364$$

$$X_{IRn} = \frac{74.9 \text{ kg inert}}{121.85 \text{ total kg}} = 0.615$$

The amount of overflow is obtained by equalizing the solute contained in this stream with that recovered from food:

$$E_1 Y_{SE1} = 0.9 R_A X_{SRA}$$

$$E_1\left(0.6\right) = 0.9\left(100\right)\left(0.251\right) \qquad E_1 = 37.65 \text{ kg}$$

The amount of solvent that must be fed to the extractor is obtained from the global balance:

$$E_{n+1} = R_n + E_1 - R_A = 59.5 \text{ kg}$$

If it is desired to calculate the number of stages required to carry out the extraction, the pole *P* must be placed in the triangular diagram before building the retention curve.

Retention curve: since solution retention is constant, then it is a straight line that has as its equation:

$$X_D = 0.385 - X_S$$

Pole P is placed according to the coordinates obtained from a balance between the inlet and outlet sections of the extractor:

$$X_{SP} = \frac{R_A X_{SRA} - E_1 Y_{SE1}}{R_A - E_1} = \frac{(100)(0.251) - (37.6)(0.6)}{100 - 37.65} = 0.04$$

$$X_{DP} = \frac{R_A X_{DRA} - E_1 Y_{DE1}}{R_A - E_1} = \frac{(100)(0) - (37.6)(0.4)}{100 - 37.65} = -0.242$$

The number of stages required to carry out the extraction is obtained graphically (Fig. 21.P3): $N_{TS} = 6$.

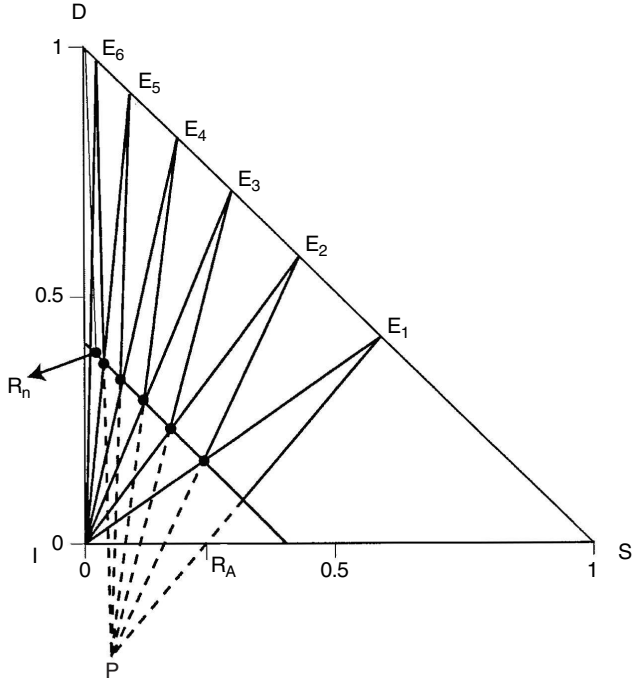

FIGURE 21.P3
Graphical calculation of theoretical stages.

21.4

During the obtainment of soluble coffee, the soluble solids are extracted with water in a solid–liquid extraction. This extraction is performed in a multistage system that operates countercurrently, where 3000 kg/h of roasted and ground coffee beans are treated. The roasted coffee contains 24% in weight of soluble solids, while the moisture content is negligible. Five percent of the soluble solids contained in the food appear in the final underflow stream, while the overflow stream contains 35% in weight of such solids.

From previous laboratory experiments, it was obtained that the amount of solution retained by inert solids is 1.6 kg solution/kg inert solids. Calculate: (a) the amount of water required to carry out this extraction; (b) the flow rate of solution extracted; and (c) the number of stages needed if the global efficiency of the system is 75%.

(a) The amount of solute and inert solids in feed is:

Solute: $$R_A X_{SRA} = (3000)(0.24) = 720 \text{ kg solute}$$

Inert solids: $$R_A X_{IRA} = (3000)(0.76) = 2280 \text{ kg inert solids}$$

Since 5% of the solute that feed contains goes to the final underflow stream, the amount of solute in this stream is:

$$R_n X_{SRn} = 0.05\, R_A X_{SRA} = (0.05)(3000)(0.24) = 36 \text{ kg solute}$$

A solute balance for the whole system yields:

$$(3000)(0.24) + 0 = (36) + E_1(0.35)$$

Hence, the final overflow stream is:

$$E_1 = 1954.3 \text{ kg}$$

Since underflow retains 1.6 kg of solution/kg of inert solids, the final underflow has R_n:

$$2280 \text{ kg inert} \frac{1.6 \text{ kg solution}}{\text{kg inert}} = 3648 \text{ kg retained solution}$$

Thus, the total amount of final underflow is:

$$R_n = 2280 \text{ kg inert solids} + 3648 \text{ kg solution} = 5928 \text{ total kg}$$

From the global balance:

$$E_{n+1} = (5928) + (1954.3) - (3000) = 4882.3 \text{ kg fresh water}$$

Retention of solution r is constant, so the retention curve in this case is a straight line that behaves according to the equation $X_D = 0.615 - X_S$.

Pole P is obtained from the balances in each section:

$$X_{SP} = \frac{R_A X_{SRA} - E_1 Y_{SE1}}{R_A - E_1} = \frac{(3000)(0.24) - (1954.3)(0.35)}{3000 - 1954.3} = 0.034$$

$$X_{DP} = \frac{R_A X_{DRA} - E_1 Y_{DE1}}{R_A - E_1} = \frac{(3000)(0) - (1954.3)(0.65)}{3000 - 1954.3} = -1.215$$

These coordinates allow one to place pole P in the triangular diagram and thus calculate the number of stages required (Fig. 21.P4), obtaining: $N_{TS} = 9$.

Since efficiency is 75%, the number of real stages is:

$$N_{RS} = \frac{(9)}{(0.75)} = 12 \text{ stages}$$

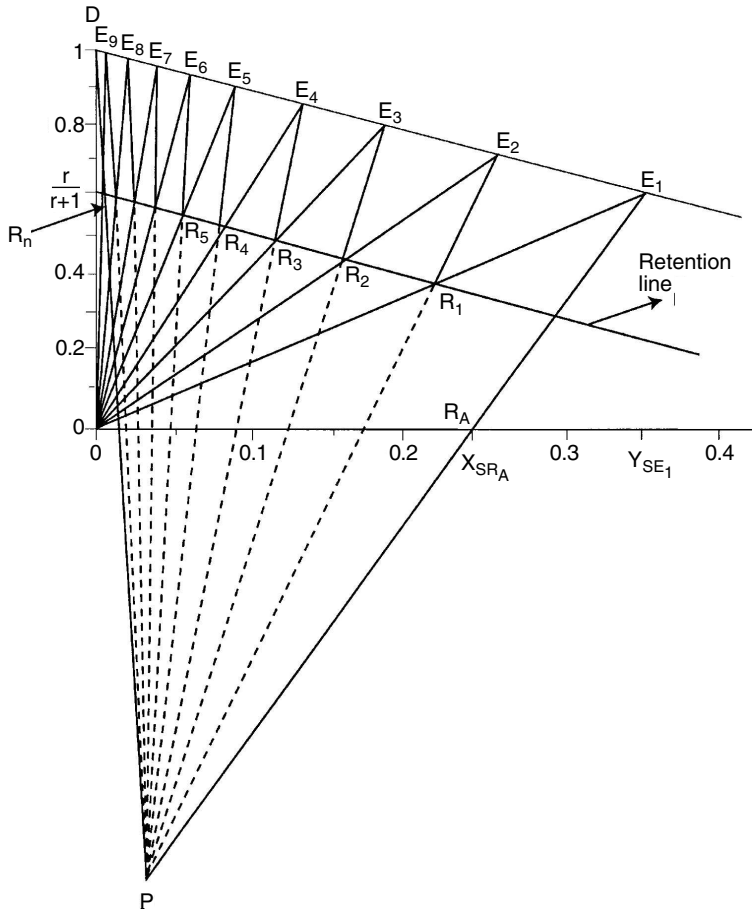

FIGURE 21.P4
Graphical calculation of theoretical stages.

22

Adsorption and Ionic Exchange

22.1 Introduction

Adsorption and ionic exchange are mass transfer unit operations in which a solute contained in a fluid phase is transferred to the solid phase due to retention on the solid's surface or to a reaction with the solid.

22.1.1 Adsorption

The solute retained in adsorption processes is called adsorbate, whereas the solid on which it is retained is called adsorbent. Solids with a large contact surface are used as adsorbents and are generally porous. Activated carbon is widely used as adsorbent, although there are synthetic polymers called molecular sieves also used for adsorption processes.

The force with which the solute is retained can be of three types: electric, Van der Waals forces, and chemical. Electric forces are due to attractions between a solute with a certain charge and points of the adsorbent with an opposite charge. The adsorption is called physical when the forces are of Van der Waals type, and adsorption is usually reversible. However, adsorption can be due to a chemical reaction between the solute and the adsorbent — a chemisorption. While in the physical adsorption the solute can be retained on any point of the surface of the adsorbent, in chemisorption the adsorbent presents active points on which the adsorbate is retained.

Adsorption is used in many cases of purification of fluids containing contaminants that give them unpleasant flavors or aromas. Limonene is a compound that confers bitter flavor to orange juice, and it can be eliminated by adsorption on polymers. In the same way, melanins and melanoidins, formed by enzymatic and nonenzymatic browning, can be eliminated by adsorption on activated carbon.

22.1.2 Ionic Exchange

Ionic exchange consists of replacing ions of a solution with others contained in a solid, which is called exchange resin. The ionic exchange can be consid-

ered a chemical adsorption, where ion exchange occurs at defined points of the resin. The mathematical treatment for calculation of exchange columns is similar to that for adsorption. Depending on the type of ions that they can exchange, resins can be anionic or cationic. One of the most important applications of ion exchange is desalination and conditioning of water.

22.2 Equilibrium Process

22.2.1 Adsorption Equilibrium

When a solid adsorbent and a fluid containing a solute come into contact, the system evolves in such a way that the solute is transferred to the surface of the solid and retained there. This process continues until reaching a dynamic equilibrium between both phases. At that moment, the fluid phase has a concentration of solute *C*, while in the solid phase the amount of solute per unit mass is *m*. The values of *C* and *m* at equilibrium depend on temperature, and the function that gives the variation of the amount of solute retained by the adsorbent (*m*) with the concentration of solute in the fluid phase (*C*) is called adsorption isotherm. This type of isotherm can have different forms. Figure 22.1 shows the typical isotherms that can be presented in different types of solute–adsorbent systems.

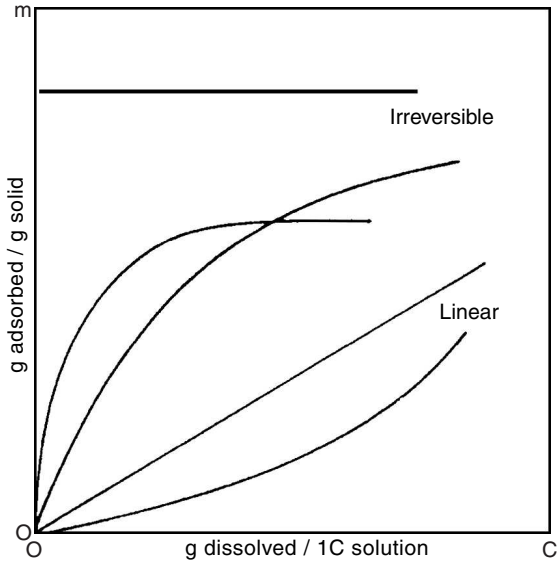

FIGURE 22.1
Types of adsorption isotherms.

The theoretical obtainment of the adsorption isotherms can be based on kinetic or thermodynamic considerations, the former more intuitive. Also, it depends on considering whether the solute is retained by the adsorbent in one or in various molecular layers.

One intuitive and simple case is adsorption of one adsorbate on one molecular layer. Thus, if it is supposed that solute A in the fluid phase is adsorbed by solid S, according to the kinetic mechanism:

$$A_{(F)} + S \underset{K_2}{\overset{K_1}{\rightleftharpoons}} S - A$$

The adsorption rate of A is expressed by the equation:

$$r_A = k_1 C_A \left(m_0 - m_A\right) - k_2 m_A \tag{22.1}$$

where:

r_A = adsorption rate of A
C_A = concentration of A in the fluid phase
m_0 = maximum concentration of A retained by the adsorbent
m_A = concentration of A retained by the adsorbent

At the adsorption equilibrium, $r_A = 0$, hence:

$$k_1 C_A \left(m_0 - m_A\right) = k_2 m_A$$

The adsorption equilibrium constant can be defined as:

$$K = \frac{k_1}{k_2} = \frac{m_A}{C_A \left(m_0 - m_A\right)} \tag{22.2}$$

Obtaining:

$$\frac{m_A}{m_0} = \frac{K C_A}{1 + K C_A} \tag{22.3}$$

This equation is called isotherm of Langmuir, and experimental data of many different systems fit well. However, another equation frequently used is the isotherm of Freundlich, which is an empirical equation of the form:

$$m_A = K(C_A)^n \tag{22.4}$$

where K and n are parameters, the values of which are a function of the type of adsorbate-adsorbent system and of temperature. The determination of these parameters should be made experimentally.

Another isotherm is that of Brunauer, Emmett, and Teller (BET), used for adsorption of one solute on multilayers (Brunauer et al., 1938; Emmett and de Witt, 1941):

$$m_A = \frac{BC_A m_A^1}{\left(C_A^S - C_A\right)\left(1-\left(B-1\right)\frac{C_A}{C_A^S}\right)} \tag{22.5}$$

where m_A is the amount of adsorbed solute per unit mass of adsorbent for the concentration C_A, C_A^S is the saturation concentration of the solute, m_A^1 is the amount of solute adsorbed per unit of adsorbent that forms a monolayer on the surface of the solid, and B is a constant representing the interaction energy with the surface.

For solutes contained in a gas phase, the BET isotherm for n layers can be expressed according to the equation:

$$\frac{m_A}{m_0} = \frac{Bx}{1-x}\,\frac{1-(n+1)\,x^n + nx^{n+1}}{1+(B-1)\,x - bX^{n+1}} \tag{22.6}$$

where:

$$x = \frac{P_A}{P_A^0} = \frac{\text{partial pressure of } A}{\text{vapor pressure of pure } A}$$

When the number of layers $n = 1$, it is obtained that:

$$\frac{m_A}{m_0} = \frac{B\,x}{1-x} \tag{22.7}$$

which coincides with the isotherm of Langmuir.

If the number of layers is high, the BET isotherm is transformed into:

$$\frac{m_A}{m_0} = \frac{B\,x}{\left(1-x\right)\left(1+(B-1)\,x\right)}$$

For low values of x, the last equation is transformed as:

$$\frac{m_A}{m_0} = \frac{Bx}{1+(B-1)x}$$

22.2.2 Ionic Exchange Equilibrium

If a fluid that contains an anion A^{n+} with charge $n+$ is available and comes into contact with a resin that can exchange a cation B^{n+} with the same charge as A, it can be considered that the following cationic exchange reaction is complied with:

$$A^{n+} + R - B \underset{K_2}{\overset{K_1}{\rightleftharpoons}} B^{n+} + R - A$$

The disappearing rate of the cation A^{n+} is:

$$\left(-r_A\right) = k_1 C_A C_{R-B} - k_2 C_B C_{R-A}$$

When equilibrium is reached, the disappearing rate of A is null, so the following is complied with:

$$K = \frac{k_1}{k_2} = \frac{C_B C_{R-A}}{C_A C_{R-B}}$$

Substitution in the last equation allows expression of the disappearing rate of A as a function of the equilibrium constant K.

The concentration in the liquid phase of the ions involved in the ionic exchange is usually expressed in equivalents/liter of solution; while in the solid phase, the concentration is expressed in equivalents of ions per unit mass of resin. In this way, if C_A^0 is the initial concentration of A in the solution and C_A is the concentration of A at a determined instant, and if C_B is the concentration of ions B that have been exchanged for A, then it is complied that $C_B = C_A^0 - C_A$. For the resin, E_A are the equivalents of A per unit mass of dry resin and E_M is the maximum capacity of the resin, expressed as equivalents of A per unit mass of dry resin that it can exchange with ions A. The concentration of B in the resin is:

$$E_B = E_M - E_A$$

Therefore, at equilibrium, it is complied that:

$$K = \frac{\left(C_A^0 - C_A\right)E_A}{C_A\left(E_M - E_A\right)} \tag{22.8}$$

If the equivalent fractions of A in the liquid and resin phases are defined as:

liquid phase: $$Y = \frac{C_A}{C_A^0}$$

resin phase: $$X = \frac{E_A}{E_M}$$

the equilibrium constant is expressed as:

$$K = \frac{(1-Y)X}{Y(1-X)} \tag{22.9}$$

This equilibrium constant is called the separation factor.

22.3 Process Kinetics

22.3.1 Adsorption Kinetics

In every adsorption process, three solute transfer stages can be considered:

1. External transfer: The solute at the fluid phase with a concentration C is transferred to the fluid–solid interphase in which the concentration is C_i. The mass flux is given by the equation:

$$N = k_F(C - C_i) \tag{22.10}$$

   where k_F is the mass transfer coefficient in the external phase.
2. Diffusion inside the solid: The mass flux on the wall of the solid for a spherical solid particle with radius r_i is expressed as:

$$N = -D_e \frac{C_S}{r} \tag{22.11}$$

   where C_S is the concentration of solute in the solid and D_e is the effective diffusivity of the solute.
3. Adsorption stage: For the simpler case, expressed before, it can be stated that:

$$r = k_1 C_S(m_0 - m_S) - k_2 m_S$$

and at equilibrium:

$$\frac{m_S}{m_0} = \frac{K\,C_S}{1 + K\,C_S}$$

Generally, the first of these stages controls the process, so it can logically be assumed that equilibrium is reached during the adsorption stage. Therefore, if the mass transfer stage controls the process, it is complied that $C_i = C_S$, and its value is constant along the whole solid.

22.3.2 Ionic Exchange Kinetics

As they occur in physical adsorption processes, different stages of mass transfer can be considered during ionic exchange:

1. External mass transfer of ion *A* from the solution to the resin's surface
2. Diffusion of ion *A* through the pores of the resin until reaching the exchange points
3. Ionic exchange reaction in which ion *A* is exchanged by ion *B* in such a way that *A* is bound to the resin while *B* passes to the fluid phase
4. Diffusion of ion *B* through the pores of the resin until reaching the resin's surface
5. External mass transfer of *B* from the surface of the resin to the solution

The slowest stage is the one that controls the ionic exchange process. Generally, the diffusion stages or the external mass transfer stages control the global process:

$$(-r) = k_A\left(C_A - C_A^i\right) = k_B\left(C_B^i - C_B\right)$$

where the superscript *i* indicates interface concentrations, and it is complied that C_A^i is in equilibrium with C_B^i.

22.4 Operation by Stages

As in other mass transfer unit operations, adsorption and ionic exchange processes can operate in stages, in batch as well as in continuous operations.

The most common ways of operation are single stage or contact and multistage, which can be repeated single contact or countercurrent multiple stage.

22.4.1 Single Simple Contact

This is the simple method of operation. As shown in Figure 22.2a, a fluid stream containing the solute and the solid stream are contacted in one stage. The solute passes to the solid stream, thereby decreasing its concentration in the fluid phase. It is assumed that the fluid and solid that leave the stage are in equilibrium; this means that an ideal stage is supposed.

The mass flows of the fluid and solid streams are F and S, respectively. Also, C and m are the concentrations in the fluid and solid streams, respectively. Generally, the mass flows of the fluid and solid streams present a

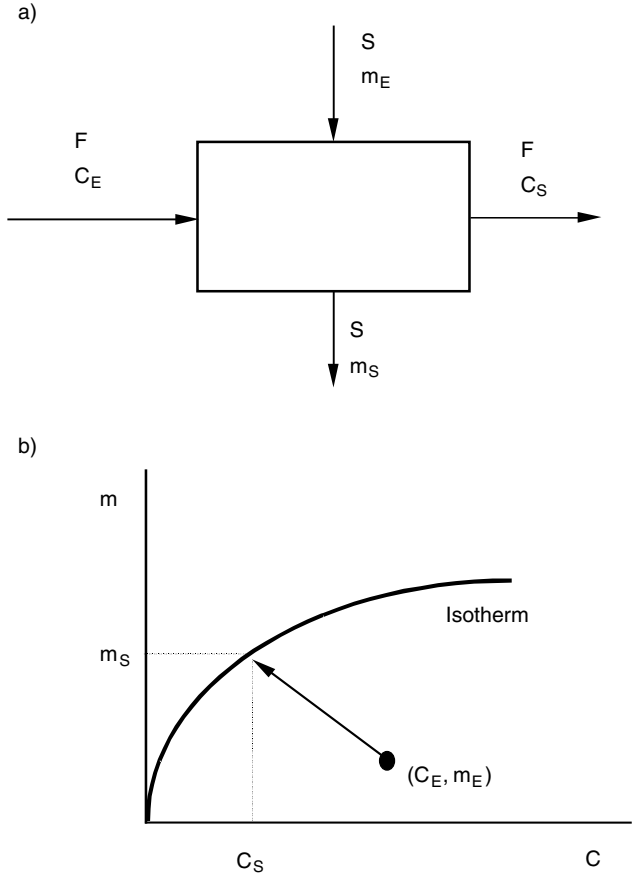

FIGURE 22.2
Single contact: (a) operation sketch; (b) operation in the equilibrium diagram.

slight variation between the inlet and outlet, so they are considered constant. When performing a solute balance in the system it is complied that:

$$F\left(C_E - C_S\right) = S\left(m_S - m_E\right)$$

where the subscript E means inlet and S means outlet. Rearranging:

$$m_S = -\frac{F}{S}C_S + \left(m_E + \frac{F}{S}C_E\right) \tag{22.12}$$

which, in the m–C diagram, is the equation of a straight line with slope $-F/S$. Therefore, if the conditions of the inlet streams are known, the concentrations of the streams that leave the stage can be determined in the m–C diagram (Figure 22.2b). For this reason, a straight line with slope $-F/S$ is traced from the point that represents the inlet streams (C_E,m_E), and the concentrations of the outlet streams (C_S,m_S) are obtained where the straight line crosses the equilibrium curve (adsorption isotherm).

For a batch operation, it is convenient to use total amounts and concentrations:

$$V\left(C_I - C_F\right) = S\left(m_F - m_I\right) \tag{22.13}$$

where V is the total volume of the fluid and S is the total amount of solid, while the subscripts I and F denote initial and final concentration, respectively.

22.4.2 Repeated Simple Contact

This is a multistage operation in which the fluid phase that leaves a stage is fed to the following stage (Figure 22.3a). It is considered that all the stages present an ideal behavior, so the concentrations of the fluid and solid streams that leave any stage are in equilibrium. Generally, the solid fed to each stage contains no solute; therefore, $m_E = 0$. In addition, the amount of solid used in each stage is the same ($S_1 = S_2 = \ldots = S_N = S$).

When performing a solute balance around any stage i:

$$F\left(C_{i-1} - C_i\right) = S\left(m_i - m_E\right)$$

Rearranging the equation:

$$m_i = -\left(\frac{F}{S}\right)C_i + \left(m_E + \left(\frac{F}{S}\right)C_{i-1}\right) \tag{22.14}$$

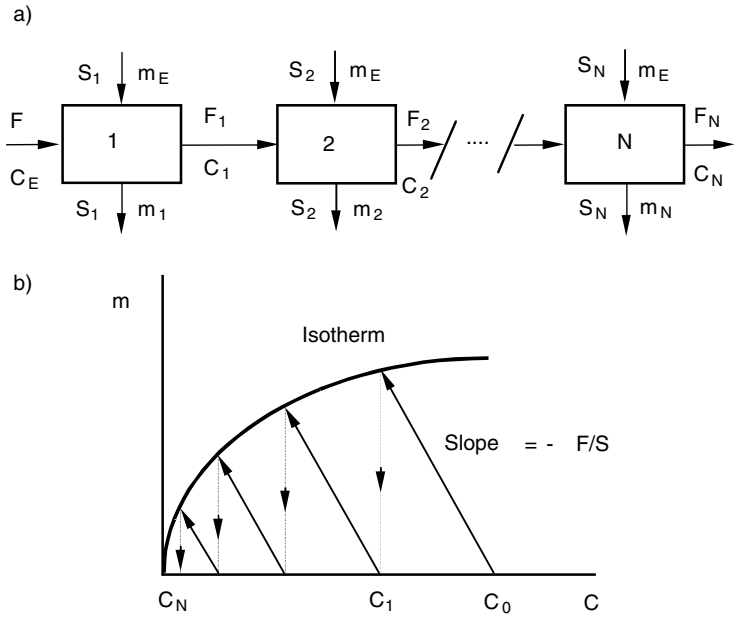

FIGURE 22.3
Repeated simple contact: (a) sketch of the operation; (b) operation in the equilibrium diagram.

If it is desired to determine the concentrations of the streams that leave each stage, one should operate as follows. The point that represents the inlet streams (m_E,C_0) is represented in the m–C diagram. A straight line with slope $-F/S$ is traced from this point. The point where this straight line crosses the equilibrium curve determines the concentrations m_1 and C_1. A straight line with the same slope is traced from the point (C_1,m_E); the point where it crosses the equilibrium curve determines the composition C_2 and m_2 of the streams that leave the second stage. The process continues until N, which allows one to obtain the concentration of solute C_N in the fluid phase (Figure 22.3b).

When the final concentration of the fluid phase is known and it is desired to determine the number of stages required, the way to operate is similar. The graphical process begins at point (C_0,m_E), and straight lines with slope $-F/S$ will be traced as described previously until exceeding the final concentration C_N. The number of straight lines of slope $-F/S$ traced is exactly the number of stages N needed to decrease the solute content in the fluid stream from C_0 to C_N.

22.4.3 Countercurrent Multiple Contact

N stages are used in this type of operation, and the fluid and solid streams circulate in opposite directions. The outlet stream of each stage is fed to the

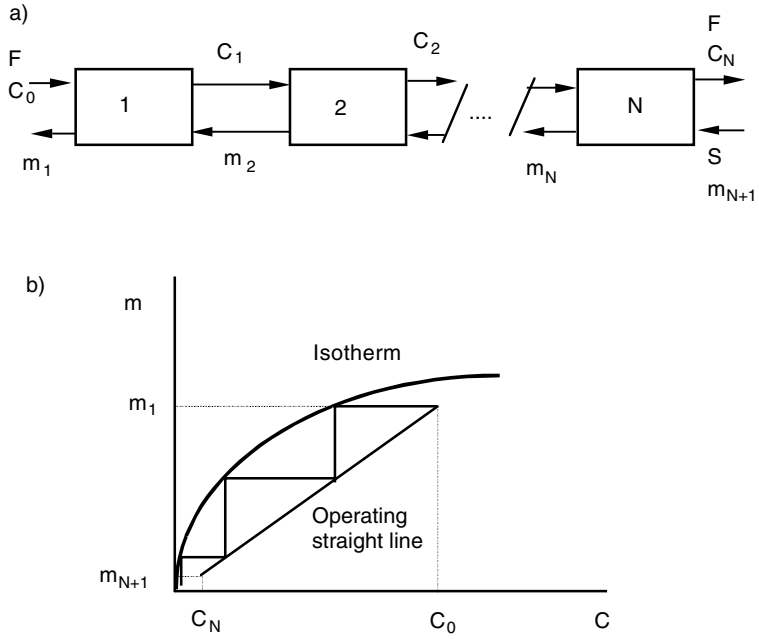

FIGURE 22.4
Countercurrent multiple contact.

following one. The fluid stream enters the system by the first stage, while the solid stream is introduced in the last stage (Figure 22.4). As in the other cases, it is supposed that the stages are ideal and that equilibrium is reached in each one.

The following equation is obtained from the global balance:

$$F\left(C_0 - C_N\right) = S\left(m_1 - m_{N+1}\right)$$

In the m–C diagram, this is the equation of a straight line with slope F/S that passes through the points (C_0,m_1) and (C_N,m_{N+1}), called the operating straight line. The number of stages required to decrease the concentration in the fluid phase from C_0 to C_{N+1} is obtained by plotting steps between the operating line and the equilibrium curve (Figure 22.4).

The maximum fluid flow to treat per unit of solid is obtained by drawing the straight line that passes through the point (C_N,m_{N+1}) and the point on the equilibrium curve with abscissa C_0. This line has a slope equal to $(F/S)_{MAX}$ (Figure 22.5a). It can occur that, when tracing the straight line with maximum slope, it crosses the equilibrium curve. In this case, the tangent to the curve should be traced and its slope is given by the relationship $(F/S)_{MAX}$ (Fig. 25.5b).

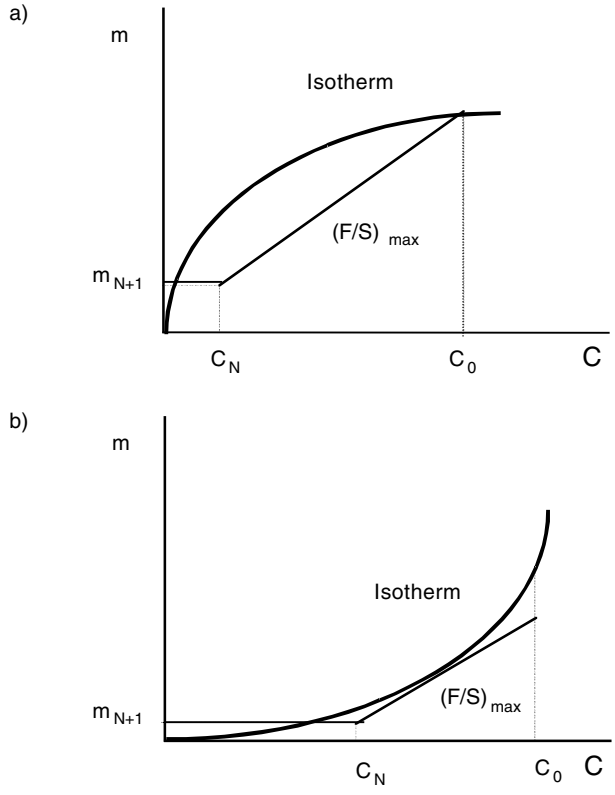

FIGURE 22.5
Countercurrent multiple stage. Conditions of maximum treatment flow: (a) convex isotherm; (b) concave isotherm.

22.5 Movable-Bed Columns

In certain cases, the adsorption or ionic exchange stage consists of a cylindrical column in which the fluid and solid phases are fed under countercurrent (Figure 22.6). It is assumed that the solid moves along the column under plug flow.

A solute balance around a differential section of height dz yields:

$$v\,A\,\varepsilon\,C = v\,A\,\varepsilon\,\left(C + dC\right) + N\,A\,dz\left(1-\varepsilon\right)a_S$$

where v is the fluid's circulation linear velocity, A is the transversal section of the column, ε is the porosity of the solid in the column, and a_S is the

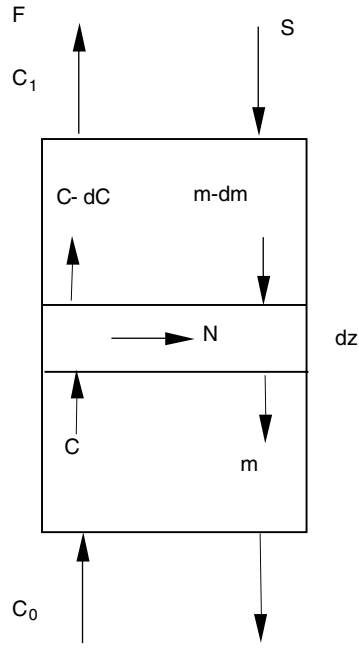

FIGURE 22.6
Moving-bed column.

specific surface of the solid bed, while N is the flux of the transferred solute, its value being:

$$N = k_F\left(C - C_i\right)$$

In this equation, k_F is the mass transfer constant and C_i is the concentration of the solute at the fluid–solid interphase. The calculation of C_i can be difficult, so it is convenient to express this transfer as a function of the concentration of the fluid C_e, which is in equilibrium with the concentration of the solid:

$$N = k_F\left(C - C_e\right)$$

Therefore, when substituting this expression in the solute's balance, the height of the column can be obtained if the resulting equation is integrated:

$$z = \int_0^z dz = \frac{v\,\varepsilon}{k_F\,a_S\left(1-\varepsilon\right)} \int_{C_1}^{C_0} \frac{dC}{C - C_e} \tag{22.15}$$

Generally, the integral does not have an analytical solution and should be solved by numerical or graphical methods.

22.6 Fixed-Bed Columns

Fixed-bed columns are the most used equipment for adsorption and ionic exchange processes. The adsorbent solid or exchange resin is contained in the column, and the fluid that contains the solute to retain or exchange is circulated through the column (Figure 22.7).

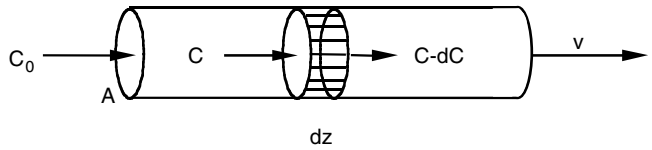

FIGURE 22.7
Fixed-bed column.

If a solute balance is performed at a column differential of height *dz*, it is observed that the inlet term is equal to the outlet term plus the part accumulated in the liquid retained in the porous fraction of *dz* and that accumulated in the solid:

$$v\,A\,\varepsilon C = v\,A\,\varepsilon\left(C - dC\right) + \frac{d}{dt}\left(\varepsilon\,A\,dz\,C + \left(1-\varepsilon\right)A\,dz\,\rho_{_P}\,m\right)$$

In this equation, v is the fluid's circulation linear velocity, A is the transversal section of the column, ε is the porosity of the solid bed, C is the concentration of solute in the fluid phase, m is the concentration of solute in the solid phase, and ρ_P is the density of the adsorbent particles or exchange resins.

When developing the accumulation term, and rearranging all the terms, the last equation can be expressed as:

$$v\frac{dC}{dz} - \frac{dC}{dt} = \frac{1-\varepsilon}{\varepsilon}\rho_{\mathrm{P}}\frac{dm}{dt} \tag{22.16}$$

This is a basic equation that allows calculation of the height of the column, although the solution method varies according to the operation conditions. Three methods to calculate the height of solid particle beds are presented next.

22.6.1 Fixed-Bed Columns with Phase Equilibrium

To solve Equation 22.16, it will be assumed that the equation does not control the mass transfer stage and also that the fluid and solid phases are in equilibrium. The rate at which a point with constant concentration moves along the column can be obtained from this equation:

$$\frac{dz}{dt} = \frac{v}{\left(1 + \frac{(1-\varepsilon)}{\varepsilon}\rho_P \frac{dm}{dC}\right)} \tag{22.17}$$

where the relationship dm/dC is the slope of the equilibrium curve.

If it is considered that a volume V of a fluid that passes at a rate v through a column with transversal section A has been treated in a time t, it is complied that: $V = A\ v\ t$.

For constant concentration, integration of Equation 22.17 allows calculation of the height of the solid bed contained in the column:

$$z = \frac{v\,t}{\left(1 + \frac{(1-\varepsilon)}{\varepsilon}\rho_P \frac{dm}{dC}\right)} = \frac{V}{A\left(1 + \frac{(1-\varepsilon)}{\varepsilon}\rho_P \frac{dm}{dC}\right)} \tag{22.18}$$

Sometimes it is desired to know the amount of solid that should be charged to the column to carry out the operation or the amount of fluid that can be treated per kg of solid contained in the column. If V is the amount of fluid to treat and S is the amount of solid in the column, it is complied that:

$$\frac{V}{S} = \frac{A\ v\ t}{z\ A(1-\varepsilon)\rho_P} = \frac{1}{(1-\varepsilon)\cdot\rho_P} + \frac{1}{\varepsilon}\frac{dm}{dt} \tag{22.19}$$

22.6.2 Rosen's Deductive Method

This is another method that allows solution of problems related to solute adsorption by fixed beds of adsorbent. It is assumed that resistance to mass transfer occurs inside the adsorbent.

When performing a solute balance for the whole column, it is supposed that all the solute that enters is accumulated on the surface of the solid. The solute's inlet and accumulation terms are:

Inlet: $$N\,A\,z\,a_S = k_F\left(C - C_e\right)A\,z\,a_S$$

Accumulation: $$\frac{d}{dt}\left[m\,A\,z\,(1-\varepsilon)^{\rho_p}\right] = A z(1-\varepsilon)\rho_p \frac{dm}{d\,t}$$

The following expression is obtained when equaling and rearranging the inlet and accumulation terms:

$$\frac{dm}{dt} = \frac{k_F\,a_S}{(1-\varepsilon)\rho_p}(C - C_e) \tag{22.20}$$

where C_e is the concentration of the fluid phase in equilibrium with the concentration in the solid phase m and is obtained from the equilibrium curve.

In the case that the isotherm is linear, $m = K_a C$, the equation has an analytical solution (Rosen, 1952; 1954). Thus, the concentration of the fluid stream that leaves the column is calculated by the expression:

$$C = C_0\left\{\frac{1}{2}\left[1 + erf\left(\frac{\frac{3\tau}{2\lambda} - 1}{2\sqrt{\frac{1+S\Gamma}{5\lambda}}}\right)\right]\right\} \tag{22.21}$$

where *erf* is the error function of Gauss, while the parameters τ, λ, and Γ are:

Time parameter: $$\tau = \frac{8D_e}{d_P^2}\left(1 - \frac{z}{v}\right) \tag{22.22}$$

Length parameter: $$\lambda = \frac{12D_e K_a (1-\varepsilon) z}{\varepsilon\ v\ d_P^2 \cdot \rho_p} \tag{22.23}$$

Resistance parameter: $$\Gamma = \frac{2D_e K_a}{d_p k_F} \tag{22.24}$$

where D_e is the effective diffusivity, K_a is the slope of the equilibrium line, k_F is the mass transfer, d_P is the diameter of the particles in the bed, v is the linear circulation velocity of the fluid, and z is the height of the column.

22.6.3 The Exchange Zone Method

The exchange zone is defined as the part of the bed of solids where the mass exchange is produced. When a fluid stream contains a solute with a concen-

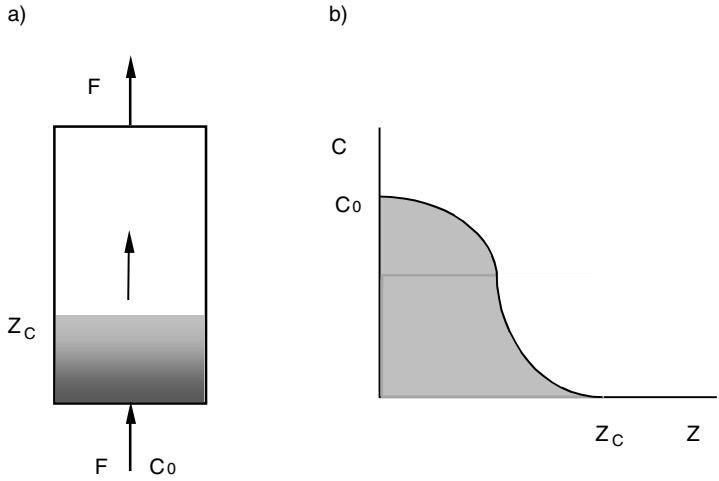

FIGURE 22.8
Exchange zone and concentration profile of the fluid stream in this zone.

tration C_0 and is introduced in a column with an adsorbent bed or exchange resin, the solute passes to the solid phase and the fluid stream leaves the column free from this solute. The upper layers of solid will fill first, and a concentration profile of the fluid phase is created in the column as shown in Figure 22.8. It can be observed that when the first layer of adsorbent is full, there is a layer at certain height z_C that still has not retained or exchanged solute, and the fluid is free from solute. The height z_C is called height of the exchange zone. The time required to form this exchange zone is the formation time t_F.

Once the zone is formed with the corresponding concentration profile, the concentration front crosses the whole column until it reaches the outlet, which occurs when this front has crossed the total column height z_T. The breakpoint is defined as the instant in which the fluid stream leaving the column starts leaving solute, although in practice it is considered that this point is reached when the concentration of the fluid stream is 5% of the inlet stream concentration. At the instant when the breakpoint is reached, the volume of fluid treated is V_R, while the elapsed time is the breakpoint time t_R. When the fluid stream that leaves the column has the same concentration as the inlet stream, the solid is completely full and the saturation point is reached, although in practice it is considered that this point has been reached when the concentration of the fluid at the column's outlet is 95% of the inlet concentration. At the saturation point, a volume of fluid V_T has been treated in a total time t_T.

Figure 22.9 is obtained by plotting the concentration of solute in the fluid stream against the volume of fluid treated. It is easy to deduce that the volume treated to form the exchange zone is the difference between the

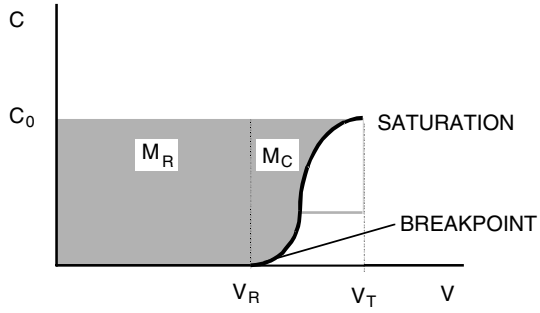

FIGURE 22.9
Volume of fluid treated under breakpoint and saturation conditions.

volume treated to reach the saturation point and that required to reach the breakpoint: $V_C = V_T - V_R$.

The amounts of solute retained or exchanged by the solid at different operation points can also be obtained. The amount of solute retained or exchanged by the solid bed to form the exchange zone is defined as M_C, while M_R is the solute retained or exchanged by the solid until the breakpoint: $M_R = V_R\ C_0$. In this equation, C_0 is the concentration of solute in the fluid stream at the column's inlet. In adsorption processes these amounts are expressed in grams or moles of solute, while in ionic exchange processes they are given in equivalents of solute.

Time t_F has been previously defined as the time needed to develop the exchange zone; however, definitions of new parameters are required. Thus, the time needed by the exchange zone to cross its own height z_C is defined as the relationship between the volume of fluid to form the exchange zone and the circulation volumetric flow rate of the fluid stream:

$$t_C = \frac{V_C}{q} = \frac{V_C}{v\,A} \tag{22.25}$$

where v is the linear velocity and A is the transversal section of the column.

In the same way, the total time required to reach the saturation point is given by the relationship between the total volume treated and the volumetric flow rate:

$$t_T = \frac{V_T}{q} = \frac{V_T}{\mathrm{v}\,A} \tag{22.26}$$

The rate with which the exchange zone moves is:

$$v = \frac{z_T}{t_T - t_F} \tag{22.27}$$

It is easy to deduce from all these definitions the relationship between the total height of the bed and the height of the exchange zone:

$$z_C = t_C\, v = t_C \frac{z_T}{t_T - t_F} \tag{22.28}$$

On the other hand, the relationship between the total time and the time required by the exchange zone to cross its own height is obtained by combining the last equations:

$$t_T = t_C \frac{V_T}{V_C} \tag{22.29}$$

The amount of solutes retained or exchanged from the breakpoint to the saturation point is obtained by integrating the variation of the concentration in this range:

$$M_C = \int_{V_R}^{V_T} \left(C_0 - C\right) dV \tag{22.30}$$

It is easy to observe that the maximum amount of solute that can be retained or exchanged in this zone is:

$$\left(M_C\right)_{MAX} = C_0 \left(V_T - V_R\right) = C_0\, V_C$$

A new parameter i is defined as a fraction of the exchange zone with capacity for retaining or exchanging:

$$i = \frac{M_C}{\left(M_C\right)_{MAX}} = \frac{\int_{V_R}^{V_T} \left(C_0 - C\right) dV}{V_C\, C_0} = 1 - \frac{\int_{V_R}^{V_T} C\, dV}{V_C\, C_0} \tag{22.31}$$

The formation time of the exchange zone and the time required by the exchange zone to cross its own height can be related according to the equation:

$$t_F = \left(1 - i\right) t_C \tag{22.32}$$

The concentration profile of the exchange zone is different according to the value of the parameter i (Figure 22.10). In the case when $i = 0.5$, it is said that the breakthrough curve is symmetrical, complying that $t_F = 0.5\ t_C$.

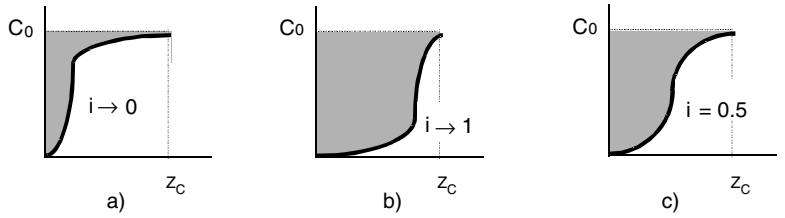

FIGURE 22.10
Concentration profile (breakthrough curve) of the exchange zone as a function of the value of *i*.

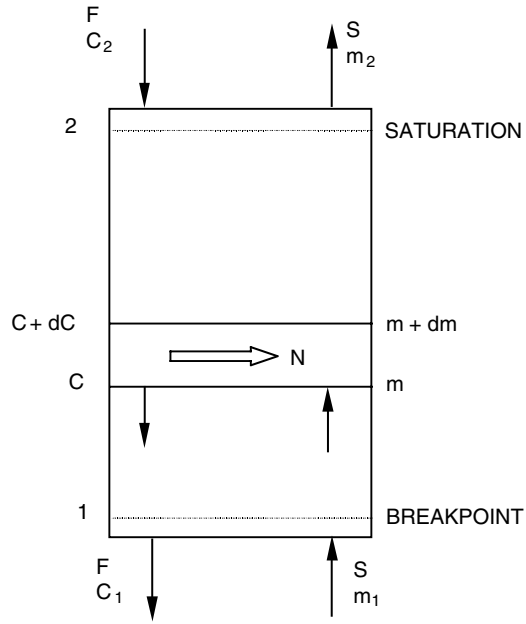

FIGURE 22.11
Conditions of the exchange zone.

22.6.3.1 Calculation of Height of Exchange Zone in an Adsorption Column

The calculation of the height of the exchange zone is made assuming that this zone is similar to a countercurrent unit of infinite height that operates under stationary conditions. Therefore, it is considered that, in this zone, the conditions represented in Figure 22.11 are given, where a fluid stream F with a solute concentration C_0 is fed by the top of the column, while a stream S of the adsorbent solid with a concentration m_1 is fed by the bottom of the column. The fluid that leaves the column has a solute concentration equal to C_1, while the solute content of solid stream is m_1.

Since the column's height is infinite, the saturation conditions will be given in zone 2 while the breakpoint conditions are in section 1. Therefore it is complied that $C_1 = 0$ and $m_2 = m_{MAX}$, where m_{MAX} is the maximum concentration of solute that the solid can adsorb.

When performing a solute balance between the bottom of the column and any column section, it is obtained that:

$$F\left(C - C_1\right) = S\left(m - m_1\right) \tag{22.33}$$

But $C_1 = 0$ and if, in addition, the adsorbent solid is free from solute when it enters into the column, $m_1 = 0$. Hence:

$$FC = Sm$$

If the solute balance is made for a dz of column, then:

$$F\,dC = k_F\left(C - C_e\right)a_S\,A\,dz$$

This equation allows calculation of the height of the exchange zone. If it is integrated with the boundary conditions marked in Figure 22.11:

$$z_C = \frac{F/A}{k_F\,a_S}\int_{C_1}^{C_2}\frac{dC}{C - C_e} \tag{22.34}$$

This equation is generally solved by graphical or numerical integration.

When the equilibrium isotherm is linear ($m = K_aC$), the equilibrium concentration C_e is:

$$C_e = \frac{m}{K_a} = \frac{FC}{S\,K_a}$$

Substitution into Equation 22.34 yields an expression easy to integrate, in which the height of the exchange zone is:

$$z_C = \frac{F/A}{K'\,k_F \cdot a_S}\ln\left(\frac{C_2}{C_1}\right) \tag{22.35}$$

where C_1 and C_2 are the concentrations of the fluid phase at the breakpoint and saturation point, respectively, while K' is a parameter defined as:

$$K' = 1 - \frac{F}{SK_a}$$

If it is considered that the following is complied at the breakpoint and saturation point:

$$C_1 = 0.05 \cdot C_0 \text{ and } C_2 = 0.95 \cdot C_0$$

then Equation 22.35 is transformed into:

$$z_C = \frac{F/A}{K' k_F a_S} \ln(19) \tag{22.36}$$

22.6.3.2 Calculation of Height of Exchange Zone in an Ionic Exchange Column

The way to operate is similar to the case of the adsorption column. From the solute balance between the bottom of the column and any column section, it is obtained that:

$$F(C - C_1) = S(m - m_1) \tag{22.33}$$

The equivalent fractions in the fluid phase (Y) and the resin (X) can be defined as:

$$Y = \frac{C}{C_0}$$

$$X = \frac{m}{m_{MAX}}$$

In this equation the concentration C of the fluid phase is expressed as equivalents of solute per liter and the concentration in the resin m is expressed as equivalents of solute per kg of resin. Also, m_{MAX} is the maximum retention capacity of the resin. The equation of the solute balance is:

$$F C_0 (Y - Y_1) = S m_{MAX} (X - X_1) \tag{22.37}$$

which is the so-called operating line in the equilibrium diagram.

If the balance is performed between the bottom and the top of the column, this equation is transformed into:

$$F C_0 (Y_2 - Y_1) = S m_{MAX} (X_2 - X_1) \tag{22.38}$$

Since sections 1 and 2 of the column correspond to the breakpoint and saturation point, respectively, it should be complied that:

Breakpoint:	$X_1 = 0$	$Y_1 = 0$
Saturation point:	$X_2 = 1$	$Y_2 = 1$

Combination of Equations 22.37 and 22.38 yields that the operating line (Equation 22.33) is a straight line with slope 1 and ordinate to the origin 0; this means $Y = X$.

When performing a solute balance around a dz of the column, it is obtained that:

$$F C_0 Y = k_F C_0 \left(Y - Y_e\right) a_S A\, dz$$

This equation allows calculation of the height of the exchange zone:

$$z_C = \frac{F/A}{k_F a_S} \int_{Y_1}^{Y_2} \frac{dY}{Y - Y_e} \tag{22.39}$$

In this case, this equation has an analytical solution, since from the operating line ($Y = X$) and the definition of the separation factor (Equation 22.9), a relationship between Y_e and Y is obtained:

$$Y_e = \frac{Y}{K\left(1 - Y\right) + Y} \tag{22.40}$$

Substitution in Equation 22.39 allows one to obtain the height of the exchange zone by integration as:

$$z_C = \frac{F/A}{k_F a_S \left(K - 1\right)} \left(K \ln\left(\frac{Y_2}{Y_1}\right) - \ln\left(\frac{1 - Y_2}{1 - Y_1}\right)\right) \tag{22.41}$$

Since in the exchange zone it is complied that the equivalent fractions of the fluid phase Y_1 and Y_2 correspond to the breakpoint and saturation point ($Y_1 = 0.05$ and $Y_2 = 0.95$), then the height of the exchange zone can be calculated using the following equation:

$$z_C = \frac{\left(F/A\right)\left(K + 1\right)}{k_F a_S \left(K - 1\right)} \ln\left(19\right) \tag{22.42}$$

Besides this method, the height of the exchange zone can also be calculated using the equation of Wilke:

$$z_C = b v^{0.51} \tag{22.43}$$

where v is the linear velocity expressed in cm/s, and b is a parameter that depends on the type of transfer. In case of an exchange of ions Ca^{2+} and Mg^{2+} by Na^{+} ions, the value of this constant is 37.4.

The height of the exchange zone can also be calculated by experimentation. For this reason, different experiments are performed with different bed heights z_T, and the volume of fluid V_T required to fill the column is determined; then, the height of the column z_T is plotted against V_T. Data are fitted to a straight line, and the value of the ordinate to the origin is the height z_C of the exchange zone.

Problems

22.1

One of the causes of deterioration of clarified juices of fruits is nonenzymatic browning due to the formation of melanoidins that can be eliminated from the juice by adsorption on activated carbon. The degree of nonenzymatic browning of a juice can be evaluated by measuring its absorbance at a wavelength of 420 nm (A_{420}). In an experimental series at the laboratory, different amounts of activated carbon (particles of 1 mm of mean diameter) are mixed with loads of 10° Brix juice, whose A_{420} is 0.646, until reaching equilibrium. Data obtained are given in the following table:

A_{420}	0.646	0.532	0.491	0.385	0.288	0.180
b	0	0.01	0.02	0.06	0.12	0.26

in which A_{420} is expressed as absorbance/kg of solution, while b is the kg of carbon/kg of solution. Determine: (a) data of the equilibrium isotherm as a table; (b) the number of stages required, operating under repeated single contact, if it is desired to decrease the A_{420} of the juice down to a value of 0.200, using in each stage 0.025 kg of carbon per each kg of 10°Brix juice; and (c) the flow of carbon that should be fed to a countercurrent moving-bed column with a juice flow of 1000 kg/h, if it operates with a carbon flow that is double the minimum, and it is desired to obtain juice with an A_{420} value not higher than 0.2.

(a) The equilibrium data are obtained from the problem statement, since the concentration of melanoidins in the liquid phase is given by the absorbance at A_{420}. A measure of the melanoidins adsorbed by the carbon is given by the difference between the initial absorbance of the juice and the absorbance that it has at a determined instant. For this reason, the melanoidin concentration in the liquid and solid phases is:

Liquid phase: $$C = A\left(\frac{\text{absorbance}}{\text{kg juice}}\right)$$

Solid phase: $$m = \frac{A_0 - A}{b}\left(\frac{\text{melanoidines adsorbed}}{\text{kg carbon}}\right)$$

Hence, the data of the equilibrium isotherm are:

$C\left(\frac{\text{absorbance}}{\text{kg juice}}\right)$	0.532	0.491	0.385	0.288	0.180
$m\left(\frac{\text{melan. adsorb.}}{\text{kg carbon}}\right)$	11.4	7.75	4.35	2.98	1.79

(b) When performing a solute balance for the first stage, in which it is supposed that the carbon that enters has no solute, it is obtained that:

$$m_1 = -\frac{L}{S}C_1 + \frac{L}{S}C_0$$

This equation indicates that, when a straight line with slope $-(L/S)$ is traced in the equilibrium diagram from the point with abscissa C_0, the values of C_1 and m_1 are obtained from the equilibrium curve.

The slope of this straight line can be easily obtained from the data in the problem statement:

$$-(L/S) = -1/0.025 = -40 \text{ kg juice/kg carbon}$$

Once C_1 has been obtained, a straight line with the same slope as before is drawn from this abscissa, which allows one to obtain the values of C_2 and m_2 on the equilibrium curve (Fig. 22.P1a). The process is repeated until exceeding the value of $C_n = 0.2$. Table 22.P1 presents the values obtained for the outlet streams of each stage.

TABLE 22.P1

Concentrations in the Stages

Stage	$C\left(\frac{\text{absorbance}}{\text{kg juice}}\right)$	$m\left(\frac{\text{melan. adsorb.}}{\text{kg carbon}}\right)$
1	0.470	7.1
2	0.365	4.0
3	0.285	2.9
4	0.225	2.2
5	0.180	1.8

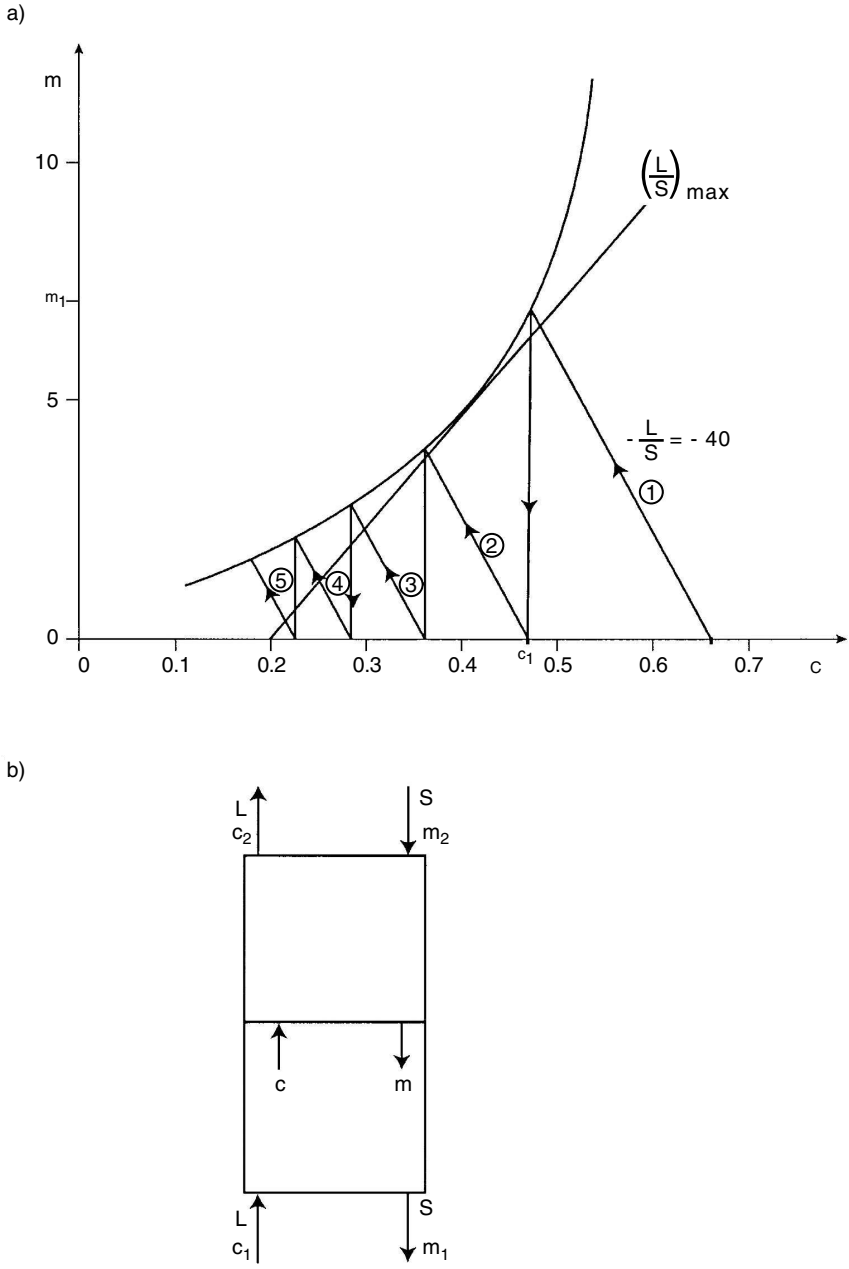

FIGURE 22.P1
(a) Graphical calculation of the stages and maximum slope; (b) movable column.

Since $C_n = 0.2$, five stages will be required.

(c) For the column that works with a moving bed, solute balance between the top of the column and any section yields:

$$m = m_2 + \frac{L}{S}\left(C - C_2\right)$$

It is assumed that the carbon entering the column is free from the solute ($m_2 = 0$) and that the concentration of the liquid stream that leaves the column is $C_2 = 0.2$. Therefore, substitution of data yields the following operation line:

$$m = \frac{L}{S}\left(C - 0.2\right)$$

The maximum slope for this straight line is obtained for $C = C_1$ in the equilibrium curve. However, this is not possible since the straight line that joins point 2 with the point at the equilibrium isotherm for $C = C_1$ will cross the curve. The value of $(L/S)_{MAX}$ is obtained by tracing a straight line tangent to the equilibrium curve from point 2, in such way that its value is:

$$\left(\frac{L}{S}\right)_{MAX} = 25.11 \text{ kg juice/kg carbon}$$

Since the juice stream that circulates by the column is $L = 1000$ kg, the minimum amount of carbon is $S_{MIN} = 39.82$ kg carbon. Since the amount of carbon required is double the minimum:

$$S = 2S_{MIN} = 79.64 \text{ kg carbon}$$

22.2

An industry that processes navel oranges obtains juice that contains 110 ppm of limonene that gives it a bitter taste. With the objective of eliminating the bitter taste from the juice, a 100 kg/h juice stream is fed to a cylindrical column (0.15 m^2 of cross section) that contains a synthetic molecular sieve that adsorbs limonene. The adsorbent solid has a density of 950 kg/m^3 of packing, with a volumetric transfer coefficient equal to 1.5×10^2 h^{-1}, and maximum retention capacity of 10 mg of limonene per kg of adsorbent. The density of the juice can be considered 1000 kg/m^3. The adsorption isotherm in the concentration range at which the column operates is linear and expressed by the equation: $m = 0.12\ C$, where C is the limonene content in the juice in mg/kg, while m is the concentration in the solid expressed in mg/kg of adsorbent. It can be assumed that the breakthrough curve is symmetrical. Calculate: (a) the height of the exchange zone; and (b) if 25 min are required for limonene in the juice stream to begin leaving the column, calculate the height that the adsorbent bed should have.

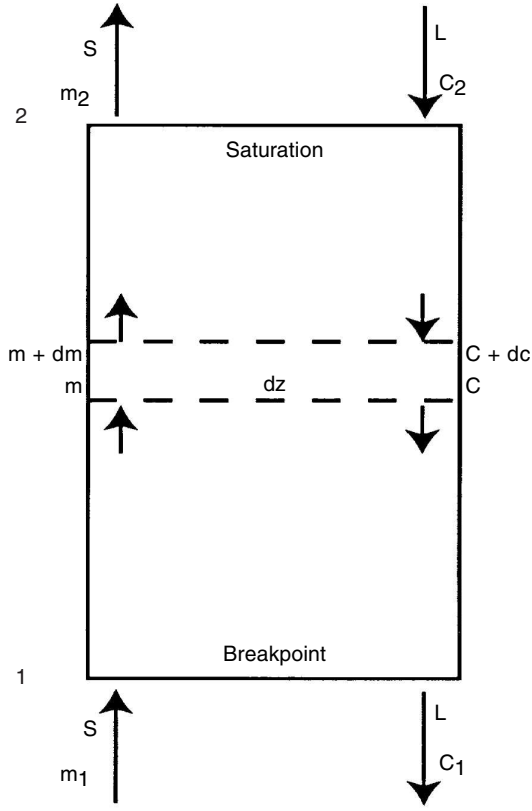

FIGURE 22.P2
Conditions of an exchange zone.

(a) The exchange zone behaves as a moving bed column with infinite height, so the saturation conditions are given on the column's top, while breakpoint conditions are on the bottom: $m_1 = 0$ and $C_1 = 0$. From the global balance of solute, it is obtained that $S = L\,C_2/m_2$. If the balance is performed between section 1 and any section: $S = L\,C/m$. Since the adsorption isotherm is linear ($m = K\,C_e$), it is possible to obtain a relationship between the equilibrium concentration and the composition of juice by combining the last equations:

$$C_e = \frac{m_2}{K\,C_2} C$$

The height of the exchange zone is obtained from the expression:

$$z_C = \frac{L/A}{K_L\,a_S} \int_{C_1}^{C_2} \frac{dC}{C - C_e} = \frac{L/A}{K_L\,a_S} \frac{KC_2}{\left(KC_2 - m_2\right)} \ln\left(\frac{C_2}{C_1}\right)$$

From data in the statement:

C_0 = 110 mg limonene/kg juice
C_1 = 0.05 C_0 = 5.5 mg limonene/kg juice
C_2 = 0.95 C_0 = 104.5 mg limonene/kg juice
$m_2 = m_0$ = 10 mg limonene/kg adsorbent

Therefore:

$$z_C = \frac{100 \text{ kg/h}}{(1000)(0.15)(150)} \frac{(0.12)(104.5)}{(0.12)(104.5)-(10)} \ln\left(\frac{0.95}{0.05}\right)$$

$$Z_C = 0.0646 \text{ m}$$

(b) The volume of the exchange zone is $V_c = z_C A = 0.00969$ m^3. The amount of limonene that enters the column with the juice stream is:

$$wC_0 = (100)(110) = 1100 \text{ mg limonene/h}$$

The breakpoint is reached when limonene begins to be present in the stream leaving the column, which occurs at 25 min (t_R = 25 min). The amount of limonene that entered during 25 min has been retained in the adsorbent in the column. If V is the volume occupied by the adsorbent in the whole column, the volume of saturated adsorbent is ($V - V_C$). Therefore, the following is complied at the breakpoint:

$$wC_0 t_R = (V - V_C)\rho_a m_0 + V_C \rho_a m_0 i$$

Substituting data:

$$(100)(110)(25/60) = (V - 0.00969)(950)(10) + (0.00969)(950)(10)(0.5)$$

Thus, the volume that the adsorbent occupies in the column is obtained:

$$V = 0.468 \text{ m}^3$$

The height of the adsorbent is $z = V/A$ = 3.12 m.

22.3

In a stage of a certain food process, 8000 kg/h of water with a magnesium salts content of 40 meq/kg are treated in an ionic exchange cylindrical column. The exchange capacity of the resin is 15 eq/kg, with a separation

factor of 50 and an apparent density of 550 kg/m^3. The column has a 30 cm diameter and contains 110 kg of resin. From previous experiments, it has been obtained that the mass transfer coefficient is $K_L \cdot a_S = 2.5 \times 10^6$ l/(h.m^3). If it is a fixed-bed column and the breakthrough curve is symmetric, determine: (a) height of the exchange zone; (b) the breakpoint and saturation times; and (c) the magnesium salts content after 75 min of operation.

If it is supposed that the density of the liquid stream is 1000 kg/m^3, then the volumetric flow rate is $q = 8$ m^3/h.

The mass transfer coefficient is expressed in proper units to facilitate later calculations:

$$K_L a_S = 2.5 \times 10^6 \ \text{l}/\left(\text{h} \cdot \text{m}^3\right) = 2500 \ \text{h}^{-1}$$

(a) The height of the exchange zone is calculated by Equation 22.42:

$$z_C = \frac{q/A}{K_L a_S} \frac{K+1}{K-1} \ln 19$$

The volume of the exchange zone can be obtained from the previous equation:

$$V_C = z_C A = \frac{(8)}{(2500)} \left(\frac{50+1}{50-1} \right) \ln 19 = 0.00981 \ \text{m}^3$$

which corresponds to an exchange zone height equal to $z_C = 0.139$ m.

The volume occupied by the resin is the total of the column:

$$V_{RESIN} = \frac{25 \ \text{kg}}{550 \ \text{kg}/\text{m}^3} = 0.04546 \ \text{m}^3$$

and a total column height equal to $z = 0.643$ m.

(b) The breakpoint time is produced when salts begin to exit with the liquid stream leaving the column. At the saturation volume, no more ions can be exchanged. Also, the exchange zone will have half of its exchange capacity.

Saturation volume: $V_S = V - V_C = 0.03565 \ \text{m}^3$

The amount of ions that entered during the breakpoint time have been retained in the volume of saturated resin and in the exchange zone, complying with the following:

$$w C_0 t_R = V_S \rho_a E_M + V_C \rho_a E_M i \left(320 \ \text{eq Mg}^{2+}/\text{h}\right) t_R$$

$$= \left(0.03565\right)\left(550\right)\left(15\right) \text{eq Mg}^{2+} + \left(0.00981\right)\left(550\right)\left(15\right)\left(0.5\right) \text{eq Mg}^{2+}$$

Thus, the breakpoint time is:

$$t_R = 1.046 \text{ h} = 63 \text{ minutes}$$

At saturation time, the resin of the column would be saturated; also, it has passed the exchange zone:

$$\begin{aligned} w C_0 t_R &= V_{RESIN} \rho_a E_M + V_C \rho_a E_M i \left(320 \text{ eq } Mg^{2+}/\text{h}\right) t_S \\ &= \left(0.04546\right)\left(550\right)\left(15\right) \text{eqMg}^{2+} + \left(0.00981\right)\left(550\right)\left(15\right)\left(0.5\right) \text{eqMg}^{2+} \end{aligned}$$

Hence, the saturation time is:

$$t_S = 1.298 \text{ h} = 78 \text{ minutes}$$

(c) Concentration after 75 min in the water stream leaving the column is obtained by linear interpolation between the breakpoint and saturation times:

$$C = C_0 \left(1 - \frac{t_S - t}{t_S - t_R}\right) = 32 \text{ meq/kg}$$

References

Adams, N. and Lodge, A.S. (1964), *Phil. Trans Roy. Soc. London,* A, 256, 149.

Aguado, M.A. and Ibarz, A. (1988), Variación de la densidad de un zumo de manzana con la temperatura y conmcentración, *Alimentación, Equipos y Tecnología,* 2/88, 209–216.

Alfa–Laval, *Heat Exchanger Guide,* Alfa–Laval AB-2nd, Sweden.

Alvarado, J.D. and Romero, C.H. (1989), *Latin Am. Appl. Res.,* 19, 15.

Andrianov, Y.P., Toerdokhleb, G.V., and Makarova, E.P. (1968), *Moloch. Prom.,* 29(8), 25.

Badger and Banchero (1970), *Introducción a la Ingeniería Química,* México. D.F.: McGraw-Hill.

Ball, C.O. (1923), *Bull. Natl. Res. Counc.,* 7(1), No. 37, 7.

Baquero, J. and Llorente, V. (1985), *Equipos para la Industria Química y Alimentaria,* Madrid: Alhambra.

Barbosa–Cánovas, G.V. and Peleg, M. (1982), Propiedades de flujo de alimentos líquidos y semilíquidos, *Rev. Tecnol. Aliment. de México,* 17(2), 4.

Barbosa–Cánovas, G.V. and Vega–Mercado, H. (1996), *Dehydration of Foods,* New York: Chapman and Hall.

Barbosa–Cánovas, G.V. and Peleg, M. (1983), Flow parameters of selected commercial semiliquid food products, *J. Texture Studies,* 14, 213.

Barbosa–Cánovas, G., Ibarz, A., and Peleg, M. (1993), *Reología de alimentos fluidos,* Revisión, Alimentaria, Mayo.

Bennet, C.O. and Meyers, J.E. (1979), *Transferencia de Cantidad de Movimiento, Calor y Materia,* Barcelona: Reverté.

Bernardini, E. (1981), *Tecnología de Aceites y Grasas,* Madrid: Alhambra.

Bertsch, A.J., Bimbenet, J.J., and Cerf, O. (1982), *Le Lait,* 62(615–616), 251.

Bhattacharya, K.R. and Sowbhagya, C.M. (1978), On viscograms and viscography. *J. Texture Stud.,* 9, 341.

Billmeyer, F.W. (1971), *Textbook of Polymer Science,* New York: Wiley-Interscience.

Bingham, E.C. (1922), *Fluidity and Plasticity,* New York: McGraw–Hill Book Co.

Bird, R.B., Stewart, W.E., and Lightfoot, E.N. (1960), *Transport Phenomena,* New York: John Wiley & Sons.

Bird, R.B., Armstrong, R.C., and Hassager, O. (1977), *Dynamics of Polymeric Liquids — Fluid Mechanics,* Vol. 1, New York: John Wiley & Sons.

Bondi, A. (1956), Theories of viscosity, in *Rheology* (F.R. Eirich, ed.), Vol. 1, New York: Academic Press, 132.

Brennan, J.G., Butters, J.R., Cowell, N.D., and Lilly, A.E.V. (1980), *Las Operaciones de la Ingeniería de los Alimentos,* Spain, Zaragoza: Acribia.

Brown, A.I. and Marco, S.M. (1970), *Transmisión de Calor,* México: CECSA.

Bruin, S. and Luyben, K. Ch.A.M. (1980), Drying of food materials, in *Advances in Drying* (A.S. Mujumdar, Ed.), Vol. 1, New York: Hemisphere Publishing.

Brunauer, S., Emmett, P.H., and Teller, E. (1938), Adsorption of gases in multimolecular layers, *J. Am. Chem. Soc.*, 60, 309.
Brunner, E. (1949), *J. Chem. Phys.*, 17, 346.
Buonopane, R.A., Troupe, R.A., and Morgan, J.C., *Chem. Eng. Prg.*, 59(7), 57.
Campanella, O.H. and Peleg, M. (1987a), Squeezing flow viscosimetry of peanut butter, *J. Food Sci.*, 52(1), 180.
Campanella, O.H. and Peleg, M. (1987b), Determination of the yield stress of semiliquid foods from squeezing flow data, *J. Food Sci.*, 52(1), 214.
Carleton, A.J., Cheng, D.C., and Whittaker, W. (1974), *Inst. Petrol. Tech.* Pap., No. 9.
Casson, N. (1959), A flow equation for pigment-oil suspensions of the printing ink type, in *Rheology of Disperse Systems* (C.C. Hill, Ed.), New York: Pergamon Press, 82.
Castaldo, D., Castaldo, D., Palmieri, L., Lo Voi, A., and Castabile, P. (1990), Flow properties of Babaco (*Carica Pentagona*) purees and concentrates, *J. Texture Stud.*, 21, 253.
Cathala, J. (1951), *Chem. Eng. Sci.*, 1, 1.
Chandarana, D.I., Gavin, A. III, and Wheaton, F.W. (1990), Particle/fluid interface heat transfer under UHT conditions at low particle/fluid relative velocities, *J. Food Process. Eng.*, 13(3), 191.
Charm, S.E. (1960), Viscometry of non-Newtonian food materials, *Food Res.*, 25, 351.
Charm, S.E. (1963), The direct determination of shear stress-shear rate behavior of foods in the presence of yield stress, *J. Food Sci.*, 28, 107.
Charm, S.E. (1963), Effect of yield stress on the power law constants of fluid materials determined in low shear rate viscometer, *Ing. Eng. Chem. (Proc. Design Dev.)*, 2, 62.
Charm, S.E. (1971), *Fundamentals of Food Engineering*, Connecticut: AVI.
Chen, C. (1985), Thermodynamic analysis of freezing and thawing of foods enthalpy and apparent specific heat, *J. Food Sci.*, 50, 1158.
Chen, C.S. and Johnson, W.H. (1969), Kinetics of moisture movement in hygroscopic materials. I. Theoretical consideration of drying phenomena, *Trans. ASAE*, 12, 109.
Cheng, D.C. (1986), Yield stress: a time dependent property and how to measure it, *Rheol. Acta*, 25, 542.
Cheng, D.C. and Evans, F. (1965), Phenomenological characterization of rheological behavior of inelastic reversible thixotropic and antithixotropic fluids, *Brit. J. Appl. Phys.*, 16, 1599.
Cheryan, M. (1986), *Ultrafiltration Handbook*, Lancaster, PA: Technomic Publishing Co., Inc.
Cheryan, M. (1992), Concentration of liquid foods by reverse osmosis, in *Handbook of Food Engineering*, (D.R. Heldman and D.B. Lund, Eds.), New York: Marcel Dekker, Inc.
Chirife, J. (1983), Fundamentals of the drying mechanism during air dehydration of foods, in *Advances in Drying*, (A.S. Mujumdar, Ed.), Vol. 2, New York: Hemisphere Publishing.
Choi, Y. and Okos, M.R. (1986a), Thermal Properties of Liquid Foods: Review. Physical and Chemical Properties of Foods (M.R. Okos, Ed.), Minnesota.
Choi, Y. and Okos, M.R. (1986b), Effects of temperature and composition on the thermal properties of foods, in *Food Engineering and Process Applications*, Vol. 1, *Transport Phenomenon* (L. Maguer and P. Jelen, Eds.), New York: Elsevier, 93.
Clark, D.F. (1974), *Chem. Eng.*, 285, May, 275.

Cleland, A.C. and Earle, R.L. (1976), A new method for prediction of surface heat transfer coefficients in freezing, *Bull. I.I.R.,* Annexe-1, 361.
Cleland, A.C. and Earle, R.L. (1979), A comparison of methods for predicting the freezing times of cylindrical and spherical foodstuffs, *J. Food Sci.,* 44, 964.
Cleland, A.C. and Earle, R.L. (1982), Freezing time prediction of foods: a simplified procedure, *Inst. J. Refrig.,* 5, 134.
Cleland, D.J., Cleland, A.C., and Earle, R.L. (1987a), Prediction of freezing and thawing times for multi-dimensional shapes by simple methods, I. Regular shapes, *Inst. J. Refrig.,* 10, 156.
Cleland, D.J., Cleland, A.C., and Earle, R.L. (1987b), Prediction of freezing and thawing times for multidimensional shapes by simple methods, II. Irregular shapes, *Inst. J. Refrig.,* 10, 234.
Cleland, A.C. (1992), Dynamic modelling of heat transfer for improvement in process design — case studies involving refrigeration, in *Advances in Food Engineering* (R.P. Singh and M.A. Wirakartakusumah, Eds.), Boca Raton, FL: CRC Press.
Committee on Dynamic Objectives for Chemical Engineering (C.D.O.Ch.E.) (1961), *Chem. Eng. Progr.,* 57, 69.
Constenla, D.T., Lozano, J.E., and Crapiste, G.H. (1989), *J. Food Sci.,* 54 (3):663.
Cooper, A. (1974), *Chem. Eng.,* 285, 280.
Cornford, S.J., Parkinson, T.L., and Robb, J. (1969), Rheological characteristics of processed whole egg, *J. Food Technol.,* 4, 353.
Costa, J. et al. (1984), *Curso de Química Técnica,* Barcelona: Reverté.
Costa, E., Calleja, Orejero, G., de Lucas, A., Aguado, J., and Uguino, M.A. (1986), *Ingeniería Química.* 4. *Transmisión de Calor,* Madrid: Alhambra.
Costa, E., Sotelo, J.L., Calleja, G., Ovejero, G., de Lucas, A., Aguado, J., and Uguina, M.A. (1983), *Ingenier a Quimica. I. Conceptos Genrales,* Madrid: Alhambra.
Costell, E. and Duran, L. (1979), Esterilización de conservas. Fundamentos teóricos y cálculo del tiempo de esterilización, *Instituto de Agroquímica y Tecnología de Alimentos (CSIC),* Información técnica general 66.
Coulson, J.M. and Richardson, J.F. (1979–1981), *Ingeniería Química,* Vols. I to VI, Barcelona: Reverté.
Cowan, C.T. (1975), *Chem. Eng.,* July, 102.
Crandall, P.G., Chen, C.S., and Carter, R.D. (1982), Models for predicting viscosity of orange juice concentrate, *Food Technol.,* May, 245.
Crapiste, G.H. and Lozano, J.E. (1988), Effect of concentration and pressure on the boiling point rise of apple juice and related sugar solutions, *J. Food Sci.,* 53(3), 865.
Davis, R.B., De Weese, D., and Gould, W.A. (1954), Consistency measurement of tomato pureé, *Food Technol.,* 8, 330.
Dickerson, R.W. (1969), Thermal properties of foods, in *The Freezing Preservation of Foods,* (D.K. Tressler, W.B. Van Arsdel, and M.J. Copley, Eds.), Vol. 2, 4th ed., Westport, CT: AVI.
Dickey, D.S. and Fenic, J.G. (1976), Dimensional analysis for fluid agitation systems, *Chem. Eng.,* 5, 139.
Dickie, A. and Kokini, J.L. (1981), Transient viscoelastic flow of fluid and semisolid food materials, presented at the 52nd Annul Meeting of the Society for Rheology, Williamsburg, VA.
Dodge, D.W. and Metzner, A.B. (1959), Turbulent flow of non-Newtonians systems, *AIChEJ,* 5(2), 189.
Earle, R.L. (1983), *Ingeniería de los Alimentos,* 2nd ed., Zaragoza, Spain: Acribia.

Edwards, M.F., Changala, A.A., and Parrot, D.L. (1974), *Chem. Eng.,* 285, 286.
Elliot, J.H. and Ganz, A.J. (1977), Salad dressings — preliminary rheological characterization, *J. Texture Stud.,* 8, 359.
Elliot, J.H. and Green, C.E. (1972), Modification of food characterization with cellulose hydrocolloids, II. The modified Bingham body, *J. Texture Stud.,* 3.
Emmett, P.H. and de Witt, T. (1941), Determination of surface areas, *Ind. Eng. Chem.* (Anal.), 13, 28.
Eolkin, D. (1957), The plastometer — a new development in continuous recording and controlling consistometers, *Food Technol.,* 11, 253.
Eyring, H. (1936), *J. Chem. Phys.,* 4, 283.
Fernández-Martín, F. (1972a), Influence of temperature and composition on some physical properties of milk concentrates, I. Viscosity, *J. Dairy Res.,* 39, 75.
Fernández–Martín, F. (1972b), *J. Dairy Res.,* 39 (1), 65.
Fernández–Martín, F. (1982), Alimentación, *Equipos y Tecnología,* 2/82, 55.
Fernández–Martín, F. and Montes, F. (1972), Milchwiss., 27(12), 772.
Fernández–Martín, F. and Montes, F. (1977), *J. Dairy Res.,* 44(1), 103.
Figoni, P.I. and Shoemaker, C.F. (1983), *J. Texture Stud.,* 14(4), 431.
Fiszman, S.M. et al. (1986), Relajación de sistemas viscoelásticos. Comparación de métodos de análisis de las curvas experimentales, *Rev. Agroquím. Tecnol. Aliment.,* 26(1), 63.
Fortes, M. and Okos, M.R. (1980), Drying theories, in *Advances in Drying* (A.S. Mujumdar, Ed.), Vol. 1, New York: Hemisphere Publishing.
Foust, A.S., Wenzel, I.A., Clump, C.W., Maus, L., and Anderson, L.B. (1980), *Principles of Unit Operations,* New York: John Wiley & Sons.
Frederickson, A.G. (1970), *Amer. Inst. Chem. Eng. J.,* 16, 436.
García, E.J. and Steffe, J.F. (1986), Optimum economic pipe diameter for pumping Herschel–Bulkley fluids in pipe flow, *J. Food Process Eng.,* 8, 117.
Garcia, E.J. and Steffe, J.F. (1987), Comparison of friction factor equations for non-Newtonian fluids in pipe flow, *J. Food Process Eng.,* 9, 93.
Geankoplis, C.J. (1978), *Transport Processes and Unit Operations,* Boston, MA: Allyn and Bacon.
Geankoplis, C.J. (1983), Drying of process materials, in *Transport Processes and Unit Operations,* 2nd ed., Boston, MA: Allyn and Bacon.
Greensmith, H.W. and Rivlin, R.S. (1953), *Phil. Trans. Roy. Soc. London* A, 245, 399.
Gregorig, R. (1968), *Cambiadores de Calor,* Bilbao: Urmo.
Gromov, M.A. (1974), *Moloch. Prom.,* 35(2), 25.
Gromov, M.A. (1979), *Moloch. Prom.,* 40(4), 37.
Hahn, S.J., Ree, T., and Eyring, H. (1959), Flow mechanism of thixotropic substances, *Ind. Eng. Chem.,* 51, 856.
Hanks, R.W. and Ricks, B.L. (1974), Laminar-turbulent transition in flow of pseudoplastic fluids with yield stresses, *J. Hydronautics,* 8(4), 163.
Harper, J.C. (1976), *Elements of Food Engineering,* Westport, CT: AVI.
Harper, J.C. and El Sarhigi, A.F. (1965), Viscometric behavior of tomato concentrates, *J. Food Sci.,* 30, 470.
Harper, J.C. and Leberman, K.W. (1962), Rheological behavior of pear purees. *Proceedings of the First International Congress of Food Science and Technology,* vol. I, 719, Newark, NJ: Gordon and Breach Science Publishers.
Harris, J. (1967), *Rheol. Acta,* 6, 6.
Heldman, D.R. (1975), *Food Process Engineering,* Westport, CT: AVI.

Heldman, D.R. (1992), Food freezing, in *Handbook of Food Engineering* (D.R. Heldman and D.B. Lund, Eds.), New York: Marcel Dekker.
Heldman, D.R. and Lund, D.B. (1992), *Handbook of Food Engineering,* New York: Marcel Dekker.
Heldman, D.R. and Singh, R.P. (1981), *Food Process Engineering,* Westport, CT: AVI.
Herranz, J. (1979), *Procesos de Transmisión de Calor*, Madrid: Castillo.
Higgs, S.J. and Norrington, R.J. (1971), Rheological properties of selected foodstuffs, *Proc. Biochem.,* 6(5), 52.
Holdsworth, S.D. (1971), Applicability of rheological models to the interpretation of flow and processing behaviour of fluid food products, *J. Texture Stud.,* 2, 393.
Huggins, M.L. (1942), The viscosity of dilute solutions of long-chain molecules, IV. Dependence on concentration, *J. Am. Chem. Soc.,* 64, 2716.
Ibarz, A. (1986), *Extracción Sólido–Líquido,* ETSEAL, Universitat Politècnica de Catalunya.
Ibarz, A. (1986), Intercambiadores de calor de placas, *Alimentación, Equipos y Tecnología,* 3/86, 119.
Ibarz, A. (1987), Un método de diseño de intercambiadores de calor de placas, *Alimentación, Equipos y Tecnología,* 2/87, 187.
Ibarz, A., Vicente, M., and Graell, J. (1987), Rheological behaviour of apple juice and pear juice and their concentrates, *J. Food Eng.,* 6, 257.
Ibarz, A. and Pagán, J. (1987), Rheology of raspberry juices, *J. Food Eng.,* 6, 269.
Ibarz, A. and Sintes, J. (1989), Rheology of egg yolk, *J. Texture Stud.,* 20, 161.
Ibarz, A. and Miguelsanz, R. (1989), *J. Food Eng.,* 10, 319.
Ibarz, A. et al. (1989), Rheological properties of clarified pear juice concentrates, *J. Food Eng.,* 10, 57.
Ibarz, A., Giner, J., Pagáu, J., and Gimeno, V. (1991), Influencia de la temperatura en la reología de zumos de kiwi, III Congreso Mundial de Tecnología de Alimentos, Barcelona.
Ibarz, A., Gonzólez, C., Esplugas, S., and Vincent, M. (1992a), Rheology of clarified fruit juices, I: Peach juices, *J. Food Eng.,* 15, 49.
Ibarz, A., Pagán, J., and Miguelsanz, R. (1992b), Rheology of clarified fruit juices, II: blackcurrant juices, *J. Food Eng.,* 15, 63.
Ilangantileke, S.G., Ruba Jr., A.B., and Joglekar, H.A. (1991), Boiling point rise of concentrated Thai tangerine juices, *J. Food Eng.,* 15, 235.
Jackson, B.W. and Tropupe, R.A. (1964), *Chem. Eng. Prg.,* 60(7), 62.
Jacob, M. (1957), *Heat Transfer,* New York: Wiley.
Jenson, V.G. and Jeffreys, G.V. (1969), *Métodos Matemáticos en Ingeniería Química,* Madrid: Alhambra.
Joye, D.D. and Poehlein, G.W. (1971), *Trans. Soc. Rheol.,* 15, 51.
Karel, M., Fennema, O.R., and Lund, D.B. (1975a), Preservation of food by storage at chilling temperatures, in *Principles of Food Science. Part II. Physical Principles of Food Preservation* (O.R. Fennema, Ed.), New York: Marcel Dekker.
Karel, M., Fennema, O.R., and Lund, D.B. (1975b), Protective packaging of foods, in *Principles of Food Science. II. Physical Principles of Food Preservation* (O.R. Fennema, Ed.), New York: Marcel Dekker.
Kemblowski, Z. and Petera, J. (1980), A generalized rheological model of thixotropic materials, *Rheolog. Acta,* 19, 529.
Kern, D.Q. (1965), *Procesos de Transferencia de Calor,* Mexico: CECSA.
Kimball, D.A. (1986), *J. Food Sci.,* 51 (2), 529.

King, C.J. (1980), *Procesos de Separación,* Barcelona: Reverté.
Kokini, J.L. and Plutchok, G.J. (1987), Viscoelastic properties of semisolid foods and their biopolymeric components, *Food Technol.,* 41(3), 89.
Kokini, J.L. (1992), Rheological properties of foods, in *Handbook of Food Engineering* (D.R. Heldman and D.B. Lund, Eds.), New York: Marcel Dekker, 1.
Kopelman, I.J. (1966), Transient heat transfer and thermal properties in food systems, Ph.D. Thesis, Michigan State University.
Kraemer, E.O. (1938), Molecular weights of cellulose and cellulose derivatives, *Ind. Eng. Chem.,* 30, 1200.
Kramer, A. and Twigg, B.A. (1970), *Quality Control for the Food Industry,* Vol. 1, Westport, CT: Avi.
Kreith, F. and Black, W.Z. (1983), *La Transmisión del Calor Principios Fundamentales,* Madrid: Alhambra.
Lana, E.P. and Tischer, R.A. (1951), Evaluation of methods for determinig quality of pumpkins for canning, *Proc. Am. Soc. Hort. Sci.,* 38, 274.
Lee, K.H. and Brodkey, R.S. (1971), *Trans. Soc. Rheol.,* 15, 627.
Letort, M., (1961), LaGénie Chimique, *Génie Chim.,* 86, 53.
Levenspiel, O. (1986), *El Omnilibro de los Reactores Químicos,* Barcelona: Reverté.
Levenspiel, O. (1993), *Flujo de Fluidos. Intercambio de Calor,* Barcelona: Reverté.
Levy, F. (1979), Enthalpy and specific heat of meat and fish in the freezing range, J. *Food Technol.,* 14, 549.
Lin, O.C.C. (1975), *J. Appl. Pol. Sci.,* 19, 199.
Longree, K. et al. (1966), Viscous behavior of custard systems, *J. Agr. Food Chem.,* 14, 653.
Lund, D.(1975), Heat transfer in foods, in *Principles of Food Science Part 2: Physical Principles of Food Preservation,* (O. Fennema, Ed.), New York: Marcel Dekker, 11.
Lutz, J.M. and Hardenburg, R.E. (1968), Agr. Handbook No 66, U.S. Department of Agriculture, Washington, D.C.: U.S. Government Printing Office.
Mafart, (1994), *Ingeniería Industrial Alimentaria,* Zaragoza, Spain: Acribia.
Manohar, B., Ramakrishna, P., and Udayasankar, K. (1991), Some physical properties of tamarind (*Tamarindus indica* L.) juice concentrates, *J. Food Eng.,* 13, 241.
Marriott, J. (1971), *Chem. Eng.,* 5, 127.
Marshall, W.R. (1954), Atomization and spray drying, *Chem. Eng. Process Monogr.* Ser., 50(2).
Martens, T. (1980), Mathematical model of heat processing in flat containers, Doctoral Thesis, Universidad Católica, Leuven, Bélgica.
Mason, J.M. and Wiley, R.C. (1958), Quick quality test for lima beans, Maryland Processor's Dept. 4, 1. Univ. Maryland, College Park, MD.
Mason, P.L., Mason, P.L., Pouti, M.P., Bistony, K.L., and Kokini, S.L. (1982), A new empirical model to simulate transient shear stress growth in semisolid foods, *J Food Proc. Eng.,* 6(4), 219.
Masters, K. (1991), *Spray Drying Handbook,* 5th ed. UK: Longman Group Limited.
McAdams, W.H. (1964), *Transmisión de Calor,* Madrid: Castillo.
McCabe, W.L. and Smith, J.C. (1968), *Operaciones Básicas de Ingeniería Química,* Barcelona: Reverté.
McCabe, W.L., Smith, J.C., and Harriott, P. (1985), *Unit Operations of Chemical Engineering,* Singapore: McGraw–Hill Book Company.
McCabe, W.L., Smith, J.C., and Harriott, P. (1991), *Operaciones Unitarias en Ingeniería Qruímica,* Madrid: McGraw–Hill/Interamericana de España, S.A.
McKennell, R. (1960), The influence of viscometer design on non-Newtonian measurements, *Anal. Chem.,* 31(11), 1458.

Miranda, L. (1975), *Ingeniería Química,* Agosto, 81–90.
Mizrahi, S. and Berk, Z. (1972), Flow behavior of concentrated orange juice: mathematical treatment, *J. Texture Stud.,* 3, 69.
Moore, F. (1959), The rheology of ceramic slips and bodies, *Trans. Proc. Ceram. Soc.,* 58, 470.
Moresi, M. and Spinosi, M. (1984), *J. Food Technol.,* 19, 519.
Morris, E.R. and Ross–Murphy, S.B. (1981), Chain flexibility of polysaccharides and glycoproteins from viscosity measurements, in *Techniques in Carbohydrate Metabolism,* Amsterdam: Elsevier, North Holland Scientific Publishers, Ltd.
Morris, G.A. and Jackson, J. (1953), *Absorption Towers,* London: Butterworths.
Muller, H.G. (1973), *An Introduction to Food Rheology,* New York: Crane, Russak & Company, Inc.
Munro, J.A. (1943), The viscosity and thixotropy of honey, *J. Econ. Entomol.,* 36, 769.
Mylins, E. and Reher, E.O. (1972), *Plaste und Kautschuk,* 19, 240.
Nagaoka, J., Takigi, S., and Hotani, S. (1955), Experiments on the freezing of fish in air-blast freezer, *Proc. 9th Int. Congr. Refrig.,* Paris, 4, 105.
Ocón, J. and Tojo, G. (1968), *Problemas de Ingeniería Química,* Madrid: Aguilar.
Ohlsson, T. (1994), Progress in pasteurization and sterilization, in *Developments in Food Engineering* (T. Yano, R. Matsuno, and K. Nakamura, Eds.), London: Chapman and Hall.
Oka, S. (1960), The principles of rheometry, in *Rheology* (F.R. Eirich, Ed.), Vol. 3, New York: Academic Press, 18.
Okos, M.R. et al. (1992), Food dehydration, in *Handbook of Food Engineering* (D.R. Heldman and D.B. Lund, Eds.), New York: Marcel Dekker.
Osorio, F.A. and Steffe, J.F. (1984), Kinetic energy calculations for non-Newtonian fluids in circular tubes, *J. Food Sci.,* 49, 1295.
Osorio, F.A. (1985), Back extrusion of power law, Bingham plastic and Herschel–Bulkley fluids, M.S. Thesis, Michigan State Univ., East Lansing, MI.
Osorio, F.A. and Steffe, J.F. (1985), Back extrusion of Herschel–Bulkley fluids — example problem, Paper No. 85-6004. *Am. Soc. Agric. Eng.,* St. Joseph, MI.
Osorio, F.A. and Steffe, J.F. (1987), Back extrusion of power law fluids, *J. Texture Stud.,* 18, 43.
Paulov, K.F., Ramakov, P.G., and Noskov, A.A. (1981), *Problems and Examples, for a Course in Bassic Operations and Equipment in Chemical Technology,* Mir, Moscow. (Cited by O. Levenspiel (1993), *Flujo de Fluidos. Intercambio de calor,* Barcelona: Reverté.)
Perry, R.H. and Chilton, C.H. (1973), *Chemical Engineer's Handbook,* New York: McGraw–Hill.
Peter, S. (1964), *Rheolog. Acta,* 3, 178.
Petrellis, N.C. and Flumerfelt, R.W. (1973), Rheological behavior of shear degradable oils: kinetic and equilibrium properties, *Can, J. Chem. Eng.,* 51, 291.
Plank, R. (1980), *El Empleo del Frío en la Industria de la Alimentación,* Barcelona: Reverté.
Prentice, J.H. (1968), Measurements of some flow properties of market cream, in *Rheology and Texture Foodstuffs,* SCI Monograph, No. 27, 265. Society of Chemical Industry, London.
Pryce–Jones, J. (1953), The rheology of honey, in *Foodstuffs: Their Plasticity, Fluidity and Consistency* (G.W. Scott Blair, Ed.), Amsterdam: North Holland, 148.
Raju, K.S.N. and Chand, J. (1980), *Chem. Eng.,* 11, 133.
Rambke, K. and Konrad, H. (1970), *Die Nägrung,* 14(2), 137.
Ranz, W.E. and Marshall, Jr., W.R. (1952a), Evaporation from drops Part I, *Chem. Eng. Prog.,* 48(3), 141.

Ranz, W.E. and Marshall, Jr., W.R. (1952b), Evaporation from drops Part II, *Chem. Eng. Prog.,* 48(4), 173.
Rao, M.A., Otoya Palomino, L.N., and Bernhardt, L.W. (1974), Flow properties of tropical fruit purees, 39, 160.
Rao, M.A. (1977), Rheology of liquid foods. A review, *J. Texture Stud.,* 8, 135.
Rao, M.A. (1980), Flow properties of fluid foods and their measurements, Paper presented at the 89th National Meeting of AIChE, August 17–20, Portland, Oregon.
Rao, M.A. (1987), Predicting the flow properties of food suspensions of plant origin, *Food Tech.,* 41(3), 85.
Rao, M.A. (1992), Transport and storage of food products, in *Handbook of Food Engineering* (D.R. Heldman and D.B. Lund, Eds.), New York: Marcel Dekker.
Rao, M.A., Cooley, H.J., and Vitali, A.A. (1984), Flow properties of concentrated juices at low temperatures, *Food Technol.,* 38(3), 113.
Rao, M.A. (1986), Rheological properties of fluid foods, in *Engineering Properties of Foods* (Rao, M.A. and S.S.H. Ed.), New York: Marcel Dekker, 1.
Rao, V.N.N., Hamann, D.D., and Humphries, E.G., (1975), *J. Texture Stud.,* 6, 197.
Ree and Eyring (1959).
Reidy, G.A. (1968), Thermal properties of foods and methods of their determination, M.S. Thesis, Food Science Dept., Michigan State University.
Reiner, M. (1971), *Advanced Rheology,* London, H.K. Lewis.
Rha, C.K. (1975), Theories and principles of viscosity, in *Theory Determination and Control of Physical Properties of Food Materials* (C.K. Rha, Ed.), Vol. 1, Dordrecht: D.-Reidel Publishing Company, 7.
Rha, C.K. (1978), Rheology of fluid foods, *Food Technol.,* 32, 77.
Riedel, L. (1949), *Chem. Ing. Tech.,* 21, 340.
Riedel, v.L. (1956), Calorimetric studies of the freezing of fresh meat, *Kaltetechnik,* 8 (12), 374.
Riedel, v.L. (1957a), Calorimetric studies of the meat freezing process, *Kaltetechnik,* 9, 38.
Riedel, v.L. (1957b), Calorimetric studies of the freezing of egg white and egg yolk, *Kaltetechnik,* 9(11), 342.
Ritter, R.A. and Govier, G.W. (1970), The development and evaluation of a theory of thixotropic behavior, *Can. J. Chem. Eng.,* 48, 505.
Rodrigo, M., Lorenzo, P., and Safon, J. (1980), Optimización de las técnicas de esterilización por calor. I. Planteamientos generales, *Rev. Agroquím. Tecnol. Aliment.,* 20(2), 149.
Rodrigo, M., Lorenzo, P., and Safon, J. (1980), Optimización de las técnicas de esterilización por calor. II. Concepto actualizado de la esterilización por calor y efectos de la misma sobre los alimentos. Cinética y parámetros, *Rev. Agroquím. Tecnol. Aliment.,* 20(4), 425.
Rosen, J.B. (1952), Kinetics of a fixed bed system for solid diffusion into spherical particles, *J. Eng. Chem.,* 20, 387.
Rutgus, R. (1958), Consistency of starch milk, *J. Sci. Food Agr.,* 9, 61.
Sáenz, C. and Costell, E. (1986), Comportamiento reológico de productos de limón. Influencia de la temperatura y de la concentración, *Rev. Agroquím. Tecnol. Aliment.,* 26(4), 581.
Saravacos, G.D. (1968), Tube viscometry of fruit purees and juices, *Food Technol.,* 22, 585.
Saravacos, G.D. (1970), Effect of temperature on viscosity of fruit juices and purees, *J. Food Sci.,* 35, 122.

Saravacos, G.D. and Moyer, J.C. (1967), Heating rates of fruit products in an agitated kettle, *Food Technol.,* 21, 372.
Sawistowski, H. and Smith, W. (1967), *Métodos de Cálculo en los Procesos de Transferencia de Materia,* Madrid: Alhambra.
Schwartzberg, H. (1982), Freeze Drying — Lecture Notes. Food Engineering Department, University of Massachussets, Amherst, MA.
Schlichting, H. (1960), *Boundary Layer Theory,* 4th ed., New York: McGraw–Hill.
Schowalter, W.R. (1978), *Mechanics of Non-Newtonian Fluids,* New York: Pergamon Press.
Scott-Blair, G.W. (1958), Rheology in food research, in *Advances in Food Research,* Vol. VIII, New York: Academic Press, Inc.
Shaw, F.V. (1994), Fresh options in drying, *Chem. Eng.,* 101(7), 76.
Sherman, P. (1966), *J. Food Sci.,* 31, 707.
Sherman, P. (1970), *Industrial Rheology,* New York: Academic Press.
Shoemaker, C.F., Lewis, J.I., and Tamura, M.S. (1987), Instrumentation for rheological measurements of food, *Food Technol.,* 41(3), 80.
Siebel, J.E. (1982), *Ice Refrig.,* 2, 256.
Singh, R.P. (1982), *Food Technol.,* 36(2), 87.
Singh, R.P. (1992), Heating and cooling processes for foods, in *Handbook of Food Engineering* (D.R. Heldman and D.B. Lund, Eds.), New York: Marcel Dekker, 247.
Singh, R.P. and Heldman D.R. (1993), *Introduction to Food Engineering,* California: Academic Press.
Singh, R.P. and Lund, D.B. (1984), *Introduction to Food Engineering,* Academic Press.
Singh, R.K. and Nelson, P.E. (1992), *Advances in Aseptic Processing Technologies,* London: Elsevier.
Skelland, A.P.H. (1967), *Non-Newtonian Flow and Heat Transfer,* New York: John Wiley & Sons, Inc.
Smith, J.M. and Van Ness, H.C. (1975), *Introduction to Chemical Engineering Thermodynamics,* New York: McGraw-Hill.
Steffe, J.F. (1992a), *Rheological Methods in Food Process Engineering,* Michigan: Freeman Press.
Steffe, J.F. (1992b), Yield stress: phenomena and measurement, in *Advances in Food Engineering* (R.P. Singh and M.A. Wirakertakusumah, Eds.), Boca Raton, FL: CRC Press, 363.
Steffe, J.F. and Morgan, R.G. (1986), Pipeline design and pump selection for non-Newtonian fluid foods, *Food Technol.,* 40(12), 78.
Steffe, J.F. and Osorio, F.A. (1987), Back extrusion of non-Newtonian fluids, *Food Technol.,* 41(3), 72.
Steffe, J.F., Mohamed, I.O., and Ford, E.W. (1984), Pressure drop across valves and fittings for pseudoplastic fluids in laminar flow, *Trans. ASAE,* 27, 616.
Stoecker, W.F. and Jones, J.W. (1982), *Refrigeration and Air Conditioning,* New York: McGraw–Hill.
Stumbo, C.R. (1973), *Thermobacteriology in Food Processing,* 2nd ed., New York: Academic Press.
Stumbo, C.R. and Longley, R.E. (1966), *Food Technol.,* 20, 109.
Stumbo, C.R. et al. (1983), *Handbook of Lethality Guides for Low-Acid Canned Foods,* Vol. I: Conduction-Heating, Boca Raton, FL: CRC Press.
Succar, J. and Hayakawa, K. (1983), Empirical formulae for predicting thermal physical properties of foods at freezing and defrosting temperatures, *Lebensm. Wiss. Technol.,* 16, 326.

Sweat, V.E. (1974), *J. Food Sci.,* 39(6), 1080.
Teixeira, A.A. and Shoemaker, C.F. (1989), *Computerized Food Processing Operations,* New York: Van Nostran Reinhold.
Teixeira (1992).
Tiu, C. and Boger, D.V. (1974), Complete rheological characterization of time-dependent food products, *J. Texture Stud.,* 5, 329.
Toledo, R.T. (1980), *Fundamentals of Food Process Engineering,* Westport, CT: AVI.
Toledo, R.T. (1993), *Fundamentals of Food Process Engineering,* New York: Chapman and Hall.
Toledo, R.T. and Chang, S-Y. (1990), Advantages of aseptic processing of fruits and vegetables, *Food Technol.,* 44(2), 75.
Troupe, R., Morgan, J.C., and Prifti, J. (1960), *Chem. Eng. Prog.,* 56(1), 124.
Tung, M.A. et al. (1970), Rheology of fresh, aged and gamma-irradiated egg white, *J. Food Sci.,* 35, 872.
U.S. Dept. Agriculture. (1953), U.S. standards for grades of tomato catsup, Agr. Marketing Service, Washington, D.C.
Usher, J.D. (1970), *Chem. Eng.,* 23, 90.
Van Arsdel, N.B. and Copley, M.J. (1963), *Food Dehydration,* Westport, CT: AVI.
Van Wazer, J.R. et al. (1963), *Viscosity and Flow Measurements. A Laboratory Handbook of Rheology,* New York: Interscience Publishers.
Vian, A. and Ocón, J. (1967), *Elementos de Ingeniería Química,* Madrid: Aguilar.
Vitali, A., Roig, S.M., and Rao, M.A. (1974), Viscosity behavior of concentrated passion fruit juice, *Confructa,* 19, 201.
Vitali, A.A. and Rao, M.A. (1984a), Flow properties of low-pulp concentrated orange juice: effect of temperature and concentration, *J. Food Sci.,* 49, 882.
Vitali, A.A. and Rao, M.A. (1984b), Flow properties of low-pulp concentrated orange juice: serum viscosity and effect of pulp content, *J. Food Sci.,* 49(3), 876.
Walters, K. (1975), *Rheometry,* New York: Wiley.
Watson, E.L. (1968), Rheological behavior of apricot purees and concentrates, *Can. Agr. Eng.,* 10, 1.
Weber, W.J. (1979), *Control de la Calidad der Agua. Procesus Fisicoquimicos,* Barcelona: Reverté.
Weltmann, R.N. (1943), Breakdown of thixotropic structure as function of time, *J. Appl. Phys.,* 14, 343.
Welty, J.R., Wicks, Ch.E., and Wilson, R.E. (1976), *Fundamentals of Momentum, Heat and Mass Transport,* New York: John Wiley & Sons.
White, G.W. (1970), Rheology in food research, *J. Food Technol.,* 5, 1.
Wilkinson, W.L. (1974), *Chem. Eng.,* 285, 289.
Windsor, M. and Barlows, S. (1984), *Introducción a los Subproductos de Pesquería,* Zaragoza, Spain: Acribia.
Zimm, B.H. and Grothers, D.M. (1962), Simplified rotating cylinder viscometer for DNA, *Proc. Natl. Acad. Sci.,* 48, 905.
Zitny, R. et al. (1978), Paper presented at 6th International CHISA Congress, Prague.

Appendix

TABLE A1

Properties of Saturated Steam

t (°C)	Vapor Pressure (kPa)	Specific volume (m^3/kg)		Enthalpy (kJ/kg)		Entropy (kJ/kg K)	
		Liquid	Vapor	Liquid	Vapor	Liquid	Vapor
0.01	0.611	0.0010002	206.14	0.00	2501.4	0.0000	9.1562
3	0.758	0.0010001	168.132	12.57	2506.9	0.0457	9.0773
6	0.935	0.0010001	137.734	25.20	2512.4	0.0912	9.0003
9	1.148	0.0010003	113.386	37.80	2517.9	0.1362	8.9253
12	1.402	0.0010005	93.784	50.41	2523.4	0.1806	8.8524
15	1.705	0.0010009	77.926	62.99	2528.9	0.2245	8.7814
18	2.064	0.0010014	65.038	75.58	2534.4	0.2679	8.7123
21	2.487	0.0010020	54.514	88.14	2539.9	0.3109	8.6450
24	2.985	0.0010027	45.883	100.70	2545.4	0.3534	8.5794
27	3.567	0.0010035	38.774	113.25	2550.8	0.3954	8.5156
30	4.246	0.0010043	32.894	125.79	2556.3	0.4369	8.4533
33	5.034	0.0010053	28.011	138.33	2561.7	0.4781	8.3927
36	5.947	0.0010063	23.940	150.86	2567.1	0.5188	8.3336
40	7.384	0.0010078	19.523	167.57	2574.3	0.5725	8.2570
45	9.593	0.0010099	15.258	188.45	2583.2	0.6387	8.1648
50	12.349	0.0010121	12.032	209.33	2592.1	0.7038	8.0763
55	15.758	0.0010146	9.568	230.23	2600.9	0.7679	7.9913
60	19.940	0.0010172	7.671	251.13	2609.6	0.8312	7.9096
65	25.03	0.0010199	6.197	272.06	2618.3	0.8935	7.8310
70	31.19	0.0010228	5.042	292.98	2626.8	0.9549	7.7553
75	38.58	0.0010259	4.131	313.93	2635.3	1.0155	7.6824
80	47.39	0.0010291	3.407	334.91	2643.7	1.0753	7.6122
85	57.83	0.0010325	2.828	355.90	2651.9	1.1343	7.5445
90	70.14	0.0010360	2.361	376.92	2660.1	1.1925	7.4791
95	84.55	0.0010397	1.982	397.96	2668.1	1.2500	7.4159
100	101.35	0.0010435	1.673	419.04	2676.1	1.3069	7.3549
105	120.82	0.0010475	1.419	440.15	2683.8	1.3630	7.2958
110	143.27	0.0010516	1.210	461.30	2691.5	1.4185	7.2387
115	169.06	0.0010559	1.037	482.48	2699.0	1.4734	7.1833
120	198.53	0.0010603	0.892	503.71	2706.3	1.5276	7.1296
125	232.1	0.0010649	0.771	524.99	2713.5	1.5813	7.0775
130	270.1	0.0010697	0.669	546.31	2720.5	1.6344	7.0269
135	313.0	0.0010746	0.582	567.69	2727.3	1.6870	6.9777
140	316.3	0.0010797	0.509	589.13	2733.9	1.7391	6.9299
145	415.4	0.0010850	0.446	610.63	2740.3	1.7907	6.8833
150	475.8	0.0010905	0.393	632.20	2746.5	1.8418	6.8379
155	543.1	0.0010961	0.347	653.84	2752.4	1.8925	6.7935

TABLE A1 (continued)

Properties of Saturated Steam

t (°C)	Vapor Pressure (kPa)	Specific volume (m^3/kg)		Enthalpy (kJ/kg)		Entropy (kJ/kg K)	
		Liquid	Vapor	Liquid	Vapor	Liquid	Vapor
160	617.8	0.0011020	0.307	675.55	2758.1	1.9427	6.7502
165	700.5	0.0011080	0.273	697.34	2763.5	1.9925	6.7078
170	791.7	0.0011143	0.243	719.21	2768.7	2.0419	6.6663
175	892.0	0.0011207	0.217	741.17	2773.6	2.0909	6.6256
180	1002.1	0.0011274	0.194	763.22	2778.2	2.1396	6.5857
190	1254.4	0.0011414	0.157	807.62	2786.4	2.2359	6.5079
200	1553.8	0.0011565	0.127	852.45	2793.2	2.3309	6.4323
225	2548	0.0011992	0.078	966.78	2803.3	2.5639	6.2503
250	3973	0.0012512	0.050	1085.36	2801.5	2.7927	6.0730
275	5942	0.0013168	0.033	1210.07	2785.0	3.0208	5.8938
300	8581	0.0010436	0.022	1344.0	2749.0	3.2534	5.7045

TABLE A2

Physical Properties of Water at Saturation Pressure

Temp. (°C)	Density (kg/m³)	β 10^{-4} (K^{-1})	c_p (kJ/kg K)	k (W/m K)	α·10^{-6} (m^2/s)	η·10^{-6} (Pa s)	ν·10^{-6} (m^2/s)
0	999.9	–0.7	4.226	0.558	0.131	1793.64	1.79
5	1000.0		4.206	0.568	0.135	1534.74	1.54
10	999.7	0.95	4.195	0.577	0.137	1296.44	1.30
15	999.1		4.187	0.587	0.141	1135.61	1.15
20	998.2	2.1	4.182	0.597	0.143	993.41	1.01
25	997.1		4.178	0.606	0.146	880.64	0.88
30	995.7	3.0	4.176	0.615	0.149	792.38	0.81
35	994.1		4.175	0.624	0.150	719.81	0.73
40	992.2	3.9	4.175	0.633	0.151	658.03	0.66
45	990.2		4.176	0.640	0.155	605.07	0.61
50	988.1	4.6	4.178	0.647	0.157	555.06	0.56
55	985.7		4.179	0.652	0.158	509.95	0.52
60	983.2	5.3	4.181	0.658	0.159	471.65	0.48
65	980.6		4.184	0.663	0.161	435.42	0.44
70	977.8	5.8	4.187	0.668	0.163	404.03	0.42
75	974.9		4.190	0.671	0.164	376.58	0.37
80	971.8	6.3	4.194	0.673	0.165	352.06	0.36
85	968.7		4.198	0.676	0.166	328.52	0.34
90	965.3	7.0	4.202	0.678	0.167	308.91	0.33
95	961.9		4.206	0.680	0.168	292.24	0.31
100	958.4	7.5	4.211	0.682	0.169	277.53	0.29
110	951.0	8.0	4.224	0.684	0.170	254.97	0.27
120	943.5	8.5	4.232	0.685	0.171	235.36	0.24
130	934.8	9.1	4.250	0.686	0.172	211.82	0.23
140	926.3	9.7	4.257	0.684	0.172	201.04	0.21
150	916.9	10.3	4.270	0.684	0.173	185.35	0.20
160	907.6	10.8	4.285	0.680	0.173	171.62	0.19
170	897.3	11.5	4.396	0.679	0.172	162.29	0.18
180	886.6	12.1	4.396	0.673	0.172	152.00	0.17
190	876.0	12.8	4.480	0.670	0.171	145.14	0.17
200	862.8	13.5	4.501	0.665	0.170	139.25	0.16
210	852.8	14.3	4.560	0.655	0.168	131.41	0.15
220	837.0	15.2	4.605	0.652	0.167	124.54	0.15
230	827.3	16.2	4.690	0.637	0.164	119.64	0.15
240	809.0	17.2	4.731	0.634	0.162	113.76	0.14
250	799.2	18.6	4.857	0.618	0.160	109.83	0.14

β is the volumetric thermal expansion coefficient, $\hat{C}_p$ is the specific heat, k is the thermal conductivity, α is the thermal diffusivity, η is the absolute viscosity, and ν is the kinematic viscosity.

TABLE A3

Properties of Liquid and Saturated Vapor of Ammonia

t	p	Enthalpy (kJ/kg)		Entropy (kJ/kg·K)		Specific volume (l/kg)	
(°C)	(kPa)	Liquid $\hat{h}$	Vapor $\hat{H}$	Liquid $\hat{s}$	Vapor $\hat{S}$	Liquid $\hat{v}$	Vapor $\hat{V}$
–60	21.99	–69.5330	1373.19	–0.10909	6.6592	1.4010	4685.080
–55	30.29	–47.5062	1382.01	–0.00717	6.5454	1.4126	3474.220
–50	41.03	–25.4342	1390.64	0.09264	6.4382	1.4245	2616.510
–45	54.74	–3.3020	1399.07	0.19049	6.3369	1.4367	1998.910
–40	72.01	18.9024	1407.26	0.28651	6.2410	1.4493	1547.360
–35	93.49	41.1883	1415.20	0.38082	6.1501	1.4623	1212.490
–30	119.90	63.5629	1422.86	0.47351	6.0636	1.4757	960.867
–28	132.02	72.5387	1425.84	0.51015	6.0302	1.4811	878.100
–26	145.11	81.5300	1428.76	0.54655	5.9974	1.4867	803.761
–24	159.22	90.5370	1431.64	0.58272	5.9652	1.4923	736.868
–22	174.41	99.5600	1434.46	0.61865	5.9336	1.4980	676.570
–20	190.74	108.599	1437.23	0.65436	5.9025	1.5037	622.122
–18	208.26	117.656	1439.94	0.68984	5.8720	1.5096	572.875
–16	227.04	126.729	1442.60	0.72511	5.8420	1.5155	528.257
–14	247.14	135.820	1445.20	0.76016	5.8125	1.5215	487.769
–12	268.63	144.929	1447.74	0.79501	5.7835	1.5276	450.971
–10	291.57	154.056	1450.22	0.82965	5.7550	1.5338	417.477
–9	303.60	158.628	1451.44	0.84690	5.7409	1.5369	401.860
–8	316.02	163.204	1452.64	0.86410	5.7269	1.5400	386.944
–7	328.84	167.785	1453.83	0.88125	5.7131	1.5432	372.692
–6	342.07	172.371	1455.00	0.89835	5.6993	1.5464	359.071
–5	355.71	176.962	1456.15	0.91541	5.6856	1.5496	346.046
–4	369.77	181.559	1457.29	0.93242	5.6721	1.5528	333.589
–3	384.26	186.161	1458.42	0.94938	5.6586	1.5561	321.670
–2	399.20	190.768	1459.53	0.96630	5.6453	1.5594	310.263
–1	414.58	195.381	1460.62	0.98317	5.6320	1.5627	299.340
0	430.43	200.000	1461.70	1.00000	5.6189	1.5660	288.880
1	446.74	204.625	1462.76	1.01679	5.6058	1.5694	278.858
2	463.53	209.256	1463.80	1.03354	5.5929	1.5727	269.253
3	480.81	213.892	1464.83	1.05024	5.5800	1.5762	260.046
4	498.59	218.535	1465.84	1.06691	5.5672	1.5796	251.216
5	516.87	223.185	1466.84	1.08353	5.5545	1.5831	242.745
6	535.67	227.841	1467.82	1.10012	5.5419	1.5866	234.618
7	555.00	232.503	1468.78	1.11667	5.5294	1.5901	226.817
8	574.87	237.172	1469.72	1.13317	5.5170	1.5936	219.326
9	595.28	241.848	1470.64	1.14964	5.5046	1.5972	212.132
10	616.25	246.531	1471.57	1.16607	5.4924	1.6008	205.221
11	637.78	251.221	1472.46	1.18246	5.4802	1.6045	198.580
12	659.89	255.918	1473.34	1.19882	5.4681	1.6081	192.196
13	682.59	260.622	1474.20	1.21515	5.4561	1.6118	186.058
14	705.88	265.334	1475.05	1.23144	5.4441	1.6156	180.154
15	729.79	270.053	1475.88	1.24769	5.4322	1.6193	174.475
16	754.31	274.779	1476.69	1.26391	5.4204	1.6231	169.009
17	779.46	279.513	1477.48	1.28010	5.4087	1.6269	163.748
18	805.25	284.255	1478.25	1.29626	5.3971	1.6308	158.683
19	831.69	289.005	1479.01	1.31238	5.3855	1.6347	153.804
20	858.79	293.762	1479.75	1.32847	5.3740	1.6386	149.106
21	886.57	298.527	1480.48	1.34452	5.3626	1.6426	144.578

TABLE A3 (continued)

Properties of Liquid and Saturated Vapor of Ammonia

t	p	Enthalpy (kJ/kg)		Entropy (kJ/kg·K)		Specific volume (l/kg)	
(°C)	(kPa)	Liquid $\hat{h}$	Vapor $\hat{H}$	Liquid $\hat{s}$	Vapor $\hat{S}$	Liquid $\hat{v}$	Vapor $\hat{V}$
22	915.03	303.300	1481.18	1.36055	5.3512	1.6466	140.214
23	944.18	308.081	1481.87	1.37654	5.3399	1.6507	136.006
24	974.03	312.870	1482.53	1.39250	5.3286	1.6547	131.950
25	1004.60	317.667	1483.18	1.40843	5.3175	1.6588	128.037
26	1035.90	322.471	1483.81	1.42433	5.3063	1.6630	124.261
27	1068.00	327.284	1484.42	1.44020	5.2953	1.6672	120.619
28	1100.70	332.104	1485.01	1.45604	5.2843	1.6714	117.103
29	1134.30	336.933	1485.59	1.47185	5.2733	1.6757	113.708
30	1168.60	341.769	1486.14	1.48762	5.2624	1.6800	110.430
31	1203.70	346.614	1486.67	1.50337	5.2516	1.6844	107.263
32	1239.60	351.466	1487.18	1.51908	5.2408	1.6888	104.205
33	1276.30	356.326	1487.66	1.53477	5.2300	1.6932	101.248
34	1313.90	361.195	1488.13	1.55042	5.2193	1.6977	98.391
35	1352.20	366.072	1488.57	1.56605	5.2086	1.7023	95.629
36	1391.50	370.957	1488.99	1.58165	5.1980	1.7069	92.958
37	1431.50	375.851	1489.39	1.59722	5.1874	1.7115	90.374
38	1472.40	380.754	1489.76	1.61276	5.1768	1.7162	87.875
39	1514.30	385.666	1489.10	1.62828	5.1663	1.7209	85.456
40	1557.00	390.587	1490.42	1.64377	5.1558	1.7257	83.115
41	1600.60	395.519	1490.71	1.65924	5.1453	1.7305	80.848
42	1645.10	400.462	1490.98	1.67470	5.1349	1.7354	78.654
43	1690.60	405.416	1491.21	1.69013	5.1244	1.7404	76.528
44	1737.00	410.382	1491.41	1.70554	5.1140	1.7454	74.468
45	1784.30	415.362	1491.58	1.72095	5.1036	1.7504	72.472
46	1832.60	420.358	1491.72	1.73635	5.0932	1.7555	70.536
47	1881.90	425.369	1491.83	1.75174	5.0827	1.7607	68.660
48	1932.20	430.399	1491.88	1.76714	5.0723	1.7659	66.840
49	1983.50	435.450	1491.91	1.78255	5.0618	1.7712	65.075
50	2035.90	440.523	1491.89	1.79798	5.0514	1.7766	63.361
51	2089.20	445.623	1491.83	1.81343	5.0409	1.7820	61.697
52	2143.60	450.751	1491.73	1.82891	5.0303	1.7875	60.081
53	2199.10	455.913	1491.58	1.84445	5.0198	1.7931	58.511
54	2255.60	461.112	1491.38	1.86004	5.0092	1.7987	56.985
55	2313.20	466.353	1491.12	1.87571	4.9985	1.8044	55.502

TABLE A4

Normalized Dimensions of Steel Tubing

Catalog Number	Nominal Diameter (in.)	External Diameter (cm)	Internal Diameter (cm)	Wall Thickness (cm)
40	⅛	1.029	0.683	0.173
80	⅛	1.029	0.546	0.241
40	¼	1.372	0.925	0.224
80	¼	1.372	0.767	0.302
40	⅜	1.715	1.252	0.231
80	⅜	1.715	1.074	0.320
40	½	2.134	1.580	0.277
80	½	2.134	1.387	0.373
40	¾	2.667	2.093	0.287
80	¾	2.667	1.885	0.391
40	1	3.340	2.664	0.338
80	1	3.340	2.431	0.455
40	1¼	4.216	3.505	0.356
80	1¼	4.216	3.246	0.485
40	1½	4.826	4.089	0.368
80	1½	4.826	3.810	0.508
40	2	6.033	5.250	0.391
80	2	6.033	4.925	0.554
40	2½	7.303	6.271	0.516
80	2½	7.303	5.900	0.701
40	3	8.890	7.793	0.549
80	3	8.890	7.366	0.762
40	3½	10.16	9.012	0.574
80	3½	10.16	8.545	0.808
40	4	11.43	10.226	0.602
80	4	11.43	9.718	0.856
40	5	14.23	12.819	0.655
80	5	14.13	12.225	0.953
40	6	16.83	15.405	0.711
80	6	16.83	14.633	1.097
40	8	21.91	20.272	0.818
80	8	21.91	19.368	1.270
40	10	27.31	25.451	0.927
80	10	27.31	24.287	1.509
40	12	32.39	30.323	1.031
80	12	32.39	28.890	1.748

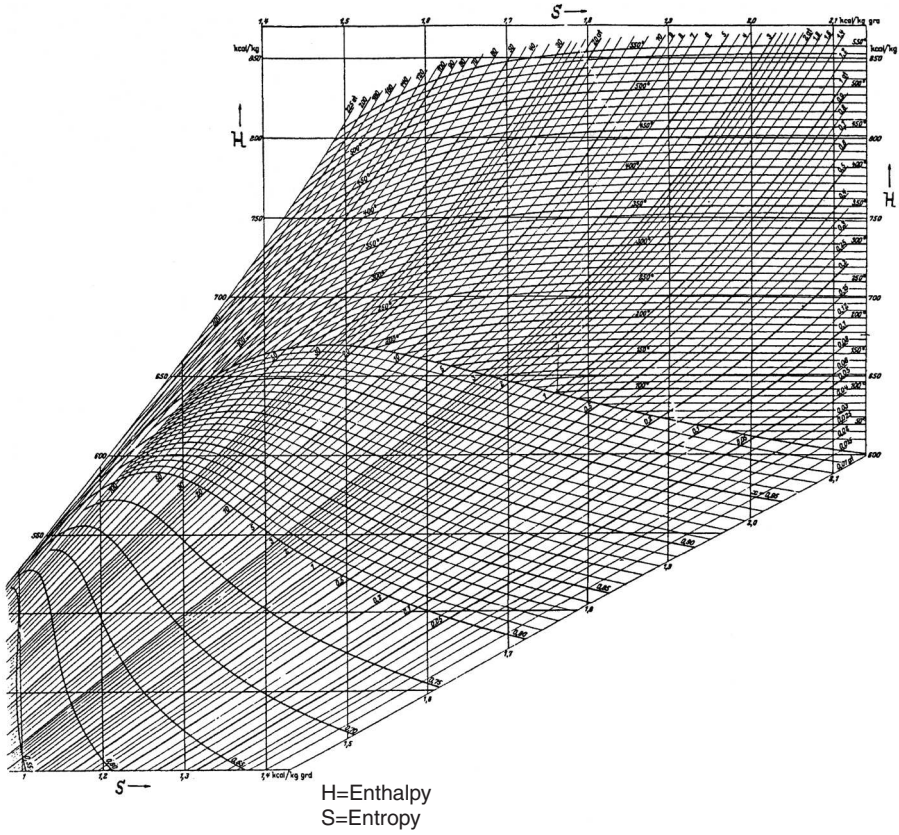

FIGURE A1
Mollier diagram for steam. H = enthalpy; S = entropy.

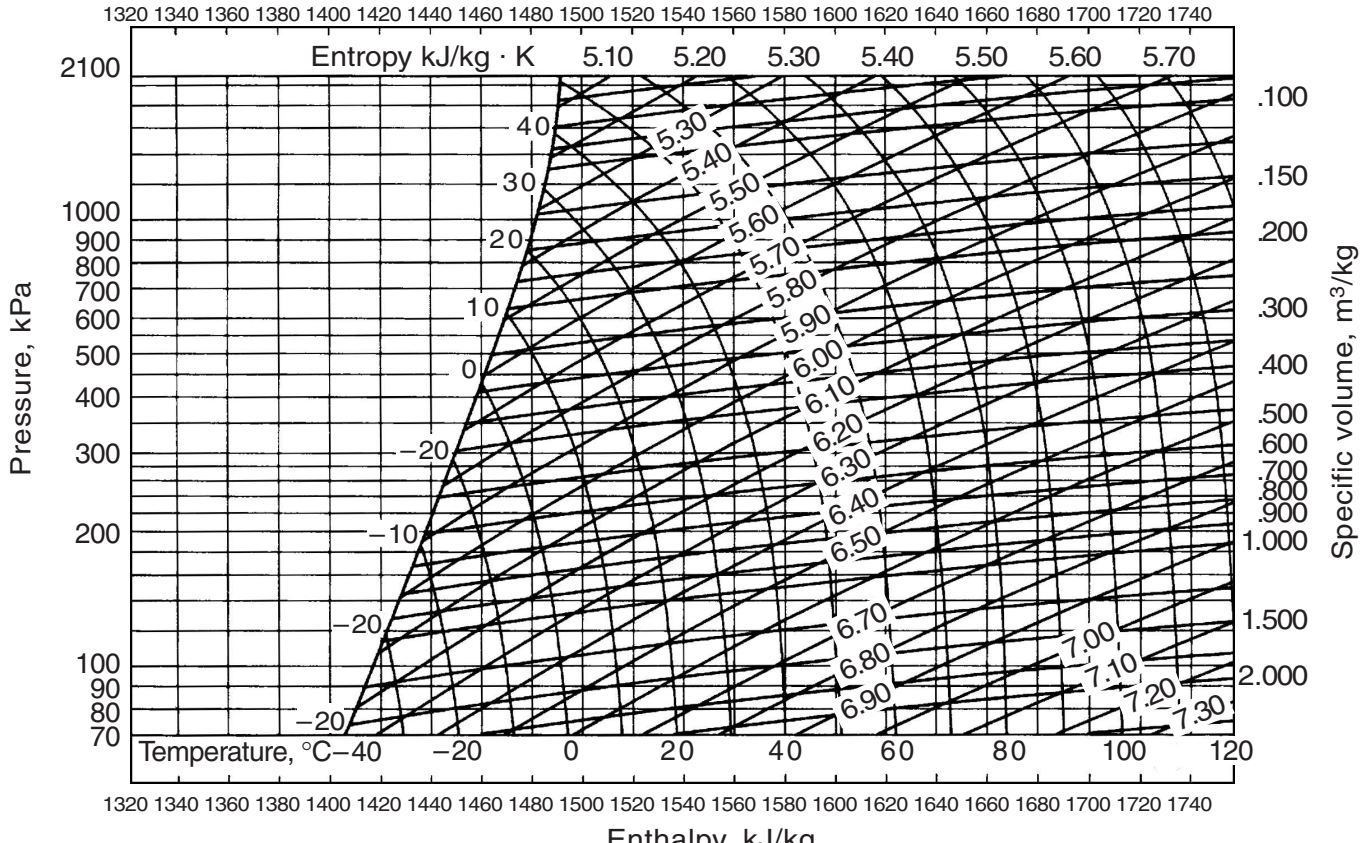

FIGURE A2
Diagram for ammonia.

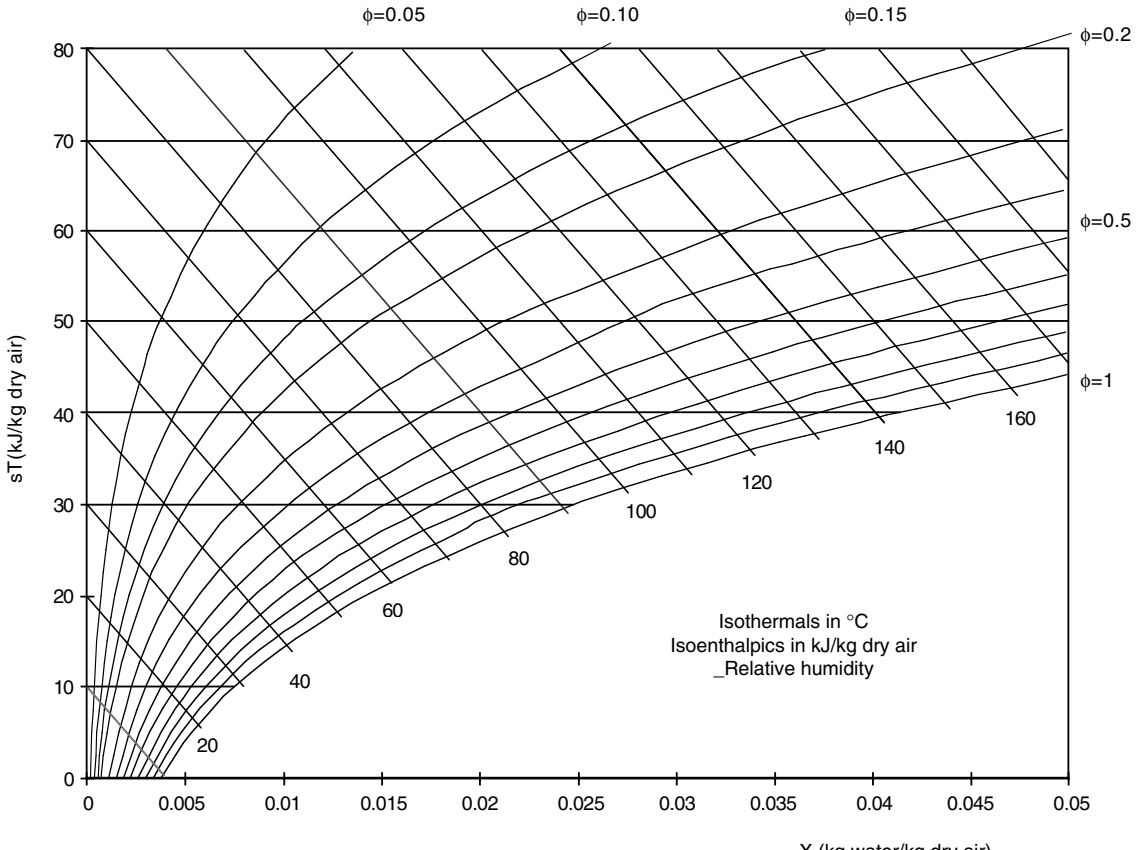

FIGURE A3
Psychrometric chart *sT–X*.